



U.S. Department  
of Transportation

**Federal Highway  
Administration**

Publication No. FHWA NHI 01-004

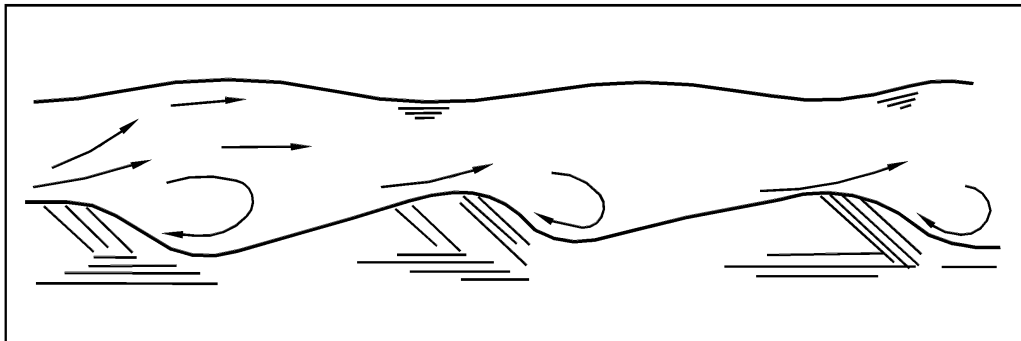
December 2001

**Hydraulic Design Series Number 6**

---

## **RIVER ENGINEERING FOR HIGHWAY ENCROACHMENTS**

### **Highways in the River Environment**



**NATIONAL HIGHWAY INSTITUTE**



1. Report No. FHWA NHI 01-004 HDS 6		2. Government Accession No.		3. Recipient's Catalog No.	
4. Title and Subtitle  RIVER ENGINEERING FOR HIGHWAY ENCROACHMENTS Highways in the River Environment				5. Report Date December 2001	
				6. Performing Organization Code	
7. Author(s)  E.V. Richardson, D.B. Simons, P.F. Lagasse				8. Performing Organization Report No.	
9. Performing Organization Name and Address  Ayres Associates 3665 JFK Parkway Building 2, Suite 200 Fort Collins, Colorado 80525				10. Work Unit No. (TRAIS)	
				11. Contract or Grant No.  DTFH61-99-T-25051	
12. Sponsoring Agency Name and Address  Office of Bridge Technology FHWA, Room 3203 400 Seventh Street, SW Washington, D.C. 20590				13. Type of Report and Period Covered	
				14. Sponsoring Agency Code	
15. Supplementary Notes  Project Manager: Philip L. Thompson Technical Assistants: Larry Arneson, J. Sterling Jones, Jorge E. Pagán-Ortiz, FHWA; P.E. Clopper, J.D. Schall, S.A. Schumm, L.W. Zevenbergen, Ayres Associates					
<p>The Federal Highway Administration document "Highways in the River Environment - Hydraulic and Environmental Design Considerations" was first published in 1975, was revised in 1990, and is now issued as Hydraulic Design Series 6, "River Engineering for Highway Encroachments." This document has proven to be a singularly authoritative document for the design of highway associated hydraulic structures in moveable boundary waterways. This revised document incorporates many technical advances that have been made in this discipline since 1990. In addition, Hydraulic Engineering Circulars (HEC) 18, 20, and 23, have been published since 1990. This document and the HECs provide detailed guidance on stream instability, scour, and appropriate countermeasures. In HDS-6, hydraulic problems at stream crossings are described in detail and the hydraulic principles of rigid and moveable boundary channels are discussed.</p> <p>In the United States, the average annual damage related to hydraulic problems at highway facilities on the Federal-aid system is \$40 million. Damages by streams can be reduced significantly by considering channel stability. The types of river changes to be carefully considered relate to: (1) lateral bank erosion; (2) degradation and aggradation of the streambed that continues over a period of years, and (3) natural short-term fluctuations of streambed elevation that are usually associated with the passage of floods. The major topics are: sediment transport, natural and human induced causes of waterway response, stream stabilization (bed and banks), hydraulic modeling and computer applications, and countermeasures. Case histories of typical human and natural impacts on waterways are analyzed.</p>					
17. Key Words  aggradation, degradation, alluvial channel, alluvial fan, river training, geomorphology, headcutting, lateral migration, riprap, sediment transport, scour, stable channel design, countermeasures			18. Distribution Statement  This document is available to the public through the National Technical Information Service, Springfield, VA 22161 (703) 487-4650 and isddc.dot.gov		
19. Security Classif. (of this report)  Unclassified		20. Security Classif. (of this page)  Unclassified		21. No. of Pages  644	22. Price





## TABLE OF CONTENTS

LIST OF FIGURES .....	xiii
LIST OF TABLES .....	xxv
ACKNOWLEDGMENTS .....	xxix
SYMBOLS .....	xxx
GLOSSARY .....	xxxvii
1. INTRODUCTION .....	1.1
1.1 CLASSIFICATION OF RIVER CROSSINGS AND ENCROACHMENTS .....	1.1
1.1.1 Types of Encroachment.....	1.2
1.1.2 Geometry of Bridge Crossings.....	1.2
1.2 DYNAMICS OF NATURAL RIVERS AND THEIR TRIBUTARIES.....	1.2
1.2.1 Historical Evidence of the Natural Instability of Fluvial Systems.....	1.3
1.2.2 Introduction to River Hydraulics and River Response .....	1.7
1.3 EFFECTS OF HIGHWAY CONSTRUCTION ON RIVER SYSTEMS.....	1.9
1.3.1 Immediate Response of Rivers to Encroachment.....	1.9
1.3.2 Delayed Response of Rivers to Encroachment.....	1.10
1.4 EFFECTS OF RIVER DEVELOPMENT ON HIGHWAY ENCROACHMENTS.....	1.11
1.5 TECHNICAL ASPECTS.....	1.13
1.5.1 Variables Affecting River Behavior.....	1.14
1.5.2 Basic Knowledge Required.....	1.14
1.5.3 Data Requirements.....	1.14
1.6 FUTURE TECHNICAL TRENDS .....	1.15
1.6.1 Adequacy of Current Knowledge .....	1.15
1.6.2 Research Needs.....	1.16
1.6.3 Training .....	1.17
1.7 OVERVIEW OF MANUAL CONTENTS .....	1.17
1.7.1 Chapter 2 - Open Channel Flow .....	1.17
1.7.2 Chapter 3 - Fundamentals of Alluvial Channel Flow.....	1.18
1.7.3 Chapter 4 - Sediment Transport .....	1.18
1.7.4 Chapter 5 - River Morphology and River Response .....	1.19
1.7.5 Chapter 6 - River Stabilization and Bank Protection .....	1.19
1.7.6 Chapter 7 - Scour at Bridges .....	1.19
1.7.7 Chapter 8 - Data Need and Data Sources .....	1.20

1.7.8	Chapter 9 - Design Considerations for Highway Encroachment and River Crossings .....	1.20
1.7.9	Chapter 10 - Overview Examples of Design for Highways in the River Environment .....	1.21
1.7.10	Chapter 11 - References .....	1.21
1.7.11	Appendices .....	1.21
1.8	DUAL SYSTEM OF UNITS .....	1.21
2.	OPEN CHANNEL FLOW .....	2.1
2.1	INTRODUCTION .....	2.1
2.1.1	Definitions .....	2.1
2.2	THREE BASIC EQUATIONS .....	2.3
2.2.1	Conservation of Mass .....	2.3
2.2.2	Conservation of Linear Momentum .....	2.6
2.2.3	Conservation of Energy .....	2.8
2.3	HYDROSTATICS .....	2.12
2.4	STEADY UNIFORM FLOW .....	2.14
2.4.1	Introduction .....	2.14
2.4.2	Shear Stress, Velocity Distribution, and Average Velocity .....	2.16
2.4.3	Other Velocity Equations .....	2.21
2.4.4	Average Boundary Shear Stress .....	2.24
2.4.5	Relation Between Shear Stress and Velocity .....	2.27
2.4.6	Energy and Momentum Coefficients for Rivers .....	2.28
2.5	UNSTEADY FLOW .....	2.32
2.5.1	Gravity Waves .....	2.32
2.5.2	Surges .....	2.34
2.5.3	Hydraulic Jump .....	2.35
2.5.4	Roll Waves .....	2.35
2.6	STEADY RAPIDLY VARYING FLOW .....	2.38
2.6.1	Flow Through Transitions .....	2.38
2.6.2	Specific Energy Diagram .....	2.39
2.6.3	Specific Discharge Diagram .....	2.40
2.6.4	Transitions With Super Critical Flows .....	2.43
2.6.5	Flow Over Drop Structures .....	2.44
2.7	FLOW IN BENDS .....	2.45
2.7.1	Types of Bends .....	2.45
2.7.2	Transverse Velocity Distribution in Bends .....	2.46

2.7.3	Subcritical Flow in Bends .....	2.47
2.7.4	Supercritical Flow in Bends .....	2.49
2.8	GRADUALLY VARIED FLOW .....	2.50
2.8.1	Introduction .....	2.50
2.8.2	Classification of Flow Profiles .....	2.50
2.8.3	Standard Step Method for the Computation of Water Surface Profiles .....	2.55
2.9	STREAM GAGING .....	2.56
2.9.1	Introduction .....	2.56
2.9.2	Gaging Station .....	2.56
2.9.3	Measuring Water Discharge .....	2.60
2.9.4	Stage-Discharge Relation .....	2.61
2.10	HYDRAULICS OF BRIDGE WATERWAYS .....	2.62
2.10.1	Introduction .....	2.62
2.10.2	Backwater Effects on Waterway Openings .....	2.63
2.10.3	Effects of a Submerged Superstructure .....	2.63
2.10.4	Effects of Supercritical Flow .....	2.63
2.10.5	Types of Flow in Bridge Openings .....	2.63
2.11	COMPUTER MODELS FOR HIGHWAY BRIDGES .....	2.65
2.11.1	One-Dimensional Computer Models .....	2.65
2.11.2	Two-Dimensional Computer Models .....	2.67
2.12	HYDRAULICS OF CULVERT FLOW .....	2.67
2.12.1	Introduction .....	2.67
2.13	ROADWAY OVERTOPPING .....	2.68
2.14	SOLVED PROBLEMS OPEN CHANNEL FLOW (SI) .....	2.68
2.14.1	PROBLEM 1 Evaluation of Correction Factors $\alpha$ and $\beta$ .....	2.68
2.14.2	PROBLEM 2 Velocity Profiles and Shear Stress .....	2.71
2.14.3	PROBLEM 3 Superelevation in Bends .....	2.74
2.14.4	PROBLEM 4 Maximum Stream Constriction Without Causing Backwater .....	2.75
2.14.5	PROBLEM 5 Maximum Water Surface Elevation Upstream of a Grade Control Structure Without Backwater .....	2.76
2.15	SOLVED PROBLEMS OPEN CHANNEL FLOW (ENGLISH) .....	2.79
2.15.1	PROBLEM 1 Evaluation of Correction Factors $\alpha$ and $\beta$ .....	2.79
2.15.2	PROBLEM 2 Velocity Profiles and Shear Stress .....	2.81
2.15.3	PROBLEM 3 Superelevation in Bends .....	2.84

2.15.4	PROBLEM 4 Maximum Stream Constriction Without Causing Backwater.....	2.85
2.15.5	PROBLEM 5 Maximum Elevation of a Grade Control Structure Without Backwater .....	2.86
3.	FUNDAMENTALS OF ALLUVIAL CHANNEL FLOW .....	3.1
3.1	INTRODUCTION .....	3.1
3.2	SEDIMENT PROPERTIES AND MEASUREMENT TECHNIQUES .....	3.1
3.2.1	Particle Size.....	3.1
3.2.2	Particle Shape .....	3.2
3.2.3	Fall Velocity .....	3.4
3.2.4	Sediment Size Distribution.....	3.6
3.2.5	Specific Weight.....	3.11
3.2.6	Porosity.....	3.11
3.2.7	Cohesion .....	3.12
3.2.8	Angle of Repose .....	3.12
3.3	FLOW IN SANDBED CHANNELS .....	3.12
3.3.1	Regimes of Flow in Alluvial Channels .....	3.13
3.3.2	Bed Configuration .....	3.15
3.3.3	Plane Bed Without Sediment Movement .....	3.17
3.3.4	Ripples.....	3.17
3.3.5	Dunes .....	3.17
3.3.6	Plane Bed With Movement .....	3.18
3.3.7	Antidunes.....	3.18
3.3.8	Chutes and Pools .....	3.19
3.3.9	Regime of Flow, Bed Configuration, and Froude Number.....	3.19
3.3.10	Bars.....	3.19
3.4	RESISTANCE TO FLOW IN ALLUVIAL CHANNELS .....	3.21
3.4.1	Depth.....	3.22
3.4.2	Slope .....	3.23
3.4.3	Apparent Viscosity and Density .....	3.23
3.4.4	Size of Bed Material.....	3.24
3.4.5	Size Gradation .....	3.25
3.4.6	Fall Velocity .....	3.25
3.4.7	Shape Factor for the Reach and Cross-Section.....	3.26
3.4.8	Seepage Force .....	3.26
3.4.9	Bed Material Concentration .....	3.26
3.4.10	Fine-Material Concentration.....	3.26
3.4.11	Bedform Predictor and Manning's n Values for Sand-Bed Streams ...	3.27
3.4.12	How Bedform Changes Affect Highways in the River Environment....	3.28
3.4.13	Alluvial Processes and Resistance to Flow in Coarse Material Streams.....	3.29

3.5	BEGINNING OF MOTION .....	3.32
3.5.1	Introduction.....	3.32
3.5.2	Theoretical Considerations .....	3.32
3.5.3	Theory of Beginning of Motion .....	3.33
3.5.4	Shields Diagram .....	3.36
3.5.5	Equations for Flow and Sediment Variables for Beginning of Motion .....	3.39
3.5.6	Tables for Determining Critical Velocities.....	3.43
3.5.7	Figures for Determining Critical Shear Stress or Velocity .....	3.44
3.5.8	Summary.....	3.45
3.6	SEDIMENT DISCHARGE MEASUREMENT.....	3.46
3.6.1	Introduction.....	3.46
3.6.2	Terminology.....	3.46
3.6.3	Suspended Sediment Discharge Measurement.....	3.47
3.6.4	Velocity Weighted Mean Suspended-Sediment Concentration .....	3.47
3.6.5	Suspended Sediment Hydrograph.....	3.49
3.6.6	Determination of Daily Suspended-Sediment Discharge.....	3.49
3.6.7	Total Sediment Discharge.....	3.51
3.7	SOLVED PROBLEMS FOR ALLUVIAL CHANNEL FLOW (SI).....	3.52
3.7.1	PROBLEM 1 Sediment Properties and Fall Velocities .....	3.52
3.7.2	PROBLEM 2 Angle of Repose.....	3.56
3.7.3	PROBLEM 3 Resistance to Flow in Alluvial Channels.....	3.57
3.7.4	PROBLEM 4 Beginning of Motion.....	3.59
3.8	SOLVED PROBLEMS FOR ALLUVIAL CHANNEL FLOW (ENGLISH) .....	3.61
3.8.1	PROBLEM 1 Sediment Properties and Fall Velocities .....	3.61
3.8.2	PROBLEM 2 Angle of Repose.....	3.62
3.8.3	PROBLEM 3 Resistance to Flow in Alluvial Channels.....	3.62
3.8.4	PROBLEM 4 Beginning of Motion.....	3.64
4.	SEDIMENT TRANSPORT .....	4.1
4.1	INTRODUCTION .....	4.1
4.2	DEFINITIONS.....	4.1
4.3	GENERAL CONSIDERATIONS.....	4.3
4.3.1	Source of Sediment Transport.....	4.3
4.3.2	Mode of Sediment Transport .....	4.4
4.3.3	Total Sediment Discharge.....	4.5
4.4	SUSPENDED BED SEDIMENT DISCHARGE.....	4.6
4.5	BED SEDIMENT DISCHARGE.....	4.10
4.5.1	Meyer-Peter and Müller Bed Load Equation .....	4.10
4.5.2	Einstein's Method of Computing Bed Sediment Discharge .....	4.13
4.5.3	Comparison of Meyer-Peter and Müller and Einstein Contact Load Equations.....	4.21
4.5.4	Colby's Method of Estimating Bed Sediment Discharge .....	4.22
4.5.5	Relative Influence of Variables .....	4.24

4.6	POWER FUNCTION RELATIONSHIPS .....	4.27
4.6.1	Introduction.....	4.27
4.6.2	Basic Power Function Relationship.....	4.27
4.6.3	Expanded Power Function Relationship.....	4.29
4.7	YANG'S EQUATIONS .....	4.30
4.8	CONVERSION FACTORS.....	4.31
4.9	APPLICATION OF SELECTED SEDIMENT TRANSPORT EQUATIONS .....	4.32
4.10	SUMMARY .....	4.34
4.11	SEDIMENT TRANSPORTATION ANALYSIS PROCEDURE.....	4.34
4.11.1	Step 1: Determine if Sediment Transport Computations are Necessary .....	4.34
4.11.2	Step 2: Determine Scope of Sediment Transport Analysis.....	4.35
4.11.3	Step 3: Determine the Type of Analysis.....	4.35
4.12	SOLVED PROBLEMS FOR SEDIMENT TRANSPORT (SI) .....	4.37
4.12.1	Introduction.....	4.37
4.12.2	Problem 1 Suspended Sediment Concentration Profile .....	4.37
4.12.3	Problem 2 Using the Meyer-Peter and Müller Equation Calculate the Bed Sediment Discharge (Bed Load).....	4.38
4.12.4	Problem 3 Application of the Einstein Method to Calculate Total Bed-Material Discharge .....	4.39
4.12.5	Problem 4 Calculation of Total Bed-Material Discharge Using Colby's Method.....	4.39
4.12.6	Problem 5 Calculation of Total Bed-Material Discharge Using the Basic Power Function Relationship.....	4.40
4.12.7	Problem 6 Calculation of Total Bed-Material Discharge Using the Expanded Power Function Relationship .....	4.40
4.12.8	Problem 7 Calculate Total Bed-Material Discharge Using Yang's Sand Equation .....	4.41
4.13	SOLVED PROBLEMS FOR SEDIMENT TRANSPORT (ENGLISH) .....	4.42
4.13.1	Introduction.....	4.42
4.13.2	Problem 1 Suspended Sediment Concentration Profile .....	4.42
4.13.3	Problem 2 Using the Meyer-Peter and Müller Equation Calculate the Bed Sediment Discharge (Bed Load).....	4.43
4.13.4	Problem 3 Application of the Einstein Method to Calculate Total Bed-Material Discharge .....	4.44
4.13.5	Problem 4 Calculation of Total Bed-Material Discharge Using Colby's Method.....	4.50
4.13.6	Problem 5 Calculation of Total Bed-Material Discharge Using the Basic Power Function Relationship.....	4.52
4.13.7	Problem 6 Calculation of Total Bed-Material Discharge Using the Expanded Power Function Relationship .....	4.53
4.13.8	Problem 7 Calculate Total Bed-Material Discharge Using Yang's Equation .....	4.53
5.	RIVER MORPHOLOGY AND RIVER RESPONSE .....	5.1
5.1	INTRODUCTION .....	5.1

5.2	FLUVIAL CYCLES AND PROCESSES .....	5.1
5.2.1	Youthful, Mature, and Old Streams.....	5.1
5.2.2	Floodplain and Delta Formations .....	5.2
5.2.3	Alluvial Fans .....	5.2
5.2.4	Nickpoint Migration and Headcutting .....	5.3
5.2.5	Geomorphic Threshold .....	5.5
5.3	VARIABILITY AND CHANGE IN ALLUVIAL RIVERS .....	5.5
5.3.1	Differences Through Time .....	5.7
5.3.2	Differences Between Reaches.....	5.8
5.3.3	Summary .....	5.12
5.4	STREAM FORM AND GEOMETRY OF ALLUVIAL CHANNELS .....	5.12
5.4.1	Classification of River Channels .....	5.13
5.4.2	Straight River Channels.....	5.17
5.4.3	Meandering River Channels.....	5.17
5.4.4	Braided River Channels .....	5.20
5.4.5	River Conditions for Meandering and Braiding.....	5.21
5.4.6	Hydraulic Geometry of Alluvial Channels .....	5.23
5.4.7	Dominant Discharge in Alluvial Rivers .....	5.27
5.4.8	River Profiles and Bed Material.....	5.28
5.5	QUALITATIVE RESPONSE OF RIVER SYSTEMS .....	5.28
5.5.1	General River Response to Change .....	5.29
5.5.2	Prediction of Channel Response to Change .....	5.32
5.5.3	River Pattern Thresholds and Response .....	5.34
5.6	MODELING OF RIVER SYSTEMS .....	5.39
5.6.1	Physical Modeling .....	5.40
5.6.2	Computer Modeling .....	5.43
5.6.3	Data Needs.....	5.47
5.7	HIGHWAY PROBLEMS RELATED TO GRADATION CHANGES .....	5.48
5.7.1	Changes Due to Human Activities .....	5.48
5.7.2	Natural Causes .....	5.50
5.7.3	Resulting Problems at Highway Crossings .....	5.51
5.8	STREAM STABILITY PROBLEMS AT HIGHWAY CROSSINGS.....	5.52
5.8.1	Bank Stability.....	5.53
5.8.2	Stability Problems Associated With Channel Relocation.....	5.54
5.8.3	Assessment of Stability for Relocated Streams .....	5.59
5.8.4	Estimation of Future Channel Stability and Behavior .....	5.60
5.8.5	Advances in Predicting Meander Migration .....	5.64

5.9	SOLVED PROBLEMS RIVER MORPHOLOGY AND RESPONSE .....	5.67
5.9.1	PROBLEM 1 Meandering and Braiding.....	5.67
5.9.2	PROBLEM 2 Classification of Alluvial Reaches .....	5.68
5.9.3	PROBLEM 3 Channel Response to Changes in Watershed Conditions .....	5.69
5.9.4	PROBLEM 4 Channel Migration Rate .....	5.69
5.9.5	PROBLEM 5 At-A-Station and Downstream Hydraulic Geometry Relationships (SI) .....	5.71
5.9.6	PROBLEM 6 At-A-Station and Downstream Hydraulic Geometry Relationships (English).....	5.73
5.9.7	PROBLEM 7 Downstream Sediment Size Distribution .....	5.74
5.9.8	PROBLEM 8 Scale Ratios for Physical Models (SI).....	5.75
5.9.9	PROBLEM 9 Scale Ratios for Physical Models (English).....	5.76
6.	RIVER STABILIZATION AND BANK PROTECTION .....	6.1
6.1	OVERVIEW .....	6.1
6.2	STREAM BANK EROSION.....	6.2
6.2.1	Causes of Streambank Failure .....	6.2
6.2.2	Bed and Bank Material.....	6.3
6.2.3	Subsurface Flow .....	6.3
6.2.4	Piping of River Banks .....	6.5
6.2.5	Mass Wasting .....	6.5
6.3	RIVER TRAINING AND STABILIZATION .....	6.6
6.3.1	Fixed Points.....	6.6
6.3.2	Radius of Curvature.....	6.6
6.3.3	Countermeasures for Channel Instability .....	6.7
6.3.4	Countermeasure Design Guidelines .....	6.8
6.3.5	Protection of Training Works .....	6.9
6.4	FLOW CONTROL STRUCTURES .....	6.10
6.4.1	Spurs.....	6.10
6.4.2	Bendway Weirs.....	6.12
6.4.3	Hardpoints .....	6.12
6.4.4	Retards.....	6.12
6.4.5	Dikes (Floodplain).....	6.14
6.4.6	Dikes (Channel).....	6.14
6.4.7	Jetties .....	6.16
6.4.8	Bulkheads.....	6.17
6.4.9	Fencing.....	6.18
6.4.10	Guide Banks .....	6.18
6.4.11	Drop Structures .....	6.19



6.5	RIPRAP DESIGN AND PLACEMENT .....	6.20
6.5.1	Factors to Consider .....	6.20
6.5.2	Stability Factor Design Methods .....	6.21
6.5.3	Velocity Profile and Tractive Force .....	6.24
6.5.4	U.S. Army Corps of Engineers Design Equation .....	6.25
6.5.5	Riprap Gradation and Thickness .....	6.28
6.5.6	Riprap Placement .....	6.30
6.5.7	Riprap Failure Modes.....	6.33
6.6	BANK PROTECTION OTHER THAN RIPRAP .....	6.36
6.6.1	Bioengineering Erosion Control .....	6.36
6.6.2	Bioengineering Countermeasures.....	6.37
6.6.3	Rock-and-Wire Mattresses .....	6.38
6.6.4	Gabions .....	6.39
6.6.5	Sacks.....	6.39
6.6.6	Articulated Concrete Block Systems (ACBs).....	6.40
6.6.7	Used Tires .....	6.41
6.6.8	Soil Cement.....	6.42
6.7	FILTERS.....	6.43
6.8	OVERTOPPING FLOW ON EMBANKMENTS .....	6.44
6.8.1	Introduction.....	6.44
6.8.2	Hydraulics of Overtopping Flow .....	6.45
6.8.3	Mechanics of Overflow Erosion.....	6.48
6.8.4	Erosion Protection in Overtoppng Flow.....	6.50
6.8.5	Overtopping Protection Systems.....	6.51
6.9	ENVIRONMENTAL CONSIDERATIONS .....	6.53
6.9.1	Environmental Impacts .....	6.53
6.9.2	Effects of Channelization .....	6.54
6.9.3	Channel Restoration and Rehabilitation .....	6.55
6.10	SOLVED PROBLEMS FOR STABILITY OF RIPRAP (SI) .....	6.55
6.10.1	PROBLEM 1 Stability of Particles Under Downslope Flow .....	6.55
6.10.2	PROBLEM 2 Riprap Design on Embankment Slopes .....	6.56
6.10.3	PROBLEM 3 Stability Factors for Riprap Design .....	6.57
6.10.4	PROBLEM 4 Riprap Design on an Abutment.....	6.60
6.11	SOLVED PROBLEMS FOR FILTER DESIGN (SI) .....	6.61
6.11.1	PROBLEM 1 Filter Design .....	6.61
6.11.2	PROBLEM 2 Filter Design .....	6.62

6.12	SOLVED PROBLEMS FOR STABILITY OF RIPRAP (ENGLISH) .....	6.64
6.12.1	PROBLEM 1 Stability of Particles Under Downslope Flow .....	6.64
6.12.2	PROBLEM 2 Riprap Design on Embankment Slopes .....	6.65
6.12.3	PROBLEM 3 Stability Factors for Riprap Design .....	6.67
6.12.4	PROBLEM 4 Riprap Design on an Abutment.....	6.68
6.13	SOLVED PROBLEMS FOR FILTER DESIGN (ENGLISH) .....	6.70
6.13.1	PROBLEM 1 Filter Design .....	6.71
6.13.2	PROBLEM 2 Filter Design .....	6.71
7.	SCOUR AT BRIDGES .....	7.1
7.1	INTRODUCTION .....	7.1
7.1.1	General.....	7.1
7.1.2	Costs of Bridge Failure From Scour.....	7.1
7.1.3	Bridge Scour Evaluation Program.....	7.2
7.1.4	Comprehensive Scour Analysis .....	7.2
7.2	TOTAL SCOUR.....	7.4
7.3	CLEAR-WATER AND LIVE-BED SCOUR .....	7.4
7.4	ARMORING.....	7.6
7.5	LONG-TERM BED ELEVATION CHANGES.....	7.6
7.6	GENERAL SCOUR.....	7.7
7.6.1	Contraction Scour .....	7.8
7.6.2	Computer Models for General Scour .....	7.12
7.7	LOCAL SCOUR AT PIERS.....	7.12
7.7.1	Introduction.....	7.12
7.7.2	Comparison of Pier Scour Equations .....	7.13
7.7.3	Colorado State University's Equation.....	7.13
7.7.4	FHWA HEC-18 Equation .....	7.16
7.7.5	Pier Scour in Cohesive Bed Material.....	7.19
7.7.6	Pier Scour for Other Pier Geometry, Flow Conditions, and Debris.....	7.20
7.7.7	Topwidth of Scour Holes.....	7.20
7.7.8	Physical Model Studies.....	7.21
7.8	LOCAL SCOUR AT ABUTMENTS.....	7.21
7.8.1	Introduction.....	7.21
7.8.2	Commentary on Abutment Scour Equations .....	7.23
7.8.3	Abutment Site Conditions .....	7.24
7.8.4	Abutment Shape.....	7.25
7.8.5	Froehlich's Live-Bed Scour Equation .....	7.25
7.8.6	1975 and 1990 HIRE Equation .....	7.26
7.9	SCOUR PROBLEMS .....	7.27

8.	DATA NEEDS AND DATA SOURCES .....	8.1
8.1	BASIC DATA NEEDS .....	8.1
8.1.1	Area Maps .....	8.1
8.1.2	Vicinity Maps.....	8.1
8.1.3	Site Maps.....	8.1
8.1.4	Aerial and Other Photographs .....	8.2
8.1.5	Field Inspection.....	8.2
8.1.6	Geologic Map .....	8.2
8.1.7	Climatologic Data.....	8.3
8.1.8	Hydraulic Data .....	8.3
8.1.9	Hydrologic Data .....	8.4
8.1.10	Environmental Data .....	8.5
8.2	CHECKLIST OF DATA NEEDS .....	8.5
8.3	DATA SOURCES .....	8.5
8.4	COMPUTERIZED LITERATURE AND DATA SEARCH.....	8.10
8.4.1	COMPENDEX.....	8.10
8.4.2	ENVIRONMENTAL BIBLIOGRAPHY.....	8.10
8.4.3	CIVIL ENGINEERING DATABASE.....	8.11
8.4.4	WATER RESOURCES ABSTRACTS.....	8.11
8.4.5	TRIS .....	8.11
8.4.6	GeoRef.....	8.12
9.	DESIGN CONSIDERATIONS FOR HIGHWAY ENCROACHMENTS AND RIVER CROSSINGS .....	9.1
9.1	INTRODUCTION .....	9.1
9.2	PRINCIPAL FACTORS TO BE CONSIDERED IN DESIGN .....	9.1
9.2.1	Types of Rivers.....	9.1
9.2.2	Location of the Crossing or Encroachment .....	9.2
9.2.3	River Characteristics.....	9.2
9.2.4	River Geometry.....	9.2
9.2.5	Hydrologic Data .....	9.3
9.2.6	Hydraulic Data .....	9.3
9.2.7	Characteristics of the Watershed.....	9.3
9.2.8	Flow Alignment .....	9.4
9.2.9	Flow on the Floodplain.....	9.4
9.2.10	Site Selection.....	9.5
9.2.11	Channel Stability Investigations .....	9.5
9.2.12	Short-Term Response .....	9.5
9.2.13	Long-Term Response .....	9.6
9.3	PROCEDURE FOR EVALUATION AND DESIGN OF RIVER CROSSINGS AND ENCROACHMENTS .....	9.6
9.3.1	Approach to River Engineering Projects .....	9.6
9.3.2	Project Initiation .....	9.7
9.4	CONCEPTUAL EXAMPLES OF RIVER ENCROACHMENTS.....	9.8

9.5	PRACTICAL EXAMPLES OF RIVER ENCROACHMENTS .....	9.20
9.5.1	Cimarron River, East of Okeene, Oklahoma (Example 1).....	9.20
9.5.2	Arkansas River, North of Bixby, Oklahoma (Example 2).....	9.20
9.5.3	Washita River, North of Maysville, Oklahoma (Example 3).....	9.20
9.5.4	Beaver River, North of Laverne, Oklahoma (Example 4) .....	9.23
9.5.5	Powder River, 40 Miles East of Buffalo, Wyoming (Example 5) .....	9.23
9.5.6	North Platte River, Near Guernsey, Wyoming (Example 6) .....	9.25
9.5.7	Coal Creek, Tributary of Powder River, Wyoming (Example 7).....	9.26
9.5.8	South Fork of Deer River at US-51 Near Halls, Tennessee (Example 8) .....	9.26
9.5.9	Elk Creek at SR-15 Near Jackson, Nebraska (Example 9).....	9.30
9.5.10	Big Elk Creek at I-90 Near Piedmont, South Dakota (Example 10)....	9.32
9.5.11	Outlet Creek at US-101 Near Longvale, California (Example 11).....	9.33
9.5.12	Nojoqui Creek at US-101 at Buellton, California (Example 12) .....	9.34
9.5.13	Turkey Creek at I-10 Near Newton, Mississippi (Example 13) .....	9.35
9.5.14	Gravel Mining on the Russian River, California (Example 14).....	9.36
9.5.15	Nowood River and Ten Sleep Creek Confluence, Wyoming (Example 15) .....	9.37
9.5.16	Middle Fork Powder River, Wyoming (Example 16).....	9.37
9.6	CONCLUDING REMARKS ON DESIGN CONSIDERATIONS .....	9.37
10.	OVERVIEW EXAMPLES OF DESIGN FOR HIGHWAYS IN THE RIVER ENVIRONMENT .....	10.1
10.1	OVERVIEW EXAMPLE 1 - BIJOU CREEK.....	10.1
10.1.1	Level 1 - Reconnaissance and Geomorphic Analysis .....	10.2
10.1.2	Level 2 - Quantitative Engineering Analysis .....	10.5
10.1.3	Riprap Design for Alternatives 1, 2, and 3.....	10.11
10.1.4	Design for Alternatives 4 and 5.....	10.13
10.2	OVERVIEW EXAMPLE 2 - RILLITO RIVER .....	10.17
10.2.1	Background .....	10.17
10.2.2	Level 1 - Qualitative Geomorphic Analysis .....	10.19
10.2.3	Level 2 - Engineering Geomorphic Analysis .....	10.23
10.2.4	Level 3 - Sediment Routing for the 100-Year Flood .....	10.31
10.2.5	Results of Analysis .....	10.32
10.3	BRI-STARS SEDIMENT TRANSPORT MODELING EXAMPLE .....	10.38
10.3.1	Background .....	10.38
10.3.2	Level 1 - Reconnaissance and Geomorphic Analysis .....	10.40
10.3.3	Level 2 - Hydraulic Engineering Analysis .....	10.41
10.3.4	Level 2 - Scour Analysis Results.....	10.43
10.3.5	Level 3 - BRI-STARS Analysis.....	10.45
11.	REFERENCES .....	11.1
	APPENDIX A - Metric System, Conversion Factors, and Water Properties .....	A.1
	APPENDIX B - Analysis of Selected Sediment Transport Relationships.....	B.1
	APPENDIX C - Index.....	C.1

## LIST OF FIGURES

Figure 1.1	Geometric properties of bridge crossings .....	1.3
Figure 1.2	Comparison of the 1884 and 1968 Mississippi River Channel near Commerce, Missouri.....	1.4
Figure 1.3	Sinuosity vs. slope with constant discharge .....	1.8
Figure 2.1	A river reach as a control volume .....	2.4
Figure 2.2	The control volume for conservation of linear momentum.....	2.6
Figure 2.3	The streamtube as a control volume.....	2.8
Figure 2.4	Pressure distribution in steady uniform and in steady nonuniform flow .....	2.13
Figure 2.5	Pressure distribution in steady uniform flow on steep slopes .....	2.13
Figure 2.6	Steady uniform flow in a unit width channel .....	2.14
Figure 2.7	Hydraulically smooth boundary .....	2.16
Figure 2.8	Hydraulically rough boundary.....	2.17
Figure 2.9	Velocities in turbulent flow .....	2.17
Figure 2.10	Einstein's multiplication factor $X$ in the logarithmic velocity equations.....	2.20
Figure 2.11	Control volume for steady uniform flow.....	2.26
Figure 2.12	Energy and momentum coefficients for a unit width of river.....	2.30
Figure 2.13	The river cross section.....	2.30
Figure 2.14	Definition sketch for small amplitude waves.....	2.32
Figure 2.15	Sketch of positive and negative surges.....	2.34
Figure 2.16	Hydraulic jump characteristics as a function of the upstream Froude number .....	2.36
Figure 2.17	Various types of hydraulic jump .....	2.36
Figure 2.18	Roll waves or slug flow .....	2.37
Figure 2.19	Transitions in open channel flow.....	2.38
Figure 2.20	Specific energy diagram .....	2.39

Figure 2.21	Changes in water surface resulting from an increase in bed elevation.....	2.41
Figure 2.22	Specific discharge diagram.....	2.41
Figure 2.23	Change in water surface elevation resulting from a change in width.....	2.42
Figure 2.24	Flow characteristics over a drop structure.....	2.44
Figure 2.25	Nappe profiles for supercritical flow .....	2.45
Figure 2.26	Schematic representation of transverse currents in a channel bed .....	2.47
Figure 2.27	Definition sketch of flow around a bend .....	2.47
Figure 2.28	Classification of water surface profiles.....	2.52
Figure 2.29	Examples of water surface profiles .....	2.54
Figure 2.30	Definition sketch for the standard step method for computation of backwater curves.....	2.55
Figure 2.31	Gaging station well and shelters .....	2.57
Figure 2.32	Typical float recording gaging station .....	2.58
Figure 2.33	Typical bubble and manometer recording gaging station.....	2.58
Figure 2.34	Stage vs. time hydrograph.....	2.59
Figure 2.35	Definition sketch of computing area and discharge at a gaging station.....	2.60
Figure 2.36	Stage-discharge relation for Schoharie Creek, New York .....	2.61
Figure 2.37	Stage-discharge relation for a sand channel (Los Gatos Creek at El Dorado Avenue, CA) .....	2.62
Figure 2.38	Three types of backwater effect associated with bridge crossings.....	2.64
Figure 2.39	Submergence of a superstructure.....	2.65
Figure 2.40	Types of flow encountered.....	2.66
Figure 2.41	Discharge coefficient for roadway overtopping .....	2.69
Figure 2.42	Weir crest length determinations for roadway overtopping .....	2.69
Figure 2.43	Sketch of backwater curve over check dam.....	2.77
Figure 2.44	Sketch of backwater curve over check dam.....	2.87

Figure 3.1	Drag coefficient $C_D$ vs. particle Reynolds number $Re_p$ for spheres and natural sediments with shape factors $S_p$ equal to 0.3, 0.5, 0.7, and 0.9 .....	3.5
Figure 3.2	Nominal diameter vs. fall velocity.....	3.6
Figure 3.3	Definition sketches for size-frequency characteristics of sediments.....	3.9
Figure 3.4	Angle of repose of non-cohesive materials.....	3.13
Figure 3.5	Forms of bed roughness in sand channels .....	3.14
Figure 3.6	Relation between water surface and bed configuration.....	3.15
Figure 3.7	Change in velocity with stream power for a sand with $D_{50} = 0.19$ mm.....	3.16
Figure 3.8	Relation between regime of flow and depth for bed material with a median size equal to or less than 0.35 mm.....	3.20
Figure 3.9	Cross-over from lower to upper flow regime based on sand size and Froude Number .....	3.20
Figure 3.10	Relation to depth to discharge for Elkhorn River near Waterloo, NE.....	3.22
Figure 3.11	Apparent kinematic viscosity of water-bentonite dispersions .....	3.23
Figure 3.12	Variation of fall velocity of several sand mixtures with percent bentonite and temperature.....	3.24
Figure 3.13	Relation between stream power, median fall diameter, and bed configuration and Manning's $n$ values.....	3.27
Figure 3.14	Change in Manning's $n$ with discharge for Padma River in Bangladesh....	3.28
Figure 3.15	Shields Diagram: dimensionless critical shear stress.....	3.36
Figure 3.16	Shields' relation for beginning of motion .....	3.37
Figure 3.17	Comparison of critical shear stress as a function of grain diameter .....	3.39
Figure 3.18	Critical shear stress as a function of grain diameter .....	3.44
Figure 3.19	Critical velocity as a function of stone size.....	3.45
Figure 3.20	Definition of sediment discharge (load) components .....	3.46
Figure 3.21	Schematic sediment and velocity profiles .....	3.48
Figure 3.22a	Suspended sediment sampler-D49.....	3.48

Figure 3.22b	Suspended sediment sampler-DH48 .....	3.49
Figure 3.23	Gage height and suspended sediment concentration hydrograph, Colorado River near San Saba, Texas, May 1-6, 1952 .....	3.50
Figure 3.24	Bed material size distribution curves.....	3.53
Figure 3.25	Size distribution curve for pebble count .....	3.56
Figure 4.1	Classification of sediment transport in streams (rivers).....	4.5
Figure 4.2	Sediment transport capacity and supply curves .....	4.6
Figure 4.3	Schematic sediment and velocity profiles .....	4.7
Figure 4.4	Graph of suspended sediment distribution.....	4.10
Figure 4.5	Einstein's $\phi_x$ vs. $\psi$ bed load function .....	4.15
Figure 4.6	Hiding factor .....	4.16
Figure 4.7	Einstein's multiplication factor X in the logarithmic velocity equations.....	4.16
Figure 4.8	Pressure correction .....	4.17
Figure 4.9	Integral $I_1$ in terms of E and Z .....	4.18
Figure 4.10	Integral $I_2$ in terms of E and Z .....	4.19
Figure 4.11	Friction loss due to channel irregularities, as a function of sediment transport .....	4.20
Figure 4.12	Comparison of the Meyer-Peter and Müller and Einstein methods for computing contact load.....	4.21
Figure 4.13	Relation of discharge of sands to mean velocity for six median sizes of bed sands, four depths of flow, and a water temperature of 60°F.....	4.22
Figure 4.14	Colby's correction curves for temperature and fine sediment.....	4.23
Figure 4.15	Bed-material size effects on bed material transport .....	4.25
Figure 4.16	Effect of slope on bed material transport .....	4.25
Figure 4.17	Effect of kinematic viscosity (temperature) on bed material transport.....	4.26
Figure 4.18	Variation of bed material load with depth of flow.....	4.26
Figure 4.19	Description of the average cross section .....	4.45



Figure 4.20	Grain size distribution of bed material.....	4.45
Figure 4.21	Comparison of the Einstein and Colby methods .....	4.52
Figure 5.1	Changing slope at fan-head leading to fan-head trenching.....	5.4
Figure 5.2	Headcuts and nickpoints.....	5.4
Figure 5.3	Relationship between flume slope and sinuosity (ratio between channel length and valley length) during flume experiments at constant water discharge.....	5.7
Figure 5.4	Sequence of channel changes as water discharge and sediment loads decrease .....	5.7
Figure 5.5	Variability of sinuosity between 1765 and 1915 for 24 Mississippi River reaches .....	5.8
Figure 5.6	Mississippi River reaches between Cairo, Illinois and Old River, Louisiana .....	5.9
Figure 5.7	Mississippi River valley profile .....	5.9
Figure 5.8	River Nile between Qena and Cairo showing six reaches of steep valley slope.....	5.11
Figure 5.9	River Nile valley profile .....	5.11
Figure 5.10	Plot of River Nile sinuosity and valley slope .....	5.12
Figure 5.11	Stream properties for classification.....	5.14
Figure 5.12	Classification of river channels .....	5.15
Figure 5.13	Channel classification showing relative stability and types of hazards encountered with each pattern.....	5.16
Figure 5.14	Planview and cross section of a meandering stream .....	5.17
Figure 5.15	Definition sketch for meanders .....	5.19
Figure 5.16	Empirical relations for meander characteristics.....	5.20
Figure 5.17	Types of multi-channel streams .....	5.21
Figure 5.18	Slope-discharge relationship for braiding or meandering in sandbed streams.....	5.22
Figure 5.19	Variation of discharge at a given river cross section and at points downstream.....	5.25

Figure 5.20	Schematic variation of width, depth, and velocity with at-a-station and downstream discharge variation .....	5.25
Figure 5.21	Changes in channel slope in response to an increase in sediment load at Point C.....	5.30
Figure 5.22	Changes in channel slope in response to a dam at Point C.....	5.31
Figure 5.23	Map of lower Chippewa River .....	5.36
Figure 5.24	Leopold and Wolman's (1957) relation between channel patterns, channel gradient, and bankfull discharge.....	5.37
Figure 5.25	Lane's (1957) relation between channel patterns, channel gradient, and mean discharge .....	5.37
Figure 5.26	Median bank erosion rate in relation to channel width for different types of streams .....	5.55
Figure 5.27	Encroachment on a meandering river .....	5.56
Figure 5.28	Erosion index in relation to sinuosity .....	5.61
Figure 5.29	Modes of meander loop development.....	5.62
Figure 5.30	Domains of meander behavior.....	5.65
Figure 5.31	Sinuuous point bar stream.....	5.67
Figure 5.32	River channels .....	5.68
Figure 5.33	Meandering river sketch .....	5.70
Figure 5.34	Estimated future location of a meandering river.....	5.70
Figure 6.1	Typical bank failure surfaces (a) noncohesive, (b) cohesive, (c) composite .....	6.4
Figure 6.2	Placement of flow control structures relative to channel banks, crossing, and floodplain.....	6.11
Figure 6.3	Perspective of hard point with section detail .....	6.12
Figure 6.4	Retard.....	6.13
Figure 6.5	Concrete or timber cribs .....	6.13
Figure 6.6	Pile dikes .....	6.15

Figure 6.7	Vane dike model, ground walnut shell bed, during low stage portion of test run .....	6.15
Figure 6.8	Typical jetty-field layout .....	6.16
Figure 6.9	Steel jacks .....	6.17
Figure 6.10	Typical guidebank.....	6.18
Figure 6.11	Definition sketch for a vertical drop.....	6.19
Figure 6.12	Flow and scour patterns at a sloping sill .....	6.20
Figure 6.13	Diagram for riprap stability conditions .....	6.21
Figure 6.14	Stability numbers for a 1.5 stability factor for horizontal flow along a side slope .....	6.24
Figure 6.15	Suggested gradation for riprap .....	6.28
Figure 6.16	Tie-in trench to prevent riprap blanket from unraveling .....	6.31
Figure 6.17	Rock-fill trench.....	6.31
Figure 6.18	Windrow revetment, definition sketch .....	6.33
Figure 6.19	Riprap failure models .....	6.35
Figure 6.20	Rock and wire mattress .....	6.38
Figure 6.21	Typical sand-cement bag revetment.....	6.40
Figure 6.22	Articulated concrete block system .....	6.41
Figure 6.23	Used tire mattress .....	6.41
Figure 6.24	Typical soil-cement bank protection.....	6.43
Figure 6.25	Hydraulic flow zones on an embankment during overtopping flow .....	6.45
Figure 6.26	Definition sketch of variables involved in overtopping flow.....	6.46
Figure 6.27	Definition sketch for application of the momentum equation for embankment overtopping flow.....	6.47
Figure 6.28	Typical embankment erosion pattern with submerged flow.....	6.48
Figure 6.29	Typical embankment erosion pattern with free flow .....	6.49

Figure 6.30	Permissible velocities of various protection materials as a function of flow duration.....	6.51
Figure 6.31	Full-scale test of an embankment overtopping protection system under steep-slope, high-velocity flow conditions .....	6.52
Figure 6.32	Definition sketch for riprap on a channel bed.....	6.56
Figure 6.33	Stability factors for various rock sizes on a side slope .....	6.59
Figure 6.34	Safety factors for various side slopes .....	6.59
Figure 6.35	Gradations of filter blanket for Problem 2 .....	6.64
Figure 6.36	Definition sketch for riprap on a channel bed.....	6.65
Figure 6.37	Stability factors for various rock sizes on a side slope .....	6.68
Figure 6.38	Safety factors for various side slopes .....	6.69
Figure 6.39	Gradations of filter blanket for Problem 2 .....	6.74
Figure 7.1	Flow chart for scour and stream stability analysis and countermeasures.....	7.3
Figure 7.2	Local scour depth at a pier as a function of time.....	7.5
Figure 7.3	Comparison of scour formulas for variable depth ratios ( $y/a$ ).....	7.14
Figure 7.4	Comparison of scour formulas with field scour measurements .....	7.14
Figure 7.5	Comparison of pier scour equations with field measurements .....	7.15
Figure 7.6	Common pier shapes.....	7.17
Figure 7.7	Topwidth of scour hole.....	7.21
Figure 7.8	Schematic representation of abutment scour.....	7.22
Figure 7.9	Comparison of laboratory flow characteristics to field flow conditions .....	7.23
Figure 7.10	Orientation of embankment angle $\theta$ to the flow.....	7.24
Figure 7.11	Abutment shape .....	7.25
Figure 9.1	Three-level analysis procedure for river engineering studies .....	9.7
Figure 9.2	Cimarron River, east of Okeene, Oklahoma (Example 1) .....	9.21
Figure 9.3	Arkansas River, north of Bixby, Oklahoma (Example 2) .....	9.22

Figure 9.4	Washita River, north of Maysville, Oklahoma (Example 3) .....	9.23
Figure 9.5	Beaver River, north of Laverne, Oklahoma (Example 4).....	9.24
Figure 9.6	Powder River, 40 miles east of Buffalo, Wyoming (Example 5) .....	9.25
Figure 9.7	North Platte River near Guernsey, Wyoming (Example 6).....	9.26
Figure 9.8	Coal Creek, tributary of Powder River, Wyoming (Example 7).....	9.27
Figure 9.9a	Map showing South Fork of Deer River at U.S. Highway 51 Crossing (Example 8) .....	9.27
Figure 9.9b	Channel modifications to South Fork of Deer River at U.S. Highway 51 Crossing near Halls, Tennessee (Example 8).....	9.28
Figure 9.9c	Elevation sketch of U.S. Highway 51 Bridge (Example 8) .....	9.29
Figure 9.10	Stage trends at Sioux City, Iowa, on the Missouri River (Example 9).....	9.31
Figure 9.11	Deflector arrangement and alignment problem on I-90 Bridge across Big Elk Creek near Piedmont, North Dakota (Example 10).....	9.32
Figure 9.12	Plan sketch of channel relocation, Outlet Creek (Example 11) .....	9.33
Figure 9.13	Plan sketch of Nojoqui Creek channel relocation (Example 12).....	9.34
Figure 9.14	Plan sketch of Turkey Creek channel relocation (Example 13).....	9.35
Figure 9.15	Case study of sand and gravel mining (Example 14) .....	9.36
Figure 9.16	Nowood River near Ten Sleep, Wyoming (Example 15) .....	9.38
Figure 9.17	Middle Fork Powder River at Kaycee, Wyoming (Example 16) .....	9.39
Figure 10.1	Topographic map of Bijou Creek study area .....	10.1
Figure 10.2	Cross sectional area versus flow depth relation .....	10.3
Figure 10.3	Wetted perimeter versus flow depth relation.....	10.4
Figure 10.4	Analysis of bed material size of Bijou Creek .....	10.4
Figure 10.5	Gumbel's method of frequency analysis .....	10.6
Figure 10.6	Proposed first alternative .....	10.6
Figure 10.7	Proposed second alternative .....	10.7

Figure 10.8 Proposed third alternative .....	10.7
Figure 10.9 Proposed fifth alternative .....	10.8
Figure 10.10 The sketch of proposed riprap design.....	10.12
Figure 10.11 Sketch of spur design .....	10.16
Figure 10.12 Rillito River system vicinity map .....	10.18
Figure 10.13 Slope-discharge relationship for Rillito River.....	10.21
Figure 10.14 Sketch of Craycroft Road crossing .....	10.22
Figure 10.15 Sabino Canyon Road crossing site .....	10.24
Figure 10.16 Flood events at Rillito River near Tucson, Arizona.....	10.25
Figure 10.17 Log-normal frequency analysis for Rillito River near Tucson .....	10.26
Figure 10.18 December 1965 flood in Rillito River and Tanque Verde Creek .....	10.26
Figure 10.19 100-year flood design hydrographs.....	10.27
Figure 10.20 Stage-discharge plot for Rillito River near Tucson .....	10.27
Figure 10.21 Rillito-Pantano-Tanque Verde bed sediment distribution .....	10.28
Figure 10.22 Bed elevation change of Rillito-Tanque Verde System (Tanque Verde flooding) .....	10.33
Figure 10.23 Bed elevation change of Rillito-Tanque Verde System (Pantano flooding).....	10.33
Figure 10.24 Alternative I for Craycroft Road Bridge crossing .....	10.34
Figure 10.25 Alternative II for Craycroft Road Bridge crossing .....	10.35
Figure 10.26 Alternative III for Craycroft Road Bridge crossing .....	10.37
Figure 10.27 General plan view of Sabino Canyon Road crossing for alternative II, III, and IV (II shown) .....	10.39
Figure 10.28 Cross section of proposed bridge .....	10.40
Figure 10.29 Equal conveyance tubes of approach section.....	10.42
Figure 10.30 Plan view of equal conveyance tubes showing velocity distribution at approach and bridge sections.....	10.42

Figure 10.31 Velocity distribution at bridge crossing .....	10.43
Figure 10.32 Plot of total scour for example problem.....	10.44
Figure 10.33 Revised plot of total scour for example problem .....	10.45
Figure 10.34 Three-day hydrograph for BRI-STARS analysis.....	10.46
Figure 10.35 Comparison longitudinal profiles from BRI-STARS .....	10.46
Figure 10.36 Comparison cross-sections from BRI-STARS.....	10.47
Figure 10.37 BRI-STARS model profiles for steady-state run.....	10.48

(page intentionally left blank)



## LIST OF TABLES

Table 1.1	Commonly Used Engineering Terms in SI and English Units.....	1.21
Table 2.1	Manning's Roughness Coefficients for Various Boundaries.....	2.22
Table 2.2	Adjustment Factors for the Determination of n Values.....	2.25
Table 2.3	Characteristics of Water Surface Profiles.....	2.53
Table 2.4	Discharge measurement notes.....	2.70
Table 2.5	Observed Velocity Data.....	2.71
Table 2.6	Velocity Profile Calculations.....	2.72
Table 2.7	Detailed Computation of Superelevation in Bends.....	2.74
Table 2.8	Discharge Measurement Notes.....	2.80
Table 2.9	Observed Velocity Data.....	2.81
Table 2.10	Velocity Profile Calculations.....	2.82
Table 2.11	Detailed Computation of Superelevation in Bends.....	2.84
Table 3.1	Sediment Grade Scale.....	3.3
Table 3.2	Guide to Size Range for Different Types of Size Analysis.....	3.6
Table 3.3	Typical Sediment Size Distribution for Gravel-Bed Stream.....	3.31
Table 3.4	Maximum Permissible Velocities Proposed by Fortier and Scobey.....	3.43
Table 3.5	Nonscour Velocities for Soils.....	3.44
Table 3.6	Sand Bed Material Size Distribution.....	3.52
Table 3.7	Sand Size Bed Material Properties.....	3.53
Table 3.8	Gravel Bed Material Size Distribution.....	3.54
Table 3.9	Gravel Bed Material Properties.....	3.55
Table 4.1	Summary of Applicability of Selected Sediment Transport Relations.....	4.27
Table 4.2	Coefficients and Exponents of Equation 4.48.....	4.30
Table 4.3	Range of Parameters Equation 4.48 Developed by Simons et al.....	4.30

Table 4.5	Concentration vs. Elevation Above the Bed .....	4.38
Table 4.6	Concentration vs. Elevation Above the Bed .....	4.43
Table 4.7	Bed Material Information for Sample Problem.....	4.44
Table 4.8	Hydraulic Calculations for Sample Problem by Applying the Einstein Procedure .....	4.46
Table 4.9	Bed-Material Load Calculations for Sample Problem by Applying the Einstein (1950) Procedure .....	4.47
Table 4.10	Bed Material Load Calculations for Sample Problem by Applying the Colby Method (Median Diameter) .....	4.49
Table 4.11	Bed Material Discharge Calculations for Sample Problem by Applying the Colby (Individual Size Fraction).....	4.50
Table 5.1	Empirical Relations for Meanders in Alluvial Valleys .....	5.20
Table 5.2	At-A-Station and Downstream Hydraulic Geometry Relationships .....	5.26
Table 5.3	Derived At-A-Station and Downstream Geometry Relationships.....	5.26
Table 5.4	Change of Variables Induced by Changes in Sediment Discharge, Size of Bed Sediment and Wash Load .....	5.32
Table 5.5	Qualitative Response of Alluvial Channels.....	5.33
Table 5.6	Chippewa River Morphology .....	5.35
Table 5.7	Scale Ratios for Similitude .....	5.42
Table 5.8	Channel Response to Changes in Watershed and River Condition .....	5.52
Table 5.9	Sediment Size Distribution in the St. Lawrence Seaway .....	5.75
Table 6.1	Factors Affecting Erosion of River Banks.....	6.2
Table 6.2	Data for Suggested Gradation .....	6.28
Table 6.3	Causes of Riprap Failure and Solutions .....	6.36
Table 6.4	Sizes of Materials.....	6.61
Table 6.5	Sizes of Materials.....	6.62
Table 6.6	Sizes of Materials.....	6.71
Table 6.7	Sizes of Materials.....	6.72

Table 7.1	Correction Factor, $K_1$ , for Pier Nose Shape.....	7.17
Table 7.2	Correction Factor, $K_2$ , for Angle of Attack, $\theta$ , of the Flow .....	7.17
Table 7.3	Increase in Equilibrium Pier Scour Depths, $K_3$ , for Bed Condition .....	7.17
Table 7.4	Abutment Shape Coefficients for Short Abutment Sections .....	7.25
Table 8.1	Checklist of Data Needs .....	8.6
Table 8.2	List of Data Sources .....	8.8
Table 9.1	River Response to Highway Encroachments and to River Development .....	9.10
Table 10.1	Summary of Computer Hydraulic Conditions .....	10.8
Table 10.2	Summary of Hydraulic Designs.....	10.10
Table 10.3	Design of Riprap Sizes .....	10.11
Table 10.4	Bank Migration for Alternative 4 .....	10.14
Table 10.5	Summary of Spur Design.....	10.14
Table 10.6	Dimension of Spurs.....	10.14
Table 10.7	Size and Filter Design for Riprap at Spur Noses and Spur Shanks.....	10.15
Table 10.8	Rillito River Near Tucson, Arizona Log-Pearson Type III Frequency Analysis by USGS .....	10.25
Table 10.9	Equilibrium Slope Calculations, Dominant Discharge.....	10.31
Table 10.10	Low Chord and Total Scour Requirements at Craycroft Road.....	10.36

(page intentionally left blank)

## ACKNOWLEDGMENTS

This manual is a major revision of the 1990 manual. The writers wish to acknowledge the contributions made by Drs. E.V. Richardson, D.B. Simons, S. Karaki, K. Mahmood, and M.A. Stevens as co-authors of the 1975 manual, as well as the review, help, and guidance given by the Steering Committee for the 1975 edition consisting of Frank L. Johnson, Roger L. Dean, Murray L. Corry, Dah-Chen Woo, Milo Cress, Lawrence J. Harrison, Herbert Gregory, Gene R. Fiala of the Federal Highway Administration and Mainard Wacker of the Wyoming Highway Department. The writers also wish to acknowledge the help of Colorado State University Professors J.F. Ruff and A.G. Mercer and Graduate Research Assistants V.M. Ponce, Larry Rundquist, and Tony Melone in the preparation of the 1975 edition.

For the 1990 manual, the writers acknowledge the contributions of Drs. E.V. Richardson, D.B. Simons, and P.Y. Julien as co-authors, the technical assistance of Philip Thompson, J. Sterling Jones, and Lawrence J. Harrison, FHWA; Mainard A. Wacker, Wyoming Highway Department, and Michael E. Zeller, Simons, Li & Associates, and CSU Graduate Research Assistant Noel E. Bormann.

Several topics have been added or expanded in this 2001 edition of the manual. Specifically, the writers acknowledge the contributions of Dr. L.W. Zevenbergen for the expanded coverage of sediment transport in Chapter 4 and Dr. L.A. Arneson for his critical review and valuable comments on that chapter. In addition, Mr. P.E. Clopper provided a new section for Chapter 6 on overtopping flow on embankments based on FHWA studies conducted in the late 1980s.

(page intentionally left blank)

## LIST OF SYMBOLS

$A$	=	surface area
$A_1$	=	cross-sectional area for the fluid entering the control volume
$A_2$	=	cross-sectional area for the fluid leaving the control volume
$A_{n2}$	=	normal cross-sectional area at the bridge crossing
$A_p$	=	projected area of a pier normal to the flow
$A_s$	=	area of a sediment particle
$a$	=	acceleration or pier width or embankment length
$a$	=	thickness of the bed layer, the unmeasured zone of flow
$a_n$	=	embankment length for relief bridge
$a_n$	=	acceleration component normal to a streamline
$a_m$	=	embankment length for main bridge
$a_o$	=	amplitude of wave
$a$	=	coefficient of width relationship
$B, B'$	=	dimensionless constants in Meyer-Peter, Müller equations
$b_s$	=	bridge opening length
$b$	=	exponent of width relationship
$C$	=	sediment concentration
$C$	=	Chezy coefficient
$C_o$	=	Chezy coefficient for steady uniform flow
$C_1$	=	constant for free vortex flow
$C_2$	=	constant for forced vortex flow
$C_D$	=	drag coefficient on a particle
$C_f$	=	concentration of fine material
$C_r$	=	overtopping discharge coefficient
$C_T$	=	bed material sediment concentration
$C_s$	=	coefficient of shear
$C$	=	average suspended sediment concentration
$c$	=	wave celerity
$c$	=	coefficient of the flow depth relationship
$D$	=	culvert diameter or sediment size
$D_{50}$	=	sediment riprap size for which 50% by weight of the particles are smaller; similarly $D_{65}$ , $D_{84}$ , $D_{90}$ represent sizes for which 65, 84, and 90% of the particles are smaller
$D_{50x}$	=	mean sediment size a distance $x$ downstream from reference location
$D_{50o}$	=	mean sediment size at the reference section
$D_m$	=	effective mean diameter of sediment or riprap
$D_s$	=	sediment size or riprap size
$dA_1$	=	differential area for the fluid entering the control volume
$dA_2$	=	differential area for the fluid leaving the control volume
$d_{rr}$	=	thickness of riprap layer
$ds$	=	displacement of a fluid particle during time $dt$
$d_s$	=	scour depth
$dt$	=	differential time interval
$E$	=	energy of a system
$E$	=	ratio of bed layer thickness to flow depth $a/y_o$
$e$	=	energy per unit mass
$e_1, e_2,$ $e_3, e_4$	=	moment arms of forces acting on a rock particle

$e_c$	=	eccentricity coefficient
$F_1, F_2$	=	pressure force acting at section one and two
$F_1(h),$ $F_2(h)$	=	functions for the transverse velocity distribution in bends
$F_B$	=	buoyant force on a particle
$F_b$	=	force exerted at the boundary
$F_c$	=	critical Froude number for the beginning of motion of sediment
$F_D$	=	drag force on a particle
$F_d$	=	drag force on a rock particle
$F_f$	=	fluid force on a particle
$F_g$	=	gravitational force on a particle
$F_P$	=	lift force on a rock particle
$F_n$	=	external forces between particles
$Fr$	=	Froude number
$F_s$	=	shear force
$F_v$	=	shear force on a particle
$F_x$	=	force acting in the x direction
$f$	=	Darcy-Weisbach friction factor
$f'_b$	=	Darcy-Weisbach friction factor for the grain roughness
$f_s$	=	seepage force
$f$	=	exponent of the flow depth relationship
$G$	=	gradation coefficient
$g$	=	acceleration due to gravity
$H$	=	total energy
$H_e$	=	entrance loss of head
$H_e$	=	average head loss over a cross-section
$H_f$	=	friction loss of head
$H_{min}$	=	minimum total energy at a critical section
$H_T$	=	total head
$H_v$	=	velocity head
$HW_2$	=	headwater at a culvert
$H_s$	=	horizontal side slope related to one unit vertically
$h_L$	=	head loss in a hydraulic jump
$h_e$	=	head loss
$h_1^*$	=	total backwater elevation
$Wh$	=	drop in water surface elevation through bridge opening
$I_1, I_2$	=	integrals in the Einstein method
$i_b$	=	fraction of the bed load for given equation
$i_s$	=	fraction of the suspended load for a given equation
$i_T$	=	fraction of total load for a given equation
$J$	=	ratio of projected area of piers to the gross constricted area $A_{n2}$
$j$	=	exponent of the bed sediment discharge relationship
$K$	=	coefficient of the Meyer-Peter and Müller equation
$K_1, K_2$	=	coefficient for the area and volume of sediment particles
$K_B, K_r$	=	coefficient in Meyer-Peter, Müller equation
$K_b$	=	base backwater coefficient
$K_e$	=	entrance loss coefficient for culverts
$WK$	=	correction coefficient for piers
$WK_e$	=	incremental correction coefficient for excentricity
$WK_p$	=	incremental correction coefficient for piers



$WK_s$	=	incremental correction coefficient for skewed flow
$k_s$	=	height of roughness elements
$k$	=	coefficient of the velocity relationship
$k^*$	=	total backwater coefficient for subcritical flow
$L$	=	length of control volume
$L$	=	length of culvert
$L_1, L_2,$		
$L_3$	=	lengths for sloping sill drop structure
$L_a$	=	length of abutment
$L_c$	=	length of a channel along the thalweg
$L_e$	=	length of embankment
$L_j$	=	length of hydraulic jump
$L_s$	=	upstream length of a guidebank
$L_s$	=	length of the roadway crest for overspill
$P$	=	pier length
$P$	=	mixing length
$P_a$	=	longest axis of particle
$P_b$	=	intermediate axis of particle
$P_c$	=	shortest axis of particle
$M$	=	bridge opening ratio
$m$	=	exponent of the velocity relationship
$M/N$	=	ratio of lift to drag moments on a particle
$n$	=	Manning's resistance coefficient
$n_b$	=	Manning's resistance coefficient of the bed
$n_o$	=	Manning's resistance coefficient for steady uniform flow
$n_w$	=	Manning's resistance coefficient of the walls
$P$	=	wetted perimeter of the flow
$p_1, p_2$	=	pressure of fluid at sections one and two
$P_b$	=	wetted perimeter of the bed
$P_E$	=	coefficient in the Einstein's total sediment discharge method
$P_i, P_o$	=	pressure of fluid inside and outside the bend
$P_w$	=	wetted perimeter of the banks
$p_i$	=	percentage by weight of a size fraction of sediment
$p$	=	coefficient of the total bed sediment discharge relationship
$p$	=	average pressure over a cross section
$Q$	=	discharge (flow rate)
$Q$	=	rate at which heat is added to the system
$Q_B$	=	bed load discharge in weight units
$Q_b$	=	water discharge quantity determining the bed load transport
$Q_c$	=	approach channel flow discharge
$Q_e$	=	approach flow discharge on the embankment
$Q_f$	=	formative discharge for a particular phenomena
$Q_n$	=	uncorrected bed sediment discharge
$Q_o$	=	overtopping discharge
$Q_s$	=	total suspended sediment discharge
$Q_{smax}$	=	maximum suspended sediment discharge
$Q_T$	=	total bed sediment discharge
$Q_T$	=	total discharge
$q$	=	unit discharge
$q_b$	=	unit bed load discharge

$q_n$	=	uncorrected unit bed sediment discharge
$q_s$	=	unit suspended sediment discharge
$q_T$	=	unit total bed sediment discharge
$R$	=	hydraulic radius
$R'_b$	=	hydraulic radius due to grain roughness
$Re$	=	Reynolds number
$Re_p$	=	Reynolds number of falling particle
$R$	=	vector $R$ of the direction of particle movement
$r$	=	radius of curvature
$r_c$	=	radius of curvature at the center of the stream
$r_i, r_o$	=	radius of curvature for inner and outer banks in a bend
$r$	=	coefficient of Manning's $n$ relationship
$S$	=	channel slope
$S_c$	=	shape factor of a cross-section
$S_f$	=	friction slope (also called the energy slope)
$S'_f$	=	friction slope to overcome grain resistance
$S_m$	=	ratio of tangents of friction angle to side slope angle
$S_n$	=	channel sinuosity
$S_o$	=	bed slope
$S_p$	=	shape factor of sediment particle
$S_R$	=	shape factor of a river reach
$S_s$	=	specific gravity of sediment particle
$S_x$	=	bed slope at a distance $x$ downstream of a reference location
$S_w$	=	slope of water surface
$s$	=	direction tangential to streamline
$T$	=	wave period
$T$	=	time
$T\hat{a}$	=	temperature
$t$	=	coefficient of the friction slope relationship
$u$	=	internal energy associated with fluid temperature
$V$	=	velocity vector
$V$	=	volume
$V_c, V_{cr}$	=	critical velocity
$V_d$	=	depth-average velocity at the vena contracta
$V_m$	=	mean stream velocity
$V_{max}$	=	maximum velocity
$V_{n2}$	=	average velocity at the bridge opening
$V_o$	=	tangential velocity in a bend
$V_p$	=	volume of a particle, or average velocity on a spallslope
$V_r$	=	reference velocity
$V_s$	=	velocity against the stone
$V_T$	=	depth-average velocity at the toe of an embankment
$V_w$	=	velocity of the wave
$V^*$	=	shear velocity
$V^*_c$	=	shear velocity in the channel
$V'^*$	=	shear velocity due to grain roughness
$V''^*$	=	shear velocity due to form roughness
$v_1, V_1$	=	velocity of the fluid entering a control volume
$v_2, V_2$	=	velocity of the fluid leaving a control volume
$v_s, v_n$	=	velocity components in the $s$ and $n$ directions

$v_x, v_y$	=	velocity components along x and y
$\bar{v}_x, \bar{v}_y$	=	average velocity components along x and y
$v'_x, v'_y$	=	velocity fluctuations
$W$	=	width of control volume or channel free surface width
$\dot{W}$	=	rate at which a fluid system does work on its surroundings
$\dot{W}_p$	=	rate of pressure work done by system
$W_s$	=	Buoyant weight of sediment particle
$\dot{W}_t$	=	rate of stress work
$\Delta WWS$	=	drop in water surface elevation at a drop structure
$w$	=	lateral location in a cross-section
$X$	=	Einstein's multiplication factor
$X$	=	function of $W/w'$ in Einstein's method
$Y$	=	pressure correction factor, a function of $D_{65}/w'$ in Einstein's method
$y$	=	vertical distance
$y_c$	=	critical depth of flow
$y_{max}$	=	maximum depth of flow
$y_n$	=	normal depth of flow
$y_o$	=	total flow depth
$y_s$	=	scour depth due to contraction
$y'$	=	vertical distance above bed at which the velocity is zero
$y$	=	exponent of the Manning's n relationship
$Z$	=	exponent of the Rouse equation
$WZ$	=	superelevation of flow in bends
$Wz$	=	drop in water surface elevation along a channel
$z$	=	elevation above arbitrary reference level
$z_i, z_o$	=	water surface elevation at inside and outside of bend
$z$	=	exponent of the friction slope relationship

### GREEK SYMBOLS

$\alpha$	=	energy correction factor
$\alpha$	=	coefficient of the downstream decrease in slope
$\alpha'$	=	energy correction factor for unit width
$\beta$	=	momentum correction factor
$\beta$	=	angle between the particle movement direction and the vertical
$\beta_1$	=	angle of the hydraulic jump in bends
$\beta'$	=	momentum correction factor for a unit width
$\beta$	=	coefficient of the downstream decrease in sediment size
$\beta_x$	=	correction term in Einstein's Method
$\gamma$	=	specific weight of the fluid
$\gamma_s$	=	specific weight of the sediment
$\Delta$	=	apparent roughness of the bed
$\Delta_o$	=	dimensionless bend angle
$\delta$	=	angle between the drag force and the particle movement direction
$\delta'$	=	thickness of the laminar sublayer in turbulent flow
$\varepsilon$	=	exponent in Laursen's equation
$\eta$	=	stability number for particles on a plane bed
$\eta_1$	=	stability number for particles on side slopes
$\theta$	=	side slope angle
$\theta$	=	inclination angle of a channel

$\theta_1$	=	bend angle in supercritical flows
$\theta_e$	=	angle of orientation of the embankment
$\kappa$	=	von Karman velocity constant
$\lambda$	=	wave length
$\lambda$	=	angle between the horizontal and the drag force vector
$\mu$	=	dynamic viscosity of a fluid
$\nu$	=	kinematic viscosity of a fluid
$\xi$	=	correction factor, a function of $D_s/X$ in Einstein's method
$\xi$	=	function of other parameters (Eq. 5.3.31)
$\rho$	=	fluid density
$\rho_1$	=	density of a fluid entering a control volume
$\rho_2$	=	density of a fluid leaving a control volume
$\rho_s$	=	density of sediment particles
$\sigma$	=	correction coefficient for piers
$\tau$	=	shear stress
$\tau_o$	=	bed shear stress
$\tau_c$	=	critical shear stress
$\phi_*$	=	dimensionless sediment transport function
$\psi$	=	uncorrected entrainment function
$\psi_*$	=	entrainment function
$\omega$	=	fall velocity of a sediment particle
$\omega_a$	=	angle of the abutment

## GLOSSARY

abrasion:	Removal of streambank material due to entrained sediment, ice, or debris rubbing against the bank.
aggradation:	General and progressive buildup of the longitudinal profile of a channel bed due to sediment deposition.
alluvial channel:	Channel wholly in alluvium; no bedrock is exposed in channel at low flow or likely to be exposed by erosion.
alluvial fan:	A fan-shaped deposit of material at the place where a stream issues from a narrow valley of high slope onto a plain or broad valley of low slope. An alluvial cone is made up of the finer materials suspended in flow while a debris cone is a mixture of all sizes and kinds of materials.
alluvial stream:	A stream which has formed its channel in cohesive or noncohesive materials that have been and can be transported by the stream.
alluvium:	Unconsolidated material deposited by a stream in a channel, floodplain, alluvial fan, or delta.
alternating bars:	Elongated deposits found alternately near the right and left banks of a channel.
anabranch:	Individual channel of an anabranching stream.
anabranching stream:	A stream whose flow is divided at normal and lower stages by large islands or, more rarely, by large bars; individual islands or bars are wider than about three times water width; channels are more widely and distinctly separated than in a braided stream.
anastomosing stream:	An anabranching stream.
angle of repose:	The maximum angle (as measured from the horizontal) at which gravel or sand particles can stand.
annual flood:	The maximum flow in one year (may be daily or instantaneous).
apron:	Protective material placed on a streambed to resist scour.
apron, launching:	An apron designed to settle and protect the side slopes of a scour hole after settlement.

armor (armoring):	Surfacing of channel bed, banks, or embankment slope to resist erosion and scour. (a) Natural process whereby an erosion-resistant layer of relatively large particles is formed on a streambed due to the removal of finer particles by streamflow; (b) placement of a covering to resist erosion.
articulated concrete mattress:	Rigid concrete slabs which can move without separating as scour occurs; usually hinged together with corrosion-resistant cable fasteners; primarily placed for lower bank protection.
average velocity:	Velocity at a given cross section determined by dividing discharge by cross sectional area.
avulsion:	A sudden change in the channel course that usually occurs when a stream breaks through its banks; usually associated with a flood or a catastrophic event.
backfill:	The material used to refill a ditch or other excavation, or the process of doing so.
backwater:	The increase in water surface elevation relative to the elevation occurring under natural channel and floodplain conditions. It is induced by a bridge or other structure that obstructs or constricts the free flow of water in a channel.
backwater area:	The low-lying lands adjacent to a stream that may become flooded due to backwater.
bank:	The sides of a channel between which the flow is normally confined.
bank, left (right):	The side of a channel as viewed in a downstream direction.
bankfull discharge:	Discharge that, on the average, fills a channel to the point of overflowing.
bank protection:	Engineering works for the purpose of protecting streambanks from erosion.
bank revetment:	Erosion-resistant materials placed directly on a streambank to protect the bank from erosion.
bar:	An elongated deposit of alluvium within a channel, not permanently vegetated.
base floodplain:	The floodplain associated with the flood with a 100-year recurrence interval.
bed:	The bottom of a channel bounded by banks.

bed form:	A recognizable relief feature on the bed of a channel, such as a ripple, dune, plane bed, antidune, or bar. Bed forms are a consequence of the interaction between hydraulic forces (boundary shear stress) and the bed sediment.
bed layer:	A flow layer, several grain diameters thick (usually two) immediately above the bed.
bed load:	Sediment that is transported in a stream by rolling, sliding, or skipping along the bed or very close to it; considered to be within the bed layer (contact load).
bed load discharge (or bed load):	The quantity of bed load passing a cross section of a stream in a unit of time.
bed material:	Material found in and on the bed of a stream (May be transported as bed load or in suspension).
bedrock:	The solid rock exposed at the surface of the earth or overlain by soils and unconsolidated material.
bed sediment discharge:	The part of the total sediment discharge that is composed of grain sizes found in the bed and is equal to the transport capability of the flow.
bed shear (tractive force):	The force per unit area exerted by a fluid flowing past a stationary boundary.
bed slope:	The inclination of the channel bottom.
blanket:	Material covering all or a portion of a streambank to prevent erosion.
boulder:	A rock fragment whose diameter is greater than 250 mm.
braid:	A subordinate channel of a braided stream.
braided stream:	A stream whose flow is divided at normal stage by small mid-channel bars or small islands; the individual width of bars and islands is less than about three times water width; a braided stream has the aspect of a single large channel within which are subordinate channels.
bridge opening:	The cross-sectional area beneath a bridge that is available for conveyance of water.
bridge waterway:	The area of a bridge opening available for flow, as measured below a specified stage and normal to the principal direction of flow.

bulk density:	Density of the water sediment mixture (mass per unit volume), including both water and sediment.
bulkhead:	A vertical, or near vertical, wall that supports a bank or an embankment; also may serve to protect against erosion.
bulking:	Increasing the water discharge to account for high concentrations of sediment in the flow.
catchment:	See drainage basin.
causeway:	Rock or earth embankment carrying a roadway across water.
caving:	The collapse of a bank caused by undermining due to the action of flowing water.
cellular-block mattress:	Interconnected concrete blocks with regular cavities placed directly on a streambank or filter to resist erosion. The cavities can permit bank drainage and the growth of vegetation where synthetic filter fabric is not used between the bank and mattress.
channel:	The bed and banks that confine the surface flow of a stream.
channelization:	Straightening or deepening of a natural channel by artificial cutoffs, grading, flow-control measures, or diversion of flow into an engineered channel.
channel diversion:	The removal of flows by natural or artificial means from a natural length of channel.
channel pattern:	The aspect of a stream channel in plan view, with particular reference to the degree of sinuosity, braiding, and anabranching.
channel process:	Behavior of a channel with respect to shifting, erosion and sedimentation.
check dam:	A low dam or weir across a channel used to control stage or degradation.
choking (of flow):	Excessive constriction of flow which may cause severe backwater effect.
clay (mineral):	A particle whose diameter is in the range of 0.00024 to 0.004 mm.
clay plug:	A cutoff meander bend filled with fine grained cohesive sediments.



clear-water scour:	Scour at a pier or abutment (or contraction scour) when there is no movement of the bed material upstream of the bridge crossing at the flow causing bridge scour.
cobble:	A fragment of rock whose diameter is in the range of 64 to 250 mm.
concrete revetment:	Unreinforced or reinforced concrete slabs placed on the channel bed or banks to protect it from erosion.
confluence:	The junction of two or more streams.
constriction:	A natural or artificial control section, such as a bridge crossing, channel reach or dam, with limited flow capacity in which the upstream water surface elevation is related to discharge.
contact load:	Sediment particles that roll or slide along in almost continuous contact with the streambed (bed load).
contraction:	The effect of channel or bridge constriction on flow streamlines.
contraction scour:	Contraction scour, in a natural channel or at a bridge crossing, involves the removal of material from the bed and banks across all or most of the channel width. This component of scour results from a contraction of the flow area at the bridge which causes an increase in velocity and shear stress on the bed at the bridge. The contraction can be caused by the bridge or from a natural narrowing of the stream channel.
Coriolis force:	The inertial force caused by the Earth's rotation that deflects a moving body to the right in the Northern Hemisphere.
countermeasure:	A measure intended to prevent, delay or reduce the severity of hydraulic problems.
crib:	A frame structure filled with earth or stone ballast, designed to reduce energy and to deflect streamflow away from a bank or embankment.
critical shear stress:	The minimum amount of shear stress required to initiate soil particle motion.
crossing:	The relatively short and shallow reach of a stream between bends; also crossover or riffle.
cross section:	A section normal to the trend of a channel or flow.
current:	Water flowing through a channel.
current meter:	An instrument used to measure flow velocity.

cut bank:	The concave wall of a meandering stream.
cutoff:	(a) A direct channel, either natural or artificial, connecting two points on a stream, thereby shortening the original length of the channel and increasing its slope; (b) A natural or artificial channel which develops across the neck of a meander loop (neck cutoff) or across a point bar (chute cutoff).
cutoff wall:	A wall, usually of sheet piling or concrete, that extends down to scour-resistant material or below the expected scour depth.
daily discharge:	Discharge averaged over one day (24 hours).
debris:	Floating or submerged material, such as logs, vegetation, or trash, transported by a stream.
degradation (bed):	A general and progressive (long-term) lowering of the channel bed due to erosion, over a relatively long channel length.
depth of scour:	The vertical distance a streambed is lowered by scour below a reference elevation.
design flow (design flood):	The discharge that is selected as the basis for the design or evaluation of a hydraulic structure.
dike:	An impermeable linear structure for the control or containment of overbank flow. A dike-trending parallel with a streambank differs from a levee in that it extends for a much shorter distance along the bank, and it may be surrounded by water during floods.
dike (groin, spur, jetty):	A structure extending from a bank into a channel that is designed to: (a) reduce the stream velocity as the current passes through the dike, thus encouraging sediment deposition along the bank (permeable dike); or (b) deflect erosive current away from the streambank (impermeable dike).
discharge:	Volume of water passing through a channel during a given time.
dominant discharge:	(a) The discharge of water which is of sufficient magnitude and frequency to have a dominating effect in determining the characteristics and size of the stream course, channel, and bed; (b) That discharge which determines the principal dimensions and characteristics of a natural channel. The dominant formative discharge depends on the maximum and mean discharge, duration of flow, and flood frequency. For hydraulic geometry relationships, it is taken to be the bankfull discharge which has a return period of approximately 1.5 years in many natural channels.

drainage basin:	An area confined by drainage divides, often having only one outlet for discharge (catchment, watershed).
drift:	Alternative term for vegetative "debris."
eddy current:	A vortex-type motion of a fluid flowing contrary to the main current, such as the circular water movement that occurs when the main flow becomes separated from the bank.
entrenched stream:	Stream cut into bedrock or consolidated deposits.
ephemeral stream:	A stream or reach of stream that does not flow for parts of the year. As used here, the term includes intermittent streams with flow less than perennial.
equilibrium scour:	Scour depth in sand-bed stream with dune bed about which live bed pier scour level fluctuates due to variability in bed material transport in the approach flow.
erosion:	Displacement of soil particles due to water or wind action.
erosion control matting:	Fibrous matting (e.g., jute, paper, etc.) placed or sprayed on a stream- bank for the purpose of resisting erosion or providing temporary stabilization until vegetation is established.
fabric mattress:	Grout-filled mattress used for streambank protection.
fall velocity:	The velocity at which a sediment particle falls through a column of still water.
fascine:	A matrix of willow or other natural material woven in bundles and used as a filter. Also, a streambank protection technique consisting of wire mesh or timber attached to a series of posts, sometimes in double rows; the space between the rows may be filled with rock, brush, or other materials.
fetch:	The area in which waves are generated by wind having a rather constant direction and speed; sometimes used synonymously with fetch length.
fetch length:	The horizontal distance (in the direction of the wind) over which wind generates waves and wind setup.
fill slope:	Side or end slope of an earth-fill embankment. Where a fill-slope forms the streamward face of a spill-through abutment, it is regarded as part of the abutment.

filter:	Layer of fabric (geotextile) or granular material (sand, gravel, or graded rock) placed between bank revetment (or bed protection) and soil for the following purposes: (1) to prevent the soil from moving through the revetment by piping, extrusion, or erosion; (2) to prevent the revetment from sinking into the soil; and (3) to permit natural seepage from the streambank, thus preventing the buildup of excessive hydrostatic pressure.
filter blanket:	A layer of graded sand and gravel laid between fine-grained material and riprap to serve as a filter.
filter fabric (cloth):	Geosynthetic fabric that serves the same purpose as a granular filter blanket.
fine sediment load:	That part of the total sediment load that is composed of particle sizes finer than those represented in the bed (wash load). Normally, the fine-sediment load is finer than 0.062 mm for sand-bed channels. Silts, clays and sand could be considered wash load in coarse gravel and cobble-bed channels.
flanking:	Erosion around the landward end of a stream stabilization countermeasure.
flashy stream:	Stream characterized by rapidly rising and falling stages, as indicated by a sharply peaked hydrograph. Typically associated with mountain streams or highly disturbed urbanized catchments. Most flashy streams are ephemeral, but some are perennial.
flood-frequency curve:	A graph indicating the probability that the annual flood discharge will exceed a given magnitude, or the recurrence interval corresponding to a given magnitude.
floodplain:	A nearly flat, alluvial lowland bordering a stream, that is subject to frequent inundation by floods.
flow-control structure:	A structure either within or outside a channel that acts as a countermeasure by controlling the direction, depth, or velocity of flowing water.
flow hazard:	Flow characteristics (discharge, stage, velocity, or duration) that are associated with a hydraulic problem or that can reasonably be considered of sufficient magnitude to cause a hydraulic problem or to test the effectiveness of a countermeasure.
flow slide:	Saturated soil materials which behave more like a liquid than a solid. A flow slide on a channel bank can result in a bank failure.

fluvial geomorphology:	The science dealing with the morphology (form) and dynamics of streams and rivers.
fluvial system:	The natural river system consisting of (1) the drainage basin, watershed, or sediment source area, (2) tributary and mainstem river channels or sediment transfer zone, and (3) alluvial fans, valley fills and deltas, or the sediment deposition zone.
freeboard:	The vertical distance above a design stage that is allowed for waves, surges, drift, and other contingencies.
Froude Number:	A dimensionless number that represents the ratio of inertial to gravitational forces in open channel flow.
gabion:	A basket or compartmented rectangular container made of wire mesh. When filled with cobbles or other rock of suitable size, the gabion becomes a flexible and permeable unit with which flow- and erosion-control structures can be built.
general scour:	General scour is a lowering of the streambed across the stream or waterway at the bridge. This lowering may be uniform across the bed or non-uniform. That is, the depth of scour may be deeper in some parts of the cross section. General scour may result from contraction of the flow or other general scour conditions such as flow around a bend.
geomorphology/ morphology:	That science that deals with the form of the Earth, the general configuration of its surface, and the changes that take place due to erosion and deposition.
grade-control structure (sill, check dam):	Structure placed bank to bank across a stream channel usually with its central axis perpendicular to flow) for the purpose of controlling bed slope and preventing scour or headcutting.
graded stream:	A geomorphic term used for streams that have apparently achieved a state of equilibrium between the rate of sediment transport and the rate of sediment supply throughout long reaches.
gravel:	A rock fragment whose diameter ranges from 2 to 64 mm.

groin:	A structure built from the bank of a stream in a direction transverse to the current to redirect the flow or reduce flow velocity. Many names are given to this structure, the most common being "spur," "spur dike," "transverse dike," "jetty," etc. Groins may be permeable, semi-permeable, or impermeable.
grout:	A fluid mixture of cement and water or of cement, sand, and water used to fill joints and voids.
guide bank:	A dike extending upstream from the approach embankment at either or both sides of the bridge opening to direct the flow through the opening. Some guidebanks extend downstream from the bridge (also spur dike).
hardpoint:	A streambank protection structure whereby "soft" or erodible materials are removed from a bank and replaced by stone or compacted clay. Some hard points protrude a short distance into the channel to direct erosive currents away from the bank. Hard points also occur naturally along streambanks as passing currents remove erodible materials leaving nonerodible materials exposed.
headcutting:	Channel degradation associated with abrupt changes in the bed elevation (headcut) that generally migrates in an upstream direction.
helical flow:	Three-dimensional movement of water particles along a spiral path in the general direction of flow. These secondary-type currents are of most significance as flow passes through a bend; their net effect is to remove soil particles from the cut bank and deposit this material on a point bar.
hydraulics:	The applied science concerned with the behavior and flow of liquids, especially in pipes, channels, structures, and the ground.
hydraulic model:	A small-scale physical or mathematical representation of a flow situation.
hydraulic problem:	An effect of streamflow, tidal flow, or wave action such that the integrity of the highway facility is destroyed, damaged, or endangered.
hydraulic radius:	The cross-sectional area of a stream divided by its wetted perimeter.
hydraulic structures:	The facilities used to impound, accommodate, convey or control the flow of water, such as dams, weirs, intakes, culverts, channels, and bridges.

hydrograph:	The graph of stage or discharge against time.
hydrology:	The science concerned with the occurrence, distribution, and circulation of water on the earth.
imbricated:	In reference to stream bed sediment particles, having an overlapping or shingled pattern.
icing:	Masses or sheets of ice formed on the frozen surface of a river or floodplain. When shoals in the river are frozen to the bottom or otherwise dammed, water under hydrostatic pressure is forced to the surface where it freezes.
incised reach:	A stretch of stream with an incised channel that only rarely overflows its banks.
incised stream:	A stream which has deepened its channel through the bed of the valley floor, so that the floodplain is a terrace.
invert:	The lowest point in the channel cross section or at flow control devices such as weirs, culverts, or dams.
island:	A permanently vegetated area, emergent at normal stage, that divides the flow of a stream. Islands originate by establishment of vegetation on a bar, by channel avulsion, or at the junction of minor tributary with a larger stream.
jack:	A device for flow control and protection of banks against lateral erosion consisting of three mutually perpendicular arms rigidly fixed at the center. Kellner jacks are made of steel struts strung with wire, and concrete jacks are made of reinforced concrete beams.
jack field:	Rows of jacks tied together with cables, some rows generally parallel with the banks and some perpendicular thereto or at an angle. Jack fields may be placed outside or within a channel.
jetty:	(a) An obstruction built of piles, rock, or other material extending from a bank into a stream, so placed as to induce bank building, or to protect against erosion; (b) A similar obstruction to influence stream, lake, or tidal currents, or to protect a harbor (also spur).
lateral erosion:	Erosion in which the removal of material is extended horizontally as contrasted with degradation and scour in a vertical direction.
launching:	Release of undercut material (stone riprap, rubble, slag, etc.) downslope or into a scoured area.

levee:	An embankment, generally landward of top bank, that confines flow during high-water periods, thus preventing overflow into lowlands.
live-bed scour:	Scour at a pier or abutment (or contraction scour) when the bed material in the channel upstream of the bridge is moving at the flow causing bridge scour.
load (or sediment load):	Amount of sediment being moved by a stream.
local scour:	Removal of material from around piers, abutments, spurs, and embankments caused by an acceleration of flow and resulting vortices induced by obstructions to the flow.
longitudinal profile:	The profile of a stream or channel drawn along the length of its centerline. In drawing the profile, elevations of the water surface or the thalweg are plotted against distance as measured from the mouth or from an arbitrary initial point.
lower bank:	That portion of a streambank having an elevation less than the mean water level of the stream.
mathematical model:	A numerical representation of a flow situation using mathematical equations (also computer model).
mattress:	A blanket or revetment of materials interwoven or otherwise lashed together and placed to cover an area subject to scour.
meander or full meander:	A meander in a river consists of two consecutive loops, one flowing clockwise and the other counter-clockwise.
meander amplitude:	The distance between points of maximum curvature of successive meanders of opposite phase in a direction normal to the general course of the meander belt, measured between center lines of channels.
meander belt:	The distance between lines drawn tangent to the extreme limits of successive fully developed meanders.
meander length:	The distance along a stream between corresponding points of successive meanders.
meander loop:	An individual loop of a meandering or sinuous stream lying between inflection points with adjoining loops.
meander ratio:	The ratio of meander width to meander length.
meander radius of curvature:	The radius of a circle inscribed on the centerline of a meander loop.



meander scrolls:	Low, concentric ridges and swales on a floodplain, marking the successive positions of former meander loops.
meander width:	The amplitude of a fully developed meander measured from midstream to midstream.
meandering stream:	A stream having a sinuosity greater than some arbitrary value. The term also implies a moderate degree of pattern symmetry, imparted by regularity of size and repetition of meander loops. The channel generally exhibits a characteristic process of bank erosion and point bar deposition associated with systematically shifting meanders.
median diameter:	The particle diameter of the 50th percentile point on a size distribution curve such that half of the particles (by weight, number, or volume) are larger and half are smaller ( $D_{50}$ .)
mid-channel bar:	A bar lacking permanent vegetal cover that divides the flow in a channel at normal stage.
middle bank:	The portion of a streambank having an elevation approximately the same as that of the mean water level of the stream.
migration:	Change in position of a channel by lateral erosion of one bank and simultaneous accretion of the opposite bank.
mud:	A soft, saturated mixture mainly of silt and clay.
natural levee:	A low ridge that slopes gently away from the channel banks that is formed along streambanks during floods by deposition.
nominal diameter:	Equivalent spherical diameter of a hypothetical sphere of the same volume as a given sediment particle.
nonalluvial channel:	A channel whose boundary is in bedrock or non-erodible material.
normal stage:	The water stage prevailing during the greater part of the year.
overbank flow:	Water movement that overtops the bank either due to stream stage or to overland surface water runoff.
oxbow:	The abandoned former meander loop that remains after a stream cuts a new, shorter channel across the narrow neck of a meander. Often bow-shaped or horseshoe-shaped.
pavement:	Streambank surface covering, usually impermeable, designed to serve as protection against erosion. Common pavements used on streambanks are concrete, compacted asphalt, and soil-cement.

paving:	Covering of stones on a channel bed or bank (used with reference to natural covering).
peaked stone dike:	Riprap placed parallel to the toe of a streambank (at the natural angle of repose of the stone) to prevent erosion of the toe and induce sediment deposition behind the dike.
perennial stream:	A stream or reach of a stream that flows continuously for all or most of the year.
phreatic line:	The upper boundary of the seepage water surface landward of a streambank.
pile:	An elongated member, usually made of timber, concrete, or steel, that serves as a structural component of a river-training structure.
pile dike:	A type of permeable structure for the protection of banks against caving; consists of a cluster of piles driven into the stream, braced and lashed together.
piping:	Removal of soil material through subsurface flow of seepage water that develops channels or "pipes" within the soil bank.
point bar:	An alluvial deposit of sand or gravel lacking permanent vegetal cover occurring in a channel at the inside of a meander loop, usually somewhat downstream from the apex of the loop.
poised stream:	A stream which, as a whole, maintains its slope, depths, and channel dimensions without any noticeable raising or lowering of its bed (stable stream). Such condition may be temporary from a geological point of view, but for practical engineering purposes, the stream may be considered stable.
probable maximum flood:	A very rare flood discharge value computed by hydrometeorological methods, usually in connection with major hydraulic structures.
quarry-run stone:	Stone as received from a quarry without regard to gradation requirements.
railbank protection:	A type of countermeasure composed of rock-filled wire fabric supported by steel rails or posts driven into streambed.
rapid drawdown:	Lowering the water against a bank more quickly than the bank can drain without becoming unstable.
reach:	A segment of stream length that is arbitrarily bounded for purposes of study.

recurrence interval:	The reciprocal of the annual probability of exceedance of a hydrologic event (also return period, exceedance interval).
regime:	The condition of a stream or its channel with regard to stability. A stream is in regime if its channel has reached an equilibrium form as a result of its flow characteristics. Also, the general pattern of variation around a mean condition, as in flow regime, tidal regime, channel regime, sediment regime, etc. (used also to mean a set of physical characteristics of a river).
regime change:	A change in channel characteristics resulting from such things as changes in imposed flows, sediment loads, or slope.
regime channel:	Alluvial channel that has attained, more or less, a state of equilibrium with respect to erosion and deposition.
regime formula:	A formula relating stable alluvial channel dimensions or slope to discharge and sediment characteristics.
reinforced-earth bulkhead:	A retaining structure consisting of vertical panels and attached to reinforcing elements embedded in compacted backfill for supporting a streambank.
reinforced revetment:	A streambank protection method consisting of a continuous stone toe-fill along the base of a bank slope with intermittent fillets of stone placed perpendicular to the toe and extending back into the natural bank.
relief bridge:	An opening in an embankment on a floodplain to permit passage of overbank flow.
retard (retarder structure):	A permeable or impermeable linear structure in a channel parallel with the bank and usually at the toe of the bank, intended to reduce flow velocity, induce deposition, or deflect flow from the bank.
revetment:	Rigid or flexible armor placed to inhibit scour and lateral erosion. (See bank revetment).
riffle:	A natural, shallow flow area extending across a streambed in which the surface of flowing water is broken by waves or ripples. Typically, riffles alternate with pools along the length of a stream channel.
riparian:	Pertaining to anything connected with or adjacent to the banks of a stream (corridor, vegetation, zone, etc.).

riprap:	Layer or facing of rock or broken concrete which is dumped or placed to protect a structure or embankment from erosion; also the rock or broken concrete suitable for such use. Riprap has also been applied to almost all kinds of armor, including wire-enclosed riprap, grouted riprap, sacked concrete, and concrete slabs.
river training:	Engineering works with or without the construction of embankment, built along a stream or reach of stream to direct or to lead the flow into a prescribed channel. Also, any structure configuration constructed in a stream or placed on, adjacent to, or in the vicinity of a streambank that is intended to deflect currents, induce sediment deposition, induce scour, or in some other way alter the flow and sediment regimes of the stream.
rock-and-wire mattress:	A flat wire cage or basket filled with stone or other suitable material and placed as protection against erosion.
roughness coefficient:	Numerical measure of the frictional resistance to flow in a channel, as in the Manning's or Chezy's formulas.
rubble:	Rough, irregular fragments of materials of random size used to retard erosion. The fragments may consist of broken concrete slabs, masonry, or other suitable refuse.
runoff:	That part of precipitation which appears in surface streams of either perennial or intermittent form.
sack revetment:	Sacks (e.g., burlap, paper, or nylon) filled with mortar, concrete, sand, stone or other available material used as protection against erosion.
saltation load:	Sediment bounced along the streambed by energy and turbulence of flow, and by other moving particles.
sand:	A rock fragment whose diameter is in the range of 0.062 to 2.0 mm.
scour:	Erosion of streambed or bank material due to flowing water; often considered as being localized (see local scour, contraction scour, total scour).
sediment or fluvial sediment:	Fragmental material transported, suspended, or deposited by water.
sediment concentration:	Weight or volume of sediment relative to the quantity of transporting (or suspending) fluid.
sediment discharge:	The quantity of sediment that is carried past any cross section of a stream in a unit of time. Discharge may be limited to certain sizes of sediment or to a specific part of the cross section.

sediment load:	Amount of sediment being moved by a stream.
sediment yield:	The total sediment outflow from a watershed or a drainage area at a point of reference and in a specified time period. This outflow is equal to the sediment discharge from the drainage area.
seepage:	The slow movement of water through small cracks and pores of the bank material.
shear stress:	See unit shear force.
shoal:	A relatively shallow submerged bank or bar in a body of water.
sill:	(a) A structure built under water, across the deep pools of a stream with the aim of changing the depth of the stream; (b) A low structure built across an effluent stream, diversion channel or outlet to reduce flow or prevent flow until the main stream stage reaches the crest of the structure.
silt:	A particle whose diameter is in the range of 0.004 to 0.062 mm.
sinuosity:	The ratio between the thalweg length and the valley length of a stream.
slope (of channel or stream):	Fall per unit length along the channel centerline or thalweg.
slope protection:	Any measure such as riprap, paving, vegetation, revetment, brush or other material intended to protect a slope from erosion, slipping or caving, or to withstand external hydraulic pressure.
sloughing:	Sliding or collapse of overlying material; same ultimate effect as caving, but usually occurs when a bank or an underlying stratum is saturated.
slope-area method:	A method of estimating unmeasured flood discharges in a uniform channel reach using observed high-water levels.
slump:	A sudden slip or collapse of a bank, generally in the vertical direction and confined to a short distance, probably due to the substratum being washed out or having become unable to bear the weight above it.
soil-cement:	A designed mixture of soil and Portland cement compacted at a proper water content to form a blanket or structure that can resist erosion.
sorting:	Progressive reduction of size (or weight) of particles of the sediment load carried down a stream.

spill-through abutment:	A bridge abutment having a fill slope on the streamward side. The term originally referred to the "spill-through" of fill at an open abutment but is now applied to any abutment having such a slope.
spread footing:	A pier or abutment footing that transfers load directly to the earth.
spur:	A permeable or impermeable linear structure that projects into a channel from the bank to alter flow direction, induce deposition, or reduce flow velocity along the bank.
spur dike:	See guide bank.
stability:	A condition of a channel when, though it may change slightly at different times of the year as the result of varying conditions of flow and sediment charge, there is no appreciable change from year to year; that is, accretion balances erosion over the years.
stable channel:	A condition that exists when a stream has a bed slope and cross section which allows its channel to transport the water and sediment delivered from the upstream watershed without aggradation, degradation, or bank erosion (a graded stream).
stage:	Water-surface elevation of a stream with respect to a reference elevation.
stone riprap:	Natural cobbles, boulders, or rock dumped or placed as protection against erosion.
stream:	A body of water that may range in size from a large river to a small rill flowing in a channel. By extension, the term is sometimes applied to a natural channel or drainage course formed by flowing water whether it is occupied by water or not.
streambank erosion:	Removal of soil particles or a mass of particles from a bank surface due primarily to water action. Other factors such as weathering, ice and debris abrasion, chemical reactions, and land use changes may also directly or indirectly lead to bank erosion.
streambank failure:	Sudden collapse of a bank due to an unstable condition such as removal of material at the toe of the bank by scour.
streambank protection:	Any technique used to prevent erosion or failure of a streambank.
suspended sediment discharge:	The quantity of sediment passing through a stream cross section above the bed layer in a unit of time suspended by the turbulence of flow (suspended load).

sub-bed material:	Material underlying that portion of the streambed which is subject to direct action of the flow. Also, substrate.
subcritical, supercritical flow:	Open channel flow conditions with Froude Number less than and greater than unity, respectively.
tetrahedron:	Component of river-training works made of six steel or concrete struts fabricated in the shape of a pyramid.
tetrapod:	Bank protection component of precast concrete consisting of four legs joined at a central joint, with each leg making an angle of $109.5^\circ$ with the other three.
thalweg:	The line extending down a channel that follows the lowest elevation of the bed.
tieback:	Structure placed between revetment and bank to prevent flanking.
timber or brush mattress:	A revetment made of brush, poles, logs, or lumber interwoven or otherwise lashed together. The completed mattress is then placed on the bank of a stream and weighted with ballast.
toe of bank:	That portion of a stream cross section where the lower bank terminates and the channel bottom or the opposite lower bank begins.
toe protection:	Loose stones laid or dumped at the toe of an embankment, groin, etc., or masonry or concrete wall built at the junction of the bank and the bed in channels or at extremities of hydraulic structures to counteract erosion.
total scour:	The sum of long-term degradation, general (contraction) scour, and local scour.
total sediment load:	The sum of suspended load and bed load or the sum of bed material load and wash load of a stream (total load).
tractive force:	The drag or shear on a streambed or bank caused by passing water which tends to move soil particles along with the streamflow.
trench-fill revetment:	Stone, concrete, or masonry material placed in a trench dug behind and parallel to an eroding streambank. When the erosive action of the stream reaches the trench, the material placed in the trench armors the bank and thus retards further erosion.

turbulence:	Motion of fluids in which local velocities and pressures fluctuate irregularly in a random manner as opposed to laminar flow where all particles of the fluid move in distinct and separate lines.
ultimate scour:	The maximum depth of scour attained for a given flow condition. May require multiple flow events and in cemented or cohesive soils may be achieved over a long time period.
uniform flow:	Flow of constant cross section and velocity through a reach of channel at a given time. Both the energy slope and the water slope are equal to the bed slope under conditions of uniform flow.
unit discharge:	Discharge per unit width (may be average over a cross section, or local at a point).
unit shear force (shear stress):	The force or drag developed at the channel bed by flowing water. For uniform flow, this force is equal to a component of the gravity force acting in a direction parallel to the channel bed on a unit wetted area. Usually in units of stress, Pa ( $\text{N/m}^2$ ) or ( $\text{lb/ft}^2$ ).
unsteady flow:	Flow of variable discharge and velocity through a cross section with respect to time.
upper bank:	The portion of a streambank having an elevation greater than the average water level of the stream.
velocity:	The time rate of flow usually expressed in m/s (ft/sec). The average velocity is the velocity at a given cross section determined by dividing discharge by cross-sectional area.
vertical abutment:	An abutment, usually with wingwalls, that has no fill slope on its streamward side.
vortex:	Turbulent eddy in the flow generally caused by an obstruction such as a bridge pier or abutment (e.g., horseshoe vortex).
wandering channel:	A channel exhibiting a more or less non-systematic process of channel shifting, erosion and deposition, with no definite meanders or braided pattern.
wandering thalweg:	A thalweg whose position in the channel shifts during floods and typically serves as an inset channel that conveys all or most of the stream flow at normal or lower stages.



wash load:	Suspended material of very small size (generally clays and colloids) originating primarily from erosion on the land slopes of the drainage area and present to a negligible degree in the bed itself.
watershed:	See drainage basin.
waterway opening width (area):	Width (area) of bridge opening at (below) a specified stage, measured normal to the principal direction of flow.
weephole:	A hole in an impermeable wall or revetment to relieve the neutral stress or pore pressure in the soil.
windrow revetment:	A row of stone placed landward of the top of an eroding streambank. As the windrow is undercut, the stone is launched downslope, thus armoring the bank.
wire mesh:	Wire woven to form a mesh; where used as an integral part of a countermeasure, openings are of suitable size and shape to enclose rock or broken concrete or to function on fence-like spurs and retards.

(page intentionally left blank)

## CHAPTER 1

### INTRODUCTION

The purpose of this chapter is to lay the groundwork for application of the concepts of open-channel flow, fluvial geomorphology, sediment transport, and river mechanics to the design, maintenance, and environmental problems associated with highway crossings and encroachments.

This manual is a basic reference for related Federal Highway Administration (FHWA) hydraulic publications and National Highway Institute (NHI) Hydraulics Courses. Some of these publications are: "Hydraulics of Bridge Waterways" (Bradley 1978), "Design of Riprap Revetment" (Brown and Clyde 1989), "Evaluating Scour at Bridges" (Richardson and Davis 2001), "Stream Stability at Highway Structures" (Lagasse et al. 2001), "Bridge Scour and Stream Instability Countermeasures - Experience, Selection and Design Guidance" (Lagasse et al. 2001). Related NHI courses include: (1) River Engineering for Highway Encroachments, (2) Stream Stability and Scour at Highway Bridges, and (3) Finite Element Surface Water Modeling System (FESWMS).

Basic definitions of terms and notations adopted for use in this document have been presented in the preceding section (Glossary) for rapid reference. Additionally, these important terms and variables are defined and explained as they are encountered.

#### 1.1 CLASSIFICATION OF RIVER CROSSINGS AND ENCROACHMENTS

The objective in this document is to consider the fluvial, hydraulic, geomorphic, sediment transport, and environmental aspects of highway encroachments, including bridge locations, alignments, longitudinal encroachments, stabilization works and road approaches. Encroachment is any occupancy of the river and floodplain for highway use. Encroachments usually present no problems during normal stages, but require special protection against floods. Flood protection requirements vary from site to site.

Some bridges and culverts must accommodate the passage of livestock and farm equipment during periods of low flow. Other bridges require low embankments for aesthetic appeal, especially in populated areas. Still other bridges require short spans with long approaches and numerous piers for economic reasons. All of these factors, and many more, contribute to the difficulty in generalizing the design for all highway encroachments.

A classification of encroachments based on prominent features is helpful. Classifying the regions requiring protection, the possible types of protection, the possible flow conditions, the possible channel shapes, and the various geometric conditions aids the engineer in selecting the design criteria for the conditions encountered.

### **1.1.1 Types of Encroachment**

In the vicinity of rivers, highways generally must impose a degree of encroachment. In some instances, particularly in mountainous regions or in river gorges and canyons, river crossings can be accomplished with absolutely no encroachment on the river. The bridge and its approaches are located far above and beyond any possible flood stage. More commonly, the economics of crossings require substantial encroachment on the river and its floodplain, the cost of a single span over the entire floodplain being prohibitive. The encroachment can be in the form of earth fill embankments on the floodplain or into the main channel itself, reducing the required bridge length; or in the form of piers and abutments or culverts in the main channel of the river.

Longitudinal encroachments may exist that are not connected with river crossings. Floodplains often appear to provide an attractive low cost alternative for highway location, even when the extra cost of flood protection is included. As a consequence, highways, including interchanges, often encroach on a floodplain over long distances. In some regions, river valleys provide the only feasible route for highways. This is true even in areas where a floodplain does not exist. In many locations the highway must encroach on the main channel itself and the channel is partly filled to allow room for the roadway. In some instances, this encroachment becomes severe, particularly as older highways are upgraded and widened. Often, a stretch of the river must be straightened to eliminate meanders to accommodate the highway.

### **1.1.2 Geometry of Bridge Crossings**

The bridge crossing is the most common type of river encroachment. The geometric properties of bridge crossings illustrated in Figure 1.1 are commonly used depending on the conditions at the site. The approaches may be skewed or normal (perpendicular) to the direction of flow or one approach may be longer than the other, producing an eccentric crossing. Abutments used for the overbank-flow case may be set back from the low-flow channel banks to provide room to pass the flood flow or simply to allow passage of livestock and machinery, or the abutments may extend up to the banks or even protrude over the banks, constricting the low-flow channel. Piers, dual bridges for multi-lane freeways, channel bed conditions, spurs and guide banks add to the list of geometric classifications.

The design procedures in this document have been derived from laboratory and field observations of bridge crossings. The design procedures include allowances made for the effects of skewness, eccentricity, scour, abutment setback, channel shape, submergence of the superstructure, debris, spurs, wind waves, ice, piers, abutment types, and flow conditions. These design procedures take advantage of the large volume of work that has been done by many people in describing the hydraulics and scour characteristics of bridge crossings.

## **1.2 DYNAMICS OF NATURAL RIVERS AND THEIR TRIBUTARIES**

Frequently, hydraulic engineers, and those involved in transportation, navigation, and flood control mistakenly consider a river to be static; that is, unchanging in shape, dimensions, and pattern. However, an alluvial river generally is continually changing its position and shape as a

consequence of hydraulic forces acting on its bed and banks. These changes may be slow or rapid and may result from natural environmental changes or from changes by human activities. When an engineer modifies a river channel locally, this local change frequently causes modification of channel characteristics both up and down the stream. The response of a river to human-induced changes often occurs in spite of attempts by engineers to keep the anticipated response under control. The points that must be stressed are that a river through time is dynamic and that human-induced change frequently sets in motion a response that can be propagated upstream or downstream for long distances.

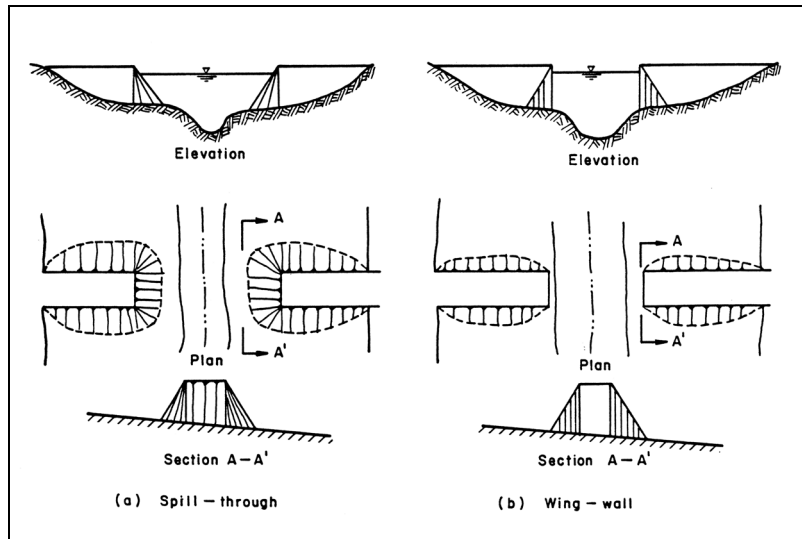


Figure 1.1. Geometric properties of bridge crossings.

In spite of their complexity, all rivers are governed by the same basic forces. The design engineer must understand, and work with these natural forces:

- Geological factors, including soil conditions
- Hydrologic factors, including possible changes in flows, runoff, and the hydrologic effects of changes in land use
- Geometric characteristics of the stream, including the probable geometric alterations that will be activated by the changes a project and future projects will impose on the channel
- Hydraulic characteristics such as depths, slopes, and velocity of streams and what changes may be expected in these characteristics in space and time.

### 1.2.1 Historical Evidence of the Natural Instability of Fluvial Systems

In order to emphasize the inherent dynamic qualities of river channels, evidence is cited below to demonstrate that most alluvial rivers are not static in their natural state. Indeed, scientists concerned with the history of landforms (geomorphologists), vegetation (botanists), and the past activities of man (archaeologists), rarely consider the landscape as unchanging. Rivers, glaciers, sand dunes, and seacoasts are highly susceptible to change with time. Over a relatively short period of time, perhaps in some cases up to 100 years, components of the

landscape may be relatively stable. Nevertheless, stability cannot be automatically assumed. Rivers are, in fact, the most actively changing of all geomorphic forms.

Evidence from several sources demonstrates that river channels are continually undergoing changes of position, shape, dimensions, and pattern. In Figure 1.2 a section of the Mississippi River as it was in 1884 is compared with the same section as observed in 1968. In the lower 9.6 km (6 mi) of river, the surface area has been reduced approximately 50 percent during this 84-year period. Some of this change has been natural and some has been the consequence of river development work.

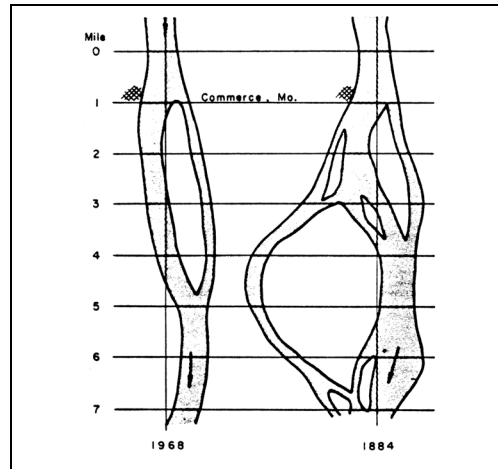


Figure 1.2. Comparison of the 1884 and 1968 Mississippi River Channel near Commerce, Missouri.

In alluvial river systems, it is the rule rather than the exception that banks will erode, sediments will be deposited and floodplains, islands, and side channels will undergo modification with time. Changes may be very slow or dramatically rapid. Fisk's (1944) report on the Mississippi River and his maps showing river position through time are sufficient to convince everyone of the innate instability of the Mississippi River. The Mississippi is our largest and most impressive river, and because of its dimensions it has sometimes been considered unique. This, of course, is not so. Hydraulic and geomorphic laws apply at all scales of comparable landform evolution. The Mississippi may be thought of as a prototype of many rivers or as a much larger than prototype model of many sandbed rivers.

Rivers change position and morphology (dimensions, shape, pattern) as a result of changes of hydrology. Hydrology can change as a result of climatic changes over long periods of time, or as a result of natural stochastic climatic fluctuations (droughts, floods), or by human modification of the hydrologic regime. For example, the major climatic changes of recent geological time (the last few million years of earth history) have triggered dramatic changes in runoff and sediment loads with corresponding channel alteration. Equally significant during this time were fluctuations of sea level. During the last continental glaciation, sea level was on the order of 120 m (400 ft) lower than at present, and this reduction of baselevel caused major incisions of river valleys near the coasts.

In recent geologic time, major river changes of different types occurred. These types are deep incision and deposition as sea level fluctuated, changes of channel geometry as a result of climatic and hydrologic changes, and obliteration or displacement of existing channels by continental glaciation. Climatic change, sea level change, and glaciation, which are interesting from an academic point of view, may also be causes of modern river instability, particularly when the 50- 100-year design life of a bridge is considered. The movement of the earth's crust is one geologic agent causing modern river instability.

The earth's surface in many parts of the world is undergoing continuous measurable change by upwarping, subsidence or lateral displacement. As a result, the study of these ongoing changes (called neotectonics) has become a field of major interest for many geologists and geophysicists. Such gradual surface changes can affect stream channels dramatically. For example, Wallace (1967) has shown that many small streams are clearly offset laterally along the San Andreas Fault in California. Progressive lateral movement of this fault on the order of 25 mm (an inch) per year has been measured. The rates of movement of faults are highly variable, but an average rate of mountain building has been estimated by Schumm (1963) to be on the order of 7.6 m (25 ft) per 1,000 years. Seemingly insignificant in human terms, this rate is actually 7.6 mm (0.3 in) per year or 76 mm (3 in) per decade. For many river systems, a change of slope of 76 mm (3 in) would be significant. For example, the slope of the energy gradient on the Lower Mississippi River is about 47 to 95 mm/km (3 to 6 in/mi).

Of course, the geologist is not surprised to see drainage patterns that have been disrupted by uplift or some complex warping of the earth's surface. In fact, complete reversals of drainage lines have been documented. In addition, convexities in the longitudinal profile of both rivers and river terraces (these profiles are concave under normal development) have been detected and attributed to upwarping. Further, the progressive shifting of a river toward one side of its valley has resulted from lateral tilting. Major shifts in position of the Brahmaputra River toward the west are attributed by Coleman (1969) to tectonic movements. Hence, neotectonics should not be ignored as a possible cause of local river instability.

Long-term climatic fluctuations have caused major changes of river morphology. Floodplains have been destroyed and reconstructed many times over. The history of semi-arid and arid valleys of the western United States is one of alternating periods of channel incision and arroyo formation followed by deposition and valley stability which have been attributed to climatic fluctuations.

It is clear that rivers can display a remarkable propensity for change of position and morphology in time periods of a century. Hence, rivers from the geomorphic point of view are unquestionably dynamic, but does this apply to modern rivers? It is probable that during a period of several years, neither neotectonics nor a progressive climate change will have a detectable influence on river character and behavior. What then causes a river to appear relatively unstable from the point of view of the highway engineer or the environmentalist? It is the slow but implacable shift of a river channel through erosion and deposition at bends, the shift of a channel to form chutes and islands, and the cutoff of a bend to form oxbow lakes. Lateral migration rates are highly variable; that is, a river may maintain a stable position for long periods and then experience rapid movement. Much, therefore, depends on flood events, bank stability, permanence of vegetation on banks and the floodplain and watershed land use. A compilation of data by Wolman and Leopold shows that rates of lateral migration for the Kosi River of India range up to approximately 760 m/yr (2,500 ft/yr). Rates of lateral migration for two major rivers in the United States are as follows: Colorado River near Needles, California, 3

to 46 m/yr (10 to 150 ft/yr); Mississippi River near Rosedale, Mississippi, 48 to 192 m/yr (158 to 630 ft/yr).

Archaeologists have also provided clear evidence of channel changes that are completely natural and to be expected. For example, the number of archaeological sites of the floodplains decreases significantly with age because the earliest sites are destroyed as floodplains are modified by river migration. Lathrop (1968), working on the Rio Ycayali in the Amazon headwaters of Peru, estimates that on the average a meander loop on this river begins to form and cuts off in 5,000 years. These loops have an amplitude of 3.2 to 9.7 km (2 to 6 mi) and an average rate of meander growth of approximately 12 m/yr (40 ft/yr).

A study by Schmudde (1963) shows that about one-third of the floodplain of the Missouri River over the 274 km (170 mi) reach between Glasgow and St. Charles, Missouri, was reworked by the river between 1879 and 1930. On the Lower Mississippi River, bend migration was on the order of 0.6 m/yr (2 ft/yr), whereas in the central and upper parts of the river, below Cairo, it was at times 305 m/yr (1,000 ft/yr) (Kolb 1963). On the other hand, a meander loop pattern of the lower Ohio River has altered very little during the past thousand years (Alexander and Nunnally 1972).

Although the dynamic behavior of perennial streams is impressive, the modification of rivers in arid and semi-arid regions and especially of ephemeral (flowing occasionally) stream channels is startling. A study of floodplain vegetation and the distribution of trees in different age groups led Everitt (1968) to the conclusion that about half of the Little Missouri River floodplain in western North Dakota was reworked in 69 years.

Historical and field studies by Smith (1940) show that floodplain destruction occurred during major floods on rivers of the Great Plains. As exceptional example of this is the Cimarron River of Southwestern Kansas, which was 15 m (50 ft) wide during the latter part of the 19th and first part of the 20th centuries (Schumm and Lichty 1957). Following a series of major floods during the 1930s it widened to 366 m (1,200 ft) and the channel occupied essentially the entire valley floor. During the decade of the 1940s a new floodplain was constructed, and the river width was reduced to about 152 m (500 ft) in 1960. Equally dramatic changes of channel dimensions have occurred along the North and South Platte Rivers in Nebraska and Colorado as a result of control of flood peaks by reservoir construction, decrease in annual flow by irrigation and restriction of channel width by bridges. In their natural state the rivers were 600 to 1,500 m (2,000 to 5,000 ft) wide but now are less than 300 m (1,000 ft). Changes of this magnitude due to changes in flow are perhaps exceptional, but emphasize the mobility of rivers and their ability to adapt to changing conditions.

Another somewhat different type of channel modification, which testifies to the rapidity of fluvial processes, is described by Shull (1922, 1944). During a major flood in 1913, a barge became stranded in a chute of the Mississippi River near Columbus, Kentucky. The barge induced deposition in the chute and an island formed. In 1919, the island was sufficiently large to be homesteaded, and a few acres were cleared for agricultural purposes. By 1933, the side channel separating the island from the mainland had filled to the extent that the island became part of Missouri. The island formed in a location protected from the erosive effects of floods but susceptible to deposition of sediment during floods. For these reasons the channel filling was rapid and progressive. It cannot be concluded that islands will always form and side channels fill at such rapid rates, but island formation and side-channel filling appear to be the normal course of events in any river transporting moderate or high sediment loads regardless of the river size. These topics are discussed in detail in Chapter 5.



In addition to changes in planform location and size with time, the bed configuration of a river can change with temperature, discharge, and concentration of silts and clays. At low flow or with warm water the bed of a sand bed stream can be dunes, but at large flows or cold temperature the bed may become plane or have antidune flow. With dunes, resistance to flow is large and bed material transport is low. Whereas, with plane bed or antidune flow the resistance to flow is small and the bed material transport is large. This topic is discussed in detail in Chapter 3.

In summary, archaeological, botanical, geological, and geomorphic evidence supports the conclusion that most rivers are subject to constant change as a normal part of their morphologic evolution. Therefore, stable or static channels are the exception in nature.

### **1.2.2 Introduction to River Hydraulics and River Response**

In the previous section, it was established that rivers are dynamic and respond to changing environmental conditions. The direction and extent of the change depends on the forces acting on the system. The mechanics of flow in rivers is a complex subject that requires special study, which is unfortunately not included in basic courses of fluid mechanics. The major complicating factors in river mechanics are: (a) the large number of interrelated variables that can simultaneously respond to natural or imposed changes in a river system and (b) the continual evolution of river channel patterns, channel geometry, bars and forms of bed roughness with changing water and sediment discharge. In order to understand the responses of a river to the actions of humans and nature, a few simple hydraulic and geomorphic concepts are presented here.

River forms are broadly classified as straight, meandering, braided or some combination of these classifications; but any changes that are imposed on a river may change its form. The dependence of river sinuosity on the slope, which may be imposed independent of the other river characteristics, is illustrated schematically in Figure 1.3. By changing the slope, it is possible to change the river from a meandering one that is relatively tranquil and easy to control to a braided one that varies rapidly with time, has high velocities, is subdivided by sandbars and carries relatively large quantities of sediment. Such a change could be caused by a natural or artificial cutoff. Conversely, it is possible that a slight decrease in slope could change an unstable braided river into a meandering one.

The significantly different channel dimensions, shapes, and patterns associated with different quantities of discharge and amounts of sediment load indicate that as these independent variables change, major adjustments of channel morphology can be anticipated. Further, if changes in sinuosity and meander wavelength as well as in width and depth are required to compensate for a hydrologic change, then a long period of channel instability can be envisioned with considerable bank erosion and lateral shifting of the channel before stability is restored. The reaction of a channel to changes in discharge and sediment load may result in channel dimension changes contrary to those indicated by many regime equations. For example, it is conceivable that a decrease in discharge together with an increase in sediment load could actuate a decrease in depth and an increase in width.

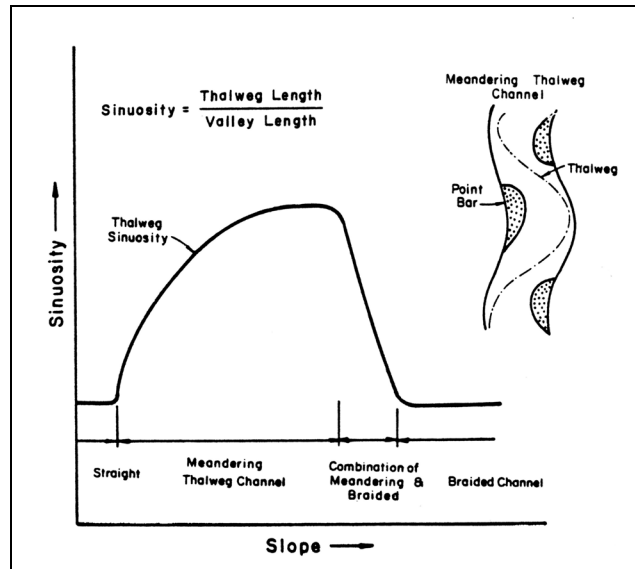


Figure 1.3. Sinuosity vs. slope with constant discharge.

Changes in sediment and water discharge at a particular point or reach in a stream may have an effect ranging from some distance upstream to a point downstream where the hydraulic and geometric conditions will have absorbed the change. Thus, it is necessary to consider a channel reach as part of a complete drainage system. Artificial controls that could benefit the reach may, in fact, cause problems in the system as a whole. For example, flood control structures can cause downstream flood damage to be greater at reduced flows if the average hydrologic regime is changed so that the channel dimensions are actually reduced. Also, where major tributaries exert a significant influence on the main channel by introducing large quantities of sediment, upstream control on the main channel may allow the tributary to intermittently dominate the system with deleterious results. If discharges in the main channel are reduced, sediments from the tributary that previously were eroded will no longer be carried away and serious aggradation with accompanying flood problems may arise.

An insight into the direction of change, the magnitude of change, and the time involved to reach a new equilibrium can be gained by:

- Studying the river in a natural condition
- Having knowledge of the sediment and water discharge
- Predicting the effects and magnitude of future human activities
- Applying knowledge of geology, soils, hydrology, and hydraulics of alluvial rivers

The current interest in ecology and the environment have made people aware of the many problems that humans can cause. Prior to this interest in environmental impacts, very few people interested in rivers ever considered the long-term changes that were possible. It is imperative that anyone working with rivers, either with localized areas or entire systems, have an understanding of the many factors involved, and of the potential for change existing in the river system.

Two methods of predicting response are physical and mathematical models. Engineers have long used small-scale hydraulic models to assist them in anticipating the effect of altering conditions in a reach of a river. With proper awareness of the large-scale effects that can exist, the results of hydraulic model testing can be extremely useful for this purpose. An alternative method of predicting short-term and long-term changes in rivers involves the use of mathematical computer models. To study a transient phenomenon in natural alluvial channels, the equations of motion and continuity for sediment laden water and the continuity equation for sediment can be used as discussed in Chapters 2, 3, 4, and 5.

### **1.3 EFFECTS OF HIGHWAY CONSTRUCTION ON RIVER SYSTEMS**

Highway construction can have significant general and local effects on the geomorphology and hydraulics of river systems. Hence, it is necessary to consider induced short-term and long-term responses of the river and its tributaries, the impact on environmental factors, the aesthetics of the river environment and short-term and long-term effects of erosion and sedimentation on the surrounding landscape and the river. The biological response of the river system should also be considered and evaluated.

#### **1.3.1 Immediate Response of Rivers to Encroachment**

Let us consider a few of the numerous and immediate responses of rivers to the construction of bridges, channel stabilization, and countermeasures.

Local changes made in the geometry or the hydraulic properties of the river might be of such a magnitude as to have an immediate impact upon the entire river system. At bridges, contraction due to the construction of encroachments usually cause contraction and local scour, and the sediments removed from this location are usually dropped in the immediate reach downstream. In the event that the contraction is extended further downstream, the river may be capable of carrying the increased sediment load an additional distance, but only until a reduction in gradient and a reduction in transport capability is encountered. The increased velocities caused by encroachments may also affect the general lateral stability of the river downstream.

In addition, the development of crossings and the contraction of river sections may have a significant effect on the water level in the vicinity and upstream of the bridge. Such changes in water level upstream of the bridge are called backwater effects. The highway engineer must be in a position to accurately assess the effects of the construction of crossings upon the water surface profile.

In many instances, to offset increased velocities and to reduce bank instabilities and related problems, the river is stabilized or channelized to some degree. When it is necessary to do this, every effort should be made to accomplish the channelization in a manner which does not degrade the river environment, including the river's aesthetic value.

As a consequence of construction, many areas become highly susceptible to erosion. The transported sediment is carried from the construction site by surface flow into the minor rills, which combine within a short distance to form larger channels leading to the river. The water

flowing from the construction site is usually a consequence of rain. The surface runoff and the accompanying erosion can significantly increase the sediment yield to the river channel unless careful control is exercised. The large sediment particles transported to the main channel may remain in the vicinity of the construction site for a long period of time or may be slowly moved away. On the other hand, the fine sediments are easily transported and generally disperse into the whole cross section of the river. The fine sediments are transported downstream to the nearest reservoir or to the sea. As will be discussed later, the sudden injection of the larger sediments into the channel may cause local aggradation, thereby steepening the channel, increasing the flow velocities and possibly causing instability in the river at that site.

The suspended fine sediments can have very significant effects on the biomass of the stream. Certain species of fish can only tolerate large quantities of suspended sediment for relatively short periods of time. This is particularly true of the eggs and fry. This type of biological response to development normally falls outside of the competence of the engineer. Yet, engineering works may be responsible for the discharge of these sediments into the system. In this regard, the engineer should utilize adequate technical assistance from experts in fisheries, biology, and other related areas to assess the consequences of sediment in a river. Only with such knowledge can one develop the necessary arguments to "sell" the case that erosion control measures must be exercised to avoid significant deterioration of the stream environment not only in the immediate vicinity of the bridge but in many instances for great distances downstream.

Another possible immediate response of the river system to construction is the loss of the recreational use of the river. In many streams, there may be an immediate drop in the quality of the fishing due to the increase of sediment load or other changed hydraulic characteristics within the channel. Some natural rivers consist of a series of pools and riffles. Both form an important part of the environment for fish. The introduction of larger quantities of sediment into the channel and changes made in the geometry of the channel may result in the loss of these pools and riffles. Along the same lines, construction work within the river may cause a loss of food essential to fish life and often it is difficult to get the food chain reestablished in the system. In contrast, construction of barbs, spurs, and other river control works to stabilize the river channel and protect a bridge crossing can decrease erosion, provide a better habitat for fish and in general improve the environment.

Construction and operation of highways in water supply watersheds present very real problems and may require special precautionary designs to protect the water supplies from highway runoff or accidental spills. Runoff from highway construction may increase sediment and turbidity of the water.

The preceding discussion is related to only a few immediate responses to construction along a river. However, they are responses that illustrate the importance of considering the environment in the design of highway encroachments.

### **1.3.2 Delayed Response of Rivers to Encroachment**

In addition to the examples of possible immediate response discussed above, there are important delayed responses of rivers to highway development. As part of this introductory

chapter, consideration is given to some of the more obvious effects that can be induced on a river system over a long time period by highway construction.

Sometimes it is necessary to employ training works in connection with highway encroachments to align the flow with bridge or culvert openings. When such training works are used, they generally straighten the channel, shorten the flow line, and increase the local velocity within the channel. Any such changes made in the system that cause an increase in the gradient may cause an increase in local velocities. The increase in velocity increases local and contraction scour with subsequent deposition downstream where the channel takes on its normal characteristics. If significant lengths of the river are trained and straightened, there can be a noticeable decrease in the elevation of the water surface profile for a given discharge in the main channel. Tributaries emptying into the main channel in such reaches are significantly affected. Having a lower water level in the main channel for a given discharge means that the tributary streams entering in that vicinity are subjected to a steeper gradient and higher velocities which cause degradation in the tributary streams. In extreme cases, degradation can be induced of such magnitude as to cause failure of structures such as bridges, culverts or other encroachments on the tributary systems. In general, any increase in transported materials from the tributaries to the main channel causes a reduction in the quality of the environment within the river. More specifically, as degradation occurs in the tributaries, bank instabilities are induced and the sediment loads are greatly increased. Increased sediment loads usually result in a deterioration of the environment.

#### **1.4 EFFECTS OF RIVER DEVELOPMENT ON HIGHWAY ENCROACHMENTS**

Some of the possible immediate and delayed responses of rivers and river systems to the construction of bridges, approaches, culverts, channel stabilization, longitudinal encroachments, and the utilization of training works have been mentioned. It is necessary also to consider the effects on highway encroachments of river development works. These works may include, for example, water diversions to and from the river system, construction of reservoirs, flood control works, cutoffs, levees, navigation works, and the mining of sand and gravel. It is essential to consider the probable long-term plans of all agencies and groups as they pertain to a river when designing crossings or when dealing with the river in any way. Let us consider a few typical responses of a crossing to different types of water resources development.

Cutoffs may develop naturally in the river system or they may be the result of human activity. The general consequence of cutoffs is to shorten the flow path and steepen the gradient of the channel. The local steepening can significantly increase the velocities and sediment transport. Also, this action can induce significant instability such as bank erosion and degradation in the reach. The material scoured in the reach affected by the cutoff is probably carried only to an adjacent downstream reach where the gradient is flatter. In this region of slower velocities, the sediment drops out rapidly. Deposition can have significant detrimental effect on the downstream reach of river, increasing the flood stage in the river itself and increasing the base level for the tributary stream, thereby causing aggradation in the tributaries.

Consider a classic example of a cutoff that was constructed on a large bend in one of the tributaries to the Mississippi. Along this bend, small towns had developed and small tributary streams entered the main channel within the bendway. It was decided to develop a cutoff

across the meander to shorten the flow line of the river, reduce the flood stage and generally improve poor hydraulic conditions in that location. Several interesting results developed.

In the vicinity of the cutoff, the bankline eroded and degradation was initiated. Within the bendway, the small tributaries continued to discharge their water and sediment. Because of the flat gradient in the bend, this channel section could not convey the sediment from these small stream systems and aggradation was initiated. Within a short period of time, sufficient aggradation had occurred so as to jeopardize water intakes and sewage outfalls. As a consequence of the adverse action in the vicinity of the cutoff and within the bendway itself, it was finally decided that it would be more beneficial to restore the river to its natural form through the bend. This action was taken and the serious problems were alleviated.

In such a haphazard program of river development, the highway engineer would be hard pressed to maintain and plan for the highway system along and over this reach of river.

Another common case occurs with the development of reservoirs for storage and flood control. These reservoirs serve as traps for the sediment normally flowing through the river system. With sediment trapped in the reservoir, essentially clear water is released downstream of the dam site. This clear water has the capacity to transport more sediment than is immediately available. Consequently the channel begins to supply this deficit with resulting degradation of the bed or banks. This degradation may significantly affect the safety of bridges in the immediate vicinity. Again, the degraded or widened main channel causes steeper gradients on tributary streams in the vicinity of the main channel. The result is degradation in the tributary streams. It is entirely possible, however that the additional sediments supplied by the tributary streams would ultimately offset the degradation in the main channel. Thus, it must be recognized that downstream of storage structures the channel may either aggrade or degrade and the tributaries will be affected in either case.

Significant responses can be induced upstream of reservoirs as well as downstream. When the stream flowing into a reservoir encounters the ponded water, its sediment load is deposited forming a delta. This deposition in the reservoir flattens the gradient of the channel upstream. The flattening of the upstream channel induces aggradation causing the bed of the river to rise, threatening highway installations and other facilities. For example, Elephant Butte Reservoir, built on the Rio Grande in New Mexico, has caused the Rio Grande to aggrade many miles upstream of the reservoir site. This change in bed level can have very significant effects upon bridges, other hydraulic structures and all types of training and stabilization works. Ultimately the river may be subjected to a flow of magnitude sufficient to overflow existing banks, causing the water to seek an entirely new channel. With the abandonment of the existing channel there would be a variety of bridges and hydraulic structures that would also be abandoned at great expense to the public.

The clear-water diversion into South Boulder Creek in Colorado is another example of river development that affects bridge crossings and encroachments as well as the environment in general. Originally the North Fork of South Boulder Creek was a small but beautiful scenic mountain stream. The banks were nicely vegetated; there was a beautiful sequence of riffles and pools, which had all the attributes of a good fishing habitat. Years ago, water was diverted from the Western Slope of the Rockies through a tunnel to the North Fork of South Boulder Creek. The normal stage in that channel was increased by a factor of 4 to 5. The extra water caused significant bank erosion and channel degradation. In fact, the additional flow gutted the river valley, changing the channel to a straight raging torrent capable of carrying large

quantities of sediment. Degradation in the system had reached as much as 5 to 6 m (15 to 20 ft) before measures were taken to stabilize the creek.

Stabilization was achieved by flattening the gradient by constructing numerous drop structures and by reforming the banks with riprap. The system has stabilized but it is a different system. The channel is straight, much of the vegetation has been washed away, and the natural sequence of riffles and pools has been destroyed. The valley may never again have the natural form and beauty it once possessed. We should bear in mind that diversions to or from the natural river system can greatly alter its geometry, beauty and utility. The river may undergo a complete change, giving rise to a multitude of problems in connection with the design and maintenance of hydraulic structures, encroachments and bridge crossings along the affected reach.

In the preceding paragraphs, possible immediate and long-term responses of river systems to various types of river development have been described, but no guidance has been given on how to determine the magnitude of these changes. This important aspect of the response of rivers to development is treated in detail in later chapters.

## **1.5 TECHNICAL ASPECTS**

Effects of river development, flood control measures and channel structures built during the last century have proven the need for considering delayed and far-reaching effects of any alteration humans make in a natural alluvial river system.

Because of the complexity of the processes occurring with natural channel flows and the accompanying erosion and deposition of material, an analytical approach to the problem can be very difficult and time consuming. Most of our river process relations have been derived empirically. Nevertheless, if a greater understanding of the principles governing the processes of river formation is to be gained, the empirically derived relations must be put in the proper context by employing an analytical approach.

Attempts at controlling large rivers have often led to the situation described by J. Hoover Mackin (1937) when he wrote:

"The engineer who alters natural equilibrium relations by diversion or damming or channel improvement measures will often find that he has the bull by the tail and is unable to let go. . . . as he continues to correct or suppress undesirable phases of the chain reaction of the stream to the initial 'stress' he will necessarily place increasing emphasis on study of the genetic aspects of the equilibrium in order that he may work with rivers, rather than merely on them."

Through such experiences, one realizes that, to prevent or reduce the detrimental effects of any modification of the natural processes and state of equilibrium on a river, one must gain an understanding of the physical laws governing them and become knowledgeable of the far-reaching effects of any attempt to control or modify a river's course.

### **1.5.1 Variables Affecting River Behavior**

Variables affecting alluvial river channels are numerous and interrelated. Their nature is such that, unlike rigid boundary hydraulic problems, it is extremely difficult to study the role of any individual variable.

Major factors affecting alluvial stream channel forms are: (1) stream discharge, viscosity, temperature; (2) sediment discharge; (3) longitudinal slope; (4) bank and bed resistance to flow; (5) vegetation; (6) geology, including types of sediments; and (7) human activity.

The fluvial processes involved are very complicated and the variables of importance are difficult to isolate. Many laboratory and field studies have been carried out in an attempt to relate these and other variables. The problem has been more amenable to an empirical solution than an analytical one.

In an analysis of flow in alluvial rivers, the flow field is complicated by the constantly changing discharge. Significant variables are, therefore, quite difficult to relate mathematically. One approach is to list measurable or computable variables which effectively describe the processes occurring and then to reduce the list by making simplifying assumptions and examining relative magnitudes of variables. When this is done, the basic equations of fluid motion may be simplified (on the basis of valid assumptions) to describe the physical processes within an acceptable balance between accuracy and limitations of obtaining data.

It is the role of the succeeding chapters to present these variables, define them, show how they interrelate, quantify their interrelations where feasible, and show how they can be applied to achieve the successful design of river crossings and encroachments.

### **1.5.2 Basic Knowledge Required**

In order for engineers to cope successfully with river engineering problems, it is necessary to have an adequate background in engineering with an emphasis on hydrology, hydraulics, erosion and sedimentation, river mechanics, soil mechanics, structures, economics, the environment and related subjects. In all aspects of bridge inspection, maintenance, design and construction an interdisciplinary approach is needed. In fact, as the public demands more comprehensive treatment of river development problems, the highway engineer must further improve his or her knowledge, and the application of it, by soliciting the cooperative efforts of the hydraulic engineer, hydrologist, geologist, geomorphologist, meteorologist, mathematician, statistician, computer programmer, systems engineer, soil physicist, soil chemist, biologist, water management staff and economist. In addition, professional organizations representing these disciplines should be encouraged to work cooperatively to achieve long-range research needs and goals relative to river development.

### **1.5.3 Data Requirements**

Large amounts of data pertaining to understanding the behavior of rivers have been acquired over a long period of time. Nevertheless, some data collection efforts have been sporadic and unfocused. Agencies should take a careful look at present data requirements needed to solve



practical problems along with existing data. A careful analysis of data requirements would make it possible to more efficiently utilize funds to collect data in the future. The basic type of information that is required includes: water discharge hydrograph, sediment discharge hydrograph, the characteristics of the sediments being transported by streams, the characteristics of the channels in which the water and sediment are transported, and the characteristics of watersheds and how they deliver water and sediment to the stream systems.

Environmental data is also needed so that proper assessment can be made of the impact of river development upon the environment and vice versa. The problem of data requirements at river crossings is of sufficient importance that it is treated in greater detail in Chapter 8.

## **1.6 FUTURE TECHNICAL TRENDS**

When considering the future, it is essential to recognize the present state of knowledge pertaining to river hydraulics and then identify inadequacies in existing theories and our understanding of the physical processes involved, and encourage further research to help correct these deficits of knowledge. In order to correct such deficits there is a need to take a careful look at existing data pertaining to rivers, future data requirements, research needs, training programs and methods of developing staff that can apply this knowledge to the solution of practical problems.

Advances have been made in developing computational software to establish hydraulic variables for scour computations, including 1- and 2-dimensional, steady and unsteady models. Most, if not all, of the commonly used scour prediction equations have been incorporated into these models. However, applications methodologies are required to facilitate the use of more appropriate hydraulic variables that can be obtained from more sophisticated computer models. World wide web sites providing hydraulic models applicable to scour computations include:

- [www.fhwa.dot.gov/bridge/hydsoft.htm](http://www.fhwa.dot.gov/bridge/hydsoft.htm)
- [www.hec.usace.army.mil/software/index.html](http://www.hec.usace.army.mil/software/index.html)

### **1.6.1 Adequacy of Current Knowledge**

The basic principles of fluid mechanics involving application of continuity, momentum and energy concepts are well known and can be effectively applied to a wide variety of river problems. Considerable work has been done on the hydraulics of rigid boundary open channels and excellent results can be expected if the principles are applied properly. The steady-state sediment transport of nearly uniform sizes of sediment in alluvial channels is well understood. There is good understanding of stable channel theory in non-cohesive materials of all sizes. The theory is adequate to enable us to design stable systems in the existing bed and bank material or, if necessary, designs can be made for appropriate types of stabilization treatments so that canals and rivers behave in a stable manner. There have been extensive studies of the fall velocity of non-cohesive sediments in static fluids to provide knowledge about the interaction between the particle and fluid so essential to the development of sediment transport theories.

The use of computers and the development of computer programs have greatly helped the hydraulic engineer to solve problems on highway crossings and encroachments. The level of effort required to apply these models to bridge and hydraulic structure design has been greatly reduced with the availability of graphical user's interfaces. These interfaces are used for model development, troubleshooting, output presentation, and review. The one-dimensional WSPRO (FHWA) or HEC-RAS (Corps of Engineers) computer programs are extremely useful to determine the water surface elevation and the velocity of the flow in a river at a highway crossing. Both the Corps' and HEC-RAS (Version 3x) and UNET models are particularly useful in unsteady flow problems. FHWA's BRI-STARS program can be used to determine flow of water and sediment through a bridge crossing. FHWA's FESWMS and the Corps of Engineers RMA-2V 2-dimensional models provide water surface elevation and local velocities in two dimensions for unsteady flows for complex problems such as tidal flows. The Corps of Engineers HEC 1 and related HEC HMS programs are of particular importance in routing water from an upstream gaging station downstream to a bridge, taking into account any increase or decrease in flow that might occur in between the station and the bridge.

Thus, available concepts and theories, which can be applied to the behavior of rivers, are extensive. However, in many instances only empirical relationships have been developed and these are pertinent to specific problems only. Consequently, a more basic theoretical understanding of flow in the river systems needs to be developed.

With respect to many aspects of river mechanics, it can be concluded that knowledge is available to cope with the majority of river problems. On the other hand, the number of individuals who are cognizant of existing theory and can apply it successfully to the solution of river problems is limited. Particularly, the number of individuals involved in the actual solution of applied river mechanics problems is very small. There is a specific reason for this deficit of trained personnel. Undergraduate engineering educators in the universities in the United States, and in the world for that matter, devote only a small amount of time to teaching hydrology, river mechanics, channel stabilization, fluvial geomorphology, and related problems.

It is not possible to obtain adequate training in these important topics except at the graduate level, and only a limited number of universities and institutions offer the required training in these subject areas. There is great need for adequately trained and experienced practitioners to cope with river problems.

### **1.6.2 Research Needs**

As knowledge of river hydraulics is reviewed, it becomes quite obvious that many things are not adequately known. Some research needs are particularly urgent and promise a rather quick return. Stabilization of rivers and bank stability of river systems needs further consideration. Also, the study of bed forms generated by the interaction between the water and sediment in the river systems deserves further study. The types of bed forms have been identified, but theories pertaining to their development are inadequate. Simple terms have been used to describe the characteristics of alluvial material of both cohesive and non-cohesive types; a comprehensive look at the characteristics of materials is warranted.

Other important research problems include the fluid mechanics of the motion of particles, secondary currents, two-dimensional velocity distributions, fall velocity of particles in turbulent flow and the application of remote sensing and geographic information system techniques to

hydrology and river mechanics. The physical modeling of rivers followed by prototype verification, mathematical modeling of river response followed by field verification, mathematical modeling of water and sediment yield from small watersheds, and studies of unsteady sediment transport are areas in which significant advances can be made.

A primary research need is the collection of field data on the flow variables and depth of scour at bridges, embankments and at river control structures. Studies are needed to better define the planform of rivers and their response to changing flow conditions. In addition, laboratory and field studies are needed to improve the equations for estimating total scour at piers and abutments.

Operational research on decision making, considering cost and risk criteria to determine the hydrologic and hydraulic design of highway structures and project alternatives, is another pressing research area. Insufficient data is frequently a problem of river mechanics analysis. A comprehensive study on information theory is needed to cope with such difficulties.

Finally the results of these efforts must be presented in such a form that it can be easily taught and easily put to practical use.

### **1.6.3 Training**

As pointed out in Section 1.6.1, engineering training is often inadequate in relation to understanding the dynamics of rivers. Better ways to train engineers and to disseminate existing knowledge in this important area need to be considered. The curriculum of university education made available to engineers should be improved, particularly at the undergraduate level. At the very minimum, such a curriculum should strive to introduce concepts of fluvial geomorphology, river hydraulics, erosion and sedimentation, environmental considerations and related topics.

Formal training should be supported with field trips and laboratory demonstrations. Laboratory demonstrations are an inexpensive method of quickly and effectively teaching the fundamentals of river mechanics and illustrating the behavior of structures. These demonstrations should be followed by field trips to illustrate similarities and differences between phenomena in the laboratory and in the field.

## **1.7 OVERVIEW OF MANUAL CONTENTS**

In the following sections a brief overview of each chapter will be given.

### **1.7.1 Chapter 2 - Open Channel Flow**

This chapter describes the fundamentals of rigid boundary open channel flow. In open channel flow, the water surface is not confined; surface configuration, flow pattern and pressure distribution within the flow depend on gravity. In rigid boundary open channel flow, no deformation of the bed and banks is considered. Mobile boundary hydraulics refers to flow, which can generate deformation of the boundary through scour and fill. Mobile

boundary hydraulics will be discussed in Chapters 3, 4, and 5. Chapter 2 is restricted to a 1-dimensional analysis of rigid boundary open channel flow, where velocity and acceleration are large only in one direction and are so small as to be negligible in all other directions.

The three basic equations of flow: continuity, energy, and momentum are derived and used. The characteristics of uniform or nonuniform, steady or unsteady, laminar or turbulent, and tranquil or rapid (subcritical or supercritical) open channel flow are described, equations derived and problems for highways in the river environment are solved. Example problems are solved at the end of the chapter in both SI and English units of measurement.

### **1.7.2 Chapter 3 - Fundamentals of Alluvial Channel Flow**

Most streams that a highway will cross or encroach upon are alluvial. That is, the rivers are formed in cohesive or non-cohesive materials that have been, and can still be, transported by the stream. The non-cohesive material generally consists of silt, sand, gravel, or cobbles, or any combination of these sizes. Silt generally is not present in appreciable quantities in streams having non-cohesive boundaries. Cohesive material consists of clays (sizes less than 0.004 mm) forming a binder with silts and sand

Chapter 3 presents the fundamentals of alluvial channel flow. It covers properties of alluvial material, methods of measuring these properties; describes flow in sandbed channels and associated bed forms; presents methods for prediction of bed forms, and Manning's  $n$  for sandbed and other natural streams; describes how bed-form changes affect highways in the river environment; presents equations, tables and figures for determining the beginning of motion of non-cohesive sediments; and describes the methods used for the physical measurement and calculation of sediment discharge. These fundamentals of alluvial channel flow are used in later chapters to develop design considerations for highway crossings and encroachments in river environments. Example problems are solved at the end of the chapter in both SI and English units of measurement.

### **1.7.3 Chapter 4 - Sediment Transport**

The quantity and quality of the sediments that a stream can transport is an important consideration for highways in the river environment. Scour at a bridge or culvert is a sediment transport process. Streambed erosion and movement is the result of sediment transport. The amount of sediment transported or deposited in a stream under a given set of conditions is the result of the interaction of two groups of variables. In the first group are those variables that determine the quantity and quality of the sediment brought down to that section of the stream (bed and bank material). In the second group are the variables that determine the capacity of the stream to transport that sediment.

Chapter 4 presents the terms that describe sediment transport, discusses the methods and fluid forces that move sediment, derives and explains the basic equations, and presents equations and computer models that other practitioners have developed. Example problems to determine the quantity and quality of sediment transport are solved at the end of the chapter in SI and English units of measurement.

#### **1.7.4 Chapter 5 - River Morphology and River Response**

Rivers have different alignments and geometry. There are meandering rivers, braided rivers, and rivers that are essentially straight. In general, braided rivers are relatively steep and meandering rivers have more gentle slopes. Meandering rivers that are not subject to rapid movement, are reasonably predictable in behavior; however, meandering rivers are generally unstable with eroding banks which may result in destruction of productive land, bridges, bridge approaches, control works, buildings, and urban properties during floods. Bank protection works are often necessary to stabilize reaches of many rivers and to improve them for other aspects of flood control and navigation.

Chapter 5 presents the fluvial geomorphology of rivers and methods to predict river response to external forces such as a bridge crossing or other natural or human induced changes. Terms such as fluvial cycles, meandering, alluvial fans, geomorphic thresholds, nick points, and head cuts are described. A simple river classification scheme is presented. A variety of methods to predict a river's response to change are given. Additional information on stream stability at highway structures can be found in HEC-20 (Lagasse et al. 2001). Example problems to determine river classification and response are given at the end of Chapter 5.

#### **1.7.5 Chapter 6 - River Stabilization and Bank Protection**

Numerous types of river control and bank stabilization devices have evolved through past experience. Concrete, brick, willow and asphalt mattresses, sacked concrete and sand, riprap grouted slope protection, sheet piles, timber piles, steel jack and brush jetties, angled and sloped rock-filled, earth-filled, and timber dikes, automobile bodies, and concrete tetrahedrons have all been used in the practice of training rivers and stabilizing river banks.

The study of river morphology and river response in Chapter 5 makes it clear that both short- and long-term changes can be expected on river systems as a result of natural and human influences. Recommended structures and design methods for river control are presented in Chapter 6. The integrated and interactive effects of these structures with the river are discussed in Chapter 9. Detailed guidelines for selection and design of stream instability and bridge scour countermeasures are presented in HEC-23 (Lagasse et al. 2001). Example problems related to riprap are solved at the end of Chapter 6 in SI and English units of measurement. However, HEC-23 has detailed design guidelines for river stabilization and protection countermeasures.

#### **1.7.6 Chapter 7 - Scour at Bridges**

Scour at highway structures is the result of the erosive action of flowing water removing bed material from around the abutments and piers which support the bridge and bed and bank material of the stream the structure crosses. Both scour at highway structures and stream migration (instability) can cause a bridge failure.

All material in a streambed will erode with time. However, some material such as granite may take hundred's of years to erode, while sandbed streams may erode to the maximum depth of scour in hours. Sandstone, shales, and other sedimentary bedrock materials can erode to the

extent that a bridge will be in danger unless the substructures are founded deep enough. Cohesive bed and bank material such as clays, silty clays, silts and silty sands or even coarser bed material such as glacial tills, which are cemented by chemical action or compression, will erode. The erosion of cohesive and other cemented material is slower than sand bed material, but their ultimate scour will be as deep if not deeper than the scour depth in a non-cohesive sandbed stream. It might take the erosive action of several major floods, but the effects of scour can be cumulative in both cohesive and non-cohesive materials.

Scour at bridge crossings is a sediment transport process. Long-term degradation, general scour, and local scour at piers and abutments result when more sediment is removed from these areas than is transported into them. If there is no transport of bed material into the bridge crossing, clear-water scour exists. Transport of appreciable bed material into the crossing results in live-bed scour. In this latter case the transport of the bed material limits the scour depth. Whereas, with clear-water scour the scour depths are limited by the critical velocity or critical shear stress of a dominant size in the bed material at the crossing. Chapter 7 presents the basic definitions of scour at bridges, and develops the basic equations for determining the scour components. However, a more detailed analysis of scour at highway bridges and detailed example problems in SI and English systems of measurement are presented in HEC-18 (Richardson and Davis 2001).

#### **1.7.7 Chapter 8 – Data Need and Data Sources**

The purpose of Chapter 8 is to identify data needed for calculations and analyses for highway crossings and encroachments of rivers. The types and amounts of data needed for planning and designing river crossings and lateral encroachments depend upon the class of the proposed highway. In addition to identifying data needed, Chapter 8 identifies sources of data.

#### **1.7.8 Chapter 9 - Design Considerations for Highway Encroachment and River Crossings**

Chapter 9 presents applications of the fundamentals of hydraulics, hydrology, fluvial geomorphology, sediment transport, and river mechanics to the hydraulic and environmental design of river crossings and highway encroachments. The principal factors to be considered in design are presented, followed by a discussion of the procedures recommended for the evaluation, analysis and design of river crossings and encroachments. The design of most complex problems in river engineering can be facilitated by a qualitative evaluation combined with a quantitative analyses. In most cases, the systematic approach of a qualitative assessment of channel response, followed by a quantitative estimate, is necessary for a meaningful analysis of complex river response problems.

Chapter 9 contains a series of conceptual examples (cases) of river environments and their response to crossings and encroachments based upon geomorphic principles given in Chapter 5. These cases indicate the trend of change in river morphology for given initial conditions. The hypothetical cases are followed by practical examples (actual case histories) for river crossings in the United States. These histories document river response to highway crossings and encroachments and illustrate river response qualitatively.

### 1.7.9 Chapter 10 - Overview Examples of Design for Highways in the River Environment

The objective of Chapter 10 is to present overview examples of the use of the principles presented in this manual in the design of highway encroachments and crossings in the river environment. A three-level design procedure is emphasized in these designs. The designs use the geomorphic, hydrologic, hydraulic, and river mechanics principles described in this manual to design safe and economical crossings that protect, maintain and restore the river environment.

Three examples are given to illustrate the application of the principles, methods, and concepts given in this manual. In the examples, the designs are determined by well-established numerical procedures; however, they also depend heavily on the judgment of the engineer.

### 1.7.10 Chapter 11 - References

Chapter 11 contains an alphabetical listing of the references cited throughout the document.

### 1.7.11 Appendices

The appendices present a discussion of the metric (SI) system (Appendix A), analysis of additional sediment transport relationships (Appendix B), and an Index (Appendix C).

## 1.8 DUAL SYSTEM OF UNITS

This manual uses dual units (SI metric and English). In Appendix A, the metric (SI) unit of measurement is explained. The conversion factors, physical properties of water in SI system of units, sediment particle size grade scale, and some common equivalent hydraulic units are also given. This edition uses for the unit of length the meter (m) or foot (ft); of mass the kilogram (kg) or slug; of weight/force the newton (N) or pound (lb); of pressure the Pascal (Pa, N/m<sup>2</sup>) or (lb/ft<sup>2</sup>); and of temperature the degree centigrade (°C) or Fahrenheit (°F). The unit of time is the same in SI as in English system (seconds, s). Sediment particle size is given in millimeters (mm), but in calculations the decimal equivalent of millimeters in meters is used (1 mm = 0.001 m) or for the English system feet (ft). The value of some hydraulic engineering terms used in the text in SI units and their equivalent English units are given in Table 1.1.

Term	SI Units	English Units
Length	1 m	3.28 ft
Volume	1 m <sup>3</sup>	35.31 ft <sup>3</sup>
Discharge	1 m <sup>3</sup> /s	35.31 ft <sup>3</sup> /s
Acceleration of Gravity	9.81 m/s <sup>2</sup>	32.2 ft/s <sup>2</sup>
Unit Weight of Water	9800 N/m <sup>3</sup>	62.4 lb/ft <sup>3</sup>
Density of Water	1000 kg/m <sup>3</sup>	1.94 slugs/ft <sup>3</sup>
Density of Quartz	2647 kg/m <sup>3</sup>	5.14 slugs/ft <sup>3</sup>
Specific Gravity of Quartz	2.65	2.65
Specific Gravity of Water	1	1
Temperature	°C = 5/9 (°F - 32)	°F

(page intentionally left blank)



## CHAPTER 2

### OPEN CHANNEL FLOW

#### 2.1 INTRODUCTION

In this chapter, the fundamentals of rigid boundary open channel flow are described. In open channel flow, the water surface is not confined; surface configuration, flow pattern and pressure distribution within the flow depend on gravity. In rigid boundary open channel flow, no deformation of the bed and banks is considered. Mobile boundary hydraulics refers to flow which can generate deformation of the boundary through scour and fill. Mobile boundary hydraulics will be discussed in later chapters. In this chapter, the discussion is restricted to a one-dimensional analysis of rigid boundary open channel flow where velocity and acceleration are large only in one direction and are so small as to be negligible in all other directions.

Open channel flow can be classified as: (1) uniform or nonuniform flow; (2) steady or unsteady flow; (3) laminar or turbulent flow; and (4) tranquil or rapid flow. In uniform flow, the depth and discharge remain constant with respect to space. Also, the velocity at a given depth does not change. In steady flow, no change occurs with respect to time at a given point. In laminar flow, the flow field can be characterized by layers of fluid, one layer not mixing with adjacent ones. Turbulent flow on the other hand is characterized by random fluid motion. Tranquil flow is distinguished from rapid flow by a dimensionless number called the Froude number,  $Fr$ . If  $Fr < 1$ , the flow is subcritical; if  $Fr > 1$ , the flow is supercritical, and if  $Fr = 1$ , the flow is called critical.

Open channel flow can be nonuniform, unsteady, turbulent and rapid at the same time. Because the classifying characteristics are independent, sixteen different types of flow can occur. These terms, uniform or nonuniform, steady or unsteady, laminar or turbulent, rapid or tranquil, and the two dimensionless numbers (the Froude number and Reynolds number) are more fully explained in the following sections.

##### 2.1.1 Definitions

Velocity: The velocity of a fluid particle is the time rate of displacement of the particle from one point to another. Velocity is a vector quantity. That is, it has magnitude and direction. The mathematical representation of the fluid velocity is a function of the increment of length  $ds$  during the infinitesimal time  $dt$ ; thus,

$$v = \frac{ds}{dt} \quad (2.1)$$

Streamline: An imaginary line within the flow which is everywhere tangent to the velocity vector is called a streamline.

Acceleration: Acceleration is the time rate of change in magnitude or direction of the velocity vector. Mathematically, acceleration  $a$  is expressed by the total derivative of the velocity vector or

$$a = \frac{dv}{dt} \quad (2.2)$$

The vector acceleration,  $a$ , has components both tangential and normal to the streamline, the tangential component embodying the change in magnitude of the velocity, and the normal component reflecting the change in direction

$$a_s = \frac{dv_s}{dt} = \frac{\partial v_s}{\partial t} + \frac{1}{2} \frac{\partial(v_s^2)}{\partial s} \quad (2.3)$$

$$a_n = \frac{dv_n}{dt} = \frac{\partial v_n}{\partial t} + \frac{v^2}{r} \quad (2.4)$$

The first terms in Equations 2.3 and 2.4 represent the change in velocity, both magnitude and direction, with time at a given point. This is called the local acceleration. The second term in each equation is the change in velocity, both magnitude and direction, with distance. This is called convective acceleration.

Uniform flow: In uniform flow the convective acceleration terms are zero.

$$\frac{\partial v_s^2}{\partial s} = 0 \text{ and } \frac{v^2}{r} = 0 \quad (2.5)$$

Nonuniform flow: In nonuniform flow, the convective acceleration terms are not equal to zero.

$$\frac{\partial v_s}{\partial s} \neq 0 \text{ and } \frac{v^2}{r} \neq 0 \quad (2.6)$$

Flow around a bend ( $v^2 / r \neq 0$ ) and flow in expansions or contractions ( $\frac{\partial v}{\partial s} \neq 0$ ) are examples of nonuniform flow.

Steady flow: In steady flow, the velocity at a point does not change with time

$$\frac{\partial v_s}{\partial t} = 0 \text{ and } \frac{\partial v_n}{\partial t} = 0 \quad (2.7)$$

Unsteady flow: In unsteady flow, the velocity at a point varies with time

$$\frac{\partial v_s}{\partial t} \neq 0 \text{ and } \frac{\partial v_n}{\partial t} \neq 0 \quad (2.8)$$

Examples of unsteady flow are channel flows with waves, flood hydrographs, and surges.

Laminar flow: In laminar flow, the mixing of the fluid and momentum transfer is by molecular activity.

Turbulent flow: In turbulent flow the mixing of the fluid and momentum transfer is related to random velocity fluctuations. The flow is laminar or turbulent depending on the value of the Reynolds number ( $Re = \rho VL/\mu$ ), which is a dimensionless ratio of the inertial forces to the viscous forces. Here  $\rho$  and  $\mu$  are the density and dynamic viscosity of the fluid,  $V$  is the fluid velocity, and

$L$  is a characteristic dimension, usually the depth (or the hydraulic radius) in open channel flow. In laminar flow, viscous forces are dominant and  $Re$  is relatively small. In turbulent flow,  $Re$  is large; that is, inertial forces are very much greater than viscous forces. Turbulent flows are predominant in nature. Laminar flow occurs very infrequently in open channel flow.

Tranquil flow: In open channel flow, the free surface configuration, in response to changes in channel geometry depends on the Froude number ( $Fr = V / \sqrt{gL}$ ), which is the ratio of inertial forces to gravitational forces. The Froude number is also the ratio of the flow velocity  $V$  to the celerity ( $c = \sqrt{gL}$ ) of a small gravity wave in the flow (this concept is detailed in Section 2.5). When  $Fr < 1$ , the flow is subcritical (or tranquil), and surface waves propagate upstream as well as downstream. The boundary condition that controls the tranquil flow depth is always located at the downstream end of the subcritical reach.

Rapid flow: When  $Fr > 1$ , the flow is supercritical (or rapid) and surface disturbances can propagate only in the downstream direction. The control section of rapid flow depth is always at the upstream end of the rapid flow region. When  $Fr = 1.0$ , the flow is critical and surface disturbances remain stationary in the flow.

## 2.2 THREE BASIC EQUATIONS

The basic equations of flow in open channels are derived from the three conservation laws. These are: (1) the conservation of mass; (2) the conservation of linear momentum; and (3) the conservation of energy. The conservation of mass is another way of stating that (except for mass-energy interchange) matter can neither be created nor destroyed. The principle of conservation of linear momentum is based on Newton's second law of motion which states that a mass (of fluid) accelerates in the direction of and in proportion to the applied forces on the mass.

In the analysis of flow problems, much simplification can result if there is no acceleration of the flow or if the acceleration is primarily in one direction, the accelerations in other directions being negligible. However, a very inaccurate analysis may occur if one assumes accelerations are small or zero when in fact they are not. The concepts explained in this chapter assume one-dimensional flow and the derivations of the equations utilize a control volume. A control volume is an isolated volume in the body of the fluid, through which mass, momentum, and energy can be convected. The control volume may be assumed fixed in space or moving with the fluid.

### 2.2.1 Conservation of Mass

Consider a short reach of river shown in Figure 2.1 as a control volume. The boundaries of the control volume are the upstream cross-section, designated section 1, the downstream cross-section, designated section 2, the free surface of the water between sections 1 and 2, and the interface between the water and the wetted perimeter (banks and bed).

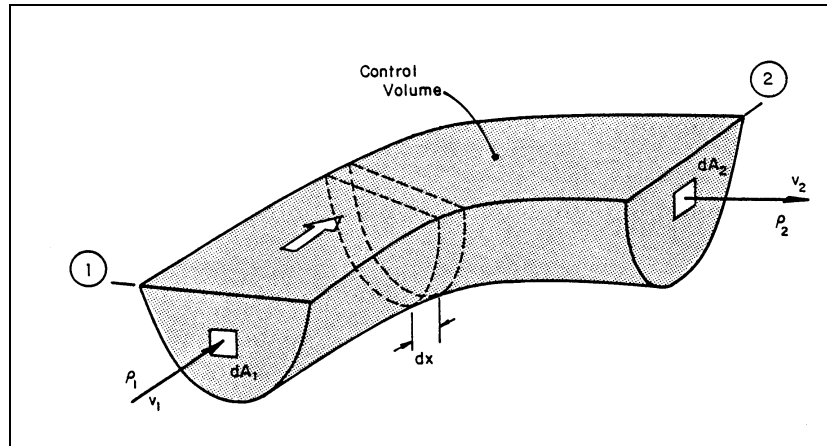


Figure 2.1. A river reach as a control volume.

The statement of the conservation of mass for this control volume is

$$\left| \begin{array}{l} \text{Mass flux} \\ \text{out of the} \\ \text{control volume} \end{array} \right| - \left| \begin{array}{l} \text{Mass flux} \\ \text{into the} \\ \text{control volume} \end{array} \right| + \left| \begin{array}{l} \text{Time rate of change} \\ \text{in mass in the} \\ \text{control volume} \end{array} \right| = 0$$

Mass can enter or leave the control volume through any or all of the control volume surfaces. Rainfall would contribute mass through the surface of the control volume and seepage passes through the interface between the water and the banks and bed. In the absence of rainfall, evaporation, seepage and other lateral mass fluxes, mass enters the control volume at section 1 and leaves at section 2.

At section 2, the mass flux out of the control volume through the differential area  $dA_2$  is  $\rho_2 v_2 dA_2$ . The values of  $\rho_2$  and  $v_2$  can vary from position to position across the width and throughout the depth of flow at section 2. The total mass flux out of the control volume at section 2 is the integral of all  $\rho_2 v_2 dA_2$  through the differential areas that make up the cross-section area  $A_2$ , and may be written as:

$$\begin{array}{l} \text{Mass flux} \\ \text{out of the} \\ \text{control volume} \end{array} = \int_{A_2} \rho_2 v_2 dA_2 \quad (2.9)$$

Similarly

$$\begin{array}{l} \text{Mass flux} \\ \text{into the} \\ \text{control volume} \end{array} = \int_{A_1} \rho_1 v_1 dA_1 \quad (2.10)$$

The amount of mass inside a differential volume  $dV$  inside the control volume is  $\rho dV$  and

Mass inside  
the control volume =  $\int_{\forall} \rho d\forall$  (2.11)

The statement of conservation of mass for the control volume calls for the time rate of change in mass. In mathematical notation,

Time rate of change  
in mass in the control volume =  $\frac{\partial}{\partial t} \int_{\forall} \rho d\forall$  (2.12)

For the reach of river, the statement of the conservation of mass becomes

$$\int_{A_2} \rho_2 v_2 dA_2 - \int_{A_1} \rho_1 v_1 dA_1 + \frac{\partial}{\partial t} \int_{\forall} \rho d\forall = 0 \quad (2.13)$$

It is often convenient to work with average conditions at a cross-section, so we define an average velocity  $V$  such that

$$V = \frac{1}{A} \int_A v dA \quad (2.14)$$

The symbol  $v$  represents the local velocity whereas the velocity  $V$  is the average velocity at the cross-section.

Because water is nearly incompressible the density  $\rho$  of the fluid is considered constant,  $\rho_1 = \rho_2 = \rho$ . When the flow is steady

$$\frac{\partial}{\partial t} \int_{\forall} \rho d\forall = 0 \quad (2.15)$$

and Equation 2.13 reduces to the statement that inflow equals outflow or

$$\rho V_2 A_2 - \rho V_1 A_1 = 0$$

That is, for steady flow of incompressible fluids

$$V_1 A_1 = V_2 A_2 = Q = VA \quad (2.16)$$

where  $Q$  is the volume flow rate or the discharge.

Equation 2.16 is the familiar form of the conservation of mass equation for steady flow in rivers. It is applicable when the fluid density is constant, the flow is steady and there is no significant lateral inflow or seepage.

## 2.2.2 Conservation of Linear Momentum

The curved reach of the river shown in Figure 2.1 is rather complex to analyze in terms of Newton's Second Law because of the curvature in the flow. Therefore, as a starting point, the differential length of reach  $dx$  is isolated as a control volume.

For this control volume, shown in Figure 2.2, the pressure terms  $p_1$  and  $p_2$  are directed toward the control volume in a direction normal to the Sections 1 and 2. The shear stress  $\tau_o$  is exerted along the interface between the water and the wetted perimeter and is acting in a direction opposite to the axis  $x$ . The statement of conservation of linear momentum is:

Flux of Momentum out of the control volume	-	Flux of momentum into the control volume	+	Time rate of change of momentum in the control volume	=	Sum of the forces acting on the fluid in the control volume
--	---	--	---	---	---	---

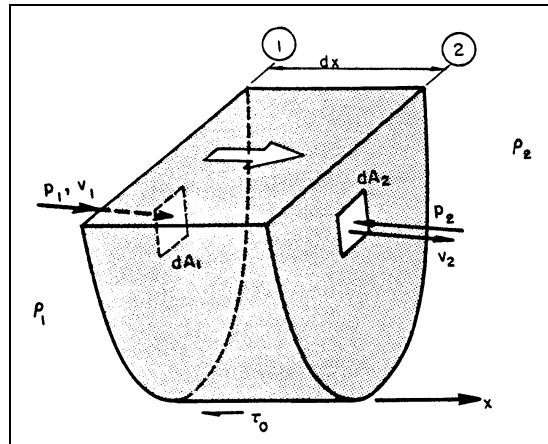


Figure 2.2. The control volume for conservation of linear momentum.

The terms in the statement are vectors so we must be concerned with direction as well as magnitude.

Consider the conservation of momentum in the direction of flow (the  $x$ -direction in Figure 2.2). At the outflow section (section 2), the flux of momentum out of the control volume through the differential area  $dA_2$  is:

$$\rho_2 v_2 dA_2 v_2 \quad (2.17)$$

Here  $\rho_2 v_2 dA_2$  is the mass flux (mass per unit of time) and  $\rho_2 v_2 dA_2 v_2$  is the momentum flux through the area  $dA_2$ .

Flux of momentum  
out of the control  
volume

$$= \int_{A_2} \rho_2 v_2 dA_2 v_2 \quad (2.18)$$

Similarly, at the inflow section (section 1),

Flux of momentum  
into the  
control volume

$$= \int_{A_1} \rho_1 v_1 dA_1 v_1 \quad (2.19)$$

The amount of momentum in the control volume is  $\int_V \rho v dV$  so

Time rate of  
change of momentum =

$$\frac{\partial}{\partial t} \left\{ \int_V \rho v dV \right\} \quad (2.20)$$

in the control volume

At the upstream section, the force acting on the differential area  $dA_1$  of the control volume is  $p_1 dA_1$  where  $p_1$  is the pressure from the upstream fluid on the differential area. The total force in the x-direction at section 1 is  $\int_{A_1} p_1 dA_1$ . Similarly, at section 2, the total force is  $\int_{A_2} p_2 dA_2$ .

There is a fluid shear stress  $\tau_0$  acting along the interface between the water and the bed and banks. The shear on the control volume is in a direction opposite to the direction of flow and results in a force  $-\tau_0 P dx$  where  $\tau_0$  is the average shear stress on the interface area,  $P$  is the average wetted perimeter and  $dx$  is the length of the control volume. The term  $P dx$  is the interface area.

The body force component acting in the x-direction is denoted  $F_b$  and will be discussed in a subsequent section. The statement of conservation of momentum in the x-direction for the control volume is:

$$\int_{A_2} p_2 v_2^2 dA_2 - \int_{A_1} p_1 v_1^2 dA_1 + \frac{\partial}{\partial t} \int_V \rho v dV = \int_{A_1} p_1 dA_1 - \int_{A_2} p_2 dA_2 - \int_L \tau_0 P dx + F_b \quad (2.21)$$

Again, as with the conservation of mass equation, it is convenient to use average velocities instead of point velocities. We define a momentum coefficient  $\beta$  so that when average velocities are used instead of point velocities, the correct momentum flux is considered. The momentum coefficient for incompressible fluids is:

$$\beta = \frac{1}{V^2 A} \int_A v^2 dA \quad (2.22)$$

For steady incompressible flow, Equation 2.21 is combined with Equation 2.22 to give

$$\rho \beta_2 V_2^2 A_2 - \rho \beta_1 V_1^2 A_1 = \int_{A_1} p_1 dA_1 - \int_{A_2} p_2 dA_2 - \int_L \tau_0 P dx + F_b \quad (2.23)$$

The pressure force and shear force terms on the right-hand side of Equation 2.23 are usually abbreviated as  $\Sigma F_x$  so:

$$\Sigma F_x = \int_{A_1} p_1 dA_1 - \int_{A_2} p_2 dA_2 - \int_L \tau_0 P dx + F_b \quad (2.24)$$

The conservation of momentum equation becomes:

$$\rho\beta_2 V_2^2 A_2 - \rho\beta_1 V_1^2 A_1 = \Sigma F_x \quad (2.25)$$

for steady flow with constant density. With Equation 2.16 the steady flow conservation of linear momentum equation takes on the familiar form

$$\rho Q(\beta_2 V_2 - \beta_1 V_1) = \Sigma F_x \quad (2.26)$$

### 2.2.3 Conservation of Energy

The First Law of Thermodynamics can be written:

$$\dot{Q} - \dot{W} = \frac{dE}{dt} \quad (2.27)$$

where:

- $\dot{Q}$  = Rate at which heat is added to a fluid system
- $\dot{W}$  = Rate at which a fluid system does work on its surroundings
- $E$  = Energy of the system

Then  $dE/dt$  is the rate of change of energy in the system.

The statement of conservation of energy for a control volume is then:

$$\left. \begin{array}{l} \text{Flux of energy} \\ \text{out of the} \\ \text{control volume} \end{array} \right| - \left. \begin{array}{l} \text{Flux of energy} \\ \text{into the control} \\ \text{volume} \end{array} \right| + \left. \begin{array}{l} \text{Time rate of change} \\ \text{of energy in the} \\ \text{control volume} \end{array} \right| = \dot{Q} - \dot{W}$$

The choice of a control volume is arbitrary. To illustrate the procedure, the control volume is reduced to the size of a streamtube connecting  $dA_1$  and  $dA_2$  as shown in Figure 2.3. The streamtube is bounded by streamlines through which no mass or momentum enters.

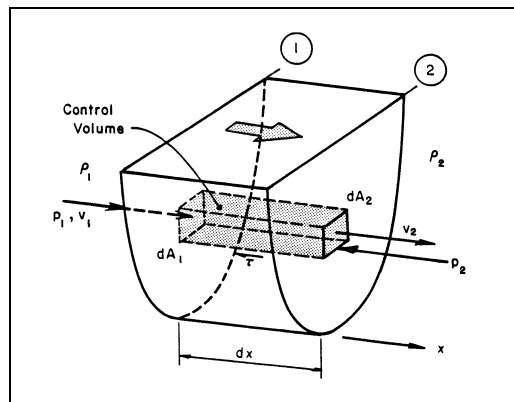


Figure 2.3. The streamtube as a control volume.



For steady flow of an incompressible fluid in the streamtube

$$\begin{array}{l} \text{Flux of energy} \\ \text{out of the} \\ \text{control volume} \end{array} = \rho_2 e_2 dA_2 v_2 \quad (2.28)$$

Similarly, at the inflow section (section 1),

$$\begin{array}{l} \text{Flux of energy} \\ \text{into the} \\ \text{control volume} \end{array} = \rho_1 e_1 dA_1 v_1 \quad (2.29)$$

and

$$\begin{array}{l} \text{Time rate of} \\ \text{change of energy} \\ \text{in the control volume} \end{array} = 0 \quad (2.30)$$

Here  $e$  is the energy per unit mass. Accordingly, the total energy  $E$  in a control volume is:

$$E = \int_{\forall} \rho e \, d\forall \quad (2.31)$$

Unless one is concerned with thermal pollution, evaporation losses, or problems concerning the formation of ice in rivers, the rate at which heat is added to the control volume can be neglected; that is:

$$\dot{Q} \approx 0 \quad (2.32)$$

The work done by the fluid in the control volume on its surroundings can be in the form of pressure work  $W_p$ , shear work  $W_\tau$ , or shaft work (mechanical work)  $W_s$ . For the streamtube shown in Figure 2.3, no shaft work is involved ( $W_s = 0$ ).

The rate at which the fluid pressure does work on the control volume surrounding through the boundary  $dA_1$  in Figure 2.3 is:

$$-p_1 dA_1 v_1$$

and on boundary  $dA_2$ , the rate of doing pressure work is

$$p_2 dA_2 v_2$$

At the other boundaries of the streamtube, there is no pressure work because there is no fluid motion normal to the boundary. Hence, for the streamtube

$$\dot{W}_p = p_2 dA_2 v_2 - p_1 dA_1 v_1 \quad (2.33)$$

Along the interior boundaries of the streamtube there is a shear stress resulting from the condition that the fluid velocity inside the streamtube may not be the same as the velocity of the fluid surrounding the streamtube. The rate at which the fluid in the streamtube does shear work on the control volume is:

$$\dot{W}_\tau = \tau P dx v \quad (2.34)$$

where  $\tau$  is the average shear stress on the streamtube boundary,  $P$  is the average perimeter of the streamtube,  $dx$  is the length of the streamtube and  $v$  is the fluid velocity at the streamtube boundary. The product  $P dx$  is the surface of the streamtube subjected to shear stresses.

Then for steady flow in the streamtube, the statement of the conservation of energy in the streamtube shown in Figure 2.3 is:

$$\rho_2 e_2 v_2 dA_2 - \rho_1 e_1 v_1 dA_1 = p_1 v_1 dA_1 - p_2 v_2 dA_2 - \tau P v dx \quad (2.35)$$

The conservation of mass for steady flow in the streamtube is (according to Equation 2.16)

$$v_2 dA_2 = v_1 dA_1 = dQ \quad (2.36)$$

Now Equation 2.35 reduces to

$$(\rho_1 e_1 + p_1) dQ - (\rho_2 e_2 + p_2) dQ = \tau P v dx \quad (2.37)$$

The energy per unit mass  $e$  is the sum of the internal, kinetic and potential energies or

$$e = u + \frac{v^2}{2} + gz \quad (2.38)$$

where:

- $u$  = Internal energy associated with the fluid temperature
- $v$  = Velocity of the mass fluid
- $g$  = Acceleration due to gravity
- $z$  = Elevation above some arbitrary reference level

This expression for  $e$  is substituted in Equation 2.37 to yield

$$u_1 + \frac{v_1^2}{2} + gz_1 \frac{\rho_1}{\rho} = u_2 + \frac{v_2^2}{2} + gz_2 + \frac{p_2}{\rho} + \frac{\tau P v dx}{\rho dQ} \quad (2.39)$$

By dividing through by  $g$  and defining the head loss  $h_\ell$  as follows:

$$h_\ell = \frac{u_2 - u_1}{g} + \frac{\tau P v dx}{\rho g dQ} \quad (2.40)$$

The energy equation for the streamtube becomes

$$\frac{v_1^2}{2g} + \frac{p_1}{\gamma} + z_1 = \frac{v_2^2}{2g} + \frac{p_2}{\gamma} + z_2 + h_\ell \quad (2.41)$$

If there is no shear stress on the streamtube boundary and if there is no change in internal energy ( $u_1 = u_2$ ), the energy equation reduces to:

$$\frac{v_1^2}{2g} + \frac{p_1}{\gamma} + z_1 = \frac{v_2^2}{2g} + \frac{p_2}{\gamma} + z_2 = \text{constant} \quad (2.42)$$

which is the Bernoulli Equation.

Generally, there is not sufficient information available to do a differential streamtube analysis of a reach of river, so appropriate changes must be made in the energy equation. A reach of river such as that shown in Figure 2.1 can be pictured as a bundle of streamtubes. We know the statement of the conservation of energy for a streamtube. It is Equation 2.41 which can be written:

$$\left( \frac{v_1^2}{2g} + \frac{p_1}{\gamma} + z_1 \right) v dA = \left( \frac{v_2^2}{2g} + \frac{p_2}{\gamma} + z_2 \right) v dA + h_\ell v dA \quad (2.43)$$

because  $v_1 dA_1 = v_2 dA_2 = v dA$  for the streamtube.

The common form of the energy equation used in open channel flow is derived by integrating Equation 2.43 over the cross-section area:

$$\int_A \left( \frac{v^2}{2g} + \frac{p}{\gamma} + z \right) v dA = \left\{ \frac{\alpha V^2}{2g} + \frac{\bar{p}}{\gamma} + \bar{z} \right\} Q \quad (2.44)$$

where:

$\alpha$  = Kinetic energy correction factor defined by the expression

$$\alpha = \frac{1}{V^3 A} \int_A v^3 dA \quad (2.45)$$

to allow the use of average velocity  $V$  rather than point velocity  $v$ . The average pressure over the cross-section is  $\bar{p}$ , defined as:

$$\bar{p} = \frac{1}{VA} \int_A p v dA \quad (2.46)$$

The term  $\bar{z}$  is the average elevation of the cross-section defined by the expression:

$$\bar{z} = \frac{1}{VA} \int_A zvdA \quad (2.47)$$

and Q is the volume flow rate or the discharge. By definition

$$Q = \int_A v dA \quad (2.48)$$

Also

$$H_L = \frac{1}{VA} \int_A h_\ell v da \quad (2.49)$$

In summary, the expression for conservation of energy for steady flow in a reach of river is written

$$\frac{\alpha_1 V_1^2}{2g} + \frac{\bar{p}_1}{\gamma} + \bar{z}_1 = \frac{\alpha_2 V_2^2}{2g} + \frac{\bar{p}_2}{\gamma} + \bar{z}_2 + H_L \quad (2.50)$$

The tendency in river work is to neglect the energy correction factor even though its value may be as large as 1.5. Usually it is assumed that the pressure is hydrostatic and the average elevation head  $\bar{z}$  is at the centroid of the cross-sectional area. However, it should be kept in mind that Equations 2.45, 2.46, and 2.47 are the correct definitions of the terms in the energy equation. An example problem illustrating the calculation of  $\alpha$  and  $\beta$  for a stream is provided in Section 2.14 (SI) and 2.15 (English).

### 2.3 HYDROSTATICS

When the only forces acting on the fluid are pressure and fluid weight, the differential equation of motion in an arbitrary direction x is

$$\frac{\partial}{\partial x} \left( \frac{p}{\gamma} + z \right) = \frac{a_x}{g} \quad (2.51)$$

In steady uniform flow (and for zero flow), the acceleration is zero and we obtain the equation of hydrostatics

$$\frac{p}{\gamma} + z = \text{Constant} \quad (2.52)$$

However, when there is acceleration, the piezometric head varies in the flow field. That is, the piezometric head is not constant in the flow. This is illustrated in Figure 2.4. In Figure 2.4a the pressure at the bed is hydrostatic and equal to  $\gamma y_0$  whereas in the curvilinear flow (Figure 2.4b) the pressure is larger than  $\gamma y_0$  because of the acceleration resulting from a change in direction.

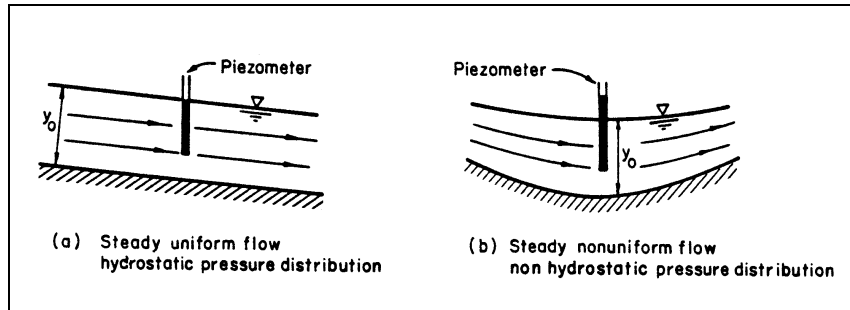


Figure 2.4. Pressure distribution in steady uniform and in steady nonuniform flow.

In general, when fluid acceleration is small (as in gradually varied flow) the pressure distribution is considered hydrostatic. However, for rapidly varying flow where the streamlines are converging, expanding or have substantial curvature (curvilinear flow), fluid accelerations are not small and the pressure distribution is not hydrostatic.

In Equation 2.52, the constant is equal to zero for gage pressure at the free surface of a liquid. For flow with hydrostatic pressure throughout (steady, uniform flow or gradually varied flow), it follows that the pressure head  $p/\gamma$  is equal to the vertical distance below the free surface. In sloping channels with steady uniform flow, the pressure head  $p/\gamma$  at a depth  $y$  below the surface is equal to

$$\frac{p}{\gamma} = y \cos \theta \quad (2.53)$$

Note that  $y$  is the depth (perpendicular to the water surface) to the point, as shown in Figure 2.5. For most channels,  $\theta$  is small and  $\cos \theta \simeq 1$ .

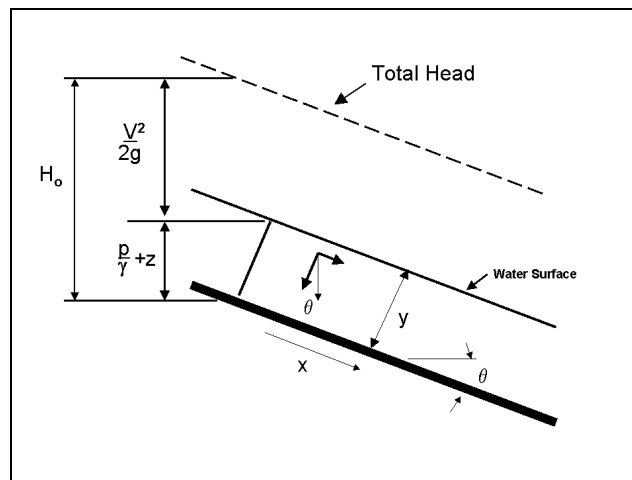


Figure 2.5. Pressure distribution in steady uniform flow on steep slopes (after Chow 1959).

## 2.4 STEADY UNIFORM FLOW

### 2.4.1 Introduction

In steady, uniform open channel flow there are no accelerations, streamlines are straight and parallel, and the pressure distribution is hydrostatic. The slope of the water surface  $S_w$  and the bed surface  $S_o$  and the energy gradient  $S_f$  are equal. Consider the unit width of channel shown in Figure 2.6 as a control volume. According to Equation 2.50, the conservation of energy for this control volume is:

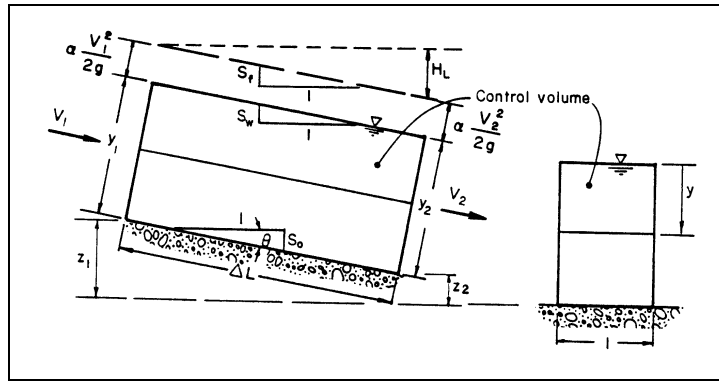


Figure 2.6. Steady uniform flow in a unit width channel.

$$\frac{\alpha_1 V_1^2}{2g} + \frac{\bar{p}_1}{\gamma} + \bar{z}_1 = \frac{\alpha_2 V_2^2}{2g} + \frac{\bar{p}_2}{\gamma} + \bar{z}_2 + H_L \quad (2.54)$$

The pressure at any point  $y$  below the surface is  $y \cos \theta$ . Then according to Equation 2.46

$$\bar{p}_1 = \frac{1}{V_1 y_1} \int_0^{y_1} \gamma y \cos \theta v_1 dy \quad (2.55)$$

Assuming only small variations in the point velocity  $v$  with  $y$  we have:

$$\bar{p}_1 \approx \frac{\gamma y_1 \cos \theta}{2} \quad (2.56)$$

Similarly,

$$\bar{p}_2 \approx \frac{\gamma y_2 \cos \theta}{2} \quad (2.57)$$

Also according to Equation 2.47

$$\bar{z}_1 \approx z_1 + \frac{y_1 \cos \theta}{2} \quad (2.58)$$

and

$$\bar{z}_2 \approx z_2 + \frac{y_2 \cos \theta}{2} \quad (2.59)$$

With the above expressions for  $\bar{p}_1$ ,  $\bar{p}_2$ ,  $\bar{z}_1$ , and  $\bar{z}_2$  the energy equation for this control volume reduces to

$$\frac{\alpha_1 V_1^2}{2g} + \frac{y_1 \cos \theta}{2} + z_1 + \frac{y_1 \cos \theta}{2} = \frac{\alpha_2 V_2^2}{2g} + \frac{y_2 \cos \theta}{2} + z_2 + \frac{y_2 \cos \theta}{2} + H_L \quad (2.60)$$

or

$$\frac{\alpha_1 V_1^2}{2g} + y_1 \cos \theta + z_1 = \frac{\alpha_2 V_2^2}{2g} + y_2 \cos \theta + z_2 + H_L \quad (2.61)$$

For most natural channels  $\theta$  is small and  $y \cos \theta \approx y$ . The velocity distribution in the vertical is normally a log function for which  $\alpha_1 \approx \alpha_2 \approx 1$ . Then the energy equation becomes:

$$\frac{V_1^2}{2g} + y_1 + z_1 = \frac{V_2^2}{2g} + y_2 + z_2 + H_L \quad (2.62)$$

and the slopes of the bed, water surface and energy grade line are respectively

$$S_o = \sin \theta = \frac{(z_1 - z_2)}{\Delta L} \quad (2.63)$$

$$S_w = \frac{(z_1 + y_1) - (z_2 + y_2)}{\Delta L} \quad (2.64)$$

and

$$S_f = \frac{H_L}{\Delta L} = \frac{\left( \frac{V_1^2}{2g} + y_1 + z_1 \right) - \left( \frac{V_2^2}{2g} + y_2 + z_2 \right)}{\Delta L} \quad (2.65)$$

Steady uniform flow is an idealized concept for open channel flow and is difficult to obtain even in laboratory flumes. For many applications, the flow is steady and the changes in width, depth or direction (resulting in nonuniform flow) are so small or occur over such a long distance that the flow can be considered uniform.

Variables of interest for steady uniform flow are: (1) the mean velocity  $V$ , (2) the discharge  $Q$ , (3) the velocity distribution  $v(y)$  in the vertical, (4) the head loss  $H_L$  through the reach, and (5) the shear stress, both local  $\tau$  and at the bed  $\tau_o$ . These variables are interrelated.

### 2.4.2 Shear Stress, Velocity Distribution, and Average Velocity

Shear stress  $\tau$  is the internal fluid stress which resists deformation. The shear stress exists only when fluids are in motion. It is a tangential stress in contrast to pressure, which is a normal stress.

The local shear stress at the interface between the boundary and the fluid can be determined quite easily if the boundary is hydraulically smooth; that is, if the roughness at the boundary is submerged in a viscous sublayer as shown in Figure 2.7.

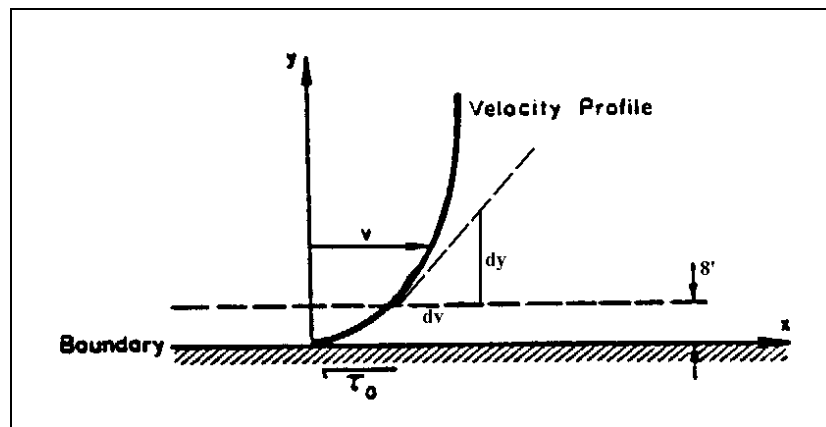


Figure 2.7. Hydraulically smooth boundary.

Here, the thickness of the laminar sublayer is denoted  $\delta'$ . In laminar flow, the shear stress at the boundary is:

$$\tau_o = \mu \left( \frac{dv}{dy} \right) \text{ at } y = 0 \quad (2.66)$$

The velocity gradient is evaluated at the boundary. The dynamic viscosity  $\mu$  is the proportionality constant relating boundary shear and velocity gradient in the viscous sublayer.

When the boundary is hydraulically rough, the thickness of the laminar sublayer is very small compared to the roughness height. The paths of fluid particles in the vicinity of the boundary are shown in Figure 2.8.

The velocity at a point near the boundary fluctuates randomly about a mean value. The random fluctuation in velocity characterizes turbulent flows. As shown in Figure 2.9a, the particle has a vertical component of velocity  $v_y$  as well as a horizontal component  $v_x$ .



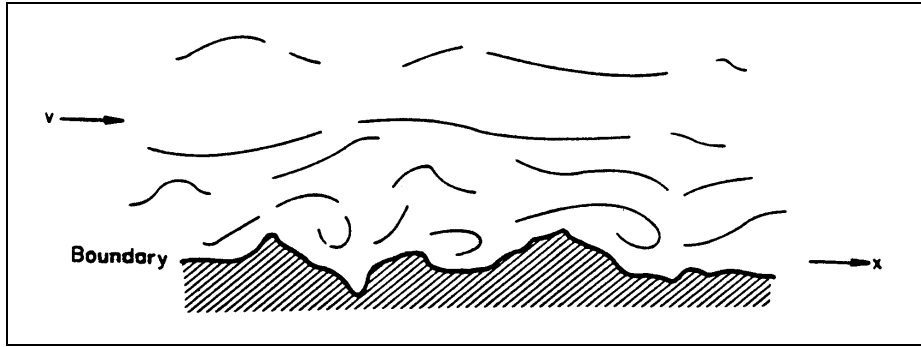


Figure 2.8. Hydraulically rough boundary.

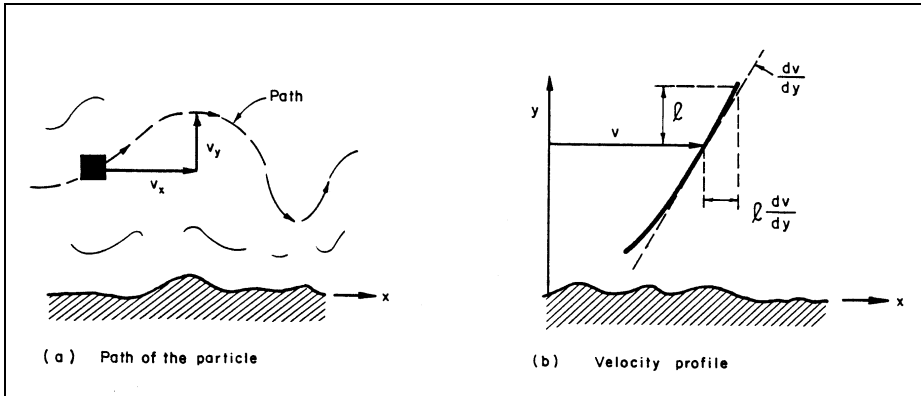


Figure 2.9. Velocities in turbulent flow.

The two components of velocity in Figure 2.9a can be written as:

$$v_x = \bar{v}_x + v'_x \quad (2.67)$$

and

$$v_y = \bar{v}_y + v'_y \quad (2.68)$$

where  $\bar{v}_x$  and  $\bar{v}_y$  are the time-averaged mean velocities in the x and y direction and  $v'_x$  and  $v'_y$  are the fluctuating components.

Through theoretical investigation it has been found that turbulence generates shear stress given by

$$\tau = -\rho \overline{v'_x v'_y} \quad (2.69)$$

The term  $\overline{v'_x v'_y}$  is the time-average of the product of  $v'_x$  and  $v'_y$  at a point in the flow. It is called the Reynolds shear stress.

Prandtl (1925) suggested that  $v'_x$  and  $v'_y$  are related to the velocity gradient  $dv/dy$  shown in Figure 2.9b. He proposed to characterize the turbulence with a dimension called the "mixing length"  $\ell$ , which is assumed to be the same in both the x and y directions. Accordingly,

$$v'_x \sim \ell \frac{dv}{dy} \quad (2.70)$$

$$v'_y \sim \ell \frac{dv}{dy} \quad (2.71)$$

and

$$\tau \sim \rho \ell^2 \left( \frac{dv}{dy} \right)^2 \quad (2.72)$$

If it is assumed that the mixing length can be represented by the product of a constant  $\kappa$  and  $y$  (i.e.,  $\ell = \kappa y$ ), then for steady uniform turbulent flow,

$$\tau = \rho \kappa^2 y^2 \left( \frac{dv}{dy} \right)^2 \quad (2.73)$$

Using different reasoning von Karman (1930) derived the same equation. Equation 2.73 can be rearranged to the form:

$$\frac{dv}{dy} = \frac{\sqrt{\tau_o / \rho}}{\kappa y} \quad (2.74)$$

where  $\kappa$  is the von Karman universal velocity coefficient. For rigid boundaries  $\kappa$  has the average value of 0.4. The term  $\tau_o$  is the bed shear stress. The term  $(\tau_o/\rho)^{1/2}$  has the dimensions of velocity and is called the shear velocity,  $V^*$ . Integration of Equation 2.74 yields

$$\frac{v}{\sqrt{\frac{\tau_o}{\rho}}} = \frac{1}{\kappa} \ln \frac{y}{y'} = \frac{2.31}{\kappa} \log \frac{y}{y'} \quad (2.75)$$

Here  $\ln$  is the logarithm to the base e and  $\log$  is the logarithm to the base 10. The term  $y'$  results from evaluation of the constant of integration assuming  $v = 0$  at some distance  $y'$  above the bed.

The term  $y'$  depends on the flow and has been experimentally determined. The many experiments have resulted in characterizing turbulent flow into three general types:

- (1) Hydraulically smooth boundary turbulent flow where the velocity distribution, mean velocity and resistance to flow are independent of the boundary roughness of the bed but depend on fluid kinematic viscosity. Then with

$$\delta' = \frac{11.6\nu}{\sqrt{\frac{\tau_o}{\rho}}} \text{ we find } y' = \frac{\delta'}{107} \quad (2.76)$$

- (2) Hydraulically rough boundary turbulent flow where velocity distribution, mean velocity and resistance to flow are independent of viscosity and depend entirely on the boundary roughness. For this case,  $y' = k_s/30.2$  where  $k_s$  is the height of the roughness element.

- (3) Transition where the velocity distribution, mean velocity and resistance to flow depend on both fluid viscosity and boundary roughness. Then

$$\frac{\delta'}{107} < y' < \frac{k_s}{30.2} \quad (2.77)$$

The boundary roughness effects can be merged into one equation by using  $y' = k_s/(30.2X)$  where  $X$  is determined from Figure 2.10. As a result, the velocity distribution  $v$ , mean velocity  $V$ , and resistance to flow equations can be written in the following dimensionless form which is related to the above flow types by Figure 2.10.

$$\frac{v}{V_*} = 5.75 \log \left( 30.2 \frac{Xy}{k_s} \right) = 2.5 \ln \left( 30.2 \frac{Xy}{k_s} \right) \quad (2.78)$$

and

$$\frac{V}{V_*} = \frac{C}{\sqrt{g}} = 5.75 \log 12.27 \frac{Xy_o}{k_s} = 2.5 \ln 12.27 \frac{Xy_o}{k_s} \quad (2.79)$$

Note that any system of units can be used as long as  $y_o$  and  $k_s$  (and  $V$ ,  $v$  and  $V_*$ ) have the same dimensions. The symbols of Equations 2.78 and 2.79 denote:

- $X$  = Coefficient given in Figure 2.10
- $k_s$  = Height of the roughness elements, for sand channels
- $v$  = Local mean velocity at depth  $y$
- $y_o$  = Depth of flow
- $V$  = Depth-averaged velocity
- $V_*$  = Shear velocity  $\sqrt{\tau_o / \rho}$  which for steady uniform flow is  $\sqrt{gRS_f}$
- $\tau_o$  = Shear stress at the boundary and for steady uniform flow the average is  
 $\tau_o = \gamma RS_f \quad (2.80)$
- $R$  = Hydraulic radius, equal to the cross-sectional area  $A$  divided by the wetted perimeter  $P$

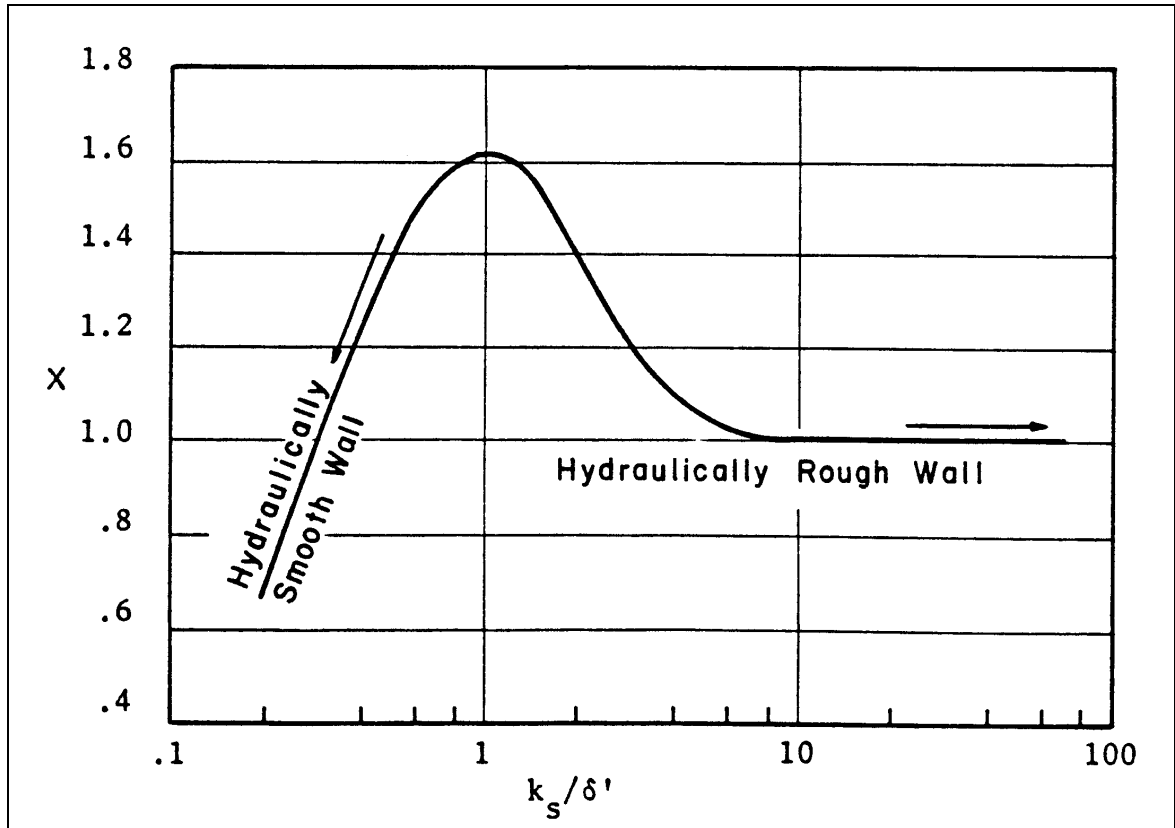


Figure 2.10. Einstein's multiplication factor  $X$  in the logarithmic velocity equations (Einstein 1950).

- $S_f$  = Slope of the energy gradeline
- $\delta'$  = Thickness of the viscous sublayer
- $\nu$  = Kinematic viscosity of fluid

$$\delta' = 11.6\nu / V.$$

$C/\sqrt{g}$  = Chezy discharge coefficient in the equation

$$V = C\sqrt{RS} \text{ or } C = \left(\frac{8g}{f}\right)^{1/2} \quad (2.81)$$

$f$  = Darcy-Weisbach resistance coefficient which is given by the expression

$$f = 8 \frac{\tau_o}{\rho V^2} \quad (2.82)$$

Any consistent set of dimensions can be used (m or ft).

### 2.4.3 Other Velocity Equations

Because of the difficulties involved in determining the shear stress and hence the velocity distribution in turbulent flows, other approaches to determine mean velocities in rivers has been prevalent. Two such equations are in common use. They are Manning's equation:

$$V = \frac{K_u}{n} R^{2/3} S_f^{1/2} \quad (2.83)$$

and Chezy's equation

$$V = CR^{1/2} S_f^{1/2} \quad (2.84)$$

where:

- V = Average velocity in the waterway cross-section in m/s, ft/s
- n = Manning's roughness coefficient
- R = Hydraulic radius in m or ft equal to the cross-sectional area A divided by the wetted perimeter P of the waterway m, ft
- S<sub>f</sub> = Friction slope m/m, ft/ft
- C = Chezy's discharge coefficient known as Chezy's C
- K<sub>u</sub> = 1.0 (SI)
- K<sub>u</sub> = 1.486 (English)

In these equations, the boundary shear stress is expressed implicitly in the roughness coefficient "n" or in the discharge coefficient C. By equating the velocity determined from Manning's equation with the velocity determined from Chezy's equation, the relation between the coefficients is

$$C = \frac{K_u}{n} R^{1/6} \quad (2.85)$$

If the flow is gradually varied, Manning's and Chezy's equations are used with the average friction slope S<sub>f,ave</sub>. The term S<sub>f,ave</sub> is determined by averaging over a short time increment at a station or over a short length increment 300 m (1,000 ft) for example at an instant of time, or both.

Over many decades, a catalog of values of Manning's n and Chezy's C has been assembled so that an engineer can estimate the appropriate value by knowing the general nature of the channel boundaries. An abbreviated list of Manning's roughness coefficients is given in Table 2.1. Additional values are given by Barnes (1967) and Chow (1959). Manning's n for sandbed and gravel-bed channels is discussed in detail in Chapter 3.

Table 2.1. Manning's Roughness Coefficients for Various Boundaries.	
	Manning's n
<b>Rigid Boundary Channels</b>	
Very smooth concrete and planed timber	0.011
Smooth concrete	0.012
Ordinary concrete lining	0.013
Wood	0.014
Vitrified clay	0.015
Shot concrete, untrowelled, and earth channels in best condition	0.017
Straight unlined earth canals in good condition	0.020
Mountain streams with rocky beds	0.040 - 0.050
<b>Minor Streams (top width at flood stage &lt; 30 m (100 ft))</b>	
Streams on Plain	
1. Clean, straight, full stage, no rifts or deep pools	0.025-0.033
2. Same as above, but more stones and weeds	0.030-0.040
3. Clean, winding, some pools and shoals	0.033-0.045
4. Same as above, but some weeds and stones	0.035-0.050
5. Same as above, lower stages, more ineffective slopes and sections	0.040-0.055
6. Same as 4, but more stones	0.045-0.060
7. Sluggish reaches, weedy, deep pools	0.050-0.080
8. Very weedy reaches, deep pools, or floodways with heavy stand of timber and underbush	0.075-0.150
Mountain Streams, no vegetation in channel, banks usually steep, trees and brush along banks submerged at high stages	
1. Bottom: gravels, cobbles, and few boulders	0.030-0.050
2. Bottom: cobbles with large boulders	0.040-0.070
<b>Floodplains</b>	
Pasture, No Brush	
1. Short Grass	0.025-0.035
2. High Grass	0.030-0.050
Cultivated Areas	
1. No Crop	0.020-0.040
2. Mature Row Crops	0.025-0.045
3. Mature Field Crops	0.030-0.050

Table 2.1. Manning's Roughness Coefficients for Various Boundaries.

	Manning's n
<b>Floodplains (continued)</b>	
Brush	
1. Scattered brush, heavy weeds	0.035-0.070
2. Light brush and trees in winter	0.035-0.060
3. Light brush and trees in summer	0.040-0.080
4. Medium to dense brush in winter	0.045-0.110
5. Medium to dense brush in summer	0.070-0.160
Trees	
1. Dense willows, summer, straight	0.110-0.200
2. Cleared land with tree stumps, no sprouts	0.030-0.050
3. Same as above, but with heavy growth of sprouts	0.050-0.080
4. Heavy stand of timber, a few down trees, little undergrowth, flood stage below branches	0.080-0.120
5. Same as above, but with flood stage reaching branches	0.100-0.160
<b>Major Streams (Top width at flood stage &gt; 30 m (100 ft))</b> The n value is less than that for minor streams of similar description, because banks offer less effective resistance.	
Regular section with no boulders or brush	0.025-0.060
Irregular and rough section	0.035-0.100
<b>Alluvial Sandbed Channels (no vegetation)<sup>1</sup></b>	
Tranquil flow, Fr < 1	
1. Plane bed	0.014 - 0.020
2. Ripples	0.018 - 0.030
3. Dunes	0.020 - 0.040
4. Washed out dunes or transition	0.014 - 0.025
5. Plane bed	0.010 - 0.013
Rapid Flow, Fr > 1	
1. Standing waves	0.010 - 0.015
2. Antidunes	0.012 - 0.020
<sup>1</sup> Data is limited to sand channels with D <sub>50</sub> < 1.0 mm, details to be discussed in Chapter 3.	

The general approach for estimating  $n$  values consists of the selection of a base roughness value for a straight, uniform, smooth channel in the materials involved, then additive values are considered for the channel under consideration:

$$n = (n_0 + n_1 + n_2 + n_3 + n_4) m_5 \quad (2.86)$$

where:

- $n_0$  = Base value for straight uniform channels
- $n_1$  = Additive value due to cross-section irregularity
- $n_2$  = Additive value due to variations of the channel
- $n_3$  = Additive value due to obstructions
- $n_4$  = Additive value due to vegetation
- $m_5$  = Multiplication factor due to sinuosity

Detailed values of the coefficients are found in Cowan (1956), Chow (1959), Benson and Dalrymple (1967) and Aldridge and Garrett (1973). Typical values are given in Table 2.2. Arcement and Schneider (1984) proposed a guide for selecting Manning's roughness coefficients for floodplains. For steeper streams, the reader is also referred to the work of Jarrett (1984, 1985).

The roughness characteristics on the floodplain are complicated by the presence of vegetation, natural and artificial irregularities, buildings, undefined direction of flow, varying slopes and other complexities. Resistance factors reflecting these effects must be selected largely on the basis of past experience with similar conditions. In general, resistance to flow is large on the floodplains. In some instances, conditions are further complicated by deposition of sediment and development of dunes and bars which affect resistance to flow and direction of flow.

The presence of ice affects channel roughness and resistance to flow in various ways. When an ice cover occurs, the open channel is more nearly comparable to a closed conduit. There is an added shear stress developed between the flowing water and the ice cover. This surface shear is much larger than the normal shear stresses developed at the air-water interface. The ice-water interface is not always smooth. In many instances, the underside of the ice is deformed so that it resembles ripples or dunes observed on the bed of sandbed channels. This may cause overall resistance to flow in the channel to be further increased.

With total or partial ice cover, the drag of ice retards flow, decreasing the average velocity and increasing the depth. Another serious effect is its influence on bank stability, in and near water structures such as docks, loading ramps, and ships. For example, the ice layer may freeze into bank stabilization materials, and when the ice breaks up, large quantities of rock and other material embedded in the ice may be floated downstream and subsequently thawed loose and dumped randomly leaving banks raw and unprotected.

#### **2.4.4 Average Boundary Shear Stress**

The average shear stress at the boundary  $\tau_0$  for steady uniform flow is determined by applying the conservation of mass and momentum principles to the control volume shown in Figure 2.11. The conservation of mass Equation 2.16 is then:



Table 2.2. Adjustment Factors for the Determination of n Values.				
		Conditions	n Value	Remarks
Cross-Section Irregularity	n <sub>1</sub>	Smooth	0	Smoothest Channel
		Minor	0.001-0.005	Slightly Eroded Side Slopes
		Moderate	0.006-0.010	Moderately Rough Bed and Banks
		Severe	0.011-0.020	Badly Sloughed & Scalloped Banks
Variations In Channel Section	n <sub>2</sub>	Gradual	0	Gradual Changes
		Alternating Occasionally	0.001-0.005	Occasional Shifts From Large to Small Sections
		Alternating Frequently	0.010-0.015	Frequent Changes in Cross-Sectional Shape
Obstructions	n <sub>3</sub>	Negligible	0-0004	Obstructions < 5% of Cross-Section Area
		Minor	0.005-0.015	Obstructions < 15% of Cross-Section Area
		Moderate	0.020-0.030	Obstructions 15-50% of Cross-Section Area
		Severe	0.040-0.060	Obstructions > 50% of Cross-Section Area
Vegetation	n <sub>4</sub>	Small	0.002-0.010	Flow Depth > 2 x Vegetation Height
		Medium	0.010-0.025	Flow Depth > Vegetation Height
		Large	0.025-0.050	Flow Depth < Vegetation Height
		Very Large	0.050-0.100	Flow Depth < 0.5 Vegetation Height
Sinuosity	m <sub>5</sub>	Minor	1.00	Sinuosity < 1.2
		Moderate	1.15	1.2 < Sinuosity < 1.5
		Severe	1.30	Sinuosity > 1.5

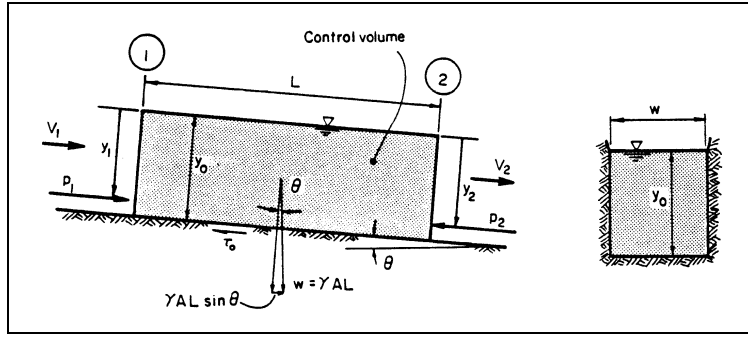


Figure 2.11. Control volume for steady uniform flow.

$$\rho y_0 W V_2 - \rho y_0 W V_1 = 0 \quad (2.87)$$

or

$$V_1 = V_2 \quad (2.88)$$

The conservation of momentum in the downstream direction is described from Equation 2.25 with  $A_1 = A_2 = Wy_0$  and  $V_1 = V_2$ . The pressure forces acting on the control boundary are approximated by:

$$F_1 = F_2 = \frac{\gamma y_0^2 W}{2} \quad (2.89)$$

The downstream component of the body force  $\gamma AL$  (equal to the weight of fluid in the control volume) in the X direction is:

$$F_b = \gamma AL \sin \theta \quad (2.90)$$

where  $\theta$  is the slope angle of the channel bed. The average boundary shear stress is  $\tau_0$  acting on the wetted perimeter  $P$ . The shear force  $F_s$  in the x-direction is:

$$F_s = \tau_0 PL \quad (2.91)$$

With the above expressions for the components, the statement of conservation of linear momentum becomes:

$$\rho \beta W y_0 V^2 - \rho \beta W y_0 V^2 = \gamma AL \sin \theta + \frac{\gamma y_0^2 W}{2} - \frac{\gamma y_0^2 W}{2} - \tau_0 PL \quad (2.92)$$

which reduces to

$$\tau_0 = \gamma \frac{A}{P} \sin \theta \quad (2.93)$$

The term  $A/P$  is the hydraulic radius  $R$ . If the channel slope angle is small,

$$\sin \theta \approx S_o \quad (2.94)$$

and for steady uniform flow the average shear stress on the boundary is

$$\tau_o = \gamma R S_o \quad (2.95)$$

If the flow is gradually varied nonuniform flow, the average boundary shear stress is

$$\tau_o = \gamma R S_f \quad (2.96)$$

where  $S_f$  is the slope of the energy grade line.

#### 2.4.5 Relation Between Shear Stress and Velocity

Measuring the average bottom shear stress directly in the field is tenuous. However, the average bottom shear stress can be computed from the expression

$$\tau_o = \gamma R S_f \quad (2.97)$$

For steady uniform flow, the local and average shear stress on the bed can be estimated by employing the velocity profile equations in Section 2.4.2. If the local velocity  $v_1$  at depth  $y_1$  is known and  $X = 1$  for hydraulically rough boundary then, from Equation 2.78 the local shear stress can be determined. The equation is:

$$\tau_o = \frac{\rho v_1^2}{\left[ 5.75 \log \left( 30.2 \frac{y_1}{k_s} \right) \right]^2} \quad (2.98)$$

This equation and the ones given below are valid for fully turbulent uniform flow over a hydraulically rough boundary in wide channels with a plane bed. Alternatively, if two point velocities in a vertical profile are known (preferably in the lower 15 percent of the depth) the local shear stress on the bed can be determined from the following equation:

$$\tau_o = \frac{\rho (v_1 - v_2)^2}{\left[ 5.75 \log \left( \frac{y_1}{y_2} \right) \right]^2} \quad (2.99)$$

If the depth of flow  $y_o$ , the grain roughness  $k_s$  and the average velocity in the vertical  $V$  are known, then the average shear stress can be determined from Equation 2.79. The equation is:

$$\tau_o = \frac{\rho V^2}{\left[ 5.75 \log \left( 12.27 \frac{y_o}{k_s} \right) \right]^2} \quad (2.100)$$

#### 2.4.6 Energy and Momentum Coefficients for Rivers

In prismatic or constructed channels it is common to assume that the energy coefficient  $\alpha$  and the momentum coefficient  $\beta$  are unity. In river channels, this is usually not the case. From Equations 2.45 and 2.22:

$$\alpha = \frac{1}{V^3 A} \int_A v^3 dA \quad (2.45)$$

and

$$\beta = \frac{1}{V^2 A} \int_A v^2 dA \quad (2.22)$$

The velocity distribution in wide channels for turbulent flow over a rough boundary is given by Equation 2.78 with  $X = 1.0$

$$\frac{v}{V_*} = 2.5 \ln(30.2 y / k_s) \quad (2.101)$$

The average velocity in the vertical is

$$V = \frac{1}{y_o} \int_0^{y_o} v dy \approx \frac{2.5V_*}{y_o - y'} \int_{y'}^{y_o} \ln(y/y') dy \quad (2.102)$$

Here, the upper limit of integration is  $y_o$ , the depth of flow and the lower limit is

$$y' = \frac{k_s}{30.2} \quad (2.103)$$

the value of  $y$  for which Equation 2.78 gives a zero velocity. The integration of Equation 2.102 yields

$$\frac{V}{V_*} = 2.5 \left\{ \frac{y_o}{y_o - y'} \left( \ln \left( \frac{y_o}{y'} \right) - 1 \right) \right\} \quad (2.104)$$

For a vertical section of unit width, the momentum coefficient  $\beta'$  is

$$\beta' = \frac{1}{V^2(y_o - y')} \int_{y'}^{y_o} v^2 dy \quad (2.105)$$

If we substitute Equations 2.78 and 2.104 into Equation 2.107 and integrate, the result is the expression

$$\beta' = \frac{1}{\left(\ln 11.11 \frac{y_o}{k_s}\right)^2} \left(\frac{y_o}{y_o - y'}\right) \left\{ \left(\ln \frac{y_o}{y'}\right)^2 - 2 \ln \left(\frac{y_o}{y'}\right) + 2 - \frac{2y'}{y_o} \right\} \quad (2.106)$$

Similarly, the energy coefficient for a vertical section unit width is

$$\alpha' = \frac{1}{V^3(y_o - y')} \int_{y'}^{y_o} v^3 dy \quad (2.107)$$

or

$$\alpha' = \frac{1}{\left(\ln 11.11 \frac{y_o}{k_s}\right)^2} \left(\frac{y_o}{y_o - y'}\right) \left\{ \left(\ln \frac{y_o}{y'}\right)^3 - 3 \left(\ln \frac{y_o}{y'}\right)^2 + 6 \ln \left(\frac{y_o}{y'}\right) - 6 + \frac{6y'}{y_o} \right\} \quad (2.108)$$

These equations (Equations 2.106 and 2.108 are rather complex, so a graph of  $\alpha'$  and  $\beta'$  vs  $y_o/k_s$  has been prepared. The relations are shown in Figure 2.12.

For the entire river cross-section (shown in Figure 2.13) Equation 2.45 can be written

$$\alpha = \frac{1}{\left(\frac{Q}{A}\right)^3 A} \left[ \int_0^W \int_0^{y_o} v^3 dy dw \right] \quad (2.109)$$

where  $W$  is the top width of the section,  $w$  is the lateral location of any vertical section,  $y_o$  is the depth of flow at location  $w$ , and  $v$  is the local velocity at the position  $y, w$ . The total discharge is  $Q$  and the total cross-sectional area is  $A$ .

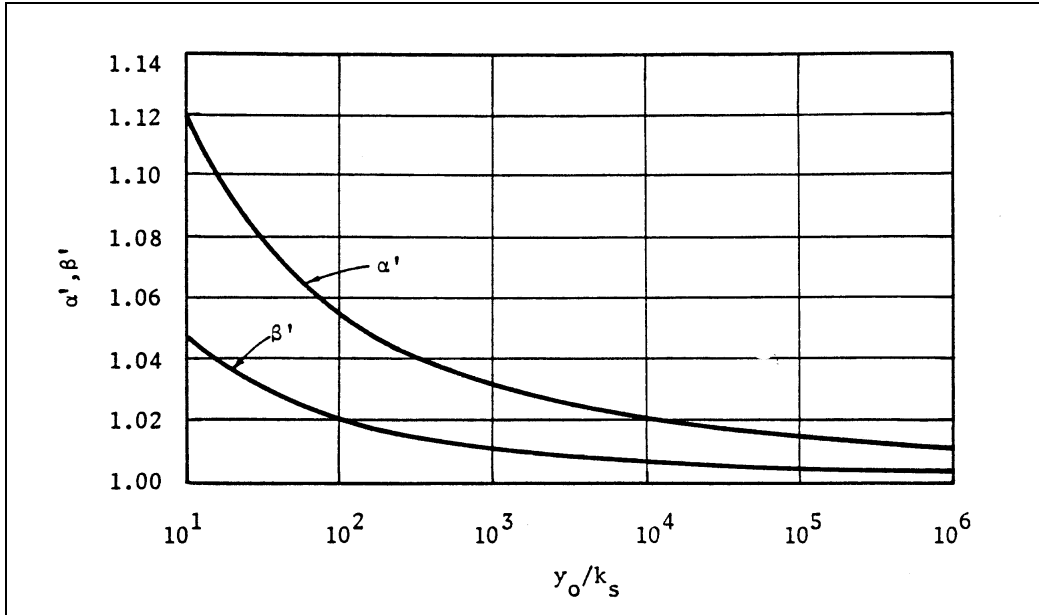


Figure 2.12. Energy and momentum coefficients for a unit width of river.

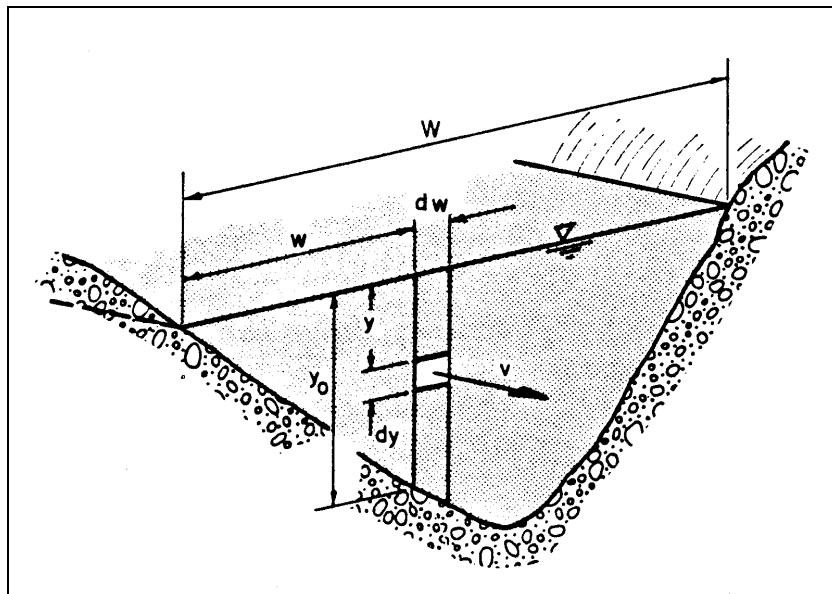


Figure 2.13. The river cross section.

The second integral term in brackets in Equation 2.109 can be written

$$\int_{y'}^{y_o} v^3 dy = \alpha' V^3 (y_o - y') \quad (2.110)$$

Here  $\alpha'$  is the energy coefficient for the vertical section  $dw$  wide and  $y_o$  deep,  $V$  is the depth-averaged velocity in this vertical section and  $y' = k_s/30.2$ .

Now, Equation 2.109 can be written

$$\alpha = \frac{A^2}{Q^3} \int_0^w \alpha' V^3 (y_o - y') dw \quad (2.111)$$

Except for cases of low flow in gravel bed rivers, the term  $y'$  is very small compared to  $y_o$  so

$$\alpha = \frac{A^2}{Q^3} \int_0^w \alpha' V^3 y_o dw \quad (2.112)$$

The discharge at a river cross-section is determined in the field by measuring the local depth and two local velocities at each of approximately 20 vertical sections. In accordance with this general stream gaging procedure, Equation 2.112 could be written as

$$\alpha = \frac{A^2}{Q^3} \sum_i \alpha'_i v_i^3 y_{oi} \Delta w_i$$

or

$$\alpha = \frac{A^2}{Q^3} \sum_i \alpha'_i v_i^2 \Delta Q_i \quad (2.113)$$

Here, the subscript  $i$  refers to the  $i$ -th vertical section, and  $\Delta Q_i$  is the river discharge associated with the  $i$ -th vertical or

$$\Delta Q_i = V_i y_{oi} \Delta w_i$$

In a similar manner, the expression for  $\beta$  is

$$\beta = \frac{A}{Q^2} \sum_i \beta'_i V_i \Delta Q_i \quad (2.114)$$

Now, with Equations 2.113 and 2.114, and Figure 2.12 we are in a position to compute  $\alpha$  and  $\beta$  for any river cross-section given the discharge measurement notes. A calculation example is presented in Section 2.14 (SI) and 2.15 (English). It is important to recognize that for river flows over floodplains, the correction factors  $\alpha$  and  $\beta$  can be significantly larger than  $\alpha'$  and  $\beta'$ .

## 2.5 UNSTEADY FLOW

Unsteady flows of interest to the designer of waterway crossings and encroachments are: (1) waves resulting from disturbances of the water surface by wind and boats; (2) waves resulting from the surface instability that exists for flows with Froude numbers close to 1.0; (3) waves resulting from flow disturbance due to change in direction of flow with Froude numbers greater than about 2.0; (4) surges or bores resulting from sudden increase or decrease in the flow by opening or closing of gates or the movement of tides on coastal streams; (5) standing waves and antidunes that occur in alluvial channel flow; and (6) flood waves resulting from the progressive movement downstream of stream runoff or gradual release from reservoirs.

Waves are an important consideration in bridge hydraulics when designing slope protection of embankments and dikes, and channel improvements. In the following paragraphs, only the basic one-dimensional analysis of waves and surges is presented. Other aspects of waves are presented in other sections.

### 2.5.1 Gravity Waves

The general equation for the celerity  $c$  (velocity of the wave relative to the velocity of flow) of a small amplitude gravity wave ( $a_o \ll \lambda$ ) is

$$c = \left\{ \frac{g\lambda}{2\pi} \tanh \frac{2\pi y_o}{\lambda} \right\}^{1/2} \quad (2.115)$$

where the terms are defined in Figure 2.14.

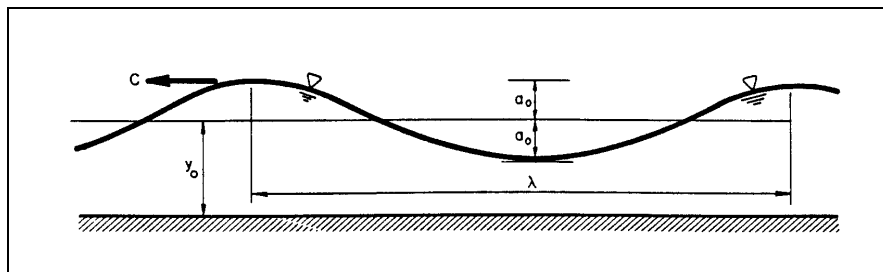


Figure 2.14. Definition sketch for small amplitude waves.

For deep water waves (short waves) defined as

$$\frac{y_o}{\lambda} > \frac{1}{2} \quad (2.116)$$



the celerity relationship (Equation 2.115) reduces to

$$c = \left\{ \frac{g\lambda}{2\pi} \right\}^{1/2} \quad (2.117)$$

For shallow water waves (long waves)

$$\frac{y_o}{\lambda} < \frac{1}{20} \quad (2.118)$$

Then Equation 2.115 reduces to

$$c = \sqrt{gy_o} \quad (2.119)$$

The time of travel of one water crest to another at a given point is called the period T and can be defined from the celerity and wave length

$$c = \lambda / T \quad (2.120)$$

In Equation 2.117, the celerity is independent of depth and depends on gravity g and wave length  $\lambda$ . This is the celerity of ocean waves. In Equation 2.119, the celerity is a function of gravity and depth which describes small amplitude waves in open channels. These two equations apply only to small amplitude waves; that is  $a_o/\lambda \ll 1$ .

The celerity of finite amplitude shallow water waves has been determined both analytically using Bernoulli's equation and experimentally, and is given by the expression

$$c = \left\{ \frac{(y_o + 2a_o)^2}{(y_o + a_o)y_o} gy_o \right\}^{1/2} \quad (2.121)$$

When  $2a_o$  is small in comparison to  $y_o$

$$c = \left\{ 1 + \frac{2a_o}{y_o} gy_o \right\}^{1/2} \quad (2.122)$$

Generally as  $2a_o/y_o$  approaches unity the crest develops a sharp peak and breaks.

In the above equations, c is measured relative to the fluid. If the wave is moving opposite to the flow then, when  $c > V$ , the waves move upstream; when  $c = V$ , the wave is stationary; and when  $c < V$ , the wave moves downstream. When  $V = c$  for small amplitude flow,

$$V = c = \sqrt{gy_o} \quad (2.123)$$

The ratio of the flow velocity to the celerity of a shallow water wave of small amplitude is defined by the Froude number:

$$Fr = \frac{V}{\sqrt{gy_0}} \quad (2.124)$$

When  $Fr < 1$  (subcritical or tranquil), a small amplitude wave moves upstream. When  $Fr > 1$  (supercritical or rapid flow), a small amplitude wave moves downstream and when  $Fr = 1$  (critical flow), a small amplitude wave is stationary. The fact that waves or surges cannot move upstream when the Froude number is equal to or greater than 1.0 is important to remember when determining when the stage-discharge relation at a cross-section can be affected by downstream conditions. The Froude number is not only the ratio of the flow velocity to the celerity of a shallow water wave, but is also the ratio of the inertia forces to the gravity forces.

### 2.5.2 Surges

A surge is a rapid increase in the depth of flow. A surge may result from sudden release of water from a dam, or from an incoming tide. If the ratio of wave height  $2a_0$  to the depth  $y_0$  is less than unity, the surge has an undulating wave form. If  $2a_0/y_0$  is greater than one, the first wave breaks and produces a discontinuous surface. The breaking wave dissipates energy and the previous equations for wave celerity are invalid. However, by applying the momentum and continuity equations for a control volume encompassing the surge shown in Figure 2.15, the equation for the celerity of a surge can be derived for flat slopes as:

$$c = \left\{ gy_1 \left[ \frac{1}{2} \frac{y_2}{y_1} \left( \frac{y_2}{y_1} + 1 \right) \right] \right\}^{1/2} \quad (2.125)$$

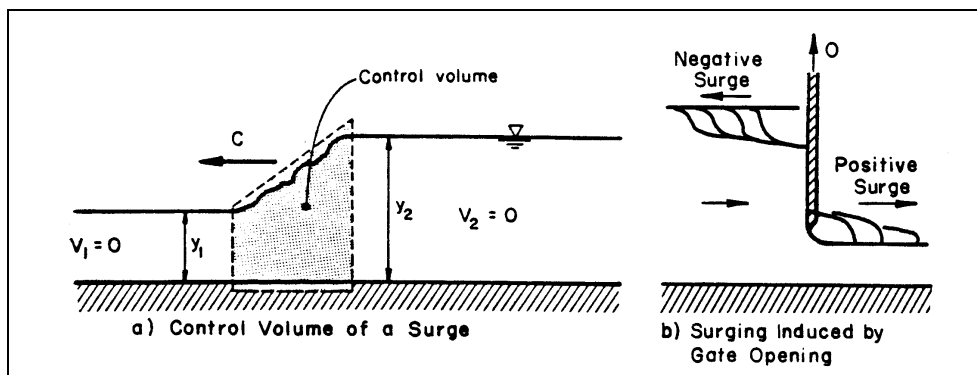


Figure 2.15. Sketch of positive and negative surges.

Equation 2.125 gives the velocity of a surge as it moves upstream as the result of a sudden total or partial closure of gates, or of an incoming tide, or of a surge that moves downstream as the result of a sudden opening of a gate. The lifting of a gate in a channel sketched in Figure 2.15b not only causes a positive surge to move downstream, it also causes a negative surge to move upstream. Equation 2.125 is approximately correct for the celerity of the negative surge if the height of the surge is small compared to the depth. As it moves upstream a negative surge quickly flattens out.

### 2.5.3 Hydraulic Jump

When the flow velocity  $V_1$  is rapid or supercritical the surge dissipates energy through a moving hydraulic jump. When  $V_1$  equals the celerity  $c$  of the surge the jump is stationary and Equation 2.125 is the equation for a hydraulic jump on a flat slope. Solutions for a hydraulic jump on a sloping channel are given in HEC-14. Equation 2.125 can be rearranged to the form:

$$\frac{V_1}{\sqrt{gy_1}} = Fr_1 = \left\{ \frac{1}{2} \frac{y_2}{y_1} \left( \frac{y_2}{y_1} + 1 \right) \right\}^{1/2} \quad (2.126)$$

or

$$\frac{y_2}{y_1} = \frac{1}{2} \left\{ (1 + 8Fr_1^2)^{1/2} - 1 \right\} \quad (2.127)$$

The corresponding energy loss in a hydraulic jump is the difference between the two specific energies. It can be shown that this head loss is:

$$h_L = \frac{(y_2 - y_1)^3}{4y_1 y_2} \quad (2.128)$$

Equation 2.128 has been experimentally verified along with the dependence of the jump length  $L_j$  and energy dissipation (head loss  $h_L$ ) on the Froude number of the approaching flow. The results of these experiments are given in Figure 2.16.

When the Froude number for rapid flow is less than 1.7, an undulating jump with large surface waves is produced. The waves are propagated for a considerable distance downstream. In addition, when the Froude number of the approaching flow is less than three, the energy dissipation of the jump is not large and jets of high velocity flow can exist for some distance downstream of the jump. These waves and jets can cause erosion a considerable distance downstream of the jump. For larger values of the Froude number, the rate of energy dissipation in the jump is very large and Figure 2.16 is recommended. The U.S. Bureau of Reclamation (Chow 1959) classifies the hydraulic jump on a flat slope into various types as illustrated in Figure 2.17. For additional information on hydraulic jumps, see HEC-14, Chow (1959) and Rouse (1950).

### 2.5.4 Roll Waves

Under certain conditions on steep slopes, surges of an intermittent nature may occur which are called roll waves or slug flow (Figure 2.18). Such flow is not at all uncommon with harmless thin sheets of flow on sloping sidewalks, for example. When these roll waves occur in large open channels, however, they may cause considerable damage, or force the operation of the channel at inefficient discharges in order to prevent damage.

Roll waves can be superposed over the normal flow in an open channel. They travel at velocities greater than the normal flow and grow in size as they progress downstream.

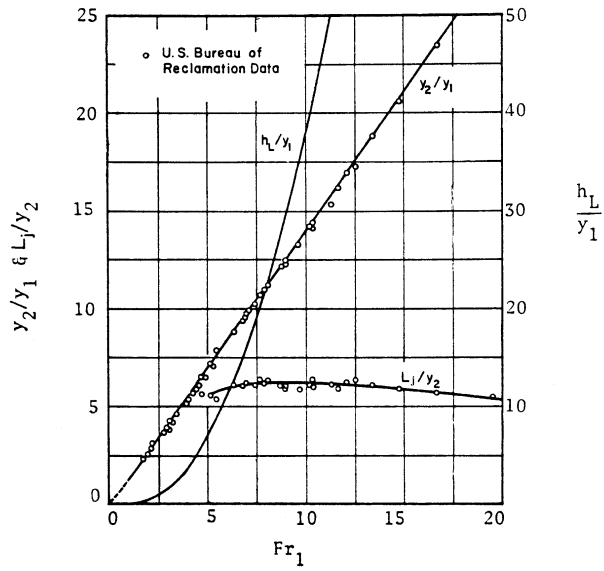


Figure 2.16. Hydraulic jump characteristics as a function of the upstream Froude number.

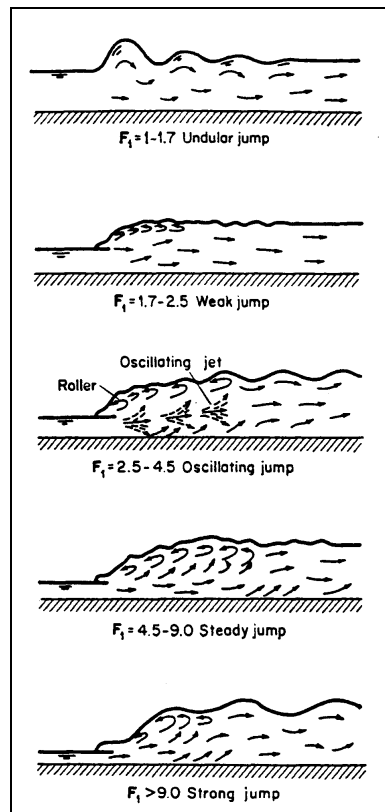


Figure 2.17. Various types of hydraulic jump (Chow 1959).

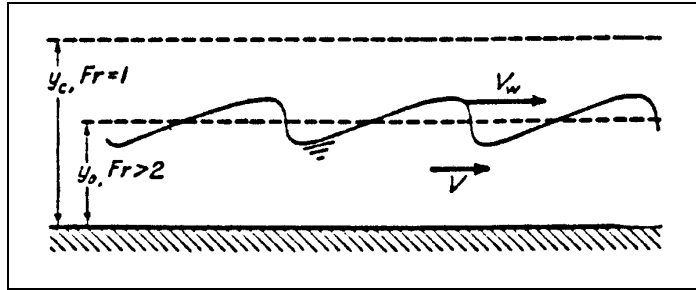


Figure 2.18. Roll waves or slug flow.

There is no simple criterion for determining the size of roll waves, since their size depends upon the magnitude of the discharge, the type of flow (laminar or turbulent), the roughness and slope of the channel, the length of the channel, and the nature and frequency of the initial disturbances which cause the waves to form. However, a necessary condition required to generate instability of the free surface and induce the formation of roll waves in turbulent flows when Chezy's equation is applicable is:

$$Fr = \frac{V}{\sqrt{gy_o}} > 2 \quad (2.129)$$

which can be expressed in alternate form for a wide channel as

$$S \geq 4 \frac{g}{C^2} \quad (2.130)$$

for turbulent flow with a rough boundary in which  $y_o$  is the normal depth,  $S$  is the slope of the channel, and  $C$  is the Chezy discharge coefficient.

When the flow in a wide channel is turbulent with a smooth boundary, roll waves can form if

$$Fr \geq 1.5 \quad (2.131)$$

$$S \geq 2.25 \frac{g}{C^2} \quad (2.132)$$

and when the flow in a wide channel is laminar, roll waves can form if

$$Fr \geq 0.5 \quad (2.133)$$

These conditions indicate that, for turbulent flow in a wide channel with a rough boundary, roll waves can occur when the flow velocity is greater than twice the celerity of a wave that is, the Froude number is greater than 2, or when the slope is four times as great as the slope required for critical depth. They can also form for turbulent flow in a wide channel with a smooth boundary if the velocity of flow is greater than 1.5 times the celerity of a wave, or the slope is 2.25 times the slope required for critical depth. By way of contrast, roll waves can form in laminar flow in a wide channel if the velocity is half the celerity of a gravity wave; in other words, the flow may never pass through critical flow ( $Fr = 1.0$ ).

## 2.6 STEADY RAPIDLY VARYING FLOW

### 2.6.1 Flow Through Transitions

Steady flow through relatively short transitions where the flow is uniform before and after the transition can be analyzed using the Bernoulli equation. Energy loss due to friction may be neglected, at least as a first approximation. Refinement of the analysis can be made in a second step by including friction loss (see HEC-14, Chapter 4). For example, the water surface elevation through a transition is determined using the Bernoulli equation and then modified by determining the friction loss effects on velocity and depth in short reaches through the transition. Energy losses resulting from flow separation cannot be neglected, and transitions where separation may occur need special treatment which may include model studies. Contracting flows (converging streamlines) are less susceptible to separation than for expanding flows. Also, any time a transition changes velocity and depth such that the Froude number approaches unity, problems such as waves, blockage, or choking of the flow may occur. If the approaching flow is supercritical, a hydraulic jump may result. Unsubmerged flow through bridges or culverts can be considered as flow through transitions.

Transitions are used to contract or expand a channel width (Figure 2.19a); to increase or decrease bottom elevation (Figure 2.19b); or to change both the width and bottom elevation. The first step in the analysis is to use the Bernoulli equation (neglecting any head loss resulting from friction or separation) to determine the depth and velocity changes of the flow through the transition. Further refinement depends on importance of freeboard, whether flow is supercritical or approaching critical conditions.

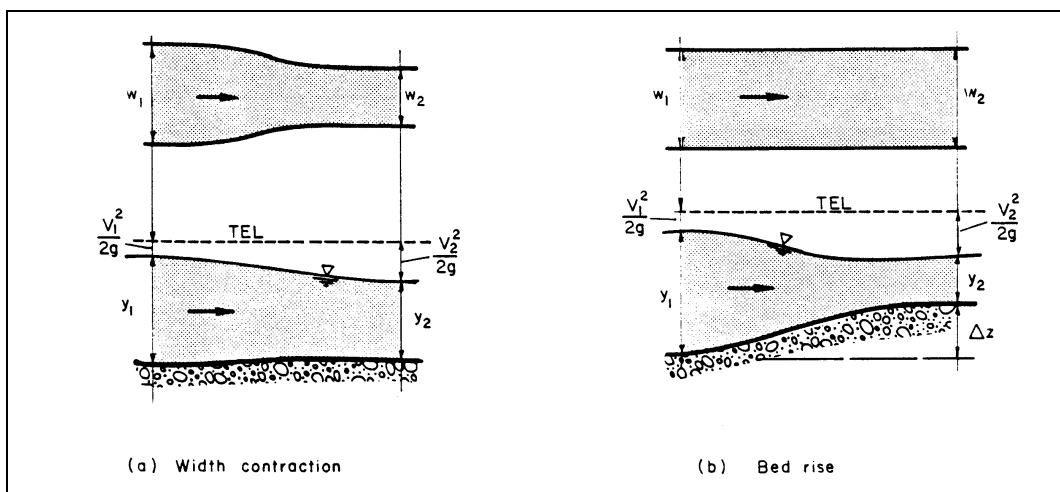


Figure 2.19. Transitions in open channel flow.

The Bernoulli equation for flow in Figure 2.19b is:

$$\frac{V_1^2}{2g} + y_1 = \frac{V_2^2}{2g} + y_2 + \Delta z \quad (2.134)$$

or

$$H_1 = H_2 + \Delta z \quad (2.135)$$

where

$$H = \frac{V^2}{2g} + y \quad (2.136)$$

The term  $H$  is called the specific head, and is the height of the total head above the channel bed.

### 2.6.2 Specific Energy Diagram

For simplicity, the following specific energy (often referred to as specific head) analysis is done on a unit width of channel so that Equation 2.136 becomes:

$$H = \frac{q^2}{2gy^2} + y \quad (2.137)$$

For a given  $q$ , Equation 2.137 can be solved for various values of  $H$  and  $y$ . When  $y$  is plotted as a function of  $H$ , Figure 2.20 is obtained (Rouse 1946). There are two possible depths called alternate depths for any  $H$  larger than a specific minimum. Thus, for specific energy larger than the minimum, the flow may have a large depth with small velocity or small depth with large velocity. Flow cannot occur with specific energy less than the minimum. The single depth of flow at the minimum specific energy is called the critical depth  $y_c$  and the corresponding velocity, the critical velocity  $V_c = q/y_c$ . To determine  $y_c$  the derivative of  $H$  with respect to  $y$  is set equal to 0.

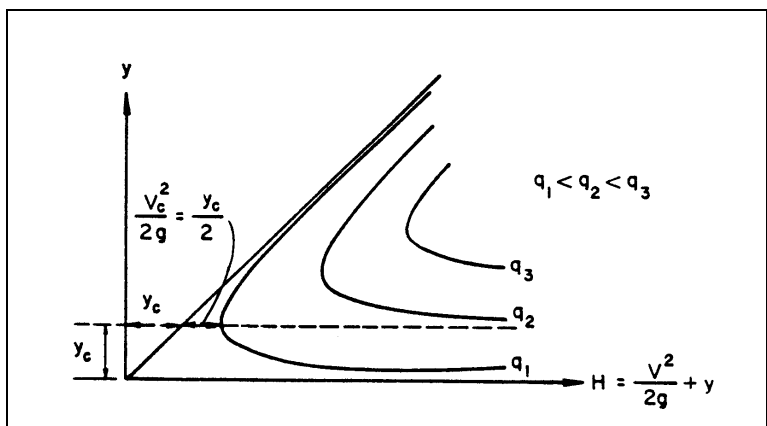


Figure 2.20. Specific energy diagram.

$$\frac{dH}{dy} = 1 - \frac{q^2}{gy^3} = 0 \quad (2.138)$$

and

$$q = (gy_c^3)^{1/2} \quad (2.139)$$

or

$$y_c = \left(\frac{q^2}{g}\right)^{1/3} = 2\frac{V_c^2}{2g} \quad (\text{see Equation 2.147}) \quad (2.140)$$

Note that

$$V_c^2 = y_c g \quad (2.141)$$

or

$$\frac{V_c}{\sqrt{gy_c}} = 1 \quad (2.142)$$

but

$$\frac{V}{\sqrt{gy}} = Fr \quad (2.143)$$

also

$$H_{\min} = \frac{V_c^2}{2g} + y_c = \frac{3}{2} y_c \quad (\text{see Equation 2.147}) \quad (2.144)$$

Thus, flow at minimum specific energy has a Froude number equal to one. Flows with velocities larger than critical ( $Fr > 1$ ) are called rapid or supercritical and flow with velocities smaller than critical ( $Fr < 1$ ) are called tranquil or subcritical. These flow conditions are illustrated in Figure 2.21, where a rise in the bed causes a decrease in depth when the flow is tranquil and an increase in depth when the flow is rapid. Furthermore, there is a maximum rise in the bed for a given  $H_1$  where the given rate of flow is physically possible. If the rise in the bed is increased beyond  $\Delta z_{\max}$  for  $H_{\min}$  then the approaching flow depth  $y_1$  would have to increase (increasing  $H$ ) or the flow would have to be decreased. Thus, for a given flow in a channel, a rise in the bed level can occur up to a  $\Delta z_{\max}$  without causing backwater.

### 2.6.3 Specific Discharge Diagram

For a constant  $H$ , Equation 2.137 can be solved for  $y$  as a function of  $q$ . By plotting  $y$  as a function of  $q$ , Figure 2.22 is obtained and for any discharge smaller than a specific maximum, two depths of flow are possible (Rouse 1946).



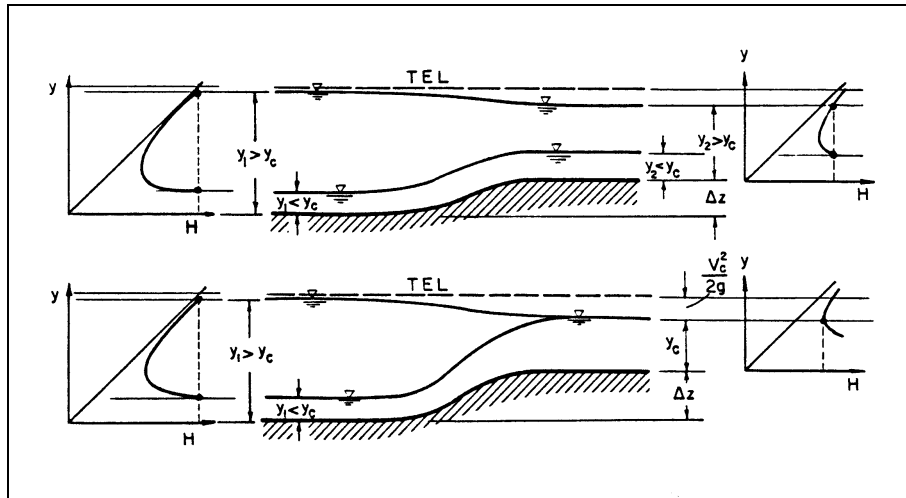


Figure 2.21. Changes in water surface resulting from an increase in bed elevation.

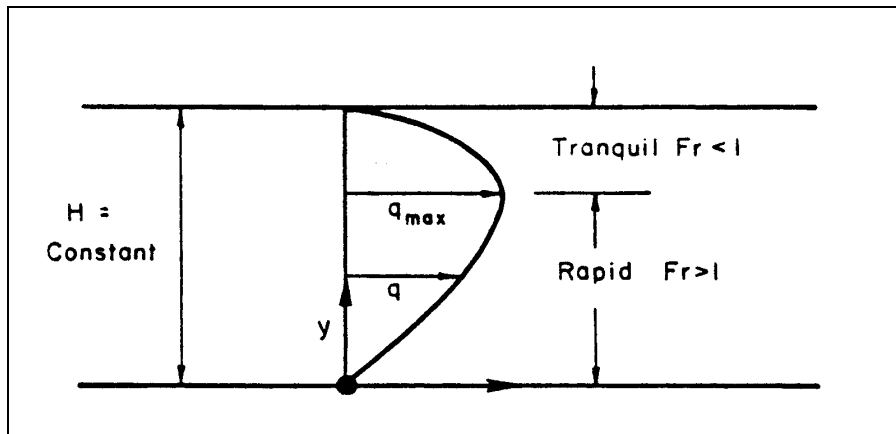


Figure 2.22. Specific discharge diagram.

To determine the value of  $y$  for  $q_{\max}$  Equation 2.137 is rearranged to obtain:

$$q = y\sqrt{2g(h-y)} \quad (2.145)$$

The differential of  $q$  with respect to  $y$  is set equal to zero.

$$\frac{dq}{dy} = 0 = \frac{q}{2} \frac{(2H-3y)}{(H-y)^{1/2}} \quad (2.146)$$

from which

$$y_c = \frac{2}{3}H = \frac{2V_c^2}{2g} \quad (2.147)$$

or

$$V_c = \sqrt{gy_c} \quad (2.148)$$

Thus for maximum discharge at constant H, the Froude number is 1.0, and the flow is critical. From this:

$$y_c = \frac{2}{3}H = \frac{2V_c^2}{2g} = \left( \frac{q_{\max}^2}{g} \right)^{1/3} \quad (\text{see Equation 2.140}) \quad (2.149)$$

For critical conditions, the Froude number is 1.0, the discharge is a maximum for a given specific head and the specific head is a minimum for a given discharge.

Flow conditions for constant specific head for a width contraction are illustrated in Figure 2.23 assuming a fixed bed and no geometrical effects such as eccentricity, skew, piers, and expansion. The contraction causes a decrease in flow depth when the flow is tranquil and an increase when the flow is rapid. The maximum possible contraction without causing backwater effects occurs when the Froude number is one, the discharge per foot of width  $q$  is a maximum, and  $y_c$  is  $2H/3$ . A further decrease in width will cause backwater. That is, an increase in depth upstream will occur to produce a larger specific energy and increase  $y_c$  in order to get the flow through the decreased width.

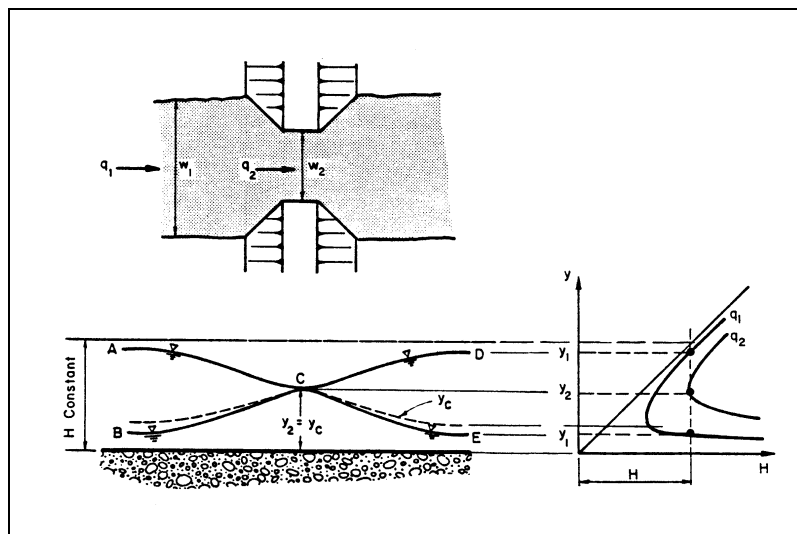


Figure 2.23. Change in water surface elevation resulting from a change in width.

The flow in Figure 2.23 can go from point A to C and then either back to D or down to E depending on the downstream boundary conditions. An increase in slope of the bed downstream from C and no separation would allow the flow to follow the line A to C to E. Similarly the flow can go from B to C and back to E or up to D depending on boundary conditions. Figure 2.23 is drawn with the side boundary forming a smooth streamline. If the contraction were due to bridge abutments, the upstream flow would follow a natural streamline to a vena contracta, but then downstream, the flow would probably separate. Tranquil approach flow could follow line A-C but the downstream flow probably would not follow either line C-D or C-E but would have an undulating hydraulic jump. There would be interaction of the flow in the separation zone and considerable energy would be lost. If the slope downstream of the abutments was the same as upstream, then the flow could not be sustained with this amount of energy loss. Backwater would occur, increasing the depth in the constriction and upstream, until the flow could go through the constriction and establish uniform flow downstream.

#### 2.6.4 Transitions With Super Critical Flows

Contractions and expansions in rapid flows produce cross wave patterns similar to those observed in curved channels (Ippen 1950 and Chow 1959). The cross waves are symmetrical with respect to the centerline of the channel. Ippen and Dawson (1951) have shown that in order to minimize the disturbance downstream of a contraction, the length of the contraction should be:

$$L = \frac{W_1 - W_2}{2 \tan \theta} \quad (2.150)$$

where  $W$  is the channel width and the subscripts 1 and 2 refer to sections upstream and downstream from the contraction. The contraction angle is  $\theta$  and should not exceed  $12^\circ$ . This requires a long transition and should not be attempted unless the structure is of primary importance. A model study should be used to determine transition geometry where a hydraulic jump is not desired. If a hydraulic jump is acceptable, the inlet structure can be designed using the procedure in HEC-14, Chapter 4B.

For an expansion, Rouse et al. (1951) found experimentally that the most satisfactory boundary form is given by:

$$\frac{w}{W_1} = \frac{1}{2} \left( \frac{x}{W_1 Fr_1} \right)^{3/2} + \frac{1}{2} \quad (2.151)$$

where  $x$  is the longitudinal distance measured from the start of the expansion or outlet section and  $w$  is the lateral coordinate measured from the channel centerline. A boundary developed from this equation diverges indefinitely. Therefore, for practical purposes, the divergent walls are followed by a transition to parallel lines. A satisfactory straight transition can be created by flaring the walls so that  $\tan \theta = 1/3 Fr$ . This criteria recommended by Blaisdel (1949) avoids creating an abrupt expansion.

## 2.6.5 Flow Over Drop Structures

Subcritical flow over vertical wall drop structures at flat slopes is illustrated in Figure 2.24. As illustrated, the flow impinging on an apron will continue downstream but at supercritical depth and velocity. Depending on downstream conditions (bed elevation and slope and down stream flow depth) the flow will continue to be supercritical or go through a hydraulic jump. If the flow impinges on an erodible bed it will scour a deep hole. Methods to calculate the depth of this scour hole are given in Chapter 3. Flow geometry and conditions of interest are:

- discharge for unit width,  $q$
- drop height,  $h$
- distance from drop wall to point of impingement,  $L_d$
- depth and velocity at impingement,  $y_1, V_1$
- pool depth under nape,  $y_p$
- sequent depth if a jump forms,  $y_2$

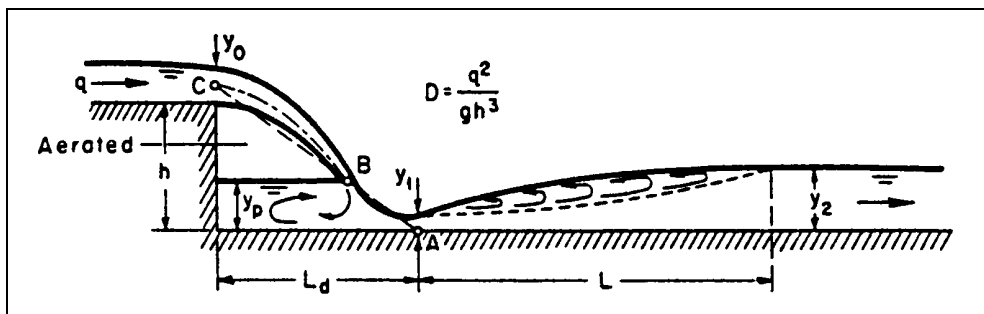


Figure 2.24. Flow characteristics over a drop structure (Chow 1959).

Chow (1959) gives equations to determine the geometric terms as functions of a drop number  $D$ . In English units of measurement these are:

$$D = \frac{q^2}{gh^3} \quad (2.152)$$

$$\frac{L_d}{h} = 4.30 D^{0.27} \quad (2.153)$$

$$\frac{y_p}{h} = 1.00 D^{0.22} \quad (2.154)$$

$$\frac{y_1}{h} = 0.54 D^{0.425} \quad (2.155)$$

$$\frac{y_2}{h} = 1.66 D^{0.27} \quad (2.156)$$

Note:

1. The equations are for a well-aerated nappe. If the nappe is poorly or not aerated, the nappe will move upstream until in contact with the vertical wall.
2. If the tailwater depth,  $y_2$ , is less than  $y_c$ , the hydraulic jump will move downstream.
3. If the tailwater depth,  $y_2$ , is larger than  $y_c$ , the jump will move upstream and the jump will be submerged.
4. For upstream subcritical flow the brink serves as the control and the subcritical approach flow goes through critical 3 to 4  $y_c$  upstream of the brink (Chow, 1959, p. 44).
5. For upstream supercritical flow the control for the flow is upstream and the profile for the nappe is a function of the approach Froude number. Ippen (1950, p. 533) gives a composite plot of nappe profiles for different values of the Froude number (Figure 2.25).

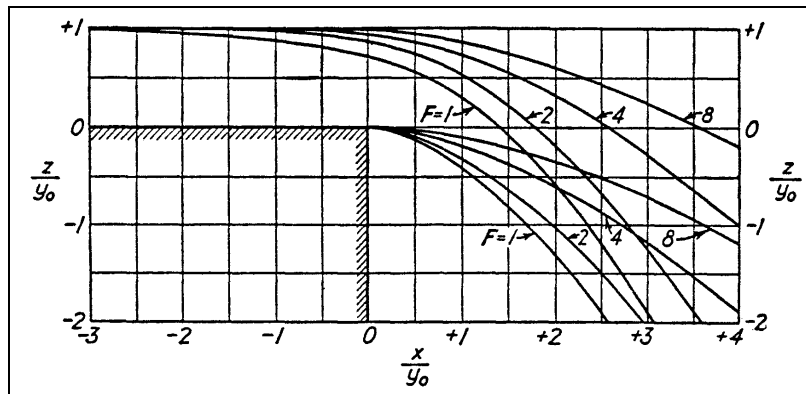


Figure 2.25. Nappe profiles for supercritical flow (Ippen 1950).

## 2.7 FLOW IN BENDS

### 2.7.1 Types of Bends

Two principal types of bends are deepened or entrenched bends and meandering surface bends. The first type includes those in which the river bends follow the curves of the valley so that each river bend includes a promontory of the parent plateau. The second type includes bends which are formed only by the river on a flat, alluvium covered valley floor, and where the slopes of the valley are not involved in the formation of such bends. This division of bends is correct and sufficiently definitive with respect to external forms of the relief and the processes of formation and development of bends. It is, however, incomplete from the standpoint of the work of the river and of the physical nature of this phenomenon. Both of these types of bends can be put into one category--the category of freely meandering channels, i.e., meandering determined only by the interaction of the stream and the bed material. Such meandering when not disturbed by the influence of external factors, proceeds at an approximately equal rate along the length of the river.

Under natural conditions, a third type of bend is often encountered. This bend occurs when the stream impinging on a erosion-resistant bank forms a forced curve which is gradually transformed into a river bend of a more constricted shape. In all cases, the effect of the character (density) of the bank material is important and, to a certain degree, determines the radius of curvature of the channel in a free bend. The radius of curvature increases with the density of the material. Considering both the action of the stream and the interaction between the stream and the channel, as well as the general laws of their formation, one can distinguish the following three types of bends of a natural river channel:

1. Free bends - Both banks are composed of alluvial floodplain material which is usually quite mobile; the free bend corresponds to the common concept of a surface bend;
2. Limited bends - The banks of the stream are composed of consolidated parent material which limits the lateral erosion by the stream. Limited bends are entrenched bends; and
3. Forced bends - The stream impinges onto an almost straight parent bank at a large angle ( $60^\circ$  to  $90^\circ$ ).

A typical feature of bends is a close relationship between the type of stream bend and the radius of curvature. The forced bend has the smallest radius of curvature. Next in size are the radii of free bends. The limited bends have the greatest radii. The average values of the ratios of the radii of curvature to the width of the stream at bankfull stage for the three types of bends are: (1) free bends 4.5 to 5.0; (2) limited bends 7.0 to 8.0; and (3) forced bends 2.5 to 3.0.

A second characteristic feature of bends is the distribution of depths along the length of the bend. In free bends and limited bends, the depth gradually increases and the maximum depth is found some distance below the apex of the bend. In the forced bend, the depth sharply increases at the beginning of the bend and then gradually diminishes. In forced bends the greatest depth is located in the middle third of the bend, where there appears to be a concentrated deep scour hole.

### **2.7.2 Transverse Velocity Distribution in Bends**

The transverse velocities in bends result from an imbalance of radial pressures on a particle of fluid traveling around the bend. In Figure 2.26, a cross section through a typical bend is shown. The radial forces acting on the shaded control volume are the centrifugal force  $mv^2/r$  in which  $r$  is the radius of curvature, and the differential hydrostatic force  $\gamma dz$  caused by the superelevation of the water surface  $dz$ . As shown in Figure 2.26a, the centrifugal force is greater near the surface where the fluid velocity  $v$  is greater and less at the bed where  $v$  is small. The differential hydrostatic force is uniform throughout the depth of the control volume. As shown in Figure 2.26b, the sum of the centrifugal and excess hydrostatic forces varies with depth and can cause a lateral velocity component. The magnitude of the transverse velocity is dependent on the radius of curvature and on the proximity of the banks. In the immediate vicinity of the banks, there can be no lateral velocity if the river is narrow and deep.

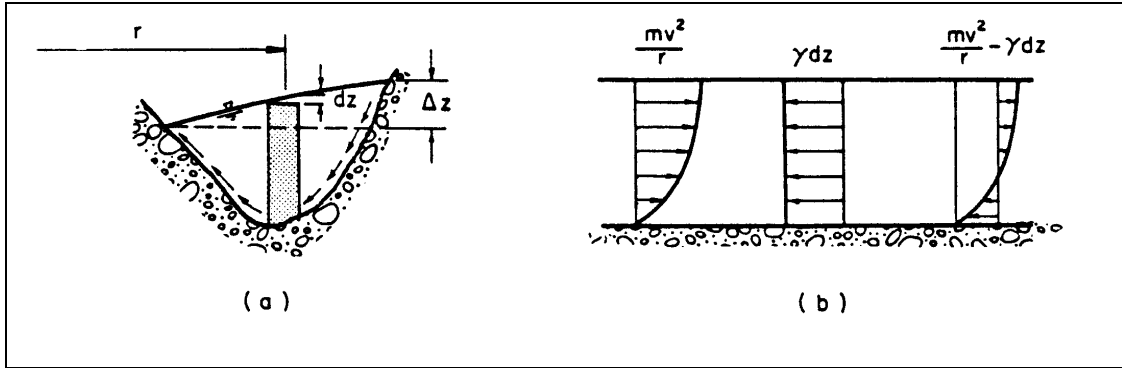


Figure 2.26. Schematic representation of transverse currents in a channel bed.

### 2.7.3 Subcritical Flow in Bends

Because of the change in flow direction which results in centrifugal forces, there is a superelevation of the water surface in river bends. The water surface is higher at the outside bank than at the inside bank. The resulting transverse slope can be evaluated quantitatively. Using cylindrical coordinates (Figure 2.27), the differential pressure in the radial direction arises from the radial acceleration or:

$$\frac{1}{\rho} \frac{\partial p}{\partial r} = \frac{V_{\theta}^2}{r} \tag{2.157}$$

To calculate the total superelevation between the outer and inner bend two assumptions are made: (1) radial and vertical velocities are small compared to the tangential velocities such that  $V_{\theta} \approx V$ ; and (2) pressure distribution in the bend is hydrostatic, i.e.,  $p = \gamma y$ .

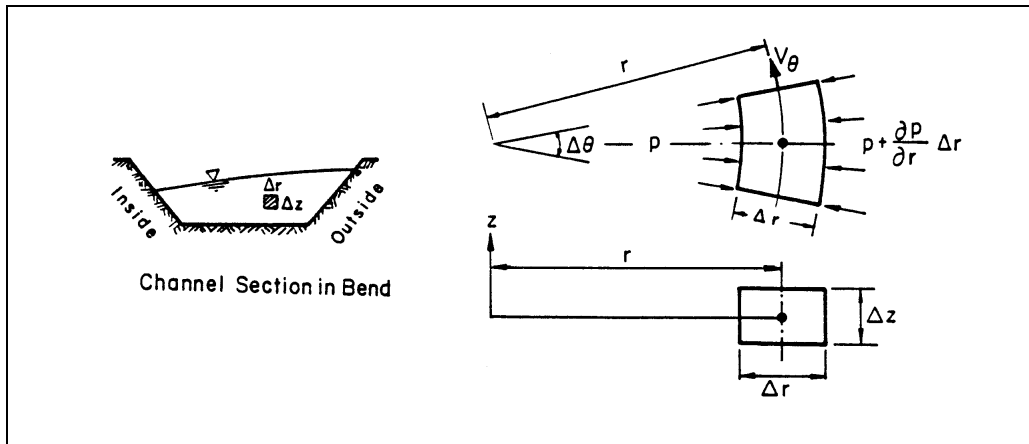


Figure 2.27. Definition sketch of flow around a bend.

Then

$$\Delta Z = \frac{1}{g} \int_{r_i}^{r_o} \frac{V^2}{r} dr \quad (2.158)$$

To solve Equation 2.158, the transverse velocity distribution along the radius of the bend must be known or assumed. The results obtained assuming various velocity distributions follow.

Woodward (1920) assumed  $V$  equal to the average velocity  $Q/A$  and  $r$  equal to the radius to the center of the stream  $r_c$ , and obtained:

$$\Delta Z = \frac{1}{g} \int_{r_i}^{r_o} \frac{V^2}{r_c} dr \quad (2.159)$$

or

$$\Delta Z = z_o - z_i = \frac{V^2}{gr_c} (r_o - r_i) \quad (2.160)$$

in which  $z_i$  and  $r_i$  are the water surface elevation and the radius at the inside of the bend, and  $z_o$  and  $r_o$  are the water surface elevation and the radius at the outside of the bend.

By assuming the velocity distribution to approximate that of a free vortex ( $V_\theta = C_1/r$ ), Shukry (1950) obtained:

$$\Delta Z = \frac{1}{g} \int_{r_i}^{r_o} \frac{C_1^2}{r^3} dr = \frac{C_1^2}{2g} \left\{ \frac{1}{r_i^2} - \frac{1}{r_o^2} \right\} \quad (2.161)$$

in which  $C_1 = rV$  is the free vortex constant. By assuming flow depth of flow upstream of the bend equal to the average depth in the bend, Ippen and Drinker (1962) reduced Equation 2.161 to:

$$\Delta Z = \frac{V^2}{2g} \frac{2W}{r_c} \left\{ \frac{1}{1 - \left( \frac{W}{2r_c} \right)^2} \right\} \quad (2.162)$$

For situations where high velocities occur near the outer bank of the channel, a forced vortex may approximate the flow pattern. With this assumption and assuming a constant average specific head, Ippen and Drinker (1962) obtained:



$$\Delta Z = \frac{V^2}{2g} \frac{2W}{r_c} \left[ \frac{1}{1 - \left( \frac{W^2}{12r_c^2} \right)} \right] \quad (2.163)$$

By assuming that the maximum velocities are close to the centerline of the channel in the bend and that the flow pattern inward and outward from the centerline can be represented as forced and free vortices, respectively, then:

$$\Delta Z = \frac{1}{g} \int_{r_i}^{r_c} \frac{C_2^2 r^2}{r} dr + \frac{1}{g} \int_{r_c}^{r_o} \frac{C_1^2}{r^3} dr \quad (2.164)$$

and when  $r = r_c$ ,  $V = V_{\max}$

Therefore,  $C_2 = \frac{V_{\max}}{r_c}$  and  $C_1 = V_{\max} r_c$

and Equation 2.164 becomes:

$$\Delta Z = \frac{V_{\max}^2}{2g} \left\{ 2 - \left( \frac{r_i}{r_c} \right)^2 - \left( \frac{r_o}{r_c} \right)^2 \right\} \quad (2.165)$$

The differences in superelevation that are obtained by using the different equations are small, and in alluvial channels the resulting erosion of the outside bank and deposition on the inside bank leads to further error in computing superelevation. Therefore, it is recommended that Equation 2.158 be used to compute superelevation in alluvial channels. For lined canals with strong curvature, superelevation should be computed using Equations 2.162 or 2.165.

An example showing how to calculate superelevation in bends from velocity measurements is presented in Section 2.14 (SI) and 2.15 (English) at the end of this chapter. The example also compares the various approximate equations included in this section.

#### 2.7.4 Supercritical Flow in Bends

Rapid flow or supercritical flow in a curved prismatic channel produces cross wave disturbance patterns which persist for long distances in a downstream direction. These disturbance patterns are the result of non-equilibrium conditions which persist because the disturbances cannot propagate upstream or even propagate directly across the stream. Therefore, the turning effect of the walls is not felt on all filaments of the flow at the same time and the equilibrium of the flow is destroyed. The waves produced form a series of troughs and crests in the water surface along the channel walls.

Two methods have been used in the design of curves for rapid flow in channels. One method is to bank the floor of the channel and the other is to provide curved vanes in the flow. Banking on the floor produces lateral forces which act simultaneously on all filaments and causes the flow to

turn without destroying the flow equilibrium. Curved vanes break up the flow into a series of small channels and since the superelevation is directly proportional to the channel width, each small channel has a smaller superelevation. If the bend is not properly shaped or designed a hydraulic jump may occur or the cross-waves can be amplified. There are design methods in the literature (Rouse 1950, Ippen 1950, Chow 1959). In most cases a physical model study is recommended.

## **2.8 GRADUALLY VARIED FLOW**

### **2.8.1 Introduction**

Thus far, two types of steady flow have been considered. They are uniform flow and rapidly varied nonuniform flow. In uniform flow, acceleration forces are zero and energy is converted to heat as a result of viscous forces within the flow. There are no changes in cross-section or flow direction, and the depth (called normal depth) is constant. In rapidly varied flow, changes in cross-section, direction, or depth take place in relatively short distances; acceleration forces are not zero; and viscous forces can be neglected (at least as a first approximation).

Different conditions prevail for each of these two types of steady flow. In steady uniform flow, the slope of the bed, the slope of the water surface and the slope of the energy gradeline are all parallel and are equal to the head loss divided by the length of the channel in which the loss occurred. In rapidly varied flow through short streamlined transitions, resistance is neglected and changes in depth due to acceleration are dominant. In this section, a third type of steady flow is considered. In this type of flow, changes in depth and velocity take place slowly over large distances, resistance to flow dominates and acceleration forces are neglected. This type of flow is called gradually varied flow.

In gradually varied flow, the actual flow depth  $y$  is either larger or smaller than the normal depth  $y_0$  and either larger or smaller than the critical depth  $y_c$ . The water surface profiles, which are often called backwater curves, depend on the magnitude of the actual depth of flow  $y$  in relation to the normal depth  $y_0$  and the critical depth  $y_c$ . Normal depth  $y_0$  is the depth of flow that would exist for steady-uniform flow as determined using the Manning or Chezy velocity equations, and the critical depth is the depth of flow when the Froude number equals 1.0. Reasons for the depth being different than the normal depth are changes in slope of the bed, changes in cross-section, obstruction to flow and imbalances between gravitational forces accelerating the flow and shear forces retarding the flow.

In working with gradually varied flow, the first step is to determine of the general characteristics of the water surface and what type of backwater curve would exist. The second step is to perform the numerical computations to determine the elevation of the water surface or depth of flow.

### **2.8.2 Classification of Flow Profiles**

The classification of flow profiles is obtained by analyzing the change of the various terms in the total head equation in the  $x$ -direction. The total head is:

$$H_T = \frac{V^2}{2g} + y + z \quad (2.166)$$

or

$$H_T = \frac{Q^2}{2gA^2} + y + z \quad (2.167)$$

Then assuming a wide channel for simplicity

$$\frac{dH_T}{dx} + \frac{q^2}{gy^3} \frac{dy}{dx} = \frac{dy}{dx} + \frac{dz}{dx} \quad (2.168)$$

The term  $dH_T/dx$  is the slope of the energy gradeline  $S_f$ , by assumption. For short distances and small changes in  $y$  the energy gradient can be evaluated using the Manning or Chezy velocity equations.

When Chezy's equation (Equation 2.84) is used the expression for  $dH_T/dx$  is

$$-\frac{dH_T}{dx} = S_f = \frac{q^2}{C^2 y^3} \quad (2.169)$$

The term  $dy/dx$  is the slope of the water surface  $S_w$ , and  $dz/dx$  is the bed slope  $-S_o$ . For steady flow, the bed slope is (from Equation 2.84)

$$S_o = \frac{-q^2}{C_o^2 y_o^3} \quad (2.170)$$

where the subscript "o" indicates the steady uniform flow values.

When Equations 2.169 and 2.170 are substituted into Equation 2.168, the familiar form of the gradually varied flow equation is obtained:

$$\frac{dy}{dx} = S_o \left\{ \frac{1 - \left( \frac{C_o}{C} \right)^2 \left( \frac{y_o}{y} \right)^3}{1 - \left( \frac{y_c}{y} \right)^3} \right\} \quad (2.171)$$

If Manning's equation is used to evaluate  $S_f$  and  $S_o$ , Equation 2.171 becomes

$$\frac{dy}{dx} = S_o \left\{ \frac{1 - \left( \frac{n}{n_o} \right)^2 \left( \frac{y_o}{y} \right)^{10/3}}{1 - \left( \frac{y_c}{y} \right)^3} \right\} \quad (2.172)$$

The slope of the water surface  $dy/dx$  depends on the slope of the bed  $S_o$ , the ratio of the normal depth  $y_o$  to the actual depth  $y$  and the ratio of the critical depth  $y_c$  to the actual depth  $y$ . The difference between flow resistance for steady uniform flow  $n_o$  to flow resistance for steady nonuniform flow  $n$  is small and the ratio is taken as 1.0. With  $n = n_o$ , there are twelve types of water surface profiles. These are illustrated in Figure 2.28 and summarized in Table 2.3.

When  $y \rightarrow y_c$ , the assumption that acceleration forces can be neglected no longer holds. Equations 2.171 and 2.172 indicate that  $dy/dx$  is perpendicular to the bed slope when  $y \rightarrow y_c$ . For cross-sections close to the cross-section where the flow is critical (a distance from [3 to 15 m (10 to 50 ft)]), curvilinear flow analysis and experimentation must be used to determine the actual values of  $y$ .

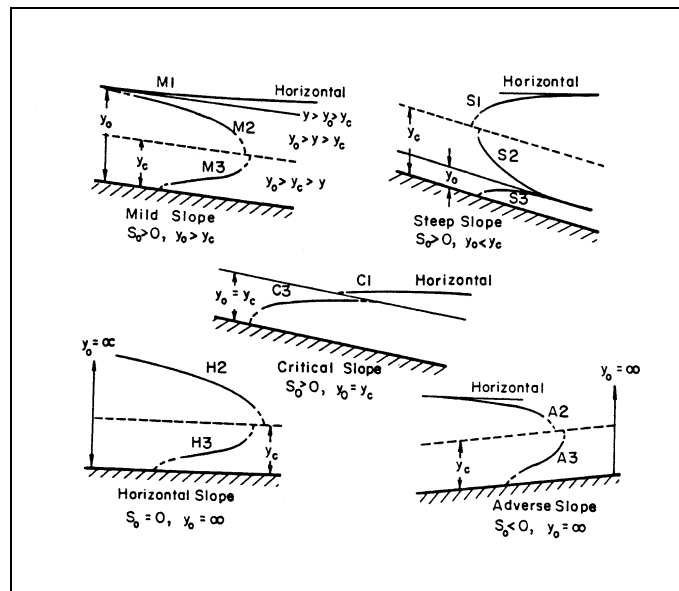


Figure 2.28. Classification of water surface profiles.

When analyzing long distances 30 to 300 m (100 to 1,000 ft) or longer one can assume qualitatively that  $y$  reaches  $y_c$ . In general, when the flow is rapid ( $Fr \geq 1$ ), the flow cannot become tranquil without a hydraulic jump occurring. In contrast, tranquil flow can become rapid (cross the critical depth line). This is illustrated in Figure 2.29.

When there is a change in cross-section or slope or an obstruction to the flow, the qualitative analysis of the flow profile depends on locating the control points, determining the type of curve upstream and downstream of the control points, and then sketching the backwater curves. It must be remembered that when flow is rapid ( $Fr > 1$ ), the control of the depth is upstream and the backwater proceeds in the downstream direction. When flow is tranquil ( $Fr < 1$ ), the depth control is downstream and the computations must proceed upstream. The backwater curves that result from a change in slope of the bed are illustrated in Figure 2.29.

Table 2.3. Characteristics of Water Surface Profiles.				
Class	Bed Slope	Depth	Type	Classification
Mild	$S_o > 0$	$y > y_o > y_c$	1	M1
Mild	$S_o > 0$	$y_o > y > y_c$	2	M2
Mild	$S_o > 0$	$y_o > y_c > y$	3	M3
Critical	$S_o > 0$	$y > y_o = y_c$	1	C1
Critical	$S_o > 0$	$y < y_o = y_c$	3	C2
Steep	$S_o > 0$	$y > y_c > y_o$	1	S1
Steep	$S_o > 0$	$y_c > y > y_o$	2	S2
Steep	$S_o > 0$	$y_c > y_o > y$	3	S3
Horizontal	$S_o = 0$	$y > y_c$	2	H2
Horizontal	$S_o = 0$	$y_c > y$	3	H3
Adverse	$S_o < 0$	$y > y_c$	2	A2
Adverse	$S_o < 0$	$y_c > y$	3	A3

Note:

- (1) With a type 1 curve (M1, S1, C1), the actual depth of flow  $y$  is greater than both the normal depth  $y_o$  and the critical depth  $y_c$ . Because flow is tranquil, control of the flow is downstream.
- (2) With a type 2 curve (M2, S2, A2, H2), the actual depth  $y$  is between the normal depth  $y_o$  and the critical depth  $y_c$ . The flow is tranquil for M2, A2 and H2 and thus the control is downstream. Flow is rapid for S2 and the control is upstream.
- (3) With a type 3 curve (M3, S3, C3, A3, H3), the actual depth  $y$  is smaller than both the normal depth  $y_o$  and the critical depth  $y_c$ . The flow is rapid and control is upstream.
- (4) For a mild slope,  $S_o$  is smaller than  $S_c$  and  $y_o > y_c$ .
- (5) For a steep slope,  $S_o$  is larger than  $S_c$  and  $y_o < y_c$ .
- (6) For a critical slope,  $S_o$  equals  $S_c$  and  $y_o = y_c$ .
- (7) For an adverse slope,  $S_o$  is negative.
- (8) For a horizontal slope,  $S_o$  equals zero.
- (9) The case where  $y \rightarrow y_c$  is of special interest. See paragraph preceding Figure 2.28.

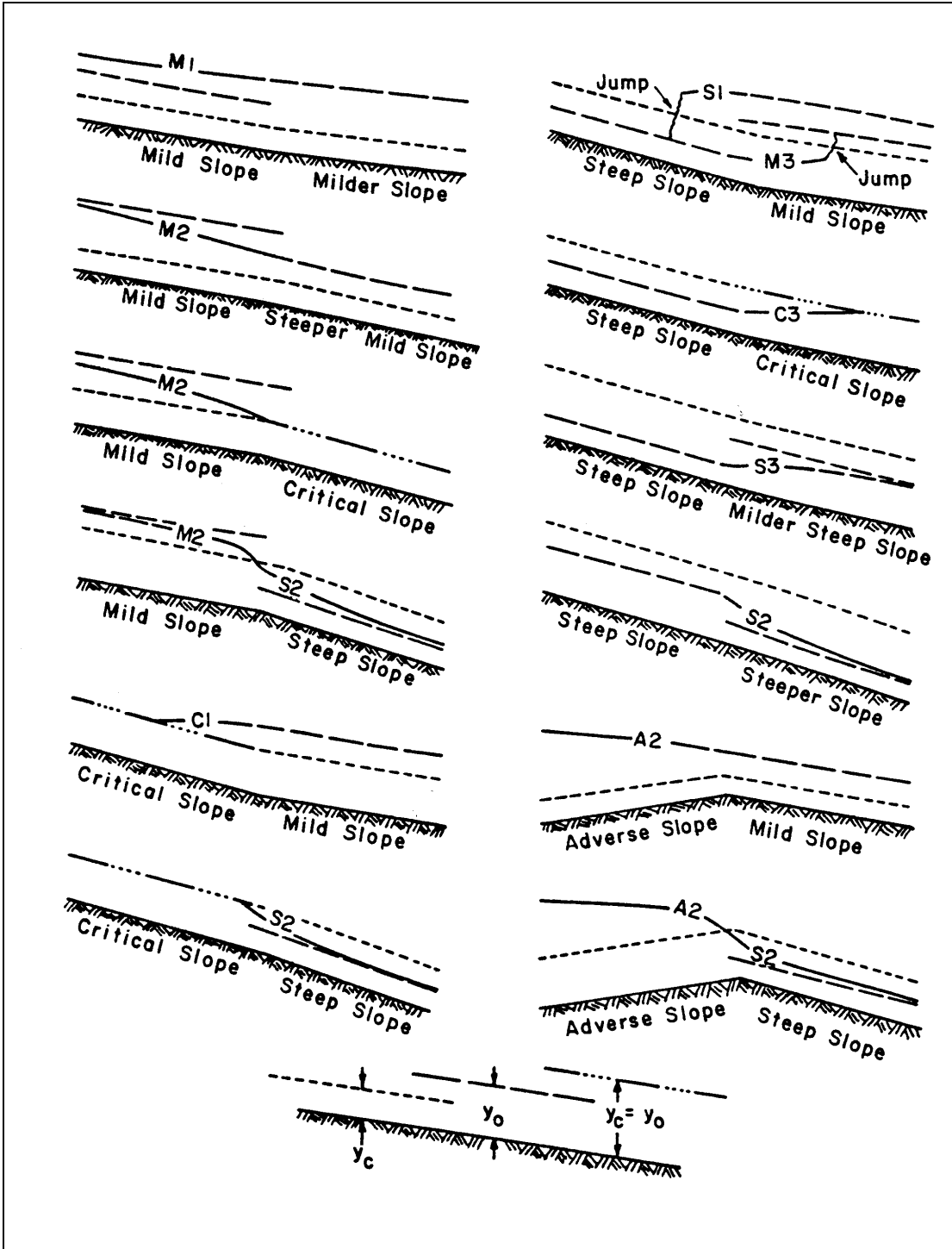


Figure 2.29. Examples of water surface profiles.

### 2.8.3 Standard Step Method for the Computation of Water Surface Profiles

The standard step method is a simple computational procedure to determine the water surface profile in gradually varied flows. Prior knowledge of the type of backwater curve as classified in Section 2.8.2 is useful to determine whether the analysis should proceed upstream or downstream.

The standard step method is derived from the energy equation

$$\frac{V_1^2}{2g} + y_1 + \Delta z = \frac{V_2^2}{2g} + y_2 + H_L \quad (2.173)$$

From Figure 2.30

$$\frac{V_1^2}{2g} + y_1 + S_o \Delta L = \frac{V_2^2}{2g} + y_2 + S_f \Delta L \quad (2.174)$$

$$H_1 + S_o \Delta L = H_2 + S_f \Delta L \quad (2.175)$$

and

$$\Delta L = \frac{H_2 - H_1}{S_o - S_f} \quad (2.176)$$

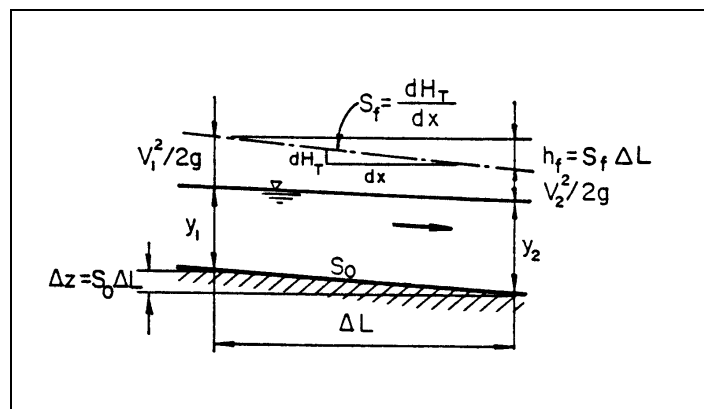


Figure 2.30. Definition sketch for the standard step method for computation of backwater curves.

The procedure is to start from some known  $y$ , which can be obtained from a stage-discharge relationship, assume another  $y$  either upstream or downstream depending on whether the flow is tranquil or rapid, and compute the distance  $\Delta L$  to the assumed depth using Equation 2.176. It is recommended that the assumed depth be kept relatively close to the known value of  $y_1$  in order to keep the interval  $\Delta L$  as short as possible to obtain better accuracy in the calculation.

## **2.9 STREAM GAGING**

### **2.9.1 Introduction**

The hydrology of the stream at a bridge crossing is determined from records obtained by State and Federal agencies. The most extensive records of streamflow are by the U.S. Geological Survey. Their records of stream flow and analysis can be obtained for any State at their District offices or from their Web Site. The USGS has been collecting stream gaging records since 1888 (Corbet 1962) and maintain over 4,000 sites in the United States in cooperation with other Federal, State, Counties, and Cities. Often a gaging station will be located near the site of a bridge crossing. If not, regional or other hydrologic tools can be used to analyze the stations in the region to obtain the hydrology for the bridge site.

The quality of the hydrologic records at a stream gaging site depends on obtaining an accurate gage height record and stage-discharge relation. These depend on stream characteristics (bed material, cross-section, and control) and, in many cases, the magnitude of the sediment transported by the stream. These terms are defined in the glossary and will be defined later in this section. For example, the hydrology used for the analysis of the 1987 I-90 bridge failure in upstate New York was excellent. There was a gaging station located 22.5 km (14 mi) upstream of the bridge. The stream at the gaging site was in bedrock with an excellent control. Thus, the stage-discharge relation was well defined with a single curve established with actual discharge measurements made over many years and large flows. The gage height record was excellent with few time gaps. The stage record for the 1987 storm was excellent. The discharge was routed to the bridge from the gage site using the U.S. Corps of Engineers HEC-1 model to obtain the hydrology of the flow at the bridge.

In contrast, the hydrology for the 1997 I-5 bridge failure in California was not well defined. The streambed was sand and there was no bed rock control, only channel control. The gage height record was good, but the stage discharge relation was poorly defined with no consistent curve. The peak discharge for the flood had to be determined using indirect methods with results that ranged from 420 to 1,140 m<sup>3</sup>/s (14,800 to 40,300 cfs). The range in discharge for the slope area measurement resulted from assumptions on Manning's n and the amount of degradation. The discharge used in the final analysis 773 m<sup>3</sup>/s (27,300 cfs) was determined from the slope-area measurement, study of the rainfall records and discharge records of other gages in the drainage basin.

A program to obtain a systematic record of the stream flow consist of (1) establishing and constructing a streamflow measurement station, (2) operating and maintaining the station, and (3) computing, compiling and publishing the stream flow data. In addition, analyses of the long-term stream flow data are made (flood frequency, low flow analysis, trends). The methods of obtaining water discharge records are described in publications of the USGS (Corbet 1962, Carter and Davidian 1968, Buchanan and Somers 1968a,b, and Kennedy 1983). In the following sections a typical gaging station, discharge measurement, stage discharge relation and the determination of the daily discharge will briefly be explained.

### **2.9.2 Gaging Station**

A gaging station consists of structures and equipment to measure and record the stage and discharge as a function of time at a given site on a stream. Stage or gage height is the height of the water surface above a chosen arbitrary datum corresponding to the zero of the gage. The zero of the gage is related to sea-level elevation. An accurate record of stage is essential for computing the discharge for any period of time. Discharge is the rate of flow in m<sup>3</sup>/s or cfs.



Typical gaging stations are illustrated in Figure 2.31 and 2.32. In many gaging stations, a manometer and gas under pressure bubbling into the stream are used to measure stage instead of a float, well and pipe intakes (Figure 2.33). The stage versus time is recorded by pen on paper, or electronically on tape, or both. Figure 2.34 illustrates a stage versus time chart. Also, at many stations the stage is transmitted over phone lines or satellite to a central location.

Discharge is measured using a current (velocity) meter by wading at low flow and from a cableway or highway bridge at high flows. The procedure for an actual current meter measurement is described in the next section. In many cases, large flows are measured by indirect methods such as a slope-area measurement using Manning's equation; however, the preferred method is to use a current meter measurement.

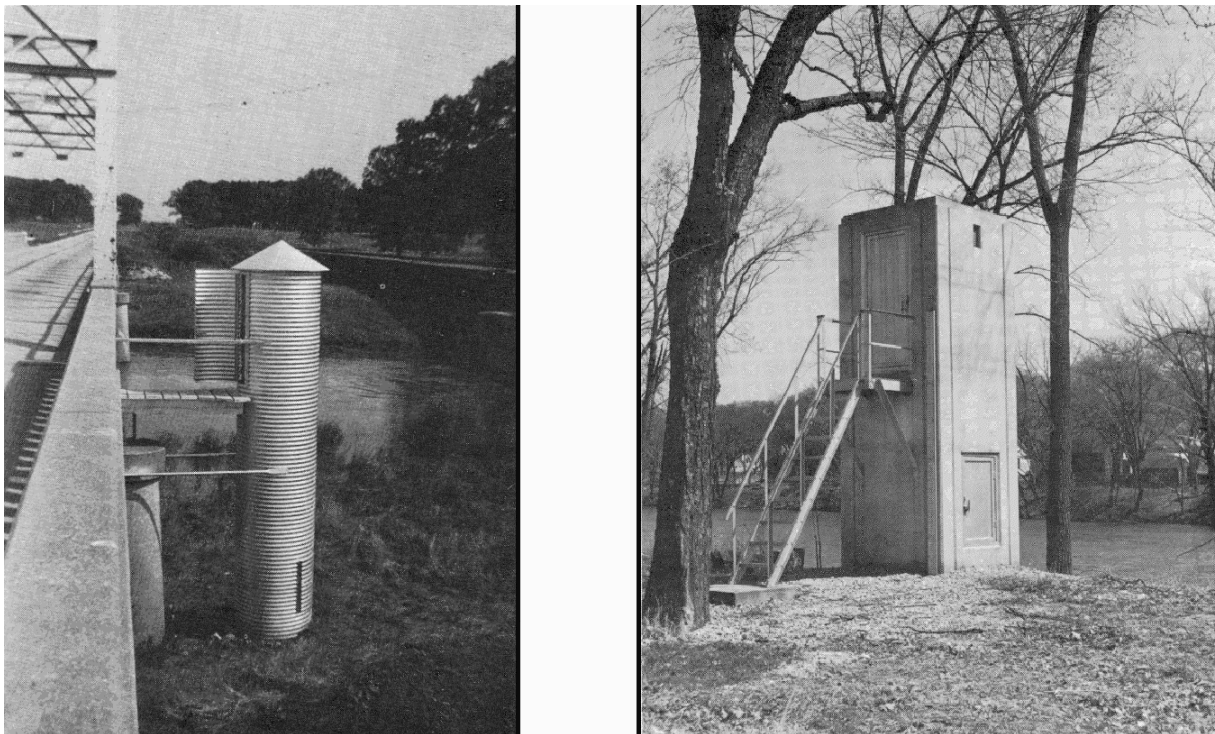


Figure 2.31. Gaging station well and shelters (from Buchanan and Somers 1968a).

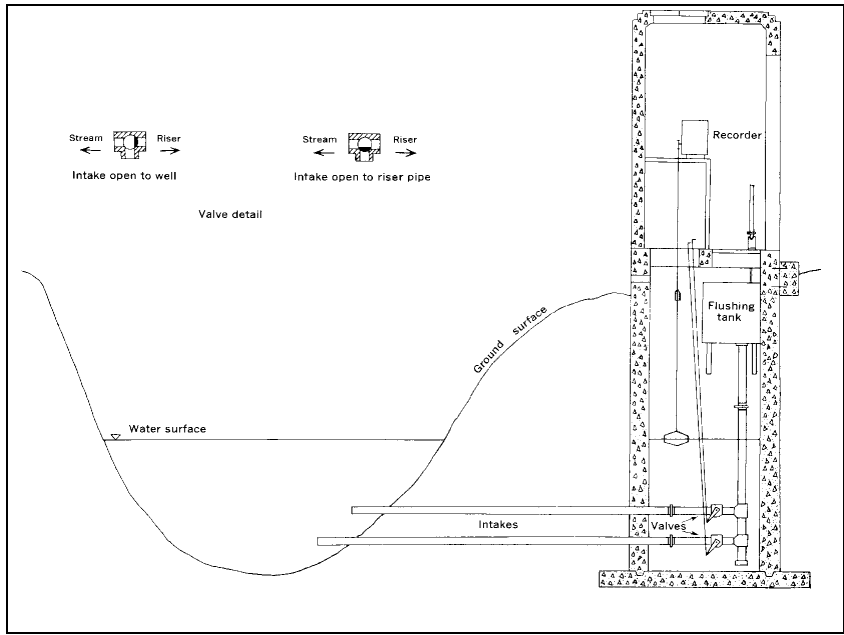


Figure 2.32. Typical float recording gaging station (from Buchanan and Somers 1968a).

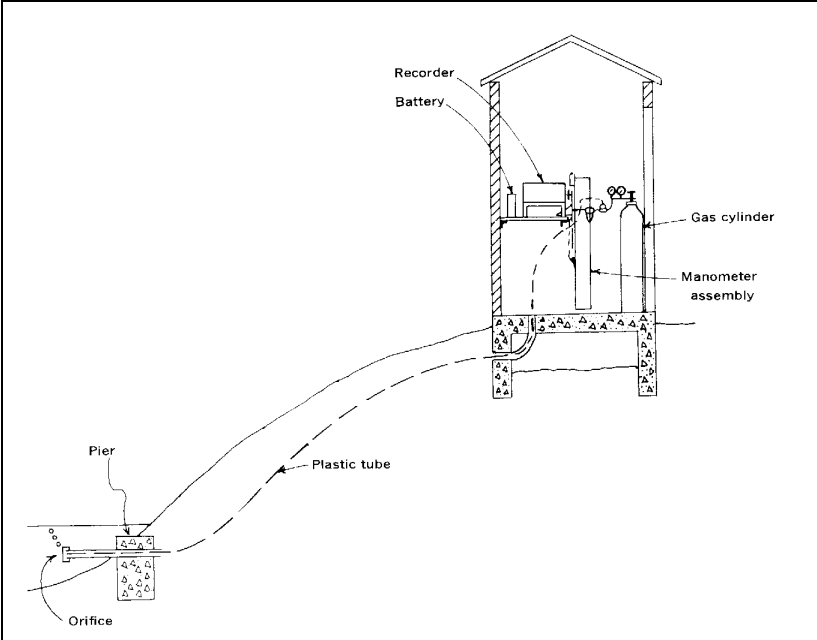


Figure 2.33. Typical bubble and manometer recording gaging station (from Buchanan and Somers 1968a).

Scale reverses at upper and lower margins

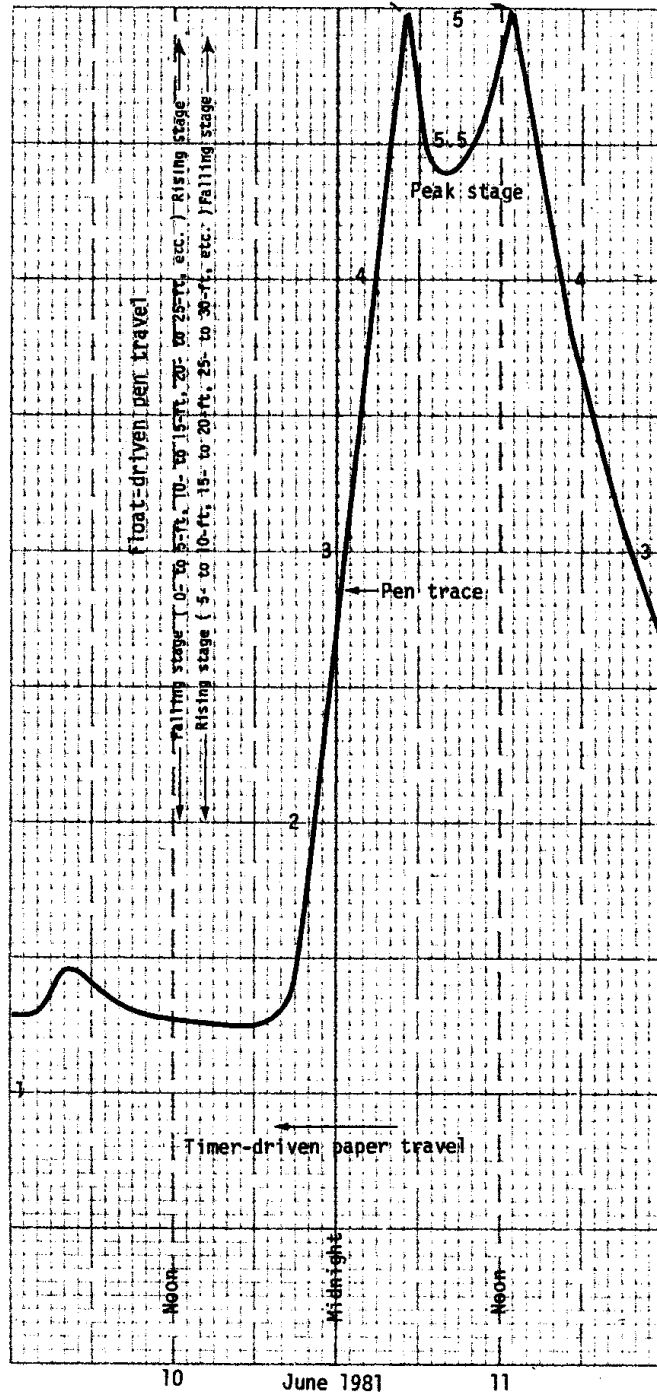


Figure 2.34. Stage vs. time hydrograph (Kennedy 1983).

### 2.9.3 Measuring Water Discharge

Generally the stream cross-section is divided into 20 sections (verticals). At each vertical the depth and velocity are measured. The velocity is measured using a vertical-axis rotor with cups (Price is typical), horizontal-axis rotor with vanes (Ott is typical) or a magnetic (Brien-Macnertry is typical) velocity meter. If the depth is less than 0.8 m (2.5 ft) the velocity is measured at 0.6 the depth below the water surface. If over 0.8 m (2.5 ft) the velocity is the average of the velocity measured at 0.2 and 0.8 the depth below the water surface. In complex velocity distributions, additional point velocities are taken, plotted, and the average velocity determined. The average velocity in the vertical (one point, two points, and etc measurement) is multiplied by the sub-area to obtain a unit discharge. The sub-area is determined by multiplying the measured depth by 0.5 times the width to the adjacent sections (Figure 2.35). Total Discharge is the sum of all the unit discharges.

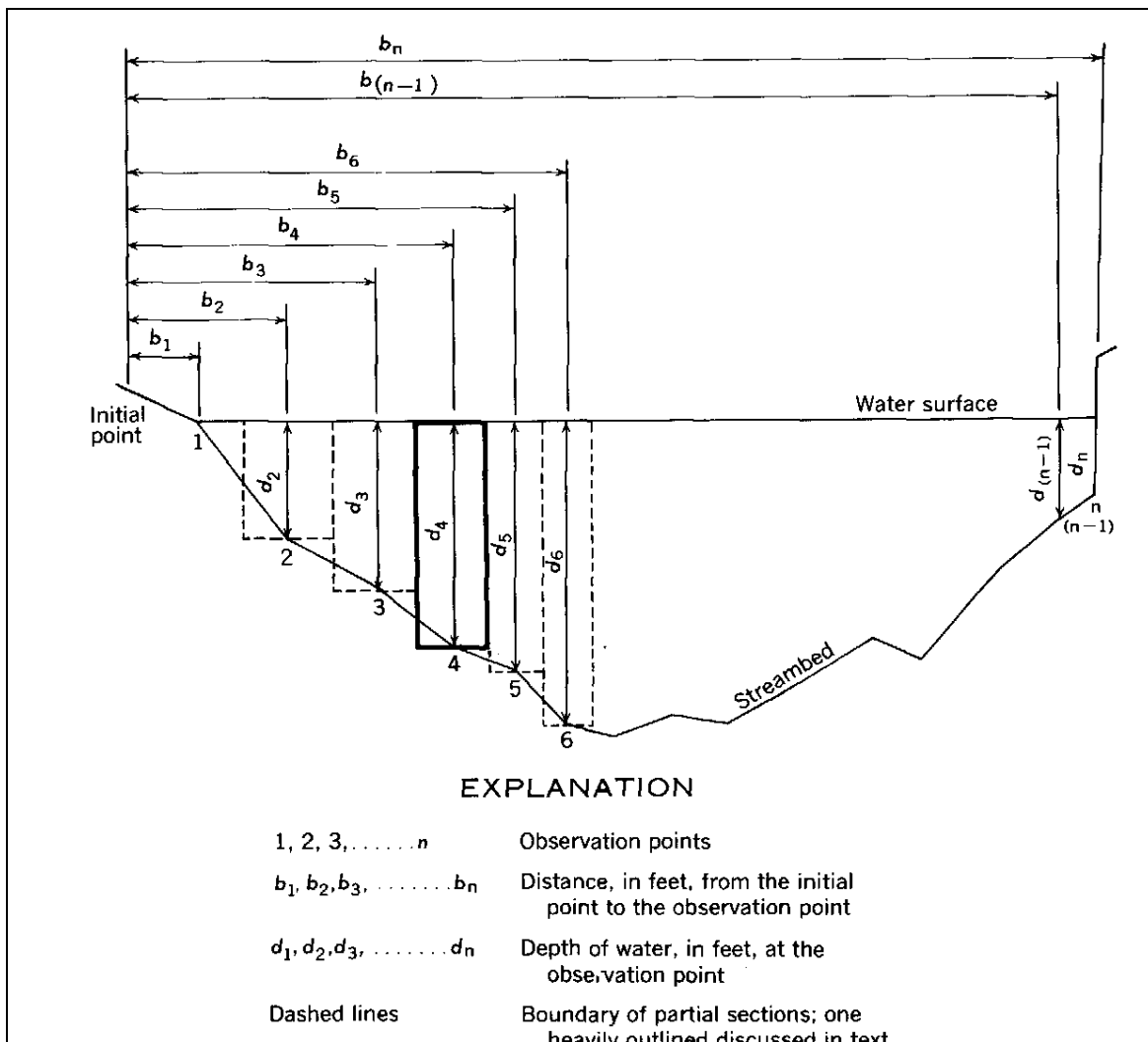


Figure 2.35. Definition sketch of computing area and discharge at a gaging station (from Buchanan and Somers 1968b).

## 2.9.4 Stage-Discharge Relation

From the recorded stage and corresponding discharge measurement of many measurements over time at a gaging station, a stage vs. discharge relation is developed. Figure 2.36 is an example of an excellent well-defined stage-discharge relation for a station with a good control. Figure 2.37 is an example of a poorly defined stage-discharge relation for a gage with a sand channel and channel control. The discharge for the first would be rated from good to excellent, and the latter from fair to poor. An additional example of a sand channel stage-discharge relation is given in Chapter 3.

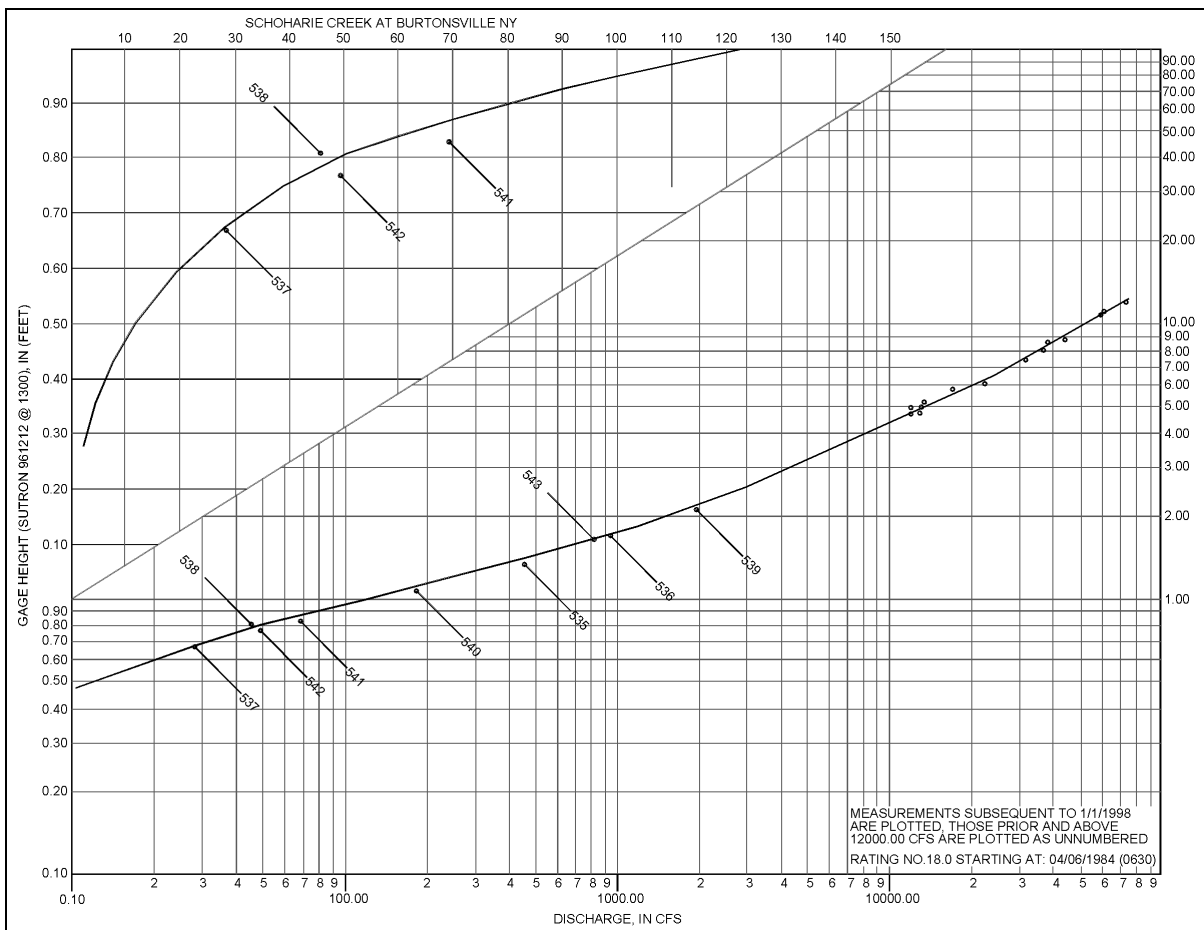


Figure 2.36. Stage-discharge relation for Schoharie Creek, New York (Butch 2000).

From the recorded stage-time record and the stage-discharge relation the daily, yearly peak, and minimum flow at the station are determined. If for a given day the stage doesn't change appreciably, the daily discharge is determined using the average gage elevation for that day. If there is a rapid change in stage with time, daily discharge is determined by converting the time-stage curve to time-discharge and by integrating over the 24 hours to determine the average daily discharge.

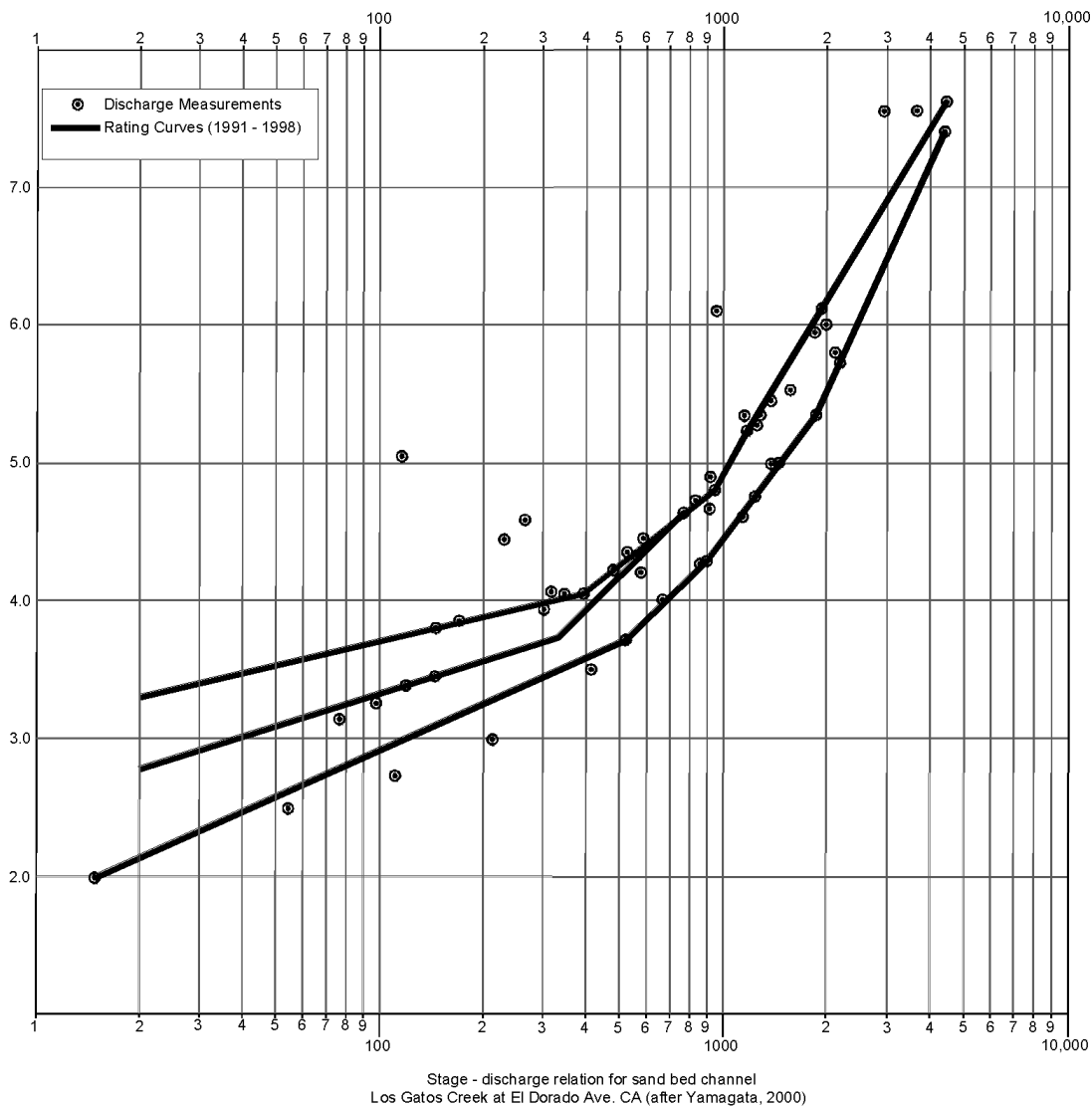


Figure 2.37. Stage-discharge relation for a sand channel (Los Gatos Creek at El Dorado Avenue, CA).

## 2.10 HYDRAULICS OF BRIDGE WATERWAYS

### 2.10.1 Introduction

As flow passes through a channel constriction most of the energy losses occur as expansion losses downstream of the contraction. This loss of energy is reflected by a rise in the water surface and the energy line upstream from the bridge. The rise in water level is referred to as the bridge backwater. Hydraulic engineers are concerned about the computation of backwater with respect to flooding upstream of the bridge. Other concerns discussed in the following chapters include the stability and scour around embankments, general scour depths due to constriction, and local scour around piers.

### **2.10.2 Backwater Effects on Waterway Openings**

It is necessary to distinguish between the following types of backwater effects.

- Backwater on a floodplain resulting from construction of a long, skewed or curved road embankment as sketched in Figure 2.38a, where the bridge opening is, in effect, located up-valley from one end of the embankment. The backwater effect along the embankment arises from ponding of water along a line running obliquely down-valley. In the case of steep rivers with wide floodplains this effect can be very large, since a large pond is created. This type of effect can be prevented by choosing a suitable location and alignment, or by providing dikes (shown on the figure) to close off the affected part of the floodplain from flood waters, or possibly by providing a relief span.
- Backwater in an incised river channel without substantial overbank flow, resulting in part from constriction of flow through an opening somewhat smaller than the natural cross section, and in part from obstructive effects of piers (Figure 2.38b). The backwater effect arising from this type is seldom large, but may be significant in developed areas.
- Backwater in a river with floodplain where the road crossing is more or less normal to the valley but the road approaches block off overbank flow (Figure 2.38c). In these cases the backwater may be significantly greater than in type b. The effect of guide banks shown in Figure 2.38c is to reduce the backwater effects by improving the hydraulic efficiency of the opening.

It is advisable to be aware of other unusual backwater effects that might occur in special circumstances, although they might never arise in ordinary bridge design practice.

### **2.10.3 Effects of a Submerged Superstructure**

If the high-water level reaches the bottom of the superstructure, the bridge will act as a short culvert. For bridges which are designed to be submersible under certain conditions, it is advisable to provide a rounded nosing on the leading edge of the girder, in order to improve the hydraulic efficiency and to reduce the tendency to catch driftwood and ice as illustrated in Figure 2.39. Also, the superstructure must be anchored to counter buoyancy.

### **2.10.4 Effects of Supercritical Flow**

In contrast to the usual drop at a constriction in subcritical flow, in supercritical flow water levels may rise suddenly at the contracted section. The phenomenon of "choking" is particularly likely if the Froude number only slightly exceeds 1.0. "Choking" may occur even in subcritical flow if the constriction is severe enough. Wider or additional openings should be designed if choking effects are expected to occur.

### **2.10.5 Types of Flow in Bridge Openings**

Three types of flow, I through III, illustrated in Figure 2.40 are often encountered in bridge waterway design. As the scale of the normal depth is the same for all flow profiles, the discharge, boundary roughness and slope of the channel must increase from Type I to Type II and to Type III.

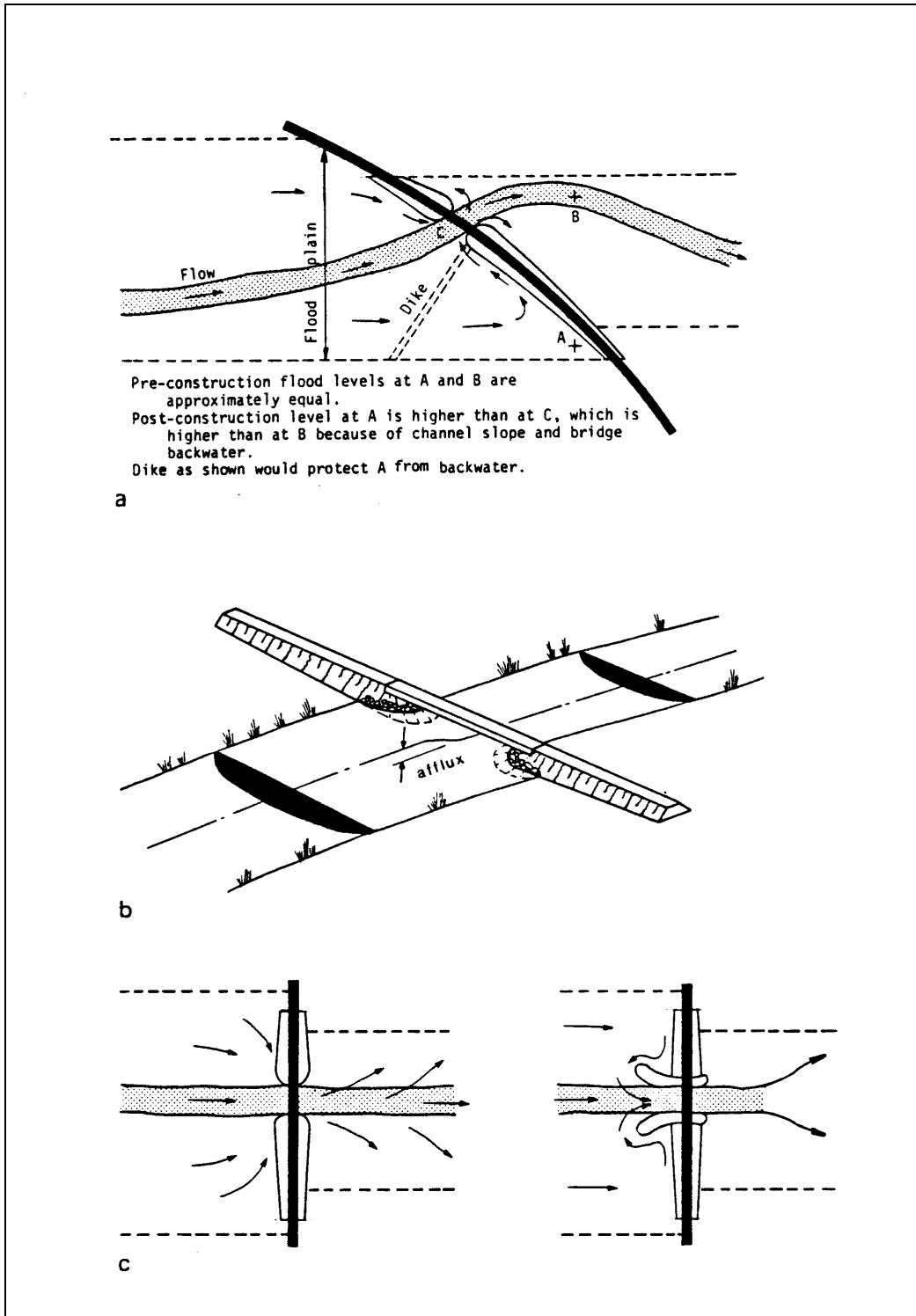


Figure 2.38. Three types of backwater effect associated with bridge crossings; (a) effect of a skewed embankment across a floodplain; (b) effect due to constriction of the channel flow; (c) effect due to constriction of the overbank flow, both without and with guide banks (after Neill 1975).



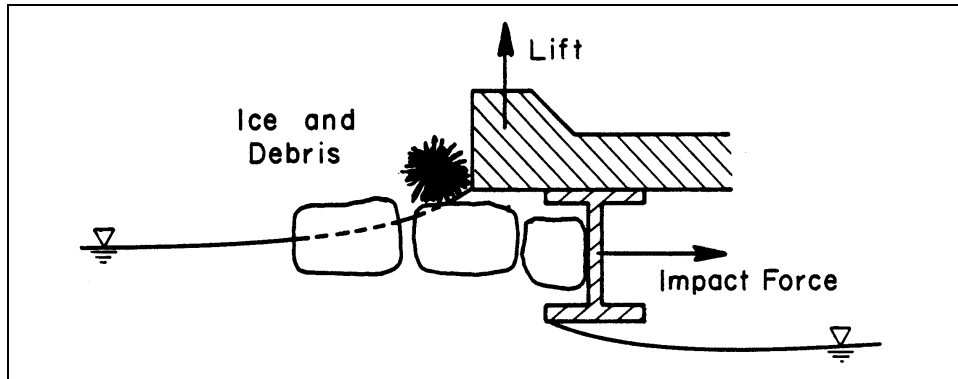


Figure 2.39. Submergence of a superstructure.

In Type I flow, the normal water surface is everywhere above critical depth and the flow is subcritical. Backwater calculations are obtained by applying the conservation of energy principle between Sections 1 and 4.

In Type II flow, subcritical flow upstream of the bridge passes through critical depth in the constriction. The backwater curve for the water surface elevation upstream from the constriction is independent of the water surface elevation downstream. An undulating hydraulic jump (with  $Fr < 2$ ) is formed when the water surface elevation dips below critical depth downstream from the contracted section (Type IIB).

Referring to Type III flow, the flow is supercritical throughout the reach as the normal water surface is everywhere below critical depth. Such conditions require steep channels as experienced in, but not limited to, mountainous regions. Backwater should not occur as long as the flow remains supercritical since the flow is controlled from upstream conditions. However, significant rise in the water surface might occur in the vicinity of the constriction due to: (1) changes in the specific energy or specific discharge diagram as indicated in Figures 2.19 and 2.21; (2) cross waves and transitions; and (3) possible hydraulic jumps near the embankments.

Solved problems are presented in Section 2.14 (SI) and 2.15 (English) to illustrate how to calculate maximum constrictions without causing backwater and to calculate water surface elevation upstream of a grade control structure.

## 2.11 COMPUTER MODELS FOR HIGHWAY BRIDGES

### 2.11.1 One-Dimensional Computer Models

Many one-dimensional computer models are available for computing water surface profiles, average depth and velocity for open channel flow. However, three have the most utility for highway bridge analysis. These are FHWA's WSPRO (Arneson and Sherman 1998). The U.S. Army Corps of Engineers (2001) HEC-RAS (River Analysis System) and UNET (Barkau 1993). HEC-RAS is the successor the Corps of Engineers HEC-2 water surface profile program. WSPRO is for steady, nonuniform flow.

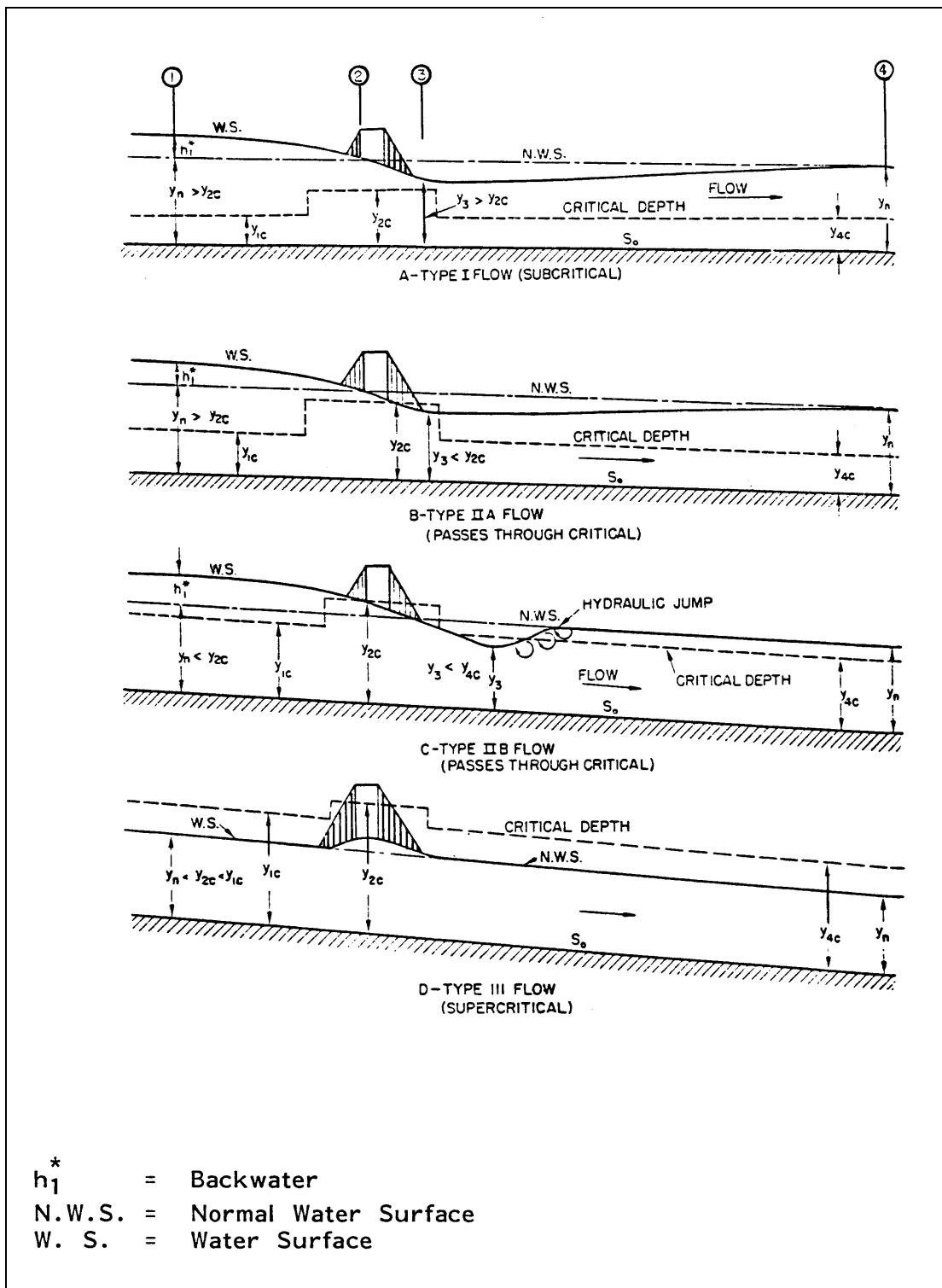


Figure 2.40. Types of flow encountered (HDS 1, Bradley 1978).

HEC-RAS performs for steady or unsteady, uniform or nonuniform flow. UNET is for unsteady, uniform, and nonuniform flow. Although one-dimensional, they can give an approximate distribution of the velocity in a cross-section. Embankment overtopping flows, in conjunction with either free surface or pressure flow through the bridge, can be computed. The programs are capable of computing profiles at stream crossings with multiple openings (including culverts), at river confluences, and mixed flow regimes. They also, incorporate the effect of wide, wooded, floodplains into the bridge backwater calculations. In addition, there are two one-dimensional computer models which include sediment transport. These are FHWA's BRI-STARS (Molinas 2000) and U.S. Army Corps of Engineers HEC-6 (1993) computer programs.

### **2.11.2 Two-Dimensional Computer Models**

Two-dimensional computer models give the water surface profile, and the depth and velocity along and across the stream. Of the many models, two have the most utility for highway bridge analysis. They are the FHWA's FESWMS (Froehlich 1996) and the U.S. Army Corps of Engineer's (1997) RMA-2V (Thomas and McAnally 1985) models. The models are for steady or unsteady and nonuniform open channel flow. They have all the capabilities of the one-dimensional programs and have the utility of giving the velocity and depth distribution along and across the channel as a function of time and distance. They can and have been used to analyze tidal flows (Zevenbergen et al. 1997, Ayres Associates 1994 and 1997, and Richardson and Lagasse 1999 pages 701 to 824) Both models require that a grid system be created for the river system. However, constructing the grid is greatly aided by the use of BYU's (2000) SMS modeling system.

## **2.12 HYDRAULICS OF CULVERT FLOW**

### **2.12.1 Introduction**

A culvert is a conduit which conveys stream flow through a roadway embankment. Most culverts are constructed of concrete, corrugated aluminum, corrugated steel, and sometimes corrugated plastics. Culvert shapes vary from circular to rectangular, and elliptical, pipe arch, arch and metal box sections are commonly used.

Two basic types of flow control are recognized depending on the location of the control section: inlet control or outlet control. The characterization of pressure, as well as subcritical and supercritical flow regimes play an important role in determining the location of the control section.

Inlet control occurs when the culvert barrel is capable of carrying more flow than the inlet will accept. Critical flow depth is located at the inlet and the flow is supercritical in the barrel.

Outlet control flow occurs when the culvert barrel is not capable of conveying as much flow as the inlet opening will accept. Under outlet control conditions, either subcritical or pressure flow exists in the culvert barrel.

The hydraulic design of culverts is given in HDS 5 (FHWA 1985) and HY8 (FHWA 1998) is a computer program for the design and analysis of culvert flows.

## 2.13 ROADWAY OVERTOPPING

Roadway overtopping will begin as the headwater rises to the elevation of the lowest point of the roadway. This type of flow is similar to flow over a broad crested weir. The length of the weir can be taken as the horizontal length across the roadway. The flow across the roadway is calculated from the broad crested weir equation

$$Q_o = K_u k_t C_r L_s (HW_r)^{1.5} \quad (2.177)$$

where:

$Q_o$	=	Overtopping discharge in $m^3/s$ ( $ft^3/s$ )
$C_r$	=	Overtopping discharge coefficient
$HW_r$	=	Flow depth above the roadway in m (ft)
$k_t$	=	Submergence factor
$L_s$	=	Length of the roadway crest along the roadway in m (ft)
$K_u$	=	1.0 (English)
$K_u$	=	$\sqrt{9.81}/\sqrt{32.2}$ or 0.552 (SI)

The charts in Figure 2.41 indicate how to evaluate the correction factors  $k_t$  and  $C_r$ .

If the elevation of the roadway crest varies, for instance where the crest is defined by a roadway sag vertical curve, the vertical curve can be approximated as a series of horizontal segments. The flow over each is calculated separately and the total flow across the roadway is the sum of the incremental flows for each segment (Figure 2.42).

The total flow across the roadway then equals the sum of the roadway overflow plus the culvert flow. A trial and error procedure is necessary to separate the amount of water passing through the culvert, if any, from the amount overtopping the roadway. Performance curves must then include both culvert flow and road overflow.

## 2.14 SOLVED PROBLEMS OPEN CHANNEL FLOW (SI)

### 2.14.1 PROBLEM 1 Evaluation of Correction Factors $\alpha$ and $\beta$

Calculate the correction factors  $\alpha$  and  $\beta$  for a cross-section given the discharge measurement during the peak flood event for the year. From Table 2.4, the following values are obtained:

$Q$	=	152.41 cms
$A$	=	138.20 $m^2$
$W$	=	49.71 m
$\sum V_i \Delta Q_i$	=	180.46 $m^4/sec^2$
$\sum V_i^2 \Delta Q_i$	=	220.88 $m^5/sec^3$

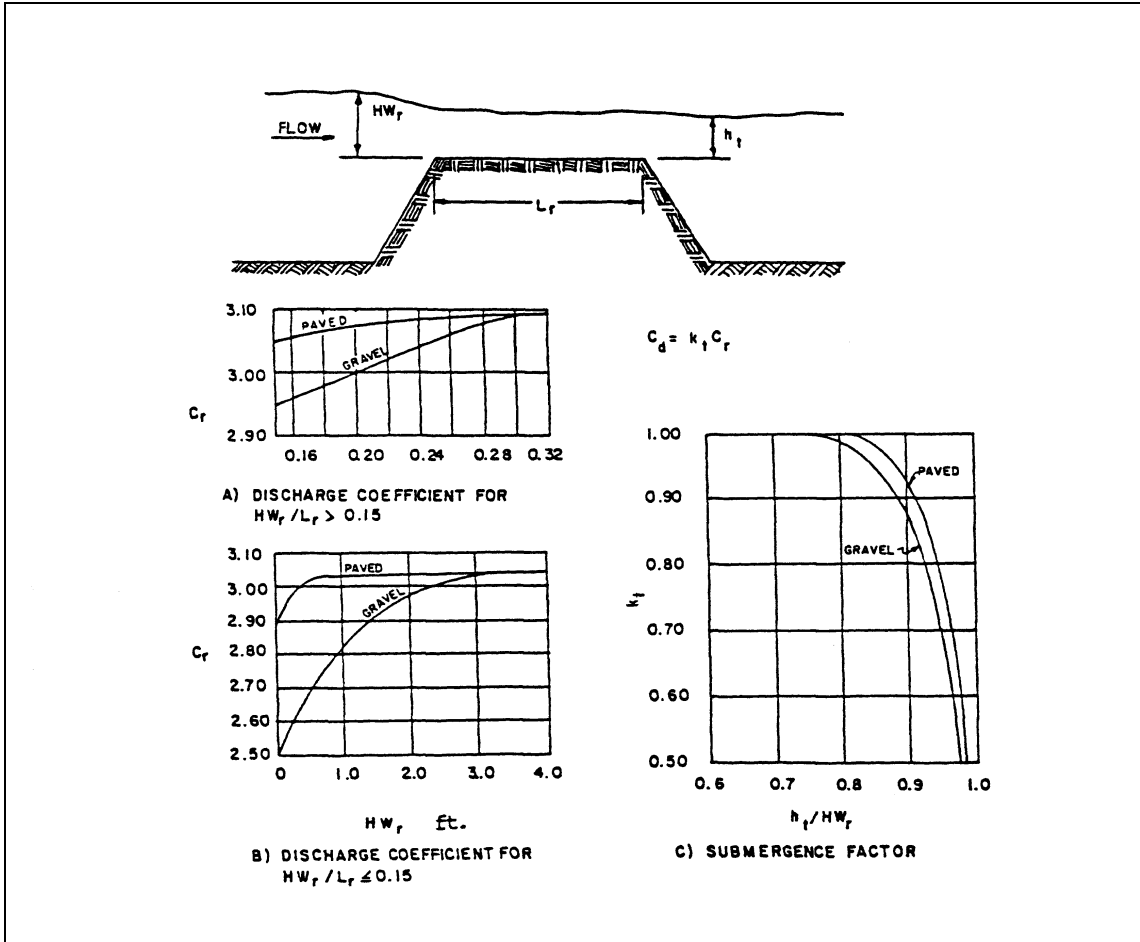


Figure 2.41. Discharge coefficient for roadway overtopping (after Petersen 1986).

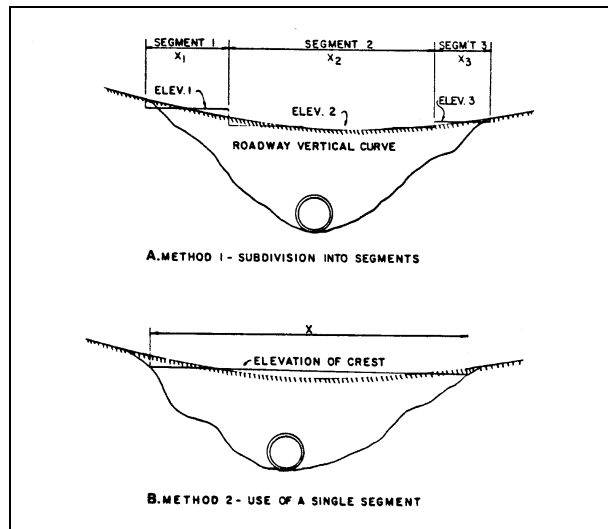


Figure 2.42. Weir crest length determinations for roadway overtopping.

Table 2.4. Discharge measurement notes <sup>1</sup> .						
$y_{oi}$ (m)	$\Delta z_i$ (m)	$V_i$ (mps)	$\Delta A_i$ (sq m)	$\Delta Q_i$ (cms)	$V_i \Delta Q_i$ (m <sup>4</sup> /sec <sup>2</sup> )	$V_i^2 \Delta Q_i$ (m <sup>5</sup> /sec <sup>3</sup> )
0.80	1.22	0.00	0.0	0.000	0.000	0.000
0.335	2.44	0.300	0.818	0.245	0.074	0.022
.793	2.44	0.165	1.93	.319	.053	.009
1.37	2.44	.195	3.34	.651	.127	.025
2.59	2.44	.732	6.32	4.626	3.386	2.479
3.35	2.44	.966	8.17	7.892	7.624	7.365
3.54	2.44	1.23	8.64	10.627	13.071	16.078
3.66	2.44	1.24	8.93	11.073	13.731	16.026
3.90	2.44	1.15	9.52	10.948	12.590	14.479
3.84	2.44	1.14	9.37	10.682	12.178	13.882
3.78	2.44	1.15	9.22	10.603	12.194	14.023
3.54	2.44	1.44	8.64	12.442	17.917	25.800
3.47	2.44	1.31	8.47	11.096	12.539	14.169
3.29	2.44	1.49	8.03	11.965	17.828	26.564
3.23	2.44	1.41	7.88	11.111	15.667	22.090
3.32	2.44	1.32	8.10	10.692	14.113	18.630
3.54	2.44	1.19	8.64	10.282	12.236	14.560
3.60	2.44	.945	8.78	8.297	7.841	7.409
2.99	2.44	.921	7.30	6.723	6.192	5.703
1.95	2.13	.515	4.15	2.137	1.101	.567
1.16	1.68	0.0	1.95	0.0	0.0	0.0
0.0	.76	0.0	0.0	0.0	0.0	0.0
TOTAL	49.71		138.20	152.411	180.462	220.88

<sup>1</sup>Simons, D.B., E.V. Richardson, M.A. Stevens, J.H. Duke, and V.C. Duke, "Stream flow, groundwater and ground response data, Hydrology Report, Vol. II, Venezuelan International Meteorological and Hydrological Experiment, Civil Engineering Dept., Colorado State University, August 1971.

The bed material at this gaging station has a  $D_{50}$  of 0.33 mm and a  $D_{65}$  of 0.45 mm and a gradation coefficient  $G$  of 3.27. If the value of  $D_{65}$  is used for  $k_s$ , then for  $y_o = 3.90$  m (the maximum depth)

$$\frac{y_o}{k_s} = \frac{3.9}{0.00045} \cong 8,700$$

and for  $y_o = .335$  m (the smallest non-zero depth)

$$\frac{y_o}{k_s} = \frac{0.335}{0.00045} \cong 750$$

Using a mean  $y_o/k_s$  of approximately 5,000, then from Figure 2.12 the average values for the energy and momentum coefficients are:

$\alpha' = 1.024$   
and  
 $\beta' = 1.008$

As it has been assumed that  $\alpha'$  and  $\beta'$  are constant across the river (for convenience), Equations 2.113 and 2.114 become:

$$\alpha = \alpha' \frac{A^2}{Q^3} \sum_i V_i^2 \Delta Q_i$$

and

$$\beta = \beta' \frac{A}{Q^2} \sum_i V_i^2 \Delta Q_i$$

With the values in Table 2.4

$$\alpha = 1.024 \frac{(138.2)^2}{(152.4)^3} (220.9) = 1.221$$

$$\beta = 1.008 \frac{(138.2)}{(152.4)^2} (180.5) = 1.083$$

These values for  $\alpha$  (1.22) and  $\beta$  (1.083) differ from unity by appreciable amounts. The difference may be important in many river channel calculations. If no data are available, the assumptions that  $\alpha = 1.22$  and  $\beta = 1.1$  should be used for river channels.

### 2.14.2 PROBLEM 2 Velocity Profiles and Shear Stress

A velocity and discharge measurement is made on the Missouri River at Sioux City. The total discharge is 923.1 cms. The average depth is 2.38 meters and the average velocity is 0.738 m/sec in a vertical section at a point 244 meters from the right bank. The velocity measurements at various distances from the bottom ( $y$ ) are shown in Table 2.5.

Also during this measurement the slope of the energy grade line was observed as 0.000206 and the bed material gradation was determined with  $D_{50} = 0.270$  mm,  $D_{65} = 0.315$  mm and  $D_{84} = 0.42$  mm.

$y$ (m)	Observed Velocity (m/sec)
0.152	0.518
0.305	0.633
0.457	0.701
0.762	0.762
1.07	0.838
1.37	0.884
1.68	0.945
1.70	0.945
2.29	0.991

## Velocity Profile Analysis

The log and power function velocity distribution functions will be used to obtain a mathematical description of the velocity profile.

### (a) Logarithmic Velocity Distribution Equation

The log velocity relation is Equation 2.75:

$$v/V_* = 1/k \ln (y/y') = 2.31/k \log (y/y')$$

Determine the value of  $k$  and  $y'$ :

$$V_* = (g y_o S_f)^{1/2} = (9.81 \times 2.38 \times 0.000206)^{1/2} = 0.069 \text{ m/sec}$$

Table 2.6 is prepared for both log and power forms with the values shown.

Using regression techniques for the logarithmic form of the equation on the values of  $v/V_*$  and  $\ln y'$  with the data in Table 2.6, obtain:

$v/V_* = 2.564 (\ln y - \ln 0.009)$  with a regression coefficient  $R = 0.996$  giving the values of  $k = 0.39$  and  $y' = 0.009$ . The final equation for the data is

$$v/V_* = 2.564 \ln (y/0.009)$$

y (m)	v (m/s)	v/V*	v/V	y/y <sub>o</sub>
0.152	0.518	7.51	0.702	0.064
0.305	0.633	9.17	0.858	0.128
0.457	0.701	10.16	0.950	0.192
0.762	0.762	11.04	1.033	0.321
1.07	0.838	12.14	1.136	0.449
1.37	0.884	12.81	1.198	0.577
1.68	0.945	13.70	1.281	0.705
1.90	0.945	13.70	1.281	0.801
2.29	0.991	14.36	1.340	0.962

### (b) Power Velocity Distribution Equation

The power form of the velocity distribution equation is:

$$v/V = a (y/y_o)^b$$

To simplify the regression calculations take the  $\ln$  transform giving:

$\ln v/V = \ln a + b \ln (y/y_o)$  using linear regression of  $\ln v/V$  vs  $\ln (y/y_o)$  calculate the values of  $a$  and  $b$ .

The results are:

$$\begin{aligned} a &= 1.368 \\ b &= 0.240 \\ R &= 0.998 \end{aligned}$$



The resulting power equation is:

$$v/0.738 = 1.37 (y/y_0)^{0.24}$$

### Shear Stress Analysis

Using the above information calculate the shear stress on the bed using the several methods given in Section 2.4.5.

#### (a) Average Shear Stress on the Bed

Calculate the average shear stress on the bed using Equation 2.97

$$\tau_0 = \gamma R S_f = 9800 \times 2.38 \times 0.000206 = 4.805 \text{ N/m}^2$$

Using  $R = y_0$  (for a wide channel)

#### (b) Local Shear Stress on the Bed Using Single Point Velocity near the Bed

Using the above information and the logarithmic velocity distribution equation derived from Equation 2.75 ( $v/V_* = 2.564 \ln (y/0.009)$ ) the shear stress on the bed using a single point velocity near the bed is:

$$\tau_0 = \frac{\rho v^2}{\left[2.564 \ln \frac{y}{0.009}\right]^2} = \frac{1000 (0.518)^2}{\left[2.564 \ln \frac{0.152}{0.009}\right]^2} = 5.11 \text{ N/m}^2$$

#### (c) Local Shear Stress on the Bed Using Two Point Velocities near the Bed

For this determination use Equation 2.99

$$\tau_0 = \frac{\rho (v_1 - v_2)^2}{\left[5.75 \log \frac{y_1}{y_2}\right]^2} = \frac{1000 (0.633 - 0.518)^2}{\left[5.75 \log \frac{0.305}{0.152}\right]^2} = 4.37 \text{ N/m}^2$$

#### (d) Shear Stress on the Bed Using Average Vertical Velocity

Using Equation 2.100 and the average depth 2.38 m, average velocity 0.738 m/sec, and a value for  $k_s$  determine the average shear stress on the bed.

Taking  $k_s$  as  $(30.2) y' = 0.27 \text{ m}$

$$\tau_0 = \frac{\rho (V)^2}{\left[5.75 \log \frac{12.27 y_0}{k_s}\right]^2} = \frac{1000 (0.738)^2}{\left[5.75 \log \frac{12.27 \times 2.38}{0.27}\right]^2} = 3.98 \text{ N/m}^2$$

(e) Summary

The average shear stress on the boundary from (a) is 4.805 newtons per square meter. This is the average stress on the entire boundary (bed and banks). The shear stress computed using velocity is the local shear stress on the bed where the velocity profile was taken. This local shear stress is calculated as 5.11 in (b), 4.37 in (c), and 3.98 in (d). Normally the use of the two point velocity equation with the velocities close to the bed is the more accurate, however, very accurate velocity measurements are required. For this example, the value from the two velocity method appears to be low. For wide channels the centerline local shear stress on the bed should generally not be lower than the average shear stress on the boundary (i.e., the value of 4.805 newtons per square meter).

**2.14.3 PROBLEM 3 Superelevation in Bends**

Calculate the superelevation of the water surface in a river bend given the velocity profile from Table 2.4. The river radius of curvature  $r_i$  is measured equal to 106.7 meters and the outer radius of curvature  $r_o$  is 156.4 meters. The detailed calculations based on Equation 2.158 are presented in Table 2.7.

Table 2.7. Detailed Computation of Superelevation in Bends.			
$\Delta r_i$ (m)	$r_i$ (m)	$V_i$ (m/s)	$\Delta Z_i = \frac{V_i^2}{g r_i} \Delta r_i$ (m)
0.61	107.3	0.00	.0000
1.82	109.1	0.300	.0002
2.44	111.6	.165	.0001
2.44	114.0	.195	.0001
2.44	116.4	.732	.0011
2.44	118.9	.966	.0020
2.44	121.3	1.23	.0031
2.44	123.7	1.24	.0031
2.44	126.2	1.15	.0026
2.44	128.6	1.14	.0025
2.44	131.1	1.15	.0025
2.44	133.5	1.44	.0038
2.44	136.0	1.31	.0031
2.44	138.4	1.49	.0040
2.44	140.9	1.41	.0035
2.44	143.3	1.32	.0030
2.44	145.8	1.19	.0024
2.44	148.2	.945	.0015
2.44	150.6	.921	.0014
2.44	153.1	.515	.0004
1.68	154.8	0.00	.0000
0.76	155.6	0.00	.0000
Total $\Delta Z$			0.0404 m

$$\Delta Z = \frac{1}{g} \sum_{r_i}^{r_o} \frac{V^2}{r} \Delta r$$

Total superelevation is 0.040 meters.

Based on relationships,  $V = Q/A = 1.10$  m/s, the following are obtained:

#### Woodward's Equation 2.160

$$\Delta Z = \frac{V^2}{g r_c} (r_o - r_i) = \frac{(1.10)^2}{9.81(131.4)} (156.4 - 106.7) = 0.047 \text{ m}$$

#### Ippen and Drinker's Equation 2.162

$$\Delta Z = \frac{V^2}{2g} \frac{2W}{r_c} \left[ \frac{1}{1 - \left(\frac{W}{2r_c}\right)^2} \right] = \frac{1.10^2}{2 \times 9.81} \times \frac{2 \times 49.7}{131.4} \left[ \frac{1}{1 - \left(\frac{49.7}{2 \times 131.4}\right)^2} \right] = 0.042 \text{ m}$$

#### Ippen and Drinker's Equation 2.163

$$\Delta Z = \frac{V^2}{2g} \frac{2W}{r_c} \left[ \frac{1}{1 - \frac{W^2}{12 r_c^2}} \right] = \frac{1.10^2}{2 \times 9.81} \times \frac{2 \times 49.7}{131.4} \left[ \frac{1}{1 - \frac{4.97^2}{12 \times 131.4^2}} \right] = 0.041 \text{ m}$$

#### Combined Free and Forced Vortex Equation 2.165

$$V_{\max} = 1.49 \text{ m/s}$$

$$\Delta Z = \frac{(V_{\max})^2}{2g} \left[ 2 - \left(\frac{r_i}{r_c}\right)^2 - \left(\frac{r_c}{r_o}\right)^2 \right] = \frac{1.49^2}{2 \times 9.81} \left[ 2 - \left(\frac{106.7}{131.4}\right)^2 - \left(\frac{131.4}{156.4}\right)^2 \right] = 0.0718 \text{ m}$$

The equations give comparable results (0.040 to 0.0718 m). Equation 2.158 which integrates across the section using the velocity distribution is the most exact. But using the value 0.072 m provides a safety factor.

#### 2.14.4 PROBLEM 4 Maximum Stream Constriction Without Causing Backwater (Neglecting Energy Losses)

A stream is rectangular in shape and 30.48 m wide. The design discharge is 141.6 cms and the uniform depth for this discharge is 3.05 m. Neglecting energy losses what is the maximum amount of constriction that a bridge can impose without causing backwater.

The upstream flow rate per unit width (q) is:

$$q = \frac{Q}{W} = \frac{141.6}{30.48} = 4.65 \text{ cfs / ft}$$

The average velocity (V) is:

$$V = \frac{Q}{A} = \frac{141.6}{92.96} = 1.52 \text{ m/s}$$

The specific head (H) is:

$$H = \frac{V^2}{2g} + y = \frac{1.52^2}{19.62} + 3.05 = 3.17 \text{ m}$$

According to Section 2.6.2 the maximum unit discharge for a given specific head (specific head equals to a constant) occurs at the critical depth  $y_c$  where the Froude number is 1. From Equation 2.149 the critical depth  $y_c$  for this specific head is:

$$y_c = \left( \frac{q_{\max}^2}{g} \right)^{1/3} = \frac{2}{3} H = \frac{2 V_c^2}{2g}$$

$$q_{\max} = \left[ g \left( \frac{2}{3} H \right)^3 \right]^{1/2} = \left[ 9.81 \left( \frac{2}{3} \times 3.17 \right)^3 \right]^{1/2} = 9.63 \text{ m}^3 / \text{s} / \text{m}$$

Therefore, the width of the channel can be contracted until the unit discharge q is a maximum. The minimum width (maximum constriction) is:

$$W_{\min} = \frac{Q}{q_{\max}} = \frac{141.6}{9.63} = 14.70 \text{ m}$$

and the maximum constriction is  $30.48 - 14.70 = 15.8 \text{ m}$

This contraction causes the flow to go to critical. This results in an undulating hydraulic jump downstream. Also, when energy losses are considered there will be some backwater at the constriction.

#### **2.14.5 PROBLEM 5 Maximum Water Surface Elevation Upstream of a Grade Control Structure Without Backwater (Neglecting Energy Losses)**

A low grade control structure (check dam) is to be placed across a stream downstream of a highway bridge. The stream is degrading. The purpose of the check dam is to maintain the elevation of the water surface at the bridge, cause deposition of bed material, protect the abutments and piers from long term degradation and contraction scour and increase the elevation of the be for

local scour. There is to be no increase in water surface elevation upstream of the bridge at the design discharge. The energy losses are expected to be small so they can be neglected.

At the bridge, the design flood discharge is 141.6 cms. The river is 30.48 m wide and has a uniform flow depth of 3.05 m for the design discharge.

**What is the maximum height of the structure that will not cause backwater at the bridge at the design discharge?**

The unit discharge ( $q$ ) in the river at design flood discharge is:

$$q = \frac{Q}{W} = \frac{141.6}{30.48} = 4.65 \text{ m}^3/\text{s}/\text{m}$$

The average velocity ( $V$ ) is

$$V = \frac{Q}{A} = \frac{141.6}{92.96} = 1.52 \text{ m/s}$$

The specific head ( $H$ ) is

$$H = \frac{V^2}{2g} + y = \frac{1.52^2}{19.62} + 3.05 = 3.17 \text{ m}$$

As a first approximation assume no energy loss in the bridge reach. Then at the check dam, the elevation of the total energy line is 3.17 m above the bed (Figure 2.43). At the dam:

$$H_{\min} + \Delta Z_{\max} = 3.17 \text{ m}$$

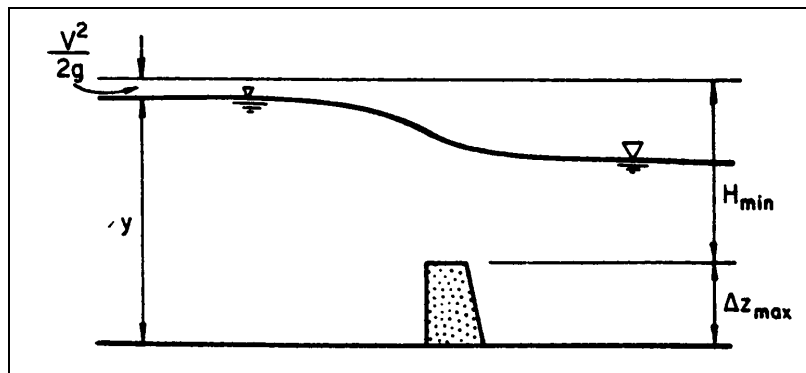


Figure 2.43. Sketch of backwater curve over check dam.

That is, the dam can be built to a height of  $\Delta Z_{\max}$  which decreases the specific head at the dam to  $H_{\min}$ . From Section 2.6.3 and Equation 2.147

$$H_{\min} = \frac{3}{2} y_c$$

From Equation 2.140

$$y_c = \left[ \frac{q^2}{g} \right]^{1/3} = \left[ \frac{4.65^2}{9.81} \right]^{1/3} = 1.30 \text{ m}$$

Then

$$H_{\min} = \frac{3}{2} y_c = \frac{3}{2} 1.30 \text{ m} = 1.95 \text{ m}$$

and

$$\Delta Z_{\max} = 3.17 - 1.95 = 1.22 \text{ m}$$

If the structure is built to a crest elevation 1.22 m above the bed, critical flow will occur at the dam for a flow of 141.6 cms and the dam will cause no backwater. At lower discharges the check dam will cause backwater. However, discharges larger than 141.6 cms at the check dam will not cause backwater. Local scour downstream of the check dam should be evaluated (see HEC-23).

**How much backwater will the dam cause for a flow of 28.37 m<sup>3</sup>/s if the normal depth for this discharge is 1.52 m and the dam height is 1.22 m?**

Upstream of the dam the discharge for foot of width (q) is,

$$q = \frac{Q}{W} = \frac{28.32}{30.48} = 0.93 \text{ m}^3 / \text{s} / \text{m}$$

The average velocity (V) is

$$V = \frac{q}{y} = \frac{0.93}{1.52} = 0.61 \text{ m} / \text{sec}$$

At the check dam the flow is critical so from Equation 2.140

$$y_c = \left[ \frac{q^2}{g} \right]^{1/3} = \left[ \frac{0.93^2}{9.81} \right]^{1/3} = 0.45 \text{ m}$$

and from Equation 2.144

$$H_{\min} = \frac{3}{2} y_c = \frac{3}{2} 0.45 \text{ m} = 0.67 \text{ m}$$

Assuming no energy loss, the specific head upstream of the dam is

$$H = H_{\min} + \Delta Z = 0.67 + 1.22 = 1.89 \text{ m}$$

To determine the depth of flow upstream of the dam ( $y$ ) solve the specific head equation (Equation 2.137)

$$H = \frac{q^2}{2gy^2} + y = \frac{0.93^2}{19.62y^2} = 1.89 \text{ m}$$

or

$$y^3 - 1.89y^2 + \frac{0.93^2}{19.62} = 0$$

The solution is

$$y = 1.87 \text{ m}$$

As the normal depth is only 1.52 m, the backwater is

$$\Delta y = 1.87 - 1.52 = 0.35 \text{ m}$$

That is, the depth upstream of the dam is increased 0.35 m by the 1.22 m high dam when the flow is 28.32 cms.

## 2.15 SOLVED PROBLEMS OPEN CHANNEL FLOW (ENGLISH)

### 2.15.1 PROBLEM 1 Evaluation of Correction Factors $\alpha$ and $\beta$

Calculate the correction factors  $\alpha$  and  $\beta$  for a cross-section given the discharge measurement during the peak flood event for the year. From Table 2.8, the following values are obtained:

$$\begin{aligned} Q &= 5,370 \text{ cfs} \\ A &= 1,485 \text{ ft}^2 \\ W &= 163 \text{ ft} \\ \sum V_i \Delta Q_i &= 21,070 \text{ ft}^4/\text{sec}^2 \\ \sum V_i^2 \Delta Q_i &= 85,500 \text{ ft}^5/\text{sec}^3 \end{aligned}$$

The bed material at this gaging station has a  $D_{50}$  of 0.33 mm and a  $D_{65}$  of 0.45 mm and a gradation coefficient  $G$  of 3.27. If the value of  $D_{65}$  is used for  $k_s$ , then for  $y_0 = 12.8$  ft (the maximum depth)

$$\frac{y_0}{k_s} = \frac{12.8}{0.45} (304.8) \cong 8,700$$

and for  $y_0 = 1.1$  ft (the smallest non-zero depth)

$$\frac{y_0}{k_s} = \frac{1.1}{0.45} (304.8) \cong 750$$

Using a mean  $y_o/k_s$  of approximately 5,000, then from Figure 2.12 the average values for the energy and momentum coefficients are:

$$\alpha' = 1.024$$

and

$$\beta' = 1.008$$

As it has been assumed that  $\alpha'$  and  $\beta'$  are constant across the river (for convenience), Equations 2.113 and 2.114 become:

$$\alpha = \alpha' \frac{A^2}{Q^3} \sum_i V_i^2 \Delta Q_i$$

$y_{oi}$ (ft)	$\Delta z_i$ (ft)	$V_i$ (fps)	$\Delta A_i$ (sq ft)	$\Delta Q_i$ (cfs)	$V_i \Delta Q_i$ (ft <sup>4</sup> /sec <sup>2</sup> )	$V_i^2 \Delta Q_i$ (ft <sup>5</sup> /sec <sup>3</sup> )
0.0	4.0	0.00	0.0	0.00	0.00	0.00
1.1	8.0	0.98	8.8	8.62	8.45	8.28
2.6	8.0	0.54	20.8	11.23	6.06	3.27
4.5	8.0	0.64	36.0	23.04	14.75	9.44
8.5	8.0	2.40	68.0	163.20	391.68	940.03
11.0	8.0	3.17	88.0	278.96	884.30	2803.24
11.6	8.0	4.02	92.8	373.06	1499.70	6028.80
12.0	8.0	4.06	96.0	389.76	1582.43	6424.65
12.8	8.0	3.78	102.4	387.07	1463.12	5530.61
12.6	8.0	3.74	100.8	376.99	1409.94	5273.19
12.4	8.0	3.78	99.2	374.98	1417.42	5357.86
11.6	8.0	4.71	92.8	437.09	2058.69	9696.45
11.4	8.0	4.30	91.2	392.16	1686.29	7251.04
10.8	8.0	4.90	86.4	423.36	2074.46	10164.87
10.6	8.0	4.63	84.8	392.62	1817.83	8416.56
10.9	8.0	4.32	87.2	376.70	1627.34	7030.13
11.4	8.0	3.89	91.2	354.77	1380.06	5368.42
11.8	8.0	3.10	94.4	292.64	907.18	2812.27
9.8	8.0	3.02	78.4	236.77	715.05	2159.44
6.4	7.0	1.69	44.8	75.71	127.95	216.24
3.8	5.5	0.0	20.9	0.0	0.0	0.0
0.0	2.5	0.0	0.0	0.0	0.0	0.0
TOTAL	163.0		1484.9	5368.74	21072.71	85494.77

<sup>1</sup>Simons, D.B., E.V. Richardson, M.A. Stevens, J.H. Duke, and V.C. Duke, "Stream flow, groundwater and ground response data, Hydrology Report, Vol. II, Venezuelan International Meteorological and Hydrological Experiment, Civil Engineering Dept., Colorado State University, August 1971.



and

$$\beta = \beta \frac{A}{Q^2} \sum V_i^2 \Delta Q_i$$

With the values in Table 2.8

$$\alpha = 1.024 \frac{(1,485)^2}{(5,369)^3} (85,490) = 1.247$$

$$\beta = 1.008 \frac{(1,485)}{(5,369)^2} (21,070) = 1.094$$

These values for  $\alpha$  (1.247) and  $\beta$  (1.094) differ from unity by appreciable amounts. The difference may be important in many river channel calculations. If no data are available, the assumptions that  $\alpha = 1.25$  and  $\beta = 1.1$  should be used for river channels.

### 2.15.2 PROBLEM 2 Velocity Profiles and Shear Stress

A velocity and discharge measurement is made on the Missouri River at Sioux City, Iowa. The total discharge is 32,600 cfs. The average depth is 7.80 feet and the average velocity is 2.42 ft/sec in a vertical section at a point 800 feet from the right bank. The velocity measurements at various distances from the bottom ( $y$ ) are shown in Table 2.9.

$y$ (ft)	Observed Velocity (ft/sec)
0.5	1.70
1.0	2.08
1.5	2.30
2.5	2.50
3.5	2.75
4.5	2.90
5.5	3.10
6.25	3.10
7.5	3.25

Also during this measurement the slope of the energy grade line was observed as 0.000206 and the bed material gradation was determined with  $D_{50} = 0.270$  mm, and  $D_{65} = 0.315$  mm.

#### Velocity Profile Analysis

The log and power function velocity distribution functions will be used to obtain a mathematical description of the velocity profile.

(a) Logarithmic Velocity Distribution Equation

The log velocity relation is Equation 2.75:

$$v/V^* = 1/k \ln (y/y') = 2.31/k \log (y/y')$$

Determine the value of k and y':

$$V^* = (g y_0 S_f)^{1/2} = (32.2 \times 7.80 \times 0.000206)^{1/2} = 0.228 \text{ ft/sec}$$

Table 2.10 is prepared for both log and power forms with the values shown.

Using regression techniques, for the logarithmic form of the equation on the values of  $V/V^*$  and  $\ln y'$  with the data in Table 2.10 obtain:

$v/V^* = 2.564 (\ln y - \ln 0.03)$  with a regression coefficient  $R = 0.996$  giving the values of  $k = 0.39$  and  $y' = 0.03$ . The final equation for the data is

$$v/V^* = 2.564 \ln (y/0.03)$$

y (ft)	v (ft/s)	$v/V^*$	$v/V$	$y/y_0$
0.50	1.70	7.46	0.702	0.064
1.00	2.08	9.12	0.860	0.128
1.50	2.30	10.09	0.950	0.192
2.50	2.50	10.96	1.033	0.321
3.50	2.75	12.06	1.136	0.449
4.50	2.90	12.71	1.198	0.577
5.50	3.10	13.60	1.281	0.705
6.25	3.10	13.60	1.281	0.801
7.50	3.25	14.25	1.340	0.962

(b) Power Velocity Distribution Equation

The power form of the velocity distribution equation is:

$$v/V = a (y/y_0)^b$$

To simplify the regression calculations take the  $\ln$  transform giving:

$\ln v/V = \ln a + b \ln (y/y_0)$  using linear regression of  $\ln v/V$  vs  $\ln (y/y_0)$  calculate the values of a and b. The results are:

$$\begin{aligned} a &= 1.368 \\ b &= 0.240 \\ R &= 0.998 \end{aligned}$$

The resulting power equation is:

$$v/2.42 = 1.38 (y/y_0)^{0.24}$$

## Shear Stress Analysis

Using the above information calculate the shear stress on the bed using the several methods given in Section 2.4.5.

### (a) Average Shear Stress on the Bed

Calculate the average shear stress on the bed using Equation 2.97

$$\tau_0 = \gamma R S_f = 62.4 \times 7.8 \times 0.000206 = 0.100 \text{ lb/ft}^2$$

Using  $R = y_o$  (for a wide channel)

### (b) Local Shear Stress on the Bed Using Single Point Velocity near the Bed

Using the above information and the logarithmic velocity distribution equation derived from Equation 2.75 ( $v/V_* = 2.564 \ln(y/0.03)$ ) the shear stress on the bed using a single point velocity near the bed is:

$$\tau_0 = \frac{\rho v^2}{\left[2.564 \ln \frac{y}{0.03}\right]^2} = \frac{1.94 (1.70)^2}{\left[2.564 \ln \frac{0.5}{0.03}\right]^2} = 0.108 \text{ lb/ft}^2$$

### (c) Local Shear Stress on the Bed Using Two Point Velocities near the Bed

For this determination use Equation 2.99

$$\tau_0 = \frac{\rho (v_1 - v_2)^2}{\left[5.75 \log \frac{y_1}{y_2}\right]^2} = \frac{1.94 (2.08 - 1.70)^2}{\left[5.75 \log \frac{1.0}{0.5}\right]^2} = 0.094 \text{ lb/ft}^2$$

### (d) Shear Stress on the Bed Using Average Vertical Velocity

Using Equation 2.100 and the average depth 7.80 ft, average velocity 2.42 ft/sec, and a value for  $k_s$  determine the average shear stress on the bed.

Taking  $k_s$  as  $(30.2) y' = 0.91$

$$\tau_0 = \frac{\rho (V)^2}{\left[5.75 \log \frac{12.27 y_o}{k_s}\right]^2} = \frac{1.94 (2.42)^2}{\left[5.75 \log \frac{12.27 \times 7.8}{0.91}\right]^2} = 0.084 \text{ lb/ft}^2$$

(e) Summary

The average shear stress on the boundary from (a) is 0.10 pound per square foot. This is the average stress on the entire boundary (bed and banks). The shear stress computed using velocity is the local shear stress on the bed where the velocity profile was taken. This local shear stress is calculated as 0.108 in (b), 0.094 in (c), 0.084, in (d). Normally the use of the two point velocity equation with the velocities close to the bed is the more accurate, however, very accurate velocity measurements are required. For this example, the value from the two velocity method appears to be low. For wide channels for the centerline local shear stress on the bed should generally not be lower than the average shear stress on the boundary, i.e., the value of 0.10 pounds per square foot.

**2.15.3 PROBLEM 3 Superelevation in Bends**

Calculate the superelevation of the water surface in a river bend given the velocity profile from Table 2.8. The river inner radius of curvature  $r_i$  is measured equal to 350 feet and the outer radius of curvature  $r_o$  is 513 feet. The detailed calculations based on Equation 2.158 are presented in Table 2.11.

Table 2.11. Detailed Computation of Superelevation in Bends.			
$\Delta r_i$ (ft)	$r_i$ (ft)	$V_i$ (ft/s)	$\Delta Z_i = \frac{V_i^2}{gr_i} \Delta r_i$ (ft)
2.0	352	0.00	.0000
6.0	358	0.98	.0005
8.0	366	0.54	.0002
8.0	374	0.64	.0003
8.0	382	2.40	.0037
8.0	390	3.17	.0064
8.0	398	4.02	.0101
8.0	406	4.06	.0101
8.0	414	3.78	.0086
8.0	422	3.74	.0082
8.0	430	3.78	.0083
8.0	438	4.71	.0126
8.0	446	4.30	.0103
8.0	454	4.90	.0131
8.0	462	4.63	.0115
8.0	470	4.32	.0099
8.0	473	3.89	.0079
8.0	486	3.10	.0049
8.0	494	3.02	.0046
7.0	502	1.69	.0014
5.5	507	0.00	.0000
2.5	512	0.00	.0000
Total $\Delta Z$			0.1330 ft

$$\Delta Z = \frac{1}{g} \sum_{r_i}^{r_o} \frac{V^2}{r} \Delta r$$

Total superelevation is 0.133 feet.

Based on relationships,  $V = Q/A = 3.61$  ft/s, the following are obtained:

**Woodward's Equation 2.160**

$$\Delta Z = \frac{V^2}{g r_c} (r_o - r_i) = \frac{(3.61)^2}{32.2 (431)} (513 - 350) = 0.153 \text{ ft}$$

**Ippen and Drinker's Equation 2.162**

$$\Delta Z = \frac{V^2}{2g} \frac{2W}{r_c} \left[ \frac{1}{1 - \left(\frac{W}{2r_c}\right)^2} \right] = \frac{3.61^2}{2 \times 32.2} \times \frac{2 \times 163}{431} \left[ \frac{1}{1 - \left(\frac{163}{2 \times 431}\right)^2} \right] = 0.158 \text{ ft}$$

**Ippen and Drinker's Equation 2.163**

$$\Delta Z = \frac{V^2}{2g} \frac{2W}{r_c} \left[ \frac{1}{1 - \frac{W^2}{12 r_c^2}} \right] = \frac{3.61^2}{2 \times 32.2} \times \frac{2 \times 163}{431} \left[ \frac{1}{1 - \frac{163^2}{12 \times 431^2}} \right] = 0.151 \text{ ft}$$

**Combined Free and Forced Vortex Equation 2.165**

$$V_{\max} = 4.90 \text{ ft/s}$$

$$\Delta Z = \frac{(V_{\max})^2}{2g} \left[ 2 - \left(\frac{r_i}{r_c}\right)^2 - \left(\frac{r_c}{r_o}\right)^2 \right] = \frac{4.90^2}{2 \times 32.2} \left[ 2 - \left(\frac{350}{431}\right)^2 - \left(\frac{431}{513}\right)^2 \right] = 0.236 \text{ ft}$$

The equations give comparable results (0.133 to 0.236 ft). Equation 2.158, which integrates across the section using the velocity distribution is the most exact. But using the value 0.24 ft provides a safety factor.

**2.15.4 PROBLEM 4 Maximum Stream Constriction Without Causing Backwater (Neglecting Energy Losses)**

A stream is rectangular in shape and 100 ft wide. The design discharge is 5,000 cfs and the uniform depth for this discharge is 10 ft. Neglecting energy losses what is the maximum amount of constriction that a bridge can impose without causing backwater.

The upstream flow rate per unit width (q) is:

$$q = \frac{Q}{W} = \frac{5,000}{100} = 50 \text{ cfs / ft}$$

The average velocity (V) is:

$$V = \frac{Q}{A} = \frac{5,000}{1,000} = 5.00 \text{ ft / s}$$

The specific head (H) is:

$$H = \frac{V^2}{2g} + y = \frac{5^2}{64.4} + 10 = 10.39 \text{ ft}$$

According to Section 2.6.2 the maximum unit discharge for a given specific head (specific head equals to a constant) occurs at the critical depth  $y_c$  where the Froude number is 1. Equation 2.149 the critical depth  $y_c$  for this specific head is:

$$y_c = \left( \frac{q_{\max}^2}{g} \right)^{1/3} = \frac{2}{3} H = \frac{2 V_c^2}{2g}$$

Solving for  $q_m$

$$q_{\max} = \left[ g \left( \frac{2}{3} H \right)^3 \right]^{1/2} = \left[ 32.2 \left( \frac{2}{3} \times 10.39 \right)^3 \right]^{1/2} = 103.4 \text{ cfs / ft}$$

Therefore, the width of the channel can be contracted until the unit discharge q is a maximum. The minimum width (maximum constriction) is:

$$W_{\min} = \frac{Q}{q_{\max}} = \frac{5,000}{103.4} = 48.3 \text{ ft}$$

and the maximum constriction is  $100 - 48.3 = 51.7 \text{ ft}$

This contraction causes the flow to go to critical. This results in an undulating hydraulic jump downstream. Also, when energy losses are considered there will be some backwater at the constriction.

### 2.15.5 PROBLEM 5 Maximum Elevation of a Grade Control Structure Without Backwater (Neglecting Energy Losses)

A low grade control structure (check dam) is to be placed across a stream downstream of a highway bridge. The stream is degrading. The purpose of the check dam is to maintain the

elevation of the water surface at the bridge, cause deposition of bed material, protect the abutments and piers from long term degradation and contraction scour and increase the elevation of the bed for local scour. There is to be no increase in water surface elevation upstream of the bridge at the design discharge. The energy losses are expected to be small so they can be neglected.

At the bridge, the design flood discharge is 5000 cfs. The river is 100 ft wide and has a uniform flow depth of 10 ft for the design discharge.

**What is the maximum height of the structure that will not cause backwater at the bridge at the design discharge?**

The unit discharge ( $q$ ) in the river at design flood discharge is:

$$q = \frac{Q}{W} = \frac{5,000}{100} = 50 \text{ cfs/ft}$$

The average velocity ( $V$ ) is

$$V = \frac{Q}{A} = \frac{5,000}{1,000} = 5.00 \text{ ft/sec}$$

The specific head ( $H$ ) is

$$H = \frac{V^2}{2g} + y = \frac{5^2}{64.4} + 10 = 10.39 \text{ ft}$$

As a first approximation assume no energy loss in the bridge reach. Then at the check dam, the elevation of the total energy line is 10.39 ft above the bed (Figure 2.44). At the dam:

$$H_{\min} + \Delta Z_{\max} = 10.39 \text{ ft}$$

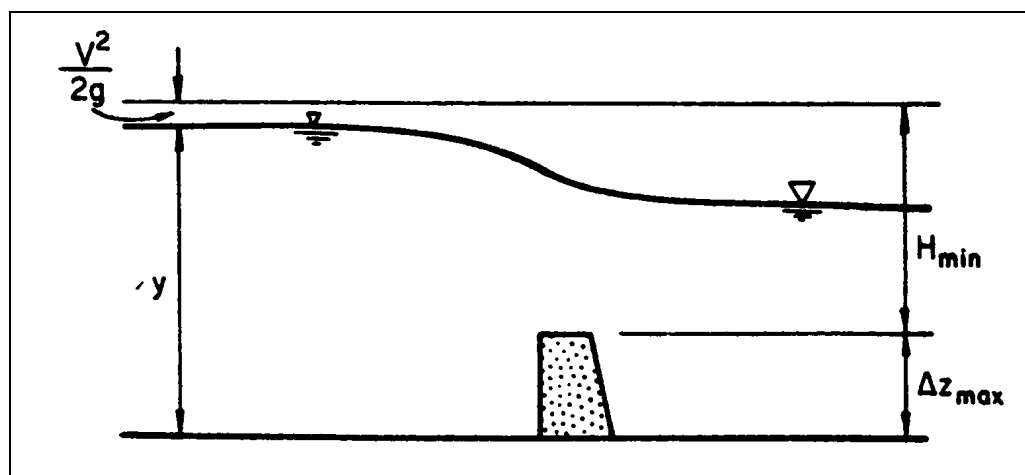


Figure 2.44. Sketch of backwater curve over check dam.

That is, the dam can be built to a height of  $\Delta Z_{\max}$  which decreases the specific head at the dam to  $H_{\min}$ . From Section 2.6.3 and Equation 2.147

$$H_{\min} = \frac{3}{2} y_c$$

From Equation 2.140

$$y_c = \left[ \frac{q^2}{g} \right]^{1/3} = \left[ \frac{50^2}{32.2} \right]^{1/3} = 4.27 \text{ ft}$$

Then

$$H_{\min} = \frac{3}{2} y_c = \frac{3}{2} 4.27 \text{ ft} = 6.40 \text{ ft}$$

and

$$\Delta Z_{\max} = 10.39 - 6.40 = 4.0 \text{ ft}$$

If the structure is built to a crest elevation 4.0 ft above the bed, critical flow will occur at the dam for a flow of 5,000 cfs and larger and the dam will cause no backwater. At lower discharges the at the check dam will cause backwater. However, discharges larger than 5,000 cfs check dam will not cause backwater. Local scour downstream of the check dam should be evaluated. HEC-23 has am problem for determining this scour.

**How much backwater will the dam cause for a flow of 1000 cfs if the normal depth for this discharge is 5 ft and the dam height is 4.0 ft?**

Upstream of the dam the discharge for foot of width ( $q$ ) is,

$$q = \frac{Q}{W} = \frac{1,000}{100} = 10 \text{ cfs/ft}$$

The average velocity ( $V$ ) is

$$V = \frac{q}{y} = \frac{10}{5} = 2.00 \text{ ft/sec}$$

At the check dam the flow is critical so from Equation 2.142

$$y_c = \left[ \frac{q^2}{g} \right]^{1/3} = \left[ \frac{10^2}{32.2} \right]^{1/3} = 1.46 \text{ ft}$$



and from Equation 2.144

$$H_{\min} = \frac{3}{2} y_c = \frac{3}{2} 1.46 \text{ ft} = 2.19 \text{ ft}$$

Assuming no energy loss, the specific head upstream of the dam is

$$H = H_{\min} + \Delta Z = 2.19 + 4.0 = 6.19 \text{ ft}$$

To determine the depth of flow upstream of the dam ( $y$ ) solve the specific head equation (Equation 2.137)

$$H = \frac{q^2}{2gy^2} + y = \frac{10^2}{64.4 y^2} + y = 6.19 \text{ ft}$$

or

$$y^3 - 6.19 y^2 + 10^2/64.4 = 0$$

The solution is

$$y = 6.14 \text{ ft}$$

As the normal depth is only 5 ft, the backwater is

$$\Delta y = 6.14 - 5.00 = 1.14 \text{ ft}$$

That is, the depth upstream of the dam is increased 1.14 ft by the 4.0 ft high dam when the flow is 1,000 cfs.

(page intentionally left blank)

## CHAPTER 3

### FUNDAMENTALS OF ALLUVIAL CHANNEL FLOW

#### 3.1 INTRODUCTION

Most streams that a highway will cross or encroach upon are alluvial. That is, the rivers are formed in cohesive or non-cohesive materials that have been, and can still be, transported by the stream. The non-cohesive material generally consists of silt, sand, gravel, or cobbles, or any combination of these sizes. Silt generally is not present in appreciable quantities in streams having non-cohesive boundaries. Cohesive material consists of clays (sizes less than 0.004 mm) forming a binder with silts and sand. Because of the electro-chemical bonding between clay particles, clays are more resistant to erosion than silts.

In alluvial rivers, bed configuration and resistance to flow are a function of the flow and can change to increase or decrease the velocity and water surface level. The river channel can shift its location so that the crossing or encroachment is unfavorably located with respect to the direction of flow. The moveable boundary of the alluvial river adds another dimension to the design problem and can compound environmental concerns. Therefore, the design of highway crossings and encroachments in the river environment requires knowledge of the mechanics of alluvial channel flow.

This chapter presents the fundamentals of alluvial channel flow. It covers properties of alluvial material, methods of measuring properties of alluvial materials, flow in sandbed channels, prediction of bed forms, Manning's  $n$  for sandbed and other natural streams, how bed-form changes affect highways in the river environment, beginning of motion, flow in coarse-material streams, and physical measurement and determination of sediment discharge in the field. These fundamentals of alluvial channel flow are used in later chapters to develop design considerations for highway crossings and encroachments in river environments.

In Chapter 4, sediment transport and physical and computer modeling of sediment transport will be covered.

#### 3.2 SEDIMENT PROPERTIES AND MEASUREMENT TECHNIQUES

A knowledge of the properties of the bed material particles is essential, as they indicate the behavior of the particles in their interaction with the flow. Several of the important bed material properties are discussed in the following sections (U.S. Interagency Subcommittee 1941, 1943, 1957; Richardson 1971).

##### 3.2.1 Particle Size

Of the various sediment properties, physical size has by far the greatest significance to the hydraulic engineer. The particle size is the most readily measured property, and other properties such as shape, fall velocity and specific gravity tend to vary with size in a roughly predictable manner. In general, size represents a sufficiently complete description of the sediment particle for many practical purposes.

Particle size  $D_s$  may be defined by its volume, diameter, weight, fall velocity, or sieve mesh size. Except for volume, these definitions also depend on the shape and density of the particle. The following definitions are commonly used to describe the particle size (U.S. Interagency Subcommittee 1943):

1. Nominal diameter - The diameter of a sphere having the same volume as the particle.
2. Sieve diameter - The diameter of a sphere equal to the length of the side of a square sieve opening through which measured quantities (by weight) of the sample will pass. As an approximation, the sieve diameter is equal to the nominal diameter.
3. Sedimentation diameter - The diameter of a sphere with the same fall velocity and specific gravity as the particle in the same fluid under the same conditions.
4. Standard fall diameter - The diameter of a sphere that has a specific gravity of 2.65 and also has the same terminal settling velocity as the particle when each is allowed to settle alone in quiescent, distilled water of infinite extent and at a temperature of 24°C.

In general, sediments have been classified into boulders, cobbles, gravels, sands, silts, and clays on the basis of their nominal or sieve diameters. The size range in each general class is given in Table 3.1. The non-cohesive material generally consists of silt (0.004-0.062 mm), sand (0.062 - 2.0 mm), gravel (2.0 - 64 mm), or cobbles (64-250 mm).

The boulder class (250 - 4000 mm) is generally of little interest in sediment problems. The cobble and gravel class plays a considerable role in the problems of local scour and resistance to flow and to a lesser extent in bed load transport. The sand class is one of the most important in alluvial channel flow. The silt and clay class is of considerable importance in the evaluation of stream sediment loads, bank stability and problems of seepage and consolidation.

### 3.2.2 Particle Shape

Generally speaking, shape refers to the overall geometrical form of a particle. Sphericity is defined as the ratio of the surface area of a sphere of the same volume as the particle to the actual surface area of the particle. Roundness is defined as the ratio of the average radius of curvature of the corners and edges of a particle to the radius of a circle inscribed in the maximum projected area of the particle. However, because of simplicity and effectiveness of correlation with the behavior of particles in flow, the most commonly used parameter to describe particle shape is the Corey shape factor,  $S_p$ , (Albertson 1953) defined as:

$$S_p = \frac{l_c}{\sqrt{l_a l_b}} \quad (3.1)$$

where:  $l_a$ ,  $l_b$ , and  $l_c$  are the dimensions of the three mutually perpendicular axes of a particle  $l_a$  the longest;  $l_b$  the intermediate; and  $l_c$  the shortest axis.

Table 3.1. Sediment Grade Scale (Brown 1950).

Size			Approximate Sieve Mesh Openings Per Inch		Class	
Millimeters	Microns	Inches	Tyler	U.S. Standard		
4000-2000	-----	-----	160-80	-----	-----	Very large boulders
2000-1000	-----	-----	80-40	-----	-----	Large boulders
1000-500	-----	-----	40-20	-----	-----	Medium boulders
500-250	-----	-----	20-10	-----	-----	Small boulders
250-130	-----	-----	10-5	-----	-----	Large cobbles
130-64	-----	-----	5-2.5	-----	-----	Small cobbles
64-32	-----	-----	2.5-1.3	-----	-----	Very coarse gravel
32-16	-----	-----	1.3-0.6	-----	-----	Coarse gravel
16-8	-----	-----	0.6-0.3	2 1/2	-----	Medium gravel
8-4	-----	-----	0.3-0.16	5	5	Fine gravel
4-2	-----	-----	0.16-0.08	9	10	Very fine gravel
2-1	2.00-1.00	2000-1000	-----	16	18	Very coarse sand
1-1/2	1.00-0.50	1000-500	-----	32	35	Coarse sand
1/2-1/4	0.50-0.25	500-250	-----	60	60	Medium sand
1/4-1/8	0.25-0.125	250-125	-----	115	120	Fine sand
1/8-1/16	0.125-0.062	125-62	-----	250	230	Very fine sand
1/16-1/32	0.062-0.031	62-31	-----			Coarse silt
1/32-1/64	0.031-0.016	31-16	-----			Medium silt
1/64-1/128	0.016-0.008	16-8	-----			Fine silt
1/128-1/256	0.008-0.004	8-4	-----			Very fine silt
1/256-1/512	0.004-0.0020	4-2	-----			Coarse clay
1/512-1/1024	0.0020-0.0010	2-1	-----			Medium clay
1/1024-1/2048	0.0010-0.0005	1-0.5	-----			Fine clay
1/2048-1/4096	0.0005-0.0002	0.5-0.24	-----			Very fine clay

### 3.2.3 Fall Velocity

The prime indicator of the interaction of sediments in suspension within the flow is the fall velocity of sediment particles. The fall velocity of a particle is defined as the velocity of that particle falling alone in quiescent, distilled water of infinite extent. In most cases, the particle is not falling alone, and the water is not distilled or quiescent. Measurement techniques are available for determining the fall velocity of groups of particles in a finite field in fluid other than distilled water. However, little is known about the effect of turbulence on fall velocity.

A particle falling at terminal velocity in a fluid is under the action of a driving force due to its buoyant weight and a resisting force due to the fluid drag. Fluid drag is the result of either the tangential shear stress on the surface of the particle, or a pressure difference on the particle or a combination of the two forces. The fluid drag on the falling particle  $F_D$  is given by the drag equation

$$F_D = C_D A_s \rho \omega^2 / 2 \quad (3.2)$$

The buoyant weight of the particle  $W_s$  is:

$$W_s = (\rho_s - \rho)gV_p \quad (3.3)$$

where:

- $C_D$  = Coefficient of drag
- $\omega$  = Terminal fall velocity of the particle
- $A_s$  = Projected area of the particle normal to the direction of flow
- $\rho$  = Fluid density
- $\rho_s$  = Particle density
- $g$  = Acceleration due to gravity
- $V_p$  = Volume of the particle

The area and volume can be written in terms of the characteristic diameter of the particle  $D_s$  or:

$$A_s = K_1 D_s^2 \quad (3.4)$$

and

$$V_p = K_2 D_s^3 \quad (3.5)$$

Where the coefficients  $K_1$  and  $K_2$  depend on the shape of sediment particles. For example,  $K_1 = \pi/4$  and  $K_2 = \pi/6$  for spherical particles. If the particle is falling at its terminal velocity,  $F_D = W_s$

$$(\rho_s - \rho) gV_p = C_D A_s \rho \omega^2 / 2 \quad (3.6)$$

By substituting Equations 3.4 and 3.5 into Equation 3.6, the expression:

$$\omega^2 = \frac{2}{C_D} \frac{K_2}{K_1} \left( \frac{\rho_s}{\rho} - 1 \right) g D_s \quad (3.7)$$

is obtained.

Four dimensionless variables describing fall velocity result from dimensional analysis of Equation 3.7:

$$f \left( \frac{\omega^2}{g D_s}, C_D, \frac{\rho_s}{\rho}, \frac{K_2}{K_1} \right) = 0 \quad (3.8)$$

The drag coefficient  $C_D$  is dependent on the particle Reynolds number ( $Re_p = \rho \omega D_s / \mu$ ), the shape, and the surface texture of the particle, where  $\mu$  is dynamic viscosity of the fluid. The ratio  $K_2/K_1$  is usually replaced by the Corey shape factor  $S_p$  (Equation 3.1).

The relations between the fall velocity of particles and the other variables are given in Figures 3.1 and 3.2.

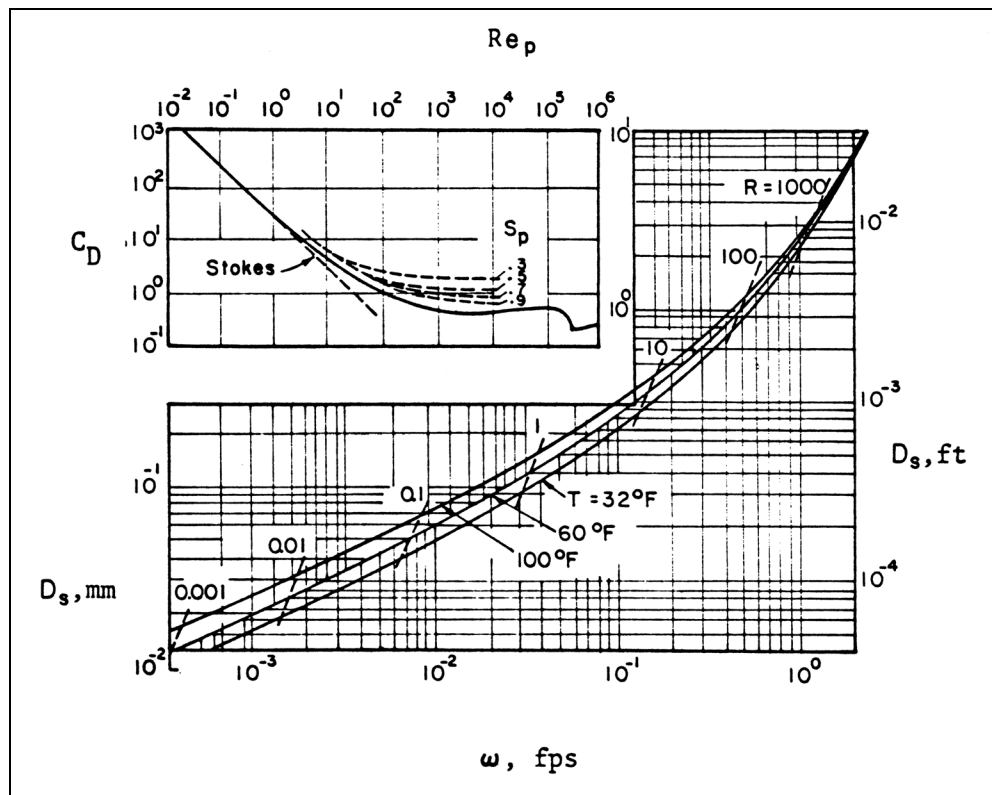


Figure 3.1. Drag coefficient  $C_D$  vs particle Reynolds number  $Re_p$  for spheres and natural sediments with shape factors  $S_p$  equal to 0.3, 0.5, 0.7, and 0.9. Also, sediment diameter  $D_s$  vs. fall velocity  $\omega$  and temperature  $T^\circ$  (Brown 1950, p. 781).

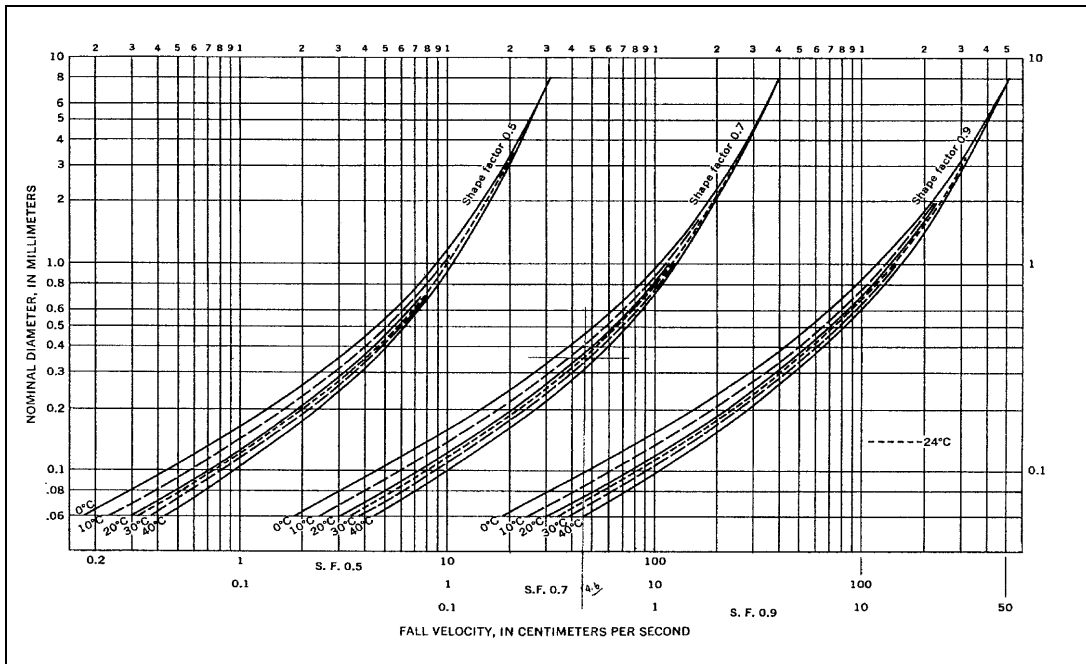


Figure 3.2. Nominal diameter vs. fall velocity (Temperature = 24°C) (Guy 1977, U.S. Interagency 1957b).

### 3.2.4 Sediment Size Distribution

Four methods of obtaining sediment size distribution are described below: Sieve analysis, visual accumulation (VA) tube analysis, pebble count method, and pipette analysis. Each method for size distribution analysis is appropriate for only a particular range of particle sizes (Table 3.2). All together the four methods provide a means of obtaining particle size distributions for most bed material samples.

	Size Range	Analysis Concentration (mg/l)	Quantity of Sediment (g) or Pebbles
Sieves	0.062-32 mm	-----	100-500
VA tube	0.062-2 mm	-----	0.05-15.0
Pipette	0.002-0.062 mm	2,000-5,000	1.0-5.0
Pebble Count	12-1000 mm	-----	100 pebbles

If the sediment sample to be analyzed (bed material or suspended sediment) has considerable fine material ( $D_s < .062$  mm) it must be separated prior to analysis. To separate the coarser from the finer sediment, the sediment should be wet-sieved using distilled water and a 250-mesh (0.062 mm) sieve. The material passing through the sieve can be analyzed by pipette analysis if further breakdown of the fine sediment is desired, or dried and included



as percent finer than 0.062 mm with the analysis of the coarser material. If it is going to be dry-sieved, the material retained on the sieve is oven dried for one hour after all visible water has been evaporated. If the material is to be analyzed by wet-sieving or with the accumulation tube, it is not dried.

Sieve Size Distribution in the sand and gravel range is generally determined by passing the sample through a series of sieves of mesh size ranging from 32 mm to 0.062 mm. A minimum of about 100 grams of sand is required for an accurate sieve analysis. More is required if the sample contains particles of 1.0 mm or larger. Standard methods employed in soil mechanics are suitable for determining the sieve sizes of sand and gravel sediment samples.

Visual Accumulation (VA) Tube is used for determining the size distribution of the sand fraction of sediment samples ( $0.062 \text{ mm} < D_s < 2.0 \text{ mm}$ ). It is a fast, economical, and accurate means of determining the fall velocity or fall diameter of the sediment. The equipment for the visual accumulation tube analysis consists of: (1) a glass funnel about 250 mm (9.8 in.) long; (2) a rubber tube connecting the funnel and the main sedimentation tube, with a special clamping mechanism serving as a "quick acting" valve; (3) glass sedimentation tubes having different sized collectors; (4) a tapping mechanism that strikes against the glass tube and helps keep the accumulation of sediment uniformly packed; (5) a special recorder consisting of a cylinder carrying a chart that rotates at a constant rate and a carriage that can be moved vertically by hand on which is mounted a recording pen and an optical instrument for tracking the accumulation; and (6) the recorder chart which has a printed form incorporating the fall diameter calibration.

In the visual accumulation tube method, the particles start falling from a common source and become stratified according to settling velocities. At a given instant, the particles coming to rest at the bottom of the tube are of one "sedimentation size" and are finer than particles that have previously settled out and are coarser than those remaining in suspension.

It has been shown that particles of a sample in the visual tube settle with greater velocities than the same particles falling individually because of the effect of mutual interaction of the particles. The visual accumulation tube apparatus is calibrated to account for the effects of this mutual interaction and the final results are given in terms of the standard fall diameter of the particles.

Visual accumulation tube method may not be suitable for some streams that transport large quantities of organic materials such as root fibers, leaf fragments, and algae. Also, extra care is needed when a stream transports large quantities of heavy or light minerals such as taconite or coal. The method is explained in detail by Guy (1977).

Pebble Count Method is used to obtain the size distribution of coarse bed materials (gravel and cobbles) which are too large to be sieved. Very often the coarser material is underlain by sands. Then, the underlying sands are analyzed by sieving. The two classes of bed material are either combined into a single distribution or used separately. The large material sizes are measured in situ by laying out a square grid. Within the grid, all the particle sizes are measured and counted by size intervals. For large samples a random selection of particles in the various classes is appropriate to develop frequency histograms of sediment sizes.

Square-Surface Sample is obtained by picking up and counting all the surface pebbles in each predetermined size class within a small enclosed area of the bed. The area is taken to be representative of the whole channel bed.

The pebble count method entails measurement of randomly selected particles in the field, often under difficult conditions. Therefore, use of the Zeiss Particle-Size Analyzer should be considered (Ritter and Helley 1968). For this method, a photograph of the stream bed is made, preferably at low flow, with a 35 mm camera supported by a tripod about 2 m (6.6 ft) above the stream bed, the height depending on the size of the bed material. A reference scale, such as a steel tape or a surveyor's rod must appear in the photograph. The photographs are printed on the thinnest paper available. An iris diaphragm, illuminated from one side, is imaged by a lens onto the plane of a Plexiglass plate. By adjusting the iris diaphragm the diameter of the sharply defined circular light spot appearing on the photograph can be changed and its area made equal to that of the individual particles. As the different diameters are registered, a puncher marks the counted particle on the photograph. An efficient operation can count up to 1,000 particles in 30 minutes.

In the line sampling method of pebble count sampling, a line is laid out or placed either across or along the stream. Particles are picked at random intervals along the line and measured. The measured particles are classified as to size or weight and a percent finer curve or table is prepared. Usually 100 particles are sufficient to give an accurate classification of the size distribution of coarse materials.

Pipette Method of determining gradation of sizes finer than 0.062 mm is one of the most widely accepted techniques utilizing the Oden theory and the dispersed system of sedimentation. The upper size limit of sediment particles which settle in water according to Stokes is about 1/16 mm or 0.062 mm. This corresponds to the lower size limit which can be determined readily by sieves. This size is the division between sand and silt (Table 3.1) and is an important division in many phases of sediment phenomena.

The fundamental principle of the pipette method is to determine the concentration of a suspension in samples withdrawn from a predetermined depth as a function of settling time. Particles having a settling velocity greater than that of the size at which separation is desired will settle below the point of withdrawal after elapse of a certain time. The time and depth of withdrawal are predetermined on the basis of Stokes law.

Satisfactory use of the pipette method requires careful and precise operation to obtain maximum accuracy in each step of the procedure. Also, for routine analysis, special apparatus can be set up for the analysis of a large number of samples. A complete description of a laboratory setup and procedure for this method is given by Guy (1969).

Frequency Curves. The presentation of sediment size analysis is made in various formats. A histogram is a graphical representation of the number, weight, or volume percentage of items in given class intervals. An example of a histogram is shown in Figure 3.3a. The abscissa scale represents the class intervals, usually in geometric progression, and the ordinate scale represents either actual concentration or percent (by number, volume, or weight) of the total sample contained in each class interval. If the class intervals are small, the shape of the histogram will approach a continuous curve. The successive sizes employed in the size analysis of sediment are usually in ratios of 2 or  $\sqrt{2}$ .

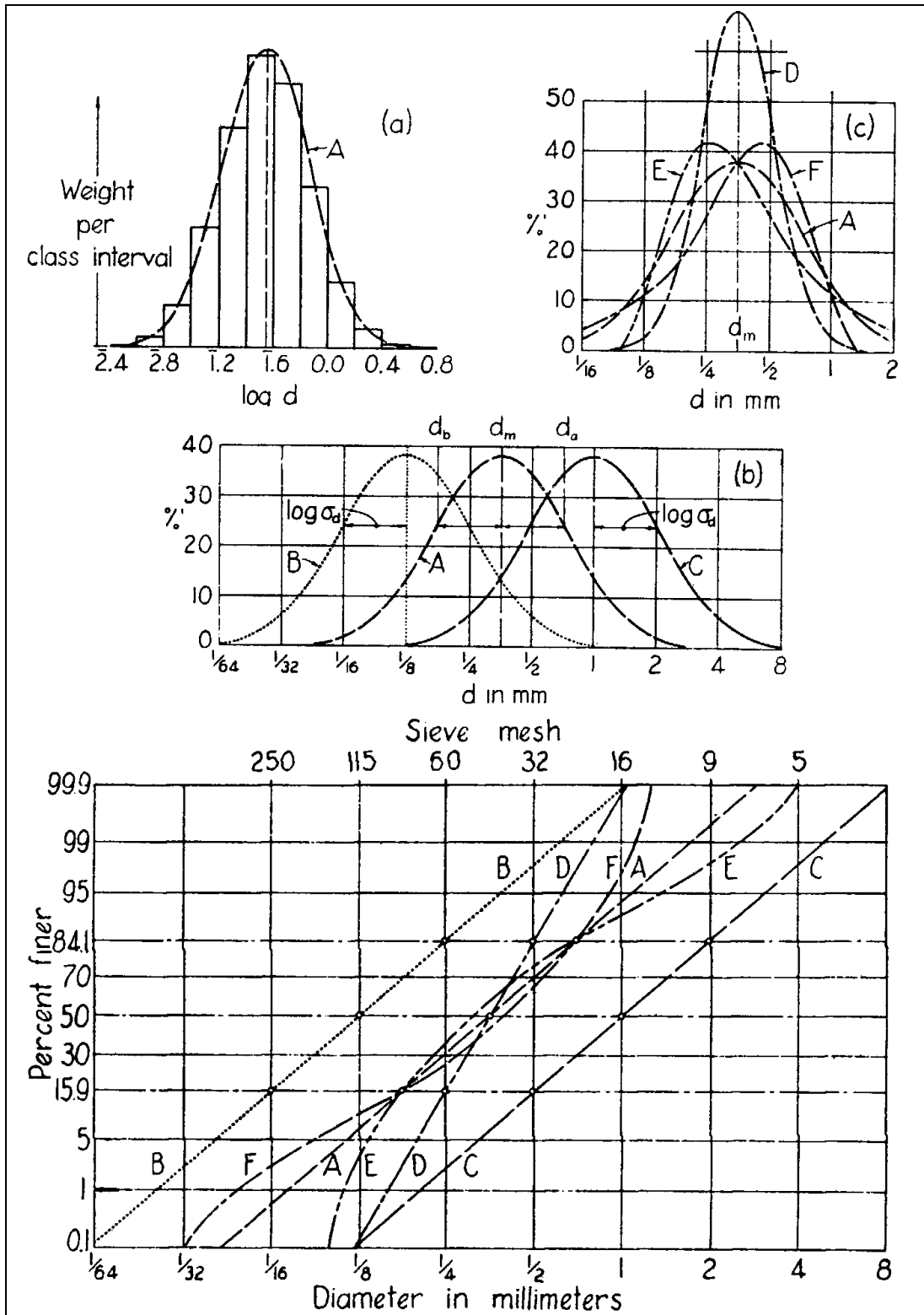


Figure 3.3. Definition sketches for size-frequency characteristics of sediments (Rouse 1940).

When the ordinates of successive classes are added and plotted against the upper limit of the size class, the cumulative percent finer distribution diagram is obtained (Figure 3.3). In this diagram, the abscissa scale (usually logarithmic) represents the intervals of the size scale and the ordinate scale is the cumulative percent by weight of the sample up to (or percent finer than) the size in question. From the cumulative percent finer the  $D_{35}$ ,  $D_{50}$ ,  $D_{85}$ ,  $D_i$ , etc. sizes can be determined.

In a size frequency distribution curve, it is possible to choose certain particle sizes as representing significant values, such as particles just larger than one-fourth of the distribution  $D_{25}$  (the first quartile), and particles just larger than three-fourths of the distribution  $D_{75}$  (the third quartile). Measures of spread are based on differences or ratios between the two quartiles. Quartile measures are confined to the central half of the frequency distribution and the values obtained are not influenced by larger or smaller sizes. Quartile measures are very readily computed, and most of the data may be obtained directly from the cumulative curve by graphic means.

In contrast to quartile measures, moment measures are influenced by each individual size class in the distribution. The first moment of a frequency curve is its center of gravity and is called the arithmetic mean and is the average size of the sediment. The second moment is a measure of the average spread of the curve and is expressed as the standard deviation of the distribution.

Commonly, the size distribution of natural sediments plots as a straight line on log probability paper. If this is true, then a natural sediment is completely described by the median diameter ( $D_{50}$  the size of sediment of which 50 percent is finer) and the slope of the cumulative frequency line on log probability paper. The slope of this line is proportional to the spread of the size distribution in a sediment sample. It is computed with the expression

$$G = \frac{1}{2} \left[ \frac{D_{50}}{D_{16}} + \frac{D_{84}}{D_{50}} \right] \quad (3.9)$$

where:

- G = Gradation coefficient
- $D_x$  = Sediment diameter particle of which x percent of sample is finer

The grain roughness used in velocity equations is taken as the  $D_{80}$ ,  $D_{85}$ , or  $D_{90}$ .

In studies of scour below culvert outlets, Stevens (1968) was able to consolidate a wide range of scour data by employing the expression.

$$k = \left\{ \frac{\sum_{i=1}^{10} D_i^3}{10} \right\}^{1/3} \quad (3.10)$$

for the effective or representative grain size of well-graded materials. Here

$$D_i(i = 1) = \frac{D_0 + D_{10}}{2} \quad (3.11)$$

$$D_i(i = 2) = \frac{D_{10} + D_{20}}{2}$$

$$D_i(i = 10) = \frac{D_{90} + D_{100}}{2}$$

The terms  $D_0, D_{10}, \dots, D_{100}$ , are the sieve diameters of the riprap for which 0 percent, 10 percent, ..., 100 percent of the material (by weight) is finer. Stevens' equation is the equivalent to utilizing the arithmetic average of the sum of the weights of the individual particles.

The effective diameter  $D_m$  is also used in sediment studies. It is defined by the following equation:

$$D_m = \frac{\sum_{i=1}^n p_i D_{si}}{100} \quad (3.12)$$

Where  $p_i$  is the percentage by weight of that fraction of the sediment with geometric mean size  $D_{si}$ . The geometric mean size is the square root of the product of the end points of a given size range.

### 3.2.5 Specific Weight

Specific weight is weight per unit volume. In the English system of units, specific weight is usually expressed in units of pounds per cubic foot and in the metric system, in grams per cubic centimeter. In connection with granular materials such as soils, sediment deposits, or water sediment mixtures, the specific weight is the weight of solids per unit volume of the material including its voids. The measurement of the specific weight of sediment deposits is determined simply by measuring the dry weight of a known volume of the undisturbed material.

### 3.2.6 Porosity

The porosity of granular materials is the ratio of the volume of void space to the total volume of an undisturbed sample. To determine porosity, the volume of the sample must be obtained in an undisturbed condition. Next, the volume of solids is determined either by liquid displacement or indirectly from the weight of the sample and the specific gravity of material. The void volume is then obtained by subtracting the volume of solids from the total volume.

### **3.2.7 Cohesion**

Cohesion is the force by which particles of clay are bound together. This force is the result of ionic attraction among individual particles, and is a function of the type of mineral, particle spacing, salt concentration in the fluid, ionic valence, and hydration and swelling properties of the constituent minerals. Cohesive soils are composed of silts and clay. Their size classification is given in Table 3.1. In the unified soil classification system, silt and clay soils have more than 50 percent by weight of particles passing the 0.075 mm sieve opening. However, cohesive soils are not classified by grain size but by their degree of plasticity, which is measured by Atterberg limits.

Clays are alumino-silicate crystals composed of two basic building sheets, the tetrahedral silicate sheet and the octahedral hydrous aluminum oxide sheet. Various types of clays result from different configurations of these sheets. The two main types of clays are kaolinite and montmorillonite. Kaolinite crystals are large (70 to 100 layers thick), held together by strong hydrogen bonds, and are not readily dispersible in water. Montmorillonite crystals are small (3 layers thick) held together by weak bonds between adjacent oxygen layers and are readily dispersible in water into extremely small particles.

Several laboratory and field measurement techniques are available for determining the magnitude of cohesion, or shear strength, of clays. Among these, the vane shear test, which is performed in the field is one of the simplest. The vane is forced into the ground and then the torque required to rotate the vane is measured. The shear strength is determined from the torque required to shear the soil along the vertical and horizontal edges of the vane.

Briaud et al. (1999) describe equipment and methods developed to determine the erosion rate of cohesive soils. Erosion rate is defined as the vertical distance scoured per unit of time. The erosion rate, expressed as mm/hr, is related to shear stress, given in  $N/m^2$ , imposed at the soil water interface using an erosion function apparatus (EFA). The EFA develops an erosion rate-shear stress curve for a soil sample taken with an ASTM standard Shelby tube with a 3.0 inches (76.2) mm outside diameter. The erosion rate-shear stress curve for samples taken at a site can then be used to determine the scour depth as a function of time.

### **3.2.8 Angle of Repose**

The angle of repose is the maximum slope angle upon which non-cohesive material will reside without moving. It is a measure of the intergranular friction of the material. Simons developed Figure 3.4 for the angle of repose for dumped granular material.

## **3.3 FLOW IN SANDBED CHANNELS**

Most larger streams flow on sandbeds for the greater part of their length. Thus, there are potentially many more opportunities for highway crossings or encroachments on sandbed streams than in cohesive or gravel streams. In sandbed rivers, the sand material is easily eroded and is continually being moved and shaped by the flow. The mobility of the sandbed creates problems for the safety of any structure placed in or over the stream, for the protection of private property along these streams, and in the preservation and enhancement of the stream environment.

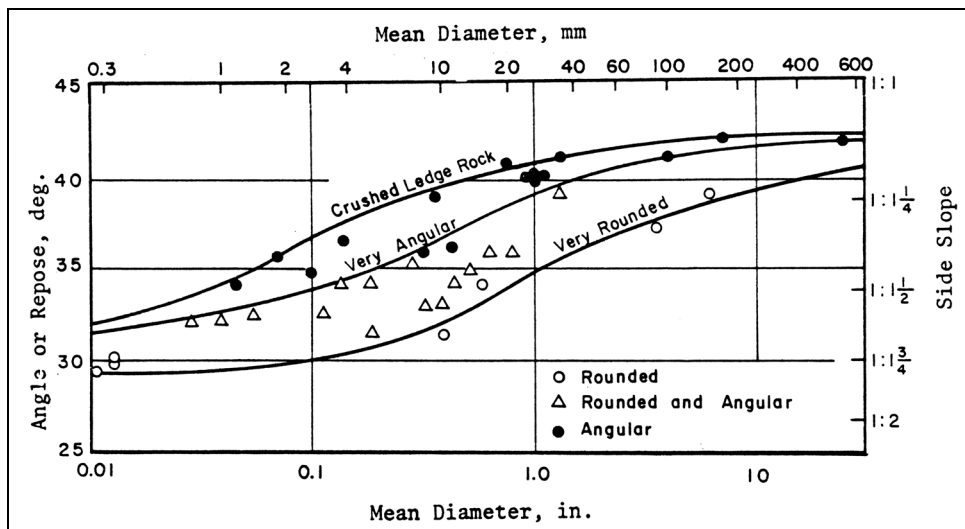


Figure 3.4. Angle of repose of non-cohesive materials (Simons 1955).

The interaction between the flow of the water-sediment mixture and the sandbed creates different bed configurations which change the resistance to flow and rate of sediment transport. The gross measures of channel flow, such as the flow depth, river stage, bed elevation and flow velocity, change with different bed configurations. In the extreme case, the change in bed configuration can cause a three-fold change in resistance to flow and a 10-to-15 fold change in concentration of bed sediment transport. For a given discharge and channel width, a three-fold increase in Manning's  $n$  results in a doubling of the flow depth.

The interaction between the flow and bed material and the interdependency among the variables makes the analysis of flow in alluvial sandbed streams extremely complex. However, with an understanding of the different types of bed forms that may occur and a knowledge of the resistance to flow and sediment transport associated with each bed form, the river engineer can better analyze alluvial channel flow.

### 3.3.1 Regimes of Flow in Alluvial Channels

The flow in alluvial channels is divided into lower and upper flow regimes separated by a transition zone (Simons and Richardson 1963, 1966). These two flow regimes are characterized by similarities in the shape of the bed configuration, mode of sediment transport, process of energy dissipation, and phase relation between the bed and water surfaces. The two regimes and their associated bed configurations shown in Figure 3.5 are:

Lower flow regime: (1) ripples; (2) dunes with ripples superposed; and (3) dunes

Transitional Flow Regime: The bed roughness ranges from dunes to plane bed or antidunes.

Upper Flow Regime: (1) plane bed; (2) antidunes, a) with standing waves, b) with breaking antidunes; and (3) chutes and pools.

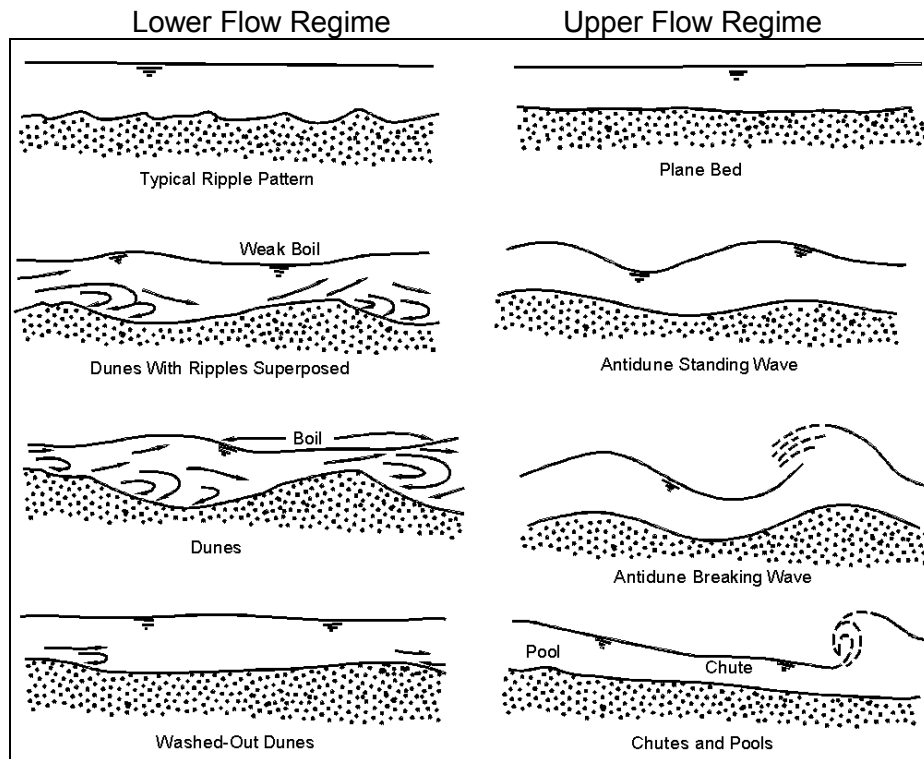


Figure 3.5. Forms of bed roughness in sand channels (Simons and Richardson 1963, 1966).

Lower Flow Regime. In the lower flow regime, resistance to flow is large and sediment transport is small. The bed form is either ripples or dunes or some combination of the two. The water-surface undulations are out of phase with the bed surface, and there is a relatively large separation zone downstream from the crest of each ripple or dune. The most common mode of bed material transport is for the individual grains to move up the back of the ripple or dune and avalanche down its face. After coming to rest on the downstream face of the ripple or dune, the particles remain there until exposed by the downstream movement of the dunes; they repeat this cycle of moving up the back of the dune, avalanching, and storage. Thus, most movement of the bed material particles is in steps. The velocity of the downstream movement of the ripples or dunes depends on their height and the velocity of the grains moving up their backs.

Transition. The bed configuration in the transition zone is erratic. It may range from that typical of the lower flow regime to that typical of the upper flow regime, depending mainly on antecedent conditions. If the antecedent bed configuration is dunes, the depth or slope can be increased to values more consistent with those of the upper flow regime without changing the bed form; or, conversely, if the antecedent bed is plane, depth and slope can be decreased to values more consistent with those of the lower flow regime without changing the bed form. Often in the transition from the lower to the upper flow regime, the dunes decrease in amplitude and increase in length before the bed becomes plane (washed-out dunes). Resistance to flow and sediment transport also have the same variability as the bed configuration in the transition. This phenomenon can be explained by the changes in resistance to flow and, consequently, the changes in depth and slope as the bed form changes. Resistance to flow is small for flow over a plane bed; so the shear stress decreases and the bed form changes to dunes. The dunes cause an increase in resistance to flow which increases the shear stress on the bed and the dunes wash out forming a plane



bed, and the cycle continues. It was the transition zone, which covers a wide range of shear values, that Brooks (1958) was investigating when he concluded that a single-valued function does not exist between velocity or sediment transport and the shear stress on the bed.

Upper Flow Regime. In the upper flow regime, resistance to flow is small and sediment transport is large. The usual bed forms are plane bed or antidunes. The water surface is in phase with bed surface except when an antidune breaks, and normally the fluid does not separate from the boundary. A small separation zone may exist downstream from the crest of an antidune prior to breaking. Resistance to flow is the result of grain roughness with the grains moving, of wave formation and subsidence, and of energy dissipation when the antidunes break. The mode of sediment transport is for the individual grains to roll almost continuously downstream in sheets one or two grain diameters thick; however, when antidunes break, much bed material is briefly suspended, then movement stops temporarily and there is some storage of the particles in the bed.

### 3.3.2 Bed Configuration

The bed configurations (roughness elements) that commonly form in sand bed channels are plane bed without sediment movement, ripples, ripples on dunes, dunes, plane bed with sediment movement, antidunes, and chutes and pools. These bed configurations are listed in their order of occurrence with increasing values of stream power ( $V\gamma_o S$ ) for bed materials having  $D_{50}$  less than 0.6 mm. For bed materials coarser than 0.6 mm, dunes form instead of ripples after beginning of motion at small values of stream power. The relation of bed form to water surface is shown in Figure 3.6.

The different forms of bed-roughness are not mutually exclusive in time and space in a stream. Different bed-roughness elements may form side-by-side in a cross-section or reach of a natural stream, giving a multiple roughness; or they may form in time sequence, producing variable roughness.

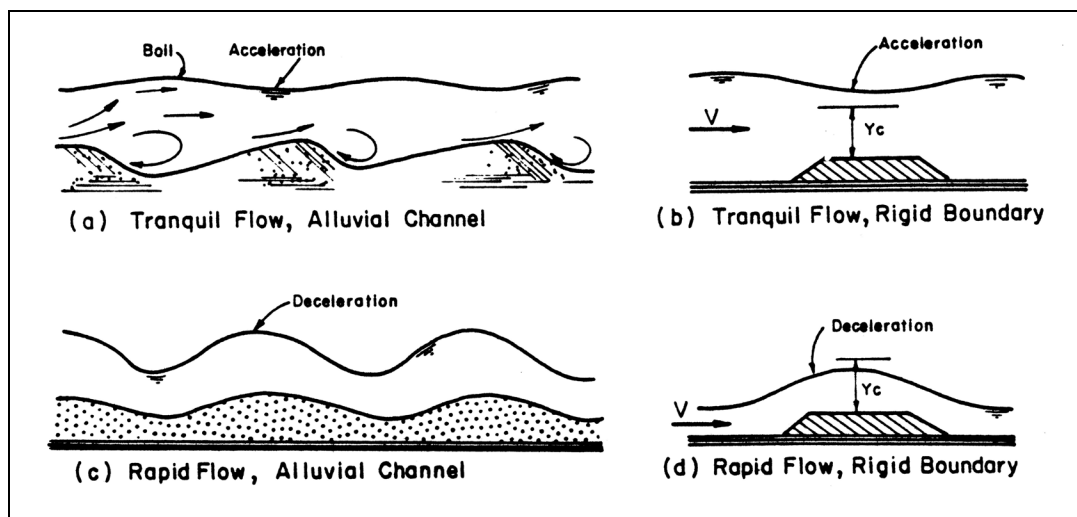


Figure 3.6. Relation between water surface and bed configuration, Richardson et al. 1975.

Multiple roughness is related to variations in shear stress ( $\gamma_0 S$ ) in a channel cross-section. The greater the width-depth ratio of a stream, the greater is the probability of a spatial variation in shear stress, stream power or bed material. Thus, the occurrence of multiple roughness is closely related to the width-depth ratio of the stream. Variable roughness is related to changes in shear stress, stream power, or reaction of bed material to a given stream power over time. A commonly observed example of the effect of changing shear stress or stream power is the change in bed form that occurs with changes in depth during a runoff event. Another example is the change in bed form that occurs with change in the viscosity of the fluid as the temperature or concentration of fine sediment varies over time. It should be noted that a transition occurs between the dune bed and the plane bed; either bed configuration may occur for the same value of stream power (Figure 3.7).

A relation between stream power, velocity, and bed configuration is shown in Figure 3.7. The relation pertains to one sand size and was determined in the 2.4 m (8-foot) flume at Colorado State University.

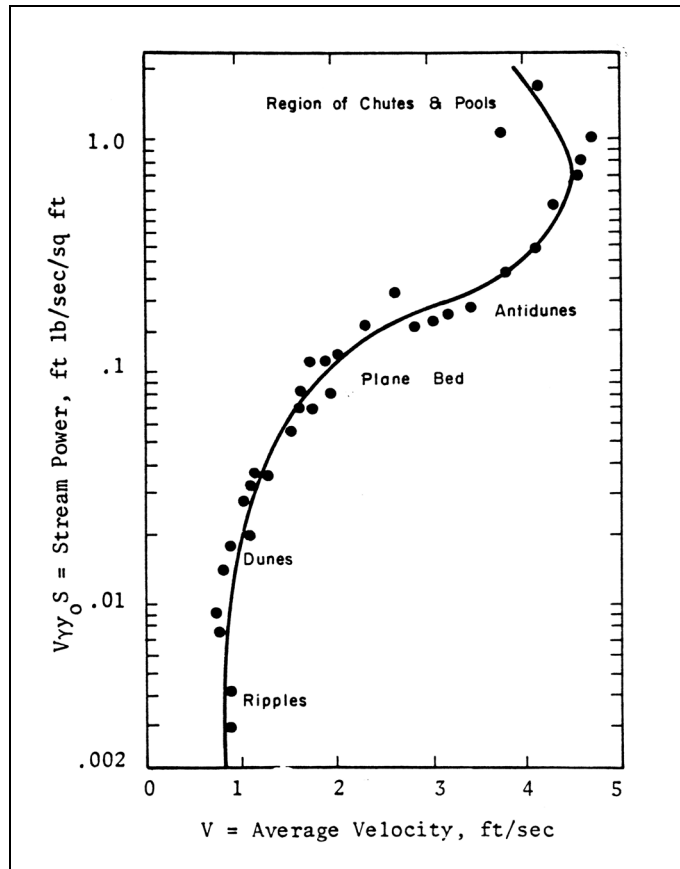


Figure 3.7. Change in velocity with stream power for a sand with  $D_{50} = 0.19$  mm (Simons and Richardson 1966).

In the following paragraphs bed configurations and their associated flow phenomena are described in the order of their occurrence with increasing stream power.

### 3.3.3 Plane Bed Without Sediment Movement

Plane bed without movement has been studied to determine the bed configuration that would form after beginning of motion. After the beginning of motion, for flat slopes and low velocity, the plane bed will change to ripples for sand material smaller than 0.6 mm, and to dunes for coarser material. Resistance to flow is small for a plane bed without sediment movement and is due solely to the sand grain roughness. Values of Manning's  $n$  range from 0.012 to 0.014 depending on the size of the bed material.

If the bed material of a stream is not moving, the bed configuration will be a remnant of the bed configuration formed when sediment was moving. The bed configurations after the beginning of motion may be those illustrated in Figure 3.5, depending on the flow and bed material. Prior to the beginning of motion, the problem of resistance to flow is one of rigid-boundary hydraulics. After the beginning of motion, the problem relates to defining bed configurations and resistance to flow.

### 3.3.4 Ripples

Ripples are small triangle-shaped elements having gentle upstream slopes and steep downstream slopes. Length ranges from 0.12 m to 0.6 m (0.4 ft to 2 ft) and height from 0.01 m to 0.06 m (0.03 ft to 0.2 ft) (Figure 3.5). Resistance to flow is relatively large (with Manning's  $n$  ranging from 0.018 to 0.030). There is a relative roughness effect associated with a ripple bed and the resistance to flow decreases as flow depth increases. The ripple shape is independent of sand size and at large values of Manning's  $n$  the magnitude of grain roughness is small relative to the form roughness. The length of the separation zone downstream of the ripple crest is about ten times the height of the ripple. Ripples cause very little, if any, disturbance on the water surface, and the flow contains very little suspended bed material. The bed material discharge concentration is small, ranging from 10 to 200 ppm.

### 3.3.5 Dunes

When the shear stress or the stream power is increased for a bed having ripples (or a plane bed without movement, if the bed material is coarser than 0.6 mm), sand waves called dunes form on the bed. At smaller shear-stress values, the dunes have ripples superposed on their backs. These ripples disappear at larger shear values, particularly if the bed material is coarse sand with  $D_{50} > 0.4$  mm.

Dunes are large triangle-shaped elements similar to ripples (Figure 3.5). Their lengths range from 0.6 m (2 ft) to many tens of meters (hundreds of feet), depending on the scale of the flow system. Dunes that formed in the 2.4 m (8-foot) wide flume used by Simons and Richardson (1963, 1966) ranged from 0.6 to 3 m (2 to 10 ft) in length and from 0.06 to 0.3 m (0.2 to 1 ft) in height; whereas, those described by Carey and Keller (1957) in the Mississippi River were 100 to 200 m (300 to 700 ft) long and as much as 12 m (40 ft) high. The maximum amplitude to which dunes can develop is approximately the average depth. Hence, in contrast with ripples, the amplitude of dunes can increase with increasing depth of flow. With dunes, the relative roughness can remain essentially constant or even increase with increasing depth of flow.

Field observations indicate that dunes can form in any sand channel, irrespective of the size of bed material, if the stream power is sufficiently large to cause general transport of the bed material without exceeding a Froude number of unity.

Resistance to flow caused by dunes is large. Manning's  $n$  ranges from 0.020 to 0.040. The form roughness for flow with dunes is equal to or larger than the sand grain roughness.

Dunes cause large separation zones in the flow. These zones, in turn, cause boils to form on the surface of the stream. Measurements of flow velocities within the separation zone show that velocities in the upstream direction exist that are  $1/2$  to  $1/3$  the average stream velocity. Boundary shear stress in the dune trough is sometimes sufficient to form ripples oriented in a direction opposite to that of the primary flow in the channel. With dunes, as with any tranquil flow over an obstruction, the water surface is out of phase with the bed surface (Figure 3.6).

### **3.3.6 Plane Bed With Movement**

As the stream power of the flow increases further, the dunes elongate and reduce in amplitude. This bed configuration is called the transition or washed out dunes. The next bed configuration with increased stream power is plane bed with movement. Dunes of fine sand (low fall velocity) are washed out at lower values of stream power than are dunes of coarser sand. With coarse sands larger slopes are required to affect the change from transition to plane bed and the result is larger velocities and larger Froude numbers. In flume studies with fine sand, the plane-bed condition commonly exists after the transition and persists over a wide range of Froude numbers ( $0.3 < F_r < 0.8$ ). If the sand is coarse and the depth is shallow, however, transition may not terminate until the Froude number is so large that the subsequent bed form may be antidunes rather than plane bed. In natural streams, because of their greater depths, the change from transition to plane bed may occur at a much lower Froude number than in flumes. Manning's  $n$  for plane bed sand channels range from 0.010 to 0.013.

### **3.3.7 Antidunes**

Antidunes form as a series or train of inphase (coupled) symmetrical sand and water waves (Figure 3.5). The height and length of these waves depend on the scale of the flow system and the characteristics of the fluid and the bed material. In a flume where the flow depth was about 0.15 m (0.5 ft) deep, the height of the sand waves ranged from 0.01 to 0.15 m (0.03 to 0.5 ft). The height of the water waves was 1.5 to 2 times the height of the sand waves and the length of the waves, from crest to crest, ranged from 1.5 to 3 m (5 to 10 ft). In natural streams, such as the Rio Grande or the Colorado River, much larger antidunes form. In these streams, surface waves 0.6 to 1.5 m (2 to 5 ft) high and 3 to 12 m (10 to 40 ft) long have been observed.

Antidunes form as trains of waves that gradually build up from a plane bed and a plane water surface. The waves may grow in height until they become unstable and break like the sea surf or they may gradually subside. The former have been called breaking antidunes, or antidunes; and the latter, standing waves. As the antidunes form and increase in height, they may move upstream, downstream, or remain stationary. Their upstream movement led Gilbert (1914) to name them antidunes.

Resistance to flow due to antidunes depends on how often the antidunes form, the area of the stream they occupy, and the violence and frequency of their breaking. If the antidunes do not break, resistance to flow is about the same as that for flow over a plane bed. If many antidunes break, resistance to flow is larger because the breaking waves dissipate a considerable amount of energy. With breaking waves, Manning's  $n$  may range from 0.012 to 0.020.

### **3.3.8 Chutes and Pools**

At very steep slopes, alluvial-channel flow changes to chutes and pools (Figure 3.5). In the 2.4 m (8-foot) wide flume at Colorado State University, this type of flow and bed configuration was studied using fine sands. The flow consisted of a long chute 3 to 9 m (10 to 30 ft) in which the flow was rapid and accelerating followed by a hydraulic jump and a long pool. The chutes and pools moved upstream at velocities of about 0.3 to 0.6 m (1 to 2 ft) per minute. The elevation of the sandbed varied within wide limits. Resistance to flow was large with Manning's  $n$  of 0.018 to 0.035.

### **3.3.9 Regime of Flow, Bed Configuration, and Froude Number**

The change from lower to upper regime flow or the reverse (that is a change from dune bed to a plane bed or plane bed to a dune bed) is not related to the Froude number. However, standing wave and antidune bed configuration in the upper flow regime only occurs with a Froude number greater than 1.0 ( $Fr > 1.0$ ), and ripples and dunes only occur in the lower flow regime at a Froude number less than 1.0 ( $Fr < 1.0$ ) (Vanoni 1977).

The misconception that the lower flow regime shifts to the upper flow regime at a Froude number of 1.0 ( $Fr = 1.0$ ) results from studies made in small flumes where the depth is shallow and large velocities are needed in order to shift from a dune bed to a plane bed. In larger flumes and in rivers the shift occurs at Froude numbers as low as 0.2 (Simons and Richardson 1966, Richardson and Simons 1967, Nordine 1964, Richardson 1965, Dawdy 1961). Figure 3.8 illustrates the relation between flow depth, Froude number and regimes of flow and Figure 3.9 conceptualizes the crossover from lower to upper flow regime in natural rivers.

### **3.3.10 Bars**

In natural channels, some other bed configurations are also found. These bed configurations are generally called bars and are related to the plan form geometry and the width of the channel (Figure 5.14).

Bars are bed forms having lengths of the same order as the channel width or greater and heights comparable to the mean depth of the generating flow. Several different types of bars are observed. They are classified as:

- (1) Point Bars which occur adjacent to the inside banks of channel bends. Their shape may vary with changing flow conditions and motion of bed particles but they do not move relative to the bends;

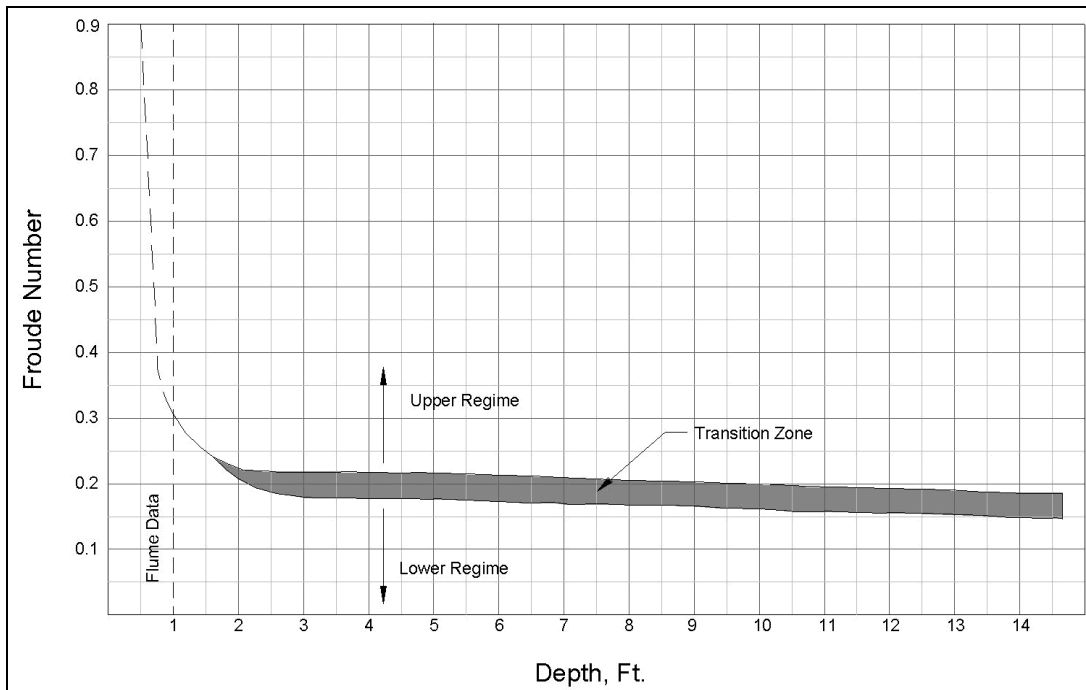


Figure 3.8. Relation between regime of flow and depth for bed material with a median size equal to or less than 0.35 mm.

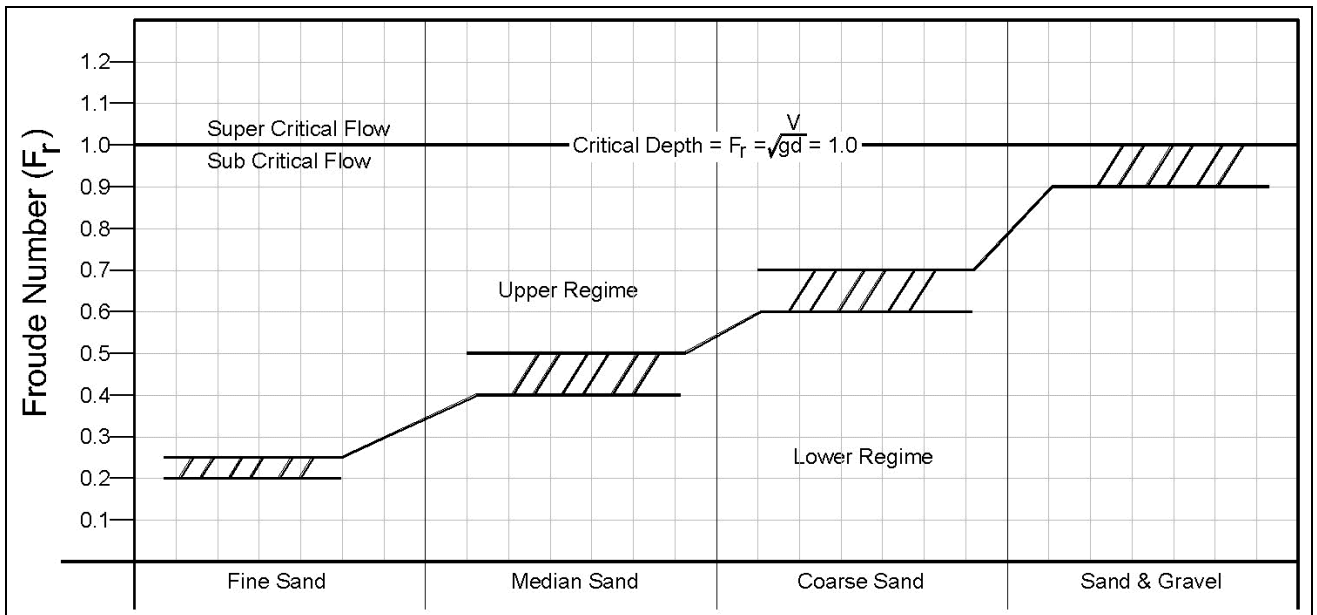


Figure 3.9 Cross-over from lower to upper flow regime based on sand size and Froude Number.

- (2) Alternate Bars which occur in somewhat straighter reaches of channels and tend to be distributed periodically along the reach, with consecutive bars on opposite sides of the channel. Their lateral extent is significantly less than the channel width. Alternate bars move slowly downstream;
- (3) Transverse Bars which also occur in straight channels. They occupy nearly the full channel width. They occur both as isolated and as periodic forms along a channel, and move slowly downstream; and
- (4) Tributary Bars which occur immediately downstream from points of lateral inflow into a channel.

In longitudinal section, bars are approximately triangular, with very long gentle upstream slopes and short downstream slopes that are approximately the same as the angle of repose. Bars appear as small barren islands during low flows. Portions of the upstream slopes of bars are often covered with ripples or dunes.

### 3.4 RESISTANCE TO FLOW IN ALLUVIAL CHANNELS

Resistance to flow in alluvial channels is complicated by the large number of variables and by the interdependency of these variables. It is difficult, especially in field studies, to tell which variables are governing the flow and which variables are the result of this flow.

The slope of the energy grade line for an alluvial stream illustrates the changing role of a variable. If a stream is in equilibrium with its environment, slope is an independent variable. In such a stream, the average slope over a period of years has adjusted so that the flow is capable of transporting only the amount of sediment supplied at the upper end of the stream and by the tributaries. If for some reason a larger or smaller quantity of sediment is supplied to the stream than the stream is capable of transporting, the slope would change and would be dependent on the amount of sediment supplied until a new equilibrium is reached.

In the following sections the variables affecting resistance to flow are discussed. The effects produced by different variables change under different conditions. These changing effects are discussed along with approximations to simplify the analysis of alluvial channel flow.

The variables that describe alluvial channel flow are:

$V$	=	velocity
$y_o$	=	depth
$S_f$	=	slope of the energy grade line
$\rho$	=	density of water-sediment mixture
$\rho_s$	=	density of sediment
$\mu$	=	apparent dynamic viscosity of the water-sediment mixture
$g$	=	gravitational acceleration
$D_s$	=	representative fall diameter of the bed material
$G$	=	gradation coefficient of the bed material
$S_p$	=	shape factor of the particles
$S_R$	=	shape factor of the reach of the stream
$S_c$	=	shape factor of the cross-section of the stream
$f_s$	=	seepage force in the bed of the stream

- $C_T$  = bed material concentration
- $C_f$  = fine-material concentration
- $\omega$  = terminal fall velocity of the particles
- $\tau_c$  = critical shear stress

In general, analysis of river problems is confined to flow of water over beds consisting of quartz particles with constant  $\rho_s$ . The gravitational acceleration  $g$  is also constant in the present context. The effect of other variables on the flow in alluvial channels is qualitatively discussed in the following sections. Most of this presentation is based on laboratory studies which have been supplemented by data from field experience when available.

### 3.4.1 Depth

With a constant slope,  $S_f$ , and bed material,  $D_s$ , an increase in depth,  $y_o$ , can change a plane bed (without movement) to ripples, and ripple-bed configuration to dunes, and a dune bed to a plane bed or antidunes. Also, a decrease in depth may cause plane bed or antidunes to change to a dune-bed configuration. A typical break in a depth-discharge relation caused by a change in bed form from dunes to plane bed or from plane bed to dunes is shown in Figure 3.10.

Often there is a gradual change in bed form and a gradual reduction in resistance to flow and this type of change prevents the break in the stage-discharge relation. Nevertheless, it is possible to experience a large increase in discharge with little or no change in stage. For this and related reasons, development of dependable stage-discharge relations in alluvial channels is very difficult.

Resistance to flow varies with depth even when the bed configurations do not change. When the bed configuration is plane bed, either with or without sediment movement or ripples, there is a decrease in resistance to flow with an increase in depth. This is a relative roughness effect.

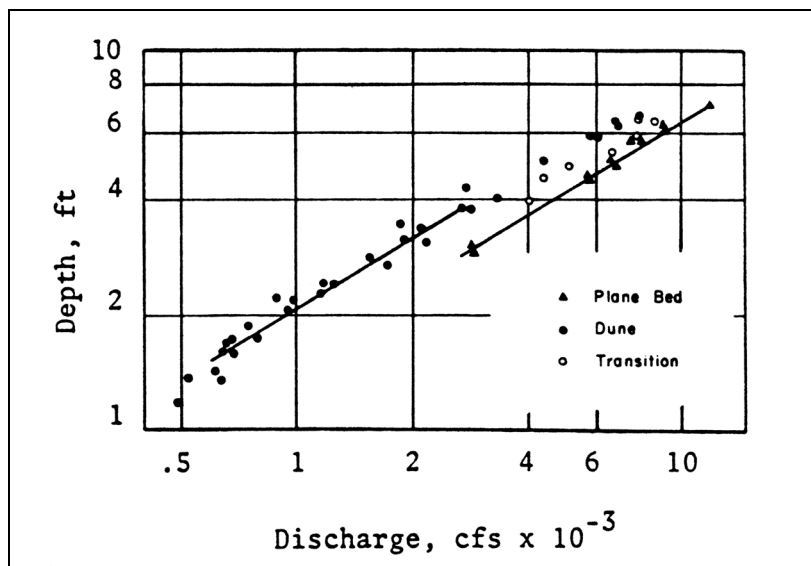


Figure 3.10. Relation of depth to discharge for Elkhorn River near Waterloo, Nebraska (after Beckman and Furness 1962).



When the bed configuration is dunes, field and laboratory studies indicate that resistance to flow may increase or decrease with an increase in depth, depending on the size of bed material and magnitude of the depth. Additional studies are needed to define the variation of resistance to flow for flow over dune beds.

When the bed configuration is antidunes, resistance to flow increases with an increase in depth to some maximum value, then decreases as depth is increased further. This increase or decrease in flow resistance is directly related to changes in length, amplitude, and activity of the antidunes as depth is increased.

### 3.4.2 Slope

The slope,  $S_i$ , is an important factor in determining the bed configuration which will exist for a given discharge. The slope provides the downstream component of the fluid weight, which in turn determines the fluid velocity and stream power. The relation between stream power, velocity and bed configuration has been illustrated in Figure 3.7.

Even when bed configurations do not change, resistance to flow is affected by a change in slope. For example, with shallow depths and the ripple-bed configuration, resistance to flow increases with an increase in slope. With the dune-bed configuration, an increase in slope increases resistance to flow for bed materials having fall velocities greater than 0.06 m/s (0.20 ft/s). For those bed materials having fall velocities less than 0.06 m/s (0.20 ft/s), the effect is uncertain.

### 3.4.3 Apparent Viscosity and Density

The effect of fine sediment (bentonite) on the apparent kinematic viscosity of the mixture is shown in Figure 3.11. The magnitude of the effect of fine sediment on viscosity is large and depends on the chemical make up of the fine sediment.

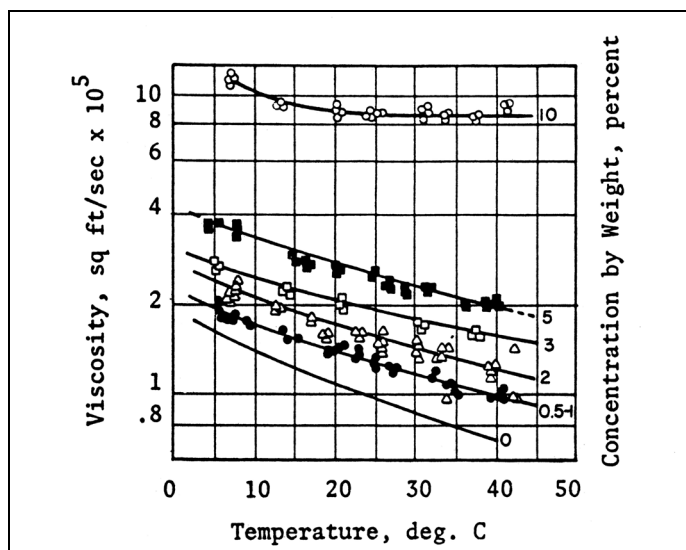


Figure 3.11. Apparent kinematic viscosity of water-bentonite dispersions (Simons and Richardson 1966).

In addition to increasing the viscosity, fine sediment suspended in water increases the mass density of the mixture ( $\rho$ ) and, consequently, the specific weight ( $\gamma$ ). The specific weight of a sediment-water mixture is computed from the relation,

$$\gamma = \frac{\gamma_w \gamma_s}{\gamma_s - C_s (\gamma_s - \gamma_w)} \quad (3.13)$$

where:

- $\gamma_w$  = Specific weight of the water [9810 N/m<sup>3</sup> (62.4 lb per cu ft)]
- $\gamma_s$  = Specific weight of the sediment [about 26,000 N/m<sup>3</sup> (165.4 lb per cu ft)]
- $C_s$  = Concentration by weight (in fraction form) of the suspended sediment

A sediment-water mixture, where  $C_s = 10$  percent, has a specific weight ( $\gamma$ ) of about 10,460 N/m<sup>3</sup> (66.5 lb per cu ft). It is clear any change in  $\gamma$  affects the boundary shear stress and the stream power.

Changes in the fall velocity of a particle caused by changes in the viscosity and the fluid density resulting from the presence of suspended bentonite clay in the water are shown in Figure 3.12a. For comparative purposes, the effect of temperature on the fall velocity of two sands in clear water is shown in Figure 3.12b.

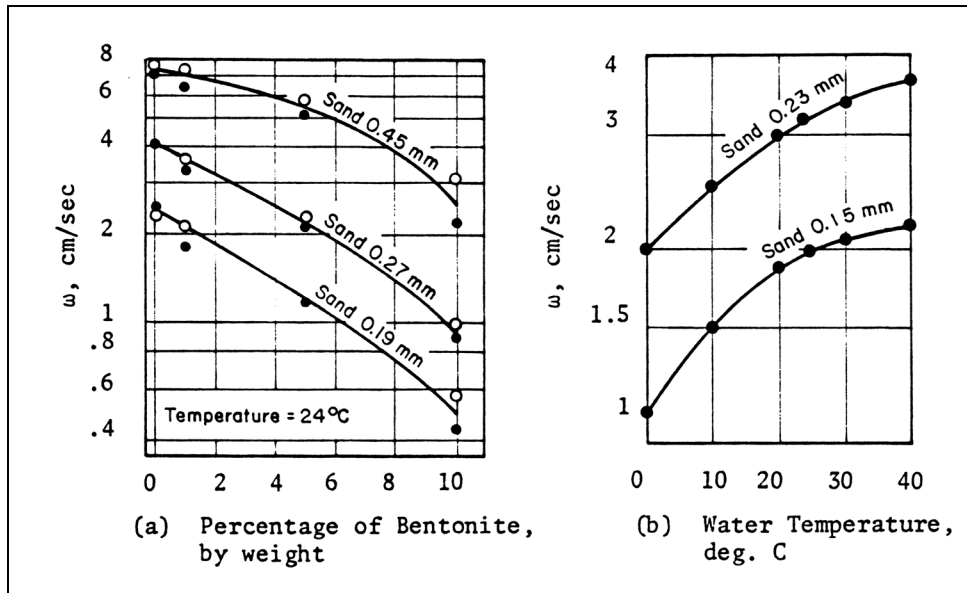


Figure 3.12. Variation of fall velocity of several sand mixtures with percent bentonite and temperature (Simons and Richardson 1966).

### 3.4.4 Size of Bed Material

The effects of the physical size of the bed material,  $D_s$ , on resistance to flow are: (1) its influence on the fall velocity,  $\omega$ , which is a measure of the interaction of the fluid and the

particle in the formation of the bed configurations; (2) its effect on grain roughness,  $K_s$ ; and (3) its effect on the turbulent structure and the velocity field of the flow.

The physical size of the bed material, as measured by the fall diameter or by sieve diameter, is a primary factor in determining fall velocity. Use of the fall diameter instead of the sieve diameter is advantageous because the shape factor and density of the particle can be eliminated as variables. That is, if only the fall diameter is known, the fall velocity of the particle in any fluid at any temperature can be computed; whereas, to do the same computation when the sieve diameter is known, knowledge of the shape factor and density of the particle are also required.

The physical size of the bed material determines the friction factor mainly for the plane-bed condition and for antidunes when they are not actively breaking. The breaking of the waves, which increases with a decrease in the fall velocity of the bed material, causes additional dissipation of energy.

The physical size of the bed material for a dune-bed configuration also has an effect on resistance to flow. The flow of fluid over the back of dunes is affected by grain roughness, although the dissipation of energy by the form roughness is the major factor. The form of the dunes is also related to the fall velocity of the bed material.

#### **3.4.5 Size Gradation**

The gradation,  $G$ , of sizes of the bed material affects bed form and resistance to flow. Flume experiments indicate that uniform sands (sands of practically the same size) have larger resistance to flow (except plane bed) than graded sands for the various bed forms. Also the transition from upper flow regime to lower flow regime occurs over a narrower range of shear values for the uniform sand. For a plane bed with motion, resistance to flow is about the same for both uniform or graded sand.

#### **3.4.6 Fall Velocity**

Fall velocity,  $\omega$ , is the primary variable that determines the interaction between the bed material and the fluid. For a given depth, and slope, the fall velocity determines the bed form that will occur, the actual dimensions of the bed form and, except for the contribution of the grain roughness, the resistance to flow.

Observations of natural streams have shown that the bed configuration and resistance to flow change with changes in fall velocity when the discharge and bed material are constant. For example, the Loup River near Dunning, Nebraska has bed roughness in the form of dunes in the summer when the water is warm and less viscous but has a nearly plane bed during the cold winter months. Similarly, two sets of data collected by Harms and Fahnestock (1965) on a stable branch of the Rio Grande at similar discharges show that when the water was cold, the bed of the stream was plane, the resistance to flow was small, the depth was relatively shallow, and the velocity was large; but when the water was warm, the bed roughness was dunes, the resistance to flow was large, the depth was large, and the velocity was low.

### 3.4.7 Shape Factor for the Reach and Cross-Section

The configuration of the reach,  $S_R$ , and the shape of the cross-section,  $S_c$ , affect the energy losses resulting from the nonuniformity of the flow in a natural stream caused by the bends and the nonuniformity of the banks. Study of these losses in natural channels has long been neglected. Also, flow phenomena, bed configuration, and resistance to flow vary with the width of the stream. In narrow channels dunes and antidunes vary mainly in the downstream direction and resistance to flow is larger than for a wide channel. Also, in wide channels more than one bed form can occur in the cross-section.

### 3.4.8 Seepage Force

A seepage force,  $f_s$ , occurs whenever there is inflow or outflow through the bed and banks of a channel in permeable alluvium. The seepage flow affects the alluvial channel phenomena by altering the velocity field in the vicinity of the bed particles and by changing the effective weight of the bed particles. Seepage may have a significant effect on bed configuration and resistance to flow. If there is inflow, the seepage force acts to reduce the effective weight of the sand and, consequently, the stability of the bed material. If there is outflow, the seepage force acts in the direction of gravity and increases the effective weight of the sand and the stability of the bed material. As a direct result of changing the effective weight, the seepage forces can influence the form of bed roughness and the resistance to flow for a given channel flow. For example, under shallow flow a bed material with median diameter of 0.5 mm will be molded into the following forms as shear stress is increased: dunes, transition, plane bed, and antidunes. If this same material was subjected to a seepage force that reduced its effective weight to a value consistent with that of medium sand (median diameter,  $D_s = 0.3$  mm), the forms of bed roughness would be transition, plane bed, and antidunes for the same range of flow conditions.

A common condition is outflow from the channel during the rising stage; this process increases the stability of the bed and bank material but stores water in the banks. During the falling stage, the situation is reversed; inflow to the channel reduces the effective weight and stability of the bed and bank material and influences the form of bed roughness and the resistance to flow.

### 3.4.9 Bed Material Concentration

The bed material concentration,  $C_T$ , affects the fluid properties by increasing the apparent viscosity and the density of the water-sediment mixture. However, the effect of the sediment on viscosity  $\mu$  and the density  $\rho$  in any resistance to flow relation is accounted for by using their values for the water-sediment mixture instead of their values for pure water. The presence of sediment in the flow causes a small change in the turbulence characteristics, velocity distribution and resistance to flow.

### 3.4.10 Fine-Material Concentration

Fine-material concentration,  $c_f$ , or washload is that part of the total sediment discharge that is not found in appreciable quantities on the bed. If significant amounts of sediment is in suspension, its effect on the viscosity of the water-sediment mixture should be taken into

account. The effect of fine sediment on resistance to flow is a result of its effect on the apparent viscosity and the density of the water-sediment mixture. Generally, the fine sediment is uniformly distributed in the stream cross-section. The method of defining and treating the fine-material load computations is discussed in Chapter 4.

### 3.4.11 Bedform Predictor and Manning's $n$ Values for Sand-Bed Streams

In Figure 3.13, the relation between stream power, median fall diameter of bed material, and form roughness is shown. This relation gives an indication of the form of bed roughness one can anticipate if the stream power and fall diameter of bed material are known. Flume data were utilized to establish the boundaries separating plane bed without sediment movement and ripples, and ripples and dunes for bed material with  $D_{50}$  finer than 0.64 mm, and plane bed without sediment movement and dunes for  $D_{50}$  coarser than 0.64 mm. The lines dividing dunes and transition and dividing transition and upper regime are based on flume data and the following field data: (1) Elkhorn River, near Waterloo, Nebraska (Beckman and Furness 1962); (2) Rio Grande, 32 km (20 mi) above El Paso, Texas; (3) Middle Loup River at Dunning, Nebraska (Hubbell and Matejka 1959); (4) Rio Grande at Cochiti, near Bernalillo and at Angostura heading, N. Mexico (Culbertson and Dawdy 1964); and (5) Punjab canal data upper regime flows that have been observed in large irrigation canals that have fine sandbeds.

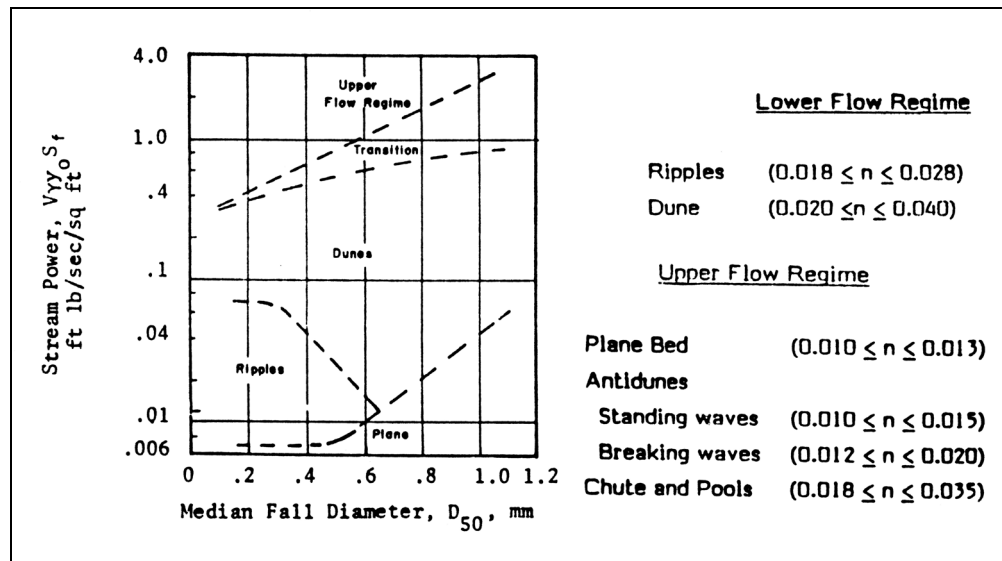


Figure 3.13. Relation between stream power, median fall diameter, and bed configuration and Manning's  $n$  values.

Observations by the authors on natural sandbed streams with bed material having a median diameter ranging from 0.1 mm to 0.4 mm indicate that the bed planes out and resistance to flow decreases whenever high flow occurs. Manning's  $n$  changes from values as large as 0.040 at low flow to as small as 0.012 at high flow. An example is given in Figure 3.14. These observations are substantiated by Dawdy (1961), Colby (1960), U.S. Army Corps of Engineers (1968) and Beckman and Furness (1962).

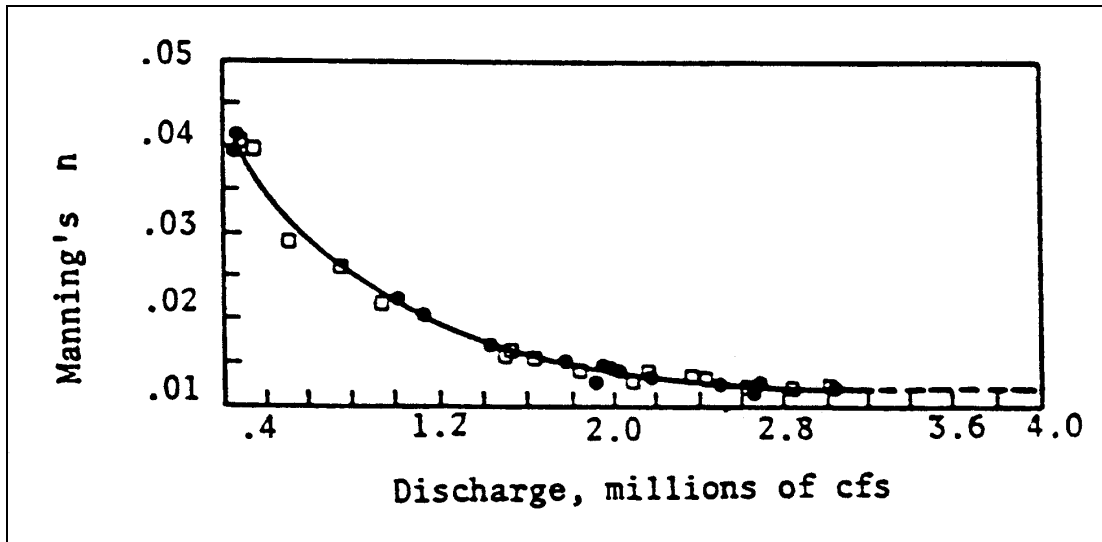


Figure 3.14. Change in Manning's  $n$  with discharge for Padma River in Bangladesh.

### 3.4.12 How Bedform Changes Affect Highways in the River Environment

At high flows, most sandbed channel streams shift from a dune bed to a transition or a plane bed configuration. The resistance to flow is then decreased two to threefold. The corresponding increase in velocity can increase scour around bridge piers, abutments, spur dikes or banks and also increases the required size of riprap. On the other hand, the decrease in stage resulting from the planing out of the bed will decrease the required elevation of the bridge crossing, the height of embankments across the floodplain, the height of any dikes, and the height of any channel control works that may be needed; and the converse is also true.

Another effect of bed form on highway crossings is that with dunes on the bed there is a fluctuating pattern of scour on the bed and around the piers, abutments, guide banks and spurs. The average height of dunes is approximately 1/2 to 1/3 the average depth of flow and the maximum height of a dune may approach the average depth of flow. If the depth of flow is 3 m (10 ft), the maximum dune height may be of the order of 3 m (10 ft), and half of this would be below the mean elevation of the bed. With the passage of this dune through a bridge section, an increase of 1.5 m (5 ft) in the local scour would be anticipated when the trough of the dune arrives at the bridge.

A very important effect of bed forms and bars is the change of flow direction in channels. At low flow the bars can be residual and cause high velocity flow along or at a pier or abutment or any of the other structures in the stream bed, causing deeper than anticipated scour. As stated previously large discharges normally experience smaller resistance to flow in a sandbed stream due to the change in bed form. However, if the bridge crossing or encroachment causes appreciable backwater, the dune bed may not plane out at large discharges and a higher resistance to flow results. This increase in resistance to flow can decrease the velocity of flow and also decrease the transport capacity of the channel so that aggradation occurs upstream of the crossing. The aggradation and the roughness increases the river stage and thus the height of any control structure or the levees. Thus, the bridge crossing can adversely affect the floodplain, due to the change in bed form that would occur.

With highways in the sandbed river environment, care must be taken in analyzing the crossing in order to foresee possible changes that may occur in the bed form and what these changes may do to the resistance coefficient, to sediment transport, and to the stability of the reach and its structures.

### **3.4.13 Alluvial Processes and Resistance to Flow in Coarse Material Streams**

The preceding discussion of alluvial channel flow is mainly related to sandbed channels; that is, channels with noncohesive bed materials of size less than 2 mm. The analysis of coarse-material channels is also pertinent to highway engineering. This classification includes all channels with noncohesive bed materials coarser than 2 mm size.

The behavior of coarse material channels is somewhat different from sandbed channels. The main distinction between the two channels lies in the spread of their bed material size distribution. In sandbed channels, for example, the bed may consist of particles from 0.02 to 2 mm; i.e., a 100-fold size range. In coarse-material channels, even if the maximum size is limited to cobbles (250 mm), the size range of particles may be 0.10 to 250 mm, which is a 2,500-fold size range. In general, coarse-material channels are less active and have slower rates of bank shifting than sandbed channels. However, the tendency for channel armoring is more pronounced in coarse material channels as discussed next.

Armoring. The phenomenon of armoring in mobile bed channels occurs by the rearrangement of bed material during movement. The bed is covered by a one particle thick layer of the coarser material underlain by the finer sizes. The absence of finer sizes from the surface layer is caused by the winnowing away of these sizes by the flow. As the spread of particle sizes available in the bed of coarse-material channels is large, these channels can armor their beds and behave as rigid boundary channels for all except the highest flows. The bed and bank forming activity in these channels is therefore limited to much smaller intervals of the annual hydrographs than the sandbed channels.

The general lack of mobility in coarse material channels also means the bed forms do not change as much or as rapidly as in sandbed channels. The roughness coefficients in coarse material channels are therefore more consistent during the annual hydrographs than in sandbed channels. Most of the resistance to flow in coarse material channels comes from the grain roughness and from bars. The river bed forms (dunes) are less important in the hydraulic behavior of coarse bed channels.

Sampling. The purpose of bed material sampling in coarse-material channels is: (1) to determine the conditions of incipient movement; (2) to assess the bed roughness related to the resistance to flow; (3) to determine the bed material load for a given flow; and (4) to determine the long and short time response of the channel to specific activities. For objectives (1) to (3), the properties of the surface layer are needed. If it is anticipated that the bed layer will be disrupted at any given stage, it is necessary to take an adequate sample of both the surface and subsurface material.

The surface sampling can be easily done on the channel bed by counting particles on a grid, as explained earlier in this chapter. However, special effort should be made to obtain an objective sample. There is a tendency to select too many large particles. The scoop sample with bed material sizes larger than 25.4 mm (an inch) or so is difficult to obtain and such samples may have to be collected from bars and other exposed areas on channel perimeter.

In the size distribution analysis of coarse-bed materials, it is sometimes necessary to obtain particle counts by number, rather than by sieving or visual accumulation tube analysis for a part of the sample. Care must be taken in the interpretation of frequency distribution of part of a sample obtained by sieving. Only if the size distribution in a sample follows log-normal probability distribution can number counts be transferred to distributions by size, volume, weight or surface areas directly. For other distributions, special numerical techniques have to be used to transform the number distributions to weight or size distributions.

If the objectives of bed material sampling include bed roughness and channel response, then the particles coarser than  $D_{84}$  or  $D_{90}$  need to be analyzed with more care. These sizes also require large samples for their determination.

Resistance to Flow. In sandbed channels, the form roughness is the primary component of channel roughness. Form roughness can be much greater than the grain roughness when the bed forms are ripples and dunes. In coarse-material channels, the ripples never form and dunes are rare. The main type of bed form roughness in such channels is the pool and riffle configuration. With coarse material channels the grain roughness is the main component of the channel roughness.

A coarse-material channel may have bed material that is only partly submerged during most of the flows. It is difficult to determine the channel roughness for such beds. For other cases, analysis of data from many rivers, canals and flumes (Anderson et al. 1968) shows that the channel roughness can be predicted by various forms of Strickler's equation:

$$n = K_u D_x^{1/6} \quad (3.14)$$

V.T. Chow (1959) (3.15)

$$K_u = 0.0417 \quad (D_{50} \text{ in meters})$$

$$K_u = 0.0342 \quad (D_{50} \text{ in feet})$$

Anderson et al. (1970) (3.16)

$$K_u = 0.0482 \quad (D_{50} \text{ in meters})$$

$$K_u = 0.0395 \quad (D_{50} \text{ in feet})$$

Lane and Carlson (1955) (3.17)

$$K_u = 0.0473 \quad (D_{75} \text{ in meters})$$

$$K_u = 0.0388 \quad (D_{75} \text{ in feet})$$

$$K_u = 0.0256 \quad (D_{75} \text{ in inches})$$

U.S. Army Corps of Engineers (1991) (3.18)

$$K_u = 0.046 \quad (D_{90} \text{ in meters})$$

$$K_u = 0.038 \quad (D_{90} \text{ in feet})$$

Equation 3.19 has been proposed by Limerinos (1970) and involves flow depth  $y_o$  as a parameter. Comparisons of several equations have been reported by Bray (1982) and Simons and Senturk (1992).



$$n = \frac{K_u y_o^{1/6}}{1.16 + 2 \log \frac{y_o}{D_{84}}} \quad (3.19)$$

$K_u = 0.113$  ( $y_o$  and  $D_{84}$  in meters)

$K_u = 0.0927$  ( $y_o$  and  $D_{84}$  in feet)

An alternative approach, valid when  $R/D_{50} > 10$ , is to evaluate the Darcy-Weisbach friction factor,  $f$ , as a function of the hydraulic radius,  $R$ , with:

$$\frac{1}{\sqrt{f}} = 1.9 \left( \frac{R}{D_{84}} \right)^{1/4} \quad (3.20)$$

$$\frac{1}{\sqrt{f}} = 2.0 \log \left( \frac{R}{D_{84}} \right) + 1.1 \quad (3.21)$$

Note:  $R$  and  $D_{84}$  in same units (meters, feet)

Manning's  $n$  can then be calculated from the relationship between  $R$  and  $f$  :

$$n = K_u R^{1/6} \sqrt{f} \quad (3.22)$$

$K_u = 0.113$  ( $R$  in meters)

$K_u = 0.0927$  ( $R$  in feet)

This approach should not be applied to river reaches with active beds or significant sediment transport.

Charlton et al. (1978) and Bray (1979) have proposed the guidelines in Table 3.3 to estimate  $D_{90}$ ,  $D_{84}$ , and  $D_{65}$ , for gravel-bed material when size distribution curves cannot be obtained from field data.

Ratio	Mean Value	Standard Deviation
$D_{90}/D_{50}$	2.1	0.46
$D_{84}/D_{50}$	1.9	0.36
$D_{65}/D_{50}$	1.3	0.08

## 3.5 BEGINNING OF MOTION

### 3.5.1 Introduction

The initiation or ceasing of motion of sediment particles is involved in many geomorphic and hydraulic problems including stream stability and scour at highway bridges, sediment transport, erosion, slope stability, stable channel design, and design of riprap. These problems can only be handled when the threshold of sediment motion is fully understood.

Beginning of motion can be related to either shear stress on the grains or the fluid velocity in the vicinity of the grains. When the grains are at incipient motion, these values are called the critical shear stress or critical velocity. The choice of shear stress or velocity depends on: (1) which is easier to determine in the field; (2) the precision with which the critical value is known or can be determined for the particle size; (3) the type of problem. In sediment transport analysis most equations use critical shear stress. In stable channel design either critical shear stress or critical velocity is used; whereas, in riprap design critical velocity is generally used.

Equations for determining the shear stress on the bed of a stream are given in Chapter 2, Section 2.4.5. The average shear stress on the boundary is given by  $\tau_0 = \gamma RS$ . Where  $\gamma$  is the unit weight of water,  $R$  is the hydraulic radius and  $S$  is the slope of the energy grade line. In wide channels (width equal to or greater than 10 times the depth)  $R \approx y$ , the depth. Other relations give the shear stress in terms of the velocity of flow.

It may not be sufficient to determine the average value of the critical shear stress or velocity because both quantities are fluctuating. For the same mean values, they may have larger values that act for a sufficiently long enough time to cause a particle to move. In addition, the forces on the particle resulting from the flowing water, waves, and seepage into or out of the bed or banks affect the beginning of motion.

In this section, the following topics are discussed: theory of beginning of motion, Shields experimental relationship and its modifications, equations to determine the relation between flow variables (depth, velocity or discharge) and sediment size, tables giving observed values between flow variables and sediment size, and figures for determining the flow or sediment variables at beginning of motion.

### 3.5.2 Theoretical Considerations

When the force of the flowing water (as measured by the shear stress or velocity) is less than some critical value, the bed material of a channel remains motionless. Then, the alluvial bed can be considered as immobile. But when the shear stress or velocity over the bed attains or exceeds its critical value, particle motion begins. In general, the observation of particle movement is difficult in nature. The most dependable data available have resulted from laboratory experiments.

The beginning of motion is difficult to define. This difficulty is a consequence of a phenomenon that is random in time and space. When the shear stress is near its critical value, it is possible to observe a few particles moving on the channel bottom. The time history of the movement of a particle involves long rest periods. In fact, it is difficult to conclude that particle motion has begun. Kramer (1935) and Buffington (1999) proposed four levels of motion of bed material.

1. None.
2. Weak movement: Only a few particles are in motion on the bed. The grains moving on one square centimeter of the bed can be counted.
3. Medium movement: The grains of mean diameter begin to move. The motion is not local in character but the bed continues to be plane.
4. General movement: All the mixture is in motion; the movement is occurring in all parts of the bed at all times. It is sufficiently vigorous to change the bed configuration.

Whether or not a plane bed can exist with weak sediment motion is debated; though positive evidence of its existence has been presented by Liu (1957) and Senturk (1969). Liu's observations may have involved such shallow flow that the Froude number was larger than 1, which would indicate antidunes not ripples. Many researchers such as Kramer (1935), Shields (1935), White (1940), Tison (1953), Simons and Richardson (1966), Gessler (1971), Vanoni (1977), have studied the problem of initiation of motion. Buffington (1999) provides an excellent review of Shields research. The studies involve both theory and experimentation. The complexity of the problem explains the diversity of experimental results. In reality, there is no truly critical condition for initiation of motion for which motion begins suddenly as the condition is reached. Data available on critical shear stress are based on arbitrary definitions of critical conditions and most definitions used have relied on subjective visual observations. Also, no evidence has shown that the mean diameter represents the composition of a mixture correctly. The engineer facing this dilemma of dealing with beginning of motion in a mixture of sediment sizes should analyze the problem very carefully. However, the equations presented in this section are theoretically sound and have proven to give reliable results. This is true, even though there is a diversity in the experimentally determined coefficients.

Water flowing over a bed of sediment exerts forces on the grains. These forces tend to move or entrain the particles. The forces that resist the entraining action of the flowing water differ depending upon the properties of bed material. For coarse sediments such as sands and gravels, the resisting forces relate mainly to the weight of the particles, but also are a function of shape of particle, its position relative to other particles, and the form of bed roughness. For cohesive bed material (generally silts and clays), chemical bonding between particles resists the beginning of motion.

When the hydrodynamic forces acting on a grain of sediment have reached a value that, if increased even slightly the grain will move, critical or threshold conditions are said to have been reached. Under critical conditions, the hydrodynamic forces acting upon a grain are just balanced by the resisting force of the particle.

### **3.5.3 Theory of Beginning of Motion**

The forces acting on an individual particle on the bed of an alluvial channel are:

1. Body force  $F_g$  due to the gravitational field,
2. External forces  $F_n$  acting at the points of contact between the grain and its neighboring grains, and

3. Fluid force  $F_f$  (lift and drag) acting on the surface of the grain. The fluid force varies with the velocity field and with the properties of the fluid.

The relative magnitude of these forces determines whether the grain moves or not.

For the individual grain, the body force is:

$$F_g = g\rho_s K_2 D_s^3 \quad (3.23)$$

where:

$$\begin{aligned} \rho_s &= \text{Density of the grain} \\ K_2 &= \text{Volumetric coefficient} \\ D_s &= \text{Grain diameter} \\ K_2 D_s^3 &= \text{Volume of the grain} \end{aligned}$$

For convenience, the fluid forces acting on the grain are divided into three components:

- (1) The form drag component  $F_D$

$$F_D = C_D K_1 D_s^2 \rho (V^2 / 2) \quad (3.24)$$

- (2) The viscous drag component  $F_V$

$$F_V = C_s K_1 D_s^2 \tau \quad (3.25)$$

- (3) The buoyant force component  $F_B$

$$F_B = g\rho K_2 D_s^3 \quad (3.26)$$

where:

$$\begin{aligned} C_D &= \text{Drag coefficient} \\ K_1 &= \text{Coefficient associated with the area of the grain subjected to form drag and shear (the term } K_1 D_s^2 \text{ represents the cross-sectional area of the grain)} \\ K_2 &= \text{Volumetric coefficient of the grain} \\ D_s &= \text{Diameter of the grain} \\ v &= \text{Velocity in the vicinity of the grain} \\ C_s &= \text{Coefficient of shear} \\ \tau &= \text{Average viscous shear stress} \end{aligned}$$

The external forces  $F_n$  depend on the values of the fluid and body forces  $F_B$ . Under conditions of no flow, the fluid force is  $F_f = F_B$ . There is no form or viscous drag. Then the external force  $F_n$  is  $F_n = F_g - F_B$  or

$$F_n = (\rho_s - \rho)gK_2 D_s^3 \quad (3.27)$$

That is, the external force is equal to the submerged weight of the grain.

The form drag can be written in terms of the shear velocity. For turbulent flow, the local velocity,  $v$  is directly proportional to the shear velocity  $V^*$ . Then, Equation 3.24 reduces to:

$$F_D \sim \rho D_s^2 V_*^2 \quad (3.28)$$

The viscous drag is also related to the shear velocity, but it is the shear velocity for laminar flow. For laminar flow:

$$\tau = \mu \frac{dv}{dy} \quad (3.29)$$

Again, by replacing  $V$  with  $V^*$  and  $y$  with  $D_s$  we can write

$$\tau \approx \mu V_* / D_s \quad (3.30)$$

With this expression for viscous shear, the shear force  $F_v$  becomes

$$F_v \sim \mu D_s V_* \quad (3.31)$$

Now, consider the ratio of the form drag force  $F_D$  to the viscous shear force  $F_v$ . According to Equations 3.28 and 3.31:

$$\frac{F_D}{F_v} \sim \frac{\rho D_s^2 V_*^2}{\mu D_s V_*}$$

or

$$\frac{F_D}{F_v} \sim \frac{D_s V_*}{\nu} \quad (3.32)$$

When the flow over the grain is turbulent, the form drag is predominant and the term  $D_s V_* / \nu$  is large. When the flow over the grain is laminar the viscous shear force is predominant and the term  $D_s V_* / \nu$  is small. Thus, the Reynolds' number of particle  $D_s V_* / \nu$  is an indicator of the characteristics of the flow in the vicinity of the grain.

As both the form drag and viscous shear are proportional to the shear velocity, the ratio of the forces tending to move the grain to the forces resisting movement is:

$$\frac{F_D}{F_n} \sim \frac{\rho D_s^2 V_*^2}{(\rho_s - \rho) g D_s^3} = \frac{\tau_o}{(\gamma_s - \gamma) D_s} \quad (3.33)$$

Recall that  $V_*^2 = \tau_o/\rho$ . The relation between  $\tau_o/(\gamma_s - \gamma) D_s$  and  $D_s V_*/\nu$  for the condition of incipient motion has been determined experimentally by Shields and others. As the relation is determined experimentally, the relation considers viscous effects. In functional form the relation (called the Shields relation) is as follows:

$$\frac{\tau_o}{(\gamma_s - \gamma) D_s} = f\left(\frac{V_* D_s}{\nu}\right) \quad (3.34)$$

### 3.5.4 Shields Diagram

Many experiments have been conducted to develop an explicit solution of the Shields relation. The earliest one is the graphical presentation given by Shields (1935). The concept of the Shields Diagram (Figure 3.15) is widely accepted and  $\tau_o/(\gamma_s - \gamma) D_s$  (often referred to as Shields parameter) is widely used to determine the shear stress at beginning of motion. For example, Gessler (1971) gave Figure 3.16 for the relation given in Equation 3.34.

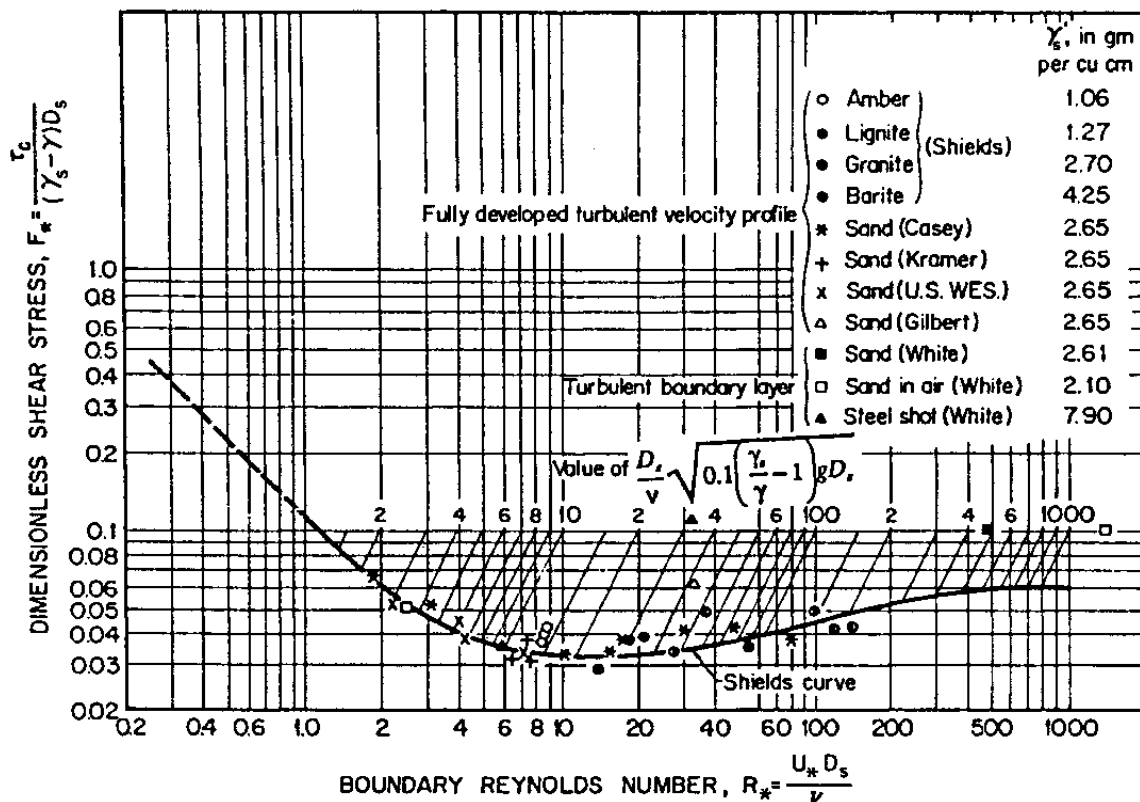


Figure 3.15. Shields Diagram: dimensionless critical shear stress.

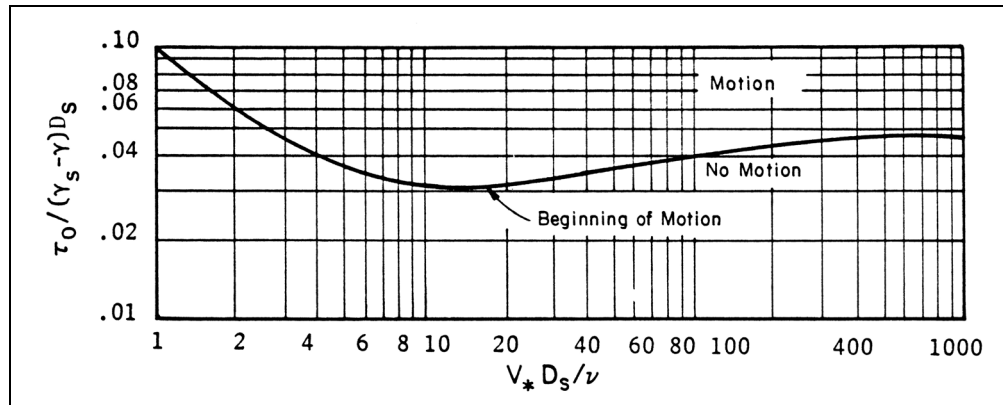


Figure 3.16. Shields' relation for beginning of motion (after Gessler 1971).

Most authors report that Shields determined this relationship (Figure 3.15) by measuring bed-load transport for various values of  $\tau/(\gamma_s - \gamma) D_s$  and then extrapolated to the point of vanishing bed load. Simons and Senturk (1992) state the values of  $\tau/(\gamma_s - \gamma) D_s$  were at least twice as large as the critical value. This indirect procedure was used to avoid the implications of the random orientation of grains and variations in local flow conditions that may result in grain movement even when  $\tau/(\gamma_s - \gamma) D_s$  is considerably below the critical value. However, Buffington (1999) discusses in great detail Shields' research and states the following:

"Nevertheless, these two passages from Shield's dissertation offer two definitions of incipient motion (bed-load extrapolation for uniform sizes versus visual observation for mixed grains. Because Shields neglected to explain which method he used and did not present sufficient data to recreate his calculations, the matter of his experimental procedure remains open to debate. However, throughout his dissertation he discussed his approach and results as being representative of uniform grains (Shields 1936c pp. 11, 14, and 16), suggesting that he employed bed-load extrapolation (the method he described for uniform sediment.)"

The Shields Diagram (Figure 3.15) was divided into three regions by Simons and Senturk (1992) as illustrated in the following.

**Region 1:**  $V_* D_s / \nu < 3.63 \sim 5.0$

In the region  $D_s < 3\delta$ , where  $\delta = 11.6\nu/V_*$ , and the boundary is considered hydraulically smooth ( $\delta$  is the thickness of the laminar boundary layer, Chapter 2). Shields estimated the portion of the diagram for  $V_* D_s / \nu < 2$ . He did not perform any experiments in that region.

According to Shields, when the value of

$$\frac{\tau_c}{(\gamma_s - \gamma) D_s} \cong 0.1 \quad (3.35)$$

then (approximately)

$$\frac{V_* D_s}{\nu} = 1.00$$

**Region 2:**  $3.63 \sim 5.0 < V_* D_s / \nu < 68.0 \sim 70.0$

In this region, the boundary is in a transitional state and  $\delta/3 < D_s < 6 \delta$ . For this region:

$$\frac{k_s}{\delta} = \frac{1}{11.6} \frac{k_s V_*}{\nu} \quad (3.36)$$

The Shields Diagram has a form similar to Darcy-Weisbach's resistance coefficient  $f$  versus Reynolds number  $R_e$ . Also, it is similar in form to the relation between the drag coefficient  $C_D$  and the Reynolds number  $R_e$  for cylindrical bodies and to the relation between  $V_* k_s / \nu$  and  $B = f(V_* k_s / \nu)$  proposed by Nikuradse (1933).

The minimum value of  $F_* = \tau_o / (\gamma_s - \gamma) D_s$  is  $0.032 \sim 0.033$  and the corresponding value of  $R_* = V_* D_s / \nu$  is about 10. If  $D_s$  is computed from these values of  $R_*$  and  $F_*$ , it can be seen that  $D_s = 0.0006 \text{ m} = 0.6 \text{ mm} = 0.002 \text{ ft}$ . For larger diameter particles, ripples do not form; dunes form on the bed.

**Region 3:**  $V_* D_s / \nu > 70$  to 500

In this region, the boundary is completely rough and  $F_*$  is independent of Reynolds number  $R_*$  and is equal to

$$\frac{\rho V_*^2}{(\gamma_s - \gamma) D_s} = 0.06 \quad (3.37)$$

The upper limit of  $R_*$  in Region 3 is subject to discussion. Some researchers have given values as high as 1,000 for  $R_*$ . Considering  $F_*$ , Meyer-Peter and Müller (1948) suggest a value of 0.047 instead of 0.06.

Experimental values of the Shields parameter for sand size (0.062 mm to 1.0 mm) bed material range from 0.030 to 0.047. For coarser bed material (gravels, cobbles and larger) the experimentally determined Shield's parameter ranges from 0.020 to 0.10. An average value of 0.039 is a good compromise for all sizes (Fiuzat and Richardson 1983, Ruff et al., 1985, 1987).

It is suggested by Simons (Simons and Senturk 1992) that collecting data on initiation of particle motion under field conditions permits selection of a more precise value for the particular channel. However, identifying initiation of particle sizes by utilizing observed values or by trapping particles in motion over a range of discharges is extremely difficult. It must be done with considerable care and with knowledge of channel geometry and hydraulic conditions at the cross section and upstream of the selected cross section. This is particularly true for gravel- and cobble-bed streams.



The variation of the critical shear stress for beginning of motion as a function of sediment size given by various investigators is shown in Figure 3.17 (Chien 1954). The spread of the representative curves shows the diversity of experimental and theoretical results. Nevertheless, equations, tables and figures given in this section provide useful tools for determining beginning of motion for sediment particles and the design of riprap.

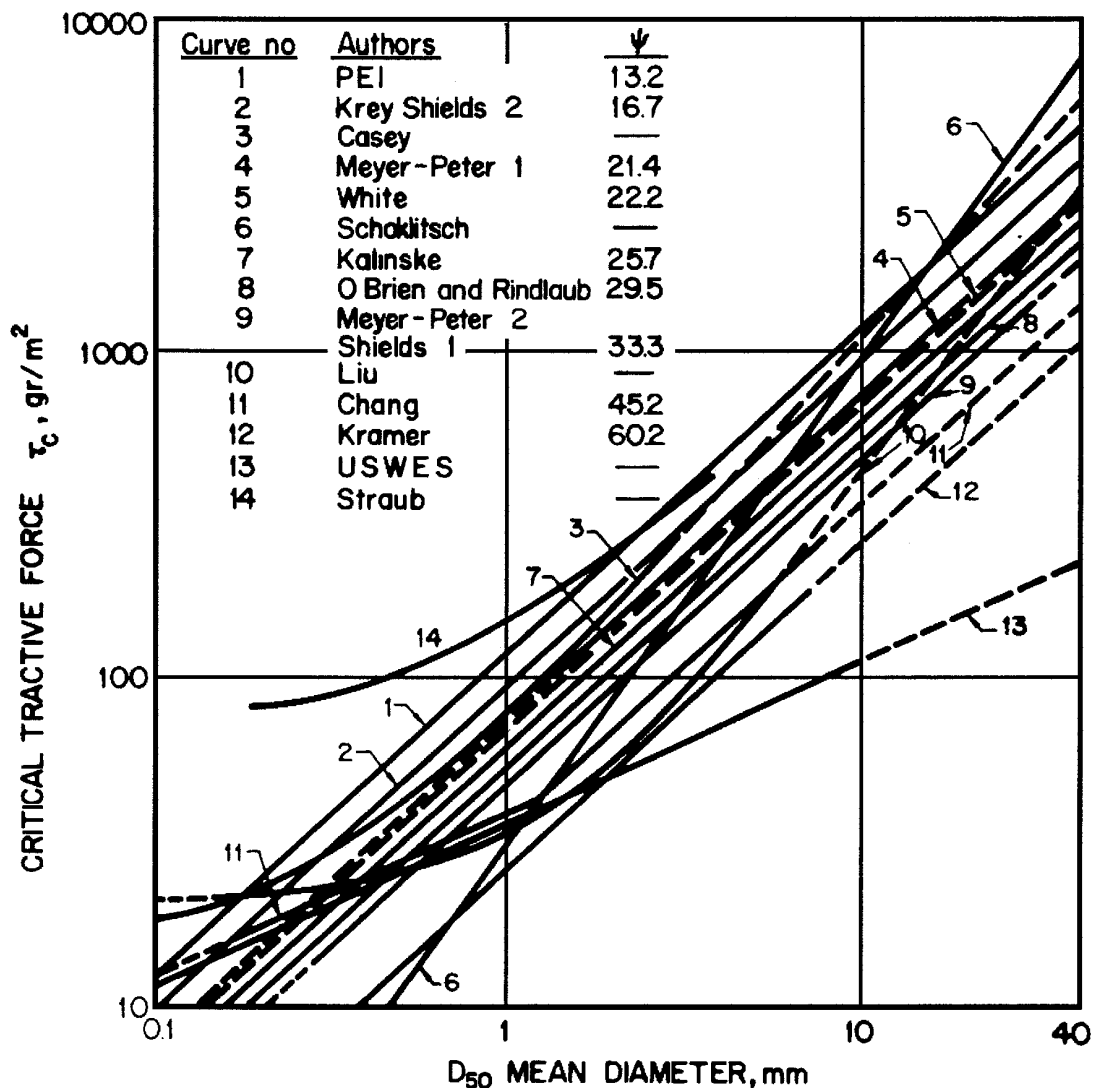


Figure 3.17. Comparison of critical shear stress as a function of grain diameter (after Chien 1954).

### 3.5.5 Equations for Flow and Sediment Variables for Beginning of Motion

Particles start to move in steady, uniform flow when the shear stress applied by the flow equals the resistance to movement of the particles. A useful relation can be developed between the flow velocity, depth, and resistance and bed material size by equating the applied shear stress to a resistance to motion shear stress. In equation form it is as follows:

$$\tau_0 = \tau_c \quad (3.38)$$

where:

$$\begin{aligned} \tau_0 &= \text{Average bed shear stress, N/m}^2, \text{ lb/ft}^2 \\ \tau_c &= \text{Critical bed shear stress at incipient motion, N/m}^2, \text{ lb/ft}^2 \end{aligned}$$

The average bed shear stress applied by the steady uniform flow, derived in Chapter 2, is as follows:

$$\tau_0 = \gamma R S_f \quad (3.39)$$

Using  $y$  for the hydraulic radius ( $R$ ) and the Manning equation to determine the slope ( $S_f$ ) The average shear stress can be expressed as follows:

$$\tau_0 = \rho g y S_f = \frac{\rho g n^2 V^2}{y^{1/3}} \quad (\text{SI}) \quad (3.40)$$

$$\tau_0 = \frac{\rho g n^2 V^2}{(1.49)^2 y^{1/3}} \quad (\text{English}) \quad (3.41)$$

For noncohesive bed materials, the Shields relation (Vanoni 1975) can be used to determine the relation between the critical shear stress and bed material size for beginning of bed material movement. The relation is as follows:

$$\tau_c = K_s (\rho_s - \rho) g D \quad (3.42)$$

At the beginning of sediment movement the applied shear stress is equal to the critical shear stress as given in Equation 3.36 ( $\tau_0 = \tau_c$ ) resulting in the following:

$$\frac{\rho g n^2 V^2}{y^{1/3}} = K_s (\rho_s - \rho) g D_s \quad (\text{SI}) \quad (3.43)$$

$$\frac{\rho g n^2 V^2}{2.22 y^{1/3}} = K_s (\rho_s - \rho) g D_s \quad (\text{English}) \quad (3.44)$$

where:

$$\begin{aligned} y &= \text{Average depth of flow, m, ft} \\ S_f &= \text{Slope of the energy grade line, m/m, ft/ft} \\ V &= \text{Average velocity, m/s, ft/s} \\ D_s &= \text{Diameter of smallest non transportable bed material particle, m, ft} \\ \gamma &= \text{Unit weight of water (9,800 N/m}^3, \text{ 62.4 lb/ft}^3) \\ n &= \text{Manning's roughness coefficient} \\ K_s &= \text{Shield's coefficient} \end{aligned}$$

- $S_s$  = Specific gravity (2.65 for quartz)
- $\rho$  = Density of water (999 kg/m<sup>3</sup>, 1.94 slugs/ ft<sup>3</sup>)
- $\rho_s$  = Density of sediment (quartz 2,647 Kg/m<sup>3</sup>, 165.4 lb/ft<sup>3</sup>)
- $g$  = Acceleration of gravity (9.81 m/s<sup>2</sup>, 32.2 ft/s<sup>2</sup>)

The relationships in Equations 3.43 and 3.44 are the fundamental relations between velocity, depth, resistance to flow (Manning's n), density and a coefficient determined experimentally for the beginning of movement of the sediment particles. This coefficient is called the Shields coefficient. The equation can be solved for the following:

1. Critical velocity for beginning of sediment movement for a given depth, roughness, Shields coefficient, and bed material size and density.
2. Critical size for a given velocity, depth, roughness, Shields coefficient, and bed material density.
3. Clear-water scour depth for a given velocity, roughness, Shields coefficient, and bed material size and density. This depth is the contraction scour depth at the end of a long contraction.

Critical Velocity for the Beginning of Bed Material Movement. Rearranging Equations 3.43 and 3.44 to give the critical velocity for beginning of motion of bed material of size D for depth y, Shield's parameter, and Manning's n results in:

$$V_c = \frac{K_s^{1/2} (S_s - 1)^{1/2} D_s^{1/2} y^{1/6}}{n} \quad (\text{SI}) \quad (3.45)$$

$$V_c = \frac{1.49 k_s^{1/2} (S_s - 1)^{1/2} D_s^{1/2} y^{1/6}}{n} \quad (\text{English}) \quad (3.46)$$

$$n = K_{nu} D_s^{1/6} \quad (3.47)$$

$$K_{nu} = 0.041 \quad (\text{SI})$$

$$K_{nu} = 0.0336 \quad (\text{English})$$

$$V_c = K_u D_s^{1/3} y^{1/6} \quad (3.48)$$

$$K_u = \frac{K_s^{1/2} (S_s - 1)^{1/2}}{K_{nu}} \quad (\text{SI}) \quad (3.49)$$

$$K_u = \frac{1.49 K_s^{1/2} (S_s - 1)^{1/2}}{K_{nu}} \quad (\text{English})$$

where:

- $V_c$  = Critical velocity above which bed material of size D and smaller will be transported, m/s, ft/s
- $K_s$  = Shields parameter

- $S_s$  = specific gravity of the bed material
- $D_s$  = Size of bed material, m, ft
- $y$  = Depth of flow, m, ft
- $n$  = Manning's roughness coefficient

The following values for  $K_u$  in Equation 3.48 can be obtained:

Metric (SI) Units (m)

Using  $K_s = 0.039$ ,  $S_s = 2.65$ ,  $K_{nu} = 0.041$

$$K_u = 6.19$$

English Units (ft)

Using  $K_s = 0.039$ ,  $S_s = 2.65$ ,  $K_{nu} = 0.0336$

$$K_u = 11.25$$

Critical Size for the Beginning of Bed Material Movement. Rearranging Equation 3.48 to give the critical bed material size  $D_s$  for beginning of motion for velocity  $V$ , depth  $y$ , Shield's parameter and Manning's  $n$  results in:

$$D_c = \frac{K_u V^3}{y^{1/2}} \tag{3.50}$$

$$K_u = \frac{1}{6.19^3} = 0.0042 \tag{SI}$$

$$K_u = \frac{1}{11.25^3} = 0.0007 \tag{English}$$

Depth of Flow For No Bed Material Movement as a function of  $V$  and  $D$ . Equation 3.48 can be solved, for the depth  $y$  for no bed material movement for a given velocity, specific density, size of bed material, Shields parameter and bed roughness. **This equation is useful to determine clear water-scour at a contraction. This is particularly true if the velocity is converted to discharge using the continuity equation.**

$$y = \frac{V^6}{K_u^6 D_s^2} = \frac{K_{yu} V^6}{D_s^2} \tag{3.51}$$

$$K_{yu} = 1.78 \times 10^{-5} \tag{SI}$$

$$K_{yu} = 4.94 \times 10^{-7} \tag{English}$$

Depth of Flow for No Bed Material Movement as Function of Q and D. The velocity V in Equation 3.51 can be replaced with the discharge Q using the continuity equation ( $Q = W y V$ ). From continuity  $V = Q/(W y)$  The relation between y, Q and D for the condition of no bed material transport is very useful in determining clear-water contraction scour as explained in Chapter 7.

Replacing V with Q in Equation 3.51 to determine the depth (y) when there is no bed material movement of size D, gives the following equation:

$$y = K_u \frac{Q^{6/7}}{D^{2/7} W^{6/7}} \quad (3.52)$$

$$K_u = K_{yu}^{1/7} = 0.210 \quad (\text{SI})$$

$$K_u = K_{yu}^{1/7} = 0.126 \quad (\text{English})$$

### 3.5.6 Tables for Determining Critical Velocities

Table 3.4 gives the permissible velocity recommended by Fortier and Scobey (1926), for channels at small slope for bed material ranging from fine sand to cobbles. Table 3.5 gives non-scour velocities for noncohesive and compact cohesive soils suggested by Keown et al. (1977) for bed material ranging from loess soils to boulders.

		Mean velocity, after aging of canals [ $y \leq 0.9$ m (3 ft)]					
Original Material excavated for canals	n	Clear water, no detritus		Water transporting colloidal silt		Water transporting noncolloidal silts, sands, gravels or rock fragments	
		ft/sec	M/sec	ft/sec	m/sec	ft/sec	m/sec
Fine sand (colloidal)	0.02	1.50	0.46	2.50	0.76	1.50	0.46
Sandy loam (noncolloidal)	0.02	1.75	0.53	2.50	0.76	2.00	0.61
Silt loam (noncolloidal)	0.02	2.00	0.61	3.00	0.91	2.00	0.61
Alluvial silt (noncolloidal)	0.02	2.00	0.61	3.50	1.07	2.00	0.61
Ordinary firm loam	0.02	2.50	0.76	3.50	1.07	2.25	0.69
Volcanic ash	0.02	2.50	0.76	3.50	1.07	2.00	0.61
Fine gravel	0.02	2.50	0.76	5.00	1.52	3.75	1.14
Stiff clay	0.025	3.75	1.14	5.00	1.52	3.00	0.91
Graded loam to Cobbles (noncolloidal)	0.03	3.75	1.14	5.00	1.52	5.00	1.52
Alluvial silt (colloidal)	0.025	3.75	1.14	5.00	1.52	3.00	0.91
Graded, silt to cobbles (colloidal)	0.03	4.00	1.22	5.50	1.68	5.00	1.52
Coarse gravel (noncolloidal)	0.025	4.00	1.22	6.00	1.83	6.50	1.98
Cobbles and shingles	0.035	5.00	1.52	5.50	1.68	6.50	1.98
Shales and hard pans	0.025	6.00	1.83	6.00	1.83	5.00	1.52

Table 3.5. Nonscour Velocities for Soils (Modified from a report by Keown et al. 1977).						
Kind of Soil	Grain Dimensions		Approximate Nonscour Velocities (feet per second)			
	(mm)	(ft)	Mean Depth			
			1.3 ft	3.3 ft	6.6 ft	9.8 ft
<b>For Noncohesive Soils</b>						
Boulders	>256	>0.840	15.1	16.7	19.0	20.3
Large cobbles	256-128	0.840-0.420	11.8	13.4	15.4	16.4
Small cobbles	128-64	0.420-0.210	7.5	8.9	10.2	11.2
Very coarse gravel	64-32	0.210-0.105	5.2	6.2	7.2	8.2
Coarse gravel	32-16	0.105-0.0525	4.1	4.7	5.4	6.1
Medium gravel	16-8.0	0.0525-0.0262	3.3	3.7	4.1	4.6
Fine gravel	8.0-4.0	0.0262-0.0131	2.6	3.0	3.3	3.8
Very fine gravel	4.0-2.0	0.0131-0.00656	2.2	2.5	2.8	3.1
Very coarse sand	2.0-1.0	0.00656-0.00328	1.8	2.1	2.4	2.7
Coarse sand	1.0-0.50	0.00328-0.00164	1.5	1.8	2.1	2.3
Medium sand	0.50-0.25	0.00164-0.000820	1.2	1.5	1.8	2.0
Fine sand	0.25-0.125	0.000820-0.000410	.98	1.3	1.6	1.8
<b>For Compact Cohesive Soils</b>						
Sandy loam (heavy)			3.3	3.9	4.6	4.9
Sandy loam (light)			3.1	3.9	4.6	4.9
Loess soils in the Conditions of finished Settlement			2.6	3.3	3.9	4.3

### 3.5.7 Figures for Determining Critical Shear Stress or Velocity

Figure 3.18 shows the relationship between critical shear stress and mean diameter as determined and/or recommended by different investigators for different soil types. The difference between investigators is possibly due to the effects of cohesion, when present, causing the particles to aggregate and not act as individual particles.

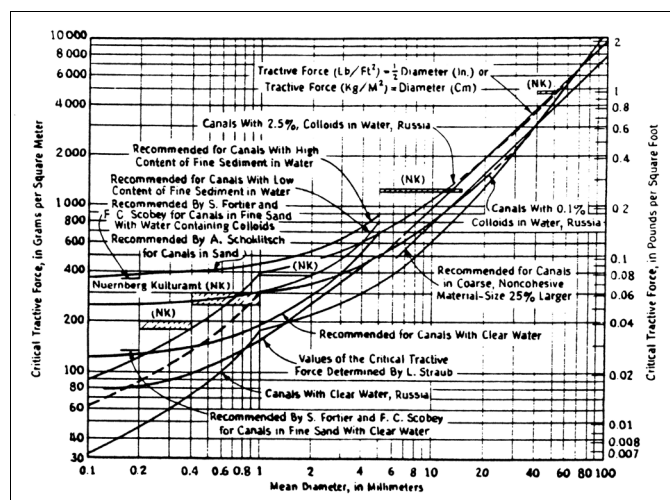


Figure 3.18. Critical shear stress as a function of grain diameter (after Lane 1953).

Figure 3.19 gives the relationship between maximum allowable velocity (critical velocity) against stone or minimum stone size that can sustain hydraulic forces without motion.

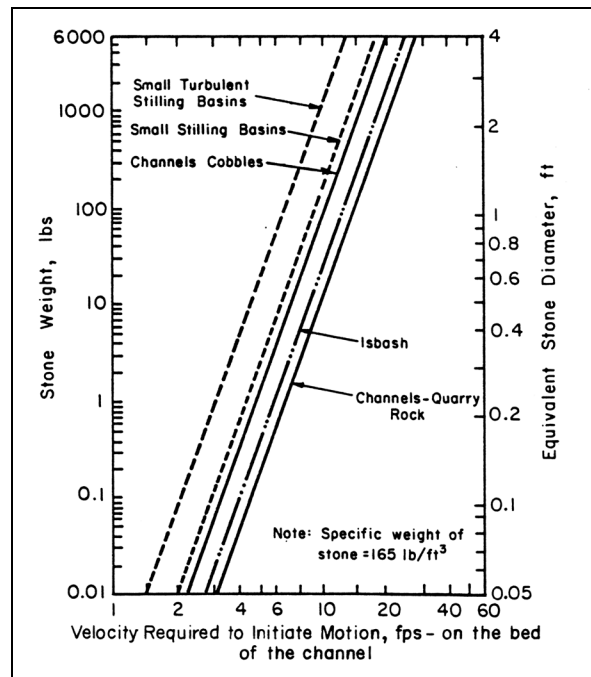


Figure 3.19. Critical velocity as a function of stone size.

### 3.5.8 Summary

Equations 3.45 and 3.46 determine critical velocity. These equations can be used to determine the critical size, and critical depth for the beginning of bed material movement based on the Manning equation, specific gravity of the bed material and Shield's parameter in metric and English units, respectively. They are for steady, uniform flow. In addition, Equation 3.52 determines the depth of flow as a function of discharge in metric and English units for these same conditions. To solve the equations Manning's  $n$ , specific gravity, and Shield's parameter must be determined as well as the other variables.

In these basic equations, reasonable values of Manning's  $n$ , specific gravity, and Shield's parameter are substituted to obtain equations for the dependent variables. These values are (1) Shield's parameter  $K_s = 0.039$ , (2) specific gravity  $S_s = 2.65$ , and (3) Manning's  $n = 0.041 D_s^{1/6}$  for metric units and  $n = 0.0336 D_s^{1/6}$  for English units. The derivations are given in sufficient detail that engineers can substitute other values for  $K_s$ ,  $S_s$ , and Manning's  $n$  to fit their specific data.

Note that the critical sediment size,  $D_c$ , is a function of  $V^3$  and the critical depth,  $y$ , is a function of  $V^6$  and  $Q^{6/7}$ .

## 3.6 SEDIMENT DISCHARGE MEASUREMENT

### 3.6.1 Introduction

In this section the basic terms and methods of measuring sediment discharge (sediment load) are described. In Chapter 4, the theory, equations, and methods of computing bed material transport are described.

### 3.6.2 Terminology

There are many terms that have developed over time to describe the many aspects of the transport of sediment by water. Sediment transport is the time rate of a quantity of sediment (by weight) moving past a cross-section of the stream. It is a discharge. Because it is measured by weight (often as tons), discharge is often referred to as sediment load. Other terms associated with sediment transport are suspended sediment discharge, bed load, bed material load, bed material discharge, and wash load.

The many terms describing sediment transport result from using or misusing and mixing terms that describe (1) the source of the sediment (bed material load and wash load), (2) mode of particle movement (suspended bed material load and bed load) and (3) measurement of sediment discharge (measured sediment discharge and unmeasured sediment discharge). The terms are defined in Chapter 4, (Section 4.2) and illustrated in Figure 3.20 from HEC-20 (Lagasse et al. 2001).

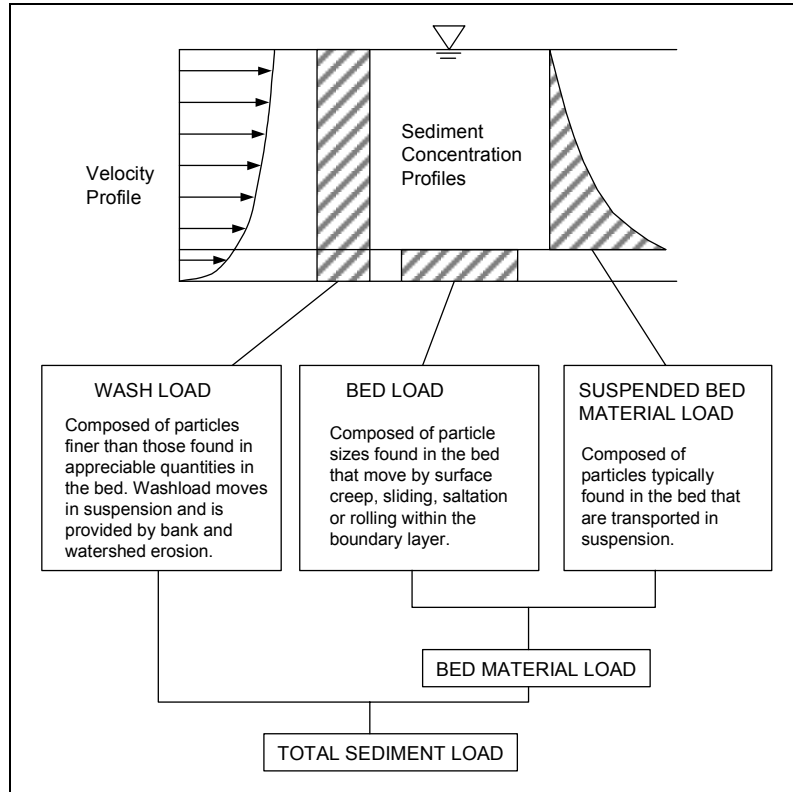


Figure 3.20. Definition of sediment discharge (load) components (Lagasse et al. 2001).



### 3.6.3 Suspended Sediment Discharge Measurement

The measurement of the suspended sediment discharge of a stream requires the time dependent measurement of the water discharge (discharge hydrograph) and velocity weighted measurement of the concentration of sediment particles moving past the cross-section. In equation form:

$$Q_s = K_u Q_w C \quad (3.53)$$

$$K_u = 0.086 \text{ (SI)}$$

$$K_u = 0.0027 \text{ (English)}$$

where:

- $Q_s$  = Suspended sediment discharge, metric or English tons per day
- $Q_w$  = Water discharge,  $m^3/s$  or cfs
- $C$  = Velocity-weighted mean concentration (by weight) of sediment, mg/l
- $k_u$  = Coefficient to convert to metric or English tons per day

The determination of water discharge was described in Chapter 2. The measurement of suspended-sediment discharge is described in detail in Techniques of Water-Resources Investigations of the United States Geological Survey (Guy 1970, 1977; Guy and Norman 1970; and Porterfield 1977). The essence of the procedure is as follows.

1. Time dependent measurement of the water discharge (discharge hydrograph). Standard stream gaging procedure described in Chapter 2.
2. Measure the velocity weighted mean suspended-sediment concentration of the flow.
3. Develop a time suspended-sediment concentration graph similar to the stage hydrograph at a gaging station (suspended sediment hydrograph).
4. Determine the daily suspended-sediment discharge in English or metric tons per day, using Equation 3.53.

### 3.6.4 Velocity Weighted Mean Suspended-Sediment Concentration

As illustrated in Figure 3.21 the velocity decreases with depth and the sediment concentration increases with depth. Very fine sediment or coarser sediment in a very turbulent stream may not decrease in concentration with depth (uniformly distributed). Whereas, very coarse sediment, or finer sediment in placid flow may have a very large increase in concentration with depth. In addition to the velocity and concentration varying with depth, they vary across the stream. The Federal Government through the Interagency Subcommittee on Sedimentation (U.S. Interagency Subcommittee 1940a,b, 1941a,b,c, 1943, 1948, and 1952; Vanoni 1977; Richardson 1994) developed samplers that take a velocity averaged suspended-sediment concentration in the vertical to 0.09 m (0.3 ft) above the bed (Figure 3.22). These samplers are used to take samples across the stream or to obtain a coefficient to be applied to a sample at a single vertical to obtain the mean discharge weighted concentration in the cross-section.

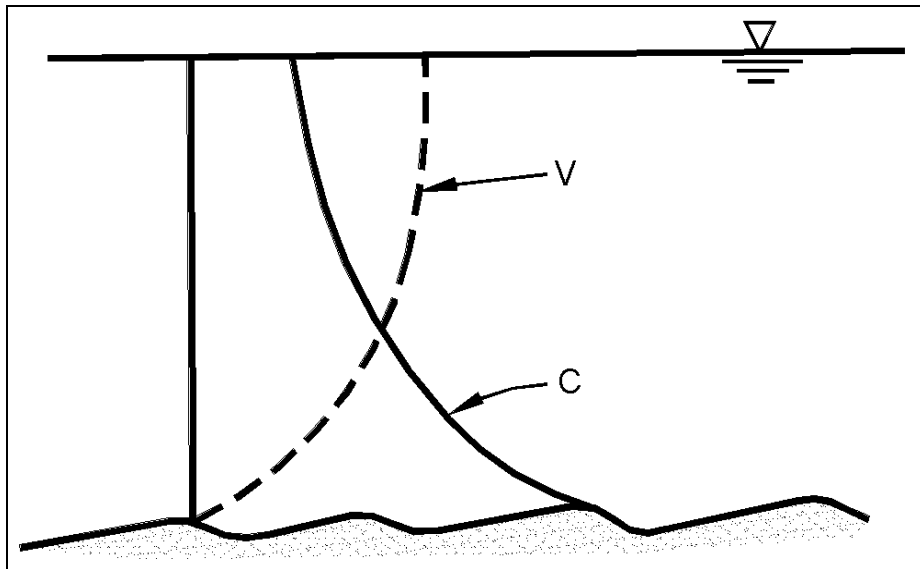


Figure 3.21. Schematic sediment and velocity profiles.

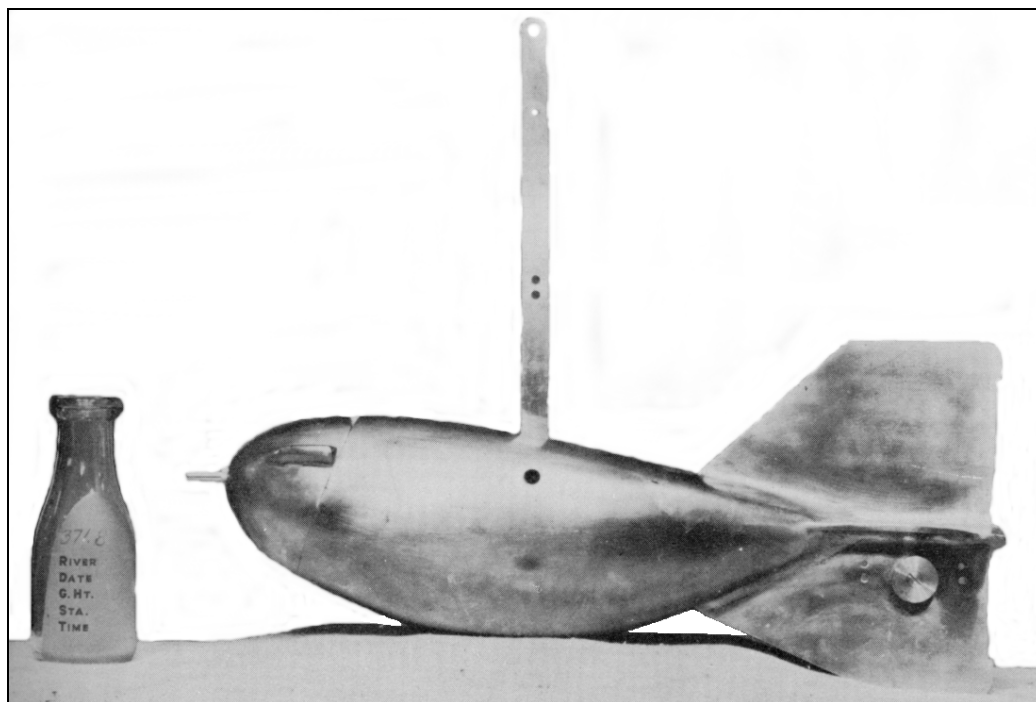


Figure 3.22a. Suspended sediment sampler-D49 (Guy and Norman 1970, U.S. Interagency 1952).

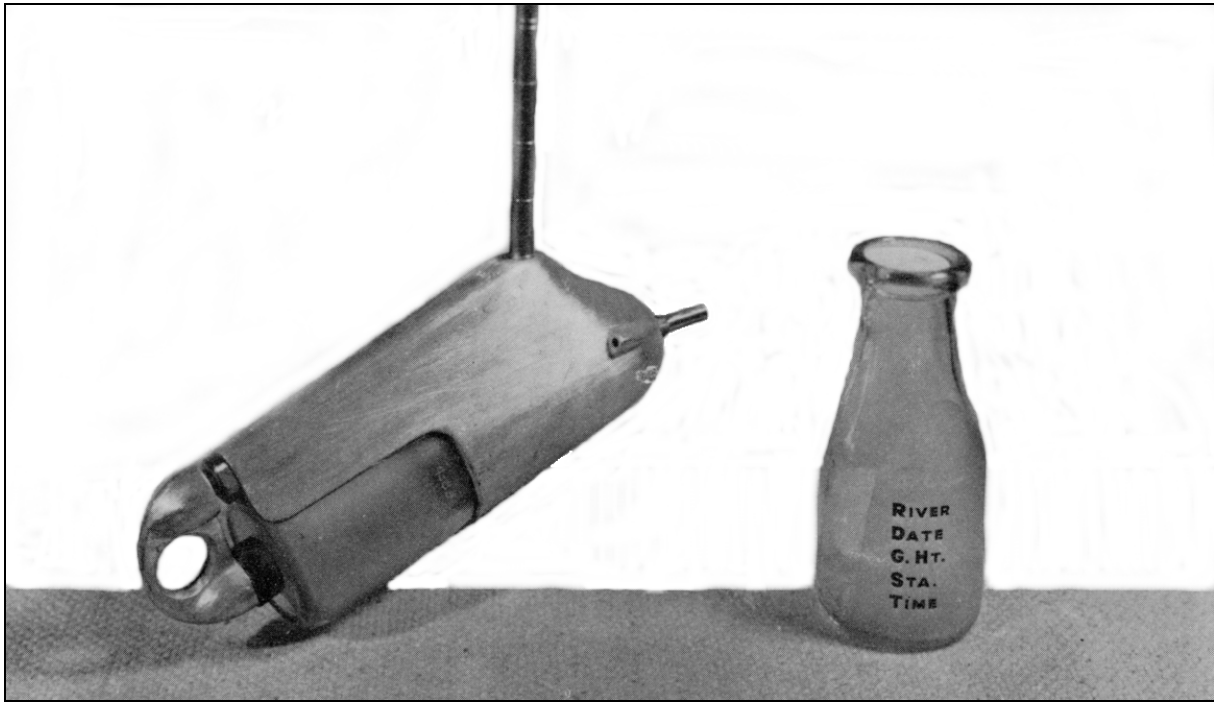


Figure 3.22b. Suspended sediment sampler-DH48 (Guy and Norman 1973, U.S. Interagency 1952).

### 3.6.5 Suspended Sediment Hydrograph

The measured suspended-sediment concentration is used to plot a concentration hydrograph (Figure 3.23). Engineering judgment, the stage hydrograph and knowledge of the stream is used in drawing the suspended-sediment hydrograph. The Techniques of Water-Resources Investigations of the United States Geological Survey, Book 3, Chapters C3 (Porterfield 1977) Computation of Fluvial-Sediment Discharge describes methods to construct a suspended-sediment hydrograph.

### 3.6.6 Determination of Daily Suspended-Sediment Discharge

Using the concentration hydrograph an average daily suspended-sediment concentration is determined. Using this concentration and the average daily water discharge in Equation 3.53 the average daily suspended-sediment discharge is determined. However, if the concentration and water discharge are changing rapidly during the day, as illustrated in Figure 3.23, the day will have to be subdivided into short time increments. The suspended-sediment discharge is determined for each time increment using Equation 3.53. Then, the suspended-sediment discharge for each time increment for the day are converted to a common time base, added up and divided by the number of common time increments to obtain the average suspended-sediment discharge for the day.

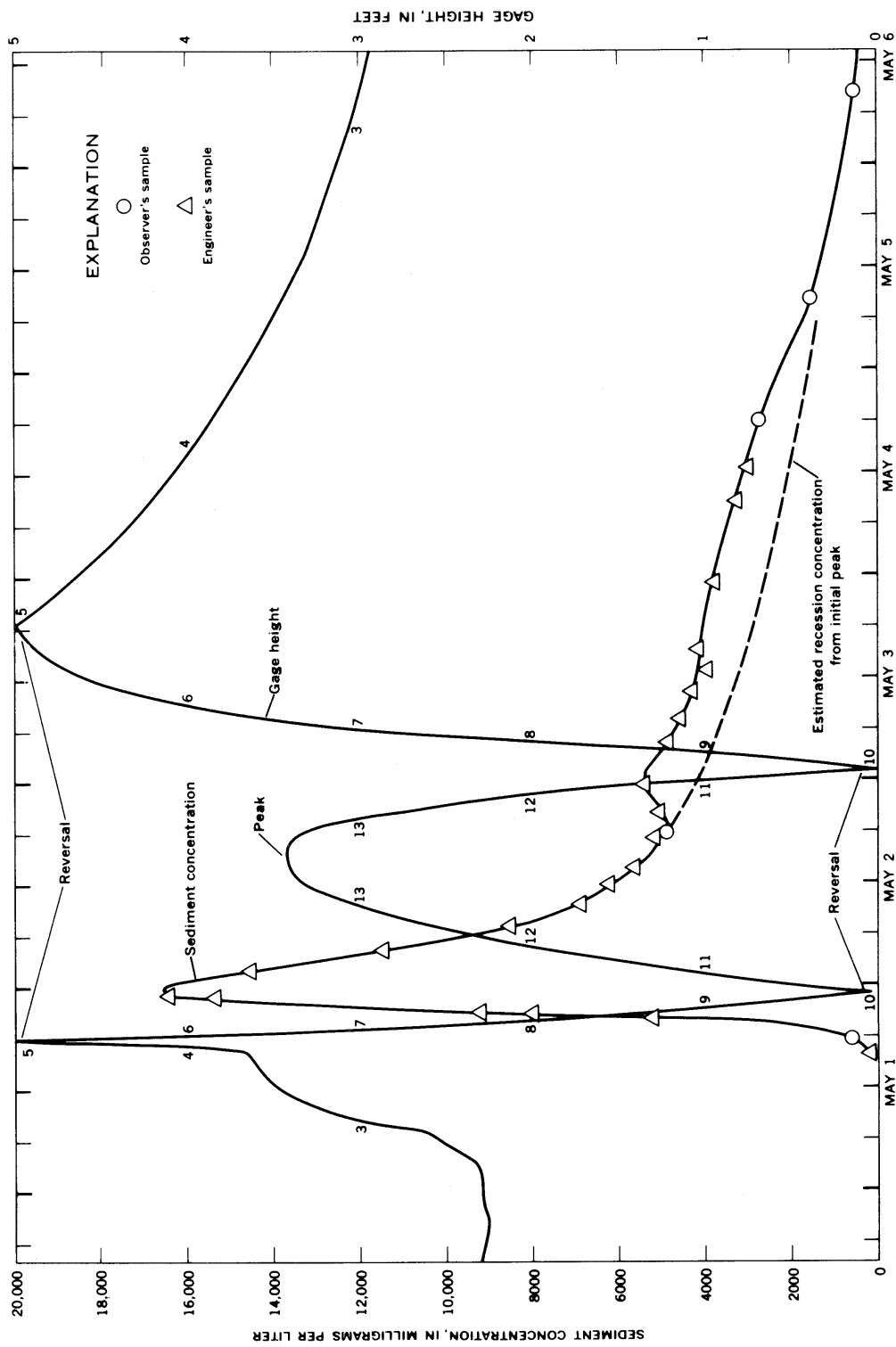


Figure 3.23. Gage height and suspended sediment concentration hydrograph, Colorado River near San Saba, Texas, May 1-6, 1952 (Porterfield 1977).

### 3.6.7 Total Sediment Discharge

The suspended-sediment discharge determination described above is the measured sediment discharge. There is the unmeasured sediment discharge composed of the sediment moving in contact with the bed (contact sediment discharge or load) and the suspended sediment discharge that the sampler doesn't sample. This unmeasured sediment discharge can be as low as 10 percent of the total sediment discharge (or total load) to as high as 50 percent or more of the total sediment discharge. The percent of the total sediment discharge that is measured depends on the turbulence of the stream, bed material size, and concentration of wash load. Streams with very large concentrations of wash load or very large turbulence and fine bed material will have very low percent of unmeasured sediment discharge.

In some stream reaches the turbulence is so large that the total sediment discharge is in suspension and each size fraction of the total sediment discharge is uniformly distributed in the vertical. Here, the suspended-sediment discharge is the total sediment discharge. Many of these streams and in some cases streams where the turbulence was artificially created were used by Colby et al. (1955, 1956, 1962) to develop the modified Einstein procedure to determine the total sediment discharge of a stream as described in Chapter 4. Burkham and Dawdy (1980) and others have further modified Colby's procedure.

As discussed in Chapter 4, the total sediment discharge has three classifications. These are:

1. By source: The bed material discharge and the wash load discharge (Figure 3.20).
2. By mode of transport: The suspended-sediment discharge and the bed (contact) sediment discharge (Figure 3.20).
3. By measurement: The measured sediment discharge and the unmeasured sediment discharge.

To determine the total sediment discharge various methods are used. Some of these are:

1. Where there is a suspended-sediment sampling program, the unmeasured sediment discharge is determined using methods described in Chapter 4 and added to the measured suspended-sediment discharge.
2. A suspended-sediment sampling program is established and the unmeasured sediment discharge determined as in 1 above and added to the measured suspended-sediment discharge.
3. The total sediment discharge is determined by the modified Einstein method described in Chapter 4 for a range of discharges and a sediment rating curve developed. The curve and a record of daily water discharge are used to determine daily and yearly total sediment discharge.
4. Computer programs are used to determine the total bed material discharge. The wash load discharge may be ignored or estimated from periodic suspended sediment measurements.

### 3.7 SOLVED PROBLEMS FOR ALLUVIAL CHANNEL FLOW (SI)

#### 3.7.1 PROBLEM 1 Sediment Properties and Fall Velocities

##### Sand Bed Channel

The bed material size distribution of a sand bed channel is shown in Table 3.6.

Size Range (mm)	Percent of Total Weight in Size Range
.002 - .0625	0.8
.0625 - .125	4.4
.125 - .250	14.2
.250 - .500	74.9
.500 - 1.00	5.0
1.00 - 2.00	0.5
2.00 - 4.00	0.2

From the grain size analysis calculate the following statistics: the geometric mean of each size range; effective diameter  $D_m$ ; the  $D_{16}$ ,  $D_{50}$ ,  $D_{84}$ ,  $D_{90}$  sizes; the gradation coefficient; and the fall velocity of each size range.

The geometric mean is calculated as the square root of the product of the end points of a given size range.

For the first size range:

$$D_i = [(0.002) (.0625)]^{1/2} = 0.011 \text{ mm.}$$

Likewise for the remainder of the size ranges, the results are summarized in Table 3.7.

The effective diameter ( $D_m$ ) of the sample distribution is calculated with the use of Equation 3.12 in Section 3.2.4.

$$D_m = \frac{\sum_{i=1}^n p_i D_{si}}{100}$$

$$D_m = \frac{\sum_{i=1}^n p_i D_{si}}{100} = \frac{(0.8)(0.011\text{mm}) + (4.44)(0.088\text{mm}) + \dots + (0.3)(2.83\text{mm})}{100}$$

$$D_m = \frac{34.2}{100} = 0.34 \text{ mm ; which lies in the sand size.}$$

Size Range (mm)	Geometric Mean Size, $D_i$ (mm)	Percent of Bed Material in this Size ( $p_i$ )	Percent Finer	$p_i D_i$	Fall Velocity (m/sec)
.002 - .0625	0.011	0.8	0.8	0.01	0.0001
.0625 - .125	0.088	4.4	5.2	0.39	0.0061
.125 - .250	0.177	14.2	19.4	2.51	0.0183
.250 - .500	0.354	74.9	94.3	26.51	0.0457
.500 - 1.00	0.707	5.0	99.3	3.54	0.0884
1.00 - 2.00	1.41	0.5	99.8	0.71	0.198
2.00 - 4.00	2.83	0.2	100.0	0.56	0.335
TOTAL		100		34.2	

The fall velocity is determined with the use of Figure 3.1 at 60° F. For the geometric mean size of the first size range  $D_i = 0.011$ mm,  $\omega = .0001$  m/s, similarly  $D_i = 0.707$  mm,  $\omega = 0.0884$  m/s etc. The results are shown in Table 3.7.

The sand size distribution is plotted on log-probability paper in Figure 3.24 from which the following values can be obtained:

- $D_{50} = 0.33$  mm
- $D_{16} = 0.24$  mm
- $D_{90} = 0.46$  mm
- $D_{84} = 0.44$  mm

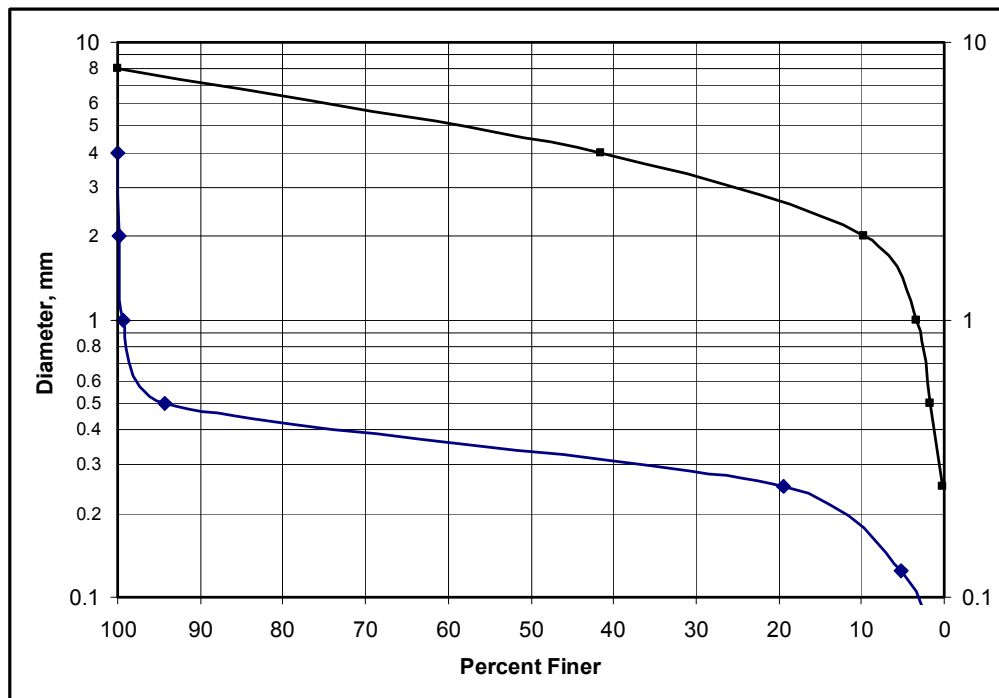


Figure 3.24. Bed material size distribution curves.

Finally, the gradation coefficient G is calculated using Equation 3.9.

$$G = \frac{1}{2} \left[ \frac{D_{50}}{D_{16}} + \frac{D_{84}}{D_{50}} \right] = \frac{1}{2} \left[ \frac{0.33\text{mm}}{0.24\text{mm}} + \frac{0.44\text{mm}}{0.33\text{mm}} \right]$$

$$G = 1.35$$

### Gravel Bed Channel

A gravel bed stream channel was sampled and the grain size analysis yielded the following results (Table 3.8):

Size Range (mm)	Percent of Total Weight in Size Range
.125 - .250	0.1
.250 - .500	1.6
.500 - 1.00	1.7
1.00 - 2.00	6.3
2.00 - 4.00	31.8
4.00 - 8.00	58.5

From this size distribution calculate the following statistics: the geometric mean of each size range; the effective diameter  $D_m$ ; the fall velocity of each size range; the  $D_m$ ,  $D_{16}$ ,  $D_{50}$ ,  $D_{84}$ ,  $D_{90}$  sizes; and the gradation coefficient.

The geometric mean size is calculated as the square root of the product of the end points of a given size range. For the largest size range:

$$D_i = [(4)(8)]^{1/2} = 5.66 \text{ mm.}$$

Likewise the rest of the size ranges are calculated, with the results shown in Table 3.9.

The effective diameter of the sample distribution is calculated with Equation 3.12:

$$D_m = \frac{\sum_{i=1}^n p_i D_{si}}{100} = \frac{(0.1)(0.177\text{mm}) + \dots + (58.5)(5.66\text{mm})}{100}$$

$$D_m = \frac{431.9}{100} = 4.32 \text{ mm}$$

The fall velocity is calculated with the use of Figure 3.1 at 60° F, for each geometric mean size. For the largest geometric mean size:  $D_i = 5.66 \text{ mm}$ ,  $\omega = 0.518 \text{ m/s}$ . Likewise the rest of the size ranges, the results are shown in Table 3.9.

The gravel bed material size distribution was plotted on log-probability paper (Figure 3.24) from which the following values were obtained:



$$D_{16} = 2.4 \text{ mm} \quad D_{84} = 6.7 \text{ mm}$$

$$D_{50} = 4.5 \text{ mm} \quad D_{90} = 7.1 \text{ mm}$$

The gradation coefficient is calculated by Equation 3.9:

$$G = \frac{1}{2} \left[ \frac{D_{50}}{D_{16}} + \frac{D_{84}}{D_{50}} \right] = \frac{1}{2} \left[ \frac{4.5 \text{ mm}}{2.4 \text{ mm}} + \frac{6.7 \text{ mm}}{4.5 \text{ mm}} \right]$$

$$G = 1.67$$

Size Range (mm)	Geometric Mean Size, $D_i$ (mm)	Percent of Bed Material in this Size ( $p_i$ )	Percent Finer	$p_i D_i$	Fall Velocity (m/s)
.125 - 0.250	0.177	0.1	0.1	0.018	0.018
.250 - 0.500	0.354	1.6	1.7	0.566	0.046
.500 - 1.00	0.707	1.7	3.4	1.20	0.088
1.00 - 2.00	1.41	6.3	9.7	8.88	0.198
2.00 - 4.00	2.83	31.8	41.5	90.0	0.335
4.00 - 8.00	5.66	58.5	100.0	331.1	0.518
TOTAL		100		431.9	

### Pebble Count

The b axis (Intermediate length) of 100 particles were randomly picked up and measured on a line in and along the flow of the Cache la Poudre River. The sampling was done by walking in a straight line and picking up and measuring the particle at the big toe at each step. The b axis lengths in meters are; 0.046, .189, .146, .436, .137, .280, .207, .226, .128, .256, .262, .067, .088, .195, .259, .216, .177, .055, .226, .113, .201, .098, .134, .082, .016, .140, .210, .159, .028, .195, .104, .192, .155, .098, .177, .146, .034, .040, .018, .256, .171, .146, .104, .226, .192, .049, .226, .015, .110, .128, .082, .180, .067, .037, .162, .195, .110, .128, .232, .021, .046, .159, .226, .177, .235, .192, .122, .015, .082, .223, .195, .070, .040, .265, .192, .113, .143, .113, .155, .110, .098, .119, .226, .073, .113, .174, .241, .012, .049, .192, .110, .082, .131, .043, .137, .171, .046, .131, .104, .192

Determine the  $D_{50}$ ,  $D_{16}$ ,  $D_{84}$ ,  $D_{90}$ , and  $G$  of the bed material.

First decide on discrete size groups and then determine the number of particles in each group.

Size Range (m)	Class No.	Percent Finer
0.305 - 0.436	1	100
0.244 - 0.305	6	94
0.198 - 0.244	14	80
0.152 - 0.198	24	56
0.091 - 0.152	27	29
0.030 - 0.091	20	9
0.012 - 0.030	8	1
TOTAL	100	

Plot on log-probability paper to determine  $D_{50}$ ,  $D_{16}$ ,  $D_{84}$ ,  $D_{90}$ , and  $G$  of the bed material (Figure 3.25).

- $D_{50} = 0.19 \text{ m (190 mm)}$
- $D_{16} = 0.23 \text{ m (120 mm)}$
- $D_{90} = 0.28 \text{ m (280 mm)}$
- $D_{84} = 0.26 \text{ m (260 mm)}$
- $D_{75} = 0.23 \text{ m (230 mm)}$

$$G = \frac{1}{2} \left[ \frac{D_{50}}{D_{16}} + \frac{D_{84}}{D_{50}} \right] = \frac{1}{2} \left[ \frac{0.19\text{m}}{0.12\text{m}} + \frac{0.26\text{m}}{0.19\text{m}} \right] = 1.48$$

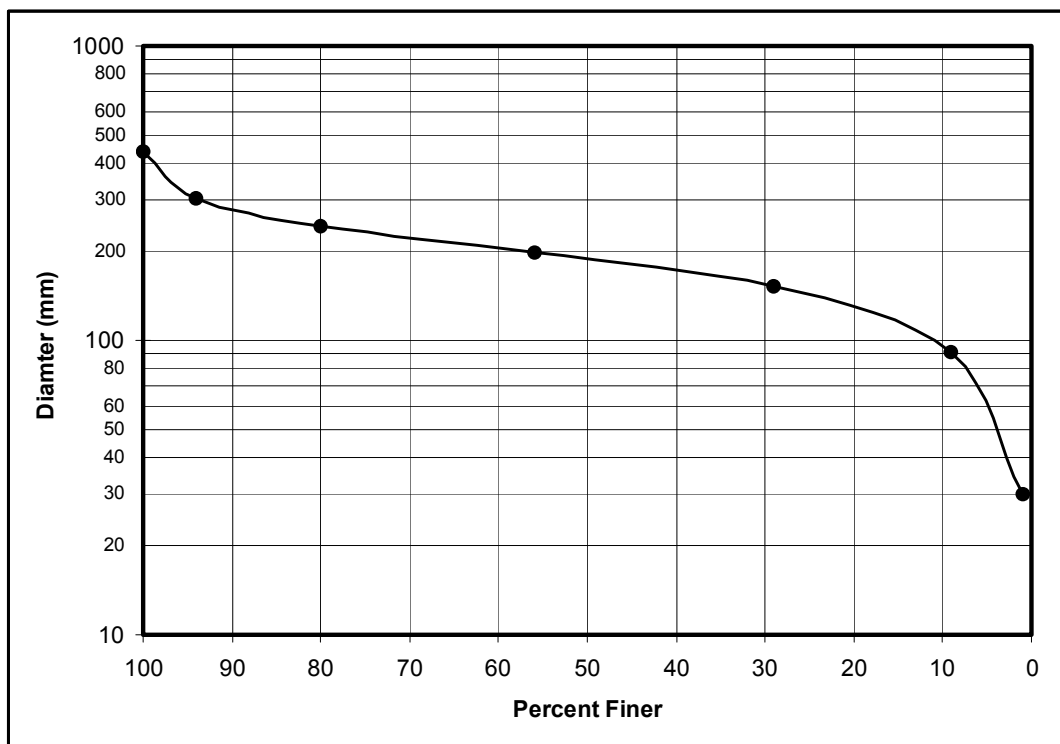


Figure 3.25. Size distribution curve for pebble count (1,000 mm = 1 m = 3.28 ft).

### 3.7.2 PROBLEM 2 Angle of Repose

Determine the angle of repose for well rounded riprap with a  $D_{30}$  of 1 ft = 305 mm. From Figure 3.4 the angle of repose is  $40^\circ$ .

### 3.7.3 PROBLEM 3 Resistance to Flow in Alluvial Channels

#### Manning's n in Sand Bed Streams

(a) Plane bed

Considering only the bed of the stream determine the following:

What is the range of Manning's n values for a plane bed sand channel stream?

Manning's n ranges from 0.010 to 0.013.

What is the Manning's n for a plane bed stream with a  $D_{50}$  of 0.32 mm.

Using the Strickler equation as an approximation:

$$n = 0.0482 D^{1/6} \text{ with } D \text{ in m} \quad n = 0.0482 (0.00032 \text{ m})^{1/6} = 0.013$$

(b) Antidune Flow

A sandbed channel is observed to have an undulating water surface, a discharge of 24.07  $\text{m}^3/\text{s}$ , an average velocity of 1.06 m/s, a channel width of 32.00 m, and a bed slope of 0.003. The stream bed has a  $D_{50}$  of 0.35 mm. An estimate of the bed form and n-value of the channel is desired.

Assuming the sieve diameter equals the fall diameter, and the bed slope equals the friction slope. Determine the stream power.

Stream power equals  $V\gamma_o S_o = (1.06) (9800) (24.07/32.00 \times 1.06) (0.003) = 22.126 \text{ N/sec-m}$ . Figure 3.13 is in English units. Therefore convert velocity and stream power to English units.

$$V = 1.06 \times 3.281 = 3.48 \text{ ft/sec}$$

$$\text{Stream Power} = 22.126 \frac{\text{N}}{\text{sec-m}} \times \frac{0.225 \text{ lb}}{\text{N}} \times \frac{1 \text{ m}}{3.281 \text{ ft}} = 152 \frac{\text{lb}}{\text{sec-ft}}$$

Figure 3.13 for this stream power indicates that upper flow regime is expected. The bed configuration should be antidunes with standing waves.

Based upon the bedform the n-value is estimated to be 0.013.

#### Manning's n in Gravel Bed Streams

Use the following gravel bed material size analysis to estimate the Manning's n-value of the stream.

$$\begin{aligned} D_{16} &= 1.8 \text{ mm} & D_{75} &= 4.0 \text{ mm} & D_{90} &= 4.9 \text{ mm} \\ D_{50} &= 3.1 \text{ mm} & D_{84} &= 4.4 \text{ mm} \end{aligned}$$

Using Equations 3.15 through 3.22

$$n = 0.0417 D_{50}^{.167} = 0.0417 (.0031)^{.167} = 0.016 \quad (3.15)$$

$$n = 0.0482 D_{50}^{.167} = 0.0482 (.0031)^{.167} = 0.018 \quad (3.16)$$

$$n = 0.0473 D_{75}^{.167} = 0.0473 (0.004)^{.167} = 0.019 \quad (3.17)$$

$$n = 0.046 D_{90}^{.167} = 0.046 (0.0049)^{.167} = 0.019 \quad (3.18)$$

(Assume  $y_o = 5.0 \text{ ft} = 1.52 \text{ m}$  and  $R = y_o$ )

$$n = \frac{0.113 y_o^{1/6}}{1.16 + 2.0 \log \left( \frac{y_o}{D_{84}} \right)} = \frac{0.113 (1.52)^{0.167}}{1.16 + 2.0 \log \left( \frac{1.52}{0.0044} \right)} = 0.019 \quad (3.19)$$

$$\frac{1}{f^{1/2}} = 1.9 \left( \frac{R}{D_{84}} \right)^{0.25} = 1.9 \left( \frac{1.52}{0.0044} \right)^{0.25} = 8.19 \quad (3.20)$$

$$f^{1/2} = 0.122$$

$$n = 0.113 R^{1/6} f^{1/2} = 0.113 (1.52)^{1/6} (0.122) = 0.015 \quad (3.22)$$

$$\frac{1}{f^{1/2}} = 2.0 \log \left( \frac{R}{D_{84}} \right) + 1.1 = 2.0 \log \left( \frac{1.52}{0.0044} \right) + 1.1 = 6.18 \quad (3.21)$$

$$f^{1/2} = 0.162$$

$$n = 0.113 R^{1/6} f^{1/2} = 0.113 (1.52)^{1/6} (0.162) = 0.020 \quad (3.22)$$

Based on the range of n-values indicated above a n-value of 0.018 is selected. Alternatively, the maximum and minimum n value could be used and a decision made on the basis of the velocity and discharge.

### Manning's n in Cobble Bed Streams

What are the Manning's n values for a cobble bed stream with the following size distribution:

- $D_{50} = 0.19 \text{ m (190 mm)}$
- $D_{16} = 0.12 \text{ m (120 mm)}$
- $D_{90} = 0.28 \text{ m (280 mm)}$
- $D_{84} = 0.25 \text{ m (250 mm)}$
- $D_{75} = 0.23 \text{ m (230 mm)}$

$$n = 0.0417 D_{50}^{1/6} \text{ with } D_{50} \text{ in meters } n = 0.0417 (0.19 \text{ m})^{1/6} = 0.032 \quad (3.15)$$

$$n = 0.0482 D_{50}^{1/6} \text{ with } D_{50} \text{ in meters } n = 0.0482 (0.19 \text{ m})^{1/6} = 0.037 \quad (3.16)$$

$$n = 0.0473 D_{75}^{1/6} \text{ with } D_{75} \text{ in meters } n = 0.0473 (0.23 \text{ m})^{1/6} = 0.037 \quad (3.17)$$

$$n = 0.046 D_{90}^{1/6} \text{ with } D_{90} \text{ in meters } n = 0.046 (0.28 \text{ m})^{1/6} = 0.037 \quad (3.18)$$

### 3.7.4 PROBLEM 4 Beginning of Motion

#### Bed Material Movement Using Shields Figure

To establish if the bed material of a channel is in motion the Shields' relationship can be used. Recall that  $\tau_o = \gamma RS$  and  $V_* = \sqrt{\tau_o / \rho}$

(a) For the following conditions determine if the bed material in a sand bed channel is in motion.

$$\begin{aligned} R &= 1.22 \text{ m} \\ S &= 0.00038 \text{ m/m} \\ D_{50} &= 0.31 \text{ mm} \\ D_{16} &= 0.24 \text{ mm} \\ D_{90} &= 0.46 \text{ mm} \\ D_{84} &= 0.42 \text{ mm} \end{aligned}$$

The shear stress on the bed, at a single vertical in the cross-section, is  $9800 \text{ N/m}^3 \times 1.22 \text{ m} \times 0.00038 = 4.543 \text{ N/m}^2$

$$\tau_o / (\gamma_s - \gamma) D_s = 4.543 / (25970 - 9800) 0.00031 = 0.91$$

$$V_* D_s / \nu = (4.543/1000)^{1/2} (0.00031) / 1.31 \times 10^{-6} = 15.95$$

This point plots above the incipient motion line in Shields (Figure 3.15) and indicates the bed of the channel is in motion.

(b) For the gravel sized material with the same values of  $\tau_o = 4.543 \text{ N/m}^2$ ;  $D_s = 3.1 \text{ mm}$  we have:

$$\tau_o / (\gamma_s - \gamma) D_s = 4.543 / (25970 - 9800) (0.0031) = 0.091$$

$$V_* D_s / \nu = (4.543/1000)^{1/2} (0.0031) / 1.31 \times 10^{-6} = 159$$

This point plots above the incipient motion line in Shields (Figure 3.15) and indicates this channel bed is in motion.

### Critical Velocity for Beginning of Bed Material Movement

(a) Sand Size Bed Material

Given depth  $y$  is 3.66 m and bed material size  $D_{50}$  is 0.31 mm, what is the critical velocity  $V_c$ ?

$$V_c = 6.19 y^{1/6} D^{1/3} = 6.19 \times 3.66^{1/6} \times 0.00031^{1/3} = 0.52 \text{ m/s}$$

(b) Gravel Size Bed Material

Given depth  $y$  is 3.66 m and bed material size  $D_{50}$  is 3.1 mm, what is the critical velocity  $V_c$ ?

$$V_c = 6.19 y^{1/6} D^{1/3} = 6.19 \times 3.66^{1/6} \times 0.0031^{1/3} = 1.12 \text{ m/s}$$

(c) Cobble size Bed Material

Given depth  $y$  is 3.66 and bed material size  $D_{50}$  is 128 mm, what is the critical velocity  $V_c$ ?

$$V_c = 6.19 y^{1/6} D^{1/3} = 6.19 \times 3.66^{1/6} \times 0.128^{1/3} = 3.88 \text{ m/s}$$

### Critical Size for Beginning of Bed Material Movement

Given depth  $y$  is 3.66 m and velocity  $V$  is 0.61 m/s, 1.22 m/s, 2.44 m/s, 3.66 m/s, and 4.88 m/s, respectively.

Determine the critical bed material size  $D_{50}$ .

$$\underline{V = 0.61 \text{ m/s}}$$

$$D_c = \frac{0.0042 V^3}{y^{1/2}} = \frac{(0.0042) 0.61^3}{3.66^{1/2}} = 0.0005 \text{ m (0.50 mm)}$$

$$\underline{V = 1.22 \text{ m/s}}$$

$$D_c = \frac{0.0042 V^3}{y^{1/2}} = \frac{(0.0042) 1.22^3}{3.66^{1/2}} = 0.00399 \text{ m (3.99 mm)}$$

$$\underline{V = 2.44 \text{ m/s}}$$

$$D_c = \frac{0.0042 V^3}{y^{1/2}} = \frac{(0.0042) 2.44^3}{3.66^{1/2}} = 0.0319 \text{ m (31.9 mm)}$$

$$\underline{V = 3.66 \text{ m/s}}$$

$$D_c = \frac{0.0042 V^3}{y^{1/2}} = \frac{(0.0042) 3.66^3}{3.66^{1/2}} = 0.108 \text{ m (108 mm)}$$

$$\underline{V = 4.88 \text{ m/s}}$$

$$D_c = \frac{0.0042 V^3}{y^{1/2}} = \frac{(0.0042) 4.88^3}{3.66^{1/2}} = 0.266 \text{ m (255 mm)}$$

### **Critical Depth When the Bed Material Movement Would Stop**

(a) Given velocity  $V$  of 0.61 m/s and bed material size  $D_{50}$  of 0.305 mm, determine the critical depth  $y$  for no bed material movement.

$$y = \frac{1.78 \times 10^{-5} V^6}{D^2} = \frac{(1.78 \times 10^{-5}) 0.61^6}{0.000305^2} = 9.86 \text{ m}$$

(b) Given velocity  $V$  of 0.61, 2.44, and 4.88 m/s and bed material size  $D_{50}$  of 152 mm, determine the critical depth  $y$  when bed material movement would stop.

$$\underline{V = 0.61 \text{ m/s}}$$

$$y = \frac{1.78 \times 10^{-5} V^6}{D^2} = \frac{(1.78 \times 10^{-5}) 0.61^6}{0.152^2} = 0.00004 \text{ m}$$

There would not be any bed material movement at this velocity.

$$\underline{V = 2.44 \text{ m/s}}$$

$$y = \frac{1.78 \times 10^{-5} V^6}{D^2} = \frac{(1.78 \times 10^{-5}) 2.44^6}{0.152^2} = 0.16 \text{ m}$$

$$\underline{V = 4.88 \text{ m/s}}$$

$$y = \frac{1.78 \times 10^{-5} V^6}{D^2} = \frac{(1.78 \times 10^{-5}) 4.88^6}{0.152^2} = 10.4 \text{ m}$$

Would this depth occur? No. Why not? The coarser material would armor the bed.

## **3.8 SOLVED PROBLEMS FOR ALLUVIAL CHANNEL FLOW (ENGLISH)**

### **3.8.1 PROBLEM 1 Sediment Properties and Fall Velocities**

Generally, sediment sizes are given in mm for the English system. Therefore, the solution to this problem is identical to the SI solution in Section 3.7.1.

### 3.8.2 PROBLEM 2 Angle of Repose

Determine the angle of repose for well rounded riprap with a  $D_{30}$  of 1 ft = 305 mm.

From Figure 3.4 the angle of repose is  $40^\circ$ .

### 3.8.3 PROBLEM 3 Resistance to Flow in Alluvial Channels

#### Manning's n in Sand Bed Streams

(a) Plane bed

Considering only the bed of the stream determine the following:

What is the range of Manning's n values for a plane bed sand channel stream?

Manning's n ranges from 0.010 to 0.013.

What is the Manning n for a plane bed stream with a  $D_{50}$  of 0.32 mm.

Using the Strickler equation as an approximation:

$$n = 0.0395 D^{1/6} \text{ with } D \text{ in ft. } n = 0.0395 (0.0010 \text{ ft})^{1/6} = 0.013$$

(b) Antidune Flow

A sandbed channel is observed to have an undulating water surface, a discharge of 850 cfs, an average velocity of 3.48 ft/sec, a channel width of 105 ft, and a bed slope of 0.003. The stream bed has a  $D_{50}$  of 0.35 mm. An estimate of the bed form and n-value of the channel is desired.

Assuming the sieve diameter equals the fall diameter, and the bed slope equals the friction slope. Determine the stream power.

Stream power equals  $V\gamma_o S_o = (3.48) (62.4) (850/105 \times 3.48) (0.003) = 1.53 \text{ lb/sec-ft}$ . Figure 3.13 for this stream power indicates that upper flow regime is expected. The bed configuration should be antidunes with standing waves.

Based upon the bedform the n-value is estimated to be 0.013.

#### Manning's n in Gravel Bed Streams

Use the following gravel bed material size analysis to estimate the Manning's n value of the stream.

$$D_{16} = 1.8 \text{ mm} \quad D_{75} = 4.0 \text{ mm} \quad D_{90} = 4.9 \text{ mm} \\ D_{50} = 3.1 \text{ mm} \quad D_{84} = 4.4 \text{ mm}$$

Using Equations 3.15 through 3.22



$$n = 0.342 D_{50}^{.167} = (0.0342) (0.0102)^{.167} = 0.016 \quad (3.15)$$

$$n = 0.395 D_{50}^{.167} = (0.0395) (0.0102)^{.167} = 0.018 \quad (3.16)$$

$$n = 0.388 D_{75}^{.167} = (0.0388) (0.0131)^{.167} = 0.019 \quad (3.17)$$

$$n = 0.038 D_{90}^{.167} = 0.038 (0.0161)^{.167} = 0.019 \quad (3.18)$$

(Assume  $y_o = 5.0$  ft and  $R = y_o$ )

$$n = \frac{0.0927 y_o^{1/6}}{1.16 + 2.0 \log \left( \frac{y_o}{D_{84}} \right)} = \frac{0.0927 (5.0)^{0.167}}{1.16 + 2.0 \log \left( \frac{5.0}{0.0144} \right)} = 0.019 \quad (3.19)$$

$$\frac{1}{f^{1/2}} = 1.9 \left( \frac{R}{D_{84}} \right) = 1.9 \left( \frac{5.00}{0.0144} \right)^{0.25} = 8.20 \quad (3.20)$$

$$f^{1/2} = 0.122$$

$$n = 0.0927 R^{1/6} f^{1/2} = 0.0927 (5.0)^{1/6} (0.122) = 0.015 \quad (3.22)$$

$$\frac{1}{f^{1/2}} = 2.0 \log \left( \frac{R}{D_{84}} \right) + 1.1 = 2.0 \log \left( \frac{5.0}{0.0144} \right) + 1.1 = 6.18 \quad (3.21)$$

$$f^{1/2} = 0.162$$

$$n = 0.0927 R^{1/6} f^{1/2} = 0.0927 (5.0)^{1/6} (0.162) = 0.020 \quad (3.22)$$

Based on the range of n-values indicated above a n-value of 0.018 is selected. Alternatively, the maximum and minimum n value could be used and a decision made based of the velocity and discharge.

### Manning's n in Cobble Bed Streams

What are the Manning's n values for a cobble bed stream with the following size distribution:

$$D_{50} = 0.62 \text{ ft (190 mm)}$$

$$D_{16} = 0.39 \text{ ft (120 mm)}$$

$$D_{90} = 0.92 \text{ ft (280 mm)}$$

$$D_{84} = 0.82 \text{ ft (250 mm)}$$

$$D_{75} = 0.75 \text{ ft (230 mm)}$$

$$n = 0.342 D_{50}^{1/6} \text{ with } D_{50} \text{ in ft. } n = 0.0342 (0.62)^{1/6} = 0.032 \quad (3.15)$$

$$n = 0.395 D_{50}^{1/6} \text{ with } D_{50} \text{ in ft. } n = 0.0395 (0.62 \text{ ft})^{1/6} = 0.037 \quad (3.16)$$

$$n = 0.388 D_{75}^{1/6} \text{ with } D_{75} \text{ in ft. } n = 0.0388 (0.75 \text{ ft})^{1/6} = 0.037 \quad (3.17)$$

$$n = 0.038 D_{90}^{1/6} \text{ with } D_{75} \text{ in ft. } n = 0.038 (0.92 \text{ ft})^{1/6} = 0.037 \quad (3.18)$$

### 3.8.4 PROBLEM 4 Beginning of Motion

#### Bed Material Movement Using Shields Figure

To establish if the bed material of a channel is in motion the Shields' relationship can be used. Recall that  $\tau_o = \gamma RS$  and  $V_* = \sqrt{\tau_o / \rho}$ .

(a) For the following conditions determine if the bed material in a sand bed channel is in motion.

$$\begin{aligned} R &= 4.0 \text{ ft} \\ S &= 0.00038 \text{ ft/ft} \\ D_{50} &= 0.31 \text{ mm} = 0.00102 \text{ ft} \\ D_{16} &= 0.24 \text{ mm} = 0.0008 \text{ ft} \\ D_{90} &= 0.46 \text{ mm} = 0.0015 \text{ ft} \\ D_{84} &= 0.42 \text{ mm} = 0.0014 \text{ ft} \end{aligned}$$

The shear stress on the bed, at a single vertical in the cross-section, is  $62.4 \text{ lb/ft}^3 \times 4.0 \text{ ft} \times 0.00038 = 0.0948 \text{ lb/ft}^2$ .

$$\tau_o / (\gamma_s - \gamma) D_s = 0.095 / (165 - 62.4) (0.00102) = 0.92$$

$$V_* D_s / \nu = (0.095 / 1.94)^{1/2} (0.001) / 1.41 \times 10^{-5} = 15.69$$

This point plots above the incipient motion line in Shields (Figure 3.15) and indicates the bed of the channel is in motion.

(b) For the gravel sized material with the same values of  $\tau_o = 0.095 \text{ lb/ft}^2$ ;  $D_s = 3.1 \text{ mm} = 0.0102 \text{ ft}$  we have:

$$\tau_o / (\gamma_s - \gamma) D_s = 0.095 / (165 - 62.4) (0.0102) = 0.091$$

$$V_* D_s / \nu = (0.095 / 1.94)^{1/2} (0.0102) / 1.41 \times 10^{-5} = 160$$

This point plots above the incipient motion line in Shields (Figure 3.15) and indicates this channel bed is in motion.

#### Critical Velocity for Beginning of Bed Material Movement

(a) Sand Size Bed Material

Given depth  $y$  is 12 ft and bed material size  $D_{50}$  is 0.31 mm = 0.00102 ft, what is the critical velocity  $V_c$ ?

$$V_c = 11.25 y^{1/6} D^{1/3} = 11.25 \times 12^{1/6} \times 0.00102^{1/3} = 1.72 \text{ ft/s}$$

(b) Gravel Size Bed Material

Given depth  $y$  is 12 ft and bed material size  $D_{50}$  is 3.1 mm = 0.0102 ft, what is the critical velocity  $V_c$ ?

$$V_c = 11.25 y^{1/6} D^{1/3} = 11.25 \cdot 12^{1/6} \times 0.0102^{1/3} = 3.70 \text{ ft/s}$$

(c) Cobble size Bed Material

Given depth  $y$  is 12 ft and bed material size  $D_{50}$  is 128 mm = 0.42 ft, what is the critical velocity  $V_c$ ?

$$V_c = 11.25 y^{1/6} D^{1/3} = 11.25 \times 12^{1/6} \times 0.42^{1/3} = 12.75 \text{ ft/s}$$

**Critical Size for Beginning of Bed Material Movement**

Given depth  $y$  is 12 ft and velocity  $V$  is 2.0 ft/s, 4 ft/s, 8.0 ft/s, 12 ft/s, and 16 ft/s, respectively.

Determine the critical bed material size  $D_{50}$ .

$V = 2.0 \text{ ft/s}$

$$D_c = \frac{0.0007 V^3}{y^{1/2}} = \frac{(0.0007) 2.0^3}{12^{1/2}} = 0.00162 \text{ ft} \quad (0.49 \text{ mm})$$

$V = 4.0 \text{ ft/s}$

$$D_c = \frac{0.0007 V^3}{y^{1/2}} = \frac{(0.0007) 4.0^3}{12^{1/2}} = 0.0129 \text{ ft} \quad (3.93 \text{ mm})$$

$V = 8 \text{ ft/s}$

$$D_c = \frac{0.0007 V^3}{y^{1/2}} = \frac{(0.0007) 8.0^3}{12^{1/2}} = 0.104 \text{ ft} \quad (31.7 \text{ mm})$$

$V = 12 \text{ ft/s}$

$$D_c = \frac{0.0007 V^3}{y^{1/2}} = \frac{(0.0007) 12.0^3}{12^{1/2}} = 0.349 \text{ ft} \quad (106 \text{ mm})$$

$V = 16 \text{ ft/s}$

$$D_c = \frac{0.0007 V^3}{y^{1/2}} = \frac{(0.0007) 16.0^3}{12^{1/2}} = 0.828 \text{ ft} \quad (252 \text{ mm})$$

### Critical Depth When the Bed Material Movement Would Stop

(a) Given velocity  $V$  of 2.0 ft/s and bed material size  $D_{50}$  of 0.305 mm = 0.001 ft, determine the critical depth  $y$  for no bed material movement.

$$y = \frac{4.94 \times 10^{-7} V^6}{D^2} = \frac{(4.94 \times 10^{-7}) 2.0^6}{0.001^2} = 31.6 \text{ ft}$$

(b) Given velocity  $V$  of 2.0, 8.0 and 16 ft/s and bed material size  $D_{50}$  of 152 mm = 0.5 ft, determine the critical depth  $y$  when bed material movement would stop.

$$\underline{V = 2 \text{ ft/s}}$$

$$y = \frac{4.94 \times 10^{-7} V^6}{D^2} = \frac{(4.94 \times 10^{-7}) 2.0^6}{0.5^2} = 0.0001 \text{ ft}$$

There would not be any bed material movement at this velocity.

$$\underline{V = 8 \text{ ft/s}}$$

$$y = \frac{4.94 \times 10^{-7} V^6}{D^2} = \frac{(4.94 \times 10^{-7}) 8.0^6}{0.5^2} = 0.52 \text{ ft}$$

$$\underline{V = 16 \text{ ft/s}}$$

$$y = \frac{4.94 \times 10^{-7} V^6}{D^2} = \frac{(4.94 \times 10^{-7}) 16.0^6}{0.5^2} = 33.28 \text{ ft}$$

Would this depth occur? No. Why not? The coarser material would armor the bed.

## CHAPTER 4

### SEDIMENT TRANSPORT

#### 4.1 INTRODUCTION

This chapter describes key terms and several methods of computing sediment transport in alluvial channels. Since a significant portion of understanding sediment transport processes centers on correct use of the terminology, the first two sections deal with definitions and general concepts. The chapter also includes the derivation of the basic suspended bed sediment transport equation to illustrate the significant physical processes of sediment entrainment into the flow. Three classic sediment transport formulae are then discussed to illustrate the application of sediment transport theory.

Simple sediment transport equations, in the form of power functions, are also presented in this chapter. The power function equations are well suited for quick estimates of sediment transport capacity and are easily adapted to field measurements. The Yang sand and gravel total load equations are also suggested as a basic approach for hand calculation. In addition, an overview of selected sediment transport equations is presented. The overview suggests the range of applicability of these equations (based on bed-material size), and provides references to those equations not discussed in detail in this chapter. Finally, a step-wise application procedure for sediment transport calculations is outlined.

Numerous sediment transport formulae have been developed with a wide range of laboratory and field conditions. Appendix B includes the results of testing several widely used sediment transport equations using a large compilation of river data.

#### 4.2 DEFINITIONS

In this section the basic terms for describing sediment load in alluvial channels are summarized.

Bed layer: The flow layer, several grain diameters thick (usually taken as two grain diameters thick), immediately above the bed.

Bed load: Sediment that moves by rolling or sliding along the bed and is essentially in contact with the stream bed in the bed layer, i.e. contact load.

Bed material: The sediment mixture of which the stream bed is composed.

Bed material discharge (load): That part of the total sediment discharge which is composed of grain sizes found in the bed, i.e. bed load (contact load) plus suspended bed material discharge (load). The total transported bed material discharge (or bed sediment discharge) is assumed equal to the transport capacity of the flow.

Contact load: Sediment particles that roll or slide along in almost continuous contact with the stream bed, i.e., bed load.

Density of water-sediment mixture: The mass per unit volume including both water and sediment.

Discharge-weighted concentration: The dry weight of sediment in a unit volume of stream discharge, or the ratio of the discharge of dry weight of sediment to the discharge by weight of water-sediment mixture normally reported in parts per million (ppm) or parts per liter (ppl).

Load (or sediment load): The sediment that is being moved by a stream.

Sediment (or fluvial sediment): Fragmentary material that originates from weathering of rocks and is transported by, suspended in, or deposited from water.

Sediment concentration (by weight or by volume): The quantity of sediment relative to the quantity of transporting fluid, or fluid-sediment mixture. The concentration may be by weight or by volume. When expressed in ppm or mg/l, the concentration is always in ratio by weight.

Sediment discharge: The quantity of sediment that is carried past any cross-section of a stream in a unit of time.

Sediment yield: The dry weight of sediment per unit volume of water-sediment mixture in place, or the ratio of the dry weight of sediment to the total weight of water-sediment mixture in a sample or a unit volume of the mixture.

Suspended load (or suspended sediment): Sediment that is supported by the upward components of turbulence in a stream and that stays in suspension for an appreciable length of time.

Suspended bed load: The portion of suspended load which is composed of grain sizes found in the bed.

Suspended-sediment discharge: The quantity of suspended sediment passing through a stream cross-section outside the bed layer in a unit of time.

Total sediment discharge: The total sediment discharge of a stream. It is the sum of the suspended-sediment discharge and the contact sediment discharge, or the sum of the bed sediment discharge and washload, or the sum of the measured sediment discharge and the unmeasured sediment discharge.

Unmeasured sediment discharge: Sediment discharge close to the bed that is not sampled by a suspended sediment sampler.

Washload: That part of the total sediment discharge (load) which is composed of particle sizes finer than those found in appreciable quantities in the bed and is determined by available bank and upstream supply rate. Also called fine sediment discharge (load).

### 4.3 GENERAL CONSIDERATIONS

The amount of material transported or deposited in the stream under a given set of conditions is the result of the interaction of two groups of variables. In the first group are those variables that influence the quantity and quality of the sediment brought down to that section of the stream. In the second group are variables that influence the capacity of the stream to transport that sediment. A list of these variables is given as follows.

Group 1 - Sediment brought down to the stream depends on the geology and topography of watershed; magnitude, intensity, duration, distribution, and season of rainfall; soil moisture conditions; vegetal cover; cultivation and grazing; surface erosion and bank cutting.

Group 2 – The capacity of a stream to transport sediment depends on hydraulic properties of the stream channel. These are fluid properties, slope, roughness, hydraulic radius, discharge, velocity, velocity distribution, turbulence, tractive force, viscosity and density of the fluid sediment mixture, and size and gradation of the sediment.

These variables are not all independent and, in some cases, their effect is not definitely known. The variables which control the amount of sediment brought down to the stream are subject to so much variation, not only between streams but at a given point of a single stream, that the quantitative analysis of any particular case is extremely difficult. It is practicable, however, to measure the sediment discharge over a long period of time and record the results, and from these records to determine a soil loss from the area.

The variables that deal with the capacity of the stream to transport solids are subject to mathematical analysis. These variables are closely related to the hydraulic variables controlling the capacity of the stream to carry water.

#### 4.3.1 Source of Sediment Transport

Einstein (1964) stated that:

Every sediment particle which passes a particular cross-section of the stream must satisfy the following two conditions: (1) it must have been eroded somewhere in the watershed above the cross-section; (2) it must be transported by the flow from the place of erosion to the cross-section.

Each of these two conditions may limit the sediment rate at the cross-section, depending on the relative magnitude of two controls: the availability of the material in the watershed and the transporting ability of the stream. In most streams, the finer part of the load, i.e., the part which the flow can easily carry in large quantities, is limited by its availability in the watershed. This part of the load is designated as washload. The coarser part of the load, i.e., the part that is more difficult to move by flowing water, is limited in its rate by the transporting ability of the flow between the source and the section. This part of the load is designated as bed sediment load.

Thus, for engineering purposes, the two sources of sediment transported by a stream are: (1) bed material that makes up the stream bed; and (2) fine material that comes from the banks and the watershed (washload). Geologically both materials come from the watershed. But for

the engineer, the distinction is important because the bed material is transported at the capacity of the stream and is functionally related to measurable hydraulic variables. The washload is not transported at the capacity of the stream. Instead, the washload depends on availability and is not functionally related to measurable hydraulic variables.

No sharp demarcation exists between washload discharge and bed material discharge. As a rule of thumb, many engineers assume that the bed material discharge is composed of sizes ( $D_s$ ) equal to or greater than 0.062 mm which is also the division point between sand and silt. The sediment discharge consisting of grain sizes smaller than 0.062 mm is considered as washload. A more reasonable criterion is to choose a sediment size finer than the smallest 10 percent of the bed material as the dividing size between washload and bed sediment load. It is important to note that in a fast flowing mountain stream with a bed of cobbles the washload may consist of coarse sand sizes. For these conditions, the transport of sand sizes is supply limited. In contrast, if the bed of a channel is silt, the rate of bed load transport of the silt sizes is less a question of supply than of capacity. The sediment transport capacity of silts has been addressed in some transport equations. This invalidates the criterion based on  $D_s < 0.062$  mm for coarse bed sediment streams, however, the criterion based on  $D_{10}$  might still be applicable.

#### 4.3.2 Mode of Sediment Transport

Sediment particles are transported by rolling or sliding on the bed (bed load or contact load) or by suspension by the turbulence of the stream. Even as there is no sharp demarcation between bed material discharge and washload there is no sharp line between contact load and suspended sediment load. A particle may move part of the time in contact with the bed and at other times be suspended by the flow. The distinction is important because the two modes of transport follow different laws. The equations for estimating the total bed material discharge of a stream are based on these laws.

A further subdivision of mode of transport of sediment, including a pictorial representation of measured load and unmeasured load follows.

When a river reaches equilibrium, its transport capacities for water and sediment are in balance with the rates supplied. In fact, most rivers are subject to some kind of control or disturbance, natural or human-induced, that give rise to non-equilibrium conditions.

Total sediment load can be expressed by three equations as illustrated in Figure 4.1 (Julien 1995):

1. By type of movement

$$L_T = L_b + L_s \quad (4.1a)$$

2. By method of measurement

$$L_T = L_m + L_u \quad (4.1b)$$

3. By source of sediment

$$L_T = L_w + L_{bm} \quad (4.1c)$$



where:

- $L_T$  = Total load
- $L_b$  = Bed load which is defined as the transport of sediment particles that are close to or maintain contact with the bed
- $L_s$  = Suspended load defined as the suspended sediment passing through a stream cross-section above the bed layer
- $L_m$  = Measured sediment
- $L_u$  = Unmeasured sediment that is the sum of bed load and a fraction of suspended load below the lowest sampling elevation
- $L_w$  = Wash load which is the fine particles not found in the bed material ( $D_s < D_{10}$ ), and originates from available bank and upstream supply
- $L_{bm}$  = Capacity limited bed material load

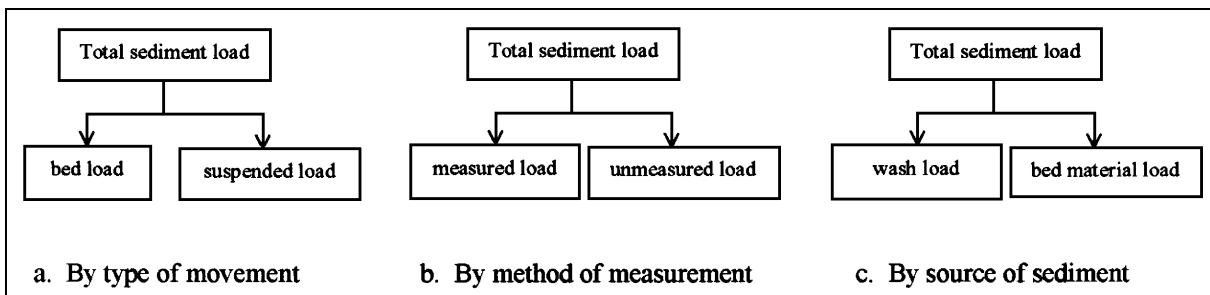


Figure 4.1. Classification of sediment transport in streams (rivers).

### 4.3.3 Total Sediment Discharge

The total sediment discharge of a stream is the sum of the bed sediment discharge (bed material load) and the fine sediment discharge (washload), or the sum of the contact sediment discharge (bed load) and suspended sediment discharge. In the former sum, the total sediment discharge is based on source of the sediments and the latter sum is based on the mode of sediment transport. Whereas suspended sediment load consists of both bed sediments and fine sediments (washload), only the bed sediment discharge can be estimated by the various equations that have been developed. The fine sediment discharge (washload) depends on its availability not on the transporting capacity of the flow and must be measured (Figure 4.2). The presence of high concentrations of wash load affects the apparent viscosity of the water-sediment mixture and reduces the fall velocity of silt and sand grains.

The sediment load that is measured by suspended-sediment samplers consists of both the washload (fine sediment load) and suspended-sediment load. The contact load is not measured, and because suspended sediment samplers cannot travel the total distance in the vertical to the bed, part of the suspended sediment in a vertical is not measured. Generally, the amount of bed material moving in contact with the bed of a large sand-bed river is from 5 to 10 percent of the bed material moving in suspension. In general, the measured suspended-sediment discharge is from 90 to 95 percent of the total sediment discharge. However, in shallow sand-bed streams with little or no washload the measured suspended-sediment load may be as small as 50 percent of the total load.

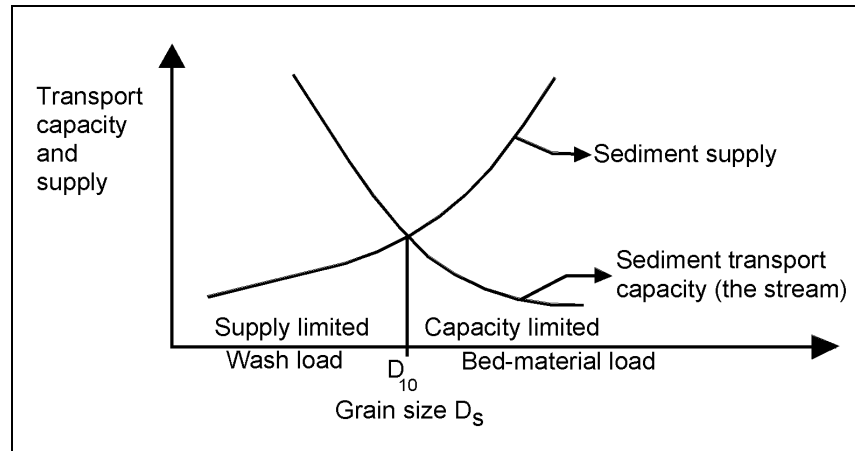


Figure 4.2. Sediment transport capacity and supply curves (Shen 1971; Simons and Sentürk 1992; Julien 1995).

The magnitude of the suspended or bed sediment discharge can be very large. Suspended-sediment concentrations as large as 600,000 ppm or 60 percent by weight have been observed. Concentrations of this magnitude are largely fine sediments. By increasing fluid properties (viscosity and density), the fine material in the flow increases the capacity of the flow to transport bed material.

The sediment load of a stream at a cross section or through a reach of a stream can be determined by measuring the suspended-sediment portion of the load using samplers and estimating the unmeasured discharge or by using one of the many methods that have been developed for computing the bed sediment load and estimating the washload. In many problems, only the bed sediment load, both in suspension and in contact with the bed, is important. In these cases, the washload can be eliminated from the measured suspended-sediment load if the size distribution of the material is known.

Many equations have been developed for the estimation of bed sediment transport. The variation between the magnitude of the bed sediment discharge predicted by different equations under the same conditions can be significant. For the same water discharge, the predicted sediment discharge can have a 100-fold difference between the smallest and the largest value. This can be expected given the number of variables, the interrelationships among them, the difficulty of measuring many of the variables and the statistical nature of bed material transport. Nevertheless, with proper use, knowledge of the river, and knowledge of the limitations of each method, useful bed material discharge information can be obtained.

#### 4.4 SUSPENDED BED SEDIMENT DISCHARGE

The sediment transport process is best described through a discussion of suspended bed sediment discharge, which usually accounts for the majority of the total load. The amount of material transported in suspension varies with depth, with the highest concentrations occurring near the bed. At equilibrium transport, the vertical exchange of sediment is balanced between particle settling (due to gravity) and turbulence (that mixes higher concentration flow up into the water column). For very fine particles, settling is small in comparison to turbulent mixing and the sediment concentration is vertically uniform. For

coarser particles, settling is rapid and particles that are in suspension tend to concentrate nearer the bed.

The suspended bed sediment discharge in Newtons or lbs per second per unit width of channel,  $q_s$ , for steady, uniform two-dimensional flow is

$$q_s = \gamma_s \int_a^{y_o} v c dy \quad (4.2)$$

where  $v$  and  $c$  vary with  $y$  and are the time-averaged flow velocity and volumetric concentrations, respectively, and  $\gamma_s$  is the weight per unit volume of the suspended sediment. The integration is taken over the depth between the distance "a" above the bed and the surface of the flow " $y_o$ ." The level "a" is generally assumed to be 2-grain diameters above the bed layer. Sediment movement below this level is considered bed load rather than suspended load.

The discharge of suspended sediment for the entire stream cross-section,  $Q_s$ , is obtained by integrating Equation 4.2 over the cross section to give

$$Q_s = \gamma_s Q \bar{C} \quad (4.3)$$

where:

$\bar{C}$  = Average suspended-sediment concentration by volume

The vertical distribution of both the velocity and the concentration vary with the mean velocity of the flow, bed roughness and size of bed material. The distributions are illustrated in Figure 4.3. Also  $v$  and  $c$  are interrelated. That is, the velocity and turbulence at a point is affected by the sediment at the point, and the sediment concentration at the point is affected by the point velocity. Normally this interrelation is neglected for low sediment concentrations or a coefficient applied to compensate for it.

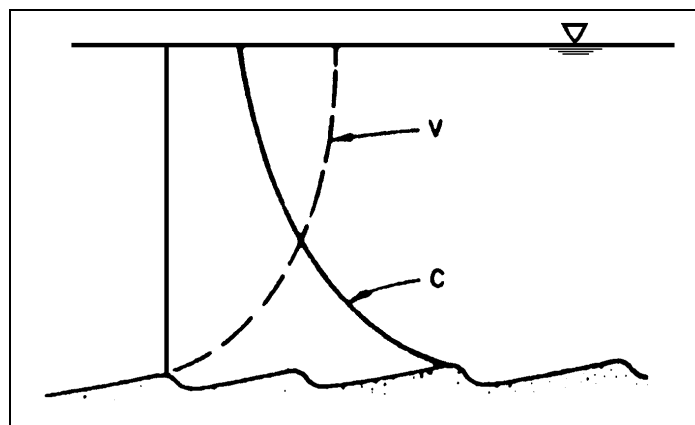


Figure 4.3. Schematic sediment and velocity profiles.

To integrate Equation 4.2,  $v$  and  $c$  must be expressed as functions of  $y$ . The one-dimensional gradient type diffusion equation is employed to obtain the vertical distribution for  $c$  and the logarithm velocity distribution is assumed for  $v$  in turbulent flows.

The one-dimensional diffusion equation describes the equilibrium condition when the quantity of sediment settling across a unit area due to the force of gravity is equal to the quantity of sediment transported upwards resulting from the vertical component of turbulence and the concentration gradient. The resulting equation for a given particle size is

$$\omega c = -\varepsilon_s dc / dy \quad (4.4)$$

where:

- $\omega$  = Fall velocity of the sediment particle at a point
- $c$  = Concentration of particles at elevation  $y$  above the bed
- $\varepsilon_s$  = Exchange coefficient, also called the mass transfer coefficient, which characterizes the magnitude of the exchange of particles across any arbitrary boundary by the turbulence
- $dc/dy$  = Concentration gradient
- $\omega c$  = Average rate of settling of the sediment particles
- $\varepsilon_s dc/dy$  = Average rate of upward sediment flow by diffusion

Integrating Equation 4.4 yields

$$c = c_a \exp\left\{-\omega \int_a^{y_0} dy / \varepsilon_s\right\} \quad (4.5)$$

where  $c_a$  is the concentration of sediment with settling velocity equal to  $\omega$  at a level  $y = a$ .

In order to determine the value of  $c$  at a given  $y$ , the value of  $c_a$  and the variation of  $\varepsilon_s$  with  $y$  must be known. To obtain an expression for  $\varepsilon_s$  the assumption is made that

$$\varepsilon_s = \beta \varepsilon_m \quad (4.6)$$

where:

$\varepsilon_m$  = Kinematic eddy viscosity or the momentum exchange coefficient defined by

$$\varepsilon_m = \frac{\tau}{\rho (dv / dy)} \quad (4.7)$$

where:

$\tau$  and  $dv/dy$  = Shear stress and velocity gradient, respectively, at point  $y$

For two-dimensional steady uniform flow

$$\tau = \gamma S (y_0 - y) = \tau_0 (1 - y / y_0) \quad (4.8)$$

and from Equation 2.74

$$\frac{dv}{dy} = \frac{\sqrt{\tau_o / \rho}}{\kappa y} = \frac{V_*}{\kappa y} \quad (4.9)$$

Thus

$$\varepsilon_s = \beta \varepsilon_m = \beta \kappa V_* y (1 - y / y_o) \quad (4.10)$$

where:

- $\beta$  = Coefficient relating  $\varepsilon_s$  to  $\varepsilon_m$
- $\kappa$  = Von Karman's velocity coefficient assumed equal to 0.4
- $V_*$  = Shear velocity equal to  $\sqrt{gRS}$  in steady uniform flow

Equation 4.10 indicates that  $\varepsilon_m$  and  $\varepsilon_s$  are zero at the bed and at the water surface, and have a maximum value at mid-depth. The substitution of Equation 4.10 into Equation 4.4 gives

$$\frac{dc}{c} = \frac{-\omega}{\beta \kappa V_*} \frac{dy}{y(1 - \frac{y}{y_o})} \quad (4.11)$$

and after integration

$$\frac{c}{c_a} = \left[ \frac{y_o - y}{y} \frac{a}{y_o - a} \right]^z \quad (4.12)$$

where:

- $c$  = Concentration at a distance  $y$  from the bed
- $c_a$  = Concentration at a point  $a$  above the bed
- $z$  =  $\omega / \beta \kappa V_*$ , the Rouse number, named after the engineer who developed the equation in 1937

Figure 4.4 shows a family of curves obtained by plotting Equation 4.12 for different values of the Rouse number  $z$ . An evaluation of the Rouse number,  $z$ , shows that for small values, the sediment distribution is nearly uniform. For large  $z$  values, little sediment is found near the water surface. The value of  $z$  is small for large shear velocities  $V_*$  or small fall velocities  $\omega$ . Thus, for small particles or for extremely turbulent flows, the concentration profiles are uniform.

The values of  $\beta$  and  $\kappa$  have been investigated. For fine particles,  $\beta$  is approximately 1.0. Also, it is well known that in clear water  $\kappa = 0.4$ , but apparently decreases with increasing sediment concentration.

Using the logarithmic velocity distribution for steady uniform flow and Equation 4.12, the equation for suspended sediment transport becomes

$$q_s = \gamma V_* c_a \int_a^{y_o} \left[ \frac{a}{y_o - a} \frac{y_o - y}{y} \right]^Z \left[ 2.5 \ln \left( 30.2 \frac{Xy}{k_s} \right) \right] dy \quad (4.13)$$

Many investigators have solved this equation through integration. The assumptions and integration made by Einstein are presented in Section 4.5.2. An example calculation for a suspended sediment concentration profile is given in Section 4.12 (SI) and 4.13 (English).

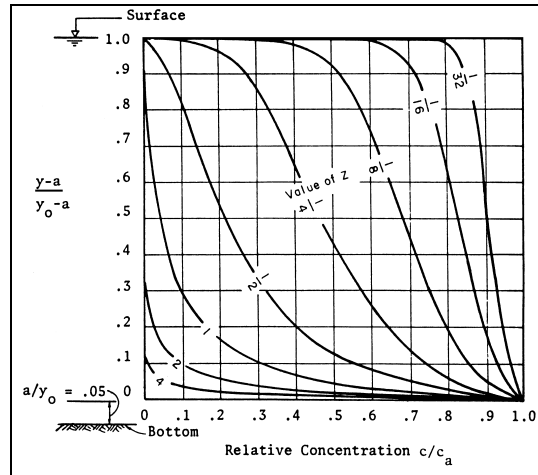


Figure 4.4. Graph of suspended sediment distribution (Rouse 1937).

## 4.5 BED SEDIMENT DISCHARGE

In this section, three classic sediment transport formulae are discussed in detail to illustrate sediment transport processes. These are the Meyer-Peter and Müller (1948), Einstein (1950), and Colby (1964) methodologies. The Meyer-Peter and Müller bedload equation (Section 4.5.1) is applicable to streams with bed material consisting of sand, gravel, and cobbles. The Einstein (Section 4.5.2) and Colby (Section 4.5.4) methods are bed material load equations used for sand-bed streams. In Section 4.7, power function sediment transport relationships are discussed to provide a practical method for quick sediment transport calculations. The Yang sand and gravel total load equations are also included (Section 4.8) because of their frequent application and wide acceptance.

### 4.5.1 Meyer-Peter and Müller Bed Load Equation

Meyer-Peter and Müller (1948) developed the following bed load equation based on experiments with sand particles of uniform sizes, sand particles of mixed sizes and density, natural gravel, lignite, and barite:

$$\left( \frac{Q_b}{Q} \right) \left( \frac{K_B}{K_r} \right)^{3/2} \gamma_o S_f = B' (\gamma_s - \gamma) D_m + B \left( \frac{\gamma}{g} \right)^{1/3} \left( \frac{\gamma_s - \gamma}{\gamma_s} \right)^{2/3} q_B^{2/3} \quad (4.14)$$

where:

- $q_B$  = Bed-load rate in weight per unit time and per unit width
- $Q_b$  = Water discharge quantity determining bed load transport
- $Q$  = Total water discharge
- $y_o$  = Depth of flow
- $S_f$  = Energy slope
- $B', B$  = Dimensionless constants

$B'$  has the value 0.047 for sediment transport and 0.034 for the case of no sediment transport.  $B$  has a value of 0.25 for sediment transport and is meaningless for no transport since  $q_B$  is zero and the last term drops out. The quantities  $K_B$  and  $K_r$  are defined by the expressions

$$K_B = \frac{V}{R^{2/3} S_f^{1/2}} \quad (4.15)$$

and

$$K_r = \frac{V}{R^{2/3} S_f'^{1/2}} \quad (4.16)$$

where:

- $S_f$  = Total energy slope
- $S_f'$  = Part of the total slope required to overcome grain resistance
- $S_f - S_f'$  = Part of the total slope required to overcome form resistance

Therefore

$$\frac{K_B}{K_r} = \sqrt{\frac{f_b'}{8}} \frac{V}{\sqrt{gRS_f}} \quad (4.17)$$

Where  $f_b'$ , the Darcy-Weisbach bed friction factor for the grain roughness,  $f_b'$  is determined from the Nikuradse pipe friction data with pipe diameter equal to four times the hydraulic radius and  $K_s = D_{90}$ . If the boundary is hydraulically rough, ( $V \cdot D_{90} / \nu \geq 100$ ),  $K_r$  is given by

$$K_r = \frac{26}{D_{90}^{1/6}} \quad (4.18)$$

where  $D_{90}$  is in meters.

Equation 4.14 is dimensionally homogeneous so that any consistent set of units may be used. Equation 4.14 was converted to units generally used in the United States in the field of sedimentation for water and quartz particles by the U.S. Bureau of Reclamation in 1960 and is expanded here for application in SI units. This equation is

$$q_B = K_{u1} \left[ K_{u2} \left( \frac{Q_b}{Q} \right) \left( \frac{D_{90}^{1/6}}{n_b} \right)^{3/2} y_o S_f - 0.627 D_m \right]^{3/2} \quad (4.19)$$

where:

$K_{u1}$	=	4.780 in SI units
$K_{u1}$	=	1.606 in English units
$K_{u2}$	=	10.846 in SI units
$K_{u2}$	=	3.306 in English units
$q_B$	=	Metric-tons/day/meter (Tons/day/foot)
$Q_b$	=	Water discharge quantity determining the bed-load transport, m <sup>3</sup> /s (cfs)
$Q$	=	Total water discharge m <sup>3</sup> /s (cfs)
$D_{90}, D_m$	=	In millimeters (both SI and English units)

The quantity  $D_m$  is the effective diameter of the sediment given by

$$D_m = \frac{\sum_i p_i D_{si}}{100} \quad (4.20)$$

where:

$p_i$  = Percentage by weight of that fraction of the bed material with geometric mean size,  $D_{si}$

The term  $n_b$  is the Manning's roughness coefficient for the bed of rectangular channels

$$n_b = n \left[ 1 + \frac{2y_o}{W} \left( 1 - \left( \frac{n_w}{n} \right)^{3/2} \right) \right]^{2/3} \quad (4.21)$$

and for trapezoidal channels

$$n_b = n \left\{ 1 + \frac{2y_o (1 + H_s^2)^{1/2}}{W} \left[ 1 - \left( \frac{n_w}{n} \right)^{3/2} \right] \right\}^{2/3} \quad (4.22)$$

where:

$n, n_b, n_w$	=	Roughness coefficients of the total stream, of the bed, and of the banks, respectively
$H_s$	=	Horizontal side slope related to one unit vertically
$W$	=	Bottom width

The ratio  $Q_b/Q$  for rectangular channels is given by

$$\frac{Q_b}{Q} = \frac{1}{1 + \left( \frac{2y_o}{W} \right) \left( \frac{n_w}{n_b} \right)^{3/2}} \quad (4.23)$$



and for trapezoidal channels is

$$\frac{Q_b}{Q} = \frac{1}{1 + \frac{2y_o(1+H_s^2)^{1/2}}{W} \left(\frac{n_w}{n_b}\right)^{3/2}} \quad (4.24)$$

The Meyer-Peter and Müller formula (Equation 4.14) is often written in the form

$$q_b = K(\tau - \tau_c)^{3/2} \quad (4.25)$$

where:

$$K = \left[ \frac{1}{B \left(\frac{\gamma}{g}\right)^{1/3} \left(\frac{\gamma_s - \gamma}{\gamma_s}\right)^{2/3}} \right]^{3/2} \cong \frac{12.9}{\gamma_s \sqrt{\rho}} \quad (4.26a)$$

$$\tau = \left(\frac{Q_b}{Q}\right) \left(\frac{K_B}{K_r}\right)^{3/2} \gamma_o S_f \quad (4.26b)$$

$$\tau_c = B'(\gamma_s - \gamma) D_m \quad (4.26c)$$

An example of sediment transport calculations using the Meyer-Peter and Müller equation is given in Section 4.12 (SI) and 4.13 (English).

#### 4.5.2 Einstein's Method of Computing Bed Sediment Discharge

Einstein's (1950) method is included in detail because the formulation provides an excellent discussion of sediment transport processes. The equations describe and incorporate the physical processes of contact load and suspended load. The method computes a contact load concentration and uses this concentration as the starting point for integrating the suspended load as presented in Section 4.4. The method also incorporates the vertical velocity distribution based on the roughness of the boundary.

The total bed sediment discharge is the sum of the contact load and the suspended load. As mentioned earlier, there is no sharp demarcation between the contact bed sediment load and the suspended bed sediment. However, this division is warranted by the fact that there is a difference in behavior of the two different loads which justifies two physical equations.

Einstein's bed sediment discharge function gives the rate at which flow of any magnitude in a given channel transports the individual sediment sizes which make up the bed material. This makes his equations extremely valuable where it is necessary to determine the change in bed material with time. Each size moves at its own rate. For each size  $D_s$  of the bed material, the contact load is given as

$$i_B q_B \quad (4.27)$$

and the suspended sediment load is given by

$$i_s q_s \quad (4.28)$$

and the total bed material discharge is

$$i_T q_T = i_s q_s + i_B q_B \quad (4.29)$$

and finally

$$Q_T = \Sigma i_T q_T \quad (4.30)$$

where  $i_T$ ,  $i_s$ , and  $i_B$  are the fractions of the total, suspended and contact bed sediment discharges  $q_T$ ,  $q_s$  and  $q_B$  for a given grain size  $D_s$ . The term  $Q_T$  is the total bed sediment transport. The suspended sediment load is related to the contact load because there is a continuous exchange of particles between the two modes of transport.

With suspended sediment load related to the contact load, Equation 4.29 becomes

$$i_T q_T = i_B q_B (1 + P_E I_1 + I_2) \quad (4.31)$$

where:

$$P_E = 2.3 \log(30.2 y_o / \Delta) \quad (4.32)$$

$I_1$  and  $I_2$  are integrals of Einstein's form of the suspended sediment Equation 4.12

$$i_B q_B = \frac{\phi \cdot i_B \gamma_s}{\left( \frac{\rho}{\rho_s - \rho} \frac{1}{g D_s^3} \right)^{1/2}} \quad (4.33)$$

and

- $\gamma_s$  = Unit weight of sediment
- $\rho$  = Density of the water
- $\rho_s$  = Density of the sediment
- $g$  = Gravitational acceleration
- $\phi \cdot$  = Dimensionless sediment transport function =  $f(\psi^*)$  given in Figure 4.5

$$\psi^* = \xi Y (\beta / \beta_x)^2 \psi = \xi Y (\log 10.6 / \beta_x)^2 \psi \quad (4.34)$$

$$\psi' = \left( \frac{\rho_s - \rho}{\rho} \right) \frac{D_s}{R_b' S_f} \quad (4.35)$$

$\xi$  = Correction factor given as a function of  $D_s / \bar{X}$  in Figure 4.6

$$\bar{X} = 0.77\Delta, \text{ if } \Delta/\delta' > 1.8 \quad (4.36a)$$

$$\bar{X} = 0.139\delta', \text{ if } \Delta/\delta' < 1.8 \quad (4.36b)$$

$\Delta$  = Apparent roughness of the bed,  $k_s / X$

$X$  = Correction factor in the logarithmic velocity distribution equation given as a function of  $k_s / \delta'$  in Figure 4.7

$$\delta' = 11.6\nu / V_*' \quad (4.37)$$

$$\nu / V_*' = \text{Einstein's velocity distribution equation} = 5.75 \log (30.2y / \Delta) \quad (4.38a)$$

$$V_*' = \text{Shear velocity due to grain roughness} = \sqrt{gR_b'S} \quad (4.38b)$$

$R_b'$  = Hydraulic radius of the bed due to grain roughness =  $R_b - R_b''$

$R_b''$  = Hydraulic radius of the bed due to channel irregularities

$S_f$  = Slope of the energy grade line normally taken as the slope of the water surface

$Y$  = Another correction term given as a function of  $D_{65} / \delta'$  in Figure 4.8

$$\beta_x = \log (10.6\bar{X} / \Delta)$$

$$I_1 = 0.216 \frac{E^{Z-1}}{(1-E)^Z} \int_E^1 \left[ \frac{1-y}{y} \right]^Z dy \quad (4.39)$$

$$I_2 = 0.216 \frac{E^{Z-1}}{(1-E)^Z} \int_E^1 \left[ \frac{1-y}{y} \right]^Z \ln y dy \quad (4.40)$$

where:

$$Z = \omega / \beta \kappa V_*' = \omega / 0.4V_*' \quad (4.41)$$

$\omega$  = Fall velocity of the particle of size  $D_s$

$E$  = Ratio of bed layer thickness to flow depth,  $a/y_0$

$y_0$  = Depth of flow

$a$  = Thickness of the bed layer,  $2D_{65}$

The two integrals  $I_1$  and  $I_2$  are given in Figures 4.9 and 4.10 as a function of  $z$  and  $E$ .

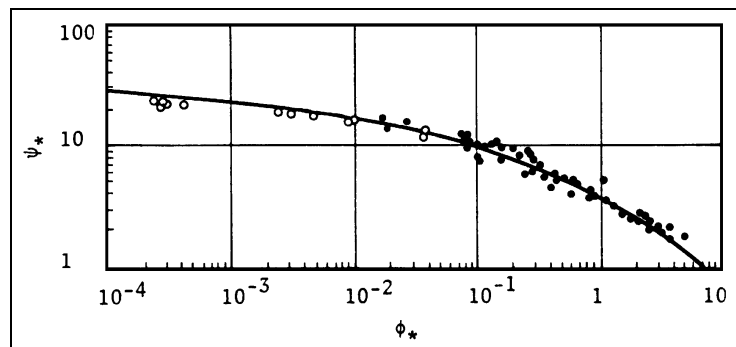


Figure 4.5. Einstein's  $\phi_*$  vs  $\psi_*$  bed load function (Einstein 1950).

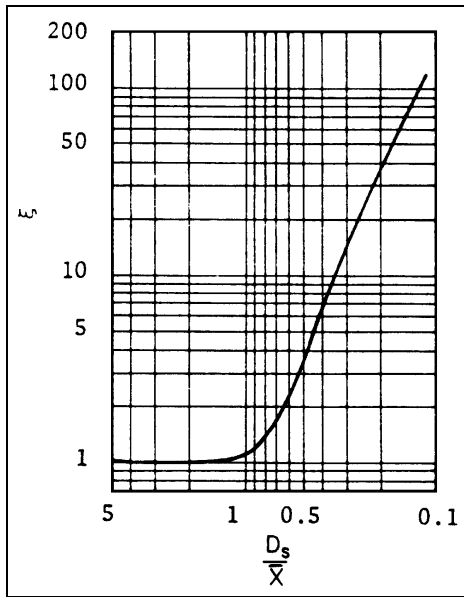


Figure 4.6. Hiding factor (Einstein 1950).

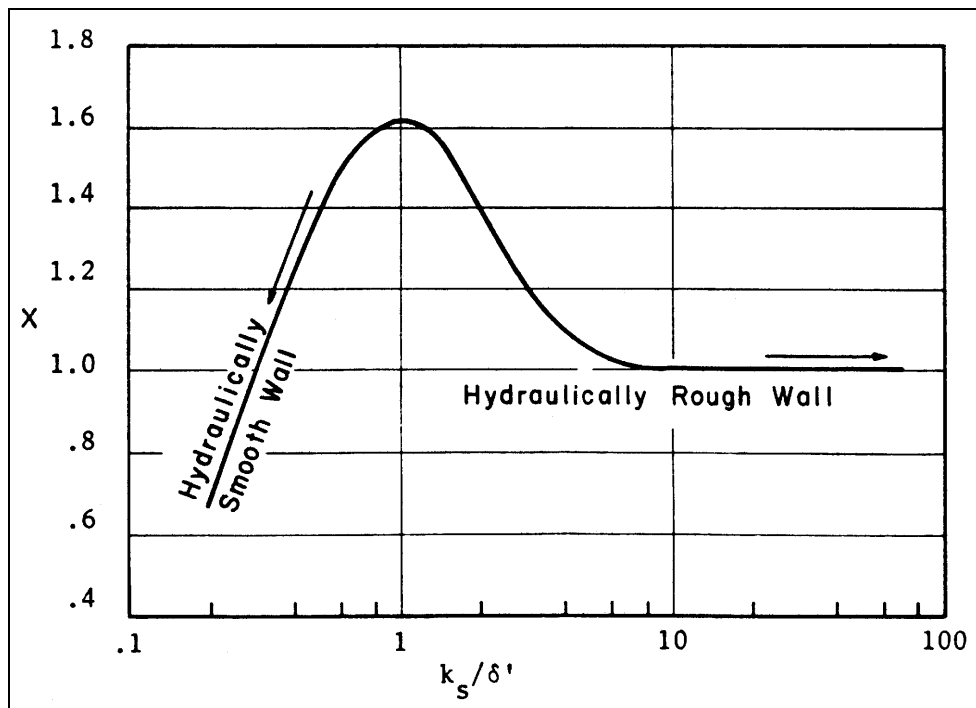


Figure 4.7. Einstein's multiplication factor  $X$  in the logarithmic velocity equations (Einstein 1950).

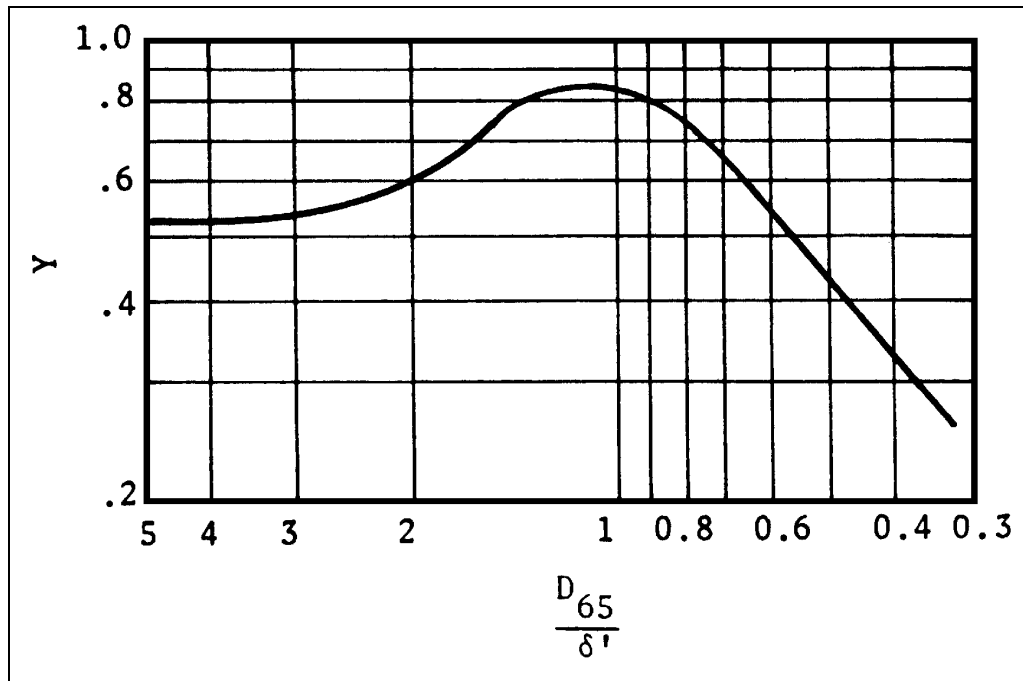


Figure 4.8. Pressure correction (Einstein 1950).

In the preceding calculations for the bed sediment load, the shear velocity is based on the hydraulic radius of the bed due to grain roughness  $R_b'$ . Its computation is explained in the following paragraph.

Total resistance to flow is composed of two parts, surface drag and form drag. The transmission of shear to the boundary is accompanied by a transformation of flow energy into energy turbulence. The part of energy corresponding to grain roughness is transformed into turbulence that stays at least for a short time in the immediate vicinity of the grains and has a great effect on the bed load motion. Whereas, the other part of the energy which corresponds to the form resistance is transformed into turbulence at the interface between wake and free stream flow, or at a considerable distance away from the grains. This energy does not contribute to the bed load motion of the particles and may be largely neglected in the sediment transportation.

Einstein's equation for mean flow velocity  $V$  in terms of  $V_*'$  is

$$V / V_*' = 5.75 \log(12.26 R_b' / \Delta) \quad (4.42a)$$

or

$$V / V_*' = 5.75 \log(12.26 R_b' / k_s X) \quad (4.42b)$$

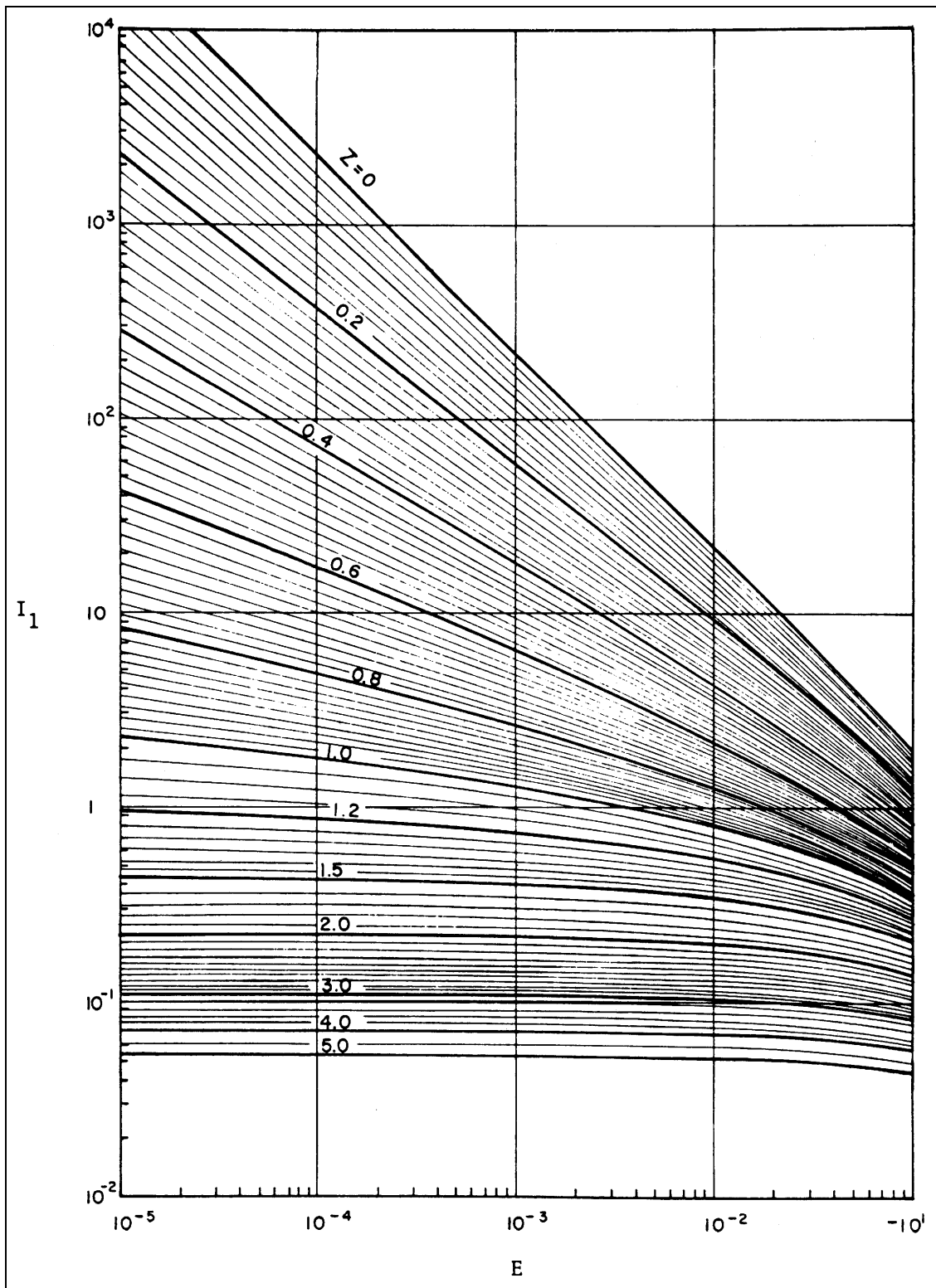


Figure 4.9. Integral  $I_1$  in terms of  $E$  and  $Z$  (Einstein 1950).

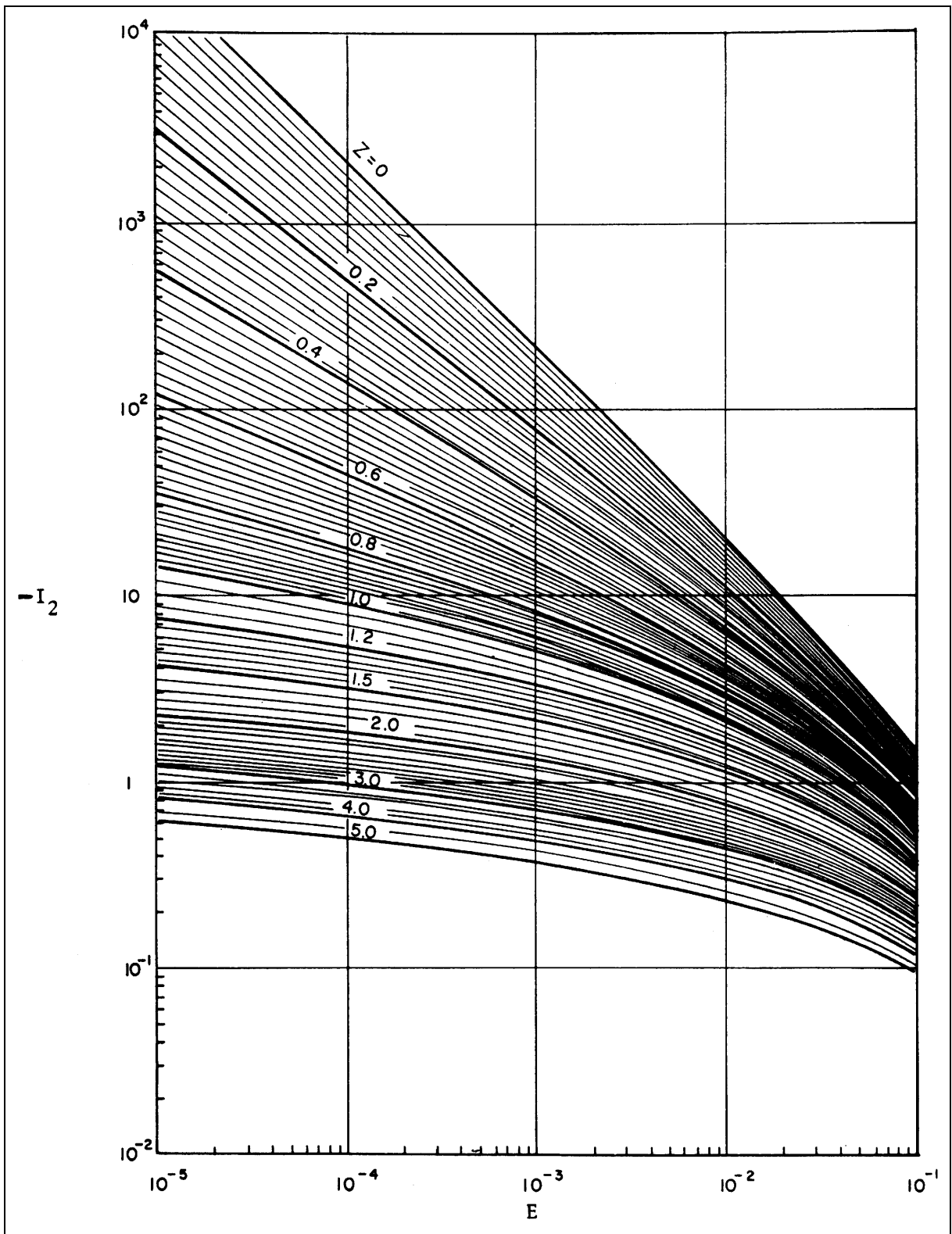


Figure 4.10. Integral  $I_2$  in terms of  $E$  and  $Z$  (Einstein 1950).

Furthermore, Einstein suggested that

$$V / V_*' = \theta[\psi'] \quad (4.43)$$

where

$$\psi' = \frac{\rho_s - \rho}{\rho} \frac{D_{35}}{R_b' S_f} \quad (4.44)$$

The relation for Equation 4.44 is given in Figure 4.11. The procedure to follow in computing  $R_b'$  depends on the information available. If mean velocity  $V$ , slope  $S$ , hydraulic radius  $R_b$  and the size of bed material are known, then  $R_b'$  is computed by trial and error using Equation 4.42 and Figure 4.11.

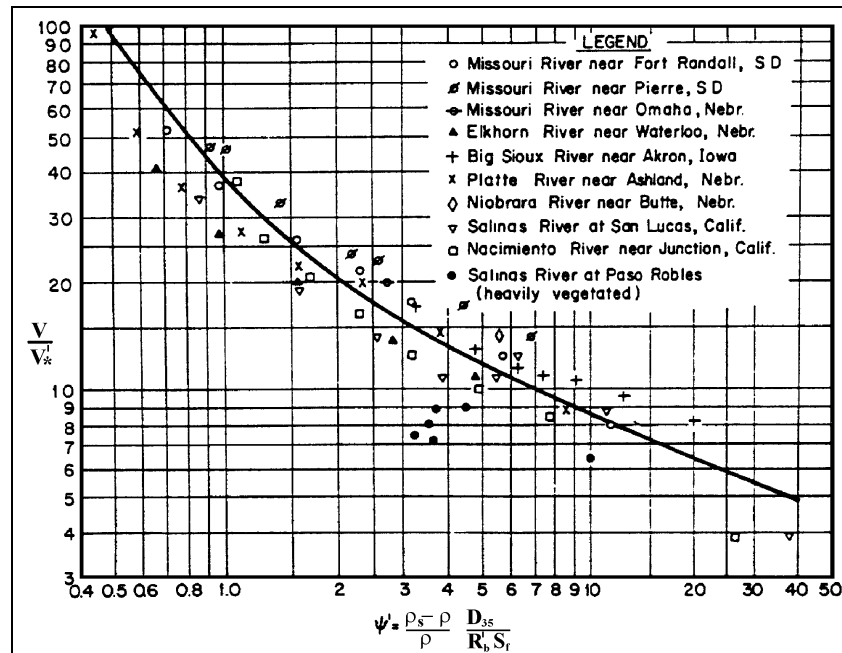


Figure 4.11. Friction loss due to channel irregularities, as a function of sediment transport (after Einstein and Barbarossa 1952).

The procedure for computing total bed sediment discharge in terms of different size fractions of the bed material is:

- (1) Calculate  $\psi_*$  using Equation 4.33 for each size fraction
- (2) Find  $\phi_*$  from Figure 4.5 for each size fraction
- (3) Calculate  $i_B q_B$  for each size fraction using Equation 4.32
- (4) Sum up the  $q_B$  across the flow to obtain  $i_B Q_b$
- (5) Sum up the size fractions to obtain  $Q_b$



For the suspended sediment discharge:

- (6) Calculate Z for each size fraction using Equation 4.41
- (7) Calculate  $E = 2D_s / y_0$  for each fraction
- (8) Determine  $l_1$  and  $l_2$  for each fraction from Figures 4.9 and 4.10
- (9) Calculate  $P_E$  using Equation 4.32
- (10) Compute the suspended discharge from  $l_B q_B (1 + P_E l_1 + l_2)$  from Equation 4.31
- (11) Sum up all the  $q_B$  and all the  $i_B$  to obtain the total suspended discharge  $Q_{ss}$

Thus, the total bed sediment discharge is computed as:

- (12) Add the results of Step 5 and 11.

A sample problem showing the calculation of the total bed sediment discharge using Einstein's procedure is presented in Section 4.13.

### 4.5.3 Comparison of Meyer-Peter and Müller and Einstein Contact Load Equations

Chien (1954) has shown that the Meyer-Peter and Müller, equation can be modified into the form

$$\phi_* = \left( \frac{4}{\psi_*} - 0.188 \right)^{3/2} \quad (4.45)$$

Figure 4.12 shows the comparison of Equation 4.45 with Einstein's  $\psi_*$  vs.  $\phi_*$  relation for uniform bed sediment size and for sediment mixtures using  $D_{35}$  in the Einstein relation and  $D_{50}$  in the Meyer-Peter and Müller relation. They show good agreement for coarse sands, but diverge for fine sands. This supports the premise that the Meyer-Peter and Müller equation is most applicable to coarse grain sizes with little or no suspended load.

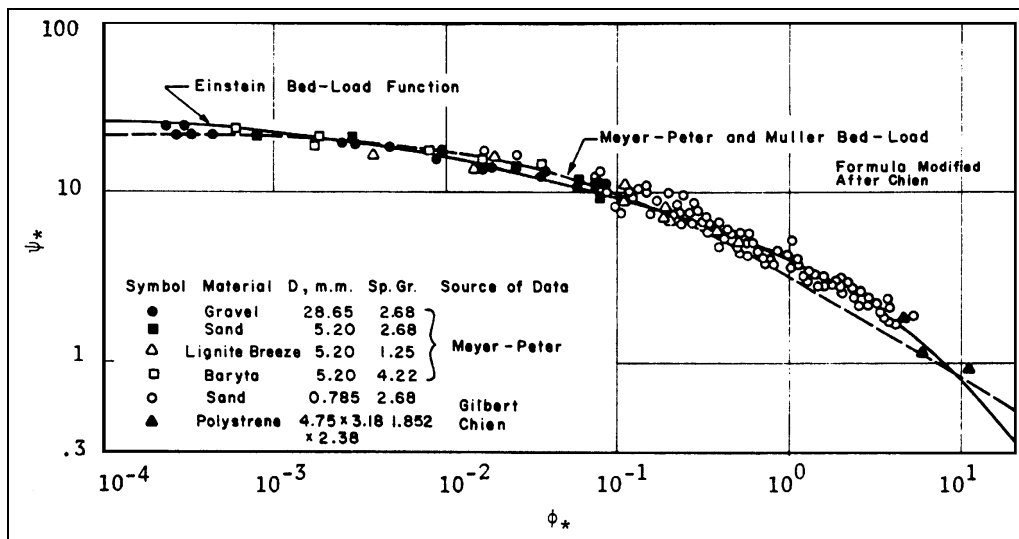


Figure 4.12. Comparison of the Meyer-Peter and Müller and Einstein methods for computing contact load (Chien 1954).

#### 4.5.4 Colby's Method of Estimating Bed Sediment Discharge

Colby's (1964) method is a graphical method for estimating total load, which can also be used to check the reasonableness of other sediment transport calculations. One very important feature of the Colby method is the inclusion of a correction factor for fine sediment (washload) concentration effects. Colby's method illustrates that washload can have a significant impact on bed material load transport capacity.

After investigating the effect of all the pertinent variables, Colby (1964) developed four graphical relations shown in Figures 4.13 and 4.14 for determining the bed sediment discharge. In arriving at his curves, Colby was guided by the Einstein bed-load function (Einstein 1950) and a large amount of data from streams and flumes. However, it should be understood that all curves for 100-foot depth, most curves of 10-foot depth and part of the curves of 1.0 and 0.1 ft are extrapolated from limited data and theory. Extrapolated curves are shown as dashed lines in Figure 4.13.

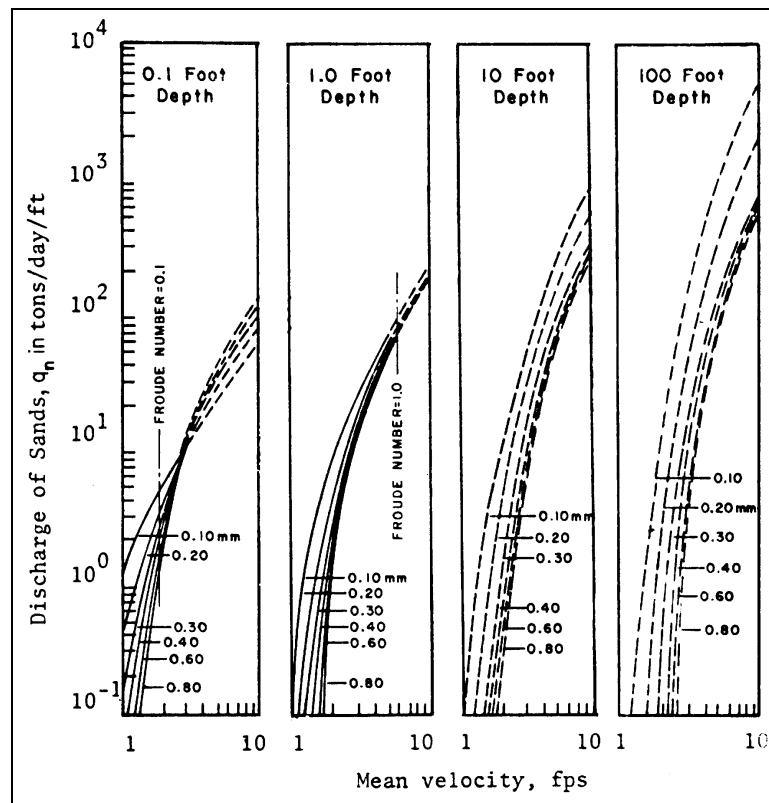


Figure 4.13. Relation of discharge of sands to mean velocity for six median sizes of bed sands, four depths of flow, and a water temperature of 60°F (Colby 1964).

In applying Figures 4.13 and 4.14 to compute the bed sediment discharge, the following procedure is used:

1. Required data are the mean velocity  $V$ , the depth  $y_0$ , the median size of bed material  $D_{50}$ , the water temperature °F and the measured fine sediment concentration  $C_f$ .

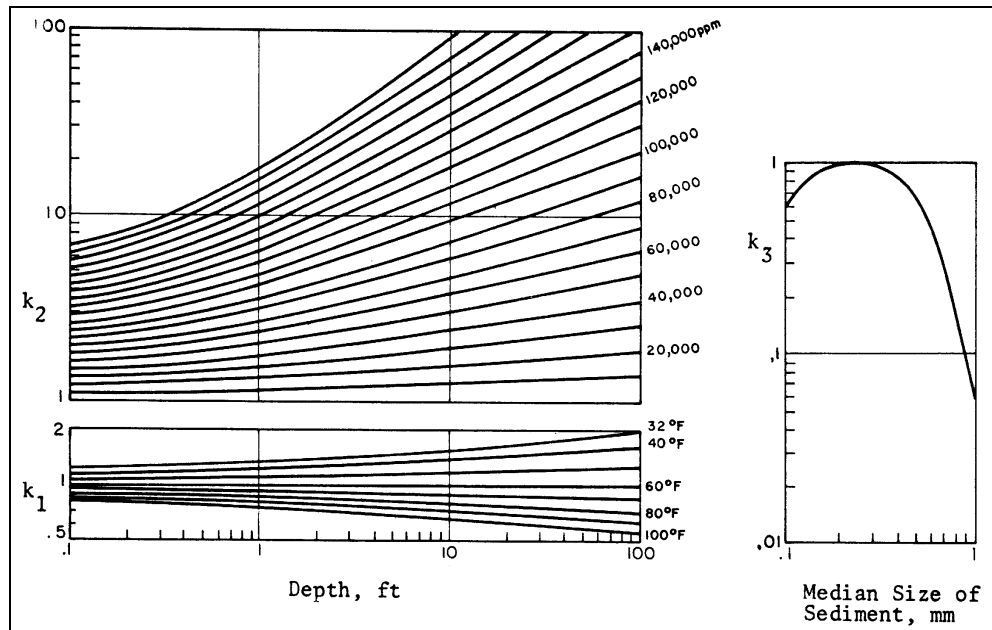


Figure 4.14. Colby's correction curves for temperature and fine sediment (Colby 1964).

2. Uncorrected sediment discharge  $q_n$  for the given  $V$ ,  $y_o$ , and  $D_{50}$  can be found from Figure 4.13 by first reading  $q_n$  knowing  $V$  and  $D_{50}$  for two depths that bracket the desired depth and then interpolating on a logarithmic graph of depth versus  $q_n$  to get the bed sediment discharge per unit width.
3. Two correction factors  $k_1$  and  $k_2$  shown in Figure 4.14 account for the effect of water temperature and fine suspended sediment on the bed sediment discharge. If the bed sediment size falls outside the 0.20 mm to 0.30 mm range, the factor  $k_3$  from Figure 4.14 is applied to correct for the effect of sediment size.
4. Unit bed sediment discharge  $q_T$  corrected for the effect of water temperature, presence of fine suspended sediment and sediment size is given by the equation

$$q_T = [1 + (k_1 k_2 - 1) k_3] q_n \quad (4.46)$$

As Figure 4.14 shows,  $k_1 = 1$  when the temperature is 60°F,  $k_2 = 1$  when the concentration of fine sediment is negligible and  $k_3 = 1$  when  $D_{50}$  lies between 0.2 mm and 0.3 mm. The total sand discharge is

$$Q_T = Wq_T \quad (4.47)$$

where:

$W$  = Width of the stream

Colby (1964) found that: "The agreement of computed and observed discharges of sands for sediment stations whose records were not used to define the graphs seemed to be about as

good as that for stations whose records were used." An example showing bed sediment discharge calculations by the Colby method is presented in Section 4.13.

#### 4.5.5 Relative Influence of Variables

The study of the relative influence of viscosity, slope, bed sediment size and depth on bed sediment and water discharge is examined in this section using Einstein's bed-load function (1950) and Colby's (1964) relationships. Einstein's bed-load function is chosen because it is the most detailed and comprehensive treatment from the point of fluid mechanics. Colby's relations are chosen because of the large amount and range of data used in their development.

The data required to compute the bed material discharge using Einstein's relations are:  $S$  = channel slope;  $D_{65}$  = size of bed material for which 65 percent is finer;  $D_{35}$  = size of bed material for which 35 percent is finer;  $D_i$  = size of bed sediment in fraction  $i$ ;  $\nu$  = kinematic viscosity;  $n_w$  = Manning's wall friction coefficient;  $A$  = cross-sectional area;  $P_b$  = wetted perimeter of the bed;  $P_w$  = wetted perimeter of the banks;  $i_B$  = percentage of bed sediment in fraction  $i$ ;  $\gamma_s$  = specific weight; and  $V$  = average velocity.

To study the relative influence of variables on bed material and water discharges, the data taken by the U.S. Geological Survey from October 1, 1940 to October 1, 1970 on the Rio Grande near Bernalillo, New Mexico are used. The width of the channel reach was 82.3 m (270 ft). In the analysis, the energy slope was varied from  $0.7S$  to  $1.5S$ , in which  $S$  is the average bed slope assumed to be equal to the average energy slope. Further, the kinematic viscosity was varied to correspond with variations in temperature from  $39.2^\circ$  to  $100^\circ\text{F}$  inclusive. The variation of  $D_{65}$ ,  $D_{50}$ ,  $D_i$ , and  $i_B$  was accomplished by using the average bed material distribution given by Nordin (1964) and shifting the curve representing the average bed sediment distribution along a line parallel to the abscissa drawn through  $D_{50}$ . The average water temperature was assumed to be equal to  $70^\circ\text{F}$  and the average energy gradient of the channel was assumed to be equal to 0.00095. The water and sediment discharges were computed independently for each variation of the variables and for three subreaches of the Rio Grande of differing width near Bernalillo. The applicability of the results depends on the reliability of the modified Einstein bed-load function and Colby's relationships used in the analysis rather than on the choice of data.

The computed water and sediment discharges are plotted in Figures 4.15, 4.16, and 4.17 and show the variation of sediment discharge due to changes in bed material size, slope and temperature for any given water discharge. Figure 4.15 shows that when the bed sediment becomes finer, the sediment discharge increases considerably. The second most important variable affecting sediment discharge is the slope variation (Figure 4.16). Temperature is third in importance (Figure 4.17). The effects of variables on sediment discharge were studied over approximately the same range of variation for each variable.

Figure 4.18 shows the variation of the sediment discharge due to changes in the depth of flow for any given discharge, computed using Colby's (1964) relations. The values of depth of flow varied from 1.0 to 10.0 ft, the median diameter of the bed sediment is maintained constant equal to 0.030 mm, the water temperature is assumed constant and the concentration of fine sediment is assumed less than 10,000 ppm. The channel width is also maintained constant at 82.3 m (270 ft). In Figure 4.18, the curves for constant depth of flow show a steep slope. This indicates that the capacity of the stream to transport sands increases very fast for a small increase of discharge at constant depth. Similar figures can be developed for other sizes of bed material, and the relations can be modified to include the effect of washload and viscosity effects.

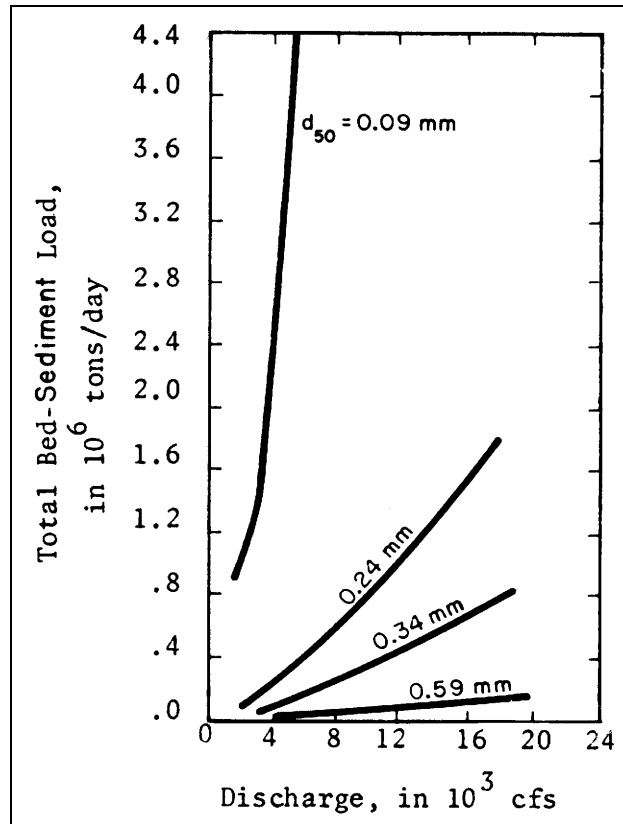


Figure 4.15. Bed-material size effects on bed material transport.

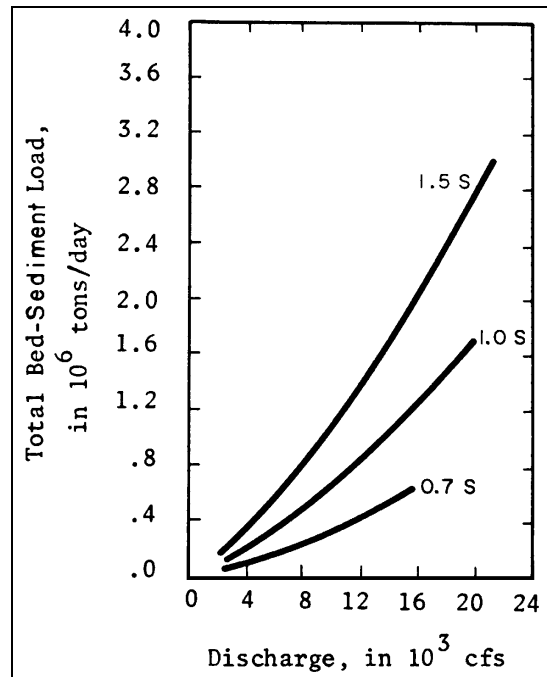


Figure 4.16. Effect of slope on bed material transport.

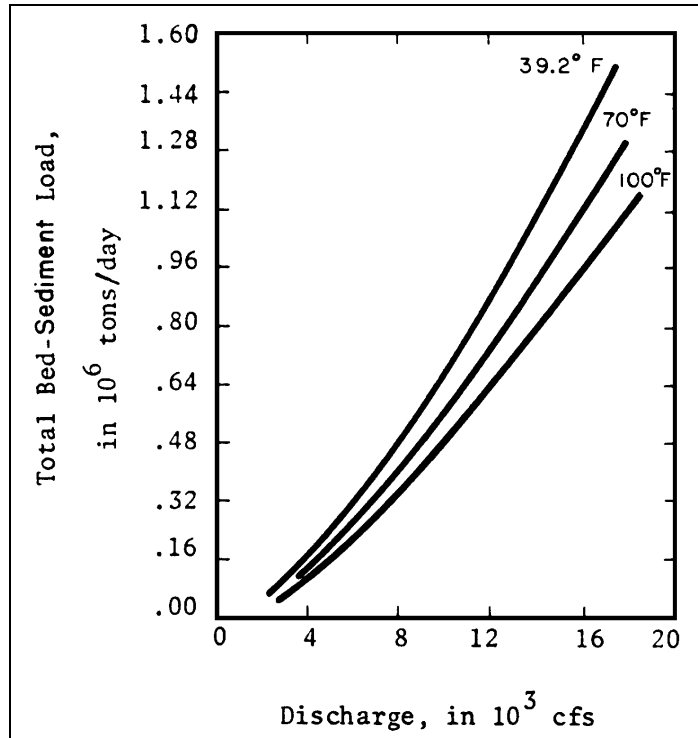


Figure 4.17. Effect of kinematic viscosity (temperature) on bed material transport.

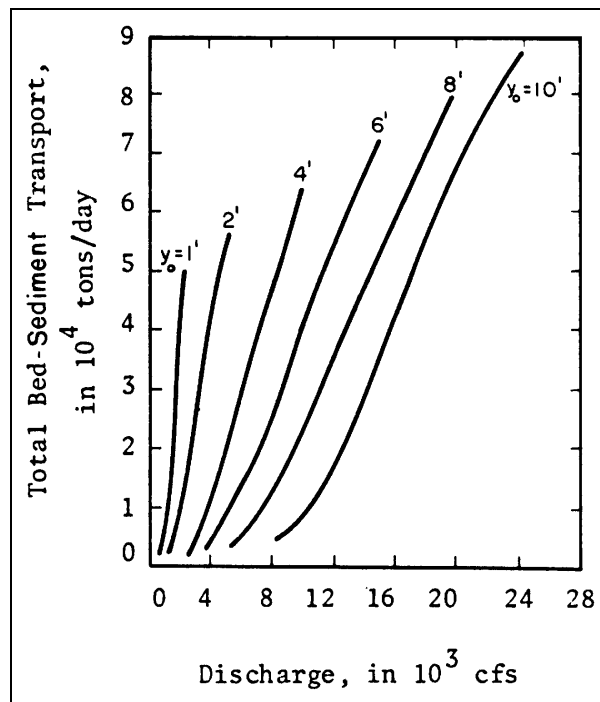


Figure 4.18. Variation of bed material load with depth of flow.

## 4.6 POWER FUNCTION RELATIONSHIPS

In Section 4.5, three classic sediment transport equations were presented. Of the three, the Meyer-Peter and Müller bedload equation is still widely used, and the Colby method provides a graphical approach that can be used as a quick check on the reasonableness of the results of other sand-bed sediment transport calculations. Both are simple enough in their application to be considered "basic" approaches for hand calculation, although, as indicated above, they can be integrated into computer solutions. To provide additional basic approaches, power function relationships are discussed in this section. These provide a practical method for quick sediment transport calculations and are readily adaptable to computer solutions.

### 4.6.1 Introduction

Power relationships relate sediment transport rates to hydraulic conditions and sediment characteristics. The value of power relationships is in (1) their ease of use, (2) application to specific flow regimes, and (3) application to site-specific conditions. Most power function relationships correlate sediment transport to velocity and flow depth. This simple relationship can be used as a first estimate of sediment transport capacity or as a comparison with the more rigorous equations. Power relationships can be developed by computing sediment transport with a more rigorous approach and fitting the results to a power function form. The Simons et al. (1981) power function was developed specifically for supercritical flow conditions on sand and fine gravel bed channels. Power relationships are also well suited for correlating measured sediment transport with observed hydraulic conditions. The resulting equation is site specific, but can be used, with judgment, to estimate sediment transport rates for hydraulic conditions outside the range of observations. HEC-20 (Chapter 6) illustrates the application of power relationships to predicting the equilibrium slope for a channel that is either sediment deficient or has an excessive sediment supply.

The following sections present the Simons et al. (1981) power function that was developed for steep sand and gravel bed channels. A more general power function relationship, by Kodoatie et al. (1999), is also presented. The Kodoatie equation can be used for silt, fine sand, medium to coarse sand, and gravel bed rivers by selecting appropriate coefficients and exponents. HEC-20 (Lagasse et al. 2001) includes a power function equation developed using the Yang (1996) sand transport equation.

In summary, power relationships empirically relate sediment transport with hydraulic conditions and sediment characteristics. They can be developed by fitting the coefficients to computed sediment transport data from more sophisticated equations or to measured data. Their utility is in their ease of use and, when developed from measured data, their site-specific accuracy.

### 4.6.2 Basic Power Function Relationship

In 1981, Simons et al. proposed an efficient method of evaluating sediment discharge. The method is based on the variables flow depth, velocity, and particle diameter, and gradation coefficient. The basic power function relationship is:

$$q_s = c_{s1} y^{c_{s2}} V^{c_{s3}} \quad (4.48)$$

where:

- $q_s$  = Unit sediment transport rate,  $ft^2/s$  ( $m^2/s$ )
- $C_{s2}, C_{s3}$  = Exponents based on mean particle diameter ( $D_{50}$ ) ranging from sand to fine gravel
- $C_{s1}$  = Coefficient based on mean particle diameter (note that  $C_{s1}$  must be adjusted for SI units)
- $y$  = Mean flow depth, ft (m)
- $V$  = Mean flow velocity, ft/s (m/s)

This relationship can be applied in steep streams with sand and fine gravel beds that normally exhibit critical or supercritical flow. This is the only transport relationship specifically developed for upper flow regime conditions. These power relationships were developed by Simons et al., from a computer solution of the Meyer-Peter and Müller bed load transport equation and the integration of the Einstein method for suspended bed material discharge (Julien 1995).

Table 4.1 provides the coefficient and exponents for Equation 4.48 (for English units) for different gradation coefficients and sizes of bed material. **Note that if sediment transport in SI units is desired,  $C_{s1}$  needs to be multiplied by a factor of 0.3048<sup>(2 - C<sub>s2</sub> - C<sub>s3</sub>)</sup>.** The term  $G_r$  in Table 4.1 is defined as the gradation coefficient of the bed material and is:

$$G_r = \frac{1}{2} \left[ \frac{D_{50}}{D_{16}} + \frac{D_{84}}{D_{50}} \right] \quad (4.49)$$

where:

- $D_n$  = Size of the bed material for which  $n$  percent of a sediment sample is finer. In this case,  $n = 84, 50,$  and  $16,$  respectively.

Table 4.1. Coefficient and Exponents of Equation 4.48 (Simons et al.).*									
		$D_{50}$ (mm)							
		0.1	0.25	0.5	1.0	2.0	3.0	4.0	5.0
$G_r = 1$	$C_{s1}$	$3.30 \times 10^{-5}$	$1.42 \times 10^{-5}$	$7.60 \times 10^{-6}$	$5.62 \times 10^{-6}$	$5.64 \times 10^{-6}$	$6.32 \times 10^{-6}$	$7.10 \times 10^{-6}$	$7.78 \times 10^{-6}$
	$C_{s2}$	0.715	0.495	0.28	0.06	-0.14	-0.24	-0.3	-0.34
	$C_{s3}$	3.3	3.61	3.82	3.93	3.95	3.92	3.89	3.87
$G_r = 2$	$C_{s1}$		$1.59 \times 10^{-5}$	$9.80 \times 10^{-6}$	$6.94 \times 10^{-6}$	$6.32 \times 10^{-6}$	$6.62 \times 10^{-6}$	$6.94 \times 10^{-6}$	
	$C_{s2}$		0.51	0.33	0.12	-0.09	-0.196	-0.27	
	$C_{s3}$		3.55	3.73	3.86	3.91	3.91	3.9	
$G_r = 3$	$C_{s1}$			$1.21 \times 10^{-5}$	$9.14 \times 10^{-6}$	$7.44 \times 10^{-6}$			
	$C_{s2}$			0.36	0.18	-0.02			
	$C_{s3}$			3.66	3.76	3.86			
$G_r = 4$	$C_{s1}$				$1.05 \times 10^{-5}$				
	$C_{s2}$				0.21				
	$C_{s3}$				3.71				

\*  $C_{s1}$  (SI units) =  $0.3048^{(2 - C_{s2} - C_{s3})} (C_{s1})$



Equation 4.48 was developed for channels with steep slopes for sand and fine gravel beds experiencing critical and super-critical flows [Simons, et al. (1981), Julien (1995)]. The range of parameters utilized to develop this equation is shown in Table 4.2.

Parameter	Value Range	SI Units
Froude Number	1 – 4	--
Velocity	1.98 – 7.92	m/s
Bed Slope	0.005 – 0.040	m/m
Unit Discharge, $q$	3.05 – 60.96	$m^2/s$
Particle Size, $D_{50}$	> 0.062	mm

As the depth increases for a given velocity, the intensity of the turbulent transfer properties decreases for these sizes. The increase in area available for suspended sediment with the increased depth does not totally counterbalance the reduced turbulent transfer characteristics. The result is an inverse dependence of transport rate on depth for these larger sizes. The sizes with no dependence ( $C_{s2} = 0$ ) on depth in their transport rate fall between these two extremes.

When applying the equations resulting from Table 4.1, care should be taken to assure that the range of parameters being used is not out of range with those used to develop the equations (Table 4.2). If conditions are within the ranges outlined in Table 4.2 the regression equations should provide results within ten percent of the values computed using the Meyer-Peter and Müller bedload and Einstein suspended load equations for the steep conditions in Table 4.2.

There are several other checks that should be made in order to ensure the equations are applicable to a given problem. The equations are based on the assumption that all the sediment sizes present can be moved by the flow. If this is not true, armoring will take place. **The equations are not applicable when armoring occurs.** Since the equations were developed for sand-bed channels, they do not apply to conditions when the bed material is cohesive. Equation 4.48 would overpredict transport rates in a cohesive channel.

An example of the application of the basic power function relationship is given in Section 4.12 (SI) and Section 4.13 (English).

### 4.6.3 Expanded Power Function Relationship

Kodoatie et al. (1999) modified a Posada (1995) equation using nonlinear optimization and the field data for different sizes of riverbed sediment. A description of the development and validation of this equation is presented in Appendix B. The resulting equation is:

$$q_t = aV^b y^c S^d \quad (4.50)$$

where:

- $q_t$  = Sediment transport rate, metric tons/m/day (tons/ft/day)
- $V$  = Mean flow velocity, m/s (ft/s)
- $y$  = Mean flow depth, m (ft)
- $S$  = Energy slope
- $a, b, c,$  and  $d$  = Regression coefficients

A summary of coefficient and exponents (for SI units) is presented in Table 4.3, depending on size of bed material. **Note that the values of "a" must be multiplied by a factor of 1.1 x 0.3048<sup>(1+b+c)</sup> for input and results in English units.**

Table 4.3. Coefficient and Exponents for Equation 4.50.				
	a*	b	c	d
Silt-bed rivers	281.4	2.622	0.182	0
Very fine to fine-bed rivers	2,829.6	3.646	0.406	0.412
Medium to very coarse sand-bed rivers	2,123.4	3.300	0.468	0.613
Gravel-bed rivers	431,884.8	1.000	1.000	2.000
*a (English Units) = 1.1 x 0.3048 <sup>(1+b+c)</sup> (a)				

An example of the application of the expanded power function relationship is given in Section 4.12 (SI) and 4.13 (English)

#### 4.7 YANG'S EQUATIONS

The Yang sand and gravel total load equations are presented because of their frequent application and wide acceptance. The Yang equations are also readily adaptable to computer solutions. Yang (1996) related total load to excess unit stream power, expressed as the product of velocity and slope. Separate equations were developed for sand and gravel bed material and solved for sediment concentration in ppm by weight. The regression equations are developed based on dimensionless combinations of unit stream power, critical unit stream power, shear velocity, fall velocity, kinematic viscosity and sediment size. Yang also developed critical velocity formulas for use with his equations. The total load equations can be used to compute sediment transport by size fraction by using the geometric mean of the size class and weighting the computed concentrations by the class interval. The sand equation, which should be used for median sizes less than 2.0 mm, is:

$$\log C_t = 5.435 - 0.286 \log \frac{\omega D_{50}}{v} - 0.457 \log \frac{V_*}{\omega} + \left( 1.799 - 0.409 \log \frac{\omega D_{50}}{v} - 0.314 \log \frac{V_*}{\omega} \right) \log \left( \frac{VS}{\omega} - \frac{V_{cr}S}{\omega} \right) \quad (4.51)$$

and the gravel equation, which should be limited to median sizes between 2.0 and 10.0 mm, is:

$$\log C_t = 6.681 - 0.633 \log \frac{\omega D_{50}}{v} - 4.816 \log \frac{V_*}{\omega} + \left( 2.784 - 0.305 \log \frac{\omega D_{50}}{v} - 0.282 \log \frac{V_*}{\omega} \right) \log \left( \frac{VS}{\omega} - \frac{V_{cr}S}{\omega} \right) \quad (4.52)$$

where:

$C_t$	=	Sediment concentration in parts per million by weight
$\omega$	=	Fall velocity of the sediment, m/s (ft/s)
$\nu$	=	Kinematic viscosity, m <sup>2</sup> /s (ft <sup>2</sup> /s)
$V_*$	=	Shear velocity ( $\sqrt{gRS}$ ), m/s (ft/s)
$V$	=	Velocity, m/s (ft/s)
$V_{cr}$	=	Critical Velocity, m/s (ft/s)
$S$	=	Energy slope

In the above equations, the dimensionless critical velocity is given by:

$$\frac{V_{cr}}{\omega} = \frac{2.5}{\log \frac{V_* D_{50}}{\nu} - 0.06} + 0.66 \quad \text{for} \quad 1.2 < \frac{V_* D_{50}}{\nu} < 70 \quad (4.53)$$

and

$$\frac{V_{cr}}{\omega} = 2.05 \quad \text{for} \quad \frac{V_* D_{50}}{\nu} \geq 70 \quad (4.54)$$

An example of calculating total bed-material discharge using Equation 4.51 is given in Section 4.12 (SI) and Section 4.13 (English).

## 4.8 CONVERSION FACTORS

There are numerous ways of expressing sediment transport. These include rate of transport and concentration. The rate of sediment transport can be expressed as a volumetric rate (m<sup>3</sup>/s, ft<sup>3</sup>/s), or mass or weight rates (metric-tons/day, tons/day). The concentration relates volume or weight of sediment to the total volume or weight of the sediment-water mixture and is converted to a rate of sediment transport by including the water discharge.

The following equations can be used to convert from a volumetric rate to a mass transport.

$$Q_s \text{ (metric-tons/day)} = Q_s \text{ (m}^3\text{/s)} \times \gamma_s / g \times 86400 / 1000 \quad (4.55)$$

$$Q_s \text{ (tons/day)} = Q_s \text{ (ft}^3\text{/s)} \times \gamma_s \times 86400 / 2000 = Q_s \text{ (ft}^3\text{/s)} \times \gamma_s \times 43.2 \quad (4.56)$$

A common unit for sediment concentration is milligrams per liter ( $C_{mg/l}$ ), which is the ratio of the mass of sediment to the total volume of water and sediment. Concentrations are often expressed as parts per million by multiplying the concentration by  $10^6$ . Four ways of expressing concentration are:

$$\text{Concentration by volume: } C_v = \text{sediment volume/total volume} \quad (4.57)$$

$$\text{Concentration by weight: } C_w = \text{sediment weight/total weight} = C_v S_g / [1+(S_g-1)C_v] \quad (4.58)$$

$$\text{Concentration as parts per millions by weight: } C_{ppm} = 10^6 C_w \quad (4.59)$$

$$\text{Concentration as mg/l: } C_{mg/l} = 10^6 C_v S_g \quad (4.60)$$

(Note that  $C_{mg/l}$  equals the ratio of the mass of sediment in milligrams to the volume of the water-sediment mixture in liters.)

In these equations,  $S_g$  is the specific gravity of the sediment ( $\gamma_s/\gamma$ ). For sediment concentrations ( $C_{ppm}$ ) less than 100,000 there is less than a 7 percent difference between  $C_{ppm}$  and  $C_{mg/l}$ . The difference is less than 1 percent for concentrations less than 10,000 ppm or mg/l. For low concentrations, they are often considered equivalent. This is because the weight of the sediment is small compared to the weight of the water. At these low concentrations, an approximate rate of sediment transport can be estimated by

$$Q_s = C_{ppm} \times 10^{-6} \times Q_{water} / S_g$$

where  $Q_s$  and  $Q_{water}$  are in  $m^3/s$  or  $ft^3/s$ .

The exact conversion is:

$$Q_s = C_{ppm} \times 10^{-6} \times Q_{water} / (S_g (1 - C_{ppm} \times 10^{-6})) \quad (4.62)$$

When sediment is eroded or deposited, the volumetric transport rate must include the void space between the sediment particles. The void space, or porosity, is the ratio of voids to the total volume and often ranges from 35 to 45 percent. The volume of eroded or deposited material for a time interval,  $\Delta t$ , is

$$V = Q_s \times \Delta t / (1 - \eta) \quad (4.63)$$

where  $Q_s$  is the rate excess (or deficit) sediment transport and  $\eta$  is the porosity of the bed material.

#### 4.9 APPLICATION OF SELECTED SEDIMENT TRANSPORT EQUATIONS

No single sediment transport equation can encompass all alluvial channel conditions. Therefore, an equation should be selected based on the particular river bed material and flow characteristics. When possible, the results of the sediment transport calculations should be compared with measured sediment transport. The equations presented in this section have broad application; however, other equations can, and should also be considered.

There are several sources for obtaining recommendations on the applicability of sediment transport equations. Appendix B includes a review of ten sediment transport equations. The review tested the equations with a large compilation of field data that encompasses a wide range of bed material, from silts to gravel, and a wide range of river sizes, from 1 m width to over 1000 meters in width. The BRI-STARS manual (Molinas 2000) presents a comparison of several sediment transport equations with a variety of measured data. The HEC-6 manual (U.S. Army Corps of Engineers) refers to Vanoni (1975) as a guide to the applicability of sediment transport equations. Another source for recommendations on suitability of various transport functions is the SAM Hydraulic Design Package for Channels (Thomas et al. 2000). If more than one equation appears suitable, one should apply the equations and determine which one provides the most reasonable results. This is most easily done using sediment transport programs such as BRI-STARS, HEC-6 and SAM. Table 4.4 includes a list of sediment transport relationships and the application of each equation.

Formula	Gravel	Sand	Very Fine Sand and Silt	See Footnotes
Ackers-White		X		1, 2, 3, 4
Bagnold		X	X	4
Brownlie		X		3, 4
Colby		X		2, 3
Dubois	X (fine)	X		2
Einstein	X	X	X	3, 4
Engelund-Hansen		X		1, 3
Karim	X	X		4
Karim and Kennedy	X	X		4
Kodoatie et al. (Power)	X	X	X	4
Laursen	X (fine)	X		2, 3, 4
Meyer-Peter and Müller	X			1, 2, 3
Molinas and Wu		X		1
Parker	X			3
Schoklitsch	X	X (coarse)		2, 3
Shen and Hung		X		4
Simons et al. (Power)	X (fine)	X		4
Toffaletti		X		2, 3, 4
Yang	X	X		1, 2, 3, 4
Yang, Molinas and Wu			X	1

1. The BRI-STARS model includes one fine sand equation (Yang, Molinas and Wu 1996), four sand equations (Engelund and Hanson 1972, Ackers and White 1973, Yang 1973, and Molinas and Wu 1996), two gravel equations (Meyer-Peter and Müller 1948, and Yang 1984) and a user specified power relationship. The power relationship can include depth, velocity, slope, sediment size and discharge.
2. The HEC-6 model includes the Toffaleti (1966), Yang (1973), Dubois (in Vanoni, 1975), Ackers and White (1973), Colby (1964), Meyer-Peter and Müller (1948), Schoklitsch (1937), several modifications to Laursen (1958), and a user specified power relationship that is a power function of the product of depth and slope. In HEC-6, the Colby (1964) correction factor for wash load concentration can be applied to most of the transport functions.
3. The U.S. Army Corps of Engineers SAM package (Thomas et al. 2000) includes Ackers and White (1973), Brownlie (1981), Colby (1964), Einstein (1950), Engelund-Hansen (1972), modified Laursen equations (1958), Meyer-Peter and Müller (1948), Parker (1990), Schoklitsch (1937), Toffaleti (1966) and Yang (1996).
4. Appendix B of this manual includes an evaluation by Kodoatie (1999) of ten equations, including Ackers and White (1973), Bagnold (1966), Brownlie (1981), Einstein (1950), Karim (1998), Karim and Kennedy (1981), Laursen (1958), Shen and Hung (1972), Toffaleti (1969), and Yang (1996). Appendix B also discusses the power function relationships by Simons et al. (1981), Posada (1995), and Kodoatie (1999).

## 4.10 SUMMARY

Computing the bed material sediment transport capacity for a river should be grounded on a firm understanding of the river channel characteristics, sources of sediment and modes of sediment movement. Equations that are well suited for the particular river conditions should be used and, if more than one are well suited, the results should be compared to assess the range of possible outcomes. For a specific river, it is recommended that the results be compared with actual measurements.

Selection of an equation for use depends on the data available and scope, objectives, and resources available for a specific project. The Colby procedure (Section 4.5.4) provides a reliable quick estimate of the bed material discharge in sand bed streams and the Meyer-Peter and Müller bed load equation (Section 4.5.1) has been widely used to estimate bed load (contact load) in coarser bed systems. The power function relationships (Section 4.6) provide a practical method for quick sediment transport calculations for sites within the range of conditions for which they were developed. The Yang sand and gravel equations (Section 4.7) are widely accepted and adaptable to both hand calculation and computer solutions. Finally, many of the sediment transport relations of Table 4.4 are frequently used in sediment transport investigations and several are represented as options in the code of sediment transport models such as HEC-6 (U.S. Army Corps of Engineers 1993), BRI-STARS (Molinas 1990, 2000), and SAM (Thomas et al. 2000).

Typical applications of sediment transport relationships include equilibrium slope and sediment continuity analyses to determine long-term trends in bed elevation change (aggradation/degradation). These applications are illustrated in HEC-20 (Lagasse et al. 2001). The next section outlines a general sediment transport analysis procedure.

## 4.11 SEDIMENT TRANSPORTATION ANALYSIS PROCEDURE

### 4.11.1 Step 1: Determine if Sediment Transport Computations are Necessary

Determine qualitatively if the sediment problem at the bridge is aggradation or degradation. If degradation, previous scour calculations may be sufficient or a sediment transport analysis using equilibrium slope or sediment continuity could provide an initial estimate of long-term degradation (see HEC-20, Lagasse et al. 2001). If aggradation or if more refined degradation estimates are required, then calculating the quantity and gradation of the sediment being transported may be necessary.

For important bridges, determining the quantity and gradation of sediment being transported can be used to:

- Check on the previous determination of long-term aggradation or degradation and contraction scour.
- Determine the type of countermeasures to solve a sedimentation problem.
- Design debris basins for aggradation problems.
- Design a check dam for degradation problems.
- Determine if there will be environmental problems upstream or downstream of the bridge from sediment transport conditions at the bridge crossing.
- Estimate the cost of methods to solve the aggradation or degradation problem.

Additional issues that need to be addressed include:

- Is the cost of a sediment transport analysis commensurate with the cost of the bridge and the accuracy of the analysis?
- Are there sediment transport data available from the USGS or other Federal or state Agencies for this stream or similar streams?

#### **4.11.2 Step 2: Determine Scope of Sediment Transport Analysis**

Determine if the need for information on the quantity of sediment being transported is for the quantity transported by the occasional high or peak flows or for the amount transported annually, i.e., determine the sediment transport design parameters.

- To check previous scour calculations, only sediment transported by high or peak flows may be needed.
- The design of a check dam or debris basin may require annual or multi-year cumulative quantities of sediment transport.
- Refining estimates of long-term aggradation or degradation will require multi-year cumulative quantities.

#### **4.11.3 Step 3: Determine the Type of Analysis**

The types of analyses available to determine the quantity and gradation of sediment transport are field measurements, computer models, and basic methods given in this chapter.

##### **Field Measurement**

Field measurement to determine sediment transport is a specialized activity and generally should be contracted for. The USGS and the U.S. Army Corps of Engineers are specialists in this type of field measurement. Field measurements used in conjunction with the modified Einstein method (Colby and Hubbell 1962, Vanoni 1977, Simons and Senturk 1992) provide the most accurate method of determining the total sediment discharge of a stream.

##### **Basic Methods for Sediment Transport Calculations**

The methods and equations given in this chapter will normally be sufficient for most determinations of the bed-material transport for a given discharge or to develop a bed-material discharge rating curve to be used with a flow duration curve to determine the annual sediment discharge. Only for the most important and costly bridges would it be necessary to use field measurements and/or computer models to determine bed-material transport.

The basic equations and methods given in this chapter and recommended for practical applications are:

- Meyer-Peter and Müller (1948) bed load equation (also USBR 1960)
- Colby's (1964) curves and method

- Simons et al. (1981) basic power function method
- Kodoatie et al. (1999) expanded power function method
- Yang (1996) sand and gravel equations

A summary of each method is given below to aid in selecting which method to use.

### **Meyer-Peter and Müller Bed Load Equation**

The Meyer-Peter and Müller bed load equation only calculates the bed material moving in contact with the bed (contact load). It does not give total bed-material discharge unless there is no bed-material in suspension. It is, therefore, best utilized for coarser bed material streams ( $D_{50}$  coarser than 2.00 mm).

### **Colby's Curves and Method**

Colby's method is only for sand size bed material ( $D_{50}$  from 0.6 to 2.00 mm). It is very good method for rapid determination of total bed-material discharge. It can be used to check or compare with the other methods. The method can be used to determine the total bed-material transport by size fraction.

### **Simons et al. (1981) Power Function Relationship**

The Simons et al. power relationship can be used for steep streams with sand and fine gravel-size bed material ( $D_{50}$  from 0.1 to 5.0 mm) that normally exhibit critical or supercritical flow. The relationship takes into consideration the size distribution of the bed material (Table 4.2). The difficulty in the method is the need to interpolate between sand sizes and gradation coefficient.

### **Kodoatie et al. (1999) Power Function Relationship**

The Kodoatie method (modified Posada (1995)) can be used for streams with bed material size ranging from silt to gravel. It provides a coefficient and exponents based on classifying streams as silt, fine sand, medium to coarse sand and gravel bed (Table 4.4). The method is useful for rapid calculations of bed-material discharge.

### **Yang (1996) Sand and Gravel Equations**

The Yang equations can be used for sand and gravel total load estimation. The equations can be applied by size fraction or to the median size. The gravel equation should be limited to median sizes between 2.0 and 10.0 mm.

### **Computer Models**

The use of computer models is beyond the scope of this manual, but programs are available. Two of the better known computer models are:

- BRI-STARS (Molinas 2000)
- HEC-6 (U.S. Army Corps of Engineers 1993)

These computer models have the ability for user-selected sediment transport relations (including most of those shown in Table 4.1 – see Section 4.6) and power relationships. The models can be used to determine the total sediment discharge for a given flow or to



determine the average annual sediment discharge. To determine the average annual total bed-material discharge the computer model is used to determine the bed-material discharge for a range of discharges to develop a sediment discharge rating curve or table. This rating curve is used in combination with a flow duration curve or table to determine the average annual bed-material discharge. BRI-STARS can be used for single event or long-term sediment transport simulations, whereas HEC-6 is better suited for long-term simulations and should be used with caution for single event simulations.

The U.S. Army Corps of Engineers SAM package (Thomas et al. 2000) includes sediment transport calculations using a wide variety of equations. The SAM package uses normal depth hydraulics and does not perform sediment routing. It is intended for basic sediment transport analysis and for developing sediment rating curves as part of a sediment yield analysis.

## 4.12 SOLVED PROBLEMS FOR SEDIMENT TRANSPORT (SI)

### 4.12.1 Introduction

The following example problems illustrate the application of concepts and equations for sediment transport. Because several of the equations are commonly given in English units (for example Einstein's equation) and the methodology is very complex, some of the examples will only be given in English units. Readers who use metric units (SI) are encouraged when encountering similar problems to convert the input variables to English units, solve the problem, and convert the results back to SI units.

### 4.12.2 Problem 1 Suspended Sediment Concentration Profile

From data observed on the Missouri River, calculate the vertical suspended sediment concentration profile for the  $D_{50}$  sediment size in mg/l.

Given:

$$y_o = 4.30 \text{ m}$$

$$V = 1.27 \text{ m/s}$$

$$S = 0.000210$$

$$\text{Temp} = 22.5^\circ\text{C} (72.5^\circ\text{F})$$

$$D_{50} = 0.000255 \text{ m}$$

$$\omega(D_{50}) = 0.0338 \text{ m/s}$$

$$\nu = 1.00 \times 10^{-6} \text{ m}^2/\text{s}$$

$$c_a = 775,000 \text{ mg/l}$$

From Equation 4.12:

$$\frac{c}{c_a} = \left[ \frac{y_o - y}{y} \frac{a}{y_o - a} \right]^z \quad \text{and} \quad z = \frac{\omega}{\beta \kappa V_*}$$

Assume:

$$\beta = 1.0$$

$$\kappa = 0.4$$

$$a = 2D_{50} = 0.00051 \text{ m}$$

Calculate:

$$V_* = (g y_o S)^{1/2} = [(9.81) (4.30) (0.00021)]^{1/2} = 0.0941 \text{ m/s}$$

$$z = \frac{\omega}{\beta \kappa V_*} = \frac{0.0338}{(1.0)(0.4)(0.0941)} = 0.898$$

Calculate the concentration versus distance profile given in Table 4.5:

y (m)	C (mg/l)
0.091	7,230
0.305	2,370
0.61	1,160
1.22	531
2.44	181
3.05	104
3.66	48
4.27	3

#### 4.12.3 Problem 2 Using the Meyer-Peter and Müller Equation Calculate the Bed Sediment Discharge (Bed Load)

In this example problem the U.S. Bureau of Reclamation formulation of the equation (Equation 4.19) will be used.

Given:

A rectangular channel and the following data:

$$D_{50} = 1.9 \text{ mm}$$

$$D_{90} = 2.8 \text{ mm}$$

$$G = 1.41$$

$$n = 0.04$$

$$n_w = 1.5 n = 0.06$$

$$y_o = 2.99 \text{ m}$$

$$S_f = 0.0005 \text{ m/m}$$

$$D_m = 2.01 \text{ mm}$$

$$W = 60.96 \text{ m}$$

Use Equation 4.19:

$$q_B = 4.780 \left[ 10.846 \left( \frac{Q_b}{Q} \right) \left( \frac{D_{90}^{1/6}}{n_b} \right)^{3/2} y_o S_f - 0.627 D_m \right]^{3/2}$$

From Equation 4.21:

$$n_b = (.04) \left\{ 1 + \frac{5.98}{60.96} \left( 1 - \left( \frac{.06}{.04} \right)^{3/2} \right) \right\}^{2/3} = 0.038$$

From Equation 4.23:

$$\frac{Q_b}{Q} = \frac{1}{1 + \frac{5.98}{60.96} \left( \frac{0.06}{0.038} \right)^{1.5}} = 0.84$$

$$q_B = 4.780 \left[ 10.846 (0.84) \left( \frac{2.8^{1/6}}{0.038} \right)^{3/2} (2.99)(.0005) - 0.627 (2.01) \right]^{3/2}$$

$$q_B = 5.65 \text{ metric-tons/day/m}$$

$$Q_s = 5.65 \times 60.96 = 344 \text{ metric-tons/day}$$

#### 4.12.4 Problem 3 Application of the Einstein Method to Calculate Total Bed-Material Discharge

The application of the Einstein method to calculate total bed material discharge is given in English units only. See Example Problem 4.13.4. The example is taken from Einstein's 1950 publication.

#### 4.12.5 Problem 4 Calculation of Total Bed-Material Discharge Using Colby's Method

The application of Colby method to calculate total bed-material discharge is given in English units only. See Example Problem 4.13.5. The example problem uses the hydraulic and sediment data given by Einstein for the purpose of comparison of the two methods.

The Colby method is easy to use. Organizations using SI units are encouraged to convert the input variables to English units, solve the problem, and convert the results back to SI units.

#### 4.12.6 Problem 5 Calculation of Total Bed-Material Discharge Using the Basic Power Function Relationship

Determine the bed-material discharge for the 100-year discharge for a stream with the following data. Note that these data are not in the  $F_r$  range of Table 4.2. Compare the result with the expanded power function application in Problem 6.

Width  $W = 60.96$  m, Depth  $y = 1.829$  m, Velocity  $V = 2.438$  m/s,  $Q = 271.83$  m<sup>3</sup>/s. Sediment properties of  $D_{50} = 0.31$  mm and size distribution factor  $G = 1.32$ .

Simons et al. (1981) Equation 4.48 is  $q_s = c_{s1} y^{C_{s2}} V^{C_{s3}}$

Use Table 4.1 and cross-interpolate to obtain the values of  $C_{s2}$  and  $C_{s3}$ . For  $C_{s1}$  in SI units use the following Equation

$$C_{s1} (\text{SI}) = C_{s1} (\text{English units}) \times 0.3048^{(2-C_{s2}-C_{s3})}$$

Cross-interpolate in Table 4.1

$$C_{s1} = 1.63 \times 10^{-5} (\text{English})$$

$$C_{s2} = 0.45$$

$$C_{s3} = 3.64$$

$$C_{s1} = 1.63 \times 10^{-5} \times 0.3048^{(2-0.45-3.64)} = 1.63 \times 10^{-5} \times 0.3048^{-2.09} = 0.000195 (\text{SI})$$

$$q_s = 0.000195 (1.829)^{0.45} (2.438)^{3.64} = 0.0066 \text{ m}^2/\text{sec}$$

$$Q_s = 60.96 \times 0.0066 = 0.402 \text{ m}^3/\text{sec}$$

Using a specific gravity of 2.65

$$Q_s = 2.65 \times 9810/9.81 \times 3600 \times 24 \times 0.402 / 1000 = 92,000 \text{ metric-tons/day}$$

#### 4.12.7 Problem 6 Calculation of Total Bed-Material Discharge Using the Expanded Power Function Relationship

Determine the bed-material discharge for the 100-yr discharge for a stream with the data given in Problem 5. The data are repeated below.

Width  $W = 60.96$  m, Depth  $y = 1.829$  m, Velocity  $V = 2.438$  m/s,  $Q = 271.83$  m<sup>3</sup>/s,  $S = .000521$ . Sediment properties of  $D_{50} = 0.31$  mm and size distribution factor  $G = 1.32$ .

Kodoatie et al. (1999) Equation 4.50 is  $q_s = a V^b y^c S^d$

The sand size places this in a medium sand bed stream in Table 4.3

From Table 4.3

$$a = 2123.4, b = 3.30, c = 0.468, d = 0.613$$

$$q_s = 2123.4 (2.438)^{3.30} (1.829)^{0.468} (0.000521)^{0.613} = 518 \text{ metric tons/m/day}$$

$$Q_s = 518 \times 60.96 = 31,580 \text{ metric-tons/day}$$

$$\text{Note } Q_s = 31,580 \text{ metric-tons/day} = 31,580 \times 2204.62/2000 = 34,800 \text{ tons/day}$$

#### 4.12.8 Problem 7 Calculate Total Bed-Material Discharge Using Yang's Sand Equation

Yang's sand equation (Equation 4.51) is as follows

$$\log C_t = 5.435 - 0.286 \log \frac{\omega D_{50}}{v} - 0.457 \log \frac{V_*}{\omega} + \left( 1.799 - 0.409 \log \frac{\omega D_{50}}{v} - 0.314 \log \frac{V_*}{\omega} \right) \log \left( \frac{VS}{\omega} - \frac{V_{cr}S}{\omega} \right)$$

$$\frac{V_{cr}}{\omega} = \frac{2.5}{\log \frac{V_* D_{50}}{v} - 0.06} + 0.66 \text{ for } 1.2 < \frac{V_* D_{50}}{v} < 70$$

and

$$\frac{V_{cr}}{\omega} = 2.05 \text{ for } \frac{V_* D_{50}}{v} \geq 70$$

Compute the bed-material transport in metric-tons/day.

Given:

$$Q = 221.39 \text{ m}^3/\text{sec}$$

$$y = 2.31 \text{ m}$$

$$V = 0.922 \text{ m/sec}$$

$$W = 103.95 \text{ m}$$

$$D_{50} = 0.32 \text{ mm}$$

$$S = 0.00022 \text{ m/m}$$

$$v = 1.16 \times 10^{-6} \text{ m}^2/\text{s}$$

$$\omega = 0.043 \text{ m/sec}$$

Calculate:

$$\tau_o = 9800 \times 2.31 \times 0.00022 = 4.98 \text{ N/m}^2$$

$$V_* = (4.98/1000)^{0.5} = 0.0706 \text{ m/s}$$

$$\frac{V_* D_{50}}{v} = 0.0706 \times 0.00032 / 1.16 \times 10^{-6} = 19.5$$

$$\frac{V_{cr}}{\omega} = \frac{2.5}{\log 19.5 - 0.06} + 0.66 = 2.69$$

$$\frac{V_{cr}S}{\omega} = 2.69 \times 0.00022 = 0.00059$$

$$\frac{VS}{\omega} = 0.922 \times 0.00022 / 0.043 = 0.00472$$

$$\frac{V_*}{\omega} = 0.0706 / 0.043 = 1.64$$

$$\frac{\omega D_{50}}{\nu} = 0.043 \times 0.00032 / 1.16 \times 10^{-6} = 11.86$$

$$\begin{aligned} \log C_t &= 5.435 - 0.286 \log 11.86 - 0.457 \log 1.64 + \\ &(1.799 - 0.409 \log 11.86 - 0.314 \log 1.64) \log(0.00472 - 0.00059) \\ &= 1.95 \end{aligned}$$

$$C_t = 10^{1.95} = 89 \text{ ppm by weight}$$

$$Q_s = 221.3 \times 89 \times 3600 \times 24 / 10^6 = 1700 \text{ metric-tons/day}$$

## 4.13 SOLVED PROBLEMS FOR SEDIMENT TRANSPORT (ENGLISH)

### 4.13.1 Introduction

The following example problems illustrate the application of concepts and equations for sediment transport.

### 4.13.2 Problem 1 Suspended Sediment Concentration Profile

From data observed on the Missouri River, calculate the vertical suspended sediment concentration profile for the  $D_{50}$  sediment size in mg/l.

Given:

$$y_o = 14.10 \text{ ft}$$

$$V = 4.164 \text{ ft/s}$$

$$S = 0.000210$$

$$\text{Temp} = 72.5^\circ\text{F} (22.5^\circ\text{C})$$

$$D_{50} = 0.255 \text{ mm} (0.000838 \text{ ft})$$

$$\omega(D_{50}) = 0.1109 \text{ ft/s}$$

$$\nu = 1.017 \times 10^{-5} \text{ ft}^2/\text{s}$$

$$c_a = 775,000 \text{ mg/l} (48.3 \text{ lb/ft}^3)$$

From Equation 4.12:

$$\frac{c}{c_a} = \left[ \frac{y_o - y}{y} \frac{a}{y_o - a} \right]^z \quad \text{and } z = \frac{\omega}{\beta \kappa V_*}$$

Assume:

$$\beta = 1.0$$

$$\kappa = 0.4$$

$$a = 2D_{50} = 0.0017 \text{ ft}$$

Calculate:

$$V_* = (g y_o S)^{1/2} = [(32.2)(14.1)(0.00021)]^{1/2} = 0.309 \text{ ft/s}$$

$$z = \frac{\omega}{\beta \kappa V_*} = \frac{0.1109}{(1.0)(0.4)(0.309)} = 0.898$$

Calculate the concentration versus distance profile given in Table 4.6:

y (ft)	C (mg/l)
0.3	7,300
1	2,360
2	1,180
4	538
8	183
10	105
12	49
14	3

#### 4.13.3 Problem 2 Using the Meyer-Peter and Müller Equation Calculate the Bed Sediment Discharge (Bed Load)

In this example problem the U.S. Bureau of Reclamation formulation of the equation (Equation 4.19) will be used.

Given:

A rectangular channel and the following data:

$$D_{50} = 1.9 \text{ mm}$$

$$D_{90} = 2.8 \text{ mm}$$

$$G = 1.41$$

$$n = 0.04$$

$$n_w = 1.5 n = 0.06$$

$$y_o = 9.8 \text{ ft}$$

$$S_f = 0.0005 \text{ (ft/ft)}$$

$$D_m = 2.01 \text{ mm}$$

$$W = 200 \text{ ft}$$

Use Equation 4.19:

$$q_B = 1.606 \left[ 3.306 \left( \frac{Q_b}{Q} \right) \left( \frac{D_{90}^{1/6}}{n_b} \right)^{3/2} y_o S_f - 0.627 D_m \right]^{3/2}$$

From Equation 4.21:

$$n_b = (.04) \left\{ 1 + \frac{19.6}{200} \left( 1 - \left( \frac{.06}{.04} \right)^{3/2} \right) \right\}^{2/3} = 0.038$$

From Equation 4.23:

$$\frac{Q_b}{Q} = \frac{1}{1 + \frac{19.6}{200} \left( \frac{0.06}{0.038} \right)^{1.5}} = 0.84$$

$$q_B = 1.606 \left[ 3.306 (0.84) \left( \frac{2.8^{1/6}}{0.038} \right)^{3/2} (9.8)(.0005) - 0.627 (2.01) \right]^{3/2}$$

$$q_B = 1.89 \text{ ton / day / ft}$$

$$Q_S = 1.89 \times 200 = 378 \text{ tons / day}$$

#### 4.13.4 Problem 3 Application of the Einstein Method to Calculate Total Bed-Material Discharge

A test reach, representative of the Big Sand Creek near Greenwood, Mississippi was used by Einstein (1950) as an illustrative example for applying his bed-load function. His numerical example is reproduced here. For simplicity, the effects due to bank friction are neglected. The reader can refer to the original example for the construction of the representative cross section and the consideration of bank friction. The characteristics of the channel cross-section follow.

The channel slope was determined to be  $S = 0.00105$ . The relations of the cross-sectional area, hydraulic radius and wetted perimeter versus stage for the representative cross section are given in Figure 4.19. For this wide and shallow channel, the wetted perimeter is assumed to equal the surface width. The averaged values of the four bed-material samples are given in Table 4.7, and the grain size distribution is presented in Figure 4.20. Note that of these composite samples, 95.8% of the bed material falls between 0.589 and 0.147 mm, which is divided into four fractions. The sediment transport calculations will be made for individual size fractions with selected representative grain sizes equal to the geometric mean grain diameter of each fraction.

The kinematic water viscosity  $\nu$  is  $1.06 \times 10^{-5} \text{ ft}^2/\text{sec}$ , and the specific gravity of the sediment is 2.65.



Grain Size Distribution, mm	Average Grain Size			Settling Velocity	
	mm	ft	%	mm/sec	fps
D > 0.589	--	--	2.4	--	--
0.589 > D > 0.417	0.495	0.00162	17.8	5.20	0.195
0.417 > D > 0.295	0.351	0.00115	40.2	3.75	0.148
0.295 > D > 0.208	0.248	0.00081	32.0	2.70	0.100
0.208 > D > 0.147	0.175	0.00057	5.8	1.70	0.064
0.147 > D	--	--	1.8	--	--

### Hydraulic Calculations

The important hydraulic parameters were calculated, as given in Table 4.8. The table headings, their meanings and calculations are explained after the table. In the calculations, Equation 4.42 and Figure 4.7 were used to evaluate the resistance to flow. Any similar relation discussed in Chapter 2 can be utilized for the same purposes.

### Bed-Material Discharge Calculations

The bed-material transport is calculated for each representative grain size of the bed material at each given flow depth. The procedure and results are given in Table 4.9, see the notes section for explanation of symbols, column by column.

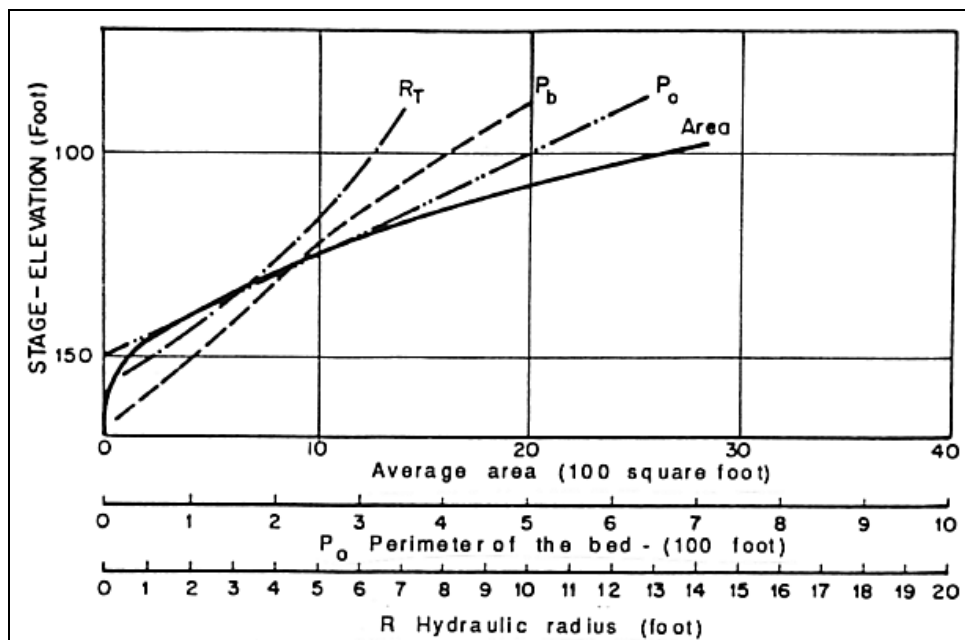


Figure 4.19. Description of the average cross section.

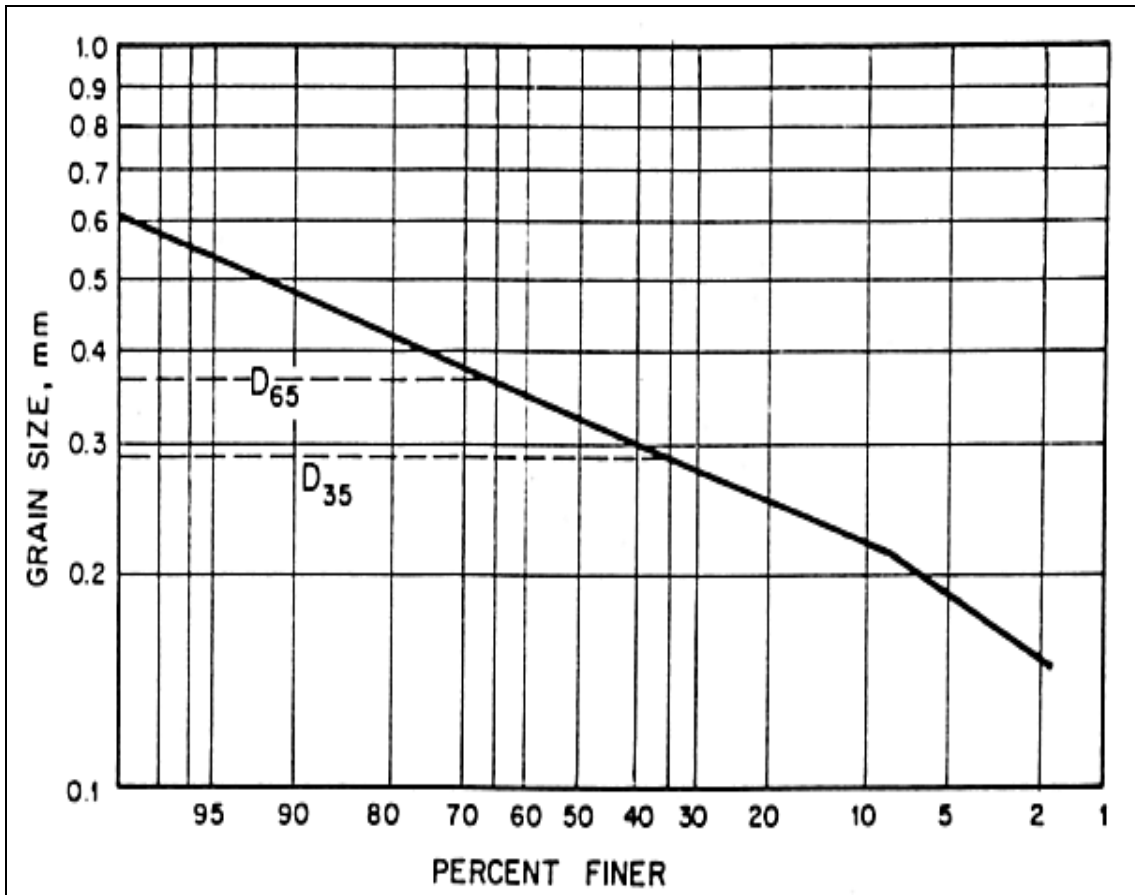


Figure 4.20. Grain size distribution of bed material.

Table 4.8. Hydraulic Calculations for Sample Problem 3. Application of the Einstein Procedure (after Einstein 1950).

$R'_b$	$V'^*$	$\delta'$	$k_s/\delta'$	X	$\Delta$	V	$\Psi'$	$V/V'^*$	$V''^*$	$R''_b$
1	2	3	4	5	6	7	8	9	10	11
0.5	0.129	0.00095	1.21	1.59	0.00072	2.92	2.98	16.8	0.17	0.86
1.0	0.184	0.00067	1.72	1.46	0.00078	4.44	1.49	27.0	0.16	0.76
2.0	0.259	0.00047	2.44	1.27	0.00091	6.63	0.75	51.0	0.13	0.50
3.0	0.318	0.00039	2.95	1.18	0.00097	8.40	0.50	87.0	0.10	0.30
4.0	0.368	0.00033	3.50	1.14	0.00101	9.92	0.37	150.0	0.07	0.14
5.0	0.412	0.00030	3.84	1.11	0.00104	11.30	0.30	240.0	0.05	0.07
6.0	0.450	0.00027	4.26	1.08	0.00107	12.58	0.25	370.0	0.03	0.03

$R_b$	$y = R_b$	Stage	A	$P_b$	Q	$\bar{X}$	Y	$\beta_x$	$(\beta/\beta_x)^2$	$P_E$
12	13	14	15	16	17	18	19	20	21	22
1.36	1.36	150.2	140	103	410	0.00132	0.84	1.29	0.63	10.97
1.76	1.76	150.9	240	136	1,065	0.00093	0.68	1.19	0.85	11.10
2.50	2.50	152.1	425	170	2,820	0.00069	0.56	0.91	1.27	11.30
3.30	3.30	153.3	640	194	5,380	0.00075	0.55	0.91	1.27	11.40
4.14	4.14	154.9	970	234	9,620	0.00079	0.54	0.91	1.27	11.70
5.07	5.07	156.9	1,465	289	16,550	0.00084	0.54	0.91	1.27	11.90
6.03	6.03	159.5	2,400	398	30,200	0.00082	0.54	0.91	1.27	12.04

Notes:

- (1)  $R'_b$  ft (bed hydraulic radius due to grain roughness), values are assumed to cover the entire desired discharge range
- (2)  $V'^* = \sqrt{gR'_b S}$  fps (shear velocity due to grain roughness)
- (3)  $\delta' = 11.6\nu / V'^*$  ft (thickness of laminar sublayer)
- (4)  $k_s = D_{65}$ , ft (roughness diameter)
- (5)  $X = f(k_s/\delta')$  (correction factor in the logarithmic velocity distribution), given in Figure 4.7
- (6)  $\Delta = k_s/X$  ft (apparent roughness diameter)
- (7)  $V = V'^* 5.75 \log(12.26 R'_b/\Delta)$  fps (average flow velocity)
- (8)  $\Psi' = (\rho_s - \rho / \rho) (D_{35}/R'_b S)$  (intensity of shear on representative particles), given by Equation 4.44
- (9)  $V/V'^* = f(\Psi')$  given in Figure 4.11
- (10)  $V''^*$  fps (shear velocity due to form roughness)
- (11)  $R''_b$  ft (bed hydraulic radius due to form roughness) from  $V''^* = \sqrt{gR''_b S}$
- (12)  $R_b = R'_b + R''_b$  ft (bed hydraulic radius), with no additional friction from the banks,  $R_b$  represents the total hydraulic radius R
- (13) y ft (average flow depth),  $y \approx R_b$  for wide shallow streams
- (14) Stage, ft, from description of cross section, Figure 4.19 for  $R = R_b$ .
- (15) A, ft<sup>2</sup>, (cross-sectional area), from Figure 4.19 for the given stage
- (16)  $P_b$  ft, (bed wetted perimeter), from Figure 4.19 for the given stage
- (17) Q = AV cfs (flow discharge), a stage-discharge relationship can be plotted by relating the computed Q to the stage
- (18)  $\bar{X}$  ft (characteristic distance), from Equation 4.36,  $\bar{X} = 0.77\Delta$  for  $\Delta/\delta' > 1.80$  and  $\bar{X} = 1.39\delta'$  for  $\Delta/\delta' < 1.8$
- (19) Y = f( $k_s/\delta'$ ) (pressure correction term), given in Figure 4.8
- (20)  $\beta_x = \log(10.6 \bar{X} / \Delta)$ , (logarithmic function)
- (21)  $\beta = \log 10.6$
- (22)  $P_E = 2.303 \log(30.2 y / \Delta)$ , (Einstein's transport parameter), given by Equation 4.32

**Table 4.9. Bed-Material Load Calculations for Sample Problem by Applying the Einstein (1950) Procedure.**

D	$i_B$	$R'_b$	$\Psi'$	$D/\bar{X}$	$\xi$	$\Psi$	$\phi$	$i_B Q_B$	$i_B Q_B$	
1	2	3	4	5	6	7	8	9	10	
0.00162	0.178	0.5	5.08	1.23	1.08	2.90	1.90	0.0267	119.0	
		1.0	2.54	1.74	1.00	1.73	4.00	0.0561	330.0	
		2.0	1.27	2.35	1.00	0.90	8.20	0.1150	845.0	
		3.0	0.85	2.16	1.00	0.60	12.80	0.1800	1,510.0	
		4.0	0.63	2.05	1.00	0.43	18.00	0.2530	2,560.0	
		5.0	0.51	2.03	1.00	0.35	22.50	0.3160	3,950.0	
0.00115	0.402	0.5	3.38	0.82	1.36	2.44	2.45	0.0471	210.0	
		1.0	1.69	1.16	1.10	1.27	5.50	0.1060	623.0	
		2.0	0.85	1.57	1.01	0.61	12.60	0.2420	1,780.0	
		3.0	0.56	1.44	1.04	0.41	19.00	0.3640	3,050.0	
		4.0	0.42	1.37	1.05	0.30	26.00	0.5000	5,050.0	
		5.0	0.34	1.35	1.05	0.25	31.50	0.6040	7,540.0	
0.00081	0.320	0.5	2.54	0.61	2.25	3.03	1.75	0.0155	69.0	
		1.0	1.27	0.87	1.26	1.09	6.80	0.0600	353.0	
		2.0	0.63	1.17	1.10	0.49	15.80	0.1390	1,020.0	
		3.0	0.42	1.08	1.12	0.33	23.50	0.2070	1,730.0	
		4.0	0.32	1.04	1.15	0.25	31.50	0.2790	2,820.0	
		5.0	0.25	1.01	1.17	0.20	39.50	0.3490	4,360.0	
0.00057	0.058	0.5	1.80	0.43	5.40	5.15	0.58	0.00056	2.5	
		1.0	0.90	0.61	2.28	1.39	5.10	0.00500	29.4	
		2.0	0.45	0.83	1.37	0.44	17.50	0.01710	126.0	
		3.0	0.30	0.76	1.52	0.32	25.00	0.02460	206.0	
		4.0	0.22	0.72	1.60	0.25	31.50	0.31000	313.0	
		5.0	0.18	0.71	1.65	0.20	39.50	0.03870	483.0	
$\sum i_B Q_B$	$10^3 E$	6.0	0.21	0.99	1.19	0.17	46.00	0.4060	6,980.0	
		Z	$I_1$	$-I_2$	$P_{E I_1+I_2+1}$	$i_T Q_T$	$i_T Q_T$	$\sum i_T Q_T$		
		11	12	13	14	15	16	17	18	19
		400	2.38	3.78	0.078	0.44	1.42	0.03800	168	670
		1335	1.84	2.65	0.131	0.74	1.71	0.09580	561	3,928
		3,771	1.30	1.88	0.240	1.27	2.44	0.28100	2,050	30,500
6,496	0.98	1.53	0.385	2.01	3.44	0.61700	5,170	113,000		
10,745	0.78	1.33	0.560	2.80	4.75	1.20000	12,100	324,000		
16,333	0.63	1.18	0.810	3.85	6.78	2.13000	26,500	800,000		
27,142	0.54	1.08	1.090	4.90	9.20	3.48000	59,800	1,940,000		
	1.69	2.88	0.117	0.68	1.60	0.07540	335			
	1.31	2.02	0.210	1.19	2.14	0.22700	1,330			
	0.92	1.44	0.450	2.33	3.76	0.91000	6,660			
	0.70	1.17	0.830	3.85	6.73	2.44000	20,400			
	0.56	1.01	1.370	5.70	11.30	5.65000	57,100			
	0.45	0.90	2.120	8.10	17.20	10.40000	129,000			
0.38	0.83	2.950	10.50	26.00	19.60000	335,000				
	1.19	1.94	0.230	1.29	2.23	0.03450	153			
	0.92	1.36	0.520	2.60	4.16	0.25000	1,460			
	0.65	0.97	1.530	6.10	12.20	1.70000	12,500			
	0.49	0.79	3.350	11.00	28.70	5.95000	49,700			
	0.39	0.68	6.200	17.50	56.00	15.00000	157,000			
	0.32	0.61	9.800	25.50	92.00	32.00000	397,000			
0.27	0.55	15.000	36.00	146.00	59.50000	1,020,000				
	0.85	1.12	0.720	3.35	5.55	0.00312	14			
	0.65	0.86	2.440	8.10	20.00	0.10000	587			
	0.46	0.61	8.400	21.50	74.40	1.26000	9,350			
	0.35	0.49	19.300	41.00	183.00	4.50000	37,600			
	0.28	0.43	32.000	63.00	312.00	9.68000	97,800			
	0.23	0.38	51.000	91.00	516.00	20.00000	248,000			
0.19	0.35	70.000	122.00	722.00	30.80000	526,000				

Table 4.9 (continued)

Notes:

- (1)  $D$  is the representative grain size, ft, given in Table 4.7
- (2)  $i_B$  is the fraction of bed material, given in Table 4.7
- (3)  $R'_b$  is the bed hydraulic radius due to grain roughness, ft, given in Table 4.8
- (4)  $\Psi'$  is the intensity of shear on a particle =  $((\rho_s - \rho)/\rho) (D/(R'_b S))$
- (5)  $D/\bar{X}$  for values of  $\bar{X}$ , see Table 4.8, Column 18
- (6)  $\xi = f(D_{65}/\bar{X})$  hiding factor, given in Figure 4.6
- (7)  $\Psi$  is the intensity of shear on individual grain size =  $\xi Y (\beta/\beta_x)^2 \Psi'$ , values of  $Y$  and  $(\beta/\beta_x)^2$  are given in Table 4.8
- (8)  $\phi$  is the intensity of sediment transport for an individual grain
- (9)  $i_B q_B$  is the bed load discharge per unit width for a size fraction, given in Equation 4.33
- (10)  $i_B Q_B$  is the bed load discharge for a size fraction for entire cross section, ton/day =  $43.2 W i_B q_B$ ,  $W = P_b$  given in Table 4.8
- (11)  $\sum i_B Q_B$  is the total bed load discharge for all size fractions for the entire cross section, tons/day
- (12)  $E$  is the ratio of bed layer thickness to water depth =  $2D/y$ . For values of  $y$ , see Table 4.8.
- (13)  $Z$  is the exponent for concentration distribution =  $\omega/(0.4 V')$  given in Equation 4.41. Values of  $\omega$  and  $V'$  are given in Tables 4.7 and 4.8.
- (14)  $I_1$  is an integral given by Equation 4.39 and read from Figure 4.9
- (15)  $-I_2$  is an integral given by Equation 4.40 and read from Figure 4.10
- (16)  $P_E I_1 + I_2 + 1$  is the factor between bed load and total load given by Equation 4.31
- (17)  $i_T q_T$  is the bed material load per unit width of stream for a size fraction lb/sec-ft =  $i_B q_B (P_E I_1 + I_2 + 1)$  given by Equation 4.31
- (18)  $i_T Q_T$  is the bed material load for a size fraction for entire cross section, tons/day =  $43.2 W i_T q_T$
- (19)  $\sum i_T Q_T$  is the total bed material load for all size fractions, tons/day

#### 4.13.5 Problem 4 Calculation of Total Bed-Material Discharge Using Colby's Method

In applying the Colby (1964) method, the required data are: the mean velocity, the depth, the median size or size distribution of the bed material, the water temperature and the fine sediment (wash load) concentration. The mean velocity and the depth of flow may be obtained by hydraulic calculations, as in Problem 3. However, to obtain best results from calculations, directly measured values of velocity and depth are required.

For purposes of comparison, the sample problem used to illustrate Einstein's method is solved using the Colby method. The required data are taken from Table 4.8 established by hydraulic calculations. In addition, the water temperature and the fine sediment concentration are assumed to equal 70°F and 10,000 ppm, respectively. For convenience, the calculations are summarized in tables. Two procedures are presented. Table 4.10 gives the calculations using the mean diameter of bed material, whereas Table 4.11 gives the calculations for individual fractions using the bed material size distribution. Note that depths,  $y$ , of 5.07 ft and 6.03 ft from Table 4.8 are not shown in Tables 4.10 and 4.11 since the corresponding velocities are greater than 10 ft/sec. The Colby curves (Figure 4.13) are limited to 10 ft/sec.

$y$	$W$	$V$	$q_n$	$k_1$	$k_2$	$k_3$	$q_T$	$Q_T$
<b>1</b>	<b>2</b>	<b>3</b>	<b>4</b>	<b>5</b>	<b>6</b>	<b>7</b>	<b>8</b>	<b>9</b>
1.36	103	2.93	14.5	0.92	1.20	0.99	16	1,648
1.76	136	4.44	50.0	0.91	1.21	0.99	56	7,616
2.50	170	6.63	135.0	0.91	1.22	0.99	150	25,500
3.30	194	8.38	220.0	0.90	1.23	0.99	243	47,142
4.14	234	9.92	325.0	0.90	1.25	0.99	365	85,410

Notes:

- (1)  $y$ , ft (mean depth), taken from Table 4.8
- (2)  $W$ , ft (surface width), taken from Table 4.8
- (3)  $V$ , fps (average velocity), taken from Table 4.8
- (4)  $q_n$  tons/day-ft (uncorrected sediment discharge per unit width of channel), taken from Figure 4.13 for the given  $V$ ,  $y$ , and  $D_{50}$
- (5)  $k_1 = f(y, T)$  (correction factor for temperature), given in Figure 4.14
- (6)  $k_2 = f(y, C_f)$  (correction factor for fine sediment concentration), given in Figure 4.14
- (7)  $k_3 = f(D_{50})$  (correction factor for sediment size), given in Figure 4.14
- (8)  $q_T = [1 + (k_1 k_2 - 1) k_3] q_n$  tons/day-ft (true bed material discharge per unit width of stream), given by Equation 4.46
- (9)  $Q_T = W q_T$  tons/day (bed material discharge for all size fractions for entire cross section)

**Table 4.11. Bed Material Discharge Calculations for Sample Problem by Applying the Colby (Individual Size Fraction).**

D	$10^2 i_b$	y	W	V	$q_n$	$k_1$
1	2	3	4	5	6	7
0.495	17.8	1.36	103	2.93	12	0.92
		1.76	136	4.44	40	0.91
		2.50	170	6.63	112	0.91
		3.30	194	8.38	193	0.90
		4.14	234	9.92	265	0.90
0.351	40.2	1.36	103	2.93	15	0.92
		1.76	136	4.44	45	0.91
		2.50	170	6.63	120	0.91
		3.30	194	8.38	210	0.90
		4.14	234	9.92	290	0.90
0.248	32.0	1.36	103	2.93	18	0.92
		1.76	136	4.44	53	0.91
		2.50	170	6.63	140	0.91
		3.30	194	8.38	240	0.90
		4.14	234	9.92	345	0.90
0.175	5.8	1.36	103	2.93	23	0.92
		1.76	136	4.44	64	0.91
		2.50	170	6.63	163	0.91
		3.30	194	8.38	305	0.90
		4.14	234	9.92	420	0.90
<b>k<sub>2</sub></b>	<b>k<sub>3</sub></b>	<b>q<sub>T</sub></b>	<b>i<sub>b</sub>q<sub>T</sub></b>	<b>i<sub>b</sub>Q<sub>T</sub></b>	<b>∑i<sub>b</sub>Q<sub>T</sub></b>	
<b>8</b>	<b>9</b>	<b>10</b>	<b>11</b>	<b>12</b>	<b>13</b>	
1.20	0.62	13	2.3	237	1,710	
1.21	0.62	43	7.7	1,050	6,908	
1.22	0.62	119	21.0	3,570	22,780	
1.23	0.62	205	37.0	7,180	45,560	
1.25	0.62	288	51.0	11,900	77,640	
1.20	0.92	16	6.4	659		
1.21	0.92	49	20.0	2,720		
1.22	0.92	132	53.0	9,010		
1.23	0.92	230	93.0	18,000		
1.25	0.92	323	130.0	30,420		
1.20	1.00	20	6.4	659		
1.21	1.00	58	19.0	2,580		
1.22	1.00	155	50.0	8,500		
1.23	1.00	266	85.0	16,500		
1.25	1.00	388	124.0	29,000		
1.20	0.97	25	1.5	155		
1.21	0.97	70	4.1	558		
1.22	0.97	180	10.0	1,700		
1.23	0.97	337	20.0	3,880		
1.25	0.97	471	27.0	6,320		

**Notes:**

- (1) D, mm (representative grain size; given in Table 4.7)
- (2)  $i_b$  (fraction of bed material), taken from Table 4.7
- (3) y, ft. (average flow depth), taken from Table 4.8, Column 13
- (4) W, ft. (top width), taken from Table 4.8, Column 16
- (5) V, fps (average velocity), taken from Table 4.8, Column 7
- (6)  $q_n$ , tons/day-ft (incorrect sediment discharge per unit width by assuming the bed is composed entirely of one sand of size D) taken from Figure 4.13 by interpolation on logarithmic paper for the given V, D, and y
- (7)  $k_1 = f(y, T)$  (correction factor for temperature), given in Figure 4.14
- (8)  $k_2 = f(y, C_f)$  (correction factor for fine sediment concentration), given in Figure 4.14
- (9)  $k_3 = f(D_{50})$  (correction factor for sediment size), given in Figure 4.14
- (10)  $q_T = [1 + (k_1 k_2 - 1) k_3] q_n$ , tons/day-ft (corrected bed material discharge per unit width by assuming the bed is composed entirely of one sand of size D)
- (11)  $i_b q_T$ , tons/day-ft, (bed material discharge per unit width for a size fraction for entire cross section)
- (12)  $i_b Q_T = W i_b q_T$ , tons/day, (bed material discharge for a size fraction for entire cross section)
- (13)  $\sum i_b Q_T$ , tons/day, (bed material discharge for all size fractions for entire cross section)

The results of the bed-material discharge calculations for the sample problem using Einstein's (1950) and Colby's (1964) methods are shown in Figure 4.21. The curves indicate that the sediment discharge increases rapidly with an increase in water discharge. In general, the two methods compare relatively well.

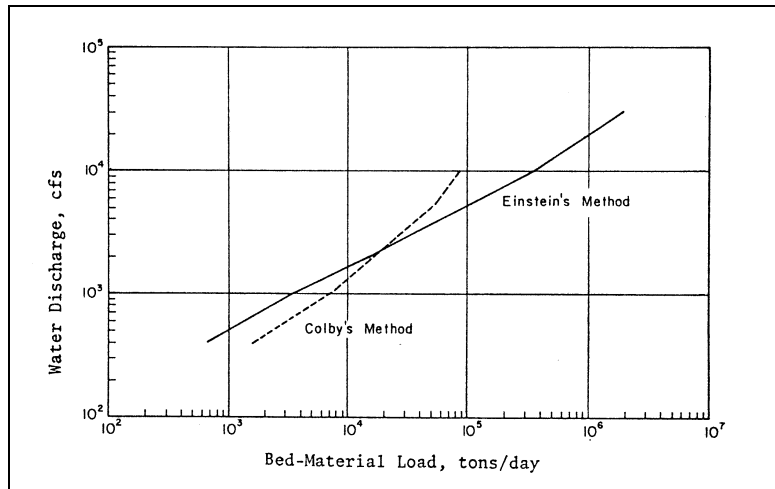


Figure 4.21. Comparison of the Einstein and Colby methods.

#### 4.13.6 Problem 5 Calculation of Total Bed-Material Discharge Using the Basic Power Function Relationship

Determine the bed-material discharge for the 100-year discharge for a stream with the following data. Note that these data are not in the  $F_r$  range of Table 4.2. Compare the result with the expanded power function application in Problem 6.

Width  $W = 200$  ft, Depth  $y = 6.0$  ft, Velocity  $V = 8.0$  ft/s,  $Q = 9600$  cfs. Sediment properties of  $D_{50} = 0.31$  mm and size distribution factor  $G = 1.32$ .

Simons et al. (1981) Equation 4.48 is  $q_s = c_{s1} y^{C_{s2}} V^{C_{s3}}$

Use Table 4.1 and cross-interpolate to obtain the values of  $C_{s2}$  and  $C_{s3}$ . Cross-interpolate in Table 4.1:

$$C_{s1} = 1.63 \times 10^{-5}$$

$$C_{s2} = 0.45$$

$$C_{s3} = 3.64$$

$$q_s = 1.63 \times 10^{-5} (6.0)^{0.45} (8.00)^{3.64} = 0.0707 \text{ ft}^2/\text{sec}$$

$$Q_s = 200 \times 0.0707 = 14.14 \text{ ft}^3/\text{sec}$$

Using a specific gravity of 2.65

$$Q_s = (2.65 \times 62.4 \times 3600 \times 24 \times 14.14) / 2000 = 101,000 \text{ tons/day}$$

$$Q_s = 101,000 \text{ tons/day} \times 2000 / 2204.62 = 91,600 \text{ metric-tons/day}$$



#### 4.13.7 Problem 6 Calculation of Total Bed-Material Discharge Using the Expanded Power Function Relationship

Determine the bed-material discharge for the 100-year discharge for a stream with the data given in Problem 5. The data are repeated below.

Width  $W = 200$  ft, Depth  $y = 6$  ft, Velocity  $V = 8$  ft/s,  $Q = 9,600$  cfs,  $S = 0.000521$ . Sediment properties of  $D_{50} = 0.31$  mm and size distribution factor  $G = 1.32$ .

Kodoatie et al. (1999) Equation 4.50 is  $q_s = a V^b y^c S^d$

The sand size places this in a medium sand bed stream in Table 4.3.

From Table 4.3

$$a = 2123.4, \quad b = 3.30, \quad c = 0.468, \quad d = 0.613$$

$$a \text{ (English units)} = 1.1 \times 0.3048^{(1+b+c)} a = 1.1 \times 0.3048^{(1+3.30+0.468)} (2123.4) = 8.095$$

$$q_s = 8.095 (8)^{3.30} (6)^{0.468} (0.000521)^{0.613} = 173.78 \text{ tons/ft/day}$$

$$Q_s = 173.78 \times 200 = 34,800 \text{ tons/day}$$

#### 4.13.8 Problem 7 Calculate Total Bed-Material Discharge Using Yang's Sand Equation

Yang's sand equation (Equation 4.51) is as follows:

$$\log C_t = 5.435 - 0.286 \log \frac{\omega D_{50}}{v} - 0.457 \log \frac{V_*}{\omega} + \left( 1.799 - 0.409 \log \frac{\omega D_{50}}{v} - 0.314 \log \frac{V_*}{\omega} \right) \log \left( \frac{VS}{\omega} - \frac{V_{cr} S}{\omega} \right)$$

$$\frac{V_{cr}}{\omega} = \frac{2.5}{\log \frac{V_* D_{50}}{v} - 0.06} + 0.66 \quad \text{for } 1.2 < \frac{V_* D_{50}}{v} < 70$$

and

$$\frac{V_{cr}}{\omega} = 2.05 \quad \text{for } \frac{V_* D_{50}}{v} \geq 70$$

Compute the bed-material transport in tons per day.

Given:

$$\begin{aligned} Q &= 7,820 \text{ ft}^3/\text{sec} \\ y &= 7.58 \text{ ft} \\ V &= 3.02 \text{ ft/sec} \end{aligned}$$

$$\begin{aligned} W &= 341 \text{ ft} \\ D_{50} &= 0.00105 \text{ ft} \\ S &= 0.00022 \end{aligned}$$

$$\begin{aligned} v &= 1.21 \times 10^{-5} \text{ ft}^2/\text{s} \\ \omega &= 0.141 \text{ ft/sec} \end{aligned}$$

Calculate:

$$\tau_o = 62.4 \times 7.58 \times 0.00022 = 1.04 \text{ lb/ft}^2$$

$$V_* = (0.104/1.94)^{0.5} = 0.232 \text{ ft/s}$$

$$\frac{V_* D_{50}}{\nu} = 0.232 \times 0.00105 / 1.121 \times 10^{-5} = 20.1$$

$$\frac{V_{cr}}{\omega} = \frac{2.5}{\log 20.1 - 0.06} + 0.66 = 2.67$$

$$\frac{V_{cr} S}{\omega} = 2.67 \times 0.00022 = 0.00059$$

$$\frac{VS}{\omega} = 3.02 \times 0.00022 / 0.141 = 0.00471$$

$$\frac{V_*}{\omega} = \frac{0.232}{0.141} = 1.64$$

$$\frac{\omega D_{50}}{\nu} = 0.141 \times 0.00105 / 1.21 \times 10^{-5} = 12.2$$

$$\begin{aligned} \log C_t &= 5.435 - 0.286 \log 12.2 - 0.457 \log 1.64 + \\ &(1.799 - 0.409 \log 12.2 - 0.314 \log 1.64) \log (0.00471 - 0.00059) \\ &= 1.96 \end{aligned}$$

$$C_t = 10^{1.96} = 91 \text{ ppm by weight}$$

$$Q_s = 7820 \times 91 \times 62.4 \times 3600 \times 24 / (2000 \times 10^6) = 1900 \text{ tons / day}$$

## CHAPTER 5

### RIVER MORPHOLOGY AND RIVER RESPONSE

#### 5.1 INTRODUCTION

Rivers and river systems have served man in many ways. Rivers are passage ways for navigation and are essential to agriculture, particularly in the arid and semiarid parts of the world. To a large degree, the flooding by rivers and the deposition of sediment on the river valleys have been a means of revitalizing the river valleys to keep them productive. Rivers have provided a means of traveling inland and developing trade. This has played a significant role in the development of all countries wherever rivers of significant size exist.

Rivers have different alignments and geometry. There are meandering rivers, braided rivers, and rivers that are essentially straight. In general, braided rivers are relatively steep and meandering rivers have more gentle slopes. Meandering rivers that are not subject to rapid movement, are reasonably predictable in behavior; however, meandering rivers are generally unstable with eroding banks which may result in destruction of productive land, bridges, bridge approaches, control works, buildings, and urban properties during floods. Bank protection works are often necessary to stabilize certain reaches of many rivers and to improve them for other aspects of flood control and navigation.

#### 5.2 FLUVIAL CYCLES AND PROCESSES

Fundamental characteristics and processes governing the formation of river systems are discussed in this section. A very general classification of rivers which considers their age is introduced. The morphology of floodplains, deltas, and alluvial fans is described as well as the processes of headcutting and nickpoint migration. The concept of geomorphic threshold completes this section on fundamentals leading to a discussion of variability and change in large alluvial rivers. Specific aspects of stream form and a simple geomorphic classification of streams are presented later in this chapter.

##### 5.2.1 Youthful, Mature, and Old Streams

One of the early methods to classify rivers was by relative age as youthful, mature, and old (Davis 1899, see King and Schumm 1980). As a general concept this has validity with steep irregular young streams becoming mature with a narrow valley, a floodplain, and a graded condition; that is, the slope and energy of the streams are just sufficient to transport the materials delivered to it. As time passes, the valley widens and a fully meandering channel of low gradient develops. Unfortunately, for this classification, the lower Mississippi River would be designated as old, when, in fact it is one of the most youthful rivers. It developed on the alluvium deposited by drainage from the continental ice sheet perhaps 10,000 years ago.

More recently, rivers have been classified based upon type of sediment load (Schumm 1977), and pattern (Brice 1982). Nevertheless, the concept of landform and channel evolution through time is a valuable one. Hydraulic Engineering Circular (HEC) No. 20 (Lagasse et al. 2001)

presents several examples of landform evolution, including the long-term cycle of erosion and evolution of incised stream channels.

In the context of a rivers age, the process of channel rejuvenation refers to an increase in erosional activities in mature or old channels caused by lowering base level elevation, tectonic activities or other causes. Rejuvenated mature or old channels then exhibit some properties of youthful channels such as channel incision and erosion processes.

### **5.2.2 Floodplain and Delta Formations**

Over time, the highlands of an area are worn down. The streams erode their banks. The material that is eroded is utilized downstream to build banks and bars to further enhance the meandering process. Streams move laterally pushing the highlands back. Low flat valley land and floodplains are formed. As the streams transport sediment to areas of flatter slopes, and in particular to bodies of water where the velocity and turbulence are too small to sustain the transport of the material, the material is deposited forming deltas. As deltas build outward the up-river portion of the channel is elevated through deposition and becomes part of the floodplain. Also, the stream channel is lengthened and the slope is further reduced. The upstream river bed is filled in and average flood elevations are increased. As they work across the river valley, these processes cause the total floodplain to raise in elevation. Hence, even old streams are far from static. Old rivers meander, are affected by changes in sea level, are influenced by movements of the earth's crust, are changed by delta formations or glaciation, and are subject to modifications due to climatological changes and as a consequence of human development.

### **5.2.3 Alluvial Fans**

Alluvial fans are very dynamic landforms that can create significant hazards to highways as a result of floods, debris flows, deposition, channel incision, and avulsion (Schumm and Lagasse 1998). They occur whenever there is a change from a steep to a flat gradient. As the bed material and water reaches the flatter section of the stream, the coarser bed materials can no longer be transported because of the sudden reduction in both slope and velocity. Consequently, a cone or fan builds out as the material is dropped. There is considerable similarity between a delta and an alluvial fan. Both result from reductions in slope and velocity and both tend to reduce upstream slopes. Alluvial fans, like deltas, are characterized by unstable channel geometries and rapid lateral movement. An action very similar to the delta develops where a steep tributary enters a main channel. The steep channel tends to drop part of its sediment load in the main channel building out into the main stream. In some instances, the main stream can be forced to make drastic changes at the time of major floods by the stream's tributaries.

Fans can be of two types, dry or mudflow fans formed by ephemeral streamflow, and wet or fluvial fans formed by perennial stream flow. Two different conditions of fan morphology are observed on modern dry fans. The first situation occurs when deposition is near the mountain front and the fan surface is undissected. The second situation occurs when sediment material is moved through a fan-head trench and deposition occurs at the toe of the fan. Good relationships exist between fan area and drainage basin area (Schumm 1977). These relationships among fan slope, area, and drainage basin characteristics are not surprising. The presence of fan-head trenches, however, is sometimes attributed to tectonic activity or climate change.

The longitudinal profile of fans may be concave. Two types of concavity are recognized. The first is due to intermittent uplift of the mountains which gradually steepens the fan head. The other case is due to trenching and the building out of a low flatter reach of recent alluvium at the toe of the fan. Normally the coarsest material is found at the fan apex, although fan-head trenching might result in a slight increase in sediment size with the fan radius.

Fluvial (wet) fans can become very large, which contrasts with dry fans. The almost random distribution of erosion and deposition patterns on the arid fan is often replaced by a progressively shifting channel. Lateral migration of streams on fluvial fans can be anticipated by the concavity of the contours (i.e., topographic lows or swales). New orientation of a river channel is also an equally possible shifting process.

The potential for avulsion, deposition, and channel blockage and channel incision are important for highway design. To minimize these impacts on highways, a reconnaissance of the fan and its drainage should be undertaken so that potential changes can be identified and countermeasures taken. The ideal result of any study of alluvial fans is a geomorphic map delineating active and inactive portions of the fan and the identification of problem sites within the active portions of the fan. For example, local aggradation in a channel can lead to avulsion because avulsion is likely to occur in places where deposition has raised the floor of the channel to a level that is nearly as high as the surrounding fan surface. This condition can be identified in the field by observation or by the surveying of cross-fan profiles (Schumm and Lagasse 1998).

Experimental studies show that growth at the fan-head is intermittent, being interrupted by periods of incision, sediment reworking and downfan distribution of sediment. The greatest variation in sediment yield is related to fan-head trenching and aggradation. Geomorphic thresholds controlling fan growth are sketched in Figure 5.1 (see also Section 5.2.5). Threshold concepts must be considered when evaluating fan-related hazards to highways. For example, identification of relatively recent debris flow deposits, which suggests very high sediment delivery from the drainage basin may, in fact, be an indication of future stability. That is, stored sediment has been flushed from the drainage basin, and it may be a very long time before sufficient sediment accumulates again to produce debris flows even under extreme rainfall. This situation has been documented along the Wasatch Mountain front north of Salt Lake City (Keaton 1995; Lowe 1993), where drainage basins that produced debris flows in 1983 do not contain sufficient stored sediment to produce debris flows at present. Therefore, not only the fan itself, but its drainage basin requires investigation.

#### **5.2.4 Nickpoint Migration and Headcutting**

Abrupt changes in the longitudinal profile of the stream are shown in Figure 5.2. This break in the profile induces a perturbation moving upstream, especially during floods. Above and below the profile break the river may be stable. As the perturbation migrates past a point, a dramatic change in channel morphology and stability occurs. These perturbations are of two types: the first is a sharp break in profile which forms an in-channel scarp called a headcut (Figure 5.2a), and the second, called a nickpoint, has a gradual change in elevation over a greater length of channel, but still represents an oversteepened reach with respect to the overall channel slope (Figure 5.2b).

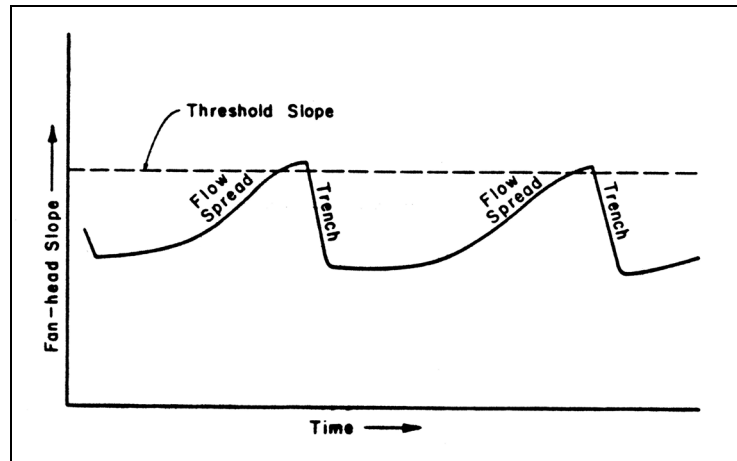


Figure 5.1. Changing slope at fan-head leading to fan-head trenching (Schumm 1977).

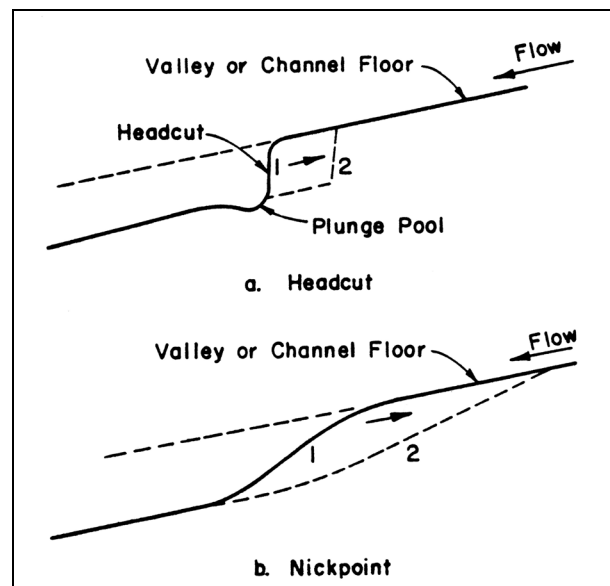


Figure 5.2. Headcuts and nickpoints.

The result of headcut or nickpoint formation and migration is, of course, lowering of the stream bed. Erosion of the bed material will be dramatic as a headcut or nickpoint migrates under a bridge. During a major flood in Tujunga Wash, California, erosion above the headwall of a gravel pit led to the failure of three highway bridges. In cohesive material or erodible rock, headcut migration normally lowers the channel abruptly to its new position. In alluvial material, however a nickpoint produces degradation that persists for some distance (Figure 5.2b). In both cases, scour continues until the gradient has been reduced and bank erosion has widened the channel to the point that deposition can begin. As the nickpoint or headcut migrates farther upstream, the quantity of sediment delivered to the reach at which a stream crossing is located increases greatly due to the erosion of the bed upstream and subsequent erosion of the banks of the stream. Therefore, a period of degradation may be followed at a site by a period of aggradation.

The most obvious way to identify nickpoints or headcuts is by the use of aerial photographs. Particularly in arid and semi-arid regions, headcuts are very easily recognizable because the upstream valley floor or channel is essentially undisturbed, whereas the channel below shows significant erosion. On topographic maps of large scale the presence of a nickpoint or headcut is indicated by closely-spaced contours. This can be verified with field surveys which show the break in the longitudinal profile of the stream. A change in the dimension of the channel and a change in the character of the bank line may indicate the presence of nickpoint or headcut migration. A low width-depth ratio below the break in slope is an indication of scour and deepening of the channel. Bank erosion is also a possible consequence and a sharp change in the bankline characteristics representing a change from stability to instability may identify the presence of a nickpoint or headcut.

### **5.2.5 Geomorphic Threshold**

Evolution of a drainage network and sediment production from drainage basins are very complex processes. Geomorphic history and climatic changes introduce a new degree of complexity into the response of watersheds and fluvial systems. Experimental studies demonstrate that within a complex natural system, one event can trigger a complex reaction as the components of the system respond to change. The magnitude of this complex response is likely to appear during early stages of an erosion cycle or during rejuvenation of high sediment producing areas. Nevertheless, these areas produce major land management and conservation problems, hence their practical interest.

It is possible to explain variations in sediment yield and channel adjustment by using the concept of geomorphic thresholds described by Schumm (1977). For example, in a given drainage area, it is possible to define a valley slope above which the valley floor is unstable. Stable valley floors above the threshold line are incipiently unstable and any major flood may eventually cause erosion and trenching of the alluvium stored in these valleys (Figure 5.1 illustrates the concept of geomorphic threshold). Another very common example of a geomorphic threshold is the progressive increase in channel sinuosity and meander amplitude until a cutoff or channel avulsion results on alluvial plains and deltas. This is due to channel lengthening and gradient reduction accompanying increases in sinuosity and delta size. Since permanent changes result only when a geomorphic threshold has been exceeded, events with high magnitude and low frequency may at times have only minor and local effect on the landscape, but at other times may produce seemingly "instantaneous" change with potentially catastrophic consequences.

## **5.3 VARIABILITY AND CHANGE IN ALLUVIAL RIVERS**

Those who work with rivers are aware of the great variability that exists among rivers and between river reaches. In addition, the impact of human activities can greatly alter the behavior, dimensions, and general morphology of a river. Large alluvial rivers have always played an important role in human affairs. All of the early great civilizations rose on the banks of large alluvial rivers such as the Nile, Indus, Yellow, and Euphrates. River engineering began early in human history to minimize the effects of floods and channel changes. Today, engineers face the same problems and they have been successful in developing flood control, navigation, and channel stabilization programs, but often at great cost and with the need to continually maintain and repair structures and channels (Schumm and Winkley 1994). In this section, historic change and channel response on the Mississippi River and the Nile are surveyed to illustrate the range of variability and change to be expected on alluvial rivers.

In order to cope with alluvial rivers, an understanding of their complexity in space and through time is necessary. Alluvial rivers differ in three ways:

1. Rivers differ among themselves depending on hydrology, sediment loads, and geologic history (in other words, rivers differ among themselves).
2. Rivers change naturally through time and as a result of climate and hydrologic change.
3. Along any one river there can be considerable variability of channel morphology as a result of geologic and geomorphic controls.

Information on these differences, especially the last two, will aid in predicting future river behavior and their response to human activities.

An important consideration in predicting future river behavior and response is the sensitivity of the channel. That is, how readily will it respond to change or how close is it to undergoing a change without an external influence? For example, individual meanders frequently develop progressively to an unstable form, and a chute or neck cutoff results, which leads to local and short-term channel adjustments. The cutting off of numerous meanders along the Mississippi River caused dramatic changes, as a result of steepening of the gradient, which led to serious bank erosion and scour (Winkley 1977). However, Brice (1980) studied the effect of cutoffs and channel alignment on numerous smaller streams, and he found that, although some responded in a manner similar to the Mississippi, many did not. Those that did not were characterized by stable banks and gentle slopes. For example, Stevens (1994) found that the Citanduy River in Java has remained relatively stable after a total of 23 cutoffs because it has very resistant clayey bed and banks. Therefore, some streams are sensitive whereas others are not. Obviously, care must be taken before the behavior and response of one stream can be extrapolated to another.

The differences among rivers is often reflected in their channel patterns. During an experimental study of a channel in a laboratory flume, the channel changed from straight, to sinuous and finally to braided, as flume slope (and thereby sediment load and stream power) increased (Figure 5.3). The relatively straight River Nile and the relatively meandering Mississippi River reflect geomorphic history as well as current geologic controls such as active tectonics, tributary contributions and other factors that affect valley slope. For example, the difference between the Nile and other large rivers may be due to the fact that the Mediterranean Sea evaporated during early Tertiary time (Hsü 1983, Said 1981). A blockage at the Straights of Gibraltar stopped the inflow of Atlantic Ocean water into the Mediterranean basin. This significant lowering of base level caused incision of streams draining into the Mediterranean, and a deep canyon was cut which formed the Nile valley. When sea level rose again, marine water entered this canyon, and marine sediments are found as far up-river as Aswan. The Nile then filled this trough with fluvial sediments at a relatively gentle slope that was needed to move water and sediment to the newly established higher base level. In contrast to this unique history, the Mississippi River developed a relatively steep valley slope as the result of the influx of outwash sediment from melting continental glaciers. After retreat of the ice, the valley slope was steeper than was required to transport the reduced sediment load, and the Mississippi developed a sinuous course in order to reduce its gradient. The difference between these two great alluvial rivers, therefore, has much to do with their geologic and geomorphic history.



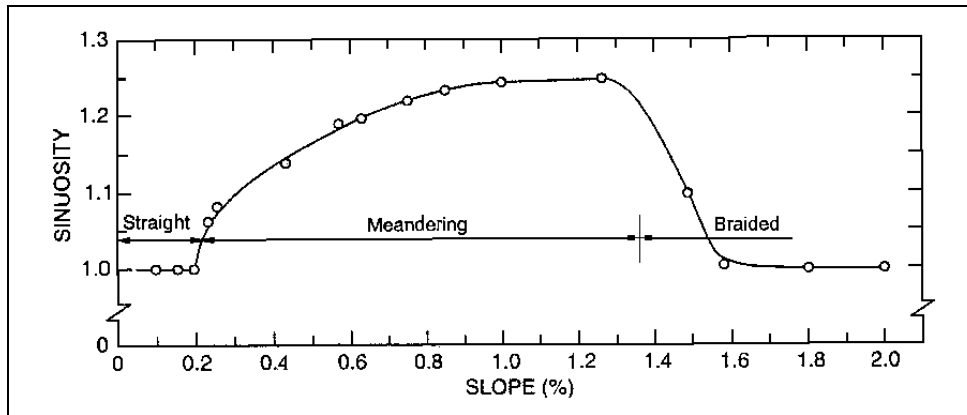


Figure 5.3. Relationship between flume slope and sinuosity (ratio between channel length and valley length) during flume experiments at constant water discharge (from Schumm and Khan 1972).

### 5.3.1 Differences Through Time

During the climate changes of Quaternary time, many rivers completely changed their morphology and behavior (Figure 5.4). This metamorphosis reflected great changes of discharge and sediment load. In addition to the Mississippi River, rivers on the Polish Plain (Kozarski and Retnicki 1977) and the Riverine Plain of Australia (Schumm 1968) underwent the same type of changes.

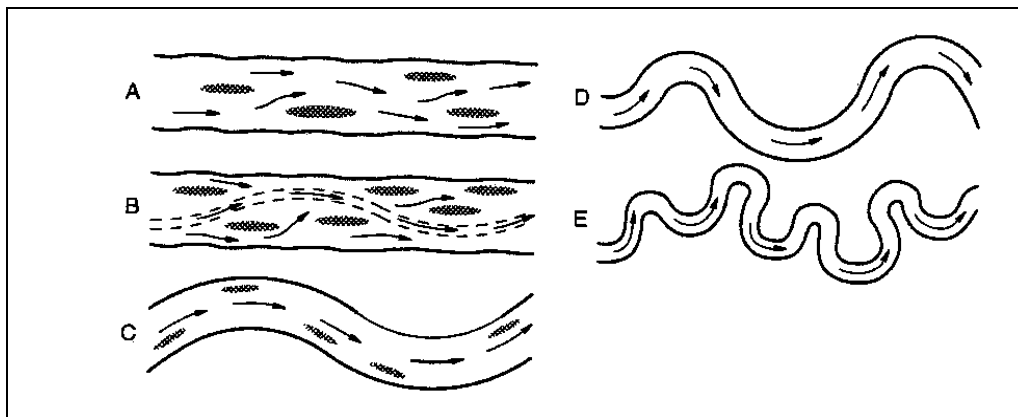


Figure 5.4. Sequence of channel changes as water discharge and sediment loads decrease. (A) braided channel; (B) transitional meandering-braided channel with well-defined thalweg; (C) low-sinuosity channel; (D) relatively narrow and deep moderately sinuous channel; and (E) multiphase meandering channel (after Schumm and Brakenridge 1987).

Perhaps of more interest here are the changes during shorter periods of time, as river bends form, grow, and cutoff. Most meandering rivers will show significant change of sinuosity through time. Figure 5.5 shows the range of sinuosity between 1765 and 1930 for 24 reaches of the lower Mississippi River. Obviously the Mississippi River is composed of very different reaches that behaved differently during the period of record. These are the types of changes to be expected with time along any active river, but the changes also can be avulsive and of a catastrophic nature with abandonment of one channel, and formation of another. This frequently occurs on deltas, and alluvial plains, and it is exemplified by great lateral shifts of the Indus River (Holmes 1968). Indeed, avulsion of the Mississippi River down the Atachafalaya River channel is only prevented by major flood-control structures.

If as a result of climatic fluctuations and human activities, the sediment load, flood peaks, and water discharge of a river are altered, a river response can be expected. However, the type of response will depend upon the nature of the river. For example, sinuous rivers could become straight, and braided rivers could become sinuous, or the changes could be very minor, depending upon the sensitivity of the river (Schumm and Beathard (1976).

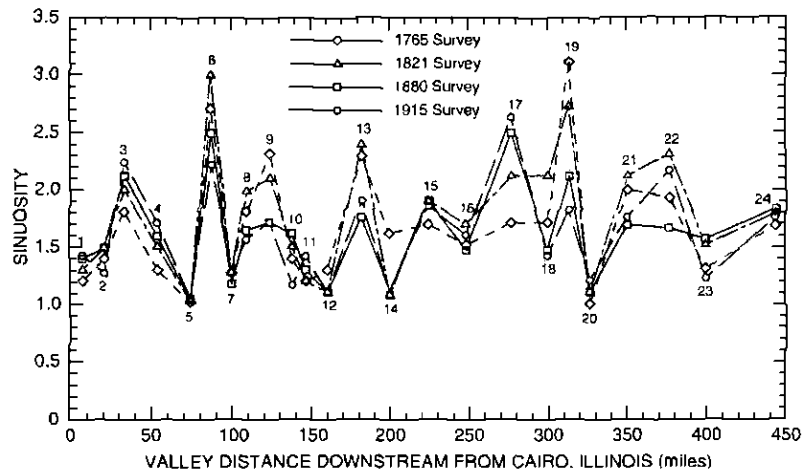


Figure 5.5. Variability of sinuosity between 1765 and 1915 for 24 Mississippi River reaches. Numbers identify the reaches of Figures 5.6 and 5.7 (after Schumm et al. 1994).

The greatest modern river changes have been the result of human activity. The Mississippi River was straightened and shortened 229 kilometers (142 miles) between 1933 and 1942. The goal was to reduce flood peaks and to improve navigation. This great river experiment yielded both beneficial and undesirable results. Floods were reduced, but channel stability decreased (Winkley 1977, 1994).

### 5.3.2 Differences Between Reaches

Perhaps of greater interest to river engineers is the variability along a single river. One could assume that large alluvial rivers should have a relatively uniform morphology because the controlling factors of water discharge and sediment load should not vary greatly. However, other factors intervene to cause considerable variability. For example, a glance at even a coarse-scale map of the pre-cutoff Mississippi River reveals great variability. In fact, 24 distinct reaches were identified between Cairo, Illinois and Old River, a distance of 768 valley kilometers (477 miles) (Figure 5.6). The reaches were identified by changes of valley slope,

channel variability through time and the pre-cutoff 1930 river pattern. Figure 5.5 shows great differences in the variability of sinuosity among reaches and for each of the reaches through time. The differences among the reaches are for the most part the result of tectonic deformation of the valley floor and the presence of more resistant materials in the bed and or banks, such as clay plugs, Pleistocene-age alluvium, and Tertiary-age bedrock. A plot of the valley (floodplain) slope, based upon the 1880 bankfull elevations (Figure 5.7) shows considerable variability, as a result of these controls. The Mississippi is characterized by a lack of uniformity in its morphology and dynamics, which has made the job of the river engineer difficult. The great variability is largely the result of geomorphic and geologic controls (Schumm et al. 1994).

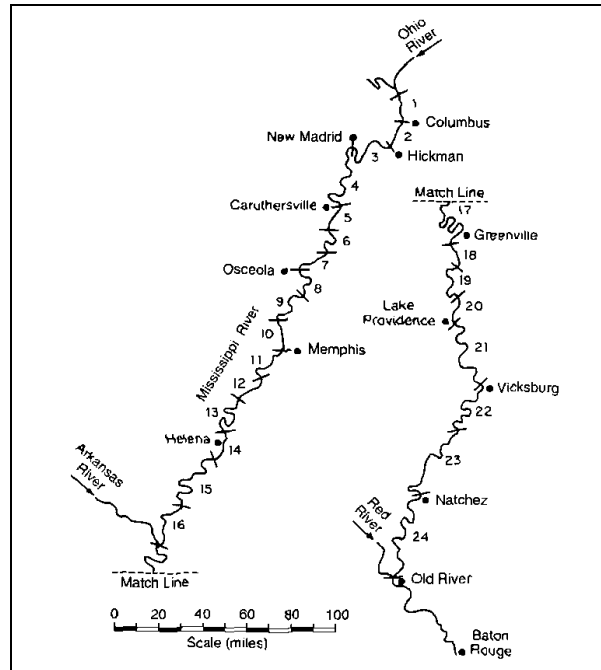


Figure 5.6. Mississippi River reaches between Cairo, Illinois and Old River, Louisiana (after Schumm et al. 1994).

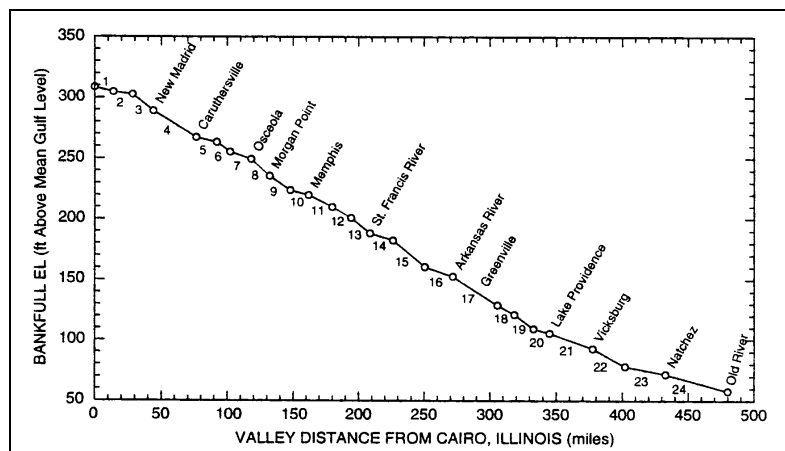


Figure 5.7. Mississippi River valley profile (after Schumm et al. 1994).

Another great alluvial river, the Nile, when studied using the same geomorphic techniques (Schumm and Galay 1994) is found to be much less variable and dynamic (Figure 5.8), but because of the great population density along its course even minor changes are of importance. There appears to have been little change of the pattern of the River Nile since mapping in the 18<sup>th</sup> century, except in the reach between El Saff and Cairo.

A plot of the Nile valley slope (Figure 5.9) shows differences similar to that of the Mississippi (Figure 5.7), but they are much less. Sinuosity does increase with increased valley slope, and valley slope actually increases downvalley (Figure 5.10). The change of valley slope and sinuosity below Qena is undoubtedly the result of the large Wadi Quena, which in the past has introduced coarse sediments into the Nile Valley. The other changes of slope are probably related to tectonics, such as faulting at Assiut.

The anticipated impact of the High Aswan Dam on hydrology and sediment loads was a matter of great concern for engineers concerned with bank stability and potential channel degradation. Perhaps of greatest concern was the potential for major degradation of the Nile following construction of the dam. Because degradation has been controversial, it was studied by many researchers prior to, and after, construction of the dam (Fathy 1956, Mostafa 1957, Shalash 1980, Shalash 1983, Richardson and Clyma 1980, Gasser et al. 1978, and El-Moatassem and El-Mottaleb 1979). The construction of the High Aswan Dam commenced in 1963 and proceeded to 1968. Pre-dam estimates of degradation ranged from 2.0 to 8.5 m (6.5 to 28 ft), but 18 years after the dam was in operation, maximum degradation was 0.70 m (2.3 ft).

Several factors account for the fact that degradation has been minimal after closure of the dam. For example, it is important to recognize that during past humid periods in Egypt, wadis delivered coarse sediments to the valley, which could act as a control of degradation depending upon their location in the valley and the depth at which they are encountered. At present, many wadis appear to contribute only relatively fine sediment that can be readily transported downstream, and the bed of the Nile is sand. However, during wetter periods of the past, the wadis probably contributed abundant coarse sediment to the river, and even today wadi flooding must introduce coarse sediments into the river. For example, there is an abundant supply of sand, gravel, and cobbles in Wadi Qena, which drains a large area to the north of Qena. A deep trench was excavated in a small wadi that enters the Nile valley at Khuzam about 30 km (18.5 mi) downstream from Armant. Boulders and cobbles are abundant in the trench, and such sediments undoubtedly were moved into the Nile during wetter periods. All of the wadis contain much stored sediment of gravel, cobble, and boulder size.

Based upon an analysis of borings in the Nile valley, Attia (1954) concluded that within the valley "coarse deposits composed of coarse sand, sand and gravel, or gravel lie beneath the fine alluvial deposits." It is well known that only a small percentage of coarse bed material can armor a bed and it appears that the minimal degradation by the River Nile in response to the High Aswan Dam is the result of coarse sediment beneath a veneer of sand.

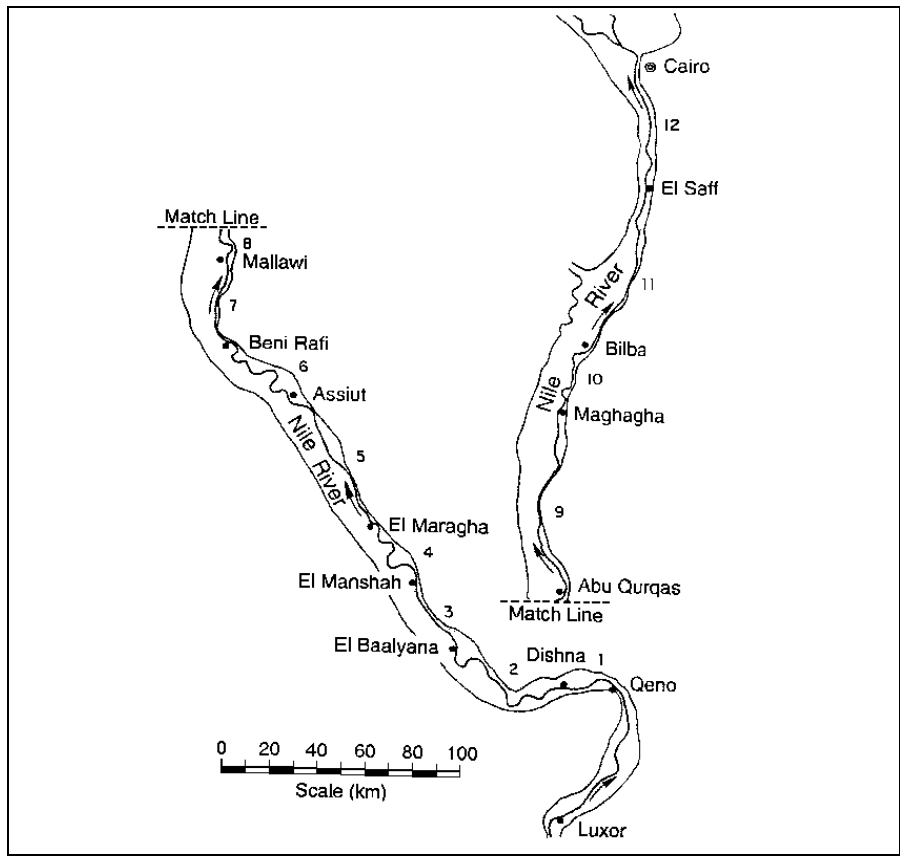


Figure 5.8. River Nile between Qena and Cairo showing six reaches of steep valley slope.

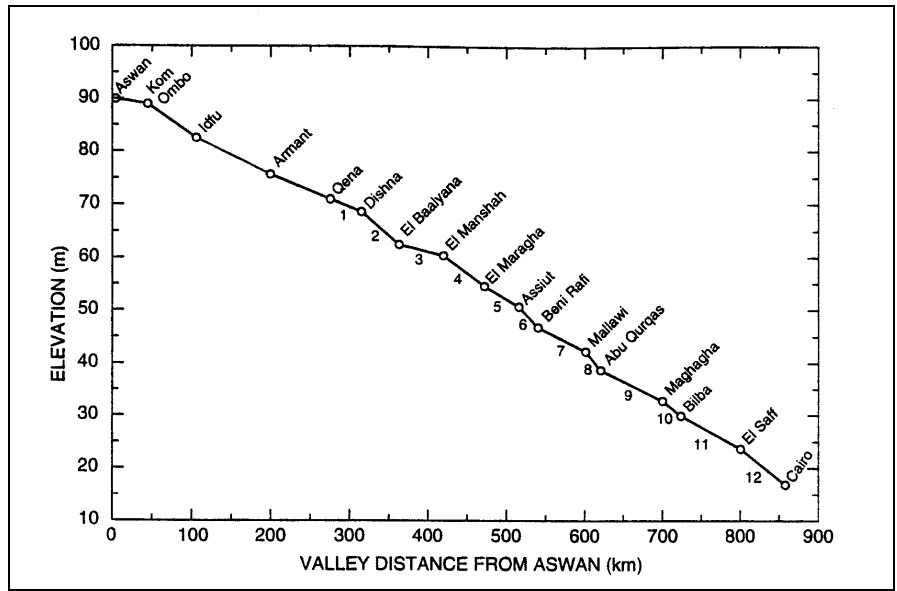


Figure 5.9. River Nile valley profile. Numbers identify reaches of Figure 5.8 (after Schumm and Galay 1994).

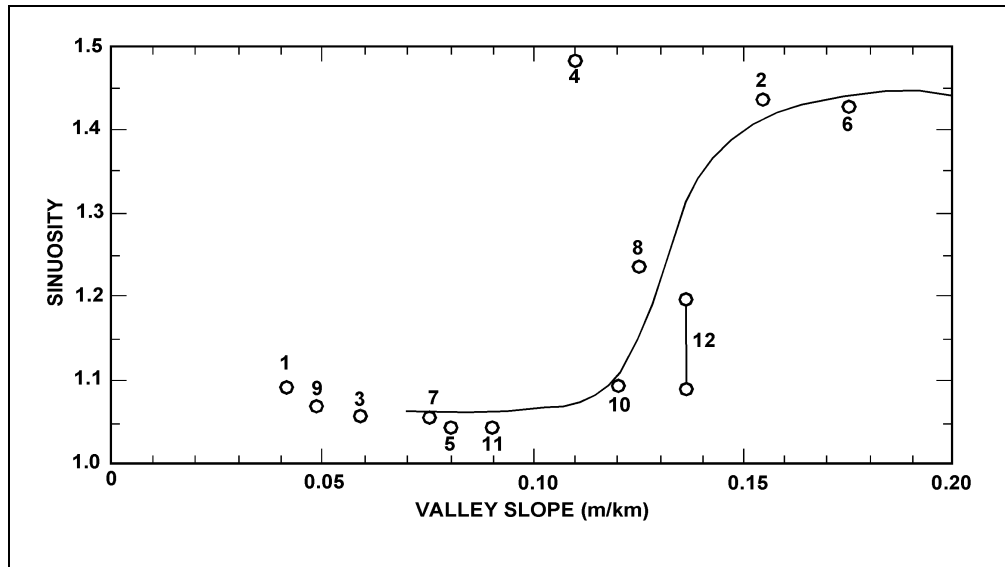


Figure 5.10. Plot of River Nile sinuosity and valley slope. Numbers represent reaches of Figure 5.9. The vertical line joining two points for Reach 12 shows the difference between 18th century and present low sinuosity (after Schumm and Galay 1994).

### 5.3.3 Summary

The contrast between the lower Mississippi River and the Nile is striking. The Nile is much less dynamic, but it too responds to geologic controls and tributary influences. Both the Mississippi and Nile Rivers have sand-beds, yet what lies beneath the sand may be of critical importance to the character and response of these great rivers. It is probable that the Mississippi is controlled totally by Tertiary-age clay and Pleistocene-age gravels, and the Nile has apparently developed an armor of gravel and cobbles beneath its sand bed. Anomalous river behavior can often be explained by factors that are related to river history. Both the Mississippi and the Nile provide support of this fact. Hence, factors that are normally beyond the engineer's range of expertise may dominate river morphology and behavior.

In order to understand alluvial rivers, one cannot limit a study to modern conditions only. In fact, past channel morphology and behavior can provide valuable information about modern river behavior. For example, although both the Mississippi and the Nile are large and transport similar sediments, they differ greatly morphologically and dynamically as a result of quite different histories. Therefore, in order to anticipate and to predict river response, both the past and the present must be combined in what could be termed a geomorphic-engineering approach to river maintenance and/or restoration.

## 5.4 STREAM FORM AND GEOMETRY OF ALLUVIAL CHANNELS

A study of the plan and profile of a stream is very useful in understanding stream morphology. Planview appearances of streams are varied and result from many interacting variables. Small

changes in a variable can change the planview and profile of a river, adversely affecting a highway crossing or encroachment. Conversely, the highway crossing or encroachment can inadvertently change the planview or profile, adversely affecting the river environment. In this section, stream form is classified and channel processes are discussed.

#### **5.4.1 Classification of River Channels**

Brice and Blodgett (1978) developed a simple classification scheme oriented primarily toward lateral stability of rivers. The common geomorphic terms for the various types of streams (e.g., meandering, braided) are shown in Figure 5.11. Each term is defined on the small sketches. This classification is also used in HEC-20 (Lagasse et al. 2001) as a basis for identifying geomorphic factors important to stream stability analyses.

Additional information on specific channel features is illustrated in Figure 5.12. Classification based on oxbow lakes is illustrated in Figure 5.12a. In Figure 5.12b, types of meander scroll formations are shown. By studying scroll formations in terms of age of vegetation the rate and direction of channel migration can be quantified. The sinuosity index is the ratio of the length of the watercourse over the valley length between the same points. Classification based on natural levees is illustrated in Figure 5.12c. Well developed levees are associated with older rivers. The floodplain that is broad in relation to the channel width is indicative of an older river. Conversely, when the river valley is narrow and confined by terraces or valley walls, the river is usually mature. In general, the growth of vegetation (tree cover) is indicative of the presence of silts and clays in the river banks and the floodplain. This is particularly true if the floodplain is well drained. With good drainage, the silt and clay are essential to the growth of vegetation because of their water holding capability.

Natural levees are a characteristic of alluvial river systems. Levees form during floods as the river stage exceeds bankfull conditions. Sediment is then deposited on the floodplain due to the reduced velocity and transporting capacity. The natural levees near the river are rather steep because coarse material drops out quickly. Farther from the river the gradients are flatter and the finer materials drop out. Beyond the levees are the swamp areas. On the lower Mississippi River, natural levees on the order of 10 ft in height are common. The rate of growth of natural levees is slower after they reach a height equal to the average annual flood stage.

A detailed knowledge of the hydraulic characteristics of different types of streams is of great value when dealing with the location of highway crossings and encroachment, training works, flood control works and other river structures. A channel classification in Figure 5.13 shows the relative stability and types of hazards encountered. Figure 5.13 is also useful in making a qualitative assessment of stream stability based on stream characteristics. It shows that straight channels are relatively stable only where flow velocities and sediment load are low. As these variables increase, flow meanders in the channel causing the formation of alternate bars and the initiation of a meandering channel pattern. Similarly, meandering channels are progressively less stable with increasing velocity and bed load. At high values of these variables, the channel becomes braided. The presence and size of point bars and middle bars are indications of the relative lateral stability of a stream channel. Bed material transport is directly related to stream power, and relative stability decreases as stream power increases as shown by Figure 5.13. An example is given in Section 5.9 (Problem 2) on how to use this classification.


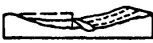










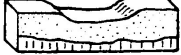


















STREAM SIZE	Small ( $< 30$ m wide)	Medium (30-150 m)		Wide ( $> 150$ m)
FLOW HABIT	Ephemeral	(Intermittant)	Perennial but flashy	Perennial
BED MATERIAL	Silt-Clay	Silt	Sand	Gravel Cobble or Boulder
VALLEY SETTING	 No valley; alluvial fan	 Low relief valley ( $< 30$ m deep)	 Moderate relief (30-300 m deep)	 High relief ( $> 300$ m deep)
FLOODPLAINS	 Little or none ( $< 2$ x channel width)	 Narrow (2-10 x channel width)	 Wide ( $> 10$ x channel width)	
NATURAL LEVEES	 Little or none	 Mainly on concave	 Well developed on both banks	
APPARENT INCISION	 Not Incised		 Probably Incised	
CHANNEL BOUNDARIES	 Alluvial	 Semi-alluvial	 Non-alluvial	
TREE COVER ON BANKS	$< 50$ percent of bankline	50-90 percent of bankline		$> 90$ percent of bankline
SINUOSITY	 Straight Sinuosity (1-1.05)	 Sinuous (1.06-1.25)	 Meandering (1.25-2.0)	 Highly Meandering ( $> 2.0$ )
BRAIDED STREAMS	 Not braided ( $< 5$ percent)	 Locally braided (5-35 percent)	 Generally braided ( $> 35$ percent)	
ANABRANCHED STREAMS	 Not anabranching ( $< 5$ percent)	 Locally anabranching (5-35 percent)	 Generally anabranching ( $> 35$ percent)	
VARIABILITY OF WIDTH AND DEVELOPMENT OF BARS	 Narrow point bars	 Equiwidth	 Wider at bends	 Random variation
		 Wide point bars	 Irregular point and lateral bars	

Figure 5.11. Stream properties for classification (after Brice and Blodgett 1978).



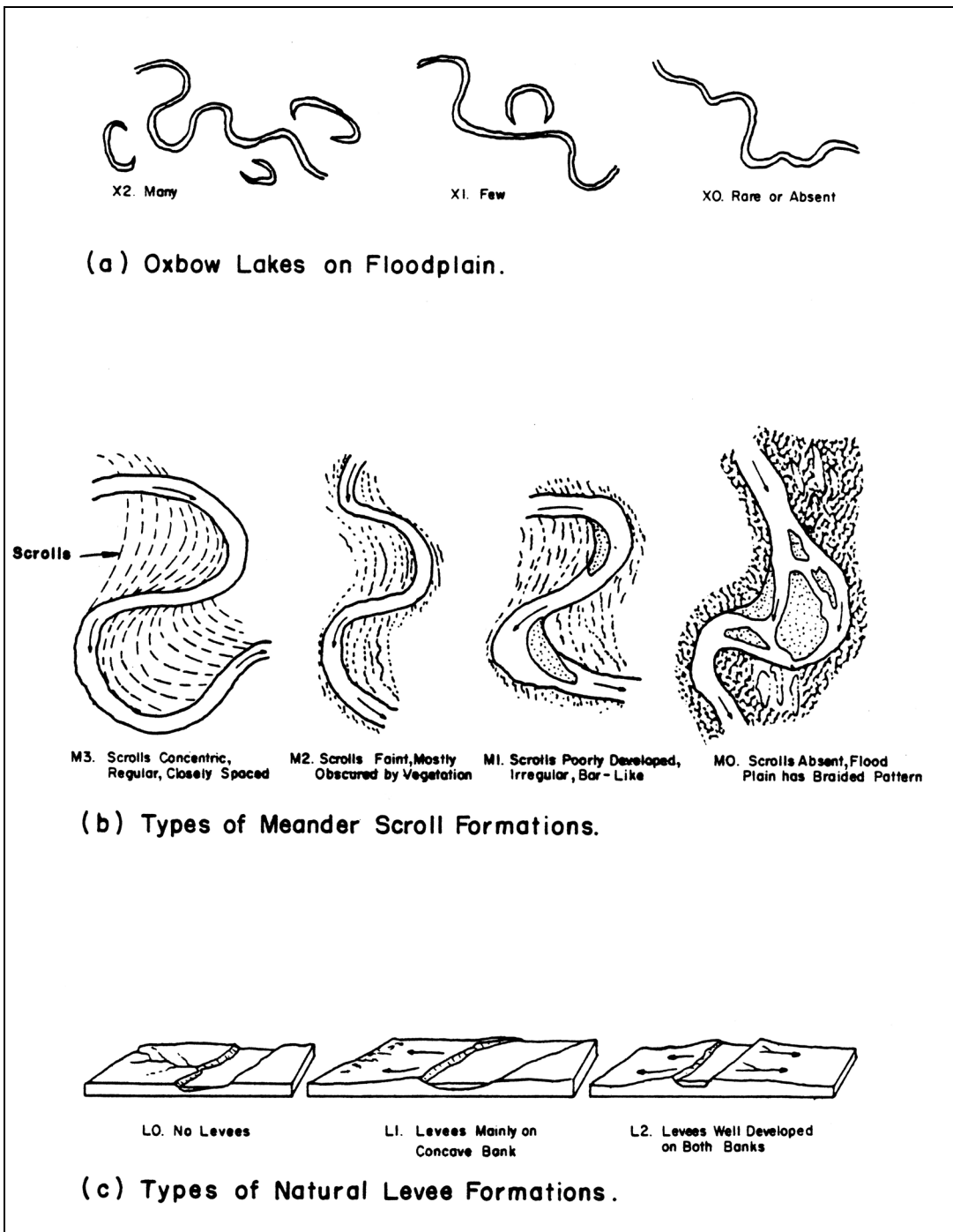


Figure 5.12. Classification of river channels (after Culbertson et al. 1967).

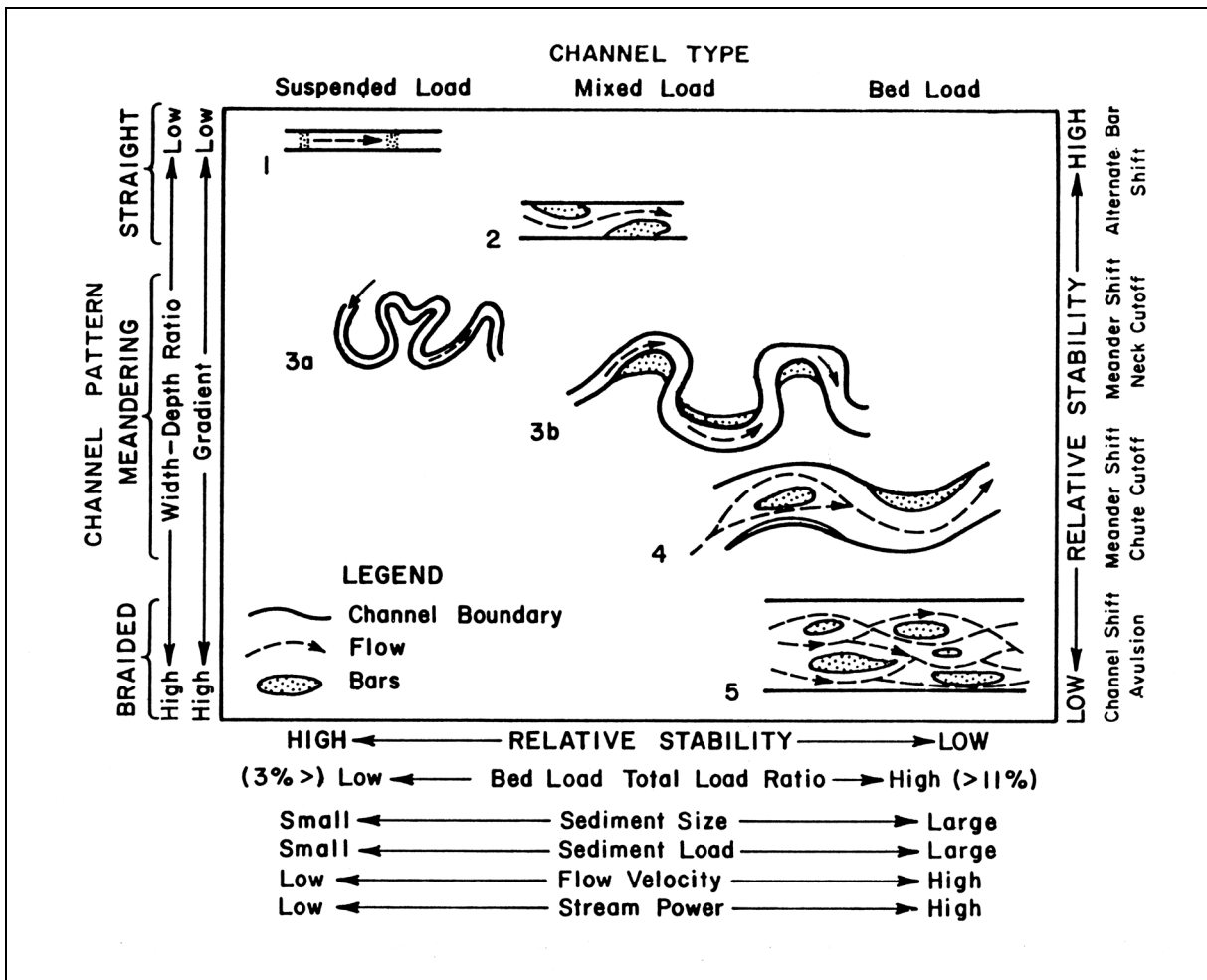


Figure 5.13. Channel classification showing relative stability and types of hazards encountered with each pattern (after Shen et al. 1981).

Additional approaches to stream channel classification including those by Brice (1975), Schumm (1977 and 1981), Montgomery and Buffington (1997), and Rosgen (1994 and 1996) are introduced in HEC-20 (Lagasse et al. 2001). Further discussion of the opportunities and limitations related to using stream classification for river analysis, engineering and management can be found in Thorne (1997).

The next sections provide a brief discussion concerning the nature and stability of straight, braided, and meandering channels. Each behaves in a slightly different way when subject to human-related or natural impacts. A knowledge of this behavior is important in anticipating and understanding stability problems.

### 5.4.2 Straight River Channels

Straight river channels can be of two types. The first forms on a low-gradient valley slope, has a low width-depth ratio channel, and is relatively stable. The second type is a steep gradient, high width-depth ratio, high energy river that has many bars, and at low flow is braided. It is relatively active. The first type of straight channel may contain alternate bars (Figure 5.14), that result in a sinuous thalweg (flow path connecting deepest points in successive cross sections) within the straight channel. The braided channel, as discussed in detail later, has numerous bars and multiple thalwegs.

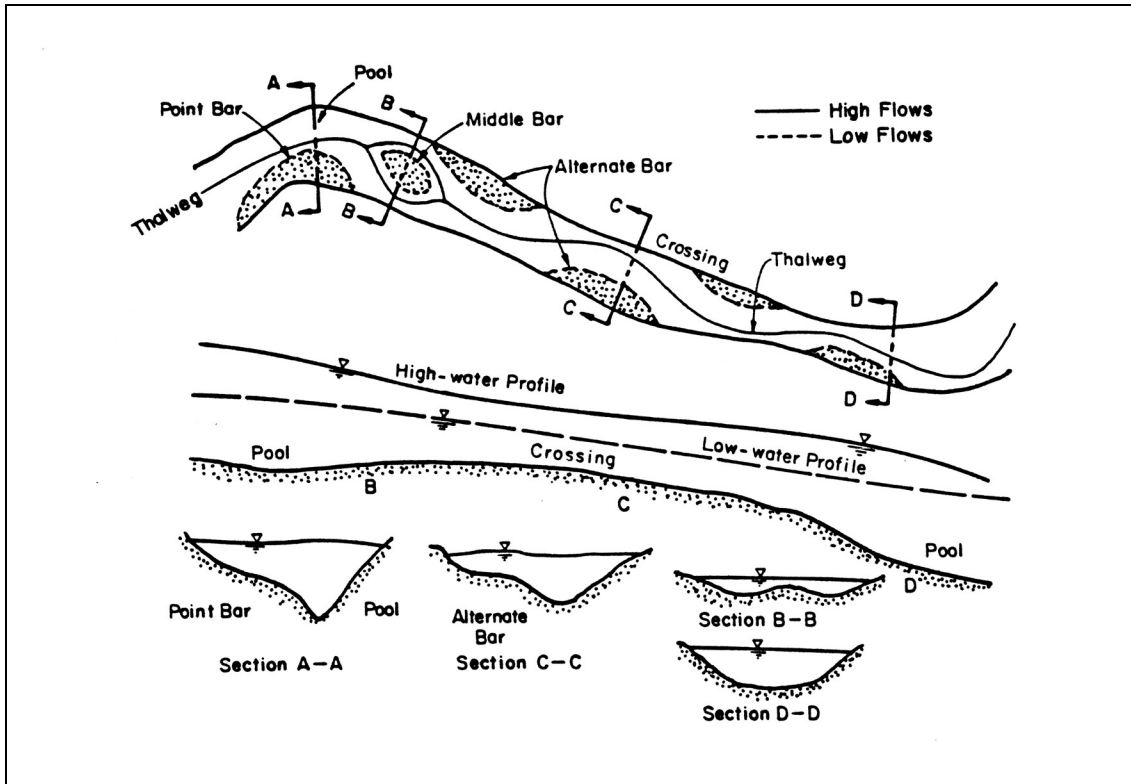


Figure 5.14. Planview and cross section of a meandering stream.

### 5.4.3 Meandering River Channels

Alluvial channels of all types deviate from a straight alignment. The thalweg oscillates transversely and initiates the formation of bends. In general, the river engineer concerned with channel stabilization should not attempt to develop straight channels fully protected with riprap. In a straight channel the alternate bars and the thalweg are continually changing; thus, the current is not uniformly distributed through the cross-section but is deflected toward one bank and then the other. Sloughing of the banks, nonuniform deposition of bed load caused by debris such as trees, and the Coriolis force due to the earth's rotation have been cited as causes for meandering of streams. When the current is directed toward a bank, the bank is eroded in the area of impingement and the current is deflected and impinges upon the opposite bank further downstream. The angle of deflection of the thalweg is affected by the curvature formed in the eroding bank and the lateral depth of erosion.

The meandering river consists of pools and crossings (Figure 5.14). The thalweg, or main current of the channel, flows from the pool through the crossing to the next pool forming the typical S-curve. In the pools, the channel cross-section is somewhat triangular. Point bars form on the inside of the bends. In the crossings, the channel cross-section is more rectangular and depths are smaller. At low flows, local slope is steeper and velocities are larger in the crossing than in the pool. At low stages, thalweg is located very close to the outside of the bend. At higher stages, thalweg tends to straighten, that is, thalweg moves away from the outside of the bend encroaching on the point bar to some degree. In the extreme case, the shifting of the current causes chute channels to develop across the point bar at high stages. In Figure 5.14, one can observe the position of the thalweg, the location of the point bars, alternate bars and the location of the pools and crossings. Note that in the crossing the channel is shallow compared to pools and the banks may be more subject to erosion.

Figure 5.14 illustrates the change in water surface profile from low to high water discharge. At low flow the water surface slope is steep in the crossing and flatter in the pool. The reverse is true at higher discharges. At higher discharges the thalweg straightens, shortening the path of travel and increasing the local friction slope. In the extreme case, river slope approaches the valley slope at flood stage. It is during high floods that the flow often cuts across the point bars, developing chute channels and a steeper channel prevails under this condition.

In general, bends are formed by the process of erosion and deposition. Erosion without deposition to assist in bend formation would result only in scalloped banks. Under these conditions the channel would simply widen until it becomes so large that the erosion would terminate. The material eroded from the bank is normally deposited over a period of time on the point bars that are formed downstream. The point bars constrict the bend and enable erosion in the bend to continue, accounting for the lateral and longitudinal migration of the meandering stream. Erosion is greatest across the channel from the point bar. As the point bars build out from the downstream sides of the bars, the bends gradually migrate down the valley. The point bars formed in the bendways clearly define the direction of flow. The bar is generally streamlined and its largest portion is oriented downstream. If there is very rapid caving in the bendways upstream, the sediment load may be sufficiently large to cause middle bars to form in the crossing.

As a meandering river system moves laterally and longitudinally, the meander limbs move at an unequal rate because of the unequal erodibility of the banks. This causes the channel to appear as a bulb form, generally skewed in a downvalley direction. The channel geometry depends upon the local slope, the bank material, and the geometry of the adjacent bends. Over time the local steep slope caused by the cutoff is distributed both upstream and downstream. Years may be required before a configuration characteristic of average conditions in the river is attained.

When a cutoff occurs, an oxbow lake is formed (Figure 5.12a). Oxbow lakes may persist for long periods of time before filling. Usually the upstream end of the lake fills quickly to bank height. Overflow during floods carries fine materials into the oxbow lake area. The lower end of the oxbow remains open and the drainage and overland flow entering the system can flow out from the lower end. The oxbow gradually fills with fine silts and clays. Fine material that ultimately fills the bendway is plastic and cohesive. As the river channel meanders it encounters old bendways filled with cohesive materials (referred to as clay plugs). These plugs are sufficiently resistant to erosion to serve as semipermanent geologic controls and can drastically affect river geometry. The variability of bank materials, and the fact that the river encounters such features as clay plugs, cause a wide variety of river forms in a meandering river.

In summary, a meandering river has regular inflections that are sinuous in plan. It consists of a series of bends connected by crossings. In the bends, deep pools are carved adjacent to the concave bank by the relatively high velocities. Because velocities are lower on the inside of the bend, sediments are deposited in this region, forming a point bar. The centrifugal force in the bend causes a transverse water surface slope, and in many cases, helicoidal flow occurs in the bend. Point bar building is enhanced when large transverse velocities occur. In so doing, they sweep the heavier concentrations of bed load toward the convex bank where they are deposited to form the point bar. Some transverse currents have a magnitude of about 15 percent of the average channel velocity. The bends are connected by crossings (short straight reaches) which are quite shallow compared to the pools in the bendways. Much of the sediment eroded from the outside bank is deposited in the crossing and on the point bar in the next bend downstream. At low flow, large sandbars form in the crossings if the channel is not well confined.

The scour in the bend causes the bend to migrate laterally and sometimes downstream. Lateral movements as large as 760 m (2,500 ft) per year have been observed in alluvial rivers. The meander belt formed by a meandering river is often fifteen to twenty times the channel width. When compared to most braided rivers, meandering rivers have relatively flat slopes.

The geometry of meandering rivers is measured quantitatively in terms of: (1) meander wavelength  $\lambda$ , (2) meander width  $W_m$ , (3) mean radius of curvature  $r_c$ , (4) meander amplitude  $A$ , and (5) bend deflection angle  $\phi$ . These variables are shown in Figure 5.15.

The actual meanders in natural rivers are obviously not as regular as indicated in Figure 5.15. The precise measurement of meander dimensions is therefore difficult in natural channels and tends to be subjective. An example on how to measure these characteristics is presented in Section 5.9 (Problem 1). The analysis of the mean meander dimension in nature shows that the meander length and meander width are both related to the width of the channels. The empirical relationships for the meander length  $\lambda$  and the bank-full channel width as well as the meander amplitude,  $A$ , and the bank-full channel width are shown in Figure 5.16 and Table 5.1.

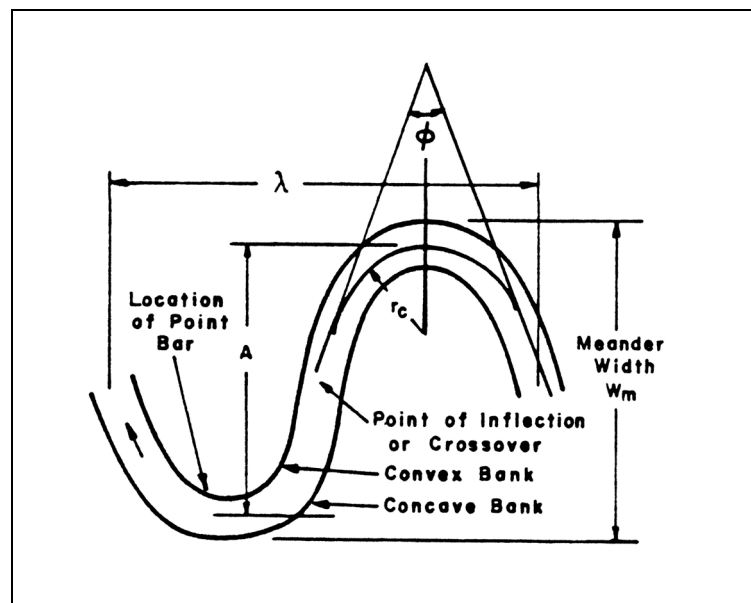


Figure 5.15. Definition sketch for meanders.

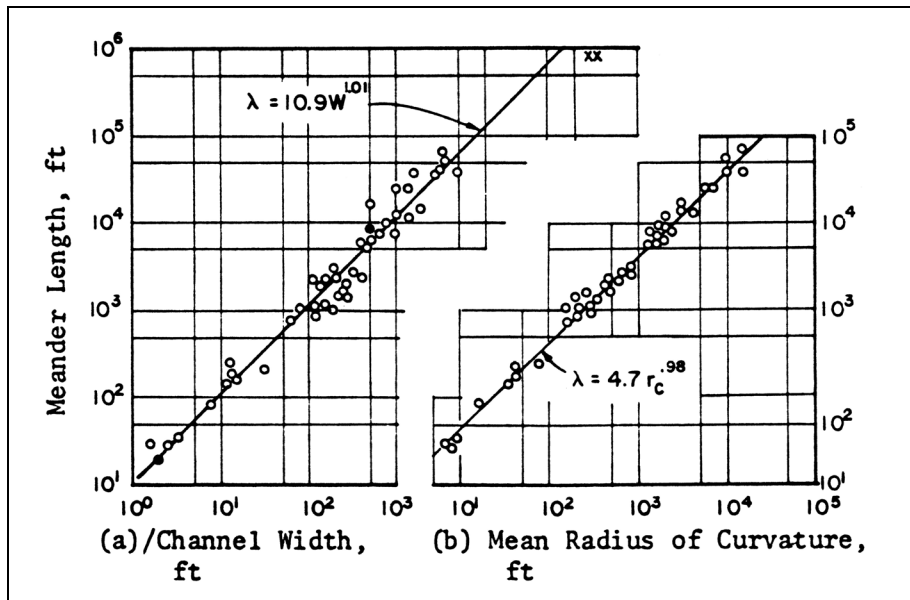


Figure 5.16. Empirical relations for meander characteristics (Leopold et al. 1964).

Table 5.1. Empirical Relations for Meanders in Alluvial Valleys.			
Meander Length to Channel Width	Amplitude to Channel Width	Meander Length to Radius of Curvature	Source
$\lambda = 6.6W^{0.99}$	$A = 18.6W^{0.99}$	-	Inglis (1949)
-	$A = 10.9W^{1.04}$	-	Inglis (1949)
$\lambda = 10.9W^{1.01}$	$A = 2.7W^{1.10}$	$\lambda = 4.7r_c^{0.98}$	Leopold and Wolman (1960)

#### 5.4.4 Braided River Channels

A braided stream is one that consists of multiple and interlacing channels (Figures 5.11 and 5.13). One cause of braiding is the large quantity of bed load. Generally, the magnitude of the bed load is more important than its size. If the channel is overloaded with sediment, deposition occurs, the bed aggrades, and the slope of the channel increases in an effort to obtain a graded state. As the channel steepens, the velocity increases, and multiple channels develop. These interlaced multiple channels cause the overall channel system to widen. Multiple channels are generally formed as bars of sediment are deposited within the main channel.

Another cause of braiding is easily eroded banks. If the banks are easily eroded, the stream widens at high flow and forms bars at low flow which become stabilized, thus forming islands. In general, a braided channel has a relatively steep slope, a large bed-material load in comparison with its suspended load, and relatively small amounts of silts and clays in the bed and banks. Figure 5.17 will assist in defining the various conditions for multiple channel streams.

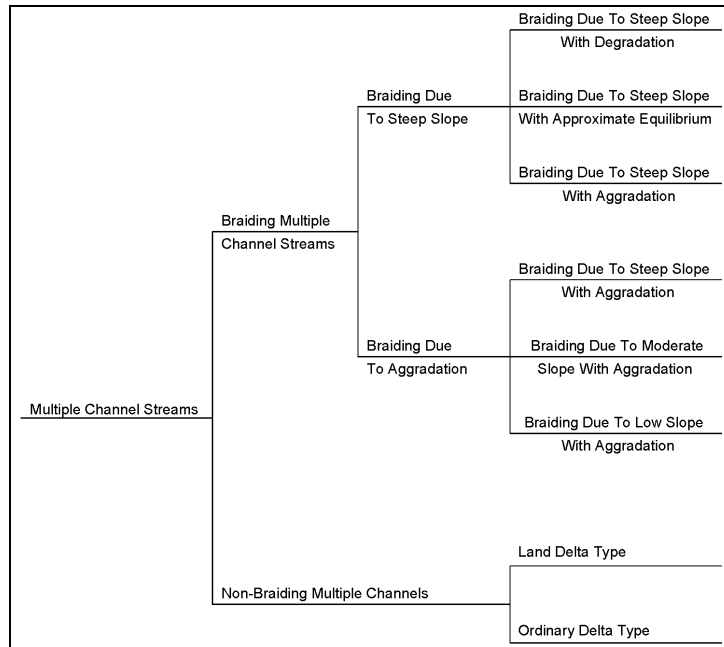


Figure 5.17. Types of multi-channel streams.

The braided stream may present difficulties for highway construction because it is unstable, changes its alignment rapidly, carries large quantities of sediment, is very wide and shallow even at flood flow and is, in general, unpredictable.

#### 5.4.5 River Conditions for Meandering and Braiding

It can be shown that changes in water discharge, sediment discharge or both can cause significant changes in channel slope (see Section 5.5). The changes in sediment discharge can be in quantity,  $Q_s$ , or sediment size,  $D_{50}$ , or both. Often, such changes can alter the planview in addition to the profile of a river.

According to Lane (1957), Figures 5.18a and b illustrate the dependence of sand bed river form on channel slope and discharge. They show that when:

$$SQ^{0.25} \leq k \tag{5.1}$$

where:

$$\begin{aligned} k &= 0.0007 \text{ SI} \\ k &= 0.0017 \text{ English} \end{aligned}$$

a sandbed channel meanders. Similarly, when:

$$SQ^{0.25} \geq k \tag{5.2}$$

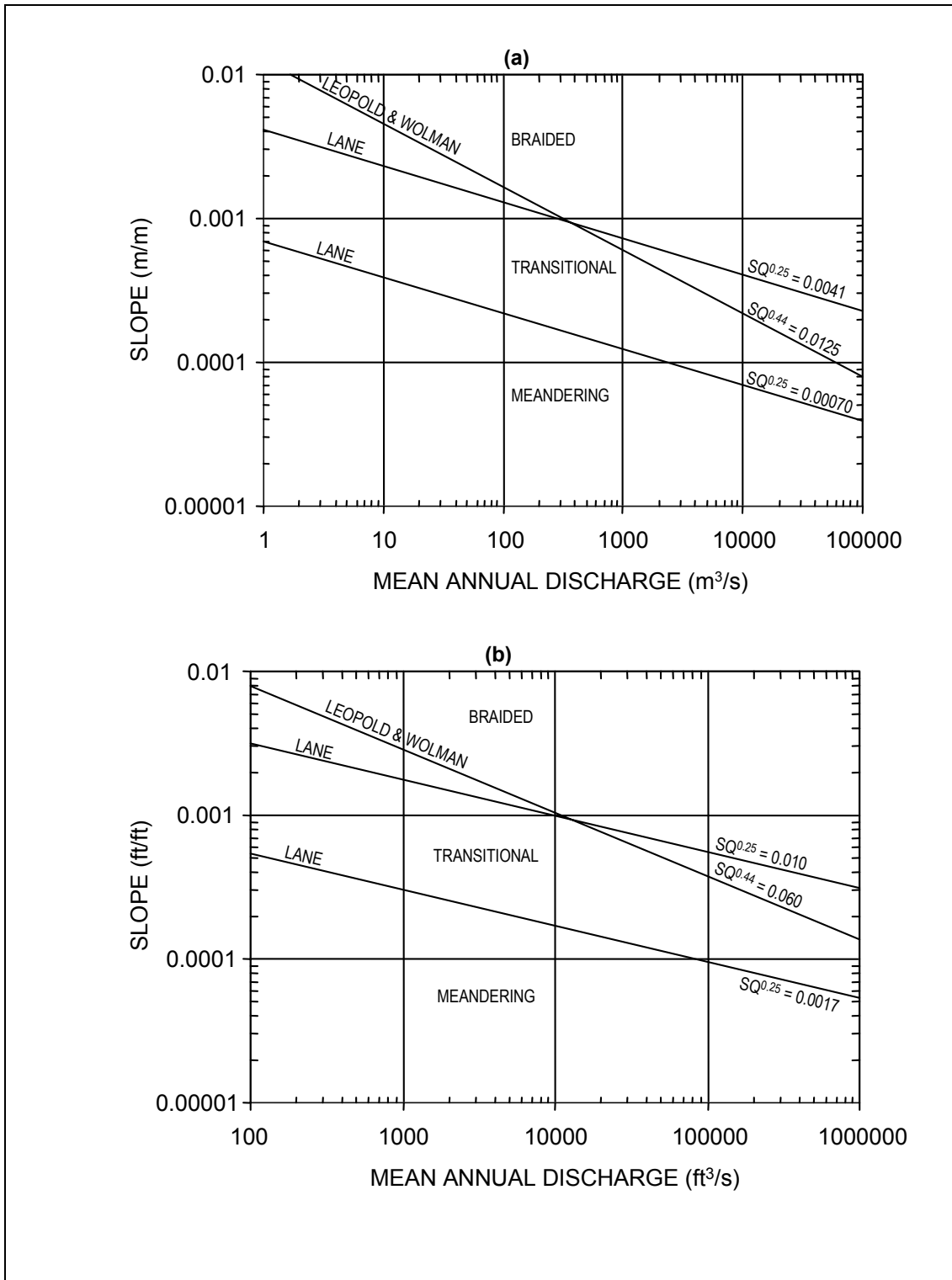


Figure 5.18a,b. Slope-discharge relationship for braiding or meandering in sandbed streams (after Lane 1957) (a = English units b = SI units).



where:

$$\begin{aligned}k &= 0.0041 \text{ SI} \\k &= 0.010 \text{ English}\end{aligned}$$

the sandbed river is braided. In these equations,  $S$  is the channel slope in m/m (ft/ft) and  $Q$  is the mean discharge in  $\text{m}^3/\text{s}$  ( $\text{ft}^3/\text{s}$ ). Between these values of  $S Q^{0.025}$  is the transitional range. Many of the U.S. rivers, classified as intermediate sandbed streams, plot in this zone. If a river is meandering but its discharge and slope border on the transitional zone a relatively small increase in channel slope may cause it to change to a transitional or braided river.

Leopold and Wolman (1960) plotted slope and discharge for a variety of natural streams. They observed that a line could separate meandering from braided streams (Figures 18a and b). The equation of this line is:

$$SQ^{0.44} = k \tag{5.3}$$

where:

$$\begin{aligned}S &= \text{Slope in m/m (ft/ft)} \\Q &= \text{Bank-full discharge in } \text{m}^3/\text{s} \text{ (ft}^3/\text{s)} \\k &= 0.0125 \text{ SI} \\k &= 0.06 \text{ English}\end{aligned}$$

Streams classified as meandering by Leopold and Wolman are those whose sinuosity is greater than 1.5. Braided streams are those which have relatively stable alluvial islands and, therefore, two or more channels. Leopold and Wolman note that sediment size is related to slope and channel pattern, but they do not try to account for the effect of sediment size on the morphology of the streams. They further note that braided and meandering streams can be differentiated based on combinations of slope, discharge, and width/depth ratio, but regard the width as a variable dependent on mainly discharge.

Leopold and Wolman recognize that their analysis treats only two of the many variables affecting morphology, therefore, they do not expect this method to apply in every condition. However, because the data were all taken from natural streams, and because the analysis obviously does indicate a significant relation between slope and discharge, the analysis should give a reasonably effective prediction of channel pattern if slope and discharge are known. Problem 1 in Section 5.9 gives an example of this type of prediction and Section 5.5.3 uses these concepts in an engineering geomorphic analysis.

#### 5.4.6 Hydraulic Geometry of Alluvial Channels

Hydraulic geometry is a general term applied to alluvial channels to denote relationships between discharge  $Q$  and the channel morphology, hydraulics and sediment transport. Channels forming in their own sediments are called alluvial channels. In alluvial channels, the morphologic, hydraulic and sedimentation characteristics of the channel are determined by a large variety of factors. The mechanics of such factors are not fully understood. However, alluvial streams do exhibit some quantitative hydraulic geometry relations. In general, these relations apply to channels within a physiographic region and can be obtained from data available on gaged rivers. It is understood that hydraulic geometry relations express the integral effect of all the hydrologic, meteorologic, and geologic variables in a drainage basin for in-bank flows.

The hydraulic geometry relations of alluvial streams are useful in river engineering. The forerunner of these relations are the regime theory equations of stable alluvial canals (see for example, Kennedy 1895, Lacy 1930, and Leliavsky 1955). Hydraulic geometry relations were developed by Leopold and Maddock (1953) for different regions in the United States and for different types of rivers. In general the hydraulic geometry relations are stated as power functions of the discharge:

$$W = aQ^b \quad (5.4)$$

$$y_o = cQ^f \quad (5.5)$$

$$V = kQ^m \quad (5.6)$$

$$Q_T = pQ^j \quad (5.7)$$

$$S_f = tQ^z \quad (5.8)$$

$$n = rQ^y \quad (5.9)$$

where:

- W = Channel width
- y<sub>o</sub> = Channel depth
- V = Average velocity of flow
- Q<sub>T</sub> = Total bed sediment load
- S<sub>f</sub> = Friction slope
- n = Manning's roughness coefficient
- Q = Discharge as defined in the following paragraphs

The coefficients a, c, k, p, t, r and exponents b, f, m, j, z, y in these equations are determined from analysis of available data on one or more streams. From the continuity equation (Q = Wy<sub>o</sub>V), it is seen that

$$a \times c \times k = 1 \quad (5.10)$$

and

$$b + f + m = 1 \quad (5.11)$$

Leopold and Maddock (1953) have shown that in a drainage basin, two types of hydraulic geometry relations can be defined: (1) relating W, y<sub>o</sub>, V and Q<sub>s</sub> to the variation of discharge at-a-station; and (2) relating these variables to the discharges of a given frequency of occurrence at various stations in a drainage basin. Because Q<sub>T</sub> is not readily available, they used Q<sub>s</sub>, the suspended sediment transport rate. The former are called **at-a-station** relationships and the latter **downstream** relationships. The distinction between at-a-station and downstream hydraulic geometry relations is illustrated in Figures 5.19 and 5.20.

Figures 5.19 and 5.20 illustrate how the hydraulic relations at-a-station and in the downstream direction may be different from one basin to another. For example, the width and depth at-a-station do not change very much in Basin A. The width to depth ratio is almost constant but the velocity increases, as it must, as the discharge increases at-a-station. In Basin B the width to depth ratio decreases with an increase in discharge. That is, the width changes very little but the depth increases significantly with discharge at-a-station. Note, that in both basins, width

increases with discharge in the downstream direction, but in Basin B, depth changes very little in the downstream direction. Leopold and Maddock (1953) show that the type of relations illustrated in Figure 5.20 exist in natural rivers.

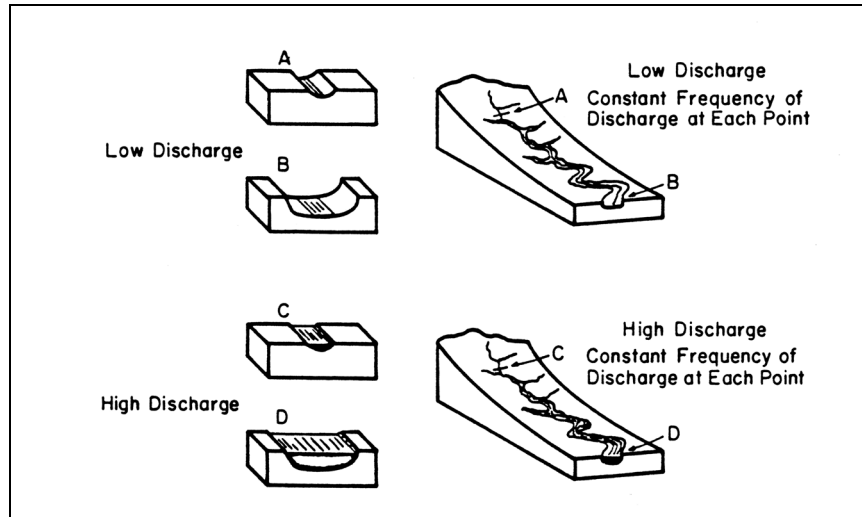


Figure 5.19. Variation of discharge at a given river cross section and at points downstream (after Leopold and Maddock 1953). At-a-station relations pertain to individual sites such as A or B. Downstream relations pertain to a channel (segment A-B) or drainage network for discharge of a given frequency of occurrence.

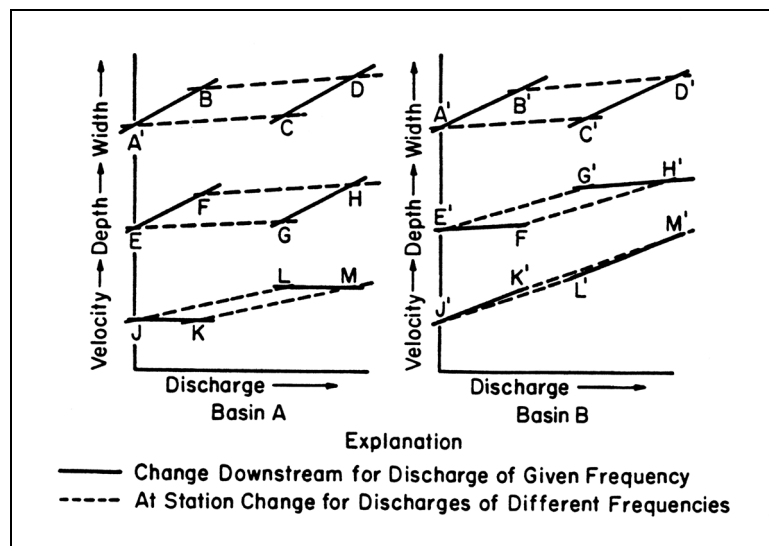


Figure 5.20. Schematic variation of width, depth, and velocity with at-a-station and downstream discharge variation (after Leopold and Maddock 1953).

The mean values of exponents b, f, m, j, z, and y as reported by Leopold et al. (1964) are given in Table 5.2. These values are based on an extensive analysis of stream data in the United States and are stream specific.

Table 5.2. At-A-Station and Downstream Hydraulic Geometry Relationships.						
Average At-A-Station Relations						
	b	f	m	j	z	y
Average values Midwestern United States	.26	.40	.34	2.5		
Brandywine Creek, PA	.04	.41	.55	2.2	.05	-.2
Ephemeral Streams in Semiarid U.S.	.29	.36	.34			
Average of 158 Gaging Stations in U.S.	.12	.45	.43			
Ten Gaging Stations on Rhine River	.13	.41	.43			
Average Downstream Relations (bank-full or mean annual flow)						
	b	f	m	j	z	y
Average values Midwestern United States	.5	.4	.1	.8	-.49	
Brandywine Creek, PA	.42	.45	.05		-1.07	-.28
Ephemeral Streams in Semiarid U.S.	.5	.3	.2	1.3	-.95	-.3
Appalachian Streams	.55	.36	.09			

In Table 5.3, derived hydraulic geometry relations for conditions at-a-station (variable discharge frequency) and in the downstream direction on the same stream at bankfull discharge (or constant frequency) are given. Note: the term "downstream" implies any other location along the channel, either upstream or downstream from a selected station. Bray (1982) and Julien and Simons (1984) determined that bed material size is an important variable in hydraulic geometry relations in alluvial gravel streams. Their relations for non-cohesive gravel-bed rivers in the downstream direction at bankfull discharge (or constant frequency) are also given in Table 5.3. Applications of these relationships are illustrated in Section 5.9 (Problems 5 and 6).

Table 5.3. Derived At-A-Station and Downstream Geometry Relationships.		
At-A-Station <sup>(1)</sup>	Downstream <sup>(1)</sup>	Downstream <sup>(2)</sup>
$y_o \approx Q^{0.40}$	$y_o \approx Q_b^{0.46}$	$y_o \approx Q_b^{0.40}$
$W \approx Q^{0.26}$	$W \approx Q^{0.46}$	$W \approx Q_b^{0.53} D_{50}^{-0.33}$
$V \approx Q^{0.34}$	$V \approx Q_b^{0.08}$	$V \approx Q_b^{0.07} D_{50}^{0.33}$
$S_f \approx Q^{0.00}$	$S_f \approx Q_b^{-0.46}$	$S_f \approx Q_b^{-0.4} D_{50}^{+1.00}$
<sup>(1)</sup> Sand bed		
<sup>(2)</sup> Gravel bed		

Work by Julien and Wargadalam (1995) has updated the theory and applications of hydraulic geometry relationships for alluvial channels. In their study, downstream hydraulic geometry of alluvial channels, in terms of bankfull width, average flow depth, mean flow velocity, and friction slope, is examined from a 3-dimensional stability analysis of noncohesive particles under 2-dimensional flows. Four exponent diagrams illustrate good agreement with several empirical regime equations found in the literature. The analytical formulations were tested with a comprehensive data set consisting of 835 field channels and 45 laboratory channels. The data set covers a wide range of flow conditions from meandering to braided sand-bed, and gravel-bed rivers.

#### 5.4.7 Dominant Discharge in Alluvial Rivers

The hydraulic geometry relations discussed in Section 5.4.6 indicate how the channel morphology and other characteristics vary with discharge at-a-station or in the downstream direction in a drainage network. In the hydraulic design of river crossings and encroachments, the relations need to be defined to determine the downstream hydraulic geometry of the channel at a site between two gaged sites. The question then arises about the frequency of discharge to be used in the hydraulic geometry relations. The downstream hydraulic geometry relations expressed in Section 5.4.6 relate to the bank-full stage, which for many humid region U.S. rivers has a frequency of occurrence of one in 1.5 years. For arid region streams, the bankfull return period may be on the order of five to ten years.

Analysis of bed sediment load estimations indicates that on most rivers, up to 90 percent of the total transport is caused by flows that are equaled or exceeded about ten percent of the time only. Thus, the average bed sediment load in a river may be described in terms of a formative discharge much larger than the mean annual flow. Also, the average channel width, depth and meander geometry may be defined in terms of different formative discharges rather than an arbitrarily chosen dominant discharge.

Research by the U.S. Army Corps of Engineers (Watson et al. 1999, Copeland and Hall 1998) suggests that the **effective discharge** is the best representation of the channel forming discharge. The effective discharge is the increment of discharge that transports the most sediment on an annual basis. This discharge may be determined by integrating a sediment transport rating curve with the annual flow-duration curve. Where possible, it is important to attempt to verify this channel-forming discharge with field indicators of bankfull discharge. Appendix A to the 1999 USACE reference cited above provides a practical guide to effective discharge calculations.

The concept of the frequency of occurrence of flows is important in the hydraulic design of highway crossings and encroachments. Both the at-a-station and downstream hydraulic geometry relations are especially useful when the hydraulic design is based on the frequency of occurrence of flows. The concept of bank-full condition corresponding to a discharge with a period of return of 1.5 years for perennial streams and five to ten years for ephemeral streams is recommended for practical use when detailed analysis of formative discharge is not possible, or feasible.

#### 5.4.8 River Profiles and Bed Material

The slope of a river channel or a river system is usually steepest in the headwater regions. The river profile is concave upward and the slope of the river profile can be represented by the equation:

$$S_x = S_o e^{-\hat{\alpha}x} \quad (5.12)$$

where:

$$\begin{aligned} S_x &= \text{Slope at any station a distance } x \text{ downstream of the reference station} \\ S_o &= \text{Slope at the reference station} \\ \hat{\alpha} &= \text{Coefficient} \end{aligned}$$

Similarly, the bed sediment size is coarser in the upper reaches where the channel slopes are steep and the bed sediment size becomes finer with distance downstream. Generally, the size of the bed material reduces with distance according to the relationship

$$D_{50_x} = D_{50_o} e^{-\hat{\beta}x} \quad (5.13)$$

where:

$$\begin{aligned} D_{50_x} &= \text{Median size of bed material at distance } x \text{ downstream of reference station} \\ D_{50_o} &= \text{Median size of bed material at the reference station} \\ \hat{\beta} &= \text{Coefficient} \end{aligned}$$

The hydraulic geometry relations are applicable to continuous channel behavior. In some cases, this behavior (in this case the slope) may become discontinuous as the channel pattern changes from meandering to braided by the formation of cutoffs. Application of Equation 5.13 is illustrated with field data in Section 5.9 (Problem 7).

### 5.5 QUALITATIVE RESPONSE OF RIVER SYSTEMS

Many rivers have achieved a state of practical equilibrium throughout long reaches. For practical engineering purposes, these stable reaches can be also called "graded" streams by geologists and "poised" streams by engineers. However, this does not preclude significant changes over a short period of time or over a period of years. Conversely, many streams contain long reaches that are actively aggrading or degrading. These aggrading and degrading channels pose a definite hazard to any highway crossing or encroachment, as compared to poised streams.

Regardless of the degree of channel stability, local human activities may produce major changes in river characteristics locally and throughout the entire reach. All too frequently the net result of a river improvement is a greater departure from equilibrium than that which originally prevailed. Good engineering design must invariably seek to enhance the natural tendency of the stream toward stable conditions. To do so, an understanding of the direction and magnitude of change in channel characteristics caused by human activity and natural processes is required. This understanding can be obtained by: (1) studying the river in a natural condition; (2) having knowledge of the sediment and water discharge; (3) being able to

predict the effects and magnitude of future human activities; and (4) applying a knowledge of geology, soils, hydrology, and hydraulics of alluvial rivers.

To predict river response to channel modifications is a very complex task. A large number of variables are involved in the analysis. These variables are interrelated and can respond to changes in a river system in the continual evolution of river form. The channel geometry, bars, and forms of bed roughness all change with changing water and sediment discharges. Because such a prediction is necessary, methods have been developed to predict the response of channel systems to changes both qualitatively and quantitatively.

### 5.5.1 General River Response to Change

Quantitative prediction of response can be made if all of the required data are known with sufficient accuracy. Usually, however, the data are not sufficient for quantitative estimates, and only qualitative estimates are possible. Examples of studies that have been undertaken by various investigators for qualitative estimates follow. Lane (1955) studied the changes in river morphology caused by modifications of water and sediment discharges. Similar but more comprehensive treatments of channel response to changing conditions in rivers have been presented by Leopold and Maddock (1953), Schumm (1971, 1977), Santos-Cayado (1972), Richards (1982), ASCE (1983), Thorne et al. (1997), Thorne (1998), and Knighton (1998). Research results support the following general statements:

1. Depth of flow is directly proportional to water discharge and inversely proportional to bed material discharge,
2. Width of channel is directly proportional to water discharge and to bed material discharge,
3. Shape of channel expressed as width-depth ratio is directly related to bed material discharge,
4. Meander wavelength is directly proportional to water discharge and to bed material discharge,
5. Slope of stream channel is inversely proportional to water discharge and directly proportional to bed material discharge and grain size, and
6. Sinuosity of stream channel is proportional to valley slope and inversely proportional to bed material discharge.

It is important to remember that these statements pertain to natural rivers and not necessarily to artificial channels with bank materials that are not representative of sediment load. In any event, the relations will help to determine the response of water conveying channels to change.

Bed material sediment transport ( $Q_s$ ) can be directly related to stream power ( $\tau_o V$ ) and inversely related to the fall diameter of bed material ( $D_{50}$ ).

$$Q_s \sim \frac{\tau_o V W C_f}{D_{50}} \quad (5.14)$$

Here  $\tau_o$  is the bed shear stress,  $V$  is the cross-sectional average velocity,  $W$  is the width of the stream and  $C_f$  is the volumetric concentration of fine sediments. Equation 5.14 can be written as:

$$Q_s \sim \frac{\gamma \gamma_o SW V C_f}{D_{50}} = \frac{\gamma QS C_f}{D_{50}} \quad (5.15)$$

If the specific weight,  $\gamma$ , is considered constant and if the concentration of wash load  $C_f$  can be incorporated in the fall diameter,  $D_{50}$ , then the relationship can be expressed as:

$$QS \sim Q_s D_{50} \quad (5.16)$$

which is the relationship originally proposed by Lane (1955), except Lane used the median diameter of the bed material as defined by sieving instead of the fall diameter. The fall diameter includes the effect of temperature on the transportability of the bed material, but use of physical diameter is sufficiently precise for most qualitative analyses.

The proportionality represented by Equation 5.16 is very useful to qualitatively predict channel response to climatological changes, river modifications, or both. Two simple example problems are analyzed using Equation 5.16.

In a first example, consider a tributary entering the main river at point C that is relatively small but carries a large sediment load (Figure 5.21). This increases the sediment discharge in the main stream from  $Q_s$  to  $Q_s^+$ . It is seen from Equation 5.16 that, for a significant increase in the sediment discharge ( $Q_s^+$ ) the channel gradient (S) below C must increase if Q and  $D_{50}$  remain constant. The line CA (indicating the original channel gradient) therefore changes with time to position C'A. Upstream of the confluence the slope will adjust over a long period of time to the original channel slope. The river bed will aggrade from C to C'. This change may induce a change in the channel morphology downstream of point C as the downstream reach may tend toward braiding. This possible change in planform geometry must be considered if any structure is to be built between points A and C'.

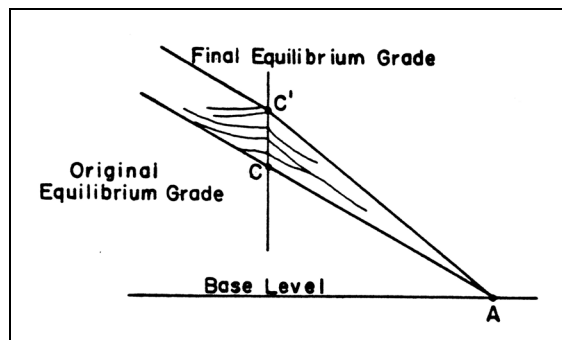


Figure 5.21. Changes in channel slope in response to an increase in sediment load at Point C.

In a second example, the construction of a dam on a river usually causes a decrease in sediment discharge downstream. Referring to Figure 5.22, and using Equation 5.16 and the earlier discussion, it can be concluded that for a decrease in bed material discharge from  $Q_s$  to  $Q_s^-$ , the slope S decreases downstream of the dam (assuming discharge and sediment size remain unchanged). In Figure 5.22, the line CA, representing the original channel gradient,



changes to C'A, indicating a decrease in bed elevation and slope in the downstream channel with time. Note, however, if the dam fills with sediment so that the incoming sediment discharge passes through, that, except for local scour at the dam, the grade line C'A would return to the line CA. Also upstream of the dam the grade would return to the original equilibrium grade but would be offset vertically by the height of the dam. Thus small reservoirs (storage capacity small in relation to annual discharge) may cause degradation below the dam and then aggradation over a relatively short period of time.

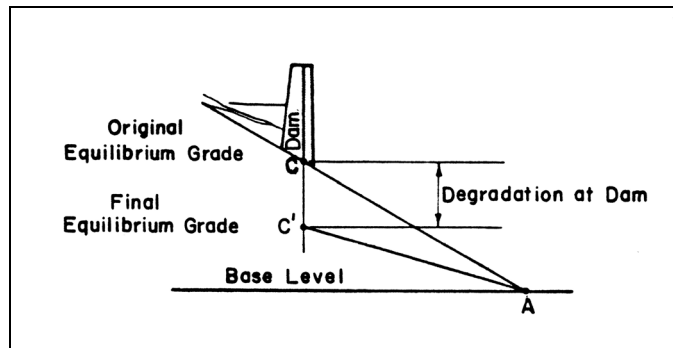


Figure 5.22. Changes in channel slope in response to a dam at point C.

The engineer is also interested in quantities in addition to qualitative trends. The geomorphic relation  $QS \sim Q_s D_{50}$  is only an initial step in analyzing long-term channel response problems. However, this initial step is useful because it warns of possible future difficulties related to channel modifications and flood protection works. The prediction of the magnitude of possible errors in flood protection design, because of changes in stage with time, requires the quantification of changes in stage. To quantify these changes, it is necessary to be able to quantify future changes in the variables that affect the stage. In this respect, knowledge of the future flow conditions is necessary.

In many instances it is important to assess the effects of changes in water and sediment discharge on specific variables such as depth of flow, channel width, characteristics of bed materials and velocity. For this type of analysis, we can use Equation 5.15 as follows:

$$Q_s D_{50} / C_f \sim SV y_o W \quad (5.17)$$

Using this form, the response of a river system to changes in specific variables is given in Table 5.4. A plus (+) sign signifies an increase in the value of the variable and a minus (-) sign signifies a decrease in the value of the variable. The letter B indicates an increase in the product  $SQ^{1/4}$  and a shift toward a braided condition and the letter M indicates a reduction in  $SQ^{1/4}$  and a shift toward the meandering condition (see Section 5.4.5). No attempt is made here to determine whether or not the channel actually braids or meanders.

Table 5.4. Change of Variables Induced by Changes in Sediment Discharge, Size of Bed Sediment and Wash Load.	
Relationship	Tendency to Braid or Meander
$Q_s^+ D_{50} / C_f \sim S^+ V^+ y_o^- W^+$	B
$Q_s^- D_{50} / C_f \sim S^- V^- y_o^+ W^-$	M
$Q_s D_{50}^+ / C_f \sim S^+ V^+ y_o^- W^+$	B
$Q_s D_{50}^- / C_f \sim S^- V^\pm y_o^\pm W^\pm$	M
$Q_s D_{50} / C_f^+ \sim S^- V^\pm y_o^\pm W^\pm$	M
$Q_s D_{50} / C_f^- \sim S^+ V^+ y_o^- W^+$	B
$Q_s^+ D_{50}^+ / C_f \sim S^+ V^+ y_o^- W^+$	B
$Q_s^- D_{50}^- / C_f \sim S^- V^\pm y_o^\pm W^-$	M
$Q_s^+ D_{50}^+ / C_f^- \sim S^+ V^+ y_o^- W^+$	B
$Q_s^- D_{50}^- / C_f^+ \sim S^- V^\pm y_o^\pm W^\pm$	M
$Q_s^+ D_{50}^+ / C_f^+ \sim S^+ V^+ y_o^- W^+$	B

Note: An increase in the value of the variable is denoted by a +; and a decrease is denoted by a -. As an example, in the first line, if the value of  $Q_s$  increases, the slope, velocity, and width will increase, the depth of flow will decrease and the channel may tend toward a braided form.

### 5.5.2 Prediction of Channel Response to Change

In Section 5.5.1, it was illustrated that the proportionality of Equation 5.16 could be used to predict changes in channel profiles caused by changes in water and sediment discharge. It is now possible to talk qualitatively about changes in channel profile, changes in river form and changes in river cross section both at-a-station and along the river channel using the other relations presented above.

This can be best illustrated by application. Referring to Table 5.5, consider the effect of an increase in discharge indicated by a plus sign on line (a) opposite discharge. The increase in discharge may affect the river form, energy slope, stability of the channel, cross-sectional area and river regime. Equations 5.1 and 5.2 or Figure 5.18 (which illustrates  $SQ^{0.25}$ ) show that an increase in discharge could change the channel form in the direction of a braided form. Whether or not the channel form changes would depend on the river form prior to the increase in discharge. With the increase in discharge the stability of the channel would be reduced, which indicates an increase in velocity. On the other hand, this prediction could be affected by changes in form of bed roughness that dictate resistance to flow.

The information presented in Chapter 4 can be used to determine the direction of change of hydraulic variables when sediment characteristics or discharges are varied. It is important to notice that Einstein, Colby, and Manning's equations apply to a cross section or reach and differ from some of the available geomorphic equations that have been derived by considering

a reach or total length of river. Einstein, Colby, and Manning's equations deal with depth of flow, width of flow and energy slope whereas most geomorphic equations deal with channel depth, channel width and channel slope.

The interdependency of top width, depth of flow, energy slope, bed-material size, and kinematic viscosity on the water and sediment discharge allows the establishment of the relative influence of those variables on stage-discharge relationships. This information can be used to establish the direction of variation of hydraulic variables as a consequence of changes imposed on the bed-material and sediment discharge as shown in Table 5.5.

Variable	Change in Magnitude of Variable	Effect On							
		Regime of Flow	River Form	Resistance to Flow	Energy Slope	Stability of Channel	Area	Stage	
Discharge	(a)	+	+	M→B	±	-	-	+	+
	(b)	-	-	B→M	±	+	+	-	-
Bed Material Size	(a)	+	-	M→B	+	+	±	+	+
	(b)	-	+	B→M	-	-	±	-	-
Bed Material Load	(a)	+	+	B→M	-	-	+	-	-
	(b)	-	-	M→B	+	+	-	+	+
Washload	(a)	+	+		-	-	±	-	-
	(b)	-	-		+	+	±	+	+
Viscosity	(a)	+	+		-	-	±	-	-
	(b)	-	-		+	+	±	+	+
Seepage Force	(a)	Outflow	-	B→M	+	-	+	+	+
	(b)	Inflow	+	M→B	-	+	-	-	-
Vegetation	(a)	+	-	B→M	+	-	+	+	+
	(b)	-	+	M→B	-	+	-	-	-
Wind	(a)	Downstream	+	M→B	-	+	-	-	-
	(b)	Upstream	-	B→M	+	-	-	+	+

Chapter 4 indicates that the wash load increases the apparent viscosity of the water and sediment mixture. This makes the bed material behave as if it were smaller. In fact, the fall diameter of the bed material is made smaller by significant concentrations of wash load. With more wash load, the bed material is more susceptible to transport and any river carrying significant wash load will change from lower to upper regime at a lower Froude number than otherwise. Also, the viscosity is affected by changes in temperature.

Seepage forces resulting from seepage losses help stabilize the channel bed and banks. With seepage inflow, the reverse is true. Vegetation adds to bank stability and increases resistance to flow, reducing the velocity. Wind can retard flow, increasing roughness and depth, when blowing upstream. The reverse is true with the wind blowing downstream. Wind generated waves and their adverse influence on channel stability are the most significant effects of wind.

In terms of channel stability, it is important to recognize that three geomorphic responses or processes can result from changes in dominant channel flow and sediment conditions. These are channel widening, channel deepening, and changing planform (a change in sinuosity or meander pattern). All of these responses will cause some level of streambank erosion.

Channel widening is evidenced through an increase in channel width, with or without an increase in channel depth. An increase in flow or sediment discharge results in a tendency toward channel widening. When both sediment discharge and flow increase, however, the channel section can be expected to increase its depth as well as its width. When only sediment load increases, width increases but the depth may decrease. In this case the channel is said to be aggrading, implying that the channel has filled in because of an excess of sediments.

Channel deepening is a process of channel degradation that increases the depth of the channel. Channel degradation can cause bank instability by producing a steeper bank angle. Whether or not instability actually occurs is a function of the properties of the bank materials and the original bank geometry. Channel deepening results from increased flow without an appreciable increase in sediment discharge. Increased flow rates can result from an overall increase in the volume of water moving through the channel or an increase in channel slope.

Changing channel planform includes changes in channel pattern and position as viewed from above. Changes in planform are most often exhibited through the downstream migration of meandering bends and changes in the sinuosity of meander bends. Other examples include the shifting of channels and the cutting off of meander bends. Generally, these changes are manifested by an adjustment of channel slope to conform with changes in flow or sediment discharge.

A reduction in sediment discharge or an increase in water discharge will result in a reduction of the channel slope. These slope reductions result from increased channel sinuosity and/or channel-bed degradation; both of which lead to a tendency toward increased bank erosion. Also, a reduction in sediment discharge will result in an increase in channel sinuosity, again, leading to increased bank erosion.

It is also important to recognize that the three geomorphic processes just discussed (channel widening, channel deepening, and changing planform) are often interrelated and can occur simultaneously or in sequence. For example, adjustments in channel slope through degradation often are accompanied by increases in channel sinuosity and bank caving or channel widening. Also, the initiation of a given process at a particular site may initiate another process either upstream or downstream. For example, an aggrading channel reach can cause an increase in sinuosity in a downstream reach.

### **5.5.3 River Pattern Thresholds and Response**

The work of Lane (1957) and Leopold and Wolman (1960) as summarized in Section 5.4.5 indicates that there is a gradient or discharge threshold above which rivers tend to be braided (Figure 5.18). The experimental work reported by Schumm and Khan (1972) shows that for a given discharge, as valley-floor slope is progressively increased, a straight river becomes sinuous and then eventually braided at high values of stream power and sediment transport (Figure 5.3). Rivers that are situated close to the meandering-braided threshold should have a history which is characterized by transitions in morphology from braided to meandering and vice versa.

If the natural range of patterns along a river can be identified, then within that range it should be possible to identify the most appropriate channel pattern and sinuosity. If so, the engineer can work with the river to produce its most efficient or most stable channel. Obviously, a river can be forced into a straight configuration or it can be made more sinuous, but there is a limit to the changes that can be induced beyond which the channel cannot function without a radical morphologic adjustment as suggested by Figure 5.4. Identification of rivers that are near the pattern threshold would be useful, because a braided river near the threshold might be converted to a more stable, meandering, single-thalweg stream. On the other hand, a meandering stream near the threshold should be identified in order that steps could be taken to prevent braiding due, perhaps, to changes of land use.

Perhaps the best qualitative guide to river stability is a comparison of the morphology of numerous reaches, and the determination of whether or not there has been a change in the position and morphology of the channel in the past. Another approach might be to determine the position of the river on the Leopold-Wolman (1957) or Lane (1957) gradient-discharge graphs (Figure 5.18). If a braided river plots among the meandering channels or vice versa, it is a likely candidate for change because it is incipiently unstable.

An example of the way that this could be done is provided by the Chippewa River of Wisconsin, a major tributary to the Mississippi River (Schumm and Beathard 1976). The Chippewa River rises in northern Wisconsin and flows 320 km (200 mi) to the Mississippi River, entering it 120 km (75 mi) below St. Paul (Figure 5.23). It is the second largest river in Wisconsin, with a drainage basin area of 24 600 km<sup>2</sup> (9,500 sq mi).

From its confluence with the Mississippi to the town of Durand 26.5 km (16.5 mi) up the valley, the Chippewa is braided (Table 5.6). The main channel is characteristically broad and shallow, and it contains shifting sand bars. The bankfull width as measured from U.S. Geological Survey topographic maps is 333 m (1,092 ft). The sinuosity of this reach is very low, being only 1.06. However, in the 68 km (42 mi) reach from Durand to Eau Claire, the Chippewa River has a meandering configuration with a bankfull width of 194 m (636 ft) and a sinuosity of 1.49. The valley slope and channel gradient are different for each reach of the river. The braided section has a gentler valley slope than the meandering reach upstream, 0.00035 as opposed to 0.00040, contrary to what is expected from Figure 5.18, but the situation is reversed for channel slope. The braided reach has a channel gradient of 0.00033, whereas the meandering reach has a gradient of 0.00028.

Location	Channel Pattern	Channel Width m (ft)	Sinuosity	Valley Slope	Channel Slope
Below Durand	Braided	333 (1,092)	1.06	0.00035	0.00033
Above Durand	Meandering	194 (636)	1.49	0.0004	0.00028
Buffalo Slough	Meandering	212 (695)	1.28	0.00035	0.00027

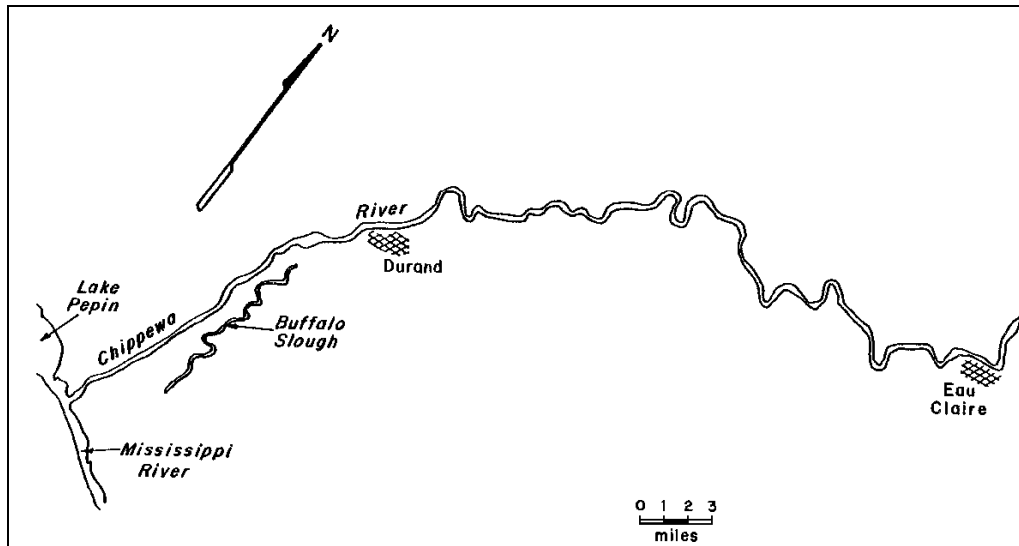


Figure 5.23. Map of lower Chippewa River. The river is braided below Durand, Wisconsin. Buffalo Slough is an old course of Chippewa River (Schumm and Beathard 1976).

There is no evidence to suggest that the Chippewa River is either progressively eroding or aggrading its channel at present. In fact, the river below Durand has remained braided during historic time. It has maintained its channel position and its pattern, but a significant narrowing as the result of the attachment of islands and the filling of chute channels has occurred downstream of Durand, which resulted in a recent decrease in channel width of over 40 percent. The only other change in the lower river is a noticeable growth of the Chippewa delta into the Mississippi valley. The delta deposits show increased vegetational cover as well as extension into the Mississippi River valley.

The relations described by Leopold and Wolman (1957) and Lane (1957), which are combined in Figure 5.18, provide a means of evaluating the relative stability of the modern channel patterns of the Chippewa River. The bankfull discharge was plotted against channel slope on Figure 5.24 (the Leopold and Wolman relationship) for both the braided and the meandering reaches of the Chippewa. The value used for the bankfull discharge is  $1,503 \text{ m}^3/\text{s}$  (53,082 cfs), which is the flood discharge having a return period of 2.33 years. The braided reach plots higher than the meandering reach, but both are well within the meandering zone, as defined by Leopold and Wolman. This suggests that the braided reach is anomalous; that is, according to this relation the lower Chippewa would be expected to display a meandering pattern rather than a braided one. Even when the 25-year flood of  $2,787 \text{ m}^3/\text{s}$  (98,416 cfs) is used, the braided reach still plots within the meandering region of Figure 5.24.

When the Chippewa data are plotted on Lane's graph (Figure 5.25) the same relation exists. The Chippewa River falls in the intermediate region, but within the range of scatter about the regression line for meandering streams. Again the braided reach is seen to be anomalous because it should plot much closer to or above the braided stream regression line. The position of the braided reach as plotted on both figures indicates that this reach should be meandering.

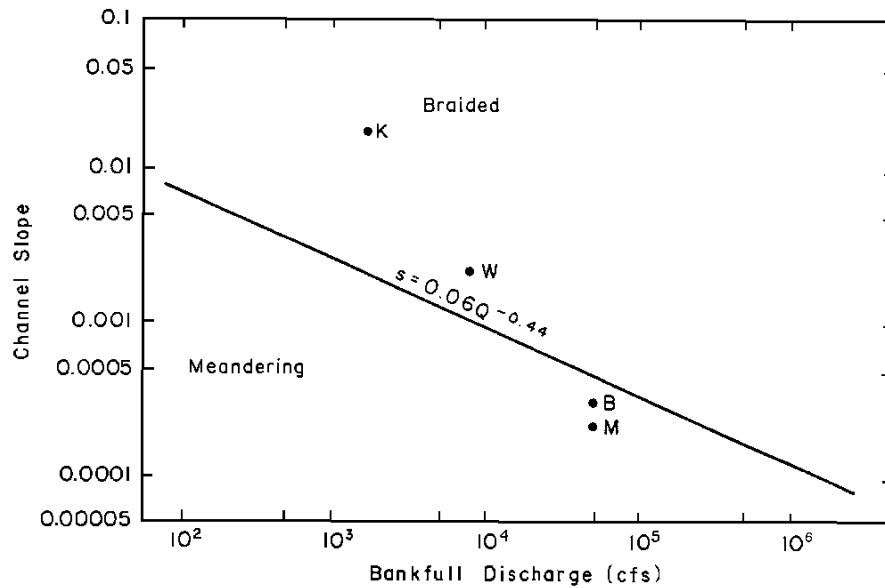


Figure 5.24. Leopold and Wolman's (1957) relation between channel patterns, channel gradient, and bankfull discharge. Letters B and M identify braided and meandering reaches of Chippewa River. Letters K and W refer to Kowhai and Wairau Rivers (Schumm and Beathard 1976).

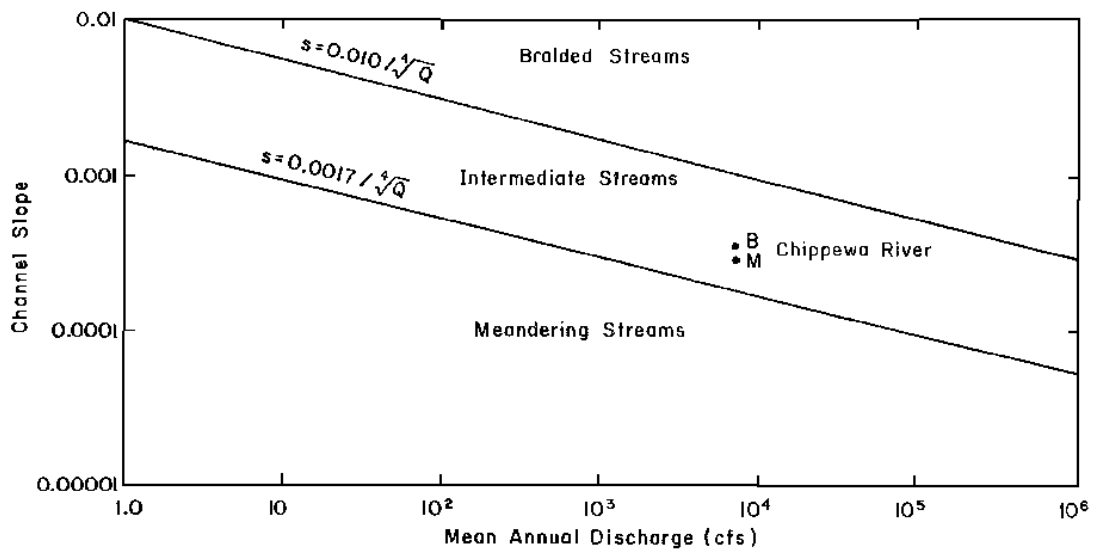


Figure 5.25. Lane's (1957) relation between channel patterns, channel gradient, and mean discharge. The regression lines were fitted to data from streams that Lane classified as highly meandering to braided. Letters B and M identify position of the braided and meandering reaches of the Chippewa River (Schumm and Beathard 1976).

This conclusion requires an explanation that can be based on the geomorphic history of Chippewa River. For example, there is a significant morphologic feature on the Chippewa River floodplain, Buffalo Slough, which occupies the southeastern edge of the floodplain (Figure 5.23). It is a sinuous remnant of the Chippewa River that was abandoned, and it is evidence of a major channel change in the Chippewa River valley (Table 5.6).

Flow through Buffalo Slough has decreased during historic time, and indeed flow was completely eliminated in 1876, when the upstream end of Buffalo Slough was permanently blocked. The abandonment of the former Buffalo Slough channel by the Chippewa River is the result of an avulsion, but one that took many years to complete. The channel shifted from Buffalo Slough to a straighter, steeper course along the northwestern edge of the floodplain. This more efficient route gradually captured more and more of the total discharge. The new Chippewa channel produced a braided configuration due to a higher flow velocity and the resulting bank erosion. As the new channel grew, the old course deteriorated and eventually its discharge was so reduced that the Mississippi was able to effectively dam the old channel mouth with natural levees and plug its outlet.

The sinuosity of Buffalo Slough is approximately 1.28. Although sinuosity is usually defined as the ratio of stream length to valley length, it is also the ratio of valley slope to channel slope. A sinuosity of 1.28 is, therefore, the ratio of the present valley slope (0.00035) to a channel slope of about 0.0027. This channel slope value is very similar to the channel slope of the meandering reach upstream of Durand (0.00028) therefore, the meandering pattern of the Buffalo Slough channel was appropriate. Although delta construction at the Mississippi River confluence was responsible for the lower valley slope of the lower Chippewa River valley, the Buffalo Slough channel had a gradient that was not appreciably different from that in the upstream reach. Channel sinuosity decreased from 1.49 to 1.28 in a downstream direction, thereby maintaining a channel gradient of about 0.00027.

This sinuous channel could not have transported the large amounts of sediment that the present braided channel carries to the Mississippi River, or it too would have followed a straight braided course. Therefore, the present sediment load carried by the Chippewa River is greater than that conveyed by the Buffalo Slough channel, but this is due almost entirely to the formation of the new straight, steep, braided channel, which is 121 m (397 ft) wider than the old sinuous Buffalo Slough channel. It appears that the lower Chippewa has not been able to adjust as yet to its new position and steeper gradient, and the resulting bed and bank erosion has supplied large amounts of sediment to the Mississippi. The normal configuration of the lower Chippewa is sinuous, and if it could be induced to assume such a pattern, the high sediment delivery from the Chippewa might be controlled. An appropriate means of channel stabilization and sediment load reduction in this case is the development of a sinuous channel.

Since the above suggestions were made (Schumm and Beathard 1976), more detailed studies of the Chippewa River basin indicate that upstream sediment production must be controlled, especially where the upper Chippewa River is cutting into the Pleistocene outwash terraces. If the contribution of sediment from these sources were reduced, the lower Chippewa could resume its sinuous course.

An indication that the pattern conversion of the Chippewa could be successful if the upstream sediment sources were controlled is provided by the Rangitata River of New Zealand. The Rangitata River is the southern most of the major rivers which traverse the



Canterbury Plains of South Island. It leaves the mountains through a bedrock gorge. Above the gorge, the valley of the Rangitata is braided, and it appears that the Rangitata should be a braided stream below the gorge, as are all the other rivers which cross the Canterbury Plain. However, below the gorge, the Rangitata is meandering. A few miles farther downstream, the river cuts into high Pleistocene outwash terraces, and it abruptly converts from a meandering to a braided stream. The braided pattern persists to the sea. If the Rangitata could be isolated from the gravel terraces, it probably could be converted to a single-thalweg sinuous channel, because the Rangitata is obviously a river near the pattern threshold.

There are other New Zealand rivers that are near the pattern threshold. and therefore, they are susceptible to pattern change. In fact, New Zealand engineers are attempting to accomplish this pattern change in order to produce 'single-thread' channels which will cause less flood damage, have greater stability at bridge crossings, and be less likely to acquire large sediment loads from their banks and terraces. For example, the engineers have had success in converting the Wairau River, a major braided stream, from its uncontrolled braided mode to that of a slightly sinuous, single-thalweg, relatively more stable channel. The increase in sinuosity is only from 1.0 to 1.05, and this was accomplished by the construction of curved training banks. On Figure 5.24 the Wairau River plots close to the threshold line, and with the reduction of sediment load produced by bank stabilization, it appears that the pattern threshold can be crossed successfully.

Farther to the south near Kaikoura, the Kowhai River is being modified in the same manner as was the Wairau. Whereas much of the sediment load in the Wairau River is derived from bank and terrace erosion which can be controlled, high sediment loads are delivered to the Kowhai River directly from steep and unstable mountain slopes. On Figure 5.24 the Kowhai River plots well above the threshold line, and without a major reduction in upstream sediment, it may be difficult to maintain a single-thalweg channel at this location.

The variability of the Rangitata River pattern indicates that braided to single-thalweg conversions should be possible for the Chippewa and Wairau Rivers. However, not all braided rivers can be so readily modified, as this depends on their position with regard to the line defining the pattern thresholds on Figures 5.24 and 5.25.

Perhaps the simplest way to determine the most likely pattern for a river is to determine its pattern from the earliest maps and aerial photographs. If the river was braiding in the past, it seems unlikely that an attempt to convert to a sinuous channel will be successful. However, if the historic river was meandering and it is now braided, although there have been no major erosional or hydrologic changes in the drainage basin, then a conversion back to a meandering pattern is appropriate. Another approach is to determine the characteristics of other nearby rivers. If the subject river is very different it may be converted to the local character if neither the sediment load or hydrologic character are significantly different.

## **5.6 MODELING OF RIVER SYSTEMS**

The necessity for quantitative prediction of river channel response is increasing. The accuracy of such a prediction depends on the quality of the data. There are generally two ways of predicting response. One is the mathematical model and the other is the physical model. Mathematical models utilize a number of mathematical equations governing the motion of water and sediments in a channel. Regardless of the potential of mathematical models, to date they have been best used to study channel response using 1-dimensional, or at most 2-dimensional, approximations. For complex three-dimensional channel processes, it is very difficult to accurately formulate mathematically what happens in a river. Studies of channel

response to development for complex situations are usually made using a physical model. The physical model is designed to achieve similar behavior as that of the prototype. The relationship of the governing physical processes and parameters must then be the same for the model as for the prototype.

### 5.6.1 Physical Modeling

Physical models are used to test the performance of a design or to study the details of a phenomenon. The performance tests of proposed structures can be made at moderate costs and small risks on small-scale (physical) models. Similarly, the interaction of a structure and the river environment can be studied in detail. In this regard, HEC-23 (Lagasse et al. 2001) discusses the use of physical modeling in bridge scour and stream instability countermeasure design.

The natural phenomena are governed by appropriate sets of governing equations. If these equations can be integrated, the prediction of a given phenomena in time and space domains can be made mathematically. In many cases related to river engineering, all the governing equations are not known. Also, the known equations cannot be directly treated mathematically for the geometries involved. In such cases, physical models are used to physically represent solutions to the governing equations.

The similitude required between a prototype and a model implies two conditions:

1. To each point, time and process in the prototype, a uniquely coordinated point, time and process exists in the model; and
2. The ratios of corresponding physical magnitudes between prototype and model are constant for each type of physical quantity.

Rigid Boundary Models. To satisfy the preceding conditions in clear water, geometric, kinematic, and dynamic similarities must exist between the prototype and the model. Geometric similarity refers to the similarity of form between the prototype and its model. Kinematic similarity refers to similarity of motion, while dynamic similarity is a scaling of masses and forces. For kinematic similarity, patterns or paths of motion between the model and the prototype should be geometrically similar. If similarity of flow is maintained between the model and prototype, mathematical equations of motion will be identical for the two. Considering the equations of motion, the dimensionless ratios of  $V / \sqrt{gy}$  (Froude number) and  $Vy/\nu$  (Reynolds number) are both significant parameters in models of rigid boundary clear water open channel flow. The Froude number represents the ratio of inertial to gravity forces in the system being modeled, while the Reynolds number represents the ratio of inertial to friction (viscosity) forces.

It is seldom possible to achieve kinematic, dynamic and geometric similarity all at the same time in a model. For instance, in open channel flow, gravitational forces predominate, and hence, the effects of the Froude number are more important than those of the Reynolds number. Therefore, the Froude criterion is used to determine the geometric scales, but only with the knowledge that some scale effects, that is, departure from strict similarity, exists in the model.

Ratios (or scales) of velocity, time, force and other characteristics of flow for two systems are determined by equating the appropriate dimensionless number which applies to a dominant force. If the two systems are denoted by the subscript m for model and p for prototype, then

the ratio of corresponding quantities in the two systems can be defined. The subscript  $r$  is used to designate the ratio of the model quantity to the prototype quantity. For example, the length ratio is given by:

$$L_r = x_m / x_p = y_m / y_p = z_m / z_p \quad (5.18)$$

for the coordinate directions,  $x$ ,  $y$ , and  $z$ . Equation 5.18 assumes a condition of exact geometric similarity in all coordinate directions.

Frequently, open channel models are distorted. A model is said to be distorted if there are variables that have the same dimension but are modeled by different scale ratios. Thus, geometrically distorted models can have different scales in horizontal ( $x$ ,  $y$ ) and vertical ( $z$ ) directions, and two equations are necessary to define the length ratios in this case.

$$L_r = x_m / x_p = y_m / y_p \quad (5.19)$$

and

$$z_r = z_m / z_p \quad (5.20)$$

If perfect similitude is to be obtained the relationships that must exist between the properties of the fluids used in the model and in the prototype are given in Table 5.7 for the Froude (gravity), Reynolds (viscosity), and Weber (surface tension) criteria. The use of this table is presented in Section 5.9, Problems 5 and 6.

In free surface flow, the length ratio is often selected arbitrarily, but with certain limitations kept in mind. The Froude number is used as a scaling criterion because gravity has a predominant effect. However, if a small length ratio is used (very shallow water depths) then surface tension forces, which are included in the Weber number ( $V / \sqrt{\sigma / \rho L}$ ), may become important and complicate the interpretations of results of the model. It is desirable that the length scale be made as large as possible so that the Reynolds number is sufficiently large that friction becomes a function of the boundary roughness (and essentially independent of the Reynolds number). A large length scale also ensures that the flow is as turbulent in the model as it is in the prototype.

The boundary roughness is characterized by Manning's roughness coefficient,  $n$ , in free surface flow. Analysis of Manning's equation and substitution of the appropriate length ratios, based upon the Froude criterion, results in an expression for the ratio of the roughness which is given by

$$n_r = L_r^{1/6} \quad (5.21)$$

It is not always possible to achieve boundary roughness in a model and prototype that corresponds to that required by Equation 5.21 and additional measures such as adjustment of the slope, may be necessary to offset disproportionately high resistance in the model.

Table 5.7. Scale Ratios for Similitude.				
Characteristic	Dimension	Re	Fr	We
Length	L	L	L	L
Area	L <sup>2</sup>	L <sup>2</sup>	L <sup>2</sup>	L <sup>2</sup>
Volume	L <sup>3</sup>	L <sup>3</sup>	L <sup>3</sup>	L <sup>3</sup>
Time	T	$\rho L^2/\mu$	$(L\rho/\gamma)^{1/2}$	$(L^3\rho/\sigma)^{1/2}$
Velocity	L/T	$\mu/L\rho$	$(L\gamma/\rho)^{1/2}$	$(\sigma/L\rho)^{1/2}$
Acceleration	L/T <sup>2</sup>	$\mu^2/\rho^2L^3$	$\gamma/\rho$	$\sigma/L^2\rho$
Discharge	L <sup>3</sup> /T	$L\mu/\rho$	$L^{5/2}(\gamma/\rho)^{1/2}$	$L^{3/2}(\sigma/\rho)^{1/2}$
Mass	M	L <sup>3</sup> ρ	L <sup>3</sup> ρ	L <sup>3</sup> ρ
Force	ML/T <sup>2</sup>	$\mu^2/\rho$	L <sup>3</sup> γ	Lσ
Density	M/L <sup>3</sup>	ρ	ρ	ρ
Specific Weight	M/L <sup>2</sup> T <sup>2</sup>	$\mu^2/L^2\rho$	γ	$\sigma/L^2$
Pressure	ML/T	$\mu^2/L^2\rho$	Lγ	$\sigma/L$
Impulse & Momentum	ML <sup>2</sup> /T <sup>2</sup>	L <sup>2</sup> μ	$L^{7/2}(\rho\gamma)^{1/2}$	$L^{5/2}(\rho\sigma)^{1/2}$
Energy and Work	ML <sup>2</sup> /T <sup>2</sup>	$L\mu^2/\rho$	L <sup>4</sup> γ	L <sup>2</sup> σ
Power	ML <sup>2</sup> /T <sup>3</sup>	$\mu^3/L\rho^2$	$L^{7/2}\gamma^{3/2}\rho^{-1/2}$	$\sigma^{3/2}(L\rho)^{1/2}$

Mobile Bed Models. In modeling highway crossings and encroachments in the river environment, two- and three-dimensional mobile bed models are often used. These models have the bed and sides molded of materials that can be moved by the model flow. Similitude in mobile bed models implies that the model reproduces the fluvial processes such as bed scour, bed deposition, lateral channel migration, and varying boundary roughness. It is generally not possible to faithfully simulate all of these processes simultaneously on scale models. Distortions of various parameters are often made in such models.

Two approaches are available to design mobile bed models. One approach is the analytical derivation of distortions explained by Einstein and Chien (1956) and the other is based on hydraulic geometry relationships given by Lacey, Blench, and others (Mahmood and Shen 1971). In both of these approaches, a first approximation of the model scales and distortions can be obtained by numerical computations. The model is built to these scales and then verified for past information obtained from the prototype. In general, the model scales need adjusting during the verification stage.

Model verification consists of the reproduction of observed prototype behavior under given conditions on the model. This is specifically directed to one or more alluvial processes of interest. For example, a model may be verified for bed-level changes over a certain reach of the river. The predictive use of the model should be restricted to the aspects for which the model has been verified. The use is based on the premise that if the model has successfully

reproduced the phenomenon of interest over a given hydrograph as observed on the prototype, it will also reproduce the future response of the river over a similar range of conditions.

The mobile bed models are more difficult to design and their theory is significantly more complicated as compared to clear water rigid bed models. However, many successful examples of their use are available. In general, important river training and control works are invariably studied on physical models. The interpretation of results from a mobile bed model requires a basic understanding of the fluvial processes and some experience with such models. Even in the many cases where it is only possible to obtain qualitative information from mobile bed models, this information is of great help in comparing the performance of different designs.

Adoption of a particular method for estimating river response depends on quality and availability of data as well as the engineer's experience. More information on physical modeling can be found in HEC-23 and reports by Gessler (1971), Yalin (1971), Shen (1979), and Richardson et al. (1987, 1989). Additional applications of physical model studies of alluvial channel flow at highway crossings can be found in: "Hydraulic, Erosion, and Channel Stability Analysis of the Schoharie Creek Bridge Failure, New York," (Richardson et al. 1987); "Flume Modeling Experimental Plan for the Replacement of the Herbert C. Bonner Bridge," (Parsons Brinkerhoff Quade and Douglas, Inc. 1996); "Laboratory Report of the Acosta Bridge Scour Study," (Stein, S.M. et al. 1990); "FHWA Hydraulics Laboratory and Partners Perform Scour Evaluation for Woodrow Wilson Bridge" (Jones, J.S. 1999); and "Local Pier Scour Model Tests for Jensen Beach Bridge," (Sheppard, D.M. 1999).

### **5.6.2 Computer Modeling**

The design engineer's interest in alluvial river response is generally focused on anticipating how the river bed and water-surface elevations will change if an existing stable or equilibrium situation is perturbed. This perturbation may be the occurrence of an unusually large annual flood that temporarily scours the bed and banks to accommodate the higher flow before returning to normal conditions. The perturbation may also be a permanent change in river discharge and sediment supply caused by upstream regulation of flows, or a change in channel geometry resulting from bank stabilization or channelization. The first type of perturbation can often be simulated using a physical scale model. Although problems arise with interpretation of the results, physical models in the hands of experience modelers can yield valuable information on local scour and deposition around structures. However, the sheer expense and space requirements of physical scale models generally disqualify them for simulation of long-term, large-scale river bed response to the second type of perturbation. This is where numerical, computer-based models, which can simulate both short- and long-term response, find their natural area of application. Another area where prediction of long-term response is desired is river stabilization and river restoration design.

Numerical models of alluvial river response are the natural outgrowth of rigid-boundary, unsteady flood propagation models that have proven so useful in engineering design. These unsteady flow models have succeeded because they are based on mathematical descriptions that incorporate all the important physical processes involved and use reliable, carefully implemented numerical methods to obtain approximate solutions to the appropriate partial-differential equations. However, alluvial river-response models have not enjoyed the success of their rigid-boundary cousins, precisely because of the weaknesses in our

understanding and mathematical formulation of the relevant physical processes. Notwithstanding this fundamental difficulty, design engineers have an immediate need for reliable numerical simulations, and hydraulic research engineers have targeted alluvial river hydraulics as a prime area for continuing fundamental and applied research. Out of this fortunate confluence of interest have arisen a variety of simulation techniques and software systems, as well as many apparently successful simulations of prototype situations.

The most basic one-dimensional description of water and sediment flow in an alluvial river consists of four relations: conservation of water; conservation of water momentum; conservation of sediment; and sediment-transport relationships. These equations form a nonlinear partial-differential system that in general cannot be solved analytically.

When the water wave propagation effects are of secondary importance for sediment-transport phenomena, the system of equations can be simplified by assuming that the water flow remains quasi-steady during a certain interval of time.

Most published 1-dimensional software systems for the solution of the water- and sediment-flow equations use one form or another of the finite-difference method, in which time and space derivatives are approximated by differences of nodal values of grid functions that replace the continuous functions, leading to a system of algebraic equations. Some authors have used the finite-element method, but in one dimension there does not appear to be any strong reason for doing so. In any case, the quality and reliability of numerical models for bed evolution are determined primarily by the sediment-transport formulation and mechanisms adopted for sorting, armoring, and so forth. The particular numerical method used, as long as it is consistent with the partial-differential equations and is stable, has only a secondary effect on simulation quality.

Whether the full unsteady set of equations or the quasi-steady set of equations is solved numerically, two basic approaches are possible: coupled or uncoupled. In the coupled case, a simultaneous solution of both water and sediment equations is sought. This is evidently the physically proper way to proceed, because the water-flow and sediment-transport processes occur simultaneously. However, the simultaneous solution may involve certain computational complications, especially when the sediment-transport flow resistance equation involves not just an analytic mathematical expression, but a whole series of procedures and computations to simulate alluvial channel processes such as armoring, sorting, and bed forms.

The uncoupled procedure has arisen essentially to circumvent the computational difficulties of the coupled approach. The uncoupling of the liquid and solid transport occurs during a short computational time step. First the water-flow equations are solved to yield new values of depth and velocity throughout the reach of interest, assuming that neither the bed elevation nor the bed-sediment characteristics change during the time step. Then the depths and velocities are taken as constant, known inputs to the sediment continuity and transport equations; these equations then become relatively easy to solve numerically, yielding the new bed elevations. When the overall model includes bed-sediment sorting or armoring, these processes are simulated in a third uncoupled computational phase using new depths, velocities, and bed elevations as known inputs. Although it is difficult to quantify the error associated with this artificial uncoupling of simultaneous, mutually dependent processes, it is intuitively obvious that the uncoupling is justified only if bed elevations and bed-material characteristics change very little during one time step. Experience in the use of uncoupled models, with both the unsteady

and quasi-steady water-flow equations, has shown that the uncoupling is not a serious obstacle to successful simulation.

Another distinguishing feature of numerical bed-evolution models is the representation of sediment sorting and bed-surface armoring. Alluvial sediments are rarely of uniform grain size. A broad range of sizes are represented, from gravels and coarse sands down to fine silt and clay in varying proportions. Finer particles are preferentially entrained into the flow as erosion occurs, so that the material remaining on the bed contains a progressively higher proportion of coarser material. This so-called sorting process tends to increase the mean bed-sediment size as degradation occurs, thus affecting the sediment-transport rate, river regime (existence of ripples and dunes), and flow resistance through both particle roughness and bed-form effects. If the original bed material contains a high enough proportion of large, non-moveable materials (coarse gravel, cobbles, and small boulders), an interlocking armor layer may form on the surface, arresting further degradation. These processes are qualitatively reversed during deposition, but become even more difficult to quantify. Some models attempt to simulate sorting effects on bed evolution; others ignore them completely. Thus another important distinguishing feature of computer-based models is the degree to which they incorporate sorting and armoring effects.

Numerical modeling of alluvial river flows has become very popular in the 1990s because of the advancement of computer technology. However, the number of computer-based, alluvial riverbed prediction models that are readily available for application to prototype cases seems to be quite small. Many of the available models have been developed for specific rivers under particular flow and alluvial river bed conditions, and many of them are, to some extent, well tuned or calibrated only for those particular rivers.

The following assessment of selected models is made for two different groups: short-term models and long-term models. The short-term models are best suited to compute changes in alluvial river bed level during a relatively short time period. Long-term models employ simpler implementations of steady-state flow equations, and thus are suited for long-term prediction of river bed level for multiple-flood events over multiple years. However, it should be recognized that the short-term models can also be applied for long-term prediction if variable time steps are employed. In that case, a shorter time step is used for highly unsteady flows and a longer time step is used otherwise.

BRI-STARS MODEL (The Bridge Stream Tube Model for Alluvial River Simulation). The BRI-STAR (Molinas 2000) model developed for the Federal Highway Administration is a semi-two-dimensional model capable of computing alluvial scour/deposition through subcritical, supercritical, and a combination of both flow conditions involving hydraulic jumps. Both energy and momentum equations are used so the water surface profile computation can be carried out through combinations of subcritical and supercritical flows without interruption. The stream tube concept is used in a semi-two-dimensional way, which allows the lateral and longitudinal variation of hydraulic conditions as well as sediment activity at various cross sections along the study reach. The sediment continuity equation and sediment transport capacity equations are used for sediment routing computations to simulate the general scour in the river bed elevation. The sediment routing is performed for each size fraction to account for the bed composition changes and the bed armoring processes. The minimum rate of energy dissipation theory is used for decisions as to whether channel adjustments taking place at a given cross section. BRI-STARS is capable of simulating channel widening/narrowing phenomenon.

The channel widening/narrowing is accomplished by coupling a stream tube computer model with a decision-making algorithm using rate of energy dissipation or total stream power minimization. The first component, the fixed-width streamtube computer model, simulates the scouring/deposition process taking place in the vertical direction across the channel. The user can select from one of seven sediment transport functions including one general function including velocity depth, discharge, energy slope, and grain size. The second component, the total stream power minimization algorithm, determines what takes place in the lateral or vertical direction. It is this component that allows the lateral changes in channel geometries. Finally, the bridge component allows the computation of the hydraulic flow variables and the resulting scour due to highway encroachments.

HEC-6. The HEC-6 program (Scour and Deposition in Rivers and Reservoirs) was developed at the Hydrologic Engineering Center of the U.S. Army Corps of Engineers (HEC 1993). The quasi-steady backwater equation is used to compute water-flow conditions uncoupled from the sediment-continuity equation, and is intended for long-term river response simulation.

The sediment-continuity equation is solved using an explicit finite-difference scheme, with sediment-transport capacities determined from water-flow conditions previously determined in the uncoupled backwater computation. The entire movable bed portion of the channel is assumed to aggrade or degrade uniformly. Sediments are routed by individual size fraction, which makes possible a detailed accounting of hydraulic sorting and development of an armored layer. The user can select from thirteen sediment transport functions including one general function including depth and slope. Bank lines are assumed to be stable and fixed in the HEC-6 computation.

HEC-6 is strictly a one-dimensional model with no provision for simulating the development of meanders or specifying a lateral distribution of sediment transport rate across the section. The model is not suitable for rapidly changing flow conditions but can be applied to predict reservoir sedimentation, degradation of the streambed downstream from a dam, and long-term trends of scour or deposition in a stream channel, including the effects of dredging. It is anticipated that future versions of HEC-RAS will incorporate sediment transport and replace HEC-6.

FLUVIAL-12. This uncoupled model was developed at San Diego State University by Chang (1998) to simulate one dimensional, unsteady, gradually varied, water and sediment flows for channels. The model also includes the capacity to simulate bank erosion and is described as an erodible-boundary model as opposed to an erodible bed model by Chang. FLUVIAL-12 first solves the unsteady, flow-continuity and flow-momentum equations in one time step by neglecting storage effects due to unsteady flow. The model uses an implicit, central-difference, numerical scheme in solving for the two unknown variables of water discharge and cross-sectional area. The flow information is then used to compute the bed sediment discharge at each section using one of six user selected sediment transport functions.

Next, the net change in cross-sectional area is obtained by solving the sediment-continuity equation using a backward-difference scheme for space and a forward-difference scheme for time. The computed cross-sectional area change is then adjusted for the effects of channel migration. Width adjustments are made in such a manner that the spatial variation in power expenditure per unit channel length is reduced along the reach by a trial and error technique. Further adjustment of cross-sectional area is made to reduce the spatial variation in power expenditure along the channel. The effect of lateral channel migration is determined by solving the sediment-continuity equation in the transverse direction, which incorporates the effect of radius of curvature of the river bend into the transverse component of the sediment transport rate.



Chang (1998) states that the actual sediment rate is obtained by considering sediment material of all size fractions already in the flow as well as the exchange of sediment load with the bed using the method by Borah et al. (1982). If the stream carries a load in excess of its capacity, it will deposit the excess material on the bed. In the case of erosion, any size fraction available for entrainment at the bed surface will be removed by the flow and added to the sediment already in transport. During sediment removal, the exchange between the flow and the bed is assumed to take place in the active layer at the surface. Thickness of the active layer is based upon the relation defined by Borah, et al. This thickness is a function of the material size and composition, but also reflects the flow condition. During degradation, several of these layers may be scoured away, resulting in the coarsening of the bed material and formation of an armor coat. However, new active layers may be deposited on the bed in the process of aggradation. Materials eroded from the channel banks, excluding that portion in the wash load size range, are included in the accounting. Bed armoring develops if bed shear stress is too low to transport any available size.

Two-Dimensional Sediment Transport Models are also available. Both finite-element and finite-difference numerical schemes have been applied. Examples of finite-element models are the SED2D (Letter et al. 1998) and Flo2DH (Froehlich 1996) models. SED2D is an uncoupled sediment transport model that generally uses RMA-2V (USACE 1997) hydraulic simulation results to compute sediment transport, scour and fill, then updates the model geometry and cycles back to RMA-2V to update the flow field. Other sources of hydraulic computations can be used as input to SED2D. Also under development are Flo2DH Version 3 and Flo1D (Arneson 2001). FESWMS Version 3 will incorporate sediment transport computations. These models are best suited for short-term sediment transport simulations although SED2D has features that allow for long-term simulations.

### **5.6.3 Data Needs**

Common to all alluvial river-flow models are requirements for the following input information: (1) accurate initial conditions, including a cross-sectional profile and bed-material size distribution at each computational cross section; (2) accurate boundary conditions such as water and sediment inflows along the boundaries, quantitative expressions of bed-load and suspended-load discharges, size distributions of boundary-sediment input, and stage hydrographs at the upstream and downstream boundaries; and (3) bed-roughness characteristics at each computational point. It is clear that a computer simulation would be meaningless without the first and second requirements, and the lack of the third requirement would yield an erroneous estimation of flow characteristics, resulting in erroneous feedback of flow information to the riverbed. Included in the first set of data are depths of alluvium and controls such as structures and bedrock outcrops.

The exclusion of even one of these three requirements may lead to serious errors in computer simulations. However, one can hardly be provided with a complete set of input data in any prototype numerical application. Therefore, a great number of assumptions often have to be made to fill the gap in the input data. Even if adequate data are provided for a study river, there still remains a need to calibrate and verify the model by means of field data. In most natural rivers, only extremely limited field data are available for high flood stages at which major riverbed changes occur, and, consequently, adequate calibration or verification of the models normally cannot be obtained. In this sense, the capability of the alluvial river-flow models can best be assessed according to how accurately they can predict riverbed changes with limited sources of input data. A numerical modeler should be aware of which input information is most important to the final result of predicting riverbed changes. The success of the numeral model depends on the capabilities of the model, the quality of the input data and the abilities of the modeler.

## 5.7 HIGHWAY PROBLEMS RELATED TO GRADATION CHANGES

Gradation problems at highway crossings include changes in the vertical dimension such as aggradation and degradation; however, lateral erosion problems often occur as a consequence of these changes. The highway problem most associated with aggradation is reduction of flow area, which increases backwater effects upstream of bridges and culverts. Problems associated with degradation are undermining of footings, pile bents, abutments, cutoff walls, and other flow-control or crossing structures. Degradation has also been found to undermine bank protection resulting in the instability of channel banks and increasing debris problems. A common problem associated with lateral erosion is bank slumping, which undermines abutments and piers located near the bank line. Another very common problem arises when meandering streams, migrate laterally and encroach upon roadways.

Causes of gradation changes that have an impact on highway crossings can be grouped into two basic categories: (1) the result of human activities; and (2) natural causes or factors. An analysis of case histories indicates that very few gradation changes were due to natural factors.

Some gradation changes should perhaps be classified as being caused by a combination of both natural and human-induced factors. However, their number is so small that a separate category is not warranted. Because human activities dominate the causes for gradation problems, they will be discussed first.

### 5.7.1 Changes Due to Human Activities

Human activities are literally changing the face of the Earth and generate accelerated erosion from watersheds. Some activities have had far-reaching consequences on streams and have caused, or contributed to aggradation and degradation problems at bridges. Construction of a bridge and approach embankments may also have consequences, but they are unlikely to be far-reaching. Human activities were found to be the major cause of streambed elevation changes. Because accelerated erosion is associated with human activities, it is often possible to anticipate many impacts on bank stability and provide adequate bank protection in advance.

From an analysis of case histories, human activities resulting in gradation problems can be grouped into the following categories: (1) channel alterations; (2) land use changes; (3) streambed mining/excavation; and (4) dams and reservoirs.

Channel Alterations. Straightening, dredging, clearing and snagging, artificial constrictions, and other alterations of natural channels are the major causes of streambed elevation changes. Channel straightening is the dominant activity. Examples of channel response to straightening are presented in Keefer et al. (1980).

Many of the straightened channels have degraded, and degradation is usually accompanied by widening of the channel, unstable banks and serious debris problems. The degradation is attributed to an increase in channel slope that results from shortening of channel length. The increase in channel slope increases the velocity and the shear stress on the bed. As a result, the channel bed degrades until the bed becomes armored or the channel widens and begins to meander to reduce the channel slope back to an equilibrium, or stable condition. There is some evidence that degradation, if it is to occur as a consequence of channel alteration, will be most rapid during a period shortly following the alteration and will thereafter occur at a decreasing rate.

Land Use Changes. Urbanization, agriculture, strip mining, and unregulated logging are other activities that cause gradation problems. Natural vegetation is extremely important in maintaining channel stability. The lateral stability of most streams in the United States, particularly in regions where agriculture or lumbering is practiced, has very probably been affected by the clearing of natural vegetation. Because this clearing has occurred more or less gradually over the past hundred years, the magnitude of the effect at a particular crossing site is sometimes difficult to assess.

The response to deforestation and agricultural activities is generally toward increased peak flows and increased sediment yield. Channel widening and reduced sinuosity are common. Grazing along the streambanks may have significant effects on bank stability.

Urbanization normally causes significant increase in the magnitude of runoff events while reducing their duration. Urban areas are also low sediment producers because of the large percentage of land covered by impervious surfaces. The combination of increased peak runoff rates and reduced sediment loads results in channel degradation, channel widening, and a reduction in channel sinuosity.

Improper construction activities, on the other hand, are known to increase both discharge and sediment load. The removal of the vegetative cover accelerates the erosion process. The response of the system to the increased discharge is to increase channel width and reduce the radius of curvature. In response to increased sediment load, the stream will increase its tendency for bank erosion.

Mining in an upland area may cause aggradation of channels, which are then subject to degradation after the mining ceases.

Streambed Mining/Excavation. If sand or gravel is removed from an alluvial channel in quantities that represent a substantial percentage of the annual bedload in transport, the channel will probably degrade. In addition, removal of gravel from pits or trenches in or along the stream may result in a change in flow alignment at a bridge.

Downstream mining can also produce headcutting through a bridge waterway, undermining the structure. Mining operations upstream of the bridge can also produce degradation at the bridge site and endanger the structure. Equation 5.28 provides a subjective tool for analysis of gradation changes.

Highway engineers should, as a minimum, consider up- and downstream factors that might cause gradation problems during scheduled bi-annual inspections of bridges.

Dams And Reservoirs. The effects of dams and reservoirs on a stream are complex. The consequences include clear-water releases; high sustained, regulated flows; backwater; low sustained, regulated flows; dam breach or removal; and high, controlled irrigation canal releases.

Downstream from a reservoir, channel degradation is to be expected because of removal of sediment. This effect has been documented for many streams (see for example, Williams and Wolman 1984 and Lagasse 1994). The total amount of degradation is difficult to predict; if a sand-bed channel becomes armored with gravel, the amount may be small. On gravel-bed streams, aggradation may occur downstream from the dam because the flow releases are

insufficient to transport gravel brought in by tributary streams. Channel avulsions, which can present a serious threat to many engineering structures, are associated with most aggrading situations. Rapid lowering of river stage may result in severe bank slumping from pore-water pressures in the banks. However, the more general effect of reservoirs is probably to reduce hydraulic problems at highway crossing bridges, both by reduction of flood peaks and a reduction of lateral erosion rates.

Interbasin transfers of flow and diversions result in periods of channel instability and bank erosion until the new channel regime is established.

### **5.7.2 Natural Causes**

Although problems resulting from natural causes are not as frequent as those resulting from human activities, it is important to recognize natural causes in both design and maintenance of highway crossings.

Natural causes and complications from gradation problems include: alluvial fans, natural armoring, braiding, meandering/migration (natural cutoffs), recurrent flooding, high stream velocity, channel bed and bank material erodibility, fire, floating debris, mud and debris flows, earthquakes, tectonic activity, volcanic activity, and landslides.

Floating Debris. Floating debris causes hydraulic problems at highway crossings nationwide. The problems are the greatest in the Pacific Northwest and the upper and lower Mississippi River Valley. Debris hazards are generally a local phenomena often associated with large floods. Most bridge destruction from debris is due to accumulation of debris against bridge components. Debris may partially or totally block waterways, create adverse hydraulic conditions that erode pier foundations and bridge abutments or may overtop roadways and cause structural damage.

Many debris problems exist in forested areas with active logging operations. Highway crossings on streams where stream slopes are mild or moderate, in contrast to headwater streams, are more vulnerable to debris related hazards. Debris hazards occur more frequently in unstable streams where bank erosion is active. Countermeasures presently used by highway agencies include: (1) sufficient freeboard, (2) proper pier spacing, (3) solid piers, (4) debris deflectors, (5) special superstructure designs, (6) flood relief structures, and (7) routine and emergency removal of debris at bridge crossings. Most debris transported in floods does not travel a great distance and often is observable locally along the streambanks upstream from the bridge prior to the flood. Debris usually moves as individual logs in a non-random path concentrating in the thalweg of the stream. Therefore, methods for evaluating its abundance and for mitigating its hazard are deemed feasible. HEC-20 (Lagasse et al. 2001) summarizes the results of studies by the U.S. Geological Survey to develop methods to estimate potential debris accumulations at bridges (Diehl 1997 and Diehl and Bryan 1993). Examples of debris control structures for culverts are given in Reihsen (1964).

Mud Flows And Debris Flows. Fast melting snowpack and overabundance of soil moisture on steep slopes throughout the Western United States causes mudflows, debris flows and landslides, threatening bridges and highway structures. There is considerable evidence of damages to highway structures in the literature. For example Hungr et al., (1984) documented a bridge for which a concrete bridge beam was demolished by point impact during a debris flow event.

In another example, the volcanic eruption from the magmatic blast of Mount St. Helens triggered a major slope failure on the north flank of the mountain. Mudflows and debris flows were generated and swept down the Toutle and Cowlitz Rivers destroying bridges, inundating buildings, and eventually blocking the navigation channel of the Columbia River. Bradley (1984) reported the Cowlitz has aggraded markedly as a result of the post eruption hyperconcentrated flows. The upper Cowlitz and the lower Toutle have shifted from meandering to braided streams, thereby causing difficulties in preventing the failure of some remaining bridges.

Examination of typical watershed behavior and response provides information on the impact of changes on the fluvial system. Channel stability assessments and possible gradation changes are indicated in Table 5.8. Those findings reflect the observations of Keefer et al. (1980). An example relating to the use of this table is presented in Section 5.9, Problem 3.

### **5.7.3 Resulting Problems at Highway Crossings**

Brown et al. (1980) reviewed design practices to evaluate crossing design procedures and the effect of grade changes on these procedures. The parameters most influenced by grade changes are those used as input to the hydraulic design procedures currently in use. These input parameters include: design discharge; channel roughness; energy slope; bed slope; velocities; shear stresses; cross-sectional geometry; base level; flow depth; and flow alignment. Other components of crossing design affected by grade changes include foundation depth, bridge deck clearance, and flow opening size.

Problems encountered at bridge crossings include bridge capacity, backwater, pier and abutment alignment, footing depth at piers and abutments, and construction depth for flow-control and debris-control structures. With respect to bridge capacity and backwater, aggradation produces the most severe problems. However, debris problems associated with degradation can also have a significant impact on flow capacity and scour. Foundation depths for piers, abutments, and flow-control structures can be influenced in two ways by grade changes: the normal streambed base level will be altered; and the "normal" hydraulic conditions at a site used as input to local scour computations will be changed. The important components of bank protection design adversely affected by grade changes are key depths and the vertical extent of bank protection above and below the streambed.

Problems encountered at culvert crossings can be the result of general grade changes produced by long-term changes in stream morphology or inadequate design and/or construction of culvert systems. The design components most often influenced are culvert capacity and structural stability. The greatest danger produced by aggradation is partial plugging of the culvert opening resulting in a damming effect and increasing the magnitude and frequency of flooding upstream of the structure. Degrading stream reaches affect culvert systems by reducing their structural stability. General streambed degradation has undermined the foundations of culverts resulting in their complete failure.

Table 5.8. Channel Response to Changes in Watershed and River Condition (after Keefer et al. 1980).				
Observed Condition	Channel Response			
	Stable	Unstable	Degrading	Aggrading
Alluvial Fan Upstream Downstream		X X	X	X
Dam and Reservoir Upstream Downstream		X X	X	X
River Form Meandering Straight Braided	X	X X X	Unknown Unknown Unknown	Unknown Unknown Unknown
Bank Erosion			Unknown	Unknown
Vegetated Banks	X		Unknown	Unknown
Headcuts		X	X	
Diversion Clear Water Diversion Overloaded with Sediment		X		X X
Channel Straightened		X	X	
Deforested Watershed		X		X
Drought Period	X			X
Wet Period		X	X	
Bed Material Size Increase Decrease		X X	Unknown	X X

## 5.8 STREAM STABILITY PROBLEMS AT HIGHWAY CROSSINGS

In the United States, the annual damage related to hydraulic problems at bridges and highways has been estimated as high as \$60 million during years of extreme floods. Damages by streams can be reduced by considering channel stability in site selection, bridge design, and countermeasure placement. Ideally, a stable channel is one that does not change in size, form, or position through time. However, all alluvial channels change to some degree and therefore have some degree of instability. For engineering purposes, an unstable channel is one whose rate or magnitude of change is great enough to be a significant factor in the

planning or maintenance of a highway crossing during the service life of the structure. The kinds of changes considered here are: (1) lateral bank erosion; (2) degradation or aggradation of the streambed that continues progressively over a period of years; and (3) natural short-term fluctuations of streambed elevation that are usually associated with the passage of a flood (scour and fill). Stability is inferred mainly from the nature of point bars, the presence or absence of cut banks, and the variability of stream width (see also HEC-20, Lagasse et al. 2001).

### **5.8.1 Bank Stability**

On a laterally unstable channel, or at actively migrating bends on an otherwise stable channel, the point bars are usually wide and unvegetated and the bank opposite to a point bar is cut and often scalloped by erosion. The crescentic scars of slumping may be visible from place to place along the bankline. The presence of a cut bank opposite of a point bar is evidence of instability, even if the point bar is vegetated. Sand or gravel on the bar appears as a light tone on airphotos. The unvegetated condition of the point bar is attributed to a rate of growth that is too rapid for vegetation to become established. However, the establishment of vegetation on a point bar is dependent on other factors besides rate of growth, such as climate and the timing of floods. If the width of an unvegetated point bar is considered as part of the channel width, the channel tends to be wider at bends. Streams whose width at bends is about twice or more the width at straight reaches are called wide-bend streams.

Oxbow lakes are formed by the cutoff of meander loops, which occurs either by gradual closure of the neck (neck cutoffs) or by a chute that cuts across the neck (chute cutoffs). Neck cutoffs are associated with relatively stable channels, and chute cutoffs with relatively unstable channels. Recently formed oxbow lakes along a channel are evidence of recent lateral migration. A recently formed lake is usually immediately adjacent to the channel and it transmits flow at high river stages. Commonly, a new meander loop soon forms at the point of cutoff and grows in the same direction as the previous meander. Cutoffs tend to induce rapid bank erosion at adjacent meander loops. The presence of abundant oxbow lakes on a floodplain does not necessarily indicate a rapid channel migration rate, because an oxbow lake may persist for hundreds of years.

Along an unstable channel, bank erosion tends to be localized at bends, and straight reaches tend to be relatively stable. However, meandering of the thalweg in a straight reach is likely to be a precursor of instability. Bars that occur alternately from one side to the other of a straight reach are somewhat analogous to point bars and are indicative of a meandering thalweg.

The following paragraphs summarize the characteristics of unstable and stable banks. For a more detailed discussion of bank stability and the mechanics of bank failure see HEC-20 (Lagasse et al. 2001).

Unstable Banks With Moderate To High Erosion Rate. The slope angle of unstable banks usually exceeds 30 percent, and a cover of woody vegetation is rarely present. At a bend, the point bar opposite of an unstable cut bank is likely to be bare at normal stage, but it may be covered with annual vegetation and low woody vegetation, especially willows. Where very rapid erosion is occurring, the bankline may have irregular indentations. Fissures, which represent the boundaries of actual or potential slump blocks along the bankline indicate the potential for very rapid bank erosion.

Unstable Banks With Slow To Moderate Erosion Rate. If a bank is partly graded (smooth slope) the degree of instability is difficult to assess and reliance is placed mainly on vegetation. The grading of a bank typically begins with the accumulation of slumped material at the base such that a slope is formed, and progresses by smoothing of the slope and the establishment of vegetation.

Stable Banks With Very Slow Erosion Rate. Stable banks tend to be graded to a smooth slope and the slope angle is usually less than about 30 percent. In most regions of the United States, the upper parts of stable banks are vegetated, but the lower part may be bare at normal stage, depending on bank height and flow regime of the stream. Where banks are low, dense vegetation may extend to the water's edge at normal stage. Mature trees on a graded bank slope are particularly convincing evidence for bank stability. Where banks are high, occasional slumps may occur on even the most stable graded banks. Shallow mountain streams that transport coarse bed sediment tend to have stable banks.

Field information on lateral migration rates for channels of different sizes has been compiled by Brice (1982). Bank erosion rates tend to increase with increasing stream size. In Figure 5.26 channel width is taken as a measure of stream size. The dashed line is drawn arbitrarily to have a slope of 1 and a position (intercept) to separate most equiwidth streams from most wide-bend and braided point-bar streams. For a given channel width, equiwidth streams tend to have the lowest erosion rates, and braided point-bar streams the highest. Braided streams without point bars (diamond symbol, Figure 5.26) plot well below the arbitrary curve because their channels are very wide relative to their discharges. Channel width is an imperfect measure of stream size, as are drainage area and discharge, particularly for the comparison of streams in arid and semiarid regions with streams in humid regions. If braided streams and braided point-bar streams (which are uncommon in most parts of the United States) are excluded, the dashed curve in Figure 5.26 provides a preliminary estimate of erosion rates that may be encountered at a particular site. An example on the use of these results is presented in Section 5.9, Problem 4.

### **5.8.2 Stability Problems Associated With Channel Relocation**

For some highway encroachments, a change in the river channel alignment is advantageous. When a river crossing site is so constrained by non-hydraulic factors that consideration of alternative sites is not possible, the engineer must attempt to improve the local situation to meet specific needs. Also, the engineer may be forced to make channel improvements in order to maintain and protect existing highway structures in or adjacent to the river.

Suppose a meandering river is to be crossed with a highway, as shown in Figure 5.27a. Assume that the alignment is fixed by constraints in the acquisition of the right-of-way. To create better flow alignment with the bridge, consideration is given to channel improvement as shown in Figure 5.27b. Similarly, consideration for improvement to the channel would also be advisable for a hypothetical lateral encroachment of a highway as depicted in Figure 5.27c. In either case, the designer's questions are how to realign the channel, and what criteria to use to establish the cross-sectional dimensions.



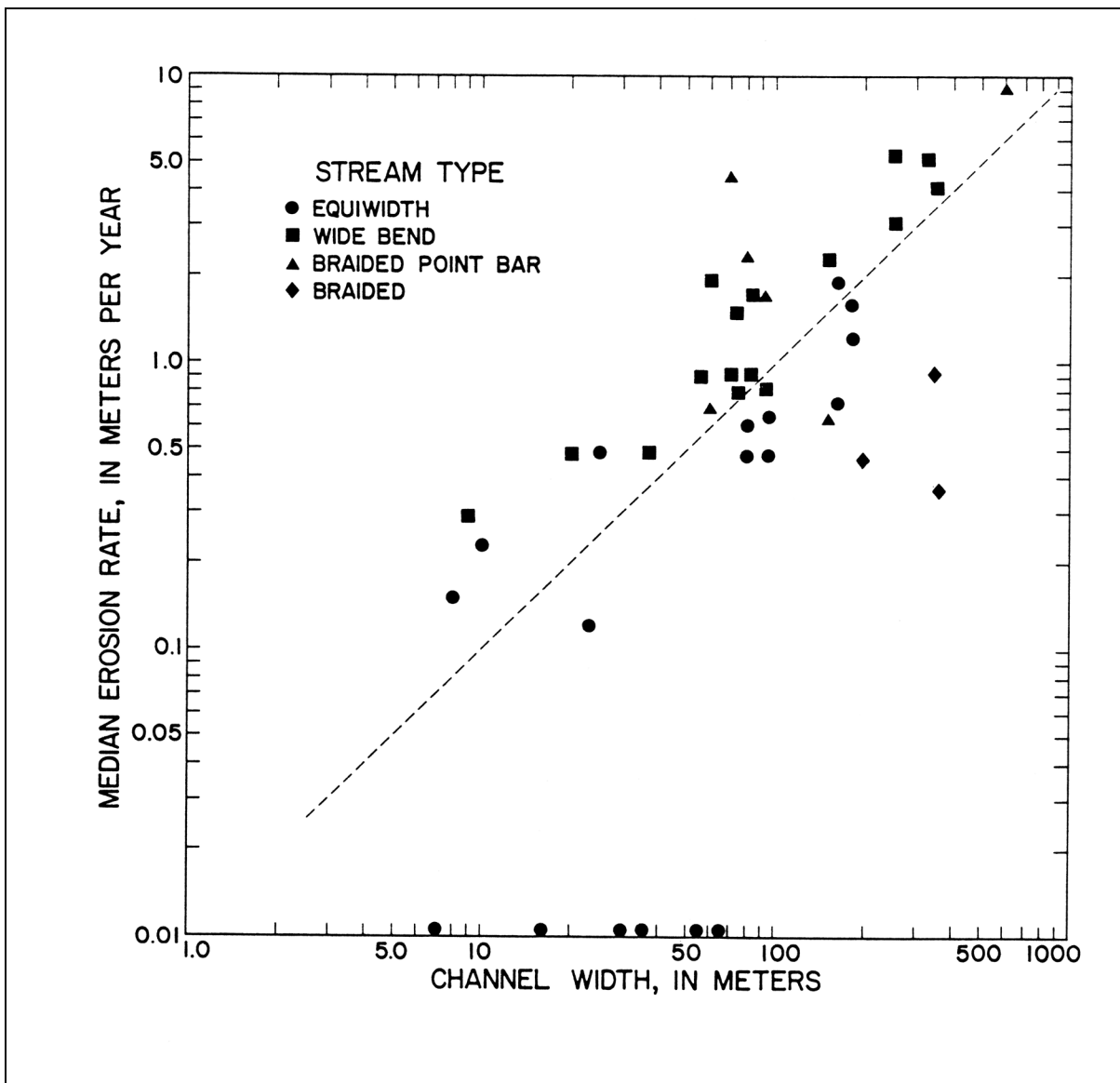


Figure 5.26. Median bank erosion rate in relation to channel width for different types of streams (after Brice 1982).

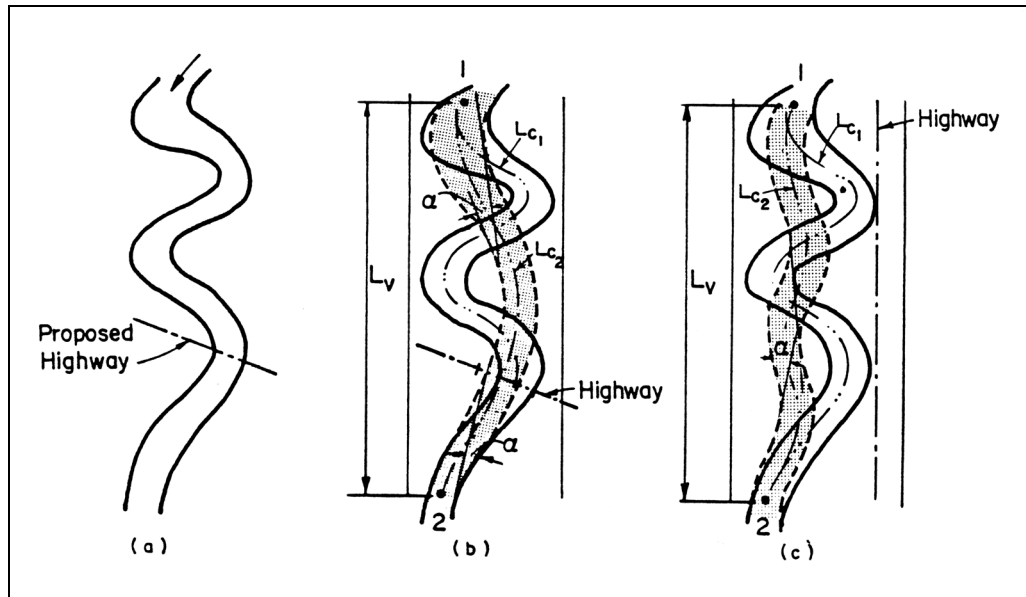


Figure 5.27. Encroachment on a meandering river.

Prior to realigning a river channel the stability of the existing channel must be examined using the methods outlined earlier. A stream classification, recent and past aerial photographs and field surveys are generally necessary. The realigned channel may be made straight without curves, or may include one or more curves. If curves are included, the radii of curvature, the number of bends, the limits of rechannelization (hence the length or slope of the channel) and the cross-sectional area are decisions which have to be made by the designer. Different rivers have different characteristics and historical background with regard to channel migration, discharge, stage, geometry and sediment transport. As indicated in the previous chapters, it is important for the designer to understand and appreciate river hydraulics and geomorphology when making decisions concerning channel relocation. It is difficult to state generalized criteria for channel relocation applicable to every river. Knowledge about river systems has not yet advanced to such a state as to make this possible. Nevertheless, it is possible to provide some principles and guidelines for the design engineer.

As the general rule, the radii of bends should be made about equal to the mean radii of bends in extended reaches of the river. When the angle  $\phi$  defined in Figure 5.15 exceeds about 40 degrees, this provides a sufficient crossing length for the thalweg to shift from one side of the channel to the other. Generally, it is necessary to stabilize the outside banks of the curves in order to hold the new alignment, and depending upon crossing length some amount of maintenance may be necessary to remove sandbars after large floods so that the channel does not develop new meander patterns in the crossings during normal flows.

The sinuosity and channel bed slope are related in the following way. The bed elevations at the ends of the reach being rechannelized, (designated 1 and 2, in Figure 5.27) are established by existing boundary conditions. Hence, the total drop in bed elevation for the new channel (subscript 2) and the old channel (subscript 1) are the same.

$$\Delta z_1 = \Delta z_2 = \Delta z \quad (5.22)$$

The length of channel measured along the thalweg is labeled  $L_c$ . Thus, the mean slope of the channel bed before relocation is:

$$S_1 = \frac{\Delta Z}{L_{c1}} \quad (5.23)$$

and after relocation is

$$S_2 = \frac{\Delta Z}{L_{c2}} \quad (5.24)$$

Sinuosity is defined as the ratio of the length of channel,  $L_c$  to the length of the valley, or

$$S_n = \frac{L_c}{L_v} \geq 1 \quad (5.25)$$

Clearly,

$$S_{n1} = \frac{L_{c1}}{L_{v1}} \quad (5.26)$$

$$S_{n2} = \frac{L_{c2}}{L_{v2}} \quad (5.27)$$

but

$$L_{v1} = L_{v2} = L_v \quad (5.28)$$

and

$$\frac{\Delta z_1}{L_{v1}} = \frac{\Delta z_2}{L_{v2}} = \frac{\Delta Z}{L_v} \quad (5.29)$$

Thus,

$$S_{n1}S_1 = \left(\frac{L_{c1}}{L_v}\right) \left(\frac{\Delta Z}{L_{c1}}\right) = \left(\frac{L_{c2}}{L_v}\right) \left(\frac{\Delta Z}{L_{c2}}\right) = S_{n2}S_2 \quad (5.30)$$

The new channel slope and channel sinuosity are inversely related. If  $S_{n2} < S_{n1}$  then  $S_2 > S_1$ . The new channel alignment, hence  $S_{n2}$ , can be chosen by the designer with due consideration given to the radii of curvature, deflection angles and tangent lengths between reversing curves. As indicated before, consideration should also be given to prevailing average conditions in the extended reach. The new slope  $S_2$  can be calculated from Equation 5.30, and the relationship for meandering (Equation 5.1) should be satisfied.

$$S_2 Q^{1/4} \leq 0.0007 \quad (\text{SI})$$

or

$$S_2 Q^{1/4} \leq 0.0017 \quad (\text{English})$$

If  $S_1$  is of such magnitude that Equation 5.1 cannot be satisfied with still larger  $S_2$ , the possibility of the river changing to a braided channel because of steeper slope should be carefully evaluated. With steeper slope, there could be an increase in sediment transport which could cause degradation, and the effect would be extended both upstream and downstream of the relocated reach. The meander patterns could change. Considerable bank protection might be necessary to contain lateral migration which is characteristic of a braided channel, and if the slope is too steep, head cuts could develop which migrate upstream with attendant effects on the geometry of the channel. Even when changes in slope are not very large, a short-term adjustment of the average river slope occurs, consistent with the sediment transport rate, flow velocities and roughnesses, beyond the upstream and downstream limits of channel improvement. For small changes in slope, the proportionality (Equation 5.16),  $Q_s \sim Q_s D_{50}$  tends toward equilibrium with slight increases in bed sediment size,  $D_{50}$ , and adjustment in the sediment transport rate,  $Q_s$ .

A small increase in the new channel width could be considered which tends to maintain the same stream power,  $\tau_o V$ , in the old and new channels. That is,

$$(\tau_o V)_1 = (\tau_o V)_2 \quad (5.31)$$

With substitution of  $\tau_o = \gamma RS$ ,  $V = Q/A$  and  $R = A/P \approx A/W$ , Equation 5.42 leads to

$$W_2 = S_2 W_1 / S_1 \quad (5.32)$$

Any designed increase in width should be limited to about 10 to 15 percent. Wider channels would be ineffective. Deposition would occur along one bank and the effort of extra excavation would be wasted. Furthermore, bar formation would be encouraged, with resultant tendencies for changes in the meander pattern leading to greater maintenance costs for bank stabilization and removal of the bars to hold the desired river alignment.

The depth of flow in the channel is dependent on discharge, effective channel width, sediment transport rate (because it affects bed form and channel roughness) and channel slope. Methods for evaluating flow depth were discussed earlier in this chapter.

The foregoing discussion pertains to alluvial channels with silt and sand sized bed materials. For streams with gravel and cobble beds, the usual concern is to provide adequate channel cross-sectional dimensions to convey flood flows. If the realigned channels are made too steep, there is an increased stream power with a consequent increase in transport rate of the bed material. The deposition of material in the reaches downstream of the crossing tends to form gravel bars and encourages changes in the planform of the channel. Short-term changes in channel slope can be expected until equilibrium is reestablished over extended reaches both upstream and downstream of the rechannelized reach. Bank stabilization may be necessary to prevent lateral migration, and periodic removal of gravel bars may also be necessary.

### 5.8.3 Assessment of Stability for Relocated Streams

Brice (1980) reported case histories for channel stability of relocated streams in different regions of the United States. Based on his study, the recommendations and conclusions presented here apply to specific aspects of the planning and construction of channel relocation. They are intended for assessment of the risk of instability and for reduction of the degree of instability connected with relocation. Serious instability resulting from relocation can be observed either when the prior natural channel is unstable or when floods of high recurrence interval occur during or soon after construction. Although there is an element of uncertainty in channel stability, the experience represented by Brice's study sites provides useful guidelines for improvement in the performance of channels relocated by highway agencies. Consideration of the following aspects of the channel relocation is recommended.

Channel Stability Prior To Relocation. Assessment of the stability of a channel prior to relocation is needed to assess erosion-control measures and risk of instability. An unstable channel is likely to respond unfavorably to relocation. Bank stability is assessed by field study and the stereoscopic examination of aerial photographs. The most useful indicators of bank instability are cut or slumped banks, fallen trees along the bankline, and wide, unvegetated, exposed point bars. Bank recession rates are measured by comparison of time-sequential aerial photographs. Vertical instability is equally important but more difficult to determine. It is indicated by changes in channel elevation at bridges and gaging stations. Serious degradation is usually accompanied by generally cut or slumped banks along a channel.

Erosion Resistance Of Channel Boundary Materials. The stability of a channel, whether natural or relocated, is partly determined by the erosion resistance of materials that form the wetted perimeter of the channel. Resistant bedrock outcrops, which extend out into the channel bottom, or that lie at shallow depths, will provide protection against degradation. Not all bedrock is resistant. Erosion of shale, or of other sedimentary rock types interbedded with shale, has been observed. Degradation was slight or undetected at most sites where bed sediment was of cobble and boulder size. However, serious degradation may result from relocation. Degradation may result from the relocation of any alluvial channel, whatever the size of bed material, but the incidence of serious degradation of channels relocated by highway agencies is slight.

The cohesion and erosion resistance of banks tend to increase with clay content. Banks of weakly coherent sand or silt are clearly subject to rapid erosion, unless protected with vegetation. No consistent relation was found between channel stability and the cohesion of bank materials, probably because of the effects of vegetation.

Length Of Relocation. The length of relocation contributes significantly to channel instability at sites where its value exceeded 250 channel widths. When the value is below 100 channel widths, the effects of length of relocation are dominated by other factors. The probability of local bank erosion at some point along a channel increases with the length of the channel. The importance of vegetation, both in appearance and in erosion control, would seem to justify a serious and possibly sustained effort to establish it as soon as possible on the graded banks.

Bank Revetment. Revetment makes a critical contribution to stability at many sites where it is placed at bends and along roadway embankments. Rock riprap is by far the most commonly used and effective revetment. Concrete slope paving is prone to failure. Articulated concrete block can be effective especially when vegetation can establish in the interstices between blocks. Bank revetment is discussed in detail in the next chapter.

Check Dams (drop structures). In general, check dams are effective in preventing channel degradation. The potential for erosion at a check dam depends on its design and construction, its height and the use of revetment on adjoining banks. A series of low check dams, less than about 0.5 m (2 ft) in height, is probably preferable to a single higher structure, because the potential for erosion and failure is reduced. By simulating rapids, low check dams may add visual interest to the flow in a channel. One critical problem arising with check dams relates to improper design for large flows. Higher flows have worked around the ends of many installations to produce failure.

Maintenance. The following problems that can be controlled by maintenance were observed along relocated channels: (1) growth of annual vegetation in channel; (2) reduction of channel conveyance by overhanging trees; (3) local bank cutting; and (4) bank slumping. The expense of routine maintenance or inspection of relocated channels beyond the highway right-of-way is probably prohibitive. However, most of the serious problems could be detected by periodic inspection, perhaps by aerial photography, during the first 5 or 10 years after construction.

Relationship Between Sinuosity And Stability. This relationship is summarized as follows: (1) Meandering does not necessarily indicate instability; an unstable stream will not remain highly sinuous for very long, because the sinuosity will be reduced by frequent meander cutoffs; (2) Where instability is present along a reach, it occurs mainly at bends; straight segments may remain stable for decades; and (3) The highest instability is for reaches whose sinuosity is in the range of 1.2 to 2 and whose type is either wide bend or braided point bar.

#### **5.8.4 Estimation of Future Channel Stability and Behavior**

One objective of stability assessment is to anticipate the migration of bends and the development of new bends. Lateral erosion is probably more frequently involved in hydraulic problems at bridges than any other stream process. Problems caused by general scour, local scour, channel degradation and accumulation of debris are somewhat less common.

The lateral stability of a stream can be measured from records of its position at two or more different times where the available records are usually maps or aerial photographs. Historic surveyed cross-sections are extremely useful and can frequently be located in bridge inspection files. It is recognized that some progress is being made on the numerical prediction of loop deformation and bend migration (see Section 5.8.5). At present, however, the best available estimates are based on past rates of lateral migration at a particular reach. However, erosion rates may fluctuate substantially from one period of years to the next.

Measurements of bank erosion on two time-sequential aerial photographs (or maps) require the identification of reference points which are common to both. Useful reference points include roads, buildings, irrigation canals, bridges and fence corners. This analysis of lateral stability is greatly facilitated by a drawing of time changes in bankline position. To prepare such a drawing, aerial photographs are matched in scale and the photographs are superimposed holding the reference points fixed. For further discussion see HEC-20 (Lagasse et al. 2001).

Bank erosion rates increase with the stream size as shown in Figure 5.26. Sinuous canaliform streams can then be expected to have the lowest erosion rates and the sinuous braided streams, the highest.

The lateral stability of different stream reaches can be compared by means of a dimensionless erosion index. The erosion index is the product of its median bank erosion rate expressed in channel widths per year, multiplied by the percent of reach along which erosion occurred, multiplied by 1,000. Erosion indexes for 41 streams in the United States are plotted against sinuosity in Figure 5.28. The length of most of these reaches is 25 to 100 times the channel width. The highest erosion index values are for reaches with sinuosity ranging between 1.2 and 2. Erosion indexes are large for sinuous braided and sinuous point bar (wide bend) streams. Equiwidth streams tended to be relatively stable. The erosion index value of 5, in Figure 5.28, is suggested as a boundary between stable and unstable reaches. Brice (1984) considers that reaches having erosion indexes values less than 5 are unlikely to cause lateral erosion problems at bridges. An example on the use of Figure 5.28 is presented in Section 5.9, Problem 4.

A general assessment of bank stability can be made considering the following aspects.

**Bank Erosion Rates.** It is theoretically possible to determine bank erosion rates from factors such as water velocity and resistance of the banks to erosion. See HEC-18 (Richardson and Davis 2001) for a discussion of recent advances in measuring erosion rates. The results in Figure 5.26 provide a first approximation of migration rate of a bend regardless of the hydraulic conditions and sediment characteristics. Past rates of erosion at a particular site provide the best estimate of future rates. In projecting past rates into the future, consideration must be given to the following factors: (1) the past flow history of the site during the period of measurement, in comparison with the probable future flow history during the life span of the highway crossing. The duration of floods, or of flows near bankfull stages, is probably more important than the magnitude of floods; and (2) human-induced factors that are likely to affect bank erosion rates. Among the most important of these are urbanization and the clearing of floodplain forests.

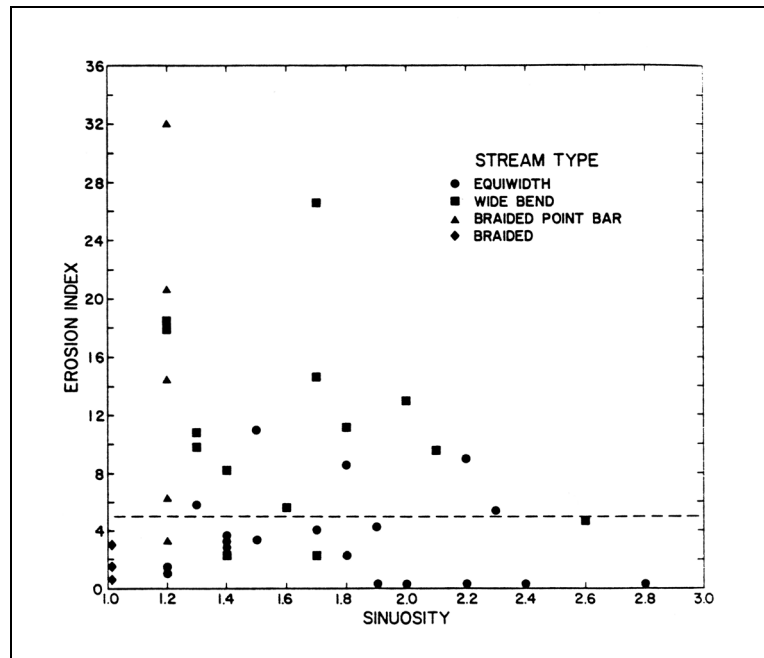


Figure 5.28. Erosion index in relation to sinuosity (Brice 1984).

Behavior Of Meander Loops. If the proposed bridge or roadway is located near a meander loop, it is useful to have some insight into the probable way in which the loop will migrate or develop, as well as its rate of growth. No two meanders will behave in exactly the same way, but the meanders on a particular stream reach tend to conform to one of the several modes of behavior illustrated in Figure 5.29.

Mode A (Figure 5.29) represents the typical development of a loop of low amplitude, which decreases in radius as it extends slightly in a downstream direction. Mode B rarely occurs unless meanders are confined by valley sides on a narrow floodplain, or are confined by artificial levees. Well developed meanders on streams that have moderately unstable banks are likely to follow Mode C. Mode D applies mainly to large loops on meandering or highly meandering streams. The meander has become too large in relation to stream size and flow, and secondary meanders develop along it, converting it to a compound loop. Mode E also applies to meandering or highly meandering streams, usually of the equiwidth point-bar type. The banks have been sufficiently stable for an elongated loop to form (without being cut off), but the neck of the loop is gradually being closed and cutoff will eventually occur at the neck. Modes F and G apply mainly to locally braided sinuous or meandering streams having unstable banks. Loops are cut off by chutes that break diagonally or directly across the neck.

Effects Of Meander Cutoff. If cutoffs seem imminent at any meanders in the vicinity of a proposed bridge crossing the probable effects of cutoff need to be considered. The local increase in channel slope due to cutoff usually results in an increase in the growth rate of adjoining meanders, and an increase in channel width at the point of cutoff. On a typical wide-bend point-bar stream the effects of cutoff do not extend very far upstream or downstream.

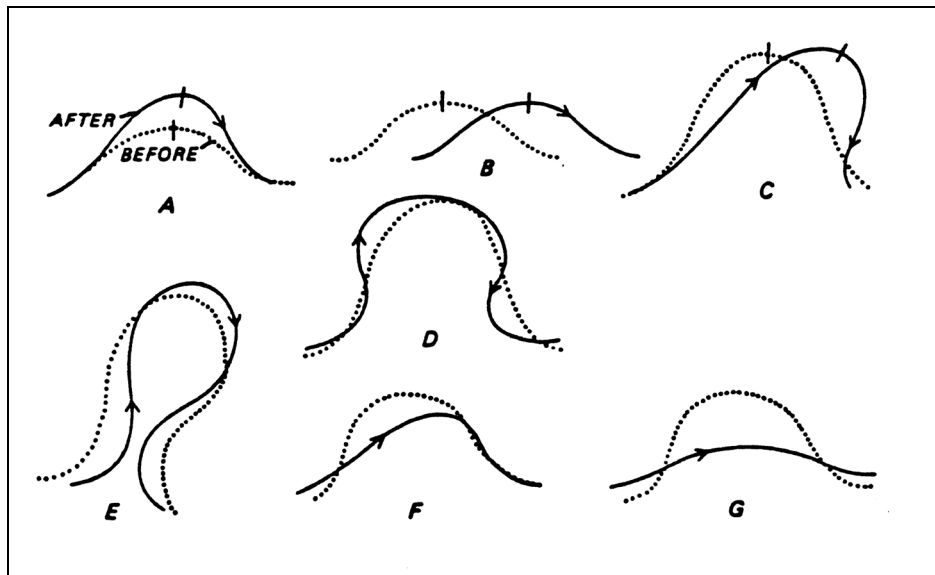


Figure 5.29. Modes of meander loop development. A, Extension. B, Translation. C, Rotation. D, Conversion to a compound loop. E, Neck cutoff by closure. F, Diagonal cutoff by chute. G, Neck cutoff by chute.



Assessment Of Degradation. Field sites having degradation problems are more numerous than sites having aggradation problems. Annual rates of degradation averaged from past records such as the closure of a dam give poor estimates of future rates of degradation. Typical situations exhibit an exponential decay function of the rate of channel degradation.

Recent evidence of degradation can be detected from field surveys or by stereo viewing of aerial photographs. Indicators of degradation are: (1) channel scarps, headcuts and nickpoints; (2) gulying of minor side tributaries; (3) high and steep unvegetated banks; (4) measurements of streambed elevation from a bridge deck; (5) changes in stream discharge relationships; and (6) measurements of longitudinal profiles.

Assessment Of Scour And Fill. Natural scour and fill refer to fluctuations of streambed elevation about an equilibrium condition. These fluctuations are associated mainly with floods and occur by three different mechanisms operating jointly or independently: (1) bed form migration; (2) convergence and divergence of flow; and (3) lateral shift of thalweg or braids.

The maximum scour induced by the migration of a dune is almost one-half the dune height, and dune heights are roughly estimated as one-third of the mean flow depth. In gravel bed streams, most migrating bed forms can be regarded as bars, the height of which is related to flow depth. The migration of a bar through a bridge waterway is mainly of concern because of the deflection and concentration of flow. Bar migration tends to be a random process and its motion can best be tracked from time-sequential aerial photographs.

Gravel bars tend to migrate on braided streams and to remain fixed at riffles on unbraided pool and riffle streams.

Flow convergence in natural streams is associated with scour, whereas divergent currents are associated with deposition. Persistent pools have the strongest convergence of flow and the greatest potential for scour. Such pools are best identified by a continuous bed profile along the thalweg. In braided streams, scour holes are found at the confluence of braids. Field measurement of cross-sectional area and flow velocity at an incised reach near bankfull stage provides a good basis for calculation of scour by extrapolation to the design flood.

Instability of the streambed that results from shift of thalweg is related to stream type and can be assessed from study of aerial photographs. On sinuous canal form streams, shift of the thalweg during flood is minimal. A greater shift of the thalweg can be expected on sinuous point-bar streams. In straight reaches, alternate bars visible on aerial photographs taken at low stage are commonly present. These alternate bars indicate the potential for thalweg shifting and also for bank erosion when the current is deflected against the bankline. Shift of the thalweg with increase in stage must be considered when determining the location of the point of maximum bed scour, bank erosion, and the alignment of piers with flood flow.

Site Selection For Highway Crossings. For most streams the magnitude of scour is substantially greater at specific places along the channel. Bends and narrow sections may scour at high stages regardless of the effect of bridge structures. Straight or gently curved reaches with stable banks are preferred.

Considerations for the selection of a crossing site on a non-sinuous reach include: (1) is the site at a pool, riffle or transition section; (2) are alternate bars visible at low stage; and (3) what is the effect of migration of mid-channel bars, if any? With respect to meandering reaches, questions requiring solution include: (1) what has been the rate and mode of migration of the meander; (2) what is the probable future behavior, as based on the past; (3) is the site at a pool, riffle or transition section; and (4) is meander cutoff probable?

### 5.8.5 Advances in Predicting Meander Migration

Meander Behavior. According to Hooke (1991), it has long been assumed that, after initial development, meanders tend towards an equilibrium of form, given stability of external conditions. These ideas were based on early experiments in flumes (Friedkin 1945) and on the analysis of process-form relations in the 1960s in which statistical relationships were established, e.g., between meander wavelengths and discharge (Carlston 1965). Much evidence has now been accumulated that many meanders exhibit no such equilibrium (Carson and Lapointe 1983, Hooke 1984).

If the behavior of individual bends on active rivers is examined (using for example, historical evidence or meander scrolls) then a continuous evolution with an increasing complexity of pattern is frequently found. Meanders may migrate at first, but then they begin to grow in amplitude, then to become compound in form. Based on analysis of historical sequences of meander change on rivers using maps and aerial photographs, models of meander development have been produced (Hooke 1991; Harvey 1989; Keller 1972).

These show a sequence from low sinuosity bends to bends of symmetrical form which tend to migrate; then bends enter a phase of rapid growth with maximum erosion at the apex leading to extension in the cross-valley direction. Beyond a certain increase in path length (Hooke and Harvey 1983) the bends start to become compound in form by development of lobes on one or both parts of the apex. These lobes may go on to develop into separate bends if there is space. This increasing asymmetry and complexity is similar to other models such as those of Brice (1974) and Hickin and Nanson (1975).

This process of growth cannot, of course, go on indefinitely. Eventually the bends are likely to intersect or spatial limits of the floodplain are reached so that cut-offs take place. Therefore, following a phase of growth, cutoffs are likely. Rivers show an early phase of increasing sinuosity then oscillating sinuosity thereafter.

Of course, not all bends exhibit complexity or rapid growth. Some simply progressively migrate or tend to stabilize at various stages. This could be for a number of reasons, e.g., slope and overall energy in the system, floodplain form, or it could simply be that changes are progressing at a very slow rate. Different domains of meander behavior can therefore be visualized (Figure 5.30). Theoretically, it should be possible to identify domains of behavior with thresholds between them. The thresholds will vary with the actual river and may be rather 'fuzzy.' Further work is needed to substantiate whether they do indeed exist, but the indication is that any single mathematical model of meander behavior will be inadequate. This is supported by problems with existing models.

The mathematical modeling of helical and cross channel flows and their related channel characteristics has proved to be difficult. Most such models are based on simplifications of the equations of continuity for water and sediment and on the Reynold's (or St. Venant's) equations of motion (Engelund 1974; Smith and McLean 1984; Odgaard 1986). As noted by several researchers (Odgaard and Bergs 1987; Yen and Ho 1990), most of these models simulate bend flow and channel topography only in the "fully developed" portions of the bend, i.e., where velocity and thalweg depth do not vary longitudinally. Other models predict these characteristics throughout the bend, even when velocity and depth change downstream (Dietrich and Smith 1983; Engelund 1974; Odgaard 1986; Yen and Ho 1990). In addition, considerable disagreement exists over the simplifications and eliminations that have been used to solve these equations (Dietrich and Smith 1983).

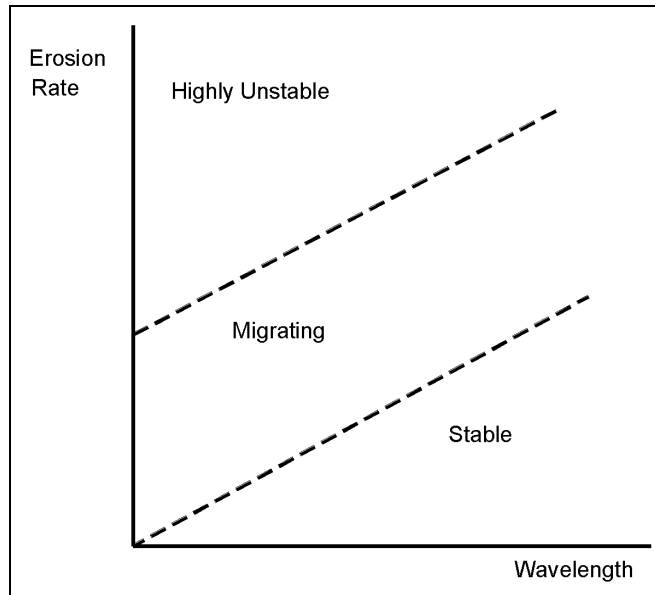


Figure 5.30. Domains of meander behavior (from Hooke 1991).

Most of the mathematical models have been tested or verified in flumes, some of which had fixed beds or constant radius of curvature segments connected to straight segments (Odgaard and Bergs 1987). Even when model testing is done on rivers with constantly-varying radii of curvature and mobile bed materials, problems with measurement accuracy of the various model components often dominate the final result (Dietrich and Smith 1983).

One difficulty is the assumption that all meanders are simple, whereas as Hooke (1991) demonstrates they are not. In addition to other controls on meander migration, the mode of bank retreat varies from grain by grain removal to mass failure (Hasegawa 1989; Knighton 1984).

There are many authors who believe that it is combinations of processes that are important (e.g., Hooke 1979; Thorne 1982; Lawler 1986). In view of the wide range of alluvial materials, riverine forms and hydroclimatic environments, the limitations of mathematical models are many and the range of validity of the models is limited. Therefore a reasonable forecast of the future planform of the river has not yet been realized successfully and remains a challenging topic (Thein 1994).

Mosselman (1995) states that the non-periodicity of meanders, which develop from a straight alignment in the numerical models of Howard and Knutson (1984) and others "suggest chaotic behavior, that is, a sensitive dependence on initial and boundary conditions." He concludes that this "chaotic behavior bears on the predictability of river meandering."

It is only by considering the great variety of meander configurations and how they influence future patterns that reasonable predictions of meander shift can be accomplished. Indeed, Howard (1996) concludes that the chaotic behavior suggests that "even the most detailed model has limited predictive power." This is perhaps because "small differences in initial geometry or boundary conditions between two identical streams will cause different meander patterns" (Howard 1996). In addition, he concludes that "predictability of future meander patterns decrease with time."

The problem appears to lie in the lack of recognition of different types of rivers with different meander behavior (Figure 5.30) and the assumption that all meanders are represented by idealized bends.

Analysis Options. A study by Johns Hopkins University (Cherry et al. 1996) for the U.S. Army Corps of Engineers Waterways Experiment Station investigated the use of both empirical and analytical approaches to provide solutions to the problem of predicting meander migration. This study evaluated empirical and analytical (computational) methods for forecasting planform change and bankline migration in flood control channels, using data originally assembled and analyzed by Brice (1982) to assess stream channel instability problems at bridges for the FHWA. Twenty-six sites were used to evaluate the predictive capabilities of bend-flow meander migration computer models. The computational bend-flow meander migration model used by Cherry et al. was developed by Garcia et al. (1994).

The Johns Hopkins study recognized that a meandering river is a complex system involving relations among many variables. The erosion rate for a meander bend is determined by the balance between the erosive forces applied to the channel bank and the resistance to erosion provided by the bank material and bank vegetation. Erosive force is a complex function of discharge, channel cross section geometry, sediment load, bed roughness, presence of bedforms and bars, and the planform geometry. Resistance to erosion is related to the properties of the bank material, the bank geometry (slope, height, shape), the presence of vegetation, and the state of the pore water in the bank (Cherry et al. 1996). Although simplified, single valued correlations between a number of variables were established empirically and expressed as power functions, Johns Hopkins concluded that they did not adequately describe meander behavior.

In regard to computer modeling, a number of authors have developed versions of the bend flow model (e.g., Parker et al. 1982; Beck and Melfi 1984; Hasegawa 1989; Odgaard and Bergs 1987; Garcia et al. 1994) and although the models have typically been tested with plots of predicted vs. observed channel form for a limited number of channels, there has been little general testing of these models over a range of hydrologic and geologic conditions (Cherry et al. 1996).

After testing the bend flow model for 26 of the meandering sites in the Brice data set, the Johns Hopkins study concluded that both the accuracy and applicability of the bend-flow meander migration model are limited by a number of simplifying assumptions. Among the most important of these are the use of a single discharge and the assumption of constant channel width, both of which prevent the model from successfully forecasting the spatial and temporal variability that appears to be inherent in the process of bend migration.

It was also concluded that much of the discrepancy between the predicted and observed distributions of erosion can be accounted for by the fact that meander migration is modeled as a smooth, continuous process. In reality, erosion occurs predominantly in discrete events, and varies greatly both temporally and spatially along the channel from bend to bend (Nanson and Hickin 1983). The Johns Hopkins study noted that the identification of local factors that influence the amount of bank erosion that occurs is a subject "that will require further investigation."

In addition to channel and bank characteristics, floodplain characteristics must also be incorporated into an analysis procedure. The floodplain characteristics that should affect meander migration include geologic controls, alluvial deposits and topographic variability. Geologic controls include bedrock outcrops and erosion resistant features along the valley sides. Alluvial deposits frequently include oxbows, meander scrolls and scars, and clay plugs, each with different erodibility characteristics. Topographic variability that should be considered include the cross valley slope of the adjacent floodplain and valley slope. These factors could be incorporated into regression equations but would be difficult to include in computer modeling of bendway migration.

## 5.9 SOLVED PROBLEMS RIVER MORPHOLOGY AND RESPONSE

### 5.9.1 PROBLEM 1 Meandering and Braiding

(a) Consider the sinuous point bar stream in Figure 5.31. Determine the following characteristics: meander wavelength  $\lambda$ ; meander width  $W_m$ ; mean radius of curvature  $r_c$ ; meander amplitude  $A$ ; and the bend deflection angle  $\phi$ .

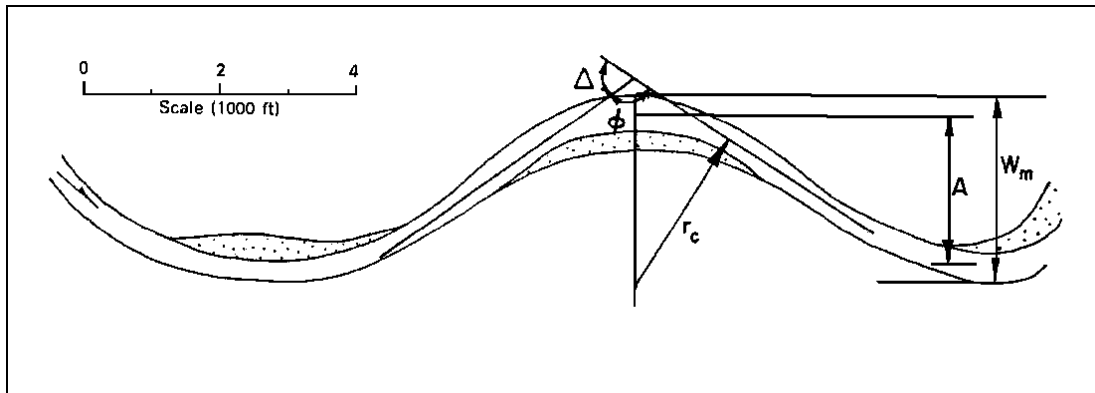


Figure 5.31. Sinuous point bar stream.

Meander wavelength  $\lambda$  is approximately 11,000 ft (3,353 m)  
 Radius of curvature  $r_c$  is approximately 2,400 ft (732 m)  
 Channel width ranges from 250 ft to 850 ft (76 to 260 m) at high stage  
 Meander amplitude  $A$  is 2,200 ft (670 m)  
 Meander width  $W_m$  is 2,700 ft (823 m)  
 Bend deflection angle  $\phi$  is  $105^\circ$   
 Sinuosity is 1.2

(b) Given the sand size  $D_{50} = 0.5\text{mm}$ , the bankfull discharge  $Q = 10,000$  cfs ( $283\text{ m}^3/\text{s}$ ) and the slope  $S = 2 \times 10^{-4}$ , determine the effect of increasing slope, discharge, sediment size and sediment discharge on the planform geometry.

The result of increasing any or several of these variables (Figure 5.18 and Table 5.4) is to promote braiding of this channel. When locating this stream on Lane's diagram (Figure 5.18) it is shown that with  $SQ^{0.25} = 0.002$  (SI = .00082), this river is very close to the line  $SQ^{0.25} = 0.0017$  (.0007 for SI) for meandering streams. Hence an increase in discharge or slope would be required to change the planform to a braided stream.

(c) Determine the effect of increased discharge of bed sediment size, bed sediment load and washload on channel stability, resistance to flow, energy slope and stage of the same river.

The Table 5.4 can be used to provide a qualitative response to these changes.

- Increase in discharge results in an increase in stage and a decrease in energy slope and channel stability.
- Increase in sediment size results in an increase in stage, energy slope and resistance to flow. The channel stability might not be changed.
- Increase in bed sediment load should increase the channel stability through a decreased resistance to flow, slope and stage.
- Effect of increasing washload is similar to that of increasing bed sediment load except for channel stability, which is uncertain.

### 5.9.2 PROBLEM 2 Classification of Alluvial Reaches

Identify the three types of alluvial river reaches sketched below. Discuss the relative stability of each channel.

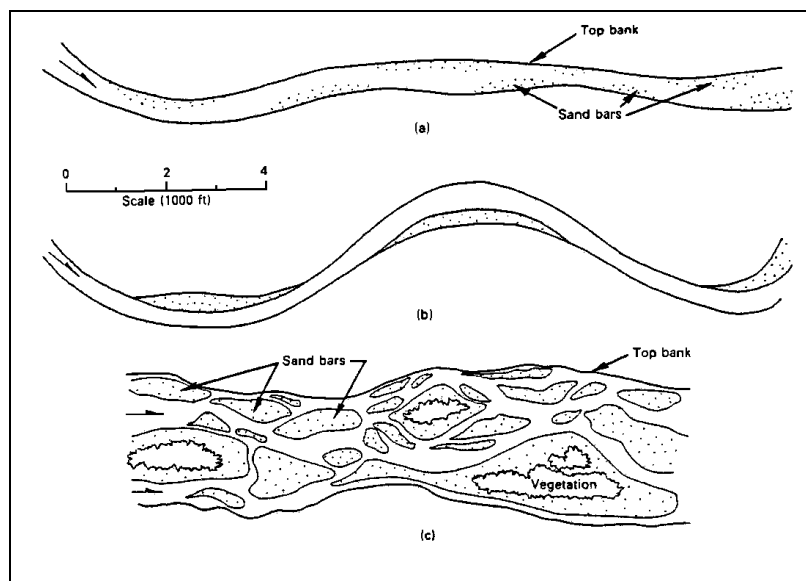


Figure 5.32. River channels (After Petersen 1986).

Based on the classification presented in Figures 5.11, 5.12, and 5.13, the first stream (a) is a straight channel with alternate bars and sinuous thalweg. This stream has a relatively low slope and low width-depth ratio. Figure 5.13 also indicates that it has an intermediate sediment size, sediment load and moderate ratio of bedload to total load (between 3 - 10 percent). This stream can be classified as relatively stable.

The second stream (b) is a sinuous point bar stream which is somewhat wider at bends. The meander bends are expected to shift gradually with possible neck cutoff. The stream is then relatively stable.

The third stream (c) is a braided sand-bed stream with multiple bars and channels. Bars are likely to be comprised of coarse sand and the large flow velocities and stream power will generate large sediment load with a large proportion transported as contact load. The overall stability of this braided channel is very low, channel shifting, and avulsions are certainly common.

### **5.9.3 PROBLEM 3 Channel Response to Changes in Watershed Conditions**

Determine the effect of watershed deforestation, bank erosion and headcutting on channel stability and gradation changes in an alluvial stream.

Referring to Table 5.8, deforestation generally causes aggradation problems and therefore channel instability. The reason for this is that deforestation increases runoff and peak runoff discharge as well as sediment transport from upland areas.

Headcutting is a degradation process. Upstream migration of headcuts induces bank failure and channel stability problems. Bank erosion has basically the same consequence on channel stability as that of headcutting. The gradation changes, however, are more difficult to assess because bank erosion changes the width-depth ratio.

### **5.9.4 PROBLEM 4 Channel Migration Rate**

(a) Determine the bank erosion rate and the erosion index of the sinuous point bar stream sketched in Figure 5.33.

The best method to estimate the rate of bank erosion is to compare two sets of aerial photographs. However, a first assessment can be obtained from Figure 5.26. Entering the figure with an average width around 150 m (492 ft), the median erosion rate should be around 2 meters (6.5 ft) per year. Wide bend streams have slightly larger erosion rates than given by the dashed line. Entering Figure 5.28 with a sinuosity of 1.2, the erosion index might be as large as 18 indicating channel instability. Erosion is to be expected on the concave side of the bends. Other means for assessing lateral migration rates such as study of past aerial photographs, scroll formation (Figure 5.12(b)) and field studies should be undertaken if any bridge crossing was to be built across this river.

(b) Sketch the likely future changes in the meandering river shown in the sketch below (Figure 5.34).

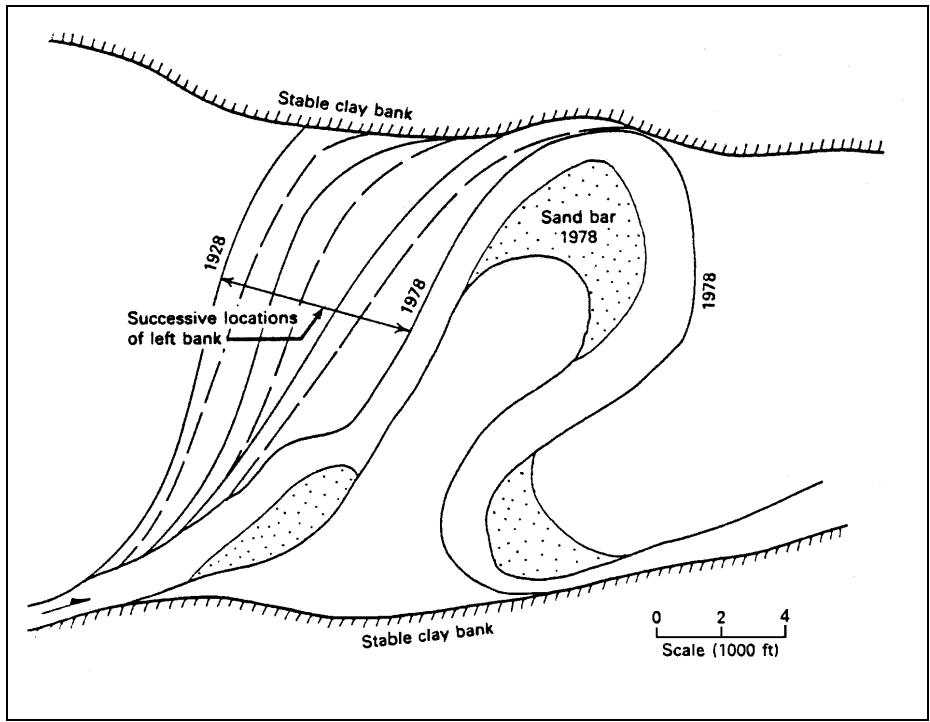


Figure 5.33. Meandering river sketch (after Petersen 1986).

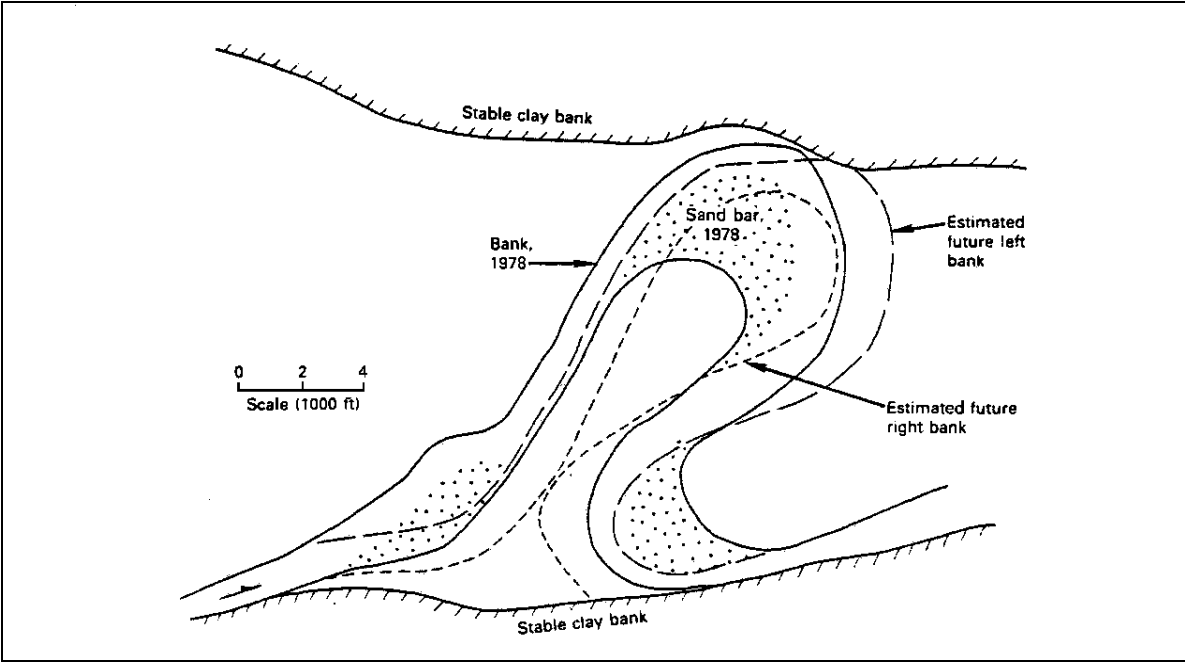


Figure 5.34. Estimated future location of a meandering river (after Petersen 1986).



The river (left bank) has moved downvalley approximately 6,000 feet (1,829 m) in 50 years or an average of 120 ft (36 m) per year. The narrowest point of the meander neck is about 2,500 ft (762 m). At its historical rate, this meandering channel will most likely lead to a cutoff in the next 15 to 20 years. The estimated position of the channel is sketched in Figure 5.34.

### 5.9.5 PROBLEM 5 At-A-Station and Downstream Hydraulic Geometry Relationships (SI)

At bankfull discharge conditions  $Q_1 = 227 \text{ m}^3/\text{s}$  and the width of a sand-bed stream ( $D_{s1} = 0.6 \text{ mm}$ ) is  $W_1 = 76 \text{ m}$ , the maximum flow depth is  $y_{o1} = 2.4 \text{ m}$ , the slope is  $S_{f1} = 2.5 \times 10^{-4}$ , and the maximum velocity is  $V_1 = 1.5 \text{ m/s}$ .

(a) Estimate the width,  $W_2$ , depth  $y_{o2}$ , slope  $S_{f2}$  and velocity  $V_2$  at the same station when the discharge  $Q_2$  is  $5.7 \text{ m}^3/\text{s}$  if the cross-sectional geometry is unknown.

The at-a-station hydraulic geometry relationships (Table 5.3) can be used when no specific field data is available.

For width:

$$W_2 = W_1 \left( \frac{Q_2}{Q_1} \right)^{0.26} = 76 \left( \frac{5.7}{227} \right)^{0.26} = 29.2 \text{ m}$$

For depth:

$$y_{o2} = y_{o1} \left( \frac{Q_2}{Q_1} \right)^{0.40} = 2.4 \left( \frac{5.7}{227} \right)^{0.40} = 0.55 \text{ m}$$

Slope is unchanged:

$$S_{f1} = S_{f2} = 2.5 \times 10^{-4}$$

For velocity:

$$V_2 = V_1 \left( \frac{Q_2}{Q_1} \right)^{0.34} = 1.5 \left( \frac{5.7}{227} \right)^{0.34} = 0.43 \text{ m/s}$$

(b) Using the same station as for part (a), estimate the width,  $W_2$ , depth  $y_{o2}$ , slope  $S_{f2}$  and velocity  $V_2$  in an upstream section of this stream if the bankfull discharge is  $14 \text{ m}^3/\text{s}$  and the bed material is gravel ( $D_{50} = 8 \text{ mm}$ ). How would the hydraulic geometry change if the bed material upstream is sand ( $D_{50} = 0.6 \text{ mm}$ )?

The "downstream" geometry relationships can be used in this case. Two types of relationships are given in Table 5.3. The sand bed relationships are a function of discharge only, whereas the gravel bed relationships are a function of both discharge and sediment size. Both methods are compared in the following.

### Flow Depth

$$\text{Sand bed: } y_{o_2} = y_{o_1} \left( \frac{Q_{b2}}{Q_{b1}} \right)^{0.46} = 2.4 \left( \frac{14}{227} \right)^{0.46} = 0.67 \text{ m}$$

$$\text{Gravel bed: } y_{o_2} = y_{o_1} \left( \frac{Q_{b2}}{Q_{b1}} \right)^{0.40} = 2.4 \left( \frac{14}{227} \right)^{0.4} = 0.79 \text{ m}$$

### Channel width

$$\text{Sand bed: } W_2 = W_1 \left( \frac{Q_{b2}}{Q_{b1}} \right)^{0.46} = 76 \left( \frac{14}{227} \right)^{0.46} = 21.1 \text{ m}$$

$$\text{Gravel bed: } W_2 = W_1 \left( \frac{Q_{b2}}{Q_{b1}} \right)^{0.53} \left( \frac{D_{s_2}}{D_{s_1}} \right)^{-0.33} = 76 \left( \frac{14}{227} \right)^{0.53} \left( \frac{8}{0.6} \right)^{-0.33} = 7.4 \text{ m}$$

### Friction slope

$$\text{Sand bed: } S_{f_2} = S_{f_1} \left( \frac{Q_{b2}}{Q_{b1}} \right)^{-0.46} = 2.5 \times 10^{-4} \left( \frac{14}{227} \right)^{-0.46} = 9 \times 10^{-4}$$

$$\text{Gravel bed: } S_{f_2} = S_{f_1} \left( \frac{Q_{b2}}{Q_{b1}} \right)^{-0.4} \left( \frac{D_{s_2}}{D_{s_1}} \right)^1 = 2.5 \times 10^{-4} \left( \frac{14}{227} \right)^{-0.4} \left( \frac{8}{0.6} \right) = 0.01$$

### Velocity

$$\text{Sand bed: } V_2 = V_1 \left( \frac{Q_{b2}}{Q_{b1}} \right)^{0.08} = 1.5 \left( \frac{14}{227} \right)^{0.08} = 1.2 \text{ m/s}$$

$$\text{Gravel bed: } V_2 = V_1 \left( \frac{Q_{b2}}{Q_{b1}} \right)^{0.07} \left( \frac{D_{s_2}}{D_{s_1}} \right)^{.33} = 1.5 \left( \frac{14}{227} \right)^{0.07} \left( \frac{8}{0.6} \right)^{.33} = 2.9 \text{ m/s}$$

The gravel bed relationships give a steeper, faster flowing and narrower channel as compared to the sand bed relationships. Unless the sediment size is markedly different for two streams, the resulting hydraulic geometry calculated from both sets of equations will be similar.

### 5.9.6 PROBLEM 6 At-A-Station and Downstream Hydraulic Geometry Relationships (English)

At bankfull discharge conditions  $Q_1 = 8000$  cfs and the width of a sand-bed stream ( $D_{s1} = 0.6$  mm) is  $W_1 = 250$  ft, the maximum flow depth is  $y_{o1} = 8$  ft, the slope is  $S_{f1} = 2.5 \times 10^{-4}$ , and the maximum velocity is  $V_1 = 5$  ft/s.

(a) Estimate the width,  $W_2$ , depth  $y_{o2}$ , slope  $S_{f2}$  and velocity  $V_2$  at the same station when the discharge  $Q_2$  is 200 cfs if the cross-sectional geometry is unknown.

The at-a-station hydraulic geometry relationships (Table 5.3) can be used when no specific field data is available.

For width:

$$W_2 = W_1 \left( \frac{Q_2}{Q_1} \right)^{0.26} = 250 \left( \frac{200}{8000} \right)^{0.26} = 96 \text{ ft}$$

For depth:

$$y_{o2} = y_{o1} \left( \frac{Q_2}{Q_1} \right)^{0.40} = 8 \left( \frac{1}{40} \right)^{0.40} = 1.8 \text{ ft}$$

Slope is unchanged:

$$S_{f1} = S_{f2} = 2.5 \times 10^{-4}$$

For velocity:

$$V_2 = V_1 \left( \frac{Q_2}{Q_1} \right)^{0.34} = 5 \left( \frac{1}{40} \right)^{0.34} = 1.4 \text{ ft/s}$$

(b) Using the same station as for part (a), estimate the width,  $W_2$ , depth  $y_{o2}$ , slope  $S_{f2}$  and velocity  $V_2$  in an upstream section of this stream if the bankfull discharge is 500 cfs and the bed material is gravel ( $D_{50} = 8$  mm). How would the hydraulic geometry change if the bed material upstream is sand ( $D_{50} = 0.6$  mm)?

The "downstream" geometry relationships can be used in this case. Two types of relationships are given in Table 5.3. The sand bed relationships are a function of discharge only, whereas the gravel bed relationships are a function of both discharge and sediment size. Both methods are compared in the following.

### Flow Depth

$$\text{Sand bed: } y_{o_2} = y_{o_1} \left( \frac{Q_{b2}}{Q_{b1}} \right)^{0.46} = 8 \left( \frac{500}{8000} \right)^{0.46} = 2.2 \text{ ft}$$

$$\text{Gravel bed: } y_{o_2} = y_{o_1} \left( \frac{Q_{b2}}{Q_{b1}} \right)^{0.40} = 8 \left( \frac{1}{16} \right)^{0.4} = 2.6 \text{ ft}$$

### Channel width

$$\text{Sand bed: } W_2 = W_1 \left( \frac{Q_{b2}}{Q_{b1}} \right)^{0.46} = 250 \left( \frac{1}{16} \right)^{0.46} = 70 \text{ ft}$$

$$\text{Gravel bed: } W_2 = W_1 \left( \frac{Q_{b2}}{Q_{b1}} \right)^{0.53} \left( \frac{D_{s_2}}{D_{s_1}} \right)^{-0.33} = 250 \left( \frac{1}{16} \right)^{0.53} \left( \frac{8}{0.6} \right)^{-0.33} = 25 \text{ ft}$$

### Friction slope

$$\text{Sand bed: } S_{f_2} = S_{f_1} \left( \frac{Q_{b2}}{Q_{b1}} \right)^{-0.46} = 2.5 \times 10^{-4} \left( \frac{1}{16} \right)^{-0.46} = 9 \times 10^{-4}$$

$$\text{Gravel bed: } S_{f_2} = S_{f_1} \left( \frac{Q_{b2}}{Q_{b1}} \right)^{-0.4} \left( \frac{D_{s_2}}{D_{s_1}} \right)^1 = 2.5 \times 10^{-4} \left( \frac{1}{16} \right)^{-0.4} \left( \frac{8}{0.6} \right) = 0.01$$

### Velocity

$$\text{Sand bed: } V_2 = V_1 \left( \frac{Q_{b2}}{Q_{b1}} \right)^{0.08} = 5 \left( \frac{1}{16} \right)^{0.08} = 4 \text{ ft/s}$$

$$\text{Gravel bed: } V_2 = V_1 \left( \frac{Q_{b2}}{Q_{b1}} \right)^{0.07} \left( \frac{D_{s_2}}{D_{s_1}} \right)^{.33} = 5 \left( \frac{1}{16} \right)^{0.07} \left( \frac{8}{0.6} \right)^{.33} = 9.7 \text{ ft/s}$$

The gravel bed relationships give a steeper, faster flowing and narrower channel as compared to the sand bed relationships. Unless the sediment size is markedly different for two streams, the resulting hydraulic geometry calculated from both sets of equations will be similar.

### **5.9.7 PROBLEM 7 Downstream Sediment Size Distribution**

Measurements of sediment size in the St.-Lawrence Seaway between Cornwall and Valleyfield are given in the following table.

Distance Downstream of Cornwall		D <sub>50</sub> (mm)
(km)	(mi)	
0	0	28
24.1	15	0.25
40.2	25	0.018
48.3	30	0.003
56.3	35	0.001

Estimate the mean sediment size D<sub>50</sub> 10 miles (16.1 km) and 20 miles (32.2 km) downstream of Cornwall.

The gradual decrease in sediment size with downstream distance can be approximated by the following equation:

$$(SI) \quad D_{50} = 28 \times 10^{-0.082x}$$

$$(English) \quad D_{50} = 28 \times 10^{-0.132x}$$

This equation was obtained by regression analysis based on Equation 5.13. At distances of 10 and 20 miles (16.1 and 32.2 km), the expected mean sediment sizes D<sub>50</sub> obtained by this relationship are, respectively, 1.34 mm and 0.064 mm.

### 5.9.8 PROBLEM 8 Scale Ratios for Physical Models (SI)

A physical model is to be built in the Hydraulics Laboratory to simulate the flow pattern around a structure in a complex multiple channel stream. About 334 m<sup>2</sup> of space (with a maximum length of 18.3 m) is available in the laboratory to model a 800 m reach. Knowing that the same fluid (water) will be used for both the model and the prototype, determine the appropriate scale ratios for time, discharge and force. Also, required is the flow depth in the model at the location where flow depth reaches 6 m in the prototype.

A fixed boundary model will be used and open channel flow modeling is scaled by similarity in Froude number. The scale ratios for  $\gamma$  and  $\rho$  equal unity and thus, scaling depends uniquely on the length scale  $L = 18.3/(800) = 2.3 \times 10^{-2}$ . The following scale ratios for time, discharge and force are calculated from the expressions shown in Table 5.7.

Parameter      Scale Ratio

Time               $(L\rho/\gamma)^{1/2} = L^{1/2} = 0.15$

Discharge         $L^{5/2} (\gamma/\rho)^{1/2} = L^{5/2} = 8.0 \times 10^{-5}$

Force              $L^3 \gamma = L^3 = 1.2 \times 10^{-5}$

The flow depth of the model at  $h = 6.0$  m is given by the product  $hL = 0.14$  m.

### 5.9.9 PROBLEM 9 Scale Ratios for Physical Models (English)

A physical model is to be built in the Hydraulics Laboratory to simulate the flow pattern around a structure in a complex multiple channel stream. About 3,600 ft<sup>2</sup> of space (with a maximum length of 60 ft) is available in the laboratory to model a 1/2-mile reach. Knowing that the same fluid (water) will be used for both the model and the prototype, determine the appropriate scale ratios for time, discharge and force. Also, required is the flow depth in the model at the location where flow depth reaches 20 ft in the prototype.

A fixed boundary model will be used and open channel flow modeling is scaled by similarity in Froude number. The scale ratios for  $\gamma$  and  $\rho$  equal unity and thus, scaling depends uniquely on the length scale  $L = 60/(0.5 \times 5280) = 2.3 \times 10^{-2}$ . The following scale ratios for time, discharge and force are calculated from the expressions shown in Table 5.7.

<u>Parameter</u>	<u>Scale Ratio</u>
Time	$(L\rho/\gamma)^{1/2} = L^{1/2} = 0.15$
Discharge	$L^{5/2} (\gamma/\rho)^{1/2} = L^{5/2} = 8.0 \times 10^{-5}$
Force	$L^3 \gamma = L^3 = 1.2 \times 10^{-5}$

The flow depth of the model at  $h = 20$  ft is given by the product  $hL = 0.45$  ft.

## CHAPTER 6

### RIVER STABILIZATION AND BANK PROTECTION

#### 6.1 OVERVIEW

From a study of river morphology and river response (Chapter 5), it should be clear that both short-term and long-term changes can be expected on river systems as a result of natural and man-made influences. Recommended structures and design methods for river control are presented in this chapter. The integrated and interactive effects of these structures with the river are discussed in Chapter 9.

Numerous types of river control and bank stabilization devices have evolved through past experience. Concrete, brick, willow, rock, and asphalt mattresses; sacked concrete and sand; riprap grouted slope protection; sheet and timber piles; steel jack and brush jetties; angled and sloped rock-filled, earth-filled, and timber dikes; automobile bodies; and concrete armor units have all been used in the practice of training, restoring, and stabilizing rivers.

An early treatise on the subject of bank and shore protection was prepared by the California Division of Highways (1959). A large number of publications on river training and stabilization have been prepared by the U.S. Army Corps of Engineers (1981, 1994a,b) and the U.S. Bureau of Reclamation. Many more publications on the subject exist in the open literature. It is not intended that an exhaustive coverage of the various types of river control structures and methods of design be made in this manual; rather, the purpose of this manual is to recommend methods and devices which provide useful alternatives to the highway engineer for the majority of circumstances which are likely to be encountered in highway practice. A treatise of great interest in relation to highway crossings is the Report FHWA-RD-78-162 and 163 on countermeasures for hydraulic problems at bridges by Brice and Blodgett (1978). The interested reader is referred to these two volumes for an analysis and assessment (Vol. 1) and 283 case histories (Vol. 2).

The Federal Highway Administration has prepared Hydraulic Engineering Circular (HEC) No. 23 (Lagasse et al. 2001) to provide experience, selection, and design guidelines for a wide range of stream instability and bridge scour countermeasures. When used in combination with HEC-20 (Lagasse et al. 2001) and HEC-18 (Richardson and Davis 2001), these three publications provide a comprehensive integrated approach to analyzing stream instability and bridge scour problems and selecting and designing countermeasures for specific problems.

Generally, changes to river alignment, river cross section, training, and bank stabilization of rivers associated with highway projects are confined to short reaches of the river. While the methods for river training and bank stabilization discussed herein are applicable to short and long reaches of the river, they are not a panacea to all problems associated with highway encroachments on rivers. An understanding of river system dynamics is essential to selection, design and successful installation of river stabilization, restoration, and bank protection works. It must also be recognized that the solution to a particular problem may generate problems elsewhere in the river system.

## 6.2 STREAM BANK EROSION

The erosion, instability, and/or retreat of a stream bank is dependent on the processes responsible for the erosion of material from the bank and the mechanisms of failure resulting from the instability created by those processes. Bank retreat is often a combination of these processes and mechanisms varying at seasonal and sub-seasonal time scales. Changes in channel geometry with time are particularly significant during periods when alluvial channels are subjected to high flows. The converse situation exists during relatively dry periods. Erosive forces during high flow periods may have a capacity approximately 100 times greater than those forces acting during periods of intermediate and low flow. In most instances when considering the instability of alluvial rivers, it can be shown that approximately 90 percent of all river changes occur during the small percentage of the time when the discharge exceeds the dominant discharge.

Regardless of the fact that the majority of bank changes occur during comparatively short time periods, there may also be regions within a river in which some degree of instability is exhibited for all flow conditions. Raw banks may develop on the outside of bends as a consequence of direct impingement of the flowing water. Sloughing banks may occur as a result of seepage and other secondary forces created by water draining back through the banks into the river. Continuous wave action, generated either naturally or by human activities, may also precipitate erosion problems.

### 6.2.1 Causes of Streambank Failure

Bank retreat processes may be grouped into three categories: weakening and weathering processes, direct fluvial entrainment, and mass failure. HEC-20 (Lagasse et al. 2001) provides more detail on these processes. The impact of these processes on bank retreat is dependent on site characteristics, especially near-bank hydraulic fields, bank height, and the geotechnical properties of the bank material. Table 1 lists factors affecting bank erosion.

A. Hydraulic Factors	B. Geomorphic Factors	C. Human Factors	D. Biological Factors	E. Climatic Factors	F. Other
Fluid Properties	River Planform	Agricultural Activities	Vegetation	Freezing	Subsurface Flows
Specific Weight	Meandering	Mining	Trees	Ice Thickness	Seepage Forces
Viscosity (Temp)	Straight	Dams	Shrubs	Duration	Piping
Flow Characteristics	Braided	Navigation	Grass	Frequency	Waves
Discharge	Anabranching	Transportation	Animals	Thawing	Wind
Magnitude	Bed and Bank Material	Urbanization	Domestic	Permafrost	Boats
Duration	Size	Drainage	Wild	Precipitation	
Frequency	Gradation	Floodplain Develop.			
Velocity	Shape	Recreational Boating			
Velocity Distrib.	Specific Weight	Commercial Boating			
Turbulence	Fall Velocity				
Shear Stress	Bank Characteristics				
Drag/Lift Forces	Cohesive				
Momentum	Noncohesive				
Energy	Stratified				
	Height				



## 6.2.2 Bed and Bank Material

Resistance of a river bank to erosion is closely related to several characteristics of the bank material. Bank material deposited in the river can be broadly classified as cohesive, noncohesive, and composite. Failure of banks for various situations is shown in Figure 6.1.

Cohesive bank material is more resistant to surface erosion and has low permeability which reduces the effects of seepage, piping, frost heaving, and subsurface flow on the stability of the banks. However, such banks when undercut and/or saturated are more likely to fail due to mass wasting processes such as sliding.

Noncohesive bank material tends to be removed grain by grain from the bank line. The rate of particle removal, and hence the rate of bank erosion, is affected by factors such as the direction and magnitude of the velocity adjacent to the bank, the turbulent fluctuations, the magnitude and fluctuations in the shear stress exerted on the banks, seepage force, piping and wave forces, many of which may act concurrently.

Composite or stratified banks are very common on alluvial rivers and generally are the product of past transport and deposition of sediment by the river. More specifically, these types of banks consist of layers of materials of various sizes, permeability, and cohesion. The layers of noncohesive material are subject to surface erosion, but may be partly protected by adjacent layers of cohesive material. This type of bank is also vulnerable to erosion and sliding as a consequence of subsurface flows and piping.

## 6.2.3 Subsurface Flow

With flow of water from the river into the adjacent banks, a stabilizing seepage force is generated. Rivers that continuously seep water into the banks tend to have smaller widths and larger depths for a particular discharge. The reverse is true of the rivers that continuously gain water by an inflow through their banks. The inflowing water creates a seepage force that makes the banks less stable. The movement of water through the bank material can be attributed to various factors.

If the water table is higher than river stage, flow will be from the banks into the river. The high water table may result from: (1) a wet period during which water draining from tributary watersheds saturates the floodplain to a higher level; (2) poor drainage conditions resulting from deterioration or failure of surface drainage systems; (3) increased infiltration resulting from changes in land use causing an increase in water level; (4) irrigated floodplains; and (5) development of the adjacent floodplain for homes and businesses that utilize septic tanks and leach fields to dispose of waste water and sewage.

With a rise in river stage an outward gradient is developed that induces flow into the banks. This can be caused by: (1) the storage and release of water for pumped storage hydropower generation which causes numerous fluctuations in river stage; (2) boat and wind waves which cause local variations in stage that introduce inflow and outflow of water from the banks; (3) predominately dry and semi-arid channels subject to intermittent floods. However, because the duration of the change in stage is small, the inflow and outflow phenomena are usually concentrated locally in the surface of the banks; and (3) the formation and loss of backwater caused by ice flows and ice jams which lead to both seepage into and out of the banks. Frequent stage fluctuations, such as may occur with hydropower operations, may exacerbate the bank erosion process.

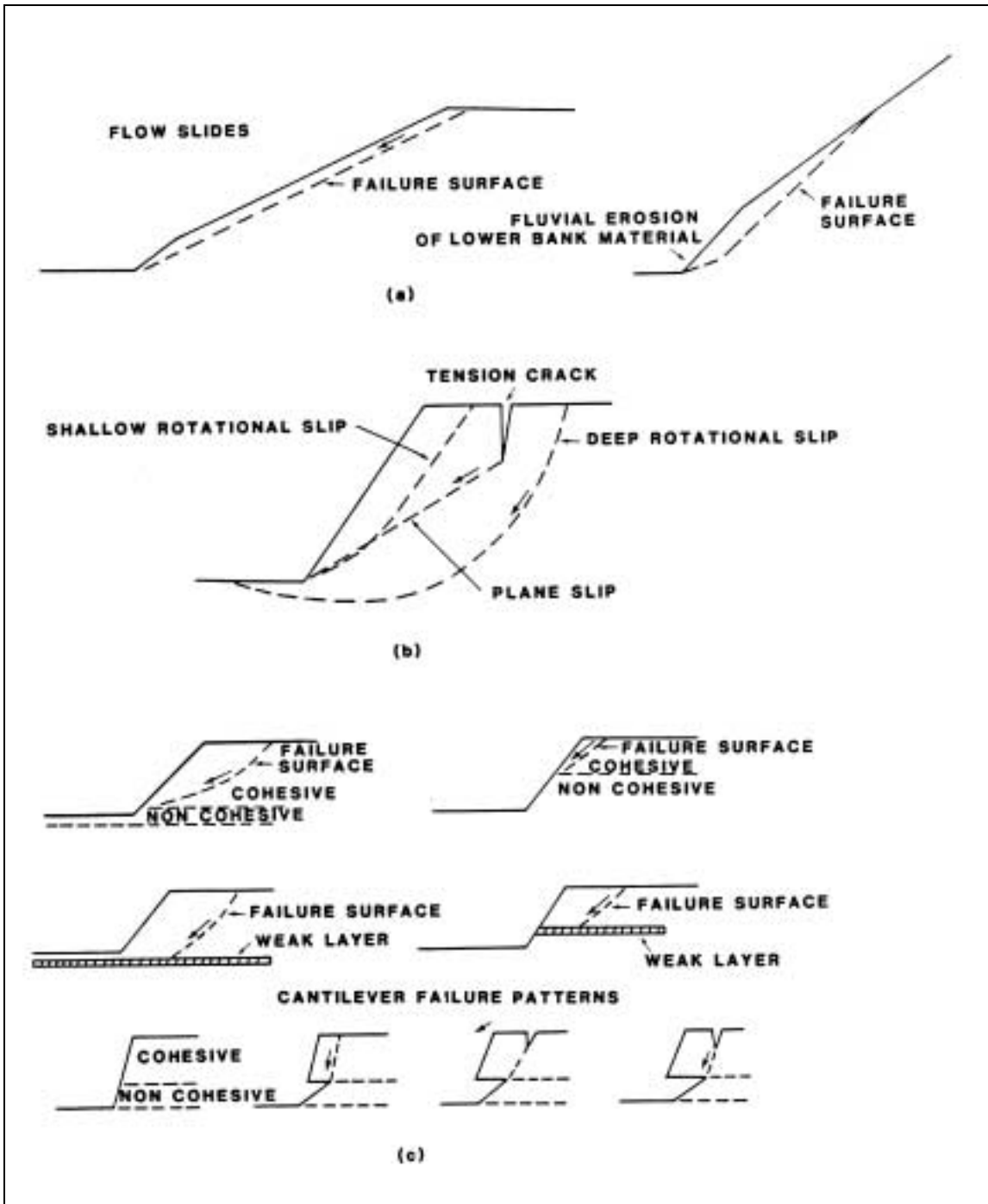


Figure 6.1. Typical bank failure surfaces (a) noncohesive, (b) cohesive, (c) composite (after Brown 1985a,b,c).

The presence of water in the banks of rivers and its movement toward or away from the river affect bank stability and bank erosion in various ways. The related erosion of banks is a consequence of seepage forces, piping, and mass wasting.

#### **6.2.4 Piping of River Banks**

Piping is another phenomenon common to the alluvial banks of rivers. With stratified banks, i.e., lenses of sand and coarser material sandwiched between a layer of finer cohesive materials, flow is induced in more permeable layers by changes in river stage and by wind- and boat-generated waves. If the flow through the permeable lenses is capable of dislodging and transporting particles from the permeable lenses, the material is slowly removed, undermining portions of the bank. Without this foundation material to support the overlying layers, a block of bank material drops down and results in the development of tension cracks sketched in Figure 6.1c. These cracks allow surface flows to enter, further reducing the stability of the affected block of bank material. Bank erosion may continue on a grain-by-grain basis or the block of bank material may ultimately slide downward and outward into the channel, causing bank failure as a result of a combination of seepage forces, piping, and mass wasting.

#### **6.2.5 Mass Wasting**

An alternative form of bank erosion is caused by local mass wasting. If the bank becomes saturated and possibly undercut by flowing water, blocks of the bank may slump or slide into the channel. Mass wasting may be further aggravated by construction of homes on river banks, operation of equipment on the floodplain adjacent to the banks, added gravitational force resulting from tree growth, location of roads that cause unfavorable drainage conditions, saturation of banks by leach fields from septic tanks, and increased infiltration of water into the floodplain as a result of changing land-use practices.

Landslides, the downslope movement of earth and organic materials, result from an imbalance of forces. Various forces are involved in mass wasting. These forces are associated with the downslope gravity component of the slope mass. Resisting these downslope forces are the shear strength of the earth's materials and any additional contributions from vegetation via root strength or engineered slope reinforcement activities. When a slope is acted upon by a stream or river, an additional set of forces is added. These forces are associated with removal of material from the toe of the slope, fluctuations in groundwater levels, and vibration of the slope. A slope may fail if stable material is removed from the toe. When the toe of a slope is removed, the slope loses more resistance by buttressing than it does by downslope gravitational forces. The slope materials may then tend to move downward into the void in order to establish a new balance of forces or equilibrium. Often this equilibrium is a slope configuration with less than original surface gradient. The toe of the failed mass can provide a new buttress against further movements. However, if this buttress is removed by stream erosion, the force equilibrium may again be upset. For slope toes acted upon by erosive stream water, the continual removal of toe material can upset the force balance.

### **6.3 RIVER TRAINING AND STABILIZATION**

Various devices and structures have been developed to control river flow along a preselected path and to stabilize the banks. Most have been developed through trial and error applications, aided in some instances by hydraulic model studies. Specific functions of bank protection and training works in relation to bridges and their approaches include: (1) stabilize eroding river banks and channel location in the case of shifting streams; (2) economize on bridge lengths by constricting the natural waterway; (3) direct flow parallel to piers and thereby minimize local scour; (4) improve the hydraulic efficiency of a waterway opening, thereby reducing backwater and scour and facilitating passage of ice and debris; (5) protect road approaches from stream attack and prevent meanders from migrating into the approaches; (6) permit construction of a well-aligned bridge crossing by diverting the channel from a skewed alignment; (7) reduce the overall cost of a road project by diverting the channel away from the base of a valley slope, thereby allowing a reduction in bridge length and height; (8) secure existing works, or to repair damage and improve initial designs; and (9) protect longitudinal encroachments.

A comprehensive bank stabilization and channel rectification program to control a river reach completely normally requires extensive work on concave banks in bends, minor work on convex bars, and control work on both banks through bridge crossings.

To minimize attack by the stream on stabilization and rectification structures, the river is shaped to an alignment consisting of a series of easy bends, with the flow directed from one bend into the next bend downstream in such a way as to maintain a direction essentially parallel to the channel flow line (see Section 5.8.4). Straight reaches and reaches of very small curvature should be avoided, insofar as practicable, because there is a tendency for flows to shift from side to side in such reaches. The optimum bend radius approximates that of relatively stable bends in the general river reach.

#### **6.3.1 Fixed Points**

One of the essential requirements in designing a system of stabilization works is that construction starts at a stable, fixed point on the bank and continues downstream to another stable location or to some point below which the river can safely be left uncontrolled. Construction of relatively short isolated stabilization work has often proved unsuccessful because eventual changes in the direction of flow inherent in bank caving in the upstream uncontrolled reach either will set up a direct attack against the isolated protective work and severely damage or destroy it, or will shift the attack to some other nearby reach of bank, requiring additional work and possible abandonment of the original work.

Revetments should be constructed on a smooth alignment, with no irregularities, in order to avoid eddies set up by disturbances to the flow that can lead to local scour and subsequent undermining of the revetment.

#### **6.3.2 Radius of Curvature**

The most appropriate radius of curvature for rectification and stabilization varies from river to river and from reach to reach for a given river. It must be determined on the basis of relatively stable natural bends for each stream (see Section 5.8.3).

The shorter the radius of curvature of a bend, the deeper the channel will be adjacent to the concave bank. The deeper the channel is, the greater the possibility of undermining bank protection work in the bend and the greater the cost of maintaining the structure. Therefore, sharp curvature of bends should be avoided to obtain the most economical control of the river.

### **6.3.3 Countermeasures for Channel Instability**

Countermeasures can be used to control both lateral and vertical channel instability and include river training structures and revetment armoring. River training structures are those which modify the flow (flow control). River training structures are distinctive in that they alter hydraulics to mitigate undesirable erosional and/or depositional conditions at a particular location or in a river reach. River training structures can be constructed of various material types and are not distinguished by their construction material, but rather, by their orientation to flow. River training structures are described as transverse, longitudinal or areal depending on their orientation to the stream flow.

To protect against lateral channel instability, flow control structures are used to:

- Direct flow from one bend into the next bend downstream
- Flair out sharp bends to a larger radius of curvature to provide a more desirable channel alignment
- Close off secondary channels and old bendways
- Concentrate flow on a limited width within a wider channel

To protect against vertical channel instability, flow control structures are used for:

- Limiting or halting long-term degradation
- Establishing a desired channel bed elevation in a bridge reach
- Arresting the migration of a head cut or nickpoint through a bridge reach

Revetments are structures parallel to the current and are used to armor the channel bank from erosive/hydraulic forces. They are usually applied in a blanket type fashion for areal coverage. Revetments can be classified as either rigid or flexible/articulating. Rigid revetments are typically impermeable and do not have the ability to conform to changes in the supporting surface. These countermeasures often fail due to undermining. Flexible/ articulating revetments can conform to changes in the supporting surface and adjust to settlement. These countermeasures often fail by removal and displacement of the armor material.

Rock riprap is probably the most widely used revetment material to stabilize river banks and protect the side slopes of embankments and river training devices. In the final report to Congress, the U.S. Army Corps of Engineers (1981) concluded that rock will likely continue to be the first choice of bank protection materials where material of sufficient size is available and affordable, because of durability, and other advantages. Because of its wide use and

importance in highway practice, a separate section (Section 6.6) is devoted to design and placement of rock riprap.

### 6.3.4 Countermeasure Design Guidelines

Hydraulic Engineering Circular (HEC) No. 23 (Lagasse et al. 2001) provides experience, selection, and design guidance for a wide range of stream instability and bridge scour countermeasures, including river training devices and revetment armoring.

HEC-23 is organized to:

- Highlight the various groups of countermeasures and identify their individual characteristics.
- For specific countermeasures, list information on their functional applicability to a particular problem, their suitability to specific river environments, the general level of maintenance resources required, and which State Highway Agencies (SHAs) have experience with specific countermeasures.
- Provide general criteria for selection of countermeasures for bridge scour and stream instability problems.
- Discuss countermeasure design concepts including design approach, hydraulic analysis, environmental permitting, special design considerations related to riprap, filters, and edge treatment, and biotechnical engineering approaches.
- Provide detailed design guidelines for specific countermeasures.

Specific design guidelines are provided in HEC-23 for the following river training devices:

- Bendway Weirs/Stream Banks
- Spurs
- Guide Banks
- Check Dams/Drop Structures

Design guidelines are also provided for the following armoring (revetment) countermeasures.

- Revetment (summary of HEC-11 guidance)
- Soil Cement
- Wire Enclosed Riprap Mattress
- Articulating Concrete Block Systems
- Articulating Grout Filled Mattress

Hydraulic Engineering Circular (HEC) No. 11 (Brown and Clyde 1989) is a comprehensive design manual for riprap revetment. HEC-11 includes discussions on erosion potential, erosion mechanisms and riprap failure modes, as well as riprap types including rock riprap, rubble riprap, gabions, preformed blocks, grouted rock, and paved linings. Design concepts included in HEC-11 are: design discharge, flow types, channel geometry, flow resistance, extent of protection, and toe depth. Detailed design guidelines are presented for rock riprap,

and design procedures are summarized in charts and examples. Design guidance is also presented for:

- Wire-enclosed rock (gabions)
- Precast concrete blocks
- Concrete paved linings

The following section (6.4) summarizes design concepts for selected flow control (river training) structures. Section 6.5 deals with riprap design and placement, and Section 6.6 describes design for revetment types other than riprap. General filter design concepts are discussed in Section 6.7 and issues related to overtopping flows on embankments are summarized in Section 6.8. Environmental considerations for streambank protection are presented in Section 6.9.

### **6.3.5 Protection of Training Works**

Granular or geosynthetic filters are essential to the performance of hydraulic countermeasures, especially armoring countermeasures such as bankline revetment or armoring used as protection for river training works such as spurs and guide banks. Filters prevent soil erosion beneath the armoring material, prevent migration of fine soil particles through voids in the armoring material, distribute the weight of the armor units to provide a more uniform settlement, and permit relief of hydrostatic pressure within the soils. Experience has indicated that the proper design of filters is critical to the stability of revetments. If openings in the filter material are too large, excessive piping through the filter can result in erosion of the subgrade beneath the armor. Conversely, if openings in the filter are too small, hydrostatic pressures can build up in the underlying soil and result in failure of the countermeasure. Guidelines for the selection, design, and specifications of filter material can be found in HEC-11 (Brown and Clyde 1989), HEC-23 (Lagasse et al. 2001), and Section 6.7.

Undermining of the edges of armoring countermeasures is another of the primary mechanisms of failure. The edges of the armoring material (head, toe, and flanks) should be designed so that undermining will not occur. For revetment slope protection, this is achieved by trenching the toe of the revetment below the channel bed to a depth which extends below the combined expected contraction scour and long-term degradation depth. When excavation to the contraction scour and degradation depth is impractical, a launching apron can be used to provide enough volume of rock to launch into the channel while maintaining sufficient protection of the exposed portion of the bank. Continuous systems, such as articulating concrete block systems and grout filled mattresses applied on side slopes, should be designed with an apron or toe trench so that the system provides protection below the combined expected contraction scour and long-term degradation depth. Tension anchors may be used to increase stability at the edges of these continuous systems. Additional guidelines on edge treatment for armoring countermeasures can be found in HEC-11 and HEC-23.

Variations in bed elevation during flow events or after bank hardening can result in the undermining of bank protection structures including longitudinal structures. Deep sections at the toe of the outer bank of a bendway are the result of scour. As discussed in Section 5.4.3, high velocity along the outer bank is caused by secondary currents and greater outer-bank depths, and together with the resultant shear stress, produce scour and cause a

difference between the sediment load entering and exiting the outer-bank zone. Since secondary currents transport sediment supplied, in large part, from outer bank erosion toward the inner bank of a bend, hardening of the outer bank by longitudinal bank protection structures may cause the channel cross section to narrow and deepen by preventing the recruitment of eroded outer bank sediments.

Experience is usually the most reliable means of estimating scour depth when designing a bank protection project for a particular stream. Lacking experience on a particular stream, scour depths may be estimated using physically based analytical models or empirical methods. Although scour-depth can be estimated analytically or empirically, empirical methods were generally found to provide better agreement with observed data.

Maynard (1996) provides an empirical method for determining scour depths on a typical bendway bank protection project. Although his studies are restricted to sand bed streams, the Maynard method agrees reasonably well with the limited number of gravel-bed data points obtained by Thorne and Abt (1993). Nonetheless, the techniques presented by Maynard are restricted to meandering channels having naturally developed widths and depths, and cannot be applied to channels that have been confined to widths significantly less than a natural system.

HEC-23 provides application guidelines for Maynard's approach to estimating toe protection requirements on stabilized bendways. HEC-23 also contains guidance for estimating scour at vertical wall structures (e.g., retards and bulkheads) from flow parallel to and impinging on the wall.

## **6.4 FLOW CONTROL STRUCTURES**

A flow control structure is defined here as a structure, either within or outside a channel that acts as a countermeasure by controlling the direction, velocity, or depth of flowing water. Structures within this category are sometimes called "river training works". Among the most important properties of a flow control structure is its degree of permeability. An impermeable structure may deflect a current entirely, whereas a permeable structure may serve mainly to reduce water velocity. As used here, the term "permeable" means that a structure has definite openings through which water is intended to pass, such as openings between adjacent boards or pilings, or the meshes of wire. Structures made of riprap, or filled with riprap, have some degree of permeability, but these are classed as impermeable because they act essentially as impermeable barriers to a rapidly moving current of water.

Types of flow control structures are distinguished on Figure 6.2.

### **6.4.1 Spurs**

A spur is a structure or embankment projected into a stream from the bank at some angle and for a short distance to deflect flowing water away from critical zones, to prevent erosion of the bank, and to establish a more desirable channel alignment or width. By deflecting the current from the bank and causing sediment deposits behind them, a spur or a series of spurs may protect the stream bank more effectively and at less cost than revetment riprap applied directly on the bank. Also, by moving the location of any scour away from the bank, failure of the riprap on the spur can often be repaired before damage is done to structures along and across the river. Conversely, failure of riprap on the bank may immediately endanger adjacent structures.



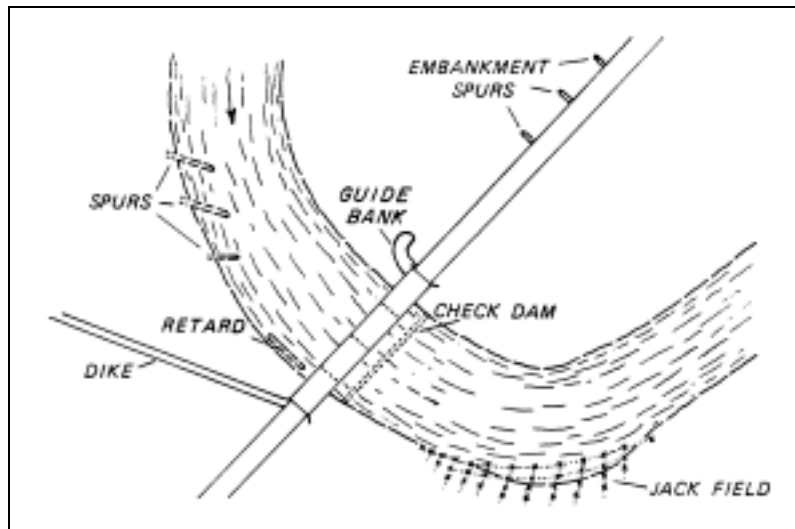


Figure 6.2. Placement of flow control structures relative to channel banks, crossing, and floodplain. Spurs, retards, dikes, and jack fields may be either upstream or downstream from the bridge (from Brice and Blodgett 1978).

Spurs are also used to protect highway embankments that form the approaches to a bridge crossing. Often these highway embankments cut off the overbank flood flows causing these flows to run parallel to the embankment enroute to the bridge opening. Spurs constructed perpendicular to the highway embankment keep the potentially erosive current away from the embankment, thus protecting it. Spurs as used in this report encompass the terms dikes, jetties, and groins, which are also used to describe these structures.

Spurs are also used to channelize a wide, poorly defined stream into a well-defined channel that neither aggrades nor degrades, thus maintaining its location from year to year. Spurs on streams with suspended sediment discharge can cause deposition to establish and maintain the new alignment. The use of spurs in this instance may decrease the length necessary for the bridge opening and may make a more suitable, stable channel approach to the bridge. This decreases the cost of the bridge structure.

Recommendations for spur design from Brown (1985) are summarized in HEC-23 (Lagasse et al. 2001). The major considerations are:

- Extent of Channelbank Protection
- Spur Length
- Spur Spacing
- Spur Angle/Orientation
- Spur Height
- Spur Crest Profile
- Channel Bed and Channel Bank Contact
- Spur Head Form

### 6.4.2 Bendway Weirs

Bendway weirs, also referred to as stream barbs, bank barbs, and reverse sills, are low elevation stone sills used to improve lateral stream stability and flow alignment problems at river bends and highway crossings. Bendway weirs are used for improving inadequate navigation channel width at bends on large navigable rivers. They are used more often for bankline protection on streams and smaller rivers. Design guidelines for bendway weirs are presented in HEC-23 (Lagasse et al. 2001).

### 6.4.3 Hardpoints

Hardpoints are an erosion control technique consisting of stone fills spaced along an eroding bank line (Figure 6.3). The structures protrude only short distances into the river channel and are supplemented with a root section extending landward into the bank to preclude flanking, should excessive erosion persist. The majority of the structure cannot be seen as the lower part consists of rock placed underwater, and the upper part is covered with topsoil and seeded with native vegetation. The structures are especially adaptable in long, straight reaches not subject to direct attack.

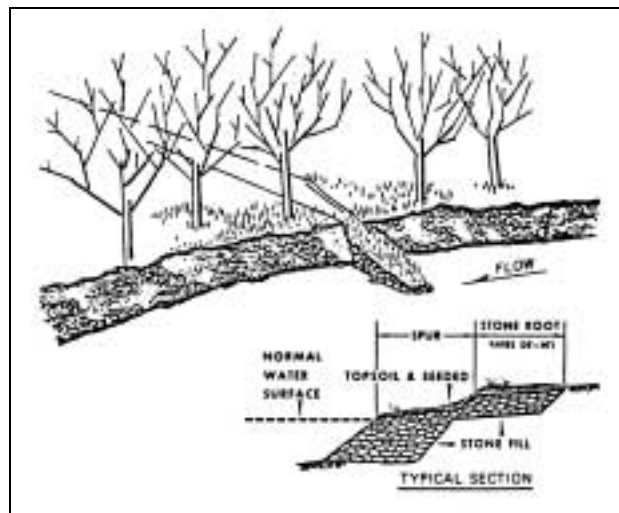


Figure 6.3. Perspective of hard point with section detail (after Brown 1985a,b,c).

### 6.4.4 Retards

Retards are devices placed parallel to embankments and river banks to decrease the stream velocities and prevent erosion (Figures 6.2 and 6.4).

Pile retards can be made of concrete, steel or timber. The design of timber pile retards is essentially the same as timber pile dikes shown in Figure 6.6. They may be used in combination with bank protection works such as riprap. The retard then serves to reduce the velocities sufficiently so that either smaller riprap can be used, or riprap can be eliminated.

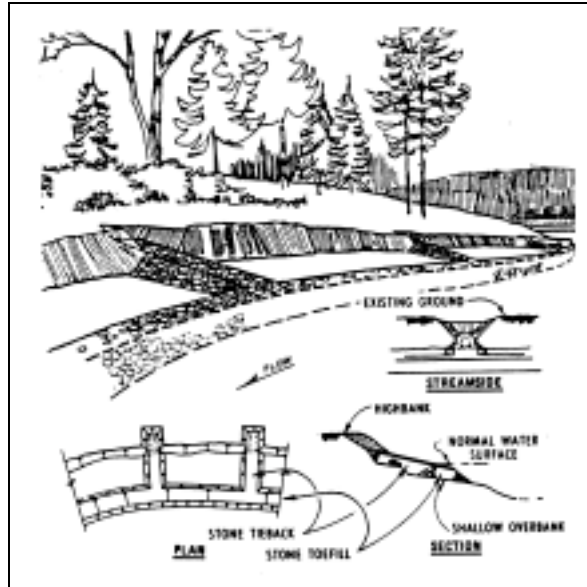


Figure 6.4. Retard.

Timber and concrete cribs are sometimes used for bulkheads and retaining walls to hold highway embankments, particularly where lateral encroachment into the river must be limited. Cribs are made up by interlocking pieces together in the manner shown in Figure 6.5. The crib may be slanted or vertical depending on height and the crib is filled with rock or earth. Reinforced concrete retaining walls are alternatives to timber cribs which can be considered. However, concrete retaining walls are expensive and are generally only used in special confined locations where space precludes other methods of bank protection. In constructing concrete retaining walls, drainage holes (weep holes) must be provided. The foundation of these walls should be placed below expected scour depths.

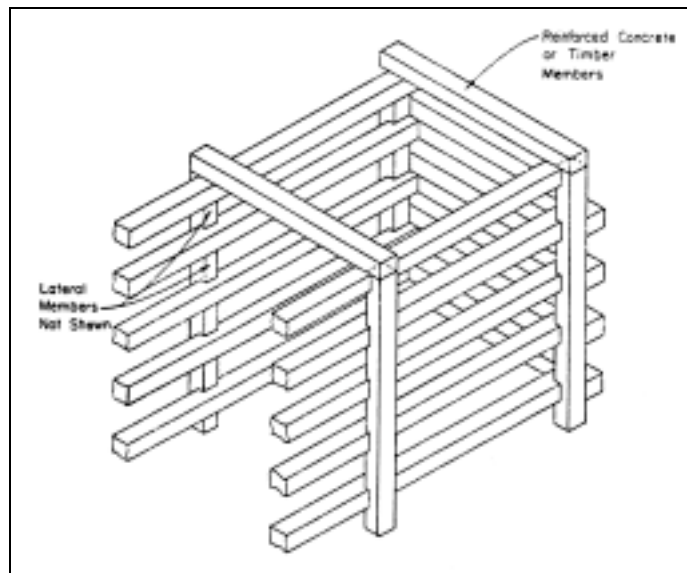


Figure 6.5. Concrete or timber cribs.

#### **6.4.5 Dikes (Floodplain)**

A floodplain dike is an impermeable linear structure for the control or containment of overbank flow. Most dikes are on floodplains (Figure 6.2) but in some situations (as on wide braided rivers or on alluvial fans) they may be within channels (see Section 6.4.6). Floodplain dikes are used to prevent flood water from bypassing a bridge, or to confine channel width and maintain channel alignment. Some dikes extend upstream from one or both sides of the bridge opening. These are similar in function to guide banks, but are usually much longer and may extend to the valley side. Such dikes are commonly called "training dikes." The use of fence-type structures for training dikes is mostly restricted to arid and semi-arid regions (Brice et al. 1978).

#### **6.4.6 Dikes (Channel)**

Both permeable and impermeable dikes are installed in channels. Permeable dikes are those which permit flow through the dike but at reduced velocities, thereby preventing further erosion of the banks and causing deposition of suspended sediment from the flow.

Timber or steel pile dikes (also retards) may consist of closely-spaced single, double, or multiple rows. There are a number of variations to this scheme. For example, wire fence may be used in conjunction with pile dikes to collect debris and thereby cause effective reduction of velocity. Double rows of piles can be placed together to form cribs, and rocks may be used to fill the space between the piles. Pile dikes are vulnerable to failure through scour. This can be overcome if the piles can be driven to a large depth to achieve safety from scour, or the base of the piles can be protected from scour with dumped rock in sufficient quantities. The various forms of pile dikes are illustrated in Figure 6.6.

The arrangement of piles depends upon the velocity of flow, quantity of suspended sediment transport, and depth and width of the river. If the velocity of flow is large, pile dikes are not likely to be very effective. Stabilization of the bank by other methods should be considered. On the other hand, in moderate flow velocities with high concentrations of suspended sediments, these dikes can be quite effective. Deposition of suspended sediments in the pile dike field is a necessary consequence of reduced velocities. If there is not sufficient concentration of suspended sediment in the flow, or the velocities in the dike fields are too large for deposition, the permeable pile dikes will only partially be effective in training the river and protecting the bends.

The length of each dike depends on channel width, position relative to other dikes, flow depth and available pile lengths. Generally, pile dikes are not used in large rivers where depths are great, although timber pile dikes have been used in the Columbia River. On the other hand, banks of wide shallow rivers can be successfully protected with dikes. The spacing between dikes varies from 3 to 20 times the length of the upstream dike, with closer spacing favored for best results.

Vane dikes are low-elevation structures designed to guide the flow away from an eroding bank line (Figure 6.7). The structures can be constructed of rock or other erosion-resistant material, the tops of which are constructed below the design water surface elevation and would not connect to the high bank. Water would be free to pass over or around the structure with the main thread of flow directed away from the eroding bank. The structures will discourage high erosive velocities next to an unprotected bank line, encourage diversity of various channel depths, and protect existing natural bottomland characteristics. The findings from a model investigation of these structures include the effects of various vane dike orientation, vane dike length, and gap length U.S. Army Corps of Engineers, 1981.

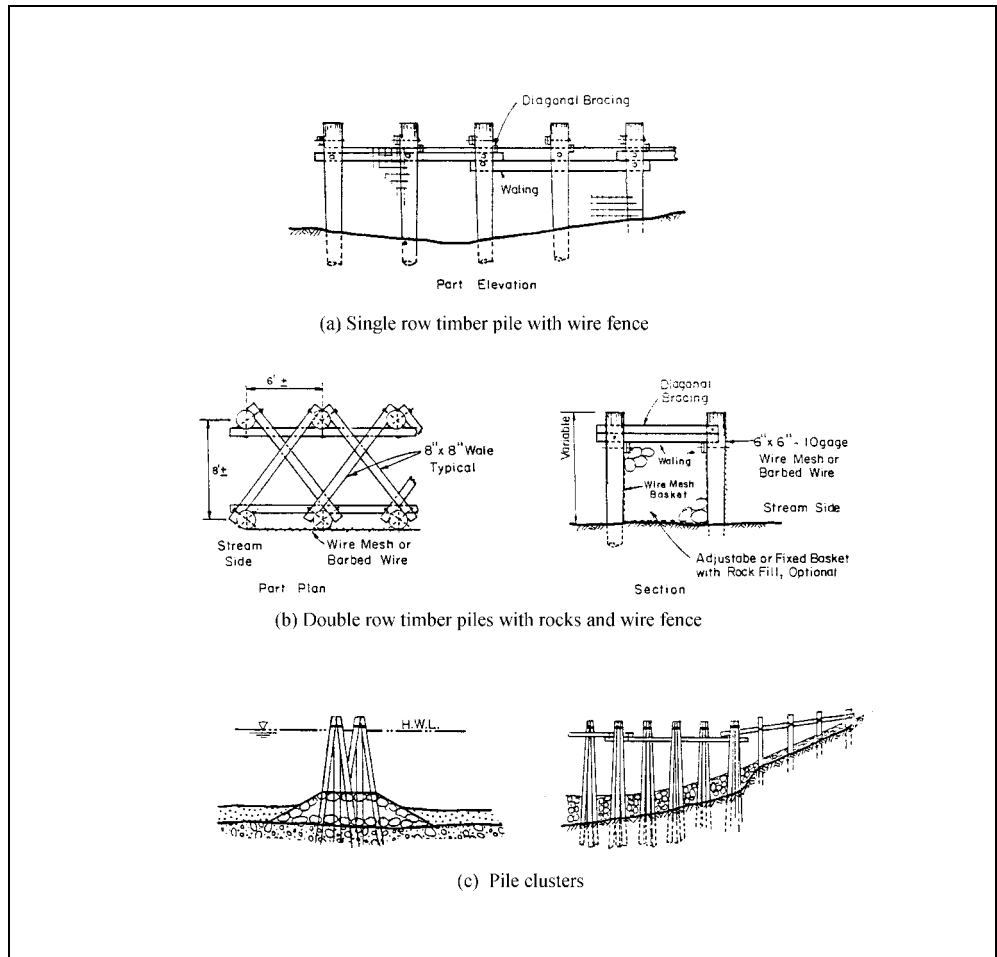


Figure 6.6. Pile dikes (retards would be similar).



Figure 6.7. Vane dike model, ground walnut shell bed, during low stage portion of test run (U.S. Army Corps of Engineers 1981).

### 6.4.7 Jetties

The purpose of a jetty field is to add roughness to a channel or overbank area to train the main stream along a selected path. The added roughness along the bank reduces the velocity and protects the bank from erosion. Jetty fields are usually made up of steel jacks tied together with cables. Both lateral and longitudinal rows of jacks are used to make up the jetty field as shown in Figure 6.8.

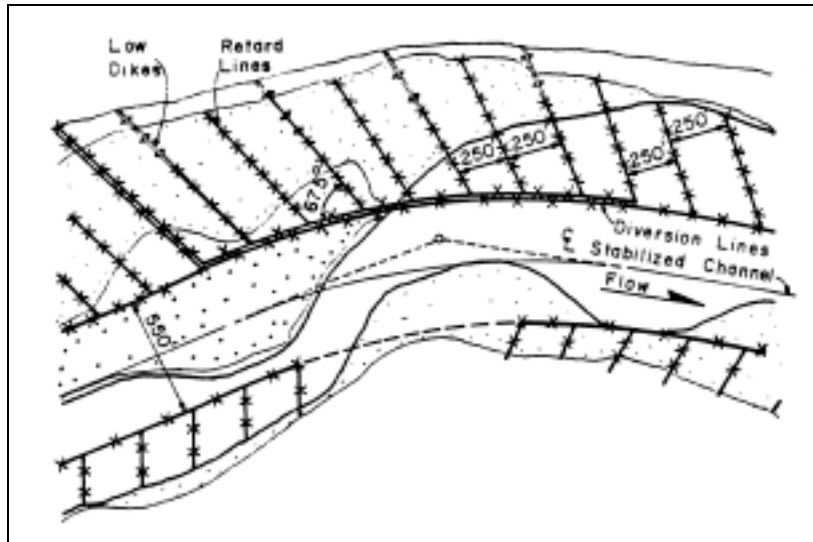


Figure 6.8. Typical jetty-field layout.

The lateral rows are usually angled about 45 to 70 degrees downstream from the bank. The spacing varies, depending upon the debris and sediment content in the stream, and may be 15 to 75 m (50 to 250 ft) apart. Jetty fields are effective only if there is a significant amount of debris carried by the stream and the suspended sediment concentration is high.

When jetty fields are used to stabilize meandering rivers, it may be necessary to use jetty fields on both sides of the river channel because in flood stage the river may otherwise develop a chute channel across the point bar. A typical layout is shown in Figure 6.8.

Steel jacks are devices with basic triangular frames tied together to form a stable unit. The resulting framework is called a tetrahedron. The tetrahedrons are placed parallel to the embankment and cabled together with the ends of the cables anchored to the bank. Wire fencing may be placed along the row of tetrahedrons. In order to function well, there must be considerable debris in the stream to collect on the fence and the suspended sediment concentration must be large so that there will be deposition behind the retard. Various forms of steel jacks may be assembled. Two types are shown in Figure 6.9. Tiebacks should be spaced every 30 m (100 ft) and space between jacks should not be greater than their width.

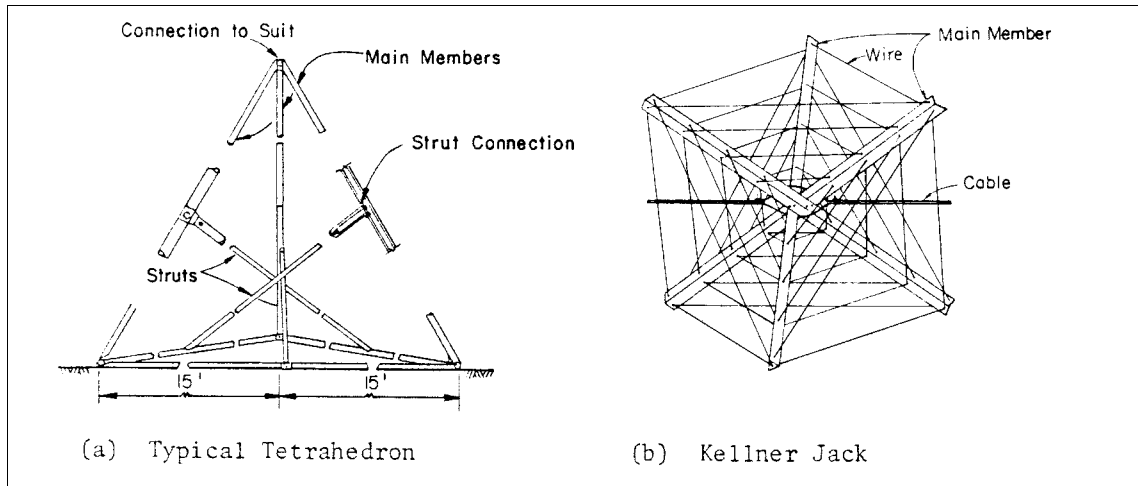


Figure 6.9. Steel jacks.

#### 6.4.8 Bulkheads

Bulkheads can be used to prevent streambank erosion or failure. As an additional benefit, a bulkhead may provide a substantial increase in waterfront area and an improvement in water/land access. Concrete, steel, timber and more recently, aluminum, corrugated asbestos, and used tires have been used to construct bulkheads. Concrete and steel bulkheads generally cost at least four times as much as a comparable bulkhead of another material; however, the service life is longer and less maintenance is required. Timber is the most commonly available material for economical bulkhead construction.

Timber bulkhead construction is similar to common fence construction except that a few precautions should be observed:

- All wood should be treated with preservative to minimize deterioration due to repetitive wetting and drying or insect activity.
- The toe of the bulkhead should always be protected with riprap. The most common cause of bulkhead failure is scour around the pilings, followed by the structure tipping over due to the pressure of the bank behind the bulkhead.
- Piles should be anchored to deadmen buried in the bank.
- Fill material placed between the bulkhead and natural bank should be free draining so that the soil behind the bulkhead will not become saturated and push the structure over.
- If there are no cracks between the planks, weepholes should be drilled in the fence at regular intervals to allow the bank to drain. Filter fabric or gravel can be placed as a filter behind openings in the fence to prevent fine soils from leaching through. A filter must be properly designed to match the filter with the soil.
- The bulkhead should be tied into the bank at the upstream and downstream end of the structure to prevent flow behind the bulkhead.

### 6.4.9 Fencing

Fencing can be used as a low-cost bank protection technique on small to medium size streams. Special structural design considerations are required in areas subject to ice and floating debris. Both longitudinal (parallel to stream) fence retards and transverse (perpendicular to stream) fences have been used in the prototype with varying degrees of success. A model investigation and literature review of longitudinal fence retards with tiebacks were conducted to identify the following important design considerations:

- Channel gradient must be stable and not be steep (tranquil flow)
- Toe scour protection can be provided by extending the support posts well below the maximum scour expected or by placing loose rock at the base of the fence to launch downward if scour occurs at the toe
- Tiebacks to the bank are important to prevent flanking of the fence and to promote deposition behind the fence
- Fence retards generally reduce attack on the bank so that vegetation can establish
- Metal or concrete fences are preferred due to ice damage and fire loss of wooden fences

### 6.4.10 Guide Banks

Guide banks are placed at or near the ends of approach embankments to guide the stream through the bridge opening. Constructed properly, flow disturbances, such as eddies and cross-flow, will be minimized to make a more efficient waterway under the bridge. They are also used to protect the highway embankment and reduce or eliminate local scour at the embankment and adjacent piers. The effectiveness of guidebanks is a function of river geometry, quantity of flow on the floodplain, and size of bridge opening. A typical guidebank at the end of an embankment is shown in Figure 6.10.

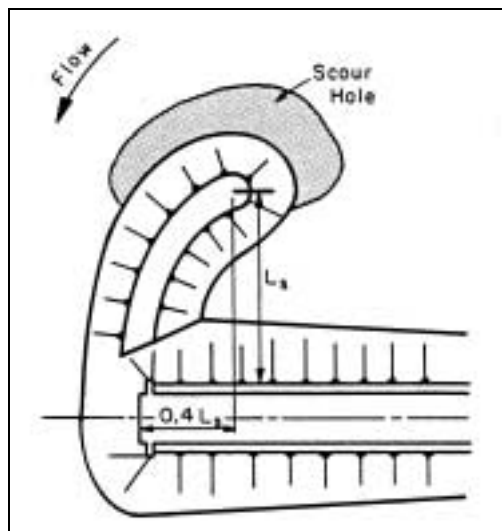


Figure 6.10. Typical guidebank.



The recommended shape of a guidebank is a quarter ellipse with a major to minor axis ratio of 2.5. The major axis should be approximately parallel to the main flow direction. For bridge crossings normal to the river, the major axis would be normal to the highway embankment. However, for skewed crossings, the guidebank should be placed at an angle with respect to the embankment with the view of streamlining the flow through the bridge opening. Design guidelines and a design chart for guide banks are provided in HEC-23 (Lagasse et al. 2001).

The length of the guide bank,  $L_s$ , required depends upon quantity of flow on the floodplain, width of bridge opening and skewness of the highway crossing. Shorter guide banks may be used where floodplain flow is small, scour potential at piers and embankment ends is small, or where trees or brush are intersected by the guidebank.

The crest elevation of guidebanks should be higher than the elevation of the design flood taking into consideration the effect of the contraction of the flow; this is because the design flow should not overtop the guidebank.

#### 6.4.11 Drop Structures

Check dams or channel drop structures are used downstream of highway crossings to arrest head cutting and maintain a stable streambed elevation in the vicinity of the bridge. Check dams are usually built of rock riprap, concrete, sheet piles, gabions, or treated timber piles. The material used to construct the structure depends on the availability of materials, the height of drop required, and the width of the channel. Definition sketches for a vertical wall and a sloping sill drop structure are shown in Figures 6.11 and 6.12. Design considerations for vertical wall or sloping sill structures are given in texts by Rouse (1950), Chow (1959), Peterson (1986), and Simons and Senturk (1992). Design guidelines for a vertical drop structure and stilling basins for drop structures are given in HEC-23 (Lagasse et al. 2001).

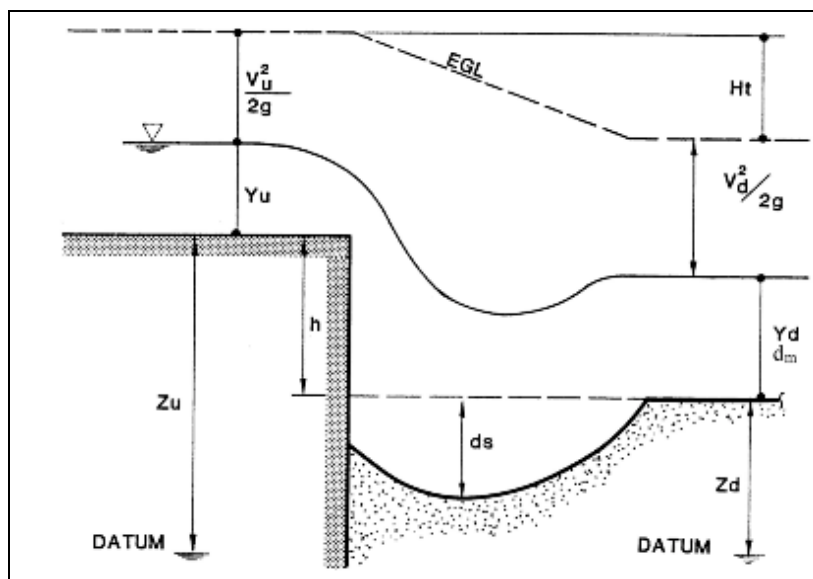


Figure 6.11. Definition sketch for a vertical drop (Lagasse et al. 2001).

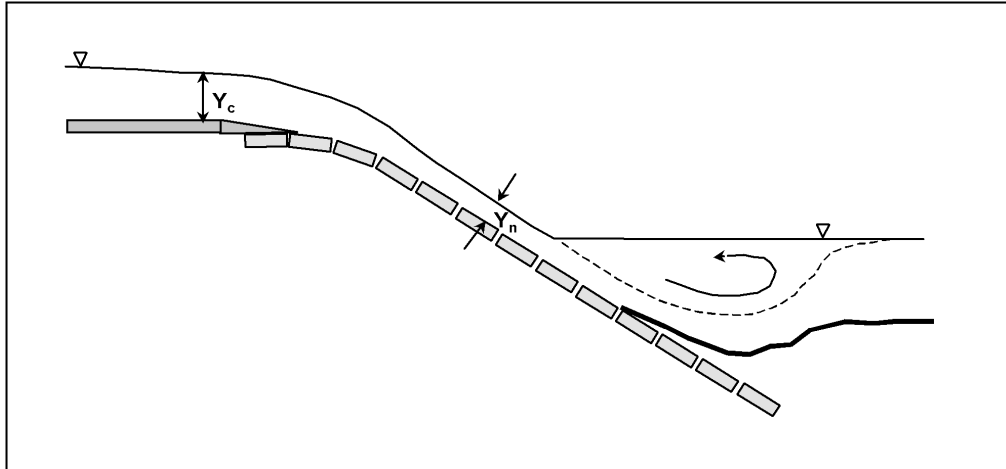


Figure 6.12. Flow and scour patterns at a sloping sill (after Laursen and Flick 1983).

## 6.5 RIPRAP DESIGN AND PLACEMENT

### 6.5.1 Factors to Consider

When available in sufficient size, rock riprap is usually the most economical material for bank protection. Rock riprap has many other advantages over other types of protection. A riprap blanket is flexible and is neither impaired nor weakened by slight movement of the bank resulting from settlement or other minor adjustments. Local damage or loss is easily repaired by the placement of more rock. Construction is not complicated so for many applications special equipment or construction practice is not necessary. Riprap is usually durable and recoverable and may be stockpiled for future use. The cost-effectiveness of locally available riprap provides a viable alternative to many other types of bank protection. Riprap stability increases with increasing thickness as more material is available to move to damaged areas and more energy is dissipated before it reaches the filter and streambank. Although riprap must be placed to the proper level below the bed, there are no special foundation requirements. The appearance of rock riprap is natural and after a period of time vegetation will grow between the rocks. Wave runup on rock slopes is usually less than on other types of bank protection.

The important factors to be considered in designing rock riprap bank protection are:

- **Durability** of the rock
- **Density** of the rock
- **Velocity** (both magnitude and direction) of the flow in the vicinity of the rock
- **Slope** of the bed and bankline being protected
- **Angle of repose** for the rock
- **Shape and angularity** of the rock
- What **shape and weight of stones will be stable** in the streamflow
- What blanket **thickness** is required
- Is a **filter** needed between the bank and the blanket to allow seepage but to prevent erosion of bank soil through the blanket

- How will the blanket be **stabilized** at the toe of the bank
- How will the blanket be **tied into the bank** at its upstream and downstream ends

### 6.5.2 Stability Factor Design Methods

Stability Factors For Riprap. In the absence of waves and seepage, the stability of rock riprap particles on a side slope is a function of: (1) the magnitude and direction of the stream velocity in the vicinity of the particles; (2) the angle of the side slope; and (3) the characteristics of the rock including the geometry, angularity and density. The functional relations between the variables are developed below. This development closely follows that given by Stevens and Simons (1971).

Consider flow along an embankment as shown in Figure 6.13. The fluid forces on a rock particle identified as P in Figure 6.13a result primarily from fluid pressure around the surface of the particles. The lift force  $F_l$  is defined herein as the fluid force normal to the plane of the embankment. The lift force is zero when the fluid velocity is zero. The drag force  $F_d$  is defined as the fluid force acting on the particle in the direction of the velocity field in the vicinity of the particle. The drag force is normal to the lift force and is zero when the fluid velocity is zero. The remaining force is the submerged weight of the rock particle  $W_s$ .

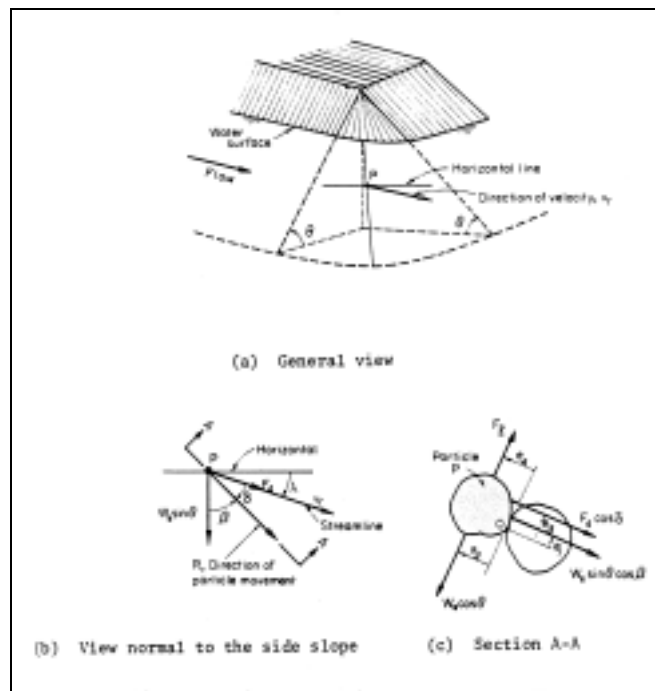


Figure 6.13. Diagram for riprap stability conditions.

Rock particles on side slopes tend to roll rather than slide, so it is appropriate to consider the stability of rock particles in terms of moments about the point of rotation. In Figure 6.13b the direction of movement is defined by the vector  $R$ . The point of contact about which rotation in the  $R$  direction occurs is identified as point "O" in Figure 6.13c.

The forces acting in the plane of the side slope are  $F_d$  and  $W_s \sin \theta$  as shown in Figure 6.13b. The angle  $\theta$  is the side slope angle. The lift force acts normal to the side slope and the component of submerged weight  $W_s \sin \theta$  acts normal to the side slope as shown in Figure 6.13c.

At incipient motion, there is a balance of moments about the point of rotation such that

$$e_2 W_s \cos \theta = e_1 W_s \sin \theta \cos \beta + e_3 F_d \cos \delta + e_4 F_\ell \quad (6.1)$$

The moment arms  $e_1$ ,  $e_2$ ,  $e_3$  and  $e_4$  are defined in Figure 6.13c and the angles  $\delta$  and  $\beta$  are defined in Figure 6.13b.

The stability factor S.F. against rotation of the particle is defined as the ratio of the moments resisting particle rotation out of the bank to the submerged weight and fluid force moments tending to rotate the particle out of its resting position. Accordingly,

$$\text{S.F.} = \frac{e_2 W_s \cos \theta}{e_1 W_s \sin \theta \cos \beta + e_3 F_d \cos \delta + e_4 F_\ell} \quad (6.2)$$

The following particle stability analysis was first derived by Stevens (1968). The analysis is also presented in Simons and Senturk (1992). This analysis shows that the stability factor for rock riprap on side slopes where the flow has a non-horizontal velocity vector is related to properties of the rock, side slope and flow by the following equations:

$$\text{S.F.} = \frac{\cos \theta \tan \phi}{\eta' \tan \phi + \sin \theta \cos \beta} \quad (6.3)$$

in which

$$\beta = \tan^{-1} \left\{ \frac{\cos \lambda}{\frac{2 \sin \theta}{\eta \tan \phi} + \sin \lambda} \right\} \quad (6.4)$$

$$\eta = \frac{21 \tau_o}{(S_s - 1) \gamma D_s} \quad (6.5)$$

and

$$\eta' = \eta \left\{ \frac{1 + \sin(\lambda + \beta)}{2} \right\} \quad (6.6)$$

Given a rock size  $D_s$ , of specific weight  $S_s$  and angle of repose  $\phi$  and given a velocity field at an angle  $\lambda$  to the horizontal producing a tractive force  $\tau_o$  on the side slope of angle  $\theta$ , the set of four equations (Equations 6.3, 6.4, 6.5, and 6.6) can be solved to obtain the stability factor S.F. If S.F. is greater than unity, the riprap is stable; if S.F. is unity, the rock is at the condition of

incipient motion; if S.F. is less than unity, the riprap is unstable. Problem F.1 in Appendix F illustrates how to determine the stability of riprap.

Simplified Design Aid For Side Slope Riprap. When the velocity along a side slope has no downslope component (i.e., the velocity factor is along the horizontal), some simple design aids can be developed.

For horizontal flow along a side slope, the equations relating the stability factor, the stability number, the side slope angle, and the angle of repose for the rock are obtained from Equations 6.4 and 6.6 with  $\lambda = 0$ .

$$\beta = \tan^{-1} \left( \frac{\eta \tan \phi}{2 \sin \theta} \right) \quad (6.7)$$

and

$$\eta' = \eta \left( \frac{1 + \sin \beta}{2} \right) \quad (6.8)$$

When Equations 6.7 and 6.8 are substituted into Equation 6.3, the expression for the stability factor for horizontal flow on a side slope is:

$$\text{S.F.} = \frac{S_m}{2} \left\{ \sqrt{\zeta^2 + 4} - \zeta \right\} \quad (6.9)$$

in which

$$\zeta = S_m \eta \sec \theta \quad (6.10)$$

and

$$S_m = \frac{\tan \phi}{\tan \theta} \quad (6.11)$$

If we solve Equations 6.9 and 6.10 for  $\eta$ , then:

$$\eta = \frac{S_m^2 - (\text{S.F.})^2}{(\text{S.F.}) S_m^2} \cos \theta \quad (6.12)$$

The interrelation of the variables in these two equations is represented in Figure 6.14. Here, the specific weight of the rock is taken as 2.65 and a stability factor of 1.5 is employed. This recommended stability factor for the design of riprap (S.F. = 1.5) is the result of studies of the riprap embankment model data obtained by Lewis. These studies were reported by Simons and Lewis (1971).

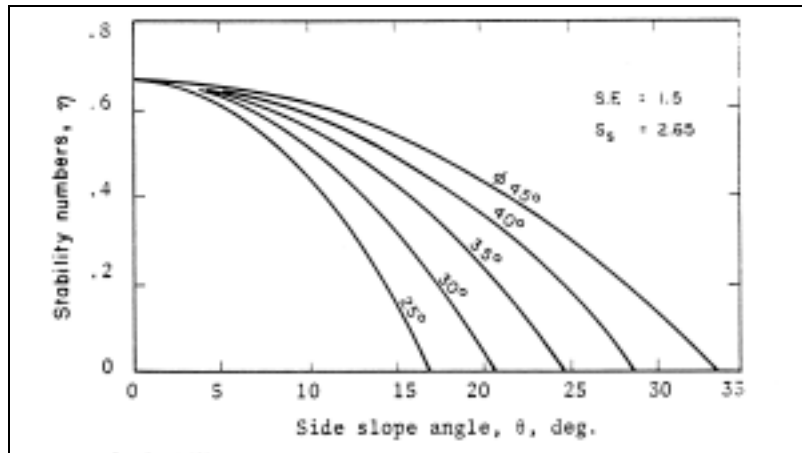


Figure 6.14. Stability numbers for a 1.5 stability factor for horizontal flow along a side slope.

The curves in Figure 6.14 are computed in the following manner: (1) Select an angle of repose  $\phi$ . For example  $\phi = 45^\circ$ ; (2) Select a side slope angle. For example  $\theta = 25^\circ$ ; (3) Compute  $S_m$  from Equation 6.11:

$$S_m = \frac{\tan 45^\circ}{\tan 25^\circ} = 2.14;$$

(4) Compute  $\eta$  from Equation 6.12 with S. F. = 1.5

$$\eta = \left( \frac{(2.14)^2 - (1.5)^2}{(1.5)(2.14)^2} \right) \cos 25^\circ = 0.31$$

(5) Repeat the above steps for the full range of interest for  $\phi$  and  $\theta$ .

If the shear stress  $\tau_o$  on the side slope is known, then, from Equation 6.5, the riprap size required is obtained from:

$$D_m = \frac{21\tau_o}{(S_s - 1) \gamma \eta} \quad (6.13)$$

where the stability number  $\eta$  is obtained from Figure 6.14.

### 6.5.3 Velocity Profile and Tractive Force

In riprap design, it is often desirable to relate the tractive force (shear stress) acting on the riprapped bed or bank to the fluid velocity in the vicinity of the riprap. For fully turbulent flow, the reference velocity  $V_r$  at a distance  $D_{50}$  above the bed is determined from Equation 6.14.

$$V_r = 2.5 V_* \ln \left( 30.2 \frac{D_{50}}{D_{50}} \right) = 8.52 V_* = 8.52 \sqrt{\frac{\tau_o}{\rho}} \quad (6.14)$$

Thus, the relation between  $V_r$  and  $\tau_o$  is:

$$\tau_o = \frac{\rho V_r^2}{72} \quad (6.15)$$

The relation is valid only for uniform flow in wide prismatic channels in which the flow is fully turbulent. For the purpose of riprap design, Equation 6.15 can be used when the flow is accelerating such as on the tip of spur dikes or abutments. The equation should not be used in areas where the flow is decelerating or below energy dissipating structures. In these areas, the shear stress is larger than calculated for Equation 6.15.

One can also demonstrate (Richardson et al. 1975) that the reference velocity  $V_r$  is related to the velocity against the stone  $V_s$  ( $V_r \approx 1.4 V_s$ ).

In summary the following expressions for  $\eta$  are equivalent:

$$\eta = \frac{21 \tau_o}{(S_s - 1) \gamma D_s} \quad (6.5)$$

$$\eta = \frac{0.30 V_r^2}{(S_s - 1) g D_s} \quad (6.16)$$

$$\eta = \frac{0.60 V_s^2}{(S_s - 1) g D_s} \quad (6.17a)$$

$$\eta = 0.30 \left\{ \frac{3.4}{\ln \left( 12.3 \frac{y_o}{D_s} \right)} \right\}^2 \frac{V^2}{(S_s - 1) g D_s} \quad (6.17b)$$

#### 6.5.4 U.S. Army Corps of Engineers Design Equation

U.S. Army Corps of Engineers design equations are based on local depth-averaged velocity ( $V$ ), local depth of flow ( $y$ ), and coefficients for a factor of safety ( $S_f$ ), stability ( $C_s$ ), vertical velocity distribution ( $C_v$ ), blanket thickness ( $C_T$ ), and side slope ( $K_1$ ). The principal equation determines the riprap size of which 30 percent is finer by weight ( $D_{30}$ ) (U.S. Army Corps of Engineers EM 1110-2-1601, 1991 and 1994a and Maynard 1988). The equation is:

$$D_{30} = S_f C_s C_v C_T y \left[ \left( \frac{\gamma}{\gamma_s - \gamma} \right)^{1/2} \frac{V}{(K_1 g y)^{1/2}} \right]^{2.5} \quad (6.18)$$

where:

$D_{30}$	=	Riprap size, m, ft
$S_f$	=	Safety factor, minimum 1.1
$C_s$	=	Stability coefficient for incipient failure, ( $D_{85}/D_{15} = 1.7$ to $5.2$ ) = 0.30 for angular rock = 0.36 for rounded rock
$D_{85}/D_{15}$	=	Gradation uniformity coefficient ( $D_{50} = D_{30} (D_{85}/D_{15})^{1/3}$ )
$C_v$	=	Vertical velocity distribution coefficient = 1.0 for straight channels, inside of bends = $1.283 - 0.2 \log (R/W)$ for outside of bends, 1 for $(R/W) > 26$ = 1.25 downstream of concrete channels and at ends of dikes
$R$	=	Centerline radius of curvature of bend (main channel only) m, ft
$W$	=	Water-surface width at upstream end of bend (main channel only) m, ft
$C_T$	=	Blanket thickness coefficient = 1.0 for thickness = $1 D_{100}$ (max) or 1.5 or $D_{50}$ (max), whichever is greater
$y$	=	Local depth of flow, m, ft
$\gamma$	=	Unit weight of water, $\text{Kg/m}^3$ , $\text{lb/ft}^3$
$\gamma_s$	=	Unit weight of rock, $\text{Kg/m}^3$ , $\text{lb/ft}^3$
$V$	=	Local depth-average velocity, m/s, ft/s
$V_{ss}$	=	Local depth average velocity on side slopes, m/s, ft/s
$V_{avg}$	=	Average velocity in the main channel, m/s, ft/s
$K_1$	=	Side slope correction factor
$g$	=	Acceleration of gravity, $9.81 \text{ m/s}^2$ , $32.2 \text{ ft/s}^2$

The use of  $D_{30}$  for the sizing of the riprap is somewhat controversial. Its use probably results in an overall increase in the sizes of the riprap in the blanket compared to using the traditional  $D_{50}$  approach. Maynard (1988) states "Stability tests conducted at a thickness of  $1 X D_{100}$ , which is the most commonly used thickness for bank protection, showed that gradations ranging from uniform, to highly nonuniform exhibited the same stability if they had the same  $D_{30}$ ." The Corps manual gives an approximate relationship between  $D_{50}$  and  $D_{30}$ . It is  $D_{50} = D_{30} (D_{85} / D_{15})^{1/3}$ .

The U.S. Army Corps of Engineers manual (1994a) states that the minimum safety factor may have to be increased for the following conditions:

- Impact forces from logs, uprooted trees, vessels, ice etc.
- Natural variations in the quality of the rock used as riprap
- Vandalism
- Placement quality
- Freeze-thaw of the riprap is anticipated
- Precision of the determination of the hydraulic variables



These factors for determining the value of the safety factor coefficient must be considered and the largest value used as the safety factor. The Corps manual (1994) provide the following additional guidance.

If the riprap design is for a channel bottom, use the local depth-averaged velocity and local depth in Equation 6.18. Determining the depth-averaged velocity to design riprap to protect side slopes is more difficult because the velocity varies greatly from the toe to the top of the bank. The Corps manual EM 1110-2-1601 uses the depth-averaged velocity at a point 20 percent up slope from the toe. This velocity can be determined by physical or computer models, empirical equations or methods, and prototype data. The Corps manual EM 1110-2-1601 gives the following equation for estimating the side slope riprap design velocity.

$$\frac{V_{ss}}{V_{avg}} = 1.74 - 0.52 \text{Log} \left( \frac{R}{W} \right) \quad (6.19)$$

Note that the value of  $V_{ss}/V_{avg}$  rarely exceeds 1.6 in alluvial or man made channels for large discharges for which riprap is designed.

$K_1$ , the side slope correction factor in Equation 6.18, is taken from the Carter et al. (1953) relation in the Corps manual EM 1110-2-1601. The relationship is:

$$K_1 = \left[ 1 - \frac{\text{Sin}^2 \theta}{\text{Sin}^2 \phi} \right]^{1/2} \quad (6.20)$$

where:

- $\theta$  = Angle of side slope with horizontal
- $\phi$  = Angle of repose of the riprap (normally 40°)

The Corps manual ME 1110-2-1601 gives an equation to determine riprap size for steep slopes (2 to 20 percent) where the unit discharge is low. A typical application is a rock-lined chute. The equation is:

$$D_{30} = \frac{1.95 S^{0.555} q^{2/3}}{g^{1/3}} \quad (6.21)$$

EM 1110-2-1601 states Equation 6.21 is applicable for thickness = 1.5  $D_{100}$ , angular rock, unit weight of 167 lb/ft<sup>3</sup>,  $D_{85}/D_{15}$  from 1.7 to 2.7, slopes from 2 to 20 percent and uniform flow with no tailwater. Also,  $q$  is determined using the bottom width of the chute.

The Corps manual 1110-2-1601 gives charts and figures as design guides and guidance for toe scour, toe scour protection, quality control, revetment top protection and revetment end protection (see also HEC-23). Termination of riprap bank protection often leads to the formation of an eddy (wake vortex) that erodes the bank. This erosion is undesirable and can initiate failure of the riprap. For this reason, end protection is needed. Maynard (1996) also gives equations and methods for toe scour estimation and toe scour and end section protection. He describes a computer program "CHANLPRO" available from the U.S. Army Engineer Waterways Experiment Station that incorporates the above riprap design and scour depth procedures as well as sizing gabion mattresses.

### 6.5.5 Riprap Gradation and Thickness

The concept of a representative grain size for riprap is simple. A uniformly graded riprap with a median size  $D_{50}$  scours to a greater depth than a well-graded mixture with the same median size. The uniformly distributed riprap scours to a depth at which the velocity is less than that required for the transportation of  $D_{50}$  size rock. The well-graded riprap, on the other hand, develops an armor plate. That is, some of the finer materials, including sizes up to  $D_{50}$  and larger, are transported by the high velocities, leaving a layer of large rock sizes which cannot be transported under the given flow conditions. Thus, the size of rock representative of the stability of the riprap is determined by the larger sizes of rock. The representative grain size  $D_m$  for riprap is larger than the median rock size  $D_{50}$ .

The recommended gradation for riprap is illustrated in Figure 6.15 in terms of  $D_{50}$ . The computations of the representative grain size  $D_m$  for the recommended gradation are given in Table 6.2.

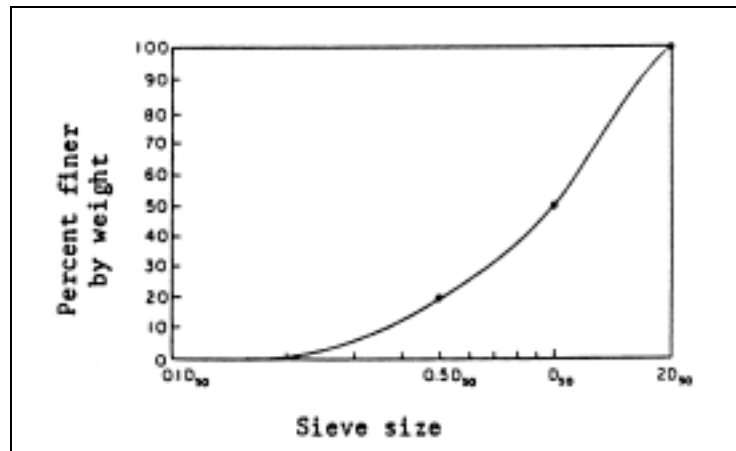


Figure 6.15. Suggested gradation for riprap.

Table 6.2. Data for Suggested Gradation.		
Percent Finer	Sieve Diameter	$D_1$
0	0.25 $D_{50}$	--
10	0.35 $D_{50}$	0.28 $D_{50}$
20	0.5 $D_{50}$	0.43 $D_{50}$
30	0.65 $D_{50}$	0.57 $D_{50}$
40	0.8 $D_{50}$	0.72 $D_{50}$
50	1.0 $D_{50}$	0.90 $D_{50}$
60	1.2 $D_{50}$	1.10 $D_{50}$
70	1.6 $D_{50}$	1.50 $D_{50}$
90	1.8 $D_{50}$	1.70 $D_{50}$
100	2.0 $D_{50}$	1.90 $D_{50}$

The rock sizes in the last column in Table 6.2 are used in the following equation (Stevens 1968) to find the representative grain size  $D_m$ . This effective grain size,  $D_m$ , of the mixture corresponds to the  $D_{65}$  size of the riprap.

$$D_m = \left[ \frac{\sum_i^{10} D_i^3}{10} \right]^{1/3} \cong 1.25 D_{50} \quad (6.22)$$

When the bed material has a log-normal distribution, the representative size of the bed material based on the weight of the particles is given by Mahmood (1973) as a function of the gradation coefficient  $G$ :

$$D_m = D_{50} \exp \left\{ \frac{3}{2} (\ln G)^2 \right\} \quad (6.23)$$

For gradation coefficients of 2 and 3,  $D_m = 0.72 D_{50}$  and  $1.81 D_{50}$  respectively.  $G$  is determined by Equation 3.9.

With a distributed size range, the interstices formed by the larger stones are filled with the smaller sizes in an interlocking fashion, preventing formation of open pockets. Riprap consisting of angular stones is more suitable than that consisting of rounded stones. Control of the gradation of the riprap is almost always made by visual inspection. If it is necessary, poor gradations of rock can be employed as riprap provided the proper filter is placed between the riprap and the bank or bed material. Where available rock size is inadequate, wire enclosed (gabion) riprap can be used.

Considering the practical problems of quarry production, a gradation band is usually specified by the U.S. Army Corps of Engineers (1981) rather than a single gradation curve, and any stone gradation within the limits is acceptable. The Corps criteria for establishing gradation limits in terms of stone weight ( $W$ ) for riprap are as follows:

- Lower limit of  $W_{50}$  stone should not be less than the weight of stone required to withstand the design shear forces.
- Upper limit of  $W_{50}$  stone should not exceed five times the lower limit of  $W_{50}$  stone, the size which can be obtained economically from the quarry, or the size that satisfies layer thickness requirements.
- Lower limit of  $W_{100}$  stone should not be less than two times the lower limit of  $W_{50}$  stone.
- Upper limit of  $W_{100}$  stone should not exceed five times the lower limit of  $W_{50}$  stone, the size which can be obtained economically from the quarry, or the size that satisfies layer thickness requirements.
- Lower limit of  $W_{15}$  stone should not be less than one-sixteenth the upper limit of  $W_{100}$  stone.
- Upper limit of  $W_{15}$  stone should be less than the upper limit of the filter material.

- Bulk volume of stone lighter than the  $W_{15}$  stone should not exceed the volume of voids in the structure without this lighter stone.

The riprap thickness should not be less than 300 mm (12 in.) for practical placement, less than the diameter of the upper limit of  $W_{100}$  stone, or less than 1.5 times the diameter of the upper limit  $W_{50}$  stone, whichever is greater. If riprap is placed under water, the thickness should be increased by 50 percent, and if it is subject to attack by large floating debris or wave action it should be increased 150 to 300 mm (6 to 12 in.).

### 6.5.6 Riprap Placement

**General.** Riprap placement is usually accomplished by dumping directly from trucks. If riprap is placed during construction of the embankment, rocks can be dumped directly from trucks from the top of the embankment. Rock should never be placed by dropping down the slope in a chute or pushed downhill with a bulldozer. These methods result in segregation of sizes. With dumped riprap there is a minimum of expensive hand work. Poorly graded riprap with slab-like rocks requires more work to form a compact protective blanket without large holes or pockets. Draglines, backhoes, and other power equipment can also be used to place the riprap.

Hand placed rock riprap is another method of riprap placement. Stones are laid out in more or less definite patterns, usually resulting in a relatively smooth top surface. This form of placement is used rarely in modern practice because it is usually more expensive than placement with power machinery, and it is more likely to fail than dumped riprap.

Dumped riprap that is keyed (or plated) by tamping has proved to be effective. Guidelines for placement of keyed riprap have been developed by the Oregon Department of Transportation and distributed by the Federal Highway Administration. In the keying of a riprap, a 1,818 kg (4,000 lb) or larger piece of steel plate is used to compact the rock into a tight mass and to smooth the revetment surface. Keyed riprap is more stable than loose riprap revetment because of reduced drag on individual stones, its angle of repose is higher, and its cost is less because a lesser volume of rock per unit area is required.

Riprap should not be used at slopes steeper than IV:1.5H. This criterion is widely followed for abutment fill-slopes, but it is sometimes disregarded for stream banks.

Broken concrete is used for riprap in many states where rock riprap is unavailable or unusually expensive. Broken concrete riprap has proven to be unsatisfactory if the material is not broken into riprap size particles.

Rounded stones less than 150 mm (6 in.) in diameter have a significantly lower angle of repose than angular stones (Figure 3.4). Although they are less desirable than angular stones, rounded stones are nevertheless effective for larger diameters.

The blanket should be stabilized at its base with a key trench or apron to prevent the stone from sliding down the bank. The upstream and downstream ends of the blanket should be tied back into the bank to prevent stream currents from unraveling the blanket. The most common method to tie into the bank is to dig a trench at the ends of the blanket. (Figure 6.16). The depth of a trench should be twice the blanket thickness and the bottom width of the trench three times the thickness.

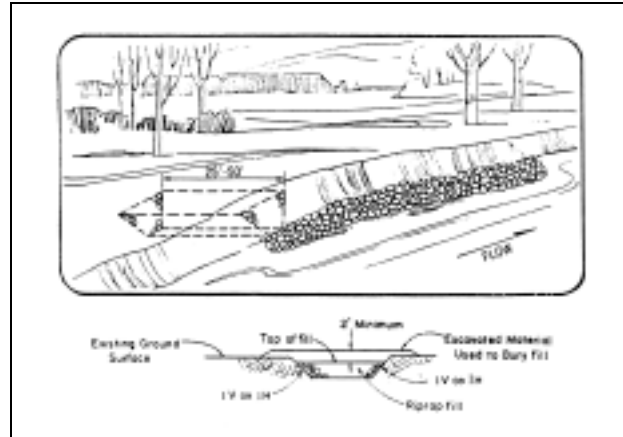


Figure 6.16. Tie-in trench to prevent riprap blanket from unraveling (after Keown 1983).

Rock-fill Trenches and Launching Aprons. Rock-fill trenches are structures used to protect banks from caving caused by erosion at the toe. A trench is excavated along the toe of the bank and filled with riprap as shown in Figure 6.17.

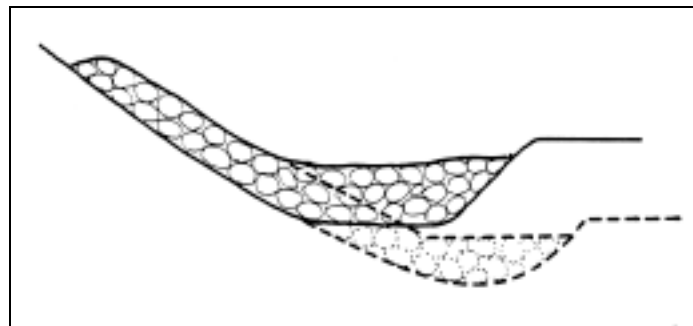


Figure 6.17. Rock-fill trench.

As the stream bed adjacent to the toe is eroded, the toe trench is undermined and the rock fill slides downward to pave the bank. The size of trench to hold the rock fill depends on expected depths of scour. It is advantageous to grade the banks before paving the slope with riprap and placing rock in the toe trench. The slope should be at such an angle that the saturated bank is stable while the river stage is falling.

The rock-fill trench need not be at the toe of the bank. An alternative method is to excavate a trench above the water line along the top of the river bank and backfill with rocks. Then as the bank erodes toward the trench, the rocks in the trench slide down and pave the bank. This method is applicable in areas of rapidly eroding banks of medium to large size rivers.

Launching aprons can provide similar protection against undermining for channel banks and revetment. A flexible launching apron is placed horizontally on the bed at the foot of the revetment, so that when scour occurs the materials will settle and cover the side of the scour hole on a natural slope. This method is generally the most economical for cohesionless channel beds where deep scour is expected. Materials used for launching aprons include

stone riprap, articulated concrete matting, concrete blocks, gabions, and wire mesh mattresses filled with stone. Stone riprap is most commonly used.

In cohesionless channel beds, the design of stone aprons should be based on the stone launching to a slope of up to IV:2H. Model tests have indicated that these slopes are realistic for sand beds, but little field confirmation seems to have been reported.

Stone sizes for launching should be the same as for slope revetment. The volume of stone should be sufficient to cover the final scoured slope to a thickness of 1.25 times the size of the largest stones in the specified grading. At the nose of a guide bank or spur, there should be sufficient stone to cover the final conical surface of the scoured slope. Piers should not be located within the launching apron slope unless it is unavoidable.

Launching aprons do not perform well on cohesive channel beds where scour occurs in the form of slumps with steep slip faces. In such cases, bank revetment should be continued down to the expected worst scour level, and the excavation then refilled.

A variation of these methods of toe protection is to pile the rocks in a "windrow" along the bank line instead of excavating a trench. Then as the bank is scoured, the rocks in the windrow drop down to pave the bank.

Windrow Revetment. Windrow revetment is an erosion control technique (Figure 6.18) consisting of the depositing of a fixed amount of erosion-resistant material (riprap) landward from the existing bank line at a predetermined location, beyond which additional erosion is to be prevented. The technique consists of burying or piling a sufficient supply of erosion-resistant material in a windrow below or on the existing land surface along the bank, then permitting the area between the natural riverbank and the windrow to erode through natural processes until the erosion reaches and undercuts the supply of rock. As the rock supply is undercut, it falls onto the eroding area, thus giving protection against further undercutting, and eventually halting further landward movement. The resulting bank line remains in a near natural state, with an irregular appearance due to intermittent lateral erosion in the windrow location. The treatment particularly lends itself to the protection of adjacent wooded areas, or placement along stretches of presently eroding, irregular bank line. The following observations and conclusions were obtained from model investigations on windrow revetments.

(1) The "application rate" is the weight of stone applied per meter (foot) of bank line. The amount of stone in the windrow indicates the degree to which lateral erosion will be permitted to occur;

(2) Various windrow shapes were investigated in the model investigations, and a rectangular cross section was the best windrow configuration. This type of windrow is most easily placed in an excavated trench of the desired width. The second best windrow shape was found to be a trapezoidal shape. This shape provides a steady supply of stone to produce a uniform blanket of stone on the eroding bank line. A triangular shape was found to be the least desirable;

(3) Studies indicated that varying the bank height did not significantly affect the final revetment; however, high banks tended to produce a nonuniform revetment alignment. Studies showed that the high banks had a tendency for large segments of the bank to break loose and rotate slightly, whereas the low banks simply "melted" or sloughed into the stream. The slight rotation of the high bank segment probably induced a tendency for ragged alignment; and

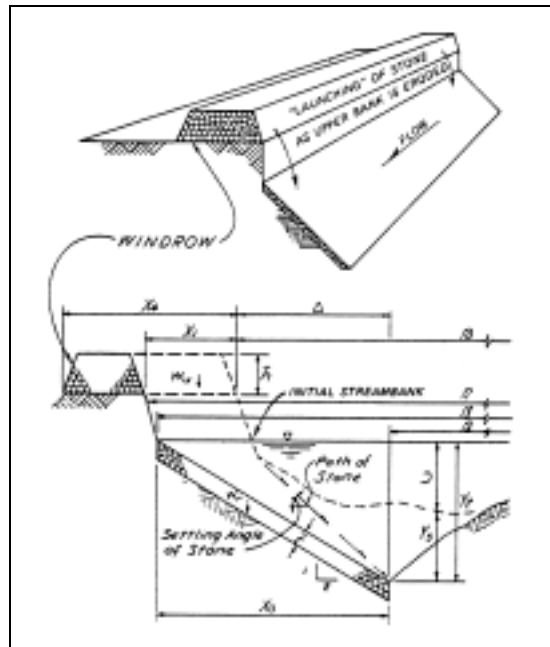


Figure 6.18. Windrow revetment, definition sketch (after U.S. Army Corps of Engineers 1981).

(4) The velocity and characteristics of the stream dictate the size of stone that must be used to form a windrow revetment. The size of stone used in the windrow was not significant as long as it was large enough to resist being transported by the stream. An important design parameter is the ratio of the relative thickness of the final revetment to the stone diameter. It was found that large stone sizes will require more material than smaller stone sizes to produce the same relative thickness. Since a filter cannot be used, a well-graded stone is important to ensure that the revetment does not fail from leaching of the underlying bank material. The stream velocity was found to have strong influence on the ultimate side slope of the revetment. It was determined that the initial bank slope was on the average approximately 15 percent steeper than the final revetment slope. In general, the greater the velocity, the steeper the side slope of the final revetment.

**Filters.** Filters are used under riprap to allow water to drain easily from the bank without carrying out soil particles. Filters must meet two basic requirements: stability and permeability. The filter material must be fine enough to prevent the base material from escaping through the filter, but it must be more permeable than the base material. Section 6.7 provides general specifications for granular and geosynthetic filters. HEC-11 (Brown and Clyde 1989) contains more detailed design guidance.

### 6.5.7 Riprap Failure Modes

In a preliminary evaluation of various riprap design techniques, Blodgett and McConaughy (1985) concluded that the procedures based on velocity as a means of estimating stresses on the boundary provide the most reliable and consistent results. The following procedures were investigated: The 1967 version of FHWA HEC-11, FHWA HEC-15, USACE (EM-1601),

Caltrans Bank and Shore Manual, Simons and Senturk, and Oregon Department of Transportation. A major shortcoming of all present design techniques is their assumption that failures of riprap revetment are due only to particle erosion. Procedures for the design of riprap protection need to consider all the various causes of failures.

Classic riprap failure modes are identified as follows: (1) particle erosion; (2) translational slide; (3) modified slump; and (4) slump. These modes of failure are illustrated in Figure 6.19.

Particle erosion is the most commonly considered erosion mechanism (Figure 6.19a). Particle erosion occurs when individual particles are dislodged by the hydraulic forces generated by the flowing water. Particle erosion can be initiated by abrasion, impingement of flowing water, eddy action/reverse flow, local flow acceleration, freeze/thaw action, ice, or toe erosion. Probable causes of particle erosion include: (1) stone size not large enough; (2) individual stones removed by impact or abrasion; (3) side slope of the bank so steep that the angle of repose of the riprap material is easily exceeded; and (4) gradation of riprap too uniform.

A translational slide is a failure of riprap caused by the downslope movement of a mass of stones, with the fault line on a horizontal plane (Figure 6.19b). The initial phases of a translational slide are indicated by cracks in the upper part of the riprap bank that extend parallel to the channel. This type of riprap failure is usually initiated when the channel bed scours and undermines the toe of the riprap blanket; this could be caused by particle erosion of the toe material, or some other mechanism which causes displacement of toe material. Any other mechanism which would cause the shear resistance along the interface between the riprap blanket and base material to be reduced to less than the gravitational force could also cause a translational slide. It has been suggested that the presence of a filter blanket may provide a potential failure plane for translational slides. Probable causes of translational slides are as follows: (1) bank side slope too steep; (2) presence of excess hydrostatic (pore) pressure; and (3) loss of foundation support at the toe of the riprap blanket caused by erosion of the lower part of the riprap blanket.

Modified slump failure of riprap (Figure 6.19c) is the mass movement of material along an internal slip surface within the riprap blanket; the underlying material supporting the riprap does not fail. This type of failure is similar in many respects to the translational slide, but the geometry of the damaged riprap is similar in shape to initial stages of failure caused by particle erosion. Probable causes of modified slump are: (1) bank side slope is so steep that the riprap is resting very near the angle of repose, and any imbalance or movement of individual stones creates a situation of instability for other stones in the blanket; and (2) material critical to the support of upslope riprap is dislodged by settlement of the submerged riprap, impact, abrasion, particle erosion, or some other cause.

Slump failure is a rotational-gravitational movement of material along a surface of rupture that has a concave upward curve (Figure 6.19d). The cause of slump failures is related to shear failure of the underlying base material that supports the riprap. The primary feature of a slump failure is the localized displacement of base material along a slip surface, which is usually caused by excess pore pressure that reduces friction along a fault line in the base material. Probable causes of slump failures are: (1) nonhomogeneous base material with layers of impermeable material that act as a fault line when subject to excess pore pressure; and (2) side slopes too steep and gravitational forces exceeding the inertia forces of the riprap and base material along a friction plane.



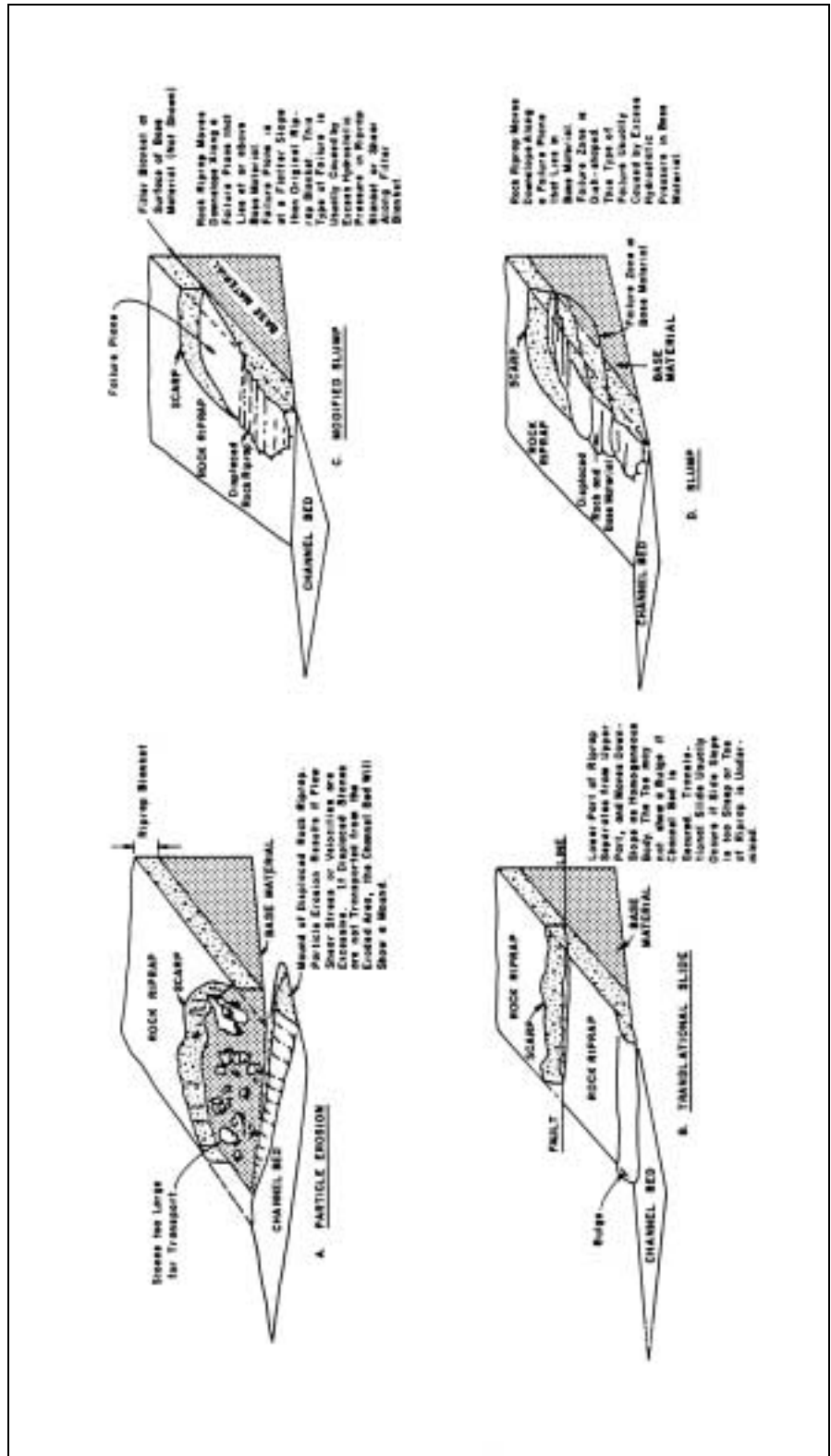


Figure 6.19. Riprap failure models (after Blodgett and McConaughy 1985).

Because of the general effectiveness of dumped riprap, a more detailed analysis of the relatively small number of cases in which it failed has been presented by Brice and Blodgett (1978). The principal causes of failure and methods of mitigation are given in Table 6.3.

Cause	Solution
Inadequate size of riprap	Larger riprap
Impingement of current directly upon riprap rather than having flow parallel to riprap	Heavier stones, flatten riprap slopes, redirect flow
Channel degradation	Provide a volume of reserve riprap at the revetment toe
Internal slope failure (slump)	Reduce the riprap slope angle
Riprap with high percentage of fines causes washing out of the fines	Follow gradation specifications

## 6.6 BANK PROTECTION OTHER THAN RIPRAP

There are many methods other than riprap that can be used for bank protection, including: vegetation, mattresses, baskets, and blocks. This section provides an overview of several of these methods. HEC-23 (Lagasse et al. 2001) and HEC-11 (Brown and Clyde 1989) provide detailed design guidance for several of these methods (see Section 6.3.4).

### 6.6.1 Bioengineering Erosion Control

Vegetation is probably the most natural method for protecting streambanks because it is relatively easy to establish and maintain, is visually attractive and environmentally more desirable.

Below a stream's waterline, vegetation can effectively protect a bank in two ways. First, the root system helps to hold the soil together and increases overall bank stability by forming a binding network. Second, the exposed stalks, stems, branches and foliage provide resistance to the streamflow, causing the flow to lose energy by deforming the plants rather than by removing soil particles. Above the waterline, vegetation prevents surface erosion by absorbing the impact of falling raindrops and reducing the velocity of overbank drainage flow and rainfall runoff. Further, vegetation takes water from the soil providing additional capacity for infiltration and may improve bank stability by water withdrawal.

Vegetation is generally divided into two broad categories: grasses and woody plants (trees and shrubs). The grasses are less costly to plant on an eroding bank above the toe and require a shorter period of time to become established. Woody plants offer greater protection against erosion because of their more extensive root systems; however, under some conditions the weight of the plant will offset the advantage of the root system. On very high banks, tree root systems do not always penetrate to the toe of the bank. If the toe becomes eroded, the weight of the tree and its root mass may cause a bank failure.

The major factor affecting species selection is the length of time required for the plant to become established on the slope.

Water-tolerant grasses such as canarygrass (*Phalaris*), reedgrass (*Calamagrostis*), cordgrass (*Spartina*), and fescue (*Festuca*) are effective in prevent erosion on upper banks which are inundated from time to time and are primarily subject to erosion due to rainfall, overland flow, and minor wave action. Along the lower bank, where erosive forces are high, grasses are generally not effective as a protective measure; however, cattails (*Typha*), bulrushes (*Scripus*), reeds (*Phragmites*), knotweed and smartweed (*Polygonum*), rushes (*Juncus*), and mannagrass (*Glyceria*) are helpful in inducing deposition and reducing velocities in shallow water or wet areas at the bank toe and in protecting the bank in some locations. Willows (*Salix*) are among the most effective woody plants in protecting low banks because they are resilient, are sufficiently dense to promote deposition of sediment, can withstand inundation, and become established easily.

Grass can be planted by hand seeding, sodding, sprigging, or by mechanical broadcasting of mulches consisting of seed, fertilizer, and other organic mixtures. Several commercial manufacturers market economical erosion control matting that will hold the seed and soil in place until new vegetation can become established. The matting is generally installed by hand and secured to the bank where plantings have been made to prevent erosion, then a fence should be placed along the top of bank. If livestock require access to the stream for watering or crossing, gates should be placed in the fence at locations where the cattle will do the least amount of damage to the planted bank; additionally, crossings should be fenced.

### **6.6.2 Bioengineering Countermeasures**

The past few decades have seen increasing use of vegetation as a bank stabilizer. It has been used primarily in stream restoration and rehabilitation projects and can be applied independently or in combination with structural countermeasures. The term bioengineering and is generally used to describe stream bank erosion countermeasures and bank stabilization methods that incorporate vegetation.

Stabilization of eroding stream banks using vegetative countermeasures has proven effective in many documented cases in Europe and the United States. However, the use of bioengineering with respect to scour and stream instability at highway bridges is a relatively new field. There is research being conducted in these fields, but these techniques have generally not been tested specifically as a countermeasure to protect bridges in the river environment.

Bioengineering erosion control is not suitable where flow velocities exceed the strength of the bank material or where pore water pressure causes failures in the lower bank. In contrast, bioengineering maybe suitable where some sort of engineered structural solution is required, but the risk associated with using just vegetation is considered too high. Nonetheless, this group of countermeasures is not as well accepted as the classical engineering approaches to bridge stability.

Design of bioengineered countermeasures to minimize rates of stream bank erosion requires accounting for hydrologic, hydraulic, geomorphic, geotechnical, vegetative, and construction factors. Although most of the literature dealing with biotechnical engineering on rivers is

associated with stream bank stabilization relative to channel restoration and rehabilitation projects, it is also generally applicable to bank stabilization associated with bridge crossings. HEC-23 (Lagasse et al. 2001) provides an overview of bioengineering approaches, a summary of design considerations, and reference to recent reports, studies, and handbooks containing design guidelines.

### 6.6.3 Rock-and-Wire Mattresses

When adequate riprap sizes are not available, rocks of cobble sizes may be placed in wire mesh mats made of galvanized fencing and placed along the bank forming a mattress. HEC-23 (Lagasse et al. 2001) contains specifications developed by the New Mexico State Highway and Transportation Department for wire enclosed riprap mattress. The individual wire units are called baskets if the thickness is greater than 300 mm (12 in.). The term mattress implies a thickness no greater than 300 mm (12 in.). Toe protection is offered by either extending the mattresses on to the channel bed as shown in Figure 6.20 or embedding the mattress to some predetermined scour depth. As the bed along the toe is scoured, the extended mattress drops into the scour hole. Special wire baskets and mattresses are manufactured and sold throughout the United States. It should be noted that when rock-and-wire mattresses are used in streams transporting cobble and rocks, the wires of the basket can be cut by abrasion rather rapidly, which will destroy the intended protection along the base of the bank. Corrosion of the wire mesh and vandalism may also be a problem.

Mattresses and baskets can be made up in large sizes in the field. These are flexible and can conform to scour holes which threaten the stability of the banks. They should be linked together to prevent separation as subsidence takes place.

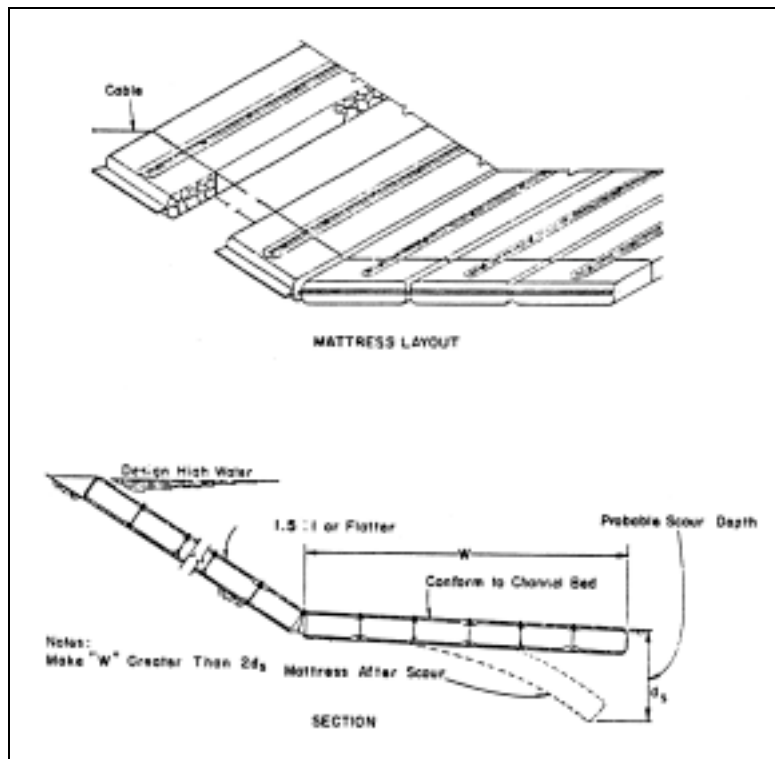


Figure 6.20. Rock and wire mattress.

The most economical combination of rock and wire for streambank protection is simply laying wire mesh over stone. The major problem with this approach is keeping the mesh in place. One successful solution has been to bend pipe or rebar into the shape of a staple and then drive it through the mesh into the bank. The major drawback is that a rock and wire mattress generally costs more to place than a comparable riprap blanket.

#### **6.6.4 Gabions**

Gabions are patented rectangular wire boxes (or baskets) filled with relatively small-size stone, usually less than 200 mm (8 in.) in diameter. Where flow velocities are such that small stone would not be stable if used in a riprap blanket, the wire boxes provide an effective restraint. Limiting recommended maximum velocity for use of gabions ranges from 2.4 to 4.6 m/s (8 to 15 ft/s), depending on the manufacturer. Gabions are used primarily for revetment-type structures, but have also been used for dikes and sills. HEC-11 (Brown and Clyde 1989) provide design guidelines for gabion revetment.

Gabions act as a large heavy porous mass having some flexibility. The baskets are commercially available in a range of standard sizes and are made of heavy galvanized wire (coated when used in a corrosive environment). They are supplied at a job site folded flat and are assembled manually, using noncorrosive wire. The baskets are normally 0.5 m deep by 1 m by 2 m (1.6 x 3.3 x 6.5 ft) and are set on a graded bank for revetments. A filter blanket or synthetic filter fabric is used, where required, to prevent leaching of base material and undermining of the baskets.

#### **6.6.5 Sacks**

Burlap sacks filled with soil or sand-cement mixtures have long been used for emergency work along levees and streambanks during floods (Figure 6.21). In recent years commercially manufactured sacks (burlap, paper, plastics, etc.) have been used to protect streambanks in areas where riprap of suitable size and quality is not available at a reasonable cost. Although most types of sacks are easily damaged and will eventually deteriorate, those sacks filled with sand-cement mixtures can provide long-term protection if the mixture has set up properly. Sand-cement sack revetment construction is not economically competitive in areas where good stone is available. However, if quality riprap must be transported over long distances, this type of sack revetment can often be placed on an eroding streambank at a lesser cost than riprap.

If a permanent revetment is to be constructed, the sacks should be filled with a mixture of 15 percent cement (minimum) and 85 percent dry sand (by weight). The filled sacks should be placed in horizontal rows like common house brick beginning at an elevation below any toe scour (alternatively, riprap can be placed at the toe to prevent undermining of the bank slope). The successive rows should be stepped back approximately 1/2-bag width to a height on the bank above which no protection is needed. The slope steepness of the completed revetment should be no more than 1:1. After the sacks have been placed on the bank, they can be hosed down for a quick set or the sand-cement mixture can be allowed to set up naturally through rainfall, seepage or condensation. If cement leaches through the sack material, a bond will form between the sacks and prevent free drainage. For this reason weepholes should be included in the revetment design. The installation of weepholes will allow drainage of groundwater from behind the revetment thus helping to prevent pressure buildup that could cause revetment failure. Detailed design guidelines for commercially available articulating grout filled mattresses are provided in HEC-23 (Lagasse et al. 2001).

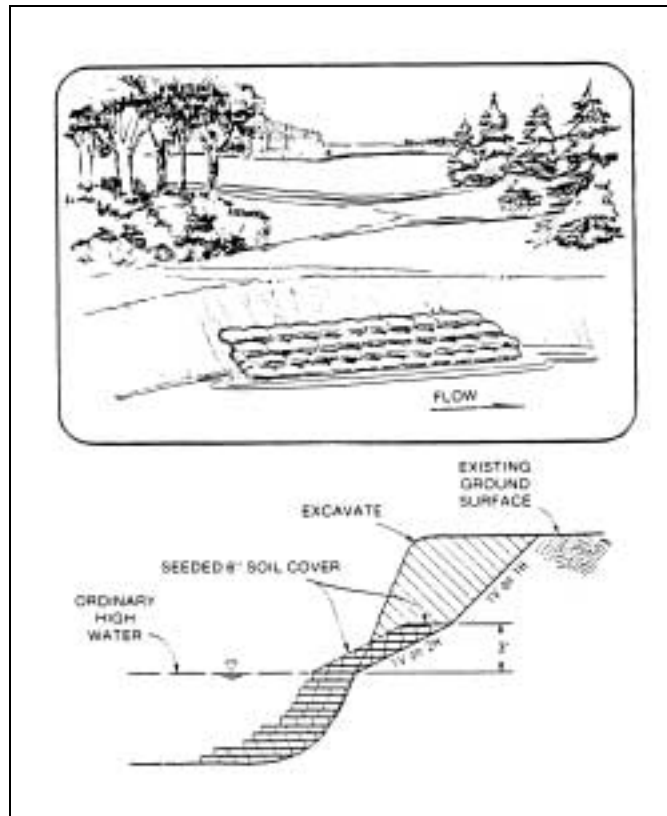


Figure 6.21. Typical sand-cement bag revetment (after Keown 1983).

### 6.6.6 Articulated Concrete Block Systems (ACBs)

Precast cellular blocks can be manufactured using locally available sand, cement, and aggregate or can be obtained from commercial sources. Cellular blocks are cast with openings to provide for drainage and to allow vegetation to grow through the blocks thus permitting the root structure to strengthen the bank. Fabric or a gravel blanket can be used as a filter under the blocks if there is any danger that the bank soil will be eroded through the block openings by streamflow or seepage. Although specialized equipment can be used to install large sections of blocks, hand placement is frequently used when mechanized apparatus is not available, access to the bank is limited, or costs need to be minimized. After the blocks have been placed, the revetment has sufficient flexibility to conform to minor changes in bank shape. Solid blocks should not be used because the bank may not be able to drain freely and failure could occur.

Small precast concrete blocks held together by steel rods or cables can be used to form a flexible mat as shown in Figure 6.22. Design guidelines for ACBs are provided in HEC-23 (Lagasse et al. 2001) and HEC-11 (Brown and Clyde 1989).

The sizes of blocks may vary to suit the contour of the bank. It is particularly difficult to make a continuous mattress of uniform sized blocks to fit sharp curves. The open spacing between blocks permits removal of bank material unless a filter blanket of gravel or geosynthetic material is placed underneath. For embankments that are subjected only to occasional flood flows, the spaces between blocks may be filled with earth and vegetation can be established.

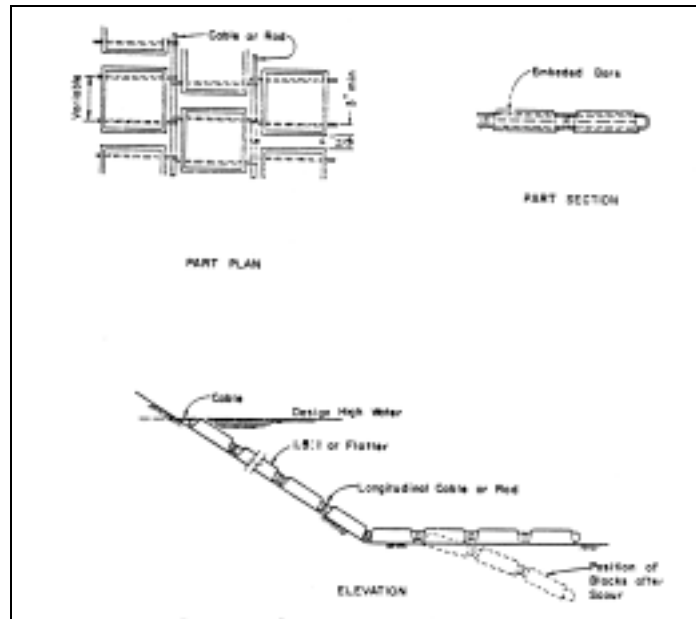


Figure 6.22 Articulated concrete block system.

### 6.6.7 Used Tires

Tires have been placed both as a mattress and stacked back against the bank. Both methods appear to have some potential as an economical approach to protect a streambank, but environmental issues and aesthetics must be considered.

During construction of a tire mattress on an eroding bank, two precautions should be considered to ensure that the mattress will stay in place.

- The tires must be banded together; alternatively, cables running the length and width of the mattress can be woven through the tires.
- The top, toe and the upstream and downstream ends of the mattress must be tied to the bank (Figure 6.23). If scour is anticipated, riprap should be placed at the toe of the mattress for additional protection.

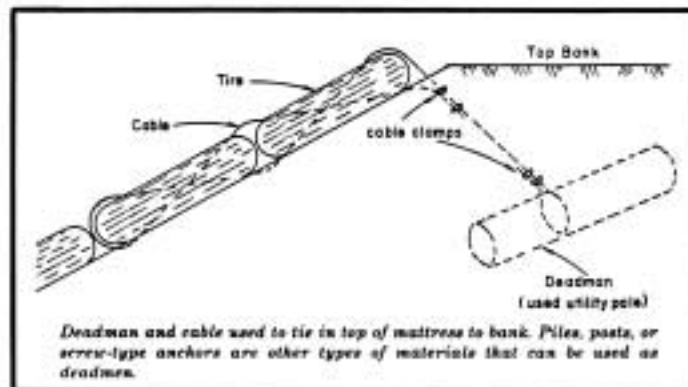


Figure 6.23. Used tire mattress (after Keown 1983).

While the precautions listed above are essential for successful construction of a stable mattress, other considerations can further improve the chances that the revetment will provide long-term bank protection.

- Holes can be cut, drilled, or burned in the tire sidewalls to prevent flotation.
- Presorting the tires by size may help to fit them together.
- Earth screw anchors (or some other type of anchor) fastened to the mattress can be placed in the bank at various points on the face of the revetment.
- The tires can be packed with stone or rubble.
- Willows can be planted inside the tires preferably at the beginning of the growing season. Once established the root system will further strengthen the bank and obscure the unsightly mattress. If willows are not readily available, other species should be planted. Possible species for use are discussed later in this text.

If the mattress effectively controls the streambank erosion and remains intact, sediment may gradually cover the revetment. If willows have not been planted, volunteer vegetation will may become established in areas with a temperate climate.

Prior to constructing a stacked-tire revetment, the bank face should be shaped so that the tires can be laid in horizontal rows on a geosynthetic filter material. The revetment should be started at the toe of the bank and stepped back 150 to 300 mm (6 to 12 in.) per row. Each tire should overlap the two tires under it. The stacked tires should be packed tightly with stone or rubble. Any space behind the tires should be filled with free-draining soil so that the soil mass will not become saturated and cause the revetment to fail. In addition, the upstream and downstream ends of the revetment should be tied into the bank so that there is no flow behind the revetment.

### **6.6.8 Soil Cement**

In areas where riprap is scarce, use of in-place soil can sometimes be combined with cement to provide a practical alternative. HEC-23 (Lagasse et al. 2001) provides design guidelines and specifications for soil cement revetments. Figure 6.24 shows a detail of a typical soil-cement construction for bank protection. For use in soil-cement, soils should be easily pulverized and contain at least five percent, but not more than 35 percent, silt and clay (material passing the No. 200 sieve). Finer textured soils usually are difficult to pulverize and require more cement as do 100 percent granular soils which have no material passing the No. 200 sieve. Soil cement can be placed and compacted on slopes as steep as one horizontal to one vertical.

A stairstep construction is recommended on channel embankments with relatively steep slopes. Placement of small quantities of soil-cement for each layer 150 mm (6-inch) layers can progress more rapidly than a large quantity of fill material. Special care should be exercised to prevent raw soil seams between successive layers of soil-cement. If uncompleted embankments are left at the end of the day, a sheep'sfoot roller should be used on the last layer to provide an interlock for the next layer. The completed soil-cement installation must be protected from drying out for a seven day hydration period. After completion, the material has sufficient strength to serve as a roadway along the embankment. Procedures for constructing soil-cement slope protection by the stairstep method can be found in "Suggested Specifications for Soil-Cement Slope Protection for Embankments (Central-Plant Mixing Method)," Portland Cement Association Publication IS052W and numerous other PCA publications.



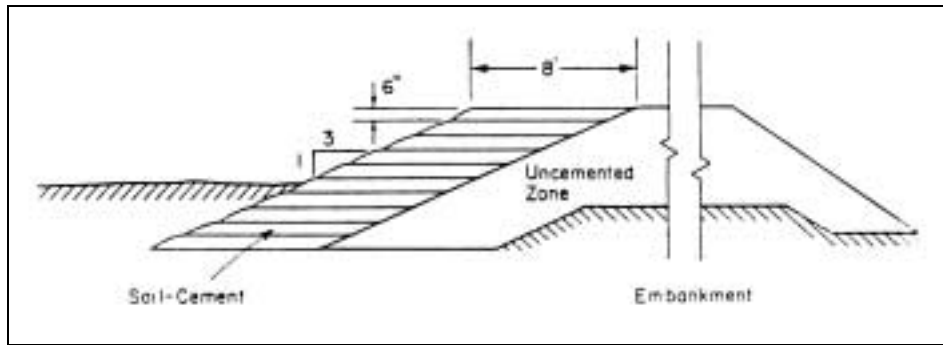


Figure 6.24. Typical soil-cement bank protection.

When velocities exceed 1.8 to 2.4 m/s (6 to 8 ft/s) and the flow carries sufficient bed load to be abrasive, special precautions are advisable. The aggregates in this case should contain at least 30 percent gravel particles retained on a No. 4 (4.75 mm) sieve. It should be emphasized that soil-cement provides a rigid bank protection. The depth of the bank protection should be sufficient to protect the installation from the anticipated total scour.

A soil cement blanket with 8 to 15 percent cement may be an economical and effective streambank protection method for use in areas where vegetation is difficult to establish and the bank material is predominately sand. The sand can be mixed with cement by hand or mechanically to a depth of at least 4 inches. The mixture should then be wet down and allowed to set up. This method has the advantage of low cost. However, there are three major disadvantages: impermeability, low strength, and susceptibility to temperature variations. If the bank behind the blanket becomes saturated and cannot drain, failure may occur. Also, because a sand-cement blanket is relatively brittle, very little if any traffic (vehicular, pedestrian, or livestock) can be sustained without cracking the thin protective veneer. In northern climates the blanket can break up during freeze-thaw cycles.

## 6.7 FILTERS

Filters are used under riprap to allow water to drain easily from the bank without carrying out soil particles. Filters must meet two basic requirements: stability and permeability. The filter material must be fine enough to prevent the base material from escaping through the filter, but it must be more permeable than the base material. There is no standard filter that can be used in all cases, see HEC-11 (Brown and Clyde 1989) for additional guidelines on filter design. Two types of filters are commonly used: granular (gravel) filters and geosynthetic filters.

Granular Filters. A layer or blanket of well-graded gravel should be placed over the embankment or riverbank prior to riprap placement. Sizes of gravel in the filter blanket should be from 5 mm (3/16 in.) to an upper limit depending on the gradation of the riprap with maximum sizes of about 76 to 89 mm (3 to 3-1/2 in.). Thickness of the filter may vary depending upon the riprap thickness but should not be less than 152 to 228 mm (6 to 9 in.). Filters that are one-half the thickness of the riprap are quite satisfactory. Suggested specifications for gradation are as follows:

$$(1) \frac{D_{50} \text{ (Filter)}}{D_{50} \text{ (Base)}} < 40 \quad (6.24)$$

$$(2) 5 < \frac{D_{15} \text{ (Filter)}}{D_{15} \text{ (Base)}} < 40 \quad (6.25)$$

$$(3) \frac{D_{15} \text{ (Filter)}}{D_{85} \text{ (Base)}} < 5 \quad (6.26)$$

If the base material is a fine-grained cohesive soil, such as fat or lean clay, these requirements are not applicable, and the stability criterion is that the  $D_{15}$  size of the filter cannot exceed 0.4 mm.

When the base material is very fine, the required filter material may also be quite fine, and more than one layer of filter (a graded filter) may be needed. In such a case, each layer must satisfy the stability and permeability requirements relative to the underlying layer.

If the filter is designed for protection against the upward flow of water, the graded filter is constructed so that each layer is coarser than the one beneath (a "reverse" or "inverted" filter).

**Geosynthetic Filters.** Geosynthetic materials are also used as filters, replacing a component of a graded filter. Detailed information on the use of geosynthetic filters can be found in Holtz et al. 1995 (FHWA HI-95-038) who define permeable geosynthetics as "geotextiles." Numerous geotextiles are on the market, with a wide variation in size and number of openings and in strength and durability. Geotextiles which provide opening areas of 25 to 30 percent are desirable to minimize the possibility of clogging and to reduce head loss.

When geotextiles are used, care must be taken not to puncture the material during construction. If the filter fabric is placed on top of the base material, gravel can sometimes be placed directly on the fabric, eliminating the need for filter sand. If the paving materials is dumped or cast stone, however, it is desirable to place a protective blanket of sand or gravel on the filter, or to take care in placing the rock, so that the filter fabric is not punctured. Stones weighing as much as 1,360 kg (3,000 lbs) have been placed on synthetic filters with no apparent damage. If a protective covering is not used, the size and drop of the rock should be limited. The sides and toe of the filter fabric must be sealed or trenched so that base material does not leach out around the filter fabric. Care is also required in joining adjacent sections of filter fabric together; sewn, overlapped, and welted seams are used. See Holtz et al. 1995 for AASHTO specifications and construction guidelines.

## 6.8 OVERTOPPING FLOW ON EMBANKMENTS

### 6.8.1 Introduction

Floodwaters which exceed the crest elevation of roadways, approach embankments, levees, and similar earth embankment structures result in a hydraulic condition referred to as overtopping flow. Overtopping flow can be broadly characterized into two categories according to the level of tailwater on the downstream side of the structure: (1) "submerged flow," where tailwater is higher than the embankment crest and presents a backwater condition sufficient to affect the discharge over the crest; and (2) "free flow," where tailwater may be present against the downstream embankment slope but at an elevation low enough such that interference with flow over the crest does not occur.

Since the mid-1980s, extensive research has been conducted on overtopping flow over embankments and on the effectiveness of alternative methods for protecting the downstream slope of embankments against erosion during overtopping events. A number of different aspects of overtopping flow have been investigated, including the hydraulic conditions of flow, the mechanics of overflow erosion, and the prevention of erosion under varying conditions of soil types, hydraulic conditions, and embankment geometry. The ASCE Task Committee on the Mechanics of Overflow Erosion on Embankments (Powledge et al. 1989b) summarizes more than 30 dam, levee and roadway embankments that experienced overtopping flows during the 1980s. Field studies and laboratory investigations conducted both at full scale and at model scales during the last two decades have contributed to the understanding of analysis and design issues associated with overtopping flow. Many of these research activities are also summarized by the Task Committee (Powledge 1989a).

### 6.8.2 Hydraulics of Overtopping Flow

**Flow Zones.** In the case where there is minimal tailwater during an overtopping event, flow over an embankment structure transitions through three zones. Zone 1 is characterized by subcritical flow over the dam crest. In this zone the total energy is essentially equal to the elevation of the low-velocity pool upstream of the embankment, and erosive energy in this flow zone is low. In Zone 1, the embankment will experience erosion only when its crest is comprised of highly erodible material. Zone 2 consists of a transition zone near the downstream shoulder where the flow transitions from subcritical to supercritical. While the total energy remains similar to that in Zone 1, an increase in velocity creates an increase in local shear stress, and the erosive energy begins to build. Zone 3 consists of supercritical flow on the downstream slope of the embankment. In this zone, the erosive energy increases significantly as the flow accelerates down the slope. The energy slope increases as well, causing high erosion potential. Figure 6.25 illustrates these flow regimes (Powledge et al. 1989b).

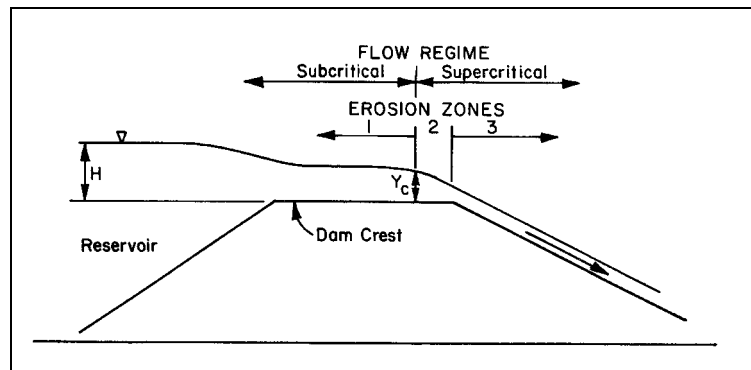


Figure 6.25. Hydraulic flow zones on an embankment during overtopping flow (Powledge et al. 1989b).

**Estimating Discharge.** Flow over an embankment can exhibit two types of behavior. Kindsvater (1964) was one of the first to classify these conditions. The first type of flow condition is known as free flow, and is characterized by tailwater conditions that are low

enough such that backwater conditions on the crest do not occur. Free flow is further subdivided into either free-plunging or free-surface flow. The term plunging flow is used when the high-velocity jet plunges under the tailwater surface, creating a hydraulic jump. Surface flow occurs when the jet separates from the downstream slope of the embankment and "rides" over the tailwater surface. The generally accepted equation for discharge over an embankment is

$$q = CH_1^{3/2} \tag{6.27}$$

where:

- q = Discharge per unit width, m<sup>2</sup>/s (ft<sup>2</sup>/s)
- C = Experimentally determined coefficient (for level-crested embankments, C ≈ 0.51 for SI units or 3.0 for English units)
- H<sub>1</sub> = Total head above the embankment crest, m (ft)

The second flow behavior is known as submerged flow. In this case, the tailwater is high enough to affect the discharge over the embankment. For the case of submerged flow, the equation becomes

$$q = CH^{3/2} \left( \frac{C_s}{C} \right) \tag{6.28}$$

where C<sub>s</sub> is the submergence coefficient and the term C<sub>s</sub>/C is dimensionless. Figure 6.26 illustrates the variables needed to describe overtopping flow (Kindsvater 1964).

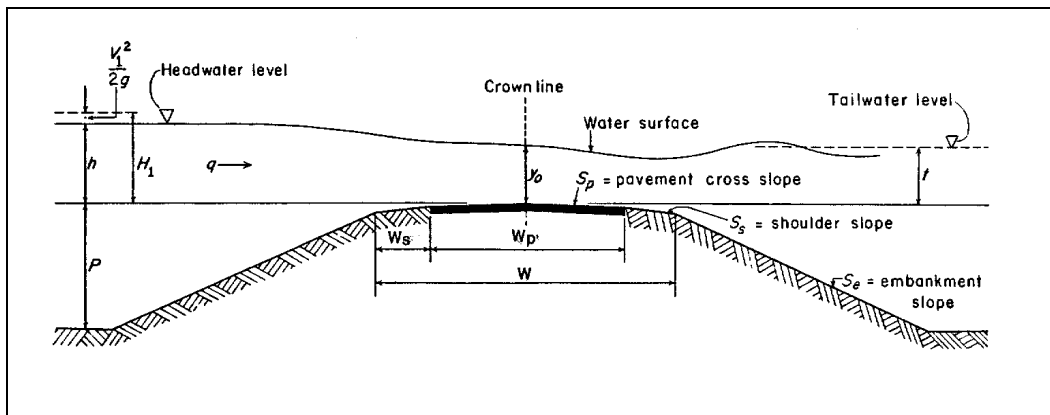


Figure 6.26. Definition sketch of variables involved in overtopping flow (Kindsvater 1964).

**Hydraulic Analysis.** In 1983, FHWA initiated research for which a full-scale testing facility was constructed in Fort Collins, Colorado. This facility was used to carry out a two-phase research project. Phase I consisted of an extensive literature review, field studies, and prototype-scale embankment tests involving different types of protection systems. Analysis of these studies developed embankment erosion equations and a computer simulation program called EMBANK (Chen and Anderson 1987). This program was used to develop

design charts that could be applied to estimate embankment erosion caused by a range of overtopping depths and tailwater conditions.

When a bare soil embankment fails, it is often directly related to the bed shear stress that is applied as the flow accelerates over and down the embankment. Clopper and Chen (1988) describe a computational approach to calculating the bed shear stress. Using the principle of the conservation of momentum, the following equation was developed for non-uniform flow on the downstream embankment slope.

$$\tau_o = \frac{\gamma}{2}(d_1 + d_2) \sin\theta + \frac{1}{L} \left[ \frac{\gamma}{2}(d_1^2 - d_2^2) \cos\theta - \rho q^2 \left( \frac{1}{d_2} - \frac{1}{d_1} \right) \right] \quad (6.29)$$

where  $\gamma$  is the unit weight of water,  $\rho$  is the unit mass of water,  $q$  is the volumetric discharge per unit width, and the remaining parameters are presented in Figure 6.27.

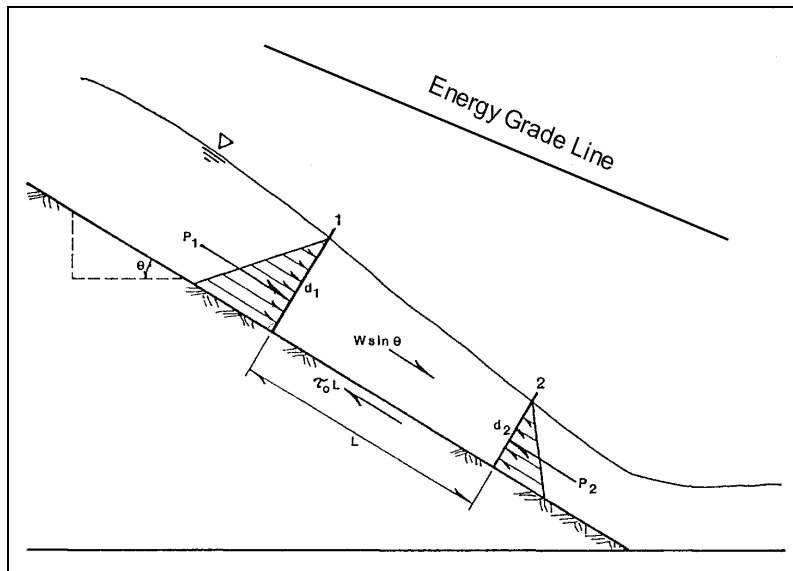


Figure 6.27. Definition sketch for application of the momentum equation for embankment overtopping flow.

If uniform flow is assumed, Manning's equation can be used to estimate the depth of flow, and shear stress calculated by

$$\tau_o = \gamma d S_f \quad (6.30)$$

It should be noted that when using Manning's equation, the assumption is made that the friction slope  $S_f$  is equal to the bed slope  $S_0$ . This assumption usually yields a conservatively high estimate of bed shear stress, unless the combination of slope length and unit discharge result in conditions which approach uniform flow.

In practice, it is recommended that a range of Manning's n values of approximately +/- 10 percent of the base value be used to calculate the range of anticipated flow conditions. The minimum value of Manning's n is used to determine the peak anticipated velocity, and the maximum value of Manning's n is used to determine peak anticipated flow depth and shear stress.

### 6.8.3 Mechanics of Overflow Erosion

Erosion Processes. When flow overtops an embankment, locally high velocities and shear stresses will create strong erosion forces, typically at the downstream shoulder and on the embankment slope, that are too great for the soil of the embankment to withstand. There are two primary processes of erosion that occur during an overtopping event.

When the overtopping flow is submerged, erosion typically begins at the downstream shoulder. This is the condition often experienced by roadways and approach embankments.

Figure 6.28 (Chen and Anderson 1987) shows the progression of this type of failure at times  $t_1$ ,  $t_2$ , and  $t_3$ . As flow accelerates over the embankment, a surging hydraulic jump is formed which causes a nick point between the shoulder and downstream slope. This nick point will begin to migrate upstream due to the high velocities and erosion will begin to move downstream. The downstream migration of the erosion is caused by the turbulence associated with the hydraulic jump. It should be noted that, depending on the tailwater conditions and embankment geometry and soil type, even events of long duration may not ultimately result in a full breach of the embankment section. This is because a balance of forces can develop once the initial embankment erosion has produced a geometry that achieves equilibrium between hydraulic forces and the erosion resistance of the remaining embankment material.

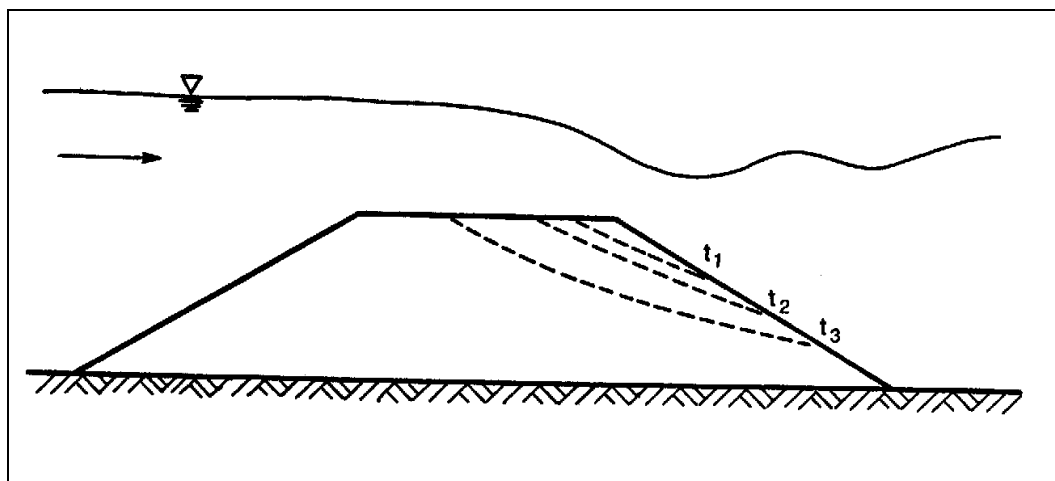


Figure 6.28. Typical embankment erosion pattern with submerged flow (Chen and Anderson 1987).

The second general erosion pattern results from the case of free flow. With low tailwater, the flow will accelerate down the slope with high velocity and shear stress associated with supercritical flow. Erosion typically initiates near the toe of the embankment, whether or not a hydraulic jump is present. Erosion progresses in the upslope and upstream direction through the embankment. Figure 6.29 (Chen and Anderson 1987) illustrates this progression. Given sufficient duration, this type of erosion pattern typically will result in a full breach of the embankment section.

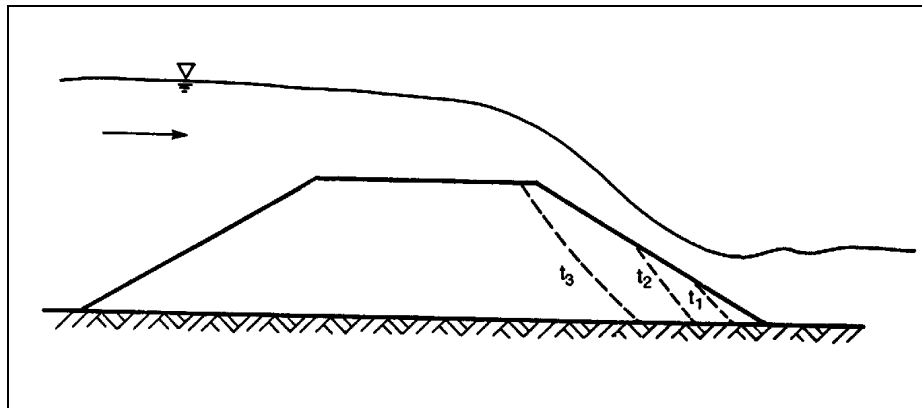


Figure 6.29. Typical embankment erosion pattern with free flow (Chen and Anderson 1987).

Erodibility Rate Equation. Many analytical equations have been presented to estimate the rate of erosion under conditions of overtopping flow. Most of these equations use the effective shear stress and/or velocity along with some measure of resistance of the embankment material to estimate the rate of soil loss. These equations were assessed (Chen and Anderson 1987) by relating the erosion rates measured during tests to those calculated by the various equations.

The erodibility rate relation developed by the Agricultural Research Laboratory was found to be the most applicable to embankment overtopping flow conditions based on these studies. This general form of the equation is:

$$E = K (\tau - \tau_c)^a \quad (6.31)$$

where:

- E = Detachment rate per unit area
- $\tau$  = Local effective shear stress based on hydraulic conditions
- $\tau_c$  = Critical shear stress of the soil
- K&a = Empirical coefficients dependent on soil properties

Local Shear Stress Calculation. For an embankment undergoing erosion, another parameter of importance is local shear stress. Chen and Anderson (1987) present the following equation (in English units) for calculating the shear stress in the immediate vicinity of the erosion location.

$$\tau = \frac{1}{8} f \rho V^2 \quad (6.32)$$

where:

$$f = \frac{116 n^2}{d^{1/3}} \quad (6.33)$$

and  $V$  is the local velocity,  $f$  is the Darcy-Weisbach coefficient, and  $\rho$  is the water density,  $n$  is Manning's resistance coefficient, and  $d$  is the local flow depth. The use of the local shear stress equation can assist in accommodating the irregular pattern of erosion and its nonuniform progression through an embankment section at various times during an overtopping event. This form of the shear stress equation is utilized in the program EMBANK, described previously in this section.

#### 6.8.4 Erosion Protection in Overtopping Flow

Materials or manufactured systems designed to protect against overtopping erosion can be selected and designed using methods based on permissible velocity, permissible shear stress, or both. Because velocity in and of itself is not a force, procedures based on permissible velocity are generally derived from extensive testing and field experience using a particular material under a variety of flow conditions, and are empirical in nature. Procedures utilizing shear stress as a fundamental variable tend to be more theoretical in nature, and are typically developed using a force-balance or moment-balance concept. Both types of methods are described in this section.

Permissible Velocity Approach. Based on a battery of tests of vegetated trapezoidal channels using various types of reinforcement materials on steep waterways, Hewlett et al (1987) present permissible velocities for reinforced grass channels. These curves are presented in Figure 6.30 as a function of duration of the overtopping event. Note that the permissible velocity of concrete-based systems are independent of duration, as shown in the figure.

Permissible Shear Stress Approach. Permissible shear stress based approaches are usually related to force-balance (sliding) or moment-balance (overturning) representations of the stability paradigm. Typically, a discrete-particle approach to the stability analysis is developed using the force- or moment-balance equations for the particular system under consideration. These approaches are presented in Hydraulic Engineering Circular No. 23 (Lagasse et al. 2001) for selected erosion control systems, e.g., articulating concrete blocks, concrete armor units, and grout-filled fabric mats.

Laboratory or field tests are recommended in order to develop the calibration parameters needed to fully describe the performance of the system. The permissible shear stress from the controlled testing program is then extended to various conditions of bed slope and side slope. Figure 6.31 shows a typical full-scale test of an articulated concrete block system in progress under steep-slope, high-velocity flow.



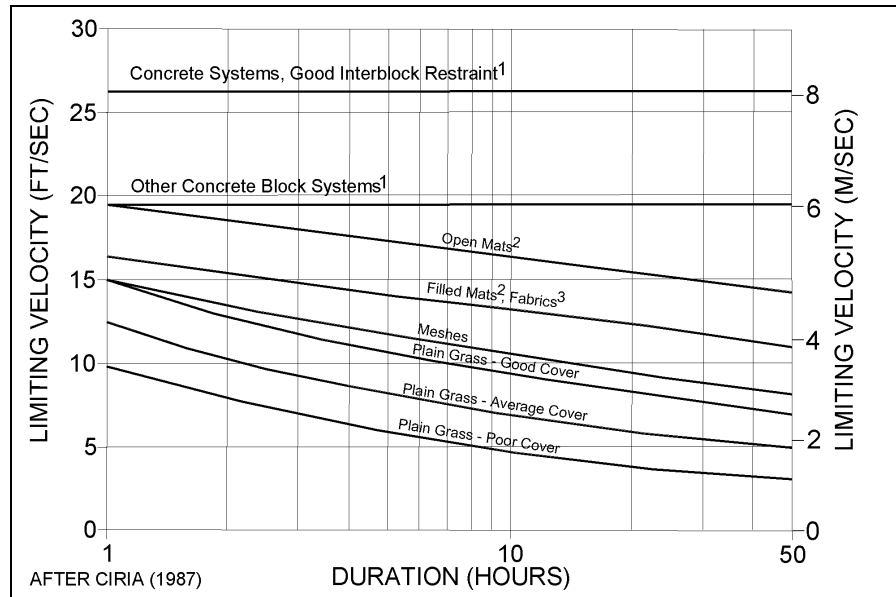


Figure 6.30. Permissible velocities of various protection materials as a function of flow duration (Hewlett et al. 1987).

Notes to Figure:

1. Minimum superficial mass  $135 \text{ kg/m}^2$  ( $28 \text{ lb/ft}^2$ )
2. Minimum nominal thickness 20 mm (0.8 inch)
3. Installed within 20 mm (0.8 inch) of soil surface, or in conjunction with a surface mesh
4. These graphs should only be used for erosion resistance to unidirectional flow. Values are based on available experience and information at the date of this report.
5. All reinforced grass values assume well established, good grass cover.
6. Other criteria (such as short-term protection, ease of installation and management, susceptibility to vandalism) must be considered in choice of reinforcement.

### 6.8.5 Overtopping Protection Systems

A number of material types and manufactured systems have been identified for use in minimizing or preventing erosion of embankments subjected to overtopping flow. Listed below are protection systems which have been the subject of various investigation over the last several decades. These systems are described in detail in a summary report issued by the ASCE Task Committee on Overtopping Protection (Oswalt et al. 1994):

1. Reinforced Vegetation
2. Roller Compacted Concrete
3. Soil Cement
4. Cast in Place Concrete
5. Articulating Concrete Blocks
6. Geotextile
7. Riprap
8. Gabions



Figure 6.31. Full-scale test of an embankment overtopping protection system under steep-slope, high-velocity flow conditions.

Each of these protection systems has its own unique mode of failure and threshold capability for erosion resistance. When using these systems, careful attention should be placed on the design of termination details at the crest, sides, and toe of the embankment. Powledge, et al. (1989a, 1989b) note that many of these systems were originally designed for uses other than the protection of embankments during overtopping flow, and have been adapted to this application as a result of a recognized need. For application of the Factor of Safety method (Section 6.5) to the design of riprap for the complex geometries often associated with overtopping flows, reference to Julien (1995) is suggested.

## **6.9 ENVIRONMENTAL CONSIDERATIONS**

Streambank protection projects should be planned, designed and constructed with consideration being given to environmental quality factors and project objectives. Environmental quality should address preservation or restoration of environmental resources within the project boundaries and avoidance of adverse impacts associated with the project. Some environmental factors are project specific and are necessarily defined during the planning phase while others are mandated by existing regulations. Streambank protection projects should strive to preserve or restore existing environmental quality to the extent possible.

### **6.9.1 Environmental Impacts**

Impacts of streambank protection projects are dependent on project location and regional characteristics. For example, in arid regions of the western United States, forested habitat may be restricted to riparian areas and be directly and extensively impacted by project construction; whereas in the southeastern United States, forested habitat may be more extensive, but changes in stream hydraulics caused by the project can result in adverse impacts throughout the floodplain ecosystem. While general categories of impacts may be stated, site-specific and regional considerations and individual project features are critical in determining the magnitude and type of environmental impact. In some cases streambank protection is performed in conjunction with other projects having different purposes, and it is difficult to isolate impacts due to streambank protection alone. Categories of environmental impacts associated with streambank protection projects include aesthetic, physical, water quality, and biological.

Aesthetic impacts most often occur because the natural appearance of the project area is disturbed or changed and replaced by an artificial appearance due to structures or channel alignment. The physical impacts of streambank protection can affect channel morphology, sediment-carrying capacity of the stream, and stream hydraulics. These physical effects tend to manifest themselves as changes in landscape diversity and associated aquatic habitat diversity or quality; for example, loss of side channels or shallow areas or replacement of natural bank with revetment. Losses or changes in habitat will affect wildlife and aquatic life either by a reduction or change in community structure; however, changes in habitat composition for a specific project can be either detrimental or beneficial depending on circumstances.

Water quality impacts from changes in turbidity together with alteration of riparian habitat (e.g., shading) affect stream temperature and photosynthetic activities that in turn may affect algae or aquatic plant populations, dissolved oxygen, and other water quality parameters. Temporary changes in water quality may occur as a result of construction activities.

Biological impacts can be broadly categorized into either terrestrial or aquatic. The major terrestrial impact involves alteration or elimination of riparian zone vegetation due to construction or project features. The riparian zone provides and supports a wide variety of plant and animal life and often provides critical habitat for certain species. Riparian vegetation also supports aquatic species by providing habitat for these species and input to the food chain. Channel stabilization can affect succession of riparian vegetation and decrease diversity. Aquatic organisms, including benthos and fish, may also be affected due to changes or reductions in required habitats as a result of project features.

Other impacts that may occur due to streambank protection projects include loss of wetlands and historic sites, changes in land use, increased recreational pressure, and economic or social impacts.

### **6.9.2 Effects of Channelization**

Patrick (1973) assessed that the stream and its floodplain constitutes an integrated system that is well designed for moderating the effects of flooding waters and for maintaining high productivity in the stream. Disturbing the system inevitably results in a reduction in diversity of species and productivity. Because the functioning of the aquatic ecosystems is impaired, the ability of the stream to cleanse itself and to assimilate wastes is lessened, and the improvement of water quality is slower. The stream, instead of being one that is aesthetically pleasing and highly productive, becomes degraded and its recreational use is minimized. The chief effects of channelization are as follows:

- Removes the natural diverse substrate materials that allow the development of many types of habitats for aquatic organisms
- Increases sediment load that decreases light penetration and primary production
- Creates a shifting bed load that is inimical to bottom-dwelling organisms
- Simplifies the current pattern and eliminates habitats of diverse currents
- Lowers the stream channel and often drains adjacent swamp areas and aquifers that help to maintain stream flow during time of low precipitation
- Destroys floodplain ponds that are the breeding ground for aquatic life and that act as a reservoir for species of the river proper
- Reduces the stability of the banks and causes cave-in of trees and other overhanging vegetation that are an important food source for stream life and whose shade reduces high stream temperatures during the summer months

Kellerhals et al. (1985) concluded that most existing engineering design criteria for river training works are in direct conflict with general concepts of fish habitat maintenance since their aims are well aligned, uniform and stable channels, with minimum local scour and no opportunity for debris jamming. The objectives of fisheries mitigation works are often quite the opposite; a degree of instability, rough and irregular banks, deep local scour holes, debris jams and overhanging vegetation. Well founded guidelines for designing such diverse and irregular

channels (particularly in larger rivers) are needed and can only be developed on the basis of studies with a far broader scope than the normal project-oriented work funded by developers.

### 6.9.3 Channel Restoration and Rehabilitation

Over the last several years, numerous agencies and practitioners have published guidelines for stream corridor restoration and channel rehabilitation design. For example, in 1998, fifteen Federal agencies and partners published a manual, Stream Corridor Restoration - Principles, Processes and Practices (Federal Interagency Stream Restoration Working Group 1998). This document represents a cooperative effort by the participating agencies to produce a common technical reference on stream corridor restoration. Recognizing that no two stream corridors and no two restoration initiatives are identical, this technical document broadly addresses the elements of restoration that apply in the majority of situations encountered. Reference is also suggested to Rosgen (1996) and U.S. Army Corps of Engineers publications such as Watson et al. 1999. HEC-20 (Lagasse et al. 2001) provides an introduction to stream restoration concepts and HEC-23 (Lagasse et al. 2001) presents guidelines and references for bioengineering bank protection treatments.

## 6.10 SOLVED PROBLEMS FOR STABILITY OF RIPRAP (SI)

### 6.10.1 PROBLEM 1 Stability of Particles Under Downslope Flow

Downslope flow over a plane bed inclined at an angle  $\hat{\theta}$  shown in Figure 6.32 is equivalent to an oblique flow on a side slope with  $\theta = \hat{\theta}$  and  $\lambda = 90^\circ$ . Then, according to Equation 6.4,  $\beta = 0$ , and from Equation 6.6,

$$\eta' = \eta \left( \frac{1 + \sin 90^\circ + 0}{2} \right) = \eta$$

It follows from Equation 6.3 that the stability factor is

$$\text{S.F.} = \frac{\cos \hat{\theta} \tan \phi}{\eta \tan \phi + \sin \hat{\theta}}$$

Alternatively, solving for  $\eta$  yields

$$\eta = \cos \hat{\theta} \left[ \frac{1}{\text{S.F.}} - \frac{\tan \hat{\theta}}{\tan \phi} \right]$$

Using this information we wish to calculate (if the angle of repose,  $\phi = 40^\circ$ ), what is the maximum bed angle  $\hat{\theta}$  at which  $\eta$  will be 5 percent different from that of a horizontal bed. Solving for  $\hat{\theta}$  with  $\eta = 0.95$ , S.F. = 1 and  $\phi = 40^\circ$  yields  $\hat{\theta} = 2.35^\circ$  or 4.1 percent.

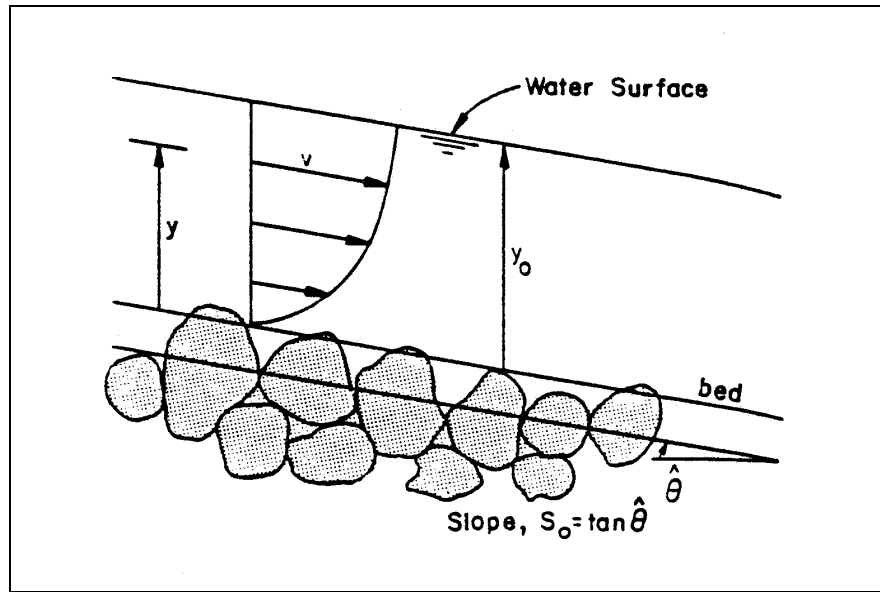


Figure. 6.32. Definition sketch for riprap on a channel bed.

### 6.10.2 PROBLEM 2 Riprap Design on Embankment Slopes

In a design situation water flows parallel to an embankment built of crushed rock riprap, ( $S_s = 2.65$ ), at a sloping angle  $\theta = 20^\circ$ .

(a) If the design shear stress is  $\tau_o = 95.8 \text{ N/m}^2$ , calculate the riprap size that gives a stability factor equal to 1.5.

Assuming angle of repose  $\phi = 40^\circ$ , the stability number  $\eta$  is obtained from Equation 6.3 or Figure 6.14 for  $\theta = 20^\circ$  ( $\eta = 0.36$ ). The stone size is then calculated from Equation 6.13.

$$D_m = \frac{21\tau_o}{(S_s - 1)\gamma\eta} = \frac{21 \times 95.8}{(2.65 - 1) 9800 \times 0.36} = 0.35 \text{ m}$$

(b) For the same design shear stress  $\tau_o = 95.8 \text{ N/m}^2$ , determine the stability factor of particle sizes  $D_m = 0.15 \text{ m}$ . From Equation 6.5

$$\eta = \frac{21\tau_o}{(S_s - 1)\gamma D_m} = \frac{21 \times 95.8}{(2.65 - 1) 9800 \times 0.15} = 0.83$$

Then, Equations 6.11, 6.10, and 6.9 are used to calculate the stability factor

$$S_m = \frac{\tan\phi}{\tan\theta} = \frac{\tan 40^\circ}{\tan 20^\circ} = 2.31$$

$$\zeta = S_m \eta \sec\theta = 2.31 \times 0.83 \sec 20^\circ = 2.04$$

$$S.F. = \frac{S_m}{2} \left( (\zeta^2 + 4) \right)^{1/2} - \zeta = \frac{2.31}{2} \left( (2.04^2 + 4) \right)^{1/2} - 2.04 = 0.94 < 1$$

This size fraction ( $D_m = 0.15$  m) is unstable.

(c) Determine riprap size  $D_m$  for a side slope. The side slope angle  $\theta = 20^\circ$ ; very angular rock with angle of repose  $\phi = 40^\circ$ ;  $V_{ss} = 3.66$  m/s;  $y = 3.05$  m;  $S.F. = 1.1$  and  $D_{85} / D_{15} = 2.0$ . From Equations 6.11, 6.12, and 6.16:

$$S_m = \frac{\tan \phi}{\tan \theta} = \frac{\tan 40}{\tan 20} = 2.31$$

$$\eta = \frac{S_m^2 - (S.F.)^2}{(S.F.) \times S_m^2} \cos \theta = \frac{2.31^2 - 1.1^2}{1.1 \times 2.31^2} \cos 20 = 0.66$$

$$D_m = \frac{0.3 V^2}{(S_s - 1) g \eta} = \frac{0.3 \times 3.66^2}{1.65 \times 9.81 \times 0.66} = 0.38 \text{ m}$$

(d) Compare the size calculated in (c) with a riprap size calculated using the U.S. Army Corps of Engineers equation (Section 6.5.4). From Equations 6.18 and 6.20:

$$D_{30} = S_f C_s C_v C_T y \left[ \left( \frac{\gamma}{\gamma_s - \gamma} \right)^{0.5} \frac{V}{(K_1 g y)^{0.5}} \right]^{2.5}$$

$$K_1 = \left[ 1 - \frac{\sin^2 \theta}{\sin^2 \phi} \right]^{1/2} = \left[ 1 - \frac{\sin^2 20}{\sin^2 40} \right]^{1/2} = 0.85$$

$$D_{30} = 1.1 \times 0.3 \times 1.0 \times 1.0 \times 3.05 \left[ \left( \frac{9800}{16,175} \right)^{0.5} \frac{3.66}{0.85 \times 9.81 \times 3.05} \right]^{2.5} = 0.24 \text{ m}$$

$$D_{50} = D_{30} \times (D_{85} / D_{15})^{1/3} = 0.24 \times (2)^{1/3} = 0.30 \text{ m}$$

### 6.10.3 PROBLEM 3 Stability Factors for Riprap Design

For flow around spill through abutments the angle between the horizontal and the velocity vector can be large (Figure 6.13). The draw down as the flow goes around the upstream end of the abutment can be very large. The draw down angle can range from 0 to 35 degrees and the reference velocity  $V_r$  in the vicinity of the riprap can be very large (Lewis 1972, Richardson et al. 1975, 1990). The following problem addresses the design of riprap for the protection of the spill through embankment.

The reference velocity  $V_r = 1.83$  m/s, and the embankment side slope angle  $\theta = 18.4^\circ$  which corresponds to a 3:1 side slope. The velocity vector angle with the horizontal  $\lambda = 20^\circ$ . If the embankment is covered with dumped rock having a specific weight  $S_s = 2.65$  and an effective rock size  $D_m = 0.305$  m, determine the stability factor.

From Equation 6.16

$$\eta = \frac{0.30 V_r^2}{(S_s - 1)gD_m} = \frac{(0.30)(1.83)^2}{(2.65 - 1)(9.81)(0.305)} = 0.203$$

This dumped rock has an angle of repose of approximately  $35^\circ$  according to Figure 3.4. Therefore, from Equation 6.4.

$$\beta = \tan^{-1} \left\{ \frac{\cos \lambda}{\frac{2 \sin \theta}{\eta \tan \phi} + \sin \lambda} \right\} = \tan^{-1} \left\{ \frac{\cos 20^\circ}{\frac{2 \sin 18.4^\circ}{0.203 \tan 35^\circ} + \sin 20^\circ} \right\} = 11^\circ$$

and from Equation 6.6

$$\eta' = \eta \left\{ \frac{1 + \sin(\lambda + \beta)}{2} \right\} = 0.203 \left\{ \frac{1 + \sin(20^\circ + 11^\circ)}{2} \right\} = 0.154$$

The stability factor for the rock is given by Equation 6.3

$$\text{S.F.} = \frac{\cos \theta \tan \phi}{\eta' \tan \phi + \sin \theta \cos \beta} = \frac{\cos 18.4^\circ \tan 35^\circ}{0.154 \tan 35^\circ + \sin 18.4^\circ \cos 11^\circ} = 1.59$$

Thus, with a stability factor of 1.59, this rock is more than adequate to withstand the flow velocity.

By repeating the above calculations over the range of interest for  $D_m$  (with  $\phi = 35^\circ$ ), the curve given in Figure 6.33 is obtained. This curve shows that the incipient motion rock size is approximately 0.107 m and the maximum stability factor is less than 2.0 on the 3:1 side slope.

The stability factor of a particular side slope riprap design can be increased by decreasing the side slope angle  $\theta$ . If the side slope angle is decreased to zero degrees, then Equation 6.3 is applicable and

$$\text{S.F.} = \frac{1}{\eta} = \frac{1}{0.203} = 4.93$$

The curve in Figure 6.34 relates the stability factor and side slope angle of the embankment (for  $\lambda = 20^\circ$ ,  $D_m = .0305$  m ft and  $V_r = 1.83$  m/s). The curve is obtained by employing Equations 6.3, 6.4, 6.16, and 6.6 for various values of  $\theta$ .



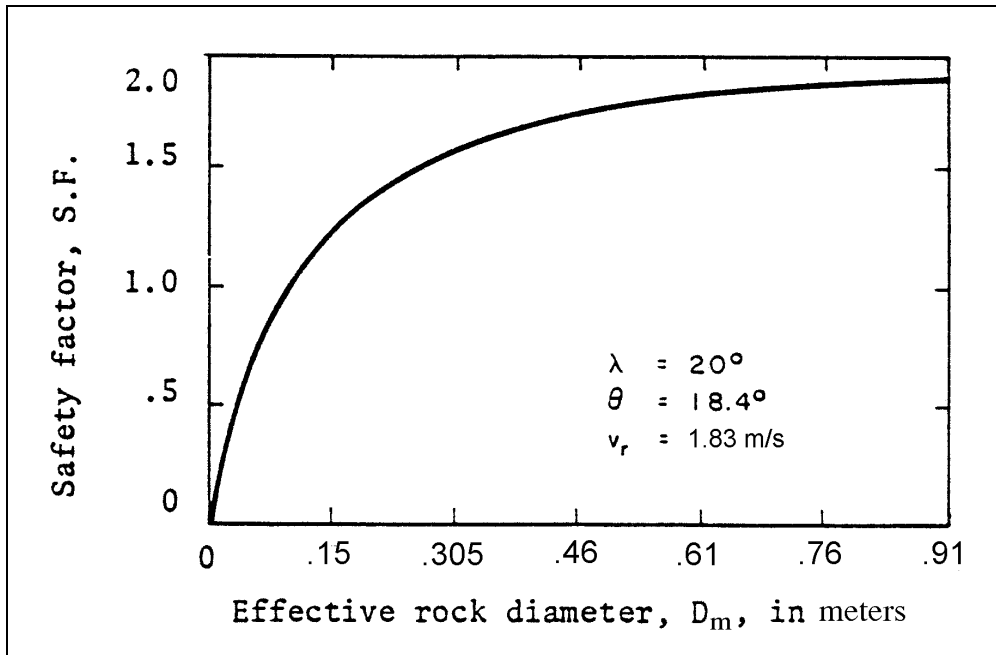


Figure 6.33. Stability factors for various rock sizes on a side slope.

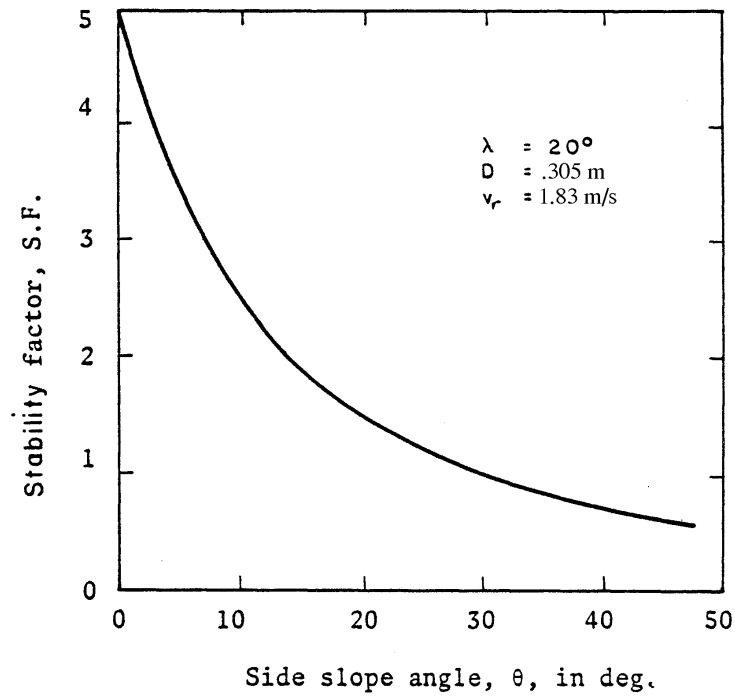


Figure 6.34. Safety factors for various side slopes.

#### 6.10.4 PROBLEM 4 Riprap Design on an Abutment

(a) Consider a spill through abutment with side slope  $\theta = 18.5^\circ$  (3:1 side slope). The flow near the surface, for the 100-year flood, has a velocity vector  $V_r$  with a magnitude of 1.83 m/s and angle with the horizontal  $\lambda = 20^\circ$ . The specific gravity of the available rock is 2.65. Determine the size of riprap in this area required to resist the erosive force of water.

The spill slope riprap rock size is obtained by iteration from assuming  $D_m$  and calculating successively Equations 6.16, 6.4, 6.6, and 6.3 until the stability factor, S.F. equals 1.5. As a first approximation, a stone size of 0.091 m is used. From Figure 3.4,  $\phi \cong 40^\circ$ .

From Equation 6.16,

$$\eta = \frac{0.3 \times 1.83^2}{(2.65 - 1) \times 9.81 \times 0.091} = 0.68$$

From Equation 6.4,

$$\beta = \tan^{-1} \left\{ \frac{\cos 20}{\frac{2 \sin 18.5}{0.68 \tan 40} + \sin 20} \right\} = 32.8$$

From Equation 6.6,

$$\eta' = 0.68 \left\{ \frac{1 + \sin (20 + 32.8)}{2} \right\} = 0.61$$

From Equation 6.3,

$$\text{S.F.} = \frac{\cos 18.5 \tan 40}{0.61 \tan 40 + \sin 18.5 \cos 32.8} = 1.02$$

The procedure is repeated with increasing stone size until S.F. = 1.5. A riprap size of 0.23 m has a S.F. slightly over 1.5.

(b) At the toe of the spill through abutment the velocity vector  $V_r$  has a magnitude of 2.88 m/s and an angle with the horizontal  $\lambda$  of 0 degrees. Determine the size of riprap to protect the toe of the abutment.

The riprap size is determined either by the same iterative procedure used in (a) or by using Equations 6.11, 6.12, and 6.16.

Using the latter method:

Equation 6.11

$$S_m = \tan\phi/\tan\theta = \tan 40/\tan 18.5 = 2.51$$

Equation 6.12

$$\eta = \left( \frac{S_m^2 - S.F.^2}{S.F. S_m^2} \right) \cos\theta = \left( \frac{(2.5)^2 - 1.5^2}{1.5 \times 2.5^2} \right) \cos 18.5 = 0.40$$

Riprap size is obtained from Equation 6.16

$$D_m = \frac{0.3 V_t^2}{(S_s - 1)g\eta} = \frac{0.3 \times (2.88)^2}{(2.65 - 1) \times 9.81 \times 0.4} = 0.38\text{m}$$

This is the size recommended.

## 6.11 SOLVED PROBLEMS FOR FILTER DESIGN (SI)

The requirements for a gravel filter are given in Section 6.7. The gradation of a filter should be such that

$$\frac{D_{50}(\text{Filter})}{D_{50}(\text{Base})} < 40 \quad (6.24)$$

$$5 < \frac{D_{15}(\text{Filter})}{D_{15}(\text{Base})} < 40 \quad (6.25)$$

$$\frac{D_{15}(\text{Filter})}{D_{85}(\text{Base})} < 5 \quad (6.26)$$

### 6.11.1 PROBLEM 1 Filter Design

The properties of the riprap and base material are given in Table 6.4. Determine if filter is needed between the riprap and the base material.

Table 6.4. Sizes of Materials.	
Base Material (Sand)	Riprap (Gravel)
$D_{85} = 1.50 \text{ mm}$	$D_{85} = 24 \text{ mm}$
$D_{50} = 0.75 \text{ mm}$	$D_{50} = 12 \text{ mm}$
$D_{15} = 0.38 \text{ mm}$	$D_{15} = 6 \text{ mm}$

In accordance with the recommended sizes for filters:

$$\frac{D_{50}(\text{Riprap})}{D_{50}(\text{Base})} = \frac{12}{0.75} = 16$$

which satisfies requirement 6.24

$$\frac{D_{15}(\text{Riprap})}{D_{15}(\text{Base})} = \frac{6}{0.38} = 16$$

which satisfies the requirement 6.25

$$\frac{D_{15}(\text{Riprap})}{D_{85}(\text{Base})} = \frac{6}{1.5} = 4$$

which satisfies the requirement 6.26.

The riprap itself satisfies the requirements for the filter so no filter is needed.

### 6.11.2 PROBLEM 2 Filter Design

The following filter design is taken from Anderson et al. (1968). The properties of the base material and the riprap are given in Table 6.5. Determine if a filter is needed.

Table 6.5. Sizes of Materials.	
Base Material (Sand)	Riprap (Rock)
$D_{85} = 1.5$ mm	$D_{85} = 400$ mm
$D_{50} = 0.5$ mm	$D_{50} = 200$ mm
$D_{15} = 0.17$ mm	$D_{15} = 100$ mm

The riprap does not contain sufficient fines to act as the filter because

$$\frac{D_{15}(\text{Riprap})}{D_{15}(\text{Base})} = \frac{100}{0.17} = 600$$

which is much greater than 40, the recommended upper limit (requirement 6.25). Also

$$\frac{D_{15}(\text{Riprap})}{D_{85}(\text{Base})} = \frac{100}{1.5} = 67$$

which is much greater than 5, the recommended upper limit (requirement 6.26).

The properties of the filter to be placed adjacent to the base are as follows:

$$(1) \quad \frac{D_{50}(\text{Filter})}{D_{50}(\text{Base})} < 40$$

$$\text{so } D_{50}(\text{Filter}) < (40)(0.5) = 20 \text{ mm}$$

$$(2) \quad \frac{D_{15}(\text{Filter})}{D_{15}(\text{Base})} < 40$$

so  $D_{15}(\text{Filter}) < (40)(0.17) = 6.8 \text{ mm}$

$$(3) \quad \frac{D_{15}(\text{Filter})}{D_{85}(\text{Base})} < 5$$

so  $D_{15}(\text{Filter}) < (5)(1.5) = 7.5 \text{ mm}$

$$(4) \quad \frac{D_{15}(\text{Filter})}{D_{15}(\text{Base})} > 5$$

so  $D_{15}(\text{Filter}) > (5)(0.17) = 0.85 \text{ mm}$

Thus, with respect to the base

$$0.85 \text{ mm} < D_{15}(\text{Filter}) < 6.8 \text{ mm}$$

and

$$D_{50}(\text{Filter}) < 2 \text{ mm}$$

The properties of the filter to be placed adjacent to the riprap are as follows:

$$(1) \quad \frac{D_{50}(\text{Riprap})}{D_{50}(\text{Filter})} < 40$$

so  $D_{50}(\text{Filter}) > \frac{200}{40} = 5 \text{ mm}$

$$(2) \quad \frac{D_{15}(\text{Riprap})}{D_{15}(\text{Filter})} > 5$$

so  $D_{15}(\text{Filter}) > \frac{100}{5} = 20 \text{ mm}$

$$(3) \quad \frac{D_{15}(\text{Riprap})}{D_{15}(\text{Filter})} < 40$$

so  $D_{15}(\text{Filter}) > \frac{100}{40} = 2.5 \text{ mm}$

$$(4) \quad \frac{D_{15}(\text{Riprap})}{D_{85}(\text{Filter})} < 5$$

so  $D_{85}(\text{Filter}) > \frac{100}{5} = 20 \text{ mm}$

Therefore, with respect to the riprap, the filter must satisfy these requirements

$$\begin{aligned} 2.5\text{mm} < D_{15}(\text{Filter}) < 20 \text{ mm} \\ D_{50}(\text{Filter}) &> 5 \text{ mm} \\ D_{85}(\text{Filter}) &> 20 \text{ mm} \end{aligned}$$

These riprap filter requirements along with those for the base material are shown in Figure 6.35. Any filter having sizes represented by the double cross-hatched area is satisfactory. For example, a good filter could have these sizes:

$$\begin{aligned} D_{85} &= 40 \text{ mm} \\ D_{50} &= 10 \text{ mm} \\ D_{15} &= 4 \text{ mm} \end{aligned}$$

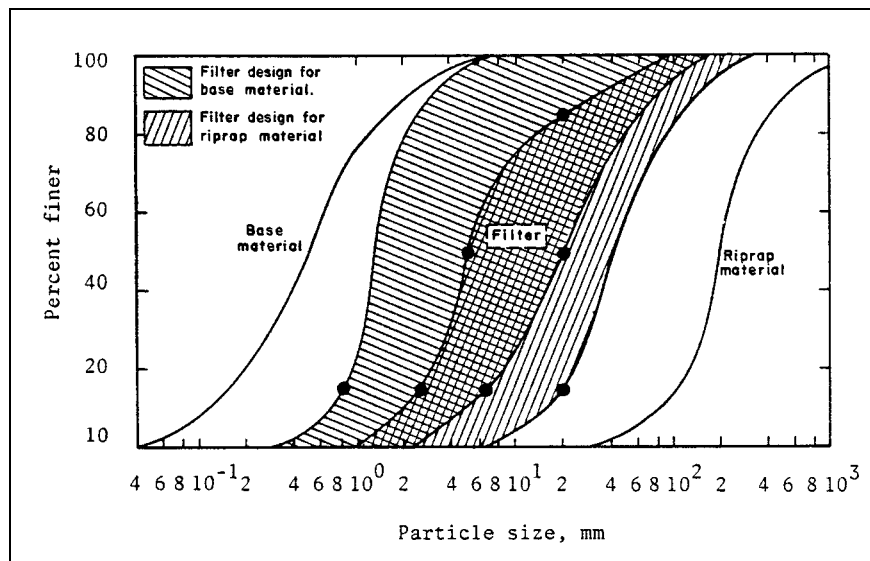


Figure 6.35. Gradations of filter blanket for Problem 2 (after Anderson et al. 1968).

## 6.12 SOLVED PROBLEMS FOR STABILITY OF RIPRAP (ENGLISH)

### 6.12.1 PROBLEM 1 Stability of Particles Under Downslope Flow

Downslope flow over a plane bed inclined at an angle  $\hat{\theta}$  shown in Figure 6.36 is equivalent to an oblique flow on a side slope with  $\theta = \hat{\theta}$  and  $\lambda = 90^\circ$ . Then, according to Equation 6.4,  $\beta = 0$ , and from Equation 6.6,

$$\eta' = \eta \left( \frac{1 + \sin 90^\circ + 0}{2} \right) = \eta$$

It follows from Equation 6.3 that the stability factor is

$$\text{S.F.} = \frac{\cos \hat{\theta} \tan \phi}{\eta \tan \phi + \sin \hat{\theta}}$$

Alternatively, solving for  $\eta$  yields

$$\eta = \cos \hat{\theta} \left[ \frac{1}{\text{S.F.}} - \frac{\tan \hat{\theta}}{\tan \phi} \right]$$

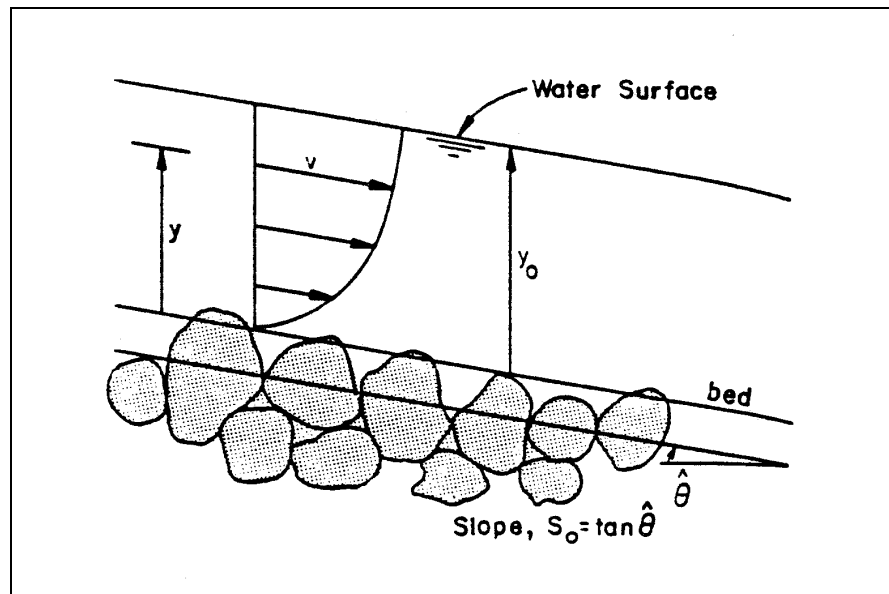


Figure. 6.36. Definition sketch for riprap on a channel bed.

Using this information we wish to calculate (if the angle of repose,  $\phi = 40^\circ$ ), what is the maximum bed angle  $\hat{\theta}$  at which  $\eta$  will be 5 percent different from that of a horizontal bed. Solving for  $\hat{\theta}$  with  $\eta = 0.95$ ,  $\text{S.F.} = 1$  and  $\phi = 40^\circ$  yields  $\hat{\theta} = 2.35^\circ$  or 4.1 percent.

### 6.12.2 PROBLEM 2 Riprap Design on Embankment Slopes

In a design situation water flows parallel to an embankment built of crushed rock riprap, ( $S_s = 2.65$ ), at a sloping angle  $\theta = 20^\circ$ .

(a) If the design shear stress is  $\tau_o = 2.0$  psf, calculate the riprap size that gives a stability factor equal to 1.5.

Assuming angle of repose  $\phi = 40^\circ$ , the stability number  $\eta$  is obtained from Equation 6.3 or Figure 6.14 for  $\theta = 20^\circ$  ( $\eta = 0.36$ ). The stone size is then calculated from Equation 6.13.

$$D_m = \frac{21\tau_o}{(S_s - 1)\gamma\eta} = \frac{21 \times 2.0}{(2.65 - 1) 62.4 \times 0.36} = 1.13 \text{ ft}$$

(b) For the same design shear stress  $\tau_o = 2.0$  psf, determine the stability factor of particle sizes  $D_m = 6$  inches. From Equation 6.5

$$\eta = \frac{21\tau_o}{(S_s - 1)\gamma D_m} = \frac{21 \times 2}{(2.65 - 1) 62.4 \times 0.5} = 0.82$$

Then, Equations 6.11, 6.10, and 6.9 are used to calculate the stability factor

$$S_m = \frac{\tan\phi}{\tan\theta} = \frac{\tan 40^\circ}{\tan 20^\circ} = 2.31$$

$$\zeta = S_m \eta \sec \theta = 2.31 \times 0.82 \sec 20 = 2.02$$

$$\text{S.F.} = \frac{S_m}{2} \left( (\zeta^2 + 4) \right)^{1/2} - \zeta = \frac{2.31}{2} \left( (2.02^2 + 4) \right)^{1/2} - 2.02 = 0.95 < 1$$

This size fraction ( $D_m = 6$  inches) is unstable.

(c) Determine riprap size  $D_m$  for a side slope. The side slope angle  $\theta = 20^\circ$ ; very angular rock with angle of repose  $\phi = 40^\circ$ ;  $V_{ss} = 12$  fps;  $y = 10$  ft; S.F. = 1.1 and  $D_{85}/D_{15} = 2.0$ . From Equations 6.11, 6.12, and 6.16

$$S_m = \frac{\tan\phi}{\tan\theta} = \frac{\tan 40}{\tan 20} = 2.31$$

$$\eta = \frac{S_m^2 - (\text{S.F.})^2}{(\text{S.F.}) \times S_m^2} \cos\theta = \frac{2.31^2 - 1.1^2}{1.1 \times 2.31^2} \cos 20 = 0.66$$

$$D_m = \frac{0.3 V^2}{(S_s - 1) g \eta} = \frac{0.3 \times 12^2}{1.65 \times 32.2 \times 0.66} = 1.25 \text{ ft}$$

(d) Compare the size calculated in (c) with a riprap size calculated using the U.S. Army Corps of Engineers equation (Section 6.5.4). From Equations 6.18 and 6.20:

$$D_{30} = S_f C_s C_v C_T y \left[ \left( \frac{\gamma}{\gamma_s - \gamma} \right)^{0.5} \frac{V}{(K_1 g y)^{0.5}} \right]^{2.5}$$



$$K_1 = \left[ 1 - \frac{\sin^2 \theta}{\sin^2 \phi} \right]^{1/2} = \left[ 1 - \frac{\sin^2 20}{\sin^2 40} \right]^{1/2} = 0.85$$

$$D_{30} = 1.1 \times 0.3 \times 1.0 \times 1.0 \times 10 \left[ \left( \frac{62.4}{102.96} \right)^{0.5} \frac{12}{0.85 \times 32.2 \times 10} \right]^{2.5} = 0.79 \text{ ft}$$

$$D_{50} = D_{30} \times (D_{85} / D_{15})^{1/3} = 0.79 \times (2)^{1/3} = 1.00 \text{ ft}$$

### 6.12.3 PROBLEM 3 Stability Factors for Riprap Design

For flow around spill through abutments the angle between the horizontal and the velocity vector can be large (Figure 6.13). The draw down as the flow goes around the upstream end of the abutment can be very large. The draw down angle can range from 0 to 35 degrees and the reference velocity  $V_r$  in the vicinity of the riprap can be very large (Lewis 1972, Richardson et al. 1975, 1990). The following problem addresses the design of riprap for the protection of the spill through embankment.

The reference velocity  $V_r = 6$  fps, and the embankment side slope angle  $\theta = 18.4^\circ$  which corresponds to a 3:1 side slope. The velocity vector angle with the horizontal  $\lambda = 20^\circ$ . If the embankment is covered with dumped rock having a specific weight  $S_s = 2.65$  and an effective rock size  $D_m = 1.0$  ft, determine the stability factor.

From Equation 6.16

$$\eta = \frac{0.30 V_r^2}{(S_s - 1)gD_m} = \frac{(0.30) (6)^2}{(2.65 - 1)(32.2)(1.0)} = 0.203$$

This dumped rock has an angle of repose of approximately  $35^\circ$  according to Figure 3.4. Therefore, from Equation 6.4.

$$\beta = \tan^{-1} \left\{ \frac{\cos \lambda}{\frac{2 \sin \theta}{\eta \tan \phi} + \sin \lambda} \right\} = \tan^{-1} \left\{ \frac{\cos 20^\circ}{\frac{2 \sin 18.4^\circ}{0.203 \tan 35^\circ} + \sin 20^\circ} \right\} = 11^\circ$$

and from Equation 6.6

$$\eta' = \eta \left\{ \frac{1 + \sin (\lambda + \beta)}{2} \right\} = 0.203 \left\{ \frac{1 + \sin (20^\circ + 11^\circ)}{2} \right\} = 0.154$$

The stability factor for the rock is given by Equation 6.3

$$S.F. = \frac{\cos \theta \tan \phi}{n' \tan \phi + \sin \theta \cos \beta} = \frac{\cos 18.4^\circ \tan 35^\circ}{0.154 \tan 35^\circ + \sin 18.4^\circ \cos 11^\circ} = 1.59$$

Thus, with a stability factor of 1.59, this rock is more than adequate to withstand the flow velocity.

By repeating the above calculations over the range of interest for  $D_m$  (with  $\phi = 35^\circ$ ), the curve given in Figure 6.37 is obtained. This curve shows that the incipient motion rock size is approximately 0.107 m and the maximum stability factor is less than 2.0 on the 3:1 side slope.

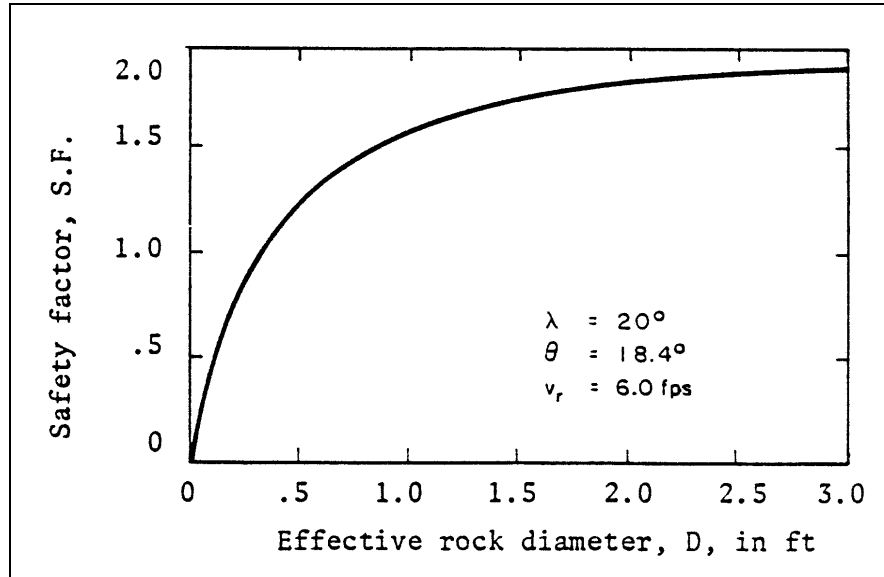


Figure 6.37. Stability factors for various rock sizes on a side slope.

The stability factor of a particular side slope riprap design can be increased by decreasing the side slope angle  $\theta$ . If the side slope angle is decreased to zero degrees, then Equation 6.3 is applicable and

$$S.F. = \frac{1}{\eta} = \frac{1}{0.203} = 4.93$$

The curve in Figure 6.38 relates the stability factor and side slope angle of the embankment (for  $\lambda = 20^\circ$ ,  $D_m = 1.0 \text{ ft}$  and  $V_r = 6.0 \text{ fps}$ ). The curve is obtained by employing Equations 6.3, 6.4, 6.16, and 6.6 for various values of  $\theta$ .

#### 6.12.4 PROBLEM 4 Riprap Design on an Abutment

(a) Consider a spill through abutment with side slope  $\theta = 18.5^\circ$  (3:1 side slope). The flow near the surface, for the 100-year flood, has a velocity vector  $V_r$  with a magnitude of 6.0 fps and angle with the horizontal  $\lambda = 20^\circ$ . The specific gravity of the available rock is 2.65. Determine the size of riprap in this area required to resist the erosive force of water.

The spill slope riprap rock size is obtained by iteration from assuming  $D_m$  and calculating successively Equations 6.16, 6.4, 6.6, and 6.3 until the stability factor, S.F. equals 1.5. As a first approximation, a stone size of 0.3 ft is used. From Figure 3.4,  $\phi \cong 40^\circ$ .

From Equation 6.16,

$$\eta = \frac{0.3 \times 6^2}{(2.65 - 1) \times (32.2) \times (0.3)} = 0.68$$

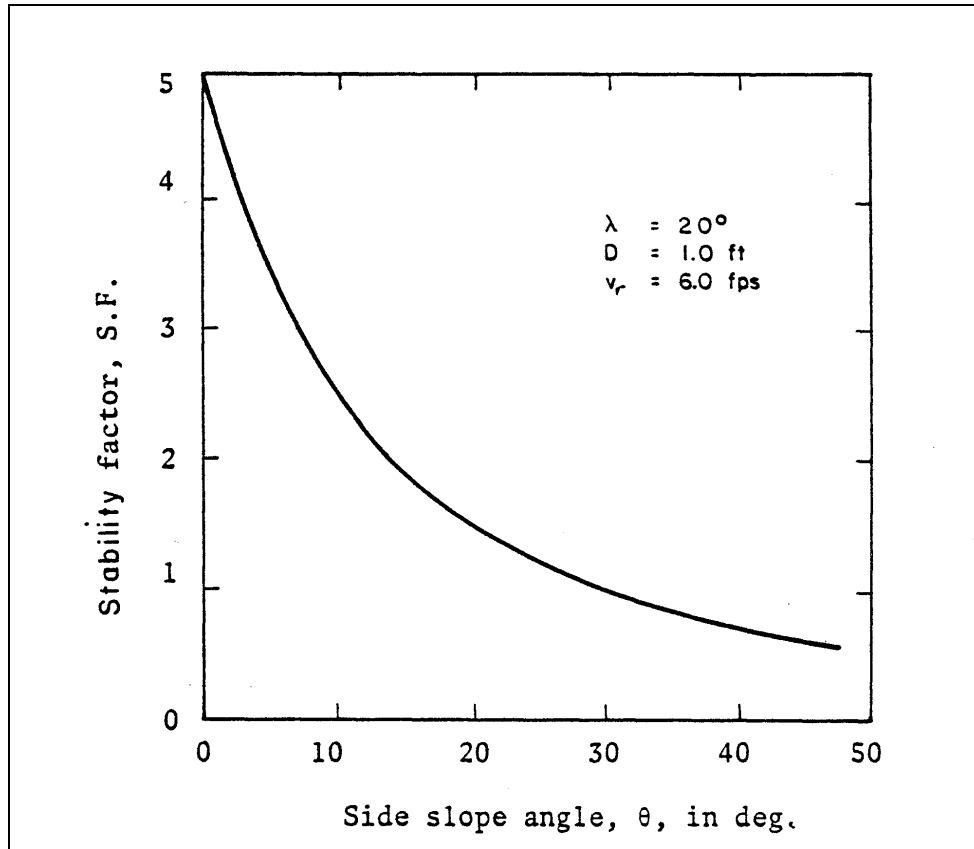


Figure 6.38. Safety factors for various side slopes.

From Equation 6.4,

$$\beta = \tan^{-1} \left\{ \frac{\cos 20}{\frac{2 \sin 18.5}{0.68 \tan 40} + \sin 20} \right\} = 32.8$$

From Equation 6.6,

$$\eta' = 0.68 \left\{ \frac{1 + \sin (20 + 32.8)}{2} \right\} = 0.61$$

From Equation 6.3,

$$\text{S.F.} = \frac{\cos 18.5 \tan 40}{0.61 \tan 40 + \sin 18.5 \cos 32.8} = 1.02$$

The procedure is repeated with increasing stone size until S.F. = 1.5. A riprap size of 9 inches would give a S.F. slightly over 1.5.

(b) At the toe of the spill through abutment the velocity vector  $V_r$  has a magnitude of 9.45 fps and an angle with the horizontal  $\lambda$  of 0 degrees. Determine the size of riprap to protect the toe of the abutment.

The riprap size is determined either by the same iterative procedure used in a or by using Equations 6.11, 6.12, and 6.16.

Using the latter method:

Equation 6.11

$$S_m = \tan \phi / \tan \theta = \tan 40 / \tan 18.5 = 2.51$$

Equation 6.12

$$\eta = \left( \frac{S_m^2 - \text{S.F.}^2}{\text{S.F.} \cdot S_m^2} \right) \cos \theta = \left( \frac{(2.5)^2 - 1.5^2}{1.5 \times 2.5^2} \right) \cos 18.5 = 0.40$$

Riprap size is obtained from Equation 6.16

$$D_m = \frac{0.3 V_r^2}{(S_s - 1) g \eta} = \frac{0.3 \times (9.45)^2}{(2.65 - 1) \times 32.2 \times 0.4} = 1.26 \text{ ft}$$

This is the size recommended.

### 6.13 SOLVED PROBLEMS FOR FILTER DESIGN (ENGLISH)

The requirements for a gravel filter are given in Section 6.7. The gradation of a filter should be such that

$$\frac{D_{50} (\text{Filter})}{D_{50} (\text{Base})} < 40 \tag{6.24}$$

$$5 < \frac{D_{15}(\text{Filter})}{D_{15}(\text{Base})} < 40 \quad (6.25)$$

$$\frac{D_{15}(\text{Filter})}{D_{85}(\text{Base})} < 5 \quad (6.26)$$

### 6.13.1 PROBLEM 1 Filter Design

The properties of the riprap and base material are given in Table 6.6. Determine if filter is needed between the riprap and the base material. Note: Generally, sediment sizes are given in mm for the English system.

Table 6.6. Sizes of Materials.	
Base Material (Sand)	Riprap (Gravel)
$D_{85} = 1.50 \text{ mm}$	$D_{85} = 24 \text{ mm}$
$D_{50} = 0.75 \text{ mm}$	$D_{50} = 12 \text{ mm}$
$D_{15} = 0.38 \text{ mm}$	$D_{15} = 6 \text{ mm}$

In accordance with the recommended sizes for filters:

$$\frac{D_{50}(\text{Riprap})}{D_{50}(\text{Base})} = \frac{12}{0.75} = 16$$

which satisfies requirement 6.24

$$\frac{D_{15}(\text{Riprap})}{D_{15}(\text{Base})} = \frac{6}{0.38} = 16$$

which satisfies the requirement 6.25

$$\frac{D_{15}(\text{Riprap})}{D_{85}(\text{Base})} = \frac{6}{1.5} = 4$$

which satisfies the requirement 6.26.

The riprap itself satisfies the requirements for the filter so no filter is needed.

### 6.13.2 PROBLEM 2 Filter Design

The following filter design is taken from Anderson et al. (1968). The properties of the base material and the riprap are given in Table 6.7. Determine if a filter is needed.

Table 6.7. Sizes of Materials.	
Base Material (Sand)	Riprap (Rock)
$D_{85} = 1.5 \text{ mm}$	$D_{85} = 400 \text{ mm}$
$D_{50} = 0.5 \text{ mm}$	$D_{50} = 200 \text{ mm}$
$D_{15} = 0.17 \text{ mm}$	$D_{15} = 100 \text{ mm}$

The riprap does not contain sufficient fines to act as the filter because

$$\frac{D_{15}(\text{Riprap})}{D_{15}(\text{Base})} = \frac{100}{0.17} = 600$$

which is much greater than 40, the recommended upper limit (requirement 6.25). Also

$$\frac{D_{15}(\text{Riprap})}{D_{85}(\text{Base})} = \frac{100}{1.5} = 67$$

which is much greater than 5, the recommended upper limit (requirement 6.26).

The properties of the filter to be placed adjacent to the base are as follows:

$$(1) \quad \frac{D_{50}(\text{Filter})}{D_{50}(\text{Base})} < 40$$

$$\text{so } D_{50}(\text{Filter}) < (40)(0.5) = 20 \text{ mm}$$

$$(2) \quad \frac{D_{15}(\text{Filter})}{D_{15}(\text{Base})} < 40$$

$$\text{so } D_{15}(\text{Filter}) < (40)(0.17) = 6.8 \text{ mm}$$

$$(3) \quad \frac{D_{15}(\text{Filter})}{D_{85}(\text{Base})} < 5$$

$$\text{so } D_{15}(\text{Filter}) < (5)(1.5) = 7.5 \text{ mm}$$

$$(4) \quad \frac{D_{15}(\text{Filter})}{D_{15}(\text{Base})} > 5$$

$$\text{so } D_{15}(\text{Filter}) > (5)(.17) = 0.85 \text{ mm}$$

Thus, with respect to the base

$$0.85 \text{ mm} < D_{15}(\text{Filter}) < 6.8 \text{ mm}$$

and

$$D_{50}(\text{Filter}) < 2 \text{ mm}$$

The properties of the filter to be placed adjacent to the riprap are as follows:

$$(1) \quad \frac{D_{50}(\text{Riprap})}{D_{50}(\text{Filter})} < 40$$

$$\text{so } D_{50}(\text{Filter}) > \frac{200}{40} = 5 \text{ mm}$$

$$(2) \quad \frac{D_{15}(\text{Riprap})}{D_{15}(\text{Filter})} > 5$$

$$\text{so } D_{15}(\text{Filter}) > \frac{100}{5} = 20 \text{ mm}$$

$$(3) \quad \frac{D_{15}(\text{Riprap})}{D_{15}(\text{Filter})} < 40$$

$$\text{so } D_{15}(\text{Filter}) > \frac{100}{40} = 2.5 \text{ mm}$$

$$(4) \quad \frac{D_{15}(\text{Riprap})}{D_{85}(\text{Filter})} < 5$$

$$\text{so } D_{85}(\text{Filter}) > \frac{100}{5} = 20 \text{ mm}$$

Therefore, with respect to the riprap, the filter must satisfy these requirements

$$\begin{aligned} 2.5 \text{ mm} < D_{15}(\text{Filter}) < 20 \text{ mm} \\ D_{50}(\text{Filter}) &> 5 \text{ mm} \\ D_{85}(\text{Filter}) &> 20 \text{ mm} \end{aligned}$$

These riprap filter requirements along with those for the base material are shown in Figure 6.39. Any filter having sizes represented by the double cross-hatched area is satisfactory. For example, a good filter could have these sizes:

$$\begin{aligned} D_{85} &= 40 \text{ mm} \\ D_{50} &= 10 \text{ mm} \\ D_{15} &= 4 \text{ mm} \end{aligned}$$

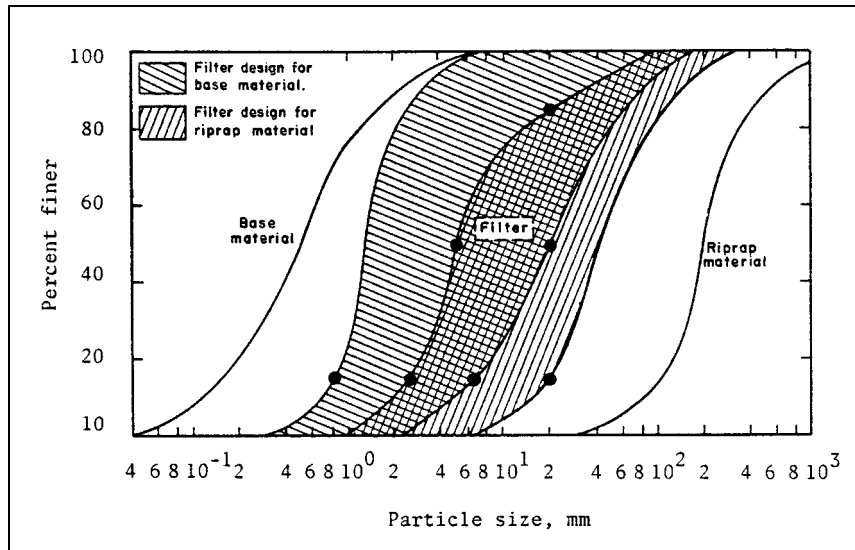


Figure 6.39. Gradations of filter blanket for Problem 2 (after Anderson et al. 1968).



## CHAPTER 7

### SCOUR AT BRIDGES

#### 7.1 INTRODUCTION

##### 7.1.1 General

Scour at highway structures is the result of the erosive action of flowing water removing bed material from around the abutments and piers which support the bridge and bed and bank material of the stream the structure crosses. Both scour at highway structures and stream migration (instability) can cause a bridge failure.

All material in a streambed will erode. It is just a matter of time. However, some material such as granite may take hundred's of years to erode. Whereas, sandbed streams will erode to the maximum depth of scour in hours. Sandstone, shales, and other sedimentary bedrock materials, although they will not erode in hours or even days will, over time, if subjected to the erosive forces of water, erode to the extent that a bridge will be in danger unless the substructures are founded deep enough. Cohesive bed and bank material such as clays, silty clays, silts and silty sands or even coarser bed material such as glacial tills, which are cemented by chemical action or compression, will erode if subjected to the forces of flowing water. The erosion of cohesive and other cemented material is slower than sand bed material, but their ultimate scour will be as deep if not deeper than the scour depth in a non-cohesive sandbed stream (Briaud et al. 1999). It might take the erosive action of several major floods but ultimately the scour hole will be equal to or greater in depth than with a sand bed material.

This does not mean that every bridge foundation must be buried below the calculated scour depth determined for non-bedrock streams. It does mean that so-called bedrock streams must be carefully evaluated.

Scour at bridge crossings is a sediment transport process. Long-term degradation, general scour, and local scour at piers and abutments result from the fact that more sediment is removed from these areas than is transported into them. If there is no transport of bed material into the bridge crossing, **clear-water** scour exists. Transport of appreciable bed material into the crossing results in **live-bed** scour. In this latter case the transport of the bed material limits the scour depth. Whereas, with clear-water scour the scour depths are limited by the critical velocity or critical shear stress of a dominant size in the bed material at the crossing.

##### 7.1.2 Costs of Bridge Failure from Scour

Hydraulic factors (scour/ice/debris) cause 60 percent of bridge failures in the United States (Shirole and Holt 1991). In the United States there are over 580,000 bridges in the National Bridge Inventory. These numbers include federal highway system, state, county and city bridges. Approximately 84 percent of these bridges are over water. Bridge failures cost millions of dollars each year as a result of both direct cost necessary to replace and restore bridges, and indirect costs related to disruption of transportation facilities. However, of even greater consequence is loss of life from bridge failures. Chang, in a 1973 study for the

Federal Highway Administration, indicated that about \$75 million was expended annually up to 1973 to repair roads and bridges that were damaged by floods. This cost does not include the additional indirect costs to highway users for fuel and operating costs resulting from temporary closure and detours and to the public for costs associated with higher tariffs, freight rates, additional labor costs and time.

Rhodes and Trent (1999) document that \$1.2 billion was expended for restoration of flood damaged highway facilities during the 1980s. They state that this amount is conservative because it (1) only includes the amount funded by the U.S. Government which ranges from 75 to 100 percent of the total restoration costs, and (2) the funds were only for disasters related to very large floods and do not include the hundreds of smaller events that occur every year. They also demonstrate that the added cost of operating a vehicle over a detour and time lost traveling when a bridge failed (only part of the indirect costs) exceed by several times the direct cost of bridge replacement or repair.

### **7.1.3 Bridge Scour Evaluation Program**

The U.S. Department of Transportation, Federal Highway Administration (FHWA) in 1988 issued Technical Advisory T5140.20 (superseded by T5140.23 in 1991) requiring the States to conduct a scour evaluation program. This program resulted from the failure of the I-90 bridge over Schoharie Creek in upstate New York which killed ten people (NTSB 1988 and Richardson et al. 1987). The evaluation is to be conducted by an interdisciplinary team of hydraulic, geotechnical and structural engineers who can make the necessary engineering judgments to determine the vulnerability of a bridge to scour. As of February 2001, the 481,313 bridges over water in the National Bridge Inventory have been screened as to their scour vulnerability (100 percent).

The evaluation program in the U.S. is on schedule and scour countermeasures are being implemented on bridges that have been identified as scour susceptible or scour critical. Replacement bridges are being constructed as rapidly as funds can be provided. Scour countermeasures include riprap protection, scour monitoring before, during and after a flood and the inspection program (Richardson and Davis 2001, Lagasse et al. 1997, 2001a, and 2001b, Schall et al. 1997a and 1997b).

### **7.1.4 Comprehensive Scour Analysis**

This chapter presents background knowledge on scour analysis. Earlier chapters give a comprehensive overview of fluvial geomorphology, sediment transport, and flow in alluvial channels and stream stability fundamentals needed to understand streams, stream instability and scour. The comprehensive procedure for scour and stream instability analyses and countermeasures to control them are given in the FHWA publications HEC-18, HEC-20, and HEC-23 (Richardson and Davis 2001; Lagasse et al. 2001a, 2001b). The interrelationships and procedures recommended in the three documents are shown in the Figure 7.1.

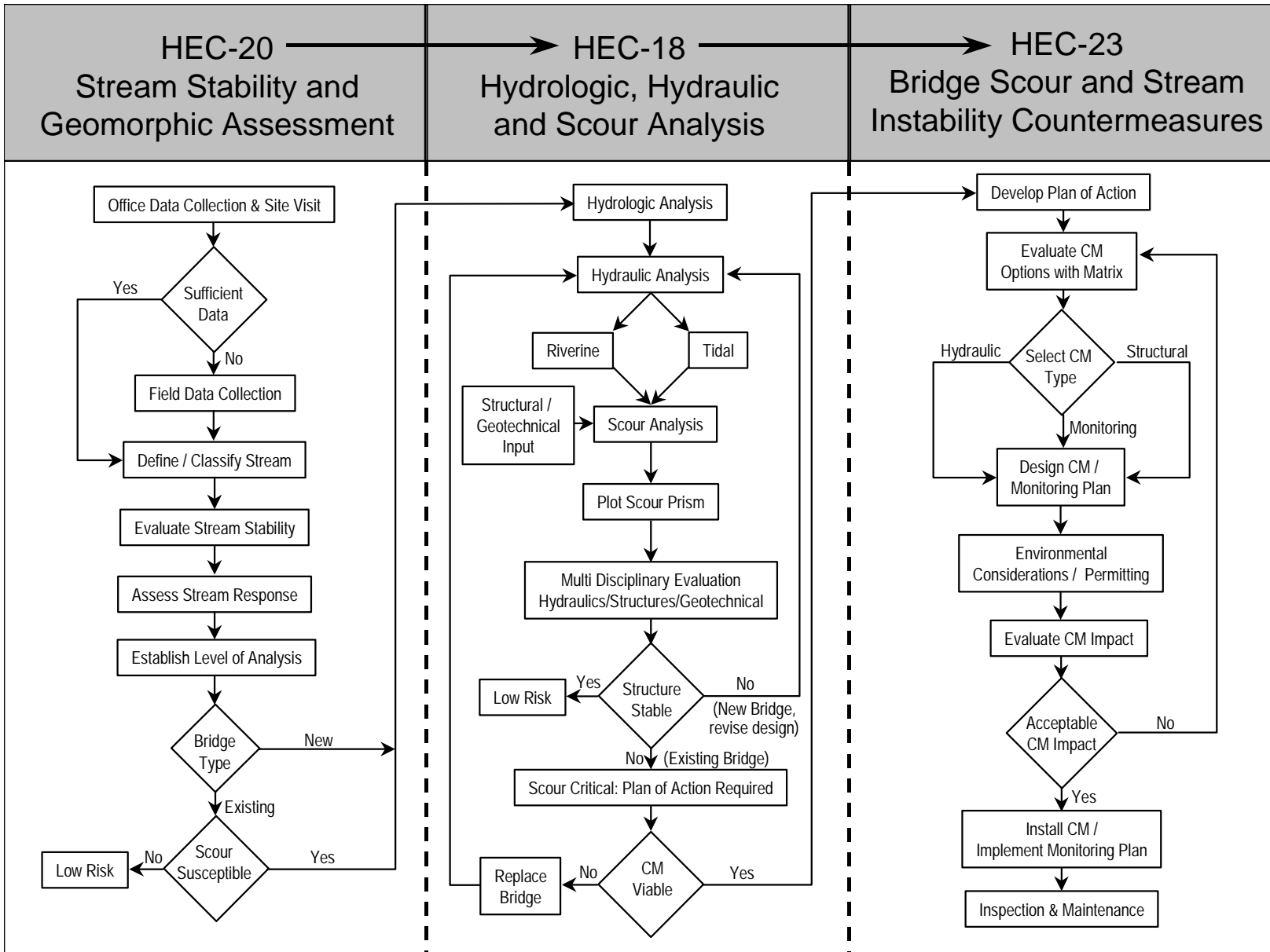


Figure 7.1. Flow chart for scour and stream stability analysis and countermeasures.

## 7.2 TOTAL SCOUR

Total scour at a highway crossing is composed of three components:

### (1) Long-Term Aggradation or Degradation

The change in river bed elevation (aggradation or degradation) over long lengths and time due to changes in controls, such as dams, changes in sediment discharge, head cuts, daily tidal flow, and changes in river geomorphology, such as changing from a meandering to a braided stream. These processes may be natural or human induced.

### (2) General Scour

The scour that results from the acceleration of the flow due to either a natural or bridge contraction or both (contraction scour). General scour may also result from the location of the bridge on the stream. For example, its location with respect to a stream bend or its location upstream from the confluence with another stream. In this latter case, the elevation of the downstream water surface will affect the backwater on the bridge, hence, the velocity and scour. General scour may occur during the passage of a flood and the stream may fill in on the falling stage. This type of scour involves the removal of material from the bed and banks across all or most of the width of a channel.

### (3) Local Scour

The scour that occurs at a pier or abutment as the result of the pier or abutment obstructing the flow. These obstructions accelerate the flow and create vortices that remove the material around them.

Generally, scour depths from local scour are much larger than long-term degradation or general scour, often by a factor of ten. But, if there are major changes in the stream conditions, such as a large dam built upstream or downstream of the bridge or severe straightening of the stream, long-term bed elevation changes can be the larger element in the total scour. Also, scour depths from severe contraction of the flow, (often causing ponding upstream of the bridge) can be larger than local scour.

### (4) Lateral Shifting of the Stream

In addition to the above, lateral shifting of the stream may also erode the approach roadway to the bridge and, by changing the angle of the flow in the waterway at the bridge crossing, change the total scour.

## 7.3 CLEAR-WATER AND LIVE-BED SCOUR

The two conditions of general and local scour are (1) clear-water scour and (2) live-bed scour.

Clear-water scour occurs when there is no movement of the bed material in the main channel of the stream upstream of the crossing, or the sediment transport in the upstream reach or floodplain is transported through the bridge opening or local scour holes in suspension. The increase in velocity by contraction of the flow by the bridge or the acceleration of the flow and vortices created by the piers or abutments causes the bed material in the bridge opening or at their base to move.

Live-bed scour occurs when the bed material upstream of the crossing is moving and moves as contact sediment discharge in the contracted bridge opening and/or into the local scour holes.

Typical clear-water scour situations include (1) coarse bed material streams, (2) flat gradient streams during low flow, (3) local deposits of larger bed materials that are larger than the biggest fraction being transported by the flow (rock riprap is a special case of this situation), (4) armored stream beds where the only locations that tractive forces are adequate to penetrate the armor layer are at piers and/or abutments, (5) vegetated channels where, again, the only locations that the cover is penetrated is at piers and/or abutments, and (6) streams with fine bed material and large velocity or shear stress whereby the bed material in transport washes through a contraction or local scour hole

Clear-water scour reaches its maximum over a longer period of time than live-bed scour (Figure 7.2). This is because clear-water scour occurs mainly on coarse bed material streams. In fact, clear-water scour may not reach its maximum until after several floods. Also, maximum clear-water scour is about 10 percent greater than the equilibrium live-bed scour. Bridges over coarse bed material streams often have clear-water scour at the lower part of a hydrograph, live-bed scour at the higher discharges, and then clear-water scour on the falling stages.

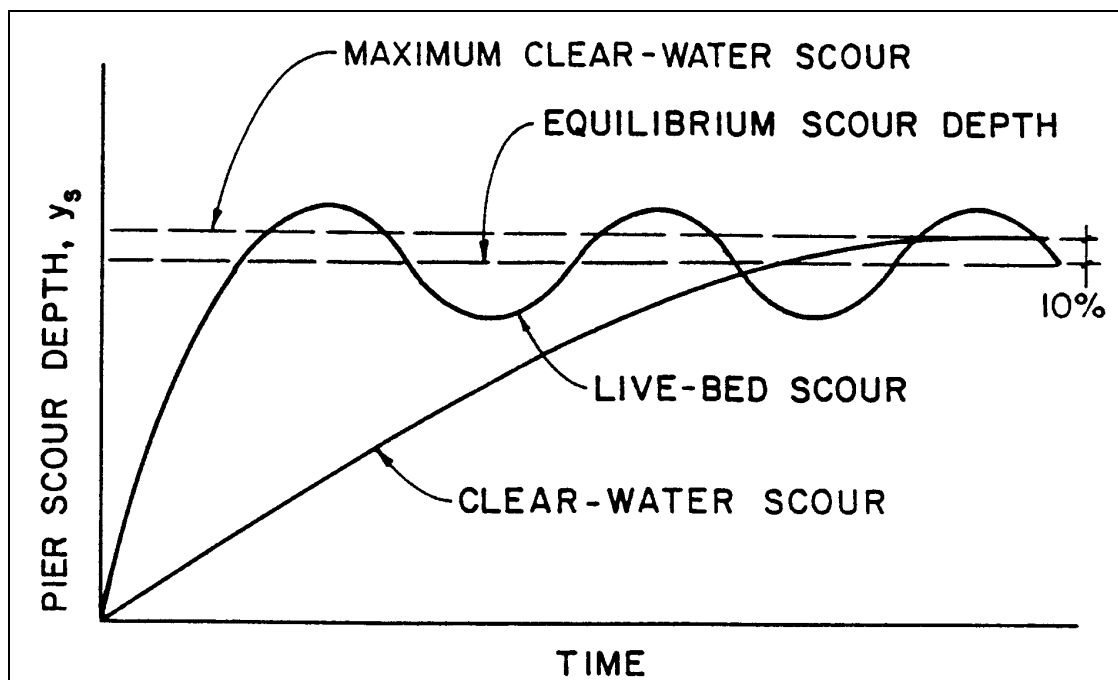


Figure 7.2. Local scour depth at a pier as a function of time.

Live-bed scour in sand bed streams with a dune bed configuration fluctuates about an equilibrium scour depth (Figure 7.2). The reason for this is the fluctuating nature of the sediment transport of the bed material in the approaching flow when the bed configuration of the stream is dunes. In this case (dune bed configuration in the channel upstream of the bridge), maximum depth of scour is about 30 percent larger than equilibrium depth of scour.

The maximum depth of scour is the same as the equilibrium depth of scour for live-bed scour with a plane bed configuration. With antidunes occurring upstream and in the bridge crossing; the maximum depth of scour, from the limited research of Jain and Fisher (1979), is from 10 to 20 percent greater than the equilibrium depth of scour. In general, with sand bed streams a dune bed changes to plane bed or antidune flow during flood flow.

#### **7.4 ARMORING**

Armoring occurs on a stream or in a scour hole when the forces of the water during a particular flood are unable to move the larger sizes of the bed material. This protects the underlying material from movement. Contraction scour or local scour around an abutment or pier may initially occur, but as the scour depth increases the coarser bed material moves down in the bridge cross-section or local scour hole and protects the bed so that the full scour potential is not reached.

When armoring occurs, the coarser bed material will tend to remain in place or quickly redeposit so as to form a layer of riprap-like armor in the cross-section or local scour hole and, thus, limit further scour for a particular discharge. When larger flows occur the armor layer can be broken and the scour depth deepened either until a new armor layer is developed or the maximum scour is reached.

#### **7.5 LONG-TERM BED ELEVATION CHANGES**

Long-term bed elevation changes (aggradation or degradation) may be the natural trend of the stream or may be the result of some modification to the stream or watershed condition. In scour analyses, only long-term degradation is considered. Aggradation, if it occurs, is not used to decrease total scour estimate.

The streambed may be aggrading, degrading or not changing (equilibrium) in the bridge crossing reach. When the bed of the stream is neither aggrading or degrading, it is in equilibrium with the sediment discharge supplied to the bridge reach and the elevation of the bed does not change. In this section, we consider long-term trends, not the cutting and filling of the bed of the stream that might occur during a runoff event. A stream may cut and fill during a runoff event and also have a long-term trend of an increase or decrease in bed elevation. The problem for the engineer is to determine what the long-term bed elevation changes will be during the lifetime of the structure. What is the current rate of change in the stream bed elevation? Is the stream bed elevation in equilibrium? Is the streambed degrading? Is it aggrading? Is there a head cut or nickpoint moving upstream? What is the future trend in the stream bed elevation?

During the life of the bridge the present trend may change. These long-term changes are the result of modifications of the state of the stream or watershed. Such changes may be the result of natural processes or the result of human activities. The engineer must assess the present state of the stream and watershed and determine future changes in the river system, and from this assessment determine the long-term stream bed elevation.

Factors that affect long-term bed elevation changes are: dams and reservoirs (up or downstream of the bridge), changes in watershed land use (urbanization, deforestation, etc.), channelization, cutoff of a meander bend (natural or human induced), changes in the

downstream base level (control) of the bridge reach, gravel mining from the stream bed, diversion of water into or out of the stream, natural lowering of the total system, movement of a bend, bridge location in reference to stream planform, and stream movement in relation to the crossing.

Analysis of long-term streambed elevation changes must be made using the principles of river mechanics in the context of a fluvial system analysis. Such analysis of a fluvial system requires the consideration of all influences upon the bridge crossing, i.e., runoff from the watershed to the channel (hydrology), the sediment delivery to the channel (erosion), the sediment transport capacity of the channel (hydraulics) and the response of the channel to these factors (geomorphology and river mechanics). Many of the largest impacts are from human activities, either in the past, the present or the future. The analysis requires a study of the past history of the river and human activities on it; a study of present water and land use and stream control activities; and, finally, contacting all agencies involved with the river to determine future changes in the river.

A method to organize such an analysis is to use a three level fluvial system approach (see Chapter 9 and HEC-20). This method provides three levels of detail in an analysis: (1) a qualitative determination based on general geomorphic and river mechanics relationships; (2) engineering geomorphic analysis using established qualitative and quantitative relationships to establish the probable behavior of the stream system to various scenarios of future conditions; and (3) quantifying the changes in bed elevation using available physical process mathematical models such as BRI-STARS (Molinas 2000) or HEC-6, (U.S. Army Corps of Engineers 1993). Methods to be used in the three levels of analysis are given in this manual, FHWA's HEC-18 (Richardson and Davis 2001) and HEC-20 (Lagasse et al. 2001).

## **7.6 GENERAL SCOUR**

General scour at a bridge can be caused by a decrease in channel width, either naturally or by the bridge, which decreases flow area and increases velocity. This is contraction scour. General scour can also be caused by short-term (daily, weekly, yearly or seasonally) changes in the downstream water surface elevation that controls the backwater and hence the velocity through the bridge opening. Because this scour is reversible it is included in general scour rather than in long-term scour. General scour can result from the location of the bridge with regard to a bend. If the bridge is located on or close to a bend, the concentration of the flow on the outer part of the channel can erode the bed.

General scour can be cyclic. That is, during a runoff event the bed scours during the rise in stage (increasing discharge) and fills on the falling stage (deposition).

General scour from a contraction occurs when the flow area of a stream is decreased from the normal either by a natural constriction or by a bridge. With the decrease in flow area there is an increase in average velocity and bed shear stress. Hence, there is an increase in stream power at the contraction and more bed material is transported through the contracted reach than is transported into the reach. The increase in transport of bed material lowers the bed elevation. As the bed elevation is lowered, the flow area increases and the velocity and shear stress decreases until equilibrium is reached, that is the bed material transported into the reach is equal to that which is transported out of the reach.

The contraction of the flow by the bridge can be caused by a decrease in flow area of the stream channel by the abutments projecting into the channel and/or the piers taking up a large portion of the flow area. Also, the contraction can be caused by the approaches to the bridge cutting off the overland flow that normally goes across the floodplain during high flow. This latter case causes clear-water scour at the bridge section because the overland flow normally does not transport any bed material sediments. This clear-water flow picks up additional sediment from the bed when it returns to the bridge crossing. In addition, if it returns to the stream channel at an abutment can increase the local scour there. A guide bank at that abutment decreases the risk from scour from this returning overbank flow. Also, relief bridges in the approaches decrease the scour problem at the bridge cross section by decreasing the amount of flow returning to the natural channel.

Other Factors that can cause contraction scour are:

- (1) a natural stream constriction
- (2) long approaches over the floodplain to the bridge
- (3) ice formation or jams
- (4) berm forming along the banks by sediment deposits
- (5) island or bar formations upstream or downstream of the bridge opening
- (6) debris
- (7) growth of vegetation in the channel or floodplain

To determine the magnitude of general scour from a variable backwater requires a study of the stream system to (1) determine if this condition exists and (2) determine the magnitude of general scour for this condition. Of particular value in determining if backwater effects exist and the magnitude of the effects on the velocity and depth is the WSPRO computer model. The difference in depth between the highest expected bed elevation and the lowest expected bed elevation for the design discharge is the value of the general scour.

General scour of the bridge opening may be concentrated in one area. If the bridge is located on or close to a bend the scour will be concentrated on the outer part of the bend. In fact, there may be deposition on the inner portion of the bend, further concentrating the flow, which increases the scour at the outer part of the bend. Also at bends, the thalweg (the part of the stream where the flow or velocity is largest) will shift toward the center of the stream as the flow increases. This can increase scour and the non-uniform distribution of the scour in the bridge opening.

Often the magnitude of general scour cannot be predicted and inspection is the solution for general scour problems. Also, a physical model study can be used to determine general scour.

### 7.6.1 Contraction Scour

Contraction Scour Conditions. Contraction scour equations are based on the principle of conservation of sediment transport (continuity). In the case of **live-bed** scour, the fully developed scour in the bridge cross section reaches equilibrium when sediment transported into the contracted section equals sediment transported out. As scour develops, the shear stress in the contracted section decreases as a result of a larger flow area and decreasing average velocity. For **live-bed** scour, maximum scour occurs when the shear stress reaches the point that bed-material transported in equals the bed-material transported out and the conditions for sediment continuity are in balance. For **clear-water** scour, the bed-material



transported into the contracted section is essentially zero and maximum scour occurs when the shear stress or velocity reaches the critical shear stress or critical velocity of the bed material in the section. Chapter 3 and HEC-18 give equations and methods for calculating critical shear stress or critical velocity.

**Live-bed** contraction scour occurs at a bridge when there is transport of bed material in the upstream reach into the bridge cross section. With live-bed contraction scour, the area of the contracted section increases until, in the limit, the transport of bed material out of the contracted section equals the bed material transported in. Normally, the width of the contracted section is constrained and depth increases until the limiting conditions are reached.

**Clear-water** contraction scour occurs in a long contraction when (1) there is no bed material transport from the upstream reach into the downstream reach or (2) the material being transported in the upstream reach is transported through the downstream reach mostly in suspension and at less than capacity of the flow. With clear-water contraction scour, the area of the contracted section increases until, in the limit, the velocity ( $V$ ) of the flow or the shear stress ( $\tau_o$ ) on the bed is equal to the critical velocity ( $V_c$ ) or the critical shear stress ( $\tau_c$ ) of a certain particle size ( $D$ ) in the bed material. Normally, the width ( $W$ ) of the contracted section is constrained and the depth ( $y$ ) increases until the limiting conditions are reached.

**Live-bed scour depths may be limited if there are appreciable amounts of large-sized particles in the bed material. It is appropriate, then, to use the clear-water scour equation in addition to the live-bed scour equation and use the smaller of the two depths. Also, it is appropriate to use the clear-water scour equation if the transport of bed material from upstream of the contraction is small in quantity or composed of fine material that washes through the contraction in suspension.**

There are four conditions (cases) of contraction scour at bridge sites depending on the type of contraction, and whether there is overbank flow or relief bridges. Regardless of the case, contraction scour can be evaluated using two basic equations: (1) **live-bed** scour, and (2) **clear-water** scour. For any case or condition, it is only necessary to determine if the flow in the main channel or overbank area upstream of the bridge, or approaching a relief bridge, is transporting bed material (live-bed) or is not (clear-water), and then apply the appropriate equation with the variables defined according to the location of contraction scour (channel or overbank).

Critical Velocity. To determine if the flow upstream of the bridge is transporting bed material, calculate the critical velocity for beginning of motion  $V_c$  of the  $D_{50}$  size of the bed material and compare it with the mean velocity  $V$  of the flow in the main channel or overbank area upstream of the bridge opening. If the critical velocity of the bed material is larger than the mean velocity ( $V_c > V$ ), then clear-water contraction scour will exist. If the critical velocity is less than the mean velocity ( $V_c < V$ ), then live-bed contraction scour will exist. To calculate the critical velocity use the equation derived in Chapter 3. This equation is:

$$V_c = K_u y^{1/6} D^{1/3} \quad (7.1)$$

where:

- $V_c$  = Critical velocity above which bed material of size  $D$  and smaller will be transported, m/s (ft/s)
- $y$  = Depth of flow, m (ft)

- D = Particle size for  $V_c$ , m (ft)
- $D_{50}$  = Particle size in a mixture of which 50 percent are smaller, m (ft)
- $K_u$  = Coefficient derived in Chapter 3
- $K_u$  = 6.19 SI units
- $K_u$  = 11.25 English units

Live-Bed Contraction Scour. A modified version of Laursen's 1960 equation for live-bed scour at a long contraction is recommended to predict the depth of scour in a contracted section. The modification is to eliminate the ratio of Manning's n (see the following Note #3).

$$\frac{y_2}{y_1} = \left[ \frac{Q_2}{Q_1} \right]^{6/7} \left[ \frac{W_1}{W_2} \right]^{k_1} \quad (7.2)$$

$$y_s = y_2 - y_o = \text{average scour depth} \quad (7.3)$$

where:

- $y_1$  = Average depth in the upstream main channel, m (ft)
- $y_2$  = Average depth in the contracted section, m (ft)
- $y_o$  = Existing depth in the contracted section before scour, m (ft) (see Note 7)
- $Q_1$  = Flow in the upstream channel transporting sediment,  $m^3/s$  ( $ft^3/s$ )
- $Q_2$  = Flow in the contracted channel,  $m^3/s$  ( $ft^3/s$ )
- $W_1$  = Bottom width of the upstream main channel, m (ft)
- $W_2$  = Bottom width of the main channel in the contracted section less pier width(s), m (ft)
- $k_1$  = Exponent determined below

$V^*/\omega$	$k_1$	Mode of Bed Material Transport
<0.50	0.59	Mostly contact bed material discharge
0.50 to 2.0	0.64	Some suspended bed material discharge
>2.0	0.69	Mostly suspended bed material discharge

- $V^*$  =  $(\tau_o/\rho)^{1/2} = (gy_1 S_1)^{1/2}$ , shear velocity in the upstream section, m/s ( $ft/s$ )
- $\omega$  = Fall velocity of bed material based on the  $D_{50}$ , m/s (Figure 3.1)  
For fall velocity in English units ( $ft/s$ ) multiply fall velocity in m/s by 3.28
- $g$  = Acceleration of gravity ( $9.81 m/s^2$ ) ( $32.2 ft/s^2$ )
- $S_1$  = Slope of energy grade line of main channel, m/m ( $ft/ft$ )
- $\tau_o$  = Shear stress on the bed, Pa ( $N/m^2$ ) ( $lb/ft^2$ )
- $\rho$  = Density of water ( $1000 kg/m^3$ ) ( $1.94 slugs/ft^3$ )

**Notes:**

1.  $Q_2$  is the total flow going through the bridge opening.
2.  $Q_1$  is the flow in the main channel upstream of the bridge, not including overbank flows.
3. The Manning's n ratio is eliminated in Laursen's live-bed equation to obtain Equation 7.2. This was done for the following reasons. The ratio can be significant for a condition of

dune bed in the main channel and a corresponding plane bed, washed out dunes or antidunes in the contracted channel. However, Laursen's equation does not correctly account for the increase in transport that will occur as the result of the bed planing out (which decreases resistance to flow, increases the velocity and the transport of bed material at the bridge). That is, Laursen's equation indicates a decrease in scour for this case, whereas in reality, there would be an increase in scour depth. In addition, at flood flows, a plane bedform will usually exist upstream and through the bridge waterway, and the values of Manning's  $n$  will be equal.

4.  $W_1$  and  $W_2$  are not always easily defined. In some cases, it is acceptable to use the topwidth of the main channel to define these widths. Whether topwidth or bottom width is used, it is important to be consistent so that  $W_1$  and  $W_2$  refer to either bottom widths or topwidths.
5. The average width of the bridge opening ( $W_2$ ) is normally taken as the bottom width, with the width of the piers subtracted.
6. Laursen's equation will overestimate the depth of scour at the bridge if the bridge is located at the upstream end of a natural contraction or if the contraction is the result of the bridge abutments and piers. At this time, however, it is the best equation available.
7. In sand channel streams where the contraction scour hole is filled in on the falling stage, the  $y_0$  depth may be approximated by  $y_1$ . Sketches or surveys through the bridge can help in determining the existing bed elevation.
8. Coarse sediments in the bed material which armor the bed may limit scour depths with live-bed contraction scour. Where coarse sediments are present, it is recommended that scour depths be calculated for live-bed scour conditions using the clear-water scour equation (given in the next section) in addition to the live-bed equation, and that the smaller calculated scour depth be used.

Clear-water Contraction Scour. The recommended clear-water contraction scour equation is based on a development suggested by Laursen (1963). Its development is presented in Chapter 3 as part of the development of the critical velocity equation. The equation is:

$$y_2 = \left[ \frac{K_u Q^2}{D_m^{2/3} W^2} \right]^{3/7} \quad (7.4)$$

$$y_s = y_2 - y_0 = (\text{average scour depth, m}) \quad (7.5)$$

where:

- $y_2$  = Average depth in the contracted section after contraction scour, m (ft)
- $Q$  = Discharge through the bridge or on the set-back overbank area at the bridge associated with the width  $W$ ,  $m^3/s$  ( $ft^3/s$ )
- $D_m$  = Diameter of the smallest nontransportable particle in the bed material ( $1.25 D_{50}$ ) in the contracted section, m (ft)
- $D_{50}$  = Median diameter of bed material, m (ft)
- $W$  = Bottom width of the contracted section less pier widths, m (ft)
- $y_0$  = Existing depth in the contracted section before scour, m (ft)
- $K$  = Coefficient derived in Chapter 3 as an extension of critical velocity

$$K_u = 0.025 \text{ SI units}$$
$$K_u = 0.0077 \text{ English units}$$

For stratified bed material the depth of scour can be determined by using the clear-water scour equation sequentially with successive  $D_m$  of the bed material layers.

## 7.6.2 Computer Models for General Scour

The above equations give satisfactory but conservative contraction scour depths. Computer models, if carefully used by competent hydraulic engineers experienced in their use, will give a more precise determination of contraction scour. These models can also be used for other general scour depth determinations. The one-dimensional models presently being used and maintained are BRI-STARS (Molinas 1990, 2000) and HEC-6 (U.S. Army Corps of Engineers 1993). Also, the one-dimensional water surface profile models HEC-RAS (U.S. Army Corps of Engineers 2001) and WSPRO (Arneson and Sherman 1998) and two-dimensional models FESWMS-2D (Froehlich 1996) and RMA-2V (Thomas and McAnally 1985; U.S. Army Corps of Engineers 2001) can be used to obtain the input variables for the contraction scour equations.

## 7.7 LOCAL SCOUR AT PIERS

### 7.7.1 Introduction

Local scour at piers is a function of bed material size, flow characteristics, fluid properties and the geometry of the pier. The subject has been studied extensively in the laboratory since the research of Dr. Laursen in the late 1940s and 1950s (Laursen 1958, 1960, 1963; Laursen and Toch 1956; Richardson and Lagasse 1999). Richardson (1999) gives a brief listing of scour investigations in the United States. As a result of the many studies there are many equations. In general, the equations are for live-bed scour in cohesionless sand bed streams, and they give widely varying results. Since 1988, through the efforts of the USGS and FHWA, a considerable number of field measurements of local pier scour depths have been collected (Landers and Mueller 1999). The data is given by Richardson and Lagasse (1999), page 585. In this section, we give two equations for determining the ultimate local pier scour and an equation to determine the topwidth of a local pier scour hole. These equations are as follows:

1. Colorado State University's (CSU) equation. (Richardson et al. 1975)
2. FHWA's HEC-18 equation (Richardson and Davis 2001)
3. Topwidth equation (Richardson and Abed 1999; Richardson and Davis 2001)

This discussion of the equations is only for simpler flow conditions and pier geometry. Equations and methods to determine local scour depths for piers in more complex flow conditions (for example tidal flow) and pier geometry (for example a pier on piles with the pile cap at the water surface) are given in HEC-18 (Richardson and Davis 2001). The HEC-18 equation is a modification of the CSU equation resulting from additional research and field measurements that have occurred since 1975.

As explained in Section 7.7.2, FHWA's HEC-18 equation is recommended for determining the ultimate scour depth for both live-bed and clear-water scour. Briaud et al. (1999) present a method for determining local pier scour depth in cohesive bed material is given for those special occasions when it is assumed that the ultimate scour depth is not needed. For

example, a bridge with foundations in clay that is to be replaced in a few years. However, as Briaud et al. (1999) point out the ultimate scour in cohesive material is as deep as in sand bed material.

### 7.7.2 Comparison of Pier Scour Equations

Jones (1983) compared many of the more common equations. His comparison of these equations is given in Figures 7.3 and 7.4. Some of the equations have velocity as a variable (normally in the form of a Froude number). However, some equations, such as Laursen's, do not include velocity. A Froude number of 0.3 was used ( $Fr = 0.3$ ) in Figure 7.3 for purposes of comparing commonly used scour equations. In Figure 7.4, the equations are compared with some field data measurements. As can be seen from Figure 7.4 the CSU equation encloses all the data points, but gives lower values of scour than the other equations. The CSU equation includes the velocity of the flow just upstream of the pier by including the Froude Number in the equation.

The equations illustrated in Figures 7.3 and 7.4 do not take into account the possibility that larger sizes in the bed material could armor the scour hole. That is, the large sizes in the bed material will at some depth of scour limit the scour depth. FHWA's HEC-18 scour depth equation has a coefficient, which is applied to the CSU equation, that decreases the scour depth when the bed material has large particles.

Mueller (1996) compared 22 scour equations using field data collected by the USGS (Landers and Mueller 1996; Landers, Mueller, and Richardson 1999). He concluded that the HEC-18 equation was good for design because it rarely under predicted measured scour depth. However, it frequently over predicted the observed scour. The data contained 384 measurements of scour at 56 bridges. Figure 7.5 gives six of his 22 comparisons. The six equations in Figure 7.5 are Shen's, Froehlich's, Laursen's, Melville and Sutherland's, HEC-18, and Mueller's modified HEC-18 equation (HEC-18BM).

### 7.7.3 Colorado State University's Equation

The Colorado State University's Equation (Richardson et al. 1975) is as follows:

$$\frac{y_s}{y_1} = 2.0 K_1 K_2 \left[ \frac{a}{y_1} \right]^{0.65} Fr_1^{0.43} \quad (7.6)$$

where:

- $y_s$  = Scour depth, m (ft)
- $y_1$  = Flow depth just upstream of the pier, m (ft)
- $K_1$  = Correction for pier shape from Table 7.1 and Figure 7.6
- $K_2$  = Correction for flow angle of attack of flow from Table 7.2 and Equation 7.8
- $a$  = Pier width, m (ft)
- $Fr_1$  = Froude number =  $V_1 / (gy_1)^{0.5}$
- $V_1$  = Velocity upstream of pier, m/s (ft/s)

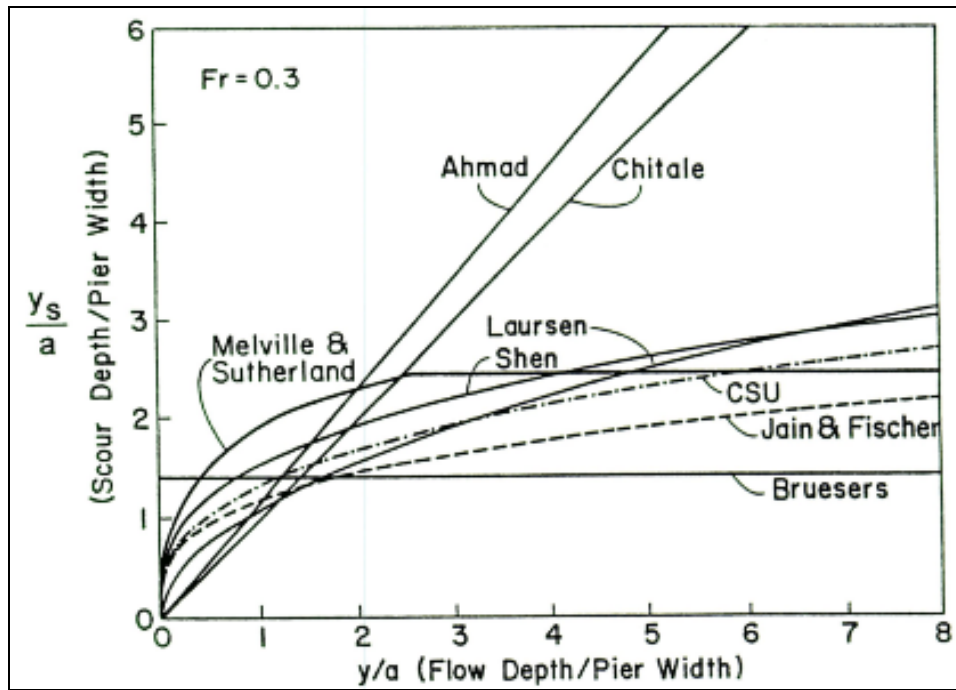


Figure 7.3 Comparison of scour formulas for variable depth ratios ( $y/a$ ) (Jones 1983).

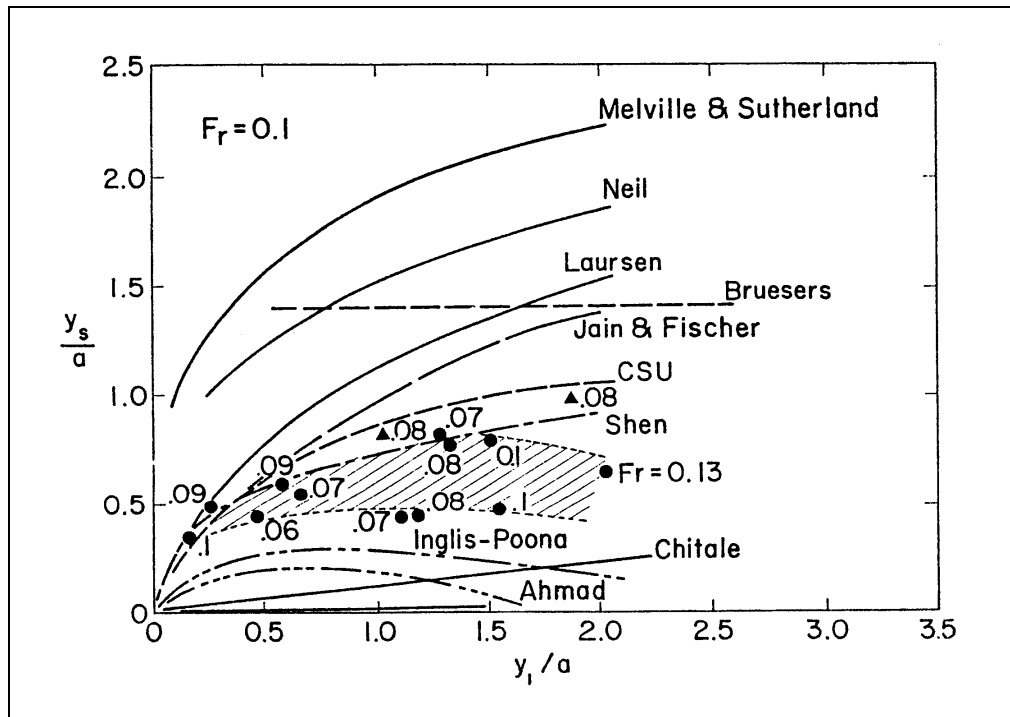


Figure 7.4. Comparison of scour formulas with field scour measurements (Jones 1983).

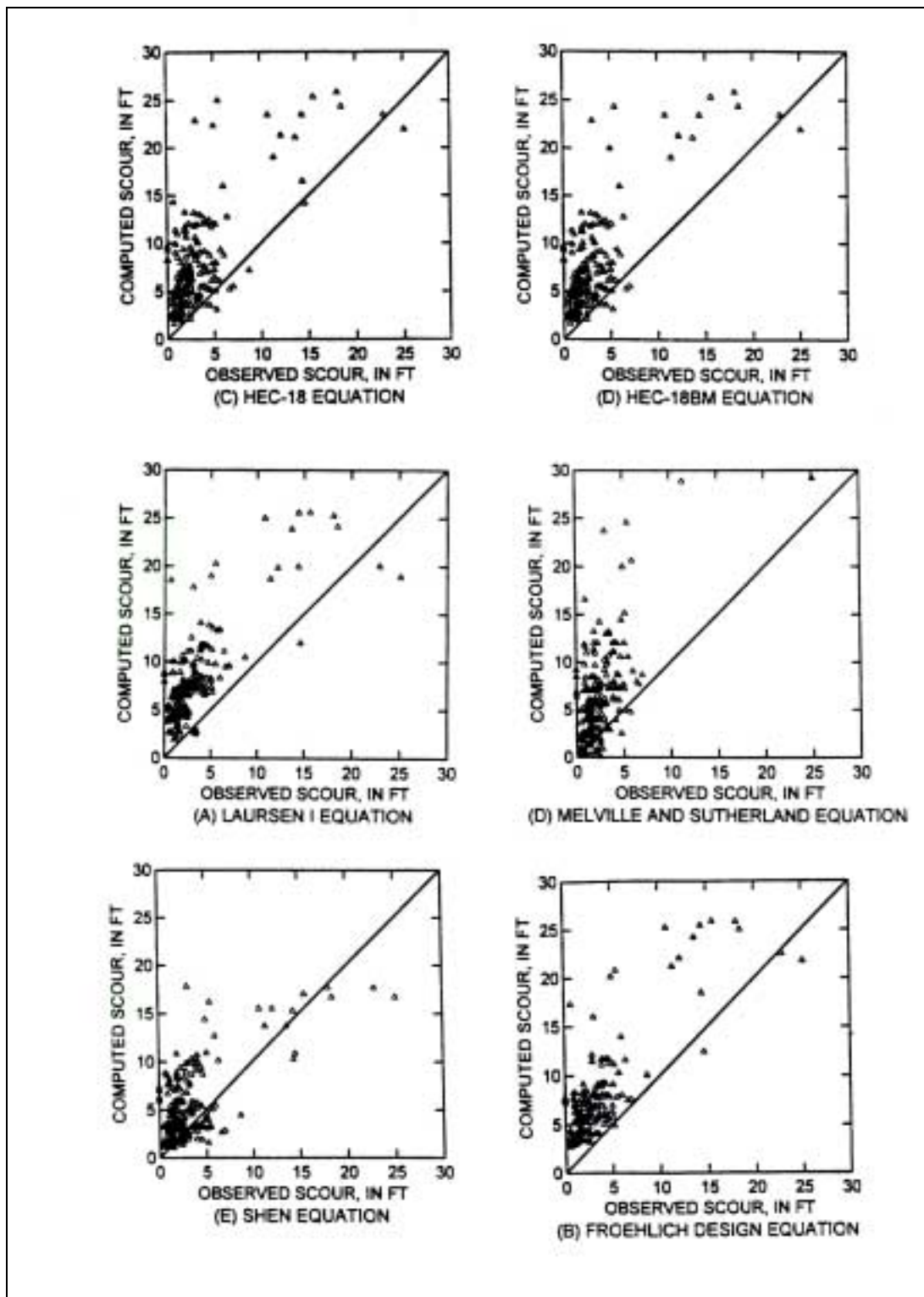


Figure 7.5. Comparison of pier scour equations with field measurements (after Mueller 1996).

#### 7.7.4 FHWA HEC-18 Equation

The FHWA HEC-18 equation (Richardson and Davis 2001) to predict local scour depths at a pier, based on the CSU equation, is recommended for both live-bed and clear-water scour. The equation predicts maximum pier scour depths. The equation is:

$$\frac{y_s}{y_1} = 2.0 K_1 K_2 K_3 K_4 K_5 \left[ \frac{a}{y_1} \right]^{0.65} Fr_1^{0.43} \quad (7.7)$$

where:

- $y_s$  = Scour depth, m (ft)
- $y_1$  = Flow depth just upstream of the pier, m (ft)
- $K_1$  = Correction for pier shape from Table 7.1 and Figure 7.6
- $K_2$  = Correction for flow angle of attack of flow from Table 7.2 and Equation 7.8
- $K_3$  = Correction factor for bed condition from Table 7.3
- $K_4$  = Correction factor for armoring by bed material size from Equation 7.9
- $K_5$  = Correction factor for pier width from Equation 7.13 or 7.14
- $L$  = Length of pier, m (ft)
- $Fr_1$  = Froude Number directly upstream of the pier =  $V_1/(gy_1)^{1/2}$
- $V_1$  = Mean velocity of flow directly upstream of the pier, m/s (ft/s)
- $g$  = Acceleration of gravity (9.81 m/s<sup>2</sup>) (32.2 ft/s<sup>2</sup>)

For round nose piers aligned with the flow the depth of scour has the following limits.

- $y_s \leq 2.4$  times the pier width (a) for  $Fr \leq 0.8$
- $y_s \leq 3.0$  times the pier width (a) for  $Fr > 0.8$

The correction factor for angle of attack of the flow  $K_2$  given in Table 7.2 can be calculated using the following equation:

$$K_2 = \left( \cos\theta + \frac{L}{a} \sin\theta \right)^{.65} \quad (7.8)$$

If  $L/a$  is larger than 12, use  $L/a = 12$  as a maximum in Equation 7.8 and Table 7.2.



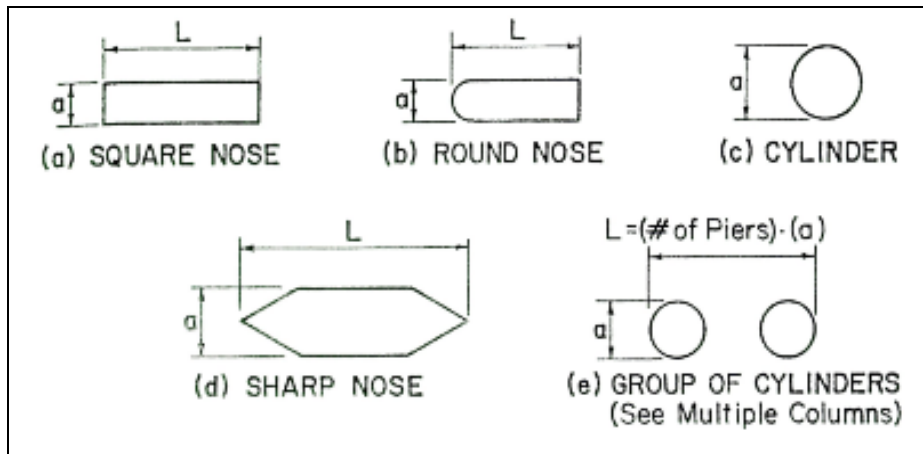


Figure 7.6. Common pier shapes.

Shape of Pier Nose	$K_1$
(a) Square nose	1.1
(b) Round nose	1.0
(c) Circular cylinder	1.0
(d) Group of cylinders	1.0
(e) Sharp nose	0.9

Angle	$L/a=4$	$L/a=8$	$L/a=12$
0	1.0	1.0	1.0
15	1.5	2.0	2.5
30	2.0	2.75	3.5
45	2.3	3.3	4.3
90	2.5	3.9	5.0

Angle = skew angle of flow  
 $L$  = length of pier, m

Bed Condition	Dune Height m	$K_3$
Clear-Water Scour	N/A	1.1
Plane bed and Antidune flow	N/A	1.1
Small Dunes	$3 > H > 0.6$	1.1
Medium Dunes	$9 > H > 3$	1.2 to 1.1
Large Dunes	$H > 9$	1.3

**Notes:**

- The correction factor  $K_1$  for pier nose shape should be determined using Table 7.1 for angles of attack up to 5 degrees. **For greater angles,  $K_2$  dominates and  $K_1$  should be considered as 1.0.** If  $L/a$  is larger than 12, use the values for  $L/a = 12$  as a maximum in Table 7.2 and Equation 7.8.

2. The values of the correction factor  $K_2$  should be applied only when the field conditions are such that the entire length of the pier is subjected to the angle of attack of the flow. Use of this factor will result in a significant over-prediction of scour if (1) a portion of the pier is shielded from the direct impingement of the flow by an abutment or another pier; or (2) an abutment or another pier redirects the flow in a direction parallel to the pier. For such cases, judgment must be exercised to reduce the value of the  $K_2$  factor by selecting the effective length of the pier actually subjected to the angle of attack of the flow.
  
3. The correction factor  $K_3$  results from the fact that for plane-bed conditions, which is typical of most bridge sites for the flood frequencies employed in scour design, the maximum scour may be 10 percent greater than computed with Equation 7.6. In the unusual situation where a dune bed configuration, with large dunes, exists at a site during flood flow, the maximum pier scour may be 30 percent greater than the predicted equation value. This may occur on very large rivers, such as the Mississippi. For smaller streams that have a dune bed configuration at flood flow, the dunes will be smaller and the maximum scour may be only 10 to 20 percent larger than.

#### Correction Factor for Bed Material Size

The correction factor  $K_4$  decreases scour depths for armoring of the scour hole for bed materials that have a  $D_{50}$  equal to or larger than 2.0 mm and  $D_{95}$  equal to or larger than 20 mm. The correction factor results from research by Molinas et al. (1998) and Mueller (1996). Molinas' research for FHWA showed that when the approach velocity ( $V_1$ ) is less than the critical velocity ( $V_{c90}$ ) of the  $D_{90}$  size of the bed material and there is a gradation in sizes in the bed material, the  $D_{90}$  will limit the scour depth. Mueller and Jones (1999) developed a  $K_4$  correction coefficient from a study of 384 field measurements of scour at 56 bridges.

if  $D_{50} \geq 2 \text{ mm}$  and  $D_{95} \geq 20 \text{ mm}$

then

$$K_4 = 0.4(V_R)^{0.15} \quad (7.9)$$

where:

$$V_R = \frac{V_1 - V_{icD_{50}}}{V_{cD_{50}} - V_{icD_{95}}} > 0 \quad (7.10)$$

and

$V_{icD_x}$  = Approach velocity corresponding to critical velocity (m/s or ft/sec) for incipient scour in the accelerated flow region at the pier for the grain size  $D_x$  (m or ft)

$$V_{icD_x} = 0.645 \left( \frac{D_x}{a} \right)^{0.053} V_{cD_x} \quad (7.11)$$

$V_{cD_x}$  = Critical velocity (m/s or ft/s) for incipient motion for the grain size  $D_x$  (m or ft)

$$V_{cD_x} = K_u y_1^{1/6} D_x^{1/3} \quad (7.12)$$

$y_1$  = Depth of flow just upstream of the pier, excluding local scour, m (ft)

$V_1$  = Velocity of the approach flow just upstream of the pier, m/s (ft/s)

$D_x$  = Grain size for which x percent of the bed material is finer, m (ft)

$K_u$  = 11.25 SI units

$K_u$  = 6.19 English units

Although this  $K_4$  provides a good fit with the field data, the velocity ratio terms are so formed that if  $D_{50}$  is held constant and  $D_{95}$  increases, the value of  $K_4$  increases rather than decreases. For field data an increase in  $D_{95}$  was always accompanied with an increase in  $D_{50}$ .

The minimum value of  $K_4$  is 0.4 and  $V_R$  must be greater than 0. The bed material size must have  $D_{50} > 2.0$  mm and  $D_{95} > 20.0$  mm.

#### Correction Factor for Wide Piers

Flume studies on scour depths at wide piers in shallow flows and field observations of scour depths at bascule piers in shallow flows indicate that existing equations, including the CSU equation, overestimate scour depths. Johnson and Torrico (1994) suggest the following equations for a  $K$  factor to be used to correct Equation 7.7 for wide piers in shallow flow. The correction factor to be applied when the ratio of depth of flow ( $y$ ) to pier width ( $a$ ) is less than 0.8 ( $y/a < 0.8$ ); the ratio of pier width ( $a$ ) to the median diameter of the bed material ( $D_{50}$ ) is greater than 50 ( $a/D_{50} > 50$ ); and the Froude Number of the flow is subcritical.

$$K_5 = 2.58 \left( \frac{y}{a} \right)^{0.34} F^{0.65} \text{ for } V/V_c < 1 \quad (7.13)$$

$$K_5 = 1.0 \left( \frac{y}{a} \right)^{0.13} F^{0.25} \text{ for } V/V_c > 1 \quad (7.14)$$

**Engineering judgment should be used in applying  $K_5$  because it is based on limited data from flume experiments. Engineering judgment should take into consideration the volume of traffic, the importance of the highway, cost of a failure (potential loss of lives and dollars) and the change in cost that would occur if the  $K_5$  factor is used.**

#### **7.7.5 Pier Scour in Cohesive Bed Material**

The rate of scour in cohesive silt and clay bed materials is many times slower than for non-cohesive materials. The maximum depth of scour at a pier will often be reached during one

runoff event in a sand bed material stream. Whereas, it will take many runoff events to get the maximum depth scour at a pier in a stream with clay bed material. However, as Briaud et al. (1999) point out, "the maximum depth of scour in sand and in clay appears to be the same; this is confirmed by the fact that the HEC-18 equation developed from sand experiments fits this data on clay quite well." This data refers to the Briaud et al. flume studies of pier scour in clay bed material. Also, in their flume studies of scour at a circular cylinder in clay bed material, the maximum scour depth occurred behind the pier.

Using an Erosion Function Apparatus (EFA) to measure scour in cohesive soils Briaud et al. (1999) demonstrated that the scour rate for sand was approximately 1,000 times faster than clay. Other researchers and field experience have also demonstrated that the scour rate in clay is many times slower than in sand. In addition, Briaud et al. describe the phenomena, bonds, and factors that give and affect cohesion in clays. They note "because of the number and complexity of these bonds, it is very difficult to predict the critical shear stress for clays empirically on the basis of a few index properties." They propose that the critical shear stress be measured for the clay bed material at the bridge site directly. The EFA was developed to measure the erosion rate directly. Briaud et al. propose a method and equations to use this measurement to predict depth of scour corresponding to the duration of the flood or the design life of the bridge.

#### 7.7.6 Pier Scour for Other Pier Geometry, Flow Conditions, and Debris

HEC-18 (Richardson and Davis 2001) gives procedures and equations to determine local pier scour depths for piers with exposed footings and piles groups. multiple columns skewed to the flow, composite pier configurations (pier on pile cap on piles exposed to the flow), debris on piers, and piers subjected to pressure flow.

#### 7.7.7 Topwidth of Scour Holes

The topwidth of a scour hole in cohesionless bed material from one side of a pier or footing can be estimated from the following equation (Richardson and Abed 1999).

$$W = y_s (K + \cot \theta) \quad (7.15)$$

where:

- $W$  = Topwidth of the scour hole from each side of the pier or footing, m (ft)
- $y_s$  = Scour depth, m (ft)
- $K$  = Bottom width of the scour hole as a fraction of scour depth
- $\theta$  = Angle of repose of the bed material ranging from about 30° to 44°

The angle of response of cohesiveness material in air ranges from about 30° to 44°. Therefore, if the bottom width of the scour hole is equal to the depth of scour  $y_s$  ( $K = 1$ ), the topwidth in cohesionless sand would vary from 2.07 to 2.80  $y_s$ . At the other extreme, if  $K = 0$ , the topwidth would vary from 1.07 to 1.8  $y_s$ . Thus, the topwidth could range from 1.0 to 2.8  $y_s$  and will depend on the bottom width of the scour hole and composition of the bed material. In general, the deeper the scour hole, the smaller the bottom width. In water, the angle of repose of cohesionless material is less than the values given for air; therefore, a topwidth of 2.0  $y_s$  is suggested for practical applications (Figure 7.7).

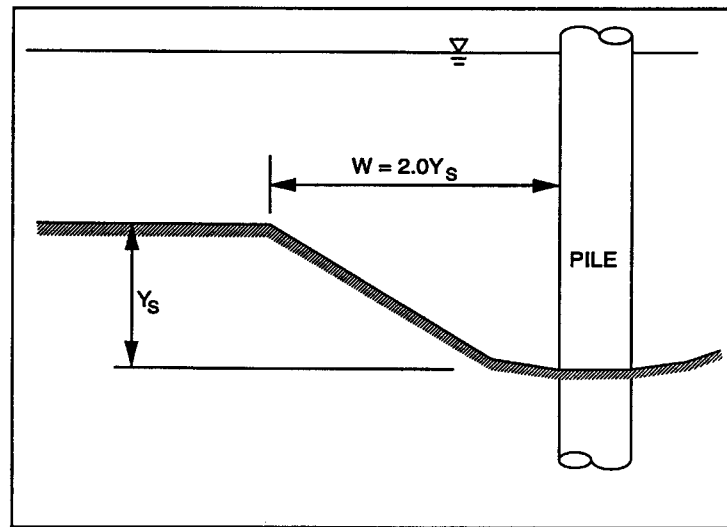


Figure 7.7. Topwidth of scour hole (HEC-18).

### 7.7.8 Physical Model Studies

For unusual or complex pier foundation configurations a physical model study should be made. The scale between model and prototype is based on the Froude criteria, that is, the Froude number for the model should be the same as for the prototype. In general, it is not possible to scale the bed material size. Also, at flood flows in sand bed streams the sediment transport conditions will be live-bed and the bed configuration will be plane bed. Whereas, in the model live-bed transport conditions may be ripples or dunes. These are incomparable pier scour conditions. Therefore, it is recommended that a bed material be used that has a critical velocity just below the model velocity (i.e., clear-water scour conditions). This will usually give the maximum scour depth; but a careful study of the results need to be made by persons with field and model scour experience. For additional discussion of the use of physical modeling in hydraulic design, see Chapter 5 and HEC-23 (Lagasse et al. 2001).

## 7.8 LOCAL SCOUR AT ABUTMENTS

### 7.8.1 Introduction

The two causes of scour when the flow is obstructed by the abutment and approach highway embankment are: (1) A horizontal vortex starting at the upstream end of the abutment and running along the toe of the abutment, and (2) a vertical wake vortex at the downstream end of the abutment (Figure 7.8).

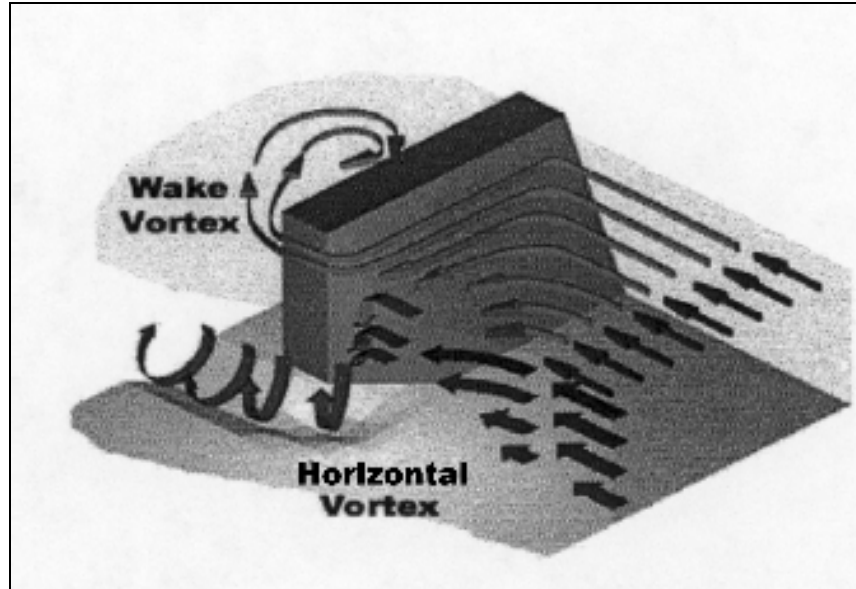


Figure 7.8. Schematic representation of abutment scour.

The horizontal vortex at the toe of the abutment is very similar to the horseshoe vortex that forms at piers, and the vertical vortex that forms at the downstream end is similar to the wake vortex that forms downstream of a pier, or that forms downstream of any flow separation. A large amount of laboratory research has been conducted to determine the depth and location of the scour hole that develops for the horizontal (so called horseshoe) vortex that occurs at the upstream end of the abutment. From this research, numerous abutment scour equations have been developed to predict this scour depth. However, very little field data exist to verify the equations. In fact, many of the equations, as explained in Section 7.8.2, are spurious correlations for the field case.

Only since 1992 has research been conducted to develop equations for the field case. Maryland SHA has developed an abutment scour program titled ABSCOUR (Chang and Davis 1999) based on Laursen's long contraction scour equations. Sturm (1999a, b) developed equations based on his research at Georgia Institute of Technology. Kouchakzadeh and Townsend (1999) and Trivino and Richardson (2000) present equations based on momentum transfer for the determination of abutment scour depths. These equations have had limited testing of computed vs. measured abutment scour and will not be given.

The wake vortex at the downstream end of the abutment also causes abutment failures. Sometimes the abutment does not fail but only the approach embankment is eroded. Research and the development of methods to determine the erosion from the wake vortex has not been conducted. Methods to protect abutments and the embankments against wake vortex erosion are given in HEC-23 (Lagasse et al. 2001b).

**In summary, engineering judgment is required in designing foundations for abutments. As a minimum, abutment foundations should be designed assuming no ground support (lateral or vertical) as a result of soil loss from long-term degradation and contraction scour. The abutment should be protected from local scour from both**

the upstream and downstream vortexes using riprap and/or guide banks. Guidelines for the design of riprap and guide banks are given in HEC-23 (Lagasse et al. 2001b). To protect the abutment and approach roadway from scour by the wake vortex several SHAs use a 15-meter (50-ft) guide bank extending from the downstream corner of the abutment. Otherwise, the downstream abutment and approach should be protected with riprap.

In the following sections, two equations from HEC-18 are presented for use in estimating scour depths as a guide in designing abutment foundations. The methods can be used for either **clear-water or live-bed** scour.

### 7.8.2 Commentary on Abutment Scour Equations

Until recently, the equations in the literature were developed using the abutment and roadway approach length as one of the variables. This approach results in excessively conservative estimates of scour depth. Richardson and Richardson (1993) pointed this out in a discussion of Melville's (1992) paper and in a 1999 paper (Richardson and Lagasse 1999, p. 457). They stated.

"The reason the equations in the literature predict excessively conservative abutment scour depths for the field situation is that, in the laboratory flume, the discharge intercepted by the abutment is directly related to the abutment length; whereas, in the field, this is rarely the case."

Figure 7.9 illustrates the difference. Thus, equations for predicting abutment scour would be more applicable to field condition if they included the discharge intercepted by the embankment rather than embankment length.

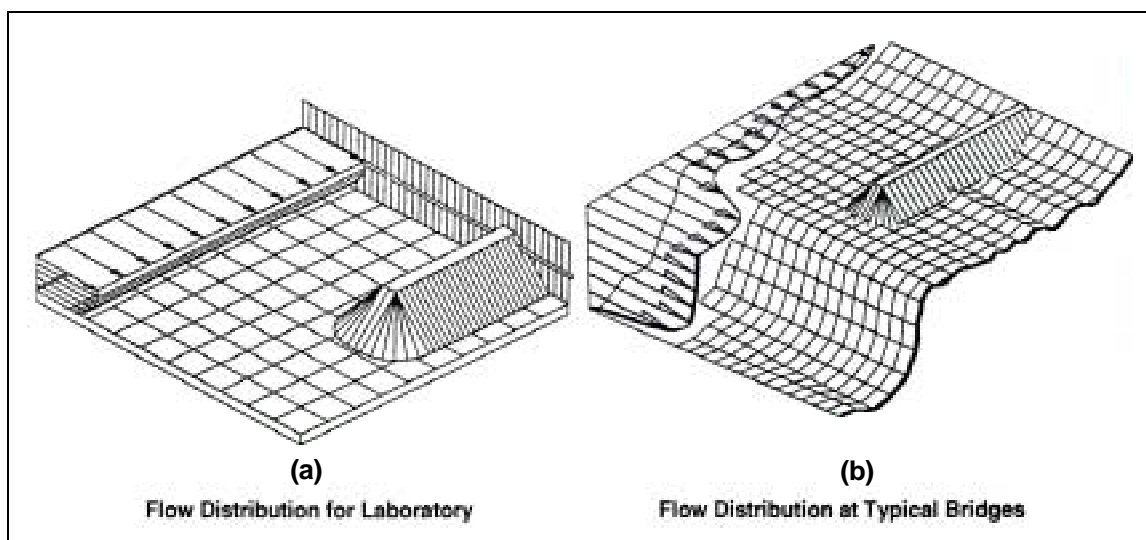


Figure 7.9. Comparison of laboratory flow characteristics to field flow conditions.

Abutment scour depends on the interaction of the flow obstructed by the abutment and roadway approach and the flow in the main channel at the abutment. The discharge returned to the main channel at the abutment is not simply a function of the abutment and roadway length in the field case. Richardson and Richardson (1993) noted that abutment scour depth depends on abutment shape, discharge in the main channel at the abutment, discharge intercepted by the abutment and returned to the main channel at the abutment, sediment characteristics, cross-sectional shape of the main channel at the abutment (especially the depth of flow in the main channel and depth of the overbank flow at the abutment), and alignment. In addition, field conditions may have tree-lined or vegetated banks, low velocities, and shallow depths upstream of the abutment. **Most of the early laboratory research failed to replicate these field conditions.**

### 7.8.3 Abutment Site Conditions

Abutments can be set back from the natural stream bank, placed at the bankline or, in some cases, actually set into the channel itself. Common designs include stub abutments placed on spill through slopes, and vertical wall abutments, with or without wingwalls. Scour at abutments can be live-bed or clear-water scour. The bridge and approach road can cross the stream and floodplain at a skew angle and this will have an effect on flow conditions at the abutment. Finally, there can be varying amounts of overbank flow intercepted by the approaches to the bridge and returned to the stream at the abutment. More severe abutment scour will occur when the majority of overbank flow returns to the bridge opening directly upstream of the bridge crossing. Less severe abutment scour will occur when overbank flows gradually return to the main channel upstream of the bridge crossing.

The skew angle for an abutment (embankment) is depicted in Figure 7.10. For an abutment angled downstream, the scour depth is decreased whereas the scour depth is increased for an abutment angled upstream.

An equation for adjusting abutment scour depth for embankment skew is given in Section 7.8.5.

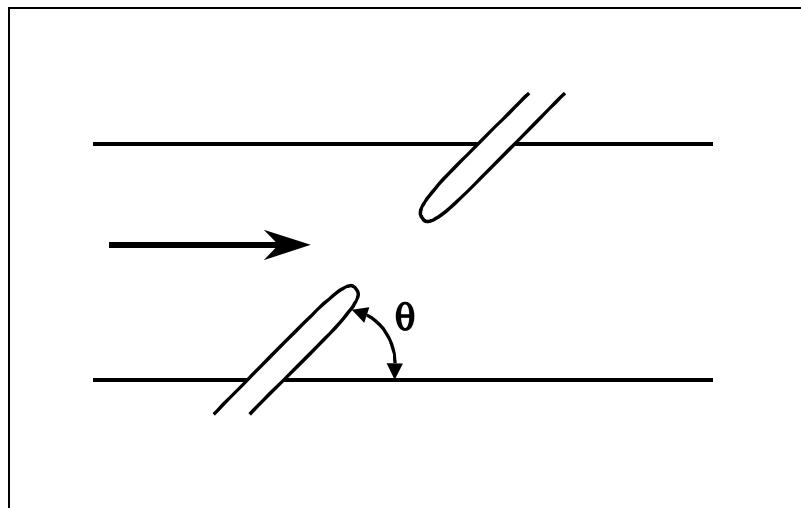


Figure 7.10. Orientation of embankment angle  $\theta$  to the flow.



### 7.8.4 Abutment Shape

The three general shapes for abutments are: (1) spill-through abutments, (2) vertical walls without wing walls, and (3) vertical-wall abutments with wing walls (Figure 7.11). These shapes can all have varying angles to the flow. As shown in Table 7.4, depth of scour is approximately double for vertical-wall abutments as compared with spill-through abutments for very short sections of the abutment and approach road. As the length of the abutment and approach road in the floodplain increase, the effect of the spill-through slope is decreased. For long approach road sections on the floodplain, this coefficient will approach a value of 1.0. Similarly, scour for vertical wall abutments with wingwalls on short abutment sections is reduced to 82 percent of the scour of vertical wall abutments without wingwalls. As the length of the abutment and approach road in the floodplain increase, the effect of the wingwall is decreased. For long approach road sections in the floodplain, this coefficient will approach a value of 1.0.

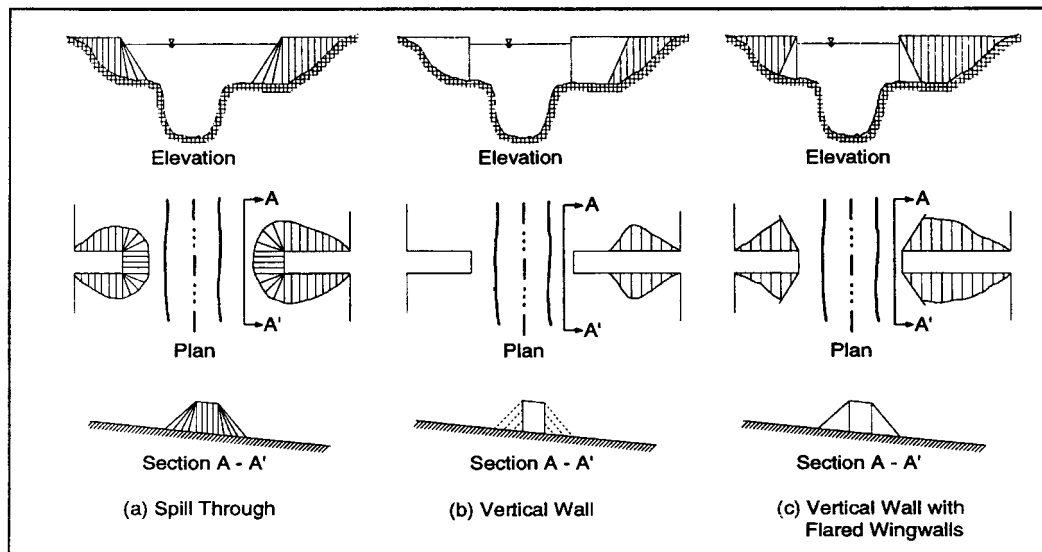


Figure 7.11. Abutment shape.

Description	$K_1$
Vertical-wall abutment	1.00
Vertical-wall abutment with wing walls	0.82
Spill-through abutment	0.55

### 7.8.5 Froehlich's Live-Bed Scour Equation

To determine the potential depth of scour at existing bridges and to aid in the design of foundations and placement of rock riprap or guide banks at new bridges, Froehlich's (1989) live-bed scour equation or an equation from HIRE (Richardson et al. 1995) can be used. Froehlich analyzed by regression analysis, 170 live-bed scour measurements in laboratory flumes to obtain the following equation:

$$\frac{y_s}{y_a} = 2.27K_1K_2 \left[ \frac{L'}{y_a} \right]^{0.43} Fr^{0.61} + 1 \quad (7.16)$$

where:

- $K_1$  = Coefficient for abutment shape (Table 7.4)
- $K_2$  = Coefficient for angle of embankment to flow
- $K_2$  =  $(\theta/90)^{0.13}$  (Figure 7.10 for definition of  $\theta$ )
  - $\theta < 90^\circ$  if embankment points downstream
  - $\theta > 90^\circ$  if embankment points upstream
- $L'$  = Length of abutment projected normal to flow, m, ft
- $A_e$  = Flow area of the approach cross section obstructed by the embankment,  $m^2$ ,  $ft^2$
- $Fr$  = Froude Number of approach flow upstream of the abutment =  $V_e/(gy_a)^{1/2}$
- $V_e$  =  $Q_e/A_e$ , m/s, ft/s
- $Q_e$  = Flow obstructed by the abutment and approach embankment,  $m^3/s$ ,  $ft^3/s$
- $y_a$  = Average depth of flow on the floodplain, m, ft
- $y_s$  = Scour depth, m, ft

Note: That as  $L'$  tends to 0,  $y_s$  also tends to 0. In a regression equation, 50 percent of the data are above or below the regression line. The 1 was added to the equation so as to encompass 98 percent of the data.

### 7.8.6 1975 and 1990 HIRE Equation

An equation in HIRE was developed from Corps of Engineers field data of scour at the end of spurs in the Mississippi River (Richardson et al. 1975, 1990). This field situation closely resembles the laboratory experiments for abutment scour in that the discharge intercepted by the spurs was a function of the spur length. The HIRE equation is applicable when the ratio of projected abutment length ( $a$ ) to the flow depth ( $y_1$ ) is greater than 25. This equation can be used to estimate scour depth ( $y_1$ ) at an abutment where conditions are similar to the field conditions from which the equation was derived: the equation is:

$$\frac{y_s}{y_1} = 4 Fr^{0.33} \frac{k_1}{0.55} \quad (7.17)$$

where:

- $y_s$  = Scour depth, m, ft
- $y_1$  = Depth of flow at the abutment on the overbank or in the main channel, m, ft
- $Fr$  = Froude Number based on the velocity and depth adjacent to and upstream of the abutment
- $K_1$  = Coefficient for abutment shape (Table 7.4)

To correct Equation 7.17 for abutments skewed to the stream, use  $K_2$  for Equation 7.16.

Clear-Water Scour at an Abutment. Use Equations 7.16 or 7.17 for live-bed scour because clear-water scour equations potentially decreases scour at abutments due to the presence of coarser material. This decrease is unsubstantiated by field data.

## **7.9 SCOUR PROBLEMS**

Solved problems for contraction, pier, and abutment scour in metric (SI) and English units are given in HEC-18 (Richardson and Davis 2001). Example problems for stream instability problems are given in HEC-20 (Lagasse et al. 2001a). In addition, guidelines for the design of scour and stream instability countermeasures are given in HEC-23 (Lagasse et al. 2001b). In Chapter 10 of this manual, three design examples are given which demonstrate the use of some of the equations and methods given in this chapter.

(page intentionally left blank)

## CHAPTER 8

### DATA NEEDS AND DATA SOURCES

The purpose of this chapter is to identify data needed for calculations and analyses which will lead to recommendations for highway crossings and encroachments of rivers. The types and amounts of data needed for planning and designing river crossings and lateral encroachments can vary from project to project depending upon the class of the proposed highway, the type of river and the geographic area.

#### 8.1 BASIC DATA NEEDS

The data, preliminary calculations, alternative route selections and analyses of these routes should be documented in a report. Such a report serves to guide the detailed designs, and provides reference background for environmental impact analysis and other needs such as application for permits and historical documentation for any litigation which may arise.

##### 8.1.1 Area Maps

An area map is needed to identify the location of the entire highway project and all streams and river crossings and encroachments involved. The purpose of the map is to orient the highway project geographically with other area features. The map may be very small scale showing towns, cities, mountain ranges, railroads and other highways and roads. The area map should be large enough to identify river systems and tributaries.

##### 8.1.2 Vicinity Maps

Vicinity maps for each river crossing or lateral encroachment are needed to layout the proposed highway alignment and alternate routes. There should be sufficient length of river included on the vicinity map to enable identification of stream type and to locate river meanders, sand bars, and braided channels. Other highways and railroads should be identified. The maps should show contours and relief. Intakes for municipal and industrial water, diversions for irrigation and power, and navigation channels should be clearly identified.

Recreational areas such as camping, picnic grounds, beaches, and recreational boat docks should be identified. Cultivated areas and urban and industrial areas, in the vicinity of towns and cities should be noted on the map. The direction of river flow should of course be clearly identified.

##### 8.1.3 Site Maps

Site maps are needed to determine details for hydraulic, roadway, and structural designs. The site map should show detailed contours (1- or 2-foot intervals), vegetation distribution and type, and other structures. The site map is used to locate highway approach embankments, piers and alignments of piers, channel changes, and protection works. High water lines should be

indicated on the site maps for the purpose of estimating flood flows and distributions across the river cross section.

#### **8.1.4 Aerial and Other Photographs**

It is highly desirable in preparing vicinity and site maps that aerial photographs be obtained. Multi-image cameras use different ranges of the light spectrum to assist in identifying various features such as sewer outfalls, groundwater inflows, types of vegetation, sizes and heights of sandbars, river thalwegs, river controls and geologic formations, existing bank protection works, old meander channels, and other features. Topographic information can also be developed from aerial photographs for vicinity and site maps where such information is not readily available. Historic aerial photographs are a valuable resource to assess river planform stability.

Land photographs (as opposed to aerial photos) of existing structures near the crossing are always helpful in documentation and evaluation of potential effects of highway construction. Photographs of water intake works likely to be affected by the highway project should be obtained, and specific data should be noted and briefly discussed. High water marks recorded photographically along with dates of occurrence are useful. Photographs aid the designer, who may not have the opportunity to visit the site, to visualize crossings and encroachments, and they aid documentation.

Conditions of the river channel in the river reach of concern are easy to record photographically, and such pictures can be very helpful in analysis of the river reach. Vegetation on floodplains and seasonal variations of vegetation should be recorded photographically. Notable geologic formations should be photographed as well and supplemented with adequate notes. All photographs should be referenced on the site or on vicinity maps.

#### **8.1.5 Field Inspection**

A field inspection of potential highway encroachment sites of rivers should be made prior to the analysis. This has been implied in the foregoing paragraphs but is emphasized again because of the underlying importance of making first hand appraisals of specific sites before conclusions and recommendations are advanced for possible highway routes. Of course, they are important in making detailed designs as well, but it is not always feasible to provide opportunities for site inspection by the entire design staff. Forms and checklists for a detailed geomorphic reconnaissance of the stream corridor are provided in HEC-20 (Lagasse et al. 2001).

#### **8.1.6 Geologic Map**

A geologic vicinity map, on which geophysical features are indicated, is a basic need. The rock formations, outcroppings, and glacial and river deposits which form control points on rivers are valuable in analysis of rivers. Soil type determines the size of sediment in transport, infiltration rates, and groundwater flows. Channel geometry and roughness are important factors in river mechanics.

Soil survey maps with engineering interpretations are available for a significant proportion of the United States. They may be helpful in selecting layouts and assessing the suitability of fill materials.

### **8.1.7 Climatologic Data**

Stream gaging stations have been established on many streams throughout the United States. However, there are some streams where either a gaging station does not exist near the project site or a gaging station does not exist at all. In such cases, it is necessary to estimate flood flows. These estimates may be based on regionalized estimating procedures or other prediction models using meteorological and watershed data inputs. These meteorological data are available from the National Weather Service (NWS) Data Center of the National Oceanic and Atmospheric Administration (NOAA), and estimates of average conditions can be made from rainfall data published by the NWS. Temperature records are helpful in making snowmelt estimates, and wind data are helpful in making wave height estimates on rivers, lakes and reservoirs as well as for coastal areas.

### **8.1.8 Hydraulic Data**

Whenever possible, sediment load data should be provided as auxiliary data for river analyses. Bed-material load, suspended load and wash load data may be obtained for some rivers in the water supply papers published by the U.S. Geological Survey, state engineers' reports, flood control and other water resources investigation reports. Information may also be obtained by direct sampling of the river.

Riverbed cross sections and profiles may be obtained with an ultrasonic depth sounder and are helpful in sediment transport and backwater studies. It is also helpful to know water temperatures. Direct measurement of flood flows should be made when historical records may be deficient. Depth and velocity measurements need to be made at a sufficient number of subsections in a cross section to determine total flow rate. Discharge measurements made at various stages at a gaging site can provide data for developing a stage-discharge rating curve.

Observations of high water marks along the river reach should be made. Each high water mark and relevant profile should be established. These are helpful in calculating historical flood discharges. Also, stages achieved by ice jams at specific locations should be noted.

Records of the performance of existing bridges and other drainage structures should be obtained. Data on scour at piers of existing bridges (or at bridges which have failed) in the vicinity should be obtained. For bridges which have failed, as much information as possible should be obtained relative to direction of flow (angle of attack) at the piers or embankment ends. Flood duration, debris in the river, distribution of flows, and magnitudes of scour are useful information. Historical records of damage to adjacent property and results of legal actions brought about because of damage are useful information also.

### 8.1.9 Hydrologic Data

The purpose of hydrologic data is to determine the stream discharge, flood magnitudes, and duration and frequencies of flood prior to analysis of river behavior and design of the river encroachments and crossings. Hydrologic data and hydraulic analyses should be documented in report form for project development. After construction, the documentation would be helpful in evaluating any damage from floods and failures, in the event they occur, and providing background for any litigation which may arise as a consequence.

Sometimes a highway crossing and/or encroachment may have a significant effect on flood hydrographs and a hydrologic analysis should be made to determine the level of significance. This analysis would involve hydrograph development and flow routing within the zone of influence of such highway structures.

The basic data needed are stream discharge data at the nearest gaging station, historical floods and highwater marks. It is also desirable to prepare a drainage map for the region upstream of the proposed highway project, with delineation of size, shape, slope, land use, and water resource facilities such as storage reservoirs for irrigation and power and flood control projects. It is desirable whenever possible to obtain flood histories of the river from residents and accounts by the news media, particularly for events prior to stream gaging records. Estimates of flood discharge can be made from these accounts which are valuable in flood-frequency analysis.

A flood-frequency curve is prepared from recorded stream flow data and augmented by estimated discharges (using Manning's equation or equivalent) from high water marks. Several methods ranging from sophisticated stochastic analysis to simple methods have been developed. The greatest difficulty in constructing a flood-frequency curve is lack of sufficient and reliable data. Approximate methods for extrapolating the range of flood-frequency curves are available but are not discussed in detail here (see HDS-2, FHWA 1961).

A simple graphical method based on extreme value theory is reasonably satisfactory. The method consists of ordering the annual peak flood discharges of record from the largest to smallest, irrespective of chronological order. The annual (flood) discharge is plotted against its recurrence interval on special probability (Gumbel, or other) paper. The recurrence interval, RI is calculated from

$$RI = \frac{n+1}{m} \quad (8.1)$$

in which  $n$  is the number of years of records, and  $m$  is the order (largest flood is ranked 1) of the flood magnitude. Thus, the highest flood discharge would have a recurrence interval of  $n + 1$  years and lowest would have a recurrence interval of  $(1+1/n)$  years. The U.S. Water Resources Council (1981) has adopted the log-Pearson III distribution for use as a base method for determining flood flow frequencies. Details of the method and plotting paper may be obtained from the U.S. Geological Survey in Bulletin 17B.

When adjusting discharge records from a nearby gaging station to the project site, the flood peaks are often prorated on the basis of drainage area ratios. Depending on drainage basin characteristics, the exponent of the ratio varies from 0.5 to 0.8. Slope-area calculations for



peak discharges can also be used. In using this method, the conveyance of the channel is calculated using the Manning equation in which the roughness coefficient,  $n$ , needs to be estimated from the discussion presented in Chapters 2 and 3. By referring to a catalog of (color) photographs, similar channel situations to the specific site can be identified and a relatively inexperienced engineer may make a reliable estimate for  $n$ .

Whatever approach is used, the reader is cautioned not to blindly accept computer printout as the final answer in estimating a flood frequency relationship. The data should be plotted on probability paper as analyzed by several commonly used methods. Sometimes paleo (ancient) hydrology techniques need to be employed to resolve historic outliers at very sensitive sites.

### **8.1.10 Environmental Data**

In making environmental impact analyses of highway projects on streams and rivers, it is necessary to obtain water quality and biological data for the streams. Such data are not readily available for many rivers. Municipal water and sewage treatment facilities and industrial plants utilizing river water should have recent records regarding river water quality which will be helpful in making comprehensive environmental analyses. Water quality data for certain rivers can be obtained from the U.S. Geological Survey. Wildlife information such as migration patterns of deer and elk should be determined and local game refuges should be located. Information regarding fishes and their river habitat should be obtainable from the state fish and game agencies. Species of trees and other vegetation should be determined, and some information regarding sensitivity of the flora to auto emissions should be obtained. Data should also be obtained in order to enable assessment of stream turbidity during and after highway construction. Information on soil type to be used in construction of embankments would be helpful in this regard.

## **8.2 CHECKLIST OF DATA NEEDS**

As an aid in collecting data preparatory to analysis of rivers and highway encroachment of rivers, the relevant types of data have been listed in Table 8.1. There may be more data items included in this table than are needed for a given project site, and some judgment is required. For data which are not available, the checklist should be helpful for planning a field investigation or other data acquisition program.

## **8.3 DATA SOURCES**

The best data sources are national data centers where the principal function is to disseminate data. But it might be necessary to collect data from a variety of other sources such as from a field investigation, interviews with local residents, and a search through library material. Detailed information on the location of these federal agencies across the U.S. is available in Appendix A of the manual HEC-19, (FHWA 1984). The list of sources in Table 8.2 is provided to serve as a guide to the data collection task.

Table 8.1. Checklist of Data Needs.

**Maps and Charts:**

- (1) Geographic
- (2) Topographic
- (3) Geologic
- (4) Navigation Charts
- (5) Potamology Surveys
- (6) County and City Plats

**Aerial and Other Photos:**

- (1) Large Scale Photos for Working Plans
- (2) Small Scale Stereo Pairs of River and Surrounding Terrain
- (3) Color Infrared Photos for Flow Patterns, Scour Zones, and Vegetation
- (4) Ground Photos
- (5) Underwater Photos

**Information on Existing Structures, Bridges, Dams, Diversion, or Outfalls:**

- (1) Plans and Details
- (2) Construction Details
- (3) Alterations and Repairs
- (4) Foundations
- (5) Piers and Abutments
- (6) Scour
- (7) Dikes
- (8) Field Investigations:
  - Bridge structure and repairs to bridge and approach
  - Damage due to ice or debris

**Hydraulic, Hydrology, and Soils:**

- (1) Discharge Records
- (2) Stage-Discharge Records
- (3) Flood Frequency Curves for Stations Near Site
- (4) Flow Duration Curves (hydrographs)
- (5) Newspaper, Radio, Television, Accounts of Large Floods
- (6) Channel Geometry:
  - Main channel
  - Side channel
  - Navigation channel
  - Floodplain
  - Slopes
  - Backwater calculation
  - Bars
  - Sinuosity
  - Type (braided, meandering, straight)
  - Controls (falls, rapids, restriction, rock outcropping dams, diversions)
- (7) Sediment Discharge:
  - Size distribution
  - Bed and Bank Material Sizes
  - Roughness Coefficient n
- (8) Ice:
  - Recorded thickness
  - Dates of freeze up and break up
  - Flow patterns and jams

Table 8.1. Checklist of Data Needs.

**Hydraulic, Hydrology, and Soils (continued):**

- (9) Regulating Structures:
  - Dams, diversions
  - Intake, outfalls
  - Scour survey around existing piers, abutments, spur dikes
  - Inspect and photograph stabilization works, riprap sizes, filter blankets
  - Check wells for groundwater levels in areas
  - Install gaging stations
- (10) Soils Information:
  - Excavation data
  - Borrow pits
  - Gravel pits
  - Cuts
  - Tunnels
  - Core boring logs
  - Well drilling logs
  - Soil tests
  - Permeability
  - Rock for riprap
- (11) Planned and Anticipated Water Resources Projects
- (12) Lakes, Tributaries, Reservoirs or Side Channel Impoundments
- (13) Field Surveys:
  - Onsite inspections and photographs
  - Samples of sediments
  - Measure water and sediment discharge
  - Observe channel changes or realignment since last maps or photos
  - Identify high water lines or debris deposits due to recent floods
  - Check magnitude of velocities and direction of flow in vicinity of proposed structure
  - Outcroppings
  - Subsurface Exploration

**Climatological Data:**

- (1) National Weather Service Records for Precipitation
- (2) Wind
- (3) Temperatures

**Land Use:**

- (1) Zoning Maps
- (2) Recent Aerial Photographs
- (3) Planning Committee Records
- (4) Urban Areas
- (5) Industrial Areas
- (6) Recreational Areas
- (7) Primitive Areas
- (8) Forests
- (9) Vegetation

Table 8.2. List of Data Sources.

Table 8.2. List of Data Sources.	
<b>Topographic Maps:</b>	
(1)	Quadrangle maps -- U.S. Department of the Interior, Geological Survey, Topographic Division; and U.S. Department of The Army, Army Map Service
(2)	River plans and profiles -- U.S. Department of the Interior, Geological Survey, Conservation Division
(3)	National parks and monuments -- U.S. Department of the Interior, National Park Service
(4)	Federal reclamation project maps -- U.S. Department of the Interior, Bureau of Reclamation
(5)	Local areas -- commercial aerial mapping firms
(6)	American Society of Photogrammetry
<b>Planimetric Maps:</b>	
(1)	Plans of public land surveys -- U.S. Department of the Interior, Bureau of Land Management
(2)	National forest maps -- U.S. Department of Agriculture, Forest Service
(3)	County maps -- State Highway Agency
(4)	City plans -- city or county recorder
(5)	Federal reclamation project maps -- U.S. Department of the Interior, Bureau of Reclamation
(6)	American Society of Photogrammetry
(7)	ASCE Journal -- Surveying and Mapping Division
<b>Aerial Photographs:</b>	
(1)	The following agencies have aerial photographs of portions of the United States: U.S. Department of the Interior, Geological Survey, Topographic Division; U.S. Department of Agriculture, Commodity Stabilization Service, Soil Conservation Service and Forest Service; U.S. Air Force; various State agencies; commercial aerial survey and mapping firms; National Oceanic and Atmospheric Administration
(2)	American Society of Photogrammetry
(3)	Photogrammetric Engineering
(4)	Earth Resources Observation System (EROS); Photographs from Gemini, Apollo, Earth Resources, Technology Satellite (ERTS) and Skylab
(5)	City or County Records
(6)	State Highway Agency
<b>Transportation Maps:</b>	
(1)	State Highway Agency.
(2)	Large Cities
<b>Triangulation and Benchmarks:</b>	
(1)	State Engineer.
(2)	State Highway Agency.
(3)	Cities
<b>Geologic Maps:</b>	
(1)	U.S. Department of the Interior, Geologic Survey, Geologic Division; and State Geological Surveys Departments. (Note - some regular quadrangle maps show geological data also.)
<b>Soil Data:</b>	
(1)	County soil survey reports -- U.S. Department of Agriculture, Soil Conservation Service.
(2)	Land use capability surveys -- U.S. Department of Agriculture, Soil Conservation Service.
(3)	Land classification reports -- U.S. Department of the Interior, Bureau of Reclamation.
(4)	Hydraulic laboratory reports -- U.S. Department of the Interior, Bureau of Reclamation.
(5)	State Universities and State Agricultural and Conservation Agencies.

Table 8.2. List of Data Sources.

<b>Climatological Data:</b>	
(1)	National Weather Service Data Center.
(2)	Hydrologic bulletin -- U.S. Department of Commerce, National Oceanic and Atmospheric Administration.
(3)	Technical papers -- U.S. Department of Commerce, National Oceanic and Atmospheric Administration.
(4)	Hydrometeorological reports -- U.S. Department of Commerce, National Oceanic and Atmospheric Administration, and U.S. Department of the Army, Corps of Engineers.
(5)	Cooperative study reports -- U.S. Department of Commerce, National Oceanic and Atmospheric Administration and U.S. Department of the Interior, Bureau of Reclamation.
<b>Stream Flow Data:</b>	
(1)	Water supply papers -- U.S. Department of the Interior, Geological Survey, Water Resources Division.
(2)	Reports of State Engineers.
(3)	Annual reports -- International Boundary and Water Commission, United States and Mexico.
(4)	Annual reports -- various interstate compact commissions.
(5)	Hydraulic laboratory reports -- U.S. Department of the Interior, Bureau of Reclamation.
(6)	Corps of Engineers, U.S. Army, Flood control studies.
(7)	Tennessee Valley Authority.
(8)	State Highway Agency.
(9)	USGS, FEMA Flood Studies.
(10)	University Studies
<b>Sedimentation Data:</b>	
(1)	Water supply papers -- U.S. Department of the Interior, Geological Survey, Quality of Water branch.
(2)	Reports -- U.S. Department of the Interior, Bureau of Reclamation; and U.S. Department of the Agriculture, Soil Conservation Service.
(3)	Geological Survey Circulars -- U.S. Department of the Interior, Geological Survey.
<b>Quality of Water Reports:</b>	
(1)	Water supply papers -- U.S. Department of the Interior, Geological Survey, Quality of Water Branch.
(2)	Reports -- U.S. Department of Health, Education, and Welfare, Public Health Service.
(3)	Reports -- State Public Health Departments.
(4)	Water Resources Publications -- U.S. Department of the Interior, Bureau of Reclamation.
(5)	Environmental Protection Agency, regional offices.
(6)	State Water Quality Agency.
<b>Irrigation and Drainage Data:</b>	
(1)	Agricultural census reports -- U.S. Department of Commerce, Bureau of the Census.
(2)	Agricultural Statistics -- U.S. Department of Agriculture, Agricultural Marketing Service.
(3)	Federal Reclamation Projects -- U.S. Department of the Interior, Bureau of Reclamation.
(4)	Reports and Progress Reports -- U.S. Department of the Interior, Bureau of Reclamation.
<b>Power Data:</b>	
(1)	Directory of Electric Utilities -- McGraw Hill Publishing Co.
(2)	Directory of Electric and Gas Utilities in the United States -- Federal Power Commission.
(3)	Reports -- various power companies, public utilities, State power commissions, etc.

Table 8.2. List of Data Sources.

**Basin and Project Reports and Special Reports:**

- (1) U.S. Department of the Army, Corps of Engineers.
- (2) U.S. Department of the Interior, Bureau of Land Management, Bureau of Mines, Bureau of Reclamation, Fish and Wildlife Service, and National Park Service.
- (3) U.S. Department of Agriculture, Soil Conservation Service.
- (4) U.S. Department of Health, Education, and Welfare, Public Health Service.
- (5) State Departments of Water Resources, Departments of Public Works, power authorities, and planning commissions.

**Environmental Data:**

- (1) Sanitation and public health -- U.S. Department of Health, Education, and Welfare, Public Health Service; State Departments of Public Health.
- (2) Fish and Wildlife -- U.S. Department of the Interior, Fish and Wildlife Service; State Game and Fish Departments.
- (3) Municipal and Industrial Water Supplies -- City Water Departments; State Universities; Bureau of Business Research; State Water Conservation Boards or State Public Works Departments; State Health Agencies; Environmental Protection Agency, Public Health Service.
- (4) Watershed Management -- U.S. Department of Agriculture, Soil Conservation Service, Forest Service; U.S. Department of the Interior, Bureau of Land Management, Bureau of Indian Affairs.
- (5) State Highway Administration.

## 8.4 COMPUTERIZED LITERATURE AND DATA SEARCH

Recent literature information can be retrieved from computerized databases of technical information. The principal databases related to highway and river environment are: COMPENDEX, ENVIRONMENTAL BIBLIOGRAPHY, CIVIL ENGINEER DATABASE, WATER RESOURCES ABSTRACTS, TRIS, and GeoRef.

### 8.4.1 COMPENDEX

1970 - Present, monthly updates (Engineering Information, Inc., Hoboken, New Jersey). The COMPENDEX database is the electronic version of the Engineering Index (Monthly/Annual), which provides abstracted information from the world's significant engineering and technological literature. The COMPENDEX database provides worldwide coverage of approximately 3,500 journals and selected government reports and books.

### 8.4.2 ENVIRONMENTAL BIBLIOGRAPHY

1971 - Present, bimonthly updates (Environmental Studies Institute of the International Academy, Santa Barbara, California). The ENVIRONMENTAL BIBLIOGRAPHY covers the fields of general human ecology, atmospheric studies, energy, land resources, water resources, and nutrition and health. More than 400 periodicals are currently indexed in ENVIRONMENTAL BIBLIOGRAPHY and the database includes more than 1,000 journals.

### **8.4.3 CIVIL ENGINEERING DATABASE**

1973 - Present, The Civil Engineering Database is designed to provide easy bibliographic access to all American Society of Civil Engineers ASCE publications. The database covers ASCE documents published since 1973. It provides access to all the journals, conference proceedings, books, standards, manuals, magazines, and newsletters. Engineering subject areas include: Aerospace Engineering, Architectural Engineering, Bridges, Cold Regions, Computer Practices, Construction, Earthquake Engineering, Education, Engineering Mechanics, Environmental Engineering, Forensic Engineering, Geotechnical Engineering, Highways, Hydrology, Hydraulics, Irrigation and Drainage, Management, Materials Engineering, Structural Engineering, Transportation, Urban Planning, Water Resources, Waterway, Port, Coastal, and Ocean Engineering.

### **8.4.4 WATER RESOURCES ABSTRACTS**

1967 - Present, monthly updates (U.S. Dept. of the Interior, Washington, D.C.) WATER RESOURCES ABSTRACTS is prepared from materials collected by over 50 water research centers and institutes in the United States. The file covers a wide range of water resource topics including water resource economics, ground and surface water hydrology, metropolitan water resources planning and management and water-related aspects of nuclear radiation and safety. The collection is particularly strong in the literature on water planning (demand, economics, cost allocations), water cycle (precipitation, snow, groundwater, lakes, erosion, etc.), and water quality (pollution, waste treatment). WRA covers predominantly English-language materials and includes monographs, journal articles, reports patents, and conference proceedings.

### **8.4.5 TRIS**

TRIS is the Transportation Research Information Services data base, a computerized information file maintained and operated by the Transportation Research Board (TRB) of the National Research Council. It is sponsored by the U.S. Department of Transportation's Federal Highway Administration, Federal Transit Administration, and National Highway Traffic Safety Administration; the highway and transportation departments of the fifty states, the District of Columbia and Puerto Rico; the U.S. Army Corps of engineers; the American Automobile Manufacturers Association; the National Asphalt Pavement Association; and the Association of American Railroads.

TRIS contains information on transportation modes and practices, including planning, design, finance, construction, maintenance, equipment, traffic, operations, management, and marketing. TRIS contains more than 350,000 abstracts of completed research and summaries of research projects in progress. More than 1,000 journals are scanned for TRIS. Primary domestic information sources include the U.S. Department of Transportation's Federal Highway Administration and Federal Transit Administration; the U.S. Congress; the U.S. General Accounting Office; trade and professional associations; universities; research institutes; and other regional and state organizations. International information sources include the International Union of Public Transport, the European Conference of Ministers of Transport, and the Organization for Economic Cooperation and Development.

#### **8.4.6 GeoRef**

GeoRef is an international resource for bibliographic information about geology and geosciences. It is a comprehensive database of citations established by the American Geological Institute (AGI) in 1966. The purpose of GeoRef is to facilitate research and development and to meet the needs of the geoscience community. GeoRef provides access to over 1.8 million references to articles, books, maps, conference papers, reports, and theses, covering the geology of North America from 1785 to the present. It includes more than 3,500 journals in 40 languages and references to all publications of the U.S. Geological Survey.



## CHAPTER 9

### DESIGN CONSIDERATIONS FOR HIGHWAY ENCROACHMENTS AND RIVER CROSSINGS

#### 9.1 INTRODUCTION

The objective of this chapter is to present applications of the fundamentals of hydraulics, hydrology, fluvial geomorphology, and river mechanics to the hydraulic and environmental design of river crossings and highway encroachments. The principal factors to be considered in design are presented, followed by a discussion of the procedures recommended for the evaluation, analysis and design of river crossings and encroachments. The design of most complex problems in river engineering can be facilitated by a qualitative evaluation combined with a quantitative analysis. In most cases, the systematic approach of a qualitative assessment of channel response, followed by a quantitative estimate, is necessary for a meaningful analysis of complex river response problems.

This chapter contains several hypothetical cases of river environments and their response to crossings and encroachments based upon geomorphic principles given in Chapter 5. These cases indicate the trend of change in river morphology for given initial conditions. The hypothetical cases are followed by actual case histories for river crossings in the United States. These histories document river response to highway crossings and encroachments and illustrate river response qualitatively.

This chapter uses two types of examples (conceptual and actual examples) related to river crossings and highway encroachments. Applications of the basic principles developed in Chapters 1 through 8 are illustrated by these conceptual examples and specific case histories related to the subject matter of this manual.

#### 9.2 PRINCIPAL FACTORS TO BE CONSIDERED IN DESIGN

Identification of the principal factors to be considered in design of river crossings and encroachments is useful. These factors are generally interrelated, and fundamental mechanisms and relationships of the governing physical processes must be clearly understood prior to design.

##### 9.2.1 Types of Rivers

In selecting the site for a crossing or an encroachment on a river it is necessary to give detailed consideration and study to the type of river or rivers involved. A sandbed river may be meandering, it may be essentially straight, or it may be braided. In addition, a meandering river may be small, medium, or large. The same channel can be classified as youthful, mature, or old. Each of these different river types requires different design procedures. For example, in designing training works for large sandbed channels (braided or meandering) it is unlikely that Kellner jetties alone will be useful to stabilize the bank alignment (see Chapter 6). It may be necessary to stabilize the banks with rock riprap and to control the overbank flows using jetties to achieve a set of specific purposes. Gravel and cobble bed channels are

normally considerably steeper than sandbed channels and in general have narrower river valleys. In the extreme are torrential rivers, the beds of which are comprised of large rocks. This type of river usually exists in a youthful or canyon type environment near the upper end of large river systems where the slopes are relatively steep.

### **9.2.2 Location of the Crossing or Encroachment**

In selecting the site of a crossing or a longitudinal encroachment, several considerations are necessary. First, the crossing or encroachment must mesh with the transportation system in the area. Second, environmental factors must be considered. In fact, unless appropriate weight is given to the environmental impacts it may not be possible to obtain permission to proceed with the project at all. Economic considerations are equally important. Depending upon the characteristics of the river and the environmental considerations, the cost of a particular crossing or encroachment can be significantly affected by its location. The length of the approaches versus the length of the crossing, the cost of real estate that must be acquired to accomplish the crossing, the maintenance cost required to keep the crossing functional over its estimated life, and the method of construction are some of the specific aspects that should be considered in locating the crossing. The cost of protective measures should also be considered in locating an encroachment.

### **9.2.3 River Characteristics**

The subclassifications of river form can be utilized to identify the range of conditions within which the particular river operates. It is necessary to determine if a river is relatively stable in form or is likely to be unstable. In Figure 1.3 of Chapter 1, it was pointed out that rivers can be essentially poised so that a small change in discharge characteristics can change a river from meandering to braided or vice versa. It is important to know the sensitivity of any river system to change. Criteria given in Chapter 5, for example Figure 5.18, or Chapter 3, Figure 3.13, can be used to predict this sensitivity. A meandering stream whose slope and discharge plot close to the braided river line in Figure 5.18 may change to a braided stream with a small increase in discharge or slope (see also Section 5.5.3).

In addition to river form, it is important to determine other characteristics of the channel: that is, the channel may have a sand bed and cohesive banks; it may be formed in cobbles or it may be formed in other combinations of these materials. Each of these river systems behaves differently depending upon the characteristics of the floodplain material, the bank material, and the bed material of the river both over the short term and the long term. Hence, a detailed survey of the characteristics of the bed and bank material coupled with river form plus other pertinent information are essential to design.

### **9.2.4 River Geometry**

For planning a river crossing or an encroachment it is important to know the river geometry and its variation with discharge and time. It is essential to know the slope of the channel and, preferably, the energy gradient through the reach. In Chapter 5, relations were presented that illustrate how width and depth vary with stage at-a-section as well as along the length of a

channel. For most rivers, if the appropriate hydraulic and hydrologic data are available, it is possible to develop simple relations showing how width and depth vary with discharge.

### **9.2.5 Hydrologic Data**

It is necessary to gather all of the hydrologic data pertinent to the behavior of the river and to the design of the river crossing or encroachment. As pointed out in Chapter 8, records of the flood flows are essential. From such information, flow duration curves can be developed, seasonal variations in the river system can be considered, and design discharge values can be established depending upon the discharge frequency criteria used in the design.

Also, it is important to consider the low flows that the river channel will be subjected to and the possible changes in flow conditions that may be imposed on the river system as a consequence of water resources development in the area. Sometimes low flows may lead to a more severe local scour situation at bridge piers and footings. Finally, in terms of hydrologic data it is usually necessary to synthesize some of the required data. Conventional techniques may be used to fill in missing records or it may be essential to synthesize records where limited hydrologic data exist. In synthesizing data it is very important to compare the particular watershed with other watersheds having similar characteristics. With this information, reasonably good estimates of what can be anticipated at the site can be established.

### **9.2.6 Hydraulic Data**

At the site of a crossing or a longitudinal encroachment, it is essential to know the discharge and its variation over time. Coupled with this, it is necessary to know the velocity distribution across the river cross-section and its variation in the river system. This involves determining the type of velocity distribution across the channel as well as in the vertical. Knowledge of the distribution of velocities should be coupled with a study of changes in position of the thalweg to estimate the severity of attack that may occur along the river banks and in the vicinity of the crossing. Furthermore, it is essential to develop stage-discharge relations since these relations fix key elevations of the structure in design and serve as bench-mark data when considering channel protection measures that may alter the stage of the river. Large changes in velocity can occur in a river system with changing discharge and stage. In a sandbed river, as flow conditions bring about a transition from lower regime to upper regime, the average velocity in the cross section may actually double. From another viewpoint, changes induced in the river system, such as those due to artificial cutoffs or channelization, may sufficiently steepen the gradient so the river operates in upper regime over its whole range of discharge. These possibilities must be considered in the detailed design.

### **9.2.7 Characteristics of the Watershed**

The water flowing in the river system and the sediment transported with the flow are usually intimately related to the watershed feeding the river system. Consequently, one needs to study the watershed considering its geology, geometry and land use. In the case of development, land uses include recreation, industrial development, urbanization, flood control, agriculture, and grazing. Similarly, one needs to consider the vegetation cover on the watershed and the watershed response to changes in vegetation cover by human activities or by climatic changes.

Significant changes in vegetation cover affect the amount of sediment delivered from the watershed to the river system. One of the most common techniques to study the sources of sediment in a watershed is to employ aerial photography and remote sensing techniques coupled with ground investigations. The utilization of remote sensing techniques enables the skilled observer to determine which areas of the watershed are stable and which are unstable. Viewing the total watershed from this perspective and using water and sediment routing techniques, it is possible to evaluate the sediment yield as a function of time.

### **9.2.8 Flow Alignment**

In order to design a safe crossing or longitudinal encroachment, it is necessary to consider the flow alignment in detail. The direction of flow must be considered as a function of time. The position of the thalweg will vary with low, intermediate and high stages. The changing characteristics of the river with stage, such as the change in velocity distribution, the position of the thalweg, and the river form can have a significant effect on the intensity of attack on the approaches, the abutments, the piers and embankments. The detailed study of the behavior of the river over time and with varying discharge is necessary for proper design of training works. Two-dimensional computer modeling, or in some cases physical modeling, as discussed in Chapter 5 can provide the detailed hydraulic data to support design. Only with this type of information can one adequately consider the intensity of attack, the duration of attack and the necessity for training works to make the river system operate within a range of conditions acceptable at the crossing or encroachment. Certainly, changes over time at a particular crossing affect the channel geometry, the geometry of the crossing itself, general scour and local scour. If the characteristics of the flow and how they vary with time are known, then the information in Chapter 6 can be utilized to design against excessive contraction and local scour in order to make the highway functional with minimum maintenance over the life of the project.

### **9.2.9 Flow on the Floodplain**

Up to this point the concern has been principally with flow in the main channel. However, design floods usually flow in both the main channel and on the floodplain. Only by studying the characteristics and geometry of the river and the floodplain can one determine the type of flows that are apt to occur on the floodplain. This particular topic should be studied in adequate detail so that the magnitude and intensity of the flows on the floodplain can be approximated. The characteristics of flow on the floodplain are especially relevant to the design of longitudinal encroachments. As an example, consider a sinuous channel. At flood stage there is a tendency for the water to flow in the main channel in such a way as to develop chute channels across the point bars. Often, the water spills over the outside of the bends onto the floodplain. Flow conditions on the floodplain and in the main channel can be greatly different at flood stage than at low flow, and this must be taken into consideration. Again, 2-dimensional computer modeling, as discussed in Chapter 5, can provide detailed hydraulic data on overbank and floodplain flows.

### **9.2.10 Site Selection**

Most of the factors cited in the preceding sections have a bearing on the final site selection. In summary, such factors as the form of the river, the alignment of the river, variations of the river form over time, the type of bed and bank material, the hydrologic and hydraulic characteristics of the river, and past, present and future watershed conditions are all important inputs to the site selection. In addition, it is necessary to consider the requirements of the area to be served and the economic and environmental factors that relate to the crossing. Having made a detailed study of possible alternate sites, and having determined the best site considering these important factors, one can then proceed with the determination of the geometry and length of the approaches to the crossing, the type and location of the abutments, the number and location of the piers, and the depth of structural support for the piers to insure against danger from local scour. The location of the longitudinal encroachment in the floodplain, the amount of allowable longitudinal encroachment into the main channel, and the requirement for river training works all need to be considered.

### **9.2.11 Channel Stability Investigations**

In conjunction with the background information discussed in the preceding paragraphs, it is essential to determine the need for bank stabilization. The location, selection, and design of various types of river training works must be considered. The selection of training works is significantly affected by the characteristics of the river and the river system itself. The magnitude of local scour at the training structure must be considered. The possible necessity of holding the river in a selected alignment must also be adequately explored. With regard to these particular issues, the principles of Chapter 6 can be applied to develop suitable designs for stabilizing the approaches and banks of the main channel, and the design of training works that assist in controlling the alignment of the river relative to the crossing or longitudinal encroachment. Hydraulic Engineering Circular (HEC) No. 23 (Lagasse et al. 2001) also provides experience, selection, and design guidance for a variety of river training works and their applicability under a range of characteristics of the river environment.

### **9.2.12 Short-Term Response**

Having completed the tentative design of the crossing or the encroachment based on river form, channel geometry, hydrologic and hydraulic data; it is essential to consider the short-term response of the river system to construction. Similarly, existing or proposed developments up- and downstream of the site and at the site itself should also be considered.

The techniques that may be utilized to investigate the short-term response at the site or in the vicinity of the crossing or encroachment involve the utilization of qualitative geomorphic relationships followed by the application of more sophisticated analyses using the principles presented in the chapters on open channel flow, sediment transport and river mechanics. As discussed in Chapter 5, it is possible to establish a mathematical model designed to route both water and sediment through the system. If this model is appropriately designed and utilized, it is possible to evaluate the response of the river system to both the construction of the crossing or encroachment and to other river development projects in the immediate area.

For example, it may be important to establish the pattern of clear-water releases from a dam upstream of a crossing. Knowing the type of flow the channel would be subjected to and that the water being released is clear, one can make an estimate of the extent of degradation in

the channel, the amount of sediment derived from the bed and bank, the instability of the banks and even the types of lateral shifting that may be induced in the river system as it affects the crossing or encroachment.

### **9.2.13 Long-Term Response**

The long-term river response at a crossing or a longitudinal encroachment and in the river system itself should be considered based on all river development projects including the highway. This type of treatment is, in general, beyond the scope of this particular manual. Nevertheless, significant advances have been made pertaining to the mathematical modeling of river systems, considering both their short and long-term response. Mathematical modeling can be time consuming and expensive, requiring a substantial amount of additional data for calibration of the model. However, this approach is worth considering on important projects where determining long-term response may be critical to project success (see Section 5.6).

## **9.3 PROCEDURE FOR EVALUATION AND DESIGN OF RIVER CROSSINGS AND ENCROACHMENTS**

This section presents a summary of a general procedure to evaluate and design river crossings and encroachments. Due to the multi-disciplined complexity of these problems, it is difficult to develop a procedure which is applicable to all situations that may be encountered. A generalized approach can be described; however, modification to this procedure must be made to tailor the procedure to an individual project.

### **9.3.1 Approach to River Engineering Projects**

The evaluation and design of river crossings should proceed from a broad evaluation of the characteristics of the river and the principles to be considered in design (described in Section 9.2) to detailed computations and analysis. The evaluation should begin with a qualitative assessment of the river. As the analysis progresses, the analysis becomes more and more detailed and subsequently more quantitative. At all stages of the investigation and design, qualitative evaluation is important to determine, if possible, the interrelationship of all aspects of the project.

The three-level procedure outlined in HEC-20 (Lagasse et al. 2001) and illustrated in Figure 9.1 is the recommended approach for evaluating projects in the river environment. The method begins with broad considerations and proceeds through a series of steps of increasing complexity to narrow down to the finer points of the project. Additionally, this approach provides for back checking or "feedback" loops to insure that the interdependence of all the variables is continually adjusted (see HEC-20, Chapters 1 and 3) (see also Figure 7.1).

In Level 1, the analysis consists of: (1) identifying the goals of the project; (2) developing several options to achieve those goals; (3) determining the problems and possible solutions to problems associated with each option; and (4) performing a qualitative assessment of all aspects of the project.

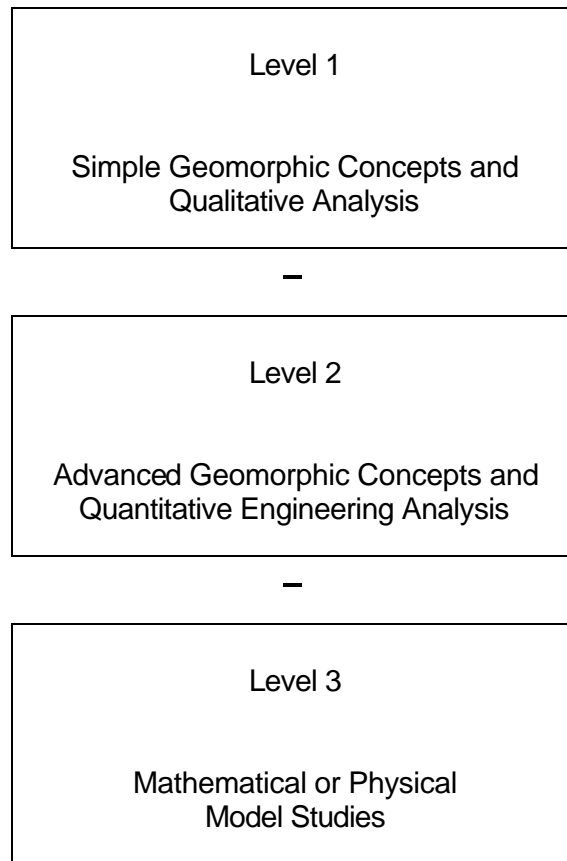


Figure 9.1. Three-level analysis procedure for river engineering studies.

A Level 2 analysis involves a more detailed qualitative analysis combined with a quantitative evaluation. Computation of water surface profiles using 1-dimensional computer models can be included in this level of analysis. In many cases, the evaluation and analysis can be considered adequate at this level if the goals are met, the interrelationship between different aspects of the project and river system are adequately explained and all of the problems resolved.

A Level 3 analysis involves mathematical or physical modeling of water and sediment. These procedures are not always necessary. Water can be modeled using a steady or unsteady flow rigid boundary flow model. In some cases, a movable boundary flow model can be employed, routing both water and sediment through the study reach. Sediment routing models will require a substantial historic data set and analysis time to calibrate and verify the model. Experienced modelers should be employed if sediment routing is to be performed.

### 9.3.2 Project Initiation

The success of a project can be dramatically influenced by careful planning in the initial stages of the project. The following guidelines will help insure the success of the project.

Develop a Project Concept. When the project is conceived the goals of the project should be carefully defined and several options to meet these goals identified. The factors discussed in Section 9.2. should be considered when identifying design options. These options will be refined as the project progresses, eventually focusing on one or two options.

Assemble Available Data. All available data should be compiled and checked. The data checklist presented in Chapter 8 should be used as a guide. Data which is unavailable or has periods of missing data should also be listed on the checklist. Missing data can be ranked according to need (i.e., essential, nonessential and optional). Field programs designed to collect the essential data could be implemented at this time, however it is recommended that a field reconnaissance and evaluation be completed prior to implementing field programs. The field reconnaissance will provide a clearer definition of the project and will influence the types and quantity of additional data requirements.

Conduct a Field Reconnaissance. An initial field reconnaissance should be performed by a small group of technical personnel. It is advisable that the group be multi-disciplined so that geologic, geomorphic, hydrologic, hydraulic, alignment and highway constraints can be identified. They should define the problems for each option and identify possible solutions to each problem. Options which are least feasible should be eliminated. Detailed procedures and check lists for a field reconnaissance that considers most geomorphic factors important to river engineering analyses are provided in HEC-20 (Lagasse et al. 2001). The field reconnaissance team should identify the most favorable options, recommend the types of analyses which will be needed, and design field programs to collect specific data which will be required by the analysis.

Collect Additional Field Data. Field programs should be designed to collect only data that will be required to analyze and design the project. The field reconnaissance discussed previously is an important tool for the design and implementation of efficient field programs. By designing and implementing field programs after the field reconnaissance, the collection of unnecessary data can be avoided, providing more time and funding for collection of essential data.

It is also advisable that the field crews be supervised in the field by personnel who will be directly involved in the analysis and design. These personnel should be completely familiar with the types of data and the methods used to collect the data, providing an interface between the field and the analysis in the office. In this way, the field work, analysis, and design can be closely coordinated.

#### **9.4 CONCEPTUAL EXAMPLES OF RIVER ENCROACHMENTS**

This section discusses conceptual examples of river response to highway encroachments. Sixteen hypothetical cases are tabulated in Table 9.1. Each individual case is identified in the first column to show the physical situation that exists prior to the construction of the highway crossing. In the following three columns some of the major effects (local, upstream, and downstream) resulting from construction of a particular crossing are given. Only the gross local, upstream and downstream effects are identified in this table. In an actual design situation, it is worthwhile first of all to consider the gross effects as listed in Table 9.1 (Level 1 analysis).



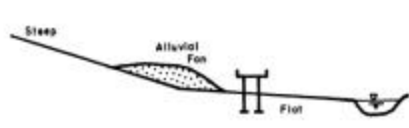
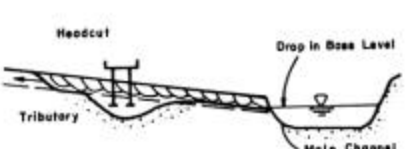
The Lane relation  $QS \sim Q_s D_{50}$  (Equation 5.28) is one method for determining qualitative river response. Having identified the qualitative response that can be anticipated, other river mechanics techniques can be used to predict the possibility of change in river form and to estimate the magnitude of local, upstream and downstream river response.

The initial river conditions in Table 9.1 include storage dams or water diversions. These examples are used as illustrations relating to common experience. In general, the effect of a storage reservoir is to cause a sudden increase of base level for the upstream section of the river. The result is aggradation of the channel upstream, degradation downstream and a modification of the flow hydrograph. Similar changes in the channel result if the base level is raised by some other mechanism, say a tectonic uplift. The effect of diversions is to decrease the river discharge downstream of the diversion with or without an overall reduction of the sediment concentration. Similarly, changes in water and sediment input to a river often occur due to river development projects upstream from the proposed crossings or due to natural causes.

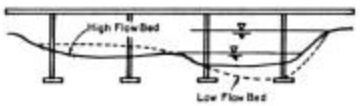
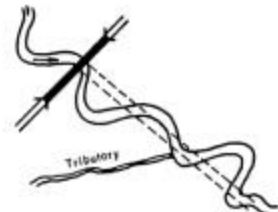
Case (1) of Figure 9.1 involves the construction of a bridge across a tributary stream downstream of where the steeper tributary stream has reached the floodplain of the parent stream. In most cases, the change in gradient of the tributary stream causes significant deposition. In the case illustrated for Case (1), an alluvial fan develops which in time can divert the river around the bridge, or, if the water continues to flow under the bridge, the waterway is significantly reduced, endangering the usefulness and stability of the structure. Usually, streams on alluvial fans shift laterally so that the future direction of the approach flow to the bridge is uncertain.

Case (2) sketched in Table 9.1 illustrates a situation where a bridge is constructed across a tributary stream. The average water surface elevation in the main channel acts as the base level for the tributary. It is assumed that at some point in time after the construction of the bridge the base level in the main channel has been lowered. Under the new condition, the local gradient of the tributary stream is significantly increased. This increased energy gradient induces head cutting and causes a significant increase in water velocities in the tributary stream. The result is bank instability, possible major changes in the geomorphic characteristics of the tributary stream and increased local scour. When the base level is raised the gradient in the tributary is decreased, resulting in deposition, lateral channel instability, increased flood levels, and a decrease in flow area under the bridge, similar to Case (1).

Case (3) illustrates a situation where a bridge supported by piers and footings is constructed across a channel that is subjected to long periods of low stage. When a river is subject to long periods of low flows, there is a tendency for the low flow to develop a new low-water thalweg in the main channel. If the low-water channel aligns itself with a given set of piers, it is possible that the depth of local scour resulting from this flow condition may be greater than the depth of local scour at high stage. There are several documented failures where bridges have been safe in terms of local scour at high stage, but have failed as a consequence of the development of greater local scour during low-flow periods.

Bridge Location	Local Effects	Upstream Effects	Downstream Effects
 <p>(1) Crossing downstream of an alluvial fan</p>	<ul style="list-style-type: none"> <li>1 - Fan reduces waterway</li> <li>2 - Direction of flow at bridge site is uncertain</li> <li>3 - Channel location is uncertain</li> </ul>	<ul style="list-style-type: none"> <li>1 - Erosion of banks</li> <li>2 - Unstable channel</li> <li>3 - Large transport rate</li> </ul>	<ul style="list-style-type: none"> <li>1 - Aggradation</li> <li>2 - Flooding</li> <li>3 - Development of tributary bar in the main channel</li> </ul>
 <p>(2) Lowering of base level for the channel</p>	<ul style="list-style-type: none"> <li>1 - Headcutting</li> <li>2 - General scour</li> <li>3 - Local scour</li> <li>4 - Bank instability</li> <li>5 - High velocities</li> </ul>	<ul style="list-style-type: none"> <li>1 - Increased velocity</li> <li>2 - Increased bed material transport</li> <li>3 - Unstable channel</li> <li>4 - Possible change of form of river</li> </ul>	<ul style="list-style-type: none"> <li>1 - Increased transport to main channel</li> <li>2 - Aggradation</li> <li>3 - Increased flood stage</li> </ul>

Case (4) illustrates a situation where artificial cutoffs have straightened the channel downstream of a particular crossing. Straightening the channel downstream of the crossing significantly increases the channel slope. This causes higher velocities, increased bed material transport, degradation and possible head cutting in the vicinity of the structure. This can result in unstable river banks and a braided streamform. The straightening of the main channel can drop the base level, adversely affecting tributary streams flowing into the straightened reach of the main channel, which was discussed in Case (2).

Bridge Location	Local Effects	Upstream Effects	Downstream Effects
 <p>(3) Channel characterized by prolonged low flows</p>	<ul style="list-style-type: none"> <li>1 - At low flow a low water channel develops in river bed</li> <li>2 - Increased danger to piers due to channelization and local scour</li> <li>3 - Bank caving</li> </ul>	-----	-----
 <p>(4) Cutoffs downstream of crossing</p>	<ul style="list-style-type: none"> <li>1 - Steeper slope</li> <li>2 - Higher velocity</li> <li>3 - Increased transport</li> <li>4 - Degradation and possible headcutting</li> <li>5 - Banks unstable</li> <li>6 - River may braid</li> <li>7 - Danger to bridge foundation from degradation and local scour</li> </ul>	See local effects	<ul style="list-style-type: none"> <li>1 - Deposition downstream of straightened channel</li> <li>2 - Increase in flood stage</li> <li>3 - Loss of channel capacity</li> <li>4 - Degradation in tributary</li> </ul>

Case (5) illustrates the situation where a bridge is constructed across a river immediately downstream of the confluence with a steep tributary. The tributary introduces relatively large quantities of bed material into the main channel. As a result, an island has formed in the main channel and divided flow exists. In order to reduce the cost of the bridge structure, the bridge is built across one subchannel to the island or bar formed by deposition, closing the secondary channel. Such a procedure forces all of the water and sediment to pass through a reduced width. This contraction of the river in general increases the local velocity, increases general and local scour, and may increase bank instability. In addition, the contraction can change the alignment of the flow in the vicinity of the bridge and affect the downstream channel for a considerable distance. A chute channel can develop across the second point bar downstream, adversely affecting several meander loops downstream. Upstream of the bridge, there is aggradation. The amount depends on the magnitude of water and sediment being introduced from the tributary. Also, there is an increase in the backwater upstream of the bridge at high flows which in turn affects other tributaries farther upstream of the crossing, see Case (2).

Case (6) illustrates a situation where the main channel is realigned in the vicinity of the bridge crossing. A cutoff is made to straighten the main channel through the selected bridge site. As discussed in Case (4), increased local gradient, local velocities, local bed material transport, and possible changes in the characteristics of the channel are expected due to the new conditions. As a result the channel may braid. A short cut off section (1 or 2 bends) can be designed to transport the same sediment loads that the river is capable of carrying upstream and downstream of the straightened reach; however, it may be difficult to achieve stability when multiple bends in a long reach are cut off.

It is possible to build modified reaches of main channels that do not introduce major adverse responses due to local steepening of the main channel. In order to design a straightened channel so that it behaves essentially as the natural channel in terms of velocities and magnitude of bed material transport, it is usually necessary to build a wider, shallower section.

Case (7) illustrates a bridge constructed across a main channel. Subsequently, the base level for the channel is raised by the construction of a dam downstream. Whenever the base level of a channel is raised, a pool is created extending a considerable distance upstream depending on the size of dam and slope of the channel. As the water and sediment being transported by the river encounter this pool, most of the sediments drop out, forming a delta-like structure at the mouth. If the bridge lies within the effects imposed by the new base level, the following response at the crossing will be expected: aggradation of the bed, a loss of waterway at the bridge site, significant changes in river geometry, and increased flood stages and lateral channel instability. This is similar to Case (1).

Case (8) considers the situation where the sediment load is reduced in the channel after a bridge has been constructed. This may happen due to the construction of a storage dam upstream of the crossing. As stated in the preceding case, the raising of the base level of a river, as in the development of storage by constructing a dam on a river, provides a sedimentation basin for the water flowing in the system. In most instances, all of the sediment coming into a reservoir drops out within the reservoir. Water released from the reservoir is mostly clear. With sediment-free flow, the channel is too steep and bed sediments are entrained from the bed and the banks causing significant degradation. If the bridge is sufficiently close to the reservoir to be affected by the degradation in the channel, the depth due to general and local scour at the bridge may be significantly increased. Also, the channel banks may become unstable due to degradation, and there is a possibility that the river, as its profile flattens, may change its form. In the extreme case, it is possible that the degradation may cause failure of the dam and the release of a flood wave.

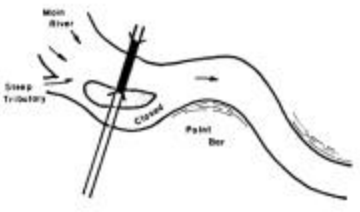
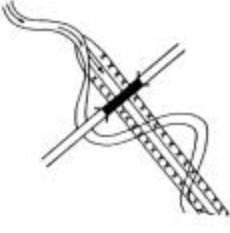
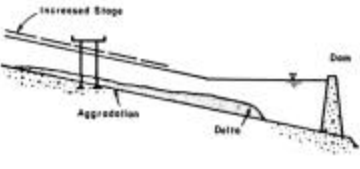
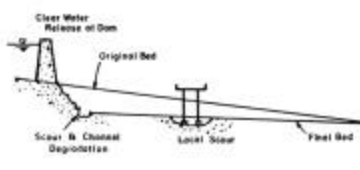
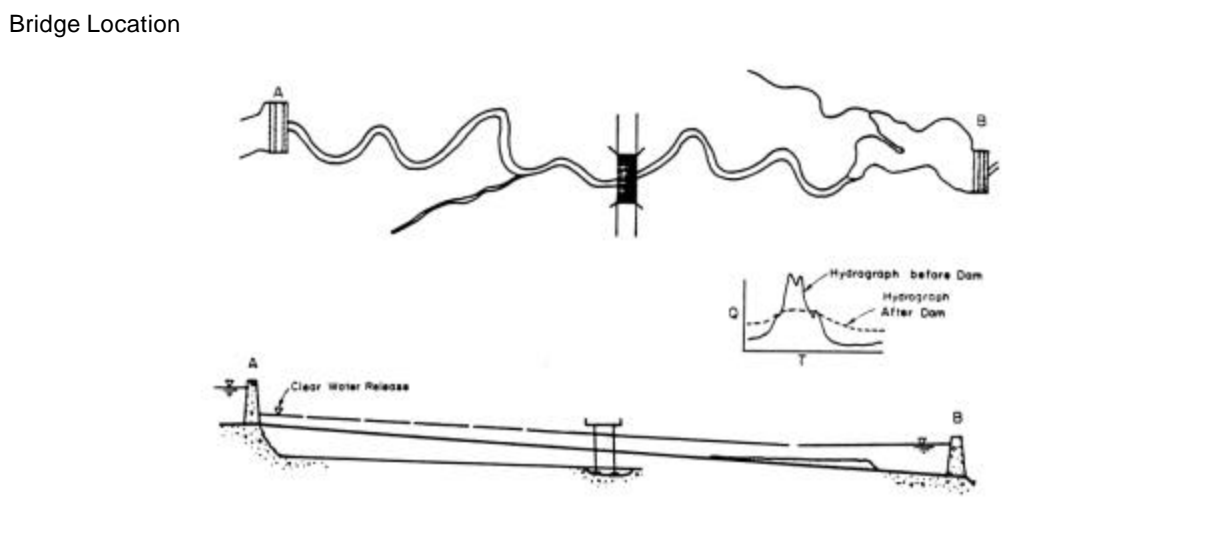
Table 9.1. River Response to Highway Encroachments and to River Development (continued).			
Bridge Location	Local Effects	Upstream Effects	Downstream Effects
 <p>(5) Excess of sediment at bridge site due to upstream tributary</p>	<ol style="list-style-type: none"> <li>1 - Contraction of the river</li> <li>2 - Increased velocity</li> <li>3 - General and local scour</li> <li>4 - Bank instability</li> </ol>	<ol style="list-style-type: none"> <li>1 - Aggradation</li> <li>2 - Backwater at flood stage</li> <li>3 - Changed response of tributaries</li> </ol>	<ol style="list-style-type: none"> <li>1 - Deposition of excess sediment eroded at downstream of the bridge</li> <li>2 - More severe attack at first bend downstream</li> <li>3 - Possible development of a chute channel across the second point bar downstream of the bridge</li> </ol>
 <p>(6) River channel relocation at crossing site</p>	<ol style="list-style-type: none"> <li>1 - None if straight section is designed to transport the sediment load of the river and if it is designed to be stable when subjected to anticipated flow. Otherwise same as in Case (4)</li> </ol>	<ol style="list-style-type: none"> <li>1 - Similar to local effects</li> </ol>	<ol style="list-style-type: none"> <li>1 - Similar to local effects</li> </ol>

Table 9.1. River Response to Highway Encroachments and to River Development (continued).			
Bridge Location	Local Effects	Upstream Effects	Downstream Effects
 <p>(7) Raising of river base level</p>	<ol style="list-style-type: none"> <li>1 - Aggradation of bed</li> <li>2 - Loss of waterway</li> <li>3 - Change in river geometry</li> <li>4 - Increased flood stage</li> <li>5 - Lateral channel instability</li> </ol>	<ol style="list-style-type: none"> <li>1 - See local effects</li> <li>2 - Change in base level for tributaries</li> <li>3 - Deposition in tributaries near confluences</li> <li>4 - Aggradation causing a perched river channel to develop or changing alignment of main channel</li> </ol>	<ol style="list-style-type: none"> <li>1 - See upstream effects</li> </ol>
 <p>(8) Reduction of sediment load upstream</p>	<ol style="list-style-type: none"> <li>1 - Channel degradation</li> <li>2 - Possible change in river form</li> <li>3 - Local scour</li> <li>4 - Possible bank instability</li> <li>5 - Possible destruction of structure due to dam failure</li> </ol>	<ol style="list-style-type: none"> <li>1 - Degradation</li> <li>2 - Reduced flood stage</li> <li>3 - Reduced base level for tributaries, increased velocity and reduced channel stability causing increased sediment transport to main channel</li> </ol>	<ol style="list-style-type: none"> <li>1 - Degradation</li> <li>2 - Increased velocity and transport in tributaries</li> </ol>

Case (9) through Case (13) illustrate a more complicated set of circumstances. These cases involve the interrelationship of Cases (1) through (8). In Case (9) the river crossing is affected by Dam A constructed upstream as well as Dam B constructed downstream. As documented in Case 8, Dam A causes significant degradation in the main channel. Dam B causes aggradation in the main channel (Case 7). The final condition at the bridge site is estimated by summing the effects of both dams on the main channel and the tributary flows. Normally, this analysis requires water and sediment routing techniques studying both long- and short-term effects of the construction of these dams, and it is necessary to consider the extreme possibilities to develop a safe design.

Table 9.1. River Response to Highway Encroachments and to River Development (continued).



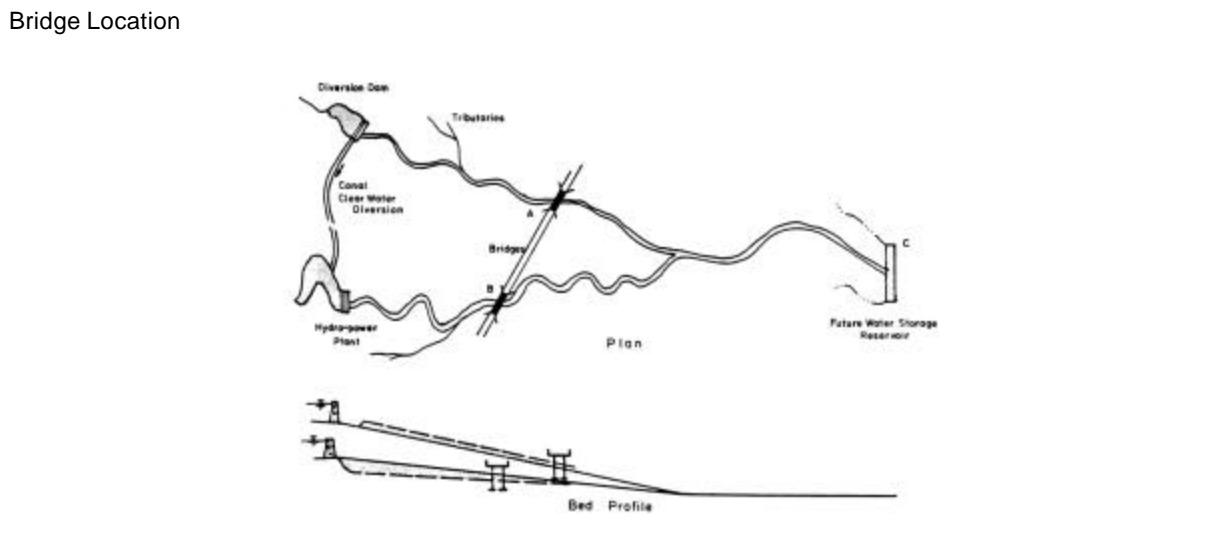
(9) Combined increase of base level and reduction of sediment load upstream

Local Effects	Upstream Effects	Downstream Effects
1 - Dam A causes degradation 2 - Dam B causes aggradation 3 - Final condition at bridge site is the combined effect of (1) and (2). Situation is complex and combined interaction of dams, main channel and tributaries must be analyzed using water and sediment routing techniques and geomorphic factors	1 - Channel could aggrade or degrade with effects similar to cases (7) and (8)	1 - See upstream effects

In Case (10) Bridges A and B cross two major tributaries a considerable distance upstream of their confluence. Upstream of Bridge A, a diversion structure is built to divert essentially clear water by canal to the adjacent tributary on which Bridge B has been constructed. Upstream of Bridge B the clear water diverted from the other channel enters the storage reservoir and the water from the tributary plus the transfer water is released through a hydro-power plant. It is anticipated that a larger storage reservoir may be constructed downstream of the confluence on the main stem at C. These changes in normal river flows give rise to several possible complex responses at bridge sites A and B, in the tributary systems as well as on the main stem. Bridge Site A may aggrade due to the excess of sediment left in that tributary when clear water is diverted. However, initially there may be

lowering of the channel bed in the vicinity of the diversion structure because of the deposition upstream of the diversion dam and the release of essentially clear water for a relatively short period of time until the sediment storage capacity of the reservoir is satisfied. Bridge site B is subjected to degradation due to the increased discharge and an essentially clear water release. However, the degradation of the channel could induce degradation in the tributaries causing them to provide additional sediment to the main channel, see Case (8). This response would to some degree counteract the degrading situation in this reach of river. Such changes in river systems are not uncommon and introduce complex responses throughout the system. Complete analysis must consider the individual effects and sum them over time to determine a safe design for the crossings.

Table 9.1. River Response to Highway Encroachments and to River Development (continued).

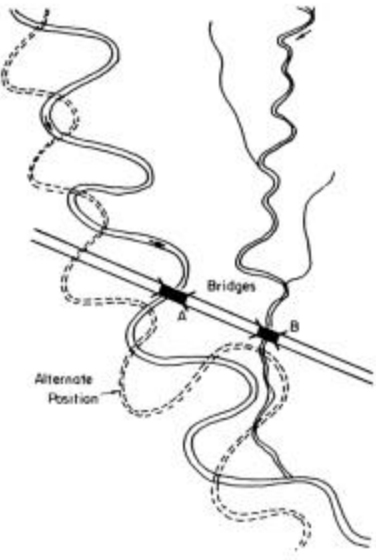


(10) Change in water discharge, no change in sediment load

Local Effects	Upstream Effects	Downstream Effects
1 - Bridge A may be subjected to aggradation due to excess sediment left in the channel by diversion of clear water 2 - Bridge B may be subjected to degradation due to increased discharge in the channel 3 - If a storage reservoir was constructed at C, it could induce aggradation in both main tributaries	1 - Upstream of Bridge A - aggradation and possible change of river form 2 - Upstream of Bridge B - degradation and change of river form 3 - Channel instabilities 4 - Significant effects on flood stage	1 - See upstream effects 2 - Construction of reservoir C could induce aggradation in the main channel and in the tributaries. Effects same as in Case 7

Case (11) shows a highway that crosses the main channel at Bridge A and its tributary at Bridge B. The confluence of the main channel and its tributary is downstream of both bridges. The alignment of the main channel is continually changing. The rate of change in the river system should be evaluated as part of the geomorphic and hydraulic analysis of the site. If the main channel shifts to the alternate position shown and moves the confluence closer to Bridge B, the gradient in the tributary is significantly increased causing degradation as well as channel instabilities and possible changes in river form. Excess sediment from the tributary causes aggradation in the main channel and possibly significant changes in channel alignment.

Table 9.1. River Response to Highway Encroachments and to River Development (continued).

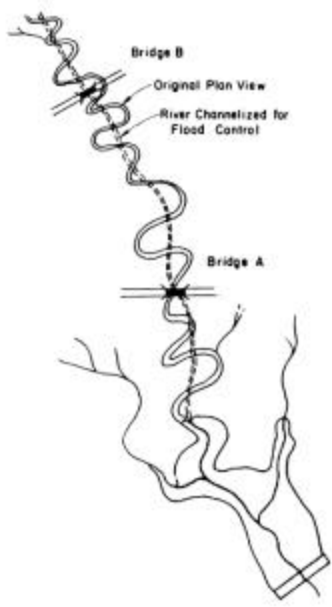
Bridge Location	Local Effects	Upstream Effects	Downstream Effects
 <p>(11) Naturally shifting river channel</p>	<ol style="list-style-type: none"> <li>1 - Rivers are dynamic (ever changing) and the rate of change with time should be evaluated as part of the geomorphic and hydraulic analysis</li> <li>2 - Alignment of main channel continually changes affecting alignment of flow with respect to Bridge A.</li> <li>3 - If the main channel shifts to the alternate position, the confluence shifts and the tributary gradient is significantly increased causing degradation in the tributary. Local effects on Bridge B same as 1, 2, 3, and 4 in Case (8)</li> <li>4 - Excess sediment from the tributary, assuming (3) causes aggradation in the main channel and possible significant changes in channel alignment</li> </ol>	<ol style="list-style-type: none"> <li>1 - The river could abandon its present channel. Changing position of the main channel may require realignment with training works.</li> </ol>	<ol style="list-style-type: none"> <li>1 - See upstream effects</li> <li>2 - Shifts in the position of the main channel relative to the position of the confluence with the tributary alternatively flattens or steepens the gradient of the tributary causing corresponding aggradation and degradation</li> <li>3 - Shifts in the position of the main channel causes aggradation, degradation and instabilities depending upon direction and magnitude of channel change</li> </ol>

Considering the possible changes in the position of the main channel, training works may be required at and upstream of Bridge A to assure a satisfactory approach of the flow to the bridge crossing. Otherwise, the river could abandon its present channel. A shift in the position of the main channel relative to the position of the confluence with the tributary also alternately flattens or steepens the gradient of the tributary causing corresponding aggradation or degradation in the tributary. This type of problem is difficult because of the continuously changing characteristics of such river systems. Rivers of this type are usually stable for several years at a time or at least between major flows. Consequently, if crossing locations are properly selected and appropriate stabilization techniques are taken, it may be possible to maintain the usefulness of the crossings for the life of the structures. However, the disadvantages associated with such locations will often require expensive solutions and these locations should be avoided if possible.

Case (12) illustrates a meandering channel with several tributaries and a major storage reservoir constructed on the main channel upstream of the reservoir. Two crossings are shown on the main channel upstream of the reservoir. It is assumed that complete channelizing of the meandering river has been authorized. This shortens the path of travel of the water by an appreciable distance. Considering local effects at the bridges, bridge site A is first subjected to possibly severe degradation and then aggradation. Bridge site B is primarily subjected to degradation. The magnitude of this degradation can be large. With the degree of straightening indicated in the sketch, severe head cutting may be initiated up the main channel as well as the tributaries. The whole system may be subjected to passage of sediment waves and the river form can dramatically change over time. The flood level in the system and the local and general scour in the vicinity of the bridges is greatly affected by the channelization.

As a result of channelization, the river reach at bridge site B could become braided. Also, in this reach the rate of sediment transport is increased, head cutting is induced and flood stages are reduced. The tributaries in the upper reach are subjected to severe degradation. For the bridge at position A, the channel would probably degrade and then significantly aggrade. Significant reactions are possible when channelization is undertaken in a river system. A detailed analysis of all of the responses is necessary before it is possible to safely design crossings such as those at location A and B.

Table 9.1. River Response to Highway Encroachments and to River Development (continued).

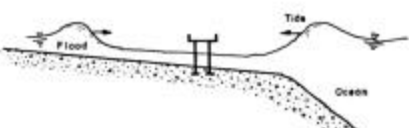
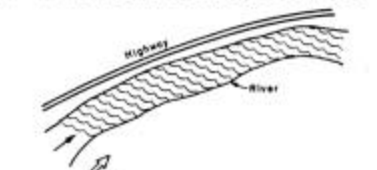
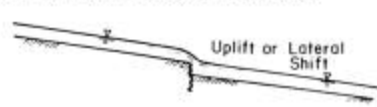
Bridge Location	Local Effects	Upstream Effects	Downstream Effects
 <p>(12) Human-induced reduction of channel length</p>	<ol style="list-style-type: none"> <li>1 - Bridge A is first subjected to degradation and then aggradation. Action can be very severe</li> <li>2 - Bridge B is primarily subjected to degradation. The magnitude can be large</li> <li>3 - The whole system is subjected to passage of sediment waves</li> <li>4 - River form could change to braided</li> <li>5 - Flood levels are reduced at B and increased at A</li> <li>6 - Local and general scour is significantly affected</li> </ol>	<ol style="list-style-type: none"> <li>1 - A change of river form from meandering to braiding is possible</li> <li>2 - Rate of sediment transport is increased</li> <li>3 - Headcutting is induced in the whole system</li> <li>4 - Upstream of B flood stage is reduced</li> <li>5 - Velocity increases</li> <li>6 - Tributaries respond to main channel changes</li> </ol>	<ol style="list-style-type: none"> <li>1 - For Bridge B see upstream effects</li> <li>2 - For Bridge A the channel first degrades and then significantly aggrades</li> <li>3 - Large quantities of bed material and wash load are carried to the reservoir</li> <li>4 - Delta forms in the reservoir</li> <li>5 - Wash load may affect water quality in the entire reservoir</li> <li>6 - Tributaries respond to main channel changes</li> </ol>



Case (13) is a series of situations, unrelated in some instances and combined in others, which can affect bridge crossings. Tidal flows, seiches and bores can have significant effects on scour and depth in the channel system. The tidal flows, seiches and bores, as well as wind waves, can rapidly and violently destroy existing bank lines.

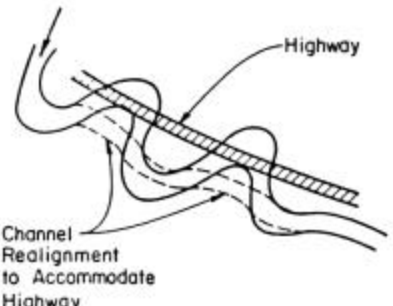
When considering earthquakes, it is of importance to examine a seismic probability map of the United States. Large portions of the United States are subjected to at least infrequent earthquakes. Associated with earthquake activity are severe landslides, mud flows, uplifts in the terrain, and liquefaction of otherwise semi-stable materials, all of which can have a profound effect upon channels and structures located within the earthquake area. Historically, several rivers have completely changed their course as a consequence of earthquakes. For example, the Brahmaputra River in Bangladesh and India shifted its course laterally a distance of some 320 km (200 miles) as a result of earthquakes that occurred approximately 200 years ago. Although it may not be possible to design for this type of natural disaster, knowledge of the probability of its occurrence is important so that certain aspects of the induced effects from earthquakes can be taken into consideration when designing the crossings and affiliated structures.

Table 9.1. River Response to Highway Encroachments and to River Development (continued).

Bridge Location	Local Effects	Upstream Effects	Downstream Effects
 <p>a. - Tidal Flows, Seiches, Bores, etc.</p>	<ol style="list-style-type: none"> <li>1 - Scour or aggradation</li> <li>2 - Bank erosion</li> <li>3 - Channel change</li> <li>4 - Bed form change</li> </ol>	<ol style="list-style-type: none"> <li>1 - See local effects</li> <li>2 - Channel erosion</li> <li>3 - Changes in channel slope</li> </ol>	<ol style="list-style-type: none"> <li>1 - See local effects</li> <li>2 - Beach erosion</li> </ol>
 <p>b. - Wind (Hurricanes, Tornadoes)</p>	<ol style="list-style-type: none"> <li>1 - Bank erosion</li> <li>2 - Inundated highway</li> <li>3 - Increase in velocity</li> <li>4 - Wave action</li> </ol>	<ol style="list-style-type: none"> <li>1 - See local effects</li> </ol>	<ol style="list-style-type: none"> <li>1 - See local effects</li> </ol>
 <p>c. - Earthquakes (see Seismic Probability Map of U.S.)</p>	<ol style="list-style-type: none"> <li>1 - Channel changes</li> <li>2 - Scour or deposition</li> <li>3 - Decrease in bank stability</li> <li>4 - Landslides</li> <li>5 - Rockslides</li> <li>6 - Mudflows</li> </ol>	<ol style="list-style-type: none"> <li>1 - See local effects</li> <li>2 - Slide lakes</li> </ol>	<ol style="list-style-type: none"> <li>1 - See local effects</li> <li>2 - Slide lakes</li> </ol>
(13) Tectonics and other natural causes			

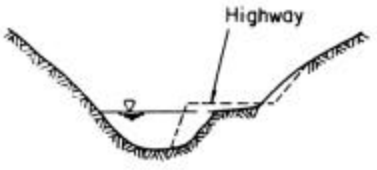
Case (14), (15), and (16) illustrate three examples of longitudinal encroachment. In Case (14), a few bends of a meandering stream have been realigned to accommodate a highway (see Case 6). There are two problems involved in channel realignment. First, the length of realigned channel is generally shorter than the original channel which results in a steeper energy gradient in the reach (Case 4). Second, the new channel bank material in the realigned reaches may have a smaller resistance to erosion. As a result of these two problems, the channel may suffer instability by the formation of a headcut from the downstream end and increased bank erosion. The realigned channel may also exhibit a tendency to regain the lost sinuosity and may approach and scour the highway embankment.

To counter these local effects one could design the realignment to maintain the original channel characteristics (length, sinuosity). Another way would be to control the slope by a series of low check dams. In any case, bank protection by riprap, jacks or spurs will be needed. The up- and downstream effects of the channel realignment will be the same as discussed for channel length reduction in Case (12). For example, as the degradation travels through the realigned reach, sediment load generation in the river by bed and bank erosion will cause aggradation downstream.

Bridge Location	Local Effects	Upstream Effects	Downstream Effects
 <p>(14) Longitudinal encroachment</p>	<ol style="list-style-type: none"> <li>1 - Increased energy gradient and potential bank and bed scour</li> <li>2 - Highway fill is subject to scour as channel tends to shift to old alignment</li> <li>3 - Reach is subject to bed degradation as headcut develops at the downstream end and travels upstream</li> <li>4 - Lateral drainage into the river is interrupted and may cause flooding and erosion</li> </ol>	<ol style="list-style-type: none"> <li>1 - Energy gradient also increased in the reach upstream and may cause change of river form from meandering to braided</li> <li>2 - Rate of sediment transport is increased. As the headcut travels upstream severe bank and bed erosion is possible</li> <li>3 - If tributaries in the zone of influence exist they will respond to lowering of base level</li> </ol>	<ol style="list-style-type: none"> <li>1 - Channel will aggrade as the sediment load coming from bed and bank erosion is received</li> <li>2 - Channel may deteriorate from meandering to braided</li> </ol>

Case (15) illustrates encroachment on the waterway of an incised stream flowing through a narrow gorge. Locally, the effect is to reduce the waterway and to increase the velocities and bank and bed erosion potential. The erosion protection of the highway slope exposed to the flow, and possibly, the opposite bank are important problems. The backwater induced by this obstruction may cause upstream aggradation and higher flood levels. On the downstream side, channel aggradation may be experienced if bed erosion occurs locally in the encroached reach.

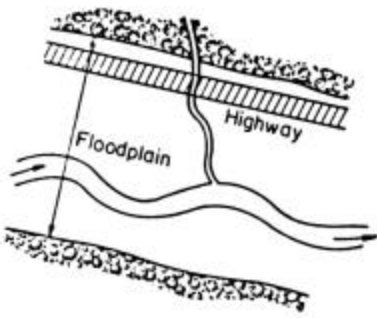
Table 9.1. River Response to Highway Encroachments and to River Development (continued).

Bridge Location	Local Effects	Upstream Effects	Downstream Effects
 <p>(15) Longitudinal encroachment</p>	<ol style="list-style-type: none"> <li>1 - Reduced waterway causes a local obstruction to flow and higher velocities</li> <li>2 - Significant erosion problem on the highway fill and induced bed degradation</li> <li>3 - Lateral drainage into the river is interrupted and may cause flooding and erosion</li> </ol>	<ol style="list-style-type: none"> <li>1 - Backwater generated by the obstruction increases flood stage</li> <li>2 - Deposition induced by the backwater</li> </ol>	<ol style="list-style-type: none"> <li>1 - Large sediment load may cause aggradation</li> <li>2 - Local scour at end of contracted section</li> </ol>

Case (16) is a case of floodplain encroachment. It is assumed that during bankfull and lower stages the highway does not interact with the flow. However, during high stages, the total flow area is decreased by the encroachment. Locally, the highway must be protected against inundation and erosion during a flood. The effect on the river channel depends on the extent of encroachment on the waterway. If the highway significantly reduces the floodplain, it may increase river stages for a given flood. If the river channel tends to shift, the highway encroachment may alter the interaction of floodplain flow and channel flow, affecting the channel floodplain flow pattern. Very often this type of encroachment has little or no effect on flood stages or on the stream upstream or downstream, however, possible adverse effects should be investigated.

In all cases of longitudinal encroachment, the lateral drainage into the river will be intercepted. An important consideration in the design of encroachments will be to provide for this drainage.

Table 9.1. River Response to Highway Encroachments and to River Development (continued).

Bridge Location	Local Effects	Upstream Effects	Downstream Effects
 <p>(16) Longitudinal encroachment</p>	<ol style="list-style-type: none"> <li>1 - Erosion of highway fill and submergence possible during floods</li> <li>2 - Pattern of overbank spill are affected by the encroachment and in highly shifting channels may change river course downstream</li> <li>3 - Lateral drainage into the river is interrupted and may cause flooding and erosion</li> </ol>	<ol style="list-style-type: none"> <li>1 - If significant encroachment on the floodplain waterway, backwater may be induced</li> </ol>	<ol style="list-style-type: none"> <li>1 - If the river channel is highly shifting, the channel alignment may change</li> <li>2 - If significant erosion experienced upstream, aggradation will occur</li> </ol>

## **9.5 PRACTICAL EXAMPLES OF RIVER ENCROACHMENTS**

In the preceding paragraphs, a series of conceptual cases were discussed. Each case considers the interactions between the river and the encroachment over a period of time. In general, the particular practical examples presented in this section are not as complex as some of the earlier conceptual cases. For example, there is no consideration of water resources development throughout the basins, including construction of reservoirs transmountain diversions, and so forth.

### **9.5.1 Cimarron River, East of Okeene, Oklahoma (Example 1)**

The bridge and a rock dike on its north abutment were built in 1934 (Figure 9.2a). A high discharge year in 1938 caused the south bank to erode. A Kellner jetty field was installed to prevent further erosion of the bank. The jetty field was ineffective due to the lack of debris and suspended sediment load. A large flood in 1957 spread out over the floodplain in several places. After the flood, seven timber pile diversion units and a riprapped dike were installed in the old jetty field location to prevent future damage to the highway (Figure 9.2b). As of 1968, the south bank had been held in line by the timber pile diversion structures and the dike (Figure 9.2c).

### **9.5.2 Arkansas River, North of Bixby, Oklahoma (Example 2)**

The bridge was built in 1938. A Kellner jetty field was installed on the north bank in 1939 to protect the north bridge abutment (Figure 9.3a). In 1948 minor floods eroded the south bank. A Kellner jetty field was installed to prevent further erosion (Figure 9.3b). Some time after, riprap was put on the south bank up- and downstream of the jetty field (Figure 9.3c). In 1959, a 50-year frequency flood eroded the north bank and washed out a section of the north approach to the bridge. The flood also washed out two sections of roadway further north on the floodplain. The approach was rebuilt and riprap was installed on the embankment. A riprapped spur dike (guide bank) was also constructed just south of the north abutment. Five pile diversion structures were built to prevent further erosion of the north bank (Figure 9.3c). As of 1968, the south bank has remained stationary, and the north bank has filled (Figure 9.3d).

### **9.5.3 Washita River, North of Maysville, Oklahoma (Example 3)**

In 1949, floods washed out the north span of the bridge. Also, both banks upstream from the bridge were damaged. A temporary structure was installed in place of the north span of the bridge. In October of 1949, two Kellner jetty fields were completed upstream from the bridge to provide bank protection (Figure 9.4a). In 1950, a new bridge was constructed just downstream from the old bridge. State Highway 74 was realigned to conform to the new bridge. In eight months of operation, the Kellner jetty field on the northeast bank had completely silted in. This was largely due to the clay content in the suspended sediment and the large amount of drift in the stream (Figure 9.4b). The floods of 1957 did very little damage to the new bridge site or the banks. Floods in 1968 and 1969 have caused bank erosion on the north bank upstream of the jetty field which could eventually cut in behind the jettyfield (Figure 9.4c).

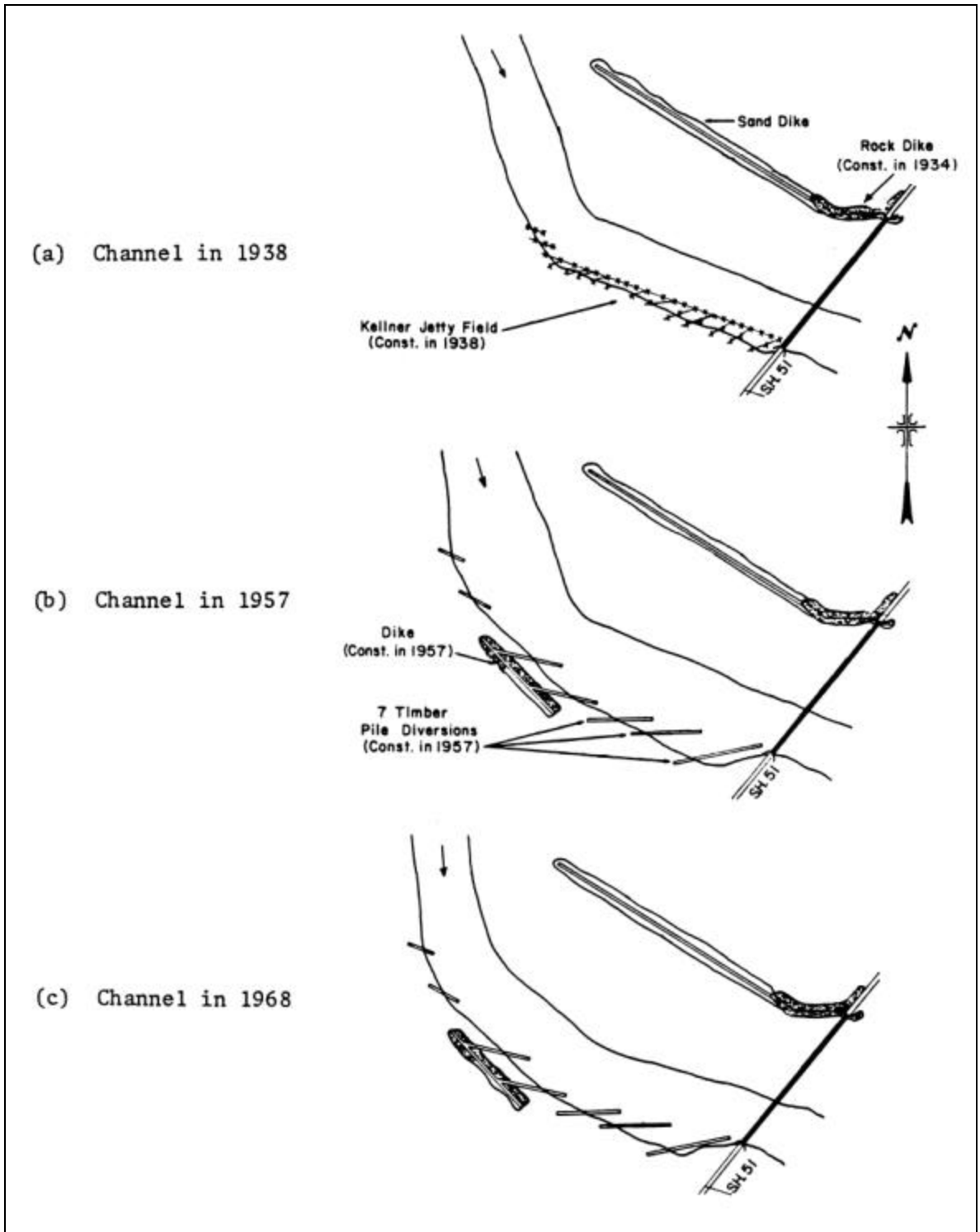


Figure 9.2. Cimarron River, east of Okeene, Oklahoma (Example 1).

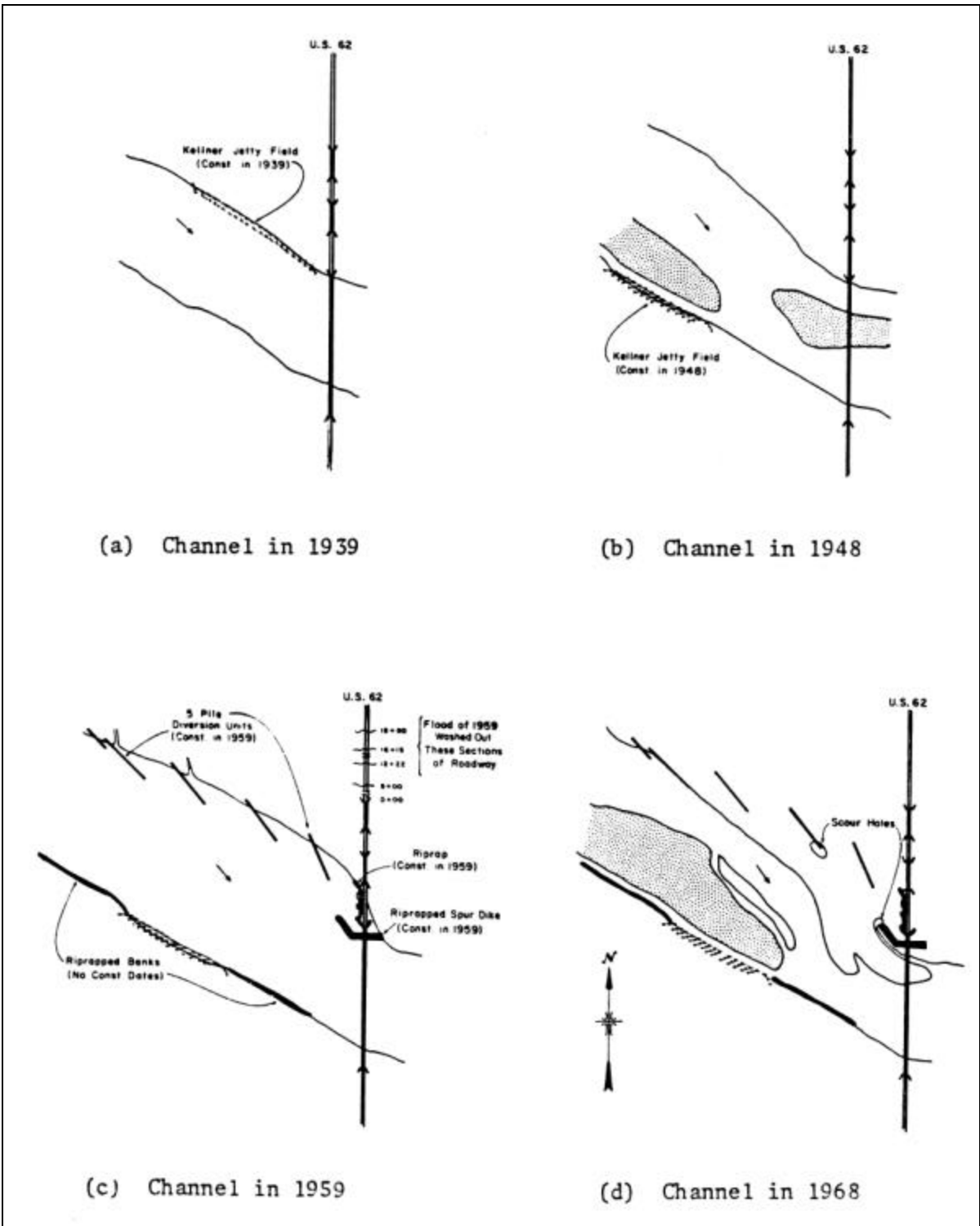


Figure 9.3. Arkansas River, north of Bixby, Oklahoma (Example 2).

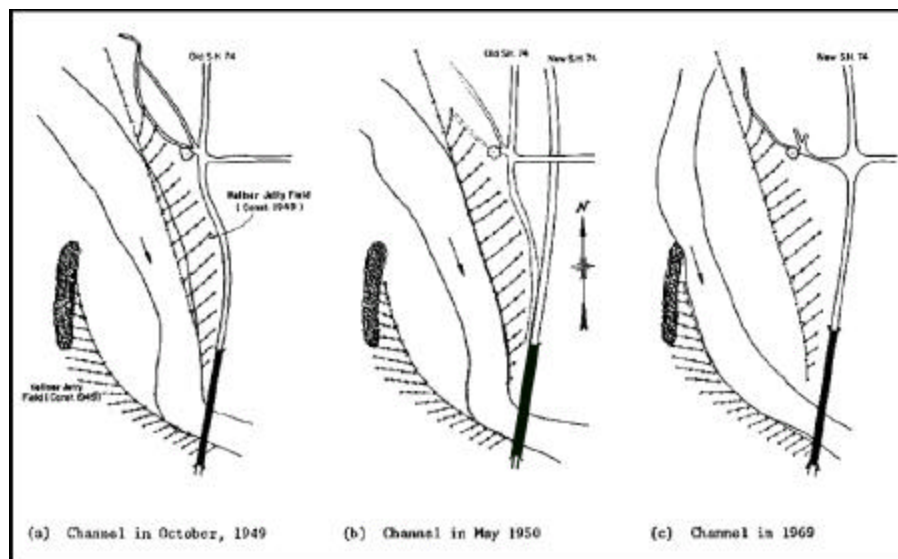


Figure 9.4. Washita River, north of Maysville, Oklahoma (Example 3).

#### 9.5.4 Beaver River, North of Laverne, Oklahoma (Example 4)

During high flows of 1938, the river washed over the south bank and damaged the approach roadway south of the bridge. The south end of the bridge was also damaged. Jetty fields were constructed in several locations upstream of the bridge in an attempt to reduce bank erosion. Two jetty lines were constructed in a side channel downstream of the bridge to discourage flow in that channel to prevent eddy currents from eroding the north embankment (Figure 9.5a). A new longer bridge was constructed in 1941. High flows in 1946 caused severe erosion on the south bank upstream from the bridge. In 1949, an earth dike and jetty field were constructed on the south bank to prevent further erosion. In 1969, the river cut through a portion of the 1949 jetty field and eroded the earth dike (Figure 9.5b). Car bodies were used as bank protection. However, car bodies are not environmentally acceptable and are difficult to hold in place unless anchored with cable or weighted down with concrete or rocks.

#### 9.5.5 Powder River, 40 Miles East of Buffalo, Wyoming (Example 5)

The Powder River has very fine bed material and a high sinuosity. The river contains dunes and antidunes at low flows. At the bridge site, there was a grove of cottonwood trees on the upstream east bank of the bridge and a dry draw coming in from the upstream left bank (Figure 9.6a). Upon completion of the bridge, a large flood occurred. The river attempted to straighten out its meanders possibly as a result of instream or floodplain mining in conjunction with the road construction. At the same time, the draw on the upstream left bank was bringing in a large amount of sediment, forcing the stream toward the upstream side of the (east) abutment. The flood flow uprooted the grove of cottonwoods which impacted on the sacked concrete riprapped spur dike (guide bank) at the east abutment and destroyed the dike (Figure 9.6b). To restore the channel to its original alignment, a training dike was constructed from the bridge upstream to a nearby bluff (Figure 9.6c). A jack jetty field was also constructed on the upstream meander to prevent the river from flowing across the point bar. The jetty field has begun to fail as a result of the streamside piles being undercut. The streamside anchors were rebuilt by driving the piles deeper in the center of small riprapped mounds.

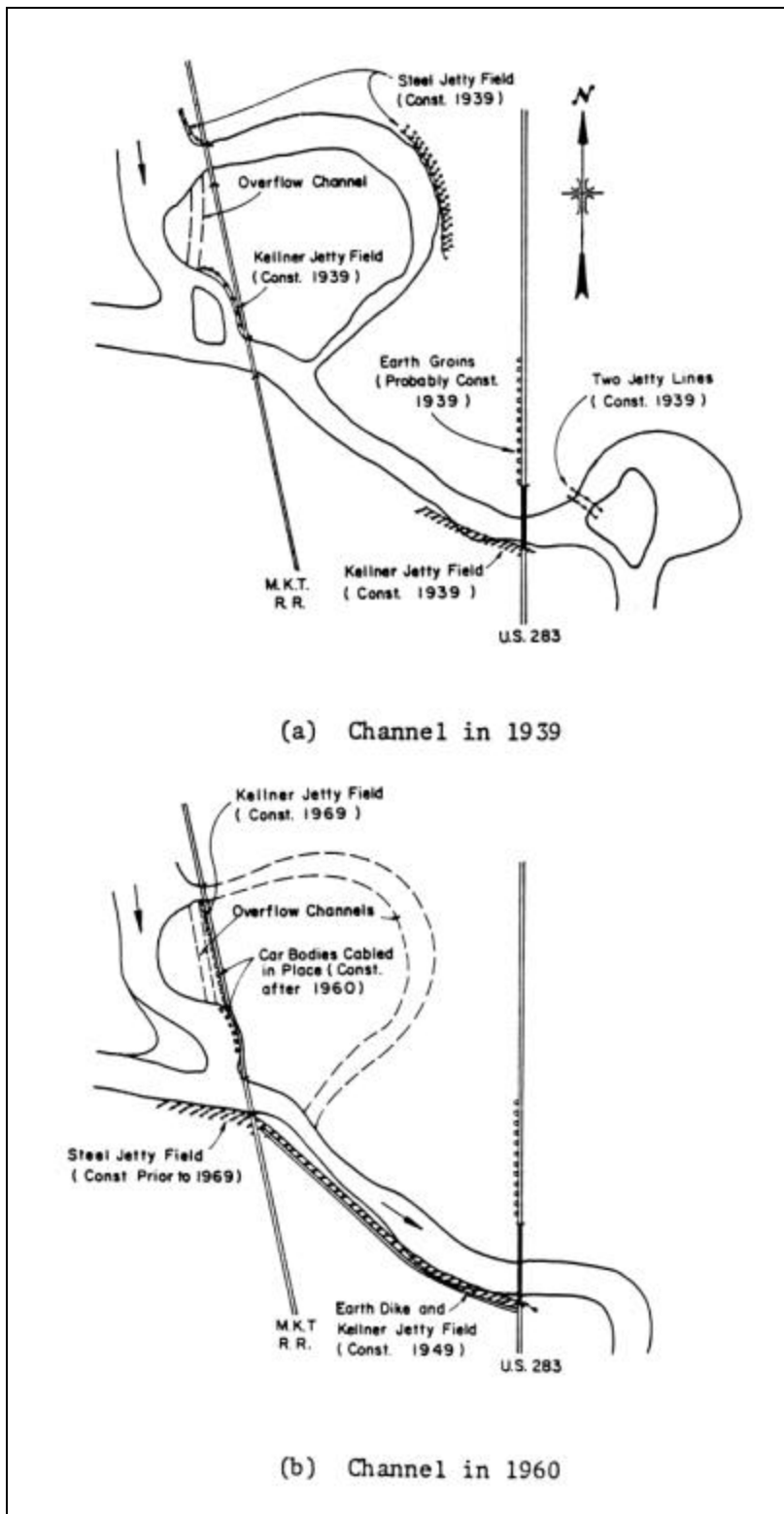


Figure 9.5. Beaver River, north of Laverne, Oklahoma (Example 4).



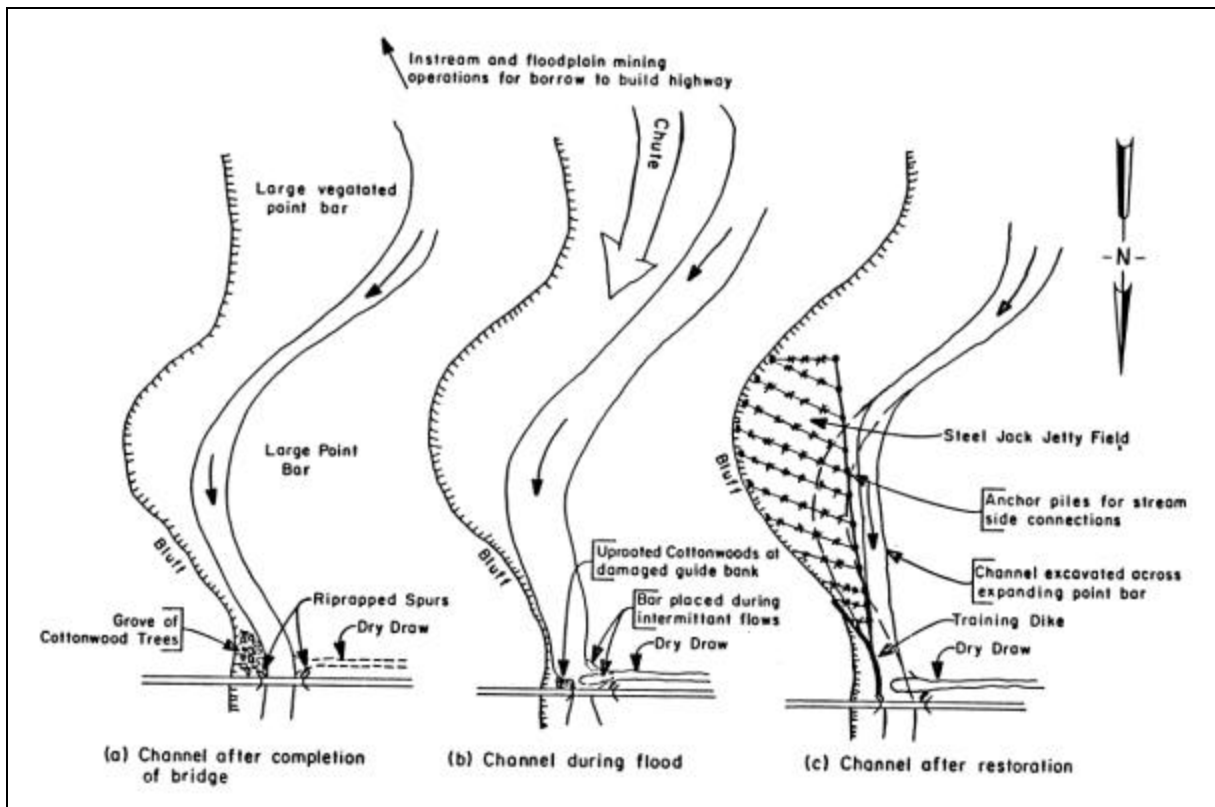


Figure 9.6. Powder River, 40 miles east of Buffalo, Wyoming (Example 5).

### 9.5.6 North Platte River, Near Guernsey, Wyoming (Example 6)

The North Platte River is a fairly stable river in this reach as a result of reservoir control upstream (Figure 9.7). The bed is coarse granular material with cobbles in evidence. It was decided at this crossing to build the bridge over the main channel and part of the island and to block off the active overflow channel on the opposite side of the island (Figure 9.7a). Two situations can occur due to this choice for the bridge crossing. One situation is that the concave bank erodes due to the high velocities resulting from the decreased area of flow under the bridge (Figure 9.7b). In fact, with extreme flows the river could erode a chute across the point bar on the first bend downstream. The other situation which may occur is that the high velocity flow carries increased sediment load and deposits this material in the eddies downstream (Figure 9.7c), which in this case would not cause any problems. The county insisted on low construction costs so the training dike had minimal riprapping as shown in the figure. As a result the dike is now eroding badly. The high bank began eroding so the property owner dumped in some broken concrete, rock and debris. The channel degraded through the opening but as expected the coarse bed has armored quite well. Except for the eroding of training dike, everything has worked well for over 30 years.

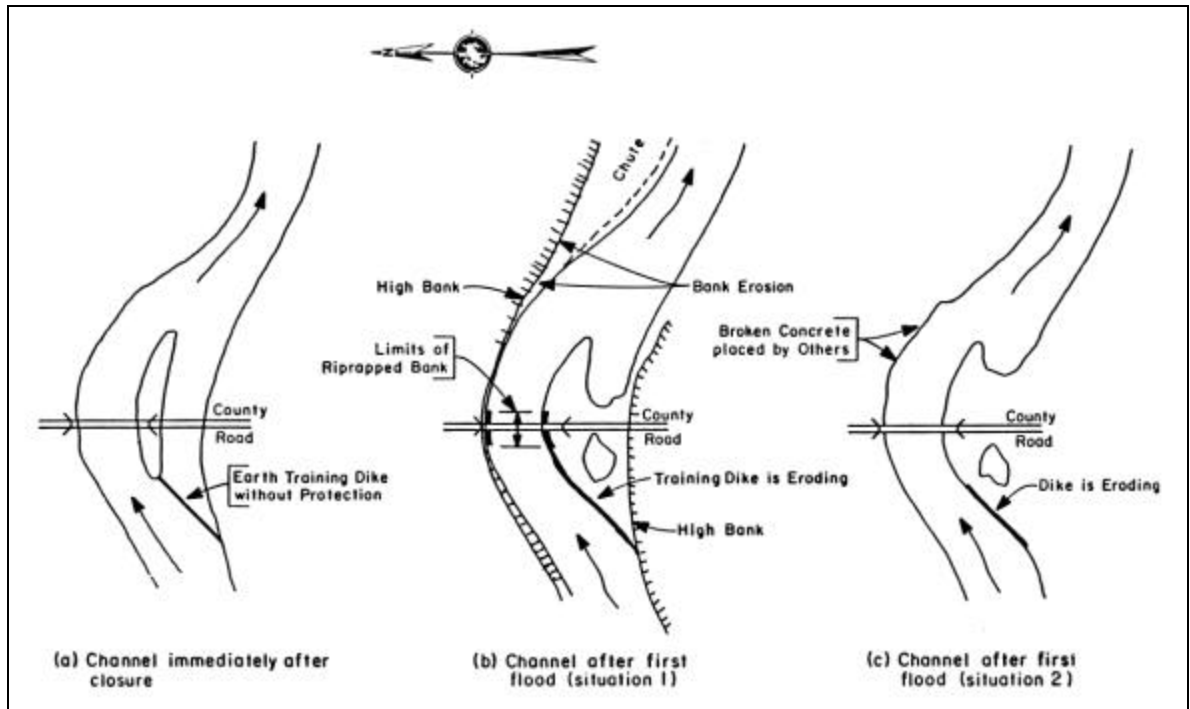


Figure 9.7. North Platte River near Guernsey, Wyoming (Example 6).

### 9.5.7 Coal Creek, Tributary of Powder River, Wyoming (Example 7)

A small bridge was constructed over Coal Creek over an intermittent tributary of the Powder River. Coal Creek is a dry draw that is incised. Head cuts existed downstream from the bridge at the time of its construction (Figure 9.8). Several headcuts were over a mile downstream. During a subsequent flood, at least one head cut moved upstream through the bridge site. This headcut almost undercut the midstream piles and exposed some of the abutment piles. To prevent further degradation under the bridge when the remaining headcuts move through, chainlink enclosed riprap was placed as shown. The lower portion was placed as articulated riprap. The migration of the downstream headcuts has since resulted in some downward articulation. A heavy steel girder fence-like device to allow the lower portion of the replaced riprap to be stable at a steeper slope was necessary to establish a larger waterway opening. The original waterway was significantly smaller than the final configuration. Other alternatives would have been to excavate the head cuts in the channel through the bridge site before the bridge construction, allowing them to move naturally upstream from there; to set the piles deeper in anticipation of the lowering of the bed elevation; or to construct a weir (check dam) control structure at the location of the headcut to prevent upstream migration.

### 9.5.8 South Fork of Deer River at US-51 Near Halls, Tennessee (Example 8)

Examples 8 through 10 were taken from Federal Highway Report Number FHWA/RD-80/038. In general, these examples are presented as in the original form. They have, however, been edited slightly and modified to fit the format of this text.

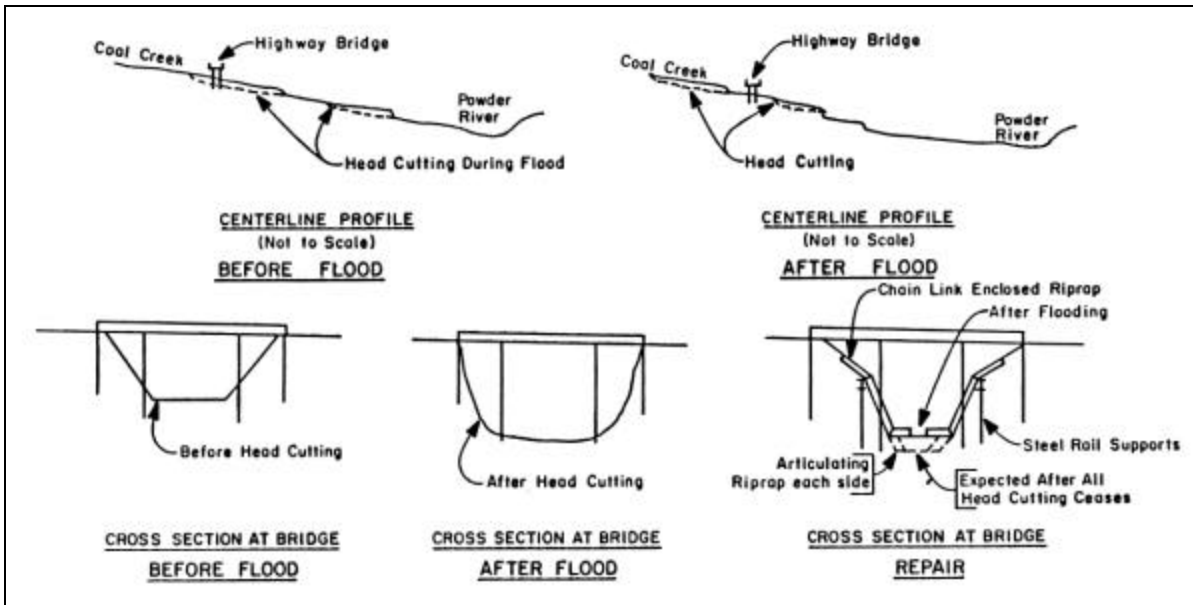


Figure 9.8. Coal Creek, tributary of Powder River, Wyoming (Example 7).

The location for Example 8 is near the Dyer and Lauderdale County line in western Tennessee (Figure 9.9a). Dual bridges were built in 1963, with a 16 m (52.5 ft) main span supported by wall-type piers in the main channel, and thirty 8 m (26 ft) approach spans supported by concrete pile bents. In 1975, both bridges over the main channel were rebuilt, with a main span of 22.5 m (73.8 ft) supported by hammerhead piers. Spill-through abutments, set back from the main channel, were protected with sacked concrete in 1963 and have remained stable.

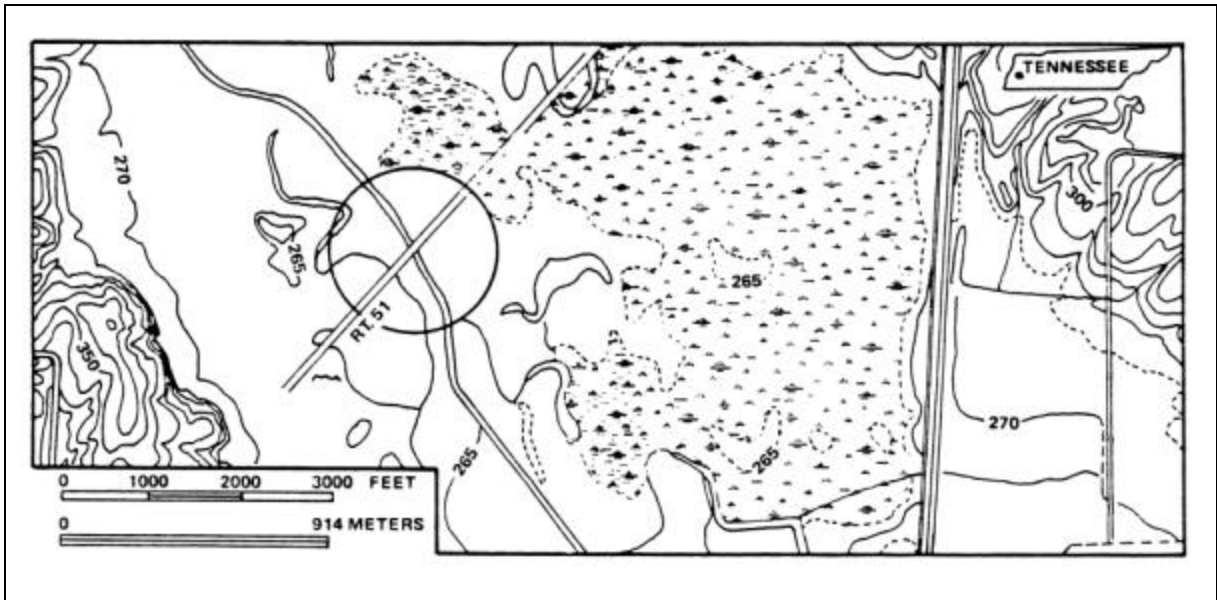


Figure 9.9a. Map showing South Fork of Deer River at U.S. Highway 51 Crossing (Example 8).

The drainage area is 2,688 km<sup>2</sup> (1,038 mi<sup>2</sup>); the bankfull discharge is 28 m<sup>3</sup>/s (989 ft<sup>3</sup>/s), and the river width (where bordered by natural vegetation) is 24 m (79 ft). The stream is perennial, alluvial, sand bed, in a valley of moderate relief and in a wide floodplain. The natural channel has a sinuosity of about 2.5 but the channel has been straightened; it is equiwidth, not incised, cut banks are rare, with silt-sand banks.

The channel was first straightened and enlarged in the 1920s by local drainage districts; but, probably because the natural floodplain forest was not cleared, the banks remained stable. In 1969, the Corps of Engineers straightened and enlarged a reach about 4.8 km (3 mi) in length downstream from the bridge, reducing the length about 20 percent. During the 1960s, and particularly early 1970s, the floodplain was cleared of trees for agricultural purposes.

Figure 9.9b illustrates the Corps of Engineers' channel modifications that reduced the channel length and increased the channel slope. Figure 9.9b also provides a profile of the channel before any modifications were made in 1975.

Between 1970 and 1971 the left bank (near bent 7) at the bridge receded an average distance of 4 m (13 ft). The peak discharge during this period was 215 m<sup>3</sup>/s (7,592 ft<sup>3</sup>/s) (1.5 year recurrence interval). Timber pile retards were built at the left bank near bent 7 and a single row of pile with wood face planks extending from the downstream end of bent 7 for a distance of 37.5 m (123 ft) upstream (Figure 9.9c).

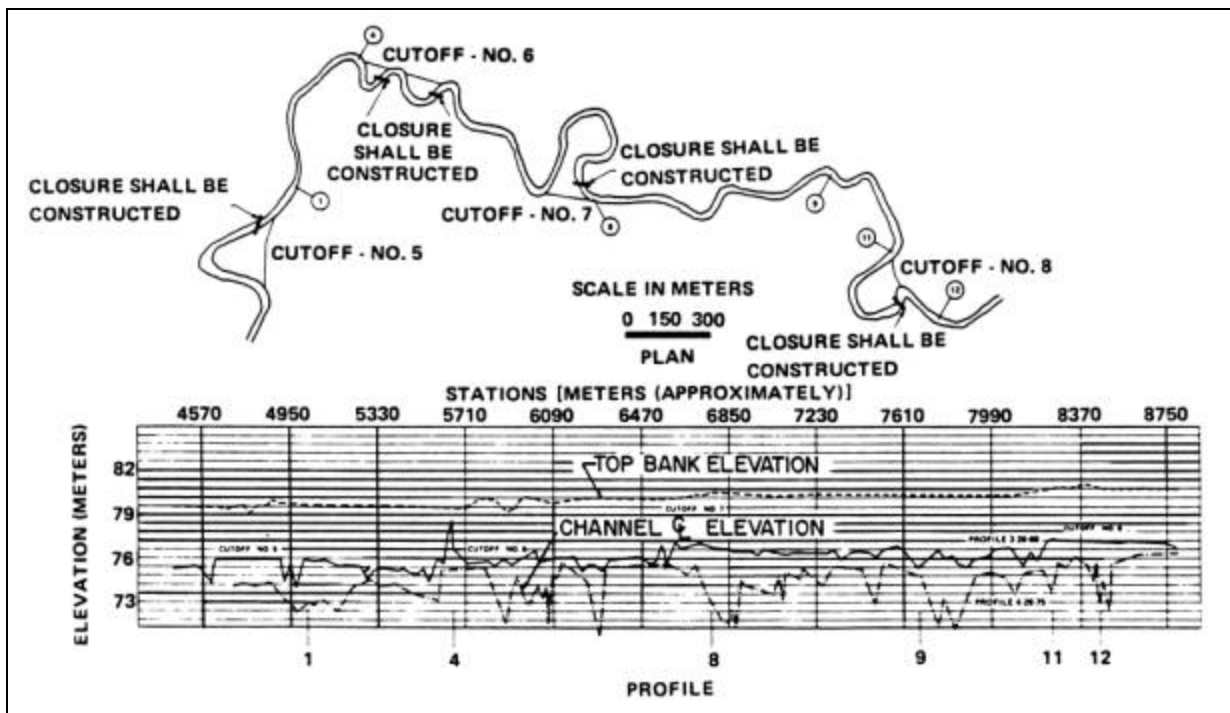


Figure 9.9b. Channel modifications to South Fork of Deer River at U.S. Highway 51 near Halls, Tennessee (Example 8).

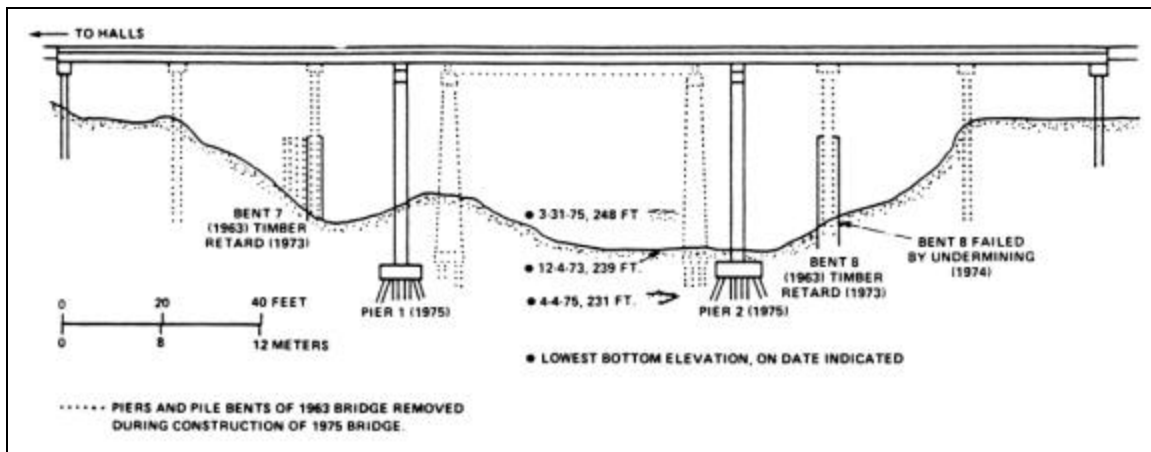


Figure 9.9c. Elevation sketch of U.S. Highway 51 Bridge (Example 8).

Between 1971 and 1973 the peak discharge was  $751 \text{ m}^3/\text{s}$  ( $26,518 \text{ ft}^3/\text{s}$ ) (17 years recurrence interval). Bankfull stage occurred several times with high flows sustained for periods of weeks. The left bank continued to erode behind the retard where the average distance of recession was about 2 m (6.5 ft) for the 3-year period. Bent 7 became exposed below the ground line. Concrete was poured at the base to prevent further erosion. Slumping from the left bank deflected flow toward the right bank, causing rapid erosion and failure of bent 8. The south lane of the bridge was closed. A detailed inspection was made in 1973, but little field data was collected. Data collected indicated a large local scour problem at the bridge. No profile data was available to evaluate the gradation problem.

In 1975 both lanes of the bridge were rebuilt, with new piers having deeper footings and less area normal to the flow (Figure 9.9c). Single-row timber pile retards were built along both banks in the vicinity of the bridge. A large scour hole in the center of the channel downstream from the bridge, attributed to flow constriction during bridge construction, was filled with gravel.

In 1977 a detailed inspection was made and cross-section data at the bridge indicated that the local scour problem was somewhat corrected and the gradation problem was fairly stable. Effectiveness of the timber pile retard had not yet been tested, and the area between the retard and the bank was not accumulating sediment. The lowermost face plank on the retard was about 1.5 m (5 ft) above the streambed. From experience face planks should be extended to, or below, streambed elevation. In addition, the upstream end of the retard seemed to be keyed into the bank for an insufficient distance. Vegetation was becoming re-established on the banks, which appeared more stable in 1977 than in the recent past.

The original bridge failed in 1974 because of channel degradation and concurrent bank recession, which are directly attributable to straightening of the channel for drainage purposes and clearing of the banks and floodplain for agricultural purposes. Channel width increased by a factor of approximately 2, between 1969 and 1976. The clearing of vegetation is apparently one of the most critical factors, because channel straightening in the 1920s which was not accompanied by extensive clearing, did not result in significant bank instability. The timber pile retard installed in 1971 was of inadequate design, in view of the seriousness of the problem.

Bank recession might have been controlled by an adequate retard or other countermeasure, but channel degradation is more difficult to control.

The site was inspected in 1973, in 1974, four times in 1975 and in 1976 by numerous federal and state agency employees. It should be pointed out that little actual field data were collected to document the progressive channel change. All inspections concluded that the channel changes were responsible for the gradation problems and other related hydraulic problems.

#### **9.5.9 Elk Creek at SR-15 Near Jackson, Nebraska (Example 9)**

Elk Creek is located in Dakota County and is a tributary of the Missouri River. It flows into the Missouri River just upstream of Sioux City, Iowa. The State Road 15 Bridge just west of Jackson is of interest. The stream is perennial but flashy, alluvial, sand-silt bed and in a valley of low relief with a wide floodplain. The channel is sinuous, incised by degradation, and has silt-clay banks.

The stream bed has degraded at least 2 m (6.6 ft) since 1955. There are two primary reasons for this degradation. First, channel modifications have been made to improve and maximize agricultural production. As a result, the channel has been straightened and changed at isolated locations. Second, and probably more important, is the general degradation below Gavins Point Dam. Missouri river stage trends, for almost 50 years for eight of the key main stream gaging stations below Sioux City, indicated at least 2 m (6.6 ft) of degradation at Sioux City, as indicated in Figure 9.10. This degradation is probably due to three main reasons as follows:

1. Between 1890 and 1960 the Missouri River length from Sioux City to Omaha has been reduced 21 percent by the Corps of Engineers. As a result the stream bed slope was increased.
2. The sediment-free water released at Gavins' Point Dam is transporting the bed sediment that is available.
3. The rather high sustained flows of the regulated Missouri River system do not allow for any aggradation or filling.

The degradation is primarily responsible for lateral instability as the channel has almost doubled in width, and degradation has exposed bridge pier footings.

Tributary degradation, resulting from degradation on the mainstream of the Missouri River is to be expected. The Missouri River has historically degraded, as indicated in the Missouri River stage trends. This condition should be evaluated on an annual basis and bridges inspected that are subject to this headcutting. This degradation should be expected on each tributary that is not protected by a grade control structure. Failure of this particular bridge due to degradation is not likely because of the great depth to which bridge foundations have been placed.

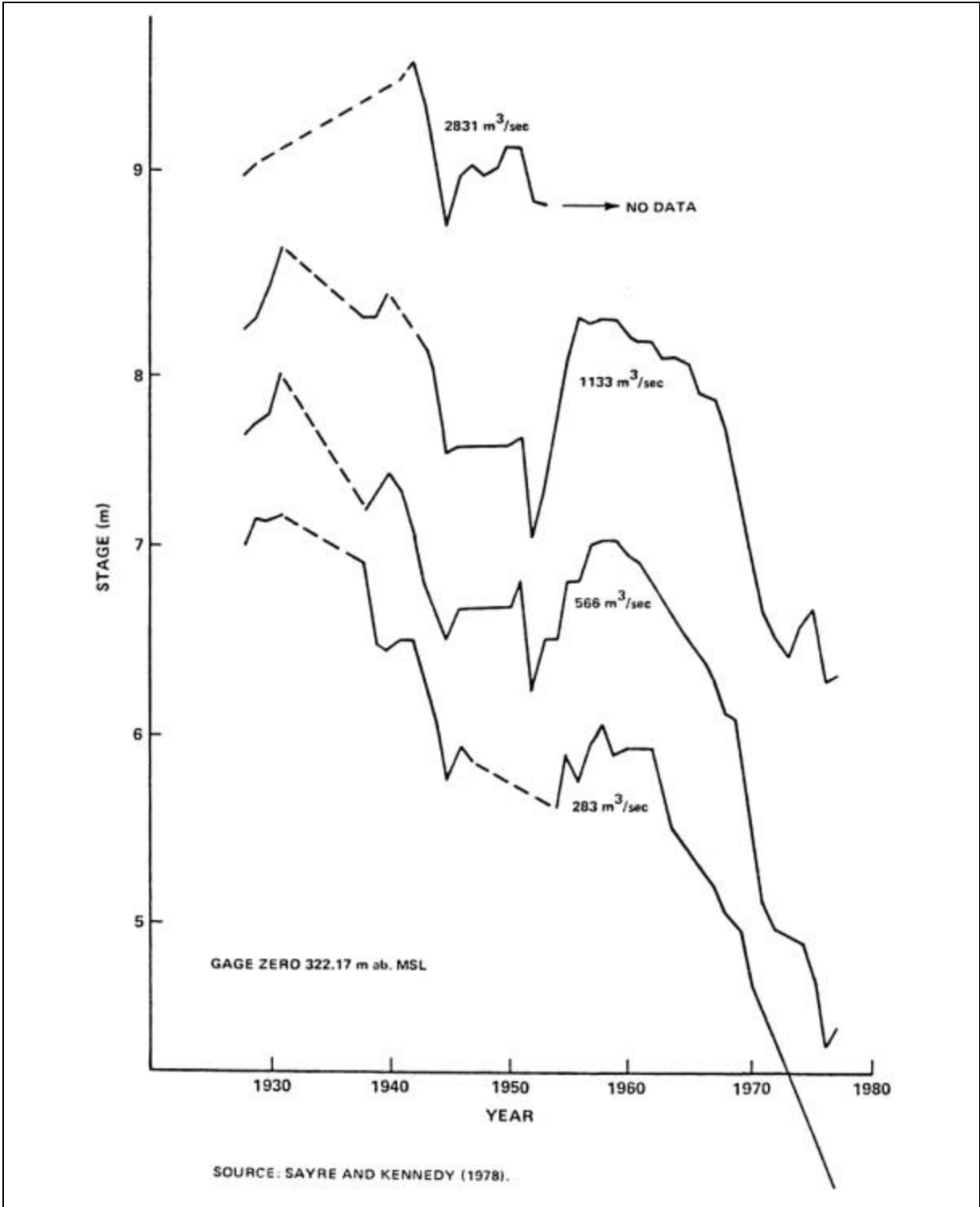


Figure 9.10. Stage trends at Sioux City, Iowa, on the Missouri River (Example 9).

### 9.5.10 Big Elk Creek at I-90 Near Piedmont, South Dakota (Example 10)

Big Elk Creek is located in Meade and Lawrence counties and is a tributary of the Cheyenne River. The headwaters of Big Elk Creek originate in the Black Hills National Forest. I-90 crosses Big Elk Creek on an alluvial fan just outside of the National Forest, where there is a significant reduction in channel slope. The bridge, built in 1964, is 54 m (177 ft) long, has pile bents with square piles, spillthrough abutments, and a concrete deck. The creek is intermittent, flashy and alluvial with cobble and gravel bed. The drainage area above I-90 is 1,300 km<sup>2</sup> (502 mi<sup>2</sup>) and the design discharge was 85 m<sup>3</sup>/s (3,000 ft<sup>3</sup>/s).

The highway crossing is located on an alluvial fan. At this location there is insufficient slope (energy) to transport the cobble and gravel material. Since 1964, it has been necessary to excavate about 20,000 m<sup>3</sup> (26,160 yd<sup>3</sup>) of deposited bed material on three occasions at an expense of hundreds of thousands of dollars. The excavation was necessary to pass the flow from the spring snowmelt runoff. The primary aggradation problem is insufficient flow area and is aggravated by too many piers in the channel as well as a bad alignment with a 67 degree skew.

In 1966 several rock and wire basket flow deflectors were installed for several hundred meters upstream of the bridge to constrict the flow and increase the transport characteristics. Figure 9.11 illustrates the deflector arrangement as well as the alignment problem. The deflectors were not very effective. They did constrict the flow and increase the velocity to transport the gravel sizes, but the cobble bed material still deposited upstream of the bridge. The constriction was not enough compensation for the reduction in slope as the creek comes out of the Black Hills.

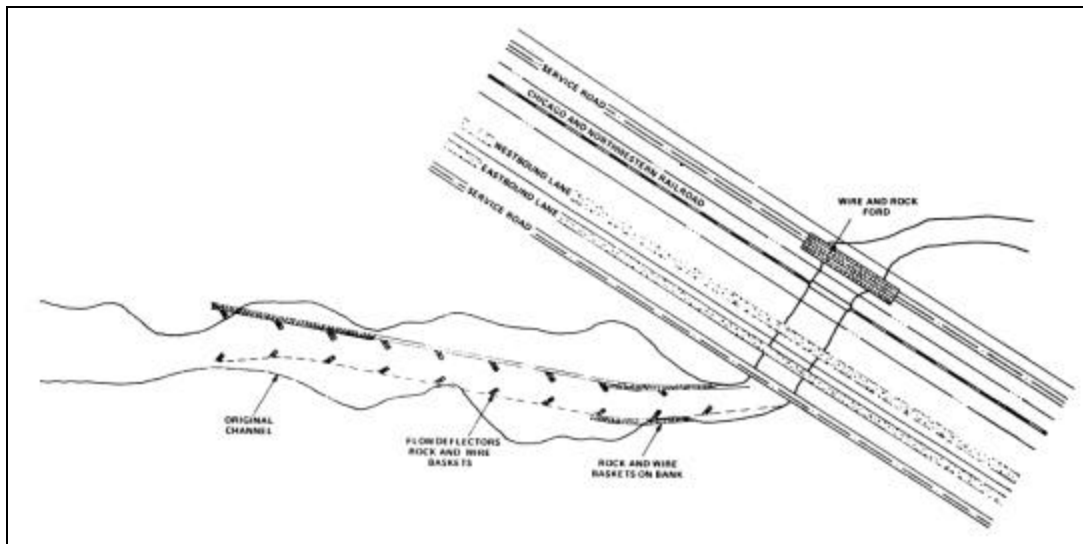


Figure 9.11. Deflector arrangement and alignment problem on I-90 Bridge across Big Elk Creek near Piedmont, North Dakota (Example 10).



The channel is not well defined as it flows onto the alluvial fan. As a result, it is difficult to locate a bridge to take into account both significant lateral channel migration and bed elevation changes. A possible solution to the problem would be to build a debris basin upstream of the bridge to trap the large-sized bed material. This would provide a source of gravel which is in demand in that area. This might be a site where a bedload transport model may be helpful in determining the solution to the aggradation problem.

### 9.5.11 Outlet Creek at US-101 Near Longvale, California (Example 11)

Examples 11 through 13 were taken from Federal Highway Administration Report No. FHWA/RD-80/158. These examples illustrate situations where the river channel was relocated to accommodate highway encroachments and crossings. These examples are reprinted from the original publication except for minor editing to conform with the format of this text.

In Example 11, the Outlet Creek channel was shortened from 435 m (1,427 ft) in length to 335 m (1,100 ft) and relocated to avoid two crossings on the realigned highway curve (Figure 9.12). The stream is semi-alluvial, and resistant bedrock crops out in the bottom of the relocated channel. The highway embankment, which forms the right bank of the relocated channel, is heavily riprapped, and the main potential for instability is at the left bank, which is a steep (3/4:1) slope cut into colluvial material. However, no erosion or slumping was observed.

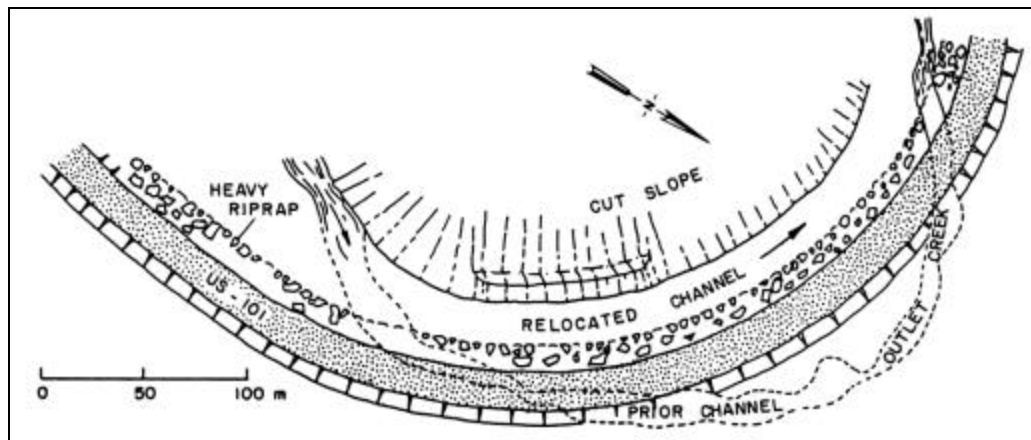


Figure 9.12. Plan sketch of channel relocation, Outlet Creek (Example 11).

The site location is on US-101, 3.2 km (2 mi) south of Longvale, California. Outlet Creek is perennial with a drainage area of about 360 km<sup>2</sup> (140 mi<sup>2</sup>) at the site and with an average discharge of 12 m<sup>3</sup>/s (424 ft<sup>3</sup>/s). The channel width is 9-15 m (30-50 ft), with a channel slope of 0.0036. The bed material is gravel and cobble, bank material is gravel and sand where alluvial.

The length of a bend in the natural channel was shortened by a factor of 0.77, and room for the relocated channel was made by grading back a steep valley side-slope. The relocated channel lies between this graded slope and the riprapped highway embankment. Riprap on the embankment includes rocks weighing several tons, and erosion of the embankment is unlikely.

Following an extreme flood in 1964, no maintenance work was needed. Small trees have become established on the riprapped highway embankment and along the base of the cut slope.

Landslides, the major potential for instability along the relocated channel, are very common in some California terrains, but are not evident here along the valley of the Outlet Creek. The lack of naturally occurring landslides, which is attributed to the resistance of the underlying bedrock, was an indication that the cut slope would not be particularly susceptible to failure by mass movement. Except for the bare upper part of the cut slope, the appearance of the relocated channel is not unnatural for a mountain stream in a narrow valley.

#### 9.5.12 Nojoqui Creek at US-101 At Buellton, California (Example 12)

The lowermost reach of this creek was relocated to enter Santa Ynez River upstream from the US-101 bridge, for purpose of avoiding a stream crossing at an interchange (Figure 9.13). The performance period of 16 years (1964-1979), during which major floods occurred in 1969 and 1978, showed no evidence of degradation or lateral erosion in the relocated channel, but a sinuous low-water channel had developed in the wide bottom of the relocated channel. Severe bank erosion occurred in the natural channel at the bend upstream from the relocation during flood of 1978, but this is not attributed to the relocation.

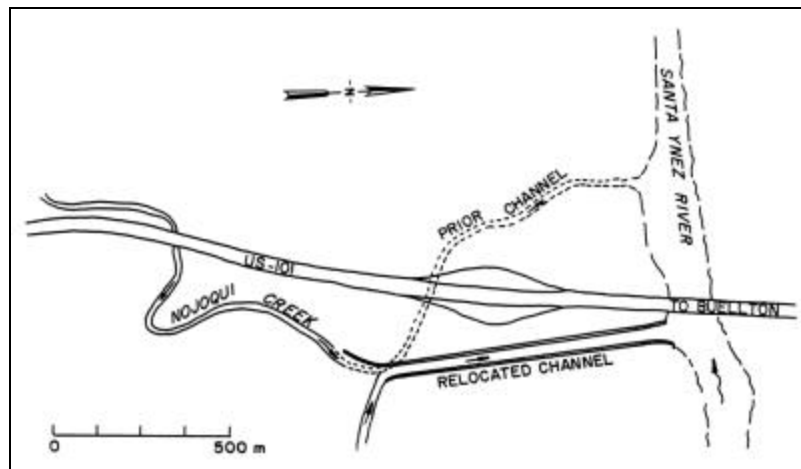


Figure 9.13. Plan sketch of Nojoqui Creek channel relocation (Example 12).

The site is located on US-101 about 1.3 km (0.8 mi) south of Buellton. Nojoqui Creek is intermittent, with a drainage area about 39 km<sup>2</sup> (15 mi<sup>2</sup>). The stream is ungaged, but an adjacent gaged stream of similar drainage area (Alisal Creek) has an average discharge of 0.15 m<sup>3</sup>/s (5.3 ft<sup>3</sup>/s), with no flow 64 percent of the time. This point-bar braided stream is generally incised into terraces. Tree cover along the channel is less than 50 percent. Bed material is gravel, cobbles, and small boulders; bank material is moderately cohesive silt, clay and gravel.

The lowermost 760 m (2,500 ft) of natural channel was relocated into a straight artificial channel 640 m (2,100 ft) in length, resulting in a length change factor of 0.84. The width of the natural channel was in the range of 15-20 m (50-65 ft). The relocated channel has a top width of 42 m (138 ft), a bottom width of 31 m (102 ft), and is bounded by riprapped dikes that rise about 1.5 m (5 ft) above the flat bottom. Slope of the natural channel was 0.0044; of the

relocated channel, 0.0053, decreasing to 0.0025 at the lower end. The dikes bounding the relocated channel are riprapped in part with large 1 m (3.2 ft) rock and in part, with 0.6 m (2 ft) rock, with the toe of riprap extending to a depth of 1.8 m (6 ft) below the channel bottom.

Floods having an estimated recurrence interval greater than 25 years occurred in 1969 and 1978. The banks of the natural channel at a bend upstream from the relocation were severely eroded in 1978, and the channel was subsequently realigned by the bulldozing of bed material against the banks. The flood apparently disrupted the riprap facing of dikes along the relocated channel, but there is no evidence that the dikes were broken. Young willows and other vegetation have become established along the dikes and, locally, in the channel bottom. Because the bottom width of the relocated channel is more than twice that of the natural channel, a sinuous low-water channel has developed, which may eventually erode laterally against the bounding dikes. In addition, the wide bottom may become overgrown with willows, which will impair its transmission of floods.

### 9.5.13 Turkey Creek at I-10 Near Newton, Mississippi (Example 13)

A reach, 625 m (2,050 ft) in length, was relocated and thereby shortened to 270 m (886 ft), for the purpose of improving the channel alignment at the bridges and to accommodate the planned roadway location (Figure 9.14). The performance period was 15 years (1964-1979). At the U.S. Geological Survey gage on nearby Chunky River, major floods occurred in April 1974 and January 1975. As specified in the plans, the relocated channel was trapezoidal in cross section, with a bottom width of 9 m (29.5 ft), and a side slope of 2:1. Channel slope as measured on the topographic map is about 0.0016. No bank protection measures were applied. In 1979, the bottom width of the relocated channel between the interstate bridges was in the range of 3-4 m (10-13 ft), resistant coherent clay was exposed in the channel bottom, and the banks were stable. The natural channel was generally stable (although choked with debris) upstream from the relocation; but downstream the bank was eroded and unstable at the outside of banks where, bordered by a pasture, the bottom width was in the range of 9-11 m (30-36 ft). Bank instability at this point was more severe than in 1955, but causes other than the relocation may have contributed to this.

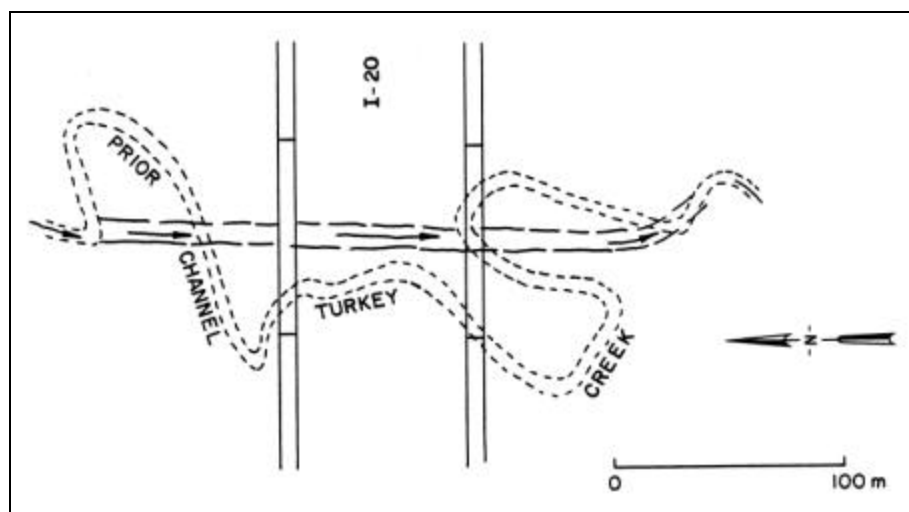


Figure 9.14. Plan sketch of Turkey Creek channel relocation (Example 13).

Stability of the relocated channel, which is substantially more narrow than specified in the plans and also more narrow than the natural channel, is attributed to the resistant clay in the bed and lower banks. Evidently because of mowing of the median area, no trees have become established along the bankline.

#### 9.5.14 Gravel Mining on the Russian River, California (Example 14)

It is essential to monitor and manage sand and gravel mining so as not to induce undesirable instabilities in the river system. In most cases, removal of sand and gravel has caused deepening and widening of the channel. These wider, deeper reaches act as sinks for the sediment loads and they may trap the finer clays and silts, altering the river environment. An interesting example of a river where excessive removal of sands and gravels has caused significant changes is in the vicinity of the confluence of Dry Creek with the Russian River. The location map is shown in Figure 9.15a. The tributary (Dry Creek) enters the river just downstream of a small dam on the Russian River. Previous sand and gravel extraction in the tributary has not exceeded the calculated safe yield, however, extraction rates in the middle reach of the Russian River significantly exceeded the safe yield for the period 1951 to 1964. This excessive extraction of sand and gravel induced a headcut that progressed upstream along the tributary, as shown in Figures 9.15b and 9.15c. This headcut was curtailed by a rock outcrop acting as a control point near a bridge approximately seven miles upstream of the confluence and essentially stabilized around 1972-1973. During the years 1946 to about 1955, the tributary channel widened (Figure 9.15d). Figure 9.15e shows the corresponding stage discharge relationships of the Russian River at the mouth of Dry Creek. Although in this example both rivers are bar-braided systems, they indicate the magnitude of possible adverse consequences from excessive sand and gravel mining on meandering streams.

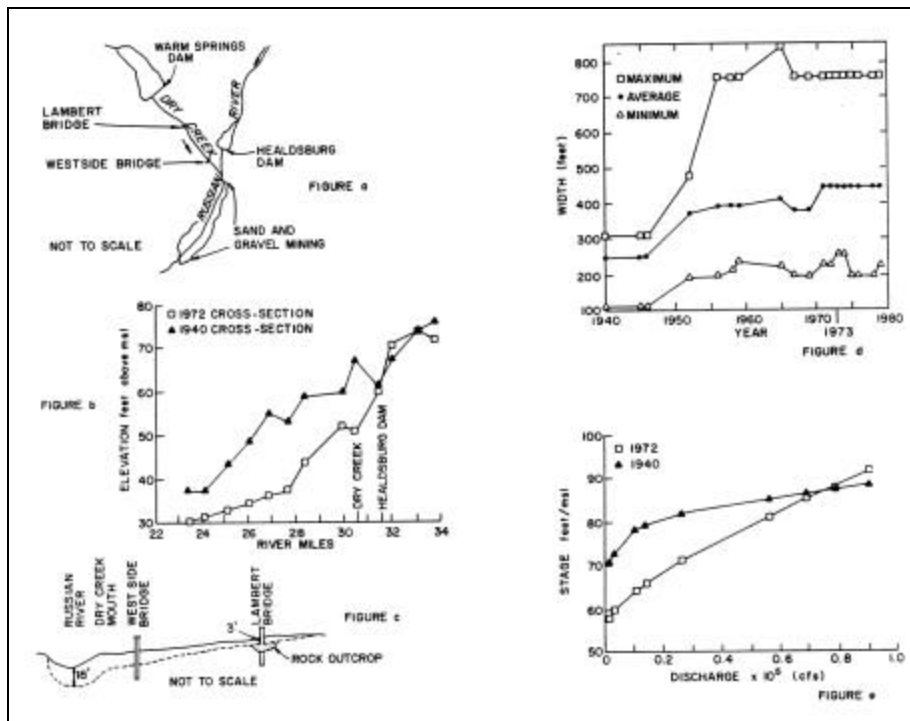


Figure 9.15. Case study of sand and gravel mining (Example 14).

### **9.5.15 Nowood River and Ten Sleep Creek Confluence, Wyoming (Example 15)**

During a site visit a unique situation was uncovered at the confluence of Ten Sleep Creek and the Nowood River in the Big Horn Basin of Wyoming. While investigating the site it was noted that the Nowood River had become unstable and considerable meandering activity was posing a threat to a rancher's numerous hay meadows. There was considerable evidence that the rancher had constructed and armored several cutoffs as well as armored incipient bendway activity to try and protect his meadows. The river had unstable banks and displayed degradation of the bed - obviously the river was in an unstable regime.

The rancher was contacted and could offer no explanation for the unusual bendway activity. He did say that prior to 1935 the Nowood River had been stable. Notably, that was the same year a highway agency had constructed the new bridge across the Nowood River. The rancher, in passing, said the 1935 bridge had replaced two bridges; one on the Nowood River and one on Ten Sleep Creek (Figure 9.16). The indiscriminate channel change employed to economize by constructing only one bridge had pushed the Nowood River past a stability threshold. The result was an unstable reach.

### **9.5.16 Middle Fork Powder River, Wyoming (Example 16)**

Significant and rapid erosion occurred immediately downstream from the new bridge across the Middle Fork Powder River at Kaycee, Wyoming. The erosion is primarily bank migration in the bendways and threatens to cause a meander cutoff (Figure 9.17). This cutoff would destroy the community's rodeo grounds.

The community blamed the highway agency's new bridge, claiming the bridge piers improperly directed flows into the downstream bendway. The highway agency's hydraulic engineers did not agree, as the new bridge was larger and more efficient than the previous structure. Aerial photos of the river reach taken several years apart through this period were obtained. New photos were obtained showing the river's present planform. Together these photos displayed a planform history.

The river was noted to be relatively stable until such time as when a downstream rancher had constructed a major cutoff to gain additional pasture land. Unfortunately the bridge was constructed about the same time as the cutoff was completed. However, the evidence was overwhelming in attributing the sudden instability to the rancher's channel change. These findings were presented to the community of Kaycee and the complaints ceased.

The erosion problem immediately downstream from the bridge is expected to continue. Should the community fail to forestall the cutoff, the rodeo grounds will be destroyed and the bridge will be in jeopardy from potential headcutting, as will an upstream trailer park.

## **9.6 CONCLUDING REMARKS ON DESIGN CONSIDERATIONS**

The dynamic features of rivers and river systems and the natural beauty of the river scenery make the design of highways in the river environment one of the most challenging and stimulating of all engineering designs.

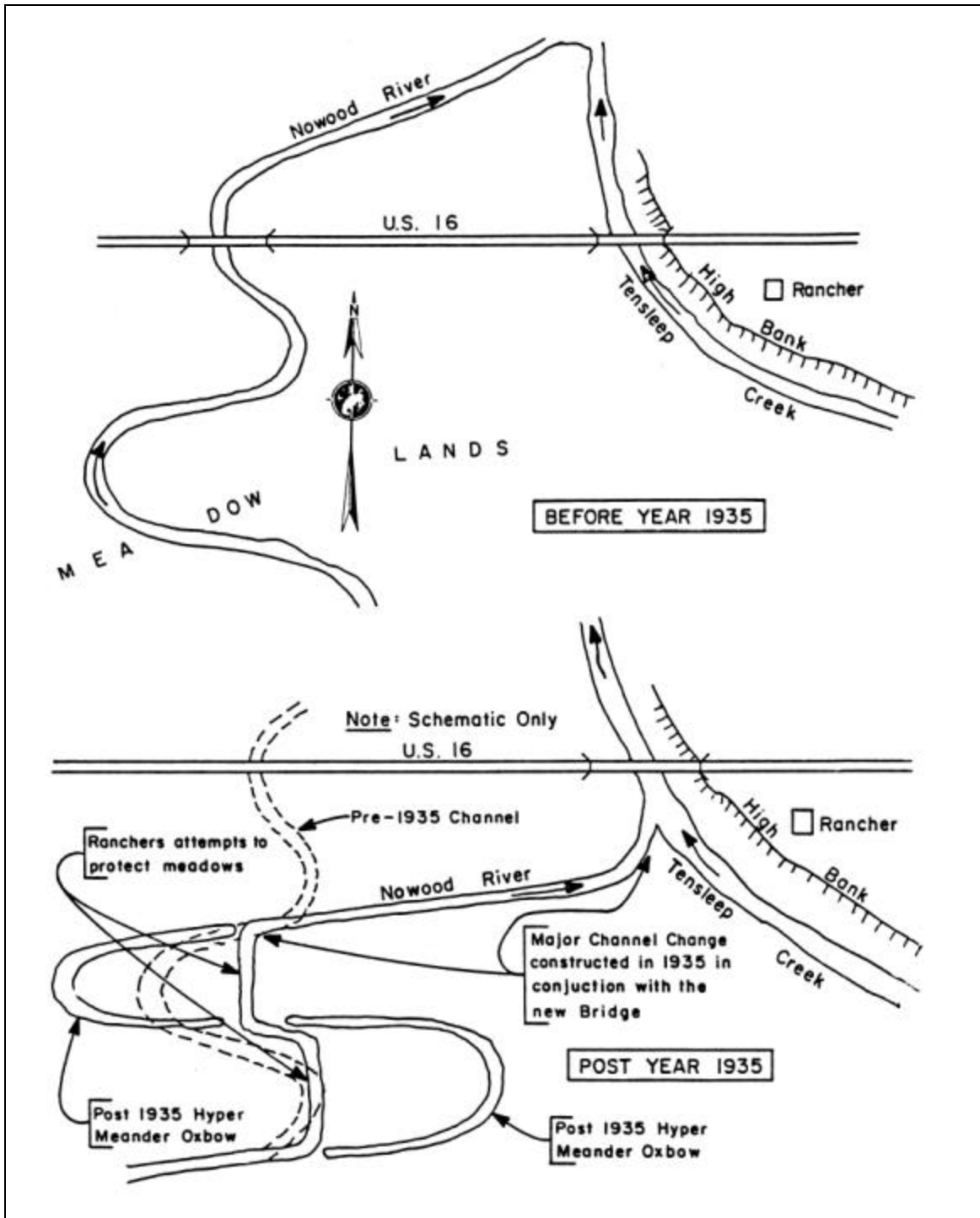


Figure 9.16. Nowood River near Ten Sleep, Wyoming (Example 15).

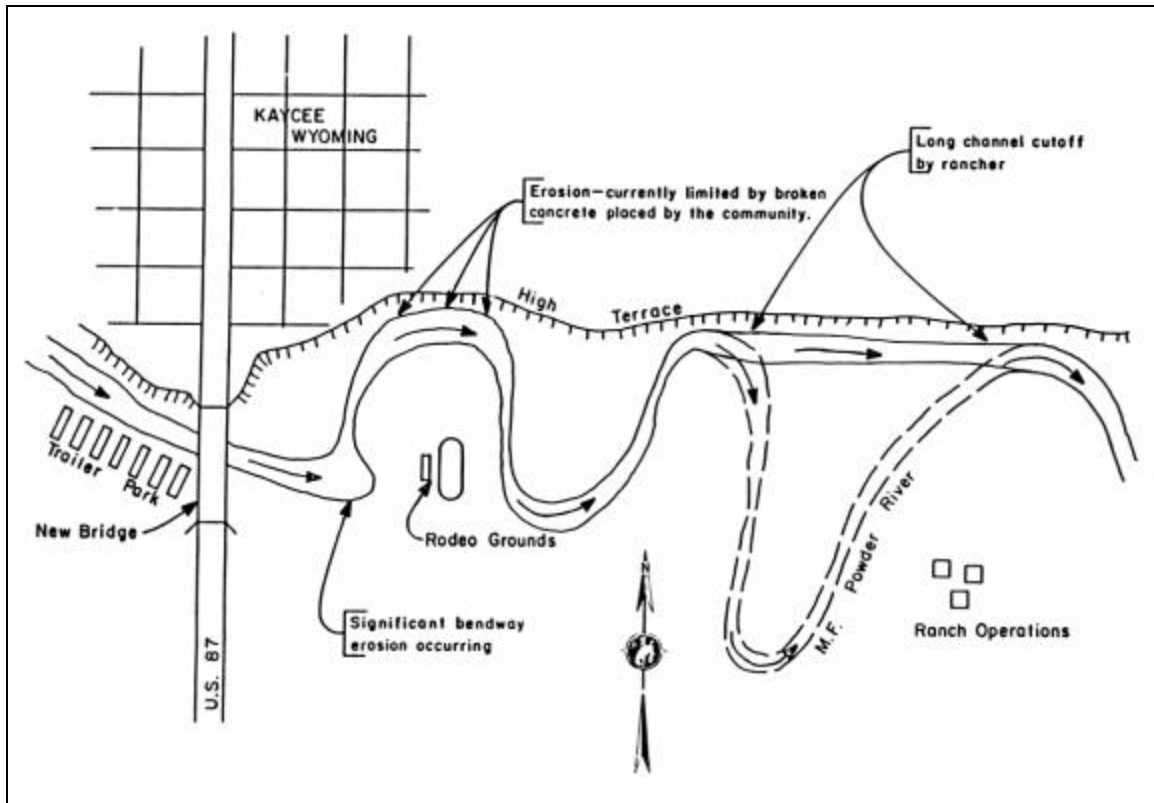


Figure 9.17. Middle Fork Powder River at Kaycee, Wyoming (Example 16).

This chapter illustrates the many interactions between rivers and highway structures. Rivers are dynamic, at times migrating rapidly across floodplains, at others lying dormant through years of low flows, only to break out of their banks during the next flood to recarve the form of the immediate landscape and, potentially, seriously impact highway structures. The design of bridges, bridge countermeasures, and river restoration must consider low, intermediate, 100-year, and super floods. The next chapter presents three design examples illustrating the application of the principles and methods given in this manual.

(page intentionally left blank)



## CHAPTER 10

### OVERVIEW EXAMPLES OF DESIGN FOR HIGHWAYS IN THE RIVER ENVIRONMENT

In this chapter, three examples are given illustrating the application of the principles, methods and concepts of previous chapters to the design of highway encroachments and crossings in the river environment. The designs encompass the use of geomorphic, hydrologic and hydraulic principles to design safe and economical crossings that protect, maintain and restore the river environment. The three-level design procedure discussed in Chapter 9 is emphasized in these designs.

In the examples, the designs are determined by well-established numerical procedures; however, they also depend heavily on the judgment of the engineer. The examples should be read and studied as an illustrative unit and not as designs from which one can choose the correct prescription for a problem at hand. River problems are much too complex for a cookbook approach, as is evident from these examples.

#### 10.1 OVERVIEW EXAMPLE 1 - BIJOU CREEK

This example presents a geomorphic, hydrologic, and hydraulic analysis of Bijou Creek, a tributary to the Narrows Unit near Fort Morgan, Colorado. The proposed location of the Union Pacific Railroad is approximately 1,500 ft (457 m) north of the creek (Figure 10.1). The purpose of the analysis is to ensure the safety of the proposed railroad location and to evaluate river engineering design alternatives. Since the data for this case study are available in English units, the figures and tables retain English unit notation. SI (metric) units are given parenthetically in the text for reference.

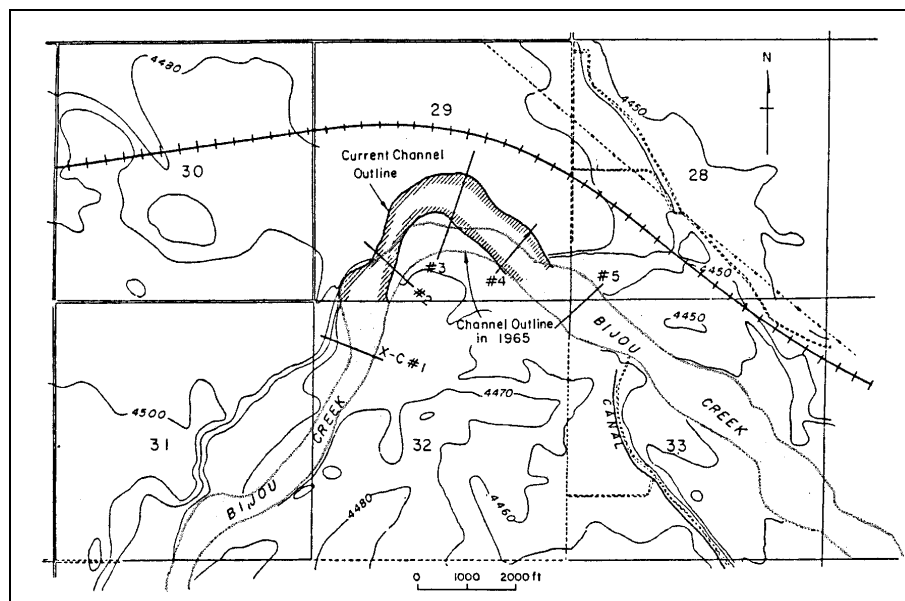


Figure 10.1. Topographic map of Bijou Creek study area.

### 10.1.1 Level 1 - Reconnaissance and Geomorphic Analysis

A Level 1 field study was conducted to obtain morphologic data for the Level 2 hydraulic analysis. The information utilized in the analysis includes the representative cross sections of the channel, the representative bed material size, and the energy slope. With these data, the flow resistance coefficient was estimated.

The representative cross section in the vicinity of the study site was developed by considering five selected cross sections established during the field study. Of these, two cross sections were similar in shape and are considered representative of the cross sections of the study reach. The dimensions of a representative cross section were established by averaging these two cross sections. The results of this analysis are shown in Figures 10.2 and 10.3.

Figure 10.2 shows the relationship between cross sectional areas and the flow depth as follows:

$$A = 242.6 y_n^{1.52}$$

in which A is the cross sectional area and  $y_n$  is the normal depth of flow measured from the thalweg level.

Figure 10.3 gives the following relationship between the wetted perimeter and the flow depth.

$$P = 682.0 y_n^{0.31}$$

The average top width of channel as estimated by field survey and topographic maps is 1,700 ft (518 m).

The results of sieve analyses of the bed material samples taken at three cross sections are shown in Figure 10.4. The average median bed material size,  $D_{50}$ , is 0.45 mm. The average  $D_{16}$  size is 0.22 mm, and the average  $D_{84}$  size is 0.91 mm. The bank material has nearly the same distribution as that of the bed material, but contains lenses of silt and clay. The bank is highly stratified and can be easily eroded.

The energy slope may be less than the channel bed slope. However, for a safer design, it is assumed that the energy slope is equal to the channel bed slope. The average channel bed slope from field surveys is 0.00252 ft/ft (m/m). This slope is adopted as the design energy slope.

The floods of June 1965 in South Platte River Basin, Bijou Creek were in upper regime, having antidunes with breaking waves. Similarly, computations show that the bed forms of Bijou Creek ( $D_{50} = 0.45$  mm) will be antidunes or standing waves during floods. Resistance to flow associated with antidunes depends on how often the antidunes form, the area of the reach which they occupy, and the violence and frequency of their breaking. If the antidunes do not break, resistance to flow is about the same as for a plane sand bed, and the discharge coefficient,  $C/(g)^{1/2}$ , (where C is the Chezy resistance coefficient and g is the gravitational acceleration) ranges from 14 to 23 (Manning's coefficient, n, is about 0.017 to 0.027 for the flow depths being considered). The acceleration and deceleration of the flow through the nonbreaking antidunes (frequently called standing waves) causes resistance to flow to be slightly more than that for flow over a plane bed. If many antidunes break, resistance to flow can be very large because the breaking waves dissipate a considerable amount of energy. With breaking waves,  $C/(g)^{1/2}$  may range from 10 to 20, and Manning's coefficient n ranges from about 0.019 to 0.038 for the flow depths being considered.

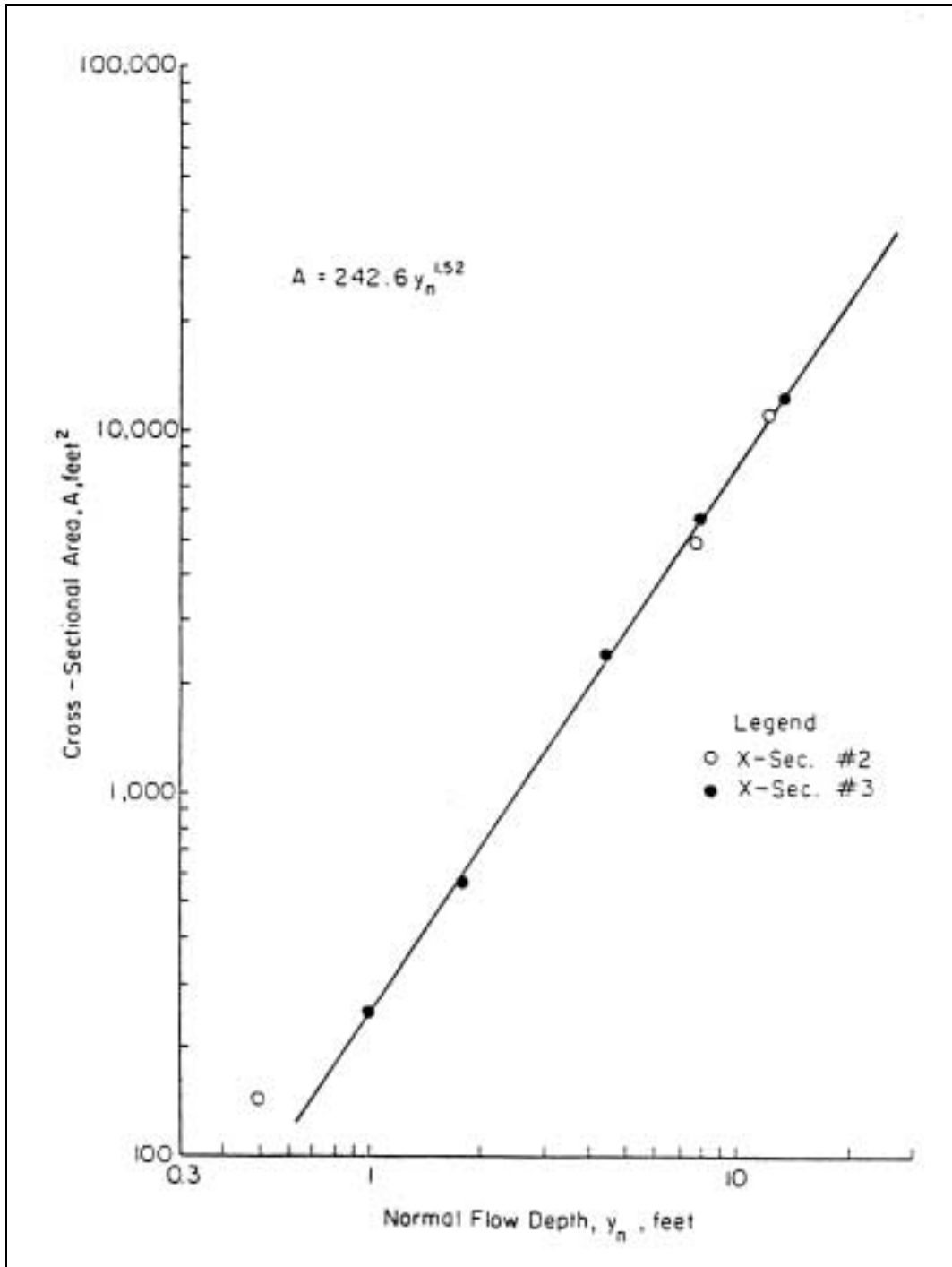


Figure 10.2. Cross sectional area versus flow depth relation.

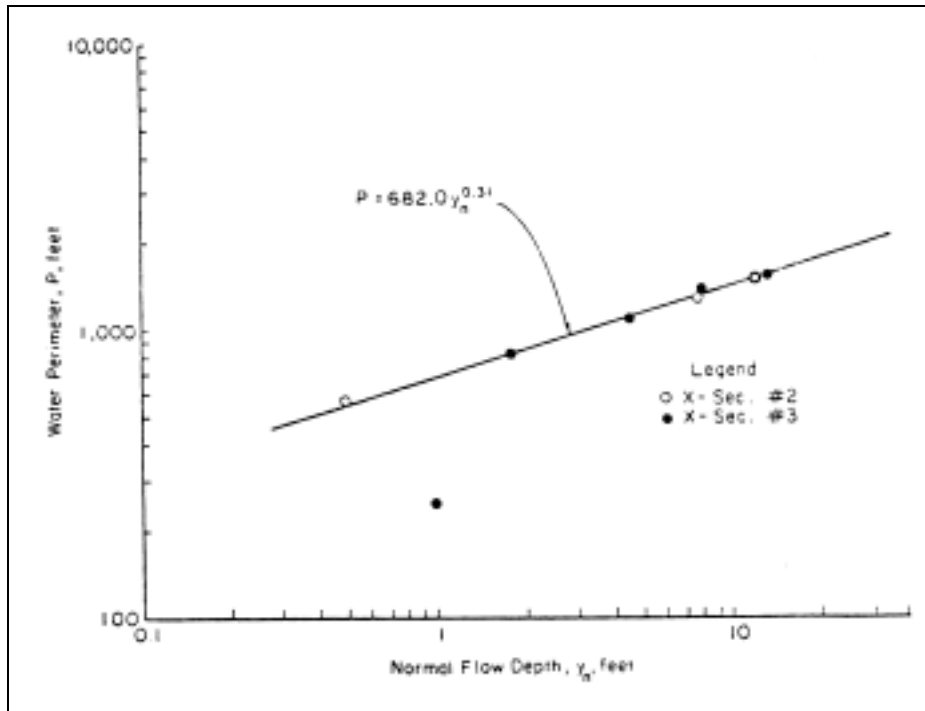


Figure 10.3. Wetted perimeter versus flow depth relation.

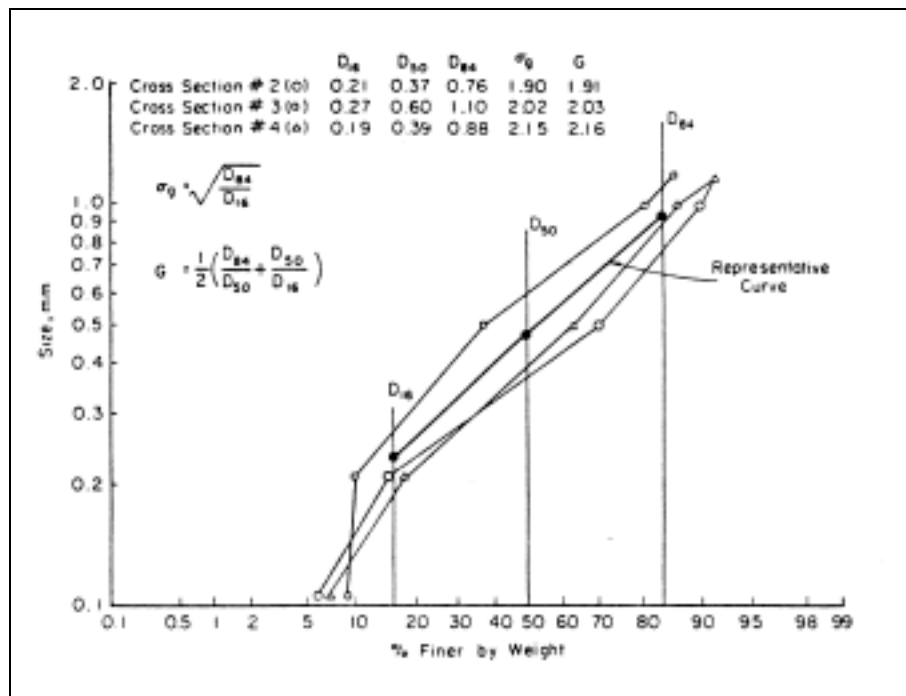


Figure 10.4. Analysis of bed material size of Bijou Creek.

From available data on the stage-discharge relation at the stream gaging station (near Wiggins, Colorado) it is estimated that the Manning roughness coefficient,  $n$ , during the design floods is about 0.023. This value of Manning's  $n$  gives a computed mean flow velocity of 18.7 ft/s (5.7 m/s) in Bijou Creek for the extreme flood of June 1965 [discharge 466,000 ft<sup>3</sup>/s (13,200 m<sup>3</sup>/s)].

### 10.1.2 Level 2 - Quantitative Engineering Analysis

Hydrologic Analysis. The hydrologic analysis identified three design floods and corresponding water surface elevations with return periods of 50, 100, and 200 years. Bank protection will be specified for each of the design floods for five channel design alternatives. The design floods were estimated using the Gumbel Method of frequency analysis and all of the available hydrologic data. The design of riprap bank protection will consider the design flood discharge, super-elevation in the bend, bedform height, local scour, bed material size, and stability of riprap materials.

The historical records show that there were two extreme floods 282,900 cfs (8,012 m<sup>3</sup>/s) and 466,000 cfs (13,200 m<sup>3</sup>/s) observed at the streamflow gaging station of Bijou Creek near Wiggins, Colorado. Historic stream flow data were plotted in Figure 10.5 using Gumbel probability paper. From this figure, the floods with various return periods can be interpolated or extrapolated. The estimated design floods with return periods of 100 and 200 years are respectively 62,000 cfs (1,756 m<sup>3</sup>/s) and 72,500 cfs (2,053 m<sup>3</sup>/s) .

Moveable Bed Hydraulic Analysis. The information on hydraulic conditions needed for designing bank protection includes the normal depth of flow, the cross sectional area of flow, the mean flow velocity, the Froude number, the bedform height, the local scour depth, the super-elevation of the flow in the bend, the local depth, and the local velocity. Moreover, different design alternatives will result in different hydraulic conditions. In this study, five design alternatives were proposed; the first alternative was to protect the existing outer bank with riprap (Figure 10.6), the second alternative was to realign the bend to its plan geometry before 1965 and to protect the outer bank with riprap (Figure 10.7), and the third alternative was to realign the bend to that of a mild bend relative to the existing channel alignment and to protect the outer bank with riprap (Figure 10.8). The fourth alternative was to determine the necessary buffer strip distance between the railroad and the present north river bank if bank protection is not utilized. The fifth alternative was to use rock riprap spurs to protect the existing river bank by realigning the channel (Figure 10.9).

As shown in Figure 10.9, the fifth alternative, to construct a series of rock riprapped spurs to guide the flow away from the existing north bank, has the same flow alignment as the second alternative (Figure 10.7).

A summary of computed hydraulic conditions in the first three basic alternatives is given in Table 10.1. The data necessary to determine riprap size are included for three values of radius of curvature,  $r_c$ , of the bend.

The following normal depth-discharge relation is determined by using Manning's equation, using the slope of energy gradient  $S = 0.00252$ , and Manning's roughness coefficient  $n = 0.023$ .

$$Q = 395.02 y_n^{2.32}$$

In this relation  $Q$  is the design discharge and  $y_n$  is the normal depth of flow measured from the thalweg level.

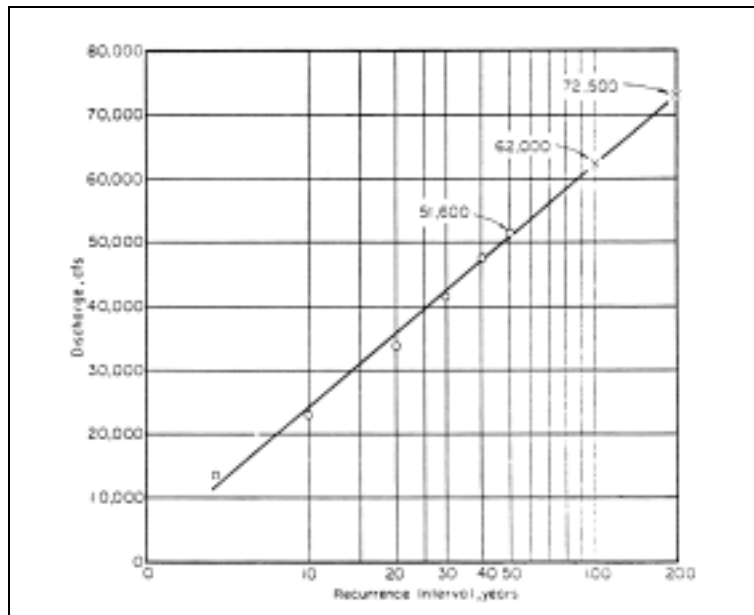


Figure 10.5. Gumbel's method of frequency analysis. Annual floods on Bijou Creek near Wiggins, Colorado.

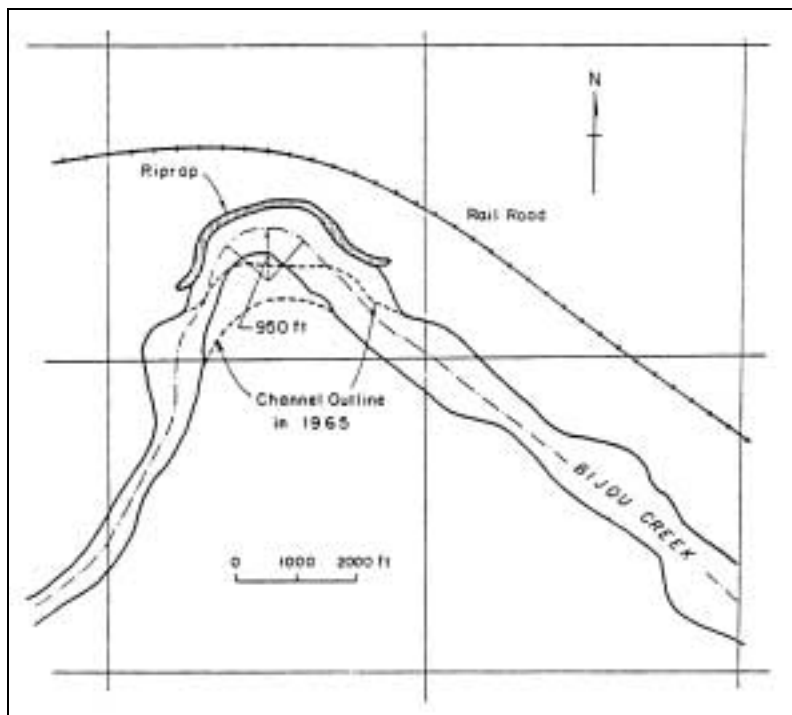


Figure 10.6. Proposed first alternative.

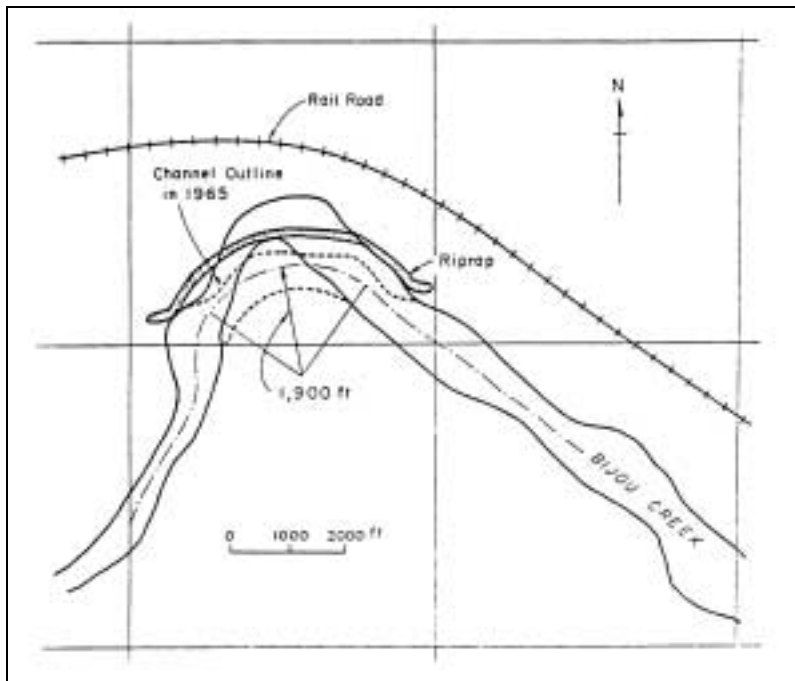


Figure 10.7. Proposed second alternative.

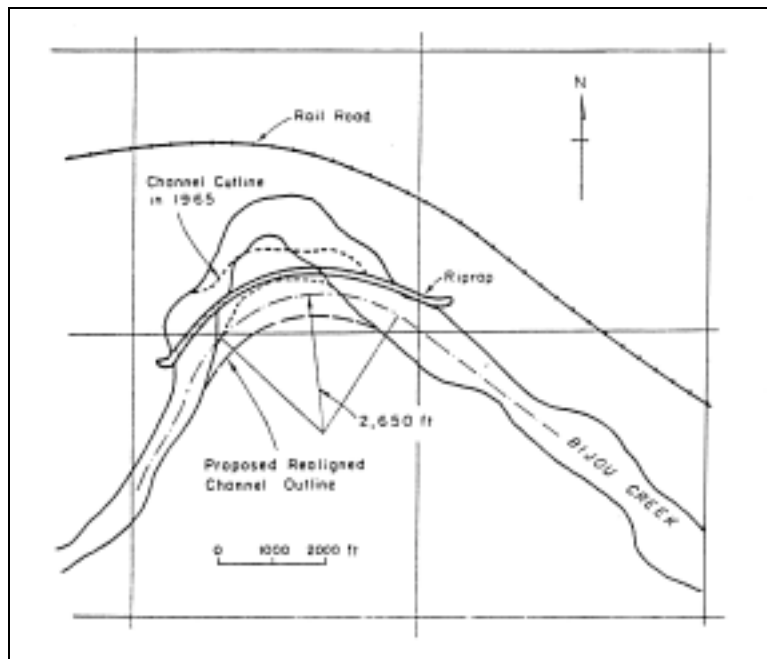


Figure 10.8. Proposed third alternative.

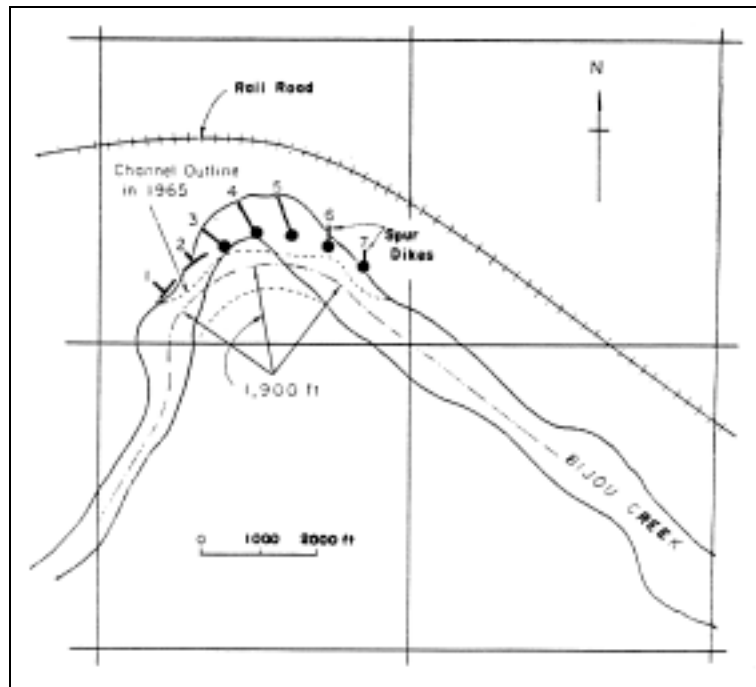


Figure 10.9. Proposed fifth alternative.

Table 10.1. Summary of Computer Hydraulic Conditions.

T yrs	Q cfs	$Y_n$ ft	A ft	V fps	F	H ft	$Y_s$ ft	$A\ell$	$r_c$ ft	$\Delta_z$ ft	$y_o$ ft	$V_o$ fps
50	51,600	8.17	5,904	8.74	0.72	1.05	8.82	1	950	4.24	12.40	17.37
								2	1,900	2.12	10.28	15.30
								3	2,650	1.52	9.69	14.70
100	62,000	8.84	6,660	9.31	0.74	1.18	9.63	1	950	4.82	13.65	18.50
								2	1,900	2.41	11.20	16.20
								3	2,650	1.73	10.57	15.60
200	72,500	9.46	7,379	9.82	0.75	1.32	10.33	1	950	5.36	14.82	19.50
								2	1,900	2.68	12.14	17.11
								3	2,650	1.92	11.38	16.40

Note: T is the return period, Q is the design discharge,  $y_n$  is the normal depth from the thalweg level, A is the cross-sectional area of flow, V is the mean flow velocity, F is the Froude number, H is the antidune height,  $y_s$  is the scour depth at the leading portion of riprap bank protection,  $A\ell$  is the alternative of designs,  $r_c$  is the radius at the center of a bend,  $\Delta_z$  is the superelevation, and  $y_o$  and  $V_o$  are the depth and velocity, respectively, for designing riprap sizes.

For design floods with return periods of 50, 100 and 200 years, the normal depths from thalweg level are determined. Then the cross sectional area and the wetted perimeter can be computed. Finally, the mean flow velocity, the hydraulic radius, and the Froude number are calculated.



As shown in Table 10.1, the average Froude number is approximately 0.74, which implies the maximum local Froude number in the center of the flow could be on the order of 1.0 to 1.2. According to Simons and Richardson (1963, 1966), these flow conditions should be in the upper regime with antidunes with breaking or nonbreaking waves. The estimated Manning's coefficient of 0.023 is correct for these flow conditions. In addition, the backwater effects are negligible because the flows are in the upper regime. The normal depth as computed should be satisfactory for design purposes.

There are many methods for determining riprap size (Simons and Senturk 1977). Among them, the method developed by Stevens et al. (1984) may be the most comprehensive and appropriate method to use. In applying their method, the depth of flow, the flow velocity and the angle between the horizontal and the velocity vector in the plane of the side slope are necessary as discussed in Chapter 6.

As mentioned in Chapter 3, the bed forms of antidunes or standing waves constitute a series of inphase symmetrical sand and water waves. These waves are in the center of the channel. Thus, the depth of flow at the bank for designing riprap sizes is taken to be the sum of the normal depth from thalweg level and the superelevation ( $y_o = y_n + \Delta_z$ ). The flow velocity for designing riprap size is computed by utilizing Manning's equation:

$$V_o = \frac{1.486}{n} y_o^{2/3} S_f^{1/2}$$

in which  $S_f$  is the energy slope. The angle between the horizontal and the velocity vector in the plane of the side slope is assumed to be negligible.

Three design alternatives based on different radii of curvature are considered in this phase of the study. Different hydraulic designs result for each of the three design alternatives and each of three different design floods. The hydraulic design includes the determination of the total length of bank protection, the minimum buffer strip distance between the railroad and the river bank, the estimated volume of earthwork, the side slope of riprapped bank, the sizes of riprap material, the thickness of riprap, the size of the gravel filters, the thickness of the gravel filters, the height of riprap protection above the existing bed level, and the depth the riprap should extend below thalweg level. Using the hydraulic data, all these values can be computed. Table 10.2 provides a summary of the hydraulic designs for different design conditions. The methods of design are described in the following sections.

From Figures 10.6, 10.7, and 10.8 the length of bank protection, minimum buffer strip distance between the railroad and the river bank, and the excavation volumes for three different design alternatives can be estimated. The minimum buffer strip distance is a measure of how far the river bank must migrate due to bank erosion to endanger the railroad. A wider minimum buffer strip distance between Bijou Creek and the railroad will provide a larger factor of safety for the railroad. However, the length of bank protection and excavation volumes increase accordingly, which in turn increase the cost of construction.

Table 10.2. Summary of Hydraulic Designs.

T yrs	Q cfs	$A_v$	L ft	$B_m$ ft	Ex $10^3$ yd <sup>3</sup>	Z	$K_{oa}$ ft	$G_x$	$t$ ft	$t_{50}^1$ mm	$G_1^1$	$t_1^1$ in	$r_{50}^2$ mm	$G_1^2$	$t_1^2$ in	$h_b$ ft	$h_b'$ ft	$h_e$ ft
50	51,600	1	4,700	700	---	2.5	1.5	1.3	3.3	6.0	3.0	10.0	60.0	2.0	10.0	14.5	10.0	5.0
		2	5,700	1,250	6.26	2.5	1.1	1.3	2.4	6.0	3.0	8.0	60.0	2.0	7.0	12.5	10.0	5.0
		3	6,250	1,500	9.42	2.5	1.0	1.3	2.2	6.0	3.0	7.0	60.0	2.0	7.0	12.0	10.0	5.0
100	62,000	1	4,700	700	---	2.5	1.7	1.3	3.7	6.0	3.0	12.0	60.0	2.0	11.0	16.0	11.0	5.0
		2	5,700	1,250	7.04	2.5	1.3	1.3	2.9	6.0	3.0	9.0	60.0	2.0	9.0	13.5	11.0	5.0
		3	6,250	1,500	10.64	2.5	1.2	1.3	2.6	6.0	3.0	8.0	60.0	2.0	8.0	13.0	11.0	5.0
200	72,500	1	4,700	700	---	2.5	2.0	1.3	4.4	6.0	3.0	14.0	60.0	2.0	13.0	17.5	12.0	5.0
		2	5,700	1,250	7.85	2.5	1.4	1.3	3.1	6.0	3.0	10.0	60.0	2.0	9.0	14.5	12.0	5.0
		3	6,250	1,500	11.91	2.5	1.3	1.3	2.9	6.0	3.0	9.0	60.0	2.0	9.0	14.0	12.0	5.0

Note: T is the return period in years, Q is the design discharge,  $A_v$  is the alternative of designs, L is the total length of riprap bank protection,  $B_m$  is the minimum buffer ship distance between the railroad and the riverbank, Ex is the estimated excavation volumes, Z is the ratio of the horizontal distance to the vertical distance for the side-slope of riprap bank,  $K_{oa}$  is the design riprap size for which 50 percent is finer by weight,  $G_x$  is the gradation coefficient of riprap,  $t$  is the thickness of riprap,  $t_{50}^1$ ,  $G_1^1$ , and  $t_1^1$  are, respectively, the gravel size for which 50 percent is finer by weight, the gradation coefficient and the thickness of the first layer of gravel filter,  $t_{50}^2$ ,  $G_1^2$ , and  $t_1^2$  are, respectively, the gravel size for which 50 percent is finer by weight, the gradation coefficient and the thickness of the second layer of gravel filter,  $h_b$  is the design height of riprap protection above the existing bed level, and  $h_b'$  and  $h_e$  are, respectively, design riprap depths in and not in the leading portion of the bank protection.

### 10.1.3 Riprap Design for Alternatives 1, 2, and 3

Side Slope of Riprap Bank. The side slope of the riprapped bank should be less than the angle of repose of the bank material. Analysis shows that the angle of side slope should be at least 5° less than the angle of repose of the bank material. The bank material is medium sand with some clay and silt with average D<sub>50</sub> of about 0.35-0.45 mm. Its angle of repose is about 29° (see Chapter 6). A side slope 2.5:1 (horizontal to vertical distance) is utilized and the corresponding angle of side slope is 21.75° (Figure 10.10).

Riprap Design. The size of riprap is determined using the method presented in Chapter 6. The method developed by the Bureau of Reclamation (1958) to determine the maximum rock size in a riprap mixture is used for comparison. The flow conditions required for designing riprap sizes were discussed earlier and given in Table 10.1.

Using a stability factor of 1.3 and an angle of repose of riprap material of 41°, the required riprap sizes with a uniform gradation are determined. The results are shown in Table 10.3.

Return Period (yrs)	Discharge (cfs)	Design Alternatives	Uniform Size by Stevens et al. (1974)	Riprap Mixture by Stevens et al. (1974)		Maximum Size by USBR (1958) (ft)
				Median Diameter (ft)	Maximum Size (ft)	
50	51,600	1	2.6	1.5	3.3	2.6
		2	2.0	1.1	2.4	2.0
		3	1.8	1.0	2.2	1.8
100	62,000	1	3.0	1.7	3.7	3.1
		2	2.2	1.3	2.9	2.2
		3	2.0	1.2	2.6	2.0
200	72,500	1	3.4	2.0	4.4	3.5
		2	2.5	1.4	3.1	2.5
		3	2.2	1.3	2.9	2.3

It is not acceptable to riprap a bank with uniform size rock, especially when large rock is required. Therefore, it is necessary to design a riprap mixture that includes an adequate range of sizes. In addition, the stability factor for determining the D<sub>50</sub> of the riprap mixture is assumed to be 1.1. According to Chapter 6, riprap gradation should follow a smooth size distribution curve with gradation coefficient of about 1.3. Riprap sizes are given in Table 10.3.

The Bureau of Reclamation (1958) developed a figure to determine the maximum rock size in a riprap mixture downstream from stilling basins. If the bottom velocity is assumed equal to the reference velocity on the top of the rock, the maximum rock sizes in the riprap mixtures for different design conditions can be estimated. The results utilizing both methods are given in Table 10.3 for comparison. The sizes obtained by use of the Stevens method given in Chapter 6 are recommended.

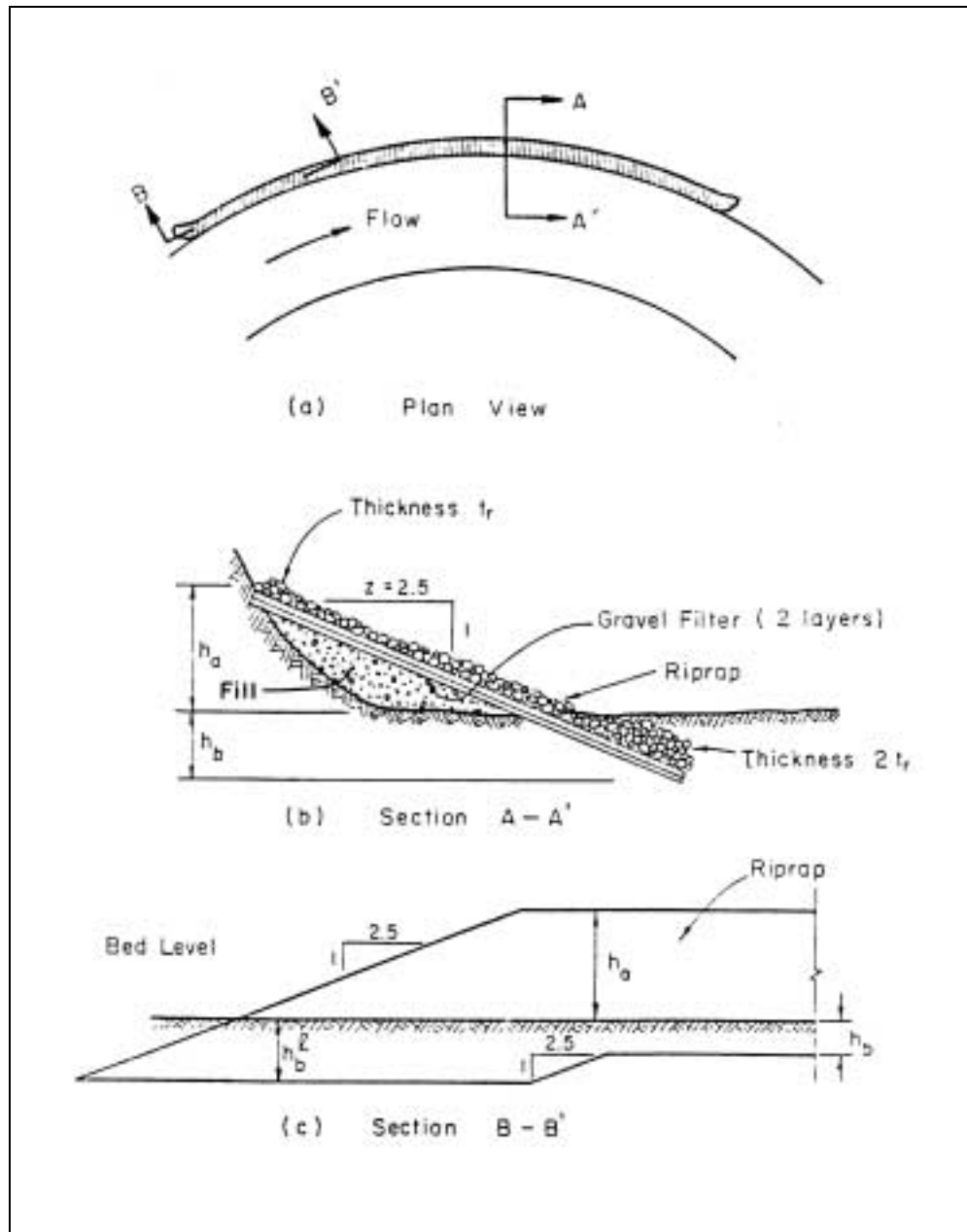


Figure 10.10. The sketch of proposed riprap design.

Gravel Filter Design. A filter should be placed under the riprap unless the material forming the core of the structure is coarse gravel or of such a mixture that it forms a natural filter. Two types of filters are commonly used: gravel and geotextile filter.

The sizes of gravel in the filter layer are calculated as explained in Chapter 6 and the results are given in Table 10.2. Two layers of filter material are required because the riprap sizes are large.

Thickness of the filters may vary depending on the riprap thickness, but should not be less than 6 to 9 in. (15 - 23 cm). Filters that are one-half the thickness of the riprap are satisfactory and provide a great degree of safety.

Height and Depth of Riprap. The design height of riprap protection above the existing bed level (Figure 10.10) must provide for freeboard, water depth, superelevation and wave height. The normal depth from the thalweg level and the superelevation were determined earlier. Because the forms of antidunes are a series of inphase symmetrical sand and water waves, the wave height at the water surface can be assumed equal to the antidune height. The minimum height required for riprap protection above the existing bed level can be determined by considering normal depth, superelevation, and antidune height. In order to provide additional protection against the breaking waves, an extra foot of freeboard is added to the required minimum height of riprap above bed level.

The riprap (Figure 10.10) must extend some distance below the thalweg level to provide safety against possible local scour, general scour, and troughs of passing sand waves. The general scour is assumed to be negligible because the proposed structures do not significantly constrict the flow. Some local scour is expected at the leading portion of the riprap revetment. Hence, a larger depth of riprap is required at this location. The minimum depth of riprap below thalweg level can be determined by considering the potential scour and the antidune height.

In general, the riprap should extend a minimum of 5 ft (1.5 m) below thalweg level in order to protect against possible long-term degradation of the river reach. If the computed depth of riprap protection below thalweg level is less than 5 ft (1.5 m), the design depth is set at 5 ft (1.5 m).

#### **10.1.4 Design for Alternatives 4 and 5**

Alternative 4. The fourth alternative is simply to provide sufficient buffer strip distance between the railroad and the existing river bank so that bank protection may not be required. The distances the north bank will migrate under different design flood conditions can be evaluated by utilizing sediment transport rates and the migration history of the 1965 flood. The estimated bank migration distances for the design floods are given in Table 10.4. In order to provide extra protection against slope failures and long-term bank migration due to smaller sizes of floods, the design buffer strip distances should be at least twice the computed migration distances (factor of safety - 2.0) because the accumulated bank migration distance due to smaller sizes of floods can be very significant.

Return Period (yrs)	Discharge (cfs)	Bank Migration Distance (ft)	Design Buffer Strip Distance* (ft)
50	51,600	562	1,124
100	62,000	629	1,258
200	72,500	715	1,430

\*The eroded bank should be restored to its present alignment after each flood to maintain an adequate buffer zone.

**Alternative 5.** The fifth alternative is to construct a series of rock riprap spurs to guide the flow away from the existing north bank (Figure 10.9). The design of the spurs includes: the form of spurs, the angle of spurs to the bank, the length of spurs, the spacing between spurs, the height or elevation of spurs, the construction materials, the crest width and slopes, and the local scour. The design of the spurs is summarized in Tables 10.5, 10.6, and 10.7. Table 10.5 gives a summary of spur designs for different design floods including buffer strip distance, number of spurs, spacing of spurs, height of spur above the existing thalweg level, riprap size at the spur nose, and riprap size in the spur shank. Table 10.6 provides the suggested design dimension of spurs including spur form, spur length, angle of spur to bank, the portion requiring riprap the same size as used on the nose, and length requiring shank protection. Table 10.7 summarizes the sizes of riprap and filter design at the nose of the spurs and for the spur shanks. HEC-23 (Lagasse et al. 2001) also provides design guidelines for a typical round nose spur recommended by FHWA.

T yrs	Q cfs	B <sub>m</sub> ft	N <sub>s</sub>	S <sub>d</sub> ft	h <sub>a</sub> ft	h <sub>b</sub> <sup>ℓ</sup> ft	K <sub>50</sub> <sup>n</sup> ft	K <sub>50</sub> <sup>s</sup> ft
50	51,600	1,250	7	600	12.5	10.0	1.1	0.6
100	62,000	1,250	7	600	13.5	11.0	1.3	0.7
200	72,500	1,250	7	600	14.5	12.0	1.4	0.7

Note: T is the flood return period in years, Q is the design discharge, B<sub>m</sub> is the minimum buffer strip distance between the railroad and the spur nose, N<sub>s</sub> is the number of spurs, S<sub>d</sub> is the spur spacing, h<sub>a</sub> is the design height of spur above the existing thalweg level, h<sub>b</sub><sup>ℓ</sup> is the design depth of spur at the spur nose below the existing thalweg level, K<sub>50</sub><sup>n</sup> is the median size of riprap at the spur nose, and K<sub>50</sub><sup>s</sup> is the size of riprap for the spur shank.

Spur No.	Spur Form	Spur Length (ft)	T-Nose Length (ft)	Angle of Spur to Bank (°)	Length Requiring Nose Riprap Size (ft)	Length Requiring Shank Protection (ft)
1	T-nose	200	400	90	20	180
2	T-nose	200	400	90	20	180
3	Round nose	500	N/A	70	200	300
4	Round nose	750	N/A	70	200	550
5	Round nose	750	N/A	70	200	550
6	Round nose	400	N/A	70	200	200
7	Round nose	200	N/A	70	200	0

Table 10.7. Size and Filter Design for Riprap at Spur Noses and Spur Shanks.										
T (yrs)	Q (cfs)	$K_{50}$ (ft)	$G_K$	$t_r$ (ft)	$f_{50}^1$ (mm)	$G_f^1$	$t_f^1$ (in.)	$f_{50}^2$ (mm)	$G_F^2$	$t_f^2$ (in.)
(a) At Spur Noses										
50	51,600	1.1	1.3	2.4	6.0	3.0	8.0	60.0	2.0	7.0
100	62,000	1.3	1.3	2.9	6.0	3.0	9.0	60.0	2.0	9.0
200	72,500	1.4	1.3	3.1	6.0	3.0	10.0	60.0	2.0	9.0
(b) At Spur Shank										
50	51,600	0.6	1.3	1.3	6.0	3.0	6.0	20.0	2.0	6.0
100	62,000	0.7	1.3	1.5	6.0	3.0	6.0	20.0	2.0	6.0
200	72,500	0.7	1.3	1.5	6.0	3.0	6.0	20.0	2.0	6.0
<p>Note: T is the return period, Q is the design discharge, <math>K_{50}</math> is the design riprap size for which 50 percent is finer by weight, <math>G_K</math> is the gradation coefficient of riprap, <math>t_r</math> is the thickness of riprap, <math>f_{50}^1</math>, <math>G_f^1</math>, and <math>t_f^1</math> are, respectively, the gravel size for which 50 percent is finer by weight, the gradation coefficient, and the thickness of the first layer of gravel filter, and <math>f_{50}^2</math>, <math>G_F^2</math>, and <math>t_f^2</math> are, respectively, the gravel size for which 50 percent is finer by weight, the gradation coefficient, and the thickness of the second layer of gravel filter.</p>										

Figure 10.11 shows the suggested spur design. The methods of design are briefly described below.

In Figure 10.9, Spurs No. 1 and 2 are T-nose spurs, and the others are round-nose spurs. The angle of spur to the bank is usually  $60^\circ$  to  $120^\circ$ . The available literature shows that the angle for T-nose spurs is normally  $90^\circ$  but the angles for round spurs varies. Mamak (1964) states that the best results for deflecting flow and trapping sediment load are obtained with spurs inclined upstream from  $100^\circ$  to  $110^\circ$ . However, the study by Franco (1967) showed that for channelization the normal or angled downstream spurs ( $60^\circ$ ) performed better than the angled upstream spurs. HEC-23 (Lagasse et al. 2001) suggests that for most applications, spurs can be oriented at  $90^\circ$  to the bank line, except for the first spur in the spur field. In this case, with a short radius bend, a moderate downstream angle is justified. Thus, judging from the purpose of spurs and flow conditions being considered, it is determined that the angles of round spurs should be constructed about  $70^\circ$  to the bank, angled downstream as shown.

The length of a spur depends on its location, amount of contraction of stream width, and purpose of the spur. The purpose of the spurs considered in this study is to guide the flow away from the bank and to provide a flow alignment similar to that of 1965. The lengths of spurs are determined to serve this purpose (Figure 10.9 and Table 10.7).

The spacing between spurs is primarily related to the length of the spur. In general, the recommended spacing is from one and one-half to six times that of the upstream projected spur length into the flow (see HEC-23 for additional guidance). For bank protection in a sharp bend, a smaller spacing should be used. For the design conditions, the spacing of spurs is taken as 600 ft (183 m).

The height or elevation of a spur is determined by considering the maximum flow depth above thalweg level. In order to provide additional protection against the breaking waves, an extra foot of freeboard was added to the design height of each spur above the existing thalweg level.

The local scour depth at the spur nose is the same as that at the leading portion of the continuous riprap revetment. The computed local scour depths for different design floods are given in Table 10.2. The minimum depth of riprap below thalweg level is determined by considering the local scour depth and the antidune heights, which also gives the design depth of spur at the spur nose below the existing thalweg level.

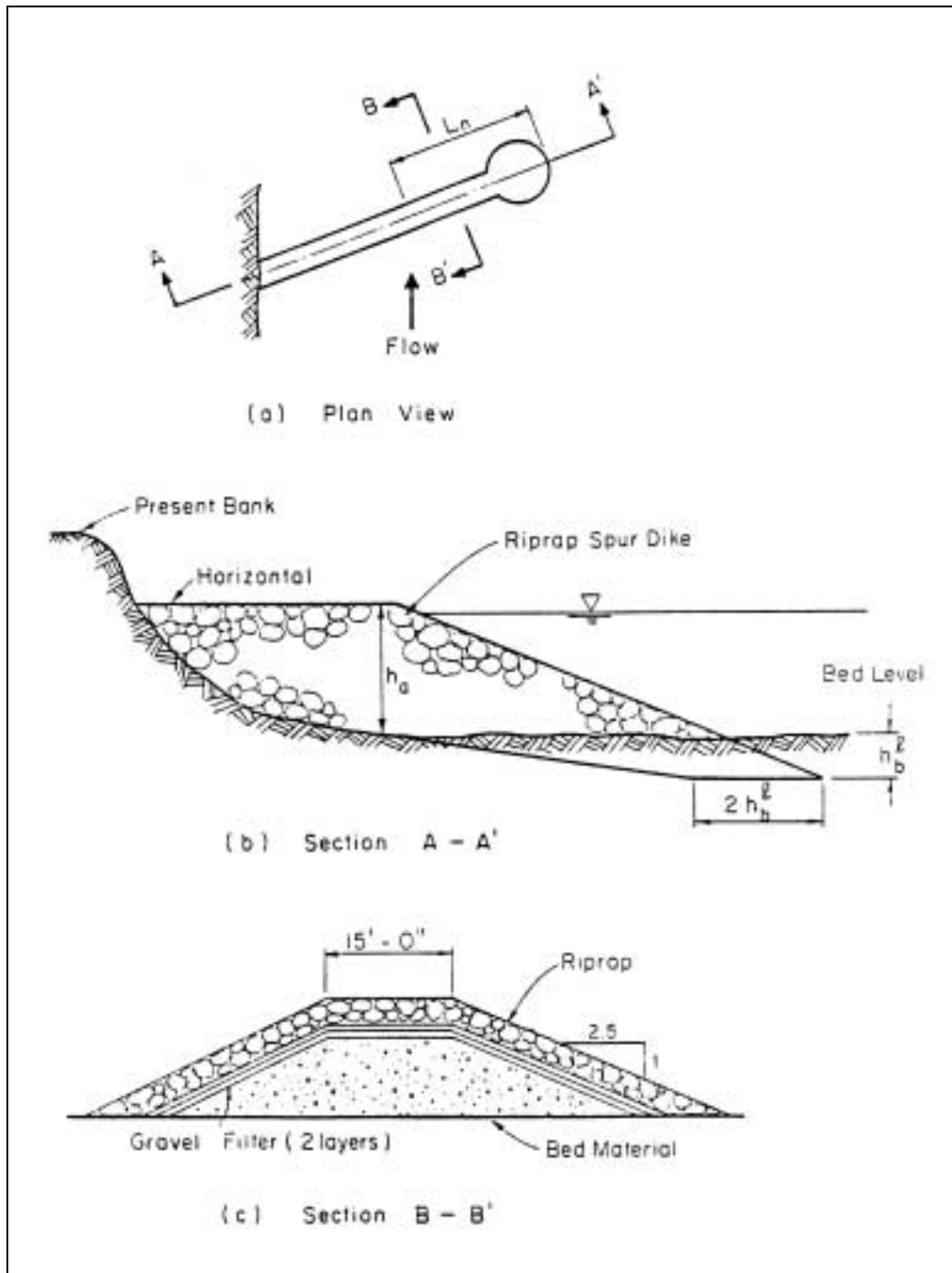


Figure 10.11. Sketch of spur design.



The construction layout is shown in Figure 10.11. The riprap design and the gravel filter design at the spur nose are the same as those used in the continuous revetment. The length requiring nose riprap size can be estimated by considering the flow separation zone. The riprap size in the shank inside this zone may use a smaller rock size. A reduction of fifty percent in rock size is determined by considering the decrease in flow velocity. The riprap at the downstream side of shank may be eliminated if a larger risk is accepted. This is because the downstream side of the shank is not expected to be subjected to a strong velocity. However, it may be subject to scour due to overtopping.

The crest width of rock riprap spurs usually ranges from 3 to 20 ft (1 to 6 m) and the side slope from 1.25:1 to 5:1. Considering the convenience in hauling and placing rock riprap, the crest width of spurs is determined to be 15 ft (5 m). The side slope was determined to be 2.5:1.

A second set of alternatives would result from replacing the rock riprap with soil-cement revetment in design alternatives 1, 2, and 3. This alternative may be of interest because large rocks can be very difficult to obtain and soil-cement revetment may be manufactured at the site without much difficulty (see Chapter 6 and HEC-23).

## **10.2 OVERVIEW EXAMPLE 2 - RILLITO RIVER**

### **10.2.1 Background**

The Rillito River System in Tucson, Arizona provides an example of the problems encountered in bridge crossing design. The objective of this example is to illustrate the methodologies used in the analysis and design of a bridge crossing, including a three-level analysis and the evaluation of conceptual alternatives. Since the data for this case study are available in English units, the figures and tables retain English unit notation. SI (metric) units are given parenthetically in the text for reference.

Two bridge sites are reviewed which provide insight into several outstanding problems characteristic of the Rillito system. These are the Sabino Canyon Road site with an existing bridge crossing (constructed 1936) and the Craycroft Road site with a dip crossing (where the roadway is at the same elevation as the channel bed). The study reach of Rillito River includes approximately 11.5 miles (18.5 km) of channel extending from Dodge Boulevard to Agua Caliente Wash (Figure 10.12). This includes 2 miles (3.2 km) on the Rillito River below Craycroft Road, 6-1/2 miles (10.5 km) upstream of Craycroft road on Tanque Verde Creek, 2 miles (3.2 km) upstream of Craycroft Road on Pantano Wash and 1 mile (1.7 km) on Sabino Creek upstream of the confluence with Tanque Verde Creek.

The history of flood events and the recent geomorphology of the Rillito system has shown that it is very dynamic and illustrates the characteristics of a braided river. The channel is steep, dropping at the rate of 21 ft per mile (3.98 m per kilometer). The bed material is predominantly in the medium to coarse sand sizes. The natural sinuosity of the river is low. Additionally, the river is generally unstable, changes alignment rapidly, and carries large quantities of sediment.

A large portion of the river system is in the metropolitan area of Tucson where human activities in, and adjacent to, the river environment have induced a number of changes in the system. Primary impacts on the system have occurred due to encroachment by urban development and channelization of segments of the river. Uncontrolled sand and gravel extraction has also led to even more rapid and significant changes in the river system. A secondary effect of urbanization is a reduction in sediment supply from tributaries draining urban areas.

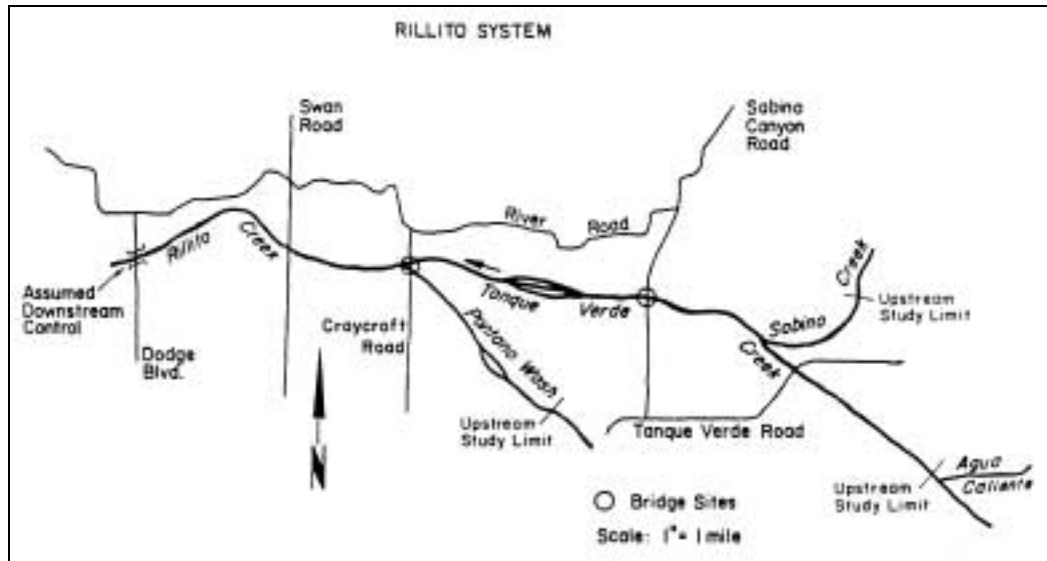


Figure 10.12. Rillito River system vicinity map.

Undeveloped land in the study area generally has little protective cover and supplies large quantities of sediment to the river system. However, extensive erosion control measures established for urban development and the creation of impermeable areas in these tributaries has reduced the sediment supply to the river system. As urbanization continues there will be a long-term decrease in sediment supply that will have a significant influence on the geomorphology of the river system.

The four bridge sites in the study area are at Dodge Boulevard, Swan Road, Sabino Canyon Road, and Tanque Verde Road (Figure 10.12). Measures have been taken at Craycroft Road to stabilize the crossing during the low flows and, as a result, the crossing is acting as a grade control on Pantano Wash. Stabilization measures have not been successful on the north side of Craycroft and no grade control has formed. Complex hydraulic conditions exist at the confluence of Tanque Verde Creek and Pantano Wash during the 100-year flood. Divided flow occurs with flood water spilling laterally into Pantano Wash from Tanque Verde Creek during a flood from that watershed, or flood water spills to Tanque Verde Creek during a flood from the Pantano watershed.

The bridges across the Rillito River and Tanque Verde Creek span a variety of channel conditions. The sedimentation and erosion processes due to the proposed bridges will depend on the extent to which the bridge influences the hydraulic conditions in the river (primarily the velocity and depth). Conversely, the changing form of the channel due to lateral migration or long-term changes in the channel profile can alter the hydraulic conditions at the bridge. The Dodge Boulevard bridge is assumed to be the downstream control for the study reach. This assumption is valid because the bridge crosses a channelized section of the Rillito River which has little influence on the water surface elevation in the channel for the 100-year flood. The downstream boundary hydraulic condition is assumed to be uniform flow.

Swan Road also crosses the Rillito River at a channelized section and has little effect on upstream water surface. Craycroft Road is one of two crossings discussed in detail later. The Sabino Canyon bridge crosses the defined channel on the Tanque Verde Creek. At the bridge

site, Tanque Verde Creek has also formed a sharp bend which will be unstable at high flow. The last bridge in the study area is at Tanque Verde Road. This bridge is on an undisturbed portion of the river system and crosses only the defined portion of the channel. Because the capacity of this channel is much less than the 100-year flood, the bridge creates a significant backwater for the 100-year flood. The roadway approaches would sustain heavy damage under these conditions.

A three-level analysis approach was applied to the river system to identify potential erosion and sedimentation problems associated with the bridge sites (see Chapter 9). First, a qualitative geomorphic analysis was performed documenting the history of the river system, the type of river form, the qualitative response of the system, and potential local problems at the bridge sites. The second level was an engineering geomorphic analysis which assesses the general quantitative response of the system, including determination of sediment supply, sediment transport rates, equilibrium slopes in the system for selected conditions, and lateral migration tendencies. The third level applied a detailed water and sediment routing procedure to evaluate the as-is conditions and various design alternatives. This three-level analysis provides the necessary information to:

1. Evaluate the stability of existing and proposed bridge structures
2. Determine the lateral migration tendencies of the channel
3. Estimate the extent of expected general channel scour
4. Determine the potential local scour around bridge piers and abutments
5. Estimate the long-term effects of sediment degradation or aggradation on the bed and water surface profiles
6. Determine the effects of debris on scour and water depth at the bridge sites

Applications of the principles of qualitative geomorphic analysis (plus basic engineering relations), and quantitative analysis (sediment routing) are demonstrated for the Craycroft site and the Sabino Canyon road bridge. Use of this three-level analysis gives a realistic bridge design for moveable bed and bank conditions resulting from the 100-year flood.

### **10.2.2 Level 1 - Qualitative Geomorphic Analysis**

General System Response. The purpose of qualitative geomorphic analysis is to identify the important physical processes which have been acting on the river system. General geomorphic relationships are used to classify the river system. Aerial photographs are compiled over a series of years as a means of constructing the recent history of the river system. Human activities including gravel mining and river training are documented and the river's response noted. A qualitative prediction of river response is developed, based on general geomorphic relationships such as the Lane relationship (see Section 5.5). The information gained by this level of analysis greatly aids in applying more rigorous methods of analysis.

The data base necessary for this type of analysis includes aerial photographs, topographic maps (1" = 100', 2' contour intervals), and site observations. With this approach, the basic characteristics of the river can be understood quickly with limited information.

Much of the system has been significantly disturbed by human activities. Observed activities include channelization, sand and gravel mining, construction of bridges, construction of grade controls, road crossings, and encroachment by urbanization. Much of the system's shape and form, then, is dictated by human activities rather than natural processes. This is especially true for the portions of the Rillito River and Pantano Wash within the study area. The Rillito River has been subjected to major channelization up- and downstream of Swan Road (Figure 10.12).

There is also a large instream gravel pit below Swan Road. The Pantano Wash system has a large instream gravel pit below, and bank stabilization works in the vicinity of Tanque Verde Road. The results of these activities have been to change these systems from their natural braided forms to defined channels. Pantano Wash still possesses a stretch of over 3,000 ft (900 m) which is braided. Tanque Verde Creek, however, has experienced less impact from human activities than the other two systems. The islands, bends and natural channel alignment observed in 1941 aerial photographs of Tanque Verde Wash are still intact.

The Tanque Verde Creek system should be classified as a braided system (see Section 5.4.5). The evidence of multiple channels, islands, and shifting alignment support this conclusion. A braided river can be identified by Equation 5.2.

$$S Q^{0.25} \geq 0.01$$

in which  $S$  is the average bed slope and  $Q$  is the dominate discharge (cfs). The mean annual flood of 5,000 cfs (142 m<sup>3</sup>/s) is assumed to represent dominant conditions in the system. The average slope for 13.1 miles (21 km) of the Tanque Verde Creek and Rillito River is 0.0044. This slope and discharge give a value of 0.037, which is well within the braided range (Figure 10.13). Pantano Wash has a slightly steeper grade, which would place it even further into the braided range. Even though much of the river has been channelized, it should be recognized that the river is in the braided range and, hence, is very dynamic.

Often, the general response of a river system to a flood event can be assessed qualitatively by studying its profile and plan view. This is especially true of a system which has been altered by human activity. This type of analysis is based on estimating the relative velocity along the system. In locations where a channel is constricted or the profile steepens, the velocity would be expected to increase. Since velocity is the dominant factor in determining sediment transport rate (when the sediment size does not change greatly), areas with large increases in velocity should degrade; areas where velocities are slowed considerably should experience aggradation. This is expressed in Lane's relationship (Equation 5.28), which can be written:

$$Q_s D_{50} \propto Q S$$

In this relationship,  $Q_s$  is the sediment transport rate,  $D_{50}$  is the median sediment size,  $Q$  is the flow rate of water and  $S$  is the slope of the bed.

For example, the instream gravel pit below Swan Road will trap sediment and reduce sediment supply to the downstream reach. This can be expressed using the Lane relationship as:

$$Q_s^- D_{50} \propto Q S^-$$

From this, one would expect an overall response of possible degradation in the reach of the Rillito River below the gravel pit to Dodge Boulevard. A similar application of the Lane relationship to various reaches in the study area indicates that over half of the channel reaches are well balanced for sediment transport. None of the reaches has a great potential for either aggradation or degradation. In all, the system should not experience large bed elevation changes except for those related to increased development and localized flow conditions. This qualitative assessment is confirmed by more detailed Level 2 analyses in the next section.

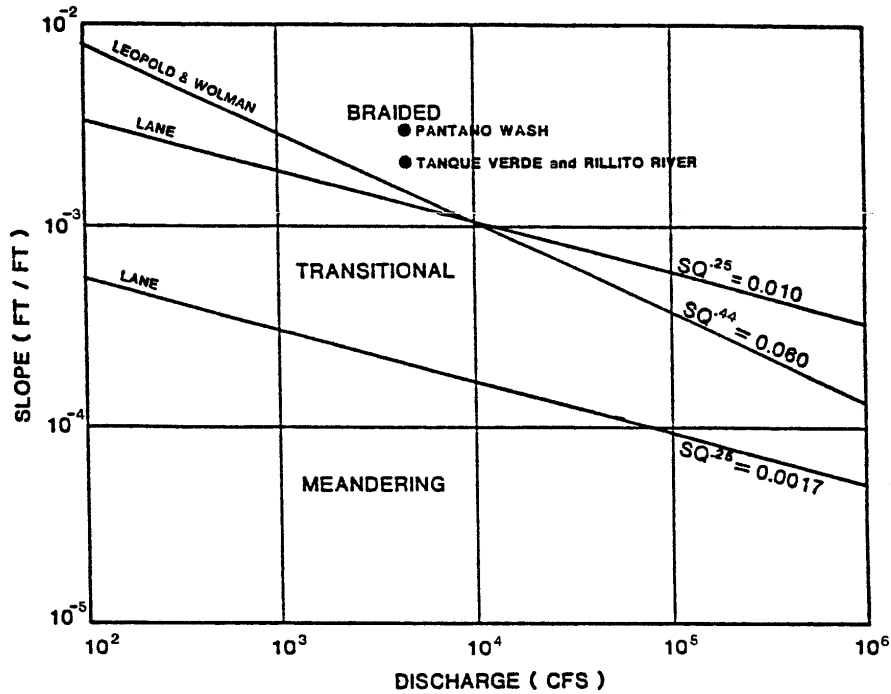


Figure 10.13. Slope-discharge relationship for Rillito River.

Each proposed or existing bridge site has possible problems associated with local erosion and sedimentation processes. These problems are identified below.

Potential Local Problems at the Craycroft Road Site. Location of a bridge at the confluence of Tanque Verde and Pantano Wash (Figure 10.14) could cause several problems. First, the confluence of two sand-bed rivers is usually very dynamic and can shift upstream or downstream and laterally quite quickly. This is especially true when an abnormal sequence of events results in a shift in the relative balance of flows between the two rivers. To compound this problem, the grade control structure (dip crossing) has created a situation in which Pantano Wash has a bed elevation several feet higher than Tanque Verde Creek at the same location. This provides an additional tendency for flows from Pantano Wash to migrate toward Tanque Verde Creek, where the flow could attack bridge piers and abutments at angles other than designed. As a result, local scour around piers and abutments of a bridge at this site could be significantly increased.

Neither Pantano Wash nor Tanque Verde Creek can contain a 100-year flood within its own channel. Since the two usually do not reach peak flows at the same time, the flow spills out of the flooding channel across the floodplain area between the two channels and into the opposite channel. In the process, the overflow deposits most of its sediment in the floodplain and the clear water entering the opposite channel causes degradation. There is also the problem of poor flow alignment past piers and abutments under these conditions. These problems are analyzed further when engineering alternatives to eliminate the problems are presented.

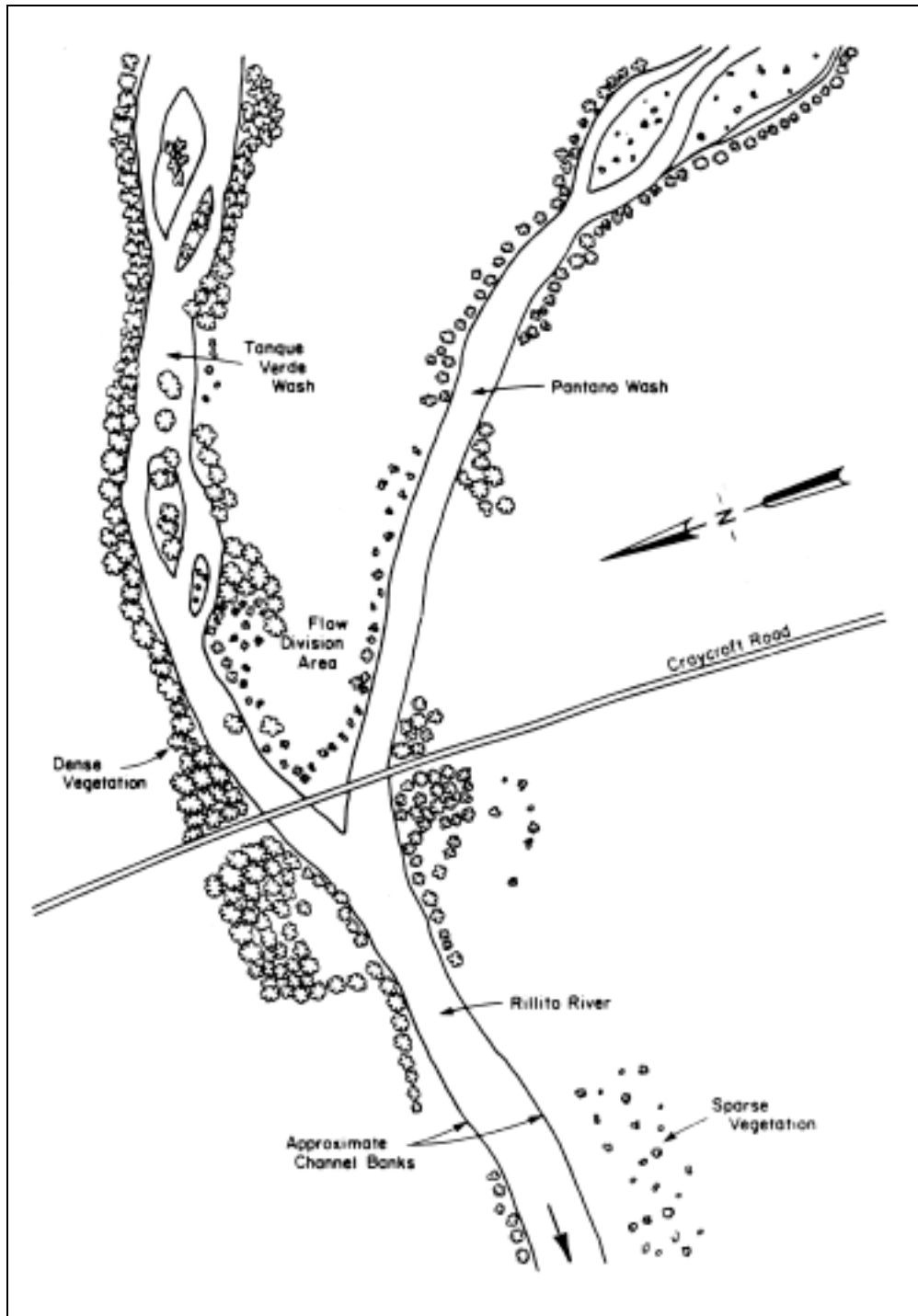


Figure 10.14. Sketch of Craycroft Road crossing.

Potential Local Problems of the Sabino Canyon Road Bridge Site. The Sabino Canyon Road bridge site (Figure 10.15) has several potential erosion and sedimentation problems that should be considered in the bridge design. The existing bridge has already experienced several such problems. The flow area of the bridge appears to be inadequate for the 100-year flood event. Over 4 ft (1.2 m) of scour has occurred around the bridge piers and abutments. In addition, the channel is located on a reach that is migrating to the left (looking downstream). This is causing the left abutment to be attacked. The migration tendency of Tanque Verde Creek is largely due to its braided nature and its lack of confinement by bank stabilization or channelization works. The lateral migration tendency is studied in more detail in the Level 2 quantitative engineering geomorphic analysis.

Considerable scour is occurring on the left side of the channel under the bridge since it is located on the outside of a bend. This is to be expected since high-velocity flow and secondary currents can scour sediment from the outside of a bend.

The final consideration is the gravel mining from the river. Currently, there is a mine approximately 3,000 ft (900 m) upstream of the bridge. The pit could act as a sediment trap and cause scour downstream of the pit near the bridge site as the water removes sediment from the bed to regain an equilibrium sediment transport rate. Because of the distance, the threat is not large from the present activity, considering the passage of the 100-year flood; however, gravel mining operations located closer to the bridge site could cause problems if not properly managed. In addition, over a long period of time the overextraction of sand and gravel can cause significant degradation for the entire reach downstream of the operating site, and possible headcuts upstream of the mining.

### **10.2.3 Level 2 - Engineering Geomorphic Analysis**

Hydrology. The Rillito River is formed by the confluence of Pantano Wash and Tanque Verde Creek northeast of Tucson and flows west-northwest about 12 miles (19.3 km) to its confluence with the Santa Cruz River. Precipitation in the Rillito River watershed is produced by three types of storms: general winter storms, general summer storms, and local thunderstorms. The general winter storms usually last for several days and result in widespread precipitation. General summer storms are often accompanied by relatively heavy precipitation over large areas for periods of up to 24 hours. Local thunderstorms can occur at any time of the year; however, they cover comparatively small areas and cause high-intensity precipitation for a few hours.

The flow in the Rillito River is intermittent and Tanque Verde Creek is almost always dry, other than during or immediately after rain. The USGS gaging station on the Rillito River near Tucson kept daily discharge records from October, 1908 to September, 1975, after which it was converted to a crest-stage partial-record station. The gage is located 4.75 mi (7.2 km) upstream of the confluence of Rillito River with the Santa Cruz River and about 4 mi (6.4 km) downstream of Dodge Boulevard (Figure 10.12).

Utilizing the USGS records at Rillito Station, all of the extreme events since 1915 are plotted in Figure 10.16. Based on these flood data the flood frequency curves are plotted on log-normal paper (Figure 10.17). The USGS log-Pearson Type III analysis is shown in Table 10.8. The hydrograph of the 1965 flood observed at the Rillito River gage near Tucson (Figure 10.18) was used to establish the 100-year flood hydrographs for Tanque Verde Creek and Pantano Wash. The design hydrographs for the 100-year flood for Tanque Verde Creek, Sabino Creek, Pantano Wash, Ventana Wash and Alamo Wash are given in Figure 10.19.

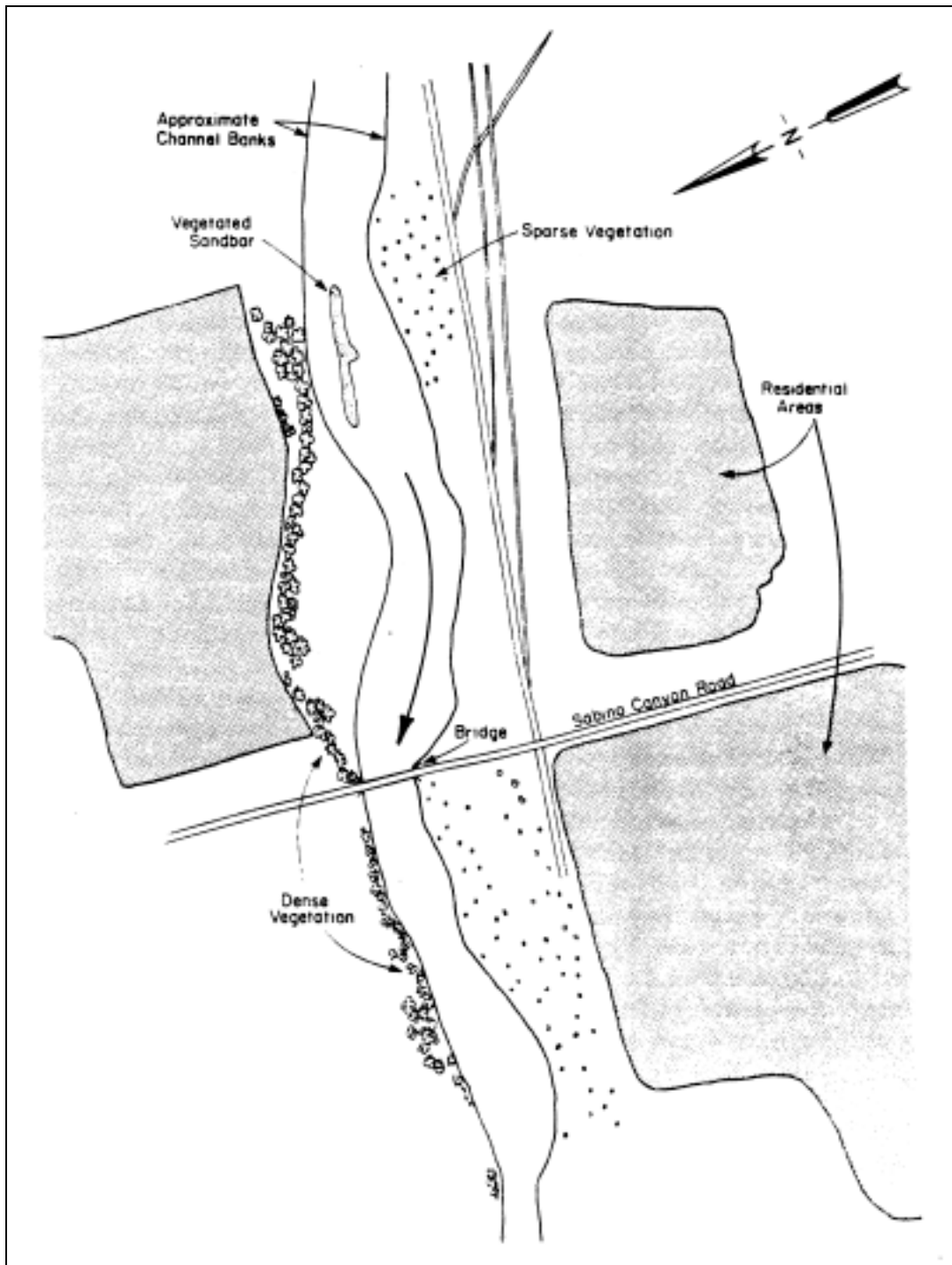


Figure 10.15. Sabino Canyon Road crossing site.



Table 10.8. Rillito River Near Tucson, Arizona Log-Pearson Type III Frequency Analysis by USGS.				
Exceedance Probability	Return Period (yr)	Expected Discharge (cfs)	95 Percent Confidence Limit (One-Sided Test)	
			Lower (cfs)	Upper (cfs)
0.5000	2	5,000	4,240	5,800
0.2000	5	9,300	7,670	11,100
0.1000	10	12,500	10,100	15,600
0.0400	25	17,200	13,300	22,000
0.0200	50	21,100	15,800	27,300
0.0100	100	25,200	18,400	33,000
0.0050	200	29,800	20,900	39,200
0.0020	500	35,700	24,400	47,800

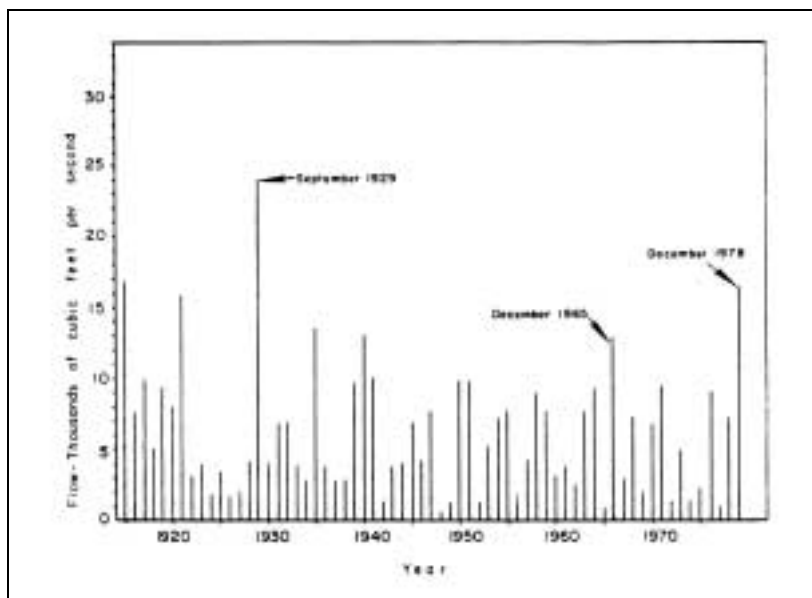


Figure 10.16. Flood events at Rillito River near Tucson, Arizona (drainage area 915 square miles).

**Hydraulics.** A complete rigid boundary hydraulic analysis was conducted prior to the moveable bed analysis. Water surface profile calculation from Dodge Boulevard to Agua Caliente Wash (Figure 10.12) was conducted using the Corps of Engineers HEC-2 program (today the Corps' HEC-RAS program would be used). The cross sectional data were modified to reduce the number of cross-sections and make the spatial resolution of the water surface computation compatible with the sediment routing model. The main channel roughness was reduced to near the lower limit of the river flow regime expected during the 100-year flood. The hydraulic conditions are predominantly subcritical up to Sabino Creek. The reach from Sabino Creek to Agua Caliente Wash increases in gradient and a mix of subcritical and supercritical hydraulic conditions is possible.

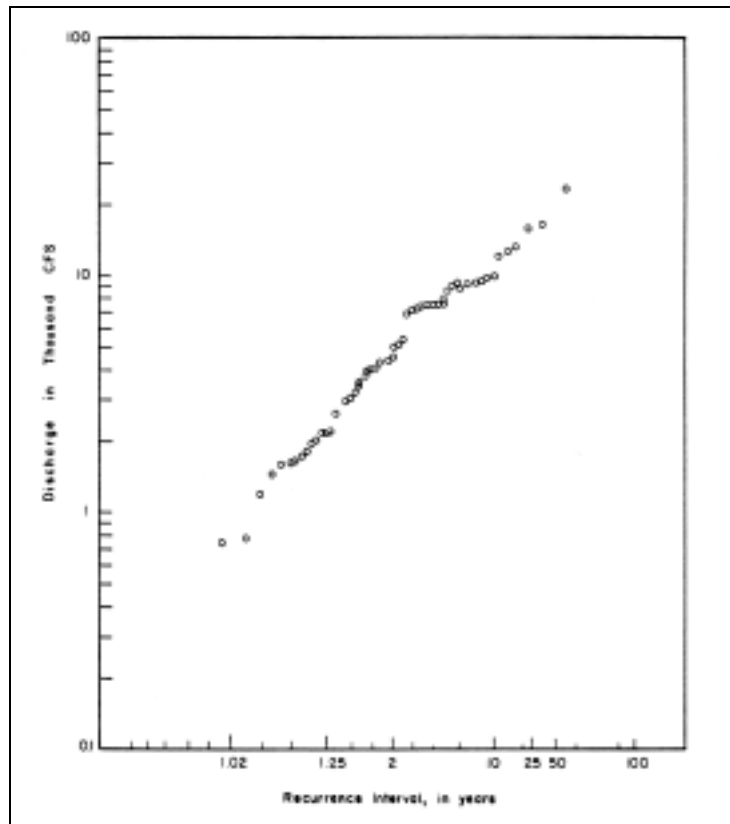


Figure 10.17. Log-normal frequency analysis for Rillito River near Tucson.

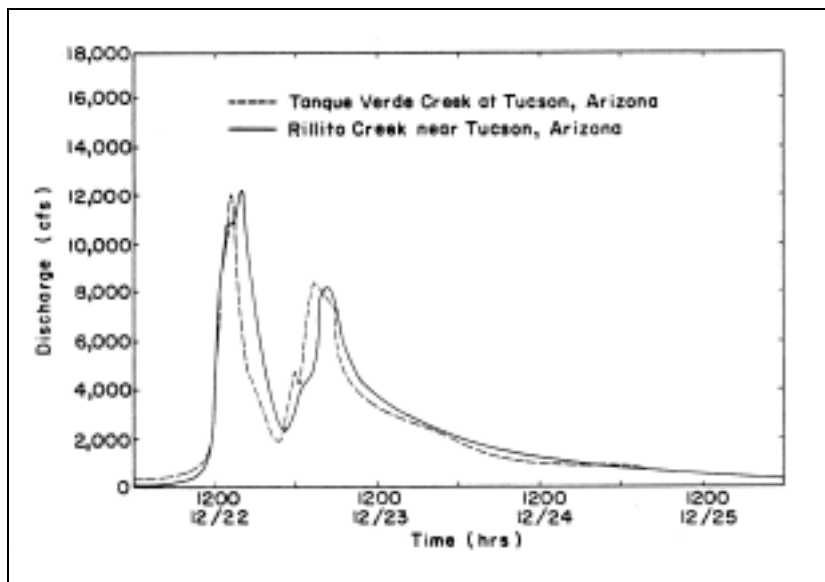


Figure 10.18. December 1965 flood in Rillito River and Tanque Verde Creek.



Spatial Design and Channel Geometry. In the quantitative geomorphic analysis, groups of cross sections were aggregated to form a typical cross section for a study reach. The geometric properties (area, wetted perimeter, top width, and hydraulic radius) of this section are determined for a series of depths. Normal depth for a given discharge, channel roughness and slope are then calculated and the hydraulic parameters (velocity and hydraulic depth) are used in the sediment transport relationship to determine the transport capacity in the reach. An equilibrium slope analysis can then be made.

A water surface profile calculation is made based on the sections utilizing HEC-2 (HEC-RAS). Hydraulic conditions in the main channel and overbank areas are based on output from HEC-2 (HEC-RAS).

Bed Material Size Distribution. Sediment size is one of the most important parameters used in evaluating sediment transport. A thorough sediment sampling survey was conducted on the river system, consisting of 41 bed material samples. Variation of the size distribution within these segments of the river did not follow an identifiable trend, and therefore an average size distribution was used and the variation from the average size distribution was assumed to be sampling error. Three size distributions were used to cover the river segments from Dodge Boulevard to Pantano Wash (including Pantano Wash), Pantano Wash to Sabino Creek and Sabino Creek to Agua Caliente Wash. Figure 10.21 shows the size distributions used for design on various segments of the river system. The size distribution of Pantano Wash is included to illustrate its similarity to the Rillito River size distribution.

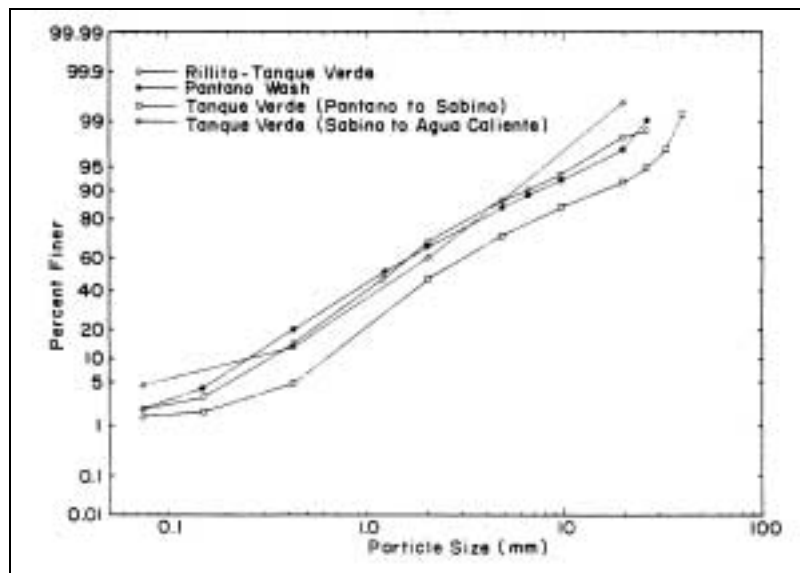


Figure 10.21. Rillito-Pantano-Tanque Verde bed sediment distribution.

A large percentage of sediment falls in the coarse sand and fine gravel range with less than 10 percent classified as medium gravel. Very coarse gravels are not present. From an analysis based on Shields' criteria, all sizes present can be easily transported by the mean annual flood. Formation of an armoring layer on the bed is unlikely since coarse, nontransportable particle sizes are missing from the distribution.

Subsurface bed material samples and bank material samples were also taken. The subsurface bed material is slightly coarser in most cases, but still lacked sizes in the nontransporting range. Bed material samples had more fine material and these distributions varied substantially from one location to the next.

Riparian Vegetation. The yield of debris to the bridge sites was determined by visual inspection of aerial photographs for the riparian zone of the system. A review of these photos indicated that large trees along the bank present the greatest problem. Trees along the banks were counted and the root zone size estimated. The root zone is the area of the tree capable of supporting the weight of the tree. This diameter is estimated as 5 to 6 ft (1.5 - 1.8 m) for trees on the Tanque Verde.

Tree yield will be from the banks of the river for large floods. The accumulation of smaller debris at a bridge is assumed to occur only in conjunction with the trapping of larger debris. Actual debris yield and trapping at a bridge were analyzed by a qualitative approach. For additional information on estimating debris accumulation, see HEC-20, Chapter 4 (Lagasse et al. 2001).

Resistance to Flow. During the December 1965 flood, the Rillito River was in upper regime, having antidunes with breaking waves. Similarly, the geomorphic analysis shows that the bed forms of the channels in the study system will be antidunes or standing waves during floods. Resistance to flow associated with antidunes depends on how often the antidunes form, the area of the reach they occupy, and the violence and frequency of their breaking. If many antidunes break, resistance to flow can be large because breaking waves dissipate a considerable amount of energy. With breaking waves,  $C/\sqrt{g}$  may range from 10 to 20, and Manning's coefficient  $n$  ranges from about 0.019 to 0.038 for the flow depths being considered.

The existing channels will not contain all of the 100-year flood flows. Some overbank flow will occur. Sparse vegetation, brush, trees and houses are in the floodplain. These elements increase the resistance to flow. For a conservative erosion and sedimentation analysis (high channel velocity), a Manning's roughness of 0.025 for the main channels was assumed for this study. For overbank flows, a higher Manning's  $n$  value of 0.05 was used from Dodge Boulevard to Sabino Creek and an  $n$  value of 0.06 was used from Sabino Creek to Agua Caliente Wash.

Sediment Transport Rates. The rate of sediment transport is the most important factor in conducting a quantitative determination of aggradation and degradation in the channel. Since very little actual data were available to calibrate the sediment transport rate determinations, there is some uncertainty inherent in the procedure used to compute sediment supply rates. Fortunately, the uncertainty in the results was reduced by several factors. An indirect check of the sediment transport rate determinations was available on Tanque Verde Creek. This area has undergone the least change in river form of all the locations in the study area. The 1941 and present aerial photographs show this portion of the system to have remained nearly unchanged. Therefore, it is expected that these reaches must have sediment transporting capacities near equilibrium. The engineering geomorphic analysis is in agreement with this conclusion.

Another factor that helped provide a reliable determination of sediment supply was the grade control structure on Pantano Wash at the Craycroft Road bridge site. A channel will quickly come to equilibrium behind such a structure since the results of an excess or imbalance in

sediment transport rate to the structure are corrected by removal or storage of material behind the structure. This process allows the channel to quickly reach equilibrium behind the structure by producing a channel bed slope that will result in a sediment transport rate equal to the incoming supply.

The method used to compute the sediment transport rate was the Meyer-Peter, Muller bed-load equation and the Einstein method for suspended bed material discharge (see Chapter 4). The shear stress on the bed of the channel was calibrated based on the grain resistance of the bed material. The method produced a total bed-material concentration which matched available data on the Rillito River and was consistent with similar sand-bed arid region rivers.

Engineering Geomorphology. To determine equilibrium channel slope and possible changes in channel alignment quantitatively, an engineering geomorphic analysis was performed. The analysis considered various river sections in the study area for a series of water discharges ranging from 5,000 cfs (mean annual flow) to 34,000 cfs (100-year flood). A multiple regression was developed for sediment transport as a function of velocity and depth. This equation was combined with Manning's equation and the water and sediment continuity equations to form a computational procedure for determining the equilibrium slope (for details see HEC-20, Chapter 6). Computation of equilibrium slopes was performed for the present sediment supply and reductions of 25 to 50 percent. Computations with the reduced sediment supplies were carried out to determine the effects of increased urbanization on the stability of the present channel system.

The calculation of equilibrium slopes was accomplished by trial and error. The results show (Table 10.9) that for the present supply condition most of the study area is close to equilibrium. The exceptions occur at the bridge sites, all of which should degrade according to the equilibrium analysis. The accuracy of the calculations at the bridge sites is less than the other locations, since the normal depth assumption may not be accurate because of local hydraulic effects caused by the bridges. In all, the calculations reflect the fact that the system is near equilibrium and should not experience significant bed elevation changes if no further disturbances are introduced. This agrees with the results of the Level 1 channel morphology analysis.

The sediment supply reduction cases result in degradation at all locations along the system. This is a crucial fact. It illustrates the severe consequences which would arise from a reduction in sediment supply by urbanization, sand and gravel mining, or other activities. The equilibrium conditions which presently exist would be destroyed and significant bed elevation changes would result. For example, a 0.0005 decrease in equilibrium slope resulting from a 25 percent reduction in supply would cause a degradation of 2.6 ft/mi (.492 m/km).

The possible extent of lateral migration was determined for Tanque Verde Creek by studying the channel alignment characteristics for 13 miles (21 km) of Tanque Verde Wash above Craycroft Road. A potentially severe lateral migration potential was identified for Tanque Verde Wash at the Sabino Canyon Road Bridge during the Level 1 analysis. In order to understand the migration process more thoroughly, a 13-mile (21 km) reach of Tanque Verde Wash above the confluence with Pantano Wash was studied closely to determine the range of channel plan geometry. Meander amplitudes, wave lengths, and radii of curvature were measured.

Table 10.9. Equilibrium Slope Calculations, Dominant Discharge.				
Location	Slope in ft/ft			
	Actual	Present Supply	25 Percent Reduction	50 Percent Reduction
Cross-Sections 32-47 (Pantano)	0.0060	Too much gravel mining to accurately estimate		
Cross-Sections 31-24 (Pantano)	0.0035	Reach assumed in equilibrium at present slope (supply reach)		
Cross-Sections 47-54 (Tanque Verde)	0.0033	Reach assumed in equilibrium at present slope (supply reach)		
Cross-Sections 46-45 (Tanque Verde-Sabino)	0.0048	0.0032	0.0026	0.0020
Cross-Sections 44-27 (Tanque Verde)	0.0036	0.0036	0.0030	0.0023
Cross-Sections 26-23 (Rillito Craycroft)	0.0043	0.0033	0.0027	0.0023
Cross-Sections 22-18 (Rillito)	0.0037	0.0032	0.0026	0.0020
Cross-Sections 17-14 (Rillito Swan Road)	0.0043	0.0032	0.0026	0.0020
Cross-Sections 13-1 (Rillito)	0.0039	0.0031	0.0025	0.0020

Meander wave length, channel width and radius of curvature ( $\lambda$ , B, and  $r_c$ ) pairs were plotted for each meander loop. These points were plotted on logarithmic scales and on linear scales. Straight lines were fitted and the following equations were obtained and adopted for the lower 13 miles (21 km) of the Tanque Verde Creek:

$$\begin{aligned}\lambda &= 2.6 r_c \\ \lambda &= 2.75 B^{1.35} \\ r_c &= 1.06 B^{1.35}\end{aligned}$$

These relationships are used to determine appropriate channel widths and bend shapes at the Sabino Canyon Road Bridge site.

Sabino Canyon Road Bridge (Figure 10.15) is currently located on a bend with a curvature that creates several problems. At low flows, scour occurs at the outside of the bend (south side) because of high velocity and secondary currents. This phenomena is evident in the present channel cross section under the bridge. At flood flows, the problem is nearly the opposite. The north side of the bridge is attacked because of the tendency of the thalweg to straighten in the bend. The amplitude of the meander bend is 300 ft (91 m). Therefore, the lateral migration tendency is on the order of 300 ft (91 m).

These facts point to the necessity for engineering control measures to be taken at Sabino Canyon Road Bridge in order to prevent future failure of the structure from lateral migration. Possible measures are bank stabilization and channelization.

#### 10.2.4 Level 3 - Sediment Routing for the 100-Year Flood

The long-term trends of the Tanque Verde, Pantano, Rillito River system were determined using a sediment routing procedure. This analysis determined the aggradation and degradation for subreaches in the respective river systems, based on sediment supply from the upstream reaches and local hydraulic conditions throughout the system. Subcritical hydraulic conditions were assumed for all backwater computations.

River and watershed information consists of upstream sediment loading information and the discretized hydrographs for the mainstem and tributaries. The mainstem hydrograph was discretized into 12 time steps with 5 time steps on the rising limb of the hydrograph. Time steps vary in length from 0.5 hours at the peak to 4.0 hours for the end of the recession limb. Time steps average typically 1.5 hours. The sediment output from the Pantano Wash was used as input to Tanque Verde at the Craycroft Road section. Two cases of sediment supply from Pantano were considered. The first case assumed stable conditions existed in the Pantano reach. This case corresponds to a no-fail grade control condition. The second case assumed the roadway grade control would fail during the 100-year flood. The sediment load resulting from the failure of the roadway was calculated independently of the routing procedure.

Four Tanque Verde sediment routing analyses were conducted for the as-is condition. The cases analyzed are:

Case I. Tanque Verde floods with overflow to the Pantano Wash and no grade control failure.

Case II. Tanque Verde floods with overflow to the Pantano Wash and the grade control fails.

Case III. Pantano Wash floods with overflow to the Tanque Verde and no grade control failure.

Case IV. Pantano Wash floods with overflow to the Tanque Verde and the grade control fails.

Figures 10.22 and 10.23 show the bed level changes over the duration of the 100-year flood for both Tanque Verde flooding and Pantano flooding. The bridge sites show only slight aggradation/degradation for the 100-year flood if the Pantano grade control structure does not fail. This agrees with the conclusion drawn from the geomorphic analysis. The major potential cause of aggradation is the failure of the existing Pantano roadway grade control. If the existing Pantano Wash roadway grade control structure fails during Pantano flooding, there is a maximum aggradation downstream of Craycroft Road of 4.6 ft (1.4 m). The erosion and/or headcut that may occur during Pantano flooding can supply significant amounts of sediment in a short period of time (Figure 10.23).

### **10.2.5 Results of Analysis**

Each of the sites evaluated has its own unique problems that must be considered in the formulation of alternative designs. This section presents several conceptual alternatives based on the analysis of the as-is conditions. Analysis of the design alternative is broken into three areas, (1) low chord criteria, (2) total scour criteria and (3) other additional considerations.

The criteria for an acceptable low chord elevation for this alternative is that the bridge can pass the 100-year flood peak with sufficient freeboard between the water surface elevation from a rigid-bed hydraulic analysis, plus additional components resulting from sand-wave movement, general aggradation, and superelevation caused by flow curvature. In addition, an increment of height is added to provide freeboard for debris passage.

When designing a bridge foundation, proper consideration of scour must be made to determine the required safe depth of piles or other supports. A design which gives adequate support for the structure when the channel bed is at its initial elevation may be inadequate after scour occurs and lowers the channel bed. The physical processes that must be considered are long-term changes in bed elevation, local scour, contraction (or general) scour, and passage of sand waves. The total scour is the sum of these, and must be subtracted from the initial design elevation to establish the design depth for all supports. The supports must have a depth of burial below this elevation sufficient to support the structure.



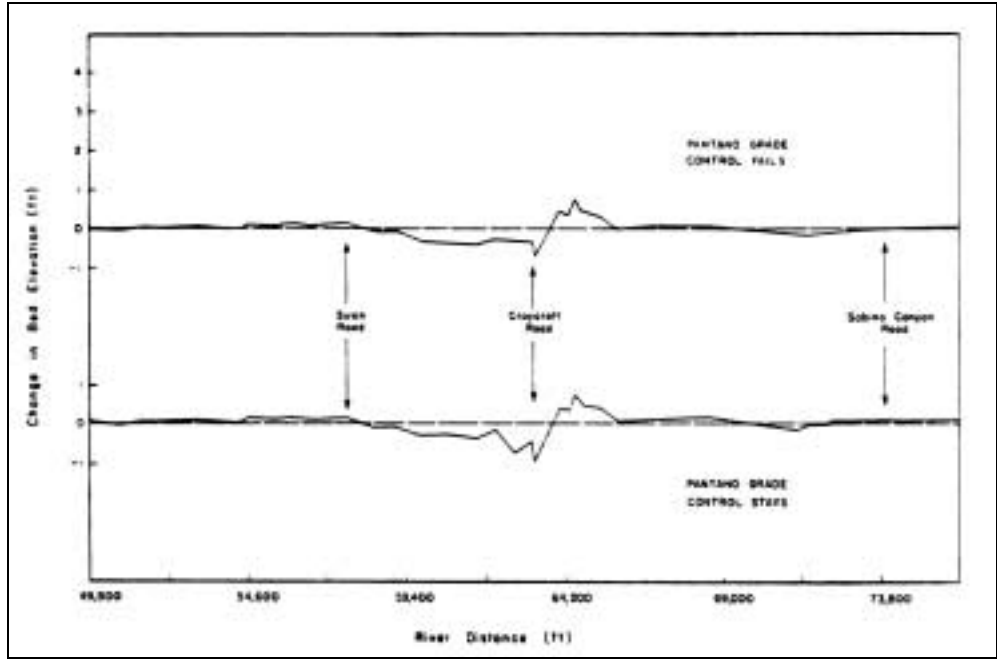


Figure 10.22. Bed elevation change of Rillito-Tanque Verde System (Tanque Verde flooding).

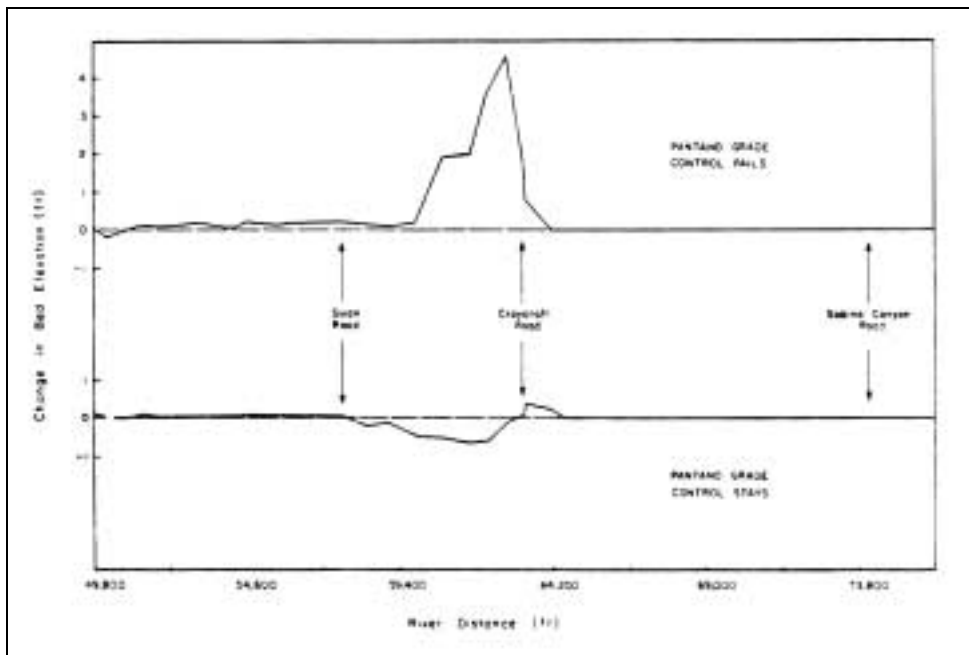


Figure 10.23. Bed elevation change of Rillito-Tanque Verde System (Pantano flooding).

Craycroft Road. Three conceptual alternatives are presented which offer various channel alignment or bridge design configurations at this site. Figure 10.24 shows Alternative I. This alternative utilizes bank protection works with the central embankment designed to guide the flow through the bridge. The pier elevations are designed according to the worst scour potential of the two branches and are the same for both tributaries. The design should also consider the condition resulting from grade control failure on Pantano and should utilize circular piers to minimize problems due to adverse flow alignment.

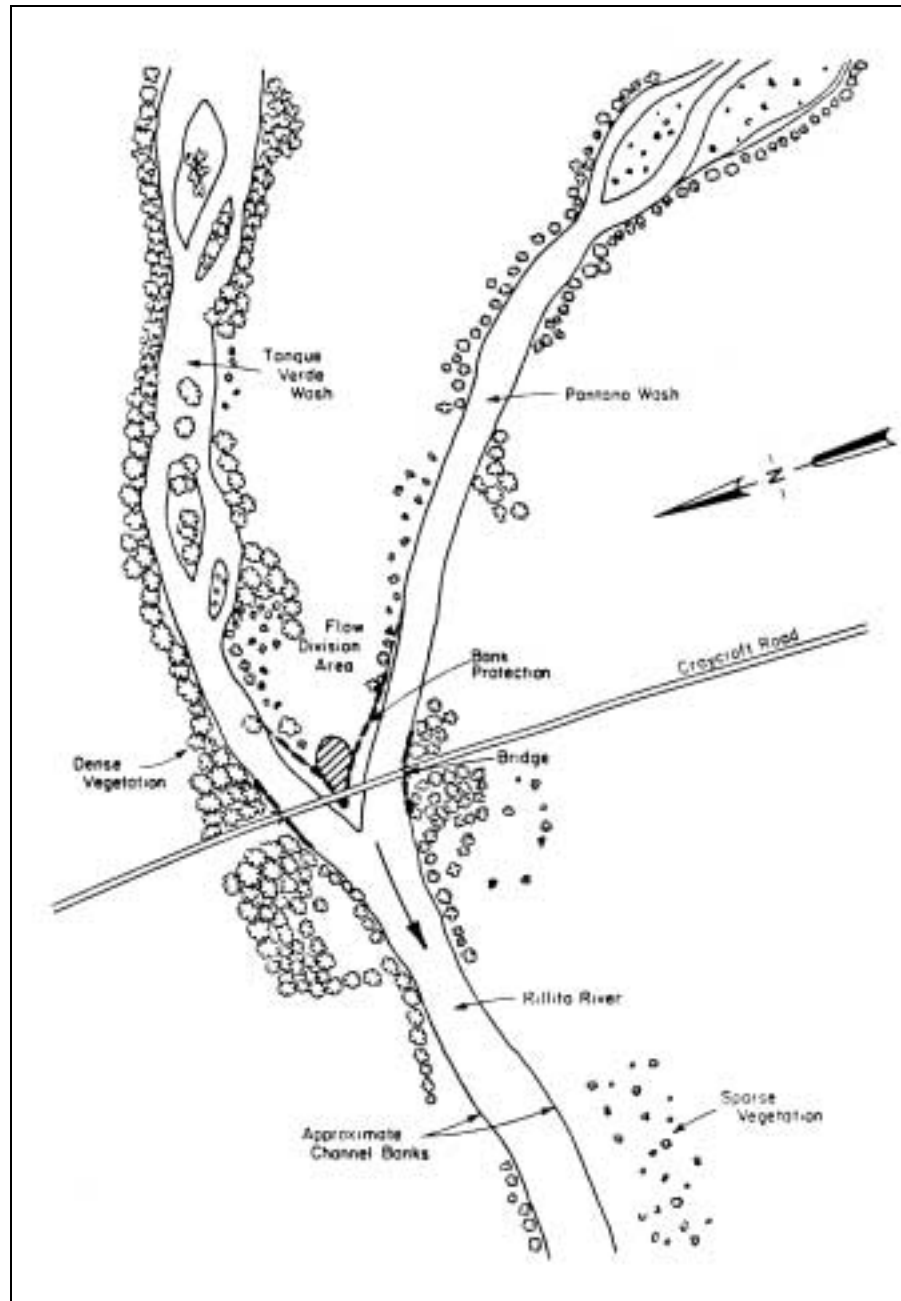


Figure 10.24. Alternative I for Craycroft Road Bridge crossing.

Alternative II conceptual design avoids some of the difficulties resulting from locating the bridge in the vicinity of the confluence. This alternative suggests relocating the bridge and road approximately 850 ft (260 m) downstream of the current right-of-way (Figure 10.25). This alternative would require only one bridge, and the piers could be properly aligned with the flow or circular piers could be used. However, the acquisition of the new right-of-way for this site may not be economically feasible.

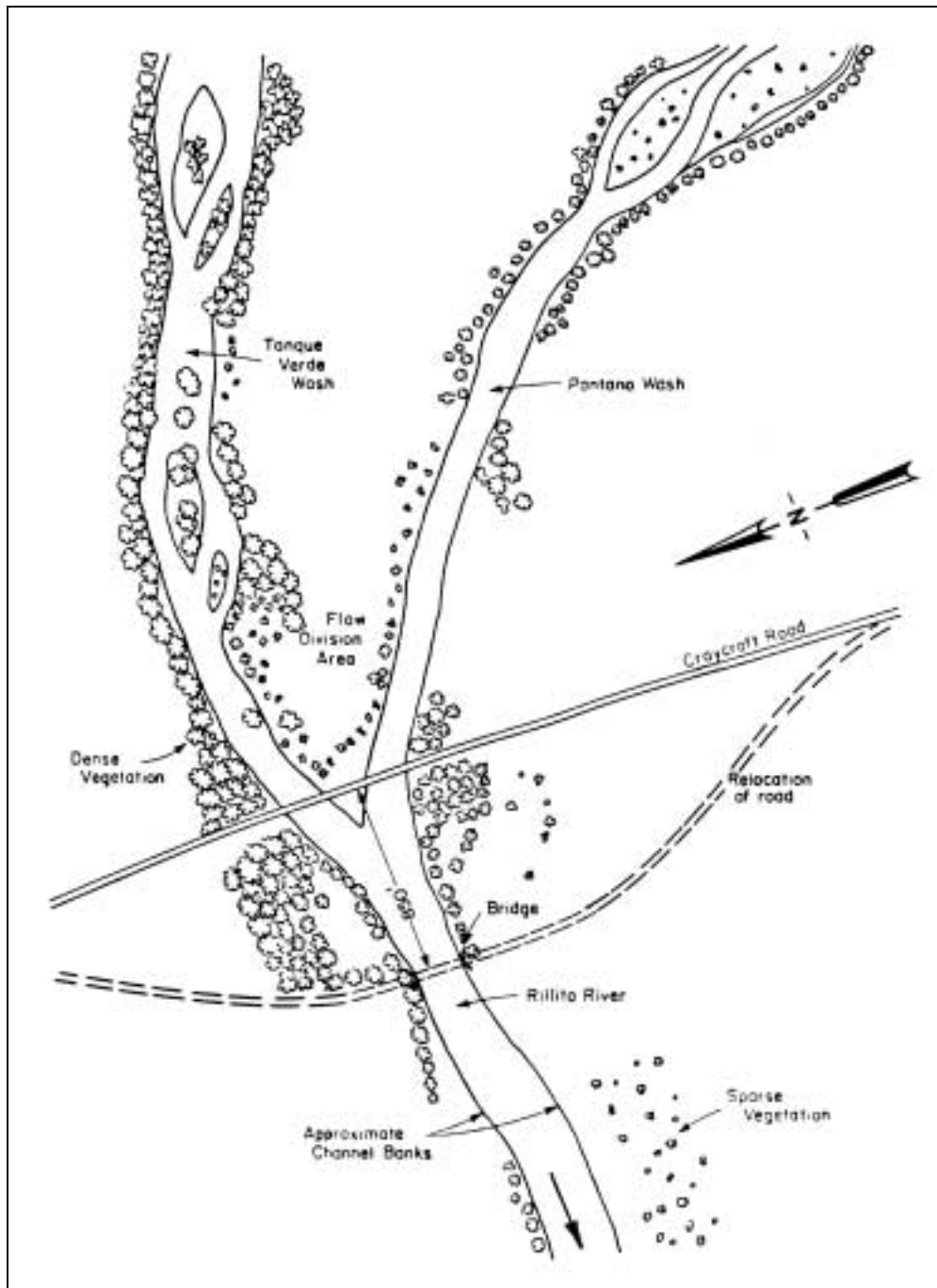


Figure 10.25. Alternative II for Craycroft Road Bridge crossing.

Alternative III suggests physically moving the confluence approximately 700 ft (213 m) upstream by modifying both branches of the tributaries with excavation, fill, and bank protection. The grade control and the deposited material behind the control would be removed. This conceptual design is shown in Figure 10.26. This alternative has most of the advantages that are provided by Alternative II and does not require relocation of the road right-of-way. However, the cost of modifying the channels can be significant and may be prohibitive.

The results of low chord and total scour analyses are presented in Table 10.10. The freeboard requirement for debris was determined qualitatively. Pier scour was estimated with and without a vegetative debris accumulation. A maximum debris width of 5 ft (1.5 m) was assumed for this analysis. Long-term degradation assuming a 25 percent reduction of sediment supply due to urbanization and gravel mining activities was added to the degradation calculated for the 100-year flood.

Alternative	Water Surface (ft)	Aggradation (ft)	Degradation (ft)		Total Abutment Scour (ft)	Total Pier Scour (ft)
			100-Year Flood	25% Reduction in Sediment Supply		
I	2435.6	1.7	0.5	2.6		
II	2431.0	4.6	0.8	2.6		
III	2434.4	0	0.8	2.6		
Vegetative Debris Freeboard (ft)	Minimum Low Chord (ft)	Abutment Local Scour (ft)	Pier Local Scour (ft)		Total Abutment Scour (ft)	Total Pier Scour (ft)
			Without Debris	With Debris		
3.0	2441.7	11.1	5.0	7.8	14.2	10.9
3.0	2437.7	13.2	7.0	10.9	16.6	14.3
3.0	2439.5	13.2	7.0	10.9	16.6	14.3

As mentioned, the grade control on Pantano Wash near the confluence with Tanque Verde Creek is temporary in nature and is likely to fail during a major flood. Sudden failure of the grade control can cause instability of the banks and the new bridge. It is recommended that the grade control be removed, or at least the bridge design should consider the consequences of its sudden failure.

The alignment of the flow is a major concern when building a bridge in the vicinity of a confluence. Poor flow alignment can cause serious local scour problems. Circular piers are strongly recommended in this situation to minimize local scour.

Although the probability of simultaneous occurrence of the two peak flows at the bridge site may be small, the impact on the proposed bridge due to such an event should be considered. One way to account for such an occurrence is to design the Craycroft Road Bridge with an extra margin of safety, both hydraulically and structurally.

In selecting the best alternatives for the Craycroft Road Bridge, economic, social and environmental constraints must be considered. Based upon this preliminary evaluation, both Alternatives I and III are more attractive than Alternative II. Alternative II has the disadvantage of a potential for both significant aggradation and degradation, which increases the cost of design. The acquisition of the right-of-way to realign the bridge in Alternative II may be prohibitive.

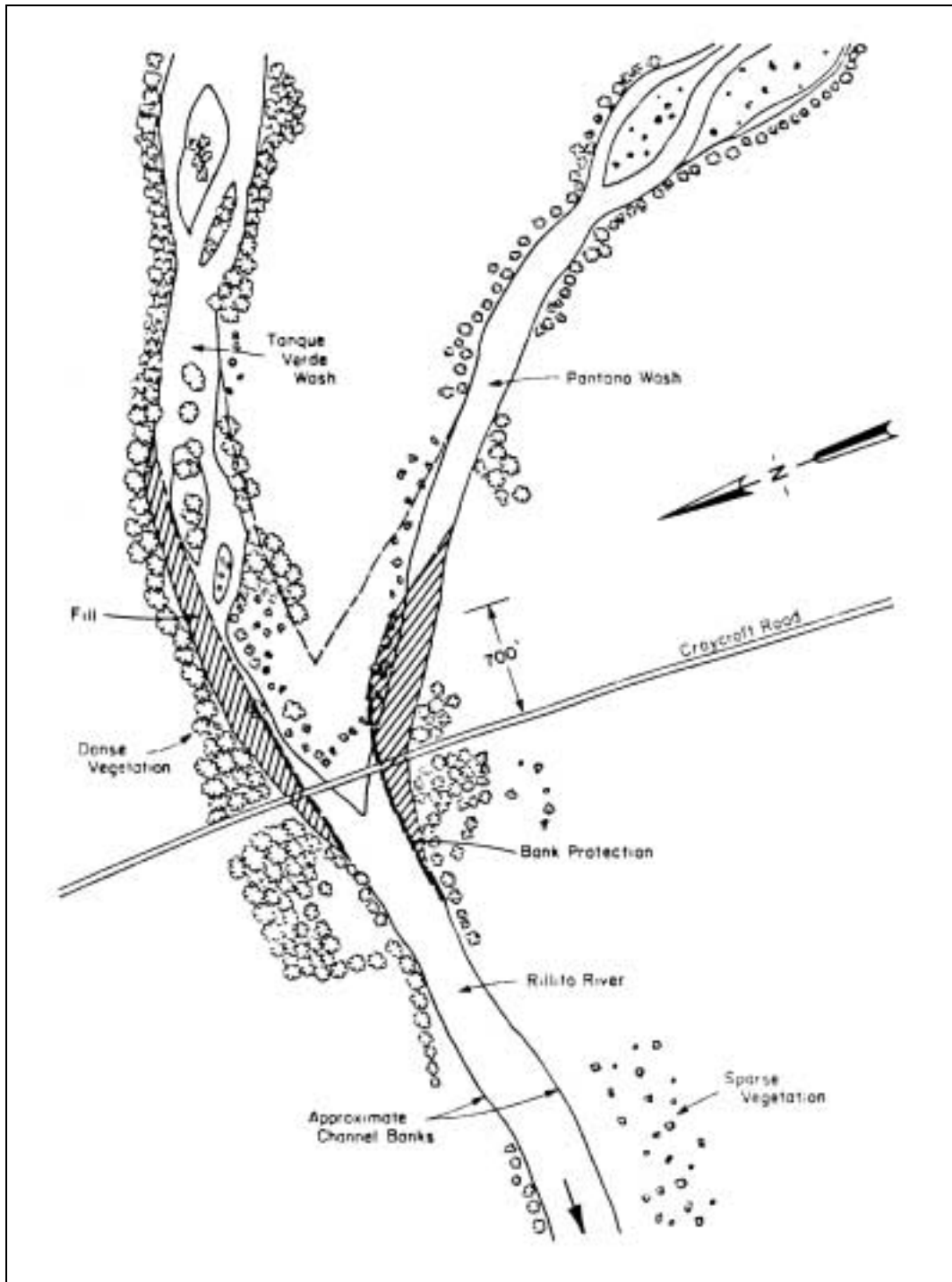


Figure 10.26. Alternative III for Craycroft Road Bridge crossing.

Sabino Canyon Road Bridge. Four alternatives for the Sabino Canyon road bridge are analyzed. Alternative I is the present condition (Figure 10.15). The other three alternatives consider variations on a similar scheme. The obvious options involve channelization downstream of the bridge to reduce water surface elevations, widening of the bridge opening, protection of the south side of the bridge by a guide bank, and bank protection at key locations. Alternatives II, III and IV consider a channel bottom width of 300, 350, and 400 ft (91, 107, and 122 m), respectively. A sketch of the basic design is presented in Figure 10.27. The drawing shows a 300-foot (91 m) channel for Alternative II.

A low chord and total scour analysis similar to the Craycroft Road site presented in Table 10.11 could be used for the analysis of the Sabino Canyon bridge. Because of the problems associated with a bridge located on a bend, Alternatives II, III, and IV include bank protection and stabilization 200 ft (60 m) up- and downstream of the bridge site. Also, additional bank protection should be provided along the south bank above Sabino Canyon Road. This latter protection will prevent the upstream bend from further migration that would cause flow alignment difficulties at the bridge. A guidebank should be constructed on the south side to protect the bridge from southward channel migration and to assist in controlling overbank flow and guiding the flow through the bridge opening (Figure 10.27).

By using the radius of bend curvature as a function of channel width determined earlier,

$$r_c = 1.06 B^{1.35}$$

the appropriate radius of curvature for each alternative can be determined. The results show that for the channelization alternatives (II, III, IV), the radius of curvature is within the stable range. However, for the present condition (Alternative I), the radius of curvature is too small. This is one cause of the present migration problem on the south bank. A very preliminary assessment concluded that Alternative II [300 ft (91 m) bottom width channelization] is probably the most feasible and practical solution for the new bridge. Very little is gained in terms of low chord and scour reduction by the wider channels; however, they would require a large amount of additional earthwork. The narrower channel would also cause less conflict with private property ownership.

## **10.3 BRI-STARS SEDIMENT TRANSPORT MODELING EXAMPLE**

### **10.3.1 Background**

Overview examples 1 and 2 illustrate the application of the three-level analysis procedure. Example 1 applied the principles and methods introduced in this manual to the design of countermeasure alternatives on a migrating alluvial channel bendway. Techniques used included a Level 1 reconnaissance and geomorphic analysis and a Level 2 quantitative engineering analysis. Example 2 developed conceptual design alternatives for two bridge crossings on a dynamic sand bed river system in the southwest using, primarily, Level 1 and 2 analysis procedures; however, the results of a Level 3 sediment routing analysis were demonstrated.

This final overview example illustrates in more detail the application of Level 3 sediment transport analysis techniques using FHWA's BRI-STARS model. This example problem is taken from a paper by Arneson et al. (1991) which is presented as the total scour comprehensive example in HEC-18 (Richardson and Davis 2001). For this problem in HEC-18, FHWA's WSPRO computer program was used to obtain the hydraulic variables. The program uses 20 stream tubes to give a quasi 2-dimensional analysis. Each stream tube has the same discharge (1/20 of the total discharge). The stream tubes provide the velocity distribution across the flow and the program has excellent bridge routines. Since the data for this case study are available in English units, the figures and tables retain English unit notation. SI (metric) units are given parenthetically in the text for reference.

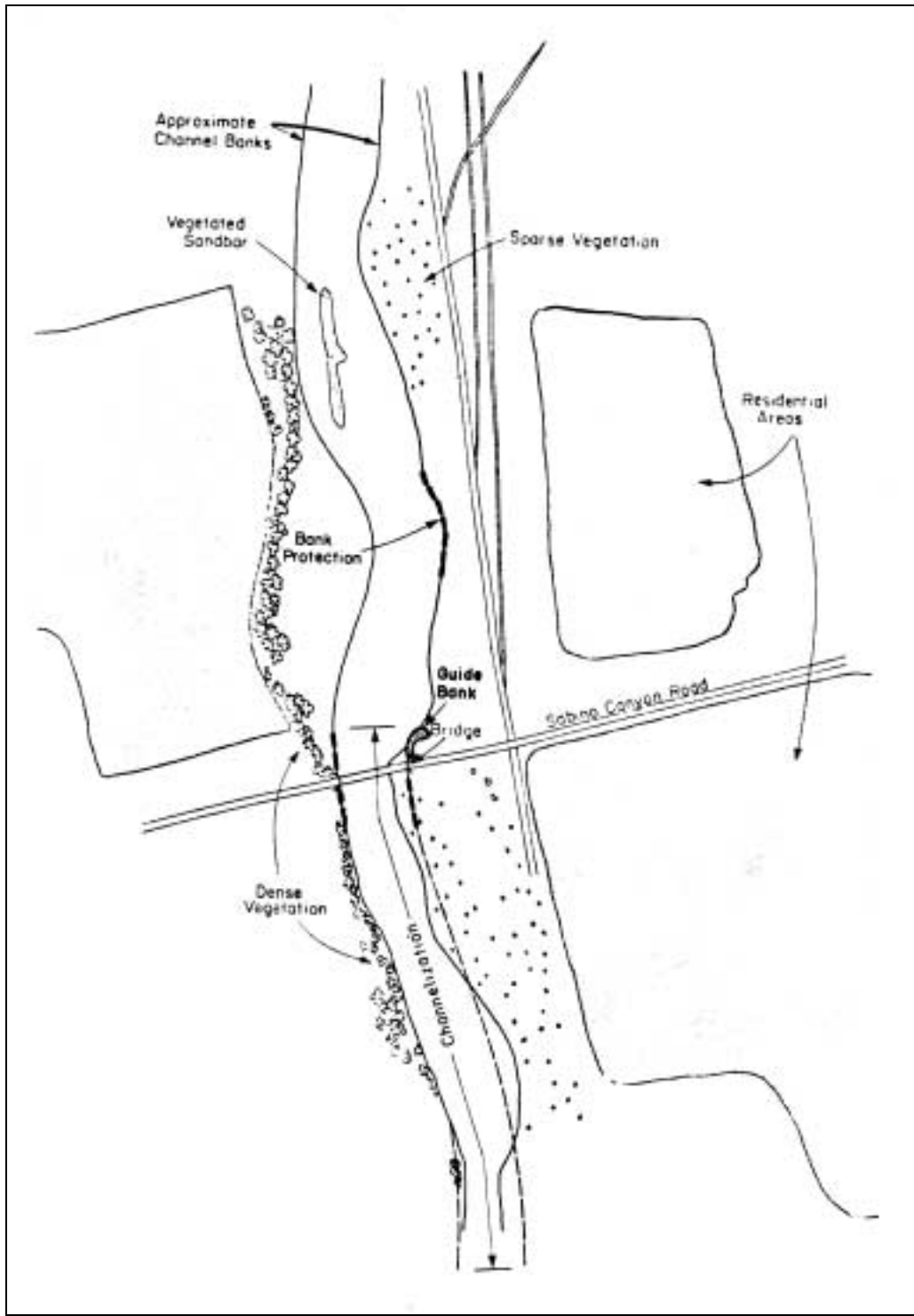


Figure 10.27. General plan view of Sabino Canyon Road crossing for alternative II, III, and IV (II Shown).

The Level 1 and 2 analysis results and total scour computations are summarized briefly in the following sections. Then the BRI-STARS model is applied to refine the initial qualitative analysis of long-term bed elevation changes.

### 10.3.2 Level 1 - Reconnaissance and Geomorphic Analysis

A 650-foot (198 m) long bridge (Figure 10.28) is to be constructed over a channel with spill-through abutments (slope of 1V:2H). The left abutment is set approximately 200 ft (60.5 m) back from the channel bank. The right abutment is set at the channel bank. The bridge deck is set at elevation 22 ft (6.71 m) and has a girder depth of 4 ft (1.22 m). Six round-nose piers are evenly spaced in the bridge opening. The piers are 5 ft (1.52 m) thick, 40 ft (12.19 m) long, and are aligned with the flow.

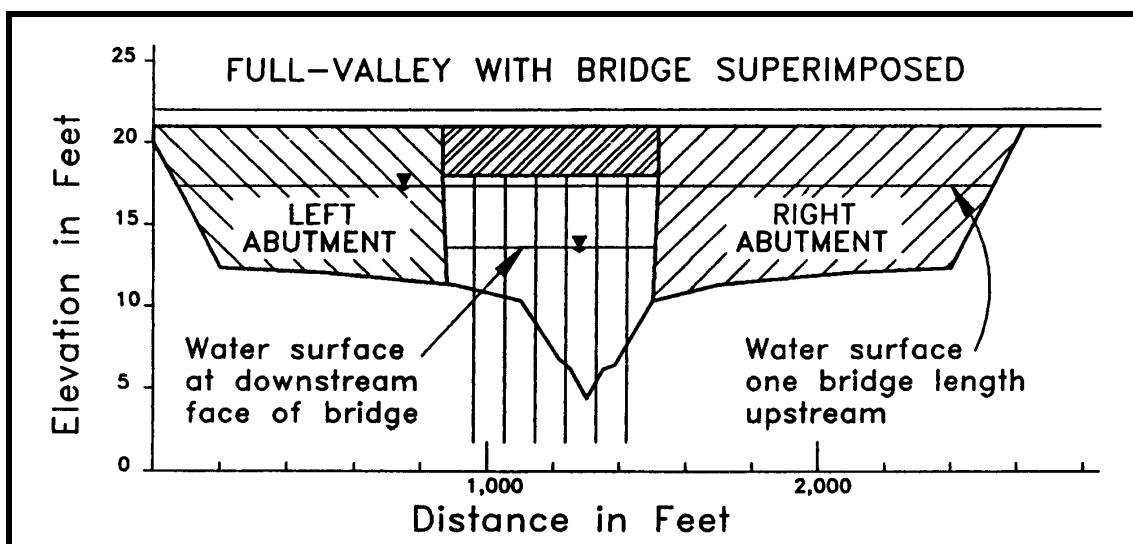


Figure 10.28. Cross section of proposed bridge.

A site investigation of the crossing was conducted to identify potential stream stability problems at this crossing. Evaluation of the site indicates that the river has a relatively wide floodplain. The floodplain is well vegetated with grass and trees; however, the presence of remnant channels indicates that there is a potential for lateral shifting of the channel. The river and crossing are located in a rural area with the primary land use consisting of agriculture and forest.

The bridge crossing is located on a relatively straight reach of channel. The channel geometry is essentially the same for approximately 1,000 ft (300 m) upstream and downstream of the bridge crossing. The  $D_{50}$  of the bed material and overbank material is approximately 2 mm. The maximum grain size of the bed material is approximately 8 mm. The specific gravity of the bed material was determined to be equal to 2.65. Since this is a sand-bed channel, no armoring potential is expected. Furthermore, the bed for this channel at low flow consists of dunes which are approximately 1 to 1.5 ft (0.3 to 0.5 m) high. At higher flows, above the  $Q_5$ , the bed will be either plane bed or antidunes.



The left and right banks are relatively well vegetated and stable; however, there are isolated portions of the bank which appear to have been undercut and are eroding. Brush and trees grow to the edge of the banks. Banks will require riprap protection if disturbed. Riprap will be required upstream of the bridge and extend downstream of the bridge.

Evaluation of stage discharge relationships and cross sectional data obtained from other agencies does not indicate progressive aggradation or degradation. Review of bridge inspection reports for bridges located upstream and downstream of the proposed crossing indicates no long-term aggradation or degradation in this reach. Based on these observations, the channel is relatively stable vertically, at present. Furthermore, there are no plans to change the local land use in the watershed. The forested areas of the watershed are government-owned and regulated to prevent wide spread fire damage, and instream gravel mining is prohibited. These observations indicate that future aggradation or degradation of the channel, due to changes in sediment delivery from the watershed, are minimal.

Based on these observations, and due to the lack of other possible impacts to the river reach, it is determined that the channel will be relatively stable vertically at the bridge crossing and long-term aggradation or degradation potential is considered to be minimal. However, there is evidence that the channel is unstable laterally.

### **10.3.3 Level 2 - Hydraulic Engineering Analysis**

Hydraulic characteristics at the bridge were determined using FHWA's WSPRO model. Three cross sections were used for this analysis and are denoted as "EXIT" for the section downstream of the bridge, "FULLV" for the full-valley section at the bridge, and "APPR" for the approach section located one bridge length upstream of the bridge. The bridge geometry was superimposed on the full-valley section and is denoted "BRDG."

The WSPRO HP2 option was used to provide hydraulic characteristics at both the bridge and approach sections. This option subdivides the cross section into 20 equal conveyance tubes. Figures 10.29 and 10.30 illustrate the location of these conveyance tubes for the approach and bridge cross sections. Figure 10.30 illustrates the average velocities in each conveyance tube and the contraction of the flow from the approach section through the bridge. Figure 10.30 also identifies the equal conveyance tubes of the approach section which are cut off by the abutments.

Contraction scour will occur both in the main channel and on the left overbank of the bridge opening. For the main channel, contraction scour could be either clear-water or live-bed depending on the magnitude of the channel velocity and the critical velocity for sediment movement. In the overbank area adjacent to the left abutment, clear-water scour will occur. This is because the overbank areas upstream of the bridge are vegetated and the velocities in these areas will be low. Thus, returning overbank flow which will pass under the bridge adjacent to the left abutment will not be transporting significant amounts of material to replenish the scour on the left overbank adjacent to the left abutment.

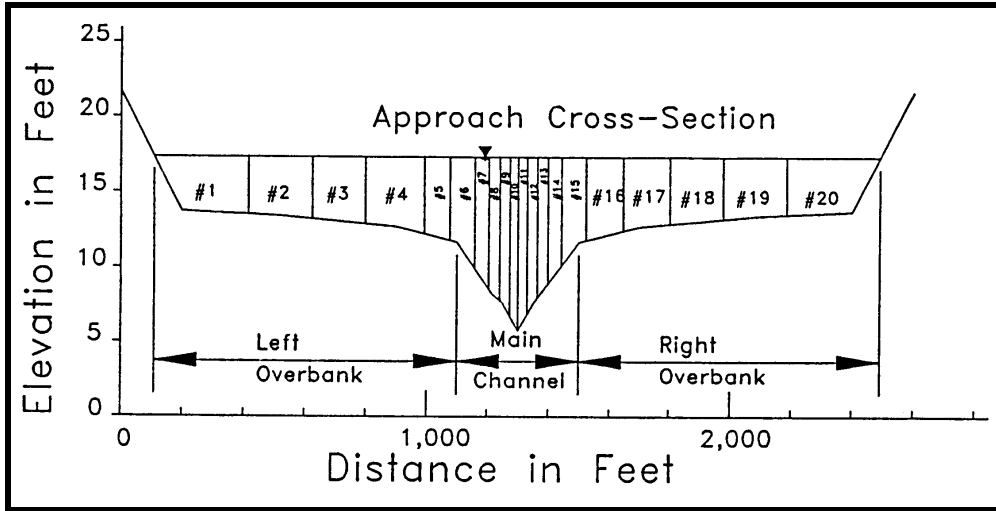


Figure 10.29. Equal conveyance tubes of approach section.

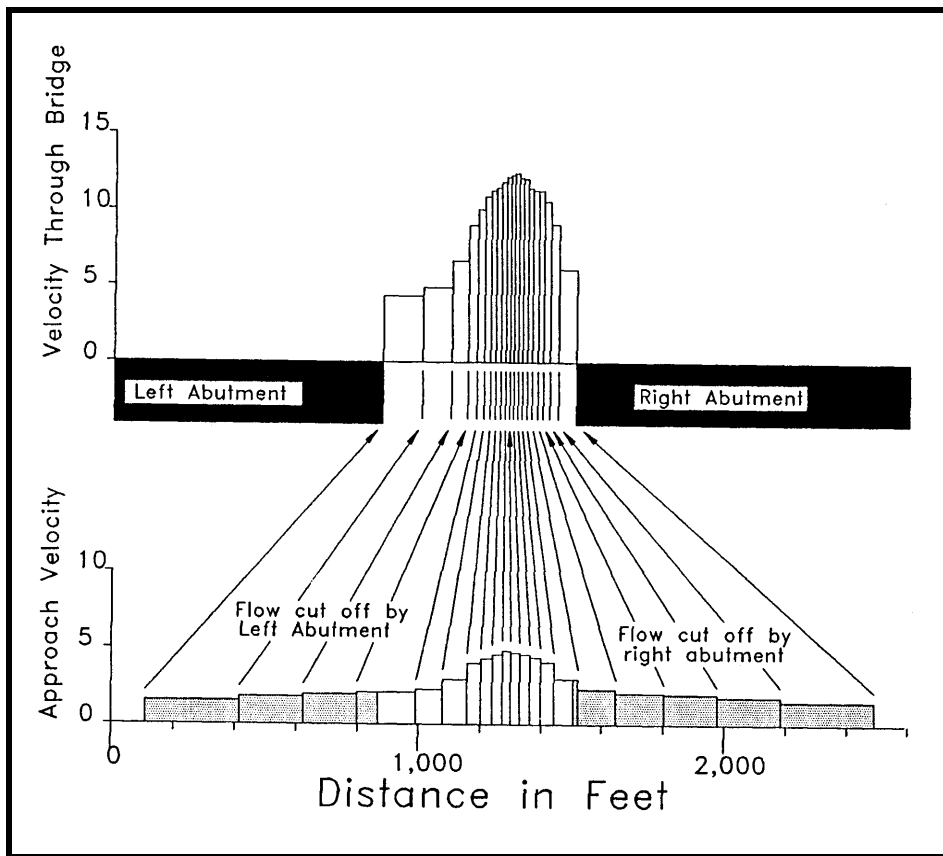


Figure 10.30. Plan view of equal conveyance tubes showing velocity distribution at approach and bridge sections.

The hydraulic variables used to estimate the local scour at the piers were determined from a plot of the velocity distribution derived from the WSPRO output (Figure 10.31). For this example the highest velocities and flow depths in the bridge cross section were used (at conveyance tube number 12). Only one pier scour computation was completed because the possibility of thalweg shifting and lateral migration requires that all of the piers be set assuming that any pier could be subjected to the maximum scour producing variables.

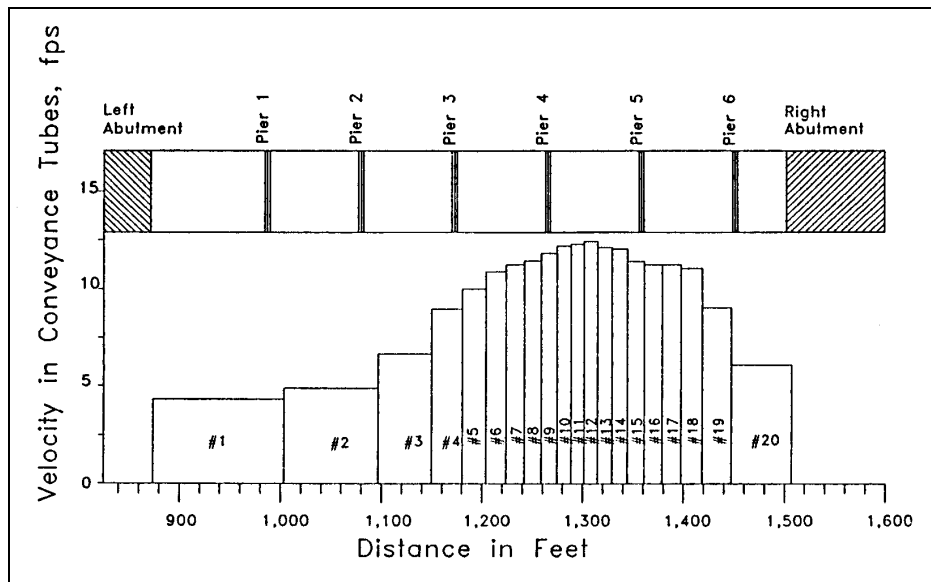


Figure 10.31. Velocity distribution at bridge crossing.

Local scour volumes at the left abutment and right abutments were estimated using the equations presented in Section 7.8.

### 10.3.4 Level 2 - Scour Analysis Results

Use of the hydraulic data from the WSPRO model in the appropriate equations of Chapter 7 resulted in the following scour estimates:

- Live-bed contraction scour in main channel (Equation 7.2) - 9.2 ft (2.8 m)
- Clear-water contraction scour on left overbank (Equation 7.4) - 1.7 ft (0.52 m)
- Local scour at piers (Equation 7.7,  $0^\circ$  angle of attack) - 11.8 ft (3.6 m)
- Local scour at piers (Equation 7.7,  $10^\circ$  angle of attack) - 19.3 ft (5.9 m)
- Local scour at left abutment (Equation 7.21) - 8.4 ft (2.6 m)
- Local scour at right abutment (Equation 7.21) - 13.3 ft (4.1 m)

The results of the scour computations should be plotted on the bridge cross section and carefully evaluated (Figure 10.32). For this example, only the computations for pier scour with piers aligned with the flow were plotted. The topwidth of the local scour holes is estimated as 2.0 times the depth of scour.

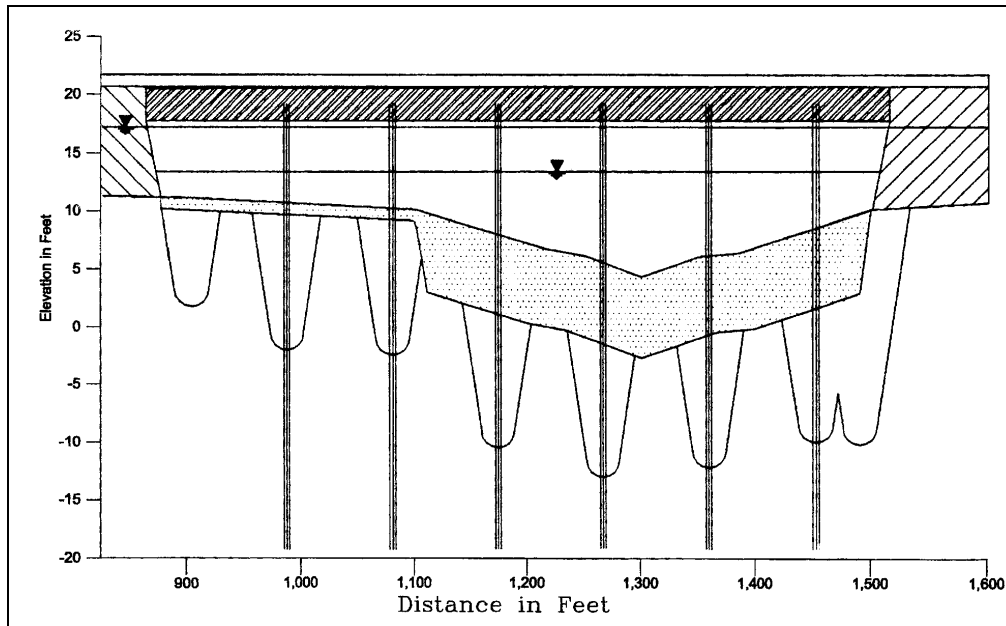


Figure 10.32. Plot of total scour for example problem.

It is important to evaluate the results of the scour computations carefully. For example, although the total scour plot indicates that the total scour at the overbank piers is less than for the channel piers, this does not indicate that the foundations for the overbank piers can be set at a higher elevation. Due to the possibility of channel and thalweg shifting identified with the Level 1 analysis, all of the piers should be set to account for the maximum total scour. Also, the computed contraction scour is distributed uniformly across the channel in Figure 10.32. However, in reality this may not occur. With the flow from the overbank area returning to the channel, the contraction scour could be deeper at both abutments. The use of guide banks would distribute the contraction scour more uniformly across the channel. This would make a strong case for guide banks in addition to the protection they would provide to the abutments. The WSPRO stream tube velocities could be used to distribute the scour depths across this section.

The plot of the total scour also indicates that there is a possibility of overlapping scour holes between the sixth pier and right abutment. Also, it is not clear from where the right abutment scour should be measured, since the abutment is located at the channel bank. Both of these uncertainties should be avoided for replacement and new bridges whenever possible. Consequently, it would be advisable to set the right abutment back from the main channel. This would also tend to reduce the magnitude of contraction scour in the main channel.

The possibility of lateral migration of the channel could also have an adverse effect on the magnitude of the pier scour. This is because lateral migration will most likely skew the flow to the piers. This problem can be minimized by using circular piers. An alternative approach would be to install guide banks to align the flow through the bridge opening.

The plot of the scour prism in Figure 10.32 should be replotted to show the potential for the scour to occur at any location in the bridge opening. This is shown in Figure 10.33.

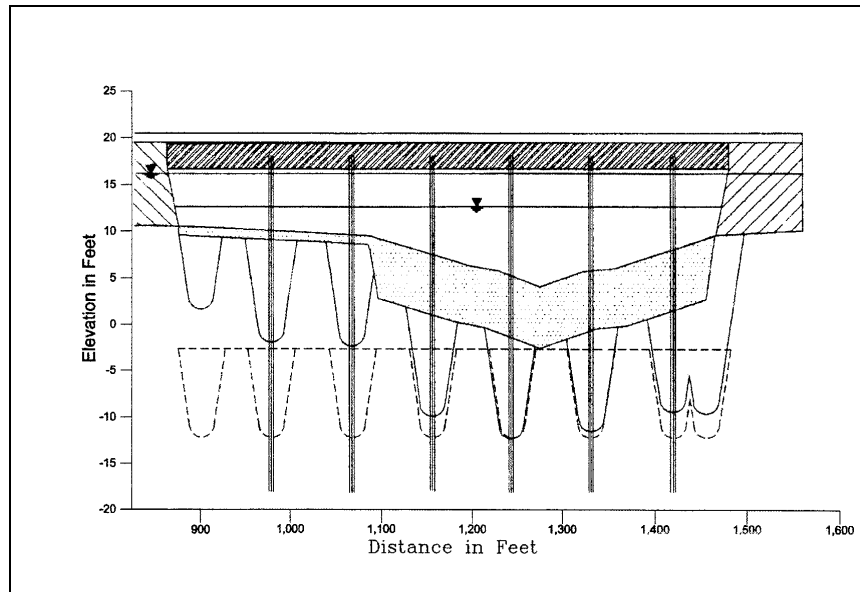


Figure 10.33. Revised plot of total scour for example problem.

### 10.3.5 Level 3 - BRI-STARS Analysis

The contraction scour computed in Section 10.3.4 using the HEC-18 (Richardson and Davis 2001) live-bed and clear-water scour equations could also be determined using the Level 3 approach of applying a sediment transport model such as BRI-STARS (see discussion in Section 5.6.2). Contraction scour occurs in a bridge when the sediment supplied from upstream is less than the sediment transport capacity in the bridge opening. The HEC-18 equations compute the ultimate amount of contraction scour that would occur if the hydraulic condition persists until the transport capacity in the bridge opening matches the upstream sediment supply.

Two BRI-STARS models were developed for the comprehensive scour example presented in HEC-18 and summarized above. The first BRI-STARS model simulated a constant flow of 30,000 cfs ( $850 \text{ m}^3/\text{s}$ ), the 100-year flow, for a 3-day period. The second model was run for a 3-day hydrograph that peaks at 30,000 cfs ( $850 \text{ m}^3/\text{s}$ ). The hydrograph is presented in Figure 10.34. The models used 1.2 hour computation intervals for a total of 60 time steps for each of the 3-day simulations (Arneson 2001).

Figure 10.35 shows the comparison thalweg profiles in the vicinity of the of the bridge, which is located between stations 1400 and 1450. Water surface and bed profiles are shown for the steady state (SS) and hydrograph (Hyd.) runs. The starting profile is a uniform slope of 0.002 ft/ft (m/m). For the steady state run, scour increases for the entire simulation and would continue well beyond the 3-day simulation time. At the end of the steady state simulation the maximum scour is approximately 4.5 ft (1.4 m) as compared with the HEC-18 (see Section 10.3.4) result of 9.2 ft (2.8 m). For the steady state run, the starting water surface profile shows approximately 1.4 ft (0.43 m) of backwater. At the maximum scour condition, however, there is virtually no backwater because the scour enlarges the bridge opening and reduces the head loss caused by the structure.

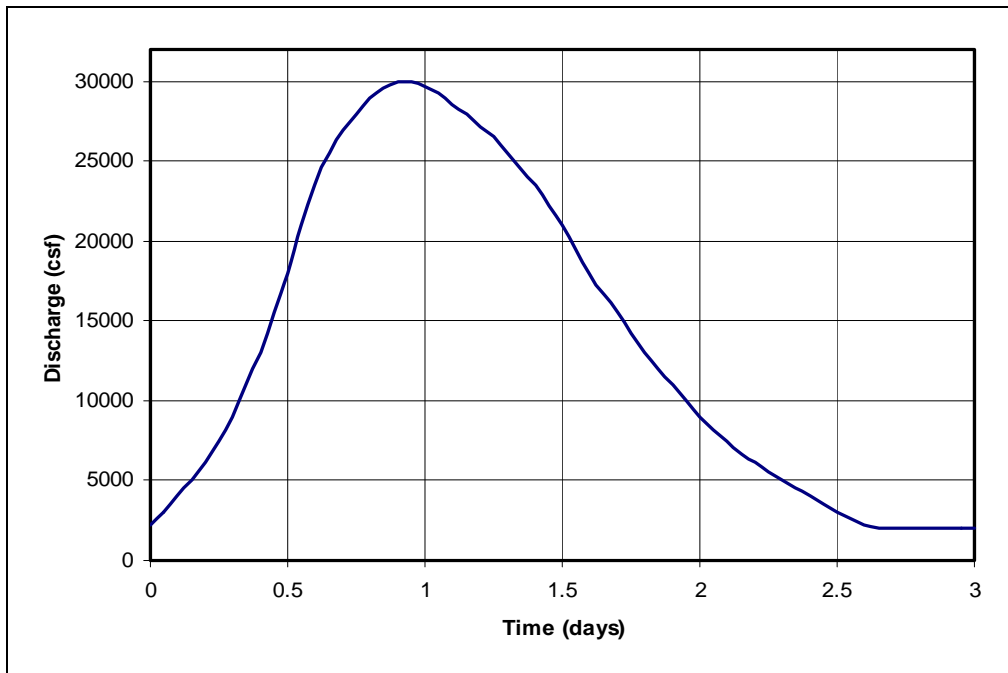


Figure 10.34. Three-day hydrograph for BRI-STARS analysis.

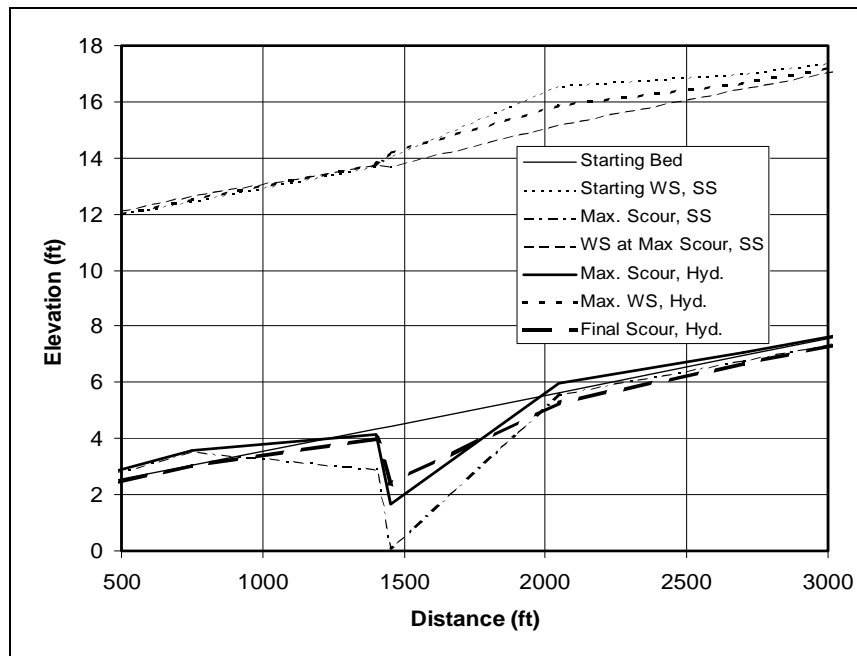


Figure 10.35 Comparison longitudinal profiles from BRI-STARS.

The hydrograph run reaches maximum scour of 2.8 ft (0.85 m) shortly after the peak flow. A different hydrograph with the same peak discharge but different shape would result in different amounts of predicted scour. This is because the sediment transport model computes scour based on the difference between rates of sediment supply and transport capacity, which vary with discharge. Also shown in Figure 10.35 is the scour at the end of the hydrograph. Some infilling of the scour hole is predicted to occur during the recession limb of the hydrograph, and the channel would be expected to return to the original condition after continued base flow. Because the hydrograph produces less scour than the steady state analysis, some backwater is predicted for peak flow conditions in this simulation.

Figure 10.36 shows a comparison of bridge cross sections from the BRI-STARS simulations. As expected, the deepest scour is in the center of the main channel. Clear-water contraction scour also occurs in the left overbank under the bridge (see Figure 10.33 for comparison). The HEC-18 clear-water contraction scour equation predicted 1.7 ft (0.52 m). The steady state model reached 0.81 ft (0.25 m) at the end of the 3-day simulation and the hydrograph model predicted a maximum scour on the left overbank of 0.17 ft (0.05 m). Figure 10.35 also shows how the scoured areas refill during the recession limb of the hydrograph.

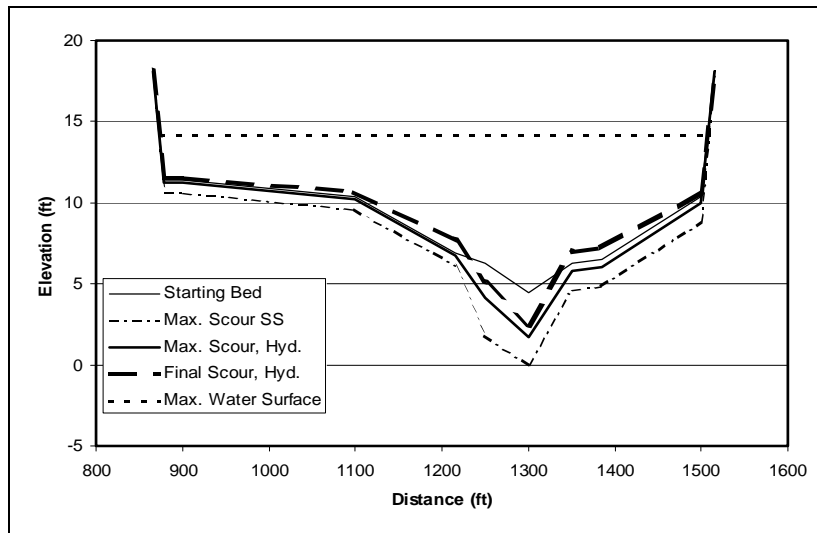


Figure 10.36 Comparison cross-sections from BRI-STARS.

Although the HEC-18 scour results are larger than those predicted by these BRI-STARS runs, the HEC-18 equation computes ultimate scour conditions using simplified relationships for sediment transport. If the BRI-STARS run had been extended, greater scour would have occurred, and since BRI-STARS does not scour the channel uniformly, the maximum scour could exceed that predicted by the HEC-18 equations.

The original WSPRO model of this bridge included one cross section downstream (EXIT) and one cross section upstream (APPROACH) of the bridge (Figure 10.29). These are the minimum number of sections required for a hydraulic analysis. Sediment transport models typically require additional sections. In addition to cross sections at the upstream and downstream bridge faces, the BRI-STARS model included two downstream cross sections and 18 upstream cross sections spaced at 650 ft (200 m) intervals along the channel.

Figure 10.37 shows the entire BRI-STARS model profile for starting and final conditions from the steady state run. By placing the upstream boundary well upstream of the bridge, no sediment inflow needed to be specified. The model eroded material from the upstream sections and maintained a stable channel upstream of the bridge. This provided the necessary sediment supply to the bridge. The model could have been set up with less length upstream of the bridge, but an appropriate amount of sediment supply would have to be entered in the input file.

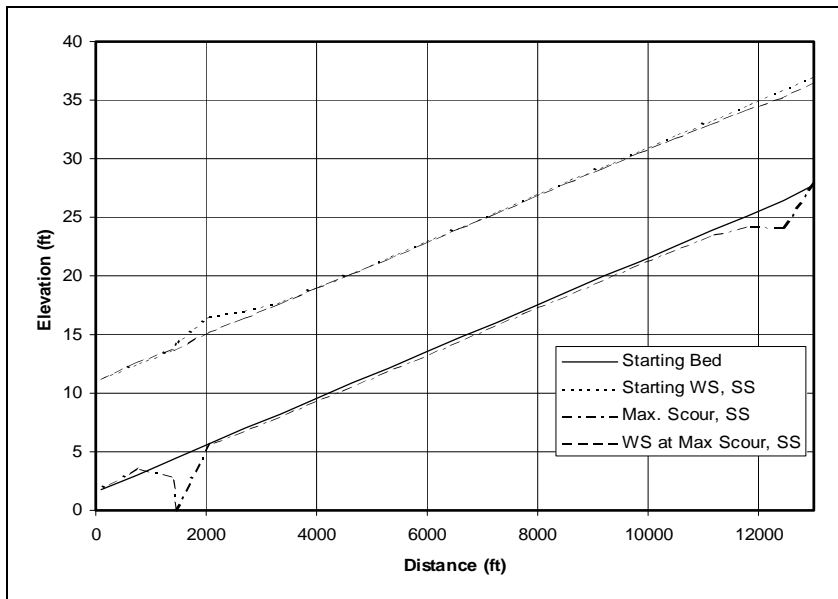


Figure 10.37. BRI-STARS model profiles for steady-state run.



## CHAPTER 11

### REFERENCES

- Ackers, P. and White, W.R., 1973, "Sediment Transport: New Approach and Analysis," ASCE Hydr. Div., Jour., Vol. 99, No. HY11, pp. 2041-60.
- Ackers, P. and White, W.R., 1980, "Bed Material Transport: a Theory for Total Load and its Verification," Proc. Intl. Sym. On River Sed, ed. by the Chinese Society of Hydraulic Engr., Vol. 1, Beijing.
- Albertson, M.L., 1953, "Effect of Shape on the Fall Velocity of Gravel Particles," Proc. 5th Hydraulics Conf., Univ. of Iowa, Hydraulics Laboratory, Iowa City, IA.
- Albertson, M.L., 1999, Personal Communication, Engineering Research Center, Colorado State University.
- Alexander, C.S. and Nunnally, N.R., "Channel Stability on the Lower Ohio River," Annals Assoc. American Geogr., Vol. 62.
- Aldridge, B.N. and Garrett, J.M., 1973, "Roughness Coefficients for Streams in Arizona," USGS Open File Report, Phoenix, AZ, 87 p.
- Alonso, C.V., Neibling, W.H., and Foster, G.R., 1982, "Estimating Sediment Transport Capacity in Watershed Modeling," Trans, ASAE, Vol. 24, No. 5, pp. 1211-1220 and 1260.
- Anderson, A. G., Painta, A. A., and Davenport, J. T., 1968, "Tentative Design Procedure for Riprap Lined Channels," Project Report No. 96, St. Anthony Falls Hydraulic Laboratory, University of Minnesota, Minneapolis, MN.
- Anderson, A. G., Painta, A. A., and Davenport, J. T., 1970, "Tentative Design Procedure for Riprap Lined Channels," NCHRP Report No. 108, TRB, National Academy of Sciences, Washington, D.C.
- Arcement, G.K. and Schneider, V.R., 1984, "Guide for Selecting Manning's Roughness Coefficients for Natural Channels and Flood Plains," FHWA Report No., FHWA-TS-84-204, Washington, D.C., 62 p.
- Arneson, L.A., 2001, Personal Communication.
- Arneson, L.A. and Sherman, J.O., 1998, "Users Manual for WSPRO- A Computer Model for Water Surface Profile Computation," Federal Highway Administration, FHWA Report No. FHWA-SA-98-080, Washington, D.C.
- Arneson, L., Shearman, J.O., and Jones, J.S., 1991, "Evaluating Scour a Bridges Using WSPRO," Unpublished paper presented at the 71st Annual transportation research Board meeting in January, Washington, D.C.
- ASCE, 1983, "River Meandering," Proc. Rivers '83, ASCE, Reston, VA.

Attia, M.I., 1954, "Deposits in the Nile Valley and the Delta," Geological Survey of Egypt, Government Press, Cairo.

Ayres Associates, 1994, "Development of Hydraulic Computer Models to Analyze, Tidal and Coastal Stream Hydraulic Conditions at Highway Structures," Final Report, Phase I, HPR552, South Carolina DOT, Columbia, SC, Ayres Associates, Fort Collins, CO.

Ayres Associates, 1997, "Development of Hydraulic Computer Models to Analyze, Tidal and Coastal Stream Hydraulic Conditions at Highway Structures," Final Report, Phase II, HPR552, South Carolina DOT, Columbia, SC, Ayres Associates, Fort Collins, CO.

Bagnold, R.A., 1966, "An Approach to the Sediment Transport Problem from General Physics," U.S. Geol. Survey Professional Paper 422-I.

Barkau, R.L., 1993, "UNET-One Dimensional Unsteady Flow Through a Full Network of Open Channels," Report CPD-66, U.S. Army Corps of Engineers, Hydrologic Engineering Center, Davis, CA.

Barnes, H.H., Jr., 1967, "Roughness Characteristics of Natural Channels," USGS Water Supply Paper 1849, Reston, VA, 213 p.

Barton, J.R. and Lin, P.P., 1955, "A Study of the Sediment Transport in Alluvial Channels," Colorado A&M College Report No. 55JRB2, Fort Collins, CO, 45 p.

Bechteler, W. and Vetter, M., 1989, "Comparison of Existing Sediment Transport Models," Proc. Fourth Intl. Sym. on River Sedimentation, Intl. Res. and Training Center on Erosion and Sed., China Ocean Press.

Beck, S. and Melfi, D.A., 1984, "Lateral Migration of the Genessee River, New York," in River Meandering, Elliott, C.M. (ed), American Soc. Civil Engrs., Reston, VA, pp. 510-517.

Beckman, M.A. and Furness, L.W., 1962, "Flow Characteristics of Elkhorn River near Waterloo, Nebraska," USGS Water Supply Paper 1498-B, Reston, VA, 34 p.

Benson, M.A. and Dalrymple, T., 1967, "General Field and Office Procedures for Indirect Discharge Measurement," USGS, Techniques of Water Resources Investigations, Book 3, Chap. A1, Reston, VA, 30 p.

Bishop, A.A., Simons D.B., and Richardson, E.V., 1965, "Total Bed Material Transport," ASCE Hydr. Div., Jour., Vol. 91, No. HY2, pp. 175-191.

Blaisdell, F. W., 1949, "Flow Through Diverging Open Channel Transitions at Supercritical Velocities," U.S. Dept. of Agr. SCS-TP-76, April.

Blodgett, J.C. and McConaughy, C.E., 1985, "Evaluation of Rock Riprap Design-Practices for Protection of Channels near Highway Structures," Phase 1 Preliminary Report, U.S. Geological Survey, Reston, VA., and Federal highway Administration, Washington, D.C.

Bledsoe, B.P., 1999, "Specific Stream Power as an Indicator of Channel Pattern, Stability and Response to Urbanization, Ph.D. Dissertation, Colorado State University.

Bogárdi, J.L., 1965, "European Concepts of Sediment Transportation," ASCE Hydr. Div., Jour., Vol. 91, No. HY1.

Bogárdi, J.L., 1974, "Sediment Transport in Alluvial Streams," Akadémiai Kiadó, Budapest.

Bondurant, D.C., 1958, Discussion of "The Total Sediment Load of Streams by E.M. Laursen (1958)," ASCE Hydr. Div., Jour., Vol. 84, No. HY6, Paper 1856, pp. 59-64.

Borah, D.K., Alonso C.V., and Prasad, S.N., 1982a, "Routing Graded Sediments in Streams: Formulation," ASCE Hydr. Div., Jour., Vol. 108, No. HY12, pp. 1486-1503.

Borah, D.K., Alonso C.V., and Prasad, S.N., 1982b, "Routing Graded Sediments in Streams: Applications," ASCE Hydr. Div., Jour., Vol. 108, No. HY12, pp. 1504-17.

Bradley, J.B., 1984, "Transition of a Meandering River to a Braided System due to High Sediment Concentration Flows," proceedings of the Conference Rivers '83, River Meandering, New Orleans, LA, 1983, pp. 89-100.

Bradley, J.N., 1978, "Hydraulics of Bridge Waterways," FHWA Hydraulic Design Series, HDS No.1, 2nd Edition, Federal Highway Administration, Washington, D.C., 110 p.

Bray, D.I., 1979, "Estimating Average Velocity in Gravel-Bed Rivers," ASCE Hydr. Div., Jour., Vol. 105, No. HY9, pp. 1103-1122.

Bray, D.I., 1982, "Flow Resistance in Gravel-Bed Rivers," Chapt. 6, Gravel-Bed Rivers, Wiley, NY, pp. 109-137.

Briaud, J-L, Ting, F.C.K., Chen, H.C., Rau, G. and Wei, G., 1999, "SRICOS: Prediction of Scour Rate in Cohesive Soils at Bridge Piers," ASCE Jour. of Geotechnical and Environmental Engineering, Vol. 124, No. 4, Reston, VA.

Brice, J.C., 1974, "Evolution of Meander Loops," Geological Society of America Bulletin 85, pp. 581-86.

Brice, J.C., 1975, "Air Photo Interpretation of the Form and Behavior of Alluvial Rivers," Final Report to the U.S. Army Research Office.

Brice, J.C., 1980, "Stability of Relocated Stream Channels," FHWA/RD-80/158, Federal Highway Administration, Washington, D.C.

Brice, J.C., 1982, "Stream Channel Stability Assessment," Federal Highway Administration Report FHWA/RD-82/021, 41 p.

Brice, J.C., 1984, "Assessment of Channel Stability at Bridge Sites," Second Bridge Engineering Conference Transportation Research Record 950, National Research Council, pp. 163-171.

Brice, J.C. and Blodgett, J.C., 1978, "Countermeasures for Hydraulic Problems at Bridges," Vol. 1, Analysis and Assessment," FHWA Report No. FHWA-RD-78-162, Federal Highway Administration, Washington, D.C.

Brice, J.C. and Blodgett, J.D., 1978, "Countermeasures for Hydraulic Problems at Bridges," Vol. 2, Case Histories for Sites 1-283," FHWA Report No. FHWA/RD-78-163, Federal Highway Administration, Washington, D.C.

Brooks, N.H., 1958, "Mechanics of Streams with Movable Beds," ASCE Trans., Vol. 123, pp. 526-594.

Brown, C.B., 1950, "Sediment Transport," Chapt. VII, Engineering Hydraulics, Rouse, Editor, John Wiley and Sons, NY.

Brown, S.A., 1985a, "Streambank Stabilization Measures for Highway Stream Crossings – Executive Summary," FHWA Report No. FHWA-RD--84-099, Washington D.C., Available through NTIS, Springfield, VA, 22161.

Brown, S.A., 1985b, "Streambank Stabilization Measures for Highway Stream Crossings – Executive Summary," FHWA Report No. FHWA-RD-84-100, Washington D.C., Available through NTIS, Springfield, VA, 22161.

Brown, S.A., 1985c, "Design of Spur-type Streambank Stabilization Structures," FHWA Report No. FHWA-RD-84-101, Washington D.C., Available through NTIS, Springfield, VA, 22161.

Brown, S.A. and Clyde, E.S., 1989, "Design of Riprap Revetment," Hydraulic Engineering Circular No. 11, FHWA Report No. FHWA-IP-016, McLean, VA. ([www.fhwa.dot.gov/bridge/hydpub.htm](http://www.fhwa.dot.gov/bridge/hydpub.htm)), see FHWA 1984, p. 11.7.

Brown, S.A., McQuivey, R.S., and Keefer, T.N., 1980, "Stream Channel Degradation and Aggradation Analysis of Impacts to Highway Crossings," Final Report FHWA/RD-80/159, Federal Highway Administration, Washington, D.C. 20590, 202 p.

Brownlie, W.R., 1981, "Prediction of Flow Depth and Sediment Discharge in Open Channels," California Institute of Technology Rept. KH-R-43A, Pasadena, CA.

Buchanan, T.J. and Somers, W.P., 1968a, "Discharge Measurements at Gaging Stations," Techniques of Water-Resources Investigations of the USGS, Book 3, Chapter A8, Reston, VA.

Buchanan, T.J. and Somers, W.P., 1968b, "Stage Measurements at Gaging Stations," Techniques of Water-Resources Investigations of the USGS, Book 3, Chapter A7, Reston, VA.

Buffington, J.M., 1999, "The Legend of A. F. Schields," ASCE Jour. of Hydr. Eng., Vol. 125, No. 4, Reston, VA, 376 p.

Burkham, D.E. and Dawdy, D.R., 1980, "General Study of the Modified Einstein Method of Computing Total Sediment Discharge," USGS Water Supply Paper 2066. Reston, VA.

Butch, G.K., 2000, USGS, Personal Communication.

BYU, 2000, "SMS Surface Water Modeling System," Version 7.0, Brigham Young University-Engineering Computer Graphics Laboratory, Provo, UT.

- California Division of Highways, 1959, "Bank and Shore Protection in California," Highway Practices," Dept of Public Works, (CALTRANS) Sacramento, CA.
- Carter, A.C., Carlson, E.J., and Lane, E.W., 1953, "Critical Tractive Forces on Channel Side Slopes in Coarse, Non-Cohesive Material," Hydr. Lab. Report No. HYD-366, U.S. Bureau of Reclamation, Denver, CO.
- Cao, Z., Wang, W., and Dong, J., 1997, "Suspended Sediment Transport Capacity of Open Channel Flow," Int'l Jour. of Sed. Res., Vol. 12, No. 3, pp. 1-10.
- Carey, W.C. and Keller, M.D., 1957, "Systematic Changes in the Beds of Alluvial Rivers," ASCE Hydr. Div., Jour., Vol. 83, No. HY3.
- Carlston, C.W., 1965, "The Relation of Free Meander Geometry to Stream Discharge and its Geomorphic Implications," American Jour. of Science Vol. 263, pp. 864-685.
- Carson, M.A. and Lapointe, M.F., 1983, "The Inherent Asymmetry of River Meander Planform, Jour. of Geology, Vol. 91, pp. 41-45.
- Carter, A.C., Carlson, E.J., and Lane, E.W., 1953, "Critical Tractive Forces on Channel Side Slopes in Coarse, Non-Cohesive Material," Hydr. Lab. Report No. HYD-366, U.S. Bureau of Reclamation, Denver, CO.
- Carter, R.W. and Davidian, J., 1968, "General Procedure for Gaging Streams," Techniques of Water-Resources Investigations of the USGS, Book 3, Chapter A6, Reston, VA.
- Chang, F.F.M., 1973, "A Statistical Summary of the Cause and Cost of Bridge Failures," Federal Highway Administration, U.S. Depart. of Transportation, Washington, D.C.
- Chang, F.F.M. and Davis, S.R., 1999, "The Maryland State Highway Administration ABSCOUR Program," Maryland SHD, Baltimore, MA.
- Chang, H.H., 1998, "Generalized Computer Program Fluvial-12 Mathematical Model for Erodible Channels," Users Manual.
- Charlton, F.G., Brown, P.M., and Benson, R.W., 1978, "The Hydraulic Geometry of Some Canal Rivers in Britain," Hydr. Research Sta. Report No. IT 180, Wallingford, England, 48p.
- Chaudry, H.M., Smith K.V.H., and Vigil, H., 1970, "Computation of Sediment Transport in Irrigation Canals," Proc. Institution of Civil Engineers, Vol. 45, Paper 7241, pp. 79-101.
- Chen, Y.H. and Anderson, B.A., 1987, "Development of a Methodology for Estimating Embankment Damage due to Flood Overtopping," FHWA Report No. [FHWA-RD-86/126](#).
- Cherry, D.S., Wilcock, P.R., and Wolman, M.G., 1996, "Evaluation of Methods for Forecasting Planform Change and Bankline Migration in Flood-Control Channels," Department of Geography and Environmental Engineering, Johns Hopkins University, prepared for U.S. Army Engineer Waterways Experiment Station, Vicksburg, MS.
- Chien, N., 1954, "The Present Status of Research in Sediment Transport," ASCE Proc. Vol. 80, Reston, VA.

Chitale, S.V., 1966, "Hydraulics of Stable Channels," Central Water and Power Commission, Ministry of Irrigation and Power, Government of India.

Chow, V.T., 1959, "Open Channel Hydraulics," McGraw-Hill, Inc, NY.

Clopper, P. E. and Chen, Y.H., 1988, "Minimizing Embankment Damage During Overtopping Flow," FHWA Report No. FHWA-RD-88/181.

Colby, B.R., 1960, "Discontinuous Rating Curves for Pigeon Roost and Cuffaw Creeks in Northern Mississippi," U.S. Dept of Agr. Research Service Report 4146, 31p.

Colby, B.R., 1964, "Practical Computations of Bed-Material Discharge," ASCE Hydr. Div., Jour., Vol. 90, No. HY2.

Colby, B.R. and Hembree, C.H., 1955, "Computations of Total Sediment Discharge, Niobrara River near Cody, Nebraska," USGS Water-Supply Paper No. 1357, Reston, VA, 187 p.

Colby, B.R. and Hubbell, D.W., 1962, "Simplified Methods for Computing Total Sediment Discharge with the Modified Einstein Procedure," USGS Water Supply Paper 1593, Reston, VA.

Colby, B.R., Hembree, C.H., and Rainwater, F., 1956, "Sedimentation and Chemical Quality of Surface Waters in the Wind River Basin, Wyoming," USGS Water Supply Paper 1373, Reston, VA.

Coleman, J.M., 1969, "Brahmaputra River; Channel Processes and Sedimentation," Sedimentary Geology, Vol. 3, pp. 129-239.

Copeland, R.R. and Thomas, W.A., 1989, "Corte Madera Creek Sediment Study Numerical Investigation," U.S. Army Engineer Waterways Experiment Station, TR HL-89-6.

Copeland, R.R. and Hall, B.R., 1998, "Channel Restoration Hydraulic Design Procedure," ASCE Proc. 1998 Wetlands Engineering and River Restoration Conf., Eng. Approaches to Ecosystem Restoration, Reston, VA.

Corbet, D.M., 1962, "Stream Gaging Procedure," USGS Water Supply Paper 888, Reston, VA.

Cowan, W.L., 1956, "Estimating Hydraulic Roughness Coefficients," Agricultural Engineering, Vol. 37, No. 7, pp. 473-475.

Culbertson, D.M., Young, L.E., and Brice, J.C, 1967, "Scour and Fill in Alluvial Channels," USGS Open File Report, Reston, VA.

Culbertson, J.K. and Dawdy, D.R., 1964, "A study of Fluvial Characteristics and Hydraulic Variables, Middle Rio Grande, New Mexico," USGS Water Supply Paper, 1498-F, Reston, VA, 74 p.

Culbertson, J.K., Scott, C.H., and Bennett, J.P., 1972, "Summary of Alluvial-Channel Data from Rio Grande Conveyance Channel, New Mexico, 1965-69," USGS Professional Paper 562-J, Reston, VA.

- Da Cunha, L.V., 1969, "River Mondego, Portugal," Personal Communication by Brownlie, Laboratorio Nacional De Engenharia Civil, Lisbon.
- Davis, W.M., 1899, "The Geographical Cycle," *Geographical Journal*, 14, pp. 481-504.
- Dawdy, D.R., 1961, "Depth-Discharge Relations of Alluvial Streams – Discontinuous Rating Curves," U.S. Geol. Survey WSP 1498-C, Reston, VA, 16p.
- Diehl, T.H., 1997, "Potential Drift Accumulation at Bridges," Federal Highway Administration Report No. FHWA-RD-97-028, Washington, D.C.
- Diehl, T.H. and Bryan, B.A., 1993, "Supply of Large Woody Debris in a Stream Channel," *ASCE Hydraulic Engineering*, Reston, VA, p 1055-1060. *Compendium of ASCE Water Resources Papers 1991 to 1998*, "Stream Stability and Scour at Highway Bridges," E.V. Richardson and P.F. Lagasse, Editors, Reston, VA, 98 p.
- Dietrich, W.E. and Smith, J.D., 1983, "Influence of the Point Bar on Flow Through Curved Channels," *Water Resource Research*, Vol. 19, pp. 1173-1192.
- Einstein, H.A., 1944, "Bed Load Transportation in Mountain Creek," U.S. Soil Conservation Service, SCS-TP-55, 50 p.
- Einstein, H.A., 1950, "The Bed Load Function for Sediment Transportation in Open Channel Flows," U.S. Dept. of Agriculture, Soil Conservation Serv., Tech. Bull. 1026.
- Einstein, H.A., 1964, "Sedimentation, Part II. River Sedimentation," Handbook of Applied Hydrology, V.T. Chow (ed), Section 17, McGraw-Hill Book Co., NY.
- Einstein, H.A. and Barbarossa, N.L., 1952, "River Channel Roughness," *Trans. ASCE*, Vol. 117, pp. 1121-1132.
- Einstein, H.A. and Chien, N., 1956, "Similarity of Distorted River Models with Movable Beds," *Transactions of the ASCE*, Vol. 121.
- El-Moatassem, M. and El-Mottaleb, F, 1979, "Effect of High Aswan Dam on the Regime of the River Downstream Essa Barrage," High Dam Side Effects Research Inst., Water Research Center, Ministry of Irrigation, Cairo, Egypt.
- Engelund, F., 1966, "Hydraulic Resistance of Alluvial Streams," *ASCE Hydr. Div., Jour.*, Vol. 92, No. HY2, Reston, VA, pp. 315-327.
- Engelund, F., 1974, "Flow and Bed Topography in Channel Bends," *ASCE Hydr. Div. Jour.*, Vol. 100, Reston, VA, pp. 1631-1648.
- Engelund, F. and Hansen, E., 1972, "A Monograph on Sediment Transport in Alluvial Streams," Teknisk Forlag, Technical Press, Copenhagen.
- Everitt, B.L., 1968, "Use of Cottonwoods in the Investigation of the Recent History of a Floodplain," *American Jour. of Science*, Vol. 206, pp. 417-439.

Fathy, A., 1956, "Some Considerations on the Degradation Problem in the Aswan High Dam Scheme," University of Alexandria, Egypt.

Federal Interagency Stream Restoration Working Group, 1998, "Stream Corridor Restoration, Principles, Processes, and Practices," National Technical Information Service, Order No. PB98-158348, Washington, D.C.

FHWA, 1961, "Peak Rates of Runoff from Small Watersheds," FHWA Hydraulic Design Series, HDS No. 2, Federal Highway Administration, Washington, D.C. ([www.fhwa.dot.gov/bridge/hydpub.htm](http://www.fhwa.dot.gov/bridge/hydpub.htm))

FHWA, 1984, "Hydrology," Hydraulic Engineering Circular 19, FHWA Report No. FHWA-IP-84-15, Washington, D.C. ([www.fhwa.dot.gov/bridge/hydpub.htm](http://www.fhwa.dot.gov/bridge/hydpub.htm))

FHWA, 1985, "Hydraulic Design of Highway Culverts," FHWA Hydraulic Design Series HDS 5, Federal Highway Administration, Washington, D.C. ([www.fhwa.dot.gov/bridge/hydpub.htm](http://www.fhwa.dot.gov/bridge/hydpub.htm))

FHWA, 1996, "Highway Hydrology," FHWA Hydraulic Design Series, HDS No. 2, Federal Highway Administration, Washington, D.C. ([www.fhwa.dot.gov/bridge/hydpub.htm](http://www.fhwa.dot.gov/bridge/hydpub.htm))

FHWA, 1997, "Introduction to Highway Hydraulics," FHWA Hydraulic Design Series, HDS No. 4, Federal Highway Administration, Washington, D.C. ([www.fhwa.dot.gov/bridge/hydpub.htm](http://www.fhwa.dot.gov/bridge/hydpub.htm))

FHWA, 1998, "HY8 Culvert Analysis Version 6.1," Computer program for design of culverts, Federal Highway Administration, Washington, D.C. ([www.fhwa.dot.gov/bridge/hydsoft.htm](http://www.fhwa.dot.gov/bridge/hydsoft.htm))

Fisk, H. M., 1944, "Geological Investigation of the Alluvial Valley of the Lower Mississippi River," Mississippi River Commission, Vicksburg, MS, 78 p.

Fiuzat, A.A. and Richardson, E.V., 1983, "Supplemental Stability Tests of Riprap in Flood Control Channels," Civil Engineering Report CER83-84AAF-EVR18, for U.S. Corps of Engineers, Colorado State University, Fort Collins, CO, 94 p.

Fortier, S. and Scobey, F.C., 1926, "Permissible Canal Velocities," ASCE Trans. Vol. 89, Reston, VA, pp. 940-956.

Franco, J.J., 1967, "Research for River Regulation Dike Design," Journal of Waterways and Harbors Division, ASCE, Vol. 93, No. WW3, pp. 71-87.

Franco, J.J., 1968, "Effects of Water Temperature on Bed-Load Movement," ASCE Waterways and Harbors Div., Jour., Vol. 94, No. WW3, pp. 343-352.

Friedkin, J.F., 1945, "A Laboratory Study of the Meandering of Alluvial Rivers," U.S. Army Corps of Engineers Waterways Experiment Station, Vicksburg, MS.

Froehlich, D.C., 1989, "Abutment Scour Prediction," Paper presented at the Annual Transportation Board Meeting, Washington, D.C., January.



Froehlich, D.C., 1996, "Finite Element Surface-Water Modeling System: Two-Dimensional Flow in a Horizontal Plane," FESWMS-2DH (FloDH), Version 2, User's Manual, U.S. Department of Transportation, Federal Highway Administration, Turner-Fairbank Highway Research Center, McLean, VA. ([www.fhwa.dot.gov/bridge/hydpub.htm](http://www.fhwa.dot.gov/bridge/hydpub.htm))

Garcia, M.H., Bittner, L.D., and Nino, 1994, "Mathematical Modeling of Meandering Streams in Illinois: A Tool for Stream Management and Engineering," Dept. Civil Engineering, University of Illinois at Urbana-Champaign, Urbana, IL.

Garde, R.J. and Rangaraju, K.G., 1966, "Resistance Relationships for Alluvial Channel Flow," ASCE Hydr. Div., Jour., Vol. 92, No. HY4, pp. 77-100.

Garde, R.J. and Albertson, M.L., 1958, Discussion of "The Total Sediment Load of Streams by E.M. Laursen (1958)," ASCE Hydr. Div., Jour., Vol. 84, No. HY6, Paper 1856, pp. 59-64.

Gasser, M.M., Hassan, W.M.A. and Helmy, M.S., 1978, "State of the Nile River Between 1964 and 1977," Hydraulic and Sediment Research Institute, Ministry of Irrigation, Delta Barrage, Egypt.

Gessler, J., 1971, "Beginning and Ceasing of Sediment Motion," Chap. 7 River Mechanics, H. W. Shen (ed), Water Resources Publication, Littleton, CO.

German Association for Water Resources and Land Improvement, 1990, "Sediment Transport in Open Channels – Calculation Procedures for the Engineering Practice," Bulletin 17, Verlag Paul Parey, Hamburg/Berlin, Germany.

Gilbert, G.K., 1914, "Transportation of Debris by Running Water," USGS Prof. Paper, No. 86, Reston, VA,

Guy, H.P., 1970, "Fluvial Sediment Concepts," Techniques of Water-Resources Investigations of the USGS, Book 3, Chapter C1, Reston, VA.

Guy, H.P., 1977, "Laboratory Theory and Methods for Sediment Analysis," Techniques of Water-Resources Investigations of the USGS, Book 5, Chapter C1, Reston, VA.

Guy, H.P. and Norman, V.W., 1970, "Field Methods for Measurement of Fluvial Sediment," Techniques of Water-Resources Investigations of the USGS, Book 3, Chapter C2, Reston, VA.

Guy, H.P., Simons, D.B., and Richardson, E.V., 1966, "Summary of Alluvial Channel Data From Flume Experiments, 1956-61," USGS Professional Paper 462-I, Reston, VA.

Harms, J.C. and Fahnestock, R.K., 1965, "Stratification, Bed Forms, and Flow Phenomena (with an example for the Rio Grande): Primary Sedimentary Structures and Their Hydrodynamic Interpretation," Society of Economic Paleontologists and Mineralogists Special Publication No. 12.

Harvey, M.D., 1989, "Meanderbelt Dynamics of the Sacramento River," California Riparian Systems Conf. Proc., USDA Forest Service General Techn. Rept. PSW-110, pp. 54-61.

Hasegawa, K., 1989, "Studies on Qualitative and Quantitative Prediction of Meander Channel Shift: in Ikeda," Parker, G. (ed) River Meandering, Amer. Geophysical Union Water Resources Monograph 12, pp. 215-236.

Hewlett, H.W.M., Boorman, L.A., and Bramley, M.E., 1987, "Design of Reinforced Grass Waterways," Construction Industry Research and Information Association, Report 116, London, United Kingdom.

Hickin, E.J. and Nanson, G., 1975, "The Character of Channel Migration on the Beatton River, Northeast British Columbia, Canada," Geological Society of America Bulletin 86, pp. 478-494.

Holmes, D.A., 1968, "The Recent History of the Indus," Geographical Jour., Vol.134 (3), pp. 367-382.

Holtz, D.H., Christopher, B.R., and Berg, R.E., 1995, "Geosynthetic Design and Construction Guidelines," Federal Highway Administration Publication No. FHWA-HI-95-038, Washington, D.C.

Hooke, J.M., 1979, "An Analysis of the Processes of River Bank Erosion," Jour. Hydrology, Vol. 42, pp. 39-62.

Hooke, J.M., 1984, "Changes in River Meanders," Progress in Physical Geography Vol. 8, pp. 473-508.

Hooke, J.M., 1991, "Changing River Channels," Geography Review Vol. 5, pp. 2-5.

Hooke, J.M. and Harvey, M.A., 1983, "Meander Changes in Relation to Bend Morphology and Secondary Flows," in Collinson, J.D. and Lewin, J. (eds), Modern and Ancient Fluvial Systems, Basil Blackwell, Oxford, pp. 121-132.

Howard, A.D., 1996, "Modeling Channel Evolution and Floodplain Morphology," in Anderson, M.G., Walling, D.E., and Bates, P.D. (eds), Floodplain Processes, Wiley, Chichester, pp. 15-62.

Howard, A.D. and Knutson, T.R., 1984, "Sufficient Conditions for River Meandering: a Simulation Approach," Water Resources Research, Vol. 20, pp. 1659-1667.

Hsü, K.J., 1983, "The Mediterranean was a Desert," A Voyage of the Glomar Challenger, Princeton Univ. Press, Princeton, N.J.

Hubbell, D.W. and Matejka, D.Q., 1959, "Investigation of Sediment Transportation, Middle Loup River at Dunning, Nebraska," USGS Water-Supply Paper No. 1476, Reston, VA.

Hungr, O., Morgan, G.C., and Kellerhals, R., 1984, "Quantitative Analysis of Debris Torrent Hazards for Design of Remedial Measures," Canadian Geotechnical Journal, Vol., 21, No. 4, pp. 663-677.

Hydrau-Tech, Inc., 1998, "Visually Interactive Sediment Transport Computation Model for Windows 95/98," Fort Collins, CO.

Hydrologic Engineering Center, 1993, "Scour and Deposition in Rivers and Reservoirs," User's Manual, HEC-6, Davis, CA.

Inglis, C.C., 1949, "The Behavior and Control of Rivers and Canals," Res. Publ., Poona (India), No. 13, 2 vols.

Ippen, A.T., 1950, "Channel Transitions and Controls," Chapt. VIII, Engineering Hydraulics, Rouse, Editor, John Wiley and Sons, NY.

Ippen, A.T. and Dawson, J.H., 1951, "Design of Channel Contractions," ASCE Trans. Vol. 116, Reston, VA, pp. 326-436.

Ippen, A.T. and Drinker, P.A., 1962, "Boundary Shear Stresses in Curved Trapezoidal Channels," ASCE Hydr. Div. Jour., Vol. 88, No. HY5, Reston, VA.

Jain, S.C. and Fischer, R.E., 1979, "Scour Around Bridge Piers at High Froude Numbers," FHWA Report No. FHWA-RD-79-104, Federal Highway Administration, Washington, D.C.

Jarrett, R.D., 1984, "Hydraulics of High-Gradient Streams," ASCE Jour. Hydr. Eng., Vol. 110, No. 11, Reston, VA.

Jarrett, R.D., "Determination of Roughness Coefficients for Streams in Colorado," USGS Water Resources Investigation Report 85-4004, Denver, CO.

Johnson, P.A. and Torrico, E.F., 1994, "Scour Around Wide Piers in Shallow Water," Transportation Research Board Record 1471, Transportation Research Board, National Academy of Science, Washington, D.C.

Jones, J.S., 1983, "Comparison of Prediction Equations for Bridge Pier and Abutment Scour," Transportation Research Record 950, Second bridge Engineering Conference Vol. 2 Transportation Research Board, National Academy of Science, Washington, D.C.

Jones, J.S. 1999, "FHWA Hydraulics Lab and Partners Perform Scour Evaluation for Woodrow Wilson Bridge", Federal Highway Administration Research and Technology Reporter, FHWA-RD-99-016, McLean, VA.

Julien, P.Y., 1995, "Erosion and Sedimentation," Cambridge University Press, Melbourne, Australia.

Julien, P.Y. and Simons, D.B., 1984, "Analysis of Hydraulic Geometry Relationships in Alluvial Channels," Report CER83-84 PYJ-DBS45, Colorado State University, Fort Collins, CO, 47 p.

Julien, P.Y. and Wargadalam, J., 1995, "Alluvial Channel Geometry: Theory and Applications," Journal of Hydraulic Engineering, Vol. 121, No. 4, April.

Kalinske, A.A. and Hsia, C.H., 1945, "Study of Transportation of Fine Sediment by Flowing Water," Iowa University Studies in Engineering, Bulletin No. 29, Iowa City, Iowa.

Karim, M.F., 1998, "Bed Material Discharge Prediction for Non-Uniform Bed Sediments," ASCE Hydr. Div., Jour., Vol. 124, No. 6, pp. 597-604.

Karim, F. and Kennedy, J.K., 1981, "Computer-based Predictors for Sediment Discharge and Friction Factor of Alluvial Streams," Iowa Institute of Hydraulic Research, Report No. 242, University of Iowa.

Keaton, J.R., 1995, "Dilemmas in Regulating Debris-Flow Hazards in Davis County, Utah," in Environmental and Engineering Geology of the Wasatch Front Region, W. R. Lund, ed. Utah Geol. Asso. Publ. 24, Salt Lake City, UT, pp. 185-192.

Keefer, T.N., McQuivey, R.S., and Simons, D.B., 1980, "Interim Report – Stream Channel Degradation and Aggradation: Causes and Consequences to Highways," Report No. FHWA/RD-80/038, Federal Highway Administration, Washington, D.C. 20590, 86 p.

Keller, E.A., 1972, "Development of Alluvial Stream Channels: a Five-Stage Model," Geol. Soc. Amer. Bull., Vol. 83, pp. 1531-1540.

Kellerhals, R., Miles, M., and Seagel, G.C., 1985, "River Channel Encroachments by Highways and Railways," Proc. Ann. Conf. and 7<sup>th</sup> Canadian Hydrotechnical Conf., Vol. 1B, Saskatoon, Canada, pp. 77-96.

Kennedy, E.J., 1983, "Computation of Continuous Records of Streamflow," Techniques of Water Resources Investigations of the USGS, Book 3, Chapter A13, Reston, VA.

Kennedy, J.F. and Brooks, N.H., 1963, "Laboratory Study of an Alluvial Stream at Constant Discharge," Proc. Federal Inter-Agency Sed. Conf., Miscellaneous Publication No. 970, Pasadena, CA, pp. 320-330.

Kennedy, R.C., 1895, "The Prevention of Silting in Irrigation Canals," Min. Proc. Instn. Civil Engr., Vol. CXIX.

Keown, M.P., 1983, "Streambank Protection Guidelines for Landowners and Local Governments," U.S. Army Corps of Engineers, Waterways Experiment Station, Vicksburg, MS, 60 p.

Keown, M.P., Oswalt, N.R., Perry, E.B., and Dordeau, E.A., 1977, "Literature Survey and Preliminary Evaluation of Streambank Protection Methods," Tech. Report H-79-9, U.S. Army Corps of Engineers, Waterways Experiment Station, Vicksburg, MS.

Kindsvater, C. E., 1964, "Discharge Characteristics of Embankment-Shaped Weirs," Studies of Flow of Water Over Weirs and Dams, USGS Water-Supply Paper 1617-A.

King, P.B. and Schumm, S.A., 1980, "The Physical Geography (Geomorphology) of W.M. Davis," Geobooks, Norwich U.K., 174 p.

Knighton, D., 1984, "Fluvial Forms and Processes," Arnold, London.

Knighton, D., 1998, "Fluvial Forms and Processes – A New Perspective," Arnold, London.

Knott, J.M., 1974, "Sediment Discharge in Trinity River Basin, California," USGS Water-Resource Investigation 49-73, 62 p.

Kodoatie, R.J., 1999, "Sediment Transport Relations in Alluvial Channels," Ph.D. Dissertation, Colorado State University, Fort Collins, CO.

Kodoatie, R.J., Simons D.B., and Albertson, M.L., 1999, "Selected Sediment Transport Relationships for Alluvial Channels," Colorado State University, Fort Collins, CO.

Kouchakzadeh, S. and Townsend, R.D., 1999, "Bridge Abutment Scour in Compound-Shaped River Channels," Compendium of ASCE Water Resources Papers 1991 to 1998, "Stream Stability and Scour at Highway Bridges," E.V. Richardson and P.F. Lagasse, Editors, Reston, VA, 311 p.

Kozarski, S. and Retnicki, K., 1977, "Valley Floors and Changes of River Channel Patterns in the North Polish Plain During the Late Würm and Holocene," *Questiones Geographicae*, Vol. 4, pp. 51-93.

Kramer, H., 1935, "Sand Mixtures and Sand Movement in Fluvial Models," *ASCE Trans.* Vol. 100, No. 1909, Reston, VA, pp. 798-878.

Lacy, G., 1930, "Stable Channels in Alluvium," *Proc. Inst. Civil Engrs.*, 229 p.

Lagasse, P.F., 1994, "Variable Response of the Rio Grande to Dam Construction," in the *Variability of Large Alluvial Rivers*, Schumm, S.A. and Winkley, B.R. (eds), ASCE Press, New York, NY.

Lagasse, P.F., Richardson, E.V., Schall, J.D., and Price, G.R. 1997, "Instrumentation for Measuring Scour at Bridge Piers and Abutments," NCHRP Report No. 396, Transportation Research Board, National Research Council, National Academy Press, Washington, D.C., Feb., 182 p.

Lagasse, P.F., Schall, J.D., and Richardson, E.V., 2001, "Stream Stability at Highway Structures," Third Edition, Hydraulic Engineering Circular No. 20, FHWA NHI 01-002, Washington, D.C. ([www.fhwa.dot.gov/bridge/hydpub.htm](http://www.fhwa.dot.gov/bridge/hydpub.htm))

Lagasse, P.F., Zevenbergen, L.W., Schall, J.D., and Clopper, P.E., 2001, "Bridge Scour and Stream Instability Countermeasures," Second Edition, Hydraulic Engineering Circular No. 23, FHWA NHI 01-003, Washington, D.C. ([www.fhwa.dot.gov/bridge/hydpub.htm](http://www.fhwa.dot.gov/bridge/hydpub.htm))

Landers, M.N., Mueller, D.S., and Richardson, E.V., 1999, "U.S. Geological Survey Field Measurements of Pier Scour," *ASCE Compendium, Stream Stability and Scour at Bridges*, Richardson and Lagasse, (eds), Reston, VA.

Lane, E.W., 1953, "Progress Report on Studies on the Design of Stable Channels of the Bureau of Reclamation," *ASCE Pro.* Vol. 79, Reston, VA.

Lane, E.W., 1955, "Design of Stable Channels," *ASCE Trans.*, Vol. 120, Paper No. 2776, pp. 1234-1260.

Lane, E.W., 1957, "A Study of the Shape of Channels Formed by Natural Streams Flowing in Erodible Material," *Missouri River Division Sediment Series No. 9*, U.S. Army Corps of Engineers, Omaha, NE.

- Lane, E.W. and Carlson, E.J., 1955, "Some Factors Affecting the Stability of Canals Constructed in Coarse Granular Materials," Internat. Assoc. Hydraulic Research, 5th Gen. Mtg., Minneapolis, MN, pp. 37-38.
- Lathrop, D.W., 1968, "Aboriginal Occupation and Changes in River Channel on the Central Vcayali, Peru," American Antiquity, Vol. 33, pp. 62-79.
- Lau, Y.L. and Krishnappan, B.G., 1985, "Sediment Transport Under Ice Cover," ASCE Hydr. Div., Jour., Vol. 54, No. 1, pp. 1-36.
- Laursen, E.M., 1958, "The Total Sediment Load of Streams," ASCE Hydr. Div., Jour., Vol. 84, No. HY1, Paper 1530, Reston, VA, pp. 1-36.
- Laursen, E.M., 1958, "Scour at Bridge Crossing," Iowa Highway Research Board Bulletin 8, Iowa Institute of Hydraulic Research, Iowa City, IA.
- Laursen, E.M., 1960, "Scour at Bridge Crossing," ASCE Hydr. Div., Jour., Vol. 86, No. HY2, Reston, VA.
- Laursen, E.M., 1963, "An Analysis of Relief Bridge Scour," ASCE Hydr. Div., Jour., Vol. 89, No. HY3, Reston, VA.
- Laursen, E.M. and Toch, A., 1956, "Scour Around Bridge Piers and Abutments," Iowa Highway Research Board Bulletin 4, Iowa Institute of Hydraulic Research, Iowa City, IA.
- Laursen, E.M. and Flick, M.W., 1983, Final Report, "Predicting Scour at Bridges, Questions not Fully Answered – Scour at Sill Structures," Report ATTI-83-6, Arizona Department of Transportation.
- Lawler, D.M., 1986, "Bank Erosion and Frost Action," in International Geomorphology, Gardner, V. (ed), Part 1, Wiley, Chichester, pp. 575-590.
- Leliavsky, S., 1955, "An Introduction to Fluvial Hydraulics," Constable & Company Ltd, London, England, 257 p.
- Leopold, L.B., 1969, "Sediment Transport Data for Various United States Rivers," Personal Communication by Brownlie.
- Leopold, L.B. and Maddock, Jr., T., 1953, "The Hydraulic Geometry of Stream Channels and Some Physiographic Implications," USGS Prof. Paper 252, Reston, VA, 57p.
- Leopold, L.B. and Wolman, M.G., 1960, "River Meanders," Geol. Soc. Am. Bull., Vol. 71.
- Leopold, L.B. and Langbein, W.B., 1962, "The Concept of Entrophy in Landscape Evolution," USGS Prof. Paper 500a, Reston, VA.
- Leopold, L.B., Wolman, M.G., and Miller, J.B., 1964, "Fluvial Processes in Geomorphology," W. H. Freeman and Co., San Francisco, CA.

Letter, Jr., J.V., Roig, L.C., Donnell, B.P., Thomas, W.A., McAnally, W.H., and Adamec, Jr., S.A., 1998, "A User's Manual for SED2D-WES, A Generalized Computer Program for Two-Dimensional, Vertically Averaged Sediment Transport."

Lewis, G.L., 1972, "Riprap Protection of Bridge Footings," Ph.D. Dissertation, Dept. of Civil Engineering, Colorado State University, Fort Collins, CO.

Limerinos, J.T., 1970, "Determination of the Manning Coefficient From Measured Bed Roughness in Natural Channels," USGS, Water Supply Paper 1898-B, Reston, VA, 47p.

Liu, H.K., 1957, "Mechanics of Sediment-Ripple Formation," ASCE Hydr. Div., Jour., Vol. 83, No. HY2, Reston, VA,

Long, Y. and Liang, G., 1994, "Data Base of Sediment Transport in the Yellow River," Institute of Hydraulic Research Tech. Report No. 94001, Yellow River Conservation Commission, Zhengzhou, P.R., China, 15 p.

Lowe, M. 1993, "Debris-Flow Hazards: A Guide for Land-Use Planning, Davis County, Utah," USGS Prof. Paper 1519, Reston, VA.

Madden, E.B., 1985, "Modified Laursen Method for Estimating Bed-material Sediment Load," U.S. Army Corps of Engineer Waterways Experiment Station HL-93-3, Vicksburg, MS.

Mahmood, K., 1973, "Log-normal Size Distribution of Particulate Matter," Jour. of Sedimentary Petrology, Vol. 43, No. 4, pp. 1161-1165.

Mahmood, K., 1979, "Selected Equilibrium-State Data from ACOP Canals," George Washington University Civil, Mechanical and Environmental Engineering Department Report No. EWR-79-2, Washington, D.C., 494 p.

Mahmood, K. and Shen, H.W., 1971, "Regime Concepts of Sediment-Transporting Canals and Rivers," River Mechanics, H.W. Shen, ed., Chapter 30, Water Resources Publ., Fort Collins, CO.

Mamak, W., 1964, "River Regulation," Department of the Interior and the National Science Foundation, Washington, D.C.

Mankin, J.H., 1937, "Concept of the Graded River," Geol. Society of America Bull., Vol. 48.

Maynard, S.T., 1988, "Stable Riprap Size for Open Channel Flows," Tech. Report HL-88-4, U.S. Army Corps of Engineers, Washington, D.C.

Maynard, S.T., 1996, "Toe Scour Estimation in Stabilized Bendways," ASCE Hydr. Div., Jour., Vol. 122, No. HY8, Reston, VA, pp. 460-464.

Mau, R.E. and Brooks, N.H., 1991, Discussion of "Test of Selected Sediment Transport Formulas by Nakato, T," ASCE Hydr. Div., Jour., Vol. 117, No. 9, pp. 1226-33.

Melville, B.W., 1992, "Local Scour at Bridge Abutments," Journal of Hydraulic Engineering, American Society of Civil Engineers, Hydraulic Division, Vol. 118, No. 4.

- Meyer-Peter, E. and Müller, R., 1948, "Formulas for Bed-Load Transport," Proc. 3d Meeting IAHR, Stockholm, pp. 39-64.
- Milhous, R.T., 1973, "Sediment Transport in a Gravel Bottom Stream," Ph.D. Dissertation, Oregon State University, 232 p.
- Molinas, A., 1990, "Bridge Stream Tube Model for Alluvial River Simulation," BRI-STARS, User's Manual, NCHRP, Project No. HR15-11, TRB, National Academy of Sciences, Washington, D.C.
- Molinas, A., 2000, "User's Manual for BRI-STARS (Bridge Stream Tube Model for Alluvial River Simulation)," FHWA Report No. FHWA-RD-99-190, Turner-Fairbank Highway Research Center, McLean, VA, 227 p. ([www.fhwa.dot.gov/bridge/hydpub.htm](http://www.fhwa.dot.gov/bridge/hydpub.htm))
- Molinas, A. and Wu, B., 1996, "Sediment Transport in Natural Rivers," Journal of Hydraulic Research, IAHR.
- Molinas, A., Abdou, M.I., Noshi, H.M., Abdeldayem, A.W., Hosni, M.M., and Reiad, N.Y., 1998, "Effects of Gradation and Cohesion on Bridge Scour," Laboratory Studies, Vol. 1 to 6, FHWA, Reston, VA and Colorado State University, Fort Collins, CO.
- Montgomery, D.R. and Buffington, J.M., 1997, "Channel-Reach Morphology in Mountain Drainage Basins," Geological Society of America Bull., Vol. 109, No. 5, pp. 596-611.
- Mosselman, E., 1995, "A Review of Mathematical Models of River Planform Changes," Earth Surface Processes and Landforms, Vol. 20, pp. 661-670.
- Mostafa, G., 1957, "River-bed Degradation Below Large-Capacity Reservoirs," ASCE Trans. Vol. 122.
- Mueller, D.S., 1996, "Local Scour at Bridge Piers in Nonuniform Sediment Under Dynamic Conditions," Ph.D. Dissertation, Colorado State University, Fort Collins, CO.
- Mueller, D.S. and Jones, J.S., 1999, "Evaluation of Recent Field and Laboratory Research on Scour at Bridge Piers in Coarse Bed Materials," Compendium of ASCE Water Resources Papers 1991 to 1998, "Stream Stability and Scour at Highway Bridges," E.V. Richardson and P.F. Lagasse, (eds), Reston, VA, 298 p.
- Nakato, T., 1990, "Test of Selected Sediment Transport Formulas," ASCE Hydr. Div., Jour., Vol. 116, No. 3, Reston, VA, pp. 362-379.
- Nakato, T., 1991, "Closure of Test of Selected Sediment Transport Formulas," ASCE Hydr. Div., Jour., Vol. 117, No. 9, Reston, VA, pp. 1235-37.
- Nanson, G.C. and Hicken, E.J., 1983, "Channel Migration and Incision on the Beatton River:" ASCE Hydr. Div. Jour. Vol. 109, Reston, VA, pp. 327-337.
- NEDECO, 1973, "Rio Magdalena and Canal del Dique Project," Mission Tecnica Colombo-Holandesa, Nedeco Report, Nedeco, The Hague.



- Neill, C.R., Editor, 1975, "Guide to Bridge Hydraulics," Canadian Project Committee on Bridge Hydr., University of Toronto Press, Toronto, Canada, 191 p.
- Nikuradse, J., 1933, "Stromungsgesetze in Rauhen Rohren," VDI – Forschungsheft, No. 361.
- Nordin, C.F., 1964, "Aspects of Flow Resistance and Sediment Transport, Rio Grande near Bernalillo, New Mexico," USGS Water Supply Paper 1498-4, 41 p.
- Nordin, C.F. and Beverage, J.P., 1965, "Sediment Transport in the Rio Grande, New Mexico," USGS Prof. Paper 462-F, Reston, VA, 35 p.
- NTSB, 1988, "Collapse of the New York Thruway (I-90) Bridge over the Schoharie Creek, Near Amsterdam, New York, April 5, 1987," NTSB/HAR-88/02, NTSB, Washington, D.C.
- Odgaard, A.J., 1986, "Meander Flow Model 1, Development," ASCE Hydr. Div., Jour., Vol. 112, pp. 1117-1136.
- Odgaard, A.J. and Bergs, M.A., 1987, "Flow in Curved Erodible Channels," IAHR Congress 1987, pp. 136-141.
- Onishi, Y., Jain, S.C., and Kennedy, J.F., 1976, "Effects of Meandering in Alluvial Streams," ASCE Hydr. Div., Jour., Vol. 102, No. HY7, pp. 899-917.
- Oswalt, N.R., Buck, L.E., Hepler, T.E., and Jackson, H.E., 1994, "Alternatives for Overtopping Protection of Dams." Report of the ASCE Task Committee on Overtopping Protection, American Society of Civil Engineers, New York, NY.
- Overbeek, H.J., 1979, "Erosion and Sedimentation," Lecture Notes, Asian Institute of Technology, Bangkok, Thailand.
- Pacheco-Ceballos, R., 1989, "Transport of Sediments: Analytical Solution," ASCE Hydr. Div., Jour., Vol. 27, No. 4, pp. 501-518.
- Parker, G., 1990, "Surface-Based Bed-load Transport Relation for Gravel Rivers, Jour. Hyd. Research, Vol. 28, No. 4, pp. 417-37.
- Parker, G., Sawai, K., and Ikeda, S., 1982, "Bend Theory of River Meanders, Part 2, Nonlinear Deformation of Finite Amplitude Bends," Jour. Fluid Mechanics, Vol. 115, pp. 303-314.
- Parsons, Brinkerhoff, Quade, and Douglas, Inc, 1996, "Flume Modeling Experimental Plan for the Replacement of the Herbert C. Bonner Bridge," Section 3 of Expert Panel Meeting Background Information, North Carolina DOT, Raleigh, NC.
- Patrick, R., 1973, "Effects of Channelization on the Aquatic Life of Streams, In Environmental Considerations in Planning Design and Construction," Special Report No. 138, Transportation Research Board, National Academy of Sciences, Washington, D.C., pp. 150-159.
- Petersen, M., 1986, "River Engineering," Prentice Hall, NY.

Porterfield, G., 1977, "Computation of Fluvial-Sediment Discharge," Techniques of Water-Resources Investigations of the USGS, Book 3, Chapter C3, Reston, VA.

Posada, G.L., 1995, "Transport of Sands in Deep Rivers," Ph.D. Dissertation, Colorado State University, Fort Collins, CO.

Powledge, G.R., Ralston, D.C., Miller, P., Chen, Y.H., Clopper, P.E., and Temple, D.M., 1989a, "Mechanics of Overflow Erosion on Embankments. I: Research Activities." Report of the ASCE Task Committee on the Mechanics of Overflow Erosion on Embankments, *Journal of Hydraulic Engineering, ASCE*, Vol. 115, No.8, pp.1040-1055.

Powledge, G.R., Ralston, D.C., Miller, P., Chen, Y.H., Clopper, P.E., and Temple, D.M., 1989b, "Mechanics of Overflow Erosion on Embankments. II: Hydraulic and Design Considerations." Report of the ASCE Task Committee on the Mechanics of Overflow Erosion on Embankments, *Journal of Hydraulic Engineering, ASCE*, Vol. 115, No. 8, pp.1056-1075.

Prandtl, L., 1925, "Uber Die Ausgebildete Turbulenz," ZAMM5 and Proc. 2nd °Intern. Cong. Appl. Mech., Zurich.

Raphelt, N.K., 1996, "An Examination of Gravel Bed-Load Functions Applied to Observed Gravel Bed-Load Discharge Measurements of Selected Streams," Ph.D. Dissertation, Colorado State University, Fort Collins, CO.

Reihesen, G., 1964, "Debris Control Structures," Hydraulic Engineering Circular No. 9, Bureau of Public Road, Department of Transportation, Washington, D.C. 20591.

Rhodes, J. and Trent, R.T., 1999, "Economics of Flood, Scour, and Bridge Failures," Compendium of ASCE Water Resources Papers 1991 to 1998, "Stream Stability and Scour at Highway Bridges," E.V. Richardson and P.F. Lagasse, (eds) Reston, VA, pp. 1013.

Richards, K., 1982, "Rivers Form and Process in Alluvial Channels," Methuen, NY, 357 p.

Richardson, E.V., 1965, "Resistance to Flow in Sand Channels," Ph.D. Dissertation, Colorado State University, Fort Collins, CO, June, Results incorporated into USGS Prof. Paper 422-J, Simons and Richardson, 1966, Reston, VA.

Richardson, E.V., 1971, "Sediment Properties," Chapter 6, River Mechanics edited by H.W. Shen, Colorado State University, Fort Collins, CO, pp. 6-1 to 6-23.

Richardson, E.V. and Clyma, W., 1980, "Egypt's High Aswan Dam-Progress or Retrogradation," Egypt Water Use and Management Project, Civil Engineering Dept. Colorado State University, Fort Collins, CO, 27 p.

Richardson, E.V., 1994, "Sediment Measurement Instrumentation-A Personal Perspective," Invited paper and lecture, ASCE Sympo. Proc. Fundamentals and Advancements in Hydr. Measurements and Experimentation, C.A. Pugh (ed), Reston, VA, pp. 94-103.

Richardson, E.V., 1999, "History of Bridge Scour Research and Evaluation in the United States," ASCE Compendium of Papers from Water Resources Engineering Conf. 1991 to 1998, Richardson, E.V. and Lagasse, P.F., (eds), Reston, VA, 15 p.

Richardson, E.V., and Simons, D.B., 1967, "Resistance to Flow in Sand Channels," Proc. XII Cong. Inter. Assoc. Hydr. Res., Vol. I, No. A 18, Fort Collins, CO, 141 p.

Richardson, E.V. and Simons, D.B., 1984, "Use of Spurs and Guidebanks for Highway Crossings," Proceedings Second Bridge Engineering Conference, Minneapolis, MN, Transportation Research Board, No. 950, TRB, NRC, Washington, D.C.

Richardson, E.V., Simons, D.B., Karaki, S., Stevens, M.A., and Mahmood, K., 1975, "Highways in the River Environment-Hydraulic and Environmental Design Considerations," Training and Design Manual, U.S. Dept. of Transportation, Federal Highway Administration, Washington, D.C.

Richardson, E.V., Lagasse, P.F., and Schall, J.D., 1987, "Hydraulic, Erosion, and Channel Stability Analysis of the Schoharie Creek Bridge Failure, New York," RCE now Ayres Associates, Inc. and Colorado State University, Fort Collins, CO.

Richardson, E.V., Brisbane, T.E., and Ruff, J.F., 1989, "Hydraulic Model Study of New Bridge, Schoharie Creek," RCE now Ayres Associates, Inc. and Colorado State University, Fort Collins, CO.

Richardson, E.V., Simons, D.B. and Julian, P.Y., 1990, "Highways in the River Environment," Design and Training Manual, U.S. Department of Transportation, Federal Highway Administration, Washington D.C. (Civil Engineering Department Report, Colorado State University, 1987).

Richardson, E.V. and Abed, L., 1999, "Top Width of Pier Scour Holes," Compendium of ASCE Water Resources Papers 1991 to 1998, "Stream Stability and Scour at Highway Bridges," E.V. Richardson and P.F. Lagasse, (eds), Reston, VA, pp. 311.

Richardson, E.V. and Lagasse, P.F., 1999, (eds), "Stream Stability and Scour at Highway Bridges," Compendium of Papers ASCE Water Resources Engineering Conferences 1991 to 1998, Reston, VA.

Richardson, E.V. and Davis, S.R. 2001, "Evaluating Scour at Bridges," Fourth Edition, Hydraulic Engineering Circular No. 18, FHWA NHI 01-001, Washington, D.C. ([www.fhwa.dot.gov/bridge/hydpub.htm](http://www.fhwa.dot.gov/bridge/hydpub.htm))

Richardson, J.R. and Richardson, E.V., 1993, Discussion of Melville, B. W., 1992 paper "Local Scour at Bridge Abutments," ASCE Hydr. Div., Jour., Vol. 119, No. 9, Reston, VA.

Richardson, J.R. and Richardson, E.V., 1999, "The Fallacy of Local Abutment Scour Equations," Compendium of ASCE Water Resources Papers 1991 to 1998, "Stream Stability and Scour at Highway Bridges," E.V. Richardson and P.F. Lagasse, (eds), Reston, VA, 457 p.

Rijn, L.C. van, 1984, "Sediment Transport Part II: Suspended Load Transport," ASCE Hydr. Div., Jour., Vol. 110, No. 11, pp. 1613-1641.

Ritter, J.R. and Helley, F.J., 1968, "An Optical Method for Determining Particle Sizes of Coarse Sediment," U.S. Geological Survey, Open-File Report, 43 p.

- Rosgen, D.L., 1994, "A Classification of Natural Rivers," *Catena*, Vol. 22, p. 169-199.
- Rosgen, D.L., 1996, "Applied River Morphology," Wildland Hydrology, 1481 Stevens Lake Road, Pagosa Springs, CO.
- Rouse, H., 1937, "Modern Conceptions of the Mechanics of Fluid Turbulence," *ASCE Trans.* Vol. 102, Reston, VA.
- Rouse, H., 1940, "Criteria for Similarity in the Transportation of Sediment," *Proc. Hydr. Conf. Univ. of Iowa Studies in Engineering*, Bull. No. 20. Iowa City, IA. Selected Writings of Hunter Rouse, Kennedy, J.F. and Macagno, E.O., (eds), 1971, Dover Publications, NY.
- Rouse, H., 1946, "Elementary Mechanics of Fluids," John Wiley and Sons, NY.
- Rouse, H., (ed), 1950, "Engineering Hydraulics," John Wiley and Sons, NY.
- Rouse, H., Bhoota, B.V., and Hsu, E.Y., 1951, "High-Velocity Flow in Open Channel Flow-Design Of Channel Expansions," *ASCE Trans.* Vol. 116, Reston, VA. Selected Writings of Hunter Rouse, Kennedy, J.F. and Macagno, E.O., (eds), 1971, Dover Pub., NY.
- Ruff, J.F., Shaikh, A., Abt, S.R., and Richardson, E.V., "1985 Riprap tests in Flood Control Channels," Civil Engineering Report CER85-86-JFR-AS-SRA-EVR-17, Colorado State University, Fort Collins, CO.
- Ruff, J.F., Shaikh, A., Abt, S.R., and Richardson, E.V., "1987 Riprap Stability in Side Sloped Channels," Civil Engineering Report for U.S. Corps of Engineers, Colorado State University, Fort Collins, CO.
- Said, R., 1981, "The Geological Evolution of the River Nile," Springer-Verlag, New York, NY.
- Samide, G.W., 1971, "Sediment Transport Measurements," Master Thesis, University of Alberta.
- Santos-Cayado, J., 1972, "State Determination for High Discharges," Ph.D. Dissertation, Dept. of Civil Engineering, Colorado State University, Fort Collins, CO.
- Schall, J.D., Price, G.R., Fisher G.A., Lagasse, P.F. and Richardson, E.V., 1997a "Sonar Scour Monitor; Installation, Operation and Fabrication Manual," NCHRP report 397A, Transportation Research Board, National Research Council, Washington D.C., 38 p.
- Schall, J.D., Price, G.R., Fisher G.A., Lagasse, P.F. and Richardson, E.V., 1997b, "Magnetic Sliding Collar Scour Monitor; Installation, Operation and Fabrication Manual," NCHRP report 397B, Transportation Research Board, National Research Council, Washington D.C., 40 p.
- Schoklitsch, A., 1930, "Handbuch des Wasserbaues," Springer, Vienna (2nd ed.), English Translation (1937) by S. Shulits.
- Schumdale, T.H., 1963, "Some Aspects of the Lower Missouri River Floodplain," *Annals Association American Geogr.*, Vol. 53, pp. 60-73.

Schumm, S.A., 1963, "The Disparity Between Present Rates of Denudation and Orogeny," USGS Prof. Paper No. 454H, Reston, VA, 17 p.

Schumm, S.A., 1968, "Speculations Concerning Paleohydrologic Controls of Terrestrial Sedimentation," Geol. Soc. Am. Bull., Vol. 79, pp. 1572-1588.

Schumm, S.A., 1977, "The Fluvial System," Wiley and Sons, 338 p.

Schumm, S.A., 1981, "Evolution and Response of the Fluvial System," Sedimentologic Implications: SEPM Special Publication 31, p. 19-19.

Schumm, S.A. and Khan, H.R., 1972, "Experimental Study of Channel Patterns," Geol. Soc. America Bull., Vol. 83, pp. 1755-1770.

Schumm, S.A. and Beathard, R.M., 1976, "Geomorphic Thresholds," ASCE Rivers 76, Vol. 1, Reston, VA, pp. 707-724.

Schumm, S.A. and Brakenridge, G.R., 1987, "River Responses" in North America and Adjacent Oceans During the Last Deglaciation, W.F. Ruddiman and H.E. Wright, Jr. (eds) Geol. Soc. America, K-3, pp. 221-240.

Schumm, S.A. and Galay, V.J., 1994, "The River Nile in Egypt," ASCE - The Variability of Large Alluvial Rivers, Reston, VA, 75 p.

Schumm, S.A., Rutherford, I.D., and Brooks, J., 1994, "Pre-Cutoff Morphology of the Lower Mississippi River," ASCE - The Variability of Large Alluvial Rivers, Reston, VA, 13 p.

Schumm, S.A. and Lagasse, P.F., 1998, "Alluvial Fan Dynamics – Hazards to Highways," ASCE Water Resources Engineering '98, Vol.1, Reston, VA, pp. 298-303.

Schumm, S.A. and Lichty, R.W., 1957, "Channel Widening and Floodplain Construction Along Cimarron River in Southwestern Kansas," USGS Prof. Paper 352-D, Reston, VA, pp. 71-88.

Seitz, H.R., 1976, "Suspended and Bed Load Sediment Transport in the Snake and Clearwater Rivers in the Vicinity of Lewiston, Idaho," USGS File Report 76-886, Boise, Idaho, 77 p.

Senturk, F., 1969, "Mechanics of Bed Formations," La Houille Blanche, No. 2.

Shalash, S., 1980, "The effects of the High Aswan Dam on the Hydrological Regime of the River Nile," Proc. of Helsinki Symp., IAHS Pub. No. 130, June.

Shalash, S., 1983, "Degradation of the River Nile," Internat. Water Power and Dam Construction, Vol. 35 (8), pp. 56-58.

Shen, H.W., 1971, "River Mechanics," Vol. I and II, Water Resources Publication, Fort Collins, CO.

Shen, H.W., 1979, "Modeling of Rivers," John Wiley and Sons, NY.

- Shen, H.W. and Hung, C.S., 1972, "An Engineering Approach to Total Bed-material Load by Regression Analysis," Proc. Sed. Sym., H.W. Shen, (ed) Chap. 14.
- Shen, H.W. and Hung, C.S., 1983, "Remodified Einstein Procedure for Sediment Load," ASCE Hydr. Div., Jour., Vol. 109, No. 4, pp. 565-578.
- Shen, H.W., Schumm, S.A., Nelson, J.D., Doehring, D.O., Skinner, M.M., and Smith, G.L., 1981, "Methods for Assessment of Stream Related Hazards to Highways and Bridges," Final Report FHWA/RD-80/160, Federal Highway Administration, Washington, D.C. 20590.
- Sheppard, D.M., 1999, "Local Pier Scour Model Tests for Jensen Beach Bridge," Final Report, Coastal and Oceanographic Engineering Dept, Univ. of Florida, Gainesville, FL.
- Shields, I.A., 1935, "Anwendung der Aenlichkeitsmechanik und der Turbulenzforschung auf die Geschiebebewegung," Berlin, Germany, translated to English by W.P. Ott and J.C. van Uchelen, California Institute of Technology, Pasadena, CA.
- Shields, I.A., 1936, "Application of Similarity Principles and Turbulence Research to Bed-Load Movement," a translation from the German by W.P. Ott and J.C. van Uchelin, U.S. Soil Consdrv. Service Coop. Lab., California Inst. of Tech., Pasadena, CA.
- Shinohara, K. and Tsubaki, T., 1979, "On the Characteristics of Sand Waves Formed Upon Beds of the Open Channels and Rivers," Reprinted from Reports of Res. Inst. of Appl. Mech., Kyushu University, Vol. VII, No. 25.
- Shirole, A.M. and Holt, R.C., 1991, "Planning for a Comprehensive Bridge Safety Assurance Program," Transportation Research Board Record 1290, Transportation Research Board, National Academy of Science, Washington, D.C., pp. 39-50.
- Shukry, A., 1950, "Flow Around Bends in Open Flums," ASCE Trans. Vol. 115, Reston, VA.
- Shull, C.A., 1922, "The Formation of a New Island in the Mississippi River," Ecology Vol. 3, pp. 202-206.
- Shull, C.A., 1944, "Observations of General Vegetational Changes on a River Island in the Mississippi River," American Midland Naturalist, Vol. 32, pp. 771-776.
- Simons, D.B., 1955, "Unpublished special paper for Emory Lane," Figure first published in 1975 edition of "Highways in the River Environment," Richardson et al.
- Simons, D.B., 1957, "Theory of Design of Stable Channels in Alluvial Materials," Ph.D. Dissertation, Colorado State University, Fort Collins, CO.
- Simons, D.B. 2000, "Personnel Communication."
- Simons, D.B. and Lewis, G.L., 1971, "Flood Protection at Bridge Crossings," report prepared for the Wyoming State Highway Department, Planning and Research Division, CER71-72DBS-GLL0, Colorado State University, Fort Collins, CO.

Simons, D.B. and Simons, R.K., 1987, "Differences Between Gravel- and Sand-Bed Rivers," *Sediment Transport in Gravel-Bed Rivers*, C.R. Thorne, J.C. Bathurst and R.D. Hey (eds), John Wiley & Sons.

Simons, D.B. and Richardson, E.V., 1963, "Forms of Bed Roughness in Alluvial Channels," *ASCE Trans.*, Vol. 128, pp. 284-323.

Simons, D.B. and Richardson, E.V., 1966, "Resistance to Flow in Alluvial Channels, USGS Prof. Paper 422-J, Reston, VA, 61 p.

Simons, D.B. and Senturk, F., 1992, "Sediment Transport Technology," Water Resources Pub., Littleton, CO.

Simons, D.B., Li R.M., and Fullerton, W., 1981, "Theoretically Derived Sediment Transport Equations for Pima County, Arizona," Simons, Li & Assoc., Fort Collins, CO.

Smith, H.T.U., 1949, "Notes on Historic Changes in Stream Courses of Western Kansas, With a Plea for Additional Data," *Kansas Acad. Sci. Trans.*, Vol. 43.

Smith, S.A. and McLean, S.R., 1984, "A Model for Flow in Meandering Streams," *Water Resources Research*, Vol. 9, pp. 1301-1315.

Stein, R.A., 1965, "Laboratory Studies of Total Load and Apparent Bed Load," *Jour. Geophysical Res.*, Vol. 70, No. 8, pp. 1831-42, April.

Stein, S.M., Kilgore, R.T., and Jones, J.S., 1990, "Lab Report of the Acosta Bridge Scour Study," Federal Highway Administration Publication No. FHWA-RD-89-114, McLean, VA.

Steven, H.H. Jr. and Yang, C.T., 1989, "Summary and Use of Selected Fluvial Sediment Discharge Formula," USGS Water Res. Investigations Rept. 89-4026, Denver, CO.

Stevens, M.A., 1968, "Scouring of Riprap at Culvert Outlets," Ph.D. Dissertation, Dept. of Civil Eng., Colorado State University, Fort Collins, CO.

Stevens, M.A., 1994, "The Citanduy, Indonesia - One Tough River," ASCE - The Variability of Large Alluvial Rivers, Reston, VA, 201 p.

Stevens, M.A. and Simons, D.B., 1971, "Stability Analysis for Coarse Granular Material on Slopes," *River Mechanics*, H.W. Shen, ed., Chapter 17, Water Resources Publications, Littleton, CO.

Stevens, M.A., Simons, D.B., and Richardson, E.V., 1984, "Riprap Stability Analysis," *Proceedings Second Bridge Engineering Conference*, Minneapolis, MN, Transportation Research Board, No. 950 TRB, NRC, Washington, D.C.

Straub, L.G., 1954, "Transportation Characteristics Missouri River Sediment," St. Anthony Falls Hydraulic Laboratory Sediment Series No. 4, Minneapolis, MN.

Straub, L.G., Anderson, A.G., and Flammer, G.H., 1958, "Experiments on the Influence of Temperature on the Sediment Load," St. Anthony Falls Hydraulic Laboratory Sediment Series No. 10, Minneapolis, MN.

Sturm, T. W., 1999a, "Abutment Scour Studies for Compound Channels," U.S. Department of Transportation, FHWA, Washington, D.C.

Sturm, T.W., 1999b, "Abutment Scour Studies in Compound Channels," Compendium of ASCE Water Resources Papers 1991 to 1998, "Stream Stability and Scour at Highway Bridges," E.V. Richardson and P.F. Lagasse, (eds), Reston, VA, 443 p.

Sturm, T.W. and Chrisochoides, A., 1998, "Abutment Scour in Compound Channel for Variable Setbacks," ASCE Water Resources Engineering Conf. Proc., Reston, VA, 174 p.

Taylor, B.D. and Vanoni, V.A., 1972, "Temperature Effects in High Transport, Flat-Bed Flows," ASCE Hydr. Div., Jour., Vol. 98, No. HY12, pp. 2191-2206.

Thein, K.N.N., 1994, "River Plan-Form Movement in an Alluvial Plain," Balkema, Rotterdam, 318 p.

Thomas, W.A. and McAnally, W.H., 1985, "Users Manual for the Generalized Computer Program System: Open Channel Flow and Sedimentation, TABS-2," U.S. Army Corps of Engineers Waterways Experiment Station, Vicksburg, MS, 671 p.

Thomas, W.A., Copeland, R.R., McComas, D.N., and Raphelt, N.K., 2000, "Hydraulic Design Package for Channels," User's Manual for the SAM, prepared for Department of the Army, U.S. Army Corps of Engineers, Washington, D.C.

Thorne, C.R., 1982, "Processes and Mechanisms of River Bank Erosion," in Gravel-Bed Rivers," Hay, R.D., Bathurst, J.C., and Thorne, C.R. (eds), John Wiley and Sons, NY, pp. 95-115.

Thorne, C.R., 1997, "Channel types and Morphological Classification," Chapter 7 in: C.R. Thorne, R.D. Hey, and M.D. Newsom (eds), Applied Fluvial Geomorphology for River Engineering and Management, John Wiley & Sons, Chichester.

Thorne, C.R., 1998, "Stream Reconnaissance Hand Book," John Wiley and Sons, NY, 133 p.

Thorne, C.R. and Abt, S.A. 1993, "Velocity and Scour Prediction in River Bends," Contract Report HL-93-1, U.S. Army Corps of Engineers, Waterways Experiment Station, Vicksburg, MS.

Thorne, C.R., Hey, R.D., and Newsom, M.D., (eds), 1997, "Applied Fluvial Geomorphology for River Engineering and Management," John Wiley and Sons, NY, 376 p.

Tison, L.J., 1953, "Studies of the Critical Tractive Force for the Entrainment of Bed Materials," Pro. Minnesota Inter. Hydraulics Conf., Minneapolis, MN.

Toffaletti, F.B., 1966, "A Procedure for Computation of Total River Sand Discharge and Detailed Distribution, Bed to Surface," Committee on Channel Stabilization, U.S. Army Corps of Engineers.

Toffaletti, F.B., 1968, "A Procedure for Computation of the Total River Sand Discharge and Detailed Distribution, Bed to Surface," U.S. Army Corps of Engineers, Technical Report No. 5., Vicksburg, MS.



Toffaleti, F.B., 1969, "Definitive Computations of Sand Discharge in Rivers," ASCE Hydr. Div., Jour., Vol. 95, No. HY1, pp. 248-255.

Triest, D.J. and Jarrett, R.D., 1987, "Roughness Coefficients in Large Floods," Proc. ASCE, Irr. and Drainage Div. Specialty Conf., Reston, VA.

Trivino, R. and Richardson, J.R., 2000, "Estimating Clear Water Abutment Scour," Civil Engineering Report, Civil Engineering Department, Univ. of Missouri, Kansas City, MO, 31 p.

Tywniuk, N., 1972, "Sediment Discharge Computation Procedures," ASCE Hydr. Div., Jour., Vol. 98, No. HY3, Proc. Paper 8783, pp. 521-40.

U.S. Army Corps of Engineers, 1968, "Missouri River Channel Regime Studies," MRD Sediment Series No. 13A, Omaha, NE.

U.S. Army Corps of Engineers, 1981, "The Streambank Erosion Control Evaluation and Demonstration Act of 1974," Section 32, Public Law 93-251: Final Report to Congress, Main Report, and Appendices A through 19, Washington, D.C.

U.S. Army Corps of Engineers, 1988, "SAM Hydraulic Design Package for Channels, Chapter 3," WES Coastal and Hydraulic Laboratory, Vicksburg, MS.

U.S. Army Corps of Engineers, 1991, 1994a, "Hydraulic Design of Flood Control Channels," EM1110-2-1601, Washington, D.C.

U.S. Army Corps of Engineers, 1994b, "Channel Stability Assessment for Flood Control Projects," EM1110-2-1418, Washington, D.C.

U.S. Army Corps of Engineers, 1993, "Scour and Deposition in Rivers and Reservoirs," User's Manual, HEC-6, Hydrologic Engineering Center, Davis, CA.

U.S. Army Corps of Engineers, 1997, "Users Guide to RMA2 WES Version 4," Waterways Experiment Station, Barbara Donnell, (ed), Vicksburg, MS.

U.S. Army Corps of Engineers, 2001, "HEC-RAS River Analysis System," User's Manual Version 3.0, Hydrologic Engineering Center, Davis, CA.

U.S. Bureau of Reclamation, 1960, "Investigation of Meyer-Peter, Müller Bedload Formulas," Sedimentation Section, Hydrology Branch, Division of Project Investigations, Denver, CO.

U.S. Department of the Interior, Bureau of Reclamation (USBR), 1958, "Total Sediment Transport Program, Lower Colorado River Basin, Interim Report," Denver, CO, 175 p.

U.S. Department of Transportation, Federal Highway Administration, 1988, "Scour at Bridges," Technical Advisory T5140.20, updated by Technical Advisory T50140.23, October 28, 1991, "Evaluating Scour at Bridges," U.S. Depart. of Transportation, Washington, D.C.

USGS, 1973a, "Field Methods for Measurement of Fluvial Sediment," Techniques of Water-Resources Investigations of the USGS, Book 3, Chapt. C2, Reston, VA.

USGS, 1973b, "Fluvial Sediment Concepts," Techniques of Water-Resources Investigations of the USGS, Book 3, Chapt. C1, Reston, VA.

USGS, 1997a, "Computation of Fluvial-Sediment Discharge," Techniques of Water-Resources Investigations of the USGS, Book 3, Chapt. C3, Reston, VA.

USGS, 1997b, Laboratory Theory and Methods for Sediment Analysis," Techniques of Water-Resources Investigations of the USGS, Book 5, Chapt. C1, Reston, VA.

U.S. Inter-Agency Subcommittee on Sedimentation, 1952, Reports, USGS, Reston, VA, District Engineer, Corps of Engineers, St. Paul, MN.

Report No. 1, 1940a, "Field Practice and Equipment Used in Sampling Suspended Sediment."

Report No. 2, 1940b, "Equipment Used for Sampling Bedload and Bed Material."

Report No. 3, 1941a, "Analytical Study of Methods of Sampling Suspended Sediment."

Report No. 4, 1941b, "Methods of Analyzing Sediment Samples."

Report No. 5, 1941c, "Laboratory Investigation of Suspended Sediment Samplers."

Report No. 6, 1952, "The Design of Improved Types of Suspended Sediment Samplers."

Report No. 7, 1943, "A Study of New Methods for Size Analysis of Suspended Sediment Samples."

Report No. 8, 1948, "Measurement of the Sediment Discharge of Streams."

Report No. 11, 1957a, "The Development and Calibration of the Visual-Accumulation Tube."

Report No. 12, 1957b, "Some Fundamentals of Particle-Size Analysis."

U.S. Water Resources Council, Hydrology Committee, 1981, "Guidelines for Determining Flood Frequency," Bulletin 17B, USGS, Reston, VA.

Vanoni, V.A. (ed), 1975, 1977, "Sedimentation Engineering," ASCE Manuals and Reports on Engineering Practice – No. 54, Reston, VA.

Vanoni, V.A., 1978, "Predicting Sediment Discharge in Alluvial Channel, Water Supply Management," Pergamon Press, Oxford, pp. 399-417.

Vanoni, V.A. and Brooks, N.H., 1957, "Laboratory Studies of the Roughness and Suspended Load of Alluvial Streams," California Institute of Technology Sedimentation Laboratory, Report No. E-68, Pasadena, CA.

Vanoni, V.A and Hwang, L.S., 1967, "Relation Between Bed Forms and Friction in Streams," ASCE Hydr. Div., Jour., Vol. 93, No. HY3, pp. 121-144.

von Karman, T., 1930, "Mechanische Aehnlichkeit und Turbulenz," Proceedings, Third International Congress for Applied Mechanics, Stockholm.

Wallace, R., "Notes on Stream Channels Offset by the San Andreas Fault," Proc. Conf. on Geologic Problems of the San Andreas Fault System, Stanford University Pub. Beol Sci., Palo Alto, CA.

Watson, C.C., Biedenharn, D.S., and Scott, S.H., 1999, "Channel Rehabilitation: Processes, Design, and Implementation (Draft)," U.S. Army Corps of Engineers, Engineering Research and Development Center, Vicksburg, MS.

White, C.M., 1940, "The Equilibrium of Grains on the Bed of a Stream." Proc. Royal Society of London, Series A, No. 958, Vol. 174, pp. 322-338.

White, W.R., Milli H., and Crabbe, A.D., 1975, "Sediment Transport Theories: a Review," Proc. Inst. Civil Eng. Part 2, Vol. 59, pp. 265-92.

Wilcock, P.R. and Southard, J.B., 1988, "Experimental Study of Incipient Motion in Mixed-Size Sediment," ASCE Jour. Water Resources Res., Vol. 24, No. 7, pp. 1137-1151.

Williams, G.P. and Rosgen, D.L., 1989, "Measured Total Sediment Loads (Suspended Loads and Bed Loads) for 93 United States Streams," U.S. Geological Survey Open-File Reports Section 89-67, Denver, CO.

Williams, D.T., 1995, "Selection and Predictability of Sand Transport Relations Based Upon a Numerical Index," Ph.D. Dissertation, Colorado State University, Fort Collins, CO.

Williams, D.T. and Julien, P.Y., 1989, "Applicability Index for Sand Transport Equations," ASCE Hydr. Div., Jour., Vol. 115, No. 11, pp. 1578-81.

Williams, G.P., 1970, "Flume Width and Water Depth Effects in Sediment-Transport Experiments," USGS Prof. Paper 562-H.

Williams, G.P. and Wolman, M.G., 1984, "Downstream Effects of Dams on Alluvial Rivers," USGS Prof. Paper No. 1286, Reston, VA.

Willis, J.C., Coleman, N.L., and Ellis, W.M., 1972, "Laboratory Study of Transport of Fine Sand," ASCE Hydr. Div., Jour., Vol. 98, No. HY3, Paper 8765, pp. 489-501.

Winkley, B.R., 1977, "Man-made Cutoffs on the Lower Mississippi River. Conception, Construction and River Response," Vicksburg Potomology Investigations Report 300-2, U.S. Army Engineer District, Vicksburg, MS.

Woodward, S.M., 1920, "Hydraulics of the Miami Flood Control Project," Tech. Reports, Miami Conservancy District, Dayton, OH.

Wu, B., 1999, "Fractional Transport of Bed-Material Load in Sand-Bed Channels," Ph.D. Dissertation, Colorado State University, Fort Collins, CO.

Yamagata, I.M., USGS, Personnel Communication.

Yang, C.T., 1973, "Incipient Motion and Sediment Transport," ASCE Hydr. Div., Jour., Vol. 99, No. HY10, pp. 1679-1704.

- Yang, C.T., 1977, "The Movement of Sediment in Rivers," Geophysical Survey 3, D. Reidel, Dordrecht, pp. 39-68.
- Yang, C.T., 1984, "Unit Stream Power Equation for Gravel," ASCE Hydr. Div., Jour., Vol. 110, No. 12, pp. 1783-97.
- Yang, C.T., 1996, Sediment Transport Theory and Practice, McGraw-Hill Companies, Inc.
- Yang, C.T. and Molinas, A., 1982, "Sediment Transport and Unit Stream Power Function," ASCE Hydr. Div., Jour., Vol. 108, No. HY6, pp. 774-793.
- Yang, C.T. and Kong, X., 1991, "Energy Dissipation Rate and Sediment Transport," ASCE Hydr. Div., Jour., Vol. 29, No. 4, pp. 457-74.
- Yang, C.T. and Wan, S., 1991, "Comparison of Selected Bed Material Load Formulas," ASCE Hydr. Div., Jour., Vol. 117, No. 8, pp. 973-989.
- Yang, C.T., Molinas, A., and Wu, B., 1996, "Sediment Transport in the Yellow River," Journal of Hydraulics Engineering, ASCE, Vol. 122, No. 5, pp. 237-244.
- Yen, C. and Ho, S., 1990, "Bed Evolution in Channel Bends," ASCE Hydr. Div. Jour. Vol. 116, HY4, pp. 544-562.
- Zevenbergen, L.W., Hunt, J.H., Byars, M.S., Edge, B.L., Richardson, E.V., and Lagasse, P.F., 1997, "Tidal Hydraulic Modeling for Bridges," Users Manual, Pooled Fund Study HPR552, Ayres Associates, Fort Collins, CO, 387 p.

## APPENDIX A

### Metric System, Conversion Factors, and Water Properties

The following information is summarized from the Federal Highway Administration, National Highway Institute (NHI) Course No. 12301, "Metric (SI) Training for Highway Agencies." For additional information, refer to the Participant Notebook for NHI Course No. 12301.

In SI there are seven base units, many derived units and two supplemental units (Table A.1). Base units uniquely describe a property requiring measurement. One of the most common units in civil engineering is length, with a base unit of meters in SI. Decimal multiples of meter include the kilometer (1000m), the centimeter (1m/100) and the millimeter (1 m/1000). The second base unit relevant to highway applications is the kilogram, a measure of mass which is the inertial of an object. There is a subtle difference between mass and weight. In SI, mass is a base unit, while weight is a derived quantity related to mass and the acceleration of gravity, sometimes referred to as the force of gravity. In SI the unit of mass is the kilogram and the unit of weight/force is the newton. Table A.2 illustrates the relationship of mass and weight. The unit of time is the same in SI as in the English system (seconds). The measurement of temperature is Centigrade. The following equation converts Fahrenheit temperatures to Centigrade,  $^{\circ}\text{C} = 5/9 (^{\circ}\text{F} - 32)$ .

Derived units are formed by combining base units to express other characteristics. Common derived units in highway drainage engineering include area, volume, velocity, and density. Some derived units have special names (Table A.3).

Table A.4 provides useful conversion factors from English to SI units. The symbols used in this table for metric units, including the use of upper and lower case (e.g., kilometer is "km" and a newton is "N") are the standards that should be followed. Table A.5 provides the standard SI prefixes and their definitions.

Table A.6 provides physical properties of water at atmospheric pressure in SI system of units. Table A.7 gives the sediment grade scale and Table A.8 gives some common equivalent hydraulic units.

Table A.1. Overview of SI Units.		
	Units	Symbol
Base units		
length	meter	m
mass	kilogram	kg
time	second	s
temperature*	kelvin	K
electrical current	ampere	A
luminous intensity	candela	cd
amount of material	mole	mol
Derived units		
Supplementary units		
angles in the plane	radian	rad
solid angles	steradian	sr
*Use degrees Celsius ( $^{\circ}\text{C}$ ), which has a more common usage than kelvin.		

Table A.2. Relationship of Mass and Weight.			
	Mass	Weight or Force of Gravity	Force
English	slug pound-mass	pound pound-force	pound pound-force
metric	kilogram	newton	newton

Table A.3. Derived Units With Special Names.			
Quantity	Name	Symbol	Expression
Frequency	hertz	Hz	$s^{-1}$
Force	newton	N	$kg \cdot m/s^2$
Pressure, stress	pascal	Pa	$N/m^2$
Energy, work, quantity of heat	joule	J	$N \cdot m$
Power, radiant flux	watt	W	$J/s$
Electric charge, quantity	coulomb	C	$A \cdot s$
Electric potential	volt	V	$W/A$
Capacitance	farad	F	$C/V$
Electric resistance	ohm	$\Omega$	$V/A$
Electric conductance	siemens	S	$A/V$
Magnetic flux	weber	Wb	$V \cdot s$
Magnetic flux density	tesla	T	$Wb/m^2$
Inductance	henry	H	$Wb/A$
Luminous flux	lumen	lm	$cd \cdot sr$
Illuminance	lux	lx	$lm/m^2$

Table A.4. Useful Conversion Factors.			
Quantity	From English Units	To Metric Units	Multiplied By*
Length	mile	km	1.609
	yard	m	0.9144
	foot	m	<u>0.3048</u>
	inch	mm	<u>25.40</u>
Area	square mile	km <sup>2</sup>	2.590
	acre	m <sup>2</sup>	4047
	acre	hectare	0.4047
	square yard	m <sup>2</sup>	0.8361
	square foot	m <sup>2</sup>	0.09290
square inch	mm <sup>2</sup>	645.2	
Volume	acre foot	m <sup>3</sup>	1233
	cubic yard	m <sup>3</sup>	0.7646
	cubic foot	m <sup>3</sup>	0.02832
	cubic foot	L (1000 cm <sup>3</sup> )	28.32
	100 board feet	m <sup>3</sup>	0.2360
	gallon	L (1000 cm <sup>3</sup> )	3.785
cubic inch	cm <sup>3</sup>	16.39	
Mass	lb	kg	0.4536
	kip (1000 lb)	metric ton (1000 kg)	0.4536
Mass/unit length	plf	kg/m	1.488
Mass/unit area	psf	kg/m <sup>2</sup>	4.882
Mass density	pcf	kg/m <sup>3</sup>	16.02
Force	lb	N	4.448
	kip	kN	4.448
Force/unit length	plf	N/m	14.59
	klf	kN/m	14.59
Pressure, stress, modulus of elasticity	psf	Pa	47.88
	ksf	kPa	47.88
	psi	kPa	6.895
	ksi	MPa	6.895
Bending moment, torque, moment of force	ft-lb	N · m	1.356
	ft-kip	kN · m	1.356
Moment of mass	lb · ft	m	0.1383
Moment of inertia	lb · ft <sup>2</sup>	kg · m <sup>2</sup>	0.04214
Second moment of area	in <sup>4</sup>	mm <sup>4</sup>	416200
Section modulus	in <sup>3</sup>	mm <sup>3</sup>	16390
Power	ton (refrig)	kW	3.517
	Btu/s	kW	1.054
	hp (electric)	W	745.7
	Btu/h	W	0.2931

\*4 significant figures; underline denotes exact conversion



Table A.4. Useful Conversion Factors (continued).			
Quantity	From English Units	To Metric Units	Multiplied by*
Volume rate of flow	ft <sup>3</sup> /s	m <sup>3</sup> /s	0.02832
	cfm	m <sup>3</sup> /s	0.0004719
	cfm	L/s	0.4719
	mgd	m <sup>3</sup> /s	0.0438
Velocity, speed	ft/s	m/s	<u>0.3048</u>
Acceleration	f/s <sup>2</sup>	m/s <sup>2</sup>	<u>0.3048</u>
Momentum	lb · ft/sec	kg · m/s	0.1383
Angular momentum	lb · ft <sup>2</sup> /s	kg · m <sup>2</sup> /s	0.04214
Plane angle	degree	rad	0.01745
		mrاد	17.45
*4 significant figures; underline denotes exact conversion			

Table A.5. Prefixes.					
Submultiples			Multiples		
deci	10 <sup>-1</sup>	d	deka	10 <sup>1</sup>	da
centi	10 <sup>-2</sup>	c	hecto	10 <sup>2</sup>	h
milli	10 <sup>-3</sup>	m	kilo	10 <sup>3</sup>	k
micro	10 <sup>-6</sup>	μ	mega	10 <sup>6</sup>	M
nano	10 <sup>-9</sup>	n	giga	10 <sup>9</sup>	G
pica	10 <sup>-12</sup>	p	tera	10 <sup>12</sup>	T
femto	10 <sup>-15</sup>	f	peta	10 <sup>15</sup>	P
atto	10 <sup>-18</sup>	a	exa	10 <sup>18</sup>	E
zepto	10 <sup>-21</sup>	z	zetta	10 <sup>21</sup>	Z
yocto	10 <sup>-24</sup>	y	yotta	10 <sup>24</sup>	Y

Table A.6. Physical Properties of Water at Atmospheric Pressure in SI Units.									
Temperature		Density	Specific Weight	Dynamic Viscosity	Kinematic Viscosity	Vapor Pressure	Surface Tension <sup>1</sup>	Bulk Modulus	
Centigrade	Fahrenheit	kg/m <sup>3</sup>	N/m <sup>3</sup>	N · s/m <sup>2</sup>	m <sup>2</sup> /s	N/m <sup>2</sup> abs.	N/m	GN/m <sup>2</sup>	
0°	32°	1,000	9,810	1.79 x 10 <sup>-3</sup>	1.79 x 10 <sup>-6</sup>	611	0.0756	1.99	
5°	41°	1,000	9,810	1.51 x 10 <sup>-3</sup>	1.51 x 10 <sup>-6</sup>	872	0.0749	2.05	
10°	50°	1,000	9,810	1.31 x 10 <sup>-3</sup>	1.31 x 10 <sup>-6</sup>	1,230	0.0742	2.11	
15°	59°	999	9,800	1.14 x 10 <sup>-3</sup>	1.14 x 10 <sup>-6</sup>	1,700	0.0735	2.16	
20°	68°	998	9,790	1.00 x 10 <sup>-3</sup>	1.00 x 10 <sup>-6</sup>	2,340	0.0728	2.20	
25°	77°	997	9,781	8.91 x 10 <sup>-4</sup>	8.94 x 10 <sup>-7</sup>	3,170	0.0720	2.23	
30°	86°	996	9,771	7.97 x 10 <sup>-4</sup>	8.00 x 10 <sup>-7</sup>	4,250	0.0712	2.25	
35°	95°	994	9,751	7.20 x 10 <sup>-4</sup>	7.24 x 10 <sup>-7</sup>	5,630	0.0704	2.27	
40°	104°	992	9,732	6.53 x 10 <sup>-4</sup>	6.58 x 10 <sup>-7</sup>	7,380	0.0696	2.28	
50°	122°	988	9,693	5.47 x 10 <sup>-4</sup>	5.53 x 10 <sup>-7</sup>	12,300	0.0679		
60°	140°	983	9,643	4.66 x 10 <sup>-4</sup>	4.74 x 10 <sup>-7</sup>	20,000	0.0662		
70°	158°	978	9,594	4.04 x 10 <sup>-4</sup>	4.13 x 10 <sup>-7</sup>	31,200	0.0644		
80°	176°	972	9,535	3.54 x 10 <sup>-4</sup>	3.64 x 10 <sup>-7</sup>	47,400	0.0626		
90°	194°	965	9,467	3.15 x 10 <sup>-4</sup>	3.26 x 10 <sup>-7</sup>	70,100	0.0607		
100°	212°	958	9,398	2.82 x 10 <sup>-4</sup>	2.94 x 10 <sup>-7</sup>	101,300	0.0589		

<sup>1</sup>Surface tension of water in contact with air

Temperature		Density	Specific Weight	Dynamic Viscosity	Kinematic Viscosity	Vapor Pressure	Surface Tension <sup>1</sup>	Bulk Modulus
Fahrenheit	Centigrade	Slugs/ft <sup>3</sup>	Weight lb/ft <sup>3</sup>	lb-sec/ft <sup>2</sup>	ft <sup>2</sup> /sec	lb/in <sup>2</sup>	lb/ft	lb/in <sup>2</sup>
32	0	1.940	62.416	0.374 X 10 <sup>-4</sup>	1.93 X 10 <sup>-5</sup>	0.09	0.00518	287,000
39.2	4.0	1.940	62.424					
40	4.4	1.940	62.423	0.323	1.67	0.12	.00514	296,000
50	10.0	1.940	62.408	0.273	1.41	0.18	.00508	305,000
60	15.6	1.939	62.366	0.235	1.21	0.26	.00504	313,000
70	21.1	1.936	62.300	0.205	1.06	0.36	.00497	319,000
80	26.7	1.934	62.217	0.180	0.929	0.51	.00492	325,000
90	32.2	1.931	62.118	0.160	0.828	0.70	.00486	329,000
100	37.8	1.927	61.998	0.143	0.741	0.95	.00479	331,000
120	48.9	1.918	61.719	0.117	0.610	1.69	.00466	332,000
140	60.0	1.908	61.386	0.0979	0.513	2.89		
160	71.1	1.896	61.006	0.0835	0.440	4.74		
180	82.2	1.883	60.586	0.0726	0.385	7.51		
200	93.3	1.869	60.135	0.0637	0.341	11.52		
212	100	1.847	59.843	0.0593	0.319	14.70		

<sup>1</sup>Surface tension of water in contact with air

Table A.8. Sediment Particles Grade Scale.						
Size			Inches	Tyler	Approximate Sieve Mesh Openings Per Inch U.S. Standard	Class
Millimeters	Microns					
4000-2000	-----	-----	160-80	----	-----	Very large boulders
2000-1000	-----	-----	80-40	----	-----	Large boulders
1000-500	-----	-----	40-20	----	-----	Medium boulders
500-250	-----	-----	20-10	----	-----	Small boulders
250-130	-----	-----	10-5	----	-----	Large cobbles
130-64	-----	-----	5-2.5	----	-----	Small cobbles
64-32	-----	-----	2.5-1.3	----	-----	Very coarse gravel
32-16	-----	-----	1.3-0.6	----	-----	Coarse gravel
16-8	-----	-----	0.6-0.3	2 1/2	-----	Medium gravel
8-4	-----	-----	0.3-0.16	5	5	Fine gravel
4-2	-----	-----	0.16-0.08	9	10	Very fine gravel
2-1	2.00-1.00	2000-1000	-----	16	18	Very coarse sand
1-1/2	1.00-0.50	1000-500	-----	32	35	Coarse sand
1/2-1/4	0.50-0.25	500-250	-----	60	60	Medium sand
1/4-1/8	0.25-0.125	250-125	-----	115	120	Fine sand
1/8-1/16	0.125-0.062	125-62	-----	250	230	Very fine sand
1/16-1/32	0.062-0.031	62-31	-----	-----	-----	Coarse silt
1/32-1/64	0.031-0.016	31-16	-----	-----	-----	Medium silt
1/64-1/128	0.016-0.008	16-8	-----	-----	-----	Fine silt
1/128-1/256	0.008-0.004	8-4	-----	-----	-----	Very fine silt
1/256-1/512	0.004-0.0020	4-2	-----	-----	-----	Coarse clay
1/512-1/1024	0.0020-0.0010	2-1	-----	-----	-----	Medium clay
1/1024-1/2048	0.0010-0.0005	1-0.5	-----	-----	-----	Fine clay
1/2048-1/4096	0.0005-0.0002	0.5-0.24	-----	-----	-----	Very fine clay

**Table A.9. Common Equivalent Hydraulic Units.**

Volume											
Unit	Equivalent										
	cubic inch	liter	u.s. gallon	cubic foot	cubic yard	cubic meter	acre-foot	sec-foot-day	gallon/minute	liter/second	meter <sup>3</sup> /second
liter	61.02	1	0.264 2	0.035 31	0.001 308	0.001	810.6 E - 9	408.7 E - 9			
U.S. gallon	231.0	3.785	1	0.133 7	0.004 951	0.003 785	3.068 E - 6	1.547 E - 6			
cubic foot	1728	28.32	7.481	1	0.037 04	0.028 32	22.96 E - 6	11.57 E - 6			
cubic yard	46 660	764.6	202.0	27	1	0.746 6	619.8 E - 6	312.5 E - 6			
meter <sup>3</sup>	61 020	1000	264.2	35.31	1.308	1	810.6 E - 6	408.7 E - 6			
acre-foot	75.27 E + 6	1 233 000	325 900	43 560	1 613	1 233	1	0.504 2			
sec-foot-day	149.3 E + 6	2 447 000	646 400	86 400	3 200	2 447	1.983	1			
Discharge (Flow Rate, Volume/Time)											
Unit	Equivalent										
	gallon/minute	liter/second	acre-foot/day	foot <sup>3</sup> /sec	million gal/day	meter <sup>3</sup> /sec	gallon/min	liter/sec	acre-foot/day	foot <sup>3</sup> /sec	meter <sup>3</sup> /sec
gallon/minute							1	0.004 419	0.002 228	0.001 440	63.09 E - 6
liter/second							15.85	0.070 05	0.035 31	0.022 82	0.001
acre-foot/day							226.3	1	0.504 2	0.325 9	0.014 28
feet <sup>3</sup> /second							448.8	1.983	1	0.646 3	0.028 32
million gal/day							694.4	3.068	1.547	1	0.043 82
meter <sup>3</sup> /second							15 850	70.04	35.31	22.82	1

(page intentionally left blank)

## APPENDIX B

### Analysis of Selected Sediment Transport Relationships

#### B.1 BACKGROUND

This appendix provides a review of several bed material load equations and provides the background for several modifications to selected equations. The equations are tested, developed, and verified using a large group of field and laboratory data for a wide range of river and bed material sizes.

Sediment transport in rivers has been studied and applied for centuries. Research continues because the analysis of bed material transport involves complex interactions among many interrelated variables (Vanoni 1977; Ackers and White 1973 and 1980; Simons and Sentürk 1992). Several sediment transport relationships for alluvial rivers have been proposed during the last 50 years. These are based upon simplified and idealized assumptions and limited field data. Due to the complexity of the problem, most existing equations are empirical and semi-empirical and/or heavily based upon laboratory data and assumptions that are not totally justified (Cao et al. 1997; Paceco-Ceballos 1989; Tywoniuk 1972). These methods have been developed based upon theoretical considerations and/or statistical interpretations of data, and some have been based upon the physics of particle motion. Other methods have been developed from experimental work, some were derived empirically, and some represent a combination of theories, experiments and empirical methods, but no comprehensive study has ever been presented for the total range of alluvial rivers for which data exist.

In practice, engineers have dealt with a variety of granular materials in applying the governing laws of transport and movement of sediments (Bogardi 1974). However, 3-dimensional, time-dependent phenomena still need to be studied, and available knowledge to conduct these analyses is still insufficient (Overbeek 1979; and Borah et al. 1982a and 1982b). In addition, field verification data have not been utilized to validate the various relationships to a significant degree (Simons and Sentürk 1992).

Rivers transporting large sediment loads are found throughout the world. Most sediment transport equations can predict with acceptable accuracy sediment transport in small rivers since the measurement of pertinent data to develop empirical relations is relatively easy. However, due to the difficulty of gathering information and required data for large rivers, extrapolation of methods to estimate sediment loads usually do not give accurate results (Posada 1995). Hence, the subject of total bed-material transport in large rivers is a challenge and needs further investigation.

Most investigators have recognized these facts. However, the sediment problem remains complex and warrants further investigation (Williams and Julien 1989). To date, accepted methodologies are not able to accurately calculate sediment transport in order to give acceptable results encompassing all alluvial channel conditions. In other words, there is no single equation which can calculate sediment transport for the entire range of conditions found in the field (Alonso et al. 1982; Shen and Hung 1983; Steven and Yang 1989; Simons and Sentürk 1992; Julien 1995). As a result, calculations of sediment transport using existing methods for specific rivers with the same input data produce a wide range of estimates of sediment transport. Because of the complexity of the problem, identification of

the best methodology is often academic. Specific equations are based upon limited data and they may not fit the whole spectrum of data from flumes, canals and rivers (Yang and Wan 1991). Therefore, engineering judgment must be used when selecting and applying the available methods. This Appendix provides additional guidance on the applicability of selected sediment transport equations based on a comparison of predicted transport rates with a large data set.

## **B.2 EVALUATION OF SELECTED SEDIMENT TRANSPORT EQUATIONS**

### **B.2.1 Introduction**

A large compilation of field data was used to test ten widely used sediment transport (bed material load) equations (Kodoatie 1999, Kodoatie et al. 1999). The data encompass a wide range of bed materials, from silts to gravels, and a wide range of river sizes, from less than 1 m width to several thousand meters in width.

The ten sediment transport equations that were evaluated are: Einstein (1950), Laursen (1958), Bagnold (1966), Toffaletti (1969), Shen and Hung (1972), Ackers and White (1973), Yang (1973) and (1984) for gravel-bed rivers, Brownlie (1981), Karim and Kennedy (1981), and Karim (1998). Field data include a total of 2,946 sets from 33 alluvial systems. Additionally, 919 sets of laboratory data from 19 sources were selected to verify the proposed methods. Tables B.1a and B.1b identify the field data and laboratory data used in the Kodoatie (1999) study.

### **B.2.2 Scope of Study**

Because no single equation can encompass all alluvial channel conditions, four subdivisions of river data were analyzed based upon bed material size. These included: gravel-bed, medium to very coarse sand-bed, very fine to fine sand-bed and silt-bed rivers. Also, the data were subdivided based upon size of river, i.e.,

- Small rivers with widths equal to or less than 10 m (33 ft) and depths equal to or less than 1 m (3.3 ft),
- Intermediate rivers with widths greater than 10 m (33 ft) and equal to or less than 50 m (164 ft) and depths greater than 1 m (3.3 ft) and equal to or less than 3 m (9.8 ft),
- Large rivers with widths greater than 50 m (164 ft) and depths of greater than 3 m (9.8 ft).

The range of field and laboratory data are identified in Table B.2. The sediment transport relations tested are summarized in Table B.3.



Table B.1a. Field Data.				
Name of River	Data Sets	No. Used	Source	Also Found In
ACOP Canal (Pakistan Canal)	151	142	Mahmood (1979)	Brownlie (1981b)
Chops Canal, West Pakistan	33	33	Chaudhry, et al. (1970)	Brownlie (1981b)
American Canal	13	12	Simons (1957)	Brownlie (1981b)
Atchafalaya River	72	72	Toffaletti (1968)	Brownlie (1981b)
Amazon and Orinoco Rivers	114	85	Posada (1995)	
Black Canal	17	7	Williams and Rosgen (1989)	
India Canal	32	32	Chitale (1966)	Brownlie (1981b)
Chippewa River	66	47	Williams and Rosgen (1989)	
Chulitna River	43	4	Williams and Rosgen (1989)	
Colorado River	131	100	USBR (1958)	Brownlie (1981b)
Hii River	38	38	Shinohara and Tsubaki (1979)	Brownlie (1981b)
Middle Loup River	38	15	Hubbel and Matajka (1959)	Brownlie (1981b)
Mississippi River	164	164	Toffaletti (1968)	Brownlie (1981b)
Mississippi River	85	85	Posada (1995)	
Mountain Creek	100	100	Einstein (1944)	Brownlie (1981b)
Niobrara River near Cody	51	19	Colby and Hembree (1955)	Brownlie (1981b)
North Fork Toutle River	10	2	Williams and Rosgen (1989)	
North Saskatchewan and Elbow Rivers	55	55	Samide (1971)	Brownlie (1981b)
Oak Creek	17	17	Milhous (1973)	Brownlie (1981b)
Red River	30	29	Toffaletti (1968)	Brownlie (1981b)
Rio Grande River	293	289	Nordin and Beverage (1965)	Brownlie (1981b)
Rio Grande Conveyance Channel	33	9	Culbertson, et al. (1972)	Brownlie (1981b)
Rio Grande River, Columbia	38	38	Toffaletti (1968)	Brownlie (1981b)
Rio Magdalena and Canal del Dique	113	75	NEDECO (1973)	Brownlie (1981b)
River data of Leopold	72	55	Leopold (1969)	Brownlie (1981b)
Portugal Rivers	219	219	Da Cunha (1969)	Brownlie (1981b)
Snake and Clearwater Rivers	21	17	Seitz (1976)	Brownlie (1981b)
Susitna River	38	2	Williams and Rosgen (1989)	
Toutle River	31	9	Williams and Rosgen (1989)	
Trinity River	4	3	Knott (1974)	Brownlie (1981b)
Wisconsin River	20	9	Williams and Rosgen (1989)	
Yampa River	24	11	Williams and Rosgen (1989)	
Yangtze River	40	40	Long and Liang (1994)	
Yellow River	2,326	1,112	Long and Liang (1995)	
TOTAL DATA	4,532	2,946		

Table B.1b. Laboratory Data.		
Number	Source	Data Sets
1	Barton and Lin (1955)	30
2	Brooks (Vanoni and Brooks 1957)	21
3	Guy (Simons and Richardson 1966)	290
4	Franco (1968)	19
5	Kalinske and Hsia (1945)	9
6	Kennedy and Brooks (1963)	9
7	Laursen (1958)	24
8	Meyer-Peter and Müller (1948)	139
9	Nomicos 1 (Toffaletti 1968) (Vanoni and Brooks 1957)	12
10	Nomicos 2 (Vanoni and Brooks 1957)	26
11	Onishi, Jain and Kennedy (1976)	14
12	Stein (1965)	57
13	Straub (1954 and 1958)	24
14	Taylor and Vanoni (1972)	6
15	Vanoni and Brooks (1957)	15
16	Vanoni and Hwang (1967)	16
17	Williams (1970)	83
18	Willis (Willis, Coleman, and Ellis 1972)	96
19	Wilcock and Southard (1988)	29
	TOTAL DATA	919

Table B.2. Field and Laboratory Data Ranges.		
Hydraulic Geometry	Field Data	Laboratory Data
Flow discharge (m <sup>3</sup> /s)	0.0009 – 235,000	0.001 – 4.614
Width (m)	0.8 – 3,338	0.267 – 2.438
Depth (m)	0.02 – 68.00	0.008 – 1.092
Slope	0.0000021 – 0.0126	0.00015 – 0.0331

Table B.3. Summary of Ten Sediment Transport Relations.

No.	Author	Equation	Comment
1	Einstein (1950)	$q_{ti} = q_{bi} (1 + P_{E1} + I_2)$	Size fraction Used graph
2	Laurson (1958)	$C_i = 0.01 \gamma \sum_i P_i \left( \frac{D_i}{V} \right)^{7/6} \left( \frac{\tau'_o}{\tau_{ci}} - 1 \right) f \left( \frac{V_c}{\omega_i} \right)$	Size fraction Used graph
3	Bagnold (1966)	$q_T = q_b + q_s = \frac{\tau_o V}{G-1} \left( \frac{e_B}{\tan \alpha} + 0.01 \frac{V}{\omega} \right)$	Based on $\tau_o V$ Used graph
4	Toffaletti (1969)	$q_{ti} = q_{bi} + q_{svi} + q_{smi} + q_{sfi}$	4 zones of depth
5	Ackers and White (1973)	$C_W = C_{AW2} G \frac{D_s}{Y} \left( \frac{V}{V_c} \right)^{C_{AW1}} \left( \frac{C_{AW5}}{C_{AW3}} - 1 \right)^{C_{AW4}}$	
6	Yang a. Sand (1973) b. Gravel (1984)	$\log C_{ppm} = 5.435 - 0.286 \log \frac{\omega D_s}{V} - 0.457 \log \frac{V_c}{\omega} + \left( 1.799 - 0.409 \log \frac{\omega D_s}{V} - 0.314 \log \frac{V_c}{\omega} \right) \log \left( \frac{VS}{\omega} - \frac{V_c S}{\omega} \right)$ $\log C_{ppm} = 6.681 - 0.633 \log \frac{\omega D_s}{V} - 4.816 \log \frac{V_c}{\omega} + \left( 2.784 - 0.305 \log \frac{\omega D_s}{V} - 0.282 \log \frac{V_c}{\omega} \right) \log \left( \frac{VS}{\omega} - \frac{V_c S}{\omega} \right)$	Based on $\frac{VS}{\omega}$
7	Shen and Hung (1972)	$\log C_{ppm} = (-107,404.459 + 324,214.747Sh - 326,309.589Sh^2 + 109,503.872Sh^3)$	Regression Based on $\frac{VS}{\omega}$
8	Brownlie (1981)	$C_{ppm} = 7115 C_B \left( \frac{V - V_c}{\sqrt{G-1} g D_s} \right)^{1.978} S_l^{0.6601} \left( \frac{R_h}{D_s} \right)^{-0.3301}$	Based on $F_{go}$ and $\tau_c$ introduced flow regime equations
9	Karim and Kennedy (1981)	$\log \frac{q_t}{\gamma_s \sqrt{(G-1) g D_s^3}} = -2.28 + 2.97 C_{k1} + 0.30 C_{k2} C_{k3} + 1.06 C_{k1} C_{k3}$	Regression
10	Karim (1998)	$\frac{q_{si}}{\sqrt{g(G-1) D_i^3}} = 0.00139 \left( \frac{V}{\sqrt{g(G-1) D_i}} \right)^{2.97} \left( \frac{V_c}{\omega_i} \right)^{1.47} \frac{P_{bi}}{\sum_{i=1}^N P_{bi}} 1.15 \frac{\omega_{50}}{V_c} \left( \frac{D_i}{D_{50}} \right)^{0.60} \frac{\omega_{50}}{V_c}$	Non-uniform sed based on size fraction

### B.2.3 Analysis of Sediment Transport Relations

The field data were divided into two categories: Group 1 for analysis of the selected sediment transport relations and proposed equations, and Group 2 for verification and validation of the proposed methods. The river data sets were divided into two parts in random order.

A comparison between computed results and field data was conducted and examined. Statistical approaches were used including the mean discrepancy ratio  $\overline{R}_D$  (Bechteler and Vetter 1989; Wu 1999; Nakato 1990; Yang and Wan 1991; and Hydraul-Tech, Inc. 1998), and the correlation coefficient  $C_c$  (Hydraul-Tech, Inc. 1998). The equations for each parameter follow:

$$\overline{R}_D = \sum \frac{R_i}{N}, R_i = \frac{X_i}{Y_i} \quad (\text{B.1})$$

$$C_c = \frac{\sum (X_i - \overline{X})(Y_i - \overline{Y})}{\sqrt{\sum (X_i - \overline{X})^2 \sum (Y_i - \overline{Y})^2}} \quad (\text{B.2})$$

For perfect fit, the values in Equations B.1 and B.2 are  $\overline{R}_D = 1$  and  $C_c = 1$ .

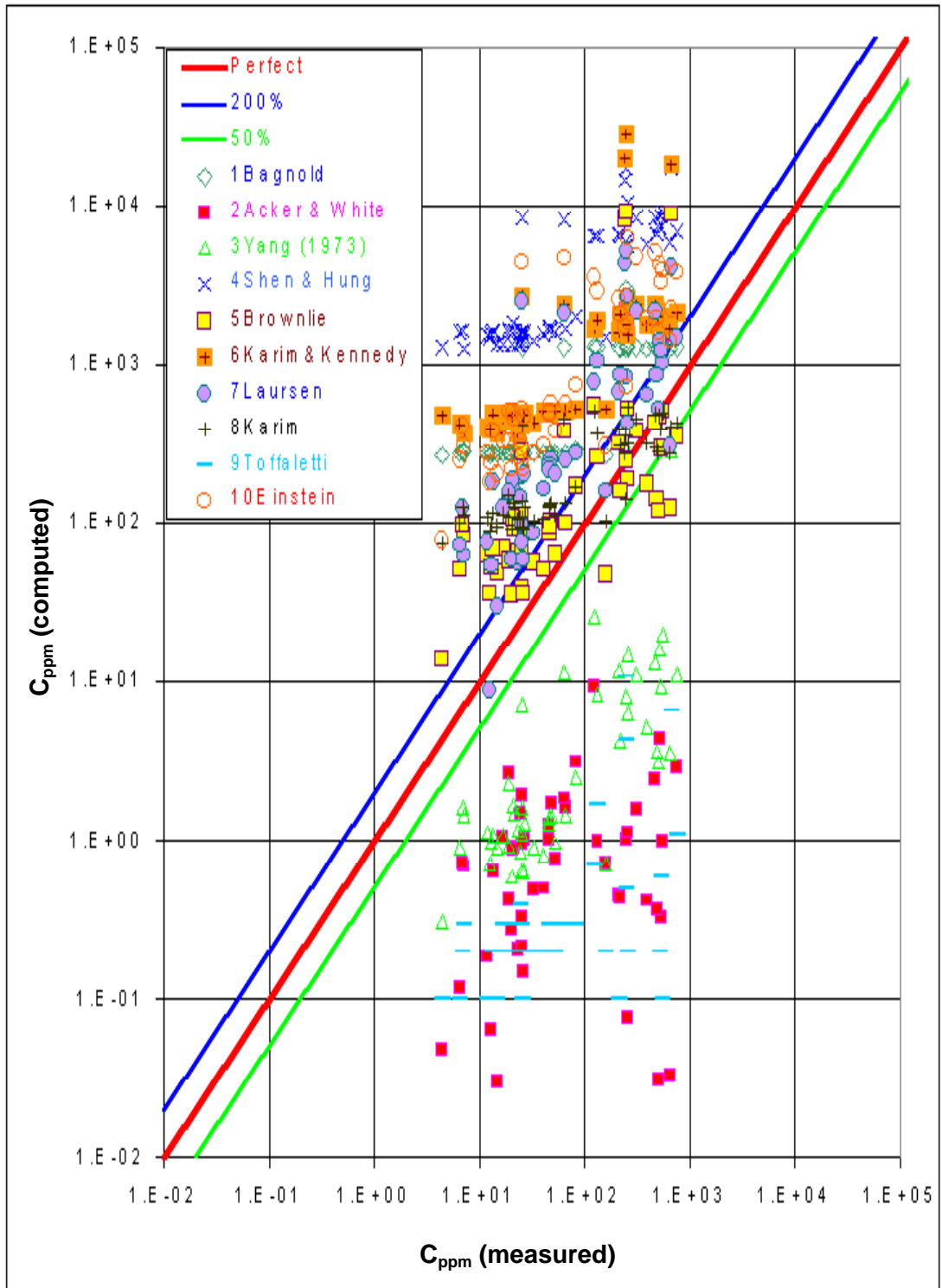
The sediment relations were used to calculate the transport of sediment using data from Group 1. The sediment load was calculated using mean diameter of riverbed material (uniform sediment size). The results of comparing computed sediment concentration ( $C_{ppm}$ ) and measured sediment concentration measured for four ranges of particle sizes and for three sizes of rivers are shown in Figure B.1a through d, and Figure B.2a through c.

### B.2.4 Summary of Applicability of Ten Sediment Relations Analyzed

The applicability of these relationships as reported by Kodoatie et al. (1999) is illustrated in Table B.4. While certain equations appear to be more applicable to particular bed characteristics or river size, each equation could, potentially, be applied with reasonable results for a specific river, if the river characteristics are compatible with those used in the equation's development. For any specific river, it is recommended that the results be compared with actual measurements. The following conclusions can be drawn from the results of this analysis:

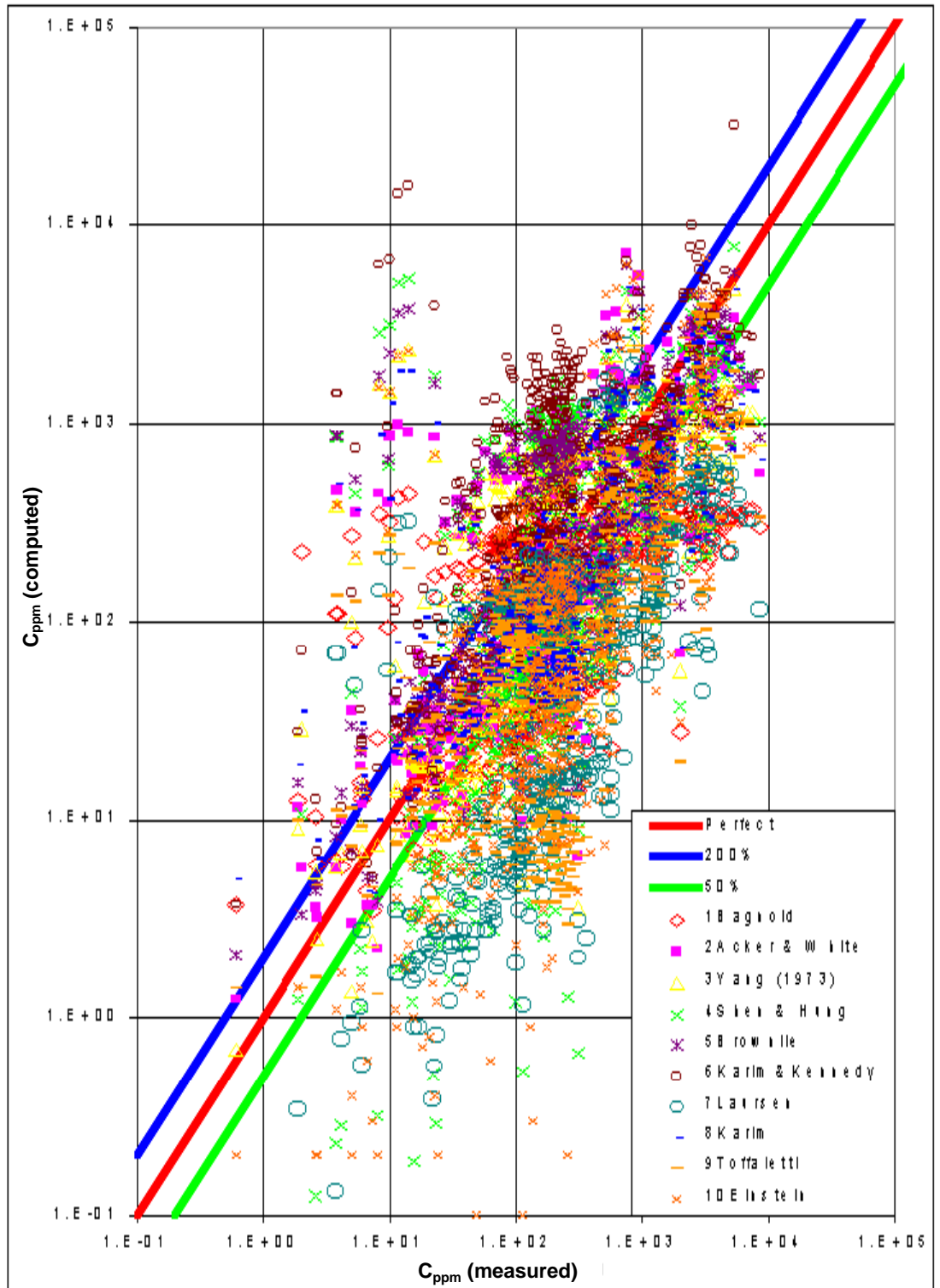
#### 1. Gravel-bed rivers ( $2 \text{ mm} < D_{50} < 64 \text{ mm}$ )

Compared to the measured values, none of the selected sediment relations can accurately predict the sediment discharge. The closest values based upon the discrepancy ratio are Ackers and White with  $\overline{R}_D = 0.33$  and Brownlie with  $\overline{R}_D = 4.25$ . However, based upon the Pearson correlation coefficient for comparison of computed to measured  $C_{ppm}$ , the best equations are Bagnold and Shen and Hung, both with  $C_c$  of 0.70. Considering gravel-bed rivers, Brownlie's equations, although developed for sand-bed rivers, are the most acceptable of the ten equations.



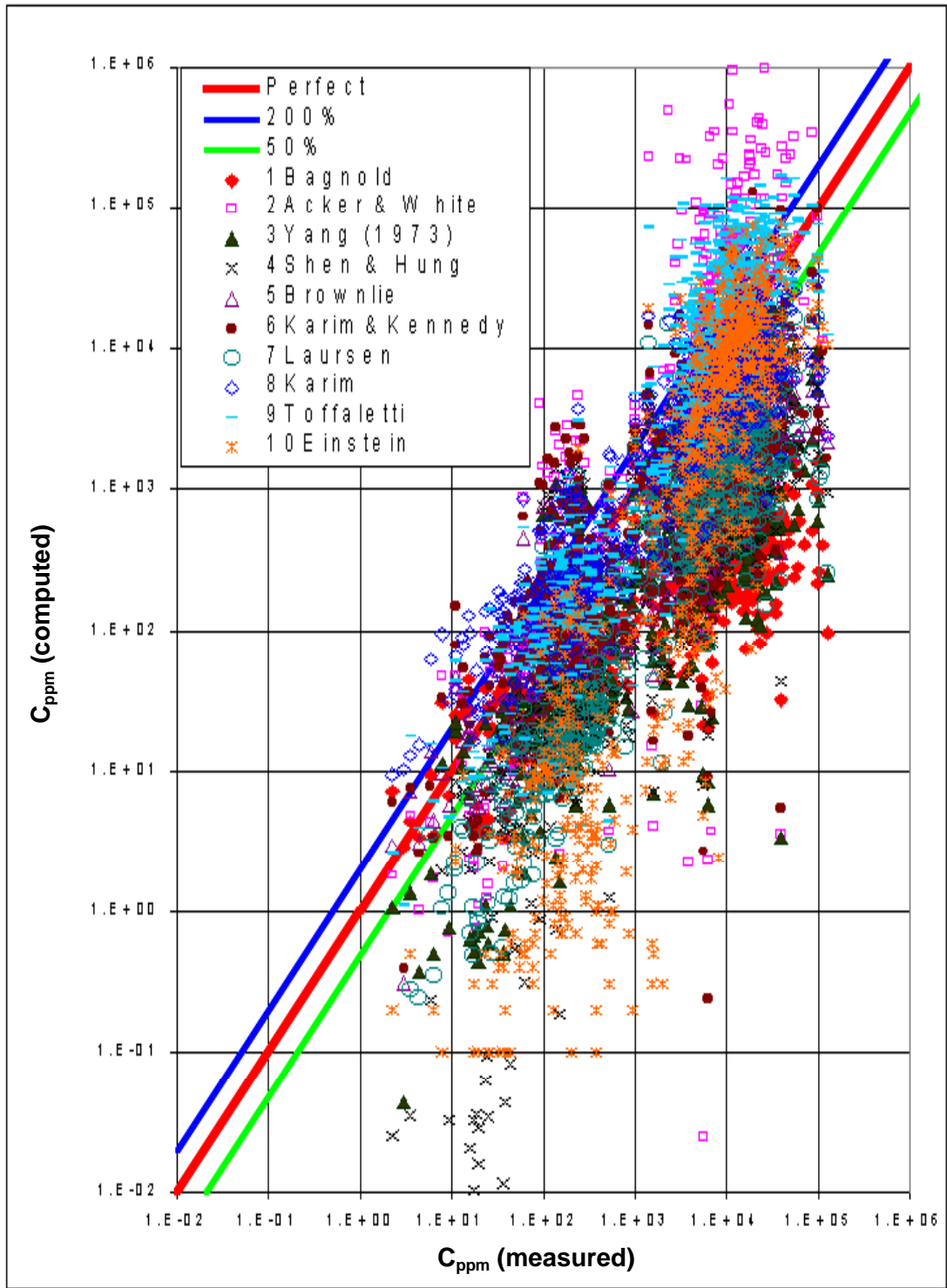
(a) gravel-bed rivers

Figure B.1. Predicted versus measured total bed-material transport considering four classifications of size of bed materials.



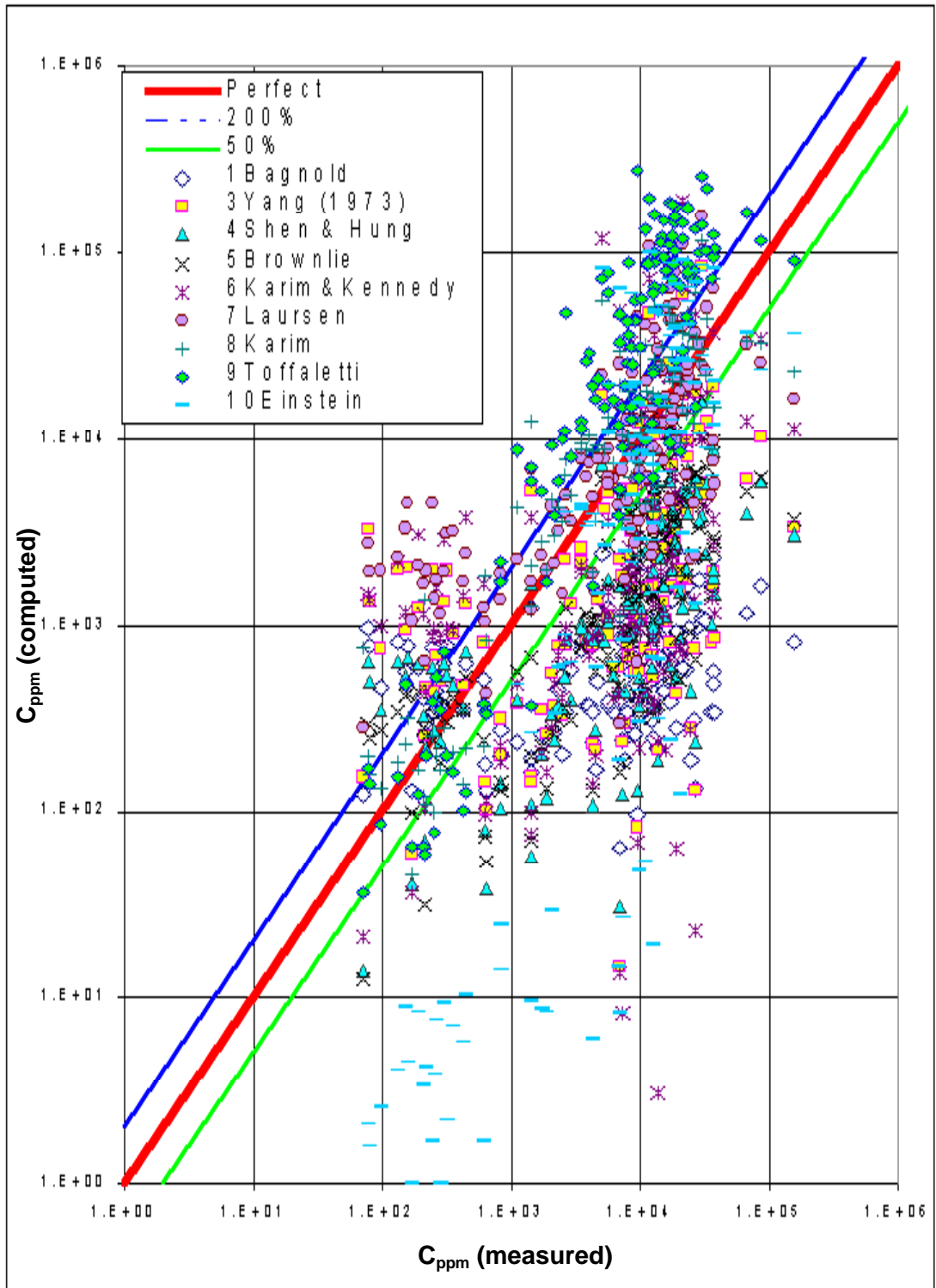
(b) medium to very coarse sand-bed rivers

Figure B.1. Predicted versus measured total bed-material transport considering four classifications of size of bed materials (continued).



( c ) very fine to fine sand-bed rivers

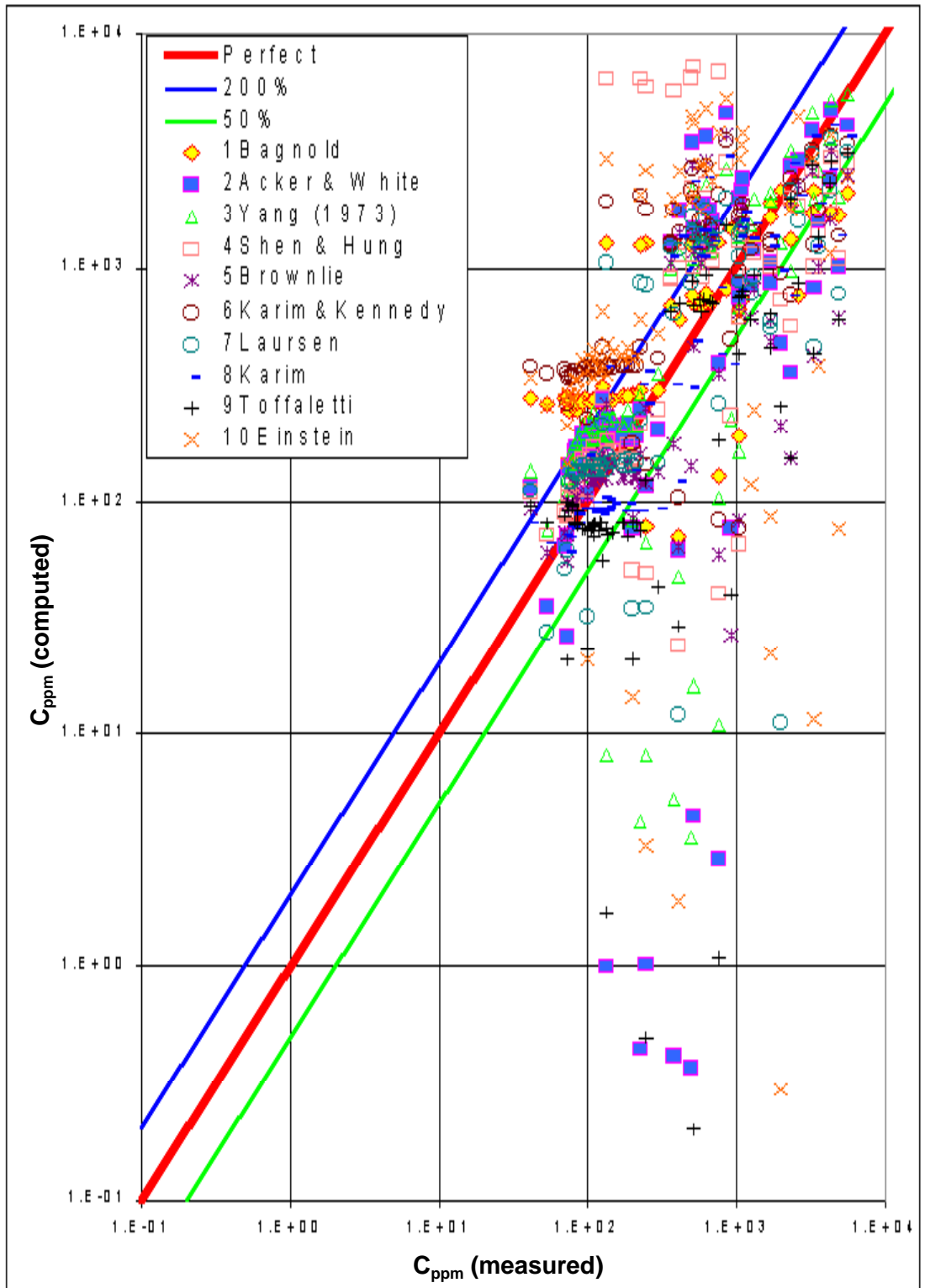
Figure B.1. Predicted versus measured total bed-material transport considering four classifications of size of bed materials (continued).



(d) silt-bed rivers (Ackers and White not plotted because values are too high)

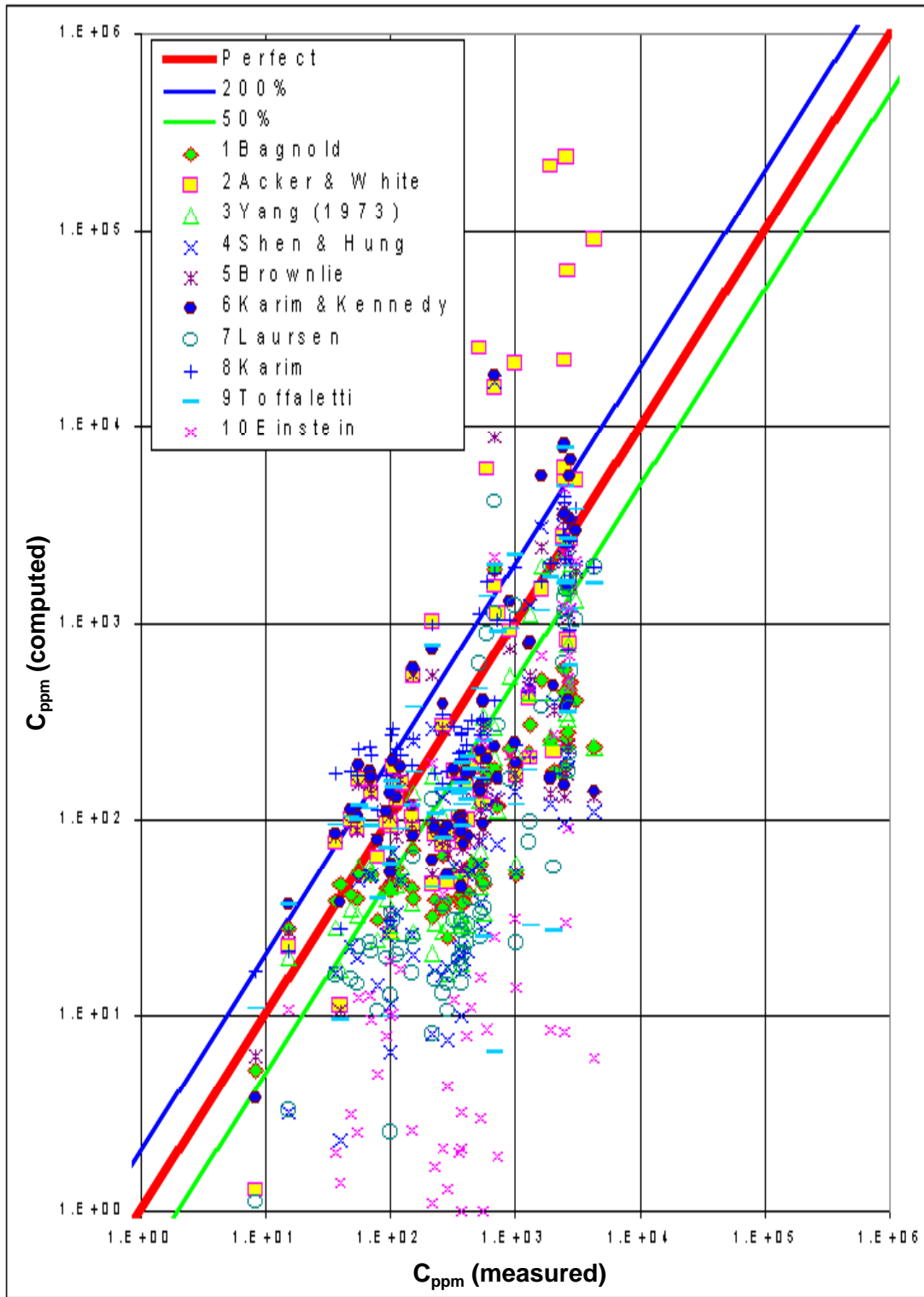
Figure B.1. Predicted versus measured total bed-material transport considering four classifications of size of bed materials (continued).





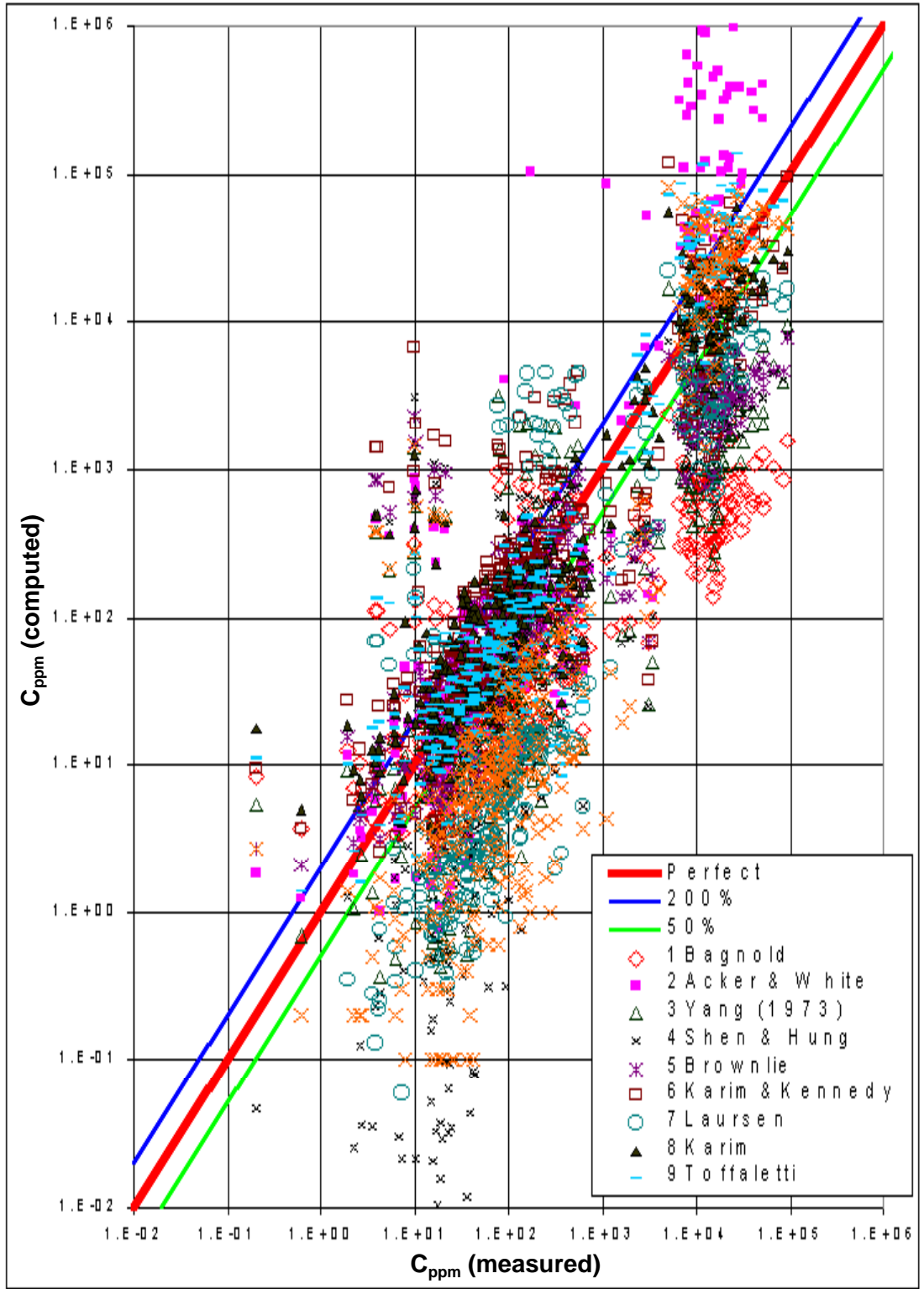
(a) small rivers

Figure B.2. Comparison  $C_{ppm}$  computed and measured for three river sets.



(b) intermediate rivers

Figure B.2. Comparison  $C_{ppm}$  computed and measured for three river sets.



( c ) large rivers

Figure B.2. Comparison  $C_{ppm}$  computed and measured for three river sets.

## 2. Medium to very coarse sand-bed rivers ( $0.250 \text{ mm} < D_{50} < 2.00 \text{ mm}$ )

For this bed material, Toffaletti with  $\overline{R_D} = 0.93$ , Laursen with  $\overline{R_D} = 0.60$ , and Bagnold with  $\overline{R_D} = 1.68$  compute  $C_{ppm}$  closest to measured values. On the other hand, based upon Pearson correlation coefficient, Karim with  $C_c = 0.66$  followed by Brownlie with  $C_c = 0.60$  best correlate measured concentrations of sediment as compared to measured values.

## 3. Very fine to fine sand-bed rivers ( $0.062 \text{ mm} < D_{50} < 0.250 \text{ mm}$ )

The most suitable equations are Karim and Kennedy with  $\overline{R_D} = 0.90$ , Karim with  $\overline{R_D} = 1.28$ , Brownlie with  $C_c = 0.58$ , and Toffaletti with  $C_c = 0.52$ .

## 4. Silt-bed rivers ( $0.004 \text{ mm} < D_{50} < 0.062 \text{ mm}$ )

For silt-bed rivers, Einstein with  $\overline{R_D} = 1.06$ , Bagnold with  $\overline{R_D} = 0.56$ , Toffaletti with  $C_c = 0.48$ , and Brownlie with  $C_c = 0.38$  are the most acceptable relationships.

## 5. Small rivers (width $\leq 10 \text{ m}$ and depth $\leq 1 \text{ m}$ )

The closest results obtained in small rivers is Brownlie with  $\overline{R_D} = 1.18$ , Karim with  $\overline{R_D} = 1.19$ , Yang with  $C_c = 0.85$  and Toffaletti with  $C_c = 0.79$ .

## 6. Intermediate rivers ( $10 \text{ m} < \text{width} \leq 50 \text{ m}$ and $1 \text{ m} < \text{depth} \leq 3 \text{ m}$ )

For intermediate rivers, Toffaletti with  $\overline{R_D} = 0.94$ , Brownlie with  $\overline{R_D} = 0.94$ , Karim with  $C_c = 0.76$ , and Yang with  $C_c = 0.70$  are the most acceptable relationships.

## 7. Large rivers (width $> 50 \text{ m}$ and depth $> 3 \text{ m}$ )

For large rivers, Bagnold with  $\overline{R_D} = 1.04$ , Laursen with  $\overline{R_D} = 1.13$ , Brownlie with  $C_c = 0.80$ , and Shen and Hung with  $C_c = 0.76$  are the most acceptable relationships. It should be noted that for silt-bed rivers and for very fine to fine sand-bed rivers, the Yellow River contributes about 77 and 63 percent of the data, respectively. As reported by many investigators, this river is an extremely heavily sediment-laden river and floods experience hyperconcentrations of sediment. Out of all rivers, this river system is unique and therefore should not be categorized as a common alluvial river.

From the analysis, it can be seen that both Ackers and White and Toffaletti have a tendency to increase the computed concentration of suspended sediment, as the median diameter of bed material becomes finer. This tendency also occurs with these relationships when the river size increases. As reported by Kodoatie et al. (1999), the applicability of the ten selected sediment transport relations based upon comparison between measured and computed sediment transport rates and results from other studies are summarized in Table B.4.

Table B.4. Summary of Applicability of Selected Sediment Transport Relations (Kodoatie et al. 1999).

	Method	Gravel	Med – Very Coarse Sand	Very Fine to Fine Sand	Silt	Small Rivers	Intermed Rivers	Large Rivers
1	Ackers and White	X	X					
2	Bagnold		X	X	X			X
3	Brownlie	X	X			X	X	
4	Einstein			X	X			
5	Karim	X		X		X		
6	Karim and Kennedy	X	X	X				
7	Laursen		X	X	X			X
8	Shen and Hung		X	X			X	
9	Toffaletti		X	X			X	X
10	Yang '73 and '84	X	X			X		

### B.3 POWER FUNCTION RELATIONSHIPS

#### B.3.1 Introduction

Power relationships empirically relate sediment transport with hydraulic conditions and sediment characteristics. They can be developed by fitting the coefficients to computed sediment transport from more sophisticated equations or to measured data. Their utility is in their ease of use and, when developed from measured data, their site-specific accuracy.

#### B.3.2 Basic Power Function Relationship

In 1981, Simons et al. proposed an efficient method of evaluating sediment discharge. The method is based on variables flow depth, velocity, and particle diameter, and gradation coefficient. It can be easily applied in steep sand and fine gravel-bed creeks and rivers that normally exhibit critical or supercritical flow. It will also be shown that a modification of this relationship can be applied to subcritical rivers. This is the only transport relationship specifically developed for upper flow regime conditions. These power relationships were developed by Simons et al., from a computer solution of the Meyer-Peter and Müller bed load transport equation and the integration of the Einstein method for suspended bed sediment discharge (Julien 1995) and expressed as

$$q_s = c_{s1} y^{c_{s2}} V^{c_{s3}} \quad (B.3)$$

where:

- $q_s$  = Unit sediment transport rate  $ft^2/s$  ( $m^2/s$ )
- $c_{s2}, c_{s3}$  = Exponents based on mean particle diameter ( $D_{50}$ ) ranging from sand to fine gravel
- $c_{s1}$  = Coefficient based on mean particle diameter (note that  $c_{s1}$  must be adjusted for SI units - see Section 4.8.2)
- $y$  = Mean flow depth, ft (m)
- $V$  = Mean velocity, ft/s (m/s)

Table B.5 provides the coefficient and exponents for Equation B.3 (for English units) for different gradation coefficients and sizes of bed material. The term  $G_r$  in Table B.5 is defined as the gradation coefficient of the bed material and is

$$G_r = \frac{1}{2} \left[ \frac{D_{50}}{D_{16}} + \frac{D_{84}}{D_{50}} \right] \quad (\text{B.4})$$

where:

$D_n$  = Size of the bed material for which  $n$  percent is finer

Equation B.3 was obtained for steep, sand- and fine gravel-bed channels experiencing critical and super-critical flows [Simons, et al. (1981), Julien (1995)]. The range of parameters utilized to develop this equation is shown in Table B.6.

The results for the total bed sediment discharge are presented in Table B.5. The high values of  $C_{s3}$  ( $3.3 < C_{s3} < 3.9$ ) show the high level of dependence that sediment transport rates have with respect to velocity. Comparatively, the influence of depth is less important ( $-0.34 < C_{s2} < 0.7$ ). For smaller sizes the exponent  $C_{s2}$  is positive since the smaller material is more easily suspended and resulting sediment concentration profiles are more uniform. Thus, the larger the depth, the more sediment will be suspended at a given velocity. For the larger sediment sizes the sediment is more difficult to suspend and keep in suspension.

Table B.5. Coefficient and Exponents of Equation B.3 (Simons et al.).									
		$D_{50}$ (mm)							
		0.1	0.25	0.5	1.0	2.0	3.0	4.0	5.0
$G_r = 1$	$C_{s1}$	$3.30 \times 10^{-5}$	$1.42 \times 10^{-5}$	$7.60 \times 10^{-6}$	$5.62 \times 10^{-6}$	$5.64 \times 10^{-6}$	$6.32 \times 10^{-6}$	$7.10 \times 10^{-6}$	$7.78 \times 10^{-6}$
	$C_{s2}$	0.715	0.495	0.28	0.06	-0.14	-0.24	-0.3	-0.34
	$C_{s3}$	3.3	3.61	3.82	3.93	3.95	3.92	3.89	3.87
$G_r = 2$	$C_{s1}$		$1.59 \times 10^{-5}$	$9.80 \times 10^{-6}$	$6.94 \times 10^{-6}$	$6.32 \times 10^{-6}$	$6.62 \times 10^{-6}$	$6.94 \times 10^{-6}$	
	$C_{s2}$		0.51	0.33	0.12	-0.09	-0.196	-0.27	
	$C_{s3}$		3.55	3.73	3.86	3.91	3.91	3.9	
$G_r = 3$	$C_{s1}$			$1.21 \times 10^{-5}$	$9.14 \times 10^{-6}$	$7.44 \times 10^{-6}$			
	$C_{s2}$			0.36	0.18	-0.02			
	$C_{s3}$			3.66	3.76	3.86			
$G_r = 4$	$C_{s1}$				$1.05 \times 10^{-5}$				
	$C_{s2}$				0.21				
	$C_{s3}$				3.71				

Table B.6. Range of Parameters Equation B.3 Developed by Simons et al.		
Parameter	Value Range	SI Units
Froude Number	1 – 4	--
Velocity	1.98 – 7.92	m/s
Bed Slope	0.005 – 0.040	m/m
Unit Discharge, $q$	3.05 – 60.96	$\text{m}^2/\text{s}$
Particle Size, $D_{50}$	> 0.062	mm

### B.3.3 Power Relationships Presented by Posada (1995)

Expanding earlier work by Nordin, Posada developed a sediment transport relation in 1995. In the simplest form, the sediment transport in sand-bed rivers varies as a function of the velocity to about the fifth power (Simons and Simons 1987). Using data from the Mississippi River (85 sets of data) and the Amazon and Orinoco River Systems (114 sets of data), Posada (1995) proposed a sediment discharge relation for sand-bed rivers as a function of velocity,

$$q_s = 30V^5 \quad (B.5)$$

where:

- $q_s$  = Unit sand discharge (metric tons/m/day)
- $V$  = Mean velocity (m/s)

This equation has an advantage for large, flat rivers in that velocity is easily measured and conversely slope is very difficult to measure accurately. This is particularly true when dealing with large, flat rivers such as the Mississippi, Padma, Amazon, and Orinoco Rivers. The application of Equation B.5 can be improved by subdividing the cross sections in the reach of channel being analyzed into similar parts, i.e., thalweg, etc. Also, better results are obtained for coarse sand and gravel if the exponent is reduced to four (4), and for silt-bed rivers if the exponent is increased to six (6).

Using Equation B.5, Posada computed the unit sand discharge for the data of the Mississippi, Amazon, and Orinoco River Systems and compared the results to the measured values. About 70 percent of the data for these river systems have a discrepancy ratio  $\bar{R}_D$  between 0.5 and 2.0. However, the quality of this relation is limited when additional sets of data from 23 river systems (2503 data points for sand-bed rivers) are included in the analysis. The results are shown in Figure B.3.

The Pearson correlation coefficient of  $q_s$  computed using Equation B.5 and  $q_s$  measured is 0.66.

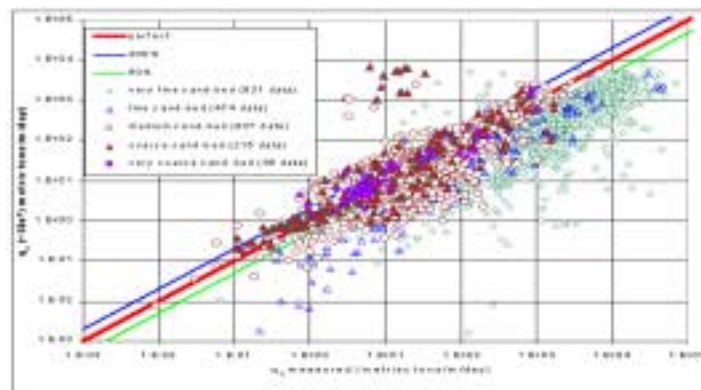


Figure B.3. Relation of unit sediment discharge  $q_s$  from measured and computed results using Equation B.5 for 2503 sets of field data.

About 60 percent of the computed unit sediment discharge is 50 percent less than the measured unit sediment discharge. Only 33 percent of computed  $q_s$  are between 70 and 200 percent of measured  $q_s$  and 7 percent of computed  $q_s$  are greater than 200 percent of the measured  $q_s$ . Accordingly, the application of Equation B.5 for a wide variety of river data is questionable, but not to the degree of several other widely utilized equations. The range of hydraulic data and particle diameters included in this analysis is shown in Table B.7.

Table B.7. Range of Data Utilized by Posada to Develop Equation B.5.						
Width (w)				Depth (d)		
< 20 m	$20 < w < 10^2$ m	$10^2 \leq w < 10^3$ m	$> 10^3$ m	< 1 m	$1 \text{ m} < d < 3 \text{ m}$	> 3 m
2.51%	6.03%	55.28%	36.18%	0.50%	10.05%	89.45%
Mean Bed Material Diameter						
< 0.125 mm		0.125 – 0.250 mm		0.250 – 2.000 mm		
5.88%		31.93%		77.39%		

Table B.7 illustrates that Posada developed Equation B.5 for large rivers with mostly medium to very coarse mean bed material (77.39 percent). Accordingly, the unit sediment discharges computed by Equation B.5 fit quite well to measured values for those conditions. For medium to very coarse sand bed rivers the discrepancy ratio between measured  $q_s$  and computed  $q_s$  is 1.12. However,  $\bar{R}_D$  is only 0.33 for very fine to fine sand-bed rivers, it is 0.18 for silt-bed rivers and it is 312.46 for gravel-bed rivers.

### B.3.4 Expanded Power Function Relationship

Considering the correlation coefficient for each variable of hydraulic geometry and the sediment characteristics, Kodoatie (1999) modified the Posada (1995) equation (Section B.3.3) using nonlinear optimization and the field data for different sizes of riverbed sediment. The resulting equation is (variables are defined in Section 4.8.3):

$$q_t = aV^b y^c S^d \quad (\text{B.6})$$

A summary of coefficients and exponents is presented in Table B.8 and depend on size of bed material. The equation was developed with one group of data (Group 1) and validated with another group of data (Group 2). Graphical comparisons for four bed material categories are shown in Figures B.4 and B.5 for the two groups of data. Discrepancy ratios and correlation coefficients based upon data from Groups 1 and 2 are shown in Tables B.9 and B.10. Comparisons between the Posada and Kodoatie et al. equations are also shown on these tables. Note that the values of "a" must be adjusted for input and results in English units (see Section 4.8.3).

Table B.8. Coefficients and Exponents for Equation B.6.				
	a	b	c	d
Silt-bed rivers	281.40	2.622	0.182	0
Very fine to fine-bed rivers	2,829.60	3.646	0.406	0.412
Medium to very coarse sand-bed rivers	2,123.40	3.300	0.468	0.613
Gravel-bed rivers	431,884.80	1.000	1.000	2.000



Table B.9. Discrepancy Ratios and Correlation Coefficients for Posada and Kodoatie Equations, Data from Group 1.				
	Posada		Kodoatie	
	$\overline{R}_D$	$C_c$	$\overline{R}_D$	$C_c$
Silt-bed rivers	0.12	0.8393	0.88	0.8018
Very fine to fine sand-bed rivers	0.33	0.6843	1.00	0.7242
Medium to very coarse sand-bed rivers	1.12	0.7274	1.00	0.8146
Gravel-bed rivers	312.46	0.2175	1.00	0.7625

Table B.10. Discrepancy Ratios and Correlation Coefficients for Posada and Kodoatie Equations, Data from Group 2.				
	Posada		Kodoatie	
	$\overline{R}_D$	$C_c$	$\overline{R}_D$	$C_c$
Silt-bed rivers	0.18	0.8393	0.88	0.8018
Very fine to fine sand-bed rivers	0.33	0.7845	1.01	0.8239
Medium to very coarse sand-bed rivers	1.12	0.7511	1.07	0.8006
Gravel-bed rivers	13.516	0.8357	0.47	0.9591

## B.4 LAURSEN AND MODIFIED LAURSEN EQUATIONS

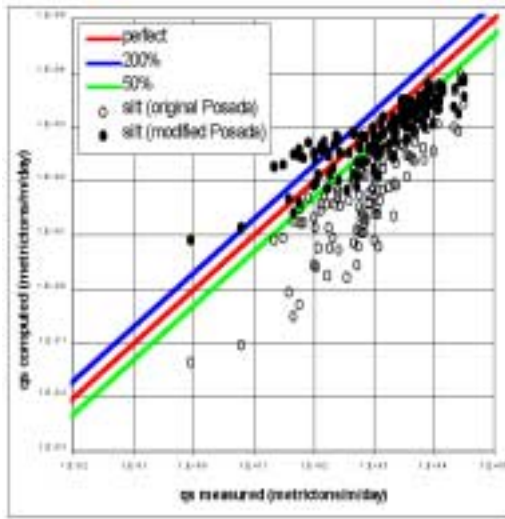
### B.4.1 Laursen Equation (1958)

Laursen (1958) working with Rouse developed the following equation. This relationship was modified by several scientists in an attempt to improve it by several scientists.

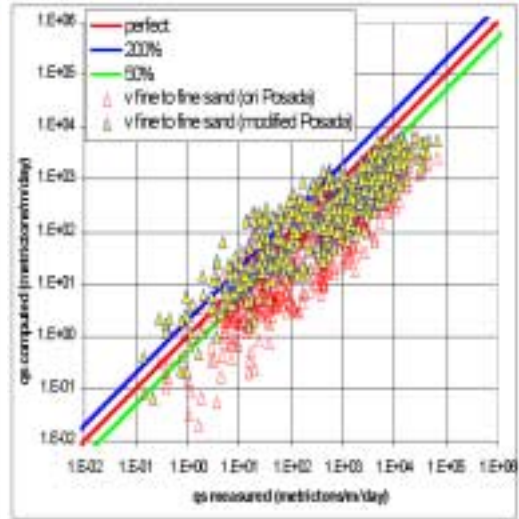
$$C_t = 0.01\gamma \sum_i p_i \left(\frac{d_i}{d}\right)^{7/6} \left(\frac{\tau'_o}{\tau_{ci}} - 1\right) f\left(\frac{V_*}{\omega_i}\right) \quad (\text{B.7})$$

### B.4.2 Modified Laursen Equation by Madden (1985) and Copeland and Thomas (1989)

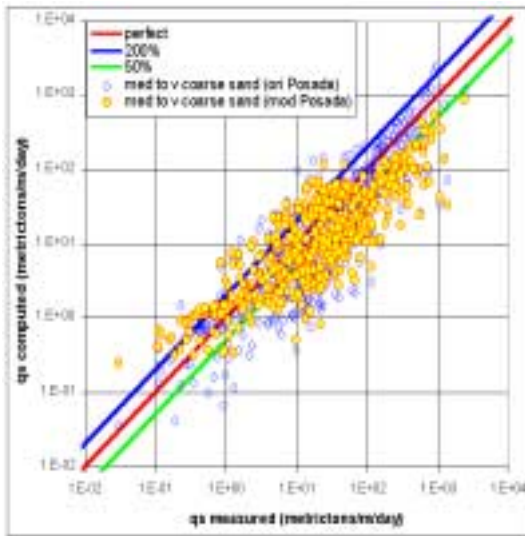
Madden (1985) modified Laursen's concepts by utilizing Arkansas River data. The modification by Madden permitted the analysis of bed material transport by size fraction. The U.S. Corps of Engineers' (1988) adopted this methodology for computing the transport in rivers with a mixture of sand and gravel forming the bed. Madden's modification to Laursen's methodology was based on three sets of sediment measurements made in the Arkansas River. The first two sets were gathered near Dardanelle in June-July 1957 and in April 1958. The third set was gathered near Morrilton in April 1958. Madden utilized the Missouri River data collected by Bondurant (1958) to validate the rating curves for the Arkansas River. The data sets resulted in best-fit curves that were parallel, but the two data sets did not overlap. The reader is reminded that the two sets of data were from two different rivers and even though they were sand-bed rivers, the methodologies produced by Bondurant and Madden were developed for specific rivers and are not generally applicable to other river systems.



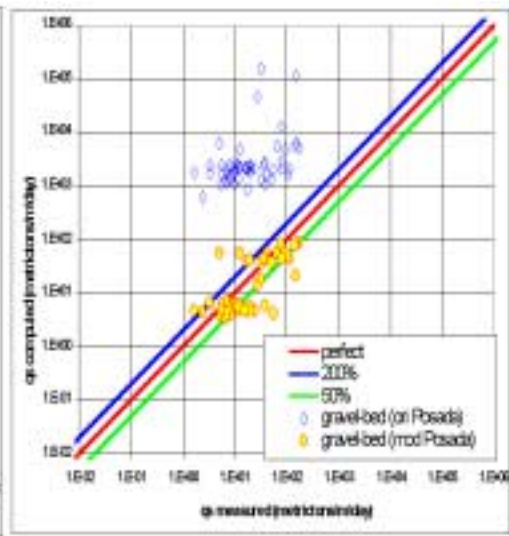
(a) silt-bed rivers



(b) very fine to fine sand bed rivers

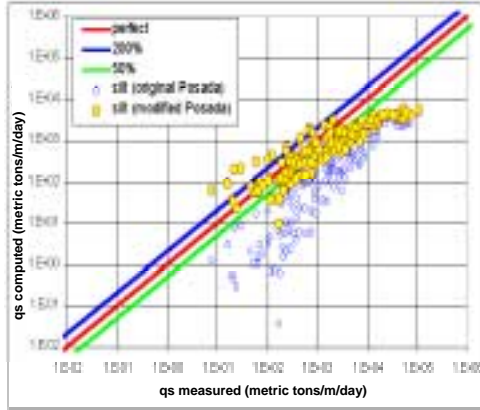


(c) medium to very coarse sand-bed rivers

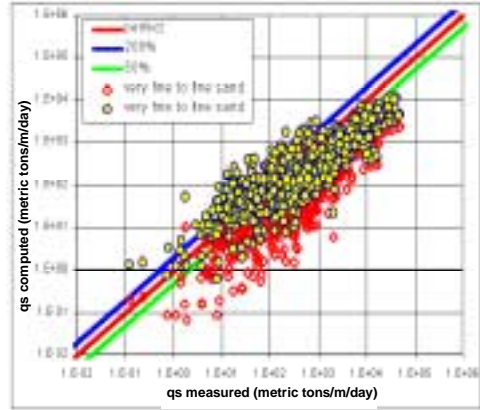


(d) gravel-bed rivers

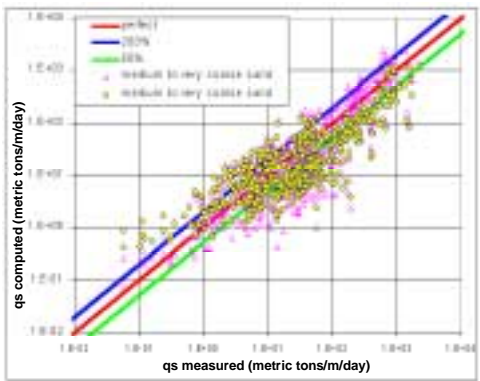
Figure B.4. Comparison of measured  $q_s$  and computed  $q_s$  using Posada and Kodoatie equations for various river-bed materials, data from Group 1.



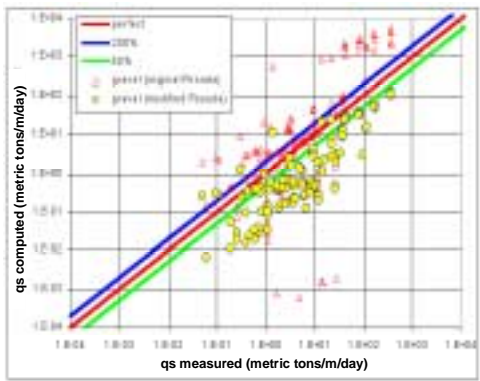
(a) silt-bed rivers



(b) very fine to fine sand-bed rivers



(c) medium to very coarse sand-bed rivers



(d) gravel-bed rivers

Figure B.5. Comparison of measured  $q_s$  and computed  $q_s$  using Posada and Kodoatie equations for various river-bed materials, data from Group 2.

An adjustment factor related to the Froude number was utilized to modify the Laursen equation by Madden as follows:

$$C_t = \sum_i p_b \left( \frac{d_i}{d} \right)^{7/6} \left( \frac{\tau'_o}{\tau_{ci}} - 1 \right) f \left( \frac{V_*'}{\omega_i} \right) \left( \frac{0.1616}{F_r^{0.904}} \right) \quad (\text{B.8})$$

In addition, Copeland and Thomas (1989) proposed a modification of Laursen's 1958 concept. This methodology was formulated to be utilized in both sand-bed rivers and, to a lesser degree, in larger gravel-bed rivers. The Laursen equation as modified by Copeland and Thomas is:

$$C_t = 0.01\gamma \sum_i p_i \left( \frac{d_i}{d} \right)^{7/6} \left( \frac{\tau'_o}{\tau_{ci}} - 1 \right) f \left( \frac{V_*'}{\omega_i} \right) \quad (\text{B.9})$$

The results of Copeland and Thomas' modification to the Laursen concepts are presented in Figure B.6. The relation between  $V_*'/\omega_i$  and  $f(V_*'/\omega_i)$  for four sizes of sediment sizes and three sizes of channels were plotted on the Laursen Graph and are presented on Figure B.7.

Many researchers have observed that more than one value of bed material transport can be obtained from the same values of  $Q$ ,  $V$ ,  $S_w$ ,  $S_f$ , and  $\tau_o$ , see for example, Brooks (1958), Simons and Sentürk (1992) and Yang (1996). Gilbert (1914) proposed the fact that different values of transport can occur for the same hydraulic parameters.

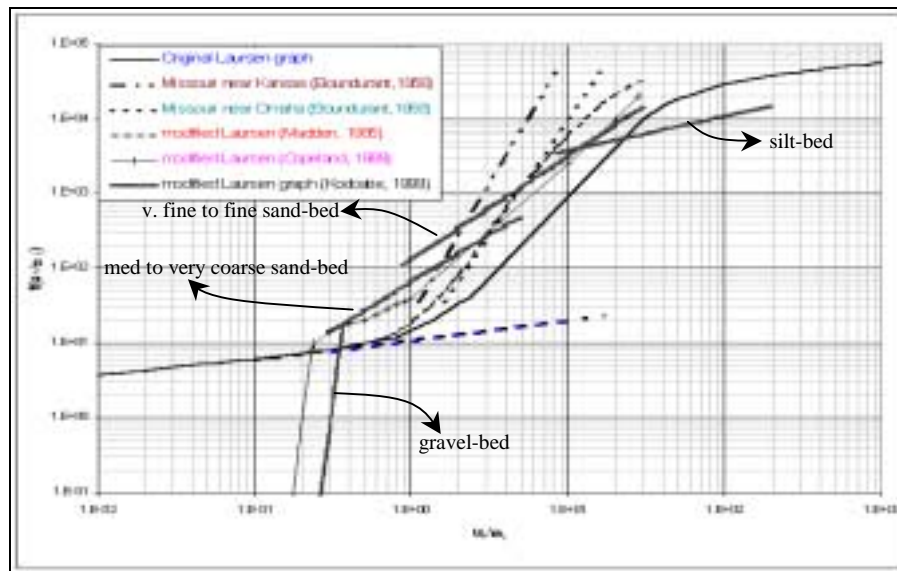
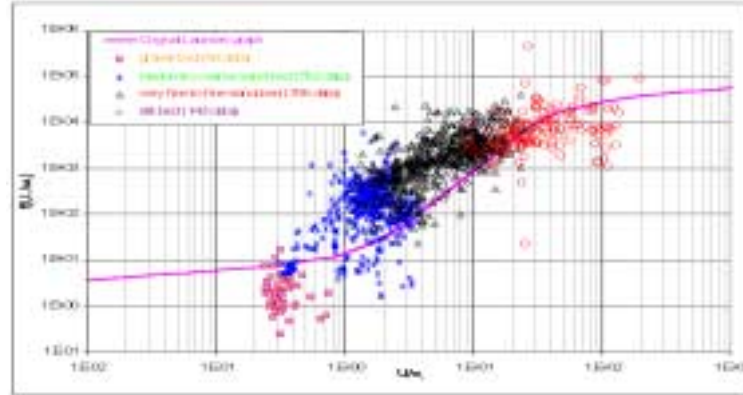
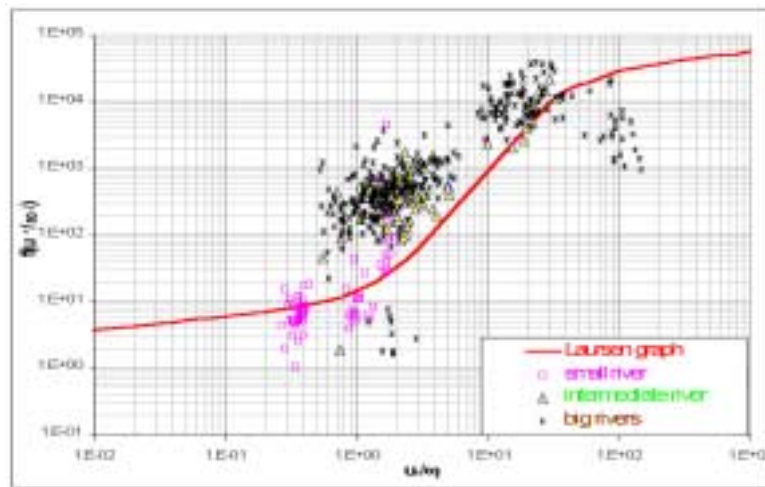


Figure B.6. Modifications of Laursen's (1958) Graph.



(a) four sizes of riverbed material



(b) three sizes of rivers

Figure B.7. Plotting  $V^*/\omega_i$  and  $f(V^*/\omega_i)$  for data from Group 1 with Laursen's Equation.

Accordingly, the validity of the assumption that total discharge for a given particle size can be determined by the proposed parameters is questionable. Lane (1955) and Bagnold (1966) first proposed the concept that stream power has a strong correlation which bed material discharge. Yang (1996) identified stream power,  $\tau V$ , as an independent variable with a strong correlation with bed material discharge. Furthermore, Yang suggested that unit stream power,  $VS$ , has a stronger relationship to bed-material discharge than stream power. Other researchers suggested that the stream power relations could be utilized in straight channels as well as channels that are in the process of changing their patterns from straight to meandering or braiding (Yang 1977 and 1996) (Vanoni 1978) (Yang and Molinas 1982). It is important to note that dimensionless unit stream power,  $VS/\omega$ , further improved the correlation with bed material discharge (Yang and Kong 1991). Kodoatie et al. 1999 verified that  $VS/\omega$  has a stronger correlation with bed-material discharge than other stream power parameters.

### B.4.3. Modified Laursen Equation by Kodoatie et al. (1999)

Kodoatie adapted the Laursen methodology for analysis because this methodology was expressed in terms which are generally recognized as important variables related to bed-material transport. Dimensionless unit stream power was used with regression analysis and nonlinear optimization techniques to improve the Laursen Equation. The modified Laursen equation resulting is (variables are defined in Section 4.9):

$$C_t = 0.01\gamma \left( \frac{D_{50}}{d} \right)^{7/6} \left( \frac{\tau_o'}{\tau_{c50}} - 1 \right) 10^{\log f \left( \frac{V_*'}{\omega_{50}} \right)} \left( \frac{VS}{\omega} \right)^a \quad (\text{B.10})$$

where the coefficient a is a variable related to mean bed material diameter as shown in Table B.11.

Bed Material	"a"
Gravel	0.0
Medium to very coarse sand	-0.2
Very fine to fine sand	0.078
Silt	0.06

In equations B.7 and B.10

- $C_t$  = Sediment concentration,  $N/m^3$  (lb/ft<sup>3</sup>)
- $\gamma$  = Unit weight of water,  $N/m^3$  (lb/ft<sup>3</sup>)
- $\rho_i$  = Fraction by weight of bed sediment mean size,  $D_i$
- $D_i$  = Bed sediment size with I percent finer, m (ft)
- $y$  = Mean flow depth, m (ft)
- $V$  = Mean velocity, m/s (ft/s)
- $V_*'$  =  $\sqrt{gRS} = \sqrt{\tau_o' / \rho}$ , m/s (ft/s)
- $\omega$  = Particle fall velocity, m/s (ft/s)
- $S$  = Slope
- $a$  = Exponent given in Table B.11
- $\tau_o'$  =  $\frac{\rho V^2}{58} \left( \frac{D_{50}}{y} \right)^{1/3}$ ,  $N/m^2$  (lb/ft<sup>2</sup>)
- $\tau_{ci}$  = Particle critical shear stress =  $k_s (\gamma_s - \gamma) D_i$ ,  $N/m^2$  (lb/ft<sup>2</sup>)
- $k_s$  = Shields parameter
- $\gamma_s$  = Unit weight of sediment,  $N/m^3$  (lb/ft<sup>3</sup>)

Note that in the modified Laursen equation an exponent equal to  $\log f(V_*/\omega_{50})$  is a significant variable. This parameter can be determined referring to Figure B.8. Comparison of modifications to the Laursen equation by Madden, Copeland, and Kodoatie et al. are presented in Table B.12.

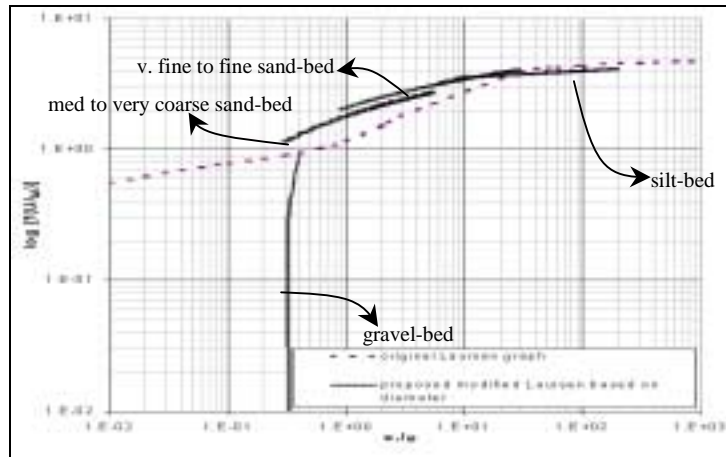


Figure B.8. Proposed graph by Kodoatie using Equation B.10.

Table B.12. Comparison of Modified Laursen Equations.

	Madden		Copeland		Kodoatie et al.
1	Used same equation, but modified using Froude No.	1	Used same equation, modified by 0.018	1	Used same equation but added dimensionless streampower as the adjustment factor
2	Used modified graph	2	Used modified graph	2	Used modified graph. More specific in particle size from silt to gravel
3	Used size fraction	3	Used size fraction	3	Used median particle diameter
4	Used Arkansas River data	4	Used both river and flume data (not specified)	4	Used 33 river systems and 18 sources of flume data (total data more than 5300 sets)
5	Graph is higher than original for sand bed; not specified for gravel and silt	5	Graph is higher than original for sand bed; for silt not specified; graph for gravel is proposed	5	Graph is higher than the original for sand bed (sand bed is more specific for very fine to fine sand and medium to very coarse sand); smaller for silt compared to original; graph for gravel is proposed

The modified Laursen equation (Kodoatie, 1999) was developed using Group 1 data and validated using Group 2 data. The following paragraphs show that this modified Laursen equation provides reasonable estimates of sediment transport for sediment sizes ranging from silt to gravel bed and rivers ranging in size from small to large.

#### B.4.3.1 Gravel-Bed Rivers

The relationship between  $V^*/\omega_i$  and  $f(V^*/\omega_i)$  of data from Group 2 (Meyer-Peter and Müller laboratory data) for gravel beds is within the range of the relationship between  $V^*/\omega_i$  and  $\log f(V^*/\omega_i)$  utilizing data from Group 1 (Figure B.9). However, since few field data sets are reported for gravel-bed rivers, which are usually bimodal, further research should be conducted in this area. The Meyer-Peter and Müller (MPM) formula may be utilized to check the results of this analysis. The MPM method is based upon almost 20 years of experimental work and is probably the most widely utilized relationship for coarse bed material (Simons and Sentürk 1992).



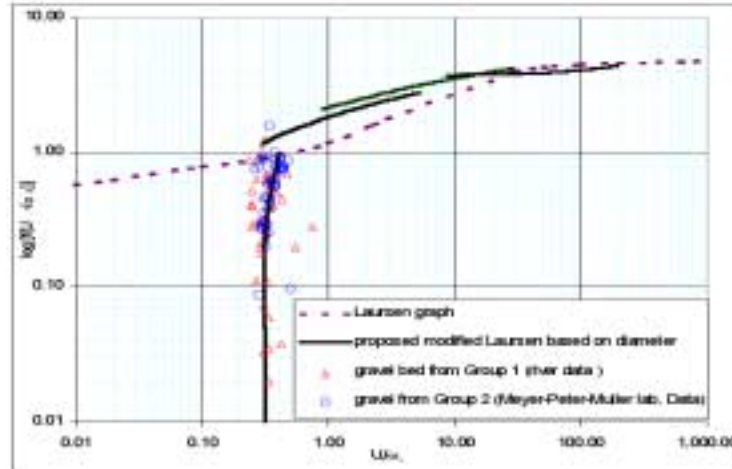


Figure B.9. Relationships between  $V^*/\omega_i$  and  $\log [f(V^*/\omega_i)]$  for gravel-bed rivers and gravel-bed Meyer-Peter and Müller laboratory data.

#### B.4.3.2 Medium to Very Coarse Sand-Bed Rivers

Comparisons of Group 2 data between measured  $C_{ppm}$  and computed  $C_{ppm}$  by the Laursen and modified Laursen equation are shown in Figure B.10 and Table B.13.

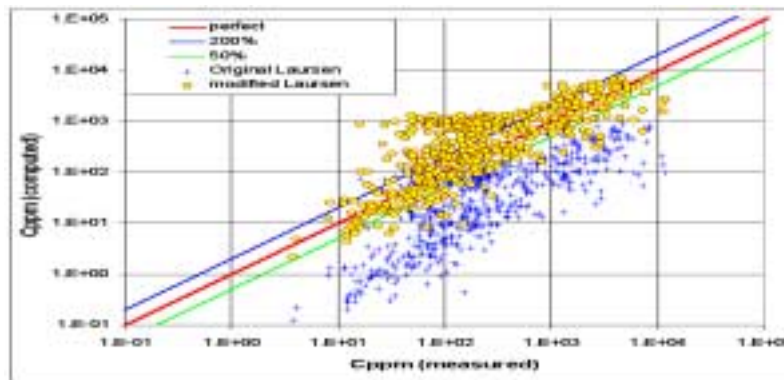


Figure B.10. Comparison of measured and computed concentration using Laursen and modified Laursen for medium to very coarse sand bed-rivers.

Table B.13. Discrepancy Ratio $\overline{R_D}$ Between $C_{ppm}$ Computed and $C_{ppm}$ Measured for Medium to Very Coarse Sand-Bed Rivers.		
	Laursen	Modified Laursen
Discrepancy Ratio $\overline{R_D}$	0.24	0.98



### B.4.3.3 Very Fine to Fine Sand-Bed Rivers

Comparison of Group 2 data between measured and computed concentrations by the Laursen and modified Laursen equation are shown in Figure B.11 and Table B.14.

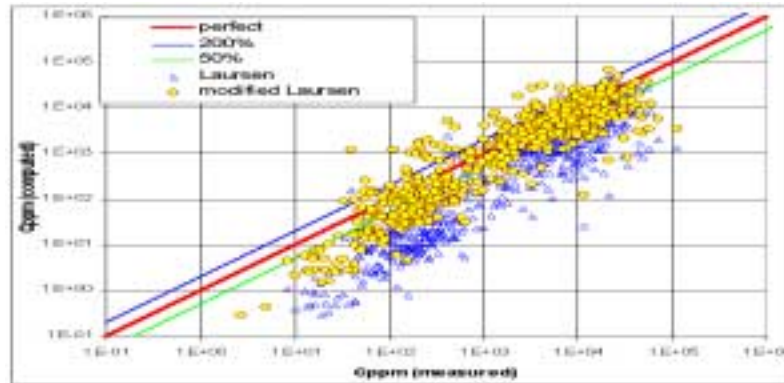


Figure B.11. Comparison of measured  $C_{ppm}$  and computed  $C_{ppm}$  using Laursen and modified Laursen equation for very fine sand bed-rivers.

Table B.14. Discrepancy Ratio $\overline{R_D}$ Between $C_{ppm}$ Computed and $C_{ppm}$ Measured for Very Fine to Fine Sand-Bed Rivers.		
	Laursen	Modified Laursen
Discrepancy Ratio $\overline{R_D}$	0.36	1.01

### B.4.3.4 Silt-Bed Rivers

Comparison of Group 2 data between measured and computed concentrations by the modified Laursen equation are shown in Figure B.12 and Table B.15.

### B.4.3.5 Channel Size

As stated in previous paragraphs, the analysis of sediment transport relations was based upon channel size subdivided into small rivers, intermediate rivers, and large rivers. From Figure B.7(b), the relationships between  $V^*/\omega_i$  and  $f(V^*/\omega_i)$  for these three channel sizes using data from Group 1 follow the proposed modified Laursen graph. Validation for this consistency is examined using data from Group 2 for three channel sizes. The relationships between  $V^*/\omega_i$  and  $f(V^*/\omega_i)$  for data from Group 2 for these three channel sizes are plotted with the Laursen graph in Figure B.13. From Figure B.13, it can be concluded that consistency between  $V^*/\omega_i$  and  $\log f(V^*/\omega_i)$  is good for several sizes of rivers based upon data from Group 2. This figure also shows that for different sizes of bed sediment (from silt to gravel) the proposed modified Laursen relation gives good results in comparison with other accepted methods.

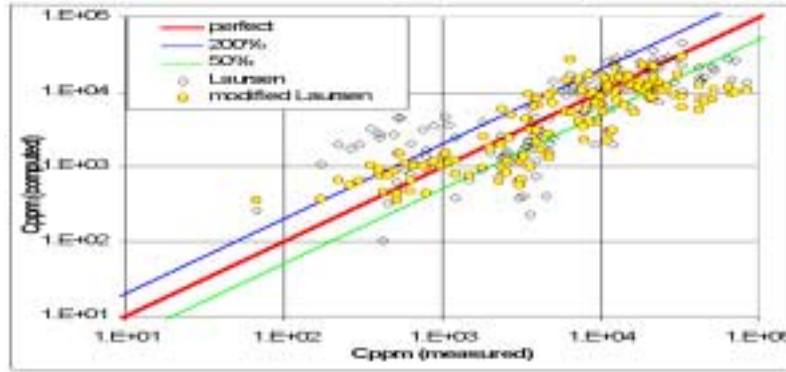


Figure B.12. Comparison of  $C_{ppm}$  measured and  $C_{ppm}$  computed using Laursen and modified Laursen equations for silt-bed rivers.

Table B.15. Discrepancy Ratio $\overline{R_D}$ Between Computed $C_{ppm}$ and Measured $C_{ppm}$ for Silt-Bed Rivers.		
	Laursen	Modified Laursen
Discrepancy Ratio $\overline{R_D}$	1.45	0.991

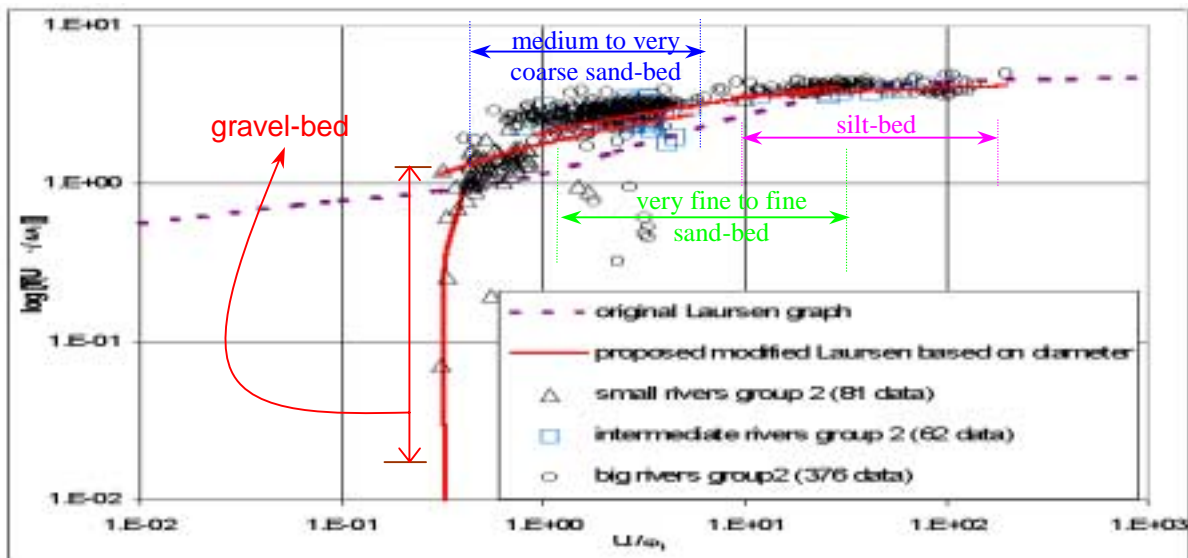


Figure B.13. Relationships between  $V^*/\omega_b$  and  $\log(V^*/\omega_b)$  for river size.

### B.5 RANGE OF DATA FOR VALIDATION

To validate the Kodoatie et al. power relationship and modified Laursen equation, data from Group 2 were used. The computed  $C_{ppm}$  from the proposed methods were compared to the measured  $C_{ppm}$ . Note that because sets of data for gravel-bed rivers were relatively small, the laboratory data of Meyer-Peter and Müller (1948) containing 139 sets of data were used

for validation and verification. The ranges of hydraulic variables of the Group 2 data are shown below.

### **B.5.1 Bed Material Size**

Gravel-Bed Rivers. The mean diameter of particle size has the range of 2.69 mm (very fine gravel) to 28.65 mm (coarse gravel). The wide range of geometric data is,

discharge, Q	: 0.001 – 4.614 m <sup>3</sup> /s
width, W	: 0.1 – 2.0 m
depth, d	: 0.01 – 1.092 m
slope, S	: 0.0004 – 0.0227

Sand-Bed Rivers. The sand-bed rivers were divided into two groups as follows: very fine to fine sand-bed rivers (0.062 mm – 0.250 mm), and medium to very coarse sand-bed rivers (0.251 mm – 2.00 mm).

Very Fine to Fine Sand-Bed Rivers (0.062 – 0.250 mm). A total of 692 data sets from Group 2 including 23 river systems were used. The range of data is:

discharge, Q	: 0.003673 – 235,000 m <sup>3</sup> /s
width, W	: 0.346 – 3,090 m
depth, d	: 0.0341 – 68.00 m
slope, S	: 0.0000027 – 0.00769

Medium to Very Coarse Sand-Bed Rivers (0.251 mm – 2.00 mm). A total of 546 data sets including 23 river systems outside of the United States and an additional 68 data sets from rivers in the United States includes: seven sets of data from the Black River near Galesville, Wisconsin; three sets data from the Chippewa River near Caryville, Wisconsin; 14 sets of data from the Chippewa River of at Durand, Wisconsin; 18 sets of data from the Chippewa River near Pepin, Wisconsin; six sets of data from the Toutle River at Tower Road near Silver Lake, Washington; nine sets of data from the Wisconsin River at Muscoda, Wisconsin; and 11 sets of data from the Yampa River at Deerlodge Park, Colorado. The range of data is as follows:

discharge, Q	: 0.0075 – 151,000 m <sup>3</sup> /s
width, W	: 1.00 – 2,608 m
depth, d	: 0.061 – 65.00 m
slope, S	: 0.0000138 – 0.0029

Silt-Bed Rivers. A total of 141 data sets from Group 2 including three river systems were used. The range of data is:

discharge, Q	: 1.15 – 41,200 m <sup>3</sup> /s
width, W	: 4.3 – 3,110 m
depth, d	: 0.55 – 13.10 m
slope, S	: 0.0000120 – 0.00087

## B.5.2 River Size

Small Rivers (width < 10 m and depth < 1.0 m). A total of 81 data sets from Group 2 including six river systems were used. The range of data is:

discharge, Q : 0.2268 – 7.35 m<sup>3</sup>/s  
mean bed diameter, D<sub>50</sub> : 0.042 mm (coarse silt) – 57.51 mm (very coarse gravel)  
slope, S : 0.000115 – 0.00745

Intermediate Rivers (10 m < width < 50 m and 1.0 m < depth < 3 m). A total of 61 data sets from Group 2 including nine river systems were used. The range of data is:

discharge, Q : 17.50 – 268.72 m<sup>3</sup>/s  
mean bed diameter, D<sub>50</sub> : 0.021 (medium silt) – 1.91 mm (very coarse sand)  
slope, S : 0.000058 – 0.0024

Large Rivers (width > 50 m and depth > 3 m). A total of 374 data sets from Group 2 including 13 river systems were used. The range of data is:

discharge, Q : 107 – 235,000 m<sup>3</sup>/s  
mean bed diameter, D<sub>50</sub> : 0.02 mm (medium silt) – 1.05 mm (coarse sand)  
slope, S : 0.0000027 – 0.000121

## APPENDIX C

### Index

<b>TERM</b>	<b>SECTION</b>
alluvial channels	3.1
alluvial channel flow	1.7.2, 3.1
alluvial fans	5.2.3
alluvial river	3.1, 5.3
anabranch	5.4.1
angle of repose	3.2.8, 3.7.2
antidunes	3.3.1, 3.3.7
average boundary shear stress	2.4.4
average velocity	2.2.1
backwater curve classification	2.8.2
bank protection	6.5, 6.6
bars	3.3.10
bends	2.7
bendway weirs	6.4.2
Bernoulli Equation	2.2.3
block revetment	6.6.6
braided river channel	5.4.4
bulkhead	6.4.8
causes of streambank failure	6.2.1
celerity	2.5.1
channel bends	2.7, 5.4
channel forms	5.4
channel relocation	6.9.3
Chenzy's equation	2.4.3
choking flow	2.6.3, 2.10.4
chutes and pools	3.3.8
clay plug	5.4.3
cohesion	3.2.7, 7.7.5
Colby Method	4.5.4
computer modeling	2.11, 5.6.2
computerized data bases	8.4
concentration conversion factors	4.8
concrete mattresses	6.6.6
conservation of energy	2.2.3
conservation of mass	2.2.1
conservation of momentum	2.2.2
contraction scour	7.2, 7.6.1

## APPENDIX C

### Index

<b>TERM</b>	<b>SECTION</b>
control volume	2.2.1
convective acceleration	2.2.1
countermeasures for hydraulic problems	6.1, 7.1
critical shear stress	3.5
critical velocity	3.5.5, 3.5.6
culvert analysis programs	2.12.1
culvert design	2.12
culvert flow	2.12
culvert hydraulics	2.12
data checklist	8.2
data needs	8.1
data sources	8.3, 8.4
debris	5.7.2, 7.7.6
dikes	6.4.5, 6.4.6
discharge diagram	2.6.3
distorted scales	5.6.1
dominant discharge	5.4.7
drag coefficient	3.5.3
drag force	3.5.3
drop structures	2.6.5, 6.4.11
dunes	3.3.1, 3.3.5
effective diameter	3.2.4
effects of human activities	1.4, 5.7.1
effects of natural changes	1.2, 5.7.2
Einstein Method	4.5.2
encroachment	1.1, 1.4
environmental impacts	6.9, 8.1.10
equation of hydrostatics	2.12
equation of motion	2.2
fall velocity	3.2.1, 3.2.3
fencing	6.4.9
filter design for riprap	6.7, 6.11.2
floodplain	5.4.1
flow classifications	2.1.1, 3.3.1
flow control structures	6.4
flow regimes	3.3.1
flow resistance	2.4, 3.4

## APPENDIX C

### Index

TERM	SECTION
forces on particles	3.5
Froude number	2.1.1, 2.5.3, 5.6.1
gabion mattresses	6.6.4
general scour	7.2, 7.6
geomorphic threshold	5.2.5
gradation coefficient	3.2.4
gradually varied flow	2.8
groins	6.4.1
guidebanks	6.4.10
hardpoints	6.4.3
headcut	5.2.4
hydraulic geometry	5.4.6
hydraulic jump	2.5.3
hydraulically rough boundary	2.4.2
hydraulically smooth boundary	2.4.2
jetties	6.4.7
kinetic energy correction factor	2.2.3, 2.4.6
laminar flow	2.1.1
limiting shear stress	3.5, 7.6.1
local acceleration	2.2.1
local scour at abutments	7.2, 7.8
local scour at drop structures	2.6.5, 6.4.11
local scour at embankments	6.8
local scour at piers	7.2, 7.7
local shear stress	2.4.5
lower flow regime	3.3.1
Manning's equation	2.4.3
mature river	5.2.1
meandering river channel	5.4.3
Meyer-Peter and Müller	4.5.1
mixing length	2.4.2
mobile bed model	5.6.1
momentum coefficient	2.2.2, 2.4.6
n-value estimate for sand bed streams	2.4.3, 3.4.11
n-value estimation	2.4.3
neotectonics	1.2.1
nickpoint	5.2.4

## APPENDIX C

### Index

TERM	SECTION
nominal diameter	3.2.1
nonuniform flow	2.2.1
open channel flow	2.1
overtopping, embankment	2.13, 6.8
pebble count	3.2.4, 3.7.1
physical modeling	5.6.1
pile retard	6.4.6
pipette method	3.2.4
plane bed	3.3.1, 3.3.6
plane bed with sediment movement	3.3.6
porosity	3.2.6
power function	4.7
pressure distribution	2.3
qualitative river response	5.5
rapid flow	2.1.1
rapidly varying flow	2.6
retards	6.4.4
revetment	6.3.3, 6.3.4
Reynolds number	5.6.1
ripples	3.3.1, 3.3.4
ripples on dunes	3.3.1
riprap	6.5
riprap design	6.5
riprap failure	6.5.7
riprap filter	6.7, 6.11.2
riprap gradation	6.5.5
riprap placement	6.5.6
riprap stability	6.5
river channel classification	5.2, 5.4.1
river channel profiles	2.8.2, 5.4.8
river morphology	5.1
river response to change	1.2, 5.5
river stabilization	6.4, 6.5
river variables	1.5.1
roadway overtopping	2.13, 6.8
rock fill trench revetment	6.5.6
roll waves	2.5.4



## APPENDIX C

### Index

TERM	SECTION
sack revetment	6.6.5
sampling bed material	3.2.4
scour due to overbank flow	2.13, 6.8
scour, general	7.2, 7.6
scour, local	7.2, 7.7, 7.8
sediment concentration conversion	4.8
sediment discharge	3.6, 4.2
sediment discharge measurement	3.6
sediment shape	3.2.2
sediment terminology	3.6.2, 4.3
sediment transport	3.6.7, 4.1
sedimentation diameter	3.2.1
shear stress relations	2.4.5
Shields' criteria	3.5.4
sieve analysis	3.2.4
sieve diameter	3.2.1, 3.2.4
similitude	5.6.1
sinuosity	5.3, 5.5.1
size classification of sediments	3.2.1
size distribution	3.2.4
soil cement revetment	6.6.8
specific discharge	2.6.3
specific energy (specific head)	2.6.2
specific weight	3.2.5
spur	6.4.1
spur angle	6.4.1
spur crest	6.4.1
spur height	6.4.1
spur length	6.4.1
spur spacing	6.4.1
stability of relocated channels	1.2, 1.3.2
stabilization measures	6.1, 6.3
standard fall diameter	3.2.1
standard fall velocity	3.2.1
standard step method	2.8.3
steady flow	2.2.1
steel jacks	6.4.7

## APPENDIX C

### Index

TERM	SECTION
stone fill dike	6.4.6, 6.5.6
straight river channel	5.4.2
stream gaging	2.9
stream power	3.4.11, 4.7, 5.5.1
stream stability	1.2, 5.1
superelevation, in rapid flow	2.7.4, 2.10.4
superelevation, in subcritical flow	2.7.3
surges	2.5.2
suspended sediment discharge	3.6, 4.4
timber crib	6.4.4
timber pile dike	6.4.6
tranquil flow	2.1.1
transition zone flow regime	2.4.2, 3.3.1
transitions	2.6, 3.3.1
transitions, in rapid flow	2.6.4
transverse velocity distribution	2.7.2
turbulent (Reynolds) shear stress	2.4.2
turbulent flow	2.1.1, 2.4.2
turbulent velocities	2.4.2
uniform flow	2.2.1
unsteady flow	2.2.1
upper flow regime	3.3.1
vane dike	6.4.6
vegetation revetment	6.6
velocity of flow on riprap	6.5.3, 6.5.4
viscous drag	3.5.3
viscous sublayer	2.4.2
visual accumulation tube	3.2.4
von Karman universal velocity coefficient	2.4.2
windrow revetment	6.5.6